frontiers | Research Topics

# Case reports in surgical oncology 2022

**Edited by**
Riccardo Bertolo, Akinfemi Akingboye, Tomoyuki Abe and Zhaolun Cai

**Published in**
Frontiers in Surgery
Frontiers in Oncology
Frontiers in Immunology

ISSN 1664-8714
ISBN 978-2-8325-3504-2
DOI 10.3389/978-2-8325-3504-2

## About Frontiers

Frontiers is more than just an open access publisher of scholarly articles: it is a pioneering approach to the world of academia, radically improving the way scholarly research is managed. The grand vision of Frontiers is a world where all people have an equal opportunity to seek, share and generate knowledge. Frontiers provides immediate and permanent online open access to all its publications, but this alone is not enough to realize our grand goals.

## Frontiers journal series

The Frontiers journal series is a multi-tier and interdisciplinary set of open-access, online journals, promising a paradigm shift from the current review, selection and dissemination processes in academic publishing. All Frontiers journals are driven by researchers for researchers; therefore, they constitute a service to the scholarly community. At the same time, the *Frontiers journal series* operates on a revolutionary invention, the tiered publishing system, initially addressing specific communities of scholars, and gradually climbing up to broader public understanding, thus serving the interests of the lay society, too.

## Dedication to quality

Each Frontiers article is a landmark of the highest quality, thanks to genuinely collaborative interactions between authors and review editors, who include some of the world's best academicians. Research must be certified by peers before entering a stream of knowledge that may eventually reach the public - and shape society; therefore, Frontiers only applies the most rigorous and unbiased reviews. Frontiers revolutionizes research publishing by freely delivering the most outstanding research, evaluated with no bias from both the academic and social point of view. By applying the most advanced information technologies, Frontiers is catapulting scholarly publishing into a new generation.

## What are Frontiers Research Topics?

Frontiers Research Topics are very popular trademarks of the *Frontiers journals series*: they are collections of at least ten articles, all centered on a particular subject. With their unique mix of varied contributions from Original Research to Review Articles, Frontiers Research Topics unify the most influential researchers, the latest key findings and historical advances in a hot research area.

Find out more on how to host your own Frontiers Research Topic or contribute to one as an author by contacting the Frontiers editorial office: frontiersin.org/about/contact

# Case reports in surgical oncology: 2022

**Topic editors**

Riccardo Bertolo — Hospital San Carlo di Nancy, Italy
Akinfemi Akingboye — Dudley Group NHS Foundation Trust, United Kingdom
Tomoyuki Abe — Higashi-hiroshima medical center, Japan
Zhaolun Cai — Sichuan University, China

**Citation**

Bertolo, R., Akingboye, A., Abe, T., Cai, Z., eds. (2024). *Case reports in surgical oncology: 2022*. Lausanne: Frontiers Media SA. doi: 10.3389/978-2-8325-3504-2

# Table of contents

frontiers | Frontiers in Oncology

TYPE Editorial
PUBLISHED 13 February 2024
DOI 10.3389/fonc.2024.1300868



OPEN ACCESS

EDITED AND REVIEWED BY
Francesco Giovinazzo,
Agostino Gemelli University Polyclinic (IRCCS), Italy

*CORRESPONDENCE
Riccardo Bertolo
riccardobertolo@hotmail.it

RECEIVED 23 September 2023
ACCEPTED 23 January 2024
PUBLISHED 13 February 2024

CITATION
Bertolo R (2024) Editorial: Case reports in surgical oncology: 2022.
*Front. Oncol.* 14:1300868.
doi: 10.3389/fonc.2024.1300868



# Editorial: Case reports in surgical oncology: 2022

Riccardo Bertolo*

Urology Unit, Azienda Ospedaliera Universitaria Integrata Verona, AUOI Verona, University of Verona, Verona, Italy

KEYWORDS

**surgical oncology, urology, case report, surgery, malignant neoplasm**

Editorial on the Research Topic
Case reports in surgical oncology: 2022

Dear readership, it is my pleasure to present you the Research Topic published on *Frontiers in Oncology* and *Frontiers in Surgery* entitled "*Case Reports in Surgical Oncology: 2022*". While editing this Research Topic, unique and/or rare cases coming from different fields of surgical oncology were selected among the submissions received. As a uro-oncologist, I am very proud to present you a selection of the 18 case reports of interest for the urologic surgeons out of the 55 submissions finally accepted. It is impressive to observe the interest and the productivity of urology researchers witnessed by such numbers. This is particularly true given the wide spectrum of diseases embraced by surgical oncology. I tried to summarize you in a few sentences the key messages from each of the articles featured in my editorial. An "organ-by-organ" sequence was followed.

Five submissions were focused on oncologic surgical interventions performed to treat diseases of the genitalia or the sacral area. Hao et al. reported the case of a 69-year-old man presenting with a growing, painless mass protruding from the penis. The patient underwent resection of the penile mass, followed by extended resection in the second operation. The diagnosis of leiomyosarcoma was verified by pathological examination. The authors underlined that immunohistochemical examination is essential for rendering this rare diagnosis. Yan et al. reported a case of superficial angiomyxoma in a 42-year-old male patient. The patient was admitted to hospital with a perineal mass found more than 1 year previously. A pelvic contrast-enhanced computed tomography scan confirmed the 6.0 cm × 8.6 cm × 4.5 cm with still clear borders seen below the penile corpus cavernosum in the perineum. Perineal mass excision was performed, and pathology report diagnosed perineal superficial angiomyxoma. Chen et al. presented a rare case of aggressive angiomyxoma in the scrotum of a 70-year-old man, underlining the importance of considering aggressive angiomyxoma in the differential diagnosis of myxoid neoplasms growing painless in male genital areas. Jiang et al. reported about the fourth ever published nuclear protein of the testis (NUT) carcinoma of probable ovarian origin. NUT is a rare subset of poorly differentiated, highly aggressive malignancy defined by NUTM1 gene rearrangements. The diagnosis is confirmed by immunohistochemistry. With their publication, the authors underlined how it is essential to think about this rare disease whenever an undifferentiated malignant neoplasm arises from the abdominopelvic cavity. Chen et al. presented the case of a 49-year-old male patient with a history of frequent and

urgent urination for 2 weeks. Radiologic studies revealed a large cystic mass in the lower abdomen. The patient underwent abdominal laparotomy, which revealed a large cystic mass arising from the distal ileum invading the sigmoid mesocolon and the bladder apex. Partial resection of the ileum along with the tumor and the adjacent bladder was performed. Macroscopic examination revealed that the cystic mass contained a large amount of foul-smelling pus and a tumor-bowel fistula. The final pathology revealed an abdominal stromal tumor. Postoperative recovery was uneventful, and adjuvant imatinib mesylate 400 mg was administered daily. The authors underlined that this is a rare presentation of the disease.

Seven submissions were focused on surgeries for renal cell carcinoma (RCC), of which two about partial nephrectomy, three about radical nephrectomy, and two about metastasectomy in metastatic RCC. Starting with partial nephrectomy, Yu et al. presented the case of a 71-year-old female patient diagnosed with a 20 x 16 cm RCC of the solitary functioning kidney. This was an imperative indication for nephron-sparing surgery. The patient initially presented with hematuria and acute urinary tract obstructive anuria caused by renal calculi. She underwent nephron-sparing surgery with success. It was a pT3 renal cancer. At 26-month follow-up renal function recovered to baseline level. No relapse was detected. Zou et al. reported the case of a 64-year-old man who was diagnosed with an extremely rare case of localized RCC in the left kidney complicated with situs viscerum inversus totalis and abdominal cocoon. The patient underwent robot-assisted partial nephrectomy. Surgery was uneventful. As regarding radical nephrectomy, Ning et al. reported the case of a female patient with low back pain diagnosed with a 7 cm left renal cystic mass. The mass was diagnosed to be a mucinous cystadenocarcinoma of the kidney after robot-assisted radical nephrectomy. This is a rare renal epithelial tumor originating from the urothelium of the pelvis. Zhang et al. reported the case of a 40-year-old woman who presented Castleman's disease arising in the renal sinus which resembled a RCC. Castleman's disease is a rare benign lymphoproliferative disease that frequently involves the mediastinal thorax and the neck lymph nodes. It rarely affects extra-thoracic presentations, with even fewer presentations in the renal sinus. In this case, the patient underwent radical nephrectomy. Histological examination revealed hyperplastic lymphoid follicles in the renal sinus and was finally diagnosed as Castleman's disease. The authors underlined that due to the low incidence of Castleman's disease at the level of the renal sinus, there is a strong likelihood of missing the diagnosis. Finally, Courcier et al. reported about a case of renal medullary carcinoma diagnosed in a 31-year-old male patient. It is a rare form of RCC with poor prognosis, known to be associated with sickle cell trait or disease, although the exact underlying mechanisms are still unclear. The diagnosis is made through immunochemical staining for SMARCB1 (INI1). The patient underwent upfront cisplatin-based cytotoxic chemotherapy before surgical removal of the right kidney and retroperitoneal lymph node dissection. Identical adjuvant chemotherapy was administered post-surgery. The disease relapses were detected in the retroperitoneal lymph nodes; these were managed with chemotherapy and surgical rechallenges until the patient died after 37 months of follow-up. The authors underlined that current management of renal medullary carcinoma relies on perioperative cytotoxic chemotherapy strategies, given that there are no known alternative therapies that have been shown to be superior to date. As aforementioned, the last two reports focused on metastatic RCC and specifically about surgical resection of unusual metastases of RCC. Shepherd et al. retrospectively analyzed 20 years of electronic records at their institution and reported about 5 patients with metastases of clear cell RCC to the thyroid. This is an uncommon location for RCC metastases, and the authors underlined about the importance to be aware they can occur. Yang et al. presented the case of a 84-year-old man who had small bowel intussusception and obstruction due to a solitary metachronous metastasis from RCC. The solitary metachronous small bowel metastases from RCC are rare. In contrast to idiopathic intussusception frequently occurring in children, adult intussusceptions are uncommon and usually indicate the presence of a malignant neoplasm. Surgical resection was performed with success. With their case, the authors underlined that life-long follow-up of RCC patients is critical due to the unpredictable behavior of the disease and the possibility of a long period of dormancy. Surgical resection is the mainstay treatment for such patients.

Four submissions were focused on surgeries for adrenal masses or at least of excision of unusual masses located in the adrenal lodge.

Feng et al. reported the case of a giant cystic pheochromocytoma in a 64-year-old woman discovered as a right abdominal mass during ultrasonography. This is the largest pheochromocytoma ever documented in China (20 cm in diameter). Atrophy of the right lobe of the liver was found at preoperative imaging and confirmed during surgical resection. The same group reported about laparoscopic resection of an adrenal myelolipoma, a commonly benign, asymptomatic, and hormonally non-secreting disease. They underlined that there is insufficient awareness of this adrenal incidentaloma among clinicians. Studies for establishing common guidelines in the management of adrenal myelolipoma are needed [Feng et al.]. Zou et al. reported the case of a 55-year-old patient incidentally diagnosed with a soft-tissue mass located in the left adrenal region. No specific abnormalities in biochemical indexes were found but the patient had a 10-year history of hypertension. The patient had undergone open splenectomy 20 years before for splenic rupture caused by traffic-accident trauma. Because of the uncertain nature of the mass, surgical treatment was recommended. During the surgery, the adrenal origin was excluded. At final pathology, the splenic corpuscle and splenic medullary structure were seen, so that an accessory spleen was diagnosed. With their report, the authors underlined that, although the diagnosis of adrenal tumours mainly depends on imaging, misdiagnosis can occur for some adrenal space-occupying lesions without specific signs/symptoms or abnormal biochemical indexes. Finally, Li et al. reported about a rare case of retroperitoneal bronchogenic cyst in a 57-year-old woman who was admitted with no clinical symptoms and found to have masses in the adrenal gland area during a routine physical examination. Abdominal computed tomography revealed a cystic lesion found in the left suprarenal region. The patient underwent a laparoscopic exploration. The histopathological finding confirmed the diagnosis

of a retroperitoneal bronchogenic cyst. The authors underlined how such disease should be considered as one of the differential diagnoses among the retroperitoneal neoplasms.

The last two reports featured covered surgical interventions for other retroperitoneal neoplasms. Namely, Wang et al. reported about the rare association between acromegalic facial features induced by a retroperitoneal hemangiopericytoma and non-islet cell tumor hypoglycemia, a rare cause of hypoglycemia caused by the overproduction of high molecular weight insulin-like growth factor (big-IGF2), which activates the insulin receptor and subsequently caused hypoglycemia. The patient underwent complete surgical resection of the diagnosed mass. Surgical pathology demonstrated a hemangiopericytoma and strong positive for IGF-2. Lastly, Su et al. reported the case of a giant retroperitoneal cystic lymphangioma. Cystic lymphangioma is a rare benign tumor of the lymphatic system, which is most observed in the neck, head, and armpit. Less than 5% of lymphangiomas occur in the abdominal cavity and even less in the retroperitoneum. The patient underwent exploratory laparotomy, and the tumor was completely removed.

This is just a taste of what you can read in this Research Topic of unique case reports in urologic oncology. I hope I have intrigued you. Please feel free to enjoy each of the summarized submission in its full text format, which is open-access. You will definitely find interesting figures, including imagings, frames from intraoperative views, and photos of anatomo-pathology specimens when going through the articles. I sincerely feel that you will appreciate the very special clinical case scenarios in the present Research Topic.

## Author contributions

RB: Writing – original draft, Writing – review & editing.

## Conflict of interest

The author declares that the research was conducted in the absence of any commercial or financial relationships that could be construed as a potential conflict of interest.

## Publisher's note

frontiers | Frontiers in Surgery

TYPE Case Report
PUBLISHED 23 August 2022
DOI 10.3389/fsurg.2022.995859



OPEN ACCESS

EDITED BY
Zhaolun Cai,
Sichuan University, China

REVIEWED BY
Rafal Czepczynski,
Poznan University of Medical Sciences, Poland
Prasanta Kumar Pradhan,
Sanjay Gandhi Post Graduate Institute of Medical Sciences (SGPGI), India
Pinaki Dutta,
Post Graduate Institute of Medical Education and Research (PGIMER), India

*CORRESPONDENCE
Chengcheng Niu
niuchengcheng@csu.edu.cn

†These authors have contributed equally to this work

SPECIALTY SECTION
This article was submitted to Surgical Oncology, a section of the journal Frontiers in Surgery

RECEIVED 16 July 2022
ACCEPTED 10 August 2022
PUBLISHED 23 August 2022

CITATION
Ye F, Liao L, Tan W, Gong Y, Li X and Niu C (2022) Case report: Large follicular thyroid carcinoma with multiple cervical lymph node metastases.
Front. Surg. 9:995859.
doi: 10.3389/fsurg.2022.995859



# Case report: Large follicular thyroid carcinoma with multiple cervical lymph node metastases

Fei Ye[1†], Liyan Liao[2†], Wanlin Tan[3,4], Yi Gong[1], Xiaodu Li[3,4] and Chengcheng Niu[3,4*]

[1]Department of Thyroid Surgery, The Second Xiangya Hospital, Central South University, Changsha, China, [2]Department of Pathology, The Second Xiangya Hospital, Central South University, Changsha, China, [3]Department of Ultrasound Diagnosis, The Second Xiangya Hospital, Central South University, Changsha, China, [4]Research Center of Ultrasonography, The Second Xiangya Hospital, Central South University, Changsha, China

**Introduction:** Follicular thyroid carcinoma (FTC) rarely metastasizes to regional lymph nodes, as they mainly metastasize through hematogenous route; in particular, a large FTC with only lateral lymph node metastasis and without distant metastasis has rarely been reported.
**Case report:** We present a 66-year-old male patient with a progressively growing thyroid for more than 20 years, causing tracheal compression and narrowing. Neck ultrasonography, computed tomography (CT), magnetic resonance (MR) imaging and positron emission tomography–computed tomography (PET/CT) were carried out to obtain images of the thyroid and surrounding tissues. Total thyroidectomy and cervical lateral and central lymph node dissection were undertaken, and histopathological, and immunohistochemical evaluations and molecular pathology confirmed the diagnosis of FTC with multiple cervical lymph node metastases.
**Conclusion:** We have reported a rare case of large FTC with diffuse nodal involvement but no distant metastases. We present the thyroid ultrasound, neck CT, MR and whole body PET/CT.

KEYWORDS
follicular thyroid carcinoma (FTC), cervical lymph node metastases, vascular invasion, PET/CT, thyroid ultrasonography, TERT promoter mutation

## Introduction

Follicular thyroid carcinoma (FTC) is a type of differentiated thyroid cancer (DTC) derived from follicular cells that accounts for 10%–15% of all thyroid cancers. Its incidence is second only to papillary thyroid carcinoma (PTC), but its mortality rate is higher than that of PTC. Some patients have bone or lung metastases during initial treatment (1, 2). FTC mainly metastasizes through the blood circulation, and usually less than 10% metastasize through lymphatic system (3, 4).

Early diagnosis and treatment and the close follow-up of patients are the main means to improve the prognosis and prolong the postoperative survival of patients with FTC. However, unlike PTC, FTC is often associated with relatively benign ultrasound features on ultrasound images and can be easily diagnosed as thyroid follicular adenoma (FA) instead, which makes clinical treatment problematic (5).

Additionally, it is difficult to obtain a diagnosis from a fine needle aspiration, and the identification of cytological markers are not developed enough currently (6). FTC is often diagnosed based on clinicopathological vascular and capsular infiltration, and is sometimes missed due to a lack of clear infiltration foci or insufficient sampling, thus the diagnosis relies on morphology combined with immunohistochemical staining and molecular pathology (7).

Here, we report on a patient with a large FTC with lateral lymph node metastasis and no distant metastasis, showing the thyroid ultrasound, CT, MR and PET/CT images of the FTC and cervical lymph nodes, which provided multimodal preoperative imaging information for FTC.

## Case report

This study was reported in agreement with principles of the CARE guidelines (8). A 66-year-old male patient presented with a progressively growing thyroid for more than 20 years, causing tracheal compression and narrowing. The neck of the patient was abnormally swollen, with engorged superficial veins. The neck ultrasound revealed diffuse and swollen heterogeneous hypo-echoic thyroid tissue (Figure 1A). Cervical lymph nodes were enlarged, round and had no hilum on grayscale sonography, with different vascular distributions on color Doppler flow imaging (CDFI) mode (Figures 1B–F). Combined with the sonographic appearance of lateral lymph nodes, the whole thyroid was highly suspicious for malignancy. The neck CT was carried out to evaluate the thyroid mass with surrounding tissues, which revealed an extremely swollen thyroid with multiple enlarged cervical lymph nodes, some of which were larger than 6 cm, and some of which had obvious cystic changes and necrosis (Figures 2A,B). Then, the neck MR was used to evaluate the degree of stenosis of the cervical trachea and the need for a tracheal stent. MR images showed uneven signal values in the enlarged thyroid and lateral lymph nodes, and the tracheal compression and narrowing was obviously observed (Figures 2C,D). The patient had a tracheal stent placed before surgery to prevent airway stenosis. Next, PET/CT with 18F-fluorodeoxyglucose (18F-FDG) was performed to assess the extent of disease in the whole body due to the large mass, which showed extensive hypermetabolic lesions in the front of the neck and partial extension to the retrosternal space (Figure 3). Fortunately, this patient had no distant metastases. In addition, the serum thyroglobulin (TG) was more than 10,000 ng/ml (normal range was 3.5–77.0 ng/ml), which was far more than the normal value. The serum anti-TG value was 1.620 IU/ml (normal range was 0.000–4.110 IU/ml).

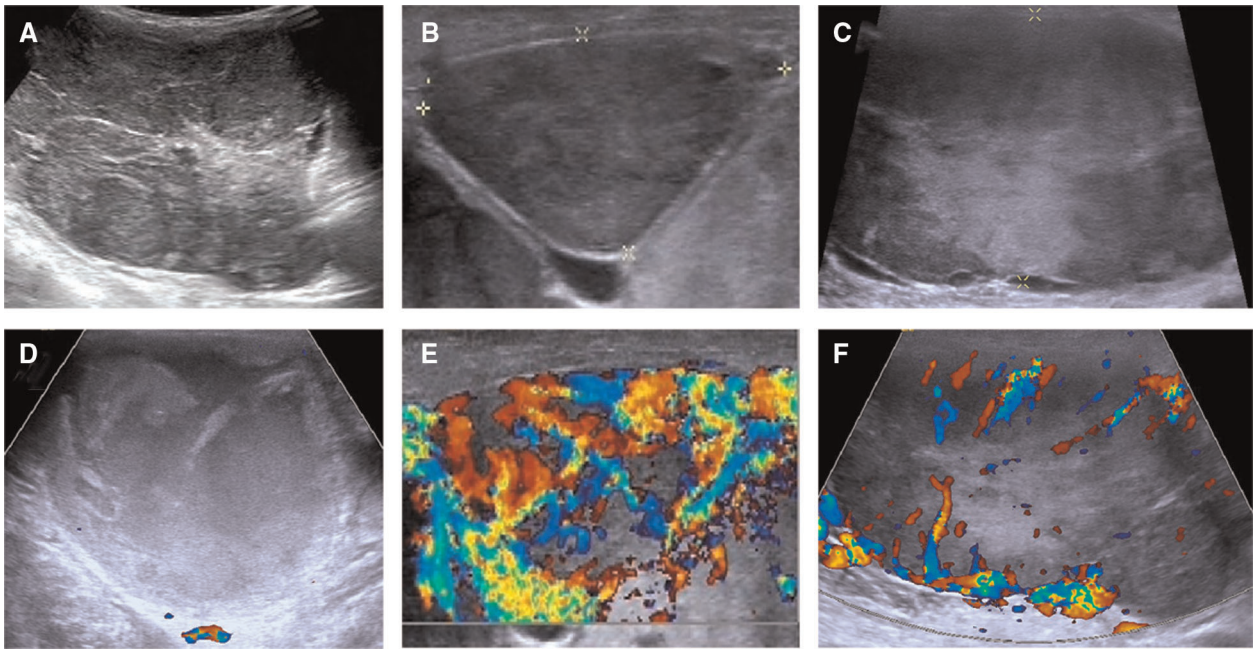


FIGURE 1
Ultrasonographic images of the thyroid and lateral lymph nodes. (A) The thyroid tissue displayed a heterogeneous echoic appearance on gray-scale sonography. (B,C) Cervical lymph nodes showed round shape and absence of hilum on gray-scale sonography. (D–F) CDFI showed different vascular distribution of cervical lymph nodes. (D) A mixed-echoic cervical lymph node with more than 90% of cystic change revealed no blood flow signal inside this lymph node. (E) A heterogeneous echoic cervical lymph node showed rich blood flow signal inside and around this lymph node. (F) A heterogeneous echoic cervical lymph node showed rich blood flow signal around this lymph node.

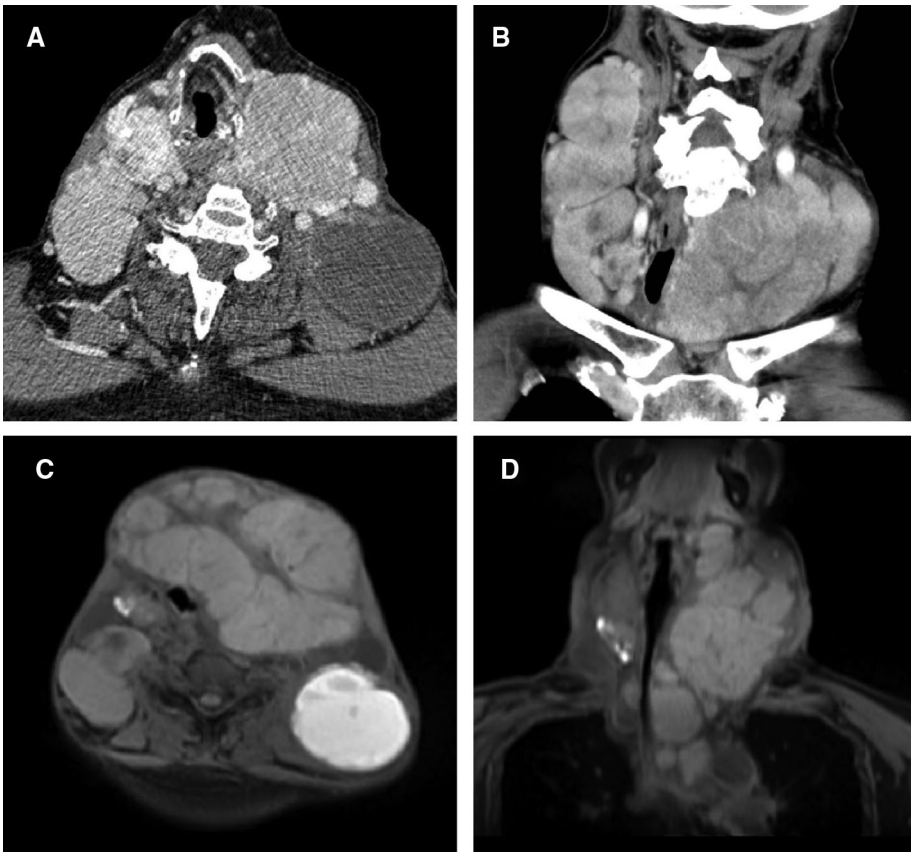


FIGURE 2
CT and MR images of the neck. (A) Transverse and (B) coronal sections of the neck revealed swelled thyroid with multiple enlarged cervical lymph nodes on CT. (C) Transverse and (D) coronal sections of the neck revealed swelled thyroid with multiple enlarged cervical lymph nodes on MR, causing the tracheal compression and narrowing.

Then, a total thyroidectomy and cervical lateral and central lymph node dissection were undertaken; this whole thyroid was completely resected and weighted 623.2 g, which was almost 30-fold higher than normal thyroid weight (Figure 4A). The pathology report revealed a large diffuse infiltrative FTC with the longest diameter of 16.0 cm and more than 4 vascular invasion lesions (tumor cells invading a vessel wall indicates with a black arrow, Figure 4C), and nine cervical lymph nodes were removed and all of them showed metastatic involvement of FTC (Figures 4K,L). According to the eighth edition of the American Joint Committee on Cancer/Tumor Lymph Node Metastasis (TNM) staging system, the patient was in TNM stage II (Any T, N1, M0) (9). The immunohistochemical stains of FTC were positive for thyroid transcription factor (TTF-1) and cytokeratin (CK) 7, partially positive for thyroglobulin (TG) and CK pan, and negative for calcitonin and parathyroid hormone (PTH), and the Ki67 proliferation index was less than 1%, which is consistent with the diagnosis of angio-invasive FTC (Figures 4D–J). Next-generation sequencing (NGS) results revealed epidermal growth factor receptor (EGFR) and telomerase reverse transcriptase (TERT) promoter region (c.-124C > T) mutations with tumor mutational burden (TMB) of 2.13 mutations/Mb.

The patient did not undergo ablative radioiodine therapy post surgery due to non-medical reasons. The TG concentration was measured 8 months after surgery and it was 300 ng/ml (the normal value after surgery should not exceed 1 ng/ml). The anti-TG was less than 1.980 IU/ml (normal range was 0.000–4.110 IU/ml), while TSH was more than 54.744 mU/L (normal range was 0.51–4.91 mU/L) because the patient reduced the doses of L-thyroxin by personal reason last 2 weeks. Enlarged bilateral cervical lymph nodes were found in neck on ultrasonography and isotope I-131 whole-body scan and SPECT that required second surgery followed by radioiodine therapy. Subsequently, the patient will be treated with suppressive doses of L-thyroxin. Fortunately, the patient has completed relevant examinations and is about to receive radioiodine therapy recently.

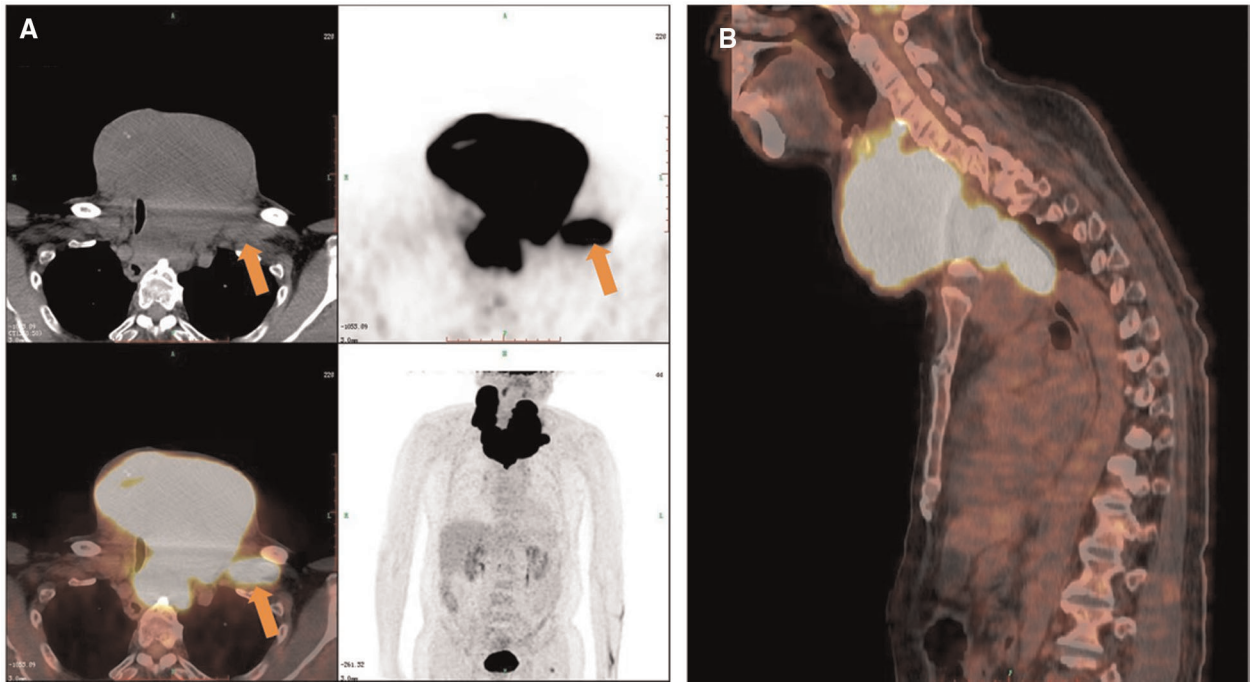


FIGURE 3
PET/CT images of the patient. Increased 18F-FDG metabolism showed in the thyroid and cervical lymph nodes on the (A) transverse, coronal and (B) sagittal sections. The orange arrow indicated one of the cervical metastatic lymph nodes.

## Discussion

FTC accounts for approximately 10% of the incidence of thyroid cancer and is prone to distant metastasis *via* blood vessels; in addition, FTC is more aggressive than PTC, develops distant metastases more frequently and shows higher mortality rate (2). Patient with FTC often experience no obvious clinical symptoms; therefore, FTC is mostly found when an ultrasound examination finds a single nodule, or when the patient is admitted to hospital due to related clinical symptoms associated with distant metastases. The most common sites of metastases are the lungs and bones, followed by the brain, liver and skin (3). In this case, this patient had a history of swollen thyroid for many years, but he had not received any treatment because there had been no obvious pressure symptoms of dyspnoea, dysphonia or dysphagia. He presented to our hospital with a progressively enlarged thyroid accompanied by tracheal compression and narrowing. Fortunately, this large FTC only had cervical metastatic lymph node involvement without distant metastases. However, lymph node metastases are rare in patients with FTC and usually have an average incidence of less than 10%; though, in this specific case, there were only lymph node metastases and no signs of haematogenic spread.

Thyroid ultrasonography is the most commonly used examination to evaluate thyroid nodules, and given that FTC and FA have similar appearances in color ultrasonography, and they may be misdiagnosed by inexperienced sonographers. Typical FTC is mainly characterized by an ill-defined shape, no fine halo, inhomogeneous echogenicity, coarse calcification and solid composition, while FA often shows a clear border, regular shape, fine halos, absence of calcification and solid composition (5, 10). In this case, thyroid ultrasonography showed a diffuse heterogeneous echoic appearance of whole thyroid tissue, which was not consistent with the sonographic findings of nodular FTC, while the postoperative pathology was confirmed as diffuse FTC. Ultrasonography is also the recommended method to evaluate benign and malignant cervical lymph nodes. In this case, all cervical lymph nodes were round and lacked a hilum, and some of them showed obvious cystic changes on grayscale sonography. Most of the lymph nodes displayed rich central and peripheral vascularity in the lymph node, the others showed peripheral vascularity, while some had no obvious vascularity when the lymph nodes had more than 90% cystic change. The ultrasonographic features of the lymph nodes were consistent with the reported sonographic findings of metastatic lymph nodes, and the postoperative pathology confirmed metastatic lymph nodes from FTC.

CT, MRI and PET/CT examinations are also important for accurate preoperative assessment (11). FTC is mainly metastasized *via* the blood circulation, and once the primary

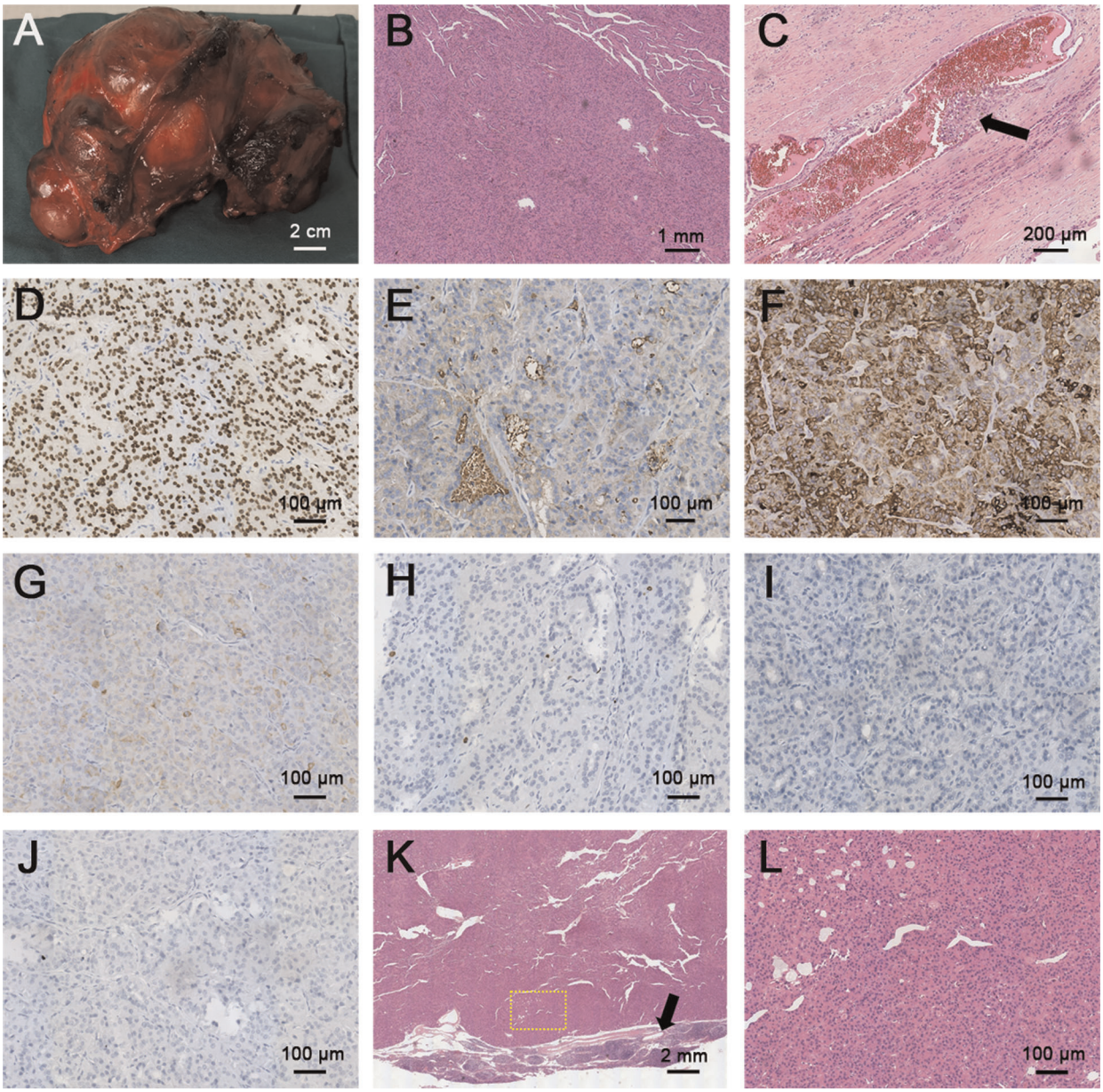


FIGURE 4
Gross and histopathological sections of follicular thyroid carcinoma and metastatic lymph node. (**A**) Gross image of follicular thyroid carcinoma. (**B**,**C**) H&E staining of follicular thyroid carcinoma (**B**, magnification × 40), black arrow indicated the vascular invasion of follicular thyroid carcinoma, the thyroid follicular epithelial cells were invaded into the blood vessel (**C**, magnification × 100). (**D**–**J**) Immunohistochemical (IHC) staining of follicular thyroid carcinoma (magnification × 200) for (**D**) TTF-1, (**E**) TG, (**F**) CK 7, (**G**) CK pan, (**H**) Ki 67, (**I**) calcitonin, (**J**) PTH. TTF-1 and CK7 were deeply stained (positive), TG and CK pan were partially stained (partial positive), Ki67 proliferation index was less than 1%, calcitonin and PTH didn't stain (negative). (**K**,**L**) H&E staining of neck metastatic lymph node: (**K**) magnification × 16, (**L**) magnification × 400. Yellow dashed circle indicated the amplification part in the picture **K**, black arrow indicated the normal part of the metastatic lymph node.

thyroid tumor is suspected to be FTC, patients with suspected FTC in other organs should undergo CT, MRI, PET/CT and other related examinations for a comprehensive evaluation. Parghane et al. reported on a 54-year-old male FTC patient presenting with cough and occasional hemoptysis for 1 year and hematuria for 6 months (12). A CT scan showed heterogeneously enhancing soft tissue lesions in the hilar region of the right lung, right lateral wall of the urinary bladder, segment III of the liver, and destruction of the left 5th rib. A PET/CT showed intense 18F-FDG metabolism in multiple mediastinal lymph node lesions, three liver lesions, and multiple left thoracic and skeletal lesions. Therefore, FTC

patients under initial treatment or those with recurrent metastasis following surgical treatment or various other local or systemic treatments, should be evaluated for their efficacy to guide the formulation of further diagnosis and treatment or follow-up strategies.

The histopathological diagnosis of FTC requires the determination of capsular and/or vascular invasion and can be divided into the following three categories: microinvasive, encapsulated vascular invasion, and diffuse invasion. The microinvasion of local blood vessels or capsules usually involves less than 4 blood vessels or capsule infiltration. Diffuse invasion usually has a poor prognosis, a high risk of recurrence and metastasis, and easily metastasizes to bone, lung, and occasionally to the soft tissue, liver or brain. In DTC, the mutation rate of RAS is second only to BRAF, and RAS mutation is the most common in FTC (13). However, RAS gene mutations can occur in both malignant and benign thyroid nodules, and the use of RAS alone in the differential diagnosis of benign and malignant thyroid nodules and the assessment of prognosis has limitations. Recent studies have found that TERT promoter mutation is closely related to high tumor aggressiveness, and TERT promoter mutated FTCs may exhibit a specific miRNA pattern that in part regulates key cancer pathways (14–16). Detection of the BRAF, RAS and TERT promoters is helpful for evaluating and predicting the biological behavior of thyroid cancer (17, 18). In this case, the patient had the TERT promoter mutation, but exhibited only cervical lymph node metastases and no distant metastases, which was rarely reported. Unfortunately, the current mechanism in this case is not very clear.

Surgery is the main treatment modality for FTC. In the ATA guidelines, there is no difference between the surgical recommendations for PTC and FTC (11). Post-surgery ablative radioiodine treatment is recommended in all FTC cases, not only the aggressive cases. Furthermore, an adequate TSH suppression prolongs survival in high-risk thyroid cancer patients (19). For FTC patients, the presence or absence of distant metastasis directly affects the survival rate. Patient age, vascular and capsular invasion, and surgical methods are all related to tumor recurrence, metastasis and prognosis (20). In this case, the patient underwent total thyroidectomy and cervical lymph node dissection. However, the patient had recurrent lymph node metastases and extremely high TG level, which required second surgery followed by radioiodine therapy.

According to ATA guidelines, this patient was classified in ATA high risk. The patient needs to receive subsequent radioiodine therapy, and the TSH levels should be suppressed with L-thyroxin to <0.1 mU/L (11).

Unfortunately, the post-surgical management of this patient was not in line with the ATA guidelines. The patient did not receive ablative radioiodine treatment for non-medical reasons. The lack of appropriate ablation has led to early recurrence in the cervical lymph nodes, after 8 months the patient had structural (enlarged bilateral cervical lymph nodes in neck on Ultrasonography and isotope I-131 labeled SPECT of the neck region) and functional (serum Tg > 300 ng/ml) evidence of loco-regional metastases, which required second surgery followed by radioiodine therapy. Subsequently, the patient will be treated with suppressive doses of L-thyroxin.

FTC is sometimes missed due to a lack of clear infiltration or to insufficient sampling; it is difficult to use ultrasonography and FNA for diagnosis; and cytological marker detection is currently not sufficiently developed. Therefore, we need to raise awareness of FTC.

## Conclusion

In this paper we have reported on a rare case of large FTC with diffuse nodal involvement but no distant metastases. We present the thyroid ultrasound, neck CT, MR and whole body PET/CT.

## Data availability statement

The original contributions presented in the study are included in the article/Supplementary Material, further inquiries can be directed to the corresponding author/s.

## Ethics statement

The studies involving human participants were reviewed and approved by the Ethics Committee of Second Xiangya Hospital, Central South University, China. The patients/participants provided their written informed consent to participate in this study. Written informed consent was obtained from the individual(s) for the publication of any potentially identifiable images or data included in this article.

## Author contributions

All authors listed have made a substantial, direct, and intellectual contribution to the work and approved it for publication. All authors contributed to the article and approved the submitted version.

## Funding

This project was funded by the National Natural Science Foundation of China (81974267), Science and Technology Innovation Program of Hunan Province (2021RC3033) and

Hunan Provincial Natural Science Foundation of China (2022JJ30827).

## Conflict of interest

The authors declare that the research was conducted in the absence of any commercial or financial relationships that could be construed as a potential conflict of interest.

## Publisher's note



## References

1. Grani G, Lamartina L, Durante C, Filetti S, Cooper SD. Follicular thyroid cancer and Hürthle cell carcinoma: challenges in diagnosis, treatment, and clinical management. *Lancet Diabetes Endocrinol*. (2018) 6(6):500–14. doi: 10.1016/s2213-8587(17)30325-x

2. Aschebrook-Kilfoy B, Grogan RH, Ward MH, Kaplan E, Devesa SS. Follicular thyroid cancer incidence patterns in the United States, 1980-2009. *Thyroid*. (2013) 23(8):1015–21. doi: 10.1089/thy.2012.0356

3. Alfalah H, Cranshaw I, Jany T, Arnalsteen L, Leteurtre E, Cardot C, et al. Risk factors for lateral cervical lymph node involvement in follicular thyroid carcinoma. *World J Surg*. (2008) 32(12):2623–6. doi: 10.1007/s00268-008-9742-2

4. Pisanu A, Deplano D, Pili M, Uccheddu A. Larger tumor size predicts nodal involvement in patients with follicular thyroid carcinoma. *Tumori*. (2011) 97 (3):296–303. doi: 10.1700/912.10025

5. Li W, Song Q, Lan Y, Li J, Zhang Y, Yan L, et al. The value of sonography in distinguishing follicular thyroid carcinoma from adenoma. *Cancer Manag Res*. (2021) 13:3991–4002. doi: 10.2147/CMAR.S307166

6. Alexander EK, Kennedy GC, Baloch ZW, Cibas ES, Chudova D, Diggans J, et al. Preoperative diagnosis of benign thyroid nodules with indeterminate cytology. *N Engl J Med*. (2012) 367(8):705–15. doi: 10.1056/NEJMoa1203208

7. Acquaviva G, Visani M, Repaci A, Rhoden KJ, de Biase D, Pession A, et al. Molecular pathology of thyroid tumours of follicular cells: a review of genetic alterations and their clinicopathological relevance. *Histopathology*. (2018) 72 (1):6–31. doi: 10.1111/his.13380

8. Riley DS, Barber MS, Kienle GS, Aronson JK, von Schoen-Angerer T, Tugwell P, et al. CARE guidelines for case reports: explanation and elaboration document. *J Clin Epidemiol*. (2017) 89:218–35. doi: 10.1016/j.jclinepi.2017.04.026

9. Lamartina L, Grani G, Arvat E, Nervo A, Zatelli MC, Rossi R, et al. 8th Edition of the AJCC/TNM staging system of thyroid cancer: what to expect (ITCO#2). *Endocr Relat Cancer*. (2018) 25(3):L7–11. doi: 10.1530/ERC-17-0453

10. Wu Q, Qu Y, Li Y, Liu Y, Shen J, Wang Y. Logistic regression analysis of contrast-enhanced ultrasound and conventional ultrasound of follicular thyroid carcinoma and follicular adenoma. *Gland Surg*. (2021) 10(10):2890–900. doi: 10.21037/gs-21-535

11. Haugen BR, Alexander EK, Bible KC, Doherty GM, Mandel SJ, Nikiforov YE, et al. 2015 American thyroid association management guidelines for adult patients with thyroid nodules and differentiated thyroid cancer: the American thyroid association guidelines task force on thyroid nodules and differentiated thyroid cancer. *Thyroid*. (2016) 26(1):1–133. doi: 10.1089/thy.2015.0020

12. Parghane RV, Basu S. Follicular thyroid carcinoma metastasizing to rare sites and exhibiting variable inter-lesional heterogeneity on (18)F-fluorodeoxyglucose positron emission tomography/computed tomography and (131)I. *World J Nucl Med*. (2021) 20(3):312–5. doi: 10.4103/wjnm.WJNM_79_20

13. Guan H, Toraldo G, Cerda S, Godley FA, Rao SR, McAneny D, et al. Utilities of RAS mutations in preoperative fine needle biopsies for decision making for thyroid nodule management: results from a single-center prospective cohort. *Thyroid*. (2020) 30(4):536–47. doi: 10.1089/thy.2019.0116

14. Paulsson JO, Zedenius J, Juhlin CC. TERT promoter mutated follicular thyroid carcinomas exhibit a distinct microRNA expressional profile with potential implications for tumor progression. *Endocr Pathol*. (2021) 32 (4):513–6. doi: 10.1007/s12022-021-09695-w

15. Bournaud C, Descotes F, Decaussin-Petrucci M, Berthiller J, de la Fouchardiere C, Giraudet AL, et al. TERT promoter mutations identify a high-risk group in metastasis-free advanced thyroid carcinoma. *Eur J Cancer*. (2019) 108:41–9. doi: 10.1016/j.ejca.2018.12.003

16. Park H, Shin HC, Yang H, Heo J, Ki CS, Kim HS, et al. Molecular classification of follicular thyroid carcinoma based on TERT promoter mutations. *Mod Pathol*. (2022) 35(2):186–92. doi: 10.1038/s41379-021-00907-6

17. Decaussin-Petrucci M, Descotes F, Depaepe L, Lapras V, Denier ML, Borson-Chazot F, et al. Molecular testing of BRAF, RAS and TERT on thyroid FNAs with indeterminate cytology improves diagnostic accuracy. *Cytopathology*. (2017) 28(6):482–7. doi: 10.1111/cyt.12493

18. Xing M, Liu R, Liu X, Murugan AK, Zhu G, Zeiger MA, et al. BRAF V600e and TERT promoter mutations cooperatively identify the most aggressive papillary thyroid cancer with highest recurrence. *J Clin Oncol*. (2014) 32 (25):2718–26. doi: 10.1200/JCO.2014.55.5094

19. Biondi B, Cooper DS. Benefits of thyrotropin suppression versus the risks of adverse effects in differentiated thyroid cancer. *Thyroid*. (2010) 20(2):135–46. doi: 10.1089/thy.2009.0311

20. O'Neill CJ, Vaughan L, Learoyd DL, Sidhu SB, Delbridge LW, Sywak MS. Management of follicular thyroid carcinoma should be individualised based on degree of capsular and vascular invasion. *Eur J Surg Oncol*. (2011) 37(2):181–5. doi: 10.1016/j.ejso.2010.11.005

frontiers | Frontiers in Surgery

TYPE Case Report
PUBLISHED 23 August 2022
DOI 10.3389/fsurg.2022.991558



OPEN ACCESS

EDITED BY
Zhaolun Cai,
Sichuan University, China

REVIEWED BY
Mihnea-Alexandru Găman,
Carol Davila University of Medicine and Pharmacy, Romania
Gaetano Thiene,
University of Padua, Italy

*CORRESPONDENCE
Xing-Lan Li
lxl19860421@126.com

SPECIALTY SECTION
This article was submitted to Surgical Oncology, a section of the journal Frontiers in Surgery

RECEIVED 11 July 2022
ACCEPTED 08 August 2022
PUBLISHED 23 August 2022

CITATION
Li J, Zhu H, Hu S-Y, Ren S-Q and Li X-L (2022) Case report: Cardiac metastatic leiomyoma in an Asian female.
Front. Surg. 9:991558.
doi: 10.3389/fsurg.2022.991558



# Case report: Cardiac metastatic leiomyoma in an Asian female

Juan Li[1,2], Hong Zhu[1,2], Shuang-Ye Hu[3], Shang-Qing Ren[2,4] and Xing-Lan Li[1,2]*

[1]Department of Pathology, Sichuan Provincial People's Hospital, University of Electronic Science and Technology of China, Chengdu, China, [2]Chinese Academy of Sciences Sichuan Translational Medicine Research Hospital, Chengdu, China, [3]Department of Pathology, Longquanyi District of Chengdu Maternity and Child Health Care Hospital, Chengdu, China, [4]Department of Robotic Minimally Invasive Surgery Center, Sichuan Provincial People's Hospital, University of Electronic Science and Technology of China, Chengdu, China

**Background:** Uterine leiomyomas are the most common gynecological tumors in women of child-bearing age and premenopausal women, while benign metastasizing leiomyomas of the heart are rare.
**Case presentation:** We report a rare case of metastasizing leiomyoma in the heart of a 54-year-old woman 10 years after a uterine leiomyoma was discovered during hysterectomy. Echocardiography, cardiac plain scan and enhanced MRI at presentation showed a soft tissue signal mass in the right ventricle. A large cardiac mass attached to the chordae of the tricuspid valve and later shown to be histopathologically consistent with uterine leiomyoma was successfully resected through a right atriotomy.
**Conclusions:** Our case report highlights a rare type of tumor of the heart and suggests that metastasizing leiomyoma should be considered in the differential diagnosis of right-sided cardiac tumors. The complete surgical resection of the tumor was considered to be the best treatment.

KEYWORDS
metastasizing leiomyoma, heart, case report, surgery, outcome

## Introduction

Primary cardiac tumors are rare, and most cardiac tumors are secondary to metastatic disease (1). Overall, smooth muscle tumors of the heart are extremely rare. Most of the smooth muscle tumors are occurring in reproductive women who have a history of uterine leiomyoma resection or hysterectomy (2). The presenting symptoms of cardiac tumor depend on the size, location of the mass, and eventual obstruction to the inflow or outflow tracts. Most cardiac tumors are asymptomatic, and diagnosis is made on the basis of heart murmur, arrythmias. Echocardiography, cardiac magnetic resonance imaging (MRI), and computed tomography (CT) usually are useful for establishing the diagnosis, although pathological diagnosis remains the gold standard for diagnostic confirmation (3). Here, we report a rare case of metastasis of uterine leiomyoma to the heart. The aim of this report is to increase awareness of this

Abbreviations
ER, estrogen receptor; PR, progesterone receptor; SMA, smooth muscle actin; FH, fumarate hydratase; TEE, transesophageal echocardiography; CT, Computed Tomography; MRI, Magnetic Resonance Imaging.

metastatic tumor. This study was reported in agreement with principles of the CARE guidelines (4).

## Case presentation

A 54-year-old woman presented to the hospital due to with a heart murmur detected at a routine examination. On physical examination, the patient's general condition and vital signs were quite unremarkable; only the 2nd to 3rd costal segment of the left margin of the sternum appeared abnormal, and 3/6 systolic blow-like murmurs could be heard; pericardial frictional sounds were not heard, and there was no edema in either lower limb. Echocardiography indicated right ventricular space occupation. Cardiac plain scan and enhanced MRI showed soft tissue signal mass shadows in the outflow tract of the right ventricle (**Figure 1**). CT angiography showed no macrovascular lesions. What's more is that patient had undergone hysterectomy in a local hospital 10 years previously due to excessive vaginal bleeding from uterine leiomyoma. The family histories were noncontributory to the diagnosis.

The patient underwent right ventricular mass resection under general anesthesia with low-temperature extracorporeal circulation. The patient recovered well after the surgery. The surgical findings showed that there was a 3 cm × 3 cm oblong tomato-like mass with a smooth surface and tough texture occupying the right ventricle. The tumor pedicle was connected to the chordae of the tricuspid valve and protruding into the right ventricular outflow tract, but other portions of the tumor had no adhesion to the heart. The specimens were laid out along their longitudinal axes and fixed in 10% neutral formalin for 12 h. Ten representative tissue samples were taken from different areas, dehydrated, embedded in paraffin, and sequentially sectioned into 3-μm-thick sections. The sections were incubated with primary antibodies against desmin, ER, PR, myogenin, MyoD1, caldesmon, pan-CK, Ki-67, SMA, CD117, FH, RB-1, MDM2, and CD34. PBS replaced the primary antibody as a negative control. DAB color development and hematoxylin counterstaining were performed. The primary antibodies and the kit were purchased from Beijing Zhongshan Jinqiao Company.

On histopathologic examination, the tumor appeared as a grayish-white tubercle, with no exact capsule; it was solid and tough and measured 3 cm × 3 cm × 1.5 cm in size (**Figure 2**). Under the microscope, the spindle cells within the tumor showed clear boundaries, mild cell morphology, fascicular arrangement, and no mitotic figures (**Figure 3**). Immunohistochemical staining for desmin, caldesmon, ER, PR and SMA was positive, and the Ki-67 index was approximately 2% (**Figure 4**). These morphologic features and the immunohistochemical staining pattern confirmed a diagnosis of benign metastasizing leiomyoma to the heart.

## Discussion

### Case review

Benign metastasizing leiomyoma is very rare. Benign metastasizing leiomyoma involving the heart was first reported by Timmis in 1980, and at least 8 other cases were subsequently reported (**Table 1**).

### Clinical manifestations, diagnosis, treatment and prognosis

Metastasizing leiomyomas of the heart are most common in middle-aged women. Most patients with metastasizing leiomyoma have a history of hysterectomy/myomectomy combined with an existing hysteromyoma. In the case described here, the patient had a history of hysteromyoma resection, and the time from the first hysteromyoma resection to the discovery of cardiac leiomyoma was 10 years. The

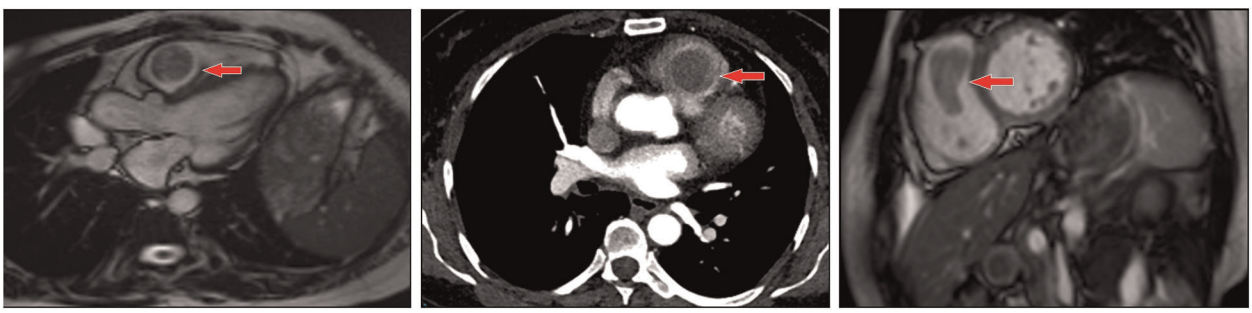

FIGURE 1
Imaging of metastasizing leiomyoma. Enhanced MRI revealed soft tissue signal mass shadows in the outflow tract of the right ventricle.

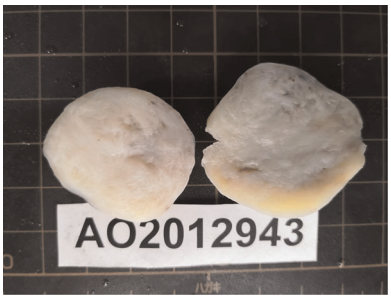


FIGURE 2
Macropathology of metastasizing leiomyoma. The leiomyoma appeared as a solid, tough, grayish-white tubercle with no exact capsule.

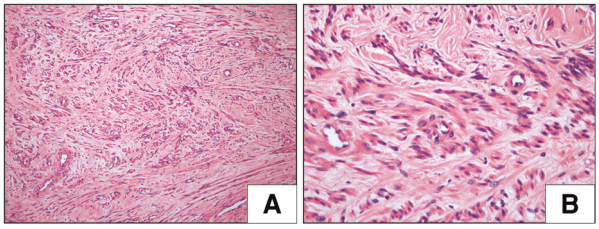


FIGURE 3
Histological examination (HE) of metastasizing leiomyoma. (**A**,**B**) The spindle cell tumor showed clear boundaries, mild cell morphology, fascicular arrangement, and no mitotic figures (H&E staining, **A**: ×100, **B**: ×400).

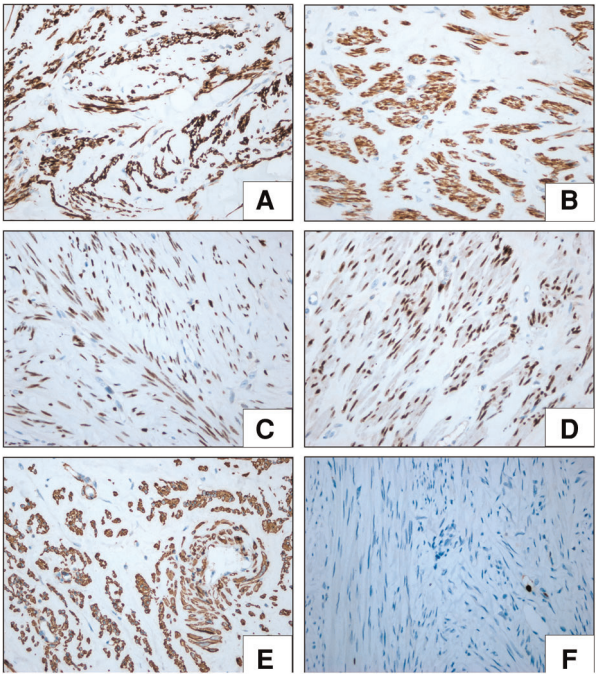


FIGURE 4
Immunohistochemical (IHC) features of metastasizing leiomyoma. (Envision × 400) The spindle cells expressed desmin (**A**), caldesmon (**B**), PR (**C**), ER (**D**) and SMA (**E**). The calculated Ki67 labeling index was less than approximately 2% (**F**).

TABLE 1 Summary of case reports of metastasizing leiomyoma in the heart.

| Patient age/ gender | Metastasis site(s) | Cardiac tumor size | Interval to metastasis | Location in heart | References |
|---|---|---|---|---|---|
| 46/F | Heart | 7.5 | 1.5 years after hysterectomy | Inferior vena cava | Timmis AD, et al. (1980) (5) |
| 44/F | Heart, lung | 4.7 | 4 years after hysterectomy | Anterior papillary muscle of right ventricle | Takemura G, et al. (1996) (6) |
| 41/F | Heart | 3.5 | 3 months after hysterectomy | Right anterior interventricular septum | Galvin SD, et al. (2010) (1) |
| 37/F | Heart, lung, soft tissue, liver and enterocoelia | NG* | 11 years after leiomyoma resection | Right cardiac chamber and cardiac wall | Cai A, et al. (2014) (7) |
| 55/F | Heart, lung | 4 | 16 years after hysterectomy | Right atrium | Consamus EN, et al. (2014) (8) |
| 51/F | Heart, lung | 4.5 | Simultaneously | Right ventricle | Williams M, et al. (2016) (9) |
| 36/F | Heart, lung | 4.7 | 12 years after hysterectomy | Abutted the pulmonary valve | Meddeb M, et al. (2018) (10) |
| 46/F | Heart, lung and Pelvic | 4.8 | 10 years after hysterectomy | The tricuspid valve | Mohamed M, et al. (2020) (11) |
| 45/F | Heart, lung | 9 | 2 years after hysterectomy | The tricuspid valve | Karnib M, et al. (2021) (12) |
| 54/F | Heart | 5 | 10 years after hysterectomy | The tricuspid valve | Current case |

*NG, not given.

clinical symptoms of metastasizing leiomyoma are nonspecific; the most common symptoms are dyspnea, syncope, edema of the lower extremities, and palpitations. The patient described here had no clinical symptoms, and the leiomyoma was found by chance during physical examination. TEE, CT and MRI can effectively assist preoperative diagnosis and guide surgical treatment. Although clinical manifestations and imaging can provide early and accurate assessment of the disease, the final diagnosis depends on postoperative pathological examination. Patients in whom there was complete tumor resection had a

good prognosis, and no postoperative recurrence or death was reported. Postoperative recurrence is common in patients with incomplete tumor resection. In cases in which the tumor cannot be completely removed, some researchers have suggested the use of antiestrogen drugs (including tamoxifen and letrozole) after surgery. Awonuga (13) and Rivera (14) found that the tumor subsided after the use of antiestrogen drugs after surgery. In our case, the patient underwent right ventricular mass resection by surgery, and have not received any medication. Postoperative cardiac MRI indicated that the mass was completely removed, and there was no recurrence after 12 months follow-up.

## Pathological etiology

The behavior of cardiac leiomyoma is benign. Microscopically, the tumor in our patient was composed of fasciculate spindle smooth muscle cells with scattered stroma in small blood vessels. No obvious bleeding or necrosis was observed, and nuclear atypia, pleomorphism and mitoses were also rare. The rare types of pathological variation previously reported include angiomyoma (15), adipose leiomyoma (16), lymphangiomyoma (17) and borderline leiomyoma (18). In our case, immunohistochemistry showed positive results for smooth muscle markers such as SMA and desmin, and the lack of expression of vimentin ruled out a myofibroblastic nature of the tumor. Intrauterine tumors have histopathological and immunohistochemical characteristics that are the same as those of cardiac leiomyomas originating in the uterus. Some researchers have conducted molecular genetic analysis of cardiac leiomyoma; the results of those studies showed that almost all of the analyzed samples had abnormal genotypes such as 45, XX, Der (14) T (12;14) (Q15; Q24) (19), However, as cardiac leiomyomas are clinically rare, their etiology remains to be further studied.

## Histological origin

At present, there are two views on the histological occurrence of leiomyomas. One is that the tumor originates from uterine fibroids and extends into veins; this is the case for the metastasizing leiomyomas reported in most studies (20–22). The second is that primary cardiac leiomyomas may originate from the smooth muscle tissue of the vein wall. In this case, the tumor extends upward along the venous system and may exceed the inferior vena cava and enter the right atrium, right ventricle and even the pulmonary artery (15). In our case, medical history, cardiac imaging findings and the immunohistochemical staining pattern confirmed a diagnosis of benign metastasizing leiomyoma originated from uterine fibroids.

## Differential diagnosis

The differential diagnosis of cardiac leiomyoma mainly includes cardiac myxoma, cardiac leiomyosarcoma, and other metastasizing cardiac tumors. Cardiac myxoma mostly occurs in the left cardiac system, with an incidence of 87.3% to 85.5%; in this respect, it differs from cardiac leiomyoma, which only affects the right cardiac system (23–25). Most atrial myxomas are pedicled to the atrial septum or wall and may be adherent to the wall. Histological morphology, preoperative imaging examination and history of uterine leiomyoma are helpful for differential diagnosis. Leiomyosarcomas in the heart are malignant tumors with similar clinical and imaging manifestations as leiomyomas of the heart, and the two need to be differentiated through postoperative pathology and immunohistochemical diagnosis. Moreover, leiomyosarcomas have the behavioral characteristics of malignant tumors and often metastasize to other organs or sites such as the lung, lymph nodes, bone, skeletal muscle, subcutaneous tissue and retroperitoneal space but do not extend and grow in the venous system (26). Other metastasizing cardiac neoplasms often invade the pericardium or myocardial tissue, and their primary foci can be determined by systemic radionuclide scanning.

# Conclusion

Although metastasizing leiomyoma is rare, this tumor should be considered in the differential diagnosis of cardiac tumors, especially in patients with a history of uterine fibroids. Future research is needed to better understand the pathogenesis and treatment of such tumors.

# Data availability statement

The raw data supporting the conclusions of this article will be made available by the authors, without undue reservation.

# Ethics statement

Written informed consent was obtained from the individual (s) for the publication of any potentially identifiable images or data included in this article.

# Author contributions

LXL and LJ contributed equally to this work; LXL and LJ wrote the manuscript; ZH and HSY was responsible for

literature search and proofreading; RSQ collected the clinicopathologic data. All authors contributed to the article and approved the submitted version.

## Funding

The Universal Application Project of Sichuan Provincial Health and Family Planning Commission of China (serial number 16PJ490). The funder is Xing-Lan Li, who wrote the manuscript. Doctoral Science Foundation of Sichuan Provincial People's Hospital (serial number 2015BS08). The funder is Xing-Lan Li, who wrote the manuscript. Key research and development projects of Sichuan Science and Technology Department (serial number 2022YFS0135). The funder is Shang-Qing Ren, who collected the clinicopathologic data.

## Conflict of interest

The authors declare that the research was conducted in the absence of any commercial or financial relationships that could be construed as a potential conflict of interest.

## Publisher's note



## References

1. Galvin SD, Wademan B, Chu J, Bunton RW. Benign metastasizing leiomyoma: a rare metastatic lesion in the right ventricle. *Ann Thorac Surg.* (2010) 89(1):279–81. doi: 10.1016/j.athoracsur.2009.06.050

2. Kayser K, Zink S, Schneider T, Dienemann H, Andre S, Kaltner H, et al. Benign metastasizing leiomyoma of the uterus: documentation of clinical, immunohistochemical and lectin-histochemical data of ten cases. *Virchows Archiv.* (2000) 437(3):284–92. doi: 10.1007/s004280000207

3. Cho JM, Danielson GK, Puga FJ, Dearani JA, McGregor CG, Tazelaar HD, et al. Surgical resection of ventricular cardiac fibromas: early and late results. *Ann Thorac Surg.* (2003) 76(6):1929–34. doi: 10.1016/S0003-4975(03)01196-2

4. Riley DS, Barber MS, Kienle GS, Aronson JK, von Schoen-Angerer T, Tugwell P, et al. CARE Guidelines for case reports: explanation and elaboration document. *J Clin Epidemiol.* (2017) 89:218–35. doi: 10.1016/j.jclinepi.2017.04.026

5. Timmis AD, Smallpeice C, Davies AC, Macarthur AM, Gishen P, Jackson G. Intracardiac spread of intravenous leiomyomatosis with successful surgical excision. *N Engl J Med.* (1980) 303(18):1043–4. doi: 10.1056/NEJM198010303031806

6. Takemura G, Takatsu Y, Kaitani K, Ono M, Ando F, Tanada S, et al. Metastasizing uterine leiomyoma. A case with cardiac and pulmonary metastasis. *Pathol Res Pract.* (1996) 192(6):622–33. doi: 10.1016/S0344-0338(96)80116-6

7. Cai A, Li L, Tan H, Mo Y, Mo Y, Zhou Y. Benign metastasizing leiomyoma. *Case report and review of the literature. Herz.* (2014) 39(7):867–70. doi: 10.1007/s00059-013-3904-1

8. Consamus EN, Reardon MJ, Ayala AG, Schwartz MR, Ro JY. Metastasizing leiomyoma to heart. *Methodist Debakey Cardiovasc J.* (2014) 10(4):251–4. doi: 10.14797/mdcj-10-4-251

9. Williams M, Salerno T, Panos AL. Right ventricular and epicardial tumors from benign metastasizing uterine leiomyoma. *J Thorac Cardiovasc Surg.* (2016) 151(2):e21–4. doi: 10.1016/j.jtcvs.2015.09.059

10. Meddeb M, Chow RD, Whipps R, Haque R. The heart as a site of metastasis of benign metastasizing leiomyoma: case report and review of the literature. *Case Rep Cardiol.* (2018) 2018:7231326. doi: 10.1155/2018/7231326

11. Gad MM, Găman MA, Bazarbashi N, Friedman KA, Gupta A. Suspicious right heart mass: a rare case of benign metastasizing leiomyoma of the tricuspid valve. *JACC Case Rep.* (2020) 2(1):51–4. doi: 10.1016/j.jaccas.2019.12.004

12. Karnib M, Rhea I, Elliott R, Chakravarty S, Al-Kindi SG. Benign metastasizing leiomyoma in the heart of a 45-year-old woman. *Tex Heart Inst J.* (2021) 48(1):e197066. doi: 10.14503/THIJ-19-7066

13. Awonuga AO, Shavell VI, Imudia AN, Rotas M, Diamond MP, Puscheck EE. Pathogenesis of benign metastasizing leiomyoma: a review. *Obstet Gynecol Surv.* (2010) 65(3):189–95. doi: 10.1097/OGX.0b013e3181d60f93

14. Rivera JA, Christopoulos S, Small D, Trifiro M. Hormonal manipulation of benign metastasizing leiomyomas: report of two cases and review of the literature. *J Clin Endocrinol Metab.* (2004) 89(7):3183–8. doi: 10.1210/jc.2003-032021

15. Tamburino C, Russo G, Incognito C, Battaglia G, Monaca V, Lomeo A, et al. Intracardiac extension of a calcified ovarian hemangioma–a case report. *Angiology.* (1992) 43(3Pt1):249–52. doi: 10.1177/000331979204300310

16. Vural C, Özen Ö, Demirhan B. Intravenous lipoleiomyomatosis of uterus with cardiac extension: a case report. *Pathol Res Pract.* (2011) 207(2):131–4. doi: 10.1016/j.prp.2010.10.004

17. Stancanelli B, Seminara G, Vita A, Pantò A, Romano M. Extension of a pelvic tumor into the right atrium. *N Engl J Med.* (1995) 333(15):1013–4. doi: 10.1056/NEJM199510123331519

18. Lam PM, Lo KW, Yu MM, Lau TK, Cheung TH. Intravenous leiomyomatosis with atypical histologic features: a case report. *Int J Gynecol Cancer.* (2003) 13(1):83–7. doi: 10.1046/j.1525-1438.2003.13008.x

19. Quade BJ, Dal Cin P, Neskey DM, Weremowicz S, Morton CC. Intravenous leiomyomatosis: molecular and cytogenetic analysis of a case. *Mod Pathol.* (2002) 15(3):351–6. doi: 10.1038/modpathol.3880529

20. Gonzalez-Lavin L, Lee RH, Falk L, Gradman MD, McFadden PM, Basso LV, et al. Tricuspid valve obstruction due to intravenous leiomyomatosis. *Am Heart J.* (1984) 108(6):1544–6. doi: 10.1016/0002-8703(84)90705-1

21. Akatsuka N, Tokunaga K, Isshiki T, Asano K, Funaki H, Mizuno M, et al. Intravenous leiomyomatosis of the uterus with continuous extension into the pulmonary artery. *Jpn Heart J.* (1984) 25(4):651–9. doi: 10.1536/ihj.25.651

22. Ohmori T, Uraga N, Tabei R, Abe M, Sumimoto T, Hamada M, et al. Intravenous leiomyomatosis: a case report emphasizing the vascular component. *Histopathology.* (1988) 13(4):470–2. doi: 10.1111/j.1365-2559.1988.tb02066.x

23. Steger CM, Hager T, Ruttmann E. Primary cardiac tumours: a single-center 41-year experience. *ISRN Cardiol.* (2012) 2012:906109. doi: 10.5402/2012/906109

24. Pacini D, Careddu L, Pantaleo A, Berretta P, Leone O, Marinelli G, et al. Primary benign cardiac tumours: long-term results. *Eur J Cardio-Thorac Surg.* (2012) 41(4):812–9. doi: 10.1093/ejcts/ezr067

25. Wang JG, Li YJ, Liu H, Li NN, Zhao J, Xing XM. Clinicopathologic analysis of cardiac myxomas: seven years' experience with 61 patients. *J Thorac Dis.* (2012) 4(3):272–83. doi: 10.3978/j.issn.2072-1439.2012.05.07

26. Canzonieri V, D'Amore ES, Bartoloni G, Piazza M, Blandamura S, Carbone A. Leiomyomatosis with vascular invasion. A unified pathogenesis regarding leiomyoma with vascular microinvasion, benign metastasizing leiomyoma and intravenous leiomyomatosis. *Virchows Archiv.* (1994) 425(5):541–5. doi: 10.1007/BF00197559

frontiers | Frontiers in Oncology

TYPE Case Report
PUBLISHED 30 August 2022
DOI 10.3389/fonc.2022.987705



OPEN ACCESS

EDITED BY
Francesco Pennestrì,
Università Cattolica del Sacro Cuore, Italy

REVIEWED BY
Pietro Locantore,
Catholic University of the Sacred Heart, Italy
Joseph M. Pappachan,
Lancashire Teaching Hospitals NHS Foundation Trust, United Kingdom

*CORRESPONDENCE
Jiwei Huang
huangjiweimd@hotmail.com

†These authors have contributed equally to this work

SPECIALTY SECTION
This article was submitted to Surgical Oncology, a section of the journal Frontiers in Oncology

RECEIVED 06 July 2022
ACCEPTED 08 August 2022
PUBLISHED 30 August 2022

CITATION
Feng Q, Li H, Qiu G, Cai Z, Li J, Zeng Y and Huang J (2022) Case report: Significant liver atrophy due to giant cystic pheochromocytoma. *Front. Oncol.* 12:987705. doi: 10.3389/fonc.2022.987705



# Case report: Significant liver atrophy due to giant cystic pheochromocytoma

Qingbo Feng[1†], Hancong Li[2†], Guoteng Qiu[1†], Zhaolun Cai[3], Jiaxin Li[1], Yong Zeng[1] and Jiwei Huang[1*]

[1]Department of Liver Surgery and Liver Transplantation Centre, West China Hospital, Sichuan University, Chengdu, China, [2]West China School of Medicine, West China Hospital, Sichuan University, Chengdu, China, [3]Department of Gastrointestinal Surgery, West China Hospital, Sichuan University, Chengdu, China

**Introduction:** Pheochromocytoma is a neuroendocrine tumor originating from chromaffin cells in the adrenal medulla. Giant pheochromocytomas with a maximum diameter of over 20 cm are particularly rare.

**Case presentation:** We present a case of giant cystic pheochromocytoma in a 64-year-old woman who was found to have a right abdominal mass during an ultrasound examination, which is the largest pheochromocytoma ever documented in China. Meanwhile, obvious atrophy of the right lobe of the liver was found in preoperative CT and during the operation. Our literature review identified 20 cases with a diameter of over 20 cm. The average age at diagnosis was 51.7 (range 17–85), and 35% of cases did not exhibit classic symptoms.

**Conclusion:** Giant pheochromocytoma is an uncommon neoplasm. It can be discovered late due to a lack of clinical manifestations. Diagnosis is dependent on imaging recognition together with catecholamine secretion. Surgical resection is the only curative treatment for such tumors.

KEYWORDS

**giant cystic pheochromocytoma, liver atrophy, case report, literature review, surgery**

## Introduction

Pheochromocytoma is an infrequent catecholamine-secreting neoplasm that arises from chromaffin tissues, which tends to occur in the adrenal medulla (1). The estimated annual incidence of pheochromocytoma is 0.4 to 9.5 per million (2). Hypertension, which can be sustained or paroxysmal, is the most common sign (3). Episodic headache, palpitations, and diaphoresis are the classical triad of clinical features, which can be seen in <25% of patients. At least one component of the triad occurs in slightly less than 50% of patients. These episodes

are connected with the catecholamine excess produced by the tumor (4). In addition, local symptoms caused by the giant tumor include stomachache, backache, abdominal distension, and some atypical gastrointestinal symptoms. Commonly, it is a solid tumor and histologically benign (5). Nevertheless, cystic pheochromocytoma is a particular rare entity and is usually asymptomatic but can be fatal due to cardiovascular complications (6). The most accurate metabolic testing for the biochemical diagnosis of this tumor is the elevated plasma-free or 24-h urinary fractionated metanephrines (7). Computed tomography (CT) or magnetic resonance imaging (MRI) is the preference for the initial anatomical localization of the tumor due to its high sensitivity (90%–100%) and reasonable specificity (70%–80%) (4). Once the pheochromocytoma is diagnosed, patients are referred to surgical extirpation, which is the only curative strategy (5). Currently, just a few cases concerning giant cystic pheochromocytomas have been reported worldwide (8). Here, a case of cystic pheochromocytoma with enormous size, a 20 × 15 × 10 cm tumor, is described. The study is reported in agreement with the principles of the CAse REport (CARE) guidelines (9). Additionally, we have performed a literature review on pheochromocytoma measuring 20 cm or greater to update the clinical features of this rare disease. To our best knowledge, this is the largest cystic pheochromocytoma in China as per the available indexed literature.

## Case presentation

On 20 April 2022, a 64-year-old woman was referred to the West China Hospital after an abdominal mass was found on ultrasound examination for mild right upper abdominal discomfort. The patient reported no significant symptoms or past medical history, while physical examination indicated a large mass measuring 20 × 15 cm was palpated at the right upper quadrant. On admission, her blood pressure was 127/89 mmHg, and her heart rate was 78 beats per minute. Initial laboratory investigations concerning biochemistry and hematology examinations were within normal limits.

Abdominal enhanced CT revealed obvious compression atrophy of the liver and a 20 cm × 13 cm mixture of cystic and solid lesions between the right lobe of the retroperitoneal liver and the right kidney (Figures 1A, B). Plasma metanephrine and catecholamine measurements were performed, and evidence of pheochromocytoma was increased upon observation of elevated metanephrines and their metabolites in serum (Table 1). The patient did not have underlying diseases such as hypertension or diabetes. Before the metabolic testing, she did not take blood pressure medications, acetaminophen, beta- and alpha-adreno receptor blocking drugs, psychotropic medications, or any drugs that might interfere with her metabolism.

Based on endocrine consultation, an alpha receptor blocker (phenoxybenzamine) was used for 2 weeks preoperatively. Three days after that, we encouraged the patient to start a salt-rich diet. In addition, an adequate fluid replacement was performed preoperatively. Blood pressure and heart rate of 139/79 mmHg and 77 beats per minute were recorded prior to surgery. The resection of the giant right adrenal pheochromocytoma was completed through a right subcostal incision under general anesthesia (Figure 1C). During the operation, the omentum majus widely adhered to the small intestine, abdominal wall,

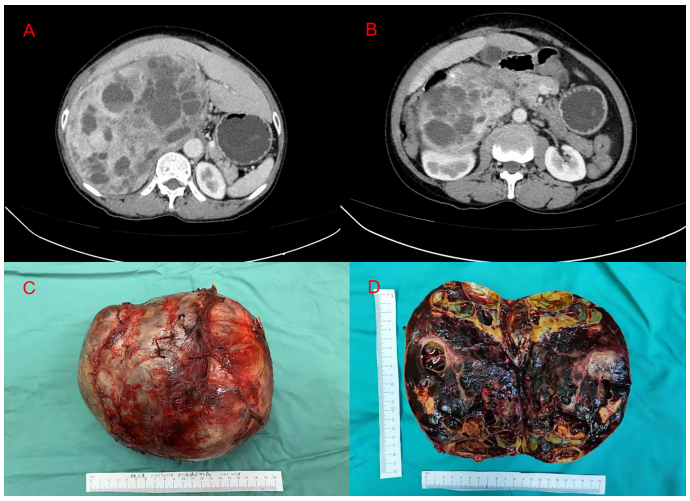


FIGURE 1
**(A, B)** Abdominal enhanced computed tomography imaging representing the huge tumor between the right lobe of the retroperitoneal liver and the right kidney. **(C)** A macroscopic image of the post-section cystic pheochromocytoma. **(D)** Excised tumor, measuring 20 × 15 × 10 cm.

TABLE 1 Plasma metanephrines measurements confirming the pheochromocytoma diagnosis.

| | Patient values | Units | Ref range | Status |
|---|---|---|---|---|
| Epinephrine | 0.76 | nmol/L | <0.34 | ↑ |
| Norepinephrine | 1.89 | nmol/L | <5.17 | |
| Dopamine | 0.02 | nmol/L | <0.31 | |
| Metanephrine | 30.72 | nmol/L | <0.42 | ↑ |
| Normetanephrine | 96.54 | nmol/L | <0.71 | ↑ |
| 3-Methoxytyramine | 48.13 | pg/ml | <18.40 | ↑ |

and liver. The right lobe of the liver was squeezed and atrophied by the retroperitoneal tumor, which was located behind the inferior vena cava. Blood pressure fluctuated intraoperatively, between 83 and 157 mmHg for the systolic pressure and between 55 and 92 mmHg for the diastolic pressure. Heart rate was measured between 57 and 87 beats per minute. After surgery, her blood pressure was stable at 112/75 mmHg, and her heart rate was 74 beats per minute. Subsequently, the patient was admitted to an intensive care unit (ICU) for 2 days and then transferred to the ward. Symptomatic supportive treatment was given while the patient was in ICU, including hemodynamic monitoring, oxygen inhalation, analgesia, infection prevention, fluid replacement, and liver function protection. On postoperative day 4, oral feeding was resumed, and the patient was discharged on the eighth day after surgery with no complications. We suggested genetic testing and developed a collaborative, multidisciplinary long-term follow-up plan. With the first outpatient visit 1 month after surgery, an annual follow-up with clinical and biochemical assessment was recommended. The individualized follow-up plan could be flexibly adjusted based on the gene detection and monitoring results.

Pathological examination of the surgical specimen indicated a necrotic change measuring 20 × 15 × 10 cm and weighing 2,240 g located in the retroperitoneum and right adrenal gland (Figure 1D). Hematoxylin–eosin (H&E) staining showed a well-circumscribed tumor surrounded by a fibrous capsule (Figures 2A, B). Immunohistochemistry showed marked pleomorphism within a few tumor cells, CD56(+), CgA (+), Syn(+), CK (Pan)(−), MART-1(−), inhibitA(−), S-100(+), INI1 (+), Desmin(−), and Myogenin(−) (Figures 2C, D). According to the immunohistochemical results, the diagnosis of pheochromocytoma was made. Based on the staging system introduced in the 8th edition of the American Joint Committee on Cancer (AJCC) staging system, the tumor was determined as T2M0N0.

## Discussion

Our case reported a rare cystic pheochromocytoma with a lack of evident endocrine symptoms, resulting in a large size and late diagnosis. The extensive necrosis of the adrenal gland, resulting in reduced production of catecholamines, and the retention of these hormones in the capsule mass after secretion may be the explanation for the absence of symptoms. As a result, the time to diagnosis was delayed, and the tumor size was larger once it was detected.

Since serious complications such as myocardial infarction, arrhythmias, dissection aortic aneurysms, heart failure, malignant hypertension, and sudden death can be caused by pheochromocytoma, it might give rise to premature mortality if overlooked (10, 11). In addition to this, cases of misdiagnosis of cystic pheochromocytoma such as pancreatic cystic tumor (12, 13), hepatic cystic tumor (14), simple adrenal cyst (15), and liver abscess (16) under CT scan have also been previously documented. Hence, it is essential to investigate the characteristics of this tumor.

To date, a total of 20 cases (5, 8, 17–33) of giant pheochromocytoma ≥20 cm were documented since the tumor was first described in 1886 by Fränke (34). We reviewed previous reports and summarized the clinical characteristics (Table 2). The average age at the discovery of giant pheochromocytoma was 51 (range 17–85) years. No significant difference was observed in gender, with slightly more women (11 cases). Additionally, similar findings were revealed in tumor histopathology (five and six cases manifested as malignant and benign, respectively). More cases had tumors that occurred on the left (11 cases) side of the abdomen than on the right (seven cases), and the rest of the articles did not explicitly state the site. Most clinical manifestations were asymptomatic (seven cases) and were often discovered occasionally during a physical examination. In addition, backache (three cases), abdominal pain (two cases), and chest pain (two cases) are relatively common chief complaints. What is more, non-endocrine manifestations, such as abdominal swelling, nausea, constipation, fatigue, and weight loss, could also be presented as the patient's chief complaints.

Till now, the largest pheochromocytoma in the world was recorded to be 45 × 20 cm originally by Grissom et al. in 1979 (17). The current case turned out to be the largest cystic pheochromocytoma in China.

One of the unusual features of the present case is the cystic components. Most of the time, pheochromocytoma is a solid neoplasm originating from the adrenal medulla (29, 35), while

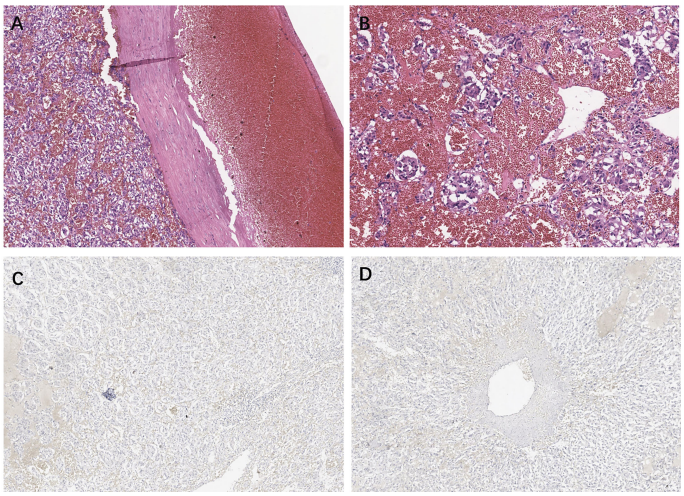


FIGURE 2
H&E staining in **(A)** ×10 view and **(B)** ×40 view. **(C, D)** CD56 staining immunohistochemistry of the tumor.

cystic pheochromocytoma is a rare neuroendocrine tumor, with only a few described in former studies (5, 18, 19, 21, 22, 25, 29, 31). Goldberg et al. and Samejimaonce et al. successively found that the cystic fluid contains high concentrations of catecholamines and metanephrines (22, 35). Extensive hemorrhage followed by necrosis with cyst formation and subsequent resorption of the contents may be the postulated mechanism for this cystic degeneration in the tumor. Furtherly, extensive hemorrhage was likely triggered by the tumor outgrowing its vascular supply (36). This cystic change has also been demonstrated in other primary adrenal neoplasms, either benign cortical adenomas and hemangioma or primary and metastatic malignant adrenal lesions (37).

Notably, despite the surgical margin being histologically negative, the nature of the cystic pheochromocytoma should be interpreted with caution.

As with many other neuroendocrine tumors, it is almost impossible to confirm whether a tumor is benign or malignant only by histological criteria (5, 38). According to 2017 WHO classification of endocrine tumors, all pheochromocytomas are deemed to have metastatic potential, replacing the previous term "malignant" (39). This approach is maintained in the 2022 WHO classification (40). Thus, many researchers are attempting to develop scoring or classification systems that would predict the future behavior of pheochromocytoma. Multifactorial assessment, including tumor size (≥5 cm), Ki-67 index, SDHB mutation, and the dopaminergic phenotype have been suggested to assess the metastatic potential (40–42). These methods for screening for SDHx mutations are reasonable for rapid identification of patients at high risk of metastasis. However, accurate genetic testing remains essential (40). In addition to this, the Pheochromocytoma of the Adrenal gland Scaled Score (PASS) system has carried out a meaningful attempt (43). This is a risk-stratification system entirely based on histological features. However, the PASS score seems to be more reliable concerning the negative predictive value for the absence of metastatic behavior (44). The Grading system for Adrenal Pheochromocytoma and Para-ganglioma (GAPP) system, based on the growth pattern, cellularity, comedo-type necrosis, and vascular or capsular invasion, complemented by the Ki-67 index and catecholamine type demonstrates good predictive performance (45).

However, the problem concerning the label "poorly differentiated" for these neoplasms that are not poorly differentiated in the context used for high-grade neuroendocrine tumors has been noted by the WHO/International Agency for Research on Cancer (IARC) classification. Currently, COmposite Pheochromocytoma/para-ganglioma (COPPS) Prognostic Score classification systems, with a sensitivity of 100% and specificity of 95%, are proposed. This score focuses on clinicopathological criteria, including tumor size (>7 cm), necrosis, vascular invasion, and SDHB immunohistochemical staining. As the study was only recently published, it has not been independently verified (40). At present, the latest version of WHO classification does not recognize any of these systems but at the same time does not discourage their use in individual practices (40). Thereby, subsequent follow-up and metastasis monitoring are still critical to patient care.

Upon suspicion of pheochromocytoma, verification can be performed by biochemical testing (46). Among hormonal assay

TABLE 2 A summary of reported giant pheochromocytomas with a maximal diameter greater than 20 cm, arranged by the largest to smallest maximum diameter.

| | First author | Year | Country | Size (cm) | Weight (g) | Sex | Age | Location | Histopathological evaluation | Operation approach | Component | Chief complaint |
|---|---|---|---|---|---|---|---|---|---|---|---|---|
| 1 | Grissom | 1979 | USA | 45 × 25 | 3,000+ | F | 54 | Left abdomen | NA | Open | NA | Asymptomatic |
| 2 | Arikan | 2021 | Turkey | 30 × 23 | NA | M | 54 | Right abdomen | Benign | Open | Cystic | Hypertension |
| 3 | Costa | 2008 | Brazil | 30 | NA | M | 46 | Right abdomen | Malignant | Open | Cystic | Abdominal pain |
| 4 | Basso | 1996 | Italy | 29 × 21 × 12 | 4,050 | M | 47 | Left abdomen | Malignant | Open | Solid | Asymptomatic |
| 5 | Karumanchery | 2012 | England | 28 × 16 × 13 | 2,300 | F | 85 | Left abdomen | NA | Open | Cystic | Back pain |
| 6 | Maharaj | 2017 | Trinidad and Tobago | 27 × 18 × 12 | 3,315 | F | 50 | Left abdomen | Low risk of malignancy | Open | NA | Back pain, fatigue, and weight loss |
| 7 | Samejima | 2019 | Japan | 27 | NA | M | 45 | Right abdomen | Benign | Open | Cystic | Abdominal swelling |
| 8 | Gupta | 2016 | India | 25 × 17 × 15 | 2,750 | F | 65 | Left abdomen | Benign | Open | Cystic | Left upper abdominal lump |
| 9 | Okada | 2016 | Japan | 24 × 23 × 16 | 5,900 | F | 43 | Abdomen | NA | Open | NA | Vulva edema |
| 10 | Díaz-Roldán | 2021 | Spain | 23 × 15 × 10 | NA | F | 57 | Right abdomen | Benign | Open | NA | Morning headache |
| 11 | Suga | 2000 | Japan | 21 × 13 × 21 | 3,900 | M | 48 | Left abdomen | NA | Open | Cystic | Asymptomatic |
| 12 | Terk | 1993 | USA | 21 × 20 × 11 | 2,870 | M | 35 | Abdominal and pelvic cavity | NA | Open | NA | Constipation |
| 13 | Arcos | 2009 | Canada | 21 × 17 × 11 | NA | F | 36 | Left abdomen | Malignant | Open | NA | Lower back pain |
| 14 | Soufi | 2012 | India | 21 × 15 | NA | F | 17 | Right abdomen | Malignant | Open | Cystic | Asymptomatic |
| 15 | Cajipe | 2017 | USA | 21 × 12 × 10.5 | 1,773 | F | 56 | Left abdomen | Benign | Open | Cystic | Nausea, vomiting, fainting spells |
| 16 | Ologun | 2017 | USA | 20.5 × 18 × 10 | 2,582 | F | 55 | Right abdomen | NA | Open | NA | Abdominal pain, chest pain, palpitation, |
| 17 | Melegh | 2002 | Hungary | 20 | NA | M | 55 | Left abdomen | NA | Open | Cystic | Asymptomatic |
| 18 | Korgali | 2014 | Turkey | 20 × 17 × 9 | 1,736 | M | 63 | Left abdomen | Malignant | Open | Solid-cystic | Chest pain, sweating, nausea |
| 19 | Current case | 2022 | China | 20 × 15 × 10 | 2,240 | F | 64 | Right abdomen | Benign | Open | Cystic | Asymptomatic |
| 20 | Jiang | 2017 | China | 20 × 14 × 5 | NA | M | 45 | Left abdomen | NA | Open | NA | Asymptomatic |

tests, elevated levels of metanephrines in 24-h urine or plasma are of the highest suggestibility (47). Anatomical imaging should be followed as the first modality if biochemical tests indicate the presence of pheochromocytomas. Abdominal or pelvic CT scans are helpful and highly recommended (47, 48). Other imaging studies, such as abdominal/pelvic multiphasic CT or MRI scans or nuclear medicine imaging, including meta-iodobenzylguanidine (MIBG) scintigraphy, FDG-PET/CT scans, and DOTA-SSA PET/CT scans, should be performed as appropriate if metastatic or multifocal disease is suspected (47). Functional imaging enables accurate diagnosis of tumor recurrence or metastasis that might go undetected by anatomical imaging (49). Regarding differential diagnosis, [$^{18}$F]-FDG can be helpful to determine whether the tumors were benign or indicate primary malignant adrenal diseases in non-functioning adrenal masses with inconclusive CT/MRI imaging (50). Further, the latest review recommends specific nuclear imaging for the different clusters of pheochromocytoma when conducting personalized surveillance and management (39, 50). Based on genetic testing, [$^{68}$Ga]-DOTA-SSA PET/CT is demonstrated as the most sensitive functional imaging modality for cluster 1A, while [$^{18}$F] FDOPA PET/CT is more sensitive for cluster 1B and cluster 2 tumors (39). Our CT image presents a sporadic isolated adrenal mass, and pheochromocytoma was highly suspected based on the imaging features. In addition, given the patient's financial situation and her wishes, we finally had no nuclear medical examination performed.

Once a pheochromocytoma is diagnosed, surgery is the preferred treatment whenever possible, regardless of its nature, component, and size. In addition to the conventional open approach, laparoscopic surgery has emerged as a favorable approach due to its ability to decrease hospitalizations, transfusion, and analgesia requirements. However, considering tumor size and location, the open operation is still recommended when tumors are with malignant potential, bilateral, and larger than 8 cm. Currently, there are four reports of laparoscopic excision of pheochromocytoma larger than 10 cm, and the maximum is 14 cm (51–54). If metastatic disease is present, primary tumor removal/debulking surgery may also be performed to alleviate symptoms and signs of catecholamine overdose or local symptoms.

Intraoperative hemodynamic monitoring, especially management of the hypertensive crisis by an experienced anesthesiologist, is essential for optimal surgical outcomes. Arrhythmias are common during the procedure, and intravenous administration of esmolol and lidocaine are effective measures. After removal of the origin of excess catecholamines in the circulation, postoperative hypotension may be intractable and is usually managed with intravenous fluid replacement (sometimes with vasopressors). Intravenous glucose prevents hypoglycemia, which occurs in 10%–15% of patients due to the elimination of the inhibitory effect of catecholamines on insulin secretion.

Postoperatively, although there has been no accurate consensus on follow-up, long-term multidisciplinary follow-up is indispensable. Since genotype–phenotype presentations have been proved to be associated with pheochromocytoma personalized management, gene detection is encouraged for patients. So far, 14 different susceptibility genes of pheochromocytomas have been documented: NF1, RET, VHL, SDHD, SDHC, SDHB, EGLN1/PHD2, KIF1β, SDH5/SDHAF2, IDH1, TMEM127, SDHA, MAX, and HIF2α (55). Among them, mutations of SDHB lead to tumor metastasis in 40% or more of affected patients (56). The 5th edition of the WHO Classification encourages routine use of SDHB immunohistochemistry (40). Vigilant imaging examinations should be performed as required.

Collectively, we reported a fairly rare case of a giant cystic pheochromocytoma and provided an up-to-date literature review of patients with such tumors larger than 20 cm. Large pheochromocytomas are usually asymptomatic and require individualized surgery. The prognosis is generally well, but long-term follow-up is required to monitor the tumor for metastasis or recurrence.

## Data availability statement

The original contributions presented in the study are included in the article/supplementary material. Further inquiries can be directed to the corresponding author.

## Ethics statement

Written informed consent was obtained from the individual for the publication of any potentially identifiable images or data included in this article.

## Author contributions

QF and HL drafted and revised the manuscript. GQ and ZC collected the data and revised the manuscript. JL revised the manuscript for content. YZ and JH designed the study and revised the manuscript. All authors contributed to the article and approved the submitted version.

## Funding

This work was supported by grants from the National Key Technologies R&D Program (2018YFC1106800), the Natural Science Foundation of China (82170621, 82070644, 81800564, and 81770615), and the 1.3.5 project for

disciplines of excellence, West China Hospital, Sichuan University (ZYJC18008).

## Conflict of interest

The authors declare that the research was conducted in the absence of any commercial or financial relationships that could be construed as a potential conflict of interest.

## Publisher's note



## References

1. Curfman KR, Di Como JA, Chung TR, Dumire RD. Functionally silent, giant pheochromocytoma presenting with varicocele. *Am Surg* (2021) 87(1):97–100. doi: 10.1177/0003134820945274

2. Lam AK. Update on adrenal tumours in 2017 world health organization (who) of endocrine tumours. *Endocr Pathol* (2017) 28(3):213–27. doi: 10.1007/s12022-017-9484-5

3. Wang X, Zhao Q, Sang H, Dong J, Bai M. Research on the damage of adrenal pheochromocytoma to patients' cardiovascular vessels and its correlation with hypertension. *J Oncol* (2022) 2022:3644212. doi: 10.1155/2022/3644212

4. Pappachan JM, Raskauskiene D, Sriraman R, Edavalath M, Hanna FW. Diagnosis and management of pheochromocytoma: a practical guide to clinicians. *Curr Hypertens Rep* (2014) 16(7):442. doi: 10.1007/s11906-014-0442-z

5. Gupta A, Bains L, Agarwal MK, Gupta R. Giant cystic pheochromocytoma: A silent entity. *Urol Ann* (2016) 8(3):384–6. doi: 10.4103/0974-7796.184886

6. Ferreira VM, Marcelino M, Piechnik SK, Marini C, Karamitsos TD, Ntusi NAB, et al. Pheochromocytoma is characterized by catecholamine-mediated myocarditis, focal and diffuse myocardial fibrosis, and myocardial dysfunction. *J Am Coll Cardiol* (2016) 67(20):2364–74. doi: 10.1016/j.jacc.2016.03.543

7. Chen H, Sippel RS, O'Dorisio MS, Vinik AI, Lloyd RV, Pacak K. The north American neuroendocrine tumor society consensus guideline for the diagnosis and management of neuroendocrine tumors: pheochromocytoma, paraganglioma, and medullary thyroid cancer. *Pancreas.* (2010) 39(6):775–83. doi: 10.1097/MPA.0b013e3181ebb4f0

8. Maharaj R, Parbhu S, Ramcharan W, Baijoo S, Greaves W, Harnanan D, et al. Giant cystic pheochromocytoma with low risk of malignancy: A case report and literature review. *Case Rep Oncol Med* (2017) 2017:4638608. doi: 10.1155/2017/4638608

9. Riley DS, Barber MS, Kienle GS, Aronson JK, von Schoen-Angerer T, Tugwell P, et al. CARE guidelines for case reports: explanation and elaboration document. *J Clin Epidemiol.* (2017) 89:218–35. doi: 10.1016/j.jclinepi.2017.04.026

10. Andreoni C, Krebs RK, Bruna PC, Goldman SM, Kater CE, Alves MT, et al. Cystic phaeochromocytoma is a distinctive subgroup with special clinical, imaging and histological features that might mislead the diagnosis. *BJU Int* (2008) 101(3):345–50. doi: 10.1111/j.1464-410X.2007.07370.x

11. Schmid H, Mussack T, Wörnle M, Pietrzyk MC, Banas B. Clinical management of large adrenal cystic lesions. *Int Urol Nephrol.* (2005) 37(4):767–71. doi: 10.1007/s11255-005-4662-7

12. Antedomenico E, Wascher RA. A case of mistaken identity: giant cystic pheochromocytoma. *Curr Surg* (2005) 62(2):193–8. doi: 10.1016/j.cursur.2004.08.015

13. Yagnik VD, Joshipura V, Sadhu R. Cystic pheochromocytoma masquerading as a cystic pancreatic tumour. *ANZ J Surg* (2019) 89(5):E195–e7. doi: 10.1111/ans.14213

14. Wu JS, Ahya SN, Reploeg MD, Singer GG, Brennan DC, Howard TK, et al. Pheochromocytoma presenting as a giant cystic tumor of the liver. *Surgery.* (2000) 128(3):482–4. doi: 10.1067/msy.2000.104113

15. Kumar S, Parmar KM, Aggarwal D, Jhangra K. Simple adrenal cyst masquerading clinically silent giant cystic pheochromocytoma. *BMJ Case Rep* (2019) 12(9). doi: 10.1136/bcr-2019-230730

16. Sarveswaran V, Kumar S, Kumar A, Vamseedharan M. A giant cystic pheochromocytoma mimicking liver abscess an unusual presentation - a case report. *Clin Case Rep* (2015) 3(1):64–8. doi: 10.1002/ccr3.149

17. Grissom JR, Yamase HT, Prosser PR. Giant pheochromocytoma with sarcoidosis. *South Med J* (1979) 72(12):1605–7. doi: 10.1097/00007611-197912000-00035

18. Arikan S, Tatar C, Emre Nayci A, Ersoz F, Baki Dogan M, Gunver F. Giant composite pheochromocytoma and gastrointestinal stromal tumor in a patient with neurofibromatosis: A case report. *North Clin Istanb.* (2021) 8(6):629–33. doi: 10.14744/nci.2020.37431

19. Costa SR, Cabral NM, Abhrão AT, Costa RB, Silva LM, Lupinacci RA. Giant cystic malignant pheochromocytoma invading right hepatic lobe: report on two cases. *Sao Paulo Med J* (2008) 126(4):229–31. doi: 10.1590/S1516-31802008000400008

20. Basso L, Lepre L, Melillo M, Fora F, Mingazzini PL, Tocchi A. Giant phaeochromocytoma: case report. *Ir J Med Sci* (1996) 165(1):57–9. doi: 10.1007/BF02942808

21. Karumanchery R, Nair JR, Hakeem A, Hardy R. An unusual case of back pain: A large pheochromocytoma in an 85 year old woman. *Int J Surg Case Rep* (2012) 3(1):16–8. doi: 10.1016/j.ijscr.2011.10.006

22. Samejima M, Taguchi S, Miyagawa S, Matsumoto R, Omura S, Ninomiya N, et al. Acute hypotension induced by suction of cystic fluid containing extremely high concentrations of catecholamines during resection of giant pheochromocytoma. *IJU Case Rep* (2019) 2(4):218–20. doi: 10.1002/iju5.12087

23. Okada R, Shimura T, Tsukida S, Ando J, Kofunato Y, Momma T, et al. Concomitant existence of pheochromocytoma in a patient with multiple endocrine neoplasia type 1. *Surg Case Rep* (2016) 2(1):84. doi: 10.1186/s40792-016-0214-x

24. Díaz-Roldán J, Díaz-Ramírez J, Franch-Arcas G, Alemán-Martín A. A new trigger in pheochromocytoma crisis: Giant leiomyoma. *Ann Endocrinol (Paris).* (2021) 82(2):124–6. doi: 10.1016/j.ando.2021.01.002

25. Suga K, Motoyama K, Hara A, Kume N, Ariga M, Matsunaga N. Tc-99m MIBG imaging in a huge clinically silent pheochromocytoma with cystic degeneration and massive hemorrhage. *Clin Nucl Med* (2000) 25(10):796–800. doi: 10.1097/00003072-200010000-00009

26. Terk MR, de Verdier H, Colletti PM. Giant extra-adrenal pheochromocytoma: magnetic resonance imaging with gadolinium-DTPA enhancement. *Magn Reson Imaging.* (1993) 11(1):47–50. doi: 10.1016/0730-725X(93)90410-F

27. Arcos CT, Luque VR, Luque JA, García PM, Jiménez AB, Muñoz MM. Malignant giant pheochromocytoma: a case report and review of the literature. *Can Urol Assoc J* (2009) 3(6):E89–91. doi: 10.5489/cuaj.1189

28. Soufi M, Lahlou MK, Benamr S, Massrouri R, Mdaghri J, Essadel A, et al. Giant malignant cystic pheochromocytoma: a case report. *Indian J Surg* (2012) 74(6):504–6. doi: 10.1007/s12262-012-0719-x

29. Cajipe KM, Gonzalez G, Kaushik D. Giant cystic pheochromocytoma. *BMJ Case Rep* (2017) 2017. doi: 10.1136/bcr-2017-222264

30. Ologun GO, Patel ZM, Adeboye A, Guduru M, Trostle D, Vandermeer T, et al. A giant adrenal mass in a super obese patient. *Cureus.* (2017) 9(8):e1572. doi: 10.7759/cureus.1572

31. Melegh Z, Rényi-Vámos F, Tanyay Z, Köves I, Orosz Z. Giant cystic pheochromocytoma located in the renal hilus. *Pathol Res Pract* (2002) 198(2):103–6. doi: 10.1078/0344-0338-00194

32. Korgali E, Dundar G, Gokce G, Kilicli F, Elagoz S, Ayan S, et al. Giant malignant pheochromocytoma with palpable rib metastases. *Case Rep Urol.* (2014) 2014:354687. doi: 10.1155/2014/354687

33. Jiang A, Zhang H, Liu X, Zhao H. Perioperative anesthetic management of a case of rare ectopic pheochromocytoma. *World J Oncol* (2017) 8(6):191–5. doi: 10.14740/wjon1065e

34. Classics in oncology. A case of bilateral completely latent adrenal tumor and concurrent nephritis with changes in the circulatory system and retinitis: Felix fränkel, 1886. *CA Cancer J Clin* (1984) 34(2):93–106. doi: 10.3322/canjclin.34.2.93

35. Goldberg A, Pautler SE, Harle C, Dennis A, Rachinsky I, Dhir A, et al. Giant cystic pheochromocytoma containing high concentrations of catecholamines and metanephrines. *J Clin Endocrinol Metab* (2011) 96(8):2308–9. doi: 10.1210/jc.2011-0465

36. Erickson LA, Lloyd RV, Hartman R, Thompson G. Cystic adrenal neoplasms. *Cancer*. (2004) 101(7):1537–44. doi: 10.1002/cncr.20555

37. Galatola R, Romeo V, Simeoli C, Guadagno E, De Rosa I, Basso L, et al. Characterization with hybrid imaging of cystic pheochromocytomas: correlation with pathology. *Quant Imaging Med Surg* (2021) 11(2):862–9. doi: 10.21037/qims-20-490

38. Adler JT, Meyer-Rochow GY, Chen H, Benn DE, Robinson BG, Sippel RS, et al. Pheochromocytoma: current approaches and future directions. *Oncologist*. (2008) 13(7):779–93. doi: 10.1634/theoncologist.2008-0043

39. Nölting S, Bechmann N, Taieb D, Beuschlein F, Fassnacht M, Kroiss M, et al. Personalized management of pheochromocytoma and paraganglioma. *Endocr Rev* (2022) 43(2):199–239. doi: 10.1210/endrev/bnab019

40. Mete O, Asa SL, Gill AJ, Kimura N, de Krijger RR, Tischler A. Overview of the 2022 WHO classification of paragangliomas and pheochromocytomas. *Endocr Pathol* (2022) 33(1):90–114. doi: 10.1007/s12022-022-09704-6

41. Lenders JWM, Kerstens MN, Amar L, Prejbisz A, Robledo M, Taieb D, et al. Genetics, diagnosis, management and future directions of research of phaeochromocytoma and paraganglioma: a position statement and consensus of the working group on endocrine hypertension of the European society of hypertension. *J Hypertens* (2020) 38(8):1443–56. doi: 10.1097/HJH.0000000000002438

42. Fassnacht M, Assie G, Baudin E, Eisenhofer G, de la Fouchardiere C, Haak HR, et al. Adrenocortical carcinomas and malignant phaeochromocytomas: ESMO-EURACAN clinical practice guidelines for diagnosis, treatment and follow-up. *Ann Oncol* (2020) 31(11):1476–90. doi: 10.1016/j.annonc.2020.08.2099

43. Thompson LD. Pheochromocytoma of the adrenal gland scaled score (PASS) to separate benign from malignant neoplasms: a clinicopathologic and immunophenotypic study of 100 cases. *Am J Surg Pathol* (2002) 26(5):551–66. doi: 10.1097/00000478-200205000-00002

44. Stenman A, Zedenius J, Juhlin CC. The value of histological algorithms to predict the malignancy potential of pheochromocytomas and abdominal paragangliomas-a meta-analysis and systematic review of the literature. *Cancers (Basel)*. (2019) 11(2):225. doi: 10.3390/cancers11020225

45. Kimura N, Takayanagi R, Takizawa N, Itagaki E, Katabami T, Kakoi N, et al. Pathological grading for predicting metastasis in phaeochromocytoma and paraganglioma. *Endocr Relat Cancer*. (2014) 21(3):405–14. doi: 10.1530/ERC-13-0494

46. Fassnacht M, Arlt W, Bancos I, Dralle H, Newell-Price J, Sahdev A, et al. Management of adrenal incidentalomas: European society of endocrinology clinical practice guideline in collaboration with the European network for the study of adrenal tumors. *Eur J Endocrinol* (2016) 175(2):G1–g34. doi: 10.1530/EJE-16-0467

47. Shah MH, Goldner WS, Benson AB, Bergsland E, Blaszkowsky LS, Brock P, et al. Neuroendocrine and adrenal tumors, version 2.2021, NCCN clinical practice guidelines in oncology. *J Natl Compr Canc Netw* (2021) 19(7):839–68. doi: 10.6004/jnccn.2021.0032

48. Hallin Thompson L, Makay Ö, Brunaud L, Raffaelli M, Bergenfelz A. Adrenalectomy for incidental and symptomatic phaeochromocytoma: retrospective multicentre study based on the eurocrine® database. *Br J Surg* (2021) 108(10):1199–206. doi: 10.1093/bjs/znab199

49. Taïeb D, Hicks RJ, Hindié E, Guillet BA, Avram A, Ghedini P, et al. European Association of nuclear medicine practice Guideline/Society of nuclear medicine and molecular imaging procedure standard 2019 for radionuclide imaging of phaeochromocytoma and paraganglioma. *Eur J Nucl Med Mol Imaging*. (2019) 46(10):2112–37. doi: 10.1007/s00259-019-04398-1

50. Lorusso M, Rufini V C, Pennestrì F, Bellantone R, Raffaelli M. Integration of molecular imaging in the personalized approach of patients with adrenal masses. *Q J Nucl Med Mol Imaging*. (2022) 66(2):104–15. doi: 10.23736/S1824-4785.22.03449-5

51. Clements HA, Wilson MS, Smith DM. Incidental giant cystic pheochromocytoma: a case report and review of the literature. *Scott Med J* (2020) 65(2):64–70. doi: 10.1177/0036933019900339

52. Mishra AK, Agarwal G, Agarwal A, Mishra SK. Laparoscopic adrenalectomy of large cystic pheochromocytoma. *Surg Endosc*. (2001) 15(2):220. doi: 10.1007/s004640040036

53. Costa Almeida CE, Silva M, Carvalho L, Costa Almeida CM. Adrenal giant cystic pheochromocytoma treated by posterior retroperitoneoscopic adrenalectomy. *Int J Surg Case Rep* (2017) 30:201–4. doi: 10.1016/j.ijscr.2016.12.018

54. Martins D, Rodrigues D, Melo M, Carrilho F. Laparoscopic adrenalectomy as an effective approach to massive bilateral pheochromocytomas. *BMJ Case Rep* (2017) 2017. doi: 10.1136/bcr-2017-221009

55. Lenders JW, Duh QY, Eisenhofer G, Gimenez-Roqueplo AP, Grebe SK, Murad MH, et al. Pheochromocytoma and paraganglioma: an endocrine society clinical practice guideline. *J Clin Endocrinol Metab* (2014) 99(6):1915–42. doi: 10.1210/jc.2014-1498

56. Amar L, Baudin E, Burnichon N, Peyrard S, Silvera S, Bertherat J, et al. Succinate dehydrogenase b gene mutations predict survival in patients with malignant pheochromocytomas or paragangliomas. *J Clin Endocrinol Metab* (2007) 92(10):3822–8. doi: 10.1210/jc.2007-0709

frontiers | Frontiers in Surgery

TYPE Case Report
PUBLISHED 05 September 2022
DOI 10.3389/fsurg.2022.1001350



OPEN ACCESS

EDITED BY
Zhaolun Cai,
West China Hospital, China

REVIEWED BY
Makoto Ide,
Takamatsu Red Cross Hospital, Japan
Hamid Pakmanesh,
Kerman University of Medical Sciences, Iran

*CORRESPONDENCE
Ning Lang
langning800129@126.com

†These authors have contributed equally to this work

SPECIALTY SECTION
This article was submitted to Surgical Oncology, a section of the journal Frontiers in Surgery

RECEIVED 23 July 2022
ACCEPTED 04 August 2022
PUBLISHED 05 September 2022

CITATION
Zhang E, Li Y and Lang N (2022) Case report: Castleman's disease involving the renal sinus resembling renal cell carcinoma.
Front. Surg. 9:1001350.
doi: 10.3389/fsurg.2022.1001350



# Case report: Castleman's disease involving the renal sinus resembling renal cell carcinoma

Enlong Zhang[1,2†], Yuan Li[1†] and Ning Lang[1*]

[1]Department of Radiology, Peking University Third Hospital, Beijing, China, [2]Department of Radiology, Peking University International Hospital, Beijing, China

**Introduction:** Castleman's disease (CD) is a rare benign lymphoproliferative disease that frequently involves the mediastinal thorax and the neck lymph nodes. It rarely affects extrathoracic presentations, with even fewer presentations in the renal sinus.
**Patient concerns:** In this report, we present a case of a 40-year-old woman with no significant past
medical history who presented Castleman's disease arising in the renal sinus.
**Diagnosis and interventions:** The patient visited our hospital with the chief complaint of left renal sinus lesion after renal ultrasonography by regular physical examination. Subsequent abdominal computed tomography urography revealed a soft tissue mass with heterogeneous obvious enhancement in the sinus of the left kidney, which was suspected to be a renal malignant tumor. Hence, the patient underwent a left radical nephrectomy. Histological examination revealed hyperplastic lymphoid follicles in the renal sinus and was finally diagnosed as Castleman's disease of the hyaline vascular type.
**Outcomes:** Five days after the surgery procedure, the patient was discharged.
**Conclusion:** Due to the low incidence of Castleman's disease in renal sinus, there is a strong likelihood of missed diagnosis or misdiagnosis, and it is, therefore, important to be aware of the risk. Heightened awareness of this disease and its radiographic manifestations may prompt consideration of this diagnosis. Therefore, we explored the radiologic findings to find out some radiologic features suggesting this condition to help clinicians to schedule nephron-sparing surgery in the future.

KEYWORDS

hyaline vascular type, renal sinus, computed tomography urography, case report, Castleman disease

## Introduction

Castleman's disease (CD), also known as giant lymph node hyperplasia, is a rare, and clinically and histopathologically heterogeneous group of disorders sharing in common an abnormal lymph node pathology of unknown etiology (1). The disease occurs in two clinical forms: unicentric CD (UCD) and multicentric CD (MCD), and is divided

Abbreviations
CD, Castleman's disease; UCD, unicentric CD; MCD, multicentric CD; CTU, computed tomography urography; HU, Hounsfield unit; CMP, corticomedullary phase; NP, nephrographic phase; EP, excretory phase.

pathologically into three types: hyaline vascular, plasma cell variants, and mixed type. UCD is the most common, occurring at a rate of 16 per million person years and occurs at any age (2); approximately 75% of these cases are hyaline vascular variant and is usually curable by surgical resection. MCD is classically associated with systemic symptoms and a poorer prognosis. CD frequently involves the mediastinal thorax and the neck lymph nodes (3). It rarely affects extrathoracic presentations, with even fewer presentations in the renal sinus. Preoperative diagnosis is difficult because diagnostic imaging alone cannot distinguish CD from other diseases due to the lack of tumor-specific signs. Here, we report a case of hyaline vascular type CD with renal sinuses involved. By reviewing the literature, we hope to find out the imaging features to assist in the preoperative qualitative diagnosis of this disease and as a reference to clinicians in the future. The present case report is developed according to the CARE checklist (4, 5).

## Case presentation

A 40-year-old female patient presented to our hospital with the chief complaint of left renal sinus lesion after renal ultrasonography was performed as part of a healthy physical examination. The patient had no symptoms of infection such as fever, night sweats, or other clinical symptoms. Physical examination also showed no obvious abnormalities. Laboratory examinations such as C-reactive protein (CRP), erythrocyte sedimentation rate (ESR), and interleukin-6 (IL-6) showed no significant abnormalities. Urinalysis findings were within normal limits, with urine cytology being normal, and 99mTc DTPA renal scintigraphy images showed normal renal blood flow (**Figure 1**). Abdominal computed tomography urography (CTU) revealed a $4.7 \times 4.0 \times 3.8$ cm soft tissue mass in the left renal sinus with heterogeneous obvious enhancement (CT: 42HUPS, 136HUCMP, 122HUNP, 85HUEP) (**Figure 2**). The mass was adjacent to the renal parenchyma, and the boundary was unclear. The left renal artery and vein, renal pelvis, and calyces showed compression changes. No obvious signs of dilated hydronephrosis were observed in the urinary tract. Multiple enlarged lymph nodes were seen retroperitoneum. A small amount of effusion was observed in the pelvic cavity. A renal malignant tumor was suspected, and the patient was scheduled for a left radical nephrectomy. She did not have a family history of renal cell carcinoma or genetic abnormalities. The cut surface of the renal sinus in the middle of the kidney revealed a grayish-yellow nodular mass (about $5.2 \times 4.0 \times 3.5$ cm) with spotty hemorrhage. The renal pelvis is unclear and the mass is adjacent to the renal parenchyma. The mucosal layers of the renal pelvis, calyces and ureter were intact, and no evidence of urothelial malignancy. Histological and immunohistochemical findings were compatible with a diagnosis of CD of the hyaline vascular type. The patient was discharged on day 5.

## Discussion and conclusion

CD is a rare disease characterized by the massive growth of the abnormal lymph node (1). The pathogenesis of CD remains unknown. The possible mechanisms include chronic low-grade inflammation, immunodeficiency state, and autoimmunity. CD can be classified clinically as UCD and MCD, and pathologically as hyaline vascular, plasma cell variants, and mixed type. UCD is the most common, occurring at the rate of 16 per million person years, occurs at any age (2), and is usually common in young individuals. The most common pathological type is hyaline vascular type, which is characterized by small and transparent vascular follicles and proliferation of capillaries between the hair follicles. Contrast-enhanced CT showed significant enhancement, even to the vascular enhancement level. The findings of UCD on 99mTc DTPA renal scintigraphy have not been well-reported. Song et al. reported a case of retroperitoneal extrarenal UCD. 99mTc DTPA renal scintigraphy shows that both kidneys are functioning normally. However, on both the posterior 2-s/frame blood flow images and the 1-min/frame functional images, UCD peaked at about the same time as the cortex of the kidneys and gradually decreased at a similar rate to the kidney activity. It seemed that the UCD exerted a mass effect and compressed the right kidney laterally (6). These findings were compatible with our case. However, the mass in our case was small, there was no obvious mass effect, and no lesions were found in the blood flow images and functional images. This type is present in 90% of patients with UCD and its most common location is the mediastinum. Usually, the diagnosis of UCD is incidental, most cases of UCD are asymptomatic, and often no laboratory abnormalities are present (7). Our patient was asymptomatic.

Surgical resection for UCD is the most appropriate first-line intervention, according to uniform panel consensus. Important considerations are the location, the resectability, and the degree to which the enlarged lymph node causes symptoms by compressing neighboring anatomy or inducing a systemic inflammatory syndrome. Recurrence of UCD after complete surgical removal is rare (7). In our case, the tumor was adjacent to the renal parenchyma, and the boundary was unclear. In addition, multiple enlarged lymph nodes were seen in the retroperitoneum. Therefore, the tumor was mistaken as a malignant lesion originating from the kidney with lymph node metastasis before the operation, so radical nephrectomy was performed. In a similar report by Radfar et al., they removed the mass laparoscopically and spared the left kidney,

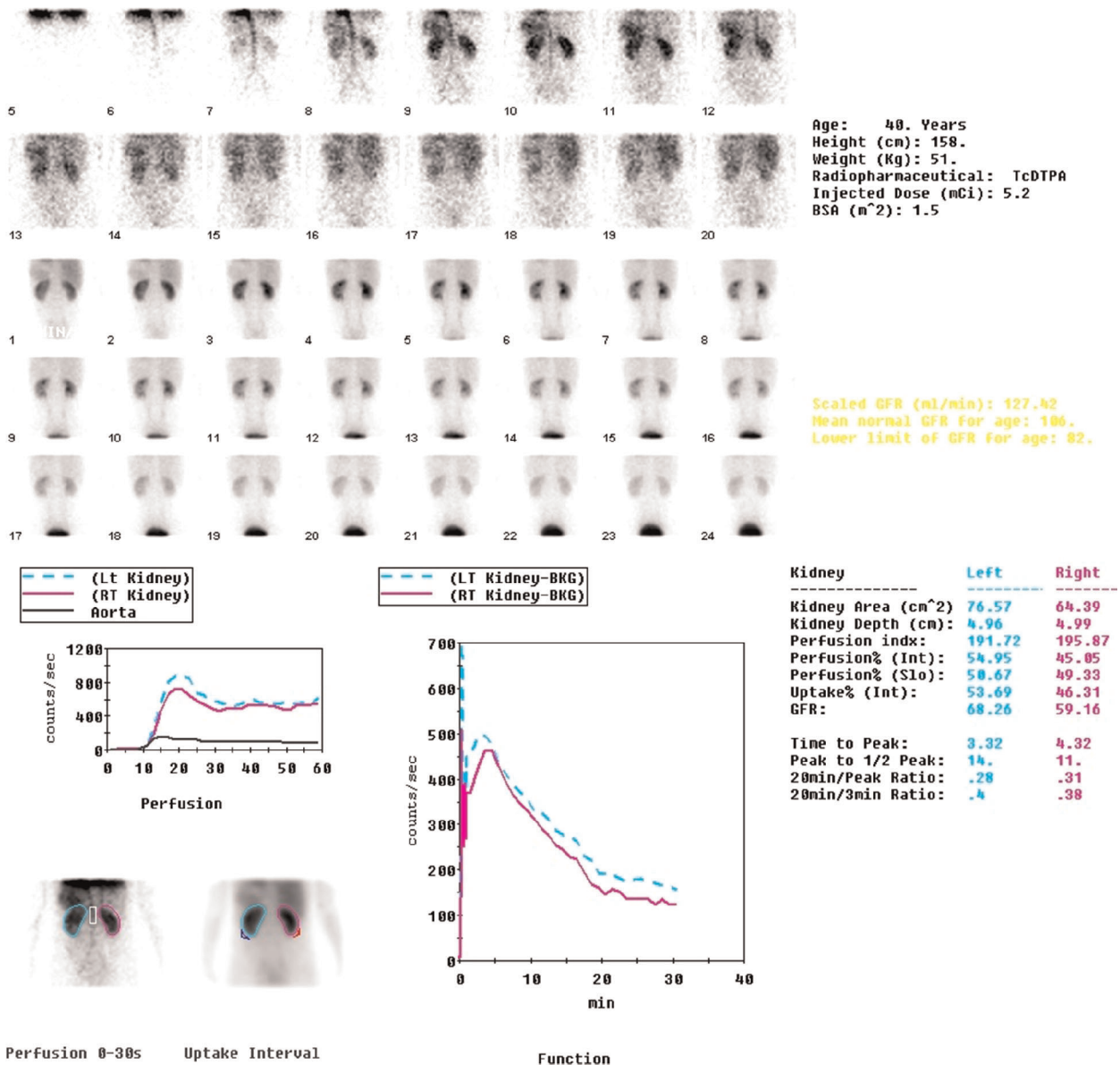


FIGURE 1
99mTc DTPA renal scintigraphy shows normal renal blood flow.

but analysis images showed a certain distance between the lesion and the renal parenchyma, suggesting that the tumor did not originate from the kidney, and radical nephrectomy was not performed (8). The plasma cell type is characterized by patches of plasmacytic between large follicles. Compared with the hyaline vascular type, it has less vascular density and is associated with many signs and symptoms. The less common MCD is usually found in older people, about 80%–90% of these cases are plasma cell variants. Most patients with MCD present with fever, malaise, anemia, elevated ESR, frequent abdominal lymph nodes enlargement, systemic symptoms, hepatosplenomegaly, and systemic lymphadenopathy. The mixed type is characterized histologically by a combination of hyaline vascular and plasma cell morphology.

CD rarely affects extrathoracic presentations, with even fewer presentations in the renal sinus. To the best of our knowledge, only a few cases have been reported (8–16). The clinicopathological features of the reported cases are shown in **Table 1**. There were 11 patients (8 males and 3 females). However, CD is generally gender-neutral. The median age of CD is 40 years old, and the mean age of sinus involvement was 62 years. The main manifestations were

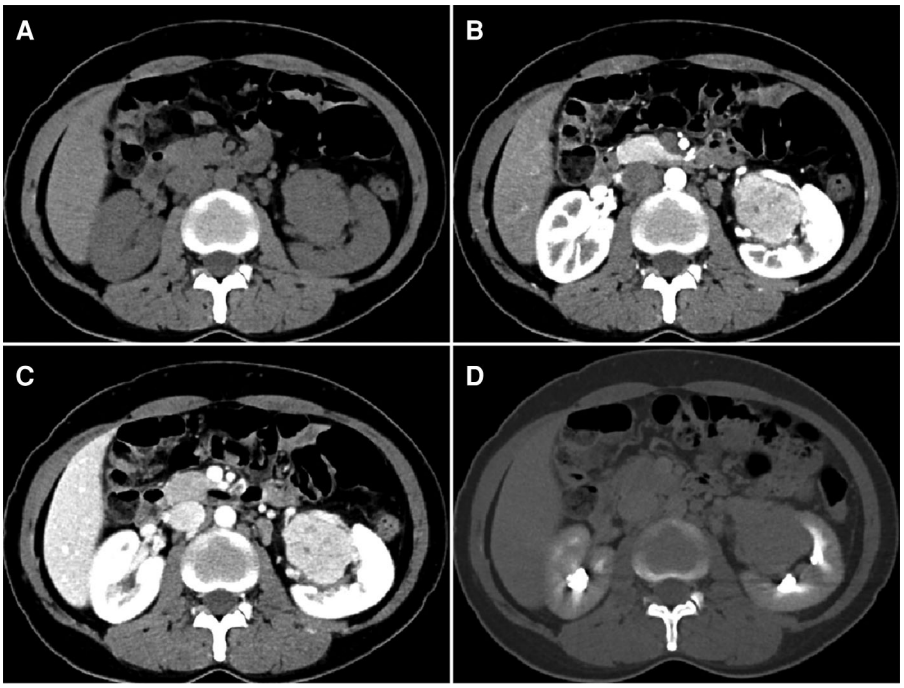


FIGURE 2
CTU reveals a soft tissue mass in the left renal sinus with heterogeneous homogeneous enhancement after injection of contrast media. (A) Unenhanced CT scan; (B) corticomedullary phase; (C) nephrographic phase; (D) excretory phase.

abdominal pain ($n = 2$), weight loss ($n = 2$), microscopic hematuria ($n = 2$), and anorexia ($n = 1$); however, five patients were asymptomatic and the clinical type was UCD. Abdominal pain can be seen both in UCD and MCD patients, weight loss almost in MCD patients, and microscopic hematuria in UCD patients. Seven cases were from a single center and four cases were multi-center. There were seven cases of plasma cell type, three cases of transparent vascular type, and one case of mixed type. The present patient, a 40-year-old female, was asymptomatic of clinically UCD and pathologically transparent vascular type. All mass sizes are less than 5 cm.

Since the treatment of CD is different from other diseases, such as renal carcinoma, lymphoma, and paraganglioma, the preoperative diagnosis of CD involving renal sinus will affect the choice of clinical treatment. UCD is mainly a hyaline vascular type, which is difficult to distinguish from other vascular-rich tumors on imaging. Most are isolated soft tissue masses with well-defined boundaries and minimal bleeding and necrosis. Satellite lesions are seen at the edge of the mass. The lesions in the corticomedullary phase are significantly enhanced, comparable to the enhancement of the aorta, so the images in this phase are easier to identify. Renal clear cell carcinoma is mostly characterized by a solid soft tissue mass with rich blood supply, which is accompanied by hemorrhage and necrosis when it is large. Most tumors show the characteristics of "fast in and fast out" on enhanced scanning, that is, the enhancement degree in the cortical phase is similar to that in the renal cortex, and the enhancement in the parenchymal phase is reduced. The above characteristics are different from UCD. Lymphoma, which includes multiple lesions, obvious enlargement of lymph nodes, fusion into masses, cystic degeneration, and necrosis can be seen, the degree of enhancement is lower than that of CD, and the surrounding blood vessels are often surrounded, that is, "vascular floating sign." Paraganglioma: mostly solid or cystic solid mass, with bleeding and fluid level, obvious enhancement, and most of them have empty blood vessels. Cystic degeneration is rare in UCD.

However, due to the low incidence of CD in renal sinus, there is a strong likelihood of missed diagnosis or misdiagnosis, and it is, therefore, important to be aware of the risk. Heightened awareness of this disease and its radiographic manifestations may prompt consideration of this diagnosis. Therefore, it is important to be aware of the risk of this condition, and the findings from this report might prove useful to clinicians in the future. Therefore, in this case, we explored the radiologic findings to find out some radiologic features suggesting this condition to help clinicians to schedule nephron-sparing surgery in the future.

TABLE 1 Clinicopathological and imaging characteristics of previously reported cases of CD with renal sinus involvement.

| References | Gender | Age (year) | Symptoms | Sinus | MRI | | | CT | | Clinical type | Pathological type |
|---|---|---|---|---|---|---|---|---|---|---|---|
| | | | | | T1WI | T2WI | DWI | Size (cm) | Enhancement | | |
| Nolan et al. (9) | M | 62 | Abdominal pain, microscopic hematuria | Unilateral | N/A | N/A | N/A | N/A | N/A | UCD | PC |
| Nagahama et al. (10) | M | 79 | Anorexia, weight loss | Left | Isointense | Hypointense | N/A | N/A | Mild | MCD | PC |
| Nishie et al. (11) | M ($n = 2$), F ($n = 1$) | 73/70/65 | Weight loss ($n = 1$), asymptomatic ($n = 2$) | Bilateral ($n = 2$), unilateral ($n = 1$) | Isointense ($n = 2$) | Hypointense ($n = 2$) | N/A | 3.0–4.5 | Mild | UCD ($n = 1$), MCD ($n = 2$) | PC ($n = 2$), MF ($n = 1$) |
| Park et al. (12) | M | 50 | Abdominal pain | Right | N/A | | | N/A | Mild | MCD | HV |
| Jang et al. (14) | M | 64 | Microscopic hematuria | Left | N/A | N/A | N/A | 2.5–4 | Mild | UCD | PC |
| Kim et al. (13) | M | 59 | Exertional dyspnea | Left | Isointense | Hypointense | Hyperintense | N/A | Mild | UCD | PC |
| Guo et al. (15) | F | 62 | Asymptomatic | Right | Isointense | Hypointense | Hyperintense | 2.8–4.5 | Mild | UCD | PC |
| Li et al. (16) | M | 56 | Asymptomatic | Right | N/A | N/A | N/A | 3.5–4 | N/A | UCD | HV |
| Radfar et al. (8) | F | 32 | Dull left flank pain | Left | N/A | N/A | N/A | 7 | N/A | N/A | N/A |
| Present | F | 40 | Asymptomatic | Left | N/A | N/A | N/A | 3.8–4.7 | Mild | UCD | HV |

M, male; F, female; N/A, not available; Sinus, the lesion in the renal sinus; MRI, magnetic resonance imaging; T1WI, T1-weighted images; T2WI, T2-weighted images; DWI, diffusion-weighted images; CT, computed tomography; HV, hyaline-vascular; PC, plasma-cell; MF, mixed form.





10.3389/fsurg.2022.1001350

## Data availability statement

The original contributions presented in the study are included in the article/Supplementary Material, further inquiries can be directed to the corresponding author/s.

## Ethics statement

The studies involving human participants were reviewed and approved by Peking University Third Hospital Medical Science Research Ethics Committee. The patients/participants provided their written informed consent to participate in this study. Written informed consent was obtained from the individual for the publication of any potentially identifiable images or data included in this article.

## Author contributions

All author roles are given as follows; design of the work by NL; acquisition of data by YL; interpretation of data by EZ; drafting and critical revision by EZ and YL; final approval by NL. All authors contributed to the article and approved the submitted version.

## Funding

This paper is supported by the National Natural Science Foundation of China under Grant No. 81971578, 81901791. The funders played a role in the study design, data collection or analysis, decision to publish, or manuscript preparation.

## Conflict of interest

The authors declare that the research was conducted in the absence of any commercial or financial relationships that could be construed as a potential conflict of interest.

## Publisher's note

All claims expressed in this article are solely those of the authors and do not necessarily represent those of their affiliated organizations, or those of the publisher, the editors and the reviewers. Any product that may be evaluated in this article, or claim that may be made by its manufacturer, is not guaranteed or endorsed by the publisher.

## References

1. Szalat R, Munshi NC. Diagnosis of Castleman disease. *Hematol Oncol Clin North Am*. (2018) 32:53–64. doi: 10.1016/j.hoc.2017.09.005

2. Simpson D. Epidemiology of Castleman disease. *Hematol Oncol Clin North Am*. (2018) 32:1–10. doi: 10.1016/j.hoc.2017.09.001

3. Cronin DM, Warnke RA. Castleman disease: an update on classification and the spectrum of associated lesions. *Adv Anat Pathol*. (2009) 16:236–46. doi: 10.1097/PAP.0b013e3181a9d4d3

4. Gagnier JJ, Kienle G, Altman DG, Moher D, Sox H, Riley D, et al. The CARE guidelines: consensus-based clinical case reporting guideline development. *BMJ Case Rep*. (2013) 2013:bcr2013201554. doi: 10.1136/bcr-2013-201554

5. Riley DS, Barber MS, Kienle GS, Aronson JK, von Schoen-Angerer T, Tugwell P, et al. CARE guidelines for case reports: explanation and elaboration document. *J Clin Epidemiol*. (2017) 89:218–35. doi: 10.1016/j.jclinepi.2017.04.026

6. Song L, Yao Q, Huang X, Zhang Y. Retroperitoneal Castleman disease on 99mTc DTPA renal scintigraphy. *Clin Nucl Med*. (2012) 37:1024–5. doi: 10.1097/RLU.0b013e3182641d19

7. van Rhee F, Oksenhendler E, Srkalovic G, Voorhees P, Lim M, Dispenzieri A, et al. International evidence-based consensus diagnostic and treatment guidelines for unicentric Castleman disease. *Blood Adv*. (2020) 4:6039–50. doi: 10.1182/bloodadvances.2020003334

8. Radfar MH, Pakmanesh H, Torbati P. Castleman disease presenting as renal hilar mass. *J Endourol Case Rep*. (2015) 1:54–5. doi: 10.1089/cren.2015.0015

9. Nolan RL, Banerjee A, Idikio H. Castleman's disease with vascular encasement and renal sinus involvement. *Urol Radiol*. (1988) 10:173–5. doi: 10.1007/BF02926563

10. Nagahama K, Higashi K, Sanada S, Nezumi M, Itou H. Multicentric Castleman's disease found by a renal sinus lesion: a case report. *Hinyokika Kiyo*. (2000) 46:95–9. http://hdl.handle.net/2433/114220. PMID: 10769797

11. Nishie A, Yoshimitsu K, Irie H, Aibe H, Tajima T, Shinozaki K, et al. Radiologic features of Castleman's disease occupying the renal sinus. *Am J Roentgenol*. (2003) 181:1037–40. doi: 10.2214/ajr.181.4.1811037

12. Park JB, Hwang JH, Kim H, Choe HS, Kim YK, Kim HB, et al. Castleman disease presenting with jaundice: a case with the multicentric hyaline vascular variant. *Korean J Intern Med*. (2007) 22:113–7. doi: 10.3904/kjim.2007.22.2.113

13. Kim TU, Kim S, Lee JW, Lee NK, Jeon UB, Ha HG, et al. Plasma cell type of Castleman's disease involving renal parenchyma and sinus with cardiac tamponade: case report and literature review. *Korean J Radiol*. (2012) 13:658–63. doi: 10.3348/kjr.2012.13.5.658

14. Jang SM, Han H, Jang KS, Jun YJ, Lee TY, Paik SS. Castleman's disease of the renal sinus presenting as a urothelial malignancy: a brief case report. *Korean J Pathol*. (2012) 46:503–6. doi: 10.4132/KoreanJPathol.2012.46.5.503

15. Guo X-W, Jia X-D, Shen S-S, Ji H, Chen Y-M, Du Q, et al. Radiologic features of Castleman's disease involving the renal sinus: a case report and review of the literature. *World J Clin Cases*. (2019) 7:1001–5. doi: 10.12998/wjcc.v7.i8.1001

16. Li Y, Zhao H, Su B, Yang C, Li S, Fu W. Primary hyaline vascular Castleman disease of the kidney: case report and literature review. *Diagn Pathol*. (2019) 14:94. doi: 10.1186/s13000-019-0870-9

frontiers | Frontiers in Oncology

TYPE Case Report
PUBLISHED 08 September 2022
DOI 10.3389/fonc.2022.933579



OPEN ACCESS

EDITED BY
Rocco Cappellesso,
University Hospital of Padua, Italy

REVIEWED BY
Antonella Brunello,
Veneto Institute of Oncology (IRCCS), Italy
Pawel Schubert,
Stellenbosch University, South Africa

*CORRESPONDENCE
Haifeng Wei
weihfspine@163.com
Shaohui He
heshaohui1025@163.com
Jianru Xiao
jianruxiao83@smmu.edu.cn

†These authors have contributed equally to this work

SPECIALTY SECTION
This article was submitted to Surgical Oncology, a section of the journal Frontiers in Oncology

RECEIVED 01 May 2022
ACCEPTED 15 August 2022
PUBLISHED 08 September 2022

CITATION
Ye C, Wei W, Tang X, Li F, Xin B, Chen Q, Wei H, He S and Xiao J (2022) Sacral Ewing sarcoma with rib, lung, and multifocal skull metastases: A rare case report and review of treatments.
*Front. Oncol.* 12:933579.
doi: 10.3389/fonc.2022.933579



# Sacral Ewing sarcoma with rib, lung, and multifocal skull metastases: A rare case report and review of treatments

Chen Ye[1,2†], Wei Wei[1,2†], Xuebin Tang[3†], Feng Li[4†], Baoquan Xin[1,2], Qianqian Chen[1], Haifeng Wei[1,2,5*], Shaohui He[2,5*] and Jianru Xiao[1,2,5*]

[1]School of Health Science and Technology, University of Shanghai for Science and Technology, Shanghai, China, [2]Spinal Tumor Center, Department of Orthopaedic Oncology, Changzheng Hospital, Second Military Medical University, Shanghai, China, [3]Department of Orthopaedics, The Second Affiliated Hospital of Xuzhou Medical University, Xuzhou, China, [4]Department of Orthopaedics, the 943rd Hospital of Joint Logistics Support Force of People's Liberation Army, Wuwei, China, [5]Department of Orthopaedics, No.905 Hospital of People's Liberation Army Navy, Second Military Medical University, Shanghai, China

Ewing sarcoma (ES) rarely derives from the sacrum or mobile spine. The discovery of primary ES with multimetastatic involvements is exceedingly less frequent in clinical practice. A 23-year-old man with initial primary sacral ES developed metastases of rib, lung, and multifocal skull after receiving surgical intervention and series of adjuvant therapies. We provide this very rare case consisting of its clinical features, imaging findings, treatments, and outcomes. Therapeutic modalities of ES are also reviewed in previous published articles. The prognosis of metastatic ES remains dismal; effective therapeutic modalities for ES require multidisciplinary collaboration, with more high-quality clinical trials to promote the optimal protocols.

KEYWORDS

**ewing sarcoma, multifocal metastases, multidisciplinary treatments, decision optimization, *en bloc* resection**

## Introduction

Ewing sarcoma (ES) is a rare sarcoma with high aggressiveness and peak occurrence during 10–20 years old (1–3). ES generally originates from the diaphysis and metaphysis of long bones, pelvis, and ribs (4, 5) and relatively uncommonly in the spinal column (6), with fairly sparse cases of contemporary distal metastatic lesion involving the lung and skull. The common sites of metastasis are the lung and bone (7). Currently, the definitions of classic ES and peripheral primitive neuroectodermal tumors are overlapping (8) and uniformly classified as ES (9), having a similar histological

appearance of uniform small round tumor cells and chromosome analysis of the most common t (10, 11)(q24; q12) translocation with functional fusion of the Ewing sarcoma breakpoint region 1 (*EWSR1*) gene and friend of leukemia virus integration site 1 gene (*FLI1*) (10, 12). ES in the sacrum and spine has worse prognosis than that in other sites (13). To the best of our knowledge, few studies reported the case of skull metastasis with or without systematic metastases (14–16). However, only one case originally arising from the sacrum was reported to develop lung and skull metastasis (17). Optimal favorable therapeutic protocols have not been established yet on such malignancy. Thus, we provide this very rare case including its clinical features, imaging findings, treatments, and outcomes. Therapeutic modalities of ES are also reviewed in previous published articles.

## Case presentation

A 23-year-old man developed initial back pain and progressively worsened in the following 6 months. It started to radiate to the hip with additional plantar numbness for 2 weeks; he came to the local hospital for medication and suggested to our department without regular treatments. However, he complained that his sleeping quality was extremely poor due to the night-increasing back pain, with weight loss of approximately 5 kg in the last half year. Physical examinations showed claudication, tenderness of the spinous process and perispinous process at L5–S1 level, paresthesia of the left lower extremity, abnormal Achilles tendon reflex, and positive Lasègue sign of the left lower limb. Magnetic resonance imaging (MRI) revealed a space-occupying lesion with abnormal signal of the sacrum at the S1 level (Figure 1). Routine blood tests revealed leukocytes as high as 17.5 * $10^9$/L (normal range 4–10 * $10^9$/L), with neutrophil–granulocyte ratio of 75.8%.

Full evaluation and written informed consent informing about the operation, as well as risks, were obtained after conducting necessary preoperative examinations. Intraoperative biopsy aiming at rapid diagnosis suggested the typical oncologic histology of uniform small round cells, so we removed the whole mass *via* an *en bloc* method, then bilateral vertebral pedicles at L4–L5 level and posterior superior iliac spine were used to accomplish spinal reconstruction. Emphasis was put on exposing the tumor margin to ensure a radical surgical procedure with a negative tumor margin. Oxaliplatin was used intraoperatively (50 ml:500 ml normal saline) for local chemotherapy on the basis of unbroken dura. The whole procedure lasted 3.5 h, with blood loss of about 1,200 ml. The postoperative physical examinations showed certain improvements of the motor and sensory functions 10 days after surgery. Subsequently, the hematoxylin–eosin (HE) and immunohistochemical staining indicated small round tumor cells with *CD99*(+), and histopathology confirmed the diagnosis of ES with molecular translocation t (10, 11)(q24;q12) with *EWSR1-FLI1* gene being identified. Postoperatively, he was transferred to the Tumor Hospital of Jiangxi Province, where he underwent two courses of external beam radiotherapy (EBRT) and four cycles of systemic chemotherapy. He received EBRT at a total dosage of 60 Gy with daily doses of 600 cGy (10 fractions in a month) and 30 Gy with daily doses of 200 cGy (15 times in a month). The chemotherapeutic protocol was cyclophosphamide, dactinomycin, vincristine, and doxorubicin (CAVD), and the blood test showed the quantity of leukocytes ranging from 2.32 to 2.55 * $10^9$/L. Good local control, satisfactory spinal reconstruction in the sacrum, and general condition of the lung without detecting metastasis were gained through physical and radiological examinations at 1, 6, and 12 months after surgery, respectively.

However, the patient had been experiencing increasing headache 13 months after sacral ES excision. Although X-ray and computed tomography (CT) images did not indicate any change of the operative region (Figure 2), the thoracic CT and MRI of the brain demonstrated metastatic lesions of the rib, left lung lobe, scalp, skull, and meninges (Figures 3, 4). Hence, besides changes in the chemotherapeutic program [vincristine, actinomycin D, and cyclophosphamide (VAC)] for six cycles, 20 Gy of whole-lung irradiation (WLI) was administered to him over 28 days in two fractions. His general condition and quality of daily life were temporarily stable without any sign of progressions at the final follow-up of 17 months. The timeline is shown in Figure 5.

## Discussion

### Epidemiology and clinical features

ES is the second most common primary malignancy of bone and soft tissue in adolescents and young adults after osteosarcoma, with an annual incidence of 1–3 persons per million and the highest morbidity during 10–20 years old (3, 18, 19). The incidence of ES among people of African and Asian ancestry is exceedingly rare (20). Both bone and soft tissue can be the primary lesions of ES with a relative incidence ratio of 7:3–17:3, and adults are prone to have extraosseous ES than children (21, 22). ES of the bone occurs mostly in the lower extremities and pelvis (1, 10), while the involvement of the spinal column only accounts for 3%–10% of all ESs (6, 22).

The common clinical features include local symptoms of mass formation, induration, pain, pathological fracture (11), and systemic characteristics of fever, anemia, fatigue, etc. (23). The typical radiographic finding is persistent osteolytic lesion with onion skin-like multilayered periosteal reaction and large soft tissue mass (24). The diagnostic histological appearance of ES is consistently small round and undifferentiated tumor cells with little cytoplasm (11) and frequent expressions of *CD99* (surface

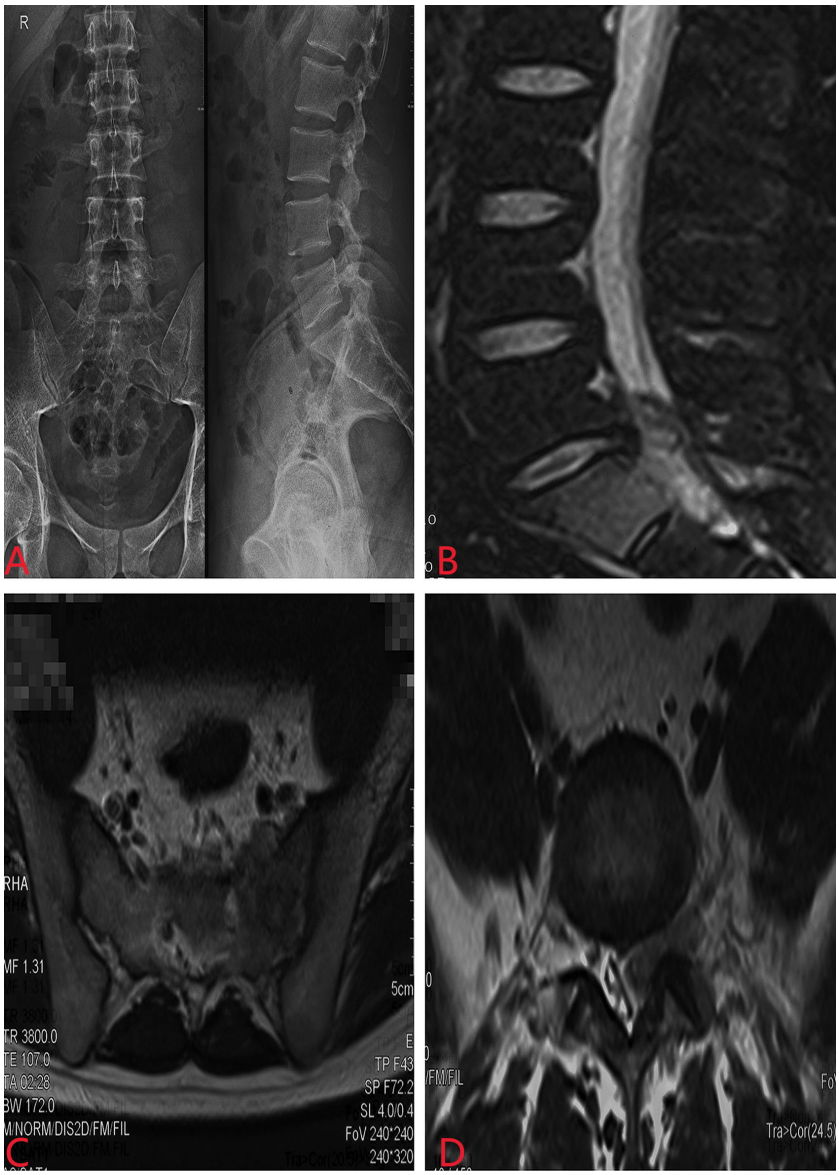


FIGURE 1
Preoperative X-ray and MRI revealed a space-occupying lesion with abnormal signal of the sacrum at the S1 level. **(A)** X-ray of the lumbosacral spine; **(B)** sagittal MRI; **(C)** coronal MRI; **(D)** lateral MRI.

antigen *MIC2*) (25). Moreover, common translocation of the *EWSR1* gene from chromosome 22 to chromosome 11 is detected in 85% of cases (2, 26), producing the fusion protein product of *EWS-FLI1* (12).

The spinal column as the primary site of ES is rare; data derived from the Japanese Orthopaedic Association indicated that 23 of 326 ESs (7%) between 2006 and 2011 arose from the spine (11). In another study, Choi et al. (27) reported 13 patients who were diagnosed as having ES family tumors (ESFTs) in the spinal region that accounted for 14.3% of 91 cases during the period of July 1988 and July 2012. Another large-sample study demonstrated that 125 of 1,277 cases (9.8%) originated from the vertebral column (6); meanwhile, the sacrum as the primary lesion was detected in 67 cases (5.2%).

The distal metastatic rate can be 20%–30% of all cases, while most of the metastases are to the lung and/or bone (7, 28). Cranial with contemporary pulmonary metastasis from a primary lesion of the sacrum is extremely rare. To our knowledge, only one case originating from the sacrum had ever been reported to develop multiple frontal lobes as well as

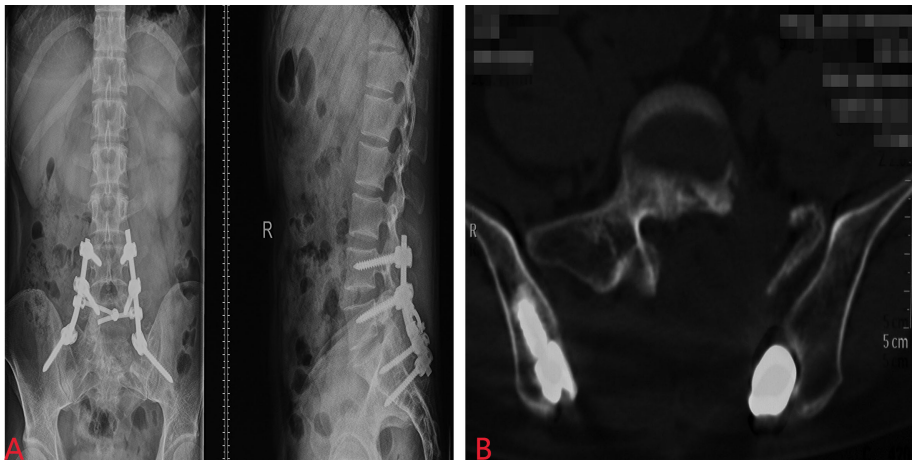


FIGURE 2
Postoperative X-ray **(A)** and CT **(B)** images did not indicate any change of the operative region.

lung metastasis (17). Turgut et al. (29) reported a 22-year-old male patient with initial primary ES from the sacroiliac joint developing brain metastasis of the temporal lobe and parietal after 24-month treatments. As was reviewed, it was estimated that bone and soft tissue sarcomas accounted for only 0.8% of all cancers presenting with brain metastasis (30). Another study demonstrated that brain metastasis from ES merely made up <1.8% of all cases, with direct extension to adjacent central neural system rates up to 32%–56% (31). Notably, *via* reverse transcriptase polymerase chain reaction (RT-PCR), 20% of patients with a diagnosis of localized ES were detected to have widespread malignant tumor cells in the bone marrow and blood (32), of whom could be presumed to have subclinical metastatic disease.

## Multidisciplinary treatments and prognosis

Currently, the overall survival rate of patients with localized disease had been improved due to the evolutionary multidisciplinary management that includes local treatments and systematic treatments, with 5-year survival rates up to around 70% (10, 33). Initially, chemotherapy is effective

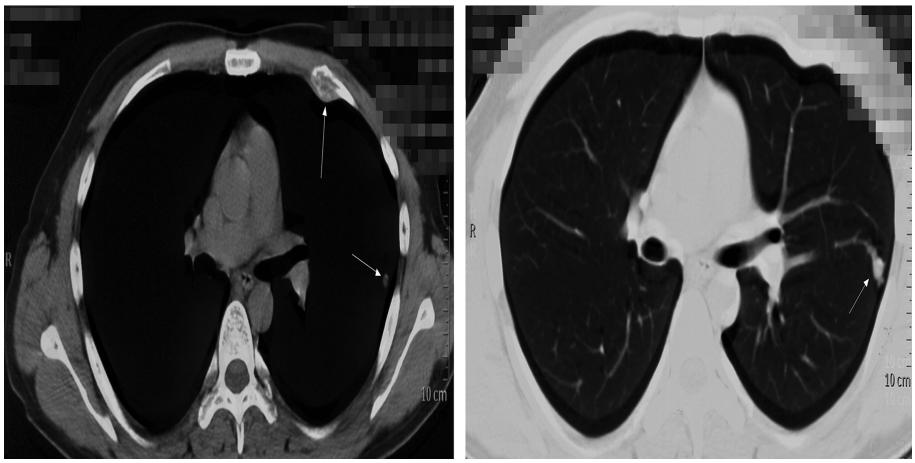


FIGURE 3
Thoracic CT demonstrated the metastatic lesions of the rib, left lung lobe. White arrows indicate the lesions.

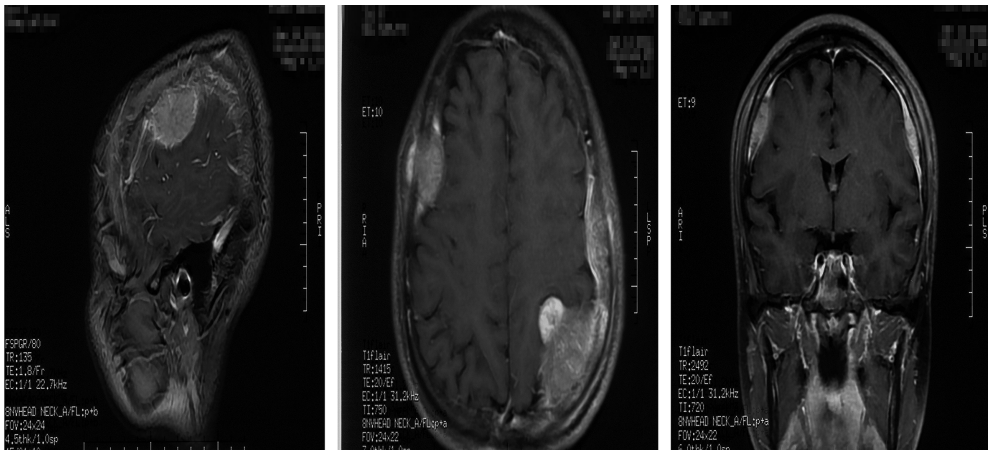

FIGURE 4
MRI of the brain showed the metastases of the scalp, skull, and meninges.

against tumors, but relapses are common both locally and distantly (1). Moreover, patients with ESFTs deriving from the mobile spine and sacrum had an inferior 5-year survival rate of 42% (13). Metastatic status was found the strongest predictor of prognosis, with a 5-year survival rate of 20%–30% reported in previous articles (34, 35). What was worse was that patients with multifocal lesions tended to have a lower survival rate of <20% (36, 37). Disseminated primary disease and relapse accompanied by extremely poor outcomes urgently demand novel multidisciplinary treatments.

## Radiotherapy

For localized ES, surgical intervention and/or radiotherapy was recommended as an optimal modality for local control. Irradiation had been the first-line therapeutic modality since ESs are sensitive to radiotherapy (38, 39). With doses ranging from 36 to 60 Gy (40, 41), radiotherapy was adopted more frequently on cases concerning spinal column involvements, considering the difficulties of surgical resection and reconstruction of central locations (42, 43). However, definitive radiotherapy resulted in unfavorable prognosis with local recurrence rates of 33%–35%, but no significant difference seen in disease-free survival and overall survival, compared to surgeries (44, 45). In contrast, opposite results were observed on another retrospective study (46).

Moreover, radiation-induced second malignancy and adverse effects on growth especially for adolescents could be overlooked (47, 48). Indeed, radiotherapy is recommended as the first consideration only for inoperable lesions, with dosage ranging from 54 to 55 Gy (49). Additionally, it is recommended as an alternative option for intralesional or questionable surgical margins (34, 50).

## Surgical intervention

Surgical interventions on localized ES played a significant role in diagnosis, local control, and reconstruction of motor function (24). Current studies demonstrated that surgical modality might present more benefits than definitive radiotherapy, especially

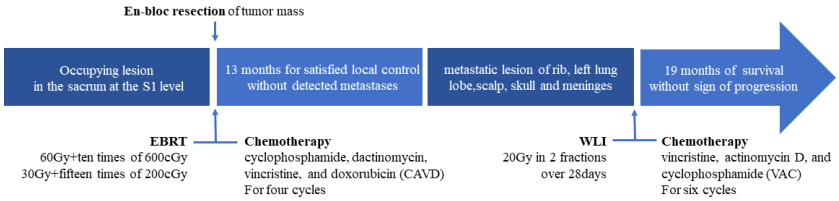


FIGURE 5
Timeline of patients undergoing multidisciplinary management.

with wide or radical margins (27, 44, 51). From our perspectives, surgical interventions were capable of directly relieving tumor-related pain for primary spinal lesions and were able to immediately release the possible existing spinal cord compression to regain ambulatory status to obtain higher local control rates and enhance the quality of life. The specific surgical modality was associated with the patient's general condition, the tumor location, the possibility for entire excision, and the patient's willingness (52). As was acknowledged, the initial tumor volume was found robustly correlated with prognosis; a maximal diameter >8 cm (53) or a volume >200 ml (54) was regarded with poor survival. In addition, for resected ES, histological response was revealed as the strongest prognostic predictor rather than the tumor volume (54). However, direct comparison and further randomized trials between surgical interventions and radiotherapy were actually infeasible because of the patient selection bias. What could be recommended was that the combination of surgery and irradiation was definitely superior to definitive radiotherapy (27), with a 5-year survival rate of 72% compared to 27% in the previous study (55). Notably, preoperative and postoperative radiotherapy should be performed in cases of inadequate surgical margin (11).

## Systemic chemotherapy

For metastatic and localized ES, systemic chemotherapy remains a significant treatment modality. The relevant therapeutic drugs included vincristine (V), ifosfamide (I), dactinomycin (A), etoposide (E), cyclophosphamide (C), and doxorubicin (D), with the recommended combination of VIDE/VAI in Europe and VDC/IE in the United States (34, 36, 56). A randomized comparison between VAI and VAC elaborated that cyclophosphamide may be able to replace ifosfamide in the treatment of standard-risk ESs, which were defined as localized ESs with either a good histological response to chemotherapy (<10% viable cells) or small tumors (<200 ml) resected at diagnosis or receiving radiotherapy alone as local treatment (56). In addition, Womer et al. (57) demonstrated that the 5-year event-free survival (EFS) rate of patients with localized ES who were assigned to 2-week interval of receiving VDC-IE chemotherapy was higher than that of those assigned to 3-week treatment interval (73% vs. 65%, $p = 0.048$). Additionally, phased results of the Euro-Ewing 2012 trial show improved overall survival without an increase in toxicity for the VDC-IC group (58).

However, outcomes of systemic chemotherapy toward metastatic ES and recurrent and primary refractory Ewing sarcoma (rEECur) remained extremely poor, where 5-year OS rates are less than 30% (7) and 15% (59). Previous study revealed that the combination of IE and VACD did not improve outcomes with an 8-year EFS and OS of 20% and 32%, respectively. In addition, no significance was found between high-dose chemotherapy plus stem cell transplantation and conventional chemotharpy (60, 61). Notably, better prognosis was confirmed in patients with isolated pulmonary metastasis than those with bone/bone marrow and multisite metastases (7, 62). In the first randomized trial of rEECur, topotecan/cyclophosphamide (TC) or high-dose ifosfamide (IFOS) was demonstrated to be promising and the trial continues to recruit participants (59). Optimal therapeutic protocols on bone/bone marrow or multimetastatic patients remained a challenge for clinicians. The management of patients with metastases, recurrences, and weak responses requires robust evidence from multicenter trials conducted internationally.

Currently, chemotherapy was administered not only for metastatic control or prevention but also for local control as a neoadjuvant and/or postoperative modality (34). The current treatment algorithm includes neoadjuvant multiagent chemotherapy followed by local treatment, which can be either surgery or radiotherapy or a combination of both. We believed that preoperative chemotherapy should be applied in order to eliminate the potential micrometastasis and create opportunities for subsequent tumor resection *via* shrinking the tumor volume.

## Targeted therapy

Since the prognosis of patients with metastatic EFSTs remains dismal, molecular targets have been applied in the preclinical and clinical treatment protocols. Because of the difficulty of targeting fusion oncoproteins mediated by chimeric transcription factors, attention was shifted to alternative mechanisms regulated by oncogenic fusion transcription factors.

TK216 was designed to bind specifically to oncoproteins in the family of ETS transcription factors. In a phase I/II study, an overall clinical benefit rate of 64% (7/11) was observed after receiving TK216 alone or with vincristine (63). Insulin-like growth factor 1 receptor (*IGF-1R*) is one of the most important targets because tumor growth, metastasis, and angiogenesis are achieved through the activated *IGF-1R* pathway (26, 64). However, the application of *IGF-1R*-directed antibodies or small-molecule inhibitors was only able to provide a transient response in a low proportion of patients in several phase I/II clinical trials (65–67). *EWS-FLT1*, expressed in most ES cells, contains a DNA-binding domain at the C-terminus and could be an optimal target for new drugs at different expression levels (10). YK-4-279, known as a typical small-molecule inhibitor of RNA helicase A (*RHA*), has the capacity to interfere with the binding between *EWS-FLT1* and *RHA* to induce apoptosis in *in vitro* and *in vivo* experiments (68–70). Poly (adenosine diphosphate–ribose) polymerase (*PARP*) inhibitors are capable of interfering with the DNA repair process of ES in preclinical models, but they do not yield any positive results in clinical trials (71, 72). In addition, combination between targeted therapy and other therapeutic

modalities may be more effective than using either alone (73). Nonetheless, although large quantities of targeted drugs had been invented and tested with definitive favorable results, more rigorous multicenter and large-scale clinical trials are required to detect the long-term effects and biological safety of molecular targeted drugs.

## Conclusions

In conclusion, effective treatment modalities for localized and metastatic ES require multidisciplinary collaboration, with more high-quality clinical trials to promote optimal therapeutic protocols.

## Data availability statement

The original contributions presented in the study are included in the article/supplementary material. Further inquiries can be directed to the corresponding authors.

## Ethics statement

Written informed consent was obtained from the individual (s) for the publication of any potentially identifiable images or data included in this article.

## Author contributions

SH and BX contributed to the implement of the treatment. WW, FL, and QC contributed to the collection and preparation of clinical data and graphic presentation, CY drafted the manuscript. JX and SH supervised and reviewed the writing. All authors approved the submitted version.

## Funding

This work was supported by a grant form the National Natural Science Foundation of China (82072971, Haifeng Wei). The funding source had no role in the study design, data gathering analysis, and interpretation, writing of the report, or the decision to submit the report for publication.

## Acknowledgments

The authors thank all the colleagues for great supports to this study and conscientious guidance.

## Conflict of interest

The authors declare that the research was conducted in the absence of any commercial or financial relationships that could be construed as a potential conflict of interest.

## Publisher's note



## References

1. Grünewald TGP, Cidre-Aranaz F, Surdez D, Tomazou EM, de Álava E, Kovar H, et al. Ewing Sarcoma. *Nat Rev Dis Primers* (2018) 4(1):5. doi: 10.1038/s41572-018-0003-x

2. Jiang Y, Ludwig J, Janku F. Targeted therapies for advanced Ewing sarcoma family of tumors. *Cancer Treat Rev* (2015) 41(5):391–400. doi: 10.1016/j.ctrv.2015.03.008

3. Burchill SA. Molecular abnormalities in ewing's sarcoma. *Expert Rev Anticancer Ther* (2008) 8(10):1675–87. doi: 10.1586/14737140.8.10.1675

4. Amaral AT, Ordonez JL, Otero-Motta AP, Garcia-Dominguez DJ, Sevillano MV, de Alava E. Innovative therapies in Ewing sarcoma. *Adv Anat Pathol* (2014) 21 (1):44–62. doi: 10.1097/pap.0000000000000003

5. Yip CM, Hsu SS, Chang NJ, Wang JS, Liao WC, Chen JY, et al. Primary vaginal extraosseous Ewing sarcoma/primitive neuroectodermal tumor with cranial metastasis. *J Chin Med Assoc* (2009) 72(6):332–5. doi: 10.1016/s1726-4901(09)70381-8

6. Ilaslan H, Sundaram M, Unni KK, Dekutoski MB. Primary ewing's sarcoma of the vertebral column. *Skeletal Radiol* (2004) 33(9):506–13. doi: 10.1007/s00256-004-0810-x

7. Grier HE, Krailo MD, Tarbell NJ, Link MP, Fryer CJ, Pritchard DJ, et al. Addition of ifosfamide and etoposide to standard chemotherapy for ewing's sarcoma and primitive neuroectodermal tumor of bone. *N Engl J Med* (2003) 348(8):694–701. doi: 10.1056/NEJMoa020890

8. Yan Y, Xu T, Chen J, Hu G, Lu Y. Intraspinal ewing's sarcoma/primitive neuroectodermal tumors. *J Clin Neurosci* (2011) 18(5):601–6. doi: 10.1016/j.jocn.2010.09.012

9. WHO Classification of Tumours Editorial Board. In: *Soft tissue and bone tumors*. Lyon (Franee): International Agency for Research on Cancer (2020) WHO classification of tumours series *5th edition* vol. 3. Available at: https://publications.iarc.fr/588

10. Riggi N, Suvà ML, Stamenkovic I. Ewing's sarcoma. *New Engl J Med* (2021) 384(2):154–64. doi: 10.1056/NEJMra2028910

11. Ozaki T. Diagnosis and treatment of Ewing sarcoma of the bone: a review article. *J Orthop Sci* (2015) 20(2):250–63. doi: 10.1007/s00776-014-0687-z

12. de Alava E, Gerald WL. Molecular biology of the ewing's sarcoma/primitive neuroectodermal tumor family. *J Clin Oncol* (2000) 18(1):204–13. doi: 10.1200/JCO.2000.18.1.204.

13. Bacci G, Boriani S, Balladelli A, Barbieri E, Longhi A, Alberghini M, et al. Treatment of nonmetastatic ewing's sarcoma family tumors of the spine and sacrum: the experience from a single institution. *Eur Spine J* (2009) 18(8):1091–5. doi: 10.1007/s00586-009-0921-0

14. Hattori T, Yamakawa H, Nakayama N, Kuroda T, Andoh T, Sakai N, et al. Skull metastasis of ewing's sarcoma–three case reports. *Neurol medico-chirurgica* (1999) 39(13):946–9. doi: 10.2176/nmc.39.946

15. Puerta P, Guillén A, Mora J, Suñol M, Ferrer E. Isolated skull metastasis of ewing's sarcoma in a child. *Austin J Cancer Clin Res* (2015) 2(5):3.

16. Rana K, Wadhwa V, Bhargava E, Batra V, Mandal S. Ewing's sarcoma multifocal metastases to temporal and occipital bone: A rare presentation. *J Clin Diagn Res* (2015) 9(6):MD04–5. doi: 10.7860/jcdr/2015/13254.6071

17. Salvati M, D'Elia A, Frati A, Santoro A. Sarcoma metastatic to the brain: a series of 35 cases and considerations from 27 years of experience. *J Neurooncol* (2010) 98(3):373–7. doi: 10.1007/s11060-009-0085-0

18. Choi EY, Gardner JM, Lucas DR, McHugh JB, Patel RM. Ewing Sarcoma. *Semin Diagn Pathol* (2014) 31(1):39–47. doi: 10.1053/j.semdp.2014.01.002

19. Esiashvili N, Goodman M, Marcus RBJr. Changes in incidence and survival of Ewing sarcoma patients over the past 3 decades: Surveillance epidemiology and end results data. *J Pediatr Hematol Oncol* (2008) 30(6):425–30. doi: 10.1097/MPH.0b013e31816e22f3

20. Worch J, Cyrus J, Goldsby R, Matthay K, Neuhaus J, DuBois S. Racial differences in the incidence of mesenchymal tumors associated with EWSR1 translocation. *Cancer epidemiol Biomarkers Prev* (2011) 20(3):449–53. doi: 10.1158/1055-9965.Epi-10-1170

21. Jawad MU, Cheung MC, Min ES, Schneiderbauer MM, Koniaris LG, Scully SP. Ewing Sarcoma demonstrates racial disparities in incidence-related and sex-related differences in outcome: an analysis of 1631 cases from the SEER database, 1973-2005. *Cancer* (2009) 115(15):3526–36. doi: 10.1002/cncr.24388

22. Hesla AC, Discacciati A, Tsagkozis P, Smedby KE. Subsequent primary neoplasms among bone sarcoma survivors; increased risks remain after 30 years of follow-up and in the latest treatment era, a nationwide population-based study. *Br J Cancer* (2020) 122(8):1242–9. doi: 10.1038/s41416-020-0748-3

23. Widhe B, Widhe T. Initial symptoms and clinical features in osteosarcoma and Ewing sarcoma. *J Bone Joint Surg Am* (2000) 82(5):667–74. doi: 10.2106/00004623-200005000-00007

24. Mar WA, Taljanovic MS, Bagatell R, Graham AR, Speer DP, Hunter TB, et al. Update on imaging and treatment of Ewing sarcoma family tumors: what the radiologist needs to know. *J Comput Assist Tomogr* (2008) 32(1):108–18. doi: 10.1097/RCT.0b013e31805c030f

25. Potratz J, Dirksen U, Jürgens H, Craft A. Ewing Sarcoma: clinical state-of-the-art. *Pediatr Hematol Oncol* (2012) 29(1):1–11. doi: 10.3109/08880018.2011.622034

26. Sand LG, Szuhai K, Hogendoorn PC. Sequencing overview of Ewing sarcoma: A journey across genomic, epigenomic and transcriptomic landscapes. *Int J Mol Sci* (2015) 16(7):16176–215. doi: 10.3390/ijms160716176

27. Choi Y, Lim do H, Lee SH, Lyu CJ, Im JH, Lee YH, et al. Role of radiotherapy in the multimodal treatment of Ewing sarcoma family tumors. *Cancer Res Treat* (2015) 47(4):904–12. doi: 10.4143/crt.2014.158

28. Paulussen M, Ahrens S, Dunst J, Winkelmann W, Exner GU, Kotz R, et al. Localized Ewing tumor of bone: final results of the cooperative ewing's sarcoma study CESS 86. *J Clin Oncol* (2001) 19(6):1818–29. doi: 10.1200/jco.2001.19.6.1818

29. Turgut M, Colak A, Gurcay O. Multiple intracranial metastases with skull and scalp involvement in ewing's sarcoma. *Cent Afr J Med* (1994) 40(4):104–6.

30. Chou YS, Liu CY, Chen WM, Chen TH, Chen PC, Wu HT, et al. Brain, the last fortress of sarcoma: similar dismal outcome but discrepancy of timing of brain metastasis in bone and soft tissue sarcoma. *J Surg Oncol* (2011) 104(7):765–70. doi: 10.1002/jso.22011

31. Shweikeh F, Bukavina L, Saeed K, Sarkis R, Suneja A, Sweiss F, et al. Brain metastasis in bone and soft tissue cancers: a review of incidence, interventions, and outcomes. *Sarcoma* (2014) 2014:475175. doi: 10.1155/2014/475175

32. Schleiermacher G, Peter M, Oberlin O, Philip T, Rubie H, Mechinaud F, et al. Increased risk of systemic relapses associated with bone marrow micrometastasis and circulating tumor cells in localized ewing tumor. *J Clin Oncol* (2003) 21(1):85–91. doi: 10.1200/JCO.2003.03.006

33. Casali P, Bielack S, Abecassis N, Aro H, Bauer S, Biagini R, et al. Bone sarcomas: ESMO-PaedCan-EURACAN clinical practice guidelines for diagnosis, treatment and follow-up. *Ann Oncol* (2018) 29:iv79–95. doi: 10.1093/annonc/mdy310

34. Gaspar N, Hawkins DS, Dirksen U, Lewis IJ, Ferrari S, Le Deley MC, et al. Ewing Sarcoma: Current management and future approaches through collaboration. *J Clin Oncol* (2015) 33(27):3036–46. doi: 10.1200/jco.2014.59.5256

35. Cotterill SJ, Ahrens S, Paulussen M, Jurgens HF, Voute PA, Gadner H, et al. Prognostic factors in ewing's tumor of bone: analysis of 975 patients from the European intergroup cooperative ewing's sarcoma study group. *J Clin Oncol* (2000) 18(17):3108–14. doi: 10.1200/JCO.2000.18.17.3108

36. Hogendoorn PC, Athanasou N, Bielack S, De Alava E, Dei Tos AP, Ferrari S, et al. Bone sarcomas: ESMO clinical practice guidelines for diagnosis, treatment and follow-up. *Ann Oncol* (2010) 21 Suppl 5:v204–13. doi: 10.1093/annonc/mdq223

37. Haeusler J, Ranft A, Boelling T, Gosheger G, Braun-Munzinger G, Vieth V, et al. The value of local treatment in patients with primary, disseminated, multifocal Ewing sarcoma (PDMES). *Cancer* (2010) 116(2):443–50. doi: 10.1002/cncr.24740

38. Cripe TP. Ewing Sarcoma: an eponym window to history. *Sarcoma* (2011) 2011:457532. doi: 10.1155/2011/457532

39. Hesla AC, Papakonstantinou A, Tsagkozis P. Current status of management and outcome for patients with Ewing sarcoma. *Cancers* (2021) 13(6):1202. doi: 10.3390/cancers13061202

40. Paulussen M, Craft AW, Lewis I, Hackshaw A, Douglas C, Dunst J, et al. Results of the EICESS-92 study: two randomized trials of ewing's sarcoma treatment–cyclophosphamide compared with ifosfamide in standard-risk patients and assessment of benefit of etoposide added to standard treatment in high-risk patients. *J Clin Oncol* (2008) 26(27):4385–93. doi: 10.1200/jco.2008.16.5720

41. Dunst J, Sauer R, Burgers JM, Hawliczek R, Kurten R, Winkelmann W, et al. Radiation therapy as local treatment in ewing's sarcoma. results of the cooperative ewing's sarcoma studies CESS 81 and CESS 86. *Cancer* (1991) 67(11):2818–25. doi: 10.1002/1097-0142(19910601)67:11<2818::aid-cncr2820671118>3.0.co;2-y

42. Schuck A, Ahrens S, von Schorlemer I, Kuhlen M, Paulussen M, Hunold A, et al. Radiotherapy in Ewing tumors of the vertebrae: treatment results and local relapse analysis of the CESS 81/86 and EICESS 92 trials. *Int J Radiat Oncol Biol Phys* (2005) 63(5):1562–7. doi: 10.1016/j.ijrobp.2005.05.036

43. Cotterill SJ, Ahrens S, Paulussen M, Jürgens HF, Voûte PA, Gadner H, et al. Prognostic factors in ewing's tumor of bone: Analysis of 975 patients from the European intergroup cooperative ewing's sarcoma study group. *J Clin Oncol* (2000) 18(17):3108–14. doi: 10.1200/jco.2000.18.17.3108

44. DuBois SG, Krailo MD, Gebhardt MC, Donaldson SS, Marcus KJ, Dormans J, et al. Comparative evaluation of local control strategies in localized Ewing sarcoma of bone: a report from the children's oncology group. *Cancer* (2015) 121(3):467–75. doi: 10.1002/cncr.29065

45. Bacci G, Longhi A, Briccoli A, Bertoni F, Versari M, Picci P. The role of surgical margins in treatment of ewing's sarcoma family tumors: experience of a single institution with 512 patients treated with adjuvant and neoadjuvant chemotherapy. *Int J Radiat oncol biol Phys* (2006) 65(3):766–72. doi: 10.1016/j.ijrobp.2006.01.019

46. Schuck A, Ahrens S, Paulussen M, Kuhlen M, Könemann S, Rübe C, et al. Local therapy in localized Ewing tumors: results of 1058 patients treated in the CESS 81, CESS 86, and EICESS 92 trials. *Int J Radiat oncol biol Phys* (2003) 55(1):168–77. doi: 10.1016/s0360-3016(02)03797-5

47. Zahlten-Hinguranage A, Bernd L, Ewerbeck V, Sabo D. Equal quality of life after limb-sparing or ablative surgery for lower extremity sarcomas. *Br J Cancer* (2004) 91(6):1012–4. doi: 10.1038/sj.bjc.6602104

48. Hardes J, von Eiff C, Streitbuerger A, Balke M, Budny T, Henrichs MP, et al. Reduction of periprosthetic infection with silver-coated megaprostheses in patients with bone sarcoma. *J Surg Oncol* (2010) 101(5):389–95. doi: 10.1002/jso.21498

49. Donaldson SS, Torrey M, Link MP, Glicksman A, Gilula L, Laurie F, et al. A multidisciplinary study investigating radiotherapy in ewing's sarcoma: end results of POG 8346. pediatric oncology group. *Int J Radiat Oncol Biol Phys* (1998) 42(1):125–35. doi: 10.1016/s0360-3016(98)00191-6

50. Granowetter L, Womer R, Devidas M, Krailo M, Wang C, Bernstein M, et al. Dose-intensified compared with standard chemotherapy for nonmetastatic Ewing sarcoma family of tumors: A children's oncology group study. *J Clin Oncol* (2009) 27(15):2536–41. doi: 10.1200/jco.2008.19.1478

51. Schuck A, Ahrens S, Paulussen M, Kuhlen M, Konemann S, Rube C, et al. Local therapy in localized Ewing tumors: results of 1058 patients treated in the CESS 81, CESS 86, and EICESS 92 trials. *Int J Radiat Oncol Biol Phys* (2003) 55(1):168–77. doi: 10.1016/s0360-3016(02)03797-5

52. Rodríguez-Galindo C, Liu T, Krasin MJ, Wu J, Billups CA, Daw NC, et al. Analysis of prognostic factors in ewing sarcoma family of tumors: review of st. Jude children's research hospital studies. *Cancer* (2007) 110(2):375–84. doi: 10.1002/cncr.22821

53. Krasin MJ, Rodriguez-Galindo C, Davidoff AM, Billups CA, Fuller CE, Neel MD, et al. Efficacy of combined surgery and irradiation for localized ewings sarcoma family of tumors. *Pediatr Blood Cancer* (2004) 43(3):229–36. doi: 10.1002/pbc.20095

54. Oberlin O, Deley MC, Bui BN, Gentet JC, Philip T, Terrier P, et al. Prognostic factors in localized ewing's tumours and peripheral neuroectodermal tumours: the third study of the French society of paediatric oncology (EW88 study). *Br J Cancer* (2001) 85(11):1646–54. doi: 10.1054/bjoc.2001.2150

55. Wilkins RM, Pritchard DJ, Burgert EOJr., Unni KK. Ewing's sarcoma of bone. experience with 140 patients. *Cancer* (1986) 58(11):2551–5. doi: 10.1002/1097-0142(19861201)58:11<2551::aid-cncr2820581132>3.0.co;2-y.

56. Le Deley MC, Paulussen M, Lewis I, Brennan B, Ranft A, Whelan J, et al. Cyclophosphamide compared with ifosfamide in consolidation treatment of standard-risk Ewing sarcoma: results of the randomized noninferiority Euro-EWING99-R1 trial. *J Clin Oncol* (2014) 32(23):2440–8. doi: 10.1200/jco.2013.54.4833

57. Womer RB, West DC, Krailo MD, Dickman PS, Pawel BR, Grier HE, et al. Randomized controlled trial of interval-compressed chemotherapy for the treatment of localized Ewing sarcoma: a report from the children's oncology group. *J Clin Oncol* (2012) 30(33):4148–54. doi: 10.1200/jco.2011.41.5703

58. Brennan B, Kirton L, Marec-Berard P, -Broto JM, Gelderblom H, Gaspar N, et al. Comparison of two chemotherapy regimens in Ewing sarcoma (ES): Overall and subgroup results of the Euro Ewing 2012 randomized trial (EE2012). *J Clin Oncol* (2020) 38(15_suppl):11500–0. doi: 10.1200/JCO.2020.38.15_suppl.11500

59. McCabe MG, Kirton L, Khan M, Fenwick N, Dirksen U, Gaspar N, et al. Results of the second interim assessment of rEECur, an international randomized controlled trial of chemotherapy for the treatment of recurrent and primary refractory Ewing sarcoma (RR-ES). *J Clin Oncol* (2020) 38(15_suppl):11502–2. doi: 10.1200/JCO.2020.38.15_suppl.11502

60. Meyers PA, Krailo MD, Ladanyi M, Chan KW, Sailer SL, Dickman PS, et al. High-dose melphalan, etoposide, total-body irradiation, and autologous stem-cell reconstitution as consolidation therapy for high-risk ewing's sarcoma does not improve prognosis. *J Clin Oncol* (2001) 19(11):2812–20. doi: 10.1200/jco.2001.19.11.2812

61. Ferrari S, Sundby Hall K, Luksch R, Tienghi A, Wiebe T, Fagioli F, et al. Nonmetastatic Ewing family tumors: high-dose chemotherapy with stem cell rescue in poor responder patients. results of the Italian sarcoma Group/Scandinavian sarcoma group III protocol. *Ann Oncol* (2011) 22(5):1221–7. doi: 10.1093/annonc/mdq573

62. Luksch R, Tienghi A, Hall KS, Fagioli F, Picci P, Barbieri E, et al. Primary metastatic ewing's family tumors: results of the Italian sarcoma group and Scandinavian sarcoma group ISG/SSG IV study including myeloablative chemotherapy and total-lung irradiation. *Ann Oncol* (2012) 23(11):2970–6. doi: 10.1093/annonc/mds117

63. Ludwig JA, Federman N, Anderson P, Macy ME, Davis LE, Riedel RF, et al. 1620O phase I study of TK216, a novel anti-ETS agent for Ewing sarcoma. *Ann Oncol* (2020) 31:S972. doi: 10.1016/j.annonc.2020.08.1846

64. Rapraeger AC. Synstatin: a selective inhibitor of the syndecan-1-coupled IGF1R-alphavbeta3 integrin complex in tumorigenesis and angiogenesis. *FEBS J* (2013) 280(10):2207–15. doi: 10.1111/febs.12160

65. Houghton P, Morton C, Gorlick R, Kolb E, Keir S, Reynolds C, et al. Initial testing of a monoclonal antibody (IMC-A12) against IGF-1R by the pediatric preclinical testing program. *Pediatr Blood Cancer* (2010) 54(7):921–6. doi: 10.1002/pbc.22367

66. Pappo A, Patel S, Crowley J, Reinke D, Kuenkele K, Chawla S, et al. R1507, a monoclonal antibody to the insulin-like growth factor 1 receptor, in patients with recurrent or refractory Ewing sarcoma family of tumors: results of a phase II sarcoma alliance for research through collaboration study. *J Clin Oncol* (2011) 29(34):4541–7. doi: 10.1200/jco.2010.34.0000

67. Malempati S, Weigel B, Ingle A, Ahern C, Carroll J, Roberts C, et al. Phase I/II trial and pharmacokinetic study of cixutumumab in pediatric patients with refractory solid tumors and Ewing sarcoma: a report from the children's oncology group. *J Clin Oncol* (2012) 30(3):256–62. doi: 10.1200/jco.2011.37.4355

68. Barber-Rotenberg JS, Selvanathan SP, Kong Y, Erkizan HV, Snyder TM, Hong SP, et al. Single enantiomer of YK-4-279 demonstrates specificity in targeting the oncogene EWS-FLI1. *Oncotarget* (2012) 3(2):172–82. doi: 10.18632/oncotarget.454

69. Erkizan H, Kong Y, Merchant M, Schlottmann S, Barber-Rotenberg J, Yuan L, et al. A small molecule blocking oncogenic protein EWS-FLI1 interaction with RNA helicase a inhibits growth of ewing's sarcoma. *Nat Med* (2009) 15(7):750–6. doi: 10.1038/nm.1983

70. Selvanathan S, Graham G, Erkizan H, Dirksen U, Natarajan T, Dakic A, et al. Oncogenic fusion protein EWS-FLI1 is a network hub that regulates alternative splicing. *Proc Natl Acad Sci United States America* (2015) 112(11):E1307–16. doi: 10.1073/pnas.1500536112

71. Brenner J, Feng F, Han S, Patel S, Goyal S, Bou-Maroun L, et al. PARP-1 inhibition as a targeted strategy to treat ewing's sarcoma. *Cancer Res* (2012) 72(7):1608–13. doi: 10.1158/0008-5472.Can-11-3648

72. Choy E, Butrynski J, Harmon D, Morgan J, George S, Wagner A, et al. Phase II study of olaparib in patients with refractory Ewing sarcoma following failure of standard chemotherapy. *BMC Cancer* (2014) 14:813. doi: 10.1186/1471-2407-14-813

73. Zhao Y, Adjei AA. Targeting angiogenesis in cancer therapy: Moving beyond vascular endothelial growth factor. *Oncologist* (2015) 20(6):660–73. doi: 10.1634/theoncologist.2014-0465

frontiers | Frontiers in Surgery

TYPE Case Report
PUBLISHED 09 September 2022
DOI 10.3389/fsurg.2022.991228



OPEN ACCESS

EDITED BY
Zhaolun Cai,
Sichuan University, China

REVIEWED BY
Adrian Fox,
St Vincent's Hospital (Melbourne), Australia
Tongyi Huang,
The First Affiliated Hospital of Sun Yat-sen University, China

*CORRESPONDENCE
Bifei Huang
hbfx711023@163.com
Lihong Wang
hustrose666@163.com

SPECIALTY SECTION
This article was submitted to Surgical Oncology, a section of the journal Frontiers in Surgery

RECEIVED 29 July 2022
ACCEPTED 25 August 2022
PUBLISHED 09 September 2022

CITATION
Zhang X, Chen J, Huang B and Wang L (2022) Case report: Hepatic epithelioid angiomyolipoma with elevated alpha-fetoprotein and a history of breast cancer. Front. Surg. 9:991228.
doi: 10.3389/fsurg.2022.991228



# Case report: Hepatic epithelioid angiomyolipoma with elevated alpha-fetoprotein and a history of breast cancer

Xiaowei Zhang[1], Jun Chen[2], Bifei Huang[1]* and Lihong Wang[3]*

[1]Department of Pathology, Affiliated Dongyang Hospital of Wenzhou Medical University, Dongyang, China, [2]Department of Nuclear Medicine, Affiliated Dongyang Hospital of Wenzhou Medical University, Dongyang, China, [3]Department of Orthopaedic Surgery, Affiliated Dongyang Hospital of Wenzhou Medical University, Dongyang, China

**Background:** Perivascular epithelioid cell tumors have characteristic histological and immunohistochemical profiles. Epithelioid angiomyolipomas in the liver have particularly rare characteristics. These tumors are relatively small and lack clinical and imaging specificity. Thus, they can be easily misdiagnosed as other primary or metastatic tumors prior to surgery. Due to the significant epithelioid morphology and atypia of hepatic epithelioid angiomyolipoma (HEAML), intraoperative frozen section pathologic diagnosis might be challenging.

**Case presentation:** A 33-year-old woman was admitted to our hospital for elevated alpha-fetoprotein (AFP) levels after a regular checkup following breast cancer surgery. Initially, liver cancer was suspected based on enhanced magnetic resonance imaging and color Doppler ultrasonography. Her serum AFP levels were 23.05 ng/ml. The patient underwent laparoscopic right hepatic tumor resection. Based on intraoperative cryopathology, hepatocellular carcinoma was considered a likely diagnosis. However, postoperative pathology confirmed a right HEAML. The patient underwent regular checkups for 23 months without exhibiting recurrence or distant metastasis.

**Conclusion:** HEAML can be easily misdiagnosed on preoperative imaging and intraoperative cryopathology. Medical professionals must be aware of this possibility and proceed with caution. Postoperative pathological examination with assessment of IHC markers was helpful in diagnosing HEAML. HEAML has low malignant potential. Surgical resection is the mainstay of treatment, and most patients have a good prognosis.

KEYWORDS

hepatocellular carcinoma, hepatic epithelioid angiomyolipoma, alpha-Fetoprotein, breast cancer, case report

Abbreviations

MRI, magnetic resonance imaging; AFP, alpha-fetoprotein; HEAML, hepatic epithelioid angiomyolipoma; IHC, immunohistochemistry; SMA, Smooth Muscle Actin; GATA3, GATA binding protein 3; HMB 45, human melanoma black 45; CK, cytokeratin.

# 1. Introduction

Hepatic epithelioid angiomyolipoma (HEAML) is a rare neoplasm and is an unusual type of the perivascular epithelioid cell tumor. On clinical and imaging examination, HEAML is often misdiagnosed as liver cancer or other types of lesions. Therefore, it is treated with mass complete resection. On pathological examination, various morphologies of HEAML resemble other benign and malignant liver tumors. Herein, we present a case of HEAML in a patient with a history of breast cancer and elevated alpha-fetoprotein (AFP) levels. To the best of our knowledge, this is the first case of HEAML presenting with elevated AFP levels. Our study describes the histopathological and immunohistochemical characteristics of the HEAML tumor and clinical and imaging manifestations of the case. The patient had no history of hepatitis or cirrhosis.

# 2. Case description

A 33-year-old woman was admitted to our hospital on January 16, 2019, for elevated AFP levels. During a routine follow-up after combination therapy for breast cancer, her serum test results showed AFP levels of 23.05 ng/ml (normal levels: <13.6 ng/ml). At that time, the patient had no abdominal pain or distension, anorexia, nausea, vomiting, acid regurgitation, yellow skin, or eyes, urine, or skin irritation, and she exhibited no features of chronic liver disease; meanwhile, there were no clinical features to suggest metastatic breast cancer. Physical examination revealed a 12 cm surgical incision due to a modified radical mastectomy of the left breast that the patient had undergone six years prior at our hospital. This surgery had been performed to treat the invasive carcinoma of her left breast after completing four cycles of postoperative chemotherapy. The extent of wound healing at the surgical site indicated no adverse events. Furthermore, no nodules were found. The liver and spleen were not swollen under the costal xiphoid process with no percussion pain in the liver area. Moreover, the abdomen was soft without tenderness.

## 2.1. Ethics declarations

This study was approved by the Dongyang Hospital, Affiliated to Wenzhou Medical University, Ethics Committee. The patient provided written informed consent to participate in this study. Additionally, written informed consent was obtained from the patient for the publication of any potentially identifiable images or data included in this article. This study was reported in agreement with principles of the CARE guidelines (1).

# 3. Diagnostic assessment

## 3.1. Imaging findings

Contrast-enhanced magnetic resonance imaging (MRI) scans of the liver revealed abnormal findings, including low signals on T1-weighted imaging and slightly elevated signals on the T2 fat saturation sequence. An area of hypodensity was observed in the right anterior segment of the liver with a 1.0 cm diameter and a clear boundary. Afterward, there was a significant enhancement in the arterial phase and a decrease in the portal phase. There was no dilatation of the intrahepatic bile duct and no lesions were detected in the region of the hepatic hilum. In addition, no swollen lymph nodes were found in the retroperitoneal area. The lesion in the right anterior segment of the liver was suggestive of hepatocellular carcinoma (**Figure 1**).

### 3.1.1. Contrast-enhanced liver ultrasound

A slightly low echo area of approximately 13 × 11 mm in size was found in the upper segment of the right anterior lobe of the liver, with an irregular shape and uneven internal echo. The ulnar vein was injected at 10 minute intervals with 1.5 ml sulfur hexafluoride as ultrasound contrast agent. Contrast-enhanced ultrasonography revealed nodules in the upper segment of the right anterior lobe of the liver that began to strengthen at 12 s, reached a peak at 20 s, and then began to subside. This showed arterial hypervascularity with washout, with a range of approximately 13 × 13 mm, suggesting a high possibility of primary hepatic carcinoma (**Figure 2**).

## 3.2. Treatment

Laparoscopic-assisted resection of the right hepatic tumor was performed. During the operation, the tumor was found to be 1.0 cm in size, with clear edges, and >1 cm from the cut edge. The tumor was completely resected. In the frozen section pathological analysis of the right liver specimen, the possibility of hepatocellular carcinoma was tested first. The patient recovered and was discharged post-operatively.

## 3.3. Histopathology

### 3.3.1. Postoperative pathology

#### *3.3.1.1. The right liver*

A 4.5 × 3.3 × 1.8 cm specimen of the liver tissue was retrieved during the operation, including a grayish-yellow mass (1.2 ×

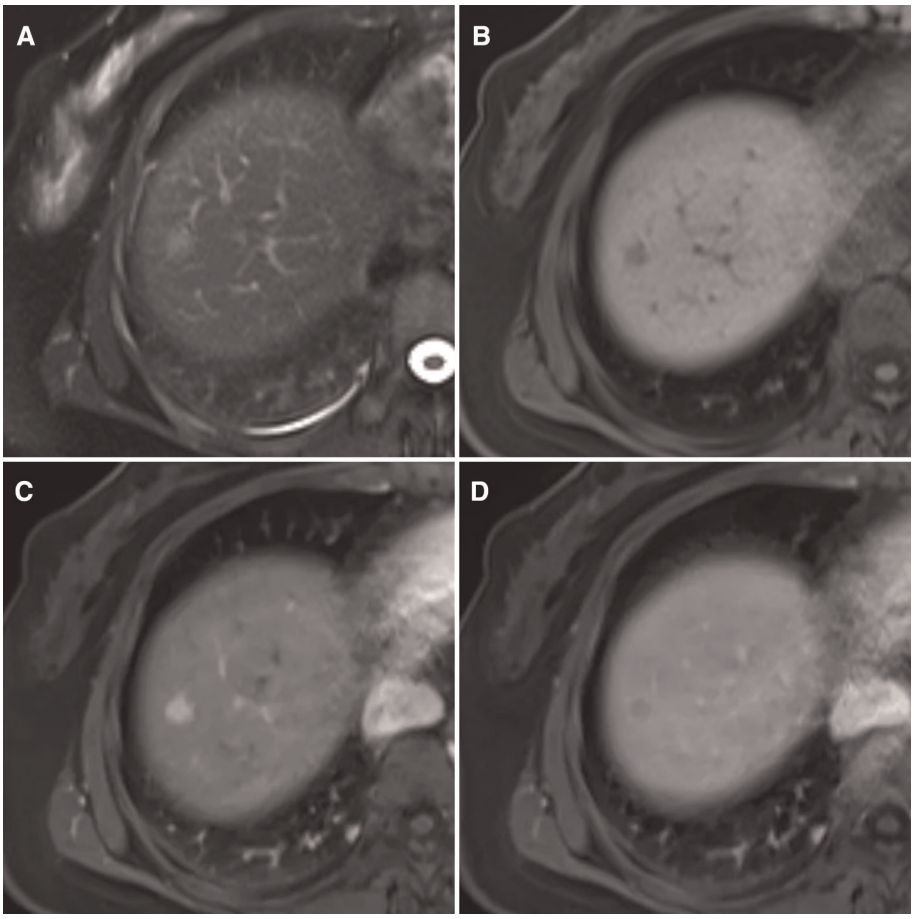


FIGURE 1
MRI findings of this case (A) heterogeneous hyperintensity on T2 lipid-pressing sequence is shown. (B) Low signal on T1 lipid-pressing sequence is shown. (C) The arterial phase is markedly enhanced. (D) Hypointensities in the portal phase are shown.

0.9 cm in size), which was soft and had a clear boundary. Light microscopy analysis showed that the liver tumor nodules were arranged by large polygonal epithelioid cells in the form of sheet nests or irregular beam cables, divided by thin-walled vessels of different sizes. The tumor cell cytoplasm was transparent, with vacuoles in the periphery. Eosinophilic granules could be seen in the cytoplasm. The nuclei were round or oval and large with clearly visible nucleoli and deep chromatin. The nodule boundaries were unclear as they grew into the surrounding liver tissue (Figures 3A–D).

#### *3.3.1.2. Pathological diagnosis*

Epithelioid angiomyolipoma of the right liver (tumor size: 1.2 × 0.9 cm) with negative incisional margins.

#### *3.3.1.3. Immunohistochemical staining results*

The tumor cells were positive for estrogen receptor (1 + 40%), progesterone receptor (2 + 10%), desmin (focal + ), E-cadherin, vimentin, and human melanoma black (HMB) 45, smooth muscle actin (SMA) (Figures 3E, F). The specimen was negative for GATA binding protein 3 (GATA3), CerbB-2, AFP, glypican-3, HepPar1, cytokeratin (CK) (AE1/AE3), cell adhesion molecule 5.2, CK20, CDX2, CK7, CK8, and S-100, with a Ki-67 index of 5%.

### 3.4. Postoperative follow-up

Over the 23 months of follow-up, no recurrence or distant metastasis was observed on computed tomography and MRI scans.

## 4. Discussion

Perivascular epithelioid cell tumors are a group of mesenchymal lesions that share similar vascular wall morphology and express melanin and smooth muscle markers. Epithelioid angiomyolipoma, which is classified as a perivascular epithelioid cell tumor, is especially unique and

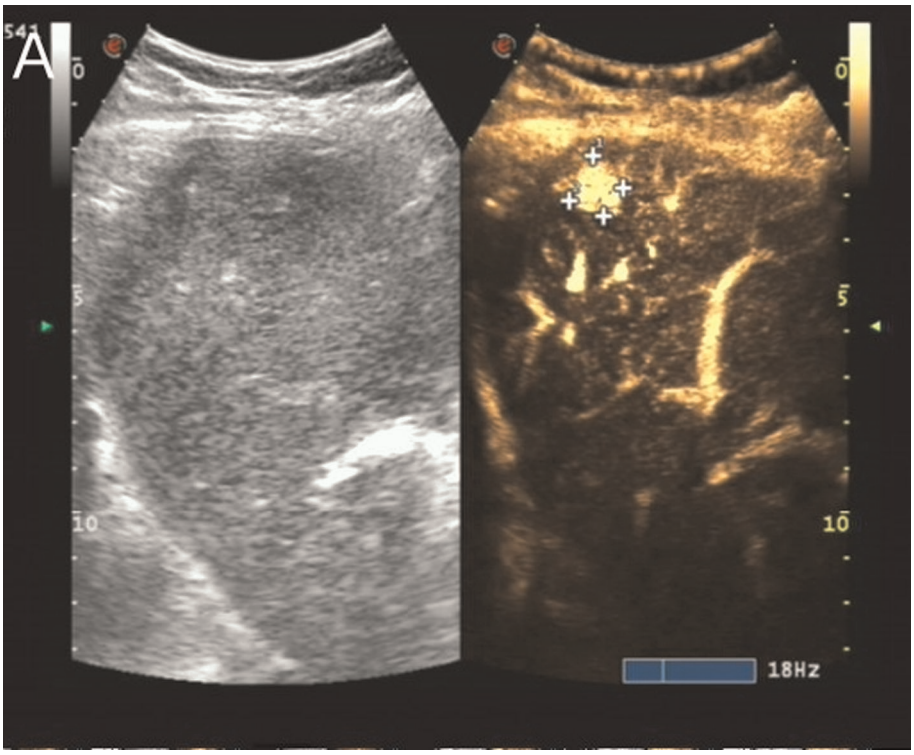


FIGURE 2
Contrast-enhanced liver ultrasound findings of this case contrast-enhanced ultrasonography of the nodules in the upper segment of the right anterior lobe of the liver showing washout performance (surrounded by crosses).

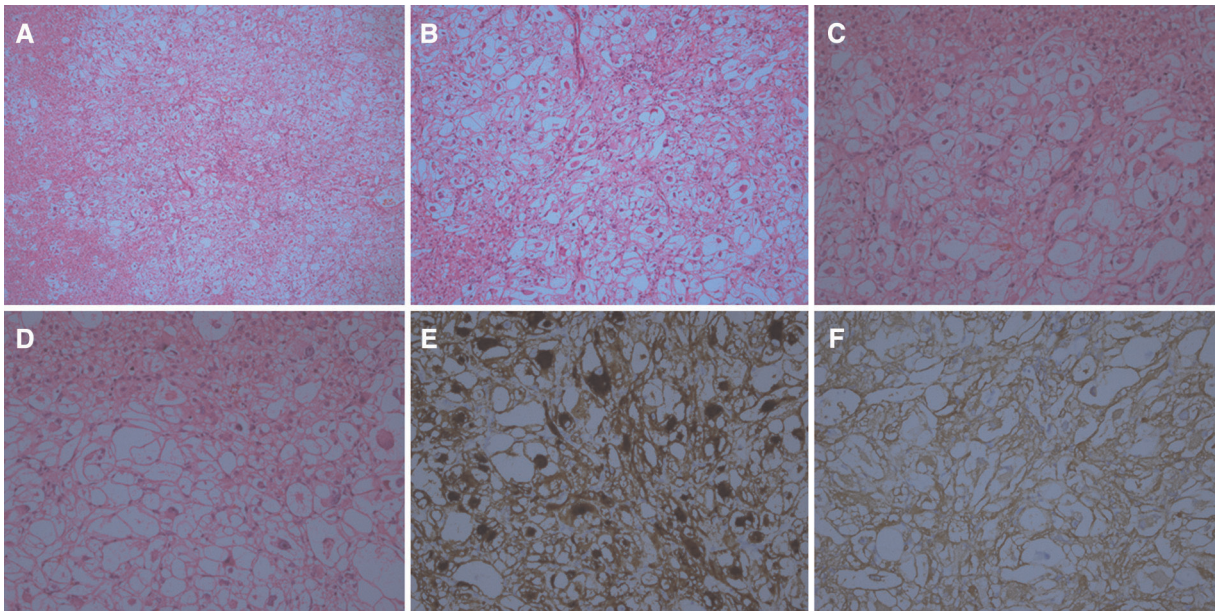


FIGURE 3
Histological findings of this case (**A–D**) hematoxylin and eosin staining of the tumor under multiple magnifications (**A**, ×50) (**B**, ×100). (**C**, ×200) (**D**, ×400). Microscopically, the tumor boundary is unclear and grows into the surrounding liver tissue. Epithelioid-like tumor cells can be seen arranged in a nest-like shape. Vascular components are visible, but adipocytes and smooth muscle components are not found. Under a high microscope objective, the tumor nuclei are round or oval with obvious nucleoli and atypia. (**E**) Tumor cells stained positive for HMB 45. Magnification at ×200. (**F**) Tumor cells stained positive for SMA. Magnification at ×200.

rare (2). In 1976, Ishak et al. first described HEAML as a rare mesenchymal tumor, mostly occurring in women, with approximately 5%–10% of these tumors being accompanied by nodular sclerosis (3). To date, the pathogenesis of HEAML is unclear. The possible etiologies of tumors include undifferentiated neural crest, differentiated smooth muscle cells, and perivascular cells. Studies have indicated that changes in the mammalian target of the mechanistic target of rapamycin (mTOR) pathway and loss of heterozygosity (LOH) of the tuberous sclerosis syndrome gene were the common pathogeneses of HEAML (4).

HEAML tends to occur in young and middle-aged women, with a male to female ratio of 1:5. Usually, these tumors are small and cause no characteristic clinical symptoms. However, when a tumor is large, the patient may experience abdominal distension and pain (5). Our patient had elevated AFP levels without experiencing any other symptoms suggestive of HEAML. The elevated AFP levels were coincidentally found during the patient's regular follow-up examination and imaging after being treated for breast cancer. Since HEAML contains only a small amount of fat or lacks it entirely, it is easily misdiagnosed for other malignant tumors during imaging examination before tumor resection (6). The preoperative liver MRI and color Doppler ultrasound in the present case suggested a possibility of liver cancer. Since the patient's AFP level was elevated, intraoperative frozen section analysis was needed to differentiate tumor type but this has the potential to be inconclusive. Thus, vigilance was needed to establish the correct diagnosis. Diagnosing HEAML by fine-needle puncture before surgery is necessary.

Although pathological examination is the gold standard for diagnosing HEAML, this patient had a history of breast cancer, and the tumor marker (AFP) was elevated, which could result in an incorrect pathological diagnosis. Microscopic analysis revealed that the HEAML cells were round or polygonal. Their cytoplasm was rich, slightly acidophilic or transparent, and sometimes contained fat vacuoles. The nuclei were median or partial, large, round or ovoid, with obvious nucleoli and rare mitotic images (7). IHC revealed that HEAML tissue was positive for melanocytic markers (HMB 45 and Melan-A) and smooth muscle cell markers (SMA and desmin) (8). Although transcription factor E3 can be expressed in some cases, there are usually no related gene expression changes. HEAML tissue does not express epithelial markers, S-100, SOX11, CD31, and CD34.

The morphology of HEAML could can be diverse making it is easy to confuse this tumor with other primary or metastatic tumors in the liver. A comprehensive IHC evaluation is required to distinguish HEAML diagnosis from other primary and metastatic liver tumors. Key ways to differentiate HEAML from other hepatic primary or metastatic tumors include the following:

First, in comparison to metastatic breast cancer, it usually presents a nest-like or glandular structure and IHC expression of markers (GATA3 and GCDFP15). Our patient had a history of breast cancer that needed to be excluded. It can sometimes be difficult to identify HEAML by evaluation using frozen section biopsy.

Second, when considering hepatocellular carcinoma, due to the significant epithelioid morphology and atypia of HEAML, it can easily be misdiagnosed as hepatocellular carcinoma, particularly based on intraoperative cryopathology diagnosis. In the present case, cryopathology analysis incorrectly identified HEAML as hepatocellular carcinoma. HEAML tissue expresses melanocytic markers, not epithelial markers. In addition, patients with hepatocellular carcinoma usually have a history of hepatitis and cirrhosis. Thus, it is easy to distinguish between the two after comprehensive analysis of postoperative pathology.

Third, HEAML demonstrates melanocyte differentiation and cell atypia, which is easily misdiagnosed as malignant melanoma. However, malignant melanoma usually expresses S-100 protein and is negative for smooth muscle cell markers. Based on patient history and IHC, malignant melanoma can be differentiated from HEAML.

Surgical resection is the preferred treatment of HEAML and should be performed as early as possible to avoid gradual growth and rupture of the tumor. It has been reported that early surgical treatment is effective in treating spontaneous rupture of hepatic angiomyolipoma with internal and peritoneal hemorrhage (9). In addition, HEAML tumors have low malignancy potential. Moreover, complete surgical resection can prevent local recurrence or metastasis (10). Approximately 10% of patients with HEAML who undergo surgical resection experience postoperative recurrence or metastasis (11). Postoperative radiotherapy and chemotherapy are ineffective, therefore, we suggest regular postoperative follow-up observation.

## 5. Conclusions

We present the case of a patient with HEAML and a history of breast cancer who presented with elevated AFP levels. Clinically, radiologically, and even pathologically, with special frozen pathological examination, HEAML can easily be misdiagnosed as other tumors. It is especially necessary to differentiate HEAML from hepatocellular carcinomas and metastatic tumors, necessitating the use of a specific IHC staining panel. Early surgical resection is the mainstay of treatment, and long-term postoperative follow-up is required.

## Patient perspective

All examination and treatment patients provided informed consent.

## Data availability statement

The original contributions presented in the study are included in the article/Supplementary Material, further inquiries can be directed to the corresponding author/s.

## Author contributions

XZ and BH acquired the data. BH analyzed the pathological data. JC analyzed the imaging data. XZ, JC, BH, and LW prepared the manuscript. All authors contributed to the article and approved the submitted version.

## Acknowledgments

The authors thank the patient who kindly agreed to provide them with the data used in this case.

## Conflict of interest

The authors declare that the research was conducted in the absence of any commercial or financial relationships that could be construed as a potential conflict of interest.

## Publisher's note



## References

1. Riley DS, Barber MS, Kienle GS, Aronson JK, Von Schoen-Angerer T, Tugwell P, et al. CARE Guidelines for case reports: explanation and elaboration document. *J Clin Epidemiol*. (2017) 89:218–35. doi: 10.1016/j.jclinepi.2017.04.026

2. Thway K, Fisher C. PEComa: morphology and genetics of a complex tumor family. *Ann Diagn Pathol*. (2015) 19:359–68. doi: 10.1016/j.anndiagpath.2015.06.003

3. Ishak K. Mesenchymal tumors of the liver. In: K Okuda, R Peter, editors. *Hepatocellular carcinoma*. New York: John Wiley & Sons (1976). p. 247–75.

4. Huang SC, Chuang HC, Chen TD, Chi CL, Ng KF, Yeh TS, et al. Alterations of the mTOR pathway in hepatic angiomyolipoma with emphasis on the epithelioid variant and loss of heterogeneity of TSC1/TSC2. *Histopathology*. (2015) 66:695–705. doi: 10.1111/his.12551

5. Liu W, Meng Z, Liu H, Li W, Wu Q, Zhang X, et al. Hepatic epithelioid angiomyolipoma is a rare and potentially severe but treatable tumor: a report of three cases and review of the literature. *Oncol Lett*. (2016) 11:3669–75. doi: 10.3892/ol.2016.4443

6. Ji JS, Lu CY, Wang ZF, Xu M, Song JJ. Epithelioid angiomyolipoma of the liver: CT and MRI features. *Abdom Imaging*. (2013) 38:309–14. doi: 10.1007/s00261-012-9911-5

7. De la Sancha C, Khan S, Alruwaii F, Cramer H, Saxena R. Hepatic angiomyolipoma with predominant epithelioid component: diagnostic clues on aspiration and core needle biopsies. *Diagn Cytopathol*. (2021) 49:E238–41. doi: 10.1002/dc.24688

8. Caliò A, Brunelli M, Marletta S, Zamboni G, Bonetti F, Pea M, et al. Epithelioid angiomyolipoma: a pathological entity discovered in Verona with the endorsement of Doctor Rosai. *Pathologica*. (2021) 113:307–15. doi: 10.32074/1591-951X-335

9. Occhionorelli S, Dellachiesa L, Stano R, Cappellari L, Tartarini D, Severi S, et al. Spontaneous rupture of a hepatic epithelioid angiomyolipoma: damage control surgery. A case report. *G Chir*. (2013) 34:320–22.

10. Tajima S, Suzuki A, Suzumura K. Ruptured hepatic epithelioid angiomyolipoma: a case report and literature review. *Case Rep Oncol*. (2014) 7:369–75. doi: 10.1159/000363690

11. Liu J, Zhang CW, Hong DF, Tao R, Chen Y, Shang MJ, et al. Primary hepatic epithelioid angiomyolipoma: a malignant potential tumor which should be recognized. *World J Gastroenterol*. (2016) 22:4908–17. doi: 10.3748/wjg.v22.i20.4908

frontiers | Frontiers in Surgery

TYPE Case Report
PUBLISHED 09 September 2022
DOI 10.3389/fsurg.2022.968891



OPEN ACCESS

EDITED BY
Akinfemi Akingboye,
Dudley Group NHS Foundation Trust,
United Kingdom

REVIEWED BY
Nguyen Minh Duc,
Pham Ngoc Thach University of Medicine,
Vietnam
Satvinder Singh Mudan,
Imperial College London, United Kingdom

*CORRESPONDENCE
Xiaojun Zhou
chowxj@126.com

SPECIALTY SECTION
This article was submitted to Surgical Oncology, a section of the journal Frontiers in Surgery

RECEIVED 14 June 2022
ACCEPTED 19 August 2022
PUBLISHED 09 September 2022

CITATION
Zhou Q, Zhou Y, Ouyang Y, Chen W and Zhou X (2022) Hepatoid adenocarcinoma of the stomach with metastatic choriocarcinoma of the liver: A case report of a rare subtype of gastric cancer with a complex treatment course.
Front. Surg. 9:968891.
doi: 10.3389/fsurg.2022.968891



# Hepatoid adenocarcinoma of the stomach with metastatic choriocarcinoma of the liver: A case report of a rare subtype of gastric cancer with a complex treatment course

Qiyang Zhou[1], Yudi Zhou[1], Yiming Ouyang[1], Weichang Chen[2] and Xiaojun Zhou[1]*

[1]Department of General Surgery, The First Affiliated Hospital of Soochow University, Suzhou, China, [2]Department of Gastroenterology, The First Affiliated Hospital of Soochow University, Suzhou, China

Gastric hepatoid adenocarcinoma and hepatic choriocarcinoma are rare diseases in clinical settings, and the case we report here is a combination of both. A 66-year-old woman presented with a chief complaint of abdominal discomfort. The patient was examined using gastroscopy and computed tomography (CT) scan, and these revealed an irregular surface ulcer on the wall of the gastric antrum. A mass, 2.0 cm in diameter, was found in the liver in April 2020. The endoscopic biopsy findings were consistent with a diagnosis of moderately to poorly differentiated hepatoid adenocarcinoma. She was then referred to our hospital for further treatment. Initially, neoadjuvant therapy was initiated for the patient. The CT scan showed that the liver metastases had progressed; hence, surgery was performed. Postoperative pathology showed that the gastric lesions were mostly hepatoid adenocarcinoma with no choriocarcinoma, while the liver lesions comprised approximately 10% hepatoid adenocarcinoma and 90% choriocarcinoma. One month later, the patient developed tumor recurrence in the liver as observed on CT imaging. Subsequently, a variety of chemotherapy regimens were tried with no obvious results. The patient eventually developed multiple organ metastasis and died in July 2021. The overall survival was 16 months. Based on findings from this case report, it appears that initial neoadjuvant therapy was not effective and radical surgery may be the best treatment for patients with hepatoid adenocarcinoma of the stomach.

KEYWORDS

gastric hepatoid adenocarcinoma, hepatic choriocarcinoma, chemotherapy, neoadjuvant therapy, radical surgery, case report

## Introduction

Hepatoid adenocarcinoma of the stomach (HAS) is a rare type of primary gastric malignant neoplasm that exhibits both adenocarcinomatous and hepatocellular differentiation and mostly produces alpha-fetoprotein (AFP). It accounts for approximately 1% of all gastric cancers. The stomach is the most commonly affected

organ, and it often occurs in the antrum accompanied by vascular invasion, lymph node metastasis, and liver metastasis (1–3). Choriocarcinoma, on the other hand, is prone to rapid hematogenous metastases, and the first clinical manifestations are often metastatic lesions (4). The characteristic laboratory finding in patients with choriocarcinoma is an elevated serum human chorionic gonadotropin (hCG) level (5). Due to the rarity and ease of metastasis associated with these neoplasms, timely diagnosis and proper treatment are of significant importance. Herein, we report a case of HAS with liver metastasis, in which the pathologic diagnosis was choriocarcinoma (90%) combined with hepatoid adenocarcinoma (10%). Furthermore, we discuss this case in the context of other similar studies, which ultimately highlight the intricacy of HAS and the need for sound treatment guidelines.

## Case presentation

This was a case of a 66-year-old female patient with a complaint of abdominal discomfort for a month with no other associated symptoms. Physical examination revealed no pathological findings. Gastroscopy and computed tomography (CT) examinations revealed an irregular surface ulcer on the wall of the gastric antrum (**Figure 1A**) and a mass of 2.0 cm in diameter was found in the liver (**Figure 1B**). The pathological diagnosis from endoscopic biopsy was consistent with a moderately to poorly differentiated hepatoid adenocarcinoma (**Figure 1C**). PET-CT examination was then performed, and this showed that the stomach and liver masses were hypermetabolic (**Figure 1D**).

Laboratory tests showed that the blood cell and biochemical values were almost within the normal range. However, serum AFP was dramatically elevated (>2,000 ng/ml). Further examination revealed the remaining tumor markers, including the carbohydrate antigen 199 (CA199) >1200 U/ml, carcinoembryonic antigen 38.17 ng/ml, and hCG 795.14 mIU/ml.

Based on the guidelines of the Chinese Society of Clinical Oncology (CSCO), the disease was classified as advanced gastric cancer with liver metastasis, and the patient underwent SOX chemotherapy regimen, which is the first-line treatment recommendation, consisting of oxaliplatin, gimeracil, and oteracil potassium capsules.

After three cycles of chemotherapy, CT revealed progression of liver metastasis (**Figure 2**). The patient had leucopenia during chemotherapy and chose surgery for the subsequent treatment. Radical gastrectomy, hepatic left lateral lobectomy, and resection of the metastatic nodule in hepatic segment V were performed. Postoperative pathology (**Figure 3**) showed that the stomach mass was hepatoid adenocarcinoma, while the mass in the liver was approximately 10% hepatoid adenocarcinoma and 90% choriocarcinoma, with lymphatic metastasis (7/26).

One month later, CT imaging revealed liver metastasis and recurrence (**Figure 4A**). Considering the poor effect of the original chemotherapy regimen, we chose the DS chemotherapy regimen, which consisted of paclitaxel, gimeracil, and oteracil potassium capsules.

After two cycles of the chemotherapy regimen, on September 14, 2020, CT reexamination showed that liver and lung metastases occurred (**Figure 4B**). We changed the chemotherapy regimen again. Sintilimab, paclitaxel, and regorafenib were selected for treatment. This chemotherapy regimen was administered three times.

Two months later, CT examination showed that the liver and lung metastases were more and larger than before (**Figure 4C**). We chose to replace the former chemotherapy scheme with FOLFOX chemotherapy regimen (oxaliplatin, folinic acid calcium salt hydrate, and 5-FU) and sintilimab as a new treatment.

On March 18, 2021, the magnetic resonance (MR) scan showed that the patient had developed brain metastases (**Figure 4D**). Then, she was treated with etoposide and KN046 (PD-L1/CTLA-4 bispecific antibody) and intracranial radiotherapy.

Overall, a variety of chemotherapy regimens were tried, and the patient developed systemic multiple organ metastasis. During the whole chemotherapy period, the indexes of tumor markers remained at high levels, including AFP, CA199, and hCG.

Finally, the patient suffered from repeated low fever, trilineage cytopenia, and her physical condition gradually worsened. She eventually rejected treatment and died in July 2021.

## Discussion

With an increasing number of articles reporting cases of HAS, the diagnosis of hepatoid adenocarcinoma is no longer a problem through laboratory examination, gastroscopy, and pathological biopsy. HAS is a rare type of primary gastric malignant neoplasm and it is accompanied by vascular invasion, lymph node metastasis, and liver metastasis. Extragenital choriocarcinomas, on the other hand, are less common, often exist with other carcinomas, and tend to occur in midline organs (4). Fernández Alonso et al. reported primary hepatic choriocarcinoma for the first time in 1992 (6). Subsequently, most patients with hepatic choriocarcinoma were reported from China (7, 8). Conversely, the histopathogenesis of extragonadal choriocarcinomas remains controversial. Some authors have reported that normal cells develop directly into choriocarcinoma (9), whereas others have reported that retrodifferentiation from pre-existing adenocarcinoma results in choriocarcinoma (10). In this case, the patient was examined through gastroscopy and biopsy and these confirmed the diagnosis of hepatoid adenocarcinoma. Since CT showed evidence of a lesion in the liver, liver

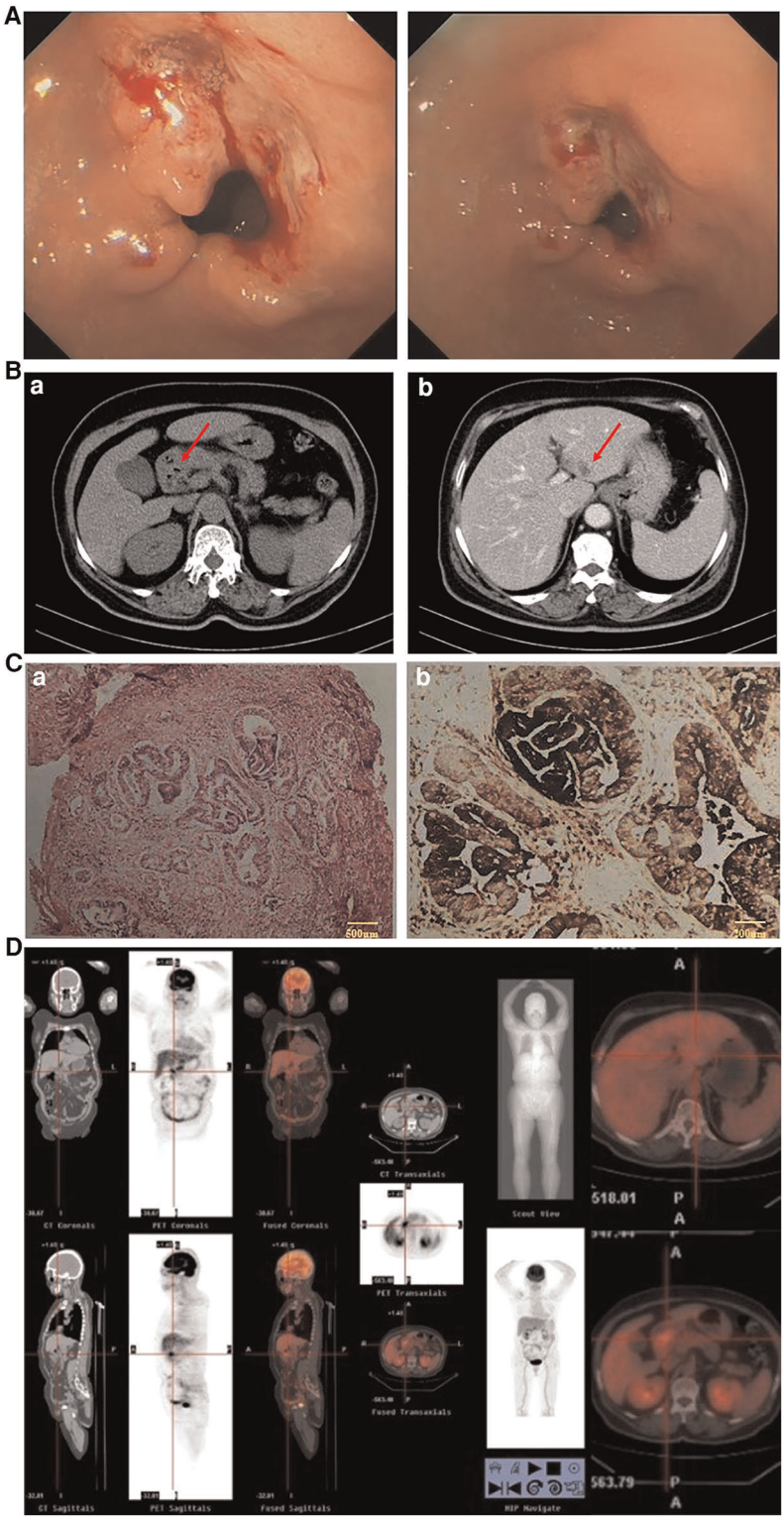


FIGURE 1
(**A**) Gastroscopy (April 1, 2020): gastric antrum ulcer. (**B**) CT (April 1, 2020): (a) Gastric antrum tumor; (b) Abnormal low density of left lateral lobe of the liver, considering metastasis. (**C**) Results of endoscopic biopsy: (a) HE staining; (b) AFP staining. (Gastric antrum) Moderately to poorly differentiated hepatoid adenocarcinoma. Immunopathology: AFP(+), HER-2(+), Ki-67(40%), PD-L1(22C3)(–), PD-1(–), CD4(+), CD8(+), MLH1(+), PMS2(+), MSH6(+), MSH2(+). (**D**) PET-CT examination: The masses of gastric antrum and left liver were hypermetabolic.

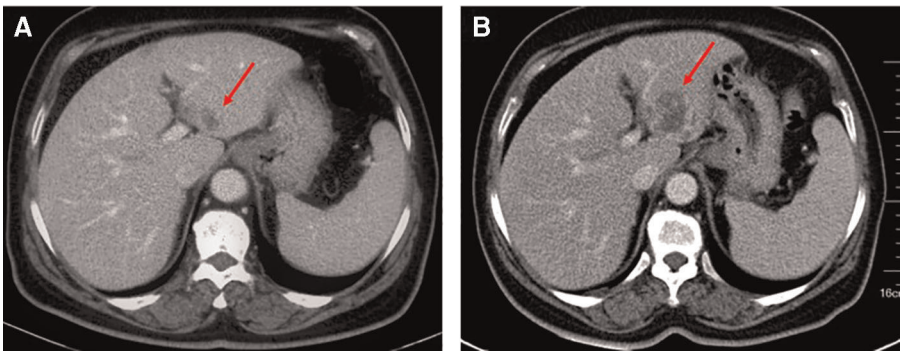


FIGURE 2
Ct examination: (A) April 1, 2020. (B) June 17, 2020. The mass of the left liver was more advanced than before.

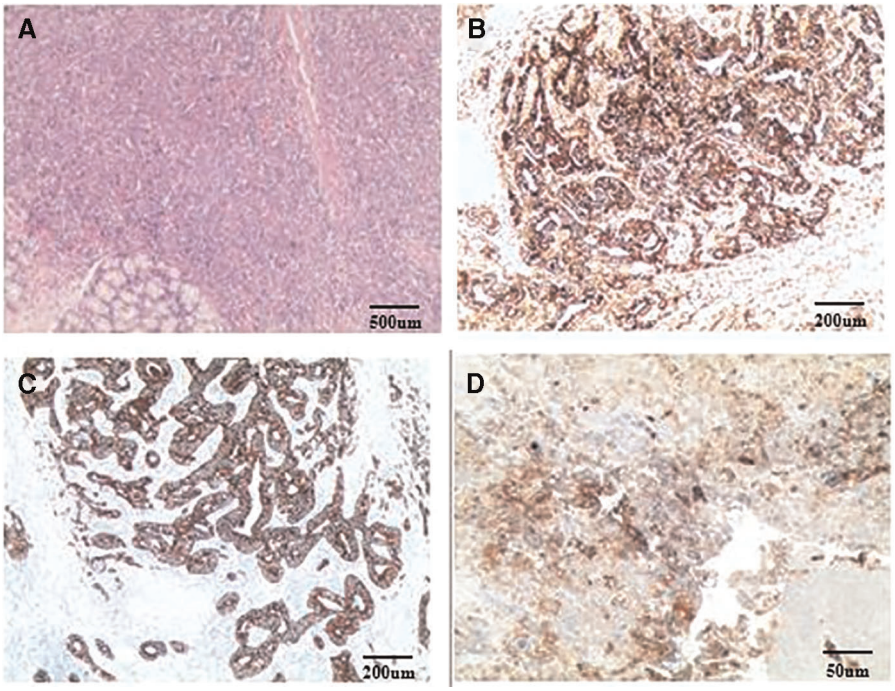


FIGURE 3
Postoperative pathology: (A) HE staining; (B) AFP staining; (C) CK staining; (D) PD-L1 staining. Routine pathology: (Stomach) Moderately to poorly differentiated adenocarcinoma, focal features of hepatoid adenocarcinoma, small necrosis, tumor invasion, tumor thrombus in the vessel; (Right liver nodule S5) cancer metastasis; (Left lateral liver) cancer metastasis, with massive necrosis, bleeding, no cancer accumulation in the liver resection margin, while the liver lesions were about 10% of hepatoid adenocarcinoma and 90% were choriocarcinoma. Immunopathology: (Stomach): CK(+), AFP(+), Glypican-3(+), MSH2(+), MSH6(+), MLH1(+), PMS2(+), MSS, Her-2(1+), Ki-67(+, 95%), PD-L1(22C3) (tumor cell: 1%–5%; microenvironment immune cells: +, 20%–30%), CD117(+), Hepa-1(–), CK7(–), CK5/6(–), P40(–), PD-1(–), CD5(–), Vimentin(–), EVB(–); (Liver): CK7 (+), Her-2(2+), Ki67(+, 95%), PD-L1(22C3)(+, >50%), MLH1(+), MSH2(+), MSH6(+), PMS2(+), MSS, AFP(–), Hepa-1(–), CD5(–), and EBV(–).

metastasis was suspected. Laboratory tests showed that in addition to the increase in AFP level (beyond 2,000 ng/ml), hCG was also significantly elevated to 795.14 mIU/ml. However, the reason for the increase in the hCG index was unclear at this point. To ensure that metastases had not occurred at other primary sites, PET-CT examination was performed and this revealed no obvious tumor in other organs. PET-CT also showed that the tumors in the stomach and liver were hypermetabolic. Therefore, we diagnosed the patient as having hepatoid gastric adenocarcinoma with liver metastasis. Postoperative pathological examinations showed that the gastric lesions were comprised mostly of hepatoid adenocarcinoma and no choriocarcinoma, while the liver lesions were approximately 10% hepatoid adenocarcinoma

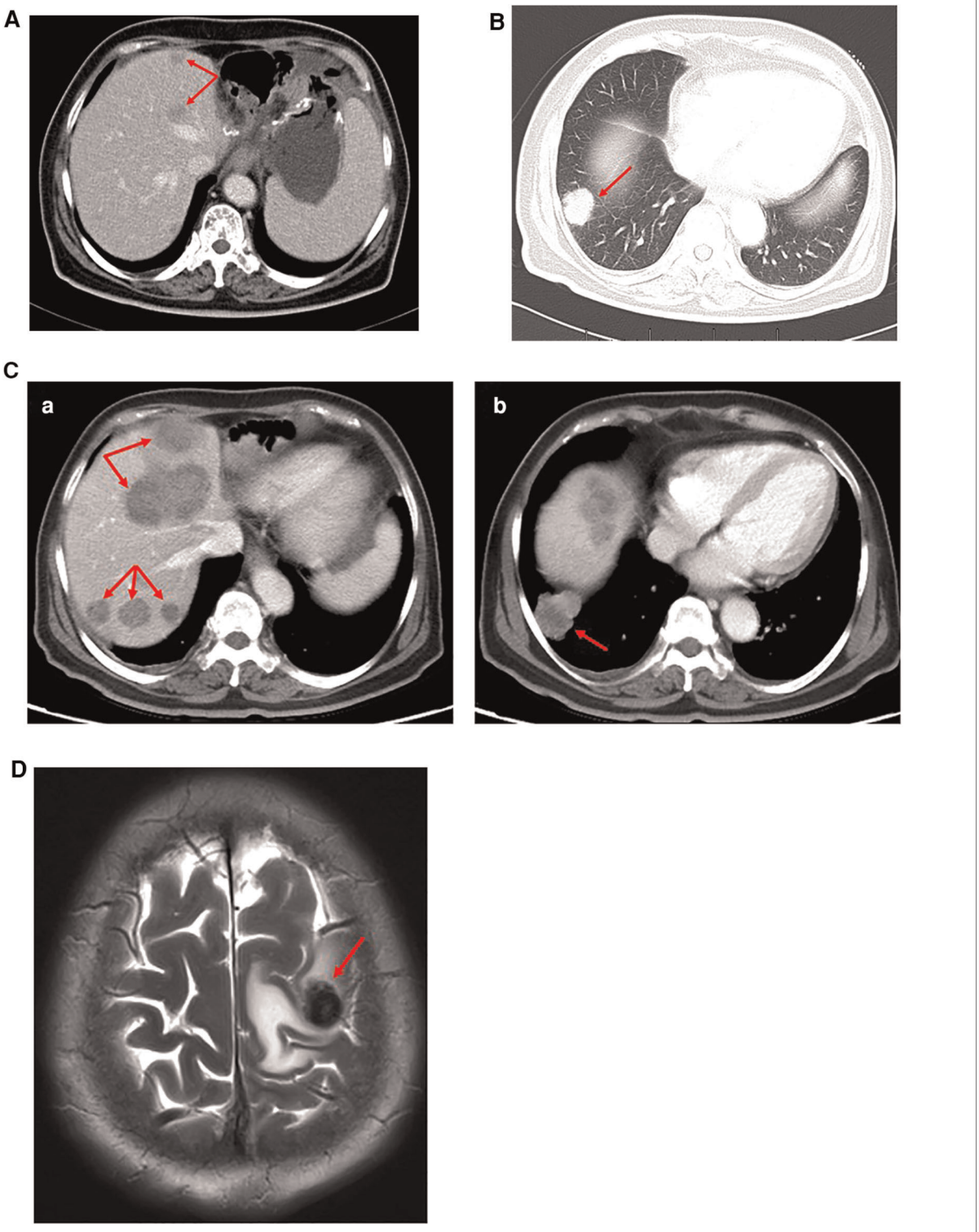


FIGURE 4
(**A**) CT examination (July 28, 2020): many slightly low-density lesions in the liver, considering metastasis. (**B**) CT examination (September 14, 2020): Right pulmonary nodule, considering metastasis. (**C**) CT examination (November 19, 2020): (a) Multiple low-density liver metastases (more and larger than before). (b) The metastatic nodules in the lower lobe of the right lung were larger than before. (**D**) MR examination (March 18, 2021): Brain metastasis.

and 90% choriocarcinoma. In fact, we were not sure whether the liver choriocarcinoma was the primary or differentiated tumor after metastasis. Liu et al. pointed out that metastatic lesions will differentiate when they metastasize to other organs (10), and the experience in this case seemed to agree with this.

The patient's condition was diagnosed as HAS with liver metastasis; hence neoadjuvant therapy was initiated first. To date, there is still no clear criterion for the treatment of HAS. Some studies have reported radical surgery as the main treatment option for patients with HAS (11, 12). However, the specific regimen of neoadjuvant or adjuvant therapy for HAS remains unclear. A recent systematic review concluded that cisplatin-based chemotherapy is the most efficient first-line systemic treatment in advanced situations, with a clinical response observed in 75% of the patients (13). Arakawa et al. recently reported a significant clinical response to ramucirumab monotherapy in a metastatic HAS (mHAS) patient with chemotherapy-resistant recurrent disease (14). The introduction of molecular targeted therapy has also brought hope to HAS patients. Hepatic choriocarcinoma, on the other hand, has no clear treatment strategy; although surgery and chemotherapy have been reported, none of the patients treated with these had good prognosis (8, 15, 16). Neoadjuvant therapy was the initial treatment option employed in this case. We used the SOX chemotherapy regimen, which consisted of oxaliplatin, gimeracil, and oteracil potassium capsules, a treatment modality not reported in the earlier literature referred; however, this is the first-line treatment for advanced metastatic gastric cancer according to our guidelines. The patient underwent simultaneous whole-genome sequencing, but the results showed that there was no new targeted drug recommended for the patient. The neoadjuvant chemotherapy did not achieve obvious results. We are puzzled whether the next treatment plan is to continue the second-line treatment plan or surgery. At that time, we assessed that the liver and stomach lesions could still be resected by operation through CT imaging. It is very difficult for us to continue to choose the second-line chemotherapy or surgery. However, the patient and her family had a strong desire for surgery; hence, surgery was performed. Nonetheless, the patient's liver tumor recurred one month after the surgery and a variety of chemotherapy regimens were tried after that, including targeted medicine and bispecific antibody with no obvious results. The disease was not controlled, multiple organ metastasis occurred, and, eventually, the patient died.

There is no standard treatment for mHAS at present. This case report discusses its clinical treatment and prognosis and helps get further knowledge and understanding of mHAS and the treatment of this rare aggressive tumor. However, a limitation of this case report may be that molecular studies were not performed; thus, HER2 gene amplification and overexpression and EGFR, KRAS, and BRAF mutation-associated tumorigenesis and gastric carcinomas that may respond to specific treatments were not able to be explored in this case report.

## Conclusion

In summary, HAS and hepatic choriocarcinoma are rare and aggressive diseases; the combination of the two is even rarer, and the diagnosis and treatment are full of challenges. Although radical surgery may be the best treatment for HAS patients, the specific systemic chemotherapy principles for patients with advanced metastasis resulting from HAS are still flawed. There is an urgent need for a large number of clinical reports to improve the understanding of HAS and hepatic choriocarcinoma.

## Data availability statement

The raw data supporting the conclusions of this article will be made available by the authors, without undue reservation.

## Ethics statement

The studies involving human participants were reviewed and approved by the Ethics Committee of The First Affiliated Hospital of Soochow University. The patients/participants provided their written informed consent to participate in this study. Written informed consent was obtained from the family of the patient for the publication of any potentially identifiable images or data included in this article.

## Author contributions

XZ and QZ put forward the content of the paper. QZ wrote the manuscript. XZ, YZ, YO, and WC reviewed literature and clinical data. All authors contributed to the article and approved the submitted version.

## Acknowledgments

The authors thank the patient and his family for consenting to report this case information.

## Conflict of interest

The authors declare that the research was conducted in the absence of any commercial or financial relationships that could be construed as a potential conflict of interest.

## Publisher's note



## References

1. Qu BG, Bi WM, Qu BT, Qu T, Han XH, Wang H, et al. PRISMA-compliant article: clinical characteristics and factors influencing prognosis of patients with hepatoid adenocarcinoma of the stomach in China. *Medicine*. (2016) 95(15): e3399. doi: 10.1097/MD.0000000000003399

2. Li T, Liu T, Wang M, Zhang M. *A*-fetoprotein producing hepatoid gastric adenocarcinoma with neuroendocrine differentiation: a case report. *Medicine*. (2018) 97(37):e12359. doi: 10.1097/MD.0000000000012359

3. Liu X, Cheng Y, Sheng W, Lu H, Xu X, Xu Y, et al. Analysis of clinicopathologic features and prognostic factors in hepatoid adenocarcinoma of the stomach. *Am J Surg Pathol*. (2010) 34(10):1465–71. doi: 10.1097/PAS.0b013e3181f0a873

4. Fine G, Smith R, Pachter M. Primary extragenital choriocarcinoma in the male subject. Case report and review of the literature. *Am J Med*. (1962) 32:776–94. doi: 10.1016/0002-9343(62)90167-5

5. Sekine R, Hyodo M, Kojima M, Meguro Y, Suzuki A, Yokoyama T, et al. Primary hepatic choriocarcinoma in a 49-year-old man: report of a case. *World J Gastroenterol*. (2013) 19(48):9485–9. doi: 10.3748/wjg.v19.i48.9485

6. Fernández Alonso J, Sáez C, Pérez P, Montaño A, Japón M. Primary pure choriocarcinoma of the liver. *Pathol Res Pract*. (1992) 188(3):375–7, discussion 378–9. doi: 10.1016/S0344-0338(11)81224-0

7. Arai M, Oka K, Nihei T, Hirota K, Kawano H, Kawasaki T, et al. Primary hepatic choriocarcinoma–a case report. *Hepato-gastroenterology*. (2001) 48 (38):424–6. PMID: 11379323.

8. Shi H, Cao D, Wei L, Sun L, Guo A. Primary choriocarcinoma of the liver: a clinicopathological study of five cases in males. *Virchows Archiv*. (2010) 456 (1):65–70. doi: 10.1007/s00428-009-0864-1

9. Okada K, Yokoyama S, Mochizuki Y, Moriuchi A, Yamashita H, Yasunaga A, et al. An autopsy case of primary gastric choriocarcinoma. *Jpn J Clin Oncol*. (1987) 17(3):263–73. PMID: 3669367.

10. Liu Z, Mira J, Cruz-Caudillo JC. Primary gastric choriocarcinoma: a case report and review of the literature. *Arch Pathol Lab Med*. (2001) 125 (12):1601–4. doi: 10.5858/2001-125-1601-PGC

11. Zeng XY, Yin YP, Xiao H, Zhang P, He J, Liu WZ, et al. Clinicopathological characteristics and prognosis of hepatoid adenocarcinoma of the stomach: evaluation of a pooled case series. *Curr Med Sci*. (2018) 38(6):1054–61. doi: 10.1007/s11596-018-1983-1

12. Søreide J. Therapeutic approaches to gastric hepatoid adenocarcinoma: current perspectives. *Ther Clin Risk Manag*. (2019) 15:1469–77. doi: 10.2147/TCRM.S204303

13. Simmet V, Noblecourt M, Lizée T, Morvant B, Girault S, Soulié P, et al. Chemotherapy of metastatic hepatoid adenocarcinoma: literature review and two case reports with cisplatin etoposide. *Oncol Lett*. (2018) 15(1):48–54. doi: 10.3892/ol.2017.7263

14. Arakawa Y, Tamura M, Aiba K, Morikawa K, Aizawa D, Ikegami M, et al. Significant response to ramucirumab monotherapy in chemotherapy-resistant recurrent alpha-fetoprotein-producing gastric cancer: a case report. *Oncol Lett*. (2017) 14(3):3039–42. doi: 10.3892/ol.2017.6514

15. Bakhshi G, Borisa A, Bhandarwar A, Tayade M, Yadav R, Jadhav Y. Primary hepatic choriocarcinoma: a rare cause of spontaneous haemoperitoneum in an adult. *Clin Pract*. (2012) 2(3):e73. doi: 10.4081/cp.2012.e73

16. Ahn Y, Kim J, Park C, Kim T, Hwang S, Lee S. Multidisciplinary approach for treatment of primary hepatic choriocarcinoma in adult male patient. *Ann J Hepatobiliary Pancreat Surg*. (2018) 22(2):164–8. doi: 10.14701/ahbps.2018.22.2.164

frontiers | Frontiers in Surgery

TYPE Case Report
PUBLISHED 09 September 2022
DOI 10.3389/fsurg.2022.984853



OPEN ACCESS

EDITED BY
Riccardo Bertolo,
Hospital San Carlo di Nancy, Italy

REVIEWED BY
Andee Dzulkarnaen Zakaria,
Universiti Sains Malaysia, Malaysia
Ketan Vagholkar,
Padmashree Dr. D.Y. Patil University, India

*CORRESPONDENCE
Qigang Li
ycliqigang@163.com

†These authors have contributed equally to this work and share first authorship

‡ORCID
Guowei Zhao
orcid.org/0000-0002-0129-7059
Wenjun Meng
orcid.org/0000-0002-6780-8720

SPECIALTY SECTION
This article was submitted to Surgical Oncology, a section of the journal Frontiers in Surgery

RECEIVED 02 July 2022
ACCEPTED 18 August 2022
PUBLISHED 09 September 2022

CITATION
Zhao G, Meng W, Bai L and Li Q (2022) Case report: An adult intussusception caused by ascending colon cancer.
Front. Surg. 9:984853.
doi: 10.3389/fsurg.2022.984853



# Case report: An adult intussusception caused by ascending colon cancer

Guowei Zhao[1†‡], Wenjun Meng[2†‡], Lian Bai[1] and Qigang Li[1*]

[1]Department of Gastrointestinal Surgery, Yongchuan Hospital, Chongqing Medical University, Chongqing, China, [2]Department of Biotherapy, Cancer Center, West China Hospital, Sichuan University, Chengdu, China

Adults with bowel intussusception caused by malignant tumors are fairly uncommon. We presented a case of a 64-year-old woman whose intussusception was secondary to ascending colon cancer. A color Doppler ultrasonography of the abdomen revealed a low echo mass in the right middle abdomen. Physical examination and digital rectal examination were both unremarkable. Computed tomography (CT) revealed a concentric circle change in the colon, as well as the mesenterium and arteries. Electronic colonoscopy discovered the colonic giant proliferative lesions and stenosis. Adenocarcinoma with moderate differentiation was discovered after a biopsy. Then laparotomy showed intussusception and the tumor was located in the ascending colon. The postoperative pathological test revealed moderately differentiated adenocarcinoma in the right colon invaded the whole layer. After hospitalization, the patient was discharged without any complications. This case highlights that rational use of CT, endoscopy, and timely surgery combines an effective strategy for the treatment of adult intussusception.

KEYWORDS
adult intussusception, colon cancer, computed tomography, colonoscopy, case report

## Introduction

Intussusception of the bowel is defined as the telescoping of a proximal segment of the gastrointestinal tract within the lumen of the adjacent segment. Adult intussusception represents 5% of all cases of intussusception and accounts for only 1%–5% of intestinal obstructions in adults (1, 2). Furthermore, adults with bowel intussusception caused by malignant tumors are fairly uncommon. To the best of our knowledge, there have only been a few reported cases of adult intussusception caused by colon cancer. Here, we presented a case of a 64-year-old woman whose intussusception was secondary to ascending colon cancer, which was diagnosed by abdominal computed tomography (CT) scan and colonoscopy.

## Case presentation

A 64-year-old woman was previously admitted to a local hospital 1 day ago for dizziness, hypodynamia, and loss of appetite. A color Doppler ultrasonography of the abdomen revealed a low echo mass in the right middle abdomen. For further

diagnosis and treatment, she was treated in our hospital with a chief complaint of the color Doppler ultrasonography finding an abdominal mass.

Anemia signs in the upper abdomen were observed, and there were no other typical pathological signs. Although color Doppler ultrasound showed an abdominal mass, no obvious mass was touched during abdominal palpation. Hemoglobin concentration: 74 g/L (normal range: 110–150 g/L), albumin concentration: 27.2 g/L (normal range: 35–55 g/L), total protein concentration: 56.2 g/L (normal range: 60–80 g/L). Based on the above information, our first clinical considerations for the abdominal mass were as follows: intestinal space-occupying lesions (possibly malignant tumors). Enhanced CT revealed a concentric circle change in the colon, as well as the mesenterium and arteries (**Figure 1**). The segment of the colon wall was edematous and thickened. To conclude, it was considered a tumor in the colon. Following an electronic colonoscopy, it was discovered that the colonic giant proliferative lesions had stenosis (**Figure 2**). Adenocarcinoma with moderate differentiation was discovered after a biopsy. After receiving the biopsy results, our medical group discussed and concluded that the patient should be treated with an operation, so elective laparoscopic right hemicolectomy was performed. During the operation, radiological examination results were confirmed. Finally, we found the tumor was located in the ascending colon, where the intestinal canal was partially inserted into the distal ascending colon. The range of lymph tissue we scavenged during the operation included the root of the ileocolic artery, the surrounding of the middle colon artery and vein, the root of the superior mesenteric artery, and the lower edge of the pancreas. We cut the transverse colon and ileum at 15 cm away from the tumor, and then anastomosed the ileum and transverse colon side-to-side. The tumor was about 7.0 cm × 6.0 cm × 2.0 cm, mass-type, hard, invaded the serosa, and occupied 2/3 circles of the intestine (**Figure 3**).

Gross examination of the resected specimen showed that the intestinal canal was 23 cm long, which contained the ascending colon tumor with a volume of 7.5 cm × 6.0 cm × 3.5 cm. The cross-section was gray-white and invaded membrana serosa. The pathological result showed a moderately differentiated adenocarcinoma invaded the whole layer; lymph nodes near the colon were negative (**Figure 4**). Immunohistochemistry: Ki67 (about 60%, +), MLH1 (+), MSH2 (+), MSH6 (+), PMS2 (+), Her-2 (weak +). The patient recovered smoothly and was discharged 12 days after the operation. She was followed up for 1 year, and there was no recurrence.

## Discussion

The incidence of adult intussusception is rare. While it is common in children, adult intussusception accounts for only 1% of intestinal obstruction and less than 5% of all cases of intussusception (1, 2). Different from children with apparent symptoms such as abdominal pain, abdominal mass, and

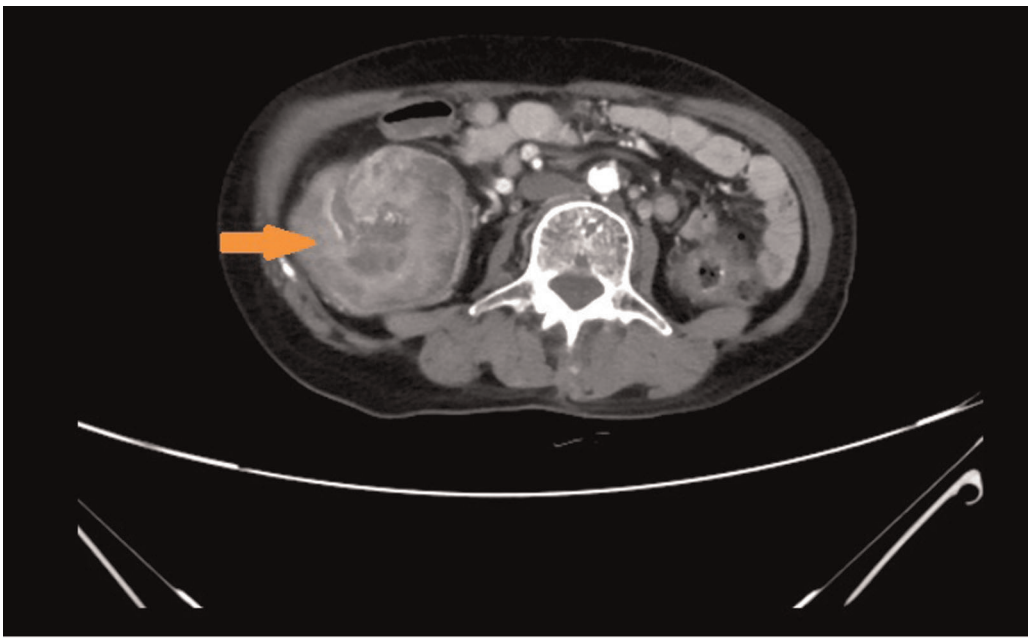

FIGURE 1
Computed tomography revealed ascending colonic intussusception.

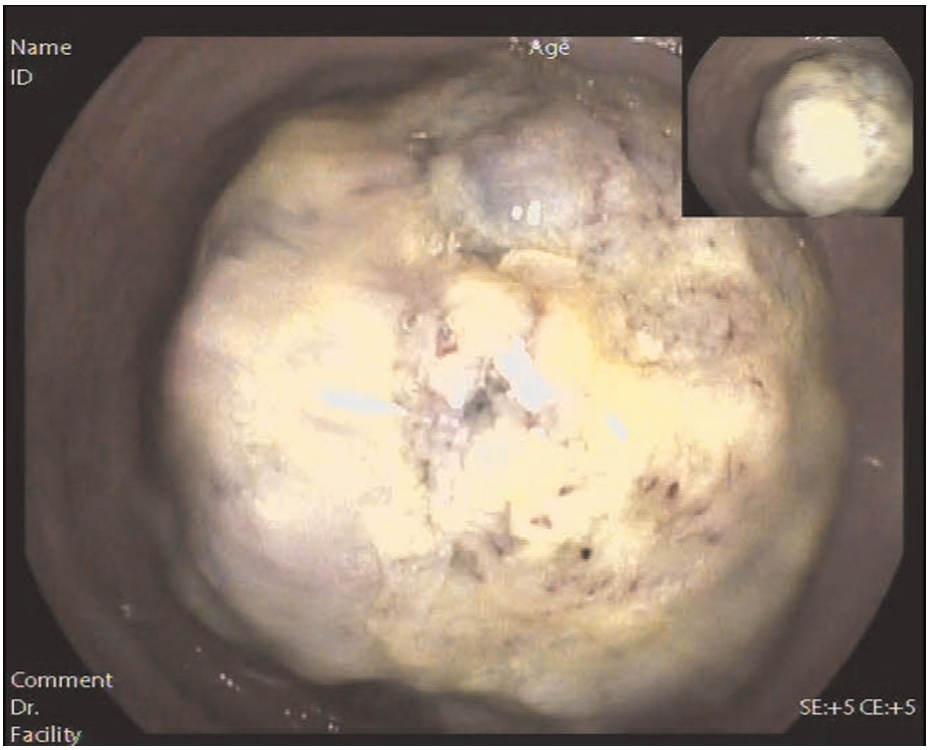


FIGURE 2
Electronic colonoscopy revealed a large proliferative lesion of the colon.

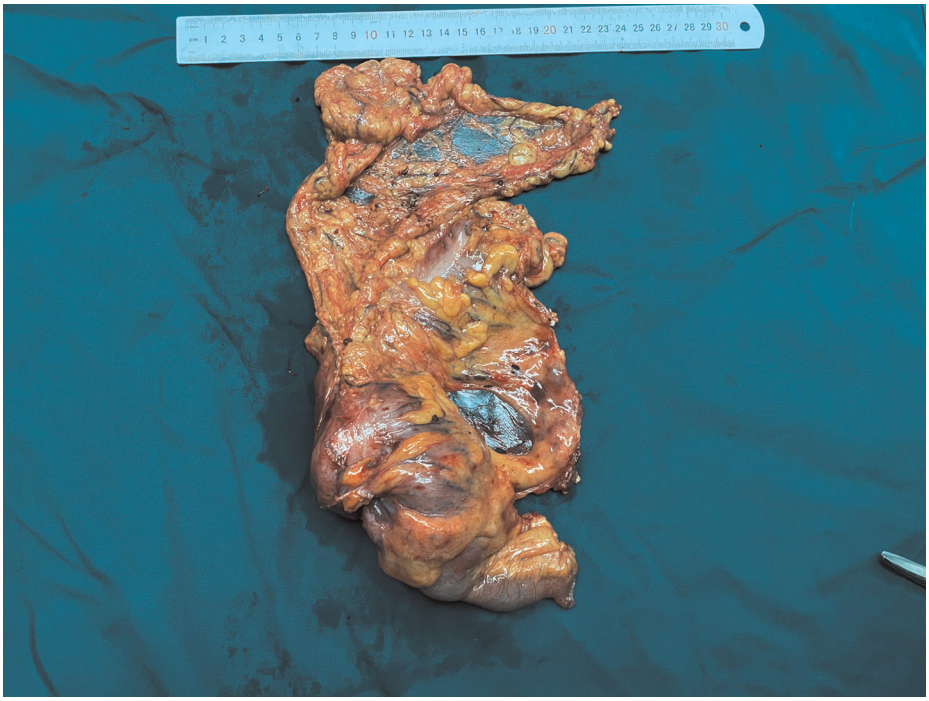

FIGURE 3
The surgical gross specimen.

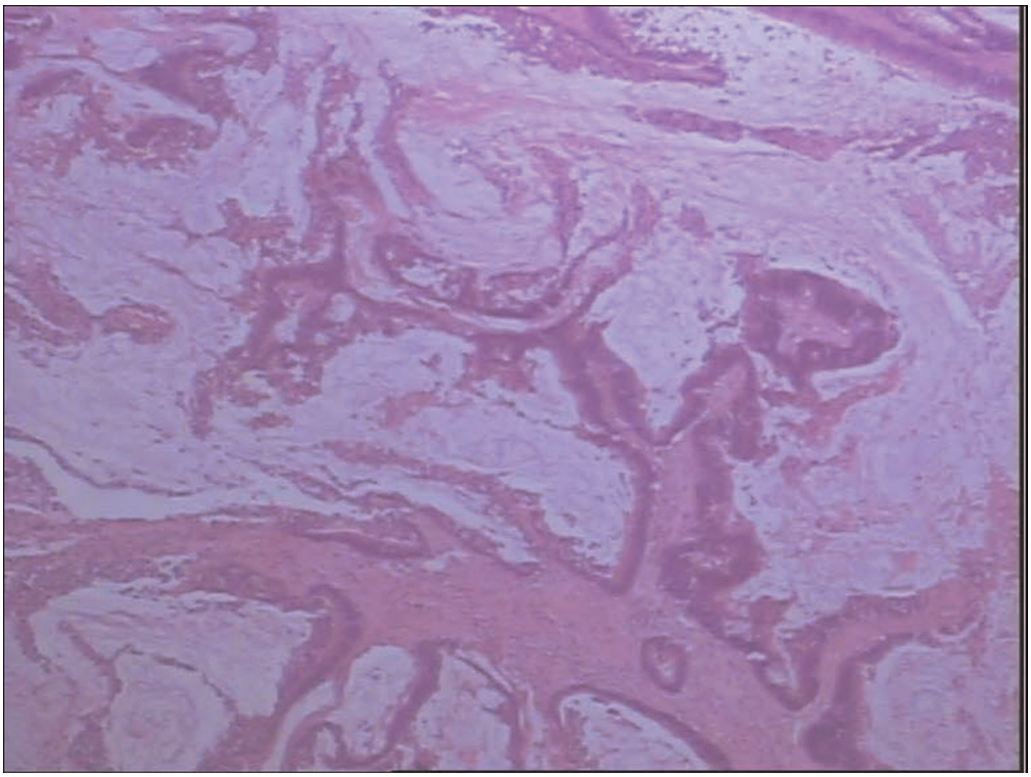

FIGURE 4
Postoperative pathological result revealed moderately differentiated adenocarcinoma in the right colon with full-thickness invasion (magnification power: 40×).

bloody stool, adults have various symptoms, which may be acute, intermittent, or chronic. Most affected adults develop pre-diagnosis episodes of intermittent abdominal pain and vomiting (3). In this case, the symptoms and signs had no obvious specificity, so it was difficult to diagnose and may have caused a delay in treatment.

In adult intussusception, 60% of cases are caused by malignant and benign neoplasms; the remaining non-idiopathic cases are usually caused by postoperative adherences, Crohn's disease, infections, intestinal ulcers, or Meckel diverticulum (2, 4). To help guide treatment decisions, it is important to diagnose the organic intussusception lesion. Enema or colonoscopy can detect and reduce intussusception, which is conducive to the qualitative diagnosis of organic lesions (5). Patients diagnosed with colonic or ileocolic intussusception are usually accompanied by tumors, and there are usually no clear clinical signs of acute abdomen. In these settings, preoperative endoscopy can be performed to confirm the presence of pathology and/or cancer (6). Compared with ultrasonography, barium enema, and colonoscopy, CT is the most accurate preoperative diagnostic method. In a recent report by Hong et al. (7), abdominal CT accurately diagnosed intussusception in 77.8% of patients. Eventually, this patient was diagnosed with intussusception by CT and confirmed benign and malignant lesions by colonoscopy biopsy. Therefore, when the clinical manifestations are difficult to diagnose, CT should be routinely performed to make a definite diagnosis. In addition, colonoscopy can also be used to distinguish benign or malignant lesions for ileocecal and colonic intussusception (8).

At present, surgery is still the main treatment for adult intussusception. It is determined according to the length of the affected intestine in patients with intussusception. In other words, if the affected portion of the small intestine is not extensive, surgery cannot reduce the intussusception. If resection of a long segment of the bowel is required, intraoperative reduction can be attempted to reduce the resection length (9). Because malignant diseases are highly correlated with intussusception in adults, surgical resection without reduction should be limited to primary malignant disease. However, when the small bowel is the only tract involved, the reduction of bowel intussusception can be attempted because of its lower rate of association with malignancy (10). Primary adenocarcinoma is the main cause of colon intussusception. Considering the high incidence of primary adenocarcinoma, it should be resected without reduction in colonic intussusception (7). When tissue diagnosis is unavailable, intussusception is located in the

colon and is highly likely to be malignant lesions, it is advisable to follow the oncology principle of colon resection as a precautionary measure to provide the best opportunity for curative resection. Most surgeons believe that laparotomy is necessary for the treatment of adult intussusception because of the high incidence of underlying malignancy colon intussusception, and the inability to differentiate benign or malignant in enteric intussusceptions (6). In a recent review article, it is reported that when there are signs and symptoms of acute abdomen, abdominal exploration is the gold standard; when there are signs of septic shock and peritonitis, emergency exploration is mandatory (6). Some surgeons believe that laparoscopic surgery can also be selected. The choice of laparoscopic surgery rather than open surgery depends on the clinical situation of patients and the experience of surgeons (11). Laparoscopic surgery cannot be selected in the following cases: (I) severe heart, lung, liver, or renal insufficiency; (II) severe coagulation dysfunction that is difficult to correct; (III) severe intestinal adhesion; and (IV) diffuse peritonitis with intestinal obstruction. In this case, a biopsy through enteroscopy confirmed that it was moderately differentiated adenocarcinoma. Therefore, laparoscopic right hemicolectomy was chosen, and total resection without reduction is performed to avoid potential intraluminal seeding or venous tumor dissemination. Eventually, right colon cancer was diagnosed, so the monitoring and evaluation of this case were also based on the right colon cancer.

In conclusion, although the optimal treatment for adult intussusception remains controversial, the definitive treatment depends on the underlying etiology and location. For stable patients without emergency indications for surgery, a thorough preoperative diagnostic evaluation and medical optimization should be performed. Because adult intussusception is highly correlated with malignant tumors, unless small bowel is the only tract involved or is proved to be benign by tissue diagnosis, it should follow the oncology principle of colon resection as a precautionary measure. When clinical manifestations are difficult to diagnose intussusception, CT is the most accurate method for a definite diagnosis. In addition, colonoscopy is recommended only when intussusception is located in the ileocecal and colon, which can not only assist the diagnosis, but also provide a reference for surgical methods.

## Data availability statement

The original contributions presented in the study are included in the article/Supplementary Material, further inquiries can be directed to the corresponding author/s.

## Ethics statement

Written informed consent was obtained from the individual(s) for the publication of any potentially identifiable images or data included in this article.

## Author contributions

Conceptualization: QL. Methodology: GZ. Writing—original draft preparation: GZ. Writing—review and editing: WM. Funding acquisition: WM. Resources: LB and QL. Supervision: QL. All authors contributed to the article and approved the submitted version.

## Funding

This work was supported by the Project of Innovative Foundation for Postgraduates in Yongchuan Hospital of Chongqing Medical University (YJSCX202012).

## Acknowledgments

We thank the funding agency for its financial support.

## Conflict of interest

The authors declare that the research was conducted in the absence of any commercial or financial relationships that could be construed as a potential conflict of interest.

## Publisher's note

## References


1. Marinis A, Yiallourou A, Samanides L, Dafnios N, Anastasopoulos G, Vassiliou I, et al. Intussusception of the bowel in adults: a review. *World J Gastroenterol*. (2009) 15(4):407–11. doi: 10.3748/wjg

2. Azar T, Berger DL. Adult intussusception. *Ann Surg*. (1997) 226(2):134–8. doi: 0.1097/00000658-199708000-00003

3. Yakan S, Caliskan C, Makay O, Denecli AG, Korkut MA. Intussusception in adults: clinical characteristics, diagnosis and operative strategies. *World J Gastroenterol*. (2009) 15(16):1985–9. doi: 10.3748/wjg.15.1985

4. Ghaderi H, Jafarian A, Aminian A, Mirjafari Daryasari SA. Clinical presentations, diagnosis and treatment of adult intussusception, a 20 years survey. *Int J Surg*. (2010) 8(4):318–20. doi: 10.1016/j.ijsu.2010.02.013

5. Omori H, Asahi H, Inoue Y, Irinoda T, Takahashi M, Saito K. Intussusception in adults: a 21-year experience in the university-affiliated emergency center and indication for nonoperative reduction. *Dig Surg*. (2003) 20:433–9. doi: 10.1159/000072712

6. Marsicovetere P, Ivatury SJ, White B, Holubar SD. Intestinal intussusception: etiology, diagnosis, and treatment. *Clin Colon Rectal Surg*. (2017) 30(1):30–9. doi: 10.1055/s-0036-1593429

7. Hong KD, Kim J, Ji W, Wexner SD. Adult intussusception: a systematic review and meta-analysis. *Tech Coloproctol*. (2019) 23:315–24. doi: 10.1007/s10151-019-01980-5

8. Wang LT, Wu CC, Yu JC, Hsiao CW, Hsu CC, Jao SW. Clinical entity and treatment strategies for adult intussusceptions: 20 years' experience. *Dis Colon Rectum*. (2007) 50(11):1941–9. doi: 10.1007/s10350-007-9048-8

9. Felix EL, Cohen MH, Bernstein AD, Schwartz JH. Adult intussusception: patient report of recurrent intussusception and review of the literature. *Am J Surg*. (1976) 131:758–61. doi: 10.1016/0002-9610(76)90196-3

10. Yalamarthi S, Smith RC. Adult intussusception: case reports and review of literature. *Postgrad Med J*. (2005) 81(953):174–7. doi: 10.1136/pgmj.2004.022749

11. Panzera F, Di Venere B, Rizzi M, Biscaglia A, Praticò CA, Nasti G, et al. Bowel intussusception in adult: prevalence, diagnostic tools and therapy. *World J Methodol*. (2021) 11(3):81–7. doi: 10.5662/wjm.v11.i3.81

frontiers | Frontiers in Surgery

TYPE Case Report
PUBLISHED 22 September 2022
DOI 10.3389/fsurg.2022.1006020



OPEN ACCESS

EDITED BY
Zhaolun Cai,
Sichuan University, China

REVIEWED BY
Roy Hajjar,
Université de Montréal, Canada
Firdaus Hayati,
University of Malaysia Sabah, Malaysia

*CORRESPONDENCE
Dingwei Chen
11118152@zju.edu.cn

†These authors have contributed equally to this work and share first authorship

SPECIALTY SECTION
This article was submitted to Surgical Oncology, a section of the journal Frontiers in Surgery

RECEIVED 28 July 2022
ACCEPTED 06 September 2022
PUBLISHED 22 September 2022

CITATION
Lin T, Bissessur AS, Liao P, Yu T and Chen D (2022) Case report: Stent-first strategy as a potential approach in the management of malignant right-sided colonic obstruction with cardiovascular risks.
Front. Surg. 9:1006020.
doi: 10.3389/fsurg.2022.1006020



# Case report: Stent-first strategy as a potential approach in the management of malignant right-sided colonic obstruction with cardiovascular risks

Tianyu Lin[1†], Abdul Saad Bissessur[2†], Pengfei Liao[1], Tunan Yu[1] and Dingwei Chen[1*]

[1]Department of General Surgery, Sir Run Run Shaw Hospital, School of Medicine, Zhejiang University, Hangzhou, China, [2]Department of Surgical Oncology, Sir Run Run Shaw Hospital, School of Medicine, Zhejiang University, Hangzhou, China

In obstructing left-sided colonic or rectal cancer, endoscopic stent placement with the purpose of decompression and bridge to elective colon resection has been widely utilized and accepted. However, in malignant right-sided colonic obstruction, stent placement prior to colectomy is still highly controversial, due to lower clinical success and high anastomotic leak. We report a case of malignant right-sided colonic obstruction based on the radiological findings of irregular thickening of ascending colon wall and dilation of proximal large bowel on enhanced computed tomography scan. The 72-year-old woman presented with obvious abdominal distension. Due to concerning cardiovascular complications as intermittent chest pain and a long history of type 2 diabetes, a three-step therapeutic plan was instigated. Initially, a self-expandable metallic stent was placed palliatively to relieve the bowel obstruction. Consecutively, coronary angiography was performed, and two coronary stents were implanted to alleviate more than 80% stenosis of two main coronary arteries. One month later, laparoscopic radical resection of right colon and lymphadenectomy were successfully performed, with a blood loss less than 50 millimeters and a harvest of 29 lymph nodes, 1 being positive. The patient was discharged one week postoperatively with no complications, and received adjuvant chemotherapy one month later. During a follow-up of more than one year, the patient was in complete remission with no recurrence and cardiovascular events. In patients presenting with malignant right-sided colonic obstruction and peril of high cardiovascular risks, we propose colonic and coronary stent-first strategy to emergency surgery as a potential approach so as to ensure sufficient cardiovascular preparation improving perioperative safety. Moreover, the anatomical location of the tumor would be significantly achievable thus granting high-quality radical colon resection and lymphadenectomy.

KEYWORDS

colonic obstruction, coronary stent, cardiovascular risk, self-expandable metallic stent, stent-first strategy, case report

## Core tip

Stenting has proven its effectiveness, predominantly in achieving a better quality of life, such as minimizing the use of colostomy, reducing medical costs and hospital stay. The role of stenting as a bridge to surgery for patients with left colonic obstruction should be debated from right-sided as stenting is strongly recommended as the alternative to emergency resection in left-sided malignant obstruction whereas its use in right-sided is still debatable and controversial. This case highlights the beneficial impact of stenting in right sided malignant colonic obstruction in a patient presenting with concurrent coronary artery stenosis.

## Introduction

Colorectal cancer is one of the most common cancers worldwide, ranking third in terms of incidence but as high as second with regard to mortality (1). Incidence rates tend to be higher in economically developed countries (2). Around one tenth of colon cancer initially present with bowel obstruction and present most commonly as abdominal pain, distention and obstipation (3). The risk of obstruction varies depending on the tumor location which is about 25% in the proximal colon compared to 75% in the left colon and colonic cancer causing obstruction tends to be at a more advanced stage (4).

Traditionally, emergency surgery, involving colectomy and colostomy has been the mainstay treatment for large bowel obstruction, a life-threatening condition (5). In the past two decades however, newer methodologies and treatment such as self-expandable metal stent (SEMS) or stoma construction (6) have proven to be more beneficial in patients with poor clinical condition and other contraindications to emergency surgery (7). However, detecting whether bowel obstruction requires definite emergency surgery is largely based on clinical signs and symptoms; high fever, tachycardia and peritonitis are suggestive of perforation or ischemia and demand urgent colectomy (3). As recommended by the European Society of Gastrointestinal Endoscopy (ESGE) Guideline 2020, colonic stenting is applicable for clinical symptoms and radiological signs of malignant large bowel obstruction, without any tip-off signs of perforation (8).

Despite SEMS followed by colectomy in patients with malignant colonic obstruction have had more favorable perioperative outcomes compared to urgent colectomy, the role of stent-first strategy in right colonic obstruction should be analyzed separately from that of left colonic obstruction, and remains unsettled and controversial (9). The use of stenting as a bridge to surgery has been extensively studied for malignant left sided obstruction, with several meta analyses and retrospective studies favoring the use of stent as an oncologically safe alternative over urgent colectomy (10–16). Interestingly, the latest update of ESGE Guideline 2020 strongly recommend the use of stenting as a bridge to surgery as an alternative to emergency resection in patients with curable left-obstructing colon cancer (8). In contrast, in patients with malignant right colonic obstruction, controversies arise and stent placement as a bridge to surgery is not yet the standard treatment approach and limited data are available on the safety and feasibility (17).

Herein, we present an elderly patient with malignant right-sided colonic obstruction and high cardiovascular risks in very poor clinical condition. The stent-first strategy brought sufficient time to manage the cardiovascular symptoms of the patient, thus improving perioperative safety. Moreover, high quality radical resection and extensive lymphadenectomy were achieved due to improvements in anatomy owing to stent placement.

TABLE 1 Patient's laboratory results of blood chemistry.

| Parameter | Results | Reference value |
|---|---|---|
| White blood cell count ($\times 10^9$/L) | 13.3 | 3.5–9.5 |
| Neutrophils (%) | 84.0 | 40.0–75.0 |
| c-reactive protein (CRP) (mg/L) | 86.4 | <6.0 |
| Hemoglobin (g/L) | 109 | 130–175 |
| Total protein (g/L) | 65.3 | 65.0–85.0 |
| Albumin (g/L) | 33.7 | 40.0–55.0 |
| Glucose (mmol/L) | 16.51 | 4.30–5.90 |
| Sodium (mmol/L) | 133 | 135–147 |
| Ferritin (ng/ml) | 358.40 | 12–150 |
| Carcinoembryonic antigen (CEA) | 1.82 | 0–5 |
| CA125 | 46.91 | <35.00 |

## Case presentation

A 72-year-old female with obvious abdominal distention and pain for half a month was admitted at our hospital. Upon admission, she had intermittent chest pain in the inferior sternal region (pectoralgia) and tenderness in abdominal right lower quadrant. She had a long history of type 2 diabetes and underwent laparoscopic cholecystectomy 3 weeks prior to admission at a local hospital. Her abdominal symptoms did not alleviate and her medical condition deteriorated. She also complained about repeated chest distress. She had no significant personal and family history. Upon physical examination, the patient's blood pressure was 143/76 mmHg, respiratory rate was 12 bpm, pulse rate was 90 bpm with a body temperature of 36.5° C. No cachexia or dehydration signs was observed. Her lung and heart auscultation were normal without apparent murmur or friction. Abdominal distention was obvious and tenderness in right lower quadrant upon palpation. The elevated laboratory

findings are shown in **Table 1**, other laboratory evaluations were normal.

Enhanced abdominal computed tomography (CT) showed irregular thickening of ascending colon wall and proximal intestinal bowel dilation (**Figure 1**), suggesting malignant right-sided colonic obstruction. CT revealed no obvious ascites, liver metastasis or mesenteric lymph nodes enlargement. After carefully evaluating the patient's symptoms given her advanced age, cardiovascular symptoms (pectoralgia and chest distress) and more than 10 years' history of diabetes, a multidisciplinary team consultation consisting of gastrointestinal surgeons, cardiologists, an endoscopist and anesthesiologist devised a three-step plan: (1) SEMS to relieve bowel obstruction, (2) coronary angiography and placement of coronary stent, and (3) right hemicolectomy 1 month later.

SEMS was placed through endoscopy (**Figure 2**) and bowel obstruction was relieved. During this primary procedure, biopsy of the tumor sample was pathologically examined and indicated tubular villous adenoma, low-grade intraepithelial neoplasia and some high-grade intraepithelial neoplasia. Due to superficial sampling, no submucosal infiltration was observed, but adenocarcinoma could not be excluded.

Consecutively, coronary angiography revealed 80% and 90% stenosis in the middle and distal left anterior descending branch of the heart (**Figure 3A**) respectively and were subsequently alleviated by two coronary stents (**Figure 3B**). One month later, the patient underwent laparoscopic right hemicolectomy and wide mesenteric excision. During the surgery, multiple adhesions were observed in the abdominal cavity, and no obvious metastasis was noted. Blood loss was less than 50 milliliters. The tumor size was $6.5 \times 5$ cm (**Figure 4A**), infiltrating into the subserosal layer. Postoperative pathological examination revealed highly to moderately differentiated adenocarcinoma (**Figure 4B**), and 1 positive lymph node (1 +/29). Immunohistochemistry findings revealed MLH1(+), MSH2(+), MSH6(+), PMS2(+) (**Figures 4C–F**). The patient was staged as T3N1aM0 (Stage IIIB, Eighth Edition AJCC).

The patient was discharged 1 week postoperatively with no complications. One month later, the patient received adjuvant chemotherapy for 6 cycles with each regimen cycle consisting of rituximab 600 mg IVGTT D1, oxaliplatin 130 mg IVGTT D1, epirubicin 90 mg IVGTT D1, vincristine 2 mg IVGTT D1 and dexamethasone 15 mg IV D1-3. One and a half year later, the patient showed no signs of recurrence on follow-up.

## Discussion

Colorectal cancer ranked third regarding incidence and second in terms of leading cause of cancer death worldwide as of 2020, accounting for 1.9 million new cases and an estimate of over 930,000 deaths (1). The burden of colorectal cancer has increased since 2012, where 1.35 million new cases were reported with an estimate of 700,000 deaths (18) and is expected to increase by 60% with more than 2.2 million new cases annually and 1.1 million deaths by 2030 (19). Occurring in about 15% of colon cancer patients, large bowel obstruction has been associated with increasing postoperative complications, mortality and a poor 5-year survival rate (20–22).

Traditionally, emergency surgery has been the mainstay treatment for malignant large bowel obstruction. However, anastomotic leak is a major postoperative burden of emergency surgery (12, 17). Reported in the early 90s by Dohmoto et al. (23) and Tejero et al. (24), stent placement as a bridge to surgery, to which we refer as stent-first strategy, has revolutionized the treatment of colon cancer, not only palliatively but also as a preoperative treatment (bridge to surgery) before final treatment approach (colectomy or colostomy) in suitable patients (25), as observed in our case. Over the years, stenting has proven its usefulness and effectiveness, predominantly in achieving a better quality of life, such as minimizing the use of temporary or permanent colostomy as well as reducing medical costs and hospital stay (12, 26–29). Moreover, in patients with inoperable tumors or presenting at advanced stages, stenting grants earlier initiation of neoadjuvant chemotherapy (30). As observed in our case, stenting also advocates minimally invasive surgery such as laparoscopic colectomy (31), thereby reducing postoperative complications and hospital stay.

However, the role of stent-first strategy or stenting as a bridge to surgery for patients with left colonic obstruction should be debated from right colonic malignant obstruction. The use of stents in left colonic cancer or rectal cancer has been extensively studied and reported favorably in several meta-analyses involving over 30 studies (11, 12) and retrospective case series (10). It is noteworthy to mention that stenting as a bridge to surgery is strongly recommended as the alternative to emergency resection in left sided malignant obstruction as per the 2020 latest guideline of ESGE (8), an upgrade compared to the 2014 Guideline by Van Hooft et al. (32) where stent placement as a bridge to surgery was still not recommended, thus proving its efficiency. Nonetheless, pertaining to malignant right-sided colonic obstruction, stent-first strategy is still controversial and currently not accepted as the standard treatment, prioritizing emergency resection and primary anastomosis (33). Limited data are accessible about the effectiveness and feasibility of stenting in right-sided colonic obstruction (17, 34).

Previous studies demonstrating the astounding safety of anastomosis in emergency resection without mechanical bowel preparation obstruction could advocate for the lack of studies of stenting in malignant right-sided colonic (33, 35). Moreover, stent placement for right colonic obstruction is technically more challenging and arduous than left sided occlusions (9), originating from the difficulty of passaging

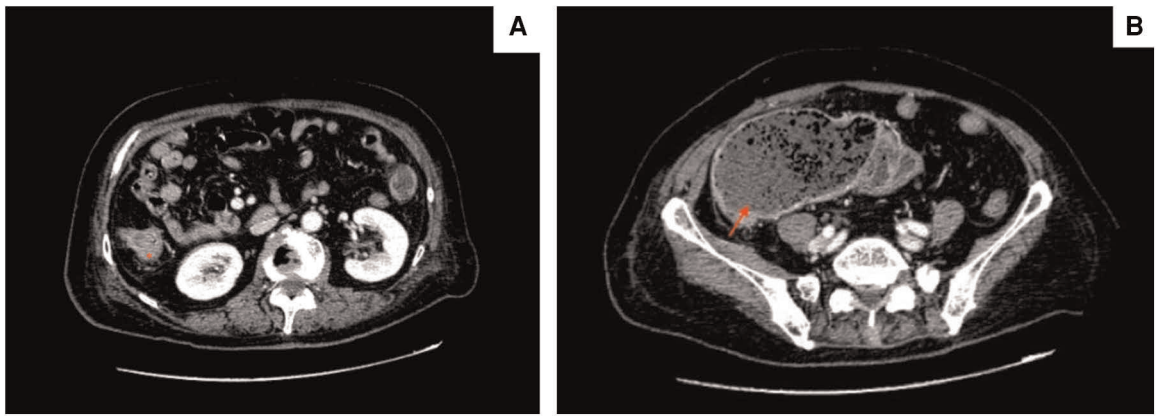


FIGURE 1
Ct scans showing (A) irregular thickening of ascending colon wall (marked by asterisk) and (B) proximal intestinal bowel distension (red arrow).

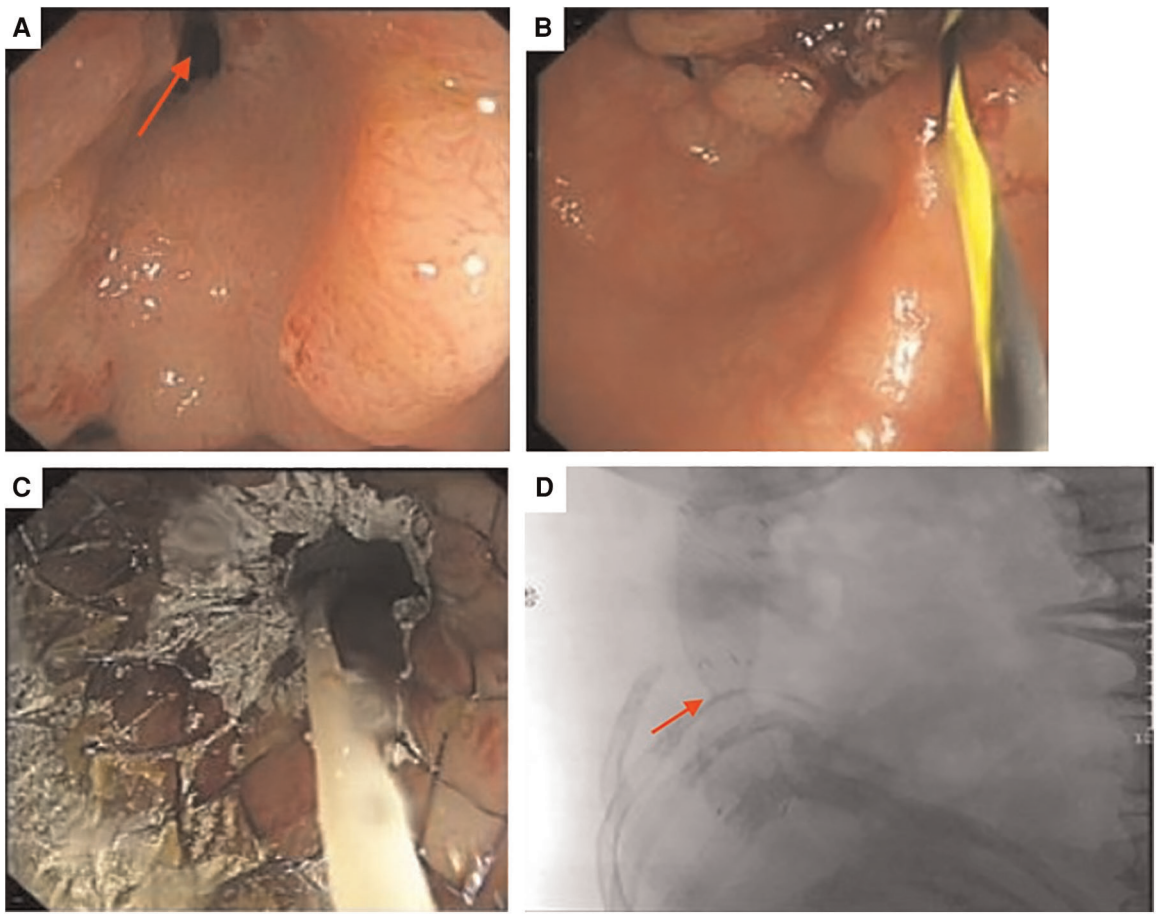


FIGURE 2
(A) Endoscopy revealing a narrowed intestinal lumen (red arrow). (B) Prior to placement of SEMS (C) successful stent placement relieving intestinal obstruction (D) x-ray showing location of stent and significant relief of intestinal obstruction.

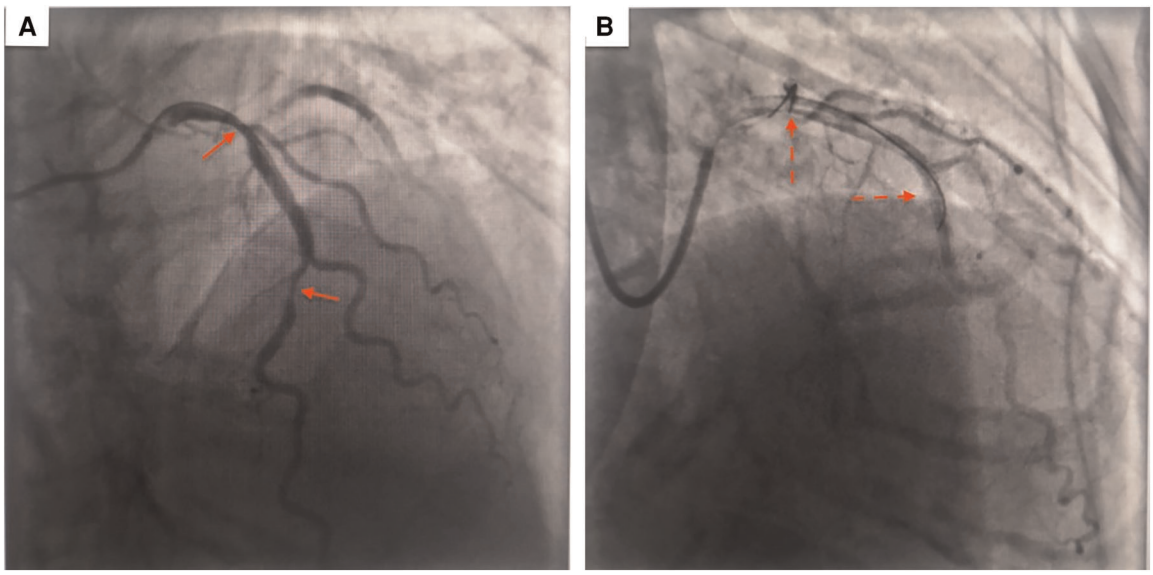


FIGURE 3
(A) Coronary angiography revealing 80% and 90% stenosis in the middle and distal left anterior descending branch of the heart (red arrow) (B) stenosis alleviated after placement of 2 stents (red dotted arrow).

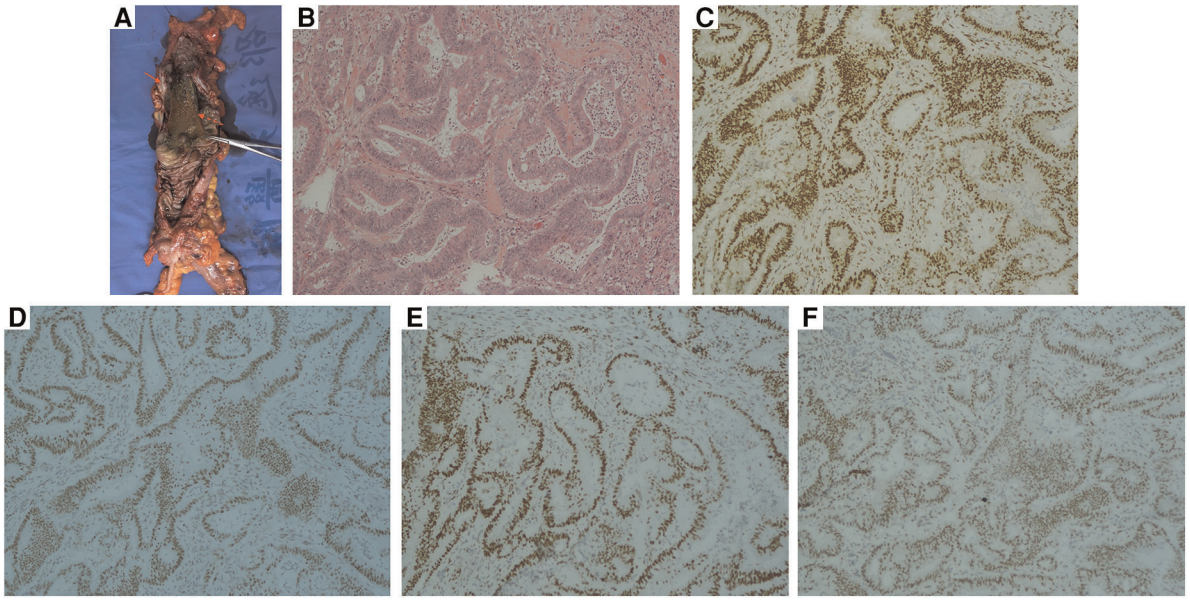


FIGURE 4
(A) A 6.5 cm × 5 cm tumor infiltrating the subserosal layer (red arrow). The previously placed stent can be observed (red dotted arrow) (B) histologic findings of right colonic adenocarcinoma following hematoxylin and eosin stain. Immunohistochemical positivity of (C) MLH1(+) (D) MSH2 (E) MSH6 (F) PMS2 (B–F, magnification ×200).

through obstructive lesions. However, recent studies (36–38) have reported a higher risk of anastomotic leak and mortality rate following emergency colectomy for malignant obstruction. These concerns elicited surgeons to find a safer approach such as stent-first strategy. A recently published meta-analysis concluded a significantly higher rate of successful primary anastomosis in stenting than the emergency surgery group (39). Stent placement also favors

mechanical bowel preparation finally resulting in end-to-end anastomosis without use of colostomy and stoma (40), thereby significantly improving quality of life. In addition, since obstructing colon cancer specifically affect elderly patients presenting with other morbidities (3, 41, 42), stent-first strategy could be life-saving, as observed in our patient.

Recent studies supported the outstanding virtue of stent-first strategy in malignant right-sided colonic obstruction. In a nationwide database study of 1,500 patients with malignant right colon obstruction, stenting followed by colectomy compared to emergency colectomy provided more beneficial perioperative outcomes such as lower morbidity, reduced need of stoma, reduced postoperative hospital stay and lesser surgical site infection (9). In a retrospective study of 98 patients who underwent stent-first strategy was associated with better operative and oncological outcomes including likelihood of laparoscopic approach, less estimated blood loss, faster post-operative restoration of gastrointestinal function, lower post-operative and wound-related complication rate (17). In a small sized study by Ji et al. (31) assessing 14 patients who successfully underwent stent placement, the rate of laparoscopic approach was higher in the stent-first group compared to the emergency group. In addition, time to resume oral food intake was shorter in the stent group. Despite its controversial use in right-sided colonic obstruction, a recent meta-analysis confers that stenting as a bridge to surgery results in a reduction of postoperative complications and mortality for right-sided malignant large bowel obstruction than emergency resection (43).

Timing of surgical resection following stent placement varies. The ESGE recommends approximately 2 weeks until resection (8). The above-mentioned retrospective study of 98 patients revealed a median interval time of 18.5 days between stenting and surgery (17), whereas the mean time for the small sized study of 14 patients was 7 days (31). In our case, since coronary stents were placed in conjunct with colonic stent, an interval of 1 month proved convenient. Nevertheless, primary colectomy after successful stent placement should be not be overly delayed as the major complications of stenting are recurrent colonic obstruction, stent migration or perforation (44). Additionally, the possible risk factors such as stent-related perforation, higher recurrence rates, permanent stoma, technical and clinical failure rates should be discussed with the patient prior to stent placement (8).

The drawbacks of stent-first strategy should not be overlooked. Previous studies concluded a higher rate of perineural invasion (45), lymphatic invasion (46) and increase in tumor cells dissemination (47) following stent placement. Moreover, a study by Maruthachalam et al. (48) revealed an increase in circulating cytokeratin 20 mRNA levels following stent placement. Stent placement also carries the risk of perforations (49) and has been associated with a worse survival rate (50), although a recent trial found no significant difference in overall survival and disease free survival between stent as bridge to surgery and emergency surgery at a minimum follow up of 3 years (51). Thus, stent placement has been recommended only in high-risk patients with an ASA score of 3 or higher and in patients older than 70 (32). Noteworthy, given that different studies brought different results and conclusions, stenting should be performed by endoscopist with adequate expertise (39). This could be a possible hypothesis as to why different studies have different conclusions.

In a nutshell, stent-first strategy was beneficial to this patient for 2 main aspects: (1) After bowel decompression, enough time was allocated for sufficient cardiovascular optimization, especially improvement of coronary stenosis, increasing anesthetic safety and reducing perioperative cardiovascular events including ischemia, myocardial infarction and lethal arrhythmia. Secondly, a 1-month interval between stenting and hemi-colectomy, tissue edema was resolved and laparoscopic approach deemed successful, increasing not only short term outcomes but also favoring oncological outcomes.

## Conclusion

In patients with malignant right-sided colonic obstruction and cardiovascular risk, stent-first strategy had the upper hand of allocating enough time for cardiovascular preparation, and improving perioperative safety. Moreover, better anatomical conditions were achieved due to stent placement, thus favoring minimally invasive surgery, which decrease postoperative complications and facilitate early recovery.

## Data availability statement

The original contributions presented in the study are included in the article/Supplementary Material, further inquiries can be directed to the corresponding author/s.

## Ethics statement

The studies involving human participants were reviewed and approved by Sir Run Run Shaw Hospital, Zhejiang University School of Medicine. The patients/participants provided their written informed consent to participate in this study. Written informed consent was obtained from the individual(s) for the publication of any potentially identifiable images or data included in this article.

## Author contributions

CD designed the study; BS, LT, YT contributed to manuscript writing and performed data analysis; BS conducted literature review; YT, LT, LP contributed in data acquisition and manuscript preparation; YT, LT, CD were responsible for patient care and data analysis; YT, CD were the patient's surgeons; CD substantively reviewed the manuscript. All authors contributed to the article and approved the submitted version.

## Funding

Supported by Major Science and Technology Projects of Zhejiang Province, China, No. 2012C13014-4 and Natural Science Foundation of Zhejiang Province, China, No. Y19H160258.

## Acknowledgments

We gratefully thank Dr Tianhong Fu (Pathologist at Sir Run Run Shaw Hospital, School of Medicine, Zhejiang University) and Xiaozhe Shi (Radiologist at Sir Run Run Shaw Hospital, School of Medicine, Zhejiang University) for providing the relevant figures included in our manuscript. We thank the reviewers for their insightful and remarkable comments.

## Conflict of interest

The authors declare that the research was conducted in the absence of any commercial or financial relationships that could be construed as a potential conflict of interest.

## Publisher's note

All claims expressed in this article are solely those of the authors and do not necessarily represent those of their affiliated organizations, or those of the publisher, the editors and the reviewers. Any product that may be evaluated in this article, or claim that may be made by its manufacturer, is not guaranteed or endorsed by the publisher.

## References

1. Sung H, Ferlay J, Siegel RL, Laversanne M, Soerjomataram I, Jemal A, et al. Global cancer statistics 2020: GLOBOCAN estimates of incidence and mortality worldwide for 36 cancers in 185 countries. *CA Cancer J Clin*. (2021) 71 (3):209–49. doi: 10.3322/caac.21660

2. Jemal A, Bray F, Center MM, Ferlay J, Ward E, Forman D. Global cancer statistics. *CA Cancer J Clin*. (2011) 61(2):69–90. doi: 10.3322/caac.20107

3. Yeo HL, Lee SW. Colorectal emergencies: review and controversies in the management of large bowel obstruction. *J Gastrointest Surg*. (2013) 17 (11):2007–12. doi: 10.1007/s11605-013-2343-x

4. Deans GT, Krukowski ZH, Irwin ST. Malignant obstruction of the left colon. *Br J Surg*. (1994) 81(9):1270–6. doi: 10.1002/bjs.1800810905

5. Byrne JJ. Large bowel obstruction. *Am J Surg*. (1960) 99:168–78. doi: 10.1016/0002-9610(60)90111-2

6. Pisano M, Zorcolo L, Merli C, Cimbanassi S, Poiasina E, Ceresoli M, et al. 2017 WSES guidelines on colon and rectal cancer emergencies: obstruction and perforation. *World J Emerg Surg*. (2018) 13:36. doi: 10.1186/s13017-018-0192-3

7. Tekkis PP, Kinsman R, Thompson MR, Stamatakis JD, Association of Coloproctology of Great Britain Ireland. The association of coloproctology of Great Britain and Ireland study of large bowel obstruction caused by colorectal cancer. *Ann Surg*. (2004) 240(1):76–81. doi: 10.1097/01.sla.0000130723.81866.75

8. van Hooft JE, Veld JV, Arnold D, Beets-Tan RGH, Everett S, Gotz M, et al. Self-expandable metal stents for obstructing colonic and extracolonic cancer: European society of gastrointestinal endoscopy (ESGE) guideline - update 2020. *Endoscopy*. (2020) 52(5):389–407. doi: 10.1055/a-1140-3017

9. Sakamoto T, Fujiogi M, Lefor AK, Matsui H, Fushimi K, Yasunaga H. Stent as a bridge to surgery or immediate colectomy for malignant right colonic obstruction: propensity-scored, national database study. *Br J Surg*. (2020) 107 (10):1354–62. doi: 10.1002/bjs.11561

10. Amelung FJ, Borstlap WAA, Consten ECJ, Veld JV, van Halsema EE, Bemelman WA, et al. Propensity score-matched analysis of oncological outcome between stent as bridge to surgery and emergency resection in patients with malignant left-sided colonic obstruction. *Br J Surg*. (2019) 106(8):1075–86. doi: 10.1002/bjs.11172

11. Jain SR, Yaow CYL, Ng CH, Neo VSQ, Lim F, Foo FJ, et al. Comparison of colonic stents, stomas and resection for obstructive left colon cancer: a meta-analysis. *Tech Coloproctol*. (2020) 24(11):1121–36. doi: 10.1007/s10151-020-02296-5

12. Arezzo A, Passera R, Lo Secco G, Verra M, Bonino MA, Targarona E, et al. Stent as bridge to surgery for left-sided malignant colonic obstruction reduces adverse events and stoma rate compared with emergency surgery: results of a systematic review and meta-analysis of randomized controlled trials. *Gastrointest Endosc*. (2017) 86(3):416–26. doi: 10.1016/j.gie.2017.03.1542

13. Yang P, Lin XF, Lin K, Li W. The role of stents as bridge to surgery for acute left-sided obstructive colorectal cancer: meta-analysis of randomized controlled trials. *Rev Invest Clin*. (2018) 70(6):269–78. doi: 10.24875/RIC.18002516

14. Quereshy FA, Poon JT, Law WL. Long-term outcome of stenting as a bridge to surgery for acute left-sided malignant colonic obstruction. *Colorectal Dis*. (2014) 16(10):788–93. doi: 10.1111/codi.12666

15. Allievi N, Ceresoli M, Fugazzola P, Montori G, Coccolini F, Ansaloni L. Endoscopic stenting as bridge to surgery versus emergency resection for left-sided malignant colorectal obstruction: an updated meta-analysis. *Int J Surg Oncol*. (2017) 2017:2863272. doi: 10.1155/2017/2863272

16. Wang X, He J, Chen X, Yang Q. Stenting as a bridge to resection versus emergency surgery for left-sided colorectal cancer with malignant obstruction: a systematic review and meta-analysis. *Int J Surg*. (2017) 48:64–8. doi: 10.1016/j.ijsu.2017.10.004

17. Zeng WG, Liu MJ, Zhou ZX, Hu JJ, Wang ZJ. Stent as a bridge to surgery versus urgent surgery for malignant right colonic obstruction: a multicenter retrospective study. *ANZ J Surg*. (2021) 91(7-8):E500–E6. doi: 10.1111/ans.16942

18. Ferlay J, Soerjomataram I, Dikshit R, Eser S, Mathers C, Rebelo M, et al. Cancer incidence and mortality worldwide: sources, methods and major patterns in GLOBOCAN 2012. *Int J Cancer*. (2015) 136(5):E359–86. doi: 10.1002/ijc.29210

19. Arnold M, Sierra MS, Laversanne M, Soerjomataram I, Jemal A, Bray F. Global patterns and trends in colorectal cancer incidence and mortality. *Gut*. (2017) 66(4):683–91. doi: 10.1136/gutjnl-2015-310912

20. Ohman U. Prognosis in patients with obstructing colorectal carcinoma. *Am J Surg*. (1982) 143(6):742–7. doi: 10.1016/0002-9610(82)90050-2

21. Irvin TT, Greaney MG. The treatment of colonic cancer presenting with intestinal obstruction. *Br J Surg*. (1977) 64(10):741–4. doi: 10.1002/bjs.1800641015

22. Mulcahy HE, Skelly MM, Husain A, O'Donoghue DP. Long-term outcome following curative surgery for malignant large bowel obstruction. *Br J Surg*. (1996) 83(1):46–50. doi: 10.1002/bjs.1800830114

23. Dohmoto M. New method-endoscopic implantation of rectal stent in palliative treatment of malignant stenosis. *Endoscopia Digestiva*. (1991) 3:1507–12.

24. Tejero E, Mainar A, Fernandez L, Tobio R, De Gregorio MA. New procedure for the treatment of colorectal neoplastic obstructions. *Dis Colon Rectum*. (1994) 37(11):1158–9. doi: 10.1007/BF02049822

25. Trompetas V. Emergency management of malignant acute left-sided colonic obstruction. *Ann R Coll Surg Engl*. (2008) 90(3):181–6. doi: 10.1308/003588408X285757

26. Han SH, Lee JH. Colonic stent-related complications and their management. *Clin Endosc*. (2014) 47(5):415–9. doi: 10.5946/ce.2014.47.5.415

27. Spannenburg L, Sanchez Gonzalez M, Brooks A, Wei S, Li X, Liang X, et al. Surgical outcomes of colonic stents as a bridge to surgery versus emergency surgery for malignant colorectal obstruction: a systematic review and meta-analysis of high quality prospective and randomised controlled trials. *Eur J Surg Oncol*. (2020) 46(8):1404–14. doi: 10.1016/j.ejso.2020.04.052

28. Tung KL, Cheung HY, Ng LW, Chung CC, Li MK. Endo-laparoscopic approach versus conventional open surgery in the treatment of obstructing left-sided colon cancer: long-term follow-up of a randomized trial. *Asian J Endosc Surg*. (2013) 6(2):78–81. doi: 10.1111/ases.12030

29. Arezzo A, Balague C, Targarona E, Borghi F, Giraudo G, Ghezzo L, et al. Colonic stenting as a bridge to surgery versus emergency surgery for malignant colonic obstruction: results of a multicentre randomised controlled trial (ESCO trial). *Surg Endosc*. (2017) 31(8):3297–305. doi: 10.1007/s00464-016-5362-3

30. Lim TZ, Chan DKH, Tan KK. Endoscopic stenting should be advocated in patients with stage IV colorectal cancer presenting with acute obstruction. *J Gastrointest Oncol*. (2018) 9(5):785–90. doi: 10.21037/jgo.2018.06.03

31. Ji WB, Kwak JM, Kang DW, Kwak HD, Um JW, Lee SI, et al. Clinical benefits and oncologic equivalence of self-expandable metallic stent insertion for right-sided malignant colonic obstruction. *Surg Endosc*. (2017) 31(1):153–8. doi: 10.1007/s00464-016-4946-2

32. van Hooft JE, van Halsema EE, Vanbiervliet G, Beets-Tan RG, DeWitt JM, Donnellan F, et al. Self-expandable metal stents for obstructing colonic and extracolonic cancer: European society of gastrointestinal endoscopy (ESGE) clinical guideline. *Endoscopy*. (2014) 46(11):990–1053. doi: 10.1055/s-0034-1390700

33. Smithers BM, Theile DE, Cohen JR, Evans EB, Davis NC. Emergency right hemicolectomy in colon carcinoma: a prospective study. *Aust N Z J Surg*. (1986) 56(10):749–52. doi: 10.1111/j.1445-2197.1986.tb02320.x

34. Repici A, Adler DG, Gibbs CM, Malesci A, Preatoni P, Baron TH. Stenting of the proximal colon in patients with malignant large bowel obstruction: techniques and outcomes. *Gastrointest Endosc*. (2007) 66(5):940–4. doi: 10.1016/j.gie.2007.04.032

35. Conrad JK, Ferry KM, Foreman ML, Gogel BM, Fisher TL, Livingston SA. Changing management trends in penetrating colon trauma. *Dis Colon Rectum*. (2000) 43(4):466–71. doi: 10.1007/BF02237188

36. Lee YM, Law WL, Chu KW, Poon RT. Emergency surgery for obstructing colorectal cancers: a comparison between right-sided and left-sided lesions. *J Am Coll Surg*. (2001) 192(6):719–25. doi: 10.1016/S1072-7515(01)00833-X

37. Hsu TC. Comparison of one-stage resection and anastomosis of acute complete obstruction of left and right colon. *Am J Surg*. (2005) 189(4):384–7. doi: 10.1016/j.amjsurg.2004.06.046

38. Kobayashi H, Miyata H, Gotoh M, Baba H, Kimura W, Kitagawa Y, et al. Risk model for right hemicolectomy based on 19,070 Japanese patients in the national clinical database. *J Gastroenterol*. (2014) 49(6):1047–55. doi: 10.1007/s00535-013-0860-8

39. Cirocchi R, Arezzo A, Sapienza P, Crocetti D, Cavaliere D, Solaini L, et al. Current Status of the self-expandable metal stent as a bridge to surgery versus emergency surgery in colorectal cancer: results from an updated systematic review and meta-analysis of the literature. *Medicina*. (2021) 57(3):5–6. doi: 10.3390/medicina57030268

40. Dionigi G, Villa F, Rovera F, Boni L, Carrafiello G, Annoni M, et al. Colonic stenting for malignant disease: review of literature. *Surg Oncol*. (2007) 16(Suppl 1):S153–5. doi: 10.1016/j.suronc.2007.10.017

41. Tanis PJ, Paulino Pereira NR, van Hooft JE, Consten EC, Bemelman WA, Dutch Surgical Colorectal Audit. Resection of obstructive left-sided colon cancer at a national level: a prospective analysis of short-term outcomes in 1,816 patients. *Dig Surg*. (2015) 32(5):317–24. doi: 10.1159/000433561

42. Cheynel N, Cortet M, Lepage C, Benoit L, Faivre J, Bouvier AM. Trends in frequency and management of obstructing colorectal cancers in a well-defined population. *Dis Colon Rectum*. (2007) 50(10):1568–75. doi: 10.1007/s10350-007-9007-4

43. Kanaka S, Matsuda A, Yamada T, Ohta R, Sonoda H, Shinji S, et al. Colonic stent as a bridge to surgery versus emergency resection for right-sided malignant large bowel obstruction: a meta-analysis. *Surg Endosc*. (2022) 36(5):2760–70. doi: 10.1007/s00464-022-09071-7

44. Lee HJ, Park SJ, Min BS, Cheon JH, Kim TI, Kim NK, et al. The role of primary colectomy after successful endoscopic stenting in patients with obstructive metastatic colorectal cancer. *Dis Colon Rectum*. (2014) 57(6):694–9. doi: 10.1097/DCR.0000000000000061

45. Kim HJ, Choi GS, Park JS, Park SY, Jun SH. Higher rate of perineural invasion in stent-laparoscopic approach in comparison to emergent open resection for obstructing left-sided colon cancer. *Int J Colorectal Dis*. (2013) 28(3):407–14. doi: 10.1007/s00384-012-1556-x

46. Balciscueta I, Balciscueta Z, Uribe N, Garcia-Granero E. Perineural invasion is increased in patients receiving colonic stenting as a bridge to surgery: a systematic review and meta-analysis. *Tech Coloproctol*. (2021) 25(2):167–76. doi: 10.1007/s10151-020-02350-2

47. Yamashita S, Tanemura M, Sawada G, Moon J, Shimizu Y, Yamaguchi T, et al. Impact of endoscopic stent insertion on detection of viable circulating tumor cells from obstructive colorectal cancer. *Oncol Lett*. (2018) 15(1):400–6. doi: 10.3892/ol.2017.7339

48. Maruthachalam K, Lash GE, Shenton BK, Horgan AF. Tumour cell dissemination following endoscopic stent insertion. *Br J Surg*. (2007) 94(9):1151–4. doi: 10.1002/bjs.5790

49. Sloothaak DA, van den Berg MW, Dijkgraaf MG, Fockens P, Tanis PJ, van Hooft JE, et al. Oncological outcome of malignant colonic obstruction in the Dutch stent-in 2 trial. *Br J Surg*. (2014) 101(13):1751–7. doi: 10.1002/bjs.9645

50. Sabbagh C, Browet F, Diouf M, Cosse C, Brehant O, Bartoli E, et al. Is stenting as "a bridge to surgery" an oncologically safe strategy for the management of acute, left-sided, malignant, colonic obstruction? A comparative study with a propensity score analysis. *Ann Surg*. (2013) 258(1):107–15. doi: 10.1097/SLA.0b013e31827e30ce

51. Arezzo A, Forcignano E, Bonino MA, Balague C, Targarona E, Borghi F, et al. Long-term oncologic results after stenting as a bridge to surgery versus emergency surgery for malignant left-sided colonic obstruction: a multicenter randomized controlled trial (ESCO trial). *Ann Surg*. (2020) 272(5):703–8. doi: 10.1097/SLA.0000000000004324

frontiers | Frontiers in Surgery

TYPE Case Report
PUBLISHED 22 September 2022
DOI 10.3389/fsurg.2022.968077



OPEN ACCESS

EDITED BY
Ulrich Ronellenfitsch,
Medical Faculty of the Martin-Luther-University Halle-Wittenberg, Germany

REVIEWED BY
Sasan Mirfakhraee,
University of Texas Southwestern Medical Center, United States
Aasim Maldar,
P. D. Hinduja Hospital and Medical Research Centre, India

*CORRESPONDENCE
Naishi Li
LNS@medmail.com.cn

†ORCID
Naishi Li
orcid.org/0000-0002-2261-7349

SPECIALTY SECTION
This article was submitted to Surgical Oncology, a section of the journal Frontiers in Surgery

RECEIVED 12 July 2022
ACCEPTED 06 September 2022
PUBLISHED 22 September 2022

CITATION
Wang X, Li N, Xie Y, Zhu L, Li J, Gu F and Xiao X (2022) Non-islet cell tumor hypoglycemia concurrent with acromegalic features: A case report and literature review.
Front. Surg. 9:968077.
doi: 10.3389/fsurg.2022.968077



# Non-islet cell tumor hypoglycemia concurrent with acromegalic features: A case report and literature review

Xiaojing Wang[1,2], Naishi Li[1*†], Yi Xie[3], Liang Zhu[4], Ji Li[5], Feng Gu[1] and Xinhua Xiao[1]

[1]Department of Endocrinology, Key Laboratory of Endocrinology of National Health Commission, Peking Union Medical College Hospital, Chinese Academy of Medical Science and Peking Union Medical College, Beijing, China, [2]Department of Endocrinology, Beijing Tsinghua Changgung Hospital, Tsinghua University, Beijing, China, [3]Department of Urology Surgery, Peking Union Medical College Hospital, Chinese Academy of Medical Science and Peking Union Medical College, Beijing, China, [4]Department of Radiology, Peking Union Medical College Hospital, Chinese Academy of Medical Science and Peking Union Medical College, Beijing, China, [5]Department of Pathology, Peking Union Medical College Hospital, Chinese Academy of Medical Science and Peking Union Medical College, Beijing, China

**Background:** Non-islet cell tumor hypoglycemia (NICTH) is a rare cause of hypoglycemia due to the overproduction of high molecular weight insulin-like growth factor (big-IGF2), which activates the insulin receptor and subsequently caused hypoglycemia. But NICTH with acromegaly had rarely been reported. We firstly reported a rare case of NICTH concurrent with acromegalic facial features induced by a retroperitoneal hemangiopericytoma and reviewed similar cases in the literature.
**Case presentation:** A 30-year old man was admitted to hospital because of recurrent unconscious, which usually occurred in the late afternoon or early morning before supper or breakfast. On one unconscious occasion, his blood glucose was 2.4 mmol/L. His consciousness recovered rapidly with intravenous 50% glucose administration. Physical examination showed that he had coarse oily facial features with acne, prominent forehead and brow, broad nose, prominent nasolabial folds. At the time of hypoglycemia, suppressed serum insulin, GH and IGF-1 levels was found. Computed Tomography further revealed a large left retroperitoneal mass measuring 7.0 cm × 12.3 cm × 13.0 cm. He underwent complete surgical resection of the mass. Surgical pathology demonstrated a hemangiopericytoma and strong positive for IGF-2. He did not experience further episodes of hypoglycemia after the operation during the 2.5 years follow-up.
**Conclusions:** Fibrous origin is the most common tumor type for NICTH with acromegaly features. NICTH should be considered in non-diabetic patients who have recurrent hypoglycemia along with suppressed serum insulin and IGF-1 levels.

KEYWORDS

non-islet cell tumor hypoglycemia, acromegaly, IGF-2, solitary fibrous tumor, hemangiopericytoma

## Introduction

Non-islet cell tumor hypoglycemia (NICTH) is a rare cause of hypoglycemia attributed to the overproduction of high molecular weight insulin-like growth factor (IGF-2), known as big-IGF2, by tumors (1). IGF-2 activates the insulin receptor, exerts insulin-like activity, and suppresses GH secretion *via* a negative feedback mechanism, resulting in hypoglycemia. In addition, IGF-2 can bind to the IGF-1 receptor, leading to acromegalic features in rare patients (1). The incidence of NICTH is estimated at one per million person-years (2). Many types of tumors have been associated with the development of NICTH (3). Although tumors of mesenchymal origin are commonly described, NICTH with acromegalic features has shown to be rare.

Here, we report a rare case of NICTH presenting with acromegaloid changes secondary to retroperitoneal hemangiopericytoma. We have also reviewed the current reports on NICTH with acromegalic features.

## Case presentation

A 30-year-old man was admitted to the outpatient Endocrinology clinic of Peking Union Medical Hospital (PUMCH) because of recurrent unconsciousness. Four months before this presentation, he had had three prior episodes of disorientation, visual changes, weakness, and palpitations in the late afternoon, and the symptoms were resolved following food intake. He did not receive any medical care. One month before admission, he was found unconscious in the early morning before eating breakfast at home and was transported by ambulance to the local hospital's emergency department. At the time of entry, his blood glucose was 2.4 mmol/L, and the patient rapidly recovered consciousness in response to intravenous 50% glucose administration. Notably, he experienced three similar episodes before this event and admission to PUMCH. He was then admitted for further evaluation and treatment following this critical information. The patient denied any history of diabetes, intake of hypoglycemic agents, and alcohol abuse. On review of his systems, he and his family noted nose enlargement, hyperhidrosis, increased acne, and coarse oily skin over approximately the last two years.

On admission, physical examination revealed a blood pressure of 146/96 mmHg, and his body mass index was 28.4 kg/m$^2$. He had coarse oily facial features with acne, a prominent forehead and brow, a broad nose, prominent nasolabial folds, and acanthosis nigricans. Furthermore, multiple skin tags were present in the neck and anterior chest.

Laboratory tests revealed that blood count, liver and renal function, tumor markers, thyroid function, and 24 h urinary catecholamine were all in normal ranges. The serum adrenocorticotropic and 24 h urinary free cortisol were high, but the low dose dexamethasone suppression test yielded a 24 h free cortisol of 1.76 ug. During a spontaneous morning hypoglycemia (2.2 mmol/L), the corresponding serum insulin level was less than 0.5 μIU/ml, C-peptide level was less than 0.05 ng/ml, proinsulin was 44 pg/ml. IGF-1 level was less than 25.0 ng/ml, and GH level was less than 0.05 ng/ml. The detailed laboratory findings are shown in **Table 1**. Based on the laboratory evaluation, the diagnoses including chronic liver disease, hypothyroidism, pheochromocytoma, adrenal insufficiency, and insulinoma were excluded, and NICTH was suspected. Contrast Computed Tomography (CT) further revealed a large left retroperitoneal mass measuring 7.0 cm × 12.3 cm × 13.0 cm with heterogeneous density, while enhanced CT scans showed moderately uneven enhancement (**Figure 1**).

Following these assessments, laparotomy was performed. Intraoperatively, an about 12 cm * 12 cm tumor with obvious varicose veins was found in the retroperitoneum, and the tumor adheres to the surrounding tissues. There was no visiable metastasis. After carefully sepatating the tumor, the patient underwent complete surgical resection of the mass (**Supplementary Figure S1**). Surgical pathology demonstrated a

TABLE 1 Laboratory findings on admission.

| | Value | Unit | Normal range |
|---|---|---|---|
| FBG | 2.2 | mmol/L | 3.9–6.1 |
| C-P | <0.05 | ng/ml | 0.8–4.2 |
| FINS | <0.5 | ng/ml | 5.2–17.2 |
| PINS | 42 | pg/ml | 30–180 |
| GH | <0.05 | ng/ml | <2.0 |
| IGF-1 | <25.0 | ng/ml | 117–329 |
| ALT | 27 | U/L | 9–50 |
| AST | 20 | U/L | 15–40 |
| Cre | 58 | μmol/L | 45–84 |
| TC | 4.03 | mmol/L | 2.85–5.70 |
| TG | 0.68 | mmol/L | 0.45–1.70 |
| HDL-c | 1.67 | mmol/L | 0.93–1.81 |
| LDL-c | 1.88 | mmol/L | <3.37 |
| Cortisol (8:AM) | 20.04 | μg/dl | 4.0–22.3 |
| ACTH (8:AM) | 92 | pg/ml | 0–46 |
| 24 hUFC | 242.06 | μg | 12.3–103.5 |
| 24 h urine DA | 300 | μg | 120.93–330.59 |
| 24 h urine E | 2.25 | μg | 1.74–6.42 |
| 24 h urine NE | 37.5 | μg | 16.69–40.65 |
| Free T3 | 4.07 | pg/ml | 1.80–4.10 |
| Free T4 | 1.21 | ng/dl | 0.81–1.89 |
| TSH | 1.568 | μIU/ml | 0.38–4.34 |

FBG, fasting blood glucose; C-P, C-peptide; FINS, fasting insulin; PINS, proinsulin; GH, growth hormone; IGF-1, insulin-like growth factor-1; ALT, alanine aminotransferase; AST, aspartate aminotransferase; TC, total cholesterol; TG, triglycerides; HDL, high density lipoprotein; LDL, low density lipoprotein; DA, dopamine; E, adrenaline; NE, Norepinephrine; ACTH, adrenocorticotrophic hormone; 24 hUFC, 24 h urinary free cortisol; FT3, free triiodothyronine; FT4, free thyroxine; TSH, thyroid stimulating hormone.

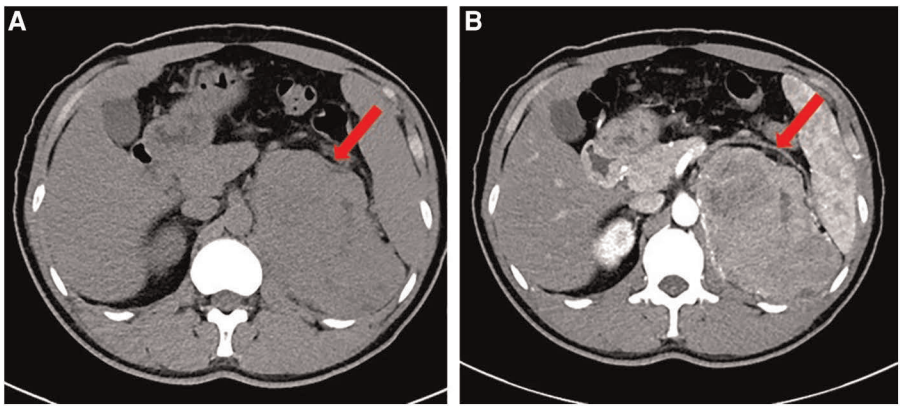


FIGURE 1
Computed tomography (CT) scan of the abdomen. (A). Non-Contrast CT. (B). Contrast CT.

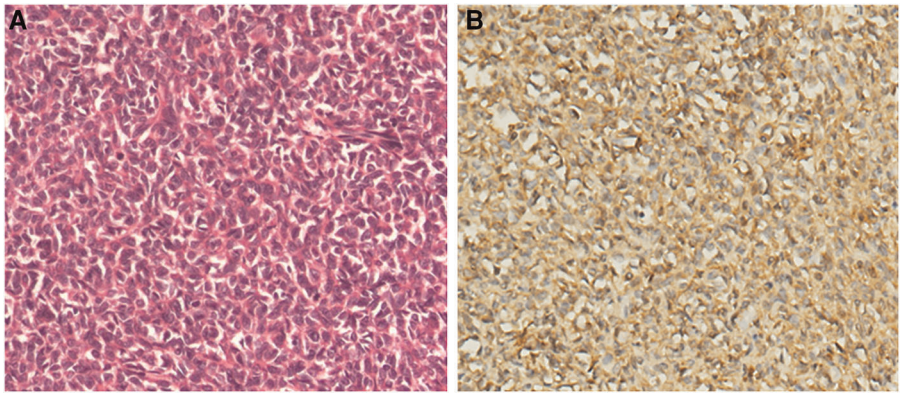


FIGURE 2
Pathological findings of the surgically resected tumors. (A). Hematoxylin-eosin (HE) staining (×150). (B). Immunostaining for IGF-2 is diffuse positive (×150).

hemangiopericytoma and a strong positive for IGF-2 (Figure 2). The ki-67 index was 15% (Supplementary Figure S2). He did not experience subsequent episodes of hypoglycemia after the operation. A CT scan of the patient's abdomen was conducted for monitoring in our hospital every six months, and a 2.5-year follow-up did not demonstrate any evidence of recurrence.

## Discussion

In 1988, Daughaday et al. reported the first case of NICTH due to IGF-2 tumor hypersecretion by thoracic leiomyosarcoma, and the recurrent severe hypoglycemia resolved after tumor resection (3). Since then, more than 200 clinical cases of NICTH have been described. It is now recognized that a comprehensive range of IGF-2-secreting tumor types is associated with hypoglycemia. Tumors of epithelial or mesenchymal origin are commonly reported, and the predominant etiology are hepatocellular carcinomas and fibrosarcomas, respectively (1). This is the first published case of NICTH with acromegalic features induced by retroperitoneal hemangiopericytoma, to the best of our knowledge.

The *IGF-2* gene, near the *INS* gene, is located on chromosome 11p15.5 and translated into the pre-pro-IGF-2 peptide, which is sequentially processed to pro-IGF2 and the 67-amino-acid mature IGF-2 (4). Typically, approximately 80% of IGF-2 is bound to IGFBP-3 and acid-labile subunit (ALS) in the circulation, forming a ternary 150-kDa complex. About 20% of IGF-2 is in a 50-kDa binary complex containing IGFBP-3 and IGF-2 (5). In IGF-2 secreting tumors, the increased IGF-2 mRNA expression produces a more considerable amount of pre-pro-IGF-2, leading to incomplete processing of pro-IGF-2 (known as big IGF-2) (6). The excessive big IGF-2 interfered with binding the pro-IGF-2-IGFBP-3 complex to ALS, and the proportion of ternary to binary complexes is reversed, with 20% ternary and 80% binary. Low levels of ALS and IGFBP-3 magnify the impaired binding of big-IGF-2 (7). The binary complexes can cross the capillary membrane and act on

TABLE 2 Reviewed current case reports on NICTH with acromegaloid changes.

| Year | Age | Sex | Tumor location | Histopathology | Tumor size | IGF-2:IGF-1 | Intervention |
|---|---|---|---|---|---|---|---|
| 2019 (11) | 60 | Male | Liver | Solitary fibrous tumors | 6 × 13 × 11 cm | 8.54 | Portal embolization + sugery + prednisone |
| 2019 (12) | 69 | Femal | Pleural | Solitary fibrous tumors | 17.5 cm | 20.4 | Sugery + prednisone + glucagon |
| 2019 (12) | 70 | Femal | Pleural | Solitary fibrous tumors | 21 cm | 31.8 | Sugery + prednisone |
| 2013 (13) | 77 | Male | Retroperitoneal mas | Fibroma | 16 × 16 cm | 23.6 | Sugery + chemotherapy + RT + prednisolone |
| 2013 (13) | 32 | Femal | Right suprarenal | Adrenocortical carcinoma | 15.3 × 12.7 × 12 cm | 8.6 | Sugery |
| 2011 (14) | 53 | Femal | Right adrenal gland | Phaeochromocytoma | 15 × 14 × 20 cm | 31.5 | Octreotide + diazoxide |
| 2006 (15) | 53 | Male | Liver | Solitary fibrous tumors | NA | NA | Sugery |
| 2000 (16) | 63 | Femal | Left lung | Pleural fibrosarcoma | 18 × 10 cm | 11.2 | Sugery |
| 1995 (17) | 60 | Male | Pelvic tumor | Clear cell sarcoma | NA | 3.3 | Sugery |

NA, not available; RT, radiation therapy.

insulin receptors in most tissues, which causes hypoglycemia (8). In addition, the suppressed GH and IGF-1 levels mediated by the negative feedback of increased IGF-2 *via* the IGF-1R in the hypothalamus also contribute to the hypoglycemic effects of IGF-2-omas. At present, a widely available assay for assessing big-IGF-2 is scarce. Although normal IGF-2 levels are frequently reported in NICTH (9), the IGF-2 to IGF-1 ratio is elevated, and the ratio exceeding 10:1 has been considered an important screening tool for NICTH (1, 10). In our case, the serum level of IGF-2 was not measured, but immunohistochemistry exhibited that the tumor cells highly expressed IGF-2. Regardless, undetectable IGF-1 and GH, along with suppressed insulin and C-peptide, strongly suggested hypoglycemia induced by IGF-2-producing tumor.

In addition to the hypoglycemia effect of IGF-2, growth-promoting changes have been described in rare instances of NICTH. In the present case, coarse acromegalic facial features were observed, which are thought to be mainly ascribed to IGF-2 activation of multiple subclasses of insulin-related and IGF-1 related receptors (1). We reviewed the literature on NICTH accompanied by acromegaliod face changes, and nine case reports were identified (11–17), see **Table 2**. The average age was 60 years (89% of patients above 50 years), with 5 females and 4 males. The most common tumor types were of mesenchymal origin, in line with previous observations. Fibrous tissue tumors (6 cases) were the most frequent among them. Pathologically, hemangiopericytoma is extremely similar to solitary fibrous tumors, but to the best of our knowledge, Hypoglycemia with acromegalic facial induced by hemangiopericytoma has not been reported. The tumors associated with NICTH are generally slow-growing and commonly quite large at the time of diagnosis (3). Fukuda et al. reported that 70% were larger than 10 cm in diameter (10). Hypoglycemia is usually the first presenting syndrome, which facilitates the identification of the tumors. In the present reviewed case series, the tumor diameter was greater than 10 cm in all patients, similar to our case. Besides, all patients had a ratio of IGF-2 to IGF-1 of more than 3, and five patients had a ratio greater than 10.

Regardless of tumor types, surgical resection is the mainstay of therapy for IGF-2-oma. Many case reports have frequently demonstrated resolution of hypoglycemia after complete resection (1). When total resection is impossible, debulking followed by chemotherapy and radiation (depending on tumor pathology) can be considered. These adjuvant treatments have also been reported to successfully ameliorate hypoglycemia (18). Except for tumor-directed therapies, glucocorticoids have been described as the most effective drugs for NICTH and are used as a "bridge" therapy to resection (19). In our reviewed case series, 4 cases included glucocorticoid treatment. One of the underlying mechanisms that glucocorticoids undertake to prevent hypoglycemia is suppressing the production of big-IGF-2 in a dose-dependent manner. Other agents such as rhGH, somatostatin analogs, and diazoxide have also been reported in a few cases (1).

In conclusion, we present a rare case of NICTH concurrent with acromegalic facial features induced by a retroperitoneal hemangiopericytoma. Data from literature indicate that fibrous origin is the most common tumor type for NICTH with acromegaly. NICTH should be considered in non-diabetic patients with recurrent hypoglycemia and suppressed serum insulin and IGF-1 levels. Earlier diagnosis of NICTH will help to completely resect the underlying tumor more successfully.

## Data availability statement

The original contributions presented in the study are included in the article/**Supplementary Material**, further inquiries can be directed to the corresponding author/s.

## Ethics statement

The studies involving human participants were reviewed and approved by PUMCH's Ethics Committee for Human Research. The patients/participants provided their written informed consent to participate in this case study. Informed consent for publication of clinical data was obtained from the patient.

## Author contributions

XJ-W wrote the manuscript. LZ analyzed and obtained pictures. JL and XH-X conducted the antibody staining and analyzed the results. YX did the surgery. NS- L and FG edited and guided writing of the manuscript. All authors contributed to the article and approved the submitted version.

## Acknowledgments

This work was funded by grants from the Beijing Natural Science Foundation (7214275), Beijing Hospital Authority Youth programme (QML20210901), and the Chinese Academy of Medical Sciences (CAMS) Innovation Fund for Medical Science (CIFMS; No. 2021-1-I2M-022). The authors thank the patient for participating the study.

## Conflict of interest

The authors declare that the research was conducted in the absence of any commercial or financial relationships that could be construed as a potential conflict of interest.

## Publisher's note



## Supplementary material

The Supplementary Material for this article can be found online at: https://www.frontiersin.org/articles/10.3389/fsurg.2022.968077/full#supplementary-material.

SUPPLEMENTARY FIGURE 1
Macroscopic view of the resected tumor.

SUPPLEMENTARY FIGURE 2
Immunostaining for Ki-67 (x150).

## References

1. Dynkevich Y, Rother KI, Whitford I, Qureshi S, Galiveeti S, Szulc A, et al. Tumors, IGF-2, and hypoglycemia: insights from the clinic, the laboratory, and the historical archive. *Endocr Rev*. (2013) 34(6):798–826. doi: 10.1210/er.2012-1033

2. Daughaday WH, Emanuele MA, Brooks MH, Barbato AL, Kapadia M, Rotwein P. Synthesis and secretion of insulin-like growth factor II by a leiomyosarcoma with associated hypoglycemia. *N Engl J Med*. (1988) 319 (22):1434–40. doi: 10.1056/NEJM198812013192202

3. Iglesias P, Diez JJ. Management of endocrine disease: a clinical update on tumor-induced hypoglycemia. *Eur J Endocrinol*. (2014) 170(4):R147–57. doi: 10.1530/EJE-13-1012

4. Sussenbach JS, Steenbergh PH, Holthuizen P. Structure and expression of the human insulin-like growth factor genes. *Growth Regul*. (1992) 2(1):1–9.

5. Zapf J. Insulinlike growth factor binding proteins and tumor hypoglycemia. *Trends Endocrinol Metab*. (1995) 6(2):37–42. doi: 10.1016/1043-2760(94)00144-S

6. Lawson EA, Zhang X, Crocker JT, Wang WL, Klibanski A. Hypoglycemia from IGF2 overexpression associated with activation of fetal promoters and loss of imprinting in a metastatic hemangiopericytoma. *J Clin Endocrinol Metab*. (2009) 94(7):2226–31. doi: 10.1210/jc.2009-0153

7. Khosravi J, Diamandi A, Mistry J, Krischna RG. The high molecular weight insulin-like growth factor-binding protein complex: epitope mapping, immunoassay, and preliminary clinical evaluation. *J Clin Endocrinol Metab*. (1999) 84(8):2826–33. doi: 10.1210/jcem.84.8.5914

8. Bond JJ, Meka S, Baxter RC. Binding characteristics of pro-insulin-like growth factor-II from cancer patients: binary and ternary complex formation with IGF binding proteins-1 to -6. *J Endocrinol*. (2000) 165(2):253–60. doi: 10.1677/joe.0.1650253

9. Cotterill AM, Holly JM, Davies SC, Coulson VJ, Price PA, Wass JA. The insulin-like growth factors and their binding proteins in a case of non-islet-cell tumour-associated hypoglycaemia. *J Endocrinol*. (1991) 131(2):303–11. doi: 10.1677/joe.0.1310303

10. Fukuda I, Hizuka N, Ishikawa Y, Yasymoto K, Murakami Y, Sata A, et al. Clinical features of insulin-like growth factor-II producing non-islet-cell tumor hypoglycemia. *Growth Horm IGF Res*. (2006) 16(4):211–6. doi: 10.1016/j.ghir.2006.05.003

11. De Los Santos-Aguilar RG, Chavez-Villa M, Contreras AG, Contreras AG, Garcia-Herrera JS, Gamboa-Dominguez A, et al. Successful multimodal treatment of an IGF2-producing solitary fibrous tumor with acromegaloid changes and hypoglycemia. *J Endocr Soc*. (2019) 3(3):537–43. doi: 10.1210/js.2018-00281

12. Jannin A, Espiard S, Benomar K, Do Cao C, Mycinski B, Porte H, et al. Non-islet-cell tumour hypoglycaemia (NICTH): about a series of 6 cases. *Ann Endocrinol (Paris)*. (2019) 80(1):21–5. doi: 10.1016/j.ando.2018.01.005

13. Dutta P, Aggarwal A, Gogate Y, Nahar U, Shah VN, Singla M, et al. Non-islet cell tumor-induced hypoglycemia: a report of five cases and brief review of the literature. *Endocrinol Diabetes Metab Case Rep*. (2013):130046. doi: 10.1530/EDM-13-0046

14. Macfarlane DP, Leese GP. Hypoglycaemia, phaeochromocytoma and features of acromegaly: a unifying diagnosis? *QJM*. (2011) 104(11):983–6. doi: 10.1093/qjmed/hcq219

15. Rabol R, Nielsen JF, Kirkegaard P, Mogensen AM, Johansen K. [Extrapancreatic tumour-induced hypoglycaemia]. *Ugeskr Laeger*. (2006) 168(5):488–9.

16. Bertherat J, Logie A, Gicquel C, Mourrieras F, Luton JP, Le Bouc Y. Alterations of the 11p15 imprinted region and the IGFs system in a case of recurrent non-islet-cell tumour hypoglycaemia (NICTH). *Clin Endocrinol (Oxf)*. (2000) 53(2):213–20. doi: 10.1046/j.1365-2265.2000.01064.x

17. Trivedi N, Mithal A, Sharma AK, Mishra SK, Pandey R, Trivedi B, et al. Non-islet cell tumour induced hypoglycaemia with acromegaloid facial and acral swelling. *Clin Endocrinol (Oxf)*. (1995) 42(4):433–5. doi: 10.1111/j.1365-2265.1995.tb02654.x

18. de Boer J, Jager PL, Wiggers T, Peter N, Machteld Wymenga AN, Pras E, et al. The therapeutic challenge of a nonresectable solitary fibrous tumor in a hypoglycemic patient. *Int J Clin Oncol*. (2006) 11(6):478–81. doi: 10.1007/s10147-006-0606-1

19. Teale JD, Wark G. The effectiveness of different treatment options for non-islet cell tumour hypoglycaemia. *Clin Endocrinol (Oxf)*. (2004) 60(4):457–60. doi: 10.1111/j.1365-2265.2004.01989.x

frontiers | Frontiers in Surgery

TYPE Case Report
PUBLISHED 23 September 2022
DOI 10.3389/fsurg.2022.963182



OPEN ACCESS

EDITED BY
Rocco Cappellesso,
University Hospital of Padua, Italy

REVIEWED BY
Liuyan Jiang,
Mayo Clinic Florida, United States
Xiaobing Liu,
The University of Hong Kong, China

*CORRESPONDENCE
Jie Li
lijiek812@yeah.net

†These authors have contributed equally to this work and share first authorship

SPECIALTY SECTION
This article was submitted to Surgical Oncology, a section of the journal Frontiers in Surgery

RECEIVED 07 June 2022
ACCEPTED 12 September 2022
PUBLISHED 23 September 2022

CITATION
Wang Z, Yuan J and Li J (2022) Case report: Ectopic thyroid tissue found in a liver with hepatocellular carcinoma.
Front. Surg. 9:963182.
doi: 10.3389/fsurg.2022.963182



# Case report: Ectopic thyroid tissue found in a liver with hepatocellular carcinoma

Zhanbo Wang†, Jing Yuan† and Jie Li*

Department of Pathology, The First Medical Center, Chinese PLA General Hospital, Beijing, China

**Background:** Concomitant intrahepatic ectopic thyroid is rare in patients with hepatocellular carcinoma. Thyroid follicular structures outside the hepatocellular carcinoma lesions are regarded as satellite nodules or intrahepatic metastases of hepatocellular carcinoma, which often leads to misdiagnosis and overtreatment of hepatocellular carcinoma patients.
**Case presentation:** We report the case of an 83-year-old man with moderately differentiated hepatocellular carcinoma (2.5 cm) whose liver contained ectopic thyroid tissue. An encapsulated, multinodular grayish-yellow mass and multiple satellite nodules were detected and removed by right hepatic lobectomy. Microscopically, the main tumor displayed a predominant trabecular, cord-like structure. Liver tissue 0.5 cm from the tumor had a benign-appearing follicular thyroid structure. The follicles contained colloid tissue and were lined with low cuboidal cells with scant cytoplasm; lymphatic tissue was also present in the area. The hepatocellular carcinoma cells were positive for hepatocyte antigen and glypican-3 and negative for cytokeratin 19. The follicular thyroid cells expressed thyroglobulin, PAX8, and thyroid transcription factor-1. A metastatic thyroid neoplasm was excluded clinically and by ultrasound and computed tomography. One month after surgery, all of the patient's serological markers were normal; no tumor recurrence or metastasis has been detected for 7 postoperative months.
**Conclusions:** The finding of ectopic thyroid tissue in the liver of a patient with hepatocellular carcinoma is very rare. The possibility of hepatocellular carcinoma forming satellite nodules and intrahepatic metastasis should be ruled out first and immunohistochemistry may be definitive in making the diagnosis. Further examination is needed to exclude thyroid cancer liver metastases.

KEYWORDS

ectopic thyroid tissue, hepatocellular carcinoma, thyroid transcription factor-1, glypican3, thyroid follicular carcinoma

## Introduction

Malignant hepatic tumors, including hepatocellular carcinoma, cholangiocarcinoma, and neuroendocrine tumors, may have a follicular thyroid structure (1, 2); ectopic thyroid tissue is rarely reported (3). Ectopic tissue in the liver may derive from structures such as the adrenal gland, pancreas, and spleen (4–6). When it is present, the possibility of thyroid cancer metastasis must be excluded by studying the patient's medical history and conducting ultrasound examination. No case of ectopic thyroid

tissue in the liver of a patient with hepatocellular carcinoma has been described in the literature. Here, we present a case of this rare condition.

## Case presentation

An 83-year-old man presented with a 6-month history of dull pain in the right abdomen. Serological examination revealed that he was negative for hepatitis B surface antigen and hepatitis C virus antibodies. On computed tomography examination, irregular and slightly low-density (~26 HU) shadows were observed in the right lobe of the liver, near the top of the diaphragm, representing a tumor measuring 29 × 23 mm with clear boundaries (**Figure 1**). Serological tests revealed that the patient had a carcinoembryonic antigen level of 5.38 μg/L (normal range, 0–5.0 μg/L), alpha fetoprotein level of 3.36 μg/L (normal range, 0–20 μg/L), carbohydrate antigen 19–9 level of 36.97 μ/ml (normal range, 0–37 μ/ml), and cancer antigen-125 level of 11.42 μ/ml (normal range, 0–35 μ/ml).

During the operation, the tumor was found to be located in the eighth segment of the right lobe of the liver; thus, the right hepatic lobe was partially resected. The tumor was a grayish-yellow mass (2.5 × 2 × 2 cm) located under the liver capsule with a clear boundary from surrounding tissues. Microscopic observation revealed that it was moderately differentiated hepatocellular carcinoma with a cord-like, trabecular structure and a pattern of local pseudoglandular growth. Some tumor cells were translucent, and multiple satellite nodules were found around the main tumor nodule (**Figures 2A,B**). An area of liver tissue (~0.3 cm) located 0.5 cm from the main tumor had a benign-appearing follicular thyroid structure (**Figures 2B,C**). The lesion was too small to appear on CT images. The follicles contained colloid tissue and were lined with low cuboidal cells with scant cytoplasm; lymphatic tissue was also present in the area.

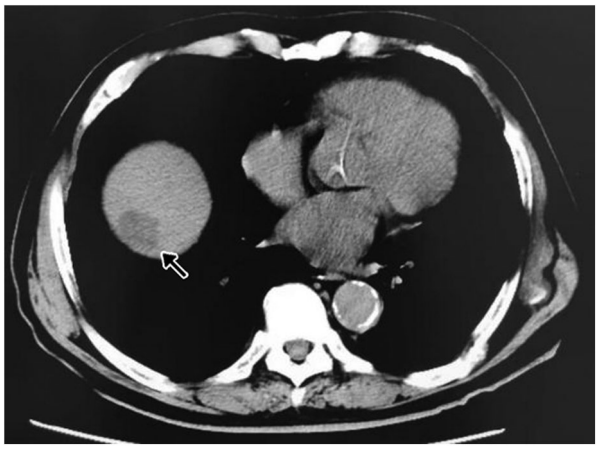

FIGURE 1
Ct image with irregular and slightly low-density shadows indicating a hepatocellular carcinoma lesion in the right lobe of the liver, near the top of the diaphragm (arrow).

Immunohistochemical (IHC) analysis of the hepatocellular carcinoma revealed hepatocyte antigen positivity, cytokeratin-19 negativity (**Figure 2D**), and glypican-3 (GPC-3) positivity (**Figure 2E**). Epithelial cells in the area with a follicular thyroid structure showed no atypia; they were negative for hepatocyte paraffin 1 (Hep Par-1) and positive for thyroglobulin (TG) (**Figure 2F**), PAX8 (**Figure 2G**), and thyroid transcription factor-1 (TTF-1; **Figure 2H**).

The patient had no history of a thyroid tumor, and thyroid function test results were normal. Thyroid hormone levels were in normal ranges (triiodothyronine, 1.27 ng/mL; thyroxine, 10.5 g/dl; free triiodothyronine, 3.84 pmol/L; and free thyroxine, 17.76 pmol/L).

Ultrasound examination showed no primary thyroid tumor. The final diagnosis was moderately differentiated hepatocellular carcinoma with heterotopic thyroid tissue in the liver. One month after surgery, all of the patient's serological markers were normal; no tumor recurrence or metastasis has been detected for 7 postoperative months.

## Discussion and conclusions

Ectopic tissue in the liver is occasionally reported; adrenal tissues and tumors of adrenal origin (i.e., adrenal heterotopia) are relatively common, found in 9.9% of unselected autopsy cases in one study (7). A search of the PubMed database yielded no report of a hepatocellular carcinoma case in which ectopic thyroid tissue was found in the liver, as in the case reported here.

Ectopic thyroid tissue is the result of abnormal embryonic development of the thyroid. Normally, the primordial thyroid base descends to a location between the thyroid cartilage and sixth tracheal cartilage ring before birth, where it develops into a normal thyroid. When this process fails, the thyroid base may remain between the foramen cecum of the tongue and the thyroid isthmus. Heterotopia of the thyroid gland is a relatively rare condition that primarily involves the liver.

The presence of ectopic thyroid tissue has no specific clinical manifestation, and preoperative diagnosis is difficult. Depending on the anatomical position of this tissue, patients may have non-specific clinical symptoms, such as wheezing and dyspnea, which are easily misdiagnosed and mistreated. The patient described here had no related symptom, and the ectopic thyroid lesion was too small to be detected by imaging.

Hepatic ectopic thyroid tissue must be differentiated from hepatic tumors and pseudolymphoma. Metastasis of a malignant thyroid tumor must be ruled out; distant metastases of thyroid cancer usually involve the lung, bone,

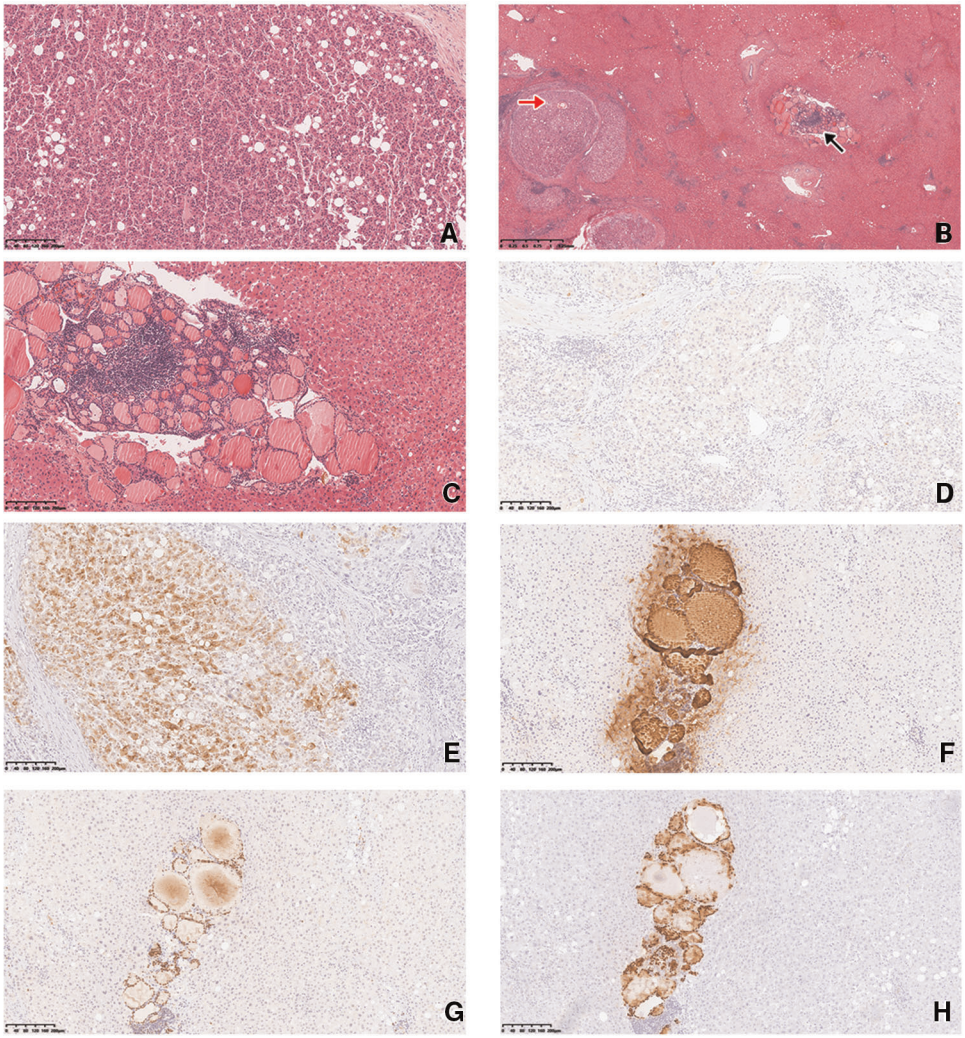


FIGURE 2
(A) The hepatocellular carcinoma had a trabecular structure, with some translucent cells. H&E staining, magnification 100×. (B) Multiple satellite nodules were present around the main tumor nodule (red arrow). Liver tissue 0.5 cm from the main tumor had a benign-appearing follicular thyroid structure (black arrow). H&E staining, magnification 20×. (C) The follicular epithelial cells showed no atypia. H&E staining, magnification 100×. (D) Immunohistochemical staining of the hepatocellular carcinoma was negative for CK-19 (D) and positive for GPC-3 (E). Magnification 100×. Immunohistochemical staining of the ectopic thyroid epithelial cells was positive for TG (F), PAX-8 (G), and TTF-1 (H). Magnification 100×.

and brain, with uncommon sites including the kidney, liver, pancreas, adrenal gland, and ovary (8). Follicular thyroid carcinoma may be difficult to differentiate from ectopic thyroid follicles; ultrasound of the thyroid gland and the patient's medical history are crucial for such differentiation. In the present case, the patient had no thyroid tumor or history thereof, and showed normal thyroid function. The structure of the ectopic thyroid follicles was normal, and the follicular epithelial cells showed no atypia. Thus, thyroid cancer metastasis could be excluded.

When ectopic thyroid tissue with a follicular structure is detected around a hepatocellular carcinoma lesion, as in the present case, the possibility of hepatic epithelial cancer with a thyroid follicular structure must be ruled out (9). Hepatocellular carcinoma that mimics the follicular thyroid structure, especially with a pseudoglandular growth pattern and bile production, is not uncommon. Intrahepatic cholangiocarcinoma and neuroendocrine tumors that mimic the thyroid structure have also been reported (1, 2). In such cases, a single IHC marker cannot be relied on; panels including Hep Par-1, GPC-3, TTF-1, PAX8, TG, synaptophysin, chromogranin A, CD56, and other indicators aid the diagnosis. In the present case, the follicular epithelium was TTF-1, PAX8, and TG positive, indicating that a malignant hepatic epithelial tumor imitating the follicular thyroid structure could be ruled out.

In conclusion, the finding of ectopic thyroid tissue in the liver of a patient with hepatocellular carcinoma is very rare. In such cases, primary tumors of the liver with follicular thyroid morphology, including hepatocellular carcinoma, intrahepatic cholangiocarcinoma, and neuroendocrine tumors, should first be ruled out. Especially in patients with primary liver malignancies, ectopic thyroid lesions may be misdiagnosed as satellite tumor nodules, which may lead to misjudgment of the patient's prognosis and over-treatment. It is also important to consider the patient's history thoroughly and to use imaging to exclude thyroid cancer metastasis.

## Data availability statement

The raw data supporting the conclusions of this article will be made available by the authors, without undue reservation.

## Ethics statement

The studies involving human participants were reviewed and approved by the Ethics Committees of the PLA General Hospital (Beijing, China). The patients/participants provided their written informed consent to participate in this study. Written informed consent was obtained from the individual for the publication of any potentially identifiable images or data included in this article.

## Author contributions

Conception and design: ZW, JY, JL; Administrative support: ZW, JY; Provision of study materials or patients: ZW; Collection and assembly of data: ZW, JY, JL; Data analysis and interpretation: ZW, JY, JL; Manuscript writing: All authors; Final approval of manuscript: All authors. All authors contributed to the article and approved the submitted version.

## Funding

This work was supported by a grant from the National Natural Science Foundation of China (no. 82072023).

## Conflict of interest

The authors declare that the research was conducted in the absence of any commercial or financial relationships that could be construed as a potential conflict of interest.

## Publisher's note

All claims expressed in this article are solely those of the authors and do not necessarily represent those of their affiliated organizations, or those of the publisher, the editors and the reviewers. Any product that may be evaluated in this article, or claim that may be made by its manufacturer, is not guaranteed or endorsed by the publisher.

## References

1. Chablé-Montero F, Shah BSA, Montante-Montes de Oca D, Angeles-Ángeles A, Henson DE, Albores-Saavedra J. Thyroid-like cholangiocarcinoma of the liver: an unusual morphologic variant with follicular, trabecular and insular patterns. *Ann Hepatol.* (2012) 11(6):961–5. doi: 10.1016/S1665-2681(19)31427-9

2. Ibrahim ME, Abadeer K, Zhai QJ, Nassar A. Primary hepatic neuroendocrine tumor with unusual thyroid follicular-like morphologic characteristics. *Case Rep Pathol.* (2017) 2017:7931975. doi: 10.1155/2017/7931975

3. Chen M, Hu J, Cai X. Ectopic thyroid gland tissue in the liver. *Clin Gastroenterol Hepatol.* (2020) 18(13):e157. doi: 10.1016/j.cgh.2019.09.042

4. Yu H, He Y. Hepatic adrenal adenoma-rare tumor on right lobe of liver: a case report and literature review. *BMC Surg.* (2020) 20(1):128. doi: 10.1186/s12893-020-00780-1

5. Limaïem F. [Intrahepatic ectopic pancreas]. *Pan Afr Med J.* (2020) 36:250. doi: 10.11604/pamj.2020.36.250.21309

6. Davidson LA, Reid IN. Intrahepatic splenic tissue. *J Clin Pathol.* (1997) 50 (6):532–3. doi: 10.1136/jcp.50.6.532

7. Honma K. Adreno-hepatic fusion. An autopsy study. *Zentralbl Pathol.* (1991) 137(2):117–22. https://pubmed.ncbi.nlm.nih.gov/1911725/

8. Yoon JH, Jeon MJ, Kim M, Hong AR, Kim HK, Shin DY, et al. Unusual metastases from differentiated thyroid cancers: a multicenter study in Korea. *PLoS One.* (2020) 15(8):e0238207. doi: 10.1371/journal.pone.0238207

9. Mullin EJ, Metcalfe MS, Maddern GJ. Differentiation of metastatic follicular thyroid cancer from hepatocellular carcinoma using Hep Par 1. *J Gastroenterol Hepatol.* (2007) 22(11):2047–8. doi: 10.1111/j.1440-1746.2006.03379.x

frontiers | Frontiers in Surgery

TYPE Case Report
PUBLISHED 23 September 2022
DOI 10.3389/fsurg.2022.1019425



OPEN ACCESS

EDITED BY
Zhaolun Cai,
Sichuan University, China

REVIEWED BY
Dorival De Carlucci,
University of São Paulo, Brazil
Qian Xiaoqin,
Jiangsu University Affiliated People's Hospital, China

*CORRESPONDENCE
Chunlei Nie
chunleinie@hrbmu.edu.cn

SPECIALTY SECTION
This article was submitted to Surgical Oncology, a section of the journal Frontiers in Surgery

RECEIVED 15 August 2022
ACCEPTED 12 September 2022
PUBLISHED 23 September 2022

CITATION
Ding Z, Chen M, Pang R, Sheng R, Zhao X and Nie C (2022) Case report: Balloon compression for cervical chyle leakage post neck dissection. Front. Surg. 9:1019425.
doi: 10.3389/fsurg.2022.1019425



# Case report: Balloon compression for cervical chyle leakage post neck dissection

Zhaoming Ding, Mengshi Chen, Rui Pang, Ruinan Sheng, Xuesong Zhao and Chunlei Nie*

Department of Thyroid Surgery, Harbin Medical University Cancer Hospital, Harbin, China

Postoperative chyle leakage (CL) is a rare but severe complication after neck dissection, and most patients with this complication can be treated conservatively. However, in patients with high-flow leakage, efficient and well-tolerated conservative treatment options are still lacking, and the treatments can be complicated. In this study, we report a case with CL of 1100 ml/day after neck dissection that was successfully treated by balloon compression.

KEYWORDS
chyle leakage, thyroid cancer, neck dissection, balloon compression, case report

## Introduction

Chyle leakage (CL) is a rare but severe complication of thyroid surgery with neck dissection, and the main cause of CL may be trauma to the thoracic duct and its main distribution (1). Prolonged CL can cause severe malnutrition, psychological depression, or even mortality. Prompt identification and treatment of CL are essential for optimal surgical outcomes (2).

Currently, there is no standardized treatment for the management of CL (3); usually, the first line of treatment is conservative management, such as a modified diet, drainage of effusion, pressure dressings, and the administration of octreotide and etilefrine (4), which are useful for most cases. However, high output fistulas (>1 L/day) or prolonged drainage with a low CL volume (a duration >7 to 14 days) will often respond unsatisfactorily to conservative management alone and require surgical intervention (5, 6). Herein, we report a case of a patient with high-volume cervical CL of 1100 ml/day who was treated successfully by balloon compression, and the patient successfully avoided reoperation. This study was reported in agreement with principles of the CARE guidelines (7).

## Case presentation

A 70-year-old man was admitted to our hospital due to the presence of a thyroid tumor and lymphadenopathy in the left lower neck diagnosed on US and CT. Fine-needle biopsy was used to make the diagnosis of PTC, clinically T1N1bM0. After discussing treatment options with the patient, total thyroidectomy with central and left lateral neck dissection was performed. During the operation, multiple metastatic

lymph nodes with a maximum diameter of 3 cm in level IV were cleared; on the premise of completing oncological resection, the trunk of the thoracic duct was preserved. In the thyroid cavity, a single drain was placed; in the left neck cavity, two drains were placed and drained out from the anterior and posterior edges of the sternocleidomastoid muscle separately. Histopathological examination revealed that a total of 43 lymph nodes were removed in the left lateral neck compartment, and 20 of them were found to have tumor metastasis. Among them, in level IV, the number of metastatic/total lymph nodes was 8/10.

Postoperatively (Figure 1), on the first postoperative day (POD1), the fluid in the lateral neck cavity drain was 200 ml/d, which was bloody in color, and this is common after surgery. On the second postoperative day (POD2), this drain produced 600 ml of milky fluid. The volume obtained from the drain increased to 1100 ml per day on POD3, even after the patient was treated with fasting, total parenteral nutrition and pressure dressings with elastic bandages. Because of the large amount of chyle, we speculated that it would be unlikely that conservative treatment would be effective, and the massive lymph loss may also be associated with mortality. Therefore, we decided to take some active interventions and designed a balloon-compression maneuver to improve the pressure dressing therapy. We removed the lateral neck drainage tube of the anterior edge of sternocleidomastoid, placed a size 14 sterile urinary catheter and retraced and connected a negative pressure drainage. The balloon was placed between the internal jugular vein and the sternal head of sternocleidomastoid, which was located by palpation. Then, 10 ml normal saline was injected into the balloon, creating local pressure at the possible lymphatic damage area at the venous angle (Figure 2). When the patient's neck moved, the balloon tended to move inward rather than fall out; therefore, we fixed the drainage tube on the chest wall skin with adhesive tape to ensure that the position of the balloon would be fixed. After balloon compression, the amount of discharge from the cervical drainage tube decreased immediately to 10 ml/24 h. On this day, we also removed the drain in the thyroid cavity, and the drain had a total drainage of 60 ml, which was hemoserous.

On POD5, we tentatively reduced the balloon volume to 5 ml, but the amount of discharge increased to 100 ml/6 h. We adjusted the balloon volume to 10 ml again, and the steady chyle leakage stopped. On POD7, we reduced the balloon volume to 5 ml, and the amount of discharge did not increase. The patient resumed a normal diet on POD8; during this time, there was still no volume of fluid that was collected. On POD9, the drainage tube was removed, the patient was discharged from the hospital on POD10, and no neck swelling was reported. No cervical chyle-related symptoms were found after one month of follow-up.

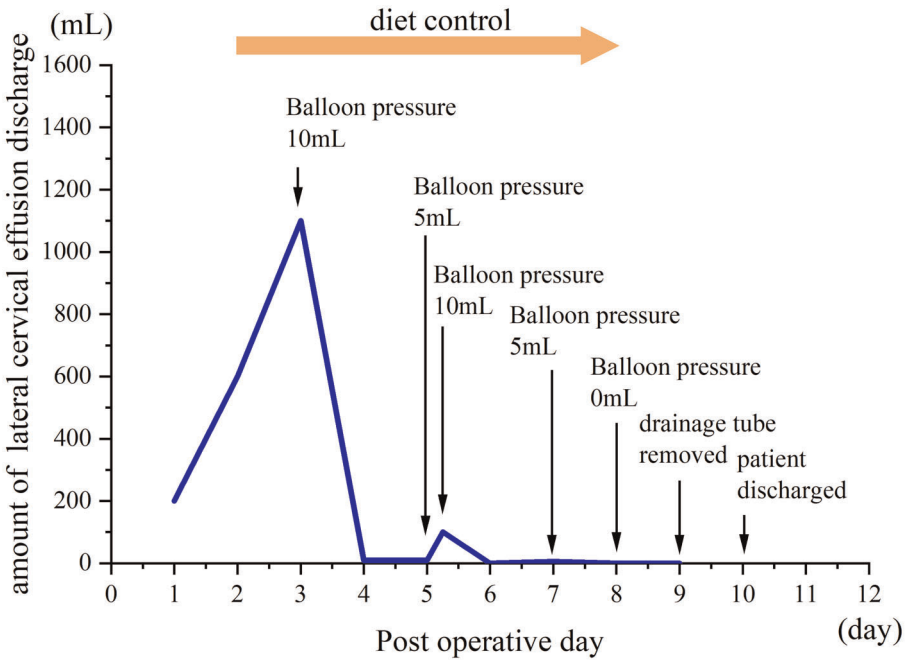


FIGURE 1
Postoperative progress and amount of discharge from lateral cervical drainage tube.

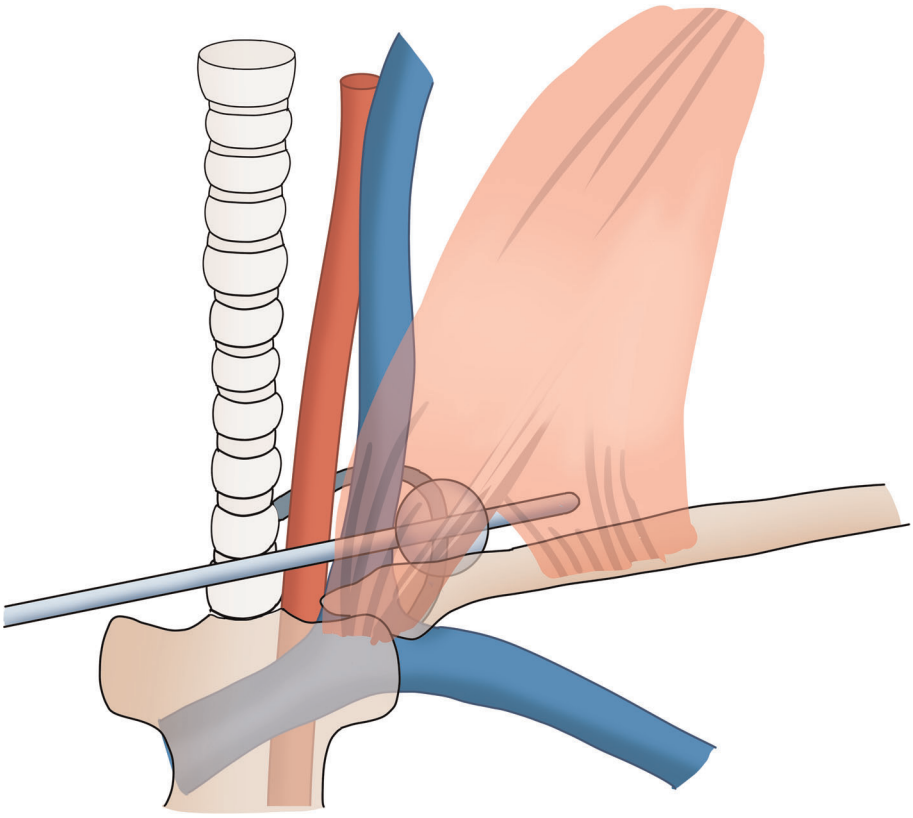

FIGURE 2
Schematic drawings of the balloon compression maneuver. Copyright © [2022] [Zhaoming Ding]: reproduced with permission.

## Discussion

Chyle leakage (CL) following neck dissection for thyroid carcinoma is infrequent but represents a serious complication. Several studies have reported chyle leakage incidences of 0.6%–1.4% after CND and 4.5%- 8.3% after lateral neck dissection (8–11). The incidence varies according to the surgical extent, and it more commonly occurs when extranodal extension is involved around the level IV compartment (12). According to the results of a previous study, a CL volume of 1 L/day is often used as a cutoff value to classify CL volumes as low and high (6). High-volume CL is a clinically inevitable and severe problem that can cause hypovolemia, malnutrition, electrolyte disturbances, metabolic imbalance, immunosuppression, dehydration, poor wound healing and prolonged length of hospital stay (13). Early identification and appropriate management of CL are imperative for optimal surgical outcomes. Meticulous protection of the thoracic duct during surgery is crucial to prevent CL, but the variation in the termination and fragility of the thoracic duct renders it difficult to avoid completely, even when the operation is performed by an experienced surgeon (14–17).

The management of CL that is detected postoperatively is challenging, and conservative management, including NPO with total parenteral nutrition, administration of medium-chain triglycerides and octreotide, repeated aspiration, negative pressure drainage, and pressure dressings (4), are the first-line treatment approaches, and these treatments are performed to promote spontaneous fistula closure by diminishing the chyle flow. However, if conservative therapy fails, invasive interventions are recommended, including lymphangiographic embolization of the thoracic duct, thoracoscopic thoracic duct ligation, and the use of local rotational muscle flaps to obliterate the leakage sites (17–19).

To date, there are no consensus guidelines on the timing of surgical exploration, and it is usually considered that surgical intervention should be decided upon within the first 4–5 days of CL when the patient does not develop a prompt response to medical management (20). Meanwhile, the surgical approach will cause patients to suffer more and is associated with an increase in complications. We aimed to find a new conservative treatment to cure CL postoperatively.

Pressure dressing is a simple, initial and effective approach that is applied in surgery to deal with hemorrhage or leakage. In the treatment of CL, pressure dressings are used to compress the

leaking chyle vessel and allow time for spontaneous closure (11, 20). However, traditional pressure dressings are ineffective for most patients when we use thick dressings with elastic bandages to put pressure on the lower neck. Since the thoracic duct is located deep in the venous angle and due to the occlusion of the anterior clavicle and sternocleidomastoid muscle, it is difficult to place an adequate amount of pressure on the precise point of leakage with only external pressure. Moreover, excessive pressure causes significant patient discomfort and affects skin flap viability (19). Interestingly, a previous study introduced a simple, finger-based pressing maneuver to stop CL, although it may be more challenging to widely adopt because of the labor required by the person carrying out continuous pressing; it is effective and comfortable compared with the traditional methods (21). In this case, we applied a new method based on balloon pressure. We used the balloon of a urinary catheter to compress the CL at the angle of the vein and accurately achieved appropriate and mild compression on the crucial pressing point.

We confirmed that the integrity of the thoracic duct trunk during the operation, as the TD route and terminations demonstrate many variations. We considered that this CL may be due to injury of an anatomical variation of TD terminations or its tributaries. Since the patient presented with high-output CL and failed to respond to conservative management, to avoid the burden of reoperation, we used a balloon to compress the venous horn to reduce the lymph exudation and provide conditions for spontaneous healing. To avoid the potential risk of chylothorax caused by excessive compression, another negative pressure drainage tube was kept indwelling until it was finally removed with the urinary catheter. In this case, our prompt treatment reduced the loss of lymph, the patient avoided reoperation, and the treatment shortened the hospital stay. To the best of our knowledge, this is the first and only case of CL treatment by balloon pressure. This treatment is simple, safe and well tolerated by patients, and the rapid reduction of drainage volume also increases the patient confidence and reduces anxiety.

This single case report had some limitations. First, we located the balloon by palpation, but this method is not accurate enough. It might be better to use guided ultrasound to locate the exact position of the damage and place the balloon. Second, we speculated where the point of leakage was located through clinical experience and intraoperative findings, and it might be better to determine the precise point of leakage before balloon pressure. Third, we overlooked the potential thrombotic risk of balloon compression on the vein; fortunately, the patient did not develop thrombosis-related complications, possibly because the mild compression did not completely compress the internal jugular vein. Ultrasound should be performed after balloon compression to confirm that the internal jugular vein is still unobstructed, and daily ultrasound should be used to confirm that there is no thrombosis in the vein. Moreover, we are not sure whether anticoagulation therapy should be used. Fourth, this was only a single case. Although the patient, who had CL of 1,100 ml/day, was managed successfully by balloon pressure, without surgical intervention, firm conclusions regarding the safety, feasibility, and efficacy of balloon pressure require further investigation in a prospective series. A suitable anatomical model to study the compression effect of pressure on lymphatic vessels is also required.

## Conclusion

In conclusion, the results of this case suggest that high-volume CL post neck dissection might be managed conservatively with balloon pressure. This technique provides a considered conservative option for treating CL.

## Data availability statement

The original contributions presented in the study are included in the article/Supplementary Material, further inquiries can be directed to the corresponding author/s.

## Ethics statement

Written informed consent was obtained from the individual(s) for the publication of any potentially identifiable images or data included in this article.

## Author contributions

ZD – Design, writing and submission; MC – Data collection, writing; RP – image collection, writing; RS – writing; literature review; DG – writing, design; XZ – literature review, image edit; CN – Design and idea. All authors contributed to the article and approved the submitted version.

## Conflict of interest

The authors declare that the research was conducted in the absence of any commercial or financial relationships that could be construed as a potential conflict of interest.

## Publisher's note



## References

1. Park I, Her N, Choe JH, Kim JS, Kim JH. Management of chyle leakage after thyroidectomy, cervical lymph node dissection, in patients with thyroid cancer. *Head Neck*. (2018) 40(1):7–15. doi: 10.1002/hed.24852

2. Delaney SW, Shi H, Shokrani A, Sinha UK. Management of chyle leak after head and neck surgery: review of current treatment strategies. *Int J Otolaryngol*. (2017) 2017:8362874. doi: 10.1155/2017/8362874

3. Molena E, King E, Davies-Husband C. Octreotide versus oral dietary modification for the treatment of chylous fistula following neck dissection: a systematic review and meta-analysis. *Clin Otolaryngol*. (2021) 46(3):474–84. doi: 10.1111/coa.13700

4. Chan JY, Wong EW, Ng SK, van Hasselt CA, Vlantis AC. Conservative management of postoperative chylous fistula with octreotide and peripheral total parenteral nutrition. *Ear Nose Throat J*. (2017) 96(7):264–7. doi: 10.1177/014556131709600720

5. Lv S, Wang Q, Zhao W, Han L, Wang Q, Batchu N, et al. A review of the postoperative lymphatic leakage. *Oncotarget*. (2017 Apr) 8(40):69062–75. doi: 10.18632/oncotarget.17297

6. Chang GH, Lee CY, Tsai YT, Fang CC, Fang KH, Tsai MS, et al. Strategic approach to massive chylous leakage after neck dissection. *Healthcare (Basel)*. (2021) 9(4):379. doi: 10.3390/healthcare9040379

7. Riley DS, Barber MS, Kienle GS, Aronson JK, von Schoen-Angerer T, Tugwell P, et al. CARE Guidelines for case reports: explanation and elaboration document. *J Clin Epidemiol*. (2017) 89:218–35. doi: 10.1016/j.jclinepi.2017.04.026

8. Kupferman ME, Patterson DM, Mandel SJ, LiVolsi V, Weber RS. Safety of modified radical neck dissection for differentiated thyroid carcinoma. *Laryngoscope*. (2004) 114(3):403–6. doi: 10.1097/00005537-200403000-00002

9. Roh JL, Yoon YH, Park CI. Chyle leakage in patients undergoing thyroidectomy plus central neck dissection for differentiated papillary thyroid carcinoma. *Ann Surg Oncol*. (2008) 15(9):2576–80. doi: 10.1245/s10434-008-0017-9

10. Lee YS, Kim BW, Chang HS, Park CS. Factors predisposing to chyle leakage following thyroid cancer surgery without lateral neck dissection. *Head Neck*. (2013) 35(8):1149–52. doi: 10.1002/hed.23104

11. Lee YS, Nam KH, Chung WY, Chang HS, Park CS. Postoperative complications of thyroid cancer in a single center experience. *J Korean Med Sci*. (2010) 25(4):541–5. doi: 10.3346/jkms.2010.25.4.541

12. Dunlap Q, Bridges M, Nelson K, King D, Stack Jr BC, Vural E, et al. Predictors for postoperative chyle leak following neck dissection, a technique-based comparison. *Otolaryngol Head Neck Surg*. (2021) 165(5):667–72. doi: 10.1177/0194599821993815

13. Ilczyszyn A, Ridha H, Durrani AJ. Management of chyle leak post neck dissection: a case report and literature review. *J Plast Reconstr Aesthet Surg*. (2011) 64(9):e223–30. doi: 10.1016/j.bjps.2010.12.018

14. Campisi CC, Boccardo F, Piazza C, Campisi C. Evolution of chylous fistula management after neck dissection. *Curr Opin Otolaryngol Head Neck Surg*. (2013) 21(2):150–6. doi: 10.1097/MOO.0b013e32835e9d97

15. Phang K, Bowman M, Phillips A, Windsor J. Review of thoracic duct anatomical variations and clinical implications. *Clin Anat*. (2014) 27(4):637–44. doi: 10.1002/ca.22337

16. Hematti H, Mehran RJ. Anatomy of the thoracic duct. *Thorac Surg Clin*. (2011) 21(2):229–38. doi: 10.1016/j.thorsurg.2011.01.002

17. Alejandre-Lafont E, Krompiec C, Rau WS, Krombach GA. Effectiveness of therapeutic lymphography on lymphatic leakage. *Acta Radiol*. (2011) 52 (3):305–11. doi: 10.1258/ar.2010.090356

18. Teksoz S, Ersen E, Arikan AE, Ferahman S, Kaynak K, Dionigi G, et al. Single port thoracoscopic treatment of thoracic duct injury after thyroidectomy with neck dissection. *Gland Surg*. (2017) 6(5):598–601. doi: 10.21037/gs.2017.07.14

19. de Gier HH, Balm AJ, Bruning PF, Gregor RT, Hilgers FJ. Systematic approach to the treatment of chylous leakage after neck dissection. *Head Neck*. (1996) 18(4):347–51. doi: 10.1002/(SICI)1097-0347(199607/08)18:4 < 347::AID-HED6 > 3.0.CO;2-Y

20. Nussenbaum B, Liu JH, Sinard RJ. Systematic management of chyle fistula: the southwestern experience and review of the literature. *Otolaryngol Head Neck Surg*. (2000) 122(1):31–8. doi: 10.1016/S0194-5998(00)70140-9

21. Xiang D, Liu Z, Yang T, Bai B, Zhang J, Wang C, et al. Finger-pressing: a simple and efficient way to stop chyle leak post neck dissection. *Endocrine*. (2020) 67(2):374–8. doi: 10.1007/s12020-019-02119-0

frontiers | Frontiers in Oncology

TYPE Case Report
PUBLISHED 05 October 2022
DOI 10.3389/fonc.2022.972883



OPEN ACCESS

EDITED BY
Riccardo Bertolo,
Hospital San Carlo di Nancy, Italy

REVIEWED BY
Nguyen Minh Duc,
Pham Ngoc Thach University of Medicine, Vietnam
Martin Huellner,
University Hospital Zürich, Switzerland
Vishal G. Shelat,
Tan Tock Seng Hospital, Singapore

*CORRESPONDENCE
Kuirong Jiang
jiangkuirong@njmu.edu.cn
Junlii Wu
junliwu1973@hotmail.com

†These authors have contributed equally to this work

SPECIALTY SECTION
This article was submitted to Surgical Oncology, a section of the journal Frontiers in Oncology

RECEIVED 19 June 2022
ACCEPTED 14 September 2022
PUBLISHED 05 October 2022

CITATION
Zhang YH, Shi GD, Meng LD, Wu J, Hu QQ, Xv D, Zhang K, Lu ZP, Wu JL and Jiang KR (2022) Laparoscopic treatment for an intrapancreatic accessory spleen: A case report. *Front. Oncol.* 12:972883. doi: 10.3389/fonc.2022.972883



# Laparoscopic treatment for an intrapancreatic accessory spleen: A case report

Yihan Zhang[1,2†], Guodong Shi[1,2†], Lingdong Meng[1,2†], Jing Wu[3], Qingqiao Hu[4], Dong Xv[1,2], Kai Zhang[1,2], Zipeng Lu[1,2], Junlii Wu[1,2*] and Kuirong Jiang[1,2*]

[1]Pancreas Center, the First Affiliated Hospital of Nanjing Medical University, Nanjing, China, [2]Pancreas Institute, Nanjing Medical University, Nanjing, China, [3]Department of Pathology, The First Affiliated Hospital of Nanjing Medical University, Nanjing, China, [4]Department of Nuclear Medicine, The First Affiliated Hospital of Nanjing Medical University, Nanjing, China

Malignant pancreatic tumors have early metastasis, aggressive behavior and poor prognosis. Surgeons often need to judge whether a patient needs prompt surgery when a pancreatic lesion is found. The accessory spleen is a congenital developmental malformation rather than a tumor and does not require surgical resection. Here, we report a 47-year-old man who underwent routine gastroscopic examination, and a submucosal eminence of the duodenal bulb was detected. The patient was asymptomatic and laboratory tests were unremarkable. Duodenal neuroendocrine neoplasm (G2) was considered following endoscopic submucosal dissection (ESD). Further examination showed a lesion in the tail of the pancreas and multiple accessory spleens. The lesion in the tail of the pancreas was Ga-68 positive and was highly considered a pancreatic neuroendocrine tumor (pNET). Based on this clinical evidence, laparoscopic spleen-preserving distal pancreatectomy (Kimura) was performed. However, the results of the postoperative pathological diagnosis indicated an intrapancreatic accessory spleen (IPAS). Given the findings of this case, we should explore more accurate diagnostic methods for IPAS to avoid unnecessary surgery.

KEYWORDS

**intrapancreatic accessory spleen, pancreatic neuroendocrine tumor, imaging diagnosis, pathological diagnosis, surgery**

## Introduction

Accessory spleen (AS) is a congenital developmental malformation that mainly occurs in the splenic hilum (62.1%) and tail of the pancreas (5.5%) (1–3). Researchers have found that approximately 10% to 40% of patients have AS at autopsy (4). A large meta-analysis of patients with AS showed that those in Oceania had the highest incidence

of AS (26.6%), followed by patients in North America (16.7%), Asia (14.1%) and Europe (12.2%) (5).

Advances in imaging diagnosis technology have helped identify an increasing number of people with pancreatic masses and, simultaneously, AS. ASs located in the pancreas are defined as intrapancreatic accessory spleens (IPASs). IPASs usually show no obvious symptoms and are often discovered in routine radiology examinations. There are no significant radiological differences between IPASs and pancreatic neuroendocrine tumors (pNETs), which may lead to a misdiagnosis. Here, we discuss methods for accurately diagnosing IPAS through a case encountered in our center.

## Case

A submucosal eminence of the duodenal bulb was discovered in a 47-year-old male patient after agreeing to undergo routine electronic gastroscopy in a local hospital. The eminence measured approximately 3*3 cm and presented with hyperemia on its surface. The patient had no chest tightness, asthma, bloating, abdominal pain or other symptoms. Ten days later, he was transferred to another hospital and underwent an abdominal enhanced CT scan as well as endoscopic submucosal dissection (ESD). The pathology results after ESD indicated that the mass was a neuroendocrine tumor (NET), the immunohistochemical report showed CgA (+), Syn (+), CD56 (+/-), SSTR2 (+), and Ki67 (4%+), and the mitotic count was 0-1/10 high-power fields (HPF). The mass was diagnosed as a NET-G2.

Given the malignant and metastatic potential of NETs and that the pathological grade of metastatic lesions may be higher than that of primary lesions, the patient underwent Ga-68 examination at a third hospital to evaluation whether other NETs were present in the abdomen and the rest of the body. Imaging revealed a high-uptake nodule in the tail of the pancreas and three accessory spleens with low uptake around the pancreas (Figure 1 and SFigures 1, 2).

For further treatment of the pancreatic tail lesion, the patient was transferred to our hospital. Neither his physical nor experimental examinations showed remarkable disorders. The patient's serum tumor markers (CA19-9, CA125, alpha fetoprotein (AFP) and carcinoembryonic antigen (CEA)) were normal. After admission, endoscopic ultrasonography (EUS) was performed. We found a quasicircular, slightly hypoechoic lesion measuring approximately 10*8 mm. The lesion was located in the tail of the pancreas, close to the splenic hilus. To further clarify the nature of the lesion and uncover other lesions, we performed dual-energy CT (DECT) of the pancreas before continuing with the next treatment steps. From the CT scan, we observed a nodular soft tissue density shadow in the tail of the pancreas measuring approximately 10*11 mm. It was significantly enhanced in the arterial phase, weakly enhanced in the venous phase and had a slightly low density in the delayed phase. Additionally, there were multiple soft tissue density shadows around the spleen, which were considered small ASs (Figure 2, SFigure 3). Although the CT results showed that the lesion was similar to the ASs outside the spleen in density and enhancement characteristics, there was a great difference between these two kinds of lesions on PET/CT (high uptake/

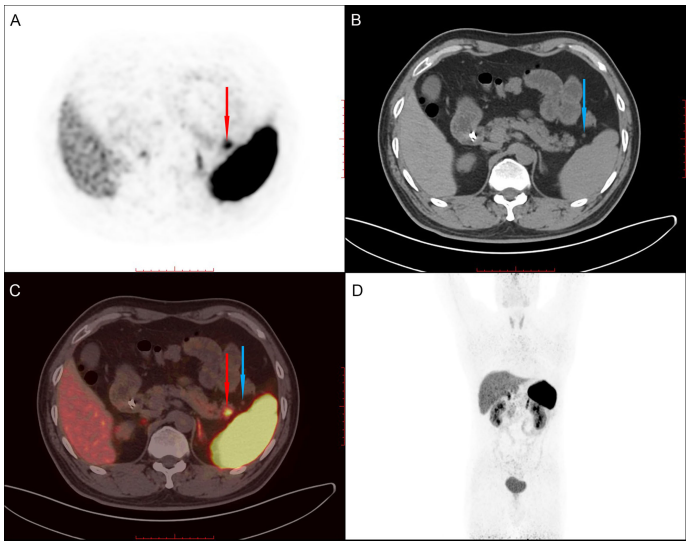


FIGURE 1
68Ga PET/CT shows a high-uptake nodule in the tail of the pancreas (red arrow) and an accessory spleen (blue arrow) with low uptake around the pancreas. **(A)**. PET image. **(B)**. CT image. **(C)** Fused PET/CT image. **(D)**. Whole-body PET image.

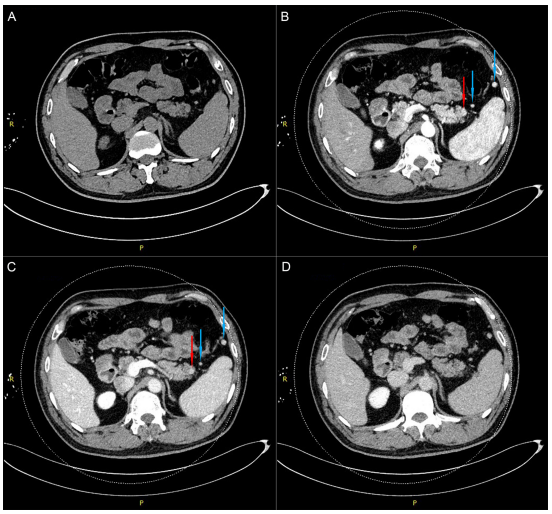


FIGURE 2
Dual-energy CT examination of the pancreas shows a nodular soft tissue density shadow in the tail of the pancreas (red arrow) and two accessory spleens near the pancreas and spleen (blue arrows). **(A)**. Plain-scan phase. **(B)**. Arterial phase. **(C)**. Venous phase. **(D)**. Delayed phase.

low uptake). Combined with the patient's history of duodenal NET, we continued to highly consider the lesion to be a pancreatic NET (pNET). Based on the results above, the patient underwent laparoscopic spleen-preserving distal pancreatectomy (Kimura). The stapler technique for stump closure was performed after left pancreatectomy. This patient had no postoperative complication including a clinically relevant postoperative pancreatic fistula (CR-POPF) and was successfully discharged on postoperative day(POD) 10. The amylase level of drain fluid was high at 15569U/L and the drains were removed on POD 9, Based on the 2016 International Study Group (ISGPS) definition and grading of POPF, it belonged to a biochemical leak, but not a CR-POPF. Postoperative pathology showed pancreatic tissue, lymphoid follicles and blood sinus-like structures (Figure 3). The immunohistochemical results showed CD20 (+), CD3 (+), CK-pan (-), and Syn (-). The lesion was considered an IPAS rather than a pNET. After a postoperative follow-up of 12 months, the patient had no recurrence.

The diagnosis of pNET by Ga-68 PET/CT mainly depends on the high expression of SSTR (mainly somatostatin receptor 2 (SSTR2) and 5 (SSTR5)). According to the earlier PET/CT results of this case, the lesion of the pancreatic tail was Ga-68 positive, indicating a highly likelihood of a misdiagnosis of NET. Therefore, we further performed additional immunohistochemical experiments. The SSTR results were SSTR2(+) and SSTR5(-) (Figure 4). In addition to SSTR, three other markers were tested, and the results were CD68(+), ERG(+), and CD8(+). Combined with hematoxylin and eosin (HE) sectioning and immunohistochemistry, this case was finally diagnosed as an intrapancreatic accessory spleen.

## Discussion

In this case, an IPAS was misdiagnosed as pNET, resulting in unnecessary surgery. However, the patient underwent relatively

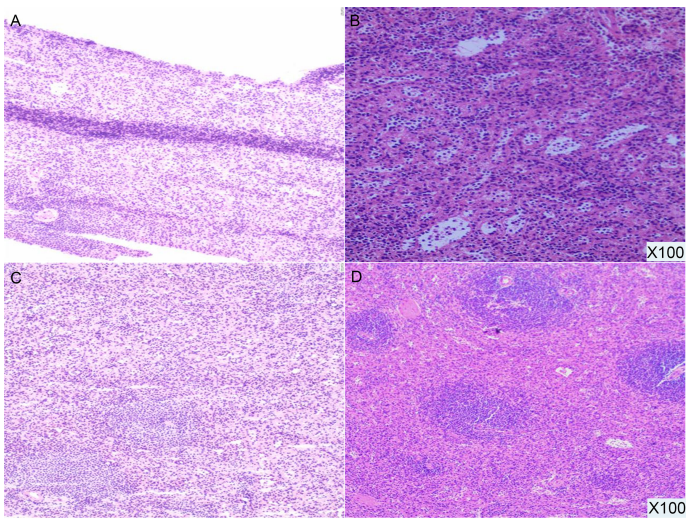


FIGURE 3
Pathological results (100X). The pancreatic tail lesion is rich in blood sinus structures, and lymphoid follicles and sinusoid-like structures can be seen.

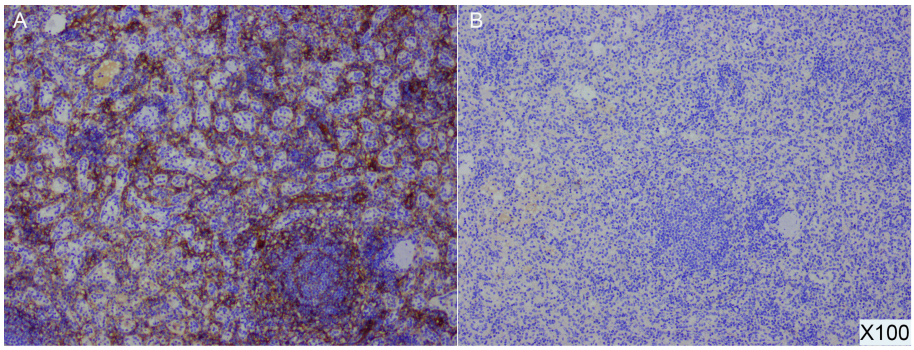


FIGURE 4
Postoperative pathological specimens and immunohistochemical results of IPAS demonstrate SSTR2(+) **(A)** and SSTR5 (-) **(B)** (100X).

sufficient examinations before the operation including radiography, endoscopy and PET/CT imaging. The preoperative examination results did not suggest the possibility of a diagnosis of IPAS, which led to the implementation of unnecessary surgery. Given the results of this case, we attempted to determine the causes of the misdiagnosis and identify better differential diagnosis methods.

Usually, CT is the first choice in the diagnosis of pancreatic masses, as it can be helpful in determining the location of the mass, analyzing the relationship between masses and blood vessels, and preliminarily evaluating the tumor stage. In this case, the pancreatic tail mass was significantly enhanced in the arterial phase. Although the enhancement was weaker in the venous phase, it was still higher than that of the surrounding tissue. These hypervascular manifestations are consistent with the radiological characteristics of pNET. However, we ignored the fact that the mass matched the density of the spleen at all phases. This feature is an important difference between IPASs and pNETs. This characteristic change in density may be difficult to detect due to a lack of individual clinical experience or inaccurate CT phase capture. We consider that additional MRI may have helped to clarify the diagnosis. IPASs match the intensity of all sequences of the spleen on MRI. Although the intensity of both pNETs and IPASs shows a low T1 and high T2, pNETs can have a ring-like enhancement (6). However, pNETs with high fibrosis have no significant or delayed intensity changes between sequences, which makes it difficult to distinguish them from IPASs (7). Val-bernal et al. reported 4 cases of pancreatic tail lesions, all of which were diagnosed as pNETs by CT and MRI. However, three of them were pathologically confirmed as IPASs *via* endoscopic ultrasound-fine needle aspiration (EUS-FNA) biopsy (8). IPAS cannot be diagnosed accurately only through imaging examinations.

EUS is helpful for making diagnoses with less invasive trauma. In this case, the endosonographers used EUS and described that the lesion was quasicircular and slightly hypoechoic with a clear boundary. However, IPASs and pNETs have similar profiles on EUS, such as round and homogenous lesions with clear and regular boundaries, which means it is still difficult to make a diagnosis excluding pNET with this imaging modality (1). To improve the accuracy of the diagnosis, biopsy *via* EUS or ESD is often needed. At present, a variety of markers are used in the pathological differential diagnosis of IPAS and pNET, such as CK-pan, Vim (epithelial and neural markers), CgA, Syn, CD56 (NET diagnostic markers) and Ki-67 (grading markers). It is worth noting that CD8 has been reported to be more conducive in improving the accuracy of the differential diagnosis between IPAS and pNET (2). We believe that CD8 staining should be added on the basis of pNET-related immunohistochemistry.

The case serves as a reminder to consider combining various methods to help to make a more precise diagnosis. Some researchers have found that the use of PET/CT can enhance the accuracy of diagnosis. 68-Ga PET/CT has an important role in the differential diagnosis of pNETs from other pancreatic lesions, and it could be used as an exclusive diagnostic method to distinguish pNETs from IPASs. However, because of the physiological radioisotope uptake of 68-Ga in splenic tissue, false positive results in Ga-68 PET/CT have been reported, leading to misdiagnoses of IPASs as pNETs (9, 10). Similarly, in our case, Ga-68 PET/CT was performed but was unable to yield a correct diagnosis. Liberini (11) et al. reported on a fully convergent iterative image reconstruction algorithm with β-values of 1000 (BSREM1000) and a data-driven gating (DDG) technique for correcting $^{68}$Ga-Dotatate PET/CT data and more effectively distinguishing pNETs from IPASs.

In addition to calibrating $^{68}$Ga PET/CT data, we also focused on finding another method. Tc-99m heat-denatured red blood cell single photon emission computed tomography has recently been shown to be a better choice for differentiating pNETs from IPASs (12). The use of this technique for diagnosing the spleen dates back to the 1980s, when Dworkin et al. (13) identified the

presence and size of a spleen in a patient with functional asplenia. This method is now used to detect the presence of ASs in patients with recurrent chronic idiopathic thrombocytopenic purpura (ITP) after splenectomy (4). It has also been reported in the diagnosis of intrathoracic splenosis (14). Because $^{99m}$Tc thermally-denatured erythrocytes only accumulate in splenic tissue rather than pNETs, some researchers believe that it can be the best method for diagnosing IPAS (14, 15).

## Conclusion

In conclusion, we believe that CT and MRI still play important roles in the localization and size evaluation of lesions, although they cannot accurately distinguish pNET from IPAS at present. Based on the imaging results in the literature, EUS-FNA should be performed to obtain satisfactory tissue for biopsy. It is suggested that CD8 staining be added on the basis of pNET-related immunohistochemistry to exclude IPAS or avoid unnecessary surgery. Tc-99m heat-denatured red blood cell single photon emission computed tomography is a promising method for diagnosing IPAS, but the number of hospitals performing this technique is relatively limited at present. Based on the factors above, we believe that CT/MRI combined with EUS-FNA can contribute to improving the accuracy of IPAS diagnosis and avoiding unnecessary surgery.

## Data availability statement

The original contributions presented in the study are included in the article/Supplementary Material. Further inquiries can be directed to the corresponding authors.

## Ethics statement

Written informed consent was obtained from the individual(s) for the publication of any potentially identifiable images or data included in this article.

## Author contributions

ZYH, SGD and MLD conceived the case and wrote the manuscript. WJ reviewed pathological results. HQQ interpreted the PET/CT results. ZK, DX and LZP interpreted CT results. WJL and JKR helped revise and polish the manuscript. All the authors contributed to the article and approved the submitted version.

## Funding

Our work was supported by the National Science Foundation for Young Scientists of China (No. 81902455); the National Natural Science Foundation of China (No. 82072706, No. 81871980); Jiangsu key Medical Discipline (General Surgery, ZDXKA2016005).

## Acknowledgments

All the authors thank the members of their research group for useful discussions.

## Conflict of interest

The authors declare that the research was conducted in the absence of any commercial or financial relationships that could be construed as a potential conflict of interest.

## Publisher's note



## Supplementary material

The Supplementary Material for this article can be found online at: https://www.frontiersin.org/articles/10.3389/fonc.2022.972883/full#supplementary-material

SUPPLEMENTARY FIGURE 1
68Ga PET/CT shows an accessory spleen (blue arrow) with low uptake near the spleen. **(A)**. PET image. **(B)**. CT image. **(C)** Fused PET/CT image. **(D)**. Whole-body PET image.

SUPPLEMENTARY FIGURE 2
68Ga PET/CT shows an accessory spleen (blue arrow) with low uptake near the splenic hilum and tail of the pancreas. **A)**. PET image. **(B)**. CT image. **(C)** Fused PET/CT image. **(D)**. Whole-body PET image.

SUPPLEMENTARY FIGURE 3
Dual-energy CT examination of the pancreas shows an accessory spleen near the splenic hilum (blue arrow). **(A).** Plain-scan phase. **(B)**. Arterial phase. **(C)**. Venous phase. **(D)**. Delayed phase.

SUPPLEMENTARY FIGURE 4
Pathological section and immunohistochemical results for SSTR2 and SSTR5 (40X).

# References

1. Kim GE, Morris JD, Anand N, DePalma F, Greenwald BD, Kim RE, et al. Recognizing intrapancreatic accessory spleen *via* EUS: Interobserver variability. *Endosc Ultrasound* (2019) 8(6):392–7. doi: 10.4103/eus.eus_35_19

2. Saunders TA, Miller TR, Khanafshar E. Intrapancreatic accessory spleen: utilization of fine needle aspiration for diagnosis of a potential mimic of a pancreatic neoplasm. *J Gastrointest Oncol* (2016) 7(Suppl 1):S62–5. doi: 10.3978/j.issn.2078-6891.2015.030

3. Lancellotti F, Sacco L, Cerasari S, Bellato V, Cicconi S, Ciardi A, et al. Intrapancreatic accessory spleen false positive to 68Ga-dotatoc: case report and literature review. *World J Surg Oncol* (2019) 17(1):117. doi: 10.1186/s12957-019-1660-2

4. García Angarita F, Sanjuanbenito Dehesa A. Intrapancreatic accessory spleen: a rare cause of recurrence of immune thrombocytopenic purpura. *Clin Case Rep* (2016) 4(10):979–81. doi: 10.1002/ccr3.642

5. Vikse J, Sanna B, Henry BM, Taterra D, Sanna S, Pękala PA, et al. The prevalence and morphometry of an accessory spleen: A meta-analysis and systematic review of 22,487 patients. *Int J Surg* (2017) 45:18–28. doi: 10.1016/j.ijsu.2017.07.045

6. Spencer LA, Spizarny DL, Williams TR. Imaging features of intrapancreatic accessory spleen. *Br J Radiol* (2010) 83(992):668–73. doi: 10.1259/bjr/20308976

7. Chiti G, Grazzini G, Cozzi D, Danti G, Matteuzzi B, Granata V, et al. Imaging of pancreatic neuroendocrine neoplasms. *Int J Environ Res Public Health* (2021) 18 (17):8895. doi: 10.3390/ijerph18178895

8. Val-Bernal JF, Martino M, Yllera-Contreras E, Castro-Senosiain B, Bueno-Ortiz P. Intrapancreatic accessory spleen. report of four cases diagnosed by ultrasound-guided fine-needle aspiration biopsy. *Rom J Morphol Embryol* (2018) 59(2):619–24.

9. Ryoo HG, Choi H, Cheon GJ. Spleen scan for $^{68}$Ga-DOTATOC PET-positive pancreatic tail lesion: Differential diagnosis of neuroendocrine tumor from accessory spleen. *Nucl Med Mol Imaging* (2020) 54(1):43–7. doi: 10.1007/s13139-019-00626-6

10. Bostancı EB, Oter V, Okten S, Küçük NO, Soydal C, Turhan N, et al. Intrapancreatic accessory spleen mimicking pancreatic neuroendocrine tumor on 68-Ga-Dotatate PET/CT. *Arch Iran Med* (2016) 19(11):816–9.

11. Liberini V, Kotasidis F, Treyer V, Messerli M, Orita E, Engel-Bicik I, et al. Impact of PET data driven respiratory motion correction and BSREM reconstruction of $^{68}$Ga-DOTATATE PET/CT for differentiating neuroendocrine tumors (NET) and intrapancreatic accessory spleens (IPAS). *Sci Rep* (2021) 11 (1):2273. doi: 10.1038/s41598-020-80855-4

12. Hagan I, Hopkins R, Lyburn I. Superior demonstration of splenosis by heat-denatured Tc-99m red blood cell scintigraphy compared with Tc-99m sulfur colloid scintigraphy. *Clin Nucl Med* (2006) 31(8):463–6. doi: 10.1097/01.rlu.0000226907.36840.b3

13. Wagman PG, Dworkin HJ. Splenic imaging in a patient with functional asplenia. *Clin Nucl Med* (1989) 14(4):264–7. doi: 10.1097/00003072-198904000-00005

14. Hagman TF, Winer-Muram HT, Meyer CA, Jennings SG. Intrathoracic splenosis: superiority of technetium Tc 99m heat-damaged RBC imaging. *Chest* (2001) 120(6):2097–8. doi: 10.1378/chest.120.6.2097

15. Barber TW, Dixon A, Smith M, Yap KS, Kalff V. Ga-68 octreotate PET/CT and Tc-99m heat-denatured red blood cell SPECT/CT imaging of an intrapancreatic accessory spleen. *J Med Imaging Radiat Oncol* (2016) 60(2):227–9. doi: 10.1111/1754-9485.12319

frontiers | Frontiers in Oncology

TYPE Case Report
PUBLISHED 12 October 2022
DOI 10.3389/fonc.2022.1011076



OPEN ACCESS

EDITED BY
Ugo Cioffi,
University of Milan, Italy

REVIEWED BY
Stefano Bona,
Humanitas Research Hospital, Italy
Marco Chiarelli,
ASST Lecco, Italy

*CORRESPONDENCE
Jiaxin Li
407723080@qq.com

†These authors have contributed equally to this work

SPECIALTY SECTION
This article was submitted to Surgical Oncology, a section of the journal Frontiers in Oncology

RECEIVED 03 August 2022
ACCEPTED 20 September 2022
PUBLISHED 12 October 2022

CITATION
Li H, Xu J, Feng Q, Cai Z and Li J (2022) Case report: The safety of laparoscopic surgery for the retroperitoneal bronchogenic cyst. *Front. Oncol.* 12:1011076. doi: 10.3389/fonc.2022.1011076



# Case report: The safety of laparoscopic surgery for the retroperitoneal bronchogenic cyst

Hancong Li[1†], Jun Xu[2,3†], Qingbo Feng[4†], Zhaolun Cai[5] and Jiaxin Li[4*]

[1]West China School of Medicine, West China Hospital, Sichuan University, Chengdu, China, [2]Department of Pancreatic Surgery, West China Hospital, Sichuan University, Chengdu, China, [3]Department of Minimal Invasive Surgery, Shangjin Nanfu Hosptial, Chengdu, China, [4]Department of Liver Surgery and Liver Transplantation Centre, West China Hospital, Sichuan University, Chengdu, China, [5]Department of Gastrointestinal Surgery, West China Hospital, Sichuan University, Chengdu, China

**Introduction:** Bronchogenic cyst is a congenital aberration of bronchopulmonary malformation with bronchial-type, pseudostratified cylindrical epithelium. They are usually discovered in the mediastinum and intrapulmonary but are rarely encountered in retroperitoneum. We report a case of the retroperitoneal bronchogenic cyst and perform a literature review to summarize the safety of laparoscopic resection for this rare disease.

**Case presentation:** We report a 57-year-old woman who was admitted to our hospital with no clinical symptoms and was found by chance to have masses in the adrenal gland area during a routine physical examination. An abdominal CT examination revealed a cystic lesion was found in the left suprarenal region. Afterward, the patient underwent a laparoscopic exploration. Histopathological findings confirmed the diagnosis of a retroperitoneal bronchogenic cyst. The patient recovered uneventfully without signs of recurrence during a 1-year follow-up period.

**Conclusion:** Bronchogenic cyst is rare in the retroperitoneal region. It should be considered as one of the differential diagnoses of a retroperitoneal neoplasm, especially in the left retroperitoneal region. Laparoscopic surgery is technically feasible and safe for the treatment of patients with a retroperitoneal bronchogenic cyst.

KEYWORDS

**bronchogenic cysts, laparoscopic surgery, retroperitoneal neoplasm, case report, retroperitoneal bronchogenic cyst**

## Introduction

Bronchogenic cysts (BCs) arise from abnormal budding of the foregut during embryogenesis, which is a benign congenital aberration of bronchopulmonary foregut malformation (1). It is typically located within the mediastinum and pulmonary parenchyma. The retroperitoneum is rarely involved (2). Particularly, retroperitoneal bronchogenic cysts(RBCs) tend to occur on the pancreas corpus or left adrenal gland (3). In most cases, BCs are asymptomatic unless they are infected, ruptured into the surrounding cavities, or enlarged enough to compress adjacent structures (4, 5). Cough, fever, pain, and dyspnea are among the most common manifestations (6). Due to the lack of characteristic clinical features, RBCs are often accidentally identified and diagnosed by imaging examinations, such as computed tomography(CT) and magnetic resonance imaging (MRI) (7). However, due to their rarity, location, variable cystic content, and non-specific imaging, they are frequently misinterpreted as cystic teratomas, adrenal tumors, or other benign and malignant retroperitoneal lesions (7–9). Although benign lesions, surgical resection is recommended to establish the diagnosis, alleviate symptoms, and prevent complications or malignant transformation (1, 10). Recently, laparoscopic procedure for RBCs has become increasingly popular for decreased scarring, less complications, shorter hospital stays, and faster recovery. Herein, we present a case of RBC, which was successfully removed through a laparoscopic excision. Additionally, we have performed a literature review to summarize the safety of laparoscopic resection for this rare disease.

## Case presentation

On January 4, 2021, a 57-year-old woman was referred to the West China Hospital for evaluation of a left adrenal neoplasm suspected of being an adrenal tumor. The patient had no symptoms and the mass was incidentally discovered on medical examination. There were no obvious abnormalities in her medical history or physical examination. Additionally, she did not have any underlying diseases or take any medications. Routine laboratory investigations such as complete blood counts and liver and kidney function tests were within normal ranges. Specifically, negative results were obtained for all adrenal gland hormones and serum tumor markers (Table 1).

CT showed an ovoid, well-defined, and heterogeneous lesion, measuring 2.2×5.8 cm in her left adrenal area (Figure 1). Based on these CT imaging characteristics, a benign lesion (most likely a cyst) was suspected. To confirm the diagnosis and determine the feature, the cyst was completely removed through the laparoscope.

During the surgery, the patient was positioned supine. Using Veress needles, a 1.5-cm incision near the upper navel edge was made to establish pneumoperitoneum with a constant pressure of 13 mm Hg. Four trocars were used: a 5 mm trocar was inserted on the left side of the umbilicus, and two 12 mm trocars were placed below the right costal margin in the midclavicular line and mid-axillary line, respectively. The rest 12 mm trocar was installed under the xiphoid process. The procedure was performed using an ultrasonic surgical aspirator (CUSA; Cavitron Lasersonic Corp., Stamford, CT, USA), an ultrasonic system (Harmonic® scalpel; Ethicon Endo-Surgery, Inc., Cincinnati, OH, USA), and a bipolar clamp coagulation system (ERBE, Tubingen, Germany). Dissociation and exposure of the mass were achieved through the ultrasound knife, along with clamping the blood vessels leading to and from the tumor by a titanium clip. Intraoperatively, a 4×3cm cyst mass was observed behind the head of the pancreas and on the left side of the abdominal aorta, which had an unclear boundary with the surrounding tissues and was closely adhered to the diaphragm. The entire mass was completely removed. Afterward, we repaired the damaged diaphragm and performed complete hemostasis of the wound. The resection specimen was collected in a plastic bag and removed *via* small incisions around the umbilical cord. An orthopedic drainage tube was inserted into the left retroperitoneal cavity, and slightly

Table 1 Laboratory tests for catecholamine metabolism and tumor marker.

| | Patient values | Units | Ref Range | Status |
|---|---|---|---|---|
| Epinephrine | 0.05 | nmol/L | <0.34 | – |
| Norepinephrine | 0.56 | nmol/L | <5.17 | – |
| Dopamine | 0.05 | nmol/L | <0.31 | – |
| Methoxypinephrine | 0.13 | nmol/L | <0.42 | – |
| Methoxy norepinephrine | 0.37 | nmol/L | <0.71 | – |
| 3-Methoxytyramine | 4.43 | pg/ml | <18.40 | – |
| AFP | 1.26 | ng/ml | <7 | – |
| CA-125 | 11.38 | U/ml | <24 | – |
| CA-199 | 16.00 | U/ml | <30 | – |
| CEA | 0.69 | ng/ml | <5 | – |

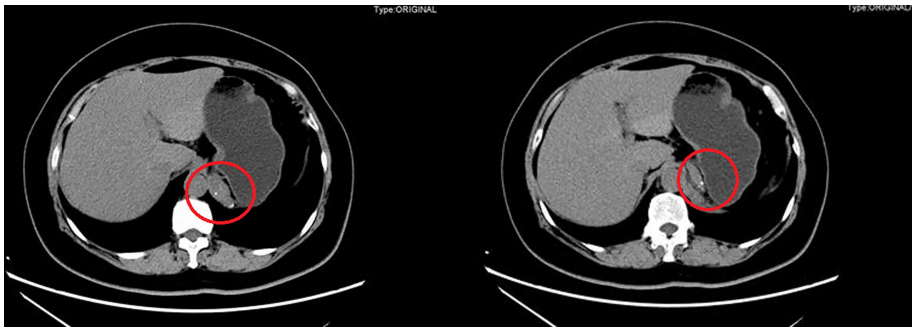

FIGURE 1
Computed tomography scan showed a 2.2×5.8 cm thin-walled water-attenuated cystic lesion in retroperitoneal region (red circle).

bloody fluid was collected. The operation lasted 200 min, and the estimated blood loss was 20 ml with no transfusion.

The postoperative period was uneventful and the patient was discharged on the 6th day after surgery with no complications. CT was repeated regularly after surgery. No recurrence, metastasis, or other complications were observed after one and a half years of follow-up.

Grossly, the cystic lesion measured 60 mm in diameter (Figure 2A). Sectioning revealed yellowish fluid within the white tough tissue. Cystic walls were about 1-2 mm thick with a smooth interior surface (Figure 2B). Pathologically, characteristic pseudostratified columnar epithelium and cartilage were identified in histological specimens (Figure 2C). It was definitively determined that a retroperitoneal bronchogenic cyst existed.

## Discussion

BCs are rare cystic lesions, with the prevalence in the general population remaining unknown (11). Men are slightly more prone to them, and they often go undetected until their 30 s or 40 s (12). They originate predominantly in the middle mediastinum and account for 10% to 15% of mediastinal tumors (13). Occasionally, they are identified in the neck, spinal canal, pleural cavity, skin, esophagus, pericardium, and retroperitoneum (1).

BCs originate from an aberrant budding of the tracheobronchial anlage of the primitive foregut between the 3$^{rd}$ and 7$^{th}$ weeks of embryonic development. The pleuroperitoneal membranes completely seal off the pericardioperitoneal canal at the end of the 7$^{th}$ week. Therefore, the abnormal lung buds are pinched off from the tracheobronchial tree by the growing diaphragm and trapped in the abdominal cavity. Eventually, the early lung buds develop into RBCs (14).

First reported by Miller et al. in 1953, RBCs are extremely rare. A thorough search of the PubMed database revealed 88 publications of retroperitoneal bronchogenic cysts reported worldwide in the English literature between 1991-2022. After screening the full texts and pathological results,40 publications reporting on 45 cases with laparoscopic RBC removal were reviewed within the study. A concise summary of the included articles was shown in Table 2.

Laparoscopic resection was first reported in 1997 by Tokuda et al. for 3 cm such cysts (51). This procedure of the cyst has been

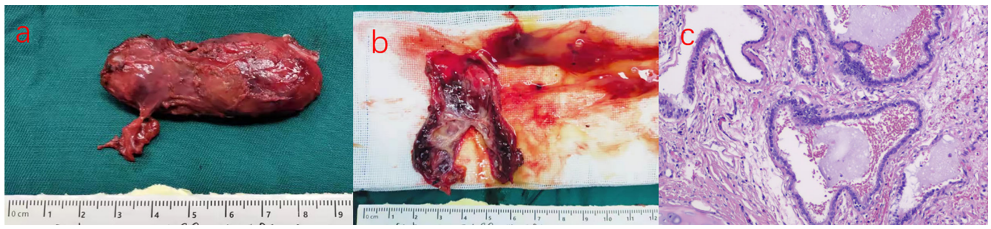


FIGURE 2
**(A)** An ovoid, well-defined, and homogeneous cystic lesion. **(B)** Mucous filled the cystic lesion. **(C)** Histopathologic section revealed the cyst lined with tall columnar epithelium and cyst wall containing thin smooth muscle bundles, seromucous glands, and mature hyaline cartilage. (Haematoxylin and eosin stain, original magnification, ×200).

Table 2 Literature review of retroperitoneal bronchogenic cyst undergoing laparoscopic surgery.

| | First Author | Year | Country | Sex | Age | Size (cm) | Location | Operation approach | Chief complaint |
|---|---|---|---|---|---|---|---|---|---|
| 1 | Hu BY (15) | 2022 | China | M | 6 | 4.5×2.8×8 | Left adrenal gland | Laparoscopic | Abdominal pain |
| 2 | Hu BY (15) | 2022 | China | M | 18 | 7.1×3.6×7 | Left adrenal gland | Laparoscopic | Asymptomatic |
| 3 | Hu BY (15) | 2022 | China | M | 27 | 3.6×3.5×3.4 | Right adrenal gland | Laparoscopic | Asymptomatic |
| 4 | Tadokoro T (16) | 2022 | Japan | F | 16 | 3.8 | Under the left diaphragm | Laparoscopic | Upper abdominal pain |
| 5 | Cowan S (17) | 2021 | New Zealand | M | 39 | 3 | Left adrenal gland | Laparoscopic | Left flank pain |
| 6 | Yuan K (18) | 2021 | China | F | 53 | 3.3×2.7×3.5 | Left adrenal gland | Laparoscopic | Back pain |
| 7 | Wu LD (2) | 2021 | China | F | 17 | 2.9×1.7×2.8 | Left adrenal gland | Laparoscopic | Epigastric pain |
| 8 | Qingyu J (19) | 2021 | China | F | 41 | 3.5×3 | Left adrenal gland | Laparoscopic | Lumbar back discomfort |
| 9 | Wen Y (20) | 2020 | China | M | 27 | 2.1×4.1 | Left adrenal gland | Laparoscopic | Asymptomatic |
| 10 | Wen Y (20) | 2020 | China | M | 33 | 3.1×5.9 | Right adrenal gland | Laparoscopic | Asymptomatic |
| 11 | Sinha V (21) | 2020 | India | M | 30 | 7×5 | Left adrenal gland | Laparoscopic | Upper abdominal pain |
| 12 | Başoğlu M (3) | 2018 | Turkey | F | 38 | NA | Left adrenal gland | Laparoscopic | Left upper abdominal pain |
| 13 | Liu Q (22) | 2018 | China | M | 33 | 4.5 | Left hepatic hilum | Robotic | Asymptomatic |
| 14 | Liu Q (22) | 2018 | China | M | 78 | 7 | Inferior of the left renal vein, left side of IVC | Robotic | Asymptomatic |
| 15 | Wang M (8) | 2017 | China | F | 48 | 8×6×5.5 | Left adrenal gland | Laparoscopic | Epigastric pain |
| 16 | Yoon YR (23) | 2015 | Korea | M | 57 | 4.8×2.5 | Left adrenal gland | Laparoscopic | Asymptomatic |
| 17 | Bulut G (24) | 2015 | Turkey | F | 25 | 4 | Left adrenal gland | Laparoscopic | Left flank pain |
| 18 | Jiang X (25) | 2015 | China | M | 52 | 2.5×2.5×0.5 | Left crus of the diaphragm | Laparoscopic | Asymptomatic |
| 19 | Trehan M (26) | 2015 | India | F | 34 | 10×6 | Right hypochondrium | Laparoscopic | Right flank heavy |
| 20 | Zhang D (27) | 2015 | China | M | 8 | 4 | Left adrenal gland | Laparoscopic | Asymptomatic |
| 21 | Terasaka T (28) | 2014 | Japan | M | 27 | 5.4×3.8 | Left adrenal gland | Laparoscopic | Asymptomatic |
| 22 | Cao DH (29) | 2014 | China | M | 51 | 4.5 | Left adrenal gland | Laparoscopic | Headache |
| 23 | Dong B (30) | 2014 | China | F | 30 | 1.5×2×2 | Left adrenal gland | Laparoscopic | Asymptomatic |
| 24 | Castro R (31) | 2013 | Portugal | F | 36 | 8 | Left upper quadrant | Laparoscopic | Abdominal pain |
| 25 | Runge T (32) | 2013 | Switzerland | F | 42 | 5×3.6×4 | Left adrenal gland | Laparoscopic | Epigastric pain |
| 26 | Cai Y (33) | 2013 | China | F | 50 | 3 | Pancreas posterior wall | Laparoscopic | Left flank pain |
| 27 | Jannasch O (34) | 2013 | Germany | M | 50 | 4 | Left adrenal gland | Laparoscopic | Left flank pain |
| 28 | O'Neal PB (35) | 2012 | USA | F | 23 | 5.2×4 | Left adrenal gland | Laparoscopic | Abdominal discomfort |
| 29 | Alguraan Z (36) | 2012 | USA | F | 23 | 4 | Right adrenal gland | Robotic | Asymptomatic |
| 30 | Díaz Nieto R (37) | 2010 | Spain | M | 67 | 6 | Gastroesophageal junction | Laparoscopic | Low back pain |
| 31 | Inaba K (38) | 2010 | Japan | F | 64 | 3×4×2 | Stomach posterior wall | Laparoscopic | Asymptomatic |
| 32 | El Youssef R (39) | 2010 | Portland | M | 44 | 3 | Left adrenal gland | Laparoscopic | Asymptomatic |
| 33 | Obando J (40) | 2009 | USA | M | 67 | 3.9×3.7 | Left upper-quadrant | Laparoscopic | Asymptomatic |
| 34 | Chung JM (41) | 2009 | Korea | F | 41 | 4.8×3.5×4.2 | Left adrenal gland | Laparoscopic | Asymptomatic |
| 35 | Roma A (42) | 2008 | USA | M | 40 | 6.2 | Left adrenal gland | Laparoscopic | Asymptomatic |
| 36 | Minei S (43) | 2007 | Japan | M | 39 | 3.5×3 | Left adrenal gland | Laparoscopic | Fever |
| 37 | Chu PY (44) | 2007 | China | M | 55 | 4×3 | Left adrenal gland | Laparoscopic | Asymptomatic |
| 38 | Terry NE (45) | 2007 | USA | F | 75 | 5 | Left adrenal gland | Laparoscopic | Abdominal pain |
| 39 | Ishizuka O (46) | 2004 | Japan | M | 36 | 5×3 | Left adrenal gland | Laparoscopic | Asymptomatic |
| 40 | Ishikawa T (47) | 2003 | Japan | F | 41 | 9.2 | Left adrenal gland | Laparoscopic | Left flank pain |
| 41 | Hedayati N (48) | 2003 | USA | F | 59 | 7×5 | Left adrenal gland | Laparoscopic | Asymptomatic(convert to open ) |
| 42 | McCrystal DJ (49) | 2002 | Australia | F | 8 | 4×3×2 | Left adrenal gland | Laparoscopic | Abdominal pain |

*(Continued)*

Continued

| | First Author | Year | Country | Sex | Age | Size (cm) | Location | Operation approach | Chief complaint |
|---|---|---|---|---|---|---|---|---|---|
| 43 | McCrystal DJ (49) | 2002 | Australia | M | 15 | 5.5×3.5×1.2 | Left adrenal gland | Laparoscopic | Left flank pain |
| 44 | Yamamoto E (50) | 1998 | Japan | F | 49 | 3.2×2.2 | Right adrenal gland | Laparoscopic | Asymptomatic |
| 45 | Tokuda N (51) | 1997 | Japan | F | 24 | 3 | Left adrenal gland | Laparoscopic | Asymptomatic |

reported most frequently in China (17cases, 37.8%), followed by Japan (8 cases,17.8%) and the United States (6 cases,13.3%). The finding concerning regional and race differences was consistent with Mike et al. (52) However, it remained unclear whether this represents a real difference in incidence among Asian patients or merely a reporting bias. There exists no discrepancy between the gender who underwent laparoscopic surgery (22 female and 23 male), with an average diagnosis age of 38.6 (range 6-78) years. To date, the largest retroperitoneal bronchial cyst of laparoscopic excision was 10×6cm, as reported by Trehan et al. in 2015 in India (26). Retroperitoneal bronchogenic cysts tend to be found on the left side of the abdomen(37cases,82.2%). The most common location of retroperitoneal bronchogenic cyst is near the left adrenal gland (31cases, 68.9%). Only 4 cases (8.9%) were discovered in the right adrenal gland. The previous review of cases has confirmed this difference (18). Based on Rud et al. (53), the left pericardioperitoneal canal closes later and is larger than the right which can explain why RBCs prefer to be located on the left side. It's worth noting that nearly half of patients (22cases, 48.9%) find a mass incidentally, with no typical clinical manifestations. Of symptomatic patients, the majority complained of abdominal pain (7 cases, 30.4%) left flank pain (6 cases,26.1%) and a small number complained of thoracic pain and back pain.

Similar literature reviews were successively performed by Cetinkurşun et al. (54), Mike et al. (52), Govaerts et al. (55), and Yuan et al. (18) in 1997, 2005, 2012, and 2021, respectively. The aforementioned studies, however, included a large number of patients undergoing surgery *via* the open approach. In addition, we enrolled the latest reports from the past two years through a more comprehensive search, and supplemented cases missed by the previous retrieval. Similar conclusions were obtained regarding the clinical characteristics of the disease, including age, symptoms, and predilection sites.

It remains difficult to diagnose RBCs before surgery. CT and MRI are the most helpful imaging modalities (13, 56). Typical CT appearances are sharply defined, homogeneous masses with attenuation coefficients to water density (0 to 20 HU). However, the attenuation coefficients can increase when protein, calcium, or anthracosis pigment are elevated within the cyst, aggravating difficulties in the differential diagnosis (14). MRI reveals the inhomogeneity of RBCs with better clarity than CT, providing a more accurate preoperative diagnosis (56). By now, only histopathology can yield a definitive diagnosis of BCs. Indispensable pathological criteria consist of secretory epithelium along with bronchial glands, smooth muscle, or hyaline cartilage (57). There is still no exact evidence that endocrine or tumor biomarkers are associated with RBCs. In only a few cases were endocrine or tumor biomarker variations recorded (8, 58, 59).

Early surgical excision of RBCs is recommended to clarify a diagnosis, relieve symptoms and prevent complications, even if asymptomatic. Due to reduced operating time, length of stay, and intraoperative blood loss, laparoscope has been increasingly ubiquitous in intraperitoneal surgery. Currently, laparoscopic resection is particularly recommended to clarify the diagnosis and apply for the treatment of retroperitoneal bronchogenic cysts. In addition, laparoscopic resection has been widely used to lessen the economic burden as well as postoperative pain of patients. More than half of patients with RBCs underwent laparoscopic resection and the majority were free of complications during the postoperative course. The present study also found laparoscopy to be safe and reliable. In particular, the retroperitoneal laparoscopic excision, which was first documented by McCrystal et al. in 2002, has gained more and more applications in recent years. Our literature review supports that the retroperitoneal approach is feasible, effective, and less invasive when treating such retroperitoneal cysts. In addition, there are only two articles reporting three cases of robotic surgery applicated to RBC patients (22, 36). Robotic surgery has overcome many limitations of traditional laparoscopic surgery and has improved in terms of dexterity, tremor reduction, and 3-dimensional visualization (60). This enables broader adaptability of robotic surgery in abdominal and retroperitoneal surgical procedures (61). However, due to the high financial cost, the application of robotic resection remains limited (22).

The prognosis of bronchogenic cysts after surgical excision is excellent. No recurrence, malignancy, or other complications are reported in all the literature we reviewed.

To our best knowledge, our review provides the largest case series in the world with such cysts to be resected laparoscopically. In conclusion, we reported a case with an ectopic bronchogenic cyst in the left retroperitoneal region. A literature review suggests that laparoscopic excision is optimal management to establish both diagnosis and treatment. The long-term outcome of this disease is excellent, with no report of recurrence.

## Data availability statement

The original contributions presented in the study are included in the article/supplementary material. Further inquiries can be directed to the corresponding author.

## Ethics statement

Written informed consent was obtained from the individual(s) for the publication of any potentially identifiable images or data included in this article.

## Author contributions

JL and QF contributed to the study concept and design. HL, JX, and QF contributed to the investigation and writing the original draft. HL, JX, and QF contributed to data collection. QF, JL and ZC revised the paper. All authors contributed to the article and approved the submitted version.

## Funding

This work was supported by the 2021 Sichuan Science and Technology Plan Project "International cooperation in science and technology innovation/technological innovation cooperation in Hong Kong, Macao and Taiwan" (2021YFH0095) and Sichuan University from 0 to 1 project (No. 2022SCUH0017).

## Conflict of interest

The authors declare that the research was conducted in the absence of any commercial or financial relationships that could be construed as a potential conflict of interest.

## Publisher's note

All claims expressed in this article are solely those of the authors and do not necessarily represent those of their affiliated organizations, or those of the publisher, the editors and the reviewers. Any product that may be evaluated in this article, or claim that may be made by its manufacturer, is not guaranteed or endorsed by the publisher.

## References

1. Limaiem F, Mlika M. *Bronchogenic cyst*. StatPearls. Treasure Island (FL: StatPearls Publishing Copyright © 2022, StatPearls Publishing LLC (2022).

2. Wu LD, Wen K, Cheng ZR, Alwalid O, Han P. Retroperitoneal bronchogenic cyst in suprarenal region treated by laparoscopic resection: A case report. *World J Clin cases* (2021) 9(24):7245–50. doi: 10.12998/wjcc.v9.i24.7245

3. Başoğlu M, Karabulut K, Özbalcı GS, Aykun N, Çamlıdağ İ, Güngör BB, et al. Laparoscopic resection of retroperitoneal bronchogenic cyst clinically presenting as adrenal cyst. *Turk J Surg* (2018), 1–3. doi: 10.5152/turkjsurg.2018.4033

4. Bolton JW, Shahian DM. Asymptomatic bronchogenic cysts: what is the best management? *Ann Thorac Surg* (1992) 53(6):1134–7. doi: 10.1016/0003-4975(92)90412-W

5. Altieri MS, Zheng R, Pryor AD, Heimann A, Ahn S, Telem DA. Esophageal bronchogenic cyst and review of the literature. *Surg Endosc* (2015) 29(10):3010–5. doi: 10.1007/s00464-015-4082-4

6. Lateef N, Kuniyoshi J, Latif A, Ahsan MJ, Shaikh K, DeVrieze B, et al. Cardiac tamponade as a complication of bronchogenic cyst. *Proc (Bayl Univ Med Cent)* (2020) 34(1):172–4. doi: 10.1080/08998280.2020.1795594

7. Tong HX, Liu WS, Jiang Y, Liu JU, Zhou JJ, Zhang Y, et al. Giant retroperitoneal bronchogenic cyst mimicking a cystic teratoma: A case report. *Oncol Lett* (2015) 9(6):2701–5. doi: 10.3892/ol.2015.3076

8. Wang M, He X, Qiu X, Tian C, Li J, Lv M. Retroperitoneal bronchogenic cyst resembling an adrenal tumor with high levels of serum carbohydrate antigen 19-9: A case report. *Med (Baltimore)* (2017) 96(31):e7678. doi: 10.1097/MD.0000000000007678

9. Kluger MD, Tayar C, Belli A, Salceda JA, van Nhieu JT, Luciani A, et al. A foregut cystic neoplasm with diagnostic and therapeutic similarities to mucinous cystic neoplasms of the pancreas. *Jop* (2013) 14(4):446–9. doi: 10.6092/1590-8577/1402

10. Sullivan SM, Okada S, Kudo M, Ebihara Y. A retroperitoneal bronchogenic cyst with malignant change. *Pathol Int* (1999) 49(4):338–41. doi: 10.1046/j.1440-1827.1999.00869.x

11. Fievet L, Gossot D, de Lesquen H, Calabre C, Merrot T, Thomas P, et al. Resection of bronchogenic cysts in symptomatic versus asymptomatic patients: An outcome analysis. *Ann Thorac Surg* (2021) 112(5):1553–8. doi: 10.1016/j.athoracsur.2020.05.031

12. Aktoğu S, Yuncu G, Halilçolar H, Ermete S, Buduneli T. Bronchogenic cysts: clinicopathological presentation and treatment. *Eur Respir J* (1996) 9(10):2017–21. doi: 10.1183/09031936.96.09102017

13. McAdams HP, Kirejczyk WM, Rosado-de-Christenson ML, Matsumoto S. Bronchogenic cyst: imaging features with clinical and histopathologic correlation. *Radiology* (2000) 217(2):441–6. doi: 10.1148/radiology.217.2.r00nv19441

14. Sumiyoshi K, Shimizu S, Enjoji M, Iwashita A, Kawakami K. Bronchogenic cyst in the abdomen. *Virchows Arch A Pathol Anat Histopathol* (1985) 408(1):93–8. doi: 10.1007/BF00739965

15. Hu BY, Yu H, Shen J (2022). A retroperitoneal bronchogenic cyst clinically mimicking an adrenal mass: three case reports and a literature review. *J. Int. Med. Res.* 50 (1):3000605211072664.

16. Tadokoro T, Misumi T, Itamoto T, Nakahara H, Matsugu Y, Ikeda S, et al. (2022). Retroperitoneal bronchogenic cyst resected by single-incision laparoscopic

surgery in an adolescent female: A case report. *Asian J. Endosc Surg.* 15 (1):206–210.

17. Cowan S, Gunawardene A, Davenport E (2021). Retroperitoneal bronchogenic cyst mistaken as an adrenal adenoma. *ANZ J. Surg.* 91 (7-8):E526–E527.

18. Yuan K, Shu M, Ma Y, Feng W, Ye J, Yuan Y. Ectopic bronchogenic cyst in the retroperitoneal region: a case report and literature review of adult patients. *BMC Surg* (2021) 21(1):347. doi: 10.1186/s12893-021-01341-w

19. Qingyu J, Xiaolong L, Ruohan Z, Licong M, Zhichao T, Qingwei C, et al. (2021). Computed tomography helps pre-operative evaluation before laparoscopic resection of retroperitoneal bronchogenic cyst: A case report. *J. Minim Access Surg.* 17 (1):95–97.

20. Wen Y, Chen W, Chen J, He X (2020). Retroperitoneal bronchogenic cyst resembling an adrenal tumor: two case reports and literature review. *J. Int. Med. Res.* 48 (5):300060520925673.

21. Sinha V, Nandi P, Shankar M, Sardana N (2020). Retroperitoneal bronchogenic cyst: A rare case study. *Cureus* 12 (9), e10421.

22. Liu Q, Gao Y, Zhao Z, Zhao G, Liu R, Lau WY. Robotic resection of benign nonadrenal retroperitoneal tumors: A consecutive case series. *Int J Surg* (2018) 55:188–92. doi: 10.1016/j.ijsu.2018.04.013

23. Yoon YR, Choi J, Lee SM, Kim YJ, Cho HD, Lee JW, et al. (2015). Retroperitoneal bronchogenic cyst presenting paraadrenal tumor incidentally detected by (18)F-FDG PET/CT. *Nucl. Med. Mol. Imaging.* 49 (1):69–72.

24. Bulut G, Bulut MD, Bahadır I, Kotan Ç (2015). Bronchogenic cyst mimicking an adrenal mass in the retroperitoneal region: report of a rare case. *Indian J. Pathol. Microbiol.* 58 (1):96–98.

25. Jiang X, Zeng H, Gong J, Huang R (2015). Unusual uptake of radioiodine in a retroperitoneal bronchogenic cyst in a patient with thyroid carcinoma. *Clin. Nucl. Med.* 40 (5):435–436.

26. Trehan M, Singla S, Singh J, Garg N, Mahajan A. A rare case of intraabdominal bronchogenic cyst- a case report. *J Clin Diagn Res* (2015) 9(11): Pd03–4. doi: 10.7860/JCDR/2015/12949.6761

27. Zhang D, Zhang Y, Liu X, Zhu J, Feng C, Yang C, et al. (2015). Challenge in preoperative diagnosis of retroperitoneal mucinous cyst in a pediatric patient. *Int. J. Clin. Exp. Med.* 8 (10):19540–19547.

28. Terasaka T, Otsuka F, Ogura-Ochi K, Miyoshi T, Inagaki K, Kobayashi Y, et al. (2014). Retroperitoneal bronchogenic cyst: a rare incidentaloma discovered in a juvenile hypertensive patient. *Hypertens. Res.* 37 (6):595–597.

29. Cao DH, Zheng S, Lv X, Yin R, Liu LR, Yang L, et al. (2014). Multilocular bronchogenic cyst of the bilateral adrenal: report of a rare case and review of literature. *Int. J. Clin. Exp. Pathol.* 7 (6):3418–3422.

30. Dong B, Zhou H, Zhang J, Wang Y, Fu Y. (2014). Diagnosis and treatment of retroperitoneal bronchogenic cysts: A case report. *Oncol Lett* 7 (6):2157–9.

31. Castro R, Oliveira MI, Fernandes T, Madureira AJ (2013). Retroperitoneal bronchogenic cyst: MRI findings. *Case Rep. Radiol.* 2013:853795.

32. Runge T, Blank A, Schäfer SC, Candinas D, Gloor B, Angst E (2013). A retroperitoneal bronchogenic cyst mimicking a pancreatic or adrenal mass. *Case Rep. Gastroenterol.* 7 (3):428–432.

33. Cai Y, Guo Z, Cai Q, Dai S, Gao W, Niu Y, et al. (2013). Bronchogenic cysts in retroperitoneal region. *Abdom Imaging.* 38 (1):211–214.

34. Jannasch O, Büschel P, Wodner C, Seidensticker M, Kuhn R, Lippert H, et al. (2013). Retroperitoneoscopic and laparoscopic removal of periadrenally located bronchogenic cysts–a systematic review. *Pol. Przegl Chir.* 85 (12):706–713.

35. O'Neal PB, Moore FD, Gawande A, Cho NL, King EE, Moalem J, et al. (2012). Bronchogenic cyst masquerading as an adrenal tumor: a case of mistaken identity. *Endocr. Pract.* 18 (5):e102–e105.

36. Alguraan Z, Agcaoglu O, El-Hayek K, Hamrahian AH, Siperstein A, Berber E. Retroperitoneal masses mimicking adrenal tumors. *Endocr Pract* (2012) 18 (3):335–41. doi: 10.4158/EP11240.OR

37. Díaz Nieto R, Naranjo Torres A, Gómez Alvarez M, Ruiz Rabelo JF, Pérez Manrique MC, Ciria Bru R, et al. (2010). Intraabdominal bronchogenic cyst. *J. Gastrointest Surg.* 14 (4):756–758.

38. Inaba K, Sakurai Y, Umeki Y, Kanaya S, Komori Y, Uyama I (2010). Laparoscopic excision of subdiaphragmatic bronchogenic cyst occurring in the retroperitoneum: Report of a case. *Surg. Laparosc Endosc Percutan Tech* 20 (6): e199–e203.

39. El Youssef R, Fleseriu M, Sheppard BC (2010). Adrenal and pancreatic presentation of subdiaphragmatic retroperitoneal bronchogenic cysts. *Arch Surg* 145 (3):302–4.

40. Obando J, Merkle E, Bean SM (2009). A retroperitoneal bronchogenic cyst. *Clin. Gastroenterol. Hepatol.* 7 (8):A24–Ae1.

41. Chung JM, Jung MJ, Lee W, Choi S (2009). Retroperitoneal bronchogenic cyst presenting as adrenal tumor in adult successfully treated with retroperitoneal laparoscopic surgery. *Urology* 73 (2):442.e13–5.

42. Roma A, Varsegi M, Magi-Galluzzi C, Ulbright T, Zhou M (2008). The distinction of bronchogenic cyst from metastatic testicular teratoma: A light microscopic and immunohistochemical study. *Am. J. Clin. Pathol.* 130 (2):265–273.

43. Minei S, Igarashi T, Hirano D (2007). A case of retroperitoneal bronchogenic cyst treated by laparoscopic surgery. *Hinyokika Kiyo.* 53 (3):171–174.

44. Chu PY, Hwang TI, Teng TH, Lee CC (2007). A retroperitoneal bronchogenic cyst successfully treated by laparoscopic surgery. *Ann. Saudi Med.* 27 (3):199–200.

45. Terry NE, Senkowski CK, Check W, Brower ST (2007). Retroperitoneal foregut duplication cyst presenting as an adrenal mass. *Am. Surg.* 73 (1):89–92.

46. Ishizuka O, Misawa K, Nakazawa M, Nishizawa O (2004). A retroperitoneal bronchogenic cyst: laparoscopic treatment. *Urol Int.* 72 (3):269–270.

47. Ishikawa T, Kawabata G, Okada H, Arakawa S, Kamidono S, Fujisawa M (2003). Retroperitoneal bronchogenic cyst managed with retroperitoneoscopic surgery. *J. Urol.* 169 (3):1078–1079.

48. Hedayati N, Cai DX, McHenry CR (2003). Subdiaphragmatic bronchogenic cyst masquerading as an "adrenal incidentaloma". *J. Gastrointest Surg.* 7 (6): 802–804.

49. McCrystal DJ, Borzi PA (2002). Retroperitoneoscopic resection of retroperitoneal bronchogenic cysts. *Pediatr. Surg. Int.* 18 (5-6):375–377.

50. Yamamoto E, Nakayama H, Ozaki N, Kitamura Y, Funatsuka M, Ueda M, et al. (1998). Laparoscopically resected foregut cyst adjacent to the right adrenal gland. *Diagn. Ther. Endosc.* 5 (1):53–56.

51. Tokuda N, Naito S, Uozumi J, Shimura H, Takayanagi R, Kumazawa J. A retroperitoneal bronchogenic cyst treated with laparoscopic surgery. *J Urol* (1997) 157(2):619. doi: 10.1016/S0022-5347(01)65220-0

52. Liang MK, Yee HT, Song JW, Marks JL. Subdiaphragmatic bronchogenic cysts: a comprehensive review of the literature. *Am Surg* (2005) 71(12):1034–41. doi: 10.1177/000313480507101210

53. Rud O, May M, Brookman-Amissah S, Moersler J, Greiner A, Gilfrich C. [Retroperitoneal bronchogenic cyst treated by laparoscopic surgery]. *Chirurg* (2010) 81(3):243–6. doi: 10.1007/s00104-009-1799-4

54. Cetinkurşun S, Oztürk H, Celasun B, Sakarya MT, Sürer I. Isolate abdominal bronchogenic cyst: A case report. *Eur J Pediatr Surg* (1997) 7(2):103–5. doi: 10.1055/s-2008-1071064

55. Govaerts K, Van Eyken P, Verswijvel G, Van der Speeten K. A bronchogenic cyst, presenting as a retroperitoneal cystic mass. *Rare Tumors* (2012) 4(1):e13. doi: 10.4081/rt.2012.e13

56. Murakami R, Machida M, Kobayashi Y, Ogura J, Ichikawa T, Kumazaki T. Retroperitoneal bronchogenic cyst: CT and MR imaging. *Abdom Imaging* (2000) 25(4):444–7. doi: 10.1007/s002610000019

57. Liang MK, Marks JL. Congenital bronchogenic cyst in the gastric mucosa. *J Clin Pathol* (2005) 58(12):1344.

58. Choi KK, Sung JY, Kim JS, Kim MJ, Park H, Choi DW, et al. Intraabdominal bronchogenic cyst: report of five cases. *Korean J Hepatobil Pancreat Surg* (2012) 16 (2):75–9. doi: 10.14701/kjhbps.2012.16.2.75

59. Doggett RS, Carty SE, Clarke MR. Retroperitoneal bronchogenic cyst masquerading clinically and radiologically as a phaeochromocytoma. *Virchows Arch* (1997) 431(1):73–6. doi: 10.1007/s004280050071

60. Giulianotti PC, Coratti A, Angelini M, Sbrana F, Cecconi S, Balestracci T, et al. Robotics in general surgery: personal experience in a large community hospital. *Arch Surg* (2003) 138(7):777–84. doi: 10.1001/archsurg.138.7.777

61. Bedirli A, Salman B, Yuksel O. Robotic versus laparoscopic resection for mid and low rectal cancers. *Jsls* (2016) 20(1). doi: 10.4293/JSLS.2015.00110

frontiers | Frontiers in Surgery

TYPE Case Report
PUBLISHED 13 October 2022
DOI 10.3389/fsurg.2022.981045



OPEN ACCESS

EDITED BY
Zhaolun Cai,
Sichuan University, China

REVIEWED BY
Anastasios Papanastasiou,
University of West Attica, Greece
Cenap Dener,
Breast and Endocrine Surgery, Turkey
Maria Sotiropoulou,
Evaggelismos General Hospital, Greece

*CORRESPONDENCE
Li Mei
523036921@qq.com
Xincai Qu
Quxc2008@126.com

†These authors have contributed equally to this work and share first authorship

SPECIALTY SECTION
This article was submitted to Surgical Oncology, a section of the journal Frontiers in Surgery

RECEIVED 29 June 2022
ACCEPTED 15 September 2022
PUBLISHED 13 October 2022

CITATION
Hu L, Qian B, Yan Z, Bing K, Mei L and Qu X (2022) Case report and literature review: Malignant adenomyoepithelioma after breast augmentation.
Front. Surg. 9:981045.
doi: 10.3389/fsurg.2022.981045



# Case report and literature review: Malignant adenomyoepithelioma after breast augmentation

Longqing Hu[1†], Bei Qian[1†], Zhecheng Yan[2], Kaijian Bing[1], Li Mei[1*] and Xincai Qu[1*]

[1]Department of Thyroid and Breast Surgery, Union Hospital, Tongji Medical College, Huazhong University of Science and Technology, Wuhan, China, [2]Department of Pathology, Union Hospital, Tongji Medical College, Huazhong University of Science and Technology, Wuhan, China

**Background:** Breast malignant adenomyoepithelioma (MAME) after breast augmentation has never been reported.
**Case summary:** We reported a case of a 55-year-old woman who was diagnosed with breast MAME 16 years after breast augmentation. Breast augmentation was performed on the patient with two 200 ml round textured prostheses in the subpectoral plane through axillary incisions in 2004. However, a breast ultrasound in 2020 revealed a suspicious malignant lump in the right breast, which was finally confirmed as MAME by pathology. Skin-sparing modified radical mastectomy and immediate breast reconstruction with expander implantation were performed. Subsequently, the patient received three cycles of chemotherapy with the regimen of anthracycline and cyclophosphamide. In the following nearly 2 years of follow-up, no tumor recurrence and metastasis were found, and the overall treatment was satisfactory for the patient.
**Conclusion:** Here, we present a unique case in which a patient was diagnosed with breast MAME after breast augmentation. Skin-sparing modified radical mastectomy and immediate breast reconstruction with expander implantation are feasible approaches that yield at least short-term oncological safety and acceptable aesthetic results. However, whether there is a potential relationship between MAME and breast implants remains to be further explored. Meanwhile, due to the rarity of breast MAME, more authoritative strategies considering both oncological safety and aesthetics to seek better long-term therapeutic effects are needed.

KEYWORDS
breast augmentation, malignant adenomyoepithelioma, MAME, prosthetic implantation, oncological safety, breast reconstruction

## Background

Breast augmentation is the most commonly performed aesthetic surgical procedure. Silicone breast implants are used in nearly 300,000 breast augmentation and 100,000 breast reconstruction operations annually in the United States (1). Although several epidemiologic pieces of evidence show no link between implants and the risk of

developing breast cancer (2), the research on breast cancer after augmentation mammoplasty is still attracting much attention. Early research suggested that cosmetic breast implants adversely affect breast cancer-specific survival following the diagnosis of such disease (3). Some authors have reported that breast cancers in augmented women present at a later stage are more aggressive tumors than those arising in nonaugmented women (4). It has also been reported that women with submuscular implants have a higher incidence of breast cancer than those with subglandular implants (5). In addition, there have been reports that women with textured breast implants are more likely to be diagnosed with anaplastic large cell lymphoma (ALCL) (6). All these studies remind a potential relationship between breast implants and breast tumors.

Adenomyoepithelioma (AME) is a rare tumor that can be seen in salivary glands, skin appendages, lungs, and breasts. Among them, AME of the breast was first reported by Hamperl in 1970 (7), which was considered to be a benign tumor formed by the biphasic proliferation of epithelial and myoepithelial cells. In the classification of breast tumors published by the World Health Organization in 2019, this kind of disease is clearly defined as breast epithelial–myoepithelial lesions. Two types of lesions composed of epithelial and myoepithelial cells in mammary ducts and/or tubules are seen under a microscope. Breast malignant adenomyoepithelioma (MAME) is a rare double-cell group lesion of mammary epithelial cells and myoepithelial cells, which means that one or both of them have malignant characteristics. So far, breast MAME after breast augmentation with implants has never been reported.

# Case description

## History of illness and physical examination

A 55-year-old female patient presented with a right breast lump by palpation without pain and nipple discharge. A medical history confirmed that the patient was implanted with two 200 ml round textured prostheses in the subpectoral plane through axillary incisions in 2004. There were no obvious adverse reactions such as infection and seroma after the breast augmentation surgery. No breast lump was detected before breast augmentation, and the family history of breast cancer was denied.

## Physical examination

Physical examination showed that bilateral breasts were symmetrical, with no nipple deviation and depression, no nipple bleeding or discharge, and no orange peel sign or dimple sign. In addition, the prosthesis could be reached in both breasts. A lump of about 3 cm could be reached under the right nipple with hard texture, unclear boundary, low mobility, and no obvious adhesion to the skin. There was no obvious mass in the left breast or enlarged lymph nodes in the bilateral axilla.

## Imaging examination

The breast ultrasound on August 21, 2020 (**Figures 1A,B**), showed a lobulated and spiculated hypoechoic solid neoplasm of 28.8*24.5*13.9 mm in the inner lower quadrant of the right breast adjacent to the nipple. The neoplasm was measured about 4.8 mm away from the body surface. According to the Breast Imaging Reporting and Data System (BI-RADS), the tumor was classified as grade 5, which meant a malignant possibility. In addition, no obvious abnormality was found in bilateral axillary lymph and the bilateral prosthesis capsule was intact.

The MRI on August 24, 2020 (**Figures 1C–E**), confirmed the existence of phyllodes lump and thickening and increase of blood vessels, suspected as a malignant tumor with a grade of 4C of BI-RADS. At the same time, several early enhanced small nodules, which were suspected as the satellite lesions of the tumor, were found in the superior external area of the lump. Moreover, chronic inflammation-like changes were reported in the surrounding tissues of the prosthesis under the pectoralis major.

## Treatment and final diagnosis

On September 2, 2020, considering the patients' aesthetic requirements, we attempted to remove the lump completely with a negative incisal margin. Unfortunately, the intraoperative pathological examination indicated the breast MAME and posterior margin of the nipple showed cancer involvement. Therefore, we had to excise the nipple–areola complex and perform the skin-sparing modified radical mastectomy. Although there was no established uniform recommendation for the time interval of replacing implants, most plastic surgeons recommend routine replacement no more than 15 years after initial placement (8). At the same time, considering the possibility of subsequent radiotherapy and chemotherapy for breast cancer, the prosthesis was removed, and immediate breast reconstruction with expander implantation was performed. As intraoperative pathological examination demonstrated that no cancer metastasis was found in four sentinel lymph nodes, therefore, the patient did not undergo axillary lymph node dissection. The pathological results are shown in **Figures 2, 3**. Immunohistochemistry shows the following tumor cells: ER (−), PR (+, about 5%, weak to moderate intensity), HER2 (1+), GATA-3 (+), AR (+, 40%, moderate intensity), E-cadherin (+), EMA (+), GCDFP-15 (−), CD-117 (focal +), Syn (−), SOX10, CK5/6, p63, S-100 and SMM-HC

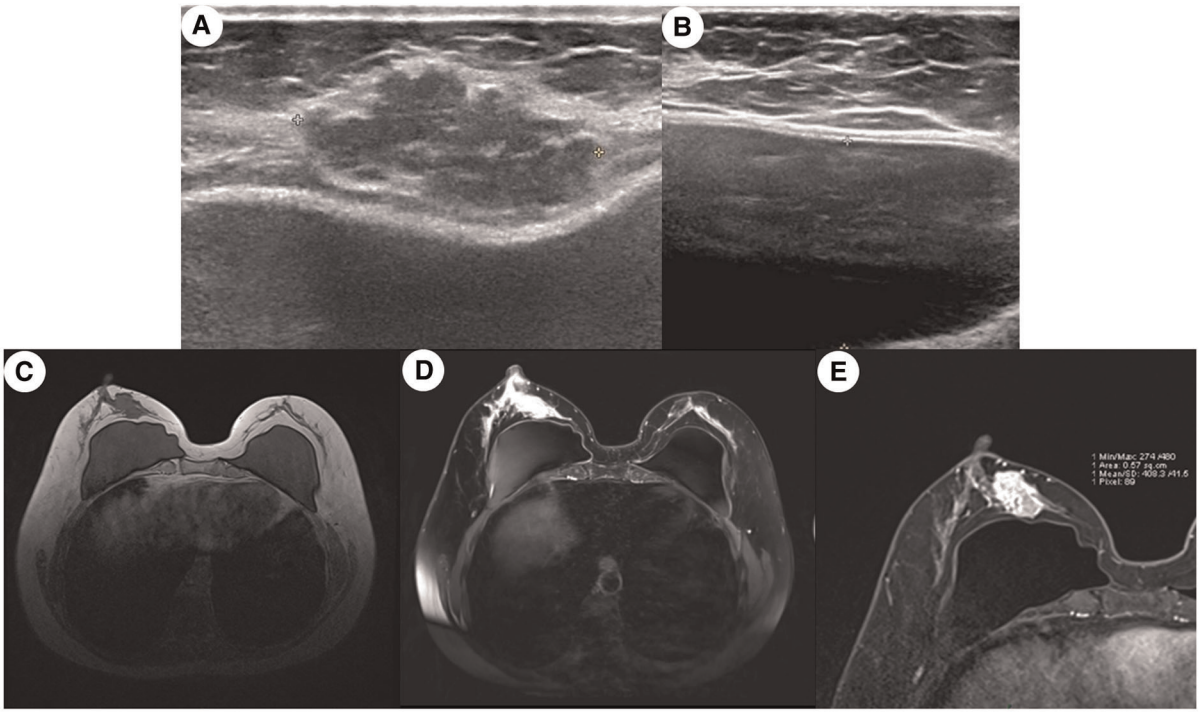


FIGURE 1
Medical imaging presentation of the breast mass. (A) Ultrasound image of a mixed-density multilobulated mass subcutaneous to the breast of an irregular shape and uneven margin; (B) ultrasound image of the pocket of breast prosthesis; (C) MRI image of the breast showing a lobulated mass in the right inner quadrant was adjacent to the margin of the prosthesis, and the vessels were increased and thickened; (D) contrast-enhanced MRI imaging showing that several early enhanced small nodules were seen in the upper posterior area of the tumor and the diffusion was limited, which seems like the satellite lesion of the tumor; (E) enlargement of the image in (D). The capsule of the prosthesis was wrinkled, and the edge of the prosthesis presented the change of chronic inflammation.

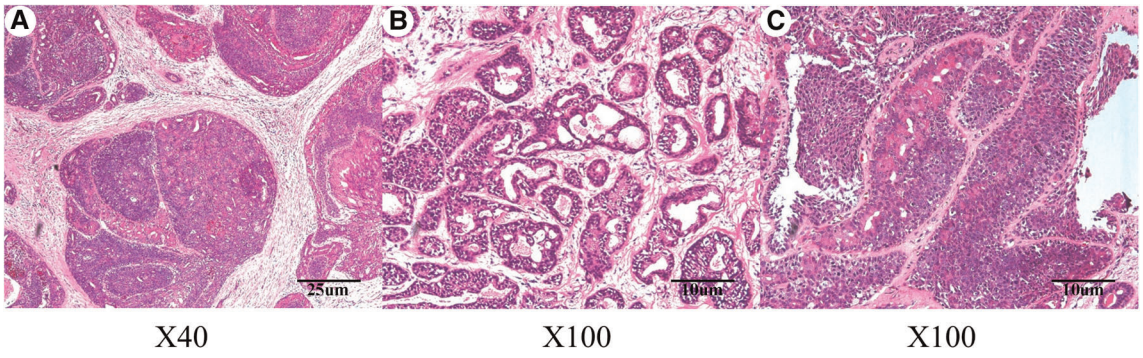


FIGURE 2
Hematoxylin–eosin staining indicated malignant adenomyoepithelioma of the breast lump. (A) Magnification of the main body of the lump (original magnification ×40); (B) magnification of the main body of the lump (original magnification ×100); (C) magnification of the different areas of the lump body (original magnification ×100).

(myoepithelial +), and Ki67 (Li: about 30%). Because of a bidirectional differentiation of glandular and myoepithelium, it was diagnosed as AME; at the same time, due to obvious cell atypia, pathological mitosis, infiltration at the tumor edge, etc., it was diagnosed as MAME.

## Outcomes and follow-up

The patient recovered well after the operation with no complications and was discharged on September 10, 2020. Since November 11, 2020, she has received three cycles of

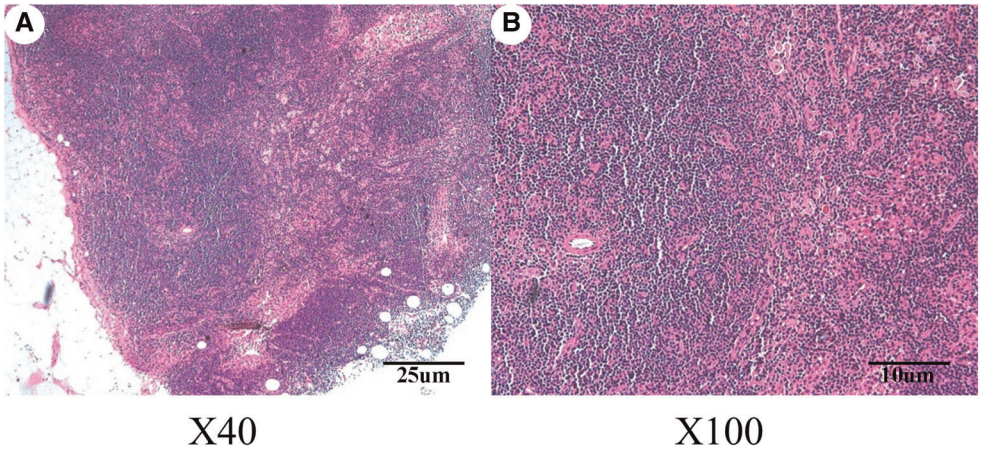


FIGURE 3
Hematoxylin–eosin staining revealed that no metastasis was observed in the sentinel lymph nodes of the right breast. (A) Magnification of the main body of the lymph nodes (original magnification ×40); (B) magnification of the main body of the lymph nodes (original magnification ×100).

chemotherapy in another hospital with the AC*4 regimen (anthracycline combined with cyclophosphamide) and then gave up on her own. There was no recurrence or metastasis in nearly 2 years of follow-up after the operation. This study was reported in agreement with the principles of the CARE guidelines (9).

## Discussion

The potential carcinogenicity of breast implants has always been a common concern for both doctors and patients. Although extensive data negate any link between the implants and an increased incidence of breast cancer (1, 10), a more rigorous recognition is that the evidence remains inconclusive about any association between silicone gel implants and long-term health outcomes (10). Moreover, the largest study of breast implants based on the long-term results of 9,9993 patients explicitly claimed that silicone implants are associated with an increased risk of certain rare harm (11). Meanwhile, Pan et al. suggested that the incidence of breast cancer for women with submuscular implants was higher than that for those with subglandular implants (5). All these views seem to support the presentation of this study to some extent. In addition, some scholars believe that cosmetic breast implants adversely affect breast cancer-specific survival following the diagnosis of such disease (3). However, some studies found that patients with implants were more likely to develop a cancer diagnosis compared with the general population. However, the data do not support breast implants being responsible for these findings. At the same time, some research studies indicated that women with breast implants have different patient demographics and lifestyles from the general population, which may also explain the finding. As for ALCL, reports from the scientific community have suggested a possible link between the disease and breast implants (6). Therefore, this study concludes that more authoritative, large-scale studies are needed to carefully elucidate the relationship between breast implants and long-term health outcomes. Also, whether there is a potential relationship between MAME and breast implants remains to be further explored.

Breast AME is a very rare breast tumor. Most of the relevant literature works are in the form of case reports. According to the statistics of AME cases reported in the literature since 2010, the age of onset of breast AME ranged from 27 to 83 years, with an average of about 60 years. Most of the cases were found in females, although male breast AME cases were also reported. The vast majority of breast AME cases are benign, and the most common site is the external superior quadrant of the breast; the longest course of the disease is 14 years, and the shortest is 4 days. The metastatic sites of AME include lymph nodes, lungs, brain, bone, thyroid, liver, kidneys, thoracic wall, soft tissue, and axillary lymph nodes (12). In the cases with metastasis, the number of distant metastases was significantly more than that of axillary lymph node metastases, so we believe that hematogenous metastasis is more common than lymph node metastasis in breast AME.

Breast AME is difficult to diagnose because of its low incidence rate. According to the clinical data, the most common clinical manifestation was a painless breast lump. Physical examination showed that the lump was medium or hard; most had no nipple discharge, but there were also records of bloody discharge. The most common ultrasound result was round or oval hypoechoic or mixed echo solid lobulated nodules with clear boundaries. Most of the breast molybdenum showed lobulated, irregular, fuzzy boundary, isodense, or slightly high-density lumps, and some of them had small central flake calcification. The clinical

manifestations and ultrasound, mammography, and MRI findings of this disease are difficult to distinguish from other breast tumors, among which the most easily misdiagnosed is breast fibroadenoma. Therefore, the main method of diagnosis is surgical resection and pathological examination: pathological diagnosis includes morphological, biological, and immunohistochemical examination. Breast AME is easy to be misdiagnosed clinically, and it should be carefully differentiated from breast fibroadenoma, benign myoepithelioma, pleomorphic adenoma, adenoid cystic carcinoma, myoepithelial carcinoma, etc.

Meanwhile, it is difficult to distinguish between benign and malignant breast AMEs. The malignant features reported in the literature that may lead to recurrence and metastasis included cellular pleomorphism, increased mitotic activity, nuclear pleomorphism, prominent nucleoli, hyperchromasia, and necrosis. The above indexes should be considered comprehensively; otherwise, it is easy to be misdiagnosed. For MAME, the biological behavior seems to be related to the degree of malignant component and tumor size (13). The two components of AME (mammary epithelium and myoepithelium) can be malignant transformation and distant metastasis. Most of the time, it is the malignant transformation of only one of the components, but cases of two components malignant transformation at the same time have also been reported (14). Immunohistochemistry showed that the tumor was bipolar; in most cases, SMA, actin, p63, CK5/6, and S-100 were positive in myoepithelial cells, while ER/PR was negative. Some think that the combination of p63 and actin/troponin immunostaining is the most suitable method for visualizing myoepithelial cells (15). Most cases are often triple negative (ER/PR/HER-2 negative) (16), so endocrine therapy and anti-Her-2 therapy are often ineffective, which also leads to the difficulty of treatment. Tavassoli (17) divided breast AMEs into three types: (1) spindle cell type, in which the lesions were mainly composed of proliferative spindle myoepithelial cells mixed with a small number of epithelial cells; (2) tubular type, in which the lesions are composed of myoepithelial cells and glandular epithelial cells around the duct, similar to sclerosing papilloma, tubular adenoma, and glandular tubular adenoma; and (3) tubular type, in which the proliferative myoepithelial cells are arranged in a solid, nest-like arrangement, and some of them are like plasma cells, the cytoplasm is dense, transparent, eosinophilic, and the nucleus moves around. Additionally, recently, breast AMEs were characterized as PIK3CA, AKT1, and HRAS mutations (18).

At present, the treatment for breast AME has not been unified, but there are literature (19) records that breast AME has the risk of recurrence and metastasis. Therefore, for benign breast AME, we recommended local lump resection and keeping a safe incisal margin, while for malignant breast AME, we recommended modified radical mastectomy to ensure a negative margin; sentinel lymph node biopsy was used to decide whether axillary lymph node dissection is necessary. There is no clear data to support the effectiveness of chemotherapy, radiation therapy, and endocrine therapy. Whether patients with MAME should receive chemotherapy and radiotherapy is still controversial. We believe that it should be considered comprehensively from the tumor's biological behavior and morphological behavior, invasion degree of surrounding tissues, lymph node metastasis, and patients' will. Two cases of chemotherapy and one case of radiotherapy were recorded: one received TC (paclitaxel liposome and cyclophosphamide) regimens with four cycles; one received one cycle of TE regimen (docetaxel and epirubicin) before operation and another cycle of TE regimen after operation; one received radiotherapy [gray (Gy) 50 total dose plus a boost of Gy 10 to the tumor bed] (20). For metastatic breast AME, there is no definite reported treatment method, and its prognosis is very poor (21). No literature proves that radiotherapy and chemotherapy have therapeutic effects on metastatic breast AME, but some scholars (22) believe that eribulin may be beneficial to patients with metastatic breast AME.

Since there is no literature on MAME after augmentation mammoplasty, this first reported study may provide experience for managing such patients. Some limitations were present in this study. First, more details of augmentation mammoplasty were unknown; Second, the follow-up time was too short to assess the long-term outcomes. Third, we are unable to present preoperative and postoperative surgical photos of the patient due to the patient's concern about privacy protection.

## Conclusion

Here, we present a unique case of a patient diagnosed with breast MAME after breast augmentation. Skin-sparing modified radical mastectomy and immediate breast reconstruction with expander implantation is a feasible approach that yields at least short-term oncological safety and acceptable aesthetic results. However, whether there is a potential relationship between MAME and breast implants remains to be further explored. Meanwhile, due to the rarity of breast MAME, more authoritative strategies considering both oncological safety and aesthetics to seek better long-term therapeutic effects are needed.

## Data availability statement

The original contributions presented in the study are included in the article/Supplementary Material, further inquiries can be directed to the corresponding author.

## Ethics statement

Ethical review and approval were not required for the study on human participants in accordance with the local legislation and institutional requirements. The patients/participants provided their written informed consent to participate in this study. Written informed consent was obtained from the individual(s) for the publication of any potentially identifiable images or data included in this article.

## Author contributions

Conception and design: all authors; administrative support: XQ and LM; provision of study materials or patients: ZcY and KjB; collection and assembly of data: LH and BQ; data analysis and interpretation: LH and BQ; pathological diagnosis: ZY; manuscript writing: all authors. All authors contributed to the article and approved the submitted version.

## Conflict of interest

The authors declare that the research was conducted in the absence of any commercial or financial relationships that could be construed as a potential conflict of interest.

## Publisher's note

All claims expressed in this article are solely those of the authors and do not necessarily represent those of their affiliated organizations, or those of the publisher, the editors and the reviewers. Any product that may be evaluated in this article, or claim that may be made by its manufacturer, is not guaranteed or endorsed by the publisher.

## References

1. Rohrich RJ, Kaplan J, Dayan E. Silicone implant illness: science versus myth? *Plast Reconstr Surg.* (2019) 144:98–109. doi: 10.1097/PRS.0000000000005710

2. Cho EH, Shammas RL, Phillips BT, Greenup RA, Hwang ES, Hollenbeck ST. Breast cancer after augmentation: oncologic and reconstructive considerations among women undergoing mastectomy. *Plast Reconstr Surg.* (2017) 139:1240e–9e. doi: 10.1097/PRS.0000000000003342

3. Lavigne E, Holowaty EJ, Pan SY, Villeneuve PJ, Johnson KC, Fergusson DA, et al. Breast cancer detection and survival among women with cosmetic breast implants: systematic review and meta-analysis of observational studies. *Br Med J.* (2013) 346:f2399. doi: 10.1136/bmj.f2399

4. Skinner KA, Silberman H, Dougherty W, Gamagami P, Waisman J, Sposto R, et al. Breast cancer after augmentation mammoplasty. *Ann Surg Oncol.* (2001) 8:138–44. doi: 10.1007/s10434-001-0138-x

5. Pan SY, Lavigne E, Holowaty EJ, Villeneuve PJ, Xie L, Morrison H, et al. Canadian breast implant cohort: extended follow-up of cancer incidence. *Int J Cancer.* (2012) 131:E1148–57. doi: 10.1002/ijc.27603

6. Leberfinger AN, Behar BJ, Williams NC, Rakszawski KL, Potochny JD, Mackay DR, et al. Breast implant-associated anaplastic large cell lymphoma: a systematic review. *JAMA Surg.* (2017) 152:1161–8. doi: 10.1001/jamasurg.2017.4026

7. Hamperl H. The myothelia (myoepithelial cells). Normal state; regressive changes; hyperplasia; tumors. *Curr Top Pathol.* (1970) 53:161–220. doi: 10.1007/978-3-662-30514-0_3

8. Fardo D, Sequeira Campos M, Pensler JM. *Breast augmentation,* Treasure Island (FL): StatPearls (2022).

9. Riley DS, Barber MS, Kienle GS, Aronson JK, von Schoen-Angerer T, Tugwell P, et al. CARE Guidelines for case reports: explanation and elaboration document. *J Clin Epidemiol.* (2017) 89:218–35. doi: 10.1016/j.jclinepi.2017.04.026

10. Balk EM, Earley A, Avendano EA, Raman G. Long-term health outcomes in women with silicone gel breast implants: a systematic review. *Ann Intern Med.* (2016) 164:164–75. doi: 10.7326/M15-1169

11. Coroneos CJ, Selber JC, Offodile 2nd AC, Butler CE, Clemens MW. US FDA breast implant postapproval studies: long-term outcomes in 99,993 patients. *Ann Surg.* (2019) 269:30–6. doi: 10.1097/SLA.0000000000002990

12. Xu J, Tang X, Iida Y, Fuchinoue F, Kusumi T, Yagihashi N, et al. Adenomyoepithelioma with carcinoma of the breast: a report of two cases and a review of the literature. *Pathol Res Pract.* (2016) 212:130–4. doi: 10.1016/j.prp.2015.09.008

13. Van Dorpe J, De Pauw A, Moerman P. Adenoid cystic carcinoma arising in an adenomyoepithelioma of the breast. *Virchows Arch.* (1998) 432:119–22. doi: 10.1007/s004280050144

14. Hungermann D, Buerger H, Oehlschlegel C, Herbst H, Boecker W. Adenomyoepithelial tumours and myoepithelial carcinomas of the breast–a spectrum of monophasic and biphasic tumours dominated by immature myoepithelial cells. *BMC Cancer.* (2005) 5:92. doi: 10.1186/1471-2407-5-92

15. Díaz Del Arco C, Estrada Muñoz L, Pascual Martín A, Pelayo Alarcón A, de Pablo Velasco D, Ortega Medina L. Adenomyoepithelioma of the breast: report of four cases and literature review. *Rev Esp Patol.* (2018) 51:55–60. doi: 10.1016/j.patol.2016.12.001

16. Delteil C, Jalaguier Coudray A, Charafe Jauffret E, Thomassin Piana J. (Adenomyoepithelioma with dominant myoepithelial contingent of the breast: a case report and literature review). *Ann Pathol.* (2015) 35:449–53. doi: 10.1016/j.annpat.2015.05.006

17. Tavassoli FA. Myoepithelial lesions of the breast. Myoepitheliosis, adenomyoepithelioma, and myoepithelial carcinoma. *Am J Surg Pathol.* (1991) 15:554–68. doi: 10.1097/00000478-199106000-00004

18. Lubin D, Toorens E, Zhang PJ, Jaffer S, Baraban E, Bleiweiss IJ, et al. Adenomyoepitheliomas of the breast frequently harbor recurrent hotspot mutations in PIK3-AKT pathway-related genes and a subset show genetic similarity to salivary gland epithelial-myoepithelial carcinoma. *Am J Surg Pathol.* (2019) 43:1005–13. doi: 10.1097/PAS.0000000000001275

19. Hayes MM. Adenomyoepithelioma of the breast: a review stressing its propensity for malignant transformation. *J Clin Pathol.* (2011) 64:477–84. doi: 10.1136/jcp.2010.087718

20. Petrozza V, Pasciuti G, Pacchiarotti A, Tomao F, Zoratto F, Rossi L, et al. Breast adenomyoepithelioma: a case report with malignant proliferation of epithelial and myoepithelial elements. *World J Surg Oncol.* (2013) 11:285. doi: 10.1186/1477-7819-11-285

21. Kihara M, Yokomise H, Irie A, Kobayashi S, Kushida Y, Yamauchi A. Malignant adenomyoepithelioma of the breast with lung metastases: report of a case. *Surg Today.* (2001) 31:899–903. doi: 10.1007/s005950170031

22. Lee S, Oh SY, Kim SH, Lee JH, Kim DC, Cho SH, et al. Malignant adenomyoepithelioma of the breast and responsiveness to eribulin. *J Breast Cancer.* (2015) 18:400–3. doi: 10.4048/jbc.2015.18.4.400

frontiers | Frontiers in Immunology

TYPE Case Report
PUBLISHED 17 October 2022
DOI 10.3389/fimmu.2022.1010490



OPEN ACCESS

EDITED BY
Zhaolun Cai,
Sichuan University, China

REVIEWED BY
Min Kyu Kim,
Sungkyunkwan University, South Korea
Antonio Simone Laganà,
University of Palermo, Italy
Giuseppe Gullo,
Azienda Ospedaliera Ospedali Riuniti Villa Sofia Cervello, Italy
Sunesh Kumar,
All India Institute of Medical Sciences, India

*CORRESPONDENCE
Dan-dan Li
lidd@sysucc.org.cn
Gong Chen
chengong@sysucc.org.cn

SPECIALTY SECTION
This article was submitted to Cancer Immunity and Immunotherapy, a section of the journal Frontiers in Immunology

RECEIVED 03 August 2022
ACCEPTED 03 October 2022
PUBLISHED 17 October 2022

CITATION
Cao D, Gao Y, Zhang R-x, Wang F-l, Li C, Wu M-q, Liu Y-f, Li D-d and Chen G (2022) Case report: Reproductive organ preservation and subsequent pregnancy for an infertility patient with lynch syndrome-associated synchronous endometrial cancer and colon cancer after treatment with a PD-1 checkpoint inhibitor.
*Front. Immunol.* 13:1010490.
doi: 10.3389/fimmu.2022.1010490



# Case report: Reproductive organ preservation and subsequent pregnancy for an infertility patient with lynch syndrome-associated synchronous endometrial cancer and colon cancer after treatment with a PD-1 checkpoint inhibitor

Di Cao[1,2], Yu Gao[3], Rong-xin Zhang[1,2], Fu-long Wang[1,2], Cong Li[1,2], Miao-qing Wu[1,2], Yi-fan Liu[1,2], Dan-dan Li[1,4]* and Gong Chen[1,2]*

[1]Sun Yat-sen University Cancer Center, State Key Laboratory of Oncology in South China, Collaborative Innovation Center for Cancer Medicine, Guangzhou, China, [2]Department of Colorectal Surgery, Sun Yat-sen University Cancer Center, Guangzhou, China, [3]Department of Obstetrics, The Sixth Affiliated Hospital of Sun Yat-sen University, Guangzhou, China, [4]Biotherapy Center, Sun Yat-sen University Cancer Center, Guangzhou, China

Currently, immune checkpoint inhibitors (ICIs) are the mainstay of treatment for Lynch syndrome patients. However, the tumor regression features in radiology and pathology are inconsistent for patients who are treated with ICIs, which sometimes confuses surgical decision-making. Here, we report a case in which a 36-year-old patient suffering from infertility was diagnosed with Lynch syndrome-associated synchronous endometrial cancer and colon cancer, and persistently enlarged left iliac paravascular lymph nodes were detected after receiving sintilimab treatment, a programmed cell death 1 (PD-1) receptor inhibitor. Fortunately, when she was about to undergo hysterectomy and bilateral salpingo-oophorectomy, intraoperative pathology examination did not reveal any cancer cells in these lymph nodes, and therefore, her reproductive organs were preserved. Later, the patient successfully conceived and gave birth to a healthy male neonate with no immune-related adverse events (irAEs) during an 11-month follow-up. This case indicates that surgeons should carefully inspect the imaging characteristics after immunotherapy and that organ preservation is possible even for patients

who fail to achieve complete clinical regression, which is especially important for female patients of childbearing age.

KEYWORDS

PD-1 inhibitor, organ preservation, lynch syndrome, pregnancy, case report

## Introduction

Lynch syndrome (LS), characterized by germline mutations of the DNA mismatch repair (MMR) system, is the most common inherited cancer syndrome (1). The global incidence of LS is approximately 1/279, and almost all LS-associated cancers present deficient MMR (dMMR) and high-level microsatellite instability (MSI-H). Colorectal cancer (CRC) and endometrial cancer (EC) are the two most common LS-associated cancers (2). There are approximately 6000 new LS-EC cases each year, accounting for 9% of all new EC cases worldwide (3, 4). Previously, the treatments for LS-EC and LS-CRC were the same as those of general EC and CRC. Surgery is the first choice if the tumor is resectable. For unresectable CRC or EC patients, receiving translational therapies is necessary, including chemotherapy, radiotherapy, targeted therapy and immunotherapy, which provides opportunities for radical resection. Understandably, surgery for LS-EC patients permanently destroys fertility. This situation hit a turning point when Le et al. demonstrated that dMMR patients were particularly sensitive to pembrolizumab, a representative ICI drug, in 2015 (5). Thus, the 2018 National Comprehensive Cancer Network (NCCN) guidelines recommended that pembrolizumab should be used in patients with MSI-H or dMMR diseases, greatly benefiting LS patients during immunotherapy.

However, the different tumor regression features in radiology and pathology of patients treated with ICIs have influenced clinical decision-making for surgeons. For female patients, reproductive organ preservation is an inevitable issue. If clinical complete regression (cCR) is not achieved according to preoperative images, patients are obliged to undergo radical resection, which leads to permanent infertility. However, if pathological complete regression (pCR) is achieved, radical surgery should be avoided.

Additionally, PD-1 inhibitors (IgG4 antibodies) may influence fetal development during pregnancy by crossing the human placenta. Using anti-PD-1 antibodies in mice weakens the immune tolerance mediated by regulatory T cells (Tregs) and significantly increases miscarriage rates (6). This finding revealed a key role of the PD-1/PD-L1 pathway in maintaining maternal-fetal immune tolerance. Thus, PD-1 antibody is classified as an FDA pregnancy Category D drug (7).

In general, this case suggests that surgeons should focus on reproductive organ preservation in female patients receiving ICI treatment rather than only considering preoperative images. In addition, our case provides additional experience in using PD-1 antibody in patients who plan to conceive. This study was reported in agreement with the principles of the CARE Guidelines (8) and includes a reporting checklist as Supplementary Material (Table S1) (9).

## Case description

The patient was a 36-year-old woman who suffered from LS-EC and LS-CRC. She conceived naturally and successfully bore a male neonate after treatment with sintilimab, a PD-1 inhibitor. The timeline is shown in Figure 1. At the age of 32, she went to Fudan University Obstetrics and Gynecology Hospital because she had failed to conceive naturally for more than one year. She underwent hysteroscopy and was found to have atypical hyperplasia of the endometrium, so she was prescribed an initial regimen of megestrol 160 mg QD in combination with metformin 0.5 g TID. Seven months later, she underwent a second hysteroscopy, which detected that the endometrium had locally progressed to grade 1 endometrioid adenocarcinoma. Due to her strong desire to conceive, the patient refused the medical advice of hysterectomy. She was referred to Peking Union Medical College Hospital, and her medication regimen was changed to enantone 3.75 mg 1/28D + letrozole 2.5 mg QD. One year later, her endometrium had reversed, and she was advised to undergo *in vitro* fertilization (IVF). However, she did not adopt this suggestion for personal reasons, and over the following year, she still failed to conceive naturally without any contraception. In December 2019, she requested IVF at Xiangya Hospital of Central South University. Preoperative hysteroscopy did not show any endometrial abnormality, but she underwent additional pelvic magnetic resonance imaging (MRI) owing to her history of endometrial cancer, which showed that the left pelvic lymph nodes (LNs) were enlarged and considered metastases. In addition, her positron emission tomography-computed tomography (PET-CT) scan showed a hypermetabolic lesion in the transverse colon, which was later confirmed as a transverse colon (TC) adenocarcinoma by colonoscopy biopsy.

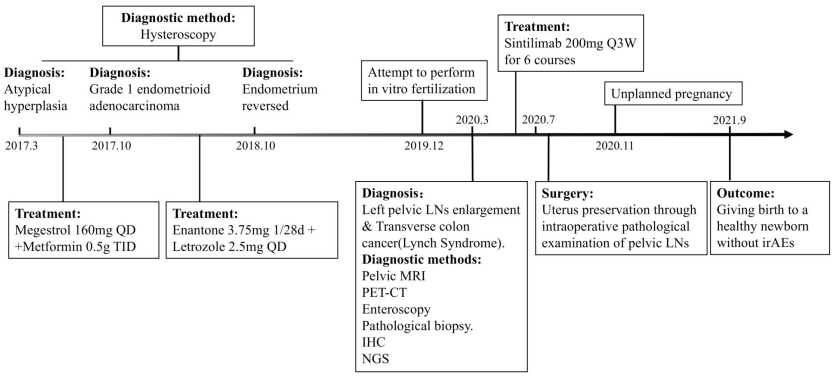


FIGURE 1
Timeline overview.

The patient came to our hospital in March 2020. We reexamined the colonoscopy results and identified the TC mass as a moderately to poorly differentiated adenocarcinoma. Of note, her immunohistochemistry (IHC) examination indicated the loss of MSH2 protein in both her EC and CRC lesions. Moreover, her father, aunt, and cousin all died of malignant tumors. Therefore, LS was highly suspected, and we conducted genetic testing, which revealed that both the EC and TC lesions were MSI-H and had somatic mutations of MSH2. More importantly, the patient also carried germline MSH2 mutations. The tumor mutation burden (TMB) of the EC lesion was 29.9 muts/Mb, and the TMB of the TC lesion was 77 muts/Mb. Based on her medical history and test results, the patient was diagnosed with LS.

Thoracoabdominal and pelvic CT were performed on March 16, 2020 (Figure 2A). CT images showed that the long diameter of the TC lesion was 32 mm, and there were enlarged LNs adjacent to the primary colon and left iliac vessels. The short diameters of the largest pelvic and pericolic LNs, which were considered metastatic LNs, were 12 mm and 18 mm, respectively. According to the results, we initiated neoadjuvant immunotherapy with sintilimab at a fixed dose of 200 mg every 3 weeks. From March to July 2020, the patient received 6 courses of immunotherapy. No significant immune-related adverse events (irAEs) were observed during the treatment. After the third course on May 5, 2020, the patient underwent enteroscopy and abdominal CT (Figure 2B). Both assessments suggested that the size of the primary and pericolic LNs had increased to 41 mm and 21 mm, respectively, compared with baseline, while the largest left pelvic LN had decreased to 8 mm. Because of our therapeutic goal of controlling the pelvic metastatic LNs, we decided to continue her neoadjuvant therapy. At the end of the sixth course on July 14, 2020, another abdominal CT was performed (Figure 2C) and showed that the TC lesion and pelvic LNs were stable, while the pericolic LNs had increased to 26 mm. In addition, her CEA serum level increased from 7.02 ng/ml to 19.17 ng/ml. At this time, we organized a multidisciplinary team (MDT) to discuss the case. According to the images, the enlarged left pelvic LNs most likely originated from EC metastasis. Although the TC lesion was confirmed as iCPD by the irRECIST method, it could reach R0 resection. Therefore, we decided to perform surgery. The surgical plan included radical TC resection, hysterectomy, bilateral salpingo-oophorectomy resection, pelvic LN dissection and retroperitoneal LN dissection.

On July 31, 2020, the patient underwent laparoscopic right hemicolectomy with radical lymphadenectomy. We did not observe any other lesions in the abdominal-pelvic cavity during intraoperative exploration. The tumor resided in the TC near the hepatic flexure and was approximately 6*5 cm in size. It possessed a tough texture and had invaded the serosa. The boundary between the tumor and the mesenteric LNs was unclear. There were several enlarged lymph nodes that extended from the left iliac vasculature to the left obturator area. Therefore, we performed an intraoperative gynecological consultation, and the gynecologist proposed total hysterectomy, bilateral salpingo-oophorectomy, and left pelvic lymphadenectomy. However, considering the patient's desire to conceive and the possible effects of immunotherapy, we decided to send the left pelvic LNs for pathological examination before resection, and none of the 7 submitted pelvic LNs contained cancer cells. Subsequently, we communicated with her family about the possibility of pathological complete regression (pCR) and the risk of EC recurrence without hysterectomy. Ultimately, her family chose to preserve her uterus and bilateral adnexa and signed an informed consent document for the fertility preservation strategy. Postoperative pathological examination confirmed that

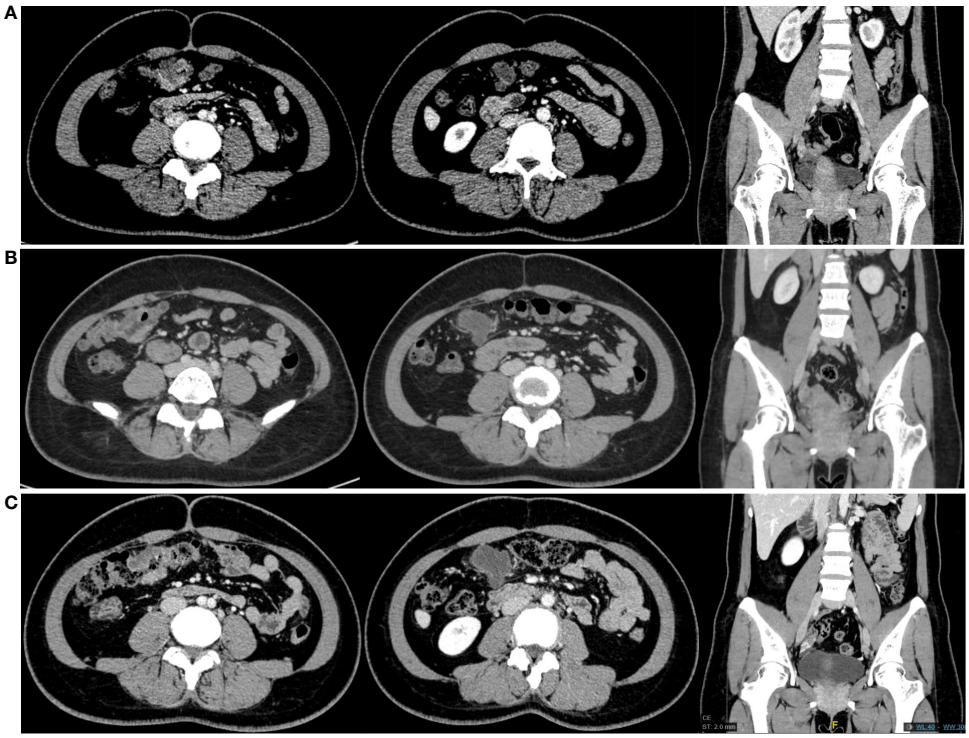


FIGURE 2
CT scans obtained from the patient. From left to right, each group of images shows the transverse colon lesion, para-transverse colon lymph nodes and the lymph nodes next to the left iliac vessels. **(A)** CT scans in March 2020. **(B)** CT scans in May 2020. **(C)** CT scans in July 2020.

the TC lesion was a poorly differentiated adenocarcinoma that had invaded through the muscularis propria into the pericolic tissues (pT3). Nerve tract invasion and intravascular cancer embolus were not observed. The resection margin was negative, and the tumor regression grade (TRG) was 2. No cancer tissue was observed in a total of 35 dissected LNs, including 28 pericolic LNs and 7 left pelvic LNs. The tumor deposits were also not detected.

After the surgery, the patient received adjuvant immunotherapy with a PD-1 inhibitor for 1 year. Although we told her to use contraception, she did not follow this advice because she had lost faith in natural conception. However, in December 2020, the patient unexpectedly found herself at 38 days' gestation. Even though we informed the patient and her family of the possible adverse influences on the fetus, they still planned to continue with the pregnancy and complied with the obstetrician's advice. There were no tumor-related conditions or gestational abnormalities, and in the 36$^{th}$ week of gestation, the patient successfully gave birth to a male neonate by cesarean section. The Apgar score of the male neonate was 9, and his serum levels of G6PD, TSH, 17-OHP and PHE were normal. There were no irAEs in either the mother or the neonate during an 11-month follow-up, and the patient is still being followed closely.

## Discussion

We report the first case in which a female LS patient suffering from both EC and CRC successfully conceived and delivered after receiving treatment with sintilimab, a PD-1 antibody. Our report mainly highlights the complexity of reproductive organ preservation for LS-EC patients. After PD-1 antibody treatment, uterine preservation is still feasible even in EC patients with pelvic LN metastases, which diverges from the previous therapeutic principle that hysterectomy is usually unavoidable for these patients.

In recent years, infertility treatment strategies have become established and various in number. Nontumorous female patients can undergo ovarian stimulation, oocyte vitrification, and IVF to treat infertility. However, these practices are still limited for patients suffering from EC, which is the most frequent gynecological malignancy and severely influences young patients without a childbearing history (10, 11). The early detection of EC is extremely important for the reproductive organ preservation of patients. Diagnostic tools for early-stage EC detection are emerging, such as relative telomere length in cell-free DNA, glandular cells detected at preoperative cervical smear, and transvaginal ultrasound (12–14). The treatment of early-stage EC is conservative and follows

the conventional regimen of medroxyprogesterone acetate (MPA) and megestrol acetate (MA) (15). Previously, type I EC at the early stage was identified as the only histological type that can be addressed with a fertility-sparing approach. Nevertheless, with a deeper understanding of molecular oncology, the importance of molecular classification for EC treatment was gradually realized, and MSI was determined to be a fair prognostic factor for fertility-sparing treatment (16, 17).

Notably, LS-EC patients featuring MSI could benefit from PD-1 antibodies, and clinicians should take into account the possibility of CR, which means that non-early-stage young patients still have a chance to preserve their reproductive organs. It is worth noting that the pathological remission rate often exceeds the radiological remission rate in patients receiving PD-1 antibody treatment. For example, 13 patients with dMMR CRC achieved pCR after pembrolizumab treatment, but among them, only 1 patient achieved cCR (18). Furthermore, some patients may develop lesion enlargement during treatment, probably caused by T-cell infiltration into the tumor stroma. These studies suggest that imaging is insufficient as an absolutely accurate standard for evaluating PD-1 efficacy. Intraoperative pathological biopsy may provide additional information for better treatment decisions.

How PD-1 antibodies influence pregnancy has always been a topic of interest. Recently, several cases have reported successful pregnancy outcomes in patients treated with PD-1 antibodies in different cancer types, including metastatic melanoma, relapsed Hodgkin's lymphoma and placental site trophoblastic tumors (6, 7, 19–27). Nevertheless, irAEs, such as intrauterine growth restriction, HELLP syndrome, placental insufficiency and low fetal heart rate, have occurred in some of these patients (28). Thus, whether conception is safe for patients after treatment with PD-1 antibody is still controversial. Current studies believe that blocking the PD-1/PD-L1 pathway will interfere with normal pregnancy because of its key role in maintaining maternal immune tolerance to the fetus, which is regarded as an allogeneic component. Fetal antigens can be processed and presented in the maternal body, leading to the activation and expansion of anti-fetus T cells (29). At the early stage of pregnancy, increased PD-L1 expression in trophoblast cells, decidual macrophages and decidual stromal cells on the maternal-fetal interface can inhibit the activity of T helper cells and the production of proinflammatory cytokines and facilitate the function of Treg cells, which mediate maternal-fetal immune tolerance. In mice, blockade of the PD-1/PD-L1 pathway inhibited Treg cell function and reduced the embryonic survival rate. In crab-eating monkeys, using high doses of nivolumab antibodies (10 mg/kg or more) resulted in significantly higher risks of fetal growth restriction and premature delivery.

However, the effect of PD-1 antibody on pregnancy is determined by multiple factors and needs comprehensive consideration. First, the administration doses and frequencies of PD-1 antibodies in clinical settings are much lower and less than those in experimental settings. Even when exposed to high doses of PD-1 antibody, animals did not present increasing risks of fetal malformations, immunodeficiencies or neurological complications (30). Second, the effect of PD-1 antibody on the fetus is subject to the interval between the last dose of the antibody and the start of pregnancy. PD-1 antibody, as an IgG antibody, requires active transport to enter the placenta where the neonatal Fc receptor (FcRn) resides. FcRn on syncytiotrophoblast cells can bind to IgG antibodies and allow them to pass through the placental barrier. However, FcRn is rarely detected during the first 14 weeks of pregnancy, which restricts the transfer of IgG antibody (31). Thus, the timing of the last administration and the pharmacokinetics of the PD-1 antibody are also involved in its effect on pregnancy. Finally, the patient's fertility intention and physical condition need to be taken into full consideration. Currently, the National Comprehensive Cancer Network guidelines recommend that all patients of reproductive age should use effective contraception during immunotherapy and maintain its use for at least 5 months after the last course of immunotherapy, which lacks adequate evidence and needs further exploration.

In conclusion, our report indicates that for young female patients with LS-EC, surgeons should be aware of the possibility of reproductive organ preservation. Intraoperative pathological biopsy is more conducive to guiding surgical decision-making for these patients. In addition, we recommend that patients should use contraception for a sufficient period after receiving PD-1 antibody treatments to reduce the incidence of irAEs.

## Data availability statement

The original contributions presented in the study are included in the article/Supplementary Material. Further inquiries can be directed to the corresponding authors.

## Ethics statement

Written informed consent was obtained from the individual(s) for the publication of any potentially identifiable images or data included in this article.

## Author contributions

DC collected the data and wrote the manuscript. DC, GY, CL, F-lW, R-xZ, D-dL, and GC was involved in the diagnosis and treatment of the disease. GY performed the histological obstetrical examination. D-dL and GC performed conception and design. GY, F-lW, R-xZ, CL, M-qW, Y-fL, D-dL, and GC reviewed and revised the manuscript. D-dL and GC supervised the review and

approved the final version of the manuscript. All authors contributed to the article and approved the submitted version.

## Acknowledgments

We appreciated the gynecologist, Ting Wan and the department of pathology for consultations during treatment.

## Conflict of interest

The authors declare that the research was conducted in the absence of any commercial or financial relationships that could be construed as a potential conflict of interest.

## Publisher's note



## Supplementary material

The Supplementary Material for this article can be found online at: https://www.frontiersin.org/articles/10.3389/fimmu.2022.1010490/full#supplementary-material

## References

1. Lynch HT, Lynch PM, Lanspa SJ, Snyder CL, Lynch JF, Boland CR. Review of the lynch syndrome: history, molecular genetics, screening, differential diagnosis, and medicolegal ramifications. *Clin Genet* (2009) 76(1):1–18. doi: 10.1111/j.1399-0004.2009.01230.x

2. Boland PM, Yurgelun MB, Boland CR. Recent progress in lynch syndrome and other familial colorectal cancer syndromes. *CA Cancer J Clin* (2018) 68(3):217–31. doi: 10.3322/caac.21448

3. Lu KH, Schorge JO, Rodabaugh KJ, Daniels MS, Sun CC, Soliman PT, et al. Prospective determination of prevalence of lynch syndrome in young women with endometrial cancer. *J Clin Oncol* (2007) 25(33):5158–64. doi: 10.1200/JCO.2007.10.8597

4. Gu B, Shang X, Yan M, Li X, Wang W, Wang Q, et al. Variations in incidence and mortality rates of endometrial cancer at the global, regional, and national levels, 1990-2019. *Gynecol Oncol* (2021) 161(2):573–80. doi: 10.1016/j.ygyno.2021.01.036

5. Le DT, Uram JN, Wang H, Bartlett BR, Kemberling H, Eyring AD, et al. PD-1 blockade in tumors with mismatch-repair deficiency. *N Engl J Med* (2015) 372 (26):2509–20. doi: 10.1056/NEJMoa1500596

6. Menzer C, Beedgen B, Rom J, Duffert CM, Volckmar AL, Sedlaczek O, et al. Immunotherapy with ipilimumab plus nivolumab in a stage IV melanoma patient during pregnancy. *Eur J Cancer* (2018) 104:239–42. doi: 10.1016/j.ejca.2018.09.008

7. Gangadhar TC, Salama AK. Clinical applications of PD-1-based therapy: A focus on pembrolizumab (MK-3475) in the management of melanoma and other tumor types. *Onco Targets Ther* (2015) 8:929–37. doi: 10.2147/OTT.S53164

8. Riley DS, Barber MS, Kienle GS, Aronson JK, von Schoen-Angerer T, Tugwell P, et al. CARE guidelines for case reports: explanation and elaboration document. *J Clin Epidemiol* (2017) 89:218–35. doi: 10.1016/j.jclinepi.2017.04.026

9. *CARE checklist - CARE case report guidelines*. care-statement.org.

10. Prapas Y, Ravanos K, Petousis S, Panagiotidis Y, Papatheodorou A, Margioula-Siarkou C, et al. GnRH antagonist administered twice the day before hCG trigger combined with a step-down protocol may prevent OHSS in IVF/ICSI antagonist cycles at risk for OHSS without affecting the reproductive outcomes: a prospective randomized control trial. *J Assist Reprod Genet* (2017) 34(11):1537–45. doi: 10.1007/s10815-017-1010-7

11. Gullo G, Petousis S, Papatheodorou A, Panagiotidis Y, Margioula-Siarkou C, Prapas N, et al. Closed vs. open oocyte vitrification methods are equally effective for blastocyst embryo transfers: Prospective study from a sibling oocyte donation program. *Gynecol Obstet Invest* (2020) 85(2):206–12. doi: 10.1159/000506803

12. Benati M, Montagnana M, Danese E, Mazzon M, Paviati E, Garzon S, et al. Aberrant telomere length in circulating cell-free DNA as possible blood biomarker with high diagnostic performance in endometrial cancer. *Pathol Oncol Res* (2020) 26(4):2281–9. doi: 10.1007/s12253-020-00819-x

13. Casarin J, Bogani G, Serati M, Pinelli C, Laganà AS, Garzon S, et al. Presence of glandular cells at the preoperative cervical cytology and local recurrence in endometrial cancer. *Int J Gynecol Pathol* (2020) 39(6):522–8. doi: 10.1097/PGP.0000000000000642

14. Capozzi VA, Rosati A, Rumolo V, Ferrari F, Gullo G, Karaman E, et al. Novelties of ultrasound imaging for endometrial cancer preoperative workup. *Minerva Med* (2021) 112(1):3–11. doi: 10.23736/S0026-4806.20.07125-6

15. Gullo G, Etrusco A, Cucinella G, Perino A, Chiantera V, Laganà AS, et al. Fertility-sparing approach in women affected by stage I and low-grade endometrial carcinoma: An updated overview. *Int J Mol Sci* (2021) 22(21):11825. doi: 10.3390/ijms222111825

16. Cavaliere AF, Perelli F, Zaami S, D'Indinosante M, Turrini I, Giusti M, et al. Fertility sparing treatments in endometrial cancer patients: The potential role of the new molecular classification. *Int J Mol Sci* (2021) 22(22):12248. doi: 10.3390/ijms222212248

17. Tanos P, Dimitriou S, Gullo G, Tanos V. Biomolecular and genetic prognostic factors that can facilitate fertility-sparing treatment (FST) decision making in early stage endometrial cancer (ES-EC): A systematic review. *Int J Mol Sci* (2022) 23(5):2653. doi: 10.3390/ijms23052653

18. Wolchok JD, Hoos A, O'Day S, Weber JS, Hamid O, Lebbé C, et al. Guidelines for the evaluation of immune therapy activity in solid tumors: immune-related response criteria. *Clin Cancer Res* (2009) 15(23):7412–20. doi: 10.1158/1078-0432.CCR-09-1624

19. Anami Y, Minami S, Kumegawa A, Matsukawa H, Nishioka K, Noguchi T, et al. Malignant melanoma treated with pembrolizumab during pregnancy: A case report and review of the literature. *Mol Clin Oncol* (2021) 15(5):242. doi: 10.3892/mco.2021.2404

20. Xu W, Moor RJ, Walpole ET, Atkinson VG. Pregnancy with successful foetal and maternal outcome in a melanoma patient treated with nivolumab in the first trimester: case report and review of the literature. *Melanoma Res* (2019) 29 (3):333–7. doi: 10.1097/CMR.0000000000000586

21. Bucheit AD, Hardy JT, Szender JB, Glitza Oliva IC. Conception and viable twin pregnancy in a patient with metastatic melanoma while treated with CTLA-4 and PD-1 checkpoint inhibition. *Melanoma Res* (2020) 30(4):423–5. doi: 10.1097/CMR.0000000000000657

22. Gambichler T, Susok L. Uncomplicated pregnancy and delivery under ongoing nivolumab therapy for metastatic melanoma. *Melanoma Res* (2022) 32 (2):131–2. doi: 10.1097/CMR.0000000000000801

23. Burotto M, Gormaz JG, Samtani S, Valls N, Silva R, Rojas C, et al. Viable pregnancy in a patient with metastatic melanoma treated with double checkpoint immunotherapy. *Semin Oncol* (2018) 45(3):164–9. doi: 10.1053/j.seminoncol.2018.03.003

24. Haiduk J, Ziemer M. Pregnancy in a patient with metastatic uveal melanoma treated with nivolumab. *J Dtsch Dermatol Ges* (2021) 19(5):762–5. doi: 10.1111/ddg.14463

25. Le-Nguyen A, Rys RN, Petrogiannis-Haliotis T, Johnson NA. Successful pregnancy and fetal outcome following previous treatment with pembrolizumab for relapsed hodgkin's lymphoma. *Cancer Rep (Hoboken)* (2022) 5(1):e1432. doi: 10.1002/cnr2.1432

26. Hutson JR, Eastabrook G, Garcia-Bournissen F. Pregnancy outcome after early exposure to nivolumab, a PD-1 checkpoint inhibitor for relapsed hodgkin's lymphoma. *Clin Toxicol (Phila)* (2022) 60(4):535–6. doi: 10.1080/15563650.2021.1981361

27. Polnaszek B, Mullen M, Bligard K, Raghuraman N, Massad LS. Term pregnancy after complete response of placental site trophoblastic tumor to immunotherapy. *Obstet Gynecol* (2021) 138(1):115–8. doi: 10.1097/AOG.0000000000004434

28. Andrikopoulou A, Korakiti AM, Apostolidou K, Dimopoulos MA, Zagouri F. Immune checkpoint inhibitor administration during pregnancy: A case series. *ESMO Open* (2021) 6(5):100262. doi: 10.1016/j.esmoop.2021.100262

29. Poulet FM, Wolf JJ, Herzyk DJ, DeGeorge JJ. An evaluation of the impact of PD-1 pathway blockade on reproductive safety of therapeutic PD-1 inhibitors. *Birth Defects Res B Dev Reprod Toxicol* (2016) 107(2):108–19. doi: 10.1002/bdrb.21176

30. Borgers J, Heimovaara JH, Cardonick E, Dierickx D, Lambertini M, Haanen J, et al. Immunotherapy for cancer treatment during pregnancy. *Lancet Oncol* (2021) 22(12):e550–61. doi: 10.1016/S1470-2045(21)00525-8

31. Pentsuk N, van der Laan JW. An interspecies comparison of placental antibody transfer: New insights into developmental toxicity testing of monoclonal antibodies. *Birth Defects Res B Dev Reprod Toxicol* (2009) 86(4):328–44. doi: 10.1002/bdrb.20201

frontiers | Frontiers in Surgery

TYPE Case Report
PUBLISHED 17 October 2022
DOI 10.3389/fsurg.2022.1017603



OPEN ACCESS

EDITED BY
Akinfemi Akingboye,
Dudley Group NHS Foundation Trust,
United Kingdom

REVIEWED BY
Boris Tadic,
University of Belgrade, Serbia
Nguyen Minh Duc,
Pham Ngoc Thach University of Medicine,
Vietnam

*CORRESPONDENCE
Gengqing Wu
genqing169@126.com
Quanliang Liu
liuquanliang2008@163.com

†These authors share first authorship

SPECIALTY SECTION
This article was submitted to Surgical Oncology, a section of the journal Frontiers in Surgery

RECEIVED 12 August 2022
ACCEPTED 28 September 2022
PUBLISHED 17 October 2022

CITATION
Zou Y, Xie X, Yan S, Wu G and Liu Q (2022) Case report: Misdiagnosis of accessory spleen in the left adrenal region as an adrenal tumour after splenectomy.
Front. Surg. 9:1017603.
doi: 10.3389/fsurg.2022.1017603



# Case report: Misdiagnosis of accessory spleen in the left adrenal region as an adrenal tumour after splenectomy

Yuhua Zou[1†], Xiaojuan Xie[2†], Sheng Yan[1], Gengqing Wu[1*] and Quanliang Liu[1*]

[1]Department of Urology, The First Affiliated Hospital of Gannan Medical University, Ganzhou, China, [2]Department of Cardiology, The First Affiliated Hospital of Gannan Medical University, Ganzhou, China

**Background:** Adrenal tumours are common in urology and endocrinology, and the diagnosis of adrenal tumours were mainly depends on imaging diagnosis. However, misdiagnosis can still occur for some adrenal space-occupying lesions without specific manifestations or abnormal biochemical indexes.
**Methods:** We report the case of a 55-year-old patient with a soft-tissue mass in the left adrenal region, and have no specific manifestations or abnormalities in biochemical indexes. The patient had undergone open splenectomy 20 years ago for splenic rupture caused by traffic-accident trauma, and had a 10-year special history of hypertension. Because of the uncertain nature of the mass, surgical treatment was recommended.
**Results:** The surgeon managed to remove the left adrenal region mass. During the surgery, the adrenal source was excluded. In the histological examination, the splenic corpuscle and splenic medullary structure were seen under the microscope, and an accessory spleen was diagnosed.
**Conclusions:** The accessory spleen was located in the adrenal region rarely, and can easily be misdiagnosed as an adrenal tumour. When the cases show abnormal adrenal space-occupying lesions in imaging examinations, non-adrenal diseases should be considered. we need to combine different imaging techniques for analysis, and think more about it, avoid misdiagnosis leading to unnecessary surgery.

KEYWORDS
accessory spleen, adrenal tumour, splenectomy, misdiagnosis, image diagnosis, case report

## Introduction

Adrenal tumours are common in urology and endocrinology (1–3). With the continuing development of different imaging techniques, such as ultrasound, computed tomography (CT) scan, magnetic resonance imaging (MRI), and detection techniques for adrenal hormone, the accuracy in localisation and qualitative diagnosis of adrenal tumours has gradually increased. However, misdiagnosis can still occur for some adrenal space-occupying lesions without specific manifestations or abnormal biochemical indexes. Clinical staff need a comprehensive analysis method to reduce

unnecessary surgery. We report a case of patient who was misdiagnosed of accessory spleen in the left adrenal region as an adrenal tumour after splenectomy.

## Case presentation

The reporting of this study conforms to CARE guidelines (4, 5). In Dec. 6, 2021, a 55-year-old patient was admitted to the department of emergency due to fallen down while working, resulting in thoracic and abdominal pain and discomfort. Subsequently, he visited the emergency department of emergency for an abdominal CT scan, which showed a left-adrenal space-occupying lesion. Consequently, enhanced scanning and hospitalisation were recommended. The patient had undergone open splenectomy 20 years ago for splenic rupture caused by traffic-accident trauma. The patient had a 10-year special history of hypertension, and his blood pressure was well controlled by regular oral antihypertensive drugs.

After admission, his maximum monitored blood pressure was 138/87 mmHg (1 mmHg = 0.133 kPa), and his monitored heart rate ranged from 86 to 103 bpm. The patient denied a history of diabetes, centripetal obesity or specific manifestations of cortisol signs, such as full-moon face and buffalo hump. All biochemical tests, including blood potassium: 3.57 mmol/L; cortisol (0AM): 1.67 μg/dl; cortisol (8AM): 7.79 μg/dl; cortisol (16PM): 4.46 μg/dl; adrenocorticotropic hormone (0AM): 2.47 pmol/L; adrenocorticotropic hormone (8AM): 3.76 pmol/L; adrenocorticotropic hormone (16PM): 2.97 pmol/L; renin (standing position): 41.68 pg/ml; aldosterone (standing position): 141 pg/ml; renin (recumbent position): 16.07 pg/ml; aldosterone (recumbent position): 129 pg/ml, and 24-h urinary 3-methoxy-4-hydroxymandelic acid, 24-h urinary catecholamines were normol. Ultrasound (US) was performed which identified a 42 × 30 × 35 mm adrenal mass in the left-adrenal region. In order to confirm the diagnosis, computed tomography (CT) scan was conducted, the CT scan confirmed the US findings, showing a 42 × 28 × 36 mm soft-tissue mass shadow in the left adrenal region, and the internal density was heterogeneity (Figures 1A,D,E). The CT value of plain scanning was 36 to 68

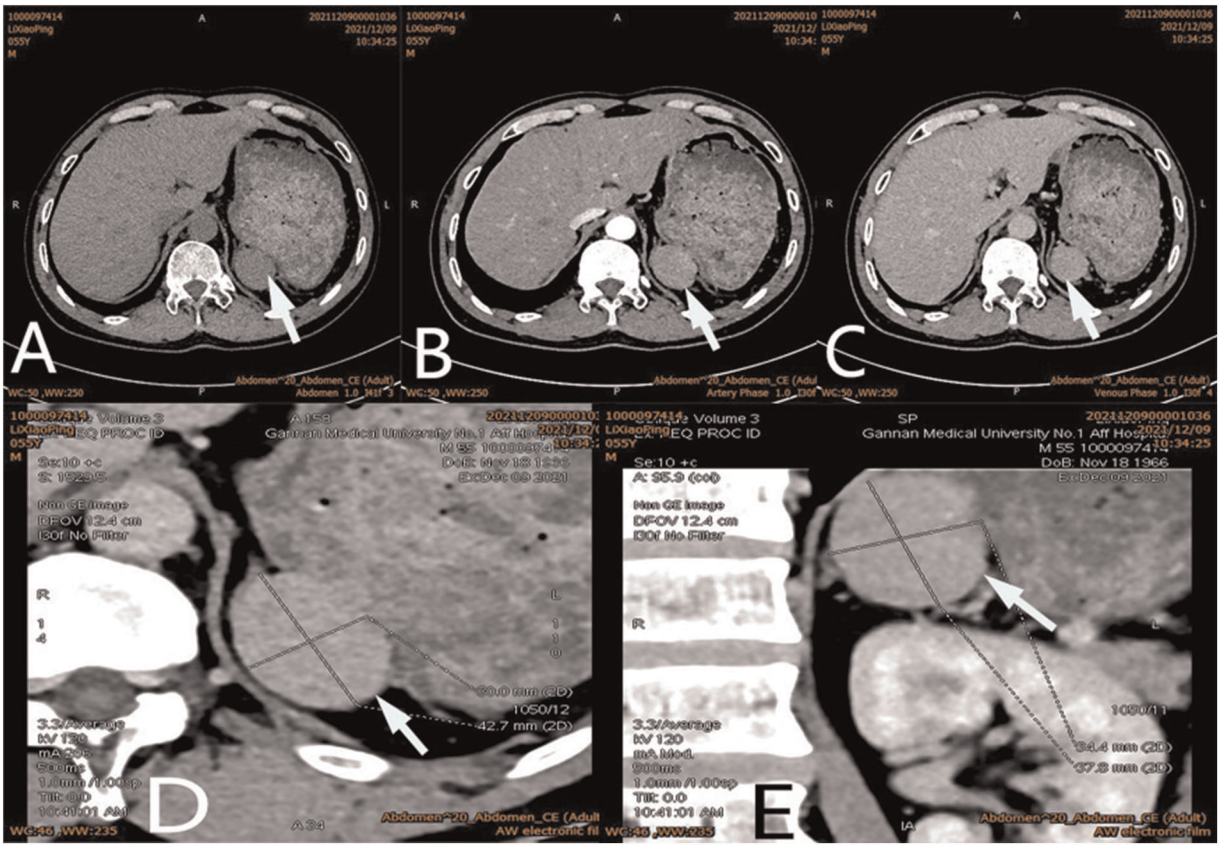


FIGURE 1
Ct scan of a mass (arrow) in the left adrenal region. The CT value of plain scanning which the internal density was heterogeneity (A), and enhanced scanning presented moderate enhancement (B), the delayed phase of the mass (C). Coronal image of the mass (D). Sagittal image of the mass (E).

HU, and enhanced scanning presented moderate enhancement (Figure 1B). The CT value in the arterial phase was 62 to 104 HU, and that in the delayed phase was 46–89 HU (Figure 1C). The lesion was considered to be a benign neoplastic lesion in the left adrenal region, possibly a left-adrenal adenoma or pheochromocytoma. According to the 2019 CUA Guidelines for Urinary Surgery (6), suspected non-functioning adrenal adenoma, which is defined as an adrenal tumour ≥3 cm, surgical treatment was recommended. The patient was placed in the right lateral decubitus position and an retroperitoneal laparoscopic approach was performed. Intraoperatively, a round dark-grey mass was observed on the upper ventral region of the retroperitoneal left kidney, with a size of about 40 mm and a surface completely covered with smooth membranous peritoneum-like tissue. The boundaries between the dorsal side of the mass and upper pole of the left kidney, left adrenal gland and surrounding adipose tissue were clear, loose and non-adhered (Figure 2A). The ventral side adhered closely to the peritoneum and provided blood supply. The mass was completely resected after partial removal of the adhered peritoneum and blocking of blood vessels (Figure 2B). The vital signs of the patient showed no significant fluctuations during tumour separation, compression and resection. The anatomopathological exam revealed a 40 × 30 mm in size, which the surface envelope was intact, and the mass was dark red and had a similar splenic structure with multiple sinusoid tissues (Figures 2C,D). In the histological examination, the splenic corpuscle and splenic medullary structure were seen under the microscope, and an accessory spleen was diagnosed (Figures 3A, B). No perioperative complications were registered and remained in the hospital for three days after surgery. The patient was satisfied with the treatment. Postoperatively, the patient was followed up for 3 months, and no lumbago or infection was observed.

## Discussion

Adrenal tumours are common in urology and endocrinology (1–3). The common clinical manifestations are secondary to excessive secretion of adrenal-gland-related hormones, such as hypertension, hyperglycaemia, myasthenia, puffiness, full-moon face, buffalo hump and irregular menstruation, but some patients may have no specific clinical

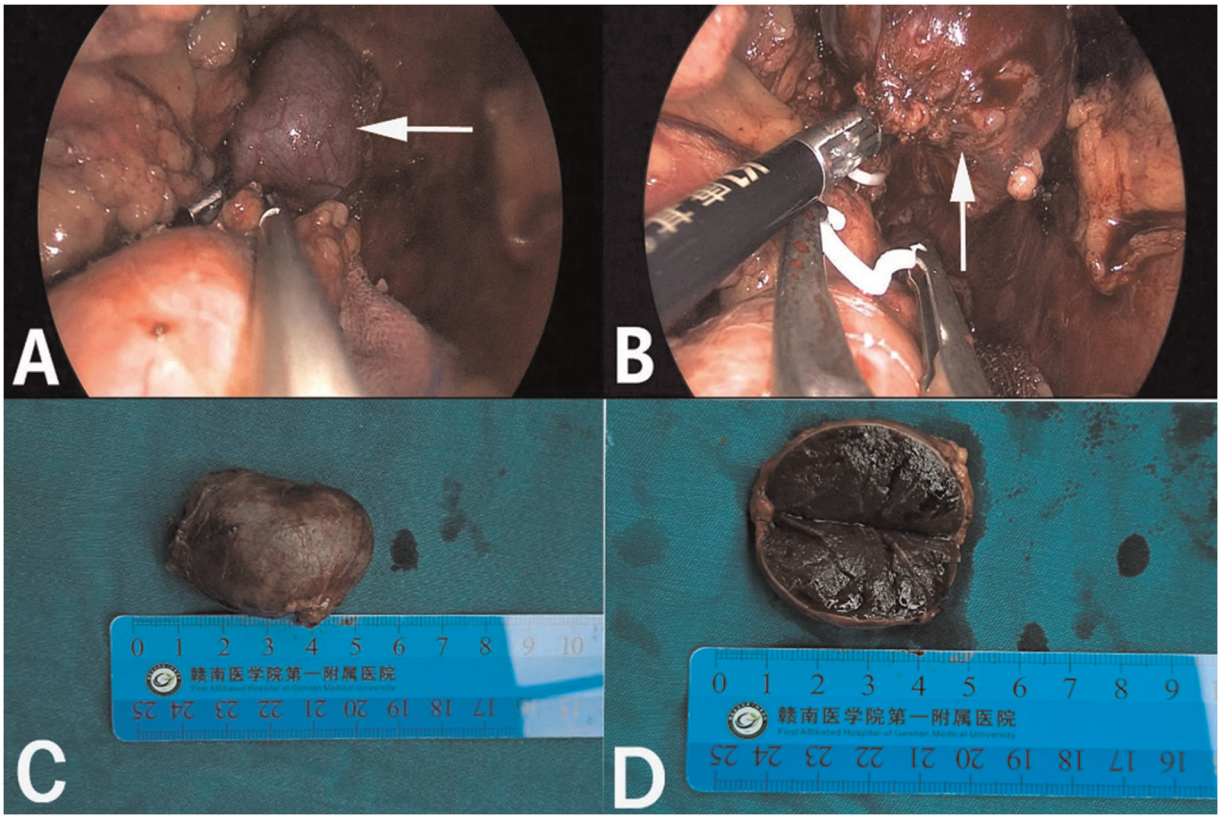


FIGURE 2
Retroperitoneal laparoscopic resection of the mass (arrow). The mass is located in the left suprarenal region, and the boundaries between the dorsal side of the mass were clear, loose and non-adhered (A), the ventral side adhered closely to the peritoneum (B). Gross appearance. The mass was dark red, and the surface envelope of the mass was intact (C), and had a similar splenic structure with multiple sinusoid tissues (D).

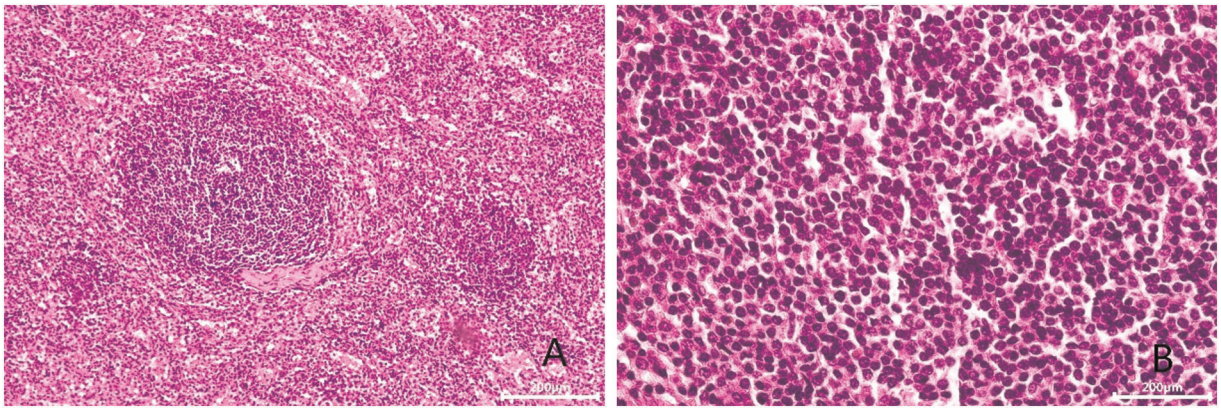


FIGURE 3
Microscopic appearance (A,B). Histologic magnification revealed accessory splenic tissue [hematoxilyn and eosin staining, ×200 (A), ×400 (B)].

manifestations (7). Clinical localisation and diagnosis of an adrenal tumour are mainly based on imaging examinations, such as ultrasound, CT and MRI. Because of the deep and hidden adrenal region, like any imaging method, an ultrasound examination is likely to be disturbed and entail the risk of misdiagnose. It is the most subjective and require considerable clinical experience and knowledge of sonographers for proper interpretation (8). Adrenal tumours often show uniform low-density shadows on CT scan, whereas an accessory spleen usually presents with uniform density, and its enhancement effect in the arterial and venous phases is always similar to that of the spleen. Our patient had undergone splenectomy 20 years ago, so we could not compare it with the normal spleen. In addition, the CT morphology of the accessory spleen in this case was similar to that of a benign adrenal tumour, with a regular shape, a clear boundary and a capsule. Moreover, The CT value of plain scanning was 36 to 68 HU, and enhanced scanning presented moderate enhancement (**Figure 1B**). The CT value in the arterial phase was 62–104 HU, and that in the delayed phase was 46–89 HU (**Figure 1C**). The CT findings were similar to those for an adrenal mass. Those findings, combined with the patient's history of hypertension, led to our suspicion of a left-adrenal tumour. Thus, surgical exploration was unavoidable.

Accessory spleen, also called supernumerary spleen, refers to tissue with the same structure and function as the normal spleen that exists in addition to the normal spleen, and it is a common congenital anatomical abnormality, with an incidence of 10%–30% (9). Accessory spleen formation is usually caused by failed fusion of some parts of an embryonic spleen bud in the mesogastrium or by independent development of partial spleen tissue that detaches from the spleen (9, 10). The location, number and size of the accessory spleen can also vary. A single accessory spleen is common, but multiple accessory spleens may also occur, and generally its diameter is 10–40 mm (11). Accessory spleen often occurs in the splenic hilum, but also in other parts of the abdomen, such as the pancreatic tail, greater omentum, hepatogastric ligament, splenogastric ligament space, gastric wall, intestinal wall and even pelvic reproductive organs, and the retroperitoneal position is extremely uncommon (12, 13). When accessory spleen was located in the adrenal region, the accessory spleen can easily be misdiagnosed as an adrenal tumour (14, 15). Compared with the left-retroperitoneal accessory spleen, the right-retroperitoneal accessory spleen is rarer but more likely to be misdiagnosed as an adrenal tumour (15).

At present, it is generally recognised that Tc-99m-labelled heat-denatured red-blood-cells scintigraphy is a reliable, sensitive and non invasive imaging method for confirm the qualitative clinical diagnosis of accessory spleen (16, 17). The diagnostic principle is that the reticuloendothelial cells of the spleen can selectively absorb and destroy the function of damaged and denatured red blood cells (RBC). Firstly, *in vitro* $^{99m}$Tc-labelled heat-denatured red blood cells ($^{99m}$Tc-DRBC) are intravenously injected into the human body and then absorbed by the spleen, followed by the liver and reticuloendothelial tissues, such as bone marrow. In these tissues, haem in RBC is destroyed, digested and metabolised to form bilirubin, so only the spleen can aggregate $^{99m}$Tc-DRBC, and has a high-uptake rate, followed by the liver and bone marrow, but other tumour tissues and lymph glands cannot. The radioactive concentration per unit volume is 2–3 times higher in the spleen than in the liver. False-negative results only are obtained in accessory spleens which were the relatively small sizes because there is no accumulation of radioactive tracers (18). $^{99m}$Tc-DRBC scintigraphy can well distinguish ectopic accessory spleen from tumour recurrence, new tumours and enlarged lymph nodes, with high accuracy (19). It is a useful nuclear medicine method to solve some of the clinical puzzles, but its development is limited in China. Moreover, the main blood

supply of the accessory spleen in the adrenal region is from splenic artery branches. Careful distinguishing between accessory spleen and adrenal tumours from the perspective of blood supply in imaging may reduce misdiagnosis to a greater extent. Therefore, when encountering suspected cases in clinics, we need to combine different imaging techniques for analysis, and think more about it, avoid misdiagnosis leading to unnecessary surgery.

Generally, the accessory spleen has no clinical symptoms and is mostly detected by physical examination or other examinations (20). Currently, it is believed that the accessory spleen needs no special treatment and requires resection only for rupture, infarction or vascular torsion that causes corresponding clinical symptoms (21). Additionally, the normal spleen and accessory spleen need to be resected together in the treatment of haematological diseases, such as idiopathic thrombocytopenic purpura, otherwise may cause recurrent disease (22). However, an enlarged accessory spleen is often clinically misdiagnosed as a tumour or enlarged lymph node for surgical treatment (23). Our patient had undergone open splenectomy for splenic rupture caused by a traffic-accident trauma 20 years ago. Due to the long time and no corresponding imaging data as a preoperative reference, we could not determine that the accessory spleen of this patient was caused by compensatory hypertrophy of the accessory spleen after splenectomy or its ectopic implantation during splenectomy. Intraoperatively, the boundaries between the dorsal side of the mass and the kidney, adrenal gland and surrounding adipose tissue were clear, loose and non-adhered (**Figures 2A**), but the ventral side adhered closely to the peritoneum (**Figures 2B**). It can be seen that the lateral peritoneum was not opened during splenectomy. Therefore, in this case, the accessory spleen was mostly caused by compensatory hypertrophy of the accessory spleen after splenectomy. After resection of the normal spleen, the ectopic accessory spleen can develop compensatory hypertrophy and play the role of the normal spleen. After splenectomy, resulting in decreased immune cells, weakened and imbalanced regulation of the immune system and increased infection, which would require special attention.

In this case, because of our lack of experience, the patient underwent unnecessary surgery. We analysed the causes of our misdiagnosis and had to admit that different imaging techniques for the suspected case were not performed, and the single examination had some defects. Additionally, this patient had a history of splenectomy, and the accessory spleen was located in the adrenal region, which is relatively rare. The patient also had a history of hypertension, which greatly interfered with the preoperative diagnosis, but the main reason was the lack of understanding of accessory spleen before surgery. During the surgery, the adrenal source was excluded, we also questioned the source of the tumour. To ensure the integrity of the tumour and the principle of "no tumour", we did not perform a frozen-section examination. However, it would be worth discussing whether a better outcome can be obtained if such tumours are subjected to frozen-section examination during surgery.

## Conclusions

In summary, the diagnosis of space-occupying lesions in the left-adrenal region remains challenging, especially in some patients who have no specific manifestations or abnormalities in biochemical indexes. When the cases show abnormal adrenal space-occupying lesions in imaging examinations, non-adrenal diseases should be considered. we need to combine different imaging techniques for analysis, and think more about it, avoid misdiagnosis leading to unnecessary surgery.

## Data availability statement

The raw data supporting the conclusions of this article will be made available by the authors, without undue reservation.

## Ethics statement

Written informed consent has been obtained from the individual to release any potentially identifiable images or data contained herein.

## Author contributions

YZ prepared and wrote the article. XX were responsible for the collection and organization of the literature. SY was directly involved in the management of the patients. QL and GW revised the manuscript and acted as corresponding authors. All authors contributed to the article and approved the submitted version.

## Acknowledgments

We would like to thank QLL for his guidance on this paper and for editing and proofreading this manuscript in English.

## Conflict of interest

The authors declare that the research was conducted in the absence of any commercial or financial relationships that could be construed as a potential conflict of interest.

## Publisher's note



## References

1. Mete O, Erickson LA, Juhlin CC, de Krijger RR, Sasano H, Volante M, et al. Overview of the 2022 WHO classification of adrenal cortical tumors. *Endocr Pathol.* (2022) 33:155–96. doi: 10.1007/s12022-022-09710-8

2. Higgs JA, Quinn AP, Seely KD, Richards Z, Mortensen SP, Crandall CS, et al. Pathophysiological link between Insulin resistance and adrenal incidentalomas. *Int J Mol Sci.* (2022) 23:4340. doi: 10.3390/ijms23084340

3. Zhang GX, Zou XF, Liu QL, Xie TP, Huang RH, Kang H, et al. MiR-193a-3p functions as a tumour suppressor in human aldosterone-producing adrenocortical adenoma by down-regulating CYP11B2. *Int J Exp Pathol.* (2018) 99:77–86. doi: 10.1111/iep.12267

4. Gagnier JJ, Kienle G, Altman DG, Moher D, Sox H, Riley D, et al. The CARE guidelines: consensus-based clinical case reporting guideline development. *Headache.* (2013) 53:1541–7. doi: 10.1111/head.12246

5. Agha RA, Franchi T, Sohrabi C, Mathew G, Kerwan A, SCARE Group. The SCARE 2020 guideline: updating consensus surgical CAse REport (SCARE) guidelines. *Int J Surg.* (2020) 84:226–30. doi: 10.1016/j.ijsu.2020.10.034

6. Huang J, Wang JY, Kong CZ, Li H, Xie LP, Zhou LQ, et al. *Chinese Association of urology guidelines 2019*. Beijing, China: Science Press[M] (2019). ISBN 9787030659798.

7. Ahmed SF, Bapir R, Fattah FH, Mahmood AG, Salih RQ, Salih AM, et al. Simultaneous pituitary and adrenal adenomas in a patient with non ACTH dependent cushing syndrome; a case report with literature review. *Int J Surg Case Rep.* (2022) 94:107038. doi: 10.1016/j.ijscr.2022.107038

8. Walczyk J, Walas MK. Errors made in the ultrasound diagnostics of the spleen. *J Ultrason.* (2013) 13:65–72. doi: 10.15557/JoU.2013.0005

9. Yildiz AE, Ariyurek MO, Karcaaltincaba M. Splenic anomalies of shape, size, and location: pictorial essay. *Sci World J.* (2013) 2013:321810. doi: 10.1155/2013/321810

10. Halpert B, Gyorkey F. Lesions observed in accessory spleens of 311 patients. *Am J Clin Pathol.* (1959) 32:165–68. doi: 10.1093/ajcp/32.2.165

11. Mohammadi S, Hedjazi A, Sajjadian M, Ghrobi N, Moghadam MD, Mohammadi M, et al. Accessory spleen in the splenic hilum: a cadaveric study with clinical significance. *Med Arch.* (2016) 70:389–91. doi: 10.5455/medarh.2016.70.389-391

12. Zhang J, Zhong JW, Lu GR, Zhou YH, Xue ZX, Ye MS, et al. Accessory spleen originating from the intrinsic muscularis of the stomach misdiagnosed as gastrointestinal stromal tumor: a case report. *J Int Med Res.* (2020) 48:300060520935304. doi: 10.1177/0300060520935304

13. Linh LT, Tra My TT, Lenh BV, Giang TV, Bang LV, Duc NM, et al. Enlarged accessory spleen after splenectomy mimicking a pancreas tumor. *Int J Surg Case Rep.* (2021) 78:214–8. doi: 10.1016/j.ijscr.2020.12.037

14. Rosenblatt G, Luthringer D, Fuchs GJ. Enlargement of accessory spleen after splenectomy can mimic a solitary adrenal tumor. *Urology.* (2010) 75:561–2. doi: 10.1016/j.urology.2009.05.070

15. Corradetti S, Duro A, Fuente LP, Wright FG, Beskow AF. Accessory spleen mimicking a right adrenal tumor. *Cir Esp (Engl Ed).* (2021) 99:321–3. doi: 10.1016/j.ciresp.2020.07.010

16. Graziani T, Baldari G, Sammartano A, Scarlattei M, Migliari S, Pescarenico MG, et al. SPECT/CT with $^{99m}$Tc labelled heat-denatured erythrocyte to detect thoracic and abdominal splenosis. *Acta Biomed.* (2020) 91:e2020098. doi: 10.23750/abm.v91i4.9270

17. Holzgreve A, Völter F, Delker A, Kunz WG, Fabritius MP, Brendel M, et al. Detection of splenic tissue using $^{99m}$Tc-labelled denatured red blood cells scintigraphy-a quantitative single center analysis. *Diagnostics (Basel).* (2022) 12:486. doi: 10.3390/diagnostics12020486

18. Gezer E, Cetinarslan B, Karakaya D, Cantürk Z, Selek A, Sözen M, et al. Differentiation of insulinoma from accessory spleen by $^{99m}$Tc-labelled heat-denaturated red blood cell scintigraphy: case report. *BMC Endocr Disord.* (2021) 21:6. doi: 10.1186/s12902-020-00671-9

19. Olmos RAV, Horenblas S, Kartachova M, Hoefnagel CA, Sivro F, Baars PC. 99mTc-labelled heat-denatured erythrocyte SPET-CT matching to differentiate accessory spleen from tumour recurrence. *Eur J Nucl Med Mol Imaging.* (2004) 31:150. doi: 10.1007/s00259-003-1419-3

20. Yoshida M, Saida T, Masuoka S, Urushibara A, Chiba F, Masumoto K. Preoperative diagnosis of a torsioned accessory spleen. *J Med Ultrasound.* (2021) 29:116–8. doi: 10.4103/JMU.JMU_35_20

21. Wang H, So H, Nah YW, Kim M, Lee TY, Seo M, et al. Acute abdominal pain due to accessory splenic infarction in an adult: a case report. *Korean J Gastroenterol.* (2021) 78:183–7. doi: 10.4166/kjg.2021.071

22. Choi YU, Dominguez EP, Sherman V, Sweeney JF. Laparoscopic accessory splenectomy for recurrent idiopathic thrombocytopenic purpura. *JSLS.* (2008) 12:314–7. PMID: 18765061

23. Palumbo V, Mannino M, Teodoro M, Menconi G, Schembari E, Corsale G, et al. An extremely rare case of an oversized accessory spleen: case report and review of the literature. *BMC Surg.* (2019) 19:45. doi: 10.1186/s12893-019-0510-z

frontiers | Frontiers in Oncology

TYPE Case Report
PUBLISHED 20 October 2022
DOI 10.3389/fonc.2022.933777



OPEN ACCESS

EDITED BY
Airazat M. Kazaryan,
Østfold Hospital, Norway

REVIEWED BY
Hai Zou,
Fudan University, China
Vagan Bokhian,
Russian Cancer Research Center NN Blokhin, Russia
Vladimir Khomiakov,
P.A. Hertsen Moscow Oncology Research Institute - Branch of the National Medical Research Radiological Centre of the Ministry of Health of the Russian Federation, Russia

*CORRESPONDENCE
Xishan Wang
wxshan_1208@126.com

†These authors have contributed equally to this work

SPECIALTY SECTION
This article was submitted to Surgical Oncology, a section of the journal Frontiers in Oncology

RECEIVED 01 May 2022
ACCEPTED 30 September 2022
PUBLISHED 20 October 2022

CITATION
Yin Y, Wang R and Wang X (2022) Laparoscopy for evaluating mesenteric lymphangiomatosis: A case report. *Front. Oncol.* 12:933777. doi: 10.3389/fonc.2022.933777



# Laparoscopy for evaluating mesenteric lymphangiomatosis: A case report

Yefeng Yin[1†], Rongdi Wang[2†] and Xishan Wang[1*]

[1]Department of Colorectal Surgery, National Cancer Center/National Clinical Research Center for Cancer/Cancer Hospital, Chinese Academy of Medical Sciences and Peking Union Medical College, Beijing, China, [2]Department of Anorectal Surgery, Dalian Municipal Central Hospital, Dalian, China

**Background:** Lymphangiomatosis is an extremely rare disease with potential soft tissue, bone, and spleen involvement, which can be characterized by lymphangioma. Only a few cases of colon and mesenteric lymphangiomatosis have been reported. We report a case presenting with fatigue, periumbilical pain, and intermittent bloody stools. This patient underwent a series of examinations. Exploratory laparoscopy, in particular, yielded very valuable images and videos for this disease, which can provide evidence for the diagnosis of this disease.

**Case summary:** The current patient had fatigue, periumbilical pain, and intermittent bloody stools. Colonoscopy indicated numerous variable-sized hyaline cysts in the colon. Submucosal puncture was performed during colonoscopy. The patient was readmitted to the hospital due to periumbilical pain. B-ultrasound and abdominal CT showed multiple hypoechoic nodules in the mesenteric area. Exploratory laparoscopy was performed, and histopathology revealed that D2-40 was positive. Based on auxiliary examination and laparoscopic biopsy, surgeons and pathologists reached the diagnosis of mesenteric lymphangiomatosis.

**Conclusion:** Clinicians need to comprehensively improve their knowledge of lymphangiomatosis, and the combination of clinical symptoms, histological characteristics, and colonoscopy biopsy findings should be considered to improve lymphangiomatosis diagnosis, thereby reducing misdiagnosis.

**Core tip:** Colon and mesenteric lymphangiomatosis is an extremely uncommon benign condition of unknown etiology and pathogenesis in adult patients. We report a case of mesenteric lymphangiomatosis in a 37-year-old woman who presented with fatigue, periumbilical pain, and intermittent bloody stools, as well as lesions in the kidney, spleen, and bones. This case provides new insights into the diagnosis and treatment of this disease.

KEYWORDS

**lymphangiomatosis, exploratory, laparoscopy, colon, mesenteric**

## Introduction

Colon and mesenteric lymphangiomatosis is an extremely uncommon benign condition of unknown etiology and pathogenesis, which could lead to compression symptoms caused by mechanical pressure. Here, we report a case of abdominal lymphangiomatosis evaluated by laparoscopy, which has not been previously reported.

## Case presentation

Colonoscopy indicated numerous variable-sized hyaline cysts, involving the ascending colon, transverse colon, and descending colon (Figure 1A), while no biopsy was carried out. Submucosal puncture was performed during colonoscopy. One year later, the patient returned with periumbilical pain. In abdominal ultrasound, multiple hypoechoic nodules with marked intranodular blood flow were observed in the spleen with a maximum size of 1.2 * 1.2 cm, with well-defined margins. In the inferior pole of the left kidney, a hypoechoic nodule was found, with an approximate diameter of 1.6 cm and no blood flow signal. Enlarged lymph nodes (1.9 * 1.1 $cm^2$) were found in the retroperitoneum (Figures 2A–C). Abdominal CT revealed multiple diffuse low-density shadowing zones without enhancement distributed in the mesenteric area, which partly surrounded the small bowel and presented a doughnut shape. The boundaries were blurred (Figure 2D). Low-density shadowing zones were observed in the left kidney, spleen, ilium, and fifth lumbar vertebra on CT scan images (Figures 2E–H). Based on the images, lymphangiomatosis was highly suspected, which was further confirmed by laparoscopic biopsy (Figure 3A). Further exploratory laparoscopy showed numerous hyalines, smooth-walled, variable-sized cystic microstructures in the root of the mesentery, involving total mesenteric excision (Figure 3B). The liquid inclusions were clear and pale yellowish (Video S1). Histopathology revealed diffuse or multi-centric proliferation of thin-walled, dilated lymphatic vessels (Figure 4A). D2-40 (a monoclonal antibody), a highly sensitive and specific marker of lymphatic endothelium in the normal tissue and a subset of vascular lesions, confirmed mesenteric lymphangiomatosis by immunoreaction (Figure 4B). D2-40-positive lymphatic vessels were shown in mesentery (Figures 4C, D). The patient was treated with sirolimus (0.8 mg/$m^2$, Bid) for 3 months, and follow-up colonoscopy was performed. Colonoscopy indicated decreased number and size of cysts compared with the condition observed 6 months before (Figure 1B).

## Discussion

In 2014, generalized lymphatic anomaly (GLA) was proposed by the International Society for the Study of Vascular Anomalies (ISSVA) as a new term for lymphangiomatosis (1).

Mesenteric lymphangiomatosis is a benign cystic tumor of lymphatic vessels that occurs rarely in adults, while its etiology and pathogenesis remain elusive (2). It has variable clinical presentations and can involve different sites, including the mesentery, bone, spleen, mediastinum, lungs, and soft tissues (3). The clinical course and compression symptoms are directly correlated to the affected sites, mechanical pressure, and extent of the disease. In most cases, these lesions are multicystic and characterized by hypodense regions on CT images, without increased vascular flow on color Doppler ultrasound. We analyzed 11 previous cases of lymphangiomatosis involving the gastrointestinal tract and summarized them in Table 1. We listed the symptom and examination procedure of these cases so

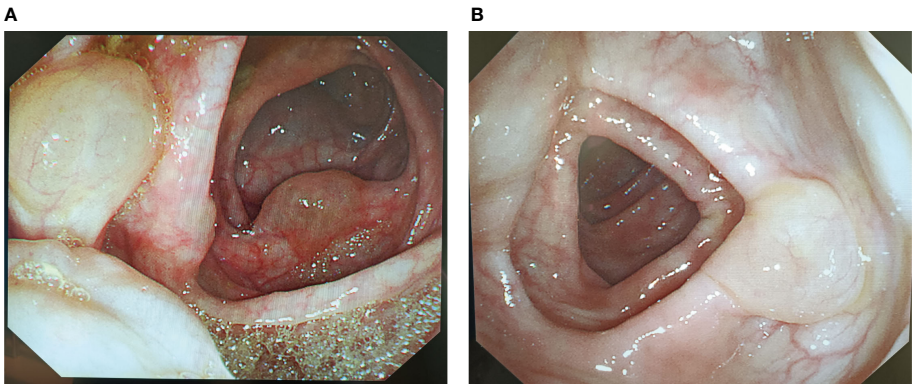


FIGURE 1
**(A)** Colonoscopy indicated numerous cysts in the ascending colon, transverse colon, and descending colon. **(B)** The patient treated with sirolimus within 3 months, and colonoscopy indicated that the number and size of cysts decreased.

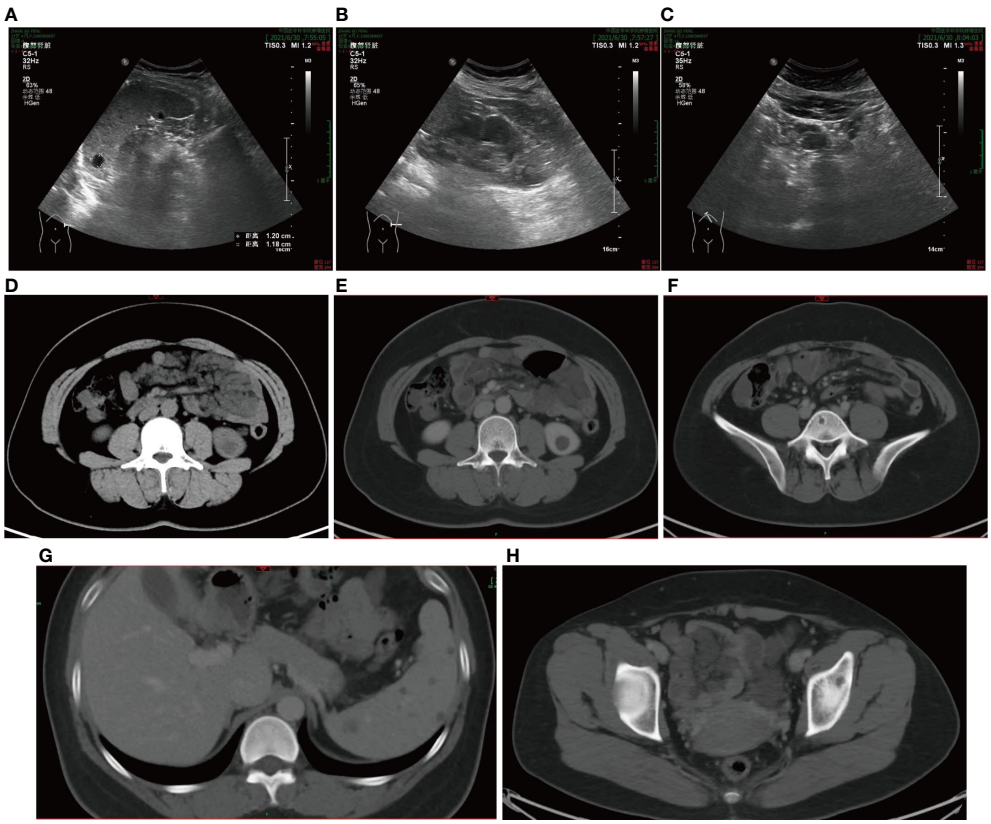


FIGURE 2
**(A–C)** Abdominal ultrasound observed multiple hypoechoic nodules in the spleen and the lower poles of the left kidney, and enlarged lymph nodes in the retroperitoneum. **(D)** Abdominal CT scan observed multiple diffuse low-density shadowing zones in the mesenteric area, which presented a doughnut shape. **(E–H)** Low-density shadowing zones can be observed in the left kidney, spleen, ilium, and the fifth lumbar vertebra in abdominal CT scan images.

that colleagues can learn more about the disease. Reviews of the literature confirm that lymphangiomatosis progresses slowly and can be well controlled with appropriate treatment.

A case report of mesenteric lymphangiomatosis indicated that surgical resection of the mesentery could be an option in case of mechanical obstruction (15). However, the defect caused by the operation may lead to internal herniation, eventually resulting in bowel obstruction and intestinal volvulus. Repairing the defect with Permacol was performed with no complications after 4 years (14). Biomaterial implant may be an option for closing the mesenteric defect caused by surgery. Lymphorrhea after open or laparoscopic biopsy is

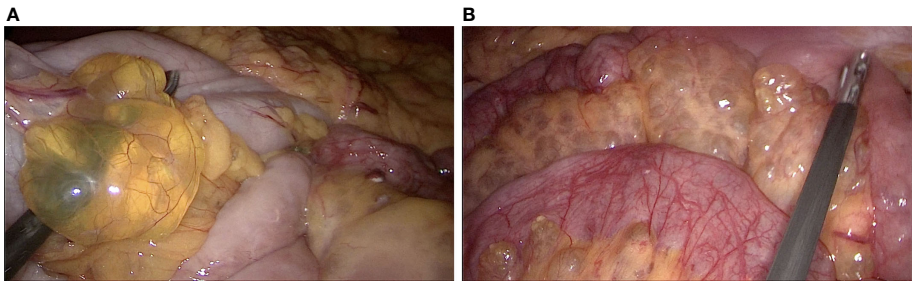


FIGURE 3
**(A, B)** Exploratory laparoscopy showed numerous hyalines, smooth-walled, variable-sized cystic microstructures in the root of the mesentery.

10.3389/fonc.2022.933777

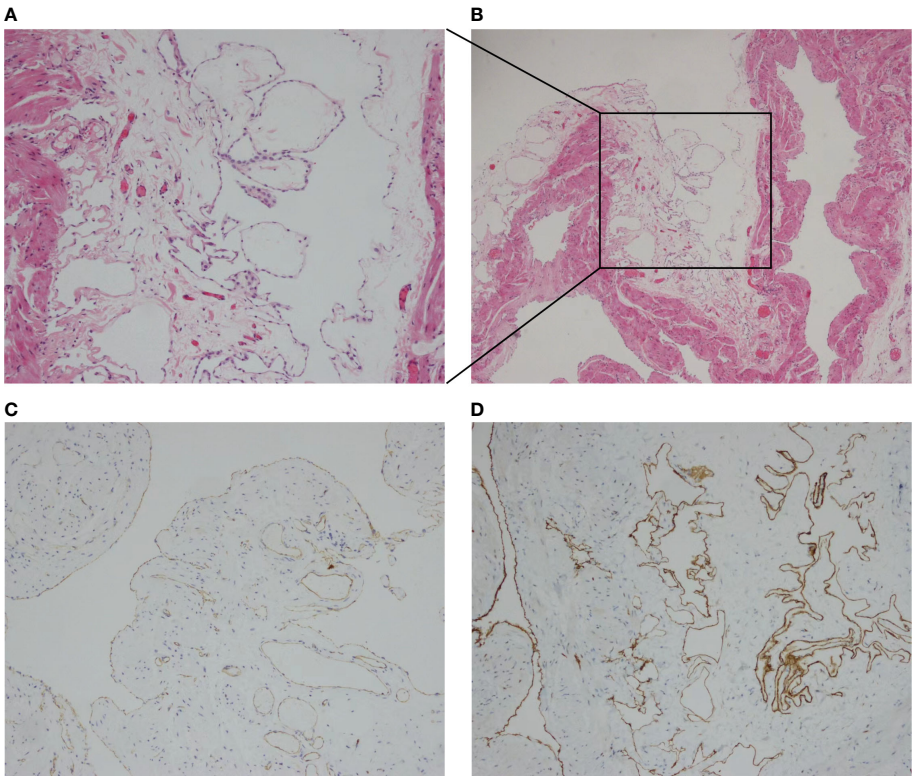


FIGURE 4
**(A, B)** Histological examination showed the positive D2-40 immunohistochemistry and confirmed mesenteric lymphangiomatosis. **(C, D)** Lymph vessels were identified imunohistochemically as D2-40-positive.

TABLE 1 Previous lymphangiomatosis-related disease cases.

| Case number | Gender | Age | Lesion location | Clinical features | Diagnostic workup | Treatment | Follow-up and outcome | Reference |
|---|---|---|---|---|---|---|---|---|
| 1 | Male | 59 | Esophagus | Choking on swallowing | Endoscopy: multiple submucosal masses, slightly translucent and whitish, covered with smooth and normal-looking mucosa;<br>Chest CT: diffuse low-density lesion;<br>Endoscopic ultrasound: multiple mixed solid and anechoic cystic lesions above the seemingly intact muscularis propria;<br>Histopathologic: lymphangioma | Observation | Progression-free | Cao et al. (4) |
| 2 | Male | 79 | Sigmoid colon | Intermittent bloody stools, abdominal discomforts | Fecal occult blood test: positive;<br>Colonoscopy: multiple cystic masses with a translucent and smooth surface, ranging from 4 to 8 mm in diameter;<br>EUS: echo-free cystic masses | Laparoscopy-assisted partial sigmoid colon resection | Progression-free | Lu et al. (5) |
| 3 | Male | 52 | Ascending colon | Intermittent bloody stools, abdominal discomforts | Endoscopy: large, balloon-like submucosal structures; | Observation | Disease progression | Mujagic et al. (6) |

*(Continued)*

TABLE 1 Continued

| Case number | Gender | Age | Lesion location | Clinical features | Diagnostic workup | Treatment | Follow-up and outcome | Reference |
|---|---|---|---|---|---|---|---|---|
| | | | | | Histology: nonspecific mild chronic inflammation | | | |
| 4 | Male | 41 | Ileum | Acute diffuse abdominal pain, nausea, vomiting and inability to pass gas or stool | Abdominal CT scan: bowel distension and multiple gas-fluid levels;<br>Diagnostic laparoscopy:ileal perforation;<br>Histology: diffuse lymphangiomatosis involving the sub-mucosa and, in some parts, the full-thickness muscular wall | Ileal resection | Not mentioned | Giuliania et al. (7) |
| 5 | Male | 71 | Jejunum | The patient underwent rectal resection and ileostomy. Follow-up examination revealed nodular jejunal and adjacent mesenteric masses | Abdominal CT scan: soft-tissue density of the nodular mass and hazy attenuations in the jejunal mesentery;<br>Contrast-enhanced CT: nodular jejunal and adjacent mesenteric masses in contrast to the barium-filled jejunum;<br>PET/CT: no remarkable FDG uptake was seen;<br>Histology: cavernous lymphangioma involving the jejunum and mesentery. | Jejunectomy | Progression-free | Hwang and Park (8) |
| 6 | Male | 31 | Jejunum, Cecum | Recurrent melena for the last 8 years and iron deficiency anemia | Colonoscopy: protruding submucosal lesions of approximately 20–30 mm in diameter at the cecum;<br>Histology: mild mononuclear infiltrate in lamina with focal prominence of goblet cells;<br>Contrast-enhanced CT: small cystic lesion in ascending colon;<br>Laparotomy: a leash of blood vessels and multiple fleshy sessile pedunculated lesions overlying serosal aspect of small bowel and small bowel mesentery starting from mid-jejunum to the ileo-cecal junction | Limited ileocecal resection | Progression-free | Rai et al. (9) |
| 7 | Male | 58 | Esophagus | Dysphagia of 7 months' duration | Esophagogastroscopy: a huge lesion grew along the esophagus; the mucosa was normal;<br>Esophageal ultrasonography: the tumor originated from the submucosal layer and the muscularis propria was found to be intact;<br>Contrast-enhanced CT: a mass localized inside the esophageal lumen and a lesion with low density was outside;<br>Histology (endoscopic biopsy specimen): mild to moderate dysplasia of the lesion mucosa;<br>Histology (resection specimen): lymphangioma | Open thoracotomy and enucleation | Progression-free | Liang et al. (10) |

*(Continued)*

TABLE 1 Continued

| Case number | Gender | Age | Lesion location | Clinical features | Diagnostic workup | Treatment | Follow-up and outcome | Reference |
|---|---|---|---|---|---|---|---|---|
| 8 | Male | 32 | Small bowel mesentery | Mild dull diffuse abdominal pain and two episodes of melena | Abdominal ultrasound: multiple anechoic cystic lesions within the abdominal cavity;<br>Abdominal CT: numerous confluent cystic lesions of variable size;<br>Cytology: few mature lymphocytes and was negative for chyle. Flow cytometry showed few B and T lymphocytes;<br>Endoscopy: no significant abnormality. | 1 g of oral paracetamol three times per day for 1 week | Progression-free | Alhasan and Daqqaq (11) |
| 9 | Female | 35 | Mediastinum, Abdomen | Abdominal pain, lymphoedema of the legs, ascites, and diarrhea | Thoracoabdominal region CT: a multilobar cystic mass in the mediastinum extending in the retroperitoneum and intraperitoneum;<br>Body MRI: multiple hyperintense cystic lesions in mediastinum and retroperitoneum on T2-weighted images;<br>Endoscopy: multiple white spots in the duodenum and jejunum.<br>Histology:no evidence of malignancy | No effect: Pan abdominal radiotherapy, sandostatin, doxycycline, beta-blockade and thalidomide;<br>Effect: sirolimus | Progression-free | Van Meerhaeghe et al. (12) |
| 10 | Female | Newborn | Right lower abdominal subcutis | None | Abdominal ultrasound: hypo-anechoic cysts in the subcutaneous tissues, extending from the umbilical to the right inguinal area, reaching the medial surface of the thigh;<br>Abdominal MRI: several lacunas with cystic appearance; the enhancement was absent.<br>Multicystic lymphangioma was diagnosed | "Wait and see" strategy, follow-up 3 years. | Progression-free | Amodeo et al. (13) |
| 11 | Female | 11 | Mesentery | Pain in the right lower quadrant of the abdomen for 2 months | Abdominal CT: infiltrative cystic mass in the mesentery;<br>Exploratory laparotomy: a broad-based multiple cystic lymphangioma within the mesentery ranging from the Treitz ligament to the transverse colon. | The lymphangiomawas completely excised saving mesenteric vessels by skeletonization. The mesenteric defect was repaired with a Permacol. | Progression-free | Kim et al. (14) |

one of the possible complications. Minor lymphatic leakage can be resolved by conservative management. Massive lymphatic leaks can be treated by embolization, but surgery may be necessary in some cases (16). Regarding the pharmacotherapy of lymphangiomatosis, sirolimus is an inhibitor of mammalian target of rapamycin (mTOR). Elisa Boscolo reached the conclusion that sirolimus suppresses the growth of lymphatic endothelial cells by inhibiting VEGF-A- and VEGF-C-driven proliferation and migration, thus impeding lymphangiogenesis (17). It is very effective in the treatment of multiple complicated vascular anomalies and has potential antitumor effects (18). Follow-up of the present case observed a significant decrease in number and size of cysts by colonoscopy.

Exploratory laparoscopy has not been utilized to evaluate mesenteric lymphangiomatosis so far, although a case report suggested that surgical resection of the mesentery could be an option in case of mechanical obstruction (14). The present case revealed the multi-systemic imaging manifestations of a rare systemic disease and highlighted the importance of exploratory laparoscopy in the diagnosis of mesenteric lymphangiomatosis.

## Data availability statement

The datasets presented in this study can be found in online repositories. The names of the repository/repositories and accession number(s) can be found in the article/Supplementary Material.

## Author contributions

XW and YY contributed to the study concept and design. YY generated the literature strategy and filtered through the identified studies. YY evaluated study quality and wrote the manuscript. RW provided critical feedback on the manuscript. All authors contributed to the article and approved the submitted version.

## Funding

National Natural Science Foundation of China, Grant Number: 82072732, 81572930; The National Key Research and Development Program of China, Grant Number: 2016YFC0905303; Beijing Science and Technology Plan, Grant Number: D171100002617004.

## Acknowledgments

We thank Dr. Hulin Ma for data acquisition and clinical assessment and thank pathologist Quan Zhou for her contribution in the diagnosis of mesenteric lymphangiomatosis.

## Conflict of interest

The authors declare that the research was conducted in the absence of any commercial or financial relationships that could be construed as a potential conflict of interest.

## Publisher's note



## Supplementary material

The Supplementary Material for this article can be found online at: https://www.frontiersin.org/articles/10.3389/fonc.2022.933777/full#supplementary-material

SUPPLEMENTARY VIDEO 1
Laparoscopic presentation of lymphangiomatosis.

## References

1. Dasgupta R, Fishman SJ. Issva classification. *Semin Pediatr Surg* (2014) 23 (4):158–61. doi: 10.1053/j.sempedsurg.2014.06.016

2. Ozeki M, Fukao T, Kondo N. Propranolol for intractable diffuse lymphangiomatosis. *New Engl J Med* (2011) 364(14):1380–2. doi: 10.1056/NEJMc1013217

3. Pauzner R. Successful thalidomide treatment of persistent chylous pleural effusion. *Ann Internal Med* (2007) 146(1):75–6. doi: 10.7326/0003-4819-146-1-200701020-00022

4. Cao D, Wang J, Guo L. Gastrointestinal: Diffuse esophageal lymphangiomatosis manifesting as multiple submucosal masses. *J Gastroenterol Hepatol* (2020) 35(2):177. doi: 10.1111/jgh.14754

5. Lu G, Li H, Li Y. Lymphangiomatosis of the sigmoid colon - a rare cause of lower gastrointestinal bleeding: A case report and review of the literature. *Oncol Lett* (2017) 13(1):339–41. doi: 10.3892/ol.2016.5399

6. Mujagic Z, Masclee AAM, Keszthelyi D. Lymphangiomatosis of the colon. *Clin Gastroenterol Hepatol* (2022) 20(2):e14–e5. doi: 10.1016/j.cgh.2020.08.037

7. Giuliani A, Romano L, Coletti G, Walid AFM, Calvisi G, Maffione F, et al. Lymphangiomatosis of the ileum with perforation: A case report and review of the literature. *Ann Med Surg (Lond)* (2019) 41:6–10. doi: 10.1016/j.amsu.2019.03.010

8. Hwang SS, Park SY, Radiology DO, Hospital SV. Cavernous mesenteric lymphangiomatosis mimicking metastasis in a patient with rectal Cancer: A case report. *World J Gastroenterol* (2009) 15(31):3947–9. doi: 10.3748/wjg.15.3947

9. Rai P, Rao RN, Chakraborthy S. Case report: Caecal lymphangioma: A rare cause of gastrointestinal blood loss. (2013) 2013:bcr2013008866. doi: 10.1136/bcr-2013-008866

10. Liang X, Wei GG, Hou J, Di G, Xiao JC. Huge lymphangiomatosis of the esophagus. *Ann Thorac Surg* (2012) 93(6):2048-51. doi: 10.1016/j.athoracsur.2011.11.021

11. Alhasan AS, Daqqaq TS. Extensive abdominal lymphangiomatosis involving the small bowel mesentery: A case report. *World J Clin Cases* (2021) 9(32):7. doi: 10.12998/wjcc.v9.i32.9990

12. Meerhaeghe TV, Vandenbroucke F, Velkeniers B. Systemic generalised lymphangiomatosis: Unknown aetiology and a challenge to treat. *BMJ Case Rep* (2021) 14(1):e237331. doi: 10.1136/bcr-2020-237331

13. Amodeo I, Cavallaro G, Raffaeli G, Colombo L, Mosca F. Abdominal cystic lymphangioma in a term newborn: A case report and update of new treatments. *Medicine* (2017) 96(8):e5984. doi: 10.1097/MD.0000000000005984

14. Kim SH, Yoon KC, Lee W, Kim HY, Jung SE. Result of using a biologic collagen implant (Permacol) for mesenteric defect repair after excision of a huge mesenteric lymphangioma in a child. *Ann Surg Treat Res* (2015) 89(6):330–3. doi: 10.4174/astr.2015.89.6.330

15. de Vries JJ, Vogten JM, de Bruin PC, Boerma D, van de Pavoordt HD, Hagendoorn J. Mesenterical lymphangiomatosis causing volvulus and intestinal obstruction. *Lymphat Res Biol* (2007) 5(4):269–73. doi: 10.1089/lrb.2007.1010

16. Lv S, Wang Q, Zhao W, Han L, Wang Q, Batchu N, et al. A review of the postoperative lymphatic leakage. *Oncotarget* (2017) 8(40):69062–75. doi: 10.18632/oncotarget.17297

17. Boscolo E, Coma S, Luks VL, Greene AK, Klagsbrun M, Warman ML, et al. Akt hyper-phosphorylation associated with Pi3k mutations in lymphatic endothelial cells from a patient with lymphatic malformation. *Angiogenesis* (2015) 18(2):151–62. doi: 10.1007/s10456-014-9453-2

18. Wu C, Song D, Guo L, Wang L. Refractory head and neck lymphatic malformation in infants treated with sirolimus: A case series. *Front Oncol* (2021) 11:616702. doi: 10.3389/fonc.2021.616702

frontiers | Frontiers in Oncology

TYPE Case Report
PUBLISHED 26 October 2022
DOI 10.3389/fonc.2022.1045458



OPEN ACCESS

EDITED BY
Zhaolun Cai,
Sichuan University, China

REVIEWED BY
Gen Lin,
Fujian Provincial Cancer Hospital, China
Brandon Peter Lucke-Wold,
University of Florida, United States
Yongfeng Yu,
Shanghai Jiao Tong University, China

*CORRESPONDENCE
Chao Zhang
drzhangchao@tmu.edu.cn

SPECIALTY SECTION
This article was submitted to Surgical Oncology, a section of the journal Frontiers in Oncology

RECEIVED 21 September 2022
ACCEPTED 10 October 2022
PUBLISHED 26 October 2022

CITATION
Xu Y, Wu H, Wang C, Ma Y and Zhang C (2022) Case report: A balance of survival and quality of life in long-term survival case of lung adenocarcinoma with synchronous bone metastasis.
*Front. Oncol.* 12:1045458.
doi: 10.3389/fonc.2022.1045458



# Case report: A balance of survival and quality of life in long-term survival case of lung adenocarcinoma with synchronous bone metastasis

Yao Xu[1,2], Haixiao Wu[1,2], Cong Wang[1], Yulin Ma[1] and Chao Zhang[1,2]*

[1]Tianjin Medical University Cancer Institute and Hospital, National Clinical Research Center for Cancer, Key Laboratory of Cancer Prevention and Therapy, Tianjin's Clinical Research Center for Cancer, Tianjin, China, [2]The Sino-Russian Joint Research Center for Bone Metastasis in Malignant Tumor, Tianjin, China

Bone metastasis is one of the comorbidities of advanced lung cancer, eventually leading to an impaired quality of life. We present a case of a lung adenocarcinoma patient with synchronous bone metastasis. The patient possessed a superior survival time of more than five years under multidisciplinary treatment. Considering the balance of life expectancy and limb function, the metastatic site on the right humerus was successively surgically managed. Based on the present case, we emphasized the importance of treatment choice between anti-tumor and bone management in the long-term survival of cancer patients with synchronous bone metastasis.

KEYWORDS

**lung adenocarcinoma, bone metastasis, survival outcome, quality of life, case report**

## Introduction

Lung cancer is the leading cause of cancer mortality worldwide. In the United States, estimated deaths of lung and bronchus cancer were up to 68,820 and 61,360 for males and females, respectively, both of which accounted for around one fifth of the total cancer deaths (1). The 3-year relative survival of lung cancer has been rising from 21.0% to 31.0%, which is attributed to the improvement of tumor screening and multidisciplinary therapy (1, 2). More than half of the newly diagnosed lung cancer patients presented with metastatic disease at initial diagnosis (3). Data from the SEER program demonstrated the corresponding 5-year relative survival rate was a dismal 6.9% for lung cancer patients with distant metastasis (4).

In this study, bone was one of the most common metastatic sites in lung cancer, and bone metastasis (BM) occurred in more than one third of the advanced patients, especially in non-small cell lung cancer (NSCLC) patients (5). Due to the longer survival expectancy and the improvement of imaging technology, the reported BM incidence of lung cancer has been increasing (6). Bone metastasis and subsequent skeletal-related events (SREs) impaired activities of daily life and reduced quality of life (QOL), which eventually deteriorated the general condition and shortened the survival time of the patients (7). The previous study concluded that the median survival of lung cancer patients with synchronous BM was 4.00 (95% CI: 3.89–4.11) months (8). In our study on lung patients with synchronous BM, a total of 938 patients were selected, and the median survival of patients was up to 11.53 months (9). With the development of therapeutic modalities, the survival outcome of advanced lung cancer patients has been improving.

Skeletal-related events (SREs) are accepted to result in impaired mobility and increased mortality in cancer patients with BM. SREs are comprised of several complications, such as bone pain, pathological bone fracture, hypercalcemia, the need for radiotherapy, and spinal cord compression (10). Bone resorption inhibitors, such as bisphosphonates and denosumab, were recommended routinely. These anti-resorptive agents have been shown to delay the occurrence of SREs and reduce the frequency of SREs by regulating bone microenvironment (11). Radiation therapy (RT) was recommended for local control and pain palliation of bone metastatic sites. The dose and fractionation of RT should be tailored to the symptom and general condition of the patients (12). As for patients with pathological fractures or spinal cord compression, surgical intervention was emphasized to palliative symptoms and stabilizes bone structure. Importantly, life expectancy should be evaluated before surgery performance (13).

In this study, we reported a female lung cancer case diagnosed with synchronous BM. Accompanied with multidisciplinary management, three operations were performed on her bone metastasis site. At the last follow-up in September 2022, the patient had lived more than 5 years after diagnosis. In this case, we emphasized the importance of treatment choice between anti-tumor and bone management in the long survival of cancer patients with synchronous bone metastasis.

## Case description

A 52-year-old woman was admitted to our department in September 2016 due to pain (VAS = 6) in her right upper arm. The study was conducted in accordance with the Declaration of Helsinki and approved by the Ethics Board of the Tianjin Medical University Cancer Institute and Hospital. The signed informed consent of the patient was obtained. The study was reported in agreement with the principles of the CARE guidelines (14). A computed tomography (CT) scan revealed the evidence of a soft tissue mass and pathologic fracture on the right humerus (Figure 1A). At the same time, a pulmonary CT presented space-occupying lesions on her left upper lobe (Figure 1B). Based on the Mirels scoring system, the patient got a 9, which indicated a high risk of pathological fracture. Thus, the patient underwent tumor resection, bone cement filling, and plate internal fixation on the right humerus. X-ray imaging after surgery is shown in Figure 1C. The postoperative pathological diagnosis was metastatic adenocarcinoma (T2aN0M1b, stage IVA), and the metastatic site was considered to have originated from the lung based on immunohistochemistry testing. Pathologic imaging is presented in Supplementary Figure 1. After recovery from surgery, five cycles of palliative chemotherapy were carried out (pemetrexed 800 mg plus carboplatin 500 mg) until stable disease of primary lung cancer was detected by a routine imaging test, accompanied by the infusion of pamidronic acid monthly.

The patient was referred to our hospital again in September 2018 because of the recurrence at the original metastatic site and severe pain (VAS = 7). A PET-CT examination was performed in order to assess the progression of the disease. The right axilla lymph node was enlarged, being diagnosed as lymphatic metastasis. Besides, several new bone destruction sites were detected, including the previous surgical site on the right head of the humerus, the fourth lumbar, the right iliac bone, and the left femur. Thus, the patient was diagnosed with multiple bone metastases (T2aN3M1c, stage IVB). The patient got a new Mirels score of 9. After the prognostic evaluation (more than 6 months) and the general condition assessment, in order to prevent pathologic fracture of the right humerus, the replacement of the right shoulder joint was performed (Figure 1D). The pathological result was confirmed to be a metastatic adenocarcinoma with poor differentiation (Supplementary Figure 2). Two cycles of chemotherapy (pemetrexed 800 mg plus carboplatin 500 mg) were performed with no remission. Thus, a new regimen of systematic chemotherapy was needed. In March 2019, the patient underwent genetic testing of postoperative paraffin-embedding tissue and the results concluded that both the mutations of EGFR, HER2, and MET and the rearrangements of ALK and ROS1 were negative. Meanwhile, the expression level of PD-L1 was less than 1%. After multidisciplinary team discussion, the chemotherapy was performed, which comprised docetaxel 110 mg and carboplatin 500 mg. Meanwhile, sintilimab 200 mg was given at the strong will of the patient. The regimen was terminated in May 2019 due to the intolerant allergy. Then, the carboplatin was replaced by nedaplatin 140 mg, and the regimen was regularly performed for four courses.

After an approximately three-year stable disease period, the patient presented to our department with the occurrence of prosthesis extrusion in April 2022. The CT imaging is shown in

10.3389/fonc.2022.1045458

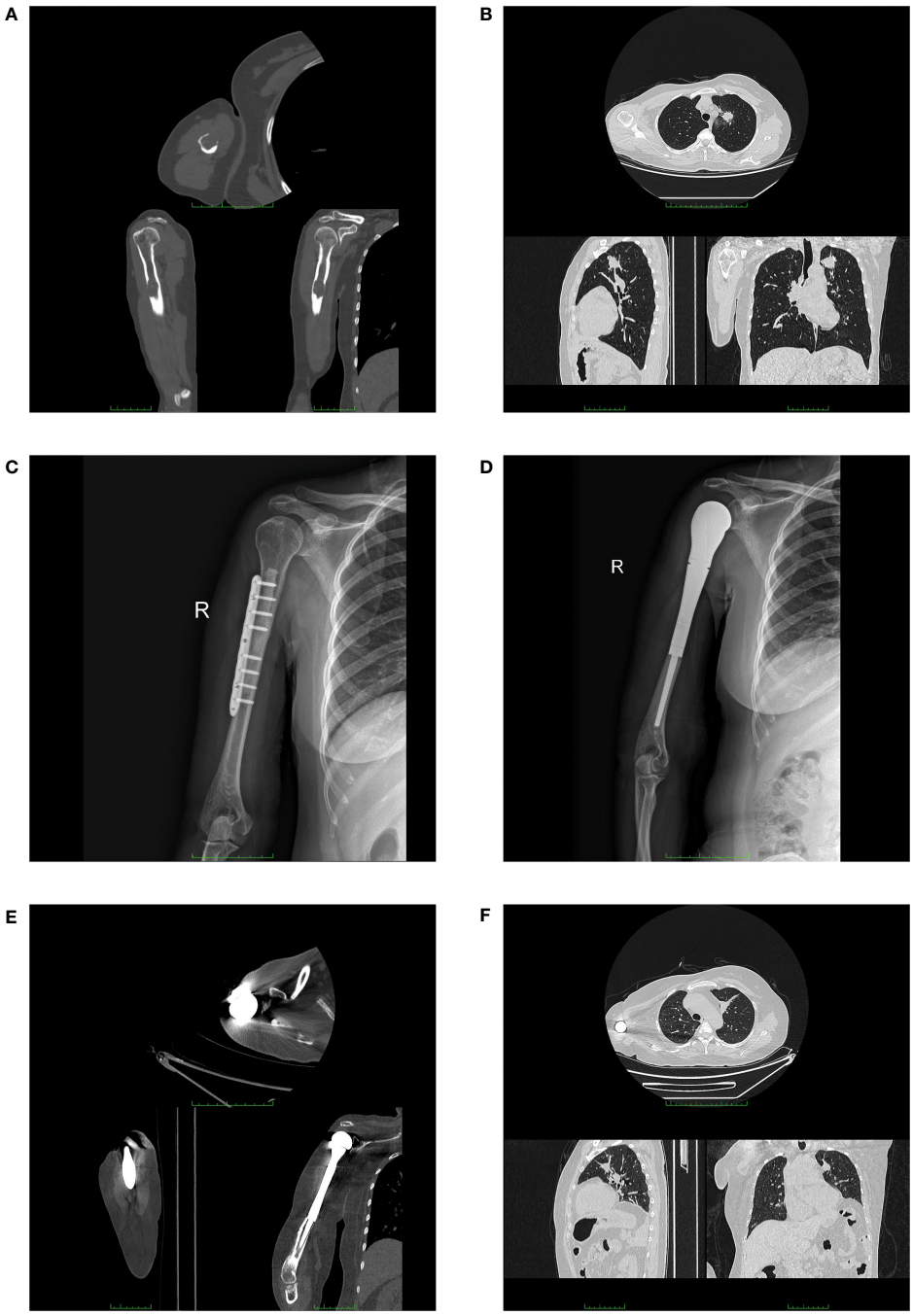


FIGURE 1
Imaging examination of the patient. Computed tomography images (upper image for axial, lower left for sagittal, and lower right for coronal, respectively) of the patient at the initial diagnosis **(A, B)**. **(A)** CT scan showed a soft tissue mass (2.4 cm × 1.8 cm) and a pathologic fracture on the right humerus of the patient. **(B)** Chest CT showed a pulmonary mass in the left upper lobe. X-ray images after the first two surgeries **(C, D)**. **(C)** X-ray image after the surgery for plate internal fixation on the right humerus. **(D)** X-ray image after the surgery for the right shoulder joint replacement. Computed tomography images (upper image for axial, lower left for sagittal, and lower right for coronal, respectively) before the surgery of shoulder disarticulation **(E, F)**. **(E)** CT scan showed the prosthesis of patient exposed out of right humerus. **(F)** Chest CT presented stable disease in the primary lung tumor.

Figure 1E. Physical examination showed a skin ulceration (5.0 cm ∗ 2.0 cm) on the previous surgical site with swelling and exudation, accompanied by no systemic symptoms of fever, sweats, or chills. The bacterial culture test of exudation was performed, and pseudomonas aeruginosa was found. The serum examination indicated an elevation of C-reactive protein (52.22 mg/L) without other abnormalities. Considering the unsatisfactory expected function of the limb and the poor general condition (Karnofsky score = 50) of the patient, the surgery of right shoulder disarticulation was performed with the consent of the patient. Early functional exercise and mental rehabilitation were applied after surgery. The patient is still in follow-up with stable disease in his primary lung tumor after long-term systematic therapy (Figure 1F). The timeline of the diagnosis and treatment course of the patient is summarized in Figure 2.

## Discussion

With the advance of targeted therapy and immunotherapy in recent years, new medications such as tyrosine kinase inhibitors (TKIs) and anti-PD1/PD-L1 agents have been approved and widely used in patients with advanced lung cancer (2). We reviewed the previous literature reporting long-term survival in lung cancer patients with synchronous BM and listed four case reports in Table 1 (15–18). Most studies were conducted before the application of targeted therapy. The treatment was restricted to conventional therapies such as systematic chemotherapy, surgical resection, and radiotherapy, which seemed to be largely out-of-data in current treatment principles. Hou et al. reported a 76-year-old female lung cancer patient presenting with metastasis on the first lumbar vertebra and the left seventh anterior rib at the initial diagnosis. The patient underwent surgery for lumbar vertebra tumor removal, bone cement filling, and pedicle screw fixation at the spine metastatic site. After surgery, the backache symptoms of the patient were significantly relieved. Two cycles of chemotherapy followed by EGFR-TKI geftinib were performed and the patient achieved an eight-year survival. In the present case, we also presented a female lung cancer patient with long-term survival. In contrast to the spinal metastatic case reported by Hou et al., our patient suffered from intolerable pain and immobility due to the metastasis on the right humerus. In the absence of individual comprehensive therapy, systematic treatment was performed to achieve a longer survival outcome. Meanwhile, the preservation and restoration of limb function in BM patients should be pursued after evaluating the balance of cancer survival and quality of life.

As shown in Figure 3, the goal of treatment for advanced-stage lung cancer is to achieve local control, minimize symptoms, and improve QOL (19). The multidisciplinary approach conducted by the team of oncologists, orthopedic surgeons, radiologists, pathologists, psychologists, and palliative medicine specialists should be emphasized before the accurate prediction of survival. Several prognostic models were reported to predict the survival of lung patients with BM, which played an important role in treatment decision-making (8, 20–22). For NSCLC patients with a predictive life expectancy of less than three months, best supportive care was recommended, which aimed to reduce suffering and support the best possible QOL (23). For BM patients with a survival time of more than 3 months, systematic therapy including bone-targeted therapy, radiotherapy, and pain management should be performed. Meanwhile, surgical intervention was recommended for patients with a survival time of more than 6 months (12). To identify targeted therapy or immunotherapy potentially benefiting survival, molecular testing should be performed and individual treatment should be planned according to the resting results (12). Notably, systemic imaging examination was emphasized for advanced cancer patients to detect unusual metastatic sites (24). Solitary suspicious lesions, especially those in uncommon locations such as the skull, should be carefully diagnosed to exclude metabolic and other diseases (25). The therapeutic regimen must be initiated under the circumstances of the right diagnosis.

The exposure of the prosthesis was one of the infrequent complications of joint replacement. Michala et al. reported a total of 130 patients who received joint replacement due to skeletal metastasis, and one case presented a prosthesis penetrating the skin (26). In the current study, the body mass index (BMI) of the patient decreased from 24.0 to 19.2 since the performance of shoulder joint replacement. Besides, the patient suffered from an impact on her right shoulder, which might have led to the rupture of the fragile fiber formed after surgery. Thus, we suspected that the prosthesis exposure was attributed to


FIGURE 2
The timeline of the diagnosis and treatment course of the patient in the present case.

TABLE 1 Summary of the previously reported long-term survival (more than five years) cases of lung cancer patients with synchronous bone metastasis.

| Publication year | Age at initial diagnosis | Gender | Pathology | Primary lung tumor treatment and systematic therapy | Bone metastatic site | Bone metastatic site treatment | Survival time |
|---|---|---|---|---|---|---|---|
| 2021 (15) | 76 | Female | Papillary adenocarcinoma, moderately differentiated | Two cycles of chemotherapy; EGFR-TKI geftinib | 1st lumbar vertebra and left 7th anterior rib | Lumbar vertebra tumor removal, bone cement filling and plate internal fxation; radiation therapy; zoledronic acid intravenous injection | Eight years survival after initial diagnosis |
| 2005 (16) | 71 | Male | Squamous cell carcinoma, well differentiated | Left lower lobe lobectomy plus six cycles of systematic chemotherapy; radiation therapy after local recurrence | Right fibula | None | Five years survival after last operation |
| | 52 | Male | Adenocarcinoma, poorly differentiated | Right upper lobe lobectomy plus three cycles of systematic chemotherapy | Left thigh | Resection of the left thigh tumor | Five years survival after last operation |
| 2005 (17) | 61 | Male | NSCLC, poorly differentiated | Chemotherapy plus radiation to the left upper lobe tumor | Right femur | Right femoral intramedullary rod placement plus radiation therapy; excision of the right femoral metastasis after recurrence | Eight years survival after initial diagnosis |
| 2004 (18) | 68 | Male | Adenocarcinoma | Left upper lobectomy and resection of partial parietal pleura | Right iliac bone | Resection of the right iliac bone tumor | Five years survival after initial diagnosis |

malnutrition and the experience of falling over. After the comprehensive discussion on the general condition, comorbidity, and economic condition of the patient, the patient chose to have disarticulation surgery. Before the disarticulation surgery, the infectious situation could not be satisfactorily controlled with the antibiotics, which were associated with the immunosuppression after long-term anti-immune treatment. The infection could increase the probability of allograft rejection, leading to the failure of revision surgery. Besides, two-time surgeries had been performed, which reduced the remaining soft tissue to cover the surgical site and increased the operational difficulty of revision surgery. Thus, disarticulation surgery, with fewer postoperative complications and a lower cost, was a more suitable choice for the patient than revision surgery.

The patient queried for the surgery of shoulder disarticulation autonomously, which reflected the pursuit of the patient for improvement of QOL. For an advanced lung cancer patient with BM, the demand of patient at initial diagnosis was cancer control and survival extension. After several invasive methods and subsequently systematic treatment, local control was achieved temporarily, which was always accompanied by cancer-associated complications and treatment-related adverse events (27). Systematic chemotherapy might cause liver dysfunction and myelosuppression alone or in combination with immunotherapy (28). It was reported that immune-related adverse effects such as thyroid disorders occurred in NSCLC patients who were receiving immunotherapy (29). As for patients undertaking surgical intervention, some of them suffered from perioperative and postoperative complications, which included pneumonia, infectious diseases, and neurological deterioration (29). Besides, the financial burden on patients and their families sustainably accumulated, which caused distress in patients and finally turned their demands from longer survival to palliating symptoms and improving QOL (30). Thus, cancer itself as well as social factors should be focused on, which urgently needs support offered by psychological consultants and medical social workers (10). The clinical management of BM was one of the major concerns worldwide (31). It was reported that the major complications of BM commonly occur within 3–6 months in patients without the treatment of bone resorption inhibitors (32). Thus, it is important to initiate a bone management program as soon as the diagnosis of BM is made, regardless of whether the patient presents SREs or not (10). Bone resorption inhibitors such as bisphosphonates and denosumab were highly recommended after the diagnosis of BM, which aimed to prevent or delay the occurrence of SREs (33). To palliate symptom of pain, oral drugs such as NSAIDs and opioid treatment and radiation therapy were effective approaches. Several options for radiation therapy are currently available, including external-beam radiation therapy (EBRT), stereotactic body irradiation therapy (SBRT), and radionuclide treatment (11).

In the current case, the patient was diagnosed with a solitary bone metastasis on the right humerus, and a surgical metastectomy was performed initially. With the development of cancer, oligometastatic disease (with a limited number of metastatic sites) was identified. Since the occurrence of disease progression, local surgical intervention was performed to prevent

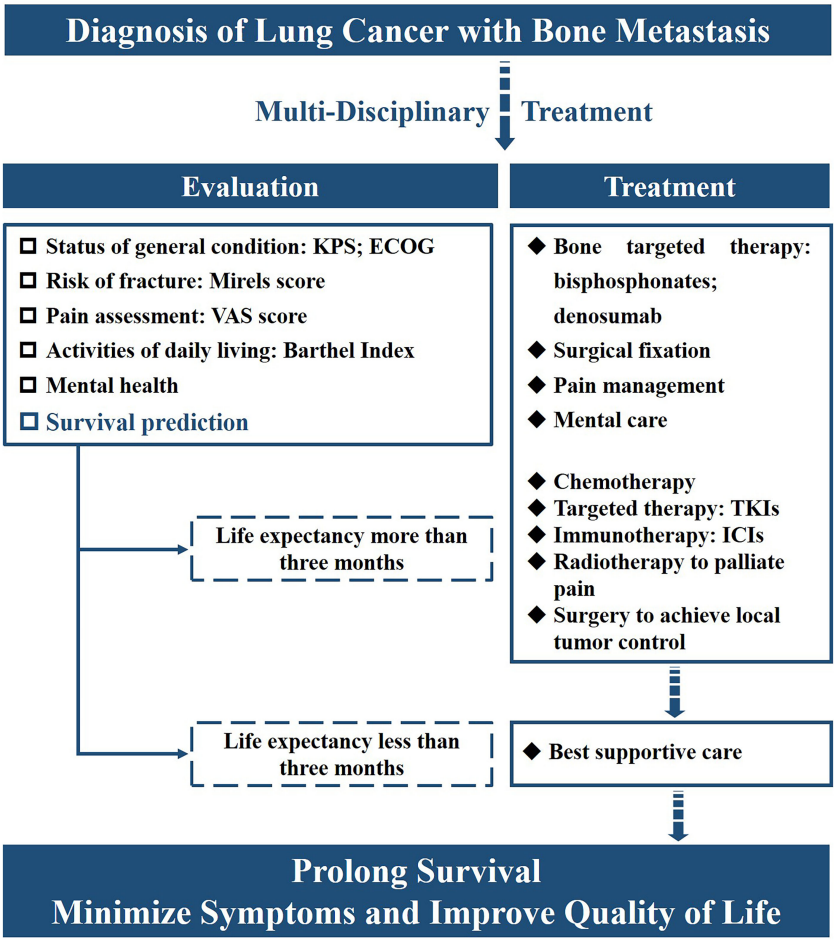


FIGURE 3
A flowchart illustrating comprehensive evaluation and treatment strategies for lung patients with bone metastasis.

pathologic fracture and systemic treatment was conducted, all of which were chosen after comprehensive evaluation of survival and limb function. As for patients with oligometastatic bone disease (OMBD), the local therapy of both primary lung cancer and bone metastatic sites should be highlighted. In a meta-analysis including 757 patients with oligometastatic NSCLC, prolonged survival was observed in patients who received consolidative local treatment (34). The aggressive surgical metastectomy and radiotherapy on bone metastasis may benefit survival in oligometastatic NSCLC patients (35, 36). Since complete pathologic fractures are a clear indication for surgery, the selected patients with impending fractures should undergo surgical intervention to prevent fractures. According to the NCCN guidelines, orthopedic stabilization accompanied by palliative radiotherapy should be performed in patients as risk of fracture on weight-bearing bone (12). Meanwhile, a previous study concluded that patients with impending pathologic fractures had a better outcome than those with complete fractures after surgical intervention (37). Thus, the optimal time to perform surgery for patients with impending fractures needs further investigation after the consideration of the benefit from surgery. As shown in Table 1, various cases suggested cancer patients could significantly benefit from the multidisciplinary treatment, even if they were diagnosed with the initial advanced stage. Thus, a multidisciplinary approach should be encouraged, and the necessary psychological counseling should be given to such patients. Currently, rarely is a study looking into the individualized needs of cancer patients with BM performed. With improved survival of cancer patients with BM, such a study would be of significance for guiding treatment plan making. At the same time, more attention should be given to the field of precise prognostication in cancer patients with BM.

In summary, we described a case of lung adenocarcinoma in the left upper lobe, diagnosed with synchronous bone metastasis. With more than 5 years of survival since the initial diagnosis, the patients obtained survival benefits from the current systematic

chemotherapy and targeted therapy. Meanwhile, the limb function of the patient was reserved as much as possible despite the multiple recurrences until the final disarticulation. The study aimed to propose the concept that treatment modalities should be tailored to the life expectancy and the individual needs of patients.

## Data availability statement

The original contributions presented in the study are included in the article/Supplementary Material. Further inquiries can be directed to the corresponding author.

## Ethics statement

This study was reviewed and approved by the Tianjin Medical University Cancer Institute and Hospital. The patients/participants provided their written informed consent to participate in this study. Written informed consent was obtained from the individual(s) for the publication of any potentially identifiable images or data included in this article.

## Author contributions

YM and CZ contributed to the conception and design of the study. YX wrote the first draft of the manuscript. HW wrote some sections of the manuscript. CW made a substantial contribution to the acquisition and interpretation of the data for the work. All authors contributed to the article and approved the submitted version.

## Conflict of interest

The authors declare that the research was conducted in the absence of any commercial or financial relationships that could be construed as a potential conflict of interest..

## Publisher's note

All claims expressed in this article are solely those of the authors and do not necessarily represent those of their affiliated organizations, or those of the publisher, the editors and the reviewers. Any product that may be evaluated in this article, or claim that may be made by its manufacturer, is not guaranteed or endorsed by the publisher.

## Supplementary material

The Supplementary Material for this article can be found online at: https://www.frontiersin.org/articles/10.3389/fonc.2022.1045458/full#supplementary-material

## References

1. Siegel RL, Miller KD, Fuchs HE, Jemal A. Cancer statistics, 2022. *CA Cancer J Clin* (2022) 72(1):7–33. doi: 10.3322/caac.21708

2. Chen R, Manochakian R, James L, Azzouqa AG, Shi H, Zhang Y, et al. Emerging therapeutic agents for advanced non-small cell lung cancer. *J Hematol Oncol* (2020) 13(1):58. doi: 10.1186/s13045-020-00881-7

3. Arbour KC, Riely GJ. Systemic therapy for locally advanced and metastatic non–small cell lung cancer. *JAMA* (2019) 322(8):764. doi: 10.1001/jama.2019.11058

4. Howlader N, Noone AM, Krapcho M, Miller D, Brest A, Yu M, et al. *SEER cancer statistics review, 1975-2018*. Bethesda, MD: National Cancer Institute. Available at: https://seer.cancer.gov/csr/1975_2018/ based on November 2020 SEER data submission, posted to the SEER web site, April 2021.

5. Chai X, Yinwang E, Wang Z, Wang Z, Xue Y, Li B, et al. Predictive and prognostic biomarkers for lung cancer bone metastasis and their therapeutic value. *Front Oncol* (2021) 11:692788. doi: 10.3389/fonc.2021.692788

6. Turpin A, Duterque-Coquillaud M, Vieillard MH. Bone metastasis: Current state of play. *Trans Oncol* (2020) 13(2):308–20. doi: 10.1016/j.tranon.2019.10.012

7. Cetin K, Christiansen CF, Jacobsen JB, Norgaard M, Sorensen HT. Bone metastasis, skeletal-related events, and mortality in lung cancer patients: a Danish population-based cohort study. *Lung Cancer* (2014) 86(2):247–54. doi: 10.1016/j.lungcan.2014.08.022

8. Zhang C, Mao M, Guo X, Cui P, Zhang L, Xu Y, et al. Nomogram based on homogeneous and heterogeneous associated factors for predicting bone metastases in patients with different histological types of lung cancer. *BMC Cancer* (2019) 19 (1):238. doi: 10.1186/s12885-019-5445-3

9. Guo X, Ma W, Wu H, Xu Y, Wang D, Zhang S, et al. Synchronous bone metastasis in lung cancer: retrospective study of a single center of 15,716 patients from tianjin, China. *BMC Cancer* (2021) 21(1):613. doi: 10.1186/s12885-021-08379-2

10. Kimura T. Multidisciplinary approach for bone metastasis: A review. *Cancers* (2018) 10(6):156. doi: 10.3390/cancers10060156

11. Aielli F, Ponzetti M, Rucci N. Bone metastasis pain, from the bench to the bedside. *Int J OF Mol Sci* (2019) 20(2):280. doi: 10.3390/ijms20020280

12. Ettinger DS, Wood DE, Aisner DL, Akerley W, Bauman JR, Bharat A, et al. Non-small cell lung cancer, version 3.2022, NCCN clinical practice guidelines in oncology. *J Natl Compr Canc Netw* (2022) 20(5):497–530. doi: 10.6004/jnccn.2022.0025

13. Dammerer D, Blum P, Krappinger D, Keiler A. Common pitfalls in the management of bone metastasis of the extremities - a current concept and systematic review of the literature. *Anticancer Res* (2021) 41(10):4665–72. doi: 10.21873/anticanres.15280

14. Riley DS, Barber MS, Kienle GS, Aronson JK, Schoen-Angerer Tv, Tugwell P, et al. CARE guidelines for case reports: explanation and elaboration document. *J OF Clin Epidemiol* (2017) 89:218–35. doi: 10.1016/j.jclinepi.2017.04.026

15. Hou WT, Xie XQ, Luo Y, Yi C, Luo F, Kang JB, et al. Long-term survival case of a non-small cell lung cancer bone metastasis patient treated with bone cement, radiation and gefitinib. *Eur Rev Med Pharmacol Sci* (2021) 25(6):2542–7. doi: 10.26355/eurrev_202103_25417

16. Hirano Y, Oda M, Tsunezuka Y, Ishikawa N, Watanabe G. Long-term survival cases of lung cancer presented as solitary bone metastasis. *Ann Thorac Cardiovasc Surg* (2005) 11(6):401–4.

17. Agarwala AK, Hanna NH. Long-term survival in a patient with stage IV non-small-cell lung carcinoma after bone metastasectomy. *Clin Lung Cancer* (2005) 6(6):367–8. doi: 10.3816/CLC.2005.n.017

18. Higashiyama M, Kodama K, Takami K, Higaki N, Yamada T, Mano M, et al. Surgical treatment of bone metastasis followed by a primary lung cancer lesion: report of a case. *Surg Today* (2004) 34(7):600–5. doi: 10.1007/s00595-004-2758-9

19. Gesthalter Y, Smyth R, Sullivan D. Treatment of advanced-stage non-small cell lung cancer. *Am J Respir Crit Care Med* (2022) 205(5):P9–P10. doi: 10.1164/rccm.2055P9

20. Zheng XQ, Huang JF, Lin JL, Chen L, Zhou TT, Chen D, et al. Incidence, prognostic factors, and a nomogram of lung cancer with bone metastasis at initial diagnosis: a population-based study. *Transl Lung Cancer Res* (2019) 8(4):367–79. doi: 10.21037/tlcr.2019.08.16

21. Fan Z, Huang Z, Tong Y, Zhu Z, Huang X, Sun H. Sites of synchronous distant metastases, prognosis, and nomogram for small cell lung cancer patients with bone metastasis: A Large cohort retrospective study. *J Oncol* (2021) 2021:1–16. doi: 10.1155/2021/9949714

22. Chen Q, Chen X, Zhou L, Chen F, Hu A, Wang K, et al. The emergence of new prognostic scores in lung cancer patients with spinal metastasis: A 12-year single-center retrospective study. *J Cancer* (2021) 12(18):5644–53. doi: 10.7150/jca.60821

23. Dans M, Kutner JS, Agarwal R, Baker JN, Bauman JR, Beck AC, et al. NCCN Guidelines(R) insights: Palliative care, version 2.2021. *J Natl Compr Canc Netw* (2021) 19(7):780–8. doi: 10.6004/jnccn.2021.0033

24. Lucke-Wold B, Bonasso PC, Cassim R. Primary colon adenocarcinoma with metastatic disease to the rectum followed by the left axilla. *Am Med Stud Res J* (2017) 4(1):57–61. doi: 10.15422/amsrj.2017.03.009

25. Turner RC, Lucke-Wold BP, Hwang R, Underwood BD. Lung cancer metastasis presenting as a solitary skull mass. *J Surg Case Rep* (2016) 2016(6) 1–3. doi: 10.1093/jscr/rjw116

26. Sorensen MS, Gregersen KG, Grum-Schwensen T, Hovgaard D, Petersen MM. Patient and implant survival following joint replacement because of metastatic bone disease. *Acta Orthopaedica* (2013) 84(3):301–6. doi: 10.3109/17453674.2013.788437

27. Dudzinska M, Szczyrek M, Wojas-Krawczyk K, Swirska J, Chmielewska I, Zwolak A. Endocrine adverse events of nivolumab in non-small cell lung cancer patients-literature review. *Cancers (Basel)* (2020) 12(8) 1–20. doi: 10.3390/cancers12082314

28. Lin LL, Lin GF, Yang F, Chen XQ. A systematic review and meta-analysis of immune-mediated liver dysfunction in non-small cell lung cancer. *Int Immunopharmacol* (2020) 83:106537. doi: 10.1016/j.intimp.2020.106537

29. Tarawneh AM, Pasku D, Quraishi NA. Surgical complications and re-operation rates in spinal metastases surgery: a systematic review. *Eur Spine J* (2021) 30(10):2791–9. doi: 10.1007/s00586-020-06647-6

30. Carrera PM, Kantarjian HM, Blinder VS. The financial burden and distress of patients with cancer: Understanding and stepping-up action on the financial toxicity of cancer treatment. *CA Cancer J Clin* (2018) 68(2):153–65. doi: 10.3322/caac.21443

31. Li H, Wu H, Abakumov MA, Xu Y, Lin Y, Chekhonin VP, et al. The 100 most cited papers on bone metastasis: A bibliometric analysis. *J Bone Oncol* (2022) 35:100443. doi: 10.1016/j.jbo.2022.100443

32. Coleman RE. Clinical features of metastatic bone disease and risk of skeletal morbidity. *Clin Cancer Res* (2006) 12(20 Pt 2):6243s–9s. doi: 10.1158/1078-0432.CCR-06-0931

33. Jehn CF, Diel IJ, Overkamp F, Kurth A, Schaefer R, Miller K, et al. Management of metastatic bone disease algorithms for diagnostics and treatment. *Anticancer Res* (2016) 36(6):2631–7.

34. Ashworth AB, Senan S, Palma DA, Riquet M, Ahn YC, Ricardi U, et al. An individual patient data metaanalysis of outcomes and prognostic factors after treatment of oligometastatic non-small-cell lung cancer. *Clin Lung Cancer* (2014) 15(5):346–55. doi: 10.1016/j.cllc.2014.04.003

35. Gomez DR, Blumenschein GJ, Lee JJ, Hernandez M, Ye R, Camidge DR, et al. Local consolidative therapy versus maintenance therapy or observation for patients with oligometastatic non-small-cell lung cancer without progression after first-line systemic therapy: a multicentre, randomised, controlled, phase 2 study. *Lancet Oncol* (2016) 17(12):1672–82. doi: 10.1016/S1470-2045(16)30532-0

36. Iyengar P, Wardak Z, Gerber DE, Tumati V, Ahn C, Hughes RS, et al. Consolidative radiotherapy for limited metastatic non-Small-Cell lung cancer: A phase 2 randomized clinical trial. *JAMA Oncol* (2018) 4(1):e173501. doi: 10.1001/jamaoncol.2017.3501

37. Johnson SK, Knobf MT. Surgical interventions for cancer patients with impending or actual pathologic fractures. *Orthopaedic Nurs* (2008) 27(3):160–71. doi: 10.1097/01.NOR.0000320543.90115.d5

frontiers | Frontiers in Surgery

TYPE Case Report
PUBLISHED 31 October 2022
DOI 10.3389/fsurg.2022.955655



OPEN ACCESS

EDITED BY
Zhaolun Cai,
Sichuan University, China

REVIEWED BY
Nguyen Minh Duc,
Pham Ngoc Thach University of Medicine, Vietnam
Nikolaos Zavras,
University General Hospital Attikon, Greece
Dimitrios Papaconstantinou,
University General Hospital Attikon, Greece

*CORRESPONDENCE
ChunKai Yu
yuchunkai2976@bjsjth.cn

SPECIALTY SECTION
This article was submitted to Surgical Oncology, a section of the journal Frontiers in Surgery

RECEIVED 29 May 2022
ACCEPTED 10 October 2022
PUBLISHED 31 October 2022

CITATION
Chen Y, Wei Y, Chang H and Yu C (2022) Case report and literature review: Rare male aggressive angiomyxoma of the scrotum. Front. Surg. 9:955655. doi: 10.3389/fsurg.2022.955655



# Case report and literature review: Rare male aggressive angiomyxoma of the scrotum

Yue Chen, YaPing Wei, Hong Chang and ChunKai Yu*

Department of Pathology, Beijing Shijitan Hospital, Capital Medical University, Beijing, China

Aggressive angiomyxoma (AAM) is an uncommon locally infiltrative tumor that frequently occurs in the pelvic soft tissues of female patients; it has a high rate of local recurrence. However, AAM is extremely rare in males. Herein, we present the case of a 70-year-old man with a gradually enlarging painless mass in the scrotum. The patient underwent local excision of the scrotal AAM, with no local relapse after 17 months of follow-up. In addition to the present case, the clinicopathological features of males with AAM reported in literature (to the best of our knowledge) are discussed in this report. The literature review revealed that the gross morphology, clinical process, and histopathology of AAM in males resemble those of AAM in females. In particular, estrogen receptor/progesterone receptor has been shown to be expressed in male patients, which may provide an option for hormone therapy. Moreover, in males, a lower recurrence rate has been observed after surgery to remove the tumor. However, more data are needed to validate this observation. This report emphasizes the importance of considering AAM as the differential diagnosis of myxoid neoplasms in male genital areas.

KEYWORDS
aggressive angiomyxoma, scrotum, local recurrence, male, soft tissue tumor

## Introduction

Aggressive angiomyxoma (AAM), a rare deep soft tissue tumor, occurs predominantly in the pelvis and perineum of women (1). The age of AAM onset in women has previously been reported to range from 6 to 77 years, with the peak incidence during the childbearing years (2). AAM is defined as a benign tumor with no malignant potential, however, AAM has a high probability of local recurrence in the form of local infiltration (3). At present, extensive surgical excision with tumor-free margins is the most commonly available treatment for AAM (2). The occurrence of this type of tumor is very rare in men. To the best of our knowledge, only 85 male AAM cases (including the present one) have been reported in literature (**Table 1**) since the disease was first described in 1983. In most of these cases, the tumors were detected in the perineal region, inguinal area, and scrotum. AAM is difficult to diagnose without pathological analysis, and misdiagnosis as prostate, testicular, or paratesticular cancer is common (4). Herein, we present the case of AAM arising from the scrotum in a 70-year-old man and describe the diagnosis and treatment procedure along with a literature review on previously reported AAM cases in males. This study was reported in agreement with principles of the CARE guidelines (5).

TABLE 1 The previously reported cases of aggressive angiomyxoma in men.

| No. | Reference | Age (y) | Size (cm) | Location | Postoperatively follow | Immunohistochemical profile |
|---|---|---|---|---|---|---|
| 1-43 | Idrees et al. (6) | 1–82 | See reference for details | | | |
| 44 | Hatano et al. (7) | 59 | 7.4 | Retrovesical area | 26 months with no recurrence | CD34 (+), desmin (+), SMA (+), S-100 (–) |
| 45 | Wu et al. (8) | 40 | 5.1 | Scrotum | 12 months with no recurrence | NA |
| 46 | Bothig et al. (9) | 46 | 20.0 | Perineum | 26 months with no recurrence | CD34 (+), desmin (+), S-100 (–), ER (+), PR (+) |
| 47 | Pai et al. (10) | 48 | 12.0 | Claviculate | 6 months with no recurrence | desmin (+), S-100 (–), ER (+), PR (–) |
| 48 | Heffernan et al. (11) | 54 | 7.4 | Thigh | 6 months with no recurrence | CD34 (+), desmin (–), S-100 (–), CD31 (–) |
| 49 | Minagawa et al. (12) | 37 | 10.0 | Inguinal area | 6 months with no recurrence | CD34 (–), desmin (–), S-100 (–), ER (–), PR (–) |
| 50 | Sylvester et al. (13) | 47 | 4.0 | Larynx | 4 years with no recurrence | CD34 (–), desmin (–), SMA (–), S-100 (–) |
| 51 | Morag et al. (14) | 64 | 19.0 | Scrotum | 3 years with no recurrence | CD34 (+), desmin (+), SMA (+), S-100 (–) |
| 52 | Plumb et al. (15) | 44 | 26.0 | Engrafted kidney | 15 months with no recurrence | desmin (+), ER (–), PR (–) |
| 53 | Sawada et al. (16) | 67 | 2.0 | Prostate | 15 months with no recurrence | CD34 (–), desmin (–), S-100 (–), ER (–), PR (+) |
| 54 | Bajaj et al. (17) | 28 | NA | Orbit | 4 years with no recurrence | CD34 (+), desmin (+), S-100 (–) |
| 55 | Rocco et al. (18) | 46 | 34.0 | Scrotum | 3 months with local recurrence | NA |
| 56 | Mishulin et al. (19) | 62 | 2.5 | Orbit | NA | NA |
| 57 | Nayal et al. (20) | 27 | 12.0 | Axillary region | 6 months with no recurrence | CD34 (–), SMA (+), S-100 (+), ER (–) |
| 58 | Gaunay et al. (21) | 40 | 5.2 | Scrotum | NA | NA |
| 59 | Karwacki et al. (22) | 81 | 5.0 | Perineum | 16 months with no recurrence | CD34 (+), desmin (+), SMA (+), ER (+), PR (+) |
| 60 | Saha et al. (23) | 17 | 25.0 | Greater omentum | NA | desmin (+) |
| 61 | Wang et al. (24) | 60 | NA | Maxilla | 2 months with no recurrence | CD34 (+), desmin (–), S-100 (–), ER (+), PR (–) |
| 62 | Caruso et al. (25) | 72 | 23.0 | Pararectal | NA | NA |
| 63 | Wang et al. (26) | 25 | 6.0 | Scrotum | NA | CD34 (+), SMA (–), S-100 (–) |
| 64 | Smith et al. (27) | 51 | 11.0 | Pelvis | 15 months with no recurrence | NA |
| 65 | Smith et al. (27) | 77 | 1.2 | Knee | NA | NA |
| 66 | Draeger et al. (28) | 73 | NA | Scrotum | No recurrence | CD34 (+), desmin (+), ER (+), PR (+) |
| 67 | Ahmed et al. (29) | <1 | 12.0 | Penis | 6 months with no recurrence | NA |
| 68 | Sharma et al. (30) | 53 | 4.0 | Scrotum | NA | NA |
| 69 | Gorsi et al. (31) | 44 | 10.5 | Engrafted kidney | Dead for pulmonary tuberculosis | CD34 (+), SMA (–), S-100 (+) |
| 70 | Damodaran et al. (32) | 62 | NA | Penis | 20 months with no recurrence | NA |
| 71 | Ismail et al. (33) | 65 | 16.0 | Scrotum | 2 years with no recurrence | CD34 (–), desmin (+), S-100 (–), ER (+), PR (–) |
| 72 | Aydin et al. (34) | 66 | 15.0 | Scrotum | 6 months with no recurrence | CD34 (+), desmin (+), S-100 (–), ER (+), PR (+) |
| 73 | Umranikar et al. (35) | 79 | 15.7 | Perineum | 4 years with no recurrence | NA |
| 74 | Hsieh et al. (36) | 46 | 20.0 | Buttock | NA | CD34 (+), desmin (–), S-100 (–), ER (+), PR (–) |
| 75 | Neyaz et al. (37) | 53 | 15.0 | Scrotum | 12 months with no recurrence | CD34 (+), desmin (+), S-100 (–), ER (–), PR (–) |
| 76 | Serao et al. (38) | 72 | 7.7 | Paratestis | No recurrence | CD34 (+), desmin (+), PR (+), ER (–) |
| 77 | Addesso et al. (39) | 56 | 7.0 | Prostate | NA | CD34 (+), desmin (+), S-100 (–), ER (+), PR (+) |
| 78 | Kirkilessis et al. (40) | 57 | 11.0 | Scrotum | 2 years with no recurrence | CD34 (+), desmin (+), S-100 (+), ER (+), PR (+) |
| 79 | Liu et al. (41) | 62 | 2.3 | Paraureteral area | 30 months with no recurrence | CD34 (–), desmin (–), SMA (–), S-100 (+) |
| 80 | Majumdar et al. (42) | 30 | 28.0 | Jaw | Intraoperative death | NA |
| 81 | Celik et al. (43) | 55 | 12.5 | Pelvic | 16 months with no recurrence | CD34 (–), desmin (+), SMA (–), S-100 (–) |
| 82 | Zhu et al. (44) | 55 | 2.0 | Prostate | 8 months with no recurrence | CD34 (+), desmin (–), S-100 (–) |
| 83 | Chen et al. (4) | 82 | 4.7 | Paratestis | 4 months with no recurrence | CD34 (+), desmin (+), S-100 (–), ER (–), PR (–) |
| 84 | Korecka et al. (45) | 11 | NA | Scrotum | Stable residual mass for 29 months | NA |
| 85 | Present case | 70 | 13.0 | Scrotum | 17 months with no recurrence | CD34 (+), desmin (+), S-100 (–), ER (+), PR (+) |

NA, not available.

# Case presentation

## Clinical findings

A 70-year-old man presented with a left scrotum mass that had been growing for the past 2 years. The mass was mobile, nonpainful, and had grown progressively larger over time. The patient was not febrile and did not present with frequent urination, urgency, pain, or hematuria. Magnetic resonance imaging (MRI) at another hospital revealed the shadow of a mass in the prostate and left scrotum. Considering the possibility of a malignant lesion, the patient visited our hospital for further diagnosis and treatment. During physical examination, a large, perineal mass approximately 15 cm in size with no obvious blood vessels on the surface was detected. MRI at our hospital revealed a well-capsulated mass protruding into the left scrotum in the left pelvis with a size of $13.2 \times 10.0 \times 4.3$ cm (Figure 1). In addition, an ill-defined mass was detected in the prostate, with a maximum cross-sectional area of $6.6 \times 5.5$ cm. The patient's total prostate-specific antigen level was 7.572 ng/ml (reference value = 0–4 ng/ml). Excisional biopsy of the scrotal mass was performed after needle biopsy revealed the mass as AAM. As the needle biopsy of the prostate revealed no malignant histological appearance, the patient was not initially treated with surgery.

## Pathological findings

The gross examination of the excisional biopsy revealed a grey–pink or grey–yellow mass measuring $13.0 \times 7.0 \times 5.5$ cm in volume, with a completely smooth capsule on the surface and soft and translucent texture in tissue sections (Figure 2A). Histologically, the tumor comprised spindle cells, myxoid matrix containing thick-walled vessels of varying sizes, and cordlike collagen fibers. The spindle cells were arranged in a wavy or parallel pattern, with no atypia or nuclear division (Figures 2B–D). Immunohistochemical staining revealed that the tumor cells were positive for vimentin, CD34 (Figure 3A), desmin (Figure 3B), estrogen receptor (ER) (Figure 3C), and progesterone receptor (PR) (Figure 3D) but negative for CK, SMA, and S-100. The tumor had a very low Ki-67 proliferation index of 1%. Based on the morphology and the immunological phenotype, the patient was diagnosed with AAM.

The hematoxylin and eosin staining of the prostate needle biopsy did not reveal prostate cancer (Supplementary Figure S1A-B), and immunohistochemical staining showed that the tumor was positive for P63 (Supplementary Figure S1C) and negative for P504S (Supplementary Figure S1D).

## Treatment and follow-up

The patient was treated surgically. First, left arc-shaped incision of the perineum was performed, the perineal skin

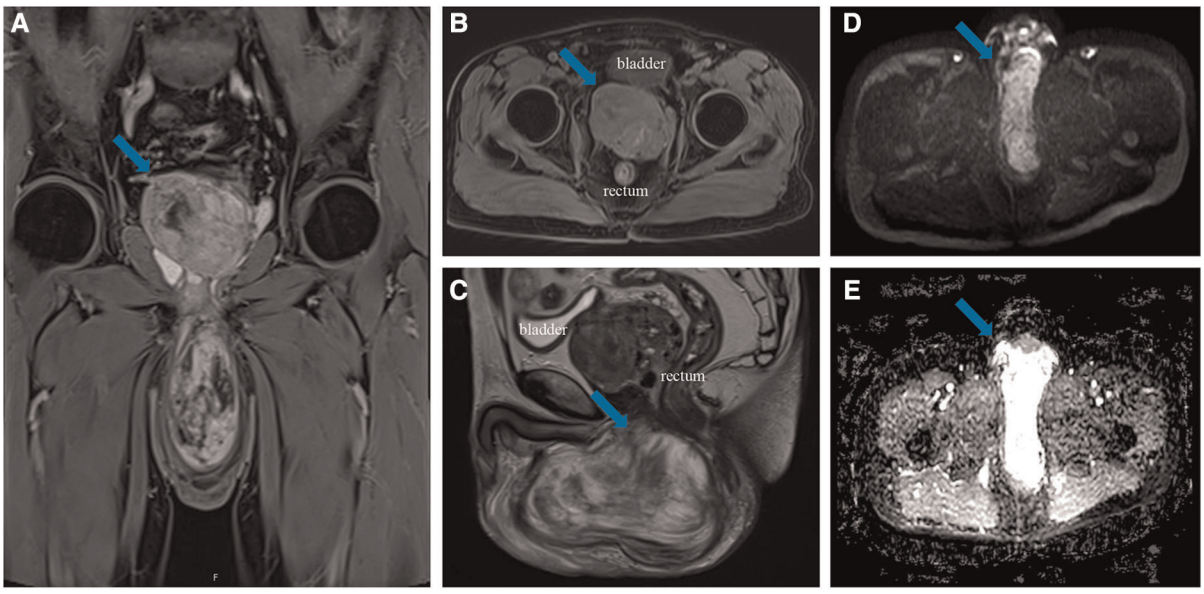


FIGURE 1
(A) coronal (weighted-sequence T1), (B) axial (weighted-sequence T1), (C) sagittal (weighted-sequence T2), (D) axial (DWI), and (E) axial (ADC) MRI reveal a well-capsulated mass protruding into the left scrotum in the left pelvis (arrows). $ADC_{mean}$ value = $2.16 \times 10^{-3}$ $mm^2/s$. MRI, magnetic resonance imaging; DWI, diffusion-weighted imaging; ADC, apparent diffusion coefficient.

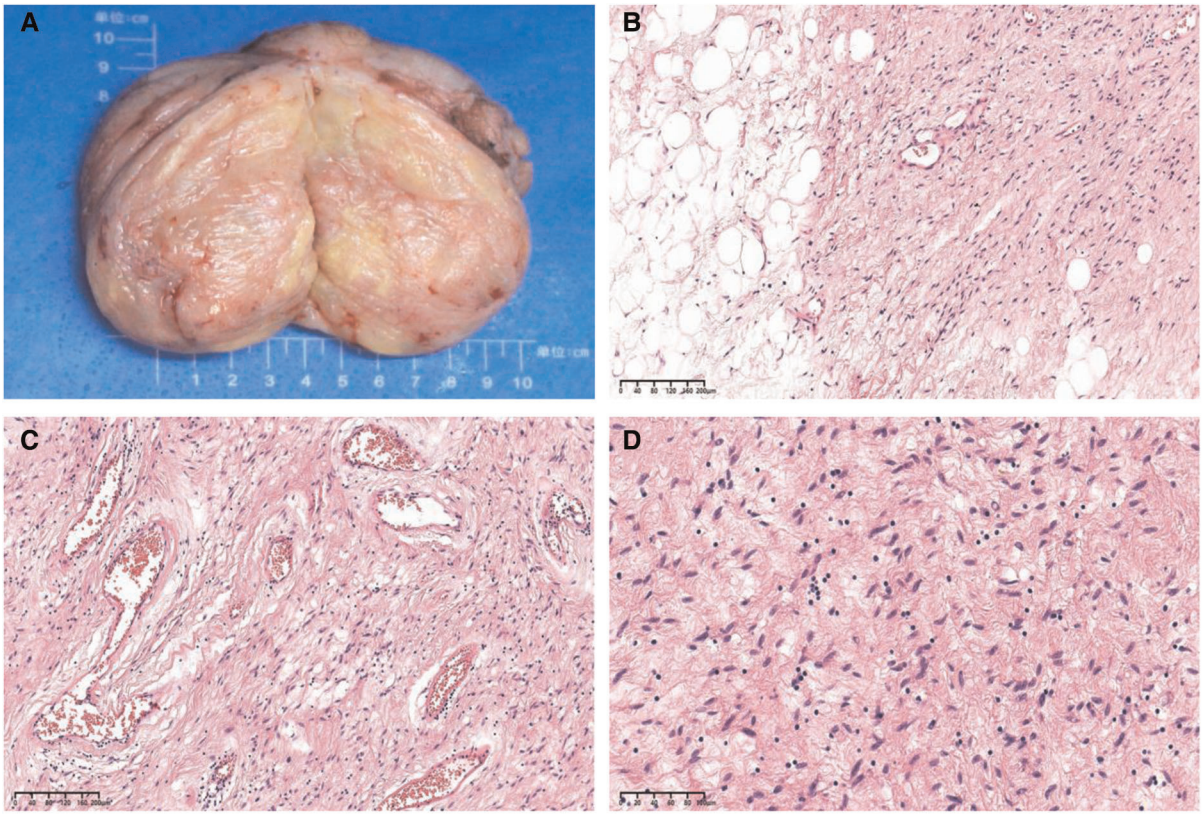


FIGURE 2
(A) A grey–pink or grey–yellow, well-circumscribed, solid mass measuring 13.0 × 7.0 × 5.5 cm. (B) Microscopic sections demonstrate a spindle cell tumor entrapping the adipose tissue (hematoxylin and eosin [H&E] stain, ×100 magnification). (C) The tumor comprises spindle cells in a loose myxoid matrix containing irregular, variably sized blood vessels and cordlike collagen fibers (H&E stain, ×100 magnification). (D) The tumor cells are eosinophilic, small, and spindle shaped, with slightly deep staining and stellate nuclei (H&E stain, ×200 magnification).

and muscles were dissected according to the anatomical level and the superficial perineal fascia was dissected. The scrotal mass was located below the urogenital diaphragm (The superior fascia of the urogenital diaphragm is adjacent to the prostate, and the inferior fascia is adjacent to the bulbar corpus cavernosum) and clearly demarcated from the surrounding tissue. The scrotal mass was then surgically removed with clear margins. A needle biopsy of the prostate was also performed intraoperatively. The patient was postoperatively followed-up for 17 months; no recurrence or metastasis has been detected.

## Discussion

AAM was first described as a separate histopathological entity by Steeper and Rosai in 1983. Considering its benign nature, the term "aggressive" was modified to "deep" in the fourth edition of the *World Health Organization Classification of Soft Tissue Tumors* in 2013 (4). In men, only case reports or case series have been reported in literature. The available cases reported in males are described in **Table 1** (4, 6–45). These men aged from 9 months to 82 years, with an average age of 49 years. The most common sites were the pelvis and genital areas, particularly the scrotum. Six tumors have been reported in the head and neck area, four in the engrafted kidney or urinary tract, three in the prostate, two in the alimentary tract, two in the lower limbs, one in the axillary region, one in the buttock, and one in the claviculate. Most of these patients were usually asymptomatic, whereas a small number of patients presented with inguinal hernia and testicular tumors. In the present case, the tumor developed in the scrotum and presented as a gradually increasing mass with no typical clinical symptoms.

Most tumors in the reviewed cases were >10 cm in size as AAMs are not easily detected early. The largest tumors found in women and men, respectively, were 60 and 28 cm in size (42, 43). Most tumors are ill defined, making complete resection difficult and resulting in frequent local recurrence. However, few tumors demonstrate partial or complete encapsulation. In most cases, the cut surface was smooth, homogeneous, soft, and gray, with few firm and cystic types

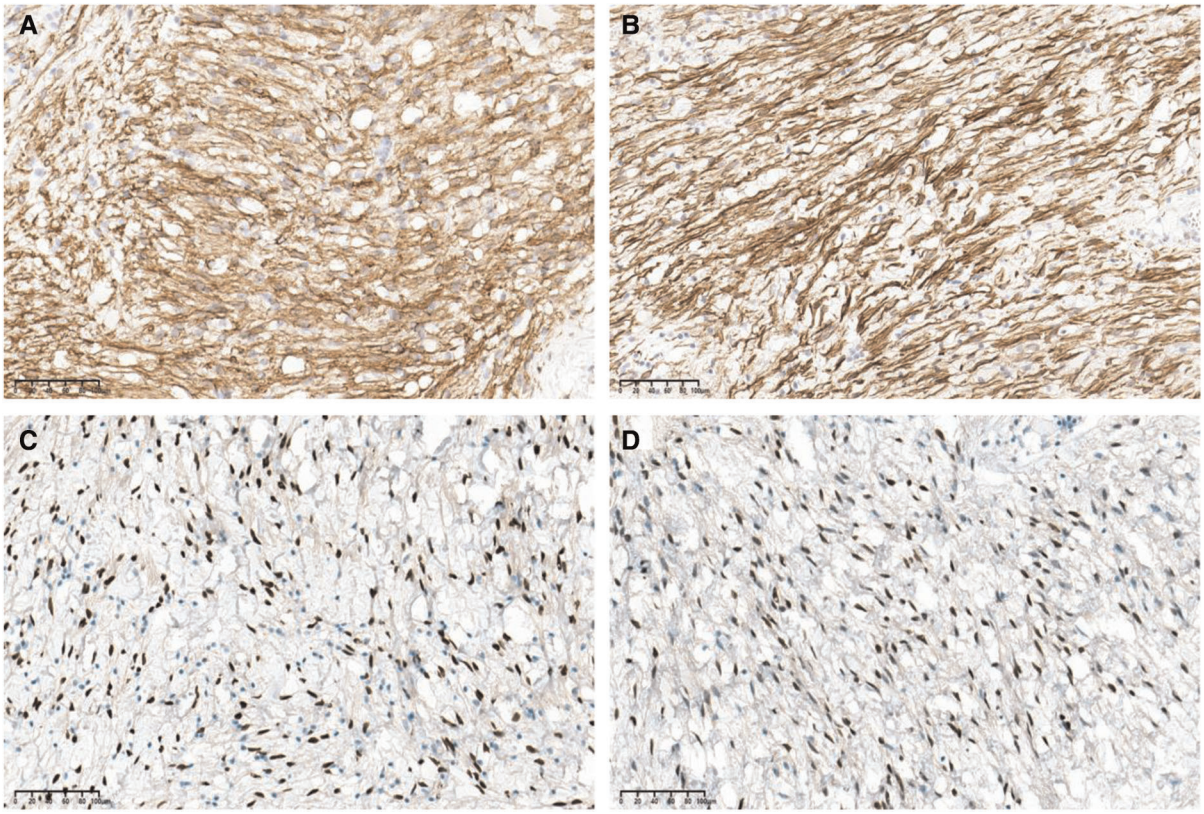


FIGURE 3
The tumor cells are positive for (A) CD34, (B) desmin, (C) estrogen receptor (ER), and (D) progesterone receptor (PR) (immunohistochemical stain, ×200 magnification).

(6). In the present case, the tumor was completely encapsulated, with a maximum diameter of 13 cm, and had a smooth, gray, soft cut surface.

Misdiagnosis in AAM is common because it can mimic other diseases, including hydrocele, inguinal hernia, or paratesticular neoplasia (4). Preoperative diagnosis is often difficult and challenging because of the rarity of these tumors and lack of specific imaging features (44). AAM is diagnosed based on the histopathological examination of postoperative specimens. The histopathological features of males with AAM reported in literature are similar to those reported in classical female cases. Microscopically, AAM comprises small-sized spindle cells or stellate cells embedded in a loose myxoid matrix with abundant collagen fibers and variably sized vessels. Blood vessels ranging from capillary-like to thick-walled vessels, which are the most prominent feature of AAM, can be observed (46). In the present case, no evidence of atypical mitotic activity or nuclear atypia was noted. While hypercellularity, cytological atypia, abundant fibrosclerotic stroma, and increased vascularity have been reported in recurrent cases (2), in the present case, the classical morphology was found. Immunohistochemical staining plays a crucial role in the diagnosis of AAM, although there is no specific immunohistochemical marker of AAM. The neoplastic cells of AAM are generally positive for desmin, vimentin, SMA, CD34, ER, and PR but negative for S-100 and CK in female patients (47). Previous studies have shown that ER and PR stains are generally negative in males with AAM compared with females (37). However, in some cases (including the present case), ER and PR may be expressed on AAM tumor, which may provide a hormonal therapeutic option (6). It is worth noting that the relationship of AAM with hormone receptor expression in males has not been well described, and more research is needed in the future. More recently, high mobility group A protein 2 (HMGA2) was revealed as a sensitive but not specific novel marker for AAM diagnosis (48). While nuclear staining can be useful in cases where cytoplasmic staining is nonspecific and of no diagnostic importance (49), the present case was diagnosed without HMGA2 staining considering the typical morphology of the tumor.

AAM should be distinguished from angiomyofibroblastoma, myxoid liposarcoma, myxoma, superficial angiomyxoma, and myxoid neurofibroma. Angiomyofibroblastoma is a benign

tumor that has recently been described as histologically similar to AAM, with myofibroblastic cells clustered in abundant myxoid stroma. This tumor contains several areas of hypo- and hypercellular cells, often clustered around blood vessels. Another key histological feature of angiomyofibroblastoma is the presence of multinucleated giant cells (50). Myxoid liposarcoma must be considered as a differential diagnosis when tumor cells infiltrate adipose tissues. It can be easily distinguished from AAM as myxoid liposarcoma is marked with adipocytes set in abundant thin-walled vessels. Myxoma, a benign tumor of the extremities, is characterized by an abundance of myxoid stroma and benign spindle and stellate cells surrounded by small blood vessels (and not blood vessels of different sizes). Superficial angiomyxoma, also known as cutaneous myxoma, usually occurs in the skin of nongenital areas. Histologically, the tumor lacks thick-walled vessels and the myxoid areas can form pools. With respect to the immunophenotype, ER and PR are generally not expressed but S-100 may be expressed in superficial angiomyxoma (51). Myxoid neurofibroma is another AAM-resembling myxoid tumor that commonly occurs in the extremities; however, the clusters of wavy nerve tumor cells are usually strongly S-100 positive.

The surgical removal of AAM with clear margins is the traditional treatment to prevent local recurrence. However, it is not clear whether the recurrence rate is associated with the surgical margin status (52). In women, the recurrence rates of 71%, 85%, and 94% have been observed within the first 3, 5, and 7 years of local excision, respectively (53). As shown in **Table 1**, 79 of the 85 male patients were followed-up after surgery, and the data revealed only 4 recurrences (4.7%), excluding 2 deaths (one died intraoperatively and one died because of pulmonary tuberculosis). The patients with recurrence were treated with wide excision, and the procedures were performed 9 months to 7 years after first surgery. Possible reasons for the lower local recurrence rate in male patients are sample limitations or lower hormone expression. It is generally known that AAM has no metastatic tendency; however, two female patients (aged 63 and 27 years) showed metastasis to the lung (54, 55). By contrast, as expected, no metastatic cases have been reported in males. Moreover, owing to the low proliferative activity of AAM, the role of radiotherapy and chemotherapy is unclear and limited. In recent years, hormonal therapy has been considered an adjunctive treatment for ER and/or PR positive female patients with primary large mass or local relapse that is not amenable to surgery (56). Unfortunately, it is not clear whether the relapse rate is higher when hormone therapy is discontinued (57). In the present case, only local resection was performed, and although the patient was both ER and PR positive, hormonal therapy was not advised as few data are available on hormonal therapy in male patients with AAM. Long-term follow-up surveillance is required because of the aggression and relapse characteristics of this tumor. At present, the patient has been followed-up for 17 months without any recurrence or metastasis.

## Conclusion

In summary, a rare case of scrotal AAM was reported and previously reported male cases with AAM were summarized. In particular, the review revealed that the clinicopathological characteristics of AAM in men are similar to those of AAM in women, including the expression of ER and PR. This provides an opportunity to treat such male patients with hormone therapy. Moreover, the literature review revealed a low recurrence rate (4.7%) in males after the surgical excision of the tumor; however, more data are needed to confirm this observation. Finally, AAM should be distinguished from myxoid neoplasms in male genital areas.

## Data availability statement

The original contributions presented in the study are included in the article/Supplementary Material, further inquiries can be directed to the corresponding author/s.

## Ethics statement

Written informed consent was obtained from the individual(s) for the publication of any potentially identifiable images or data included in this article.

## Author contributions

C-KY: conceptualization. Y-PW and HC: data curation. YC: investigation, validation, and writing of the original draft. All authors contributed to the article and approved the submitted version.

## Conflict of interest

The authors declare that the research was conducted in the absence of any commercial or financial relationships that could be construed as a potential conflict of interest.

## Publisher's note

All claims expressed in this article are solely those of the authors and do not necessarily represent those of

their affiliated organizations, or those of the publisher, the editors and the reviewers. Any product that may be evaluated in this article, or claim that may be made by its manufacturer, is not guaranteed or endorsed by the publisher.

## Supplementary material

The Supplementary Material for this article can be found online at: https://www.frontiersin.org/articles/10.3389/fsurg.2022.955655/full#supplementary-material.

## References

1. Altinmakas E, Dogan H, Temur M, Guneyli S. Incidentally detected perineal aggressive angiomyxoma in an asymptomatic patient with uterine leiomyomas. *J Obstet Gynaecol*. (2021) 41(7):1178–9. doi: 10.1080/01443615.2020.1849070

2. Magro G, Angelico G, Michal M, Broggi G, Zannoni GF, Covello R, et al. The wide morphological spectrum of deep (aggressive) angiomyxoma of the vulvo-vaginal region: a clinicopathologic study of 36 cases, including recurrent tumors. *Diagnostics (Basel)*. (2021) 11(8):1360. doi: 10.3390/diagnostics11081360

3. Kanao H, Aoki Y, Tanigawa T, Matoda M, Okamoto S, Nomura H, et al. En bloc resection of an aggressive angiomyxoma by a novel combination laparoscopic and open perineal approach. *J Minim Invasive Gynecol*. (2019) 26(4):598–9. doi: 10.1016/j.jmig.2018.07.008

4. Chen CF, Wang TY, Chen M, Lin YC. Rare paratesticular aggressive angiomyxoma mimicking an epididymal tumor in an 82-year-old man: case report. *Open Med (Wars)*. (2021) 16(1):973–7. doi: 10.1515/med-2021-0317

5. Riley DS, Barber MS, Kienle GS, Aronson JK, von Schoen-Angerer T, Tugwell P, et al. Care guidelines for case reports: explanation and elaboration document. *J Clin Epidemiol*. (2017) 89:218–35. doi: 10.1016/j.jclinepi.2017.04.026

6. Idrees MT, Hoch BL, Wang BY, Unger PD. Aggressive angiomyxoma of male genital region. Report of 4 cases with immunohistochemical evaluation including hormone receptor status. *Ann Diagn Pathol*. (2006) 10(4):197–204. doi: 10.1016/j.anndiagpath.2005.09.002

7. Hatano K, Tsujimoto Y, Ichimaru N, Miyagawa Y, Nonomura N, Okuyama A. Rare case of aggressive angiomyxoma presenting as a retrovesical tumor. *Int J Urol*. (2006) 13(7):1012–4. doi: 10.1016/j.urology.2020.05.028

8. Wu CC, Yang SS, Chin DT, Hsieh CH, Hsueh YM, Tsai YC. Scrotal aggressive angiomyxoma mimicking inguinal hernia. *Asian J Androl*. (2007) 9 (5):723–5. doi: 10.1111/j.1745-7262.2007.00286.x

9. Bothig R, Ahyai S, Kuhn K, Pramono S. Aggressive angiomyxoma in a male patient: a case report. *Aktuelle Urol*. (2008) 39(1):64–7. doi: 10.1055/s-2007-959216

10. Pai CY, Nieh S, Lee JC, Lo CP, Lee HS. Aggressive angiomyxoma of supraclavicular fossa: a case report. *Head Neck*. (2008) 30(6):821–4. doi: 10.1002/hed.20747

11. Heffernan EJ, Hayes MM, Alkubaidan FO, Clarkson PW, Munk PL. Aggressive angiomyxoma of the thigh. *Skeletal Radiol*. (2008) 37(7):673–8. doi: 10.1007/s00256-008-0465-0

12. Minagawa T, Matsushita K, Shimada R, Takayama H, Hiraga R, Uehara T, et al. Aggressive angiomyxoma mimicking inguinal hernia in a man. *Int J Clin Oncol*. (2009) 14(4):365–8. doi: 10.1007/s10147-008-0850-7

13. Sylvester DC, Kortequee S, Moor JW, Woodhead CJ, Maclennan KA. Aggressive angiomyxoma of larynx: case report and literature review. *J Laryngol Otol*. (2010) 124(7):793–5. doi: 10.1017/S0022215109992350

14. Morag R, Fridman E, Mor Y. Aggressive angiomyxoma of the scrotum mimicking huge hydrocele: case report and literature review. *Case Rep Med*. (2009) 2009:157624. doi: 10.1155/2009/157624

15. Plumb A, Shanks JH, Kochhar R. Development of aggressive angiomyxoma like tumour in a renal transplant. *Clin Radiol*. (2010) 65(5):423–6. doi: 10.1016/j.crad.2010.01.012

16. Sawada Y, Ito F, Nakazawa H, Tsushima N, Tomoe H, Aiba M. A rare benign genitourinary tumor in a Japanese male: urinary retention owing to aggressive angiomyxoma of the prostate. *Rare Tumors*. (2010) 2(1):e15. doi: 10.4081/rt.2010.e15

17. Bajaj MS, Mehta M, Kashyap S, Pushker N, Lohia P, Chawla B, et al. Clinical and pathologic profile of angiomyxomas of the orbit. *Ophthalmic Plast Reconstr Surg*. (2011) 27(2):76–80. doi: 10.1097/IOP.0b013e3181c53d53

18. Rocco F, Cozzi G, Spinelli MG, Rocco BM, Albo G, Finkelberg E, et al. Massive recurring angiomyxoma of the scrotum in a obese man. *Rare Tumors*. (2011) 3(3):e31. doi: 10.4081/rt.2011.e31

19. Mishulin A, Lever JF, Porter W, Servat JJ, Gladstone G, Black E. Aggressive glabellar angiomyxoma with orbital extension. *Orbit*. (2012) 31(5):361–3. doi: 10.3109/01676830.2012.710925

20. Nayal B, Rao L, Rao AC, Sharma S, Shenoy R. Extragenital aggressive angiomyxoma of the axilla and the chest wall. *J Clin Diagn Res*. (2013) 7 (4):718–20. doi: 10.7860/JCDR/2013/5458.2891

21. Gaunay GS, Barazani Y, Kagen AC, Stember DS. Aggressive angiomyxoma of the scrotum. *Clin Imaging*. (2013) 37(6):1122–4. doi: 10.1016/j.clinimag.2013.06.007

22. Karwacki GM, Stockli M, Kettelhack C, Mengiardi B, Studler U. Radiographic diagnosis and differentiation of an aggressive angiomyxoma in a male patient. *J Radiol Case Rep*. (2013) 7(7):1–6. doi: 10.3941/jrcr.v7i7.1154

23. Saha K, Sarkar S, Jash D, Chatterjee S, Saha AK. Aggressive angiomyxoma of greater omentum with pleural effusion in a young male. *J Cancer Res Ther*. (2014) 10(2):371–3. doi: 10.4103/0973-1482.136661

24. Wang Z, Liu Y, Yang L, Gu L, He Y, Huang D, et al. Maxillary aggressive angiomyxoma showing ineffective to radiotherapy: a rare case report and review of literature. *Int J Clin Exp Pathol*. (2015) 8(1):1063–7. PMID: 25755820

25. Caruso F, Terrier P, Bonvalot S. Lessons from an aggressive angiomyxoma unrecognized and treated as rectal prolapse. *Int J Colorectal Dis*. (2015) 30 (7):993–4. doi: 10.1007/s00384-014-2084-7

26. Wang Z, Wei YB, Yin Z, Yan B, Li D, Zhou KQ, et al. Diagnosis and management of scrotal superficial angiomyxoma with the aid of a scrotoscope: case report and literature review. *Clin Genitourin Cancer*. (2015) 13(4):e311–e3. doi: 10.1016/j.clgc.2014.11.009

27. Smith HG, Thway K, Messiou C, Barton DP, Thomas JM, Hayes AJ, et al. Selective marginal resections in the management of aggressive angiomyxomas. *J Surg Oncol*. (2016) 114(7):828–32. doi: 10.1002/jso.24420

28. Draeger DL, Protzel C, Hakenberg OW. Aggressive angiomyxoma as a rare differential diagnosis of enlargement of the scrotum. *Clin Genitourin Cancer*. (2016) 14(2):e237–9. doi: 10.1016/j.clgc.2015.12.022

29. Ahmed MAM, Uehelie MA, Rage AMA, Mohey A, Noureldin YA. Aggressive angiomyxoma of the penis: the first case report in a 9-month-old infant. *Urology*. (2017) 104:187–90. doi: 10.1016/j.urology.2016.12.045

30. Sharma N, Tomar TS, Mathew AP, Chandramohan K, Preethi R, Mony RP. Aggressive angiomyxoma of inguinoscrotal region mimicking inguinal hernia: a case report. *Indian J Surg*. (2017) 79(6):571–3. doi: 10.1007/s12262-017-1659-2

31. Gorsi U, Naranje P, Rathi M, Nada R, Khandelwal N. Aggressive angiomyxoma of transplanted kidney mimicking posttransplant lymphoproliferative disorder. *Saudi J Kidney Dis Transpl*. (2017) 28(2):425–7. doi: 10.4103/1319-2442.202778

32. Damodaran S, Gengan D, Walling ST. Aggressive angiomyxoma involving penis and urethra - a case report. *Urol Case Rep*. (2017) 13:110–2. doi: 10.1016/j.eucr.2017.03.019

33. Ismail MI, Wong YP, Tan GH, Fam XI. Paratesticular aggressive angiomyxoma: a rare case. *Urol Ann*. (2017) 9(2):197–9. doi: 10.4103/UA.UA_168_16

34. Aydin AM, Katipoglu K, Baydar DE, Bilen CY. Long-standing aggressive angiomyxoma as a paratesticular mass: a case report and review of literature. *SAGE Open Med Case Rep*. (2017) 5:2050313X17712090. doi: 10.1177/2050313X17712090

35. Umranikar S, Ubee S, Williams G. Aggressive angiomyxoma of the perineum: a rare presentation in a male with 4 years follow up. *J Surg Case Rep*. (2017) 2017(8):rjx086. doi: 10.1093/jscr/rjx086

36. Hsieh F, Chuang KT, Wu YT, Lin CH. Aggressive angiomyxoma-report of a rare male buttock lesion. *Plast Reconstr Surg Glob Open*. (2018) 6(8):e1879. doi: 10.1097/GOX.0000000000001879

37. Neyaz A, Husain N, Anand N, Srivastava P. Rare paratesticular aggressive angiomyxoma with negative oestrogen and progesterone receptors in a male patient. *BMJ Case Rep*. (2018) 2018:bcr2017222164. doi: 10.1136/bcr-2017-222164

38. Serao A, Tiranti D, Ferraro M, Malinaric R, Re P, Calamaro P. Incidental finding of paratesticular aggressive angiomyxoma in a 72-year-old monorchid male. *Urologia*. (2020) 87(4):194–8. doi: 10.1177/0391560319881082

39. Addesso M, Caputo A, D'Antonio A, Napodano G, Sanseverino R. A large paraprostatic mass in a man: rare presentation of aggressive angiomyxoma. *Urology*. (2020) 143:e3–4. doi: 10.1016/j.urology.2020.06.014

40. Kirkilessis G, Kakavia K, Bougiouklis D, Papadopoulos A, Lampropoulos C, Kirkilessis I. Aggressive angiomyxoma to 57-year old man. *J Surg Case Rep*. (2020) 2020(9):rjaa313. doi: 10.1093/jscr/rjaa313

41. Liu M, Zhai TS, Zhao XF, Feng LJ, Lyu XS, Hu LT, et al. Incidental para-ureteral aggressive angiomyxoma: a rare case report and literature review. *BMC Urol*. (2020) 20(1):182. doi: 10.1186/s12894-020-00755-7

42. Majumdar SK, Hussain M, Raha A, Barman S. "Gigantic aggressive angiomyxoma" of the jaws: a rare case report. *J Oral Maxillofac Pathol*. (2021) 25(1):205. doi: 10.4103/jomfp.JOMFP_233_20

43. Celik SU, Hesimov I, Kutlu B, Erkek AB. Aggressive angiomyxoma: a rare tumor of male pelvic cavity. *Acta Med Port*. (2018) 31(11):693–6. doi: 10.20344/amp.9062

44. Zhu Z, Yan J, Tang G. Aggressive angiomyxoma of the prostate: a case report. *Medicine (Baltimore)*. (2018) 97(51):e13716. doi: 10.1097/MD.0000000000013716

45. Korecka KK, Hyla-Klekot LE, Kudela GP, Palen PA, Kajor MW, Koszutski TK. Aggressive angiomyxoma in an 11-year-old boy - diagnostic and therapeutic dilemmas: an unusual case report and review of the literature. *Urology*. (2020) 144:205–7. doi: 10.1016/j.urology.2020.05.028

46. Xu H, Sun P, Xu R, Wang L, Shi Y. Aggressive angiomyxoma in pregnancy: a case report and literature review. *J Int Med Res*. (2020) 48(7):300060520936414. doi: 10.1177/0300060520936414

47. Xie Y, Qian Y, Zou B. A giant aggressive angiomyxoma of vulva in a young woman: a case report. *Medicine (Baltimore)*. (2019) 98(2):e13860. doi: 10.1097/MD.0000000000013860

48. Harkness R, McCluggage WG. Hmga2 is a useful marker of vulvovaginal aggressive angiomyxoma but may be positive in other mesenchymal lesions at this site. *Int J Gynecol Pathol*. (2021) 40(2):185–9. doi: 10.1097/PGP.0000000000000068

49. McCluggage WG, Connolly L, McBride HA. Hmga2 is a sensitive but not specific immunohistochemical marker of vulvovaginal aggressive angiomyxoma. *Am J Surg Pathol*. (2010) 34(7):1037–42. doi: 10.1097/PAS.0b013e3181e32a11

50. Sutton BJ, Laudadio J. Aggressive angiomyxoma. *Arch Pathol Lab Med*. (2012) 136(2):217–21. doi: 10.5858/arpa.2011-0056-RS

51. McCluggage WG. A review and update of morphologically bland vulvovaginal mesenchymal lesions. *Int J Gynecol Pathol*. (2005) 24(1):26–38. PMID: 15626915

52. Chan YM, Hon E, Ngai SW, Ng TY, Wong LC. Aggressive angiomyxoma in females: is radical resection the only option? *Acta Obstet Gynecol Scand*. (2000) 79 (3):216–20. PMID: 10716303

53. Zou R, Xu H, Shi Y, Wang J, Wang S, Zhu L. Retrospective analysis of clinicopathological features and prognosis for aggressive angiomyxoma of 27 cases in a tertiary center: a 14-year survey and related literature review. *Arch Gynecol Obstet*. (2020) 302(1):219–29. doi: 10.1007/s00404-020-05592-5

54. Siassi RM, Papadopoulos T, Matzel KE. Metastasizing aggressive angiomyxoma. *N Engl J Med*. (1999) 341(23):1772. doi: 10.1056/NEJM199912023412315

55. Blandamura S, Cruz J, Vergara LF, Puerto IM, Ninfo V. Aggressive angiomyxoma: a second case of metastasis with patient's death. *Hum Pathol*. (2003) 34(10):1072–4. doi: 10.1016/S0046-8177(03)00419-2

56. Pannier D, Cordoba A, Ryckewaert T, Robin Y-M, Penel N. Hormonal therapies in uterine sarcomas, aggressive angiomyxoma, and desmoid-type fibromatosis. *Crit Rev Oncol Hematol*. (2019) 143:62–6. doi: 10.1016/j.critrevonc.2019.08.007

57. Song M, Glasgow M, Murugan P, Rivard C. Aggressive angiomyxoma of the vulva and bladder. *Obstet Gynecol*. (2017) 130(4):885–8. doi: 10.1097/aog.0000000000002254

frontiers | Frontiers in Oncology

TYPE Case Report
PUBLISHED 02 November 2022
DOI 10.3389/fonc.2022.1035058



OPEN ACCESS

EDITED BY
Riccardo Bertolo,
Hospital San Carlo di Nancy, Italy

REVIEWED BY
Giovanna Riccipetitoni,
San Matteo Hospital Foundation (IRCCS), Italy
Stacey Schutte,
University of Cincinnati, United States

*CORRESPONDENCE
Qiong Luo
luoq@zju.edu.cn
Baihui Zhao
zhaobh@zju.edu.cn

†These authors have contributed equally to this work and share first authorship

SPECIALTY SECTION
This article was submitted to Surgical Oncology, a section of the journal Frontiers in Oncology

RECEIVED 02 September 2022
ACCEPTED 19 October 2022
PUBLISHED 02 November 2022

CITATION
Ding Y, Yang M, Lv M, Jiang Y, Dong T, Zhao B and Luo Q (2022) The ex-utero intrapartum treatment (EXIT) strategy for fetal giant sacrococcygeal teratoma with cardiac insufficiency: A case report and review of the literature. *Front. Oncol.* 12:1035058. doi: 10.3389/fonc.2022.1035058



# The ex-utero intrapartum treatment (EXIT) strategy for fetal giant sacrococcygeal teratoma with cardiac insufficiency: A case report and review of the literature

Yunping Ding†, Mengmeng Yang†, Min Lv, Ying Jiang, Tian Dong, Baihui Zhao* and Qiong Luo*

Department of Obstetrics, Women's Hospital, Zhejiang University School of Medicine, Hangzhou, China

**Background:** Antenatally diagnosed sacrococcygeal teratoma has been associated with risks of perinatal complications and death, especially when the foetus has symptoms of cardiac insufficiency, hydrops or anemia *in utero*; however, the method of intervention remains controversial.

**Case:** A 25-year-old pregnant woman was found to have a cystic and solid tumor in the fetal sacrococcygeal region at 16 weeks of gestation. As the tumour grew, the mother developed polyhydramnios accompanied with gestational diabetes. Fetal and tumorous hemodynamics were closely monitored by ultrasound. Abnormal cardiac function was detected at 31 weeks' gestation, and we creatively performed pre-emptive delivery through the ex-utero intrapartum treatment with debulking. The teratoma was removed with utero-placental circulation support. The operation proceeded smoothly with favourable prognosis for both mother and newborn.

**Conclusion:** The ex-utero intrapartum treatment may improve the prognosis for fetuses with heart failure when they reach viable gestation.

KEYWORDS

**ex-utero intrapartum treatment (EXIT), sacrococcygeal teratoma (SCT), cardiac insufficiency, fetal tumor, prenatal diagnosis**

## Introduction

Sacrococcygeal teratoma (SCT) is the most common congenital tumour in fetuses and neonates, with an incidence of 1 in 40,000 live births (1). SCT diagnosed postnatally has been associated with an excellent prognosis after surgical excision. In contrast,the mortality excluding terminations in the fetuses with prenatally diagnosed SCT ranges between 35% and 62%, furthermore, for fetuses with tumor volume to fetal weight ratio(TFR) >0.12 prior to 24 weeks gestation, more than 80% of them have poor prognosis (2–4), especially in fetuses with large tumours, rapid growth, and rich blood flow, is still related to a high risk of death.

The two main pathophysiological mechanisms of perinatal death in fetal SCT are the mass effect of the tumour, which can result in preterm delivery or tumor rupture either prior to or at the time of delivery, and the tumour vascular steal phenomenon, which can lead to anaemia and high-output cardiac failure caused by compensatory hypervolemia (5, 6). High-output failure is a more common perinatal complication in clinical practice, which may cause polyhydramnios, hydrops, intrauterine fetal demise and preterm birth.

As a result, to avoid these risks, different surgical approaches have been attempted including open fetal surgery and various minimally invasive therapies, which we will elaborate later in the literature review and discussion. All are aimed at interrupting tumor perfusion, slowing tumor growth and halting or reversing hydrops progression to get good outcomes. If fetal heart failure occurs after viability, early delivery and timely surgery may be the best option to avoid intrauterine death.

The aim of this paper is to demonstrate that a multidisciplinary approach to these tumours with close ultrasound monitoring and timely termination of pregnancy through ex-utero intrapartum treatment(EXIT) may bring positive outcomes for both mother and infant. And also we reviewd the literature regarding therapeutic options in order to assist obstetricians with the reasonable follow-up planning and decision making for achieving a good prognosis for these rare high-risk tumours.

## Case presentation

The case was a 25-year-old woman, gravida 2, para 0, with a spontaneous abortion 3 years previously. She had no family history of birth defects or genetic disorders, and she had no alcohol or smoking habits. She had a normal first trimester scan at 12 weeks; however, a sonographic examination revealed a 32 × 22 × 33 mm exophytic, mixed echogenic mass arising from the sacrococcygeal region at 16 weeks. The inner solid size was approximately 23 × 23 × 16 mm, with high vascularization seen on Doppler flow. No other abnormalities were detected, and non-invasive prenatal testing was at low risk. The parents requested to continue the pregnancy after being extensively counselled by our antenatal diagnostic centre regarding the diagnosis, treatment, and prognosis of high-risk SCT. The tumour grew in parallel with the foetus, measuring 107 × 106 × 93 mm and with polyhydramnios (amniotic fluid index 25.4) appearing at 24 weeks. Furthermore, the mother developed gestational diabetes with no other symptoms. Magnetic resonance imaging was performed at 27 weeks (Figure 1). There was no evidence of possible invasion to the foetal pelvis or abdomen. The intact spine, foetal kidneys, and bladder were normal. Based on the MRI findings, a diagnosis of type I in the Altman classification was confirmed.

The gradual growth of the SCT was identified by weekly or biweekly sonography, with no signs of foetal cardiac failure until 31 weeks and one day, and the foetal echocardiogram showed that the combined cardiac output increased to 679 ml/kg/min, accompanied by an enlarged cardiothoracic ratio and a full dilation of the inferior vena cava. Multiple large blood vessels arising from the middle sacral artery were supplying the teratoma. Doppler ultrasound, echocardiography and MRI findings are recorded in Table 1. Fortunately, the middle cerebral artery-peak systolic velocity(MCA-PSV) was in normal state all the time. Considering the possibility of foetal heart failure, we conducted a multidisciplinary consultation to avoid irreversible complications in succession. Thus, a premature caesarean section and EXIT procedure were scheduled at 32 weeks' gestation.

A multidisciplinary team, including obstetricians, anaesthesiologists, neonatologists, and assistant nurses, was organised for the procedure. After combined epidural and general anesthesia with sevoflurane inhalation was administered as the primary anaesthetic technique, laparotomy was performed with a classic Pfannenstiel approach considering the posterior placenta. The uterine incisions were clamped to reduce bleeding. Once the foetal head and neck were exposed, the uterine cavity was filled continuously with warm physiological saline solution to maintain an adequate uterine volume to avoid placental abruption and compression of the umbilical cord (Figures 2A, B). Meanwhile, IV nitroglycerin (NTG) was used to keep the uterus adequately relaxed. Amniotic fluid was slowly released, and the foetus was slowly delivered (Figure 2C). The placental circulation was maintained for a total of 32 min until the intact teratoma was excised without rupture (Figure 2D). Foetal health signs were stable through $SpO_2$ monitoring and foetal ultrasonography during the entire operation. The newborn was then transferred to the neonatal operating table for further suturing and evaluation. The maternal perioperative blood loss was 700 mL, and gauze filled in uterus was removed after 24h to prevent postpartum atony and haemorrhage.

A male infant was born with an SCT of 200 mm in diameter. The weight of the baby was 2200 g, and the teratoma weighed 2065 g. His Apgar score was 8-8. On account of premature delivery, the baby was discharged 19 days after birth with normal MRI results of the abdomen, cerebrum, and kidneys. During the

10.3389/fonc.2022.1035058

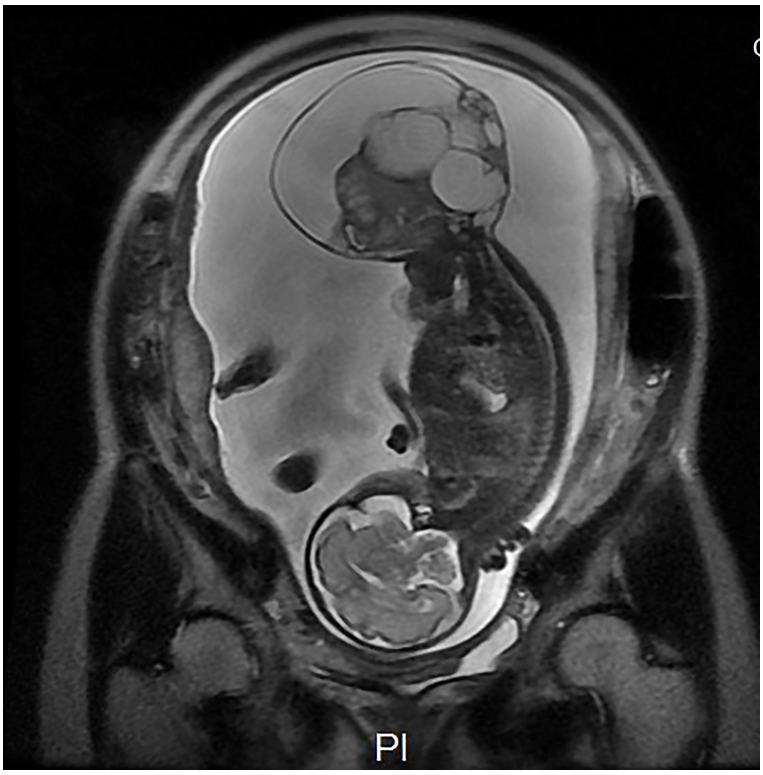


FIGURE 1
Magnetic resonance imaging was performed at 27 weeks. There was no evidence of possible invasion to the foetal pelvis or abdomen. The intact spine, foetal kidneys, and bladder were normal. A diagnosis of type I in the Altman classification was confirmed. Ax DWI b = 600.

TABLE 1 Measurements in the case.

| EGA weeks | Mass volume ml | AFIcm | CCO ml/kg/min | cardiothoracic ratio | Tei index of the left ventricle | Tei index of the right ventricle | S/D ratio | Study |
|---|---|---|---|---|---|---|---|---|
| 16 2/7 | 11.6 | 10.3 | - | - | - | - | - | US |
| 20 3/7 | 39.8 | 15.4 | - | - | - | - | 3.5 | US |
| 24 | 527.4 | 25.4 | 462 | 0.46 | 0.32 | 0.33 | 2.9 | US +echo |
| 26 3/7 | 792.5 | 25.1 | - | - | - | - | 3.2 | US |
| 27 | 824.5 | 10.9 (AFV) | - | - | - | - | - | MR |
| 28 5/7 | 1288.6 | 32.2 | 537 | 0.45 | - | - | 2.3 | US +echo |
| 31 1/7 | 1384.8 | 35.4 | 679 | 0.50 | 0.28 | 0.22 | 4.5 | US +echo |
| 32 | 1413.2 | 33.5 | 705 | 0.52 | 0.38 | 0.43 | 4.7 | US +echo |

EGA, Estimated gestational age; AFI, amniotic fluid index.
CCO, combined cardiac output ; S/D, systolic/diastolic ratio.
AFV, amniotic fluid volume; MR, magnetic resonance.
US, ultrasonography; ech, fetal echocardiography.

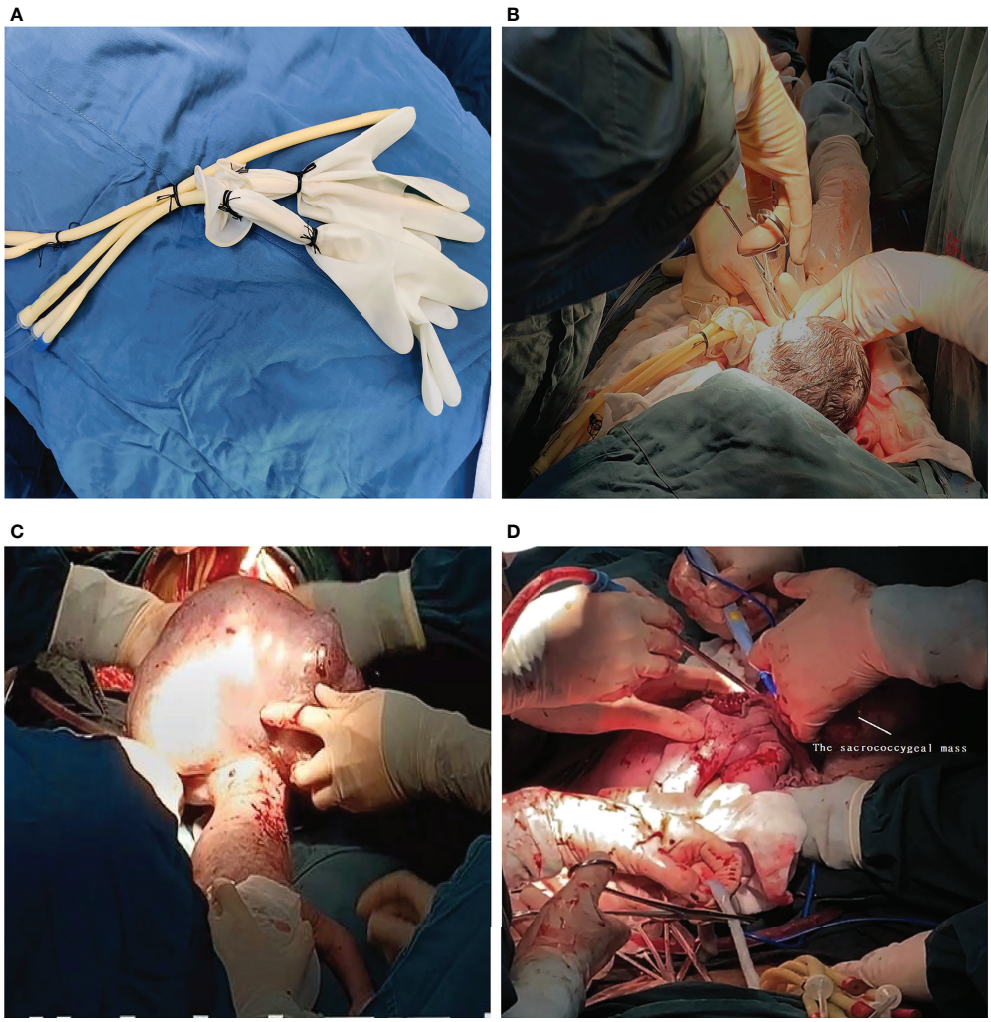


FIGURE 2
**(A)** The simple homemade balloon. **(B)** Once the foetal head and neck were exposed, the uterine cavity was filled with a homemade balloon continuously infused with warm physiological saline solution. **(C)** The newborn in posterior view with the presence of the sacrococcygeal mass during the EXIT. **(D)** The placental circulation was maintained for a total of 32 min until the intact teratoma was excised without rupture. The umbilical cord was cut immediately upon completion of the tumor debulking procedure.

hospital stay, the baby's condition was stable, and there were no tumour-related complications. Pathological findings revealed an immature teratoma and no malignant elements. Comfortingly, he showed normal development with good heart function and no postoperative complications within 18 months. His mother also did not suffer from postpartum bleeding or infection, and she was discharged without any complications.

## Literature review

With institutional approval, we described our experience with operative treatment in a fetus with large cystic solid SCT and cardiovascular compromise, and reviewed the literature about the perinatal management and postnatal outcomes for fetus with prenatally diagnosed sacrococcygeal teratoma with cardiac insufficiency. We used a list of keywords: (fetal OR prenatal OR antenatal OR fetus) AND (sacrococcygeal teratoma OR sacro-coccygeal teratoma OR SCT) to search the Medline and Cochrane Library computer databases from 2000 to 2020. Only articles in English and cases of neonates or infants with abnormity in hemodynamics were included. The treatment procedure followed ethical principles and approval was obtained from the Institutional Review Board. Written informed consent was obtained from the couple before the procedure and manuscript publication.

TABLE 2 Overview of literature review of SCT with cardiac insufficiency.

| Reference | Cases | Diagnosis GA | Intervention GA | Interventionmethod | Histology | Outcome | Comments |
|---|---|---|---|---|---|---|---|
| Graf et al. (7) | 1 | 17 | 23 | In utero SCT resection | immature with few malignant yolk sac elements | survived | Cesarean section at 28 weeks' gestation due to uncontrollable preterm birth |
| Den Otter (11) | 1 | 27 | 27 | Surgical tumor resection on the second day of life | partly mature and partly immature | survived | Defecation problems developed after 2 months. A second resection of remnants of the SCT took place. |
| Roybal et al. (8) | 8 | 18-28 | 26-31 | Four underwent SCT resection;<br>One EXIT | two immature; two mature; no data for the rest | five NND; three survived | The only surviving patient delivered before 28 weeks underwent an EXIT procedure. |
| Goto et al. (9) | 1 | 23 | 27 | Underwent SCT resection | immature | NND | The day after birth the baby suffered non-resuscitable cardiac and pulmonary arrest. |
| Van Mieghem et al. (10) | 5 | 17-26 | 17-26 | RFA; superficial laser; interstitial laser | two immature; no data for the rest | one NND, two IUFD, two survived | Three cases resulted in preterm labor within 10 days of surgery. One neonate died. Two survived had long-term morbidity related to prematurity. |
| Baumgarten et al. (12) | 11 | 19-30 | 27-32 | Four underwent debulking and complete resection at 2 months;<br>Five complete resection after delivery; | no data | two NND nine survived | One death was due to severe pulmonary hypoplasia;<br>The second death was due to in utero tumor rup-ture;<br>One patient required additional surgery due to residual tumor, and another required additional surgery for a persistent urogenital sinus. |
| Present case | 1 | 16 | 32 | EXIT | Immature | survived | He has reached all age-appropriate neurodevelopmental and motor milestones. |

GA, gestational age; IUFD, intrauterine fetal death; NND, neonatal death; RFA, radiofrequency ablation.

There are 6 published articles of SCT with operative treatment for fetal giant sacrococcygeal teratoma with cardiac insufficiency founded in literature search, which are case reports or case series. The characteristics of the cases are summarized in Table 2 (7–12).

The series of review comprised 27 fetuses with different degrees of cardiac insufficiency. We reviewed a case of open fetal surgery performed at 23 weeks' gestation which rarely succeeded after three failed cases (7). Even so, this successful case suffered from premature rupture of membranes and uncontrollable preterm labor at 28 weeks' gestation. Fortunately, the fetus survived and the routine SCT follow-up was normal. But the majority of other fetuses were not so lucky and ended up with unsatisfactory outcomes due to premature birth, infection, embolism, etc. Therefore, in recent years, new interventions have emerged for giant solid SCT, including ultrasound-guided percutaneous radiofrequency ablation (including vascular ablation and tissue ablation) and laser ablation. The fetal survival rate with minimally invasive treatment was 40% (2/5), but the surviving neonates suffered from long-term complications such as chronic lung disease and developmental delay (10).

In addition, early delivery and immediate resection for fetuses with high-risk SCT have also been proposed (8, 12). In the literature we reviewed, 20 cases underwent premature termination and postnatal tumor resection had a survival rate of 55%(11/20), and 45% (5/11) of the neonates required reoperation due to tumor-related complications (8, 9, 11, 12). An EXIT procedure was performed in only one case at 27 weeks' gestation, in which the fetus survived, but intraspinal metastasis of the tumor resulted in central nervous system injury (8).

## Discussion

With the improvement of prenatal diagnosis technology, the incidence and detection rate of fetal sacrococcygeal teratoma have increased gradually in recent years (13). Meanwhile, with our further understanding of the disease, people no longer blindly elect termination of pregnancy. However, prenatally diagnosed SCTs are challenging to manage due to their unpredictable nature. No uniform indications for prenatal intervention for SCT have yet been established. According to the summary of previous cases, in cases of singleton, normal fetal karyotype, no other major malformations, evidence of high-output heart failure, gestational age <30 weeks, type I or II, no maternal risk factors for open surgery and contraindications to anesthesia, open surgery may be attempted (14). But there are

some common complications such as preterm birth, premature rupture of membranes, and infection after open fetal surgery. Besides, different methods of minimally invasive treatment do not have good outcomes either. In fact, prognosis for these high-risk tumors is uncertain once the fetus has symptoms of heart failure and is in a gestational age that cannot survive after birth, no matter it is open fetal surgery or intrauterine treatment. In order to improve treatment outcome for such patients, it's not only required to modify intervention measures, but also more about grasping the timing of intervention. Close and dynamic monitoring of fetal hemodynamic changes largely contributed to the success of our case. If there is obvious fetal hydrops or even anemia, surgery may be difficult to reverse the adverse situation.

Although the SCT was detected early in this case, fortunately, the tumor didn't grow unpredictably rapidly. With our close monitoring, the incipient signs of fetal heart failure were detected in time. As a result, we had to terminate the pregnancy early and rapidly remove the tumour with placental blood flow during delivery, so as to reduce the foetal cardiac load and enable the newborn to establish a normal stable cardiopulmonary circulation system. Theoretically, the foetuses face risk of tumour rupture and bleeding during neonatal transport, EXIT can reduce such risk. In particular, when the foetus has heart failure, it can reduce the incidence of neonatal cardiopulmonary collapse and a series of complications caused by ischemia and hypoxia. EXIT is the most direct and rapid way to break off the blood supply to the tumour and remedy high-output heart failure. During the EXIT, a systematic anaesthetic management can provide profound uterine relaxation, continuous uteroplacental blood flow as well as foetal anaesthesia. Due to the special surgical position of such fetuses, the difficulty of endotracheal intubation increases accordingly, and the implementation of EXIT greatly reduced the possibility of fetal asphyxia caused by failure of intubation. Moreover, the blood supply to the placenta can compensate for foetal blood loss during tumourectomy. For example, one of the high-risk SCT foals studied by Roybal et al (8) underwent the EXIT procedure and survived after surgery. However, the prognosis was poor due to massive invasion of the spinal canal by the tumour. Due to the rarity and unpredictability of SCT, EXIT has rarely been used to treat SCT successfully. Nevertheless, our case report illustrates the successful use of EXIT on fetus with heart failure.

From the above case, it can be concluded that compared with traditional neonatal surgery, EXIT can allow early intervention and safe delivery of patients with SCT. In addition, anaesthesia and foetal ultrasound monitoring during EXIT are conducive to safe and effective operation. The foetal surgical incision is small or does not result in scar formation (15). In comparison with intrauterine surgery, EXIT can avoid the risks such as intrauterine infection, placental abruption, very early premature rupture of membranes and premature delivery. Comfortingly, it can greatly reduce the mental trauma for the family, and its acceptance by patients is higher than that of intrauterine surgery. However, the amount of maternal blood loss during EXIT is higher than that during general caesarean section. MacKenzie et al (16) summarised 31 cases of EXIT and reported that the maternal blood loss was 843 ± 574 mL, which was higher than that during general caesarean section. EXIT may also increase the risk of maternal infection and prolong postpartum recovery time. Hopefully, adverse outcomes will decrease with the application of new surgical instruments and the improvement of techniques (17), such as uterine staplers or modified staplers to avoid the potential of hemorrhage from the relaxed uterus during EXIT and intraoperative uterine packing to prevent postpartum hemorrhage. In addition, the maternal complications associated with EXIT procedures are manageable; indeed, these adverse outcomes had no effect on maternal recovery in our case. Future improvement should be focused on reducing the blood loss associated with the uterine incision, shortening the operation time, and controlling the speed of amniotic fluid loss.

In conclusion, the fetus with giant SCT and heart failure generally has a poor prognosis, so close monitoring by multidiscipline team is critical. When the fetus reaches viable gestation, EXIT procedure would be a good option to improve maternal and perinatal outcomes.

## Data availability statement

The original contributions presented in the study are included in the article/supplementary material. Further inquiries can be directed to the corresponding authors.

## Ethics statement

Written informed consent was obtained from the individual (s), and minor(s)' legal guardian/next of kin, for the publication of any potentially identifiable images or data included in this article.

## Author contributions

QL, and BZ contributed to the project development and surgical management. ML, TD and YJ were responsible for data acquisition and analysis. YD and MY wrote the manuscript. QL and YD revised the manuscript. All authors read and approved the final version of the manuscript. All authors contributed to the article and approved the submitted version.

## Funding

This study was supported by the center of prenatal diagnosis in Zhejiang province. Funding for this study was provided by the Health Major Science and Technology Project of Zhejiang province grant WKJ-ZJ-2126.

## Acknowledgments

The authors would like to thank Jinhu Wang's team, doctors from Children's Hospital Affiliated to Zhejiang University School of Medicine, for their surgery support.

## Conflict of interest

The authors declare that the research was conducted in the absence of any commercial or financial relationships that could be construed as a potential conflict of interest.

## Publisher's note



## References

1. Avni FE, Guibaud L, Robert Y, Segers V, Ziereisen F, Delaet MH, et al. MR imaging of fetal sacrococcygeal teratoma: Diagnosis and assessment. *Am J Roentgenol* (2002) 178(1):179–83. doi: 10.2214/ajr.178.1.1780179

2. Bond SJ, Harrison MR, Schmidt KG, Silverman NH, Flake AW, Slotnick RN, et al. Death due to high-output cardiac failure in fetal sacrococcygeal teratoma. *J Pediatr Surg* (1990) 25:1287–91. doi: 10.1016/0022-3468(90)90535-H

3. Ayed A, Tonks AM, Lander A, Kilby MD. A review of pregnancies complicated by congenital sacrococcygeal teratoma in the West Midlands region over an 18-year period: population-based, cohort study. *Prenatal Diag* (2015) 35 (11):1037–47. doi: 10.1002/pd.4641

4. Akinkuotu AC, Coleman A, Shue E, Sheikh F, Hirose S, Lim FY, et al. Predictors of poor prognosis in prenatally diagnosed sacrococcygeal teratoma: A multiinstitutional review. *J Pediatr Surg* (2015) 50(5):771–4. doi: 10.1016/j.jpedsurg.2015.02.034

5. Gebb JS, Khalek N, Qamar H, Moldenhauer JS, Oliver ER, Coleman BG, et al. High tumor volume to fetal weight ratio is associated with worse fetal outcomes and increased maternal risk in fetuses with sacrococcygeal teratoma. *Fetal Diagn Ther* (2019) 45(2):94–101. doi: 10.1159/000486782

6. Hambraeus M, Hagander L, Stenström P, Börjesson A, Arnbjörnsson E. Long-term outcome of sacrococcygeal teratoma: A controlled cohort study of urinary tract and bowel dysfunction and predictors of poor outcome. *J Pediatr Surg* (2018) 198:131–136.e2. doi: 10.1016/j.jpeds.2018.02.031

7. Graf JL, Albanese CT, Jennings RW, Farrell JA, Harrison MR. Successful fetal sacrococcygeal teratoma resection in a hydropic fetus. *J Pediatr Surg* (2000) 35 (10):1489–91. doi: 10.1053/jpsu.2000.16420

8. Roybal JL, Moldenhauer JS, Khalek N, Bebbington MW, Johnson MP, Hedrick HL, et al. Early delivery as an alternative management strategy for selected high-risk fetal sacrococcygeal teratomas. *J Pediatr Surg* (2011) 46 (7):1325–32. doi: 10.1016/j.jpedsurg.2010.10.020

9. Goto S, Suzumori N, Obayashi S, Ozaki Y, Sugiura-Ogasawara M. Two cases of prenatally diagnosed sacrococcygeal teratoma type I with different clinical features. *Congenit Anom* (2013) 53(2):92–4. doi: 10.1111/j.1741-4520.2012.00369.x

10. Van Mieghem T, Al-Ibrahim A, Deprest J, Lewi L, Langer JC, Baud D, et al. Minimally invasive therapy for fetal sacrococcygeal teratoma: case series and systematic review of the literature. *Ultrasound Obstet Gynecol* (2014) 43(6):611–9. doi: 10.1002/uog.13315

11. Den Otter SCM, De Mol AC, Eggink AJ, Van Heijst AFJ, De Bruijn D, Wijnen RMH. Major sacrococcygeal teratoma in an extreme premature infant: A multidisciplinary approach. *Fetal Diagn Ther* (2008) 23(1):41–5. doi: 10.1159/000109225

12. Baumgarten HD, Gebb JS, Khalek N, Moldenhauer JS, Johnson MP, Peranteau WH, et al. Preemptive delivery and immediate resection for fetuses with high-risk sacrococcygeal teratomas. *Fetal Diagn Ther* (2019) 45(3):137–44. doi: 10.1159/000487542

13. Pauniaho S-L, Heikinheimo O, Vettenranta K, Salonen J, Stefanovic V, Ritvanen A, et al. High prevalence of sacrococcygeal teratoma in Finland – a nationwide population-based study. *Acta Paediatr* (2013) 102:e251–6. doi: 10.1111/apa.12211

14. Hedrick HL, Flake AW, Crombleholme TM, Howell LJ, Johnson MP, Wilson RD, et al. Sacrococcygeal teratoma: prenatal assessment, fetal intervention, and outcome. *J Pediatr Surg* (2004) 39(3):430–8. doi: 10.1016/j.jpedsurg.2003.11.005

15. Makoto T, Wendy L, Mayumi I. Wound healing and skin regeneration. cold spring harb perspect med. *Cold Spring Harbor perspectives in medicine* (2015) 5(1): a023267. doi: 10.1101/cshperspect.a023267

16. Mac Kenzie TC, Crombleholme TM, Flake AW. The ex-utero intra-partum treatment. *Curt Opin Pediatr* (2002) 14(4):453–8. doi: 10.1097/00008480-200208000-00018

17. Erfani H, Nassr AA, Espinoza J, Lee TC, Shamshirsaz AA. A novel approach to ex-utero intrapartum treatment (EXIT) in a case with complete anterior placenta. *Eur J Obstet Gynecol Reprod Biol* (2018) 228:335–6. doi: 10.1016/j.ejogrb.2018.06.029

frontiers | Frontiers in Surgery

TYPE Case Report
PUBLISHED 02 November 2022
DOI 10.3389/fsurg.2022.1009119



OPEN ACCESS

EDITED BY
Tomoyuki Abe,
Higashi-Hiroshima Medical Center, Japan

REVIEWED BY
Mostafa Kotb,
Alexandria University, Egypt
Simone Guadagni,
University of Pisa, Italy

*CORRESPONDENCE
Yang Xiaojun
yangxjmd@aliyun.com

SPECIALTY SECTION
This article was submitted to Surgical Oncology, a section of the journal Frontiers in Surgery

RECEIVED 01 August 2022
ACCEPTED 10 October 2022
PUBLISHED 02 November 2022

CITATION
Xusheng Z, Yuke Y, Yun M, Huijun G, Jiangshan P, Xueqin D and Xiaojun Y (2022) Primary gastric choriocarcinoma: A case report. Front. Surg. 9:1009119. doi: 10.3389/fsurg.2022.1009119



# Primary gastric choriocarcinoma: A case report

Zhang Xusheng[1,2], Yan Yuke[2,3,4,5], Meng Yun[1,2], Guo Huijun[1,2], Peng Jiangshan[1,2], Du Xueqin[2,6] and Yang Xiaojun[2,3,4,5]*

[1]The 1st Clinical Medicine College, Gansu University of Chinese Medicine, Lanzhou, China, [2]Department of General Surgery, Gansu Provincial Hospital, Lanzhou, China, [3]School of People's Clinical Medicine, Lanzhou University, Lanzhou, China, [4]Gansu Key Laboratory of Molecular Diagnostics and Precision Medicine for Surgical Oncology, Gansu Provincial Hospital, Lanzhou, China, [5]Gansu Research Center of Prevention and Control Project for Digestive Oncology, Gansu Provincial Hospital, Lanzhou, China, [6]College of Clinical Medicine, Ningxia Medical University, Yinchuan, China

**Background:** Choriocarcinoma is a malignant tumour of trophoblastic origin. Most are gestational choriocarcinomas, which usually occur in women with an epithelial origin of the placental chorionic villi and are associated with pregnancy. It mainly originates in the gonads such as the ovaries and testes. However, it rarely occurs in the stomach and is known as primary choriocarcinoma (PGC).

**Case presentation:** A 69-year-old man complained of abdominal distention for 3 years, which worsened 1 week later. Gastroscopy showed chronic atrophic gastritis C1 (C1: indicates atrophic gastritis involving the sinus region); the pathology report of the gastroscopic specimen showed high-grade epithelial tumours in the mucosal glands. We diagnosed an occupying lesion in the stomach and performed a laparoscopically assisted distal gastrectomy and Billroth type 1 anastomosis. Postoperative pathology showed "gastric choriocarcinoma with cancerous tissue invading the entire gastric wall". The patient was discharged on the 11th postoperative day as there were no postoperative complications. The patient was followed up until June 2022 with a good recovery and no recurrence.

**Conclusion:** We encountered a case of Primary Gastric Choriocarcinoma, where the cancerous tissue invades the full thickness of the gastric wall.

KEYWORDS

choriocarcinoma, primary gastric choriocarcinoma, pathology, treatment, case report

## Background

Choriocarcinoma is a malignant tumour of trophoblastic origin (1). The vast majority of choriocarcinomas are associated with pregnancy, most commonly in the uterus, and originate mainly in the ovaries, testes and other gonads. However, primary gastric choriocarcinoma is is a rare malignancy, accounting for approximately 1% of gastric cancers (2, 3). Here, we report a case of primary gastric choriocarcinoma in which cancerous tissue invaded the entire gastric wall.

## Case report

A 69-year-old male presented to our hospital complaining of abdominal distension and discomfort for 3 years, worsening for 1 week. His medical history included chronic appendicitis and he had undergone an appendectomy 2 years ago. Recently, there was no significant change in weight. One week ago, the patient felt a marked increase in abdominal distension and pain, mainly in the upper and middle abdomen, and presented to our hospital. The results of the examination were as follows: normal vital signs, fecal occult blood test (++), ALB: 33.05 g/L, Hb: 96 g/L and HCG-β: 66.12 mIU/ml. Liver and kidney function, electrolytes and blood glucose were normal. Abdominal Doppler ultrasound showed a solid mass in the upper abdomen, which was suspected to be gastric cancer (**Figure 1A**). Gastroscopy revealed chronic atrophic gastritis stage C1 (C1: indicates atrophic gastritis involving the gastric sinus region) (**Figure 1B**). Pathological examination of the specimen taken under gastroscopy revealed high-grade intraepithelial neoplasia in the (sinus) mucosal glands (**Figures 2A–D**). Tumour marker examination showed normal tumour series CEA, AFP and CA199 except CA72-4: 10.07 U/ml (0–6 U/ml). MRI of the abdomen showed that the gastric sinus was occupied, with the main lesion located outside the gastric wall (**Figure 3A**). Biopsy consultation at another hospital showed a moderate chronic mucosal inflammation with mild intestinal metaplasia. Considering the patient's current relevant investigations and findings, we considered a gastric occupying lesion (suspected mesenchymal tumour). The patient was stable and had clear indications for surgery. We therefore performed a laparoscopic-assisted distal gastrectomy and a Billroth type 1 anastomosis. The postoperative gross specimen showed a mass measuring approximately 9 cm × 7 cm × 6 cm, which was reddish-grey in section, suggestive of solid soft tissue (**Figures 4A,B**). Pathology of the postoperative specimen showed PGC cancerous tissue invading the entire gastric wall (T4aN0M0). Metastases were found only in the vascular system and no other system had been identified. No tumour was found at either side of the resection margins. Microscopic examination showed marked tumour heterogeneity with visible cancerous areas, tumour cells of variable size, ovoid or polygonal in shape, with clear, lightly stained or granular cytoplasm, a single vacuolated nucleus with a distinct nucleolus, many nuclear fission signs, some cells could appear multinucleated, with abundant cytoplasm and large nuclear heterogeneity. The cells are of cytotrophoblastic and syncytial trophoblastic origin and are devoid of villous structures (**Figures 4C–F**). Immunohistochemistry showed CD10 (+) (**Figure 5A**), ck8/18 (+) (**Figure 5B**), CK19 (+) (**Figure 5C**), CKP (+) (**Figure 5D**) and a Ki-67 labelling index of 60% (+) (**Figure 5E**). Histochemical staining showed PAS (+) (**Figure 5F**), while immunohistochemistry showed positive for HCG antibodies (**Figure 6**). A postoperative blood HCG-β (β-human chorionic gonadotropin) test was performed at 66.12 mIU/ml, followed by cranial MRI and chest and abdominal CT, which showed no signs of distant metastases. The diagnosis of PGC was now almost clear. The patient was discharged on the 11th postoperative day and was followed up until June 2022, with good recovery and no recurrence.

## Discussion and conclusions

Primary gastric choriocarcinoma was first described by Davidsohn in 1905 (4) and accounts for approximately 0.8%

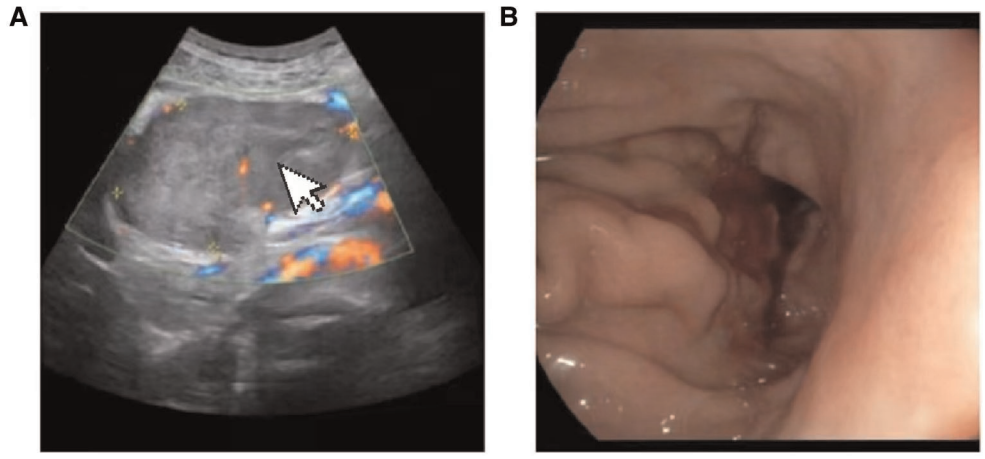


FIGURE 1
(A) Doppler ultrasound:upper abdominal solid mass. (B) Gastroscopy: chronic atrophic gastritis C1: gastric antrum mass (to be examined).

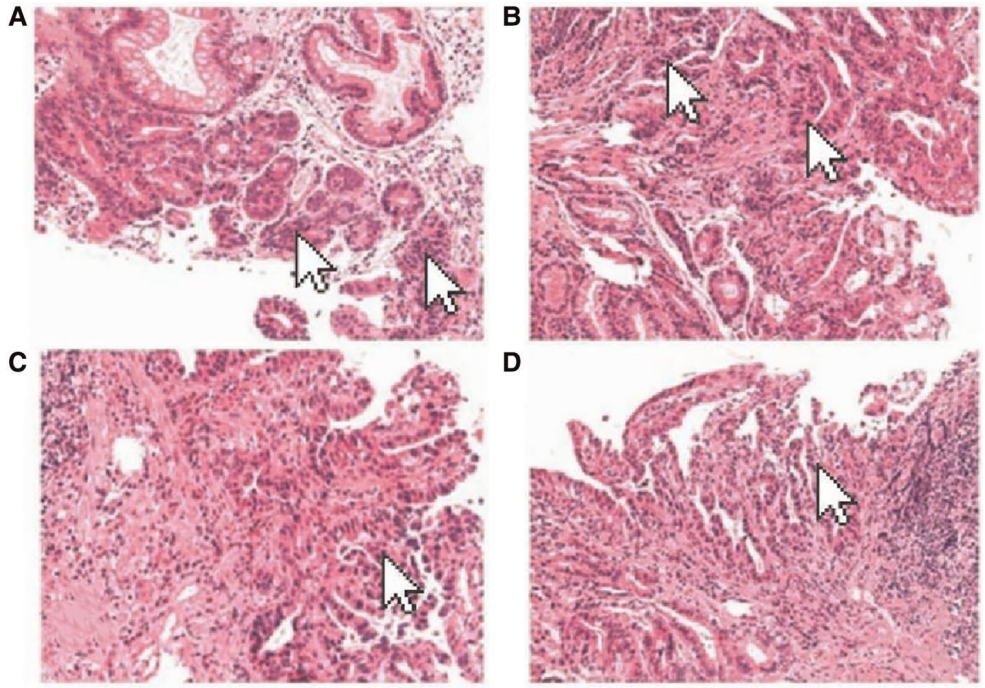


FIGURE 2
Pathological examination of the specimen taken under gastroscopy revealed high-grade intraepithelial neoplasia in the (sinus) mucosal glands (arrow). (HE×100).

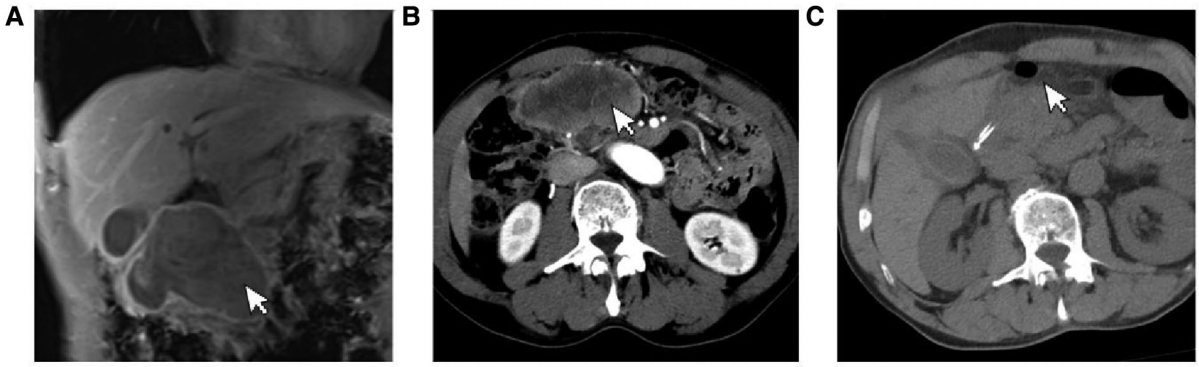


FIGURE 3
(A) The gastric antrum occupies space, the main lesion is located outside the gastric wall. (B) Patient's preoperative CT showed obvious lesions. (C) Postoperative CT of the patient showed significant resection of the lesion.

of all gastric cancers (5). PGC is most commonly seen in older men, with a male to female ratio of 2.3:1 (6). The tumour is mainly located in the gastric sinus, followed by the gastric body and least in the cardia (7, 8). The clinical presentation is similar to that of gastric adenocarcinoma, with only 25% of patients developing choriocarcinoma (9). However, primary gastric choriocarcinoma is more likely to cause gastrointestinal bleeding than other tumours (10). Very few cases of primary gastric choriocarcinoma have been reported in China, most of which are associated with elevated serum β-HCG (human chorionic gonadotropin) levels, nausea, vomiting and gynaecomastia (7). The pathogenesis of the disease is unclear and several theories exist. The most accepted mechanism is Pick's theory of dedifferentiation, which states that primary gastric choriocarcinoma originates from the reverse differentiation of gastric adenocarcinoma. This theory suggests that existing gastric adenocarcinoma cells differentiate into embryonic stages and become trophoblast cells, which in turn

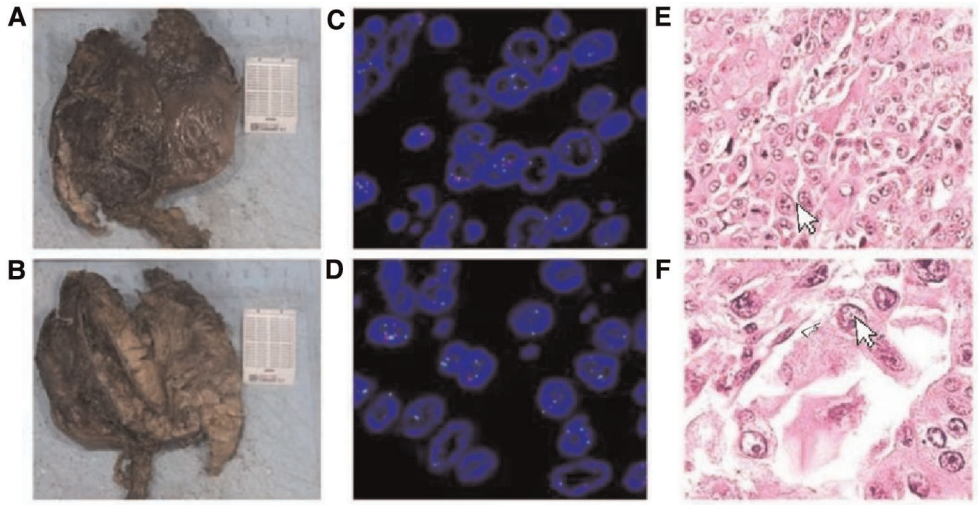


FIGURE 4
(A,B) Specimen: the size of the mass is about 9 cm × 7 cm × 6 cm, and the surface of the slice is red and gray, indicating solid, soft tissue. (C–F) Primary choriocarcinoma of the stomach, with Ovoid or polygonal, with hyaline, lightly stained or granular cytoplasm and a single vacuolated nucleus (HE ×100).

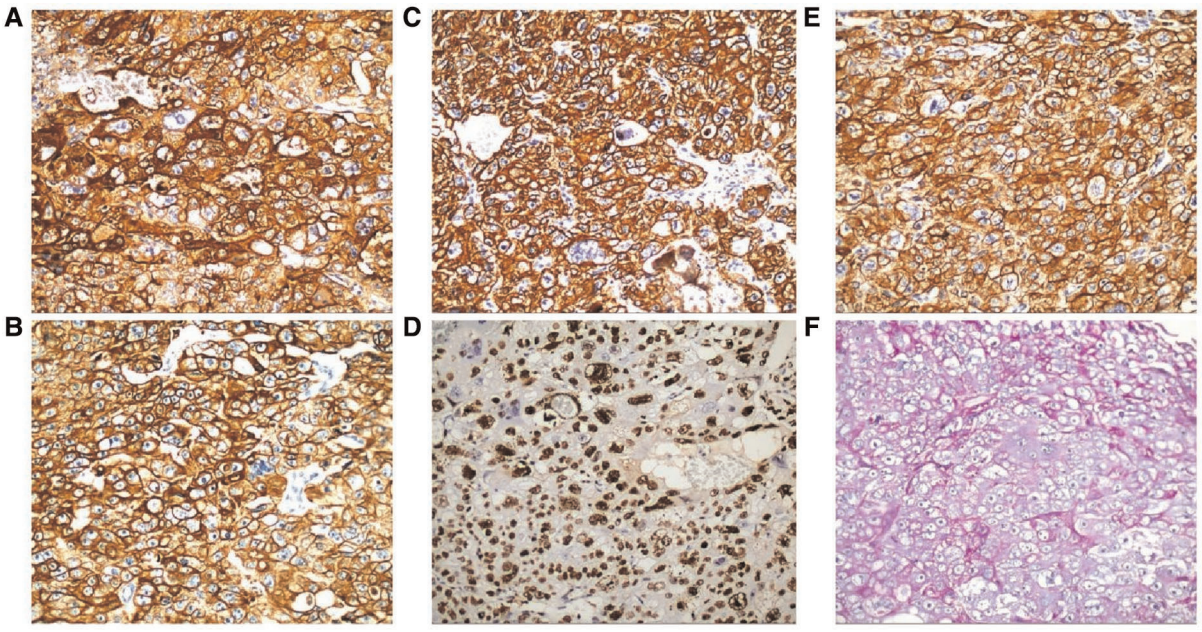


FIGURE 5
Immunohistochemistry: CD10 (+) (A), ck8/18 (+) (B), CK19 (+) (C), CKP (+) (D) and Ki-67 labelling index of 60% (+) (E) (HE ×200). Histochemical staining: PAS (+) (F) (SP ×200).

differentiate into choriocarcinoma (11). Its diagnosis remains very difficult. The diagnosis of PGC must be made with great caution and the following conditions must be met: firstly, the presence of a tumour in the stomach must be excluded from any other occult primary site; secondly, the morphology of the tumour is similar to that of choriocarcinoma in other sites and the tumour cells express HCG by immunohistochemistry; and finally, HCG is elevated in serum and urine preoperatively but decreases to normal levels after gastrectomy and chemotherapy. Therefore, when preoperative gastroscopy

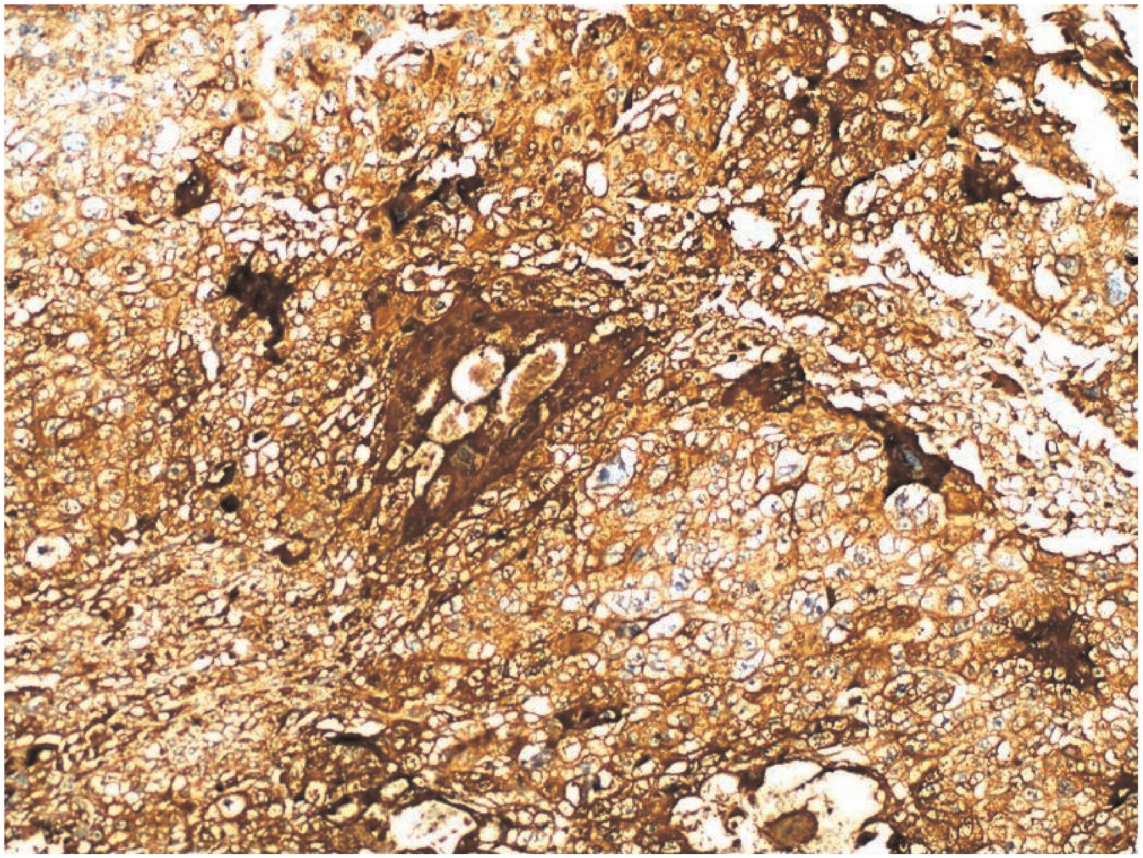

FIGURE 6
Immunohistochemistry: HCG(+) (SP ×100).

reveals a malignant gastric ulcer, a tissue biopsy is required to improve the preoperative diagnosis. The diagnosis of primary gastric choriocarcinoma is then made postoperatively based on pathological features and immunohistochemical findings. In this case the preoperative gastroscopic pathology showed only high-grade intraepithelial neoplasia of the mucosal glands, yet the postoperative pathology report showed gastric choriocarcinoma. The serum HCG level decreased from 66.12 miu/ml postoperatively to 42.86 miu/ml (one week postoperatively). We then performed various imaging examinations such as cranial MRI and chest CT to exclude other tumours. We eventually combined the imaging findings, postoperative pathological features, immunohistochemical results and serological tests to make a final diagnosis of primary gastric choriocarcinoma. Its histopathology was rapid in most patients with PGC, with a poor prognosis. Most patients survive for 6 months (12) and usually die of blood transmission within the first year of diagnosis. Lymph nodes, liver, peritoneum and lung are common sites of metastasis (5). Poor prognostic factors affecting overall survival are mainly liver metastases, which usually lead to liver failure, residual tumour after surgery, and lack of chemotherapy (13). Due to its combination of gastric and choriocarcinoma characteristics, there is no standard treatment protocol. For early stage patients, postoperative chemotherapy is the treatment of choice after gastrectomy and lymph node dissection (13). For patients with locally advanced disease, systemic chemotherapy can be followed by radical gastrectomy combined with postoperative chemotherapy. For patients with advanced cancer, systemic chemotherapy is primarily used. Previous case reports have described (5) the use of VIP, BEP (bleomycin, etoposide, and cisplatin), EMA/CO (eto-poside, methotrexate, actinomycin D, cyclophosphamide, and vincristine), and fluorouracil plus cisplatin, but their efficacy was poor. However, Ceilesh A et al. (2) found that VIP chemotherapy regimens were effective in the early treatment of metastatic primary gastric choriocarcinoma. Picazo (14) found that two patients who received chemotherapy had a mean survival of 120 days. Monitoring of serum HCG levels may help to assess the effectiveness of treatment and tumour recurrence. As a rare disease, PGC is particularly important to diagnose early and

accurately through various tests as its clinical presentation is very similar to that of other tumours. To date, there is no standard treatment for patients with PGC, so it is important to explore standard treatment options. In this case, the postoperative blood HCG-β test was 66.12 mIU/ml: since then, the HCG-β level has been measured regularly (1 week postoperative: 42.86 mIU/ml; 2 months postoperative: 15.56 mIU/ml), showing a gradual decrease and a stable trend, and together with imaging examinations (cranial MRI, chest and abdominal CT), suggesting that there are no signs of recurrence or metastasis, but close follow-up is still needed. The patient should be followed up closely.

## Data availability statement

The original contributions presented in the study are included in the article/Supplementary Material, further inquiries can be directed to the corresponding author/s.

## Ethics statement

Written informed consent was obtained from the patient and legal guardian for the publication of any identifiable data/care reports.

## Author contributions

ZXS wrote the paper. YYK provided the cases. YYK provided the images. YXJ reviewed and edited the manuscript. All authors contributed to the article and approved the submitted version.

## Funding

Funded by key projects in the National Scientific Research Cultivation Program, No.: 2019-216; Gansu Innovation Base and Talent Project, No.: 20JR10RA433; Key research and development projects of Gansu Provincial Science and Technology Plan, No.: 21YF5WA027; Gansu Province Health Industry Scientific Research Plan, No.: GSWSKY2020-45; Gansu Provincial People's Hospital-Internal Scientific Research Youth Project, No.: 20GSSY4-12.

## Acknowledgements

ZXS would like to thank everyone who has helped through the researching and preparing of this article, especially thank Professor Xiaojun Yang, who reviewed the manuscript and Yan, who provided the case and images. They would also like to sincerely thank their friends and family who have given considerable encouragement and financial support.

## Conflict of interest

The authors declare that the research was conducted in the absence of any commercial or financial relationships that could be construed as a potential conflict of interest.

## Publisher's note



## References

1. Wierzchniewska A, Romanowicz-Makowska H. Kosmówczak [choriocarcinoma]. *Ginekol Pol.* (1995) 66(9):537–40.

2. Ceilesh A, Burroughs S, Majeed N, Klein L. Primary gastric choriocarcinoma: a case report of early successful treatment outcome. *JCO Oncol Pract.* (2020) 16 (9):608–10. doi: 10.1200/OP.20.00008

3. Yoon JH, Kim MS, Kook EH, Ahn SH, Jeong SY, Han MS, et al. Primary gastric choriocarcinoma: two case reports and review of the literatures. *Cancer Res Treat.* (2008) 40(3):145–50. doi: 10.4143/crt.2008.40.3.145

4. Davidson C. Chorionepitherion und magenkrebs, eine seltene vershmelzung zweierbosartiger geschwulste. *Carite Ann.* (1905) 29:426–37.

5. Kobayashi A, Hasebe T, Endo Y, Sasaki S, Konishi M, Sugito M, et al. Primary gastric choriocarcinoma: two case reports and a pooled analysis of 53 cases. *Gastric Cancer.* (2005) 8(3):178–85. doi: 10.1007/s10120-005-0332-9

6. Takahashi K, Tsukamoto S, Saito K, Ohkohchi N, Hirayama K. Complete response to multidisciplinary therapy in a patient with primary gastric choriocarcinoma. *World J Gastroenterol.* (2013) 19(31):5187–94. doi: 10.3748/wjg.v19.i31.5187

7. Jindrak K, Bochetto JF, Alpert LI. Primary gastric choriocarcinoma: case report with review of world literature. *Hum Pathol.* (1976) 7(5):595–604. doi: 10.1016/s0046-8177(76)80105-0

8. Noguchi T, Takeno S, Sato T, Takahashi Y, Uchida Y, Yokoyama S. A patient with primary gastric choriocarcinoma who received a correct preoperative diagnosis and achieved prolonged survival. *Gastric Cancer.* (2002) 5(2):112–7. doi: 10.1007/s101200200019

9. Shastri A, Daver NG, Hayes TG. Primary gastric chorioadenocarcinoma: a needle in a haystack. *Rare Tumors.* (2011) 3(2):e19. doi: 10.4081/rt.2011.e19

10. Seckl MJ, Sebire NJ, Fisher RA, Golfier F, Massuger L. Sessa C; ESMO guidelines working group. Gestational trophoblastic disease: eSMO clinical

practice guidelines for diagnosis, treatment and follow-up. *Ann Oncol.* (2013) 24 (Suppl 6):vi39–50. doi: 10.1093/annonc/mdt345

11. Pick L. Uber die chorioepthelahnlich metastasierende from des magencarcinomas [in German]. *Klin Wochenschr.* (1926) 5:1728.

12. Baraka BA, Al Kharusi SS, Al Bahrani BJ, Bhathagar G. Primary gastric chorioadenocarcinoma. *Oman Med J.* (2016) 31(5):381–3. doi: 10.5001/omj.2016.75

13. Raghavapuram R, Veerankutty FH, Anandakumar M. Primary choriocarcinoma of the stomach. A case report and review of the literature. *Indian J Surg Oncol.* (2016) 7(1):119–23. doi: 10.1007/s13193-016-0494-4

14. Picazo Ferrera K, Herrera Servin MÁ, Hernández Guerrero AI. Primary gastric choriocarcinoma. *Rev Esp Enferm Dig.* (2020) 112(3):241. doi: 10.17235/reed.2020.6478/2019

frontiers | Frontiers in Surgery

TYPE Case Report
PUBLISHED 07 November 2022
DOI 10.3389/fsurg.2022.1037312



OPEN ACCESS

EDITED BY
Riccardo Bertolo,
Hospital San Carlo di Nancy, Italy

REVIEWED BY
Artur Rebelo,
University Hospital in Halle, Germany
Tuerhongjiang Tuxun,
First Affiliated Hospital of Xinjiang Medical University, China

*CORRESPONDENCE
Uchenna Okakpu
ucify007@gmail.com

SPECIALTY SECTION
This article was submitted to Surgical Oncology, a section of the journal Frontiers in Surgery

RECEIVED 05 September 2022
ACCEPTED 10 October 2022
PUBLISHED 07 November 2022

CITATION
Sharma NK, Okakpu U, Murthy J, Wei LM, Lopez-Solis R, Schmidt C, Badhwar V and Marsh JW (2022) Case report: Surgical resection of a retro-hepatic leiomyosarcoma involving atrial reconstruction, cardiopulmonary bypass, *ex vivo* tumor resection, and liver re-implantation. Front. Surg. 9:1037312. doi: 10.3389/fsurg.2022.1037312



# Case report: Surgical resection of a retro-hepatic leiomyosarcoma involving atrial reconstruction, cardiopulmonary bypass, *ex vivo* tumor resection, and liver re-implantation

Neel K. Sharma[1], Uchenna Okakpu[2]*, Jeevan Murthy[2], Lawrence M. Wei[3], Roberto Lopez-Solis[1], Carl Schmidt[1], Vinay Badhwar[3] and J. Wallis Marsh[1]

[1]Department of Surgery, West Virginia University, Morgantown, WV, United States, [2]School of Medicine, West Virginia University, Morgantown, WV, United States, [3]Cardiovascular and Thoracic Surgery, West Virginia University, Morgantown, WV, United States

**Introduction:** Leiomyosarcomas (LMS) involving the inferior vena cava (IVC) is a clinically rare entity, accounting for approximately 0.5% of all adult sarcomas.
**Case presentation:** A 67-year-old male presented to the emergency department with mild back and lower abdominal pain. During the workup, a computed tomography scan without contrast showed an area of decreased attenuation within the liver adjacent to the intrahepatic IVC. Magnetic resonance imaging confirmed the involvement of the retro-hepatic IVC; biopsy confirmed the diagnosis of LMS. Given the location of the involvement of the retro-hepatic IVC, liver explantation was deemed necessary for adequate tumor resection. The superior extension of the tumor toward the heart necessitated Cardio-Pulmonary (CPB). The patient successfully underwent a complex surgical procedure involving liver explantation with *ex vivo* back-table resection of the retro-hepatic LMS, replacement of the retro-hepatic vena cava with a ringed Gore-Tex graft, liver re-implantation, and hepatic vein-atrial reconstruction under cardiopulmonary bypass. There were no intraoperative or post-op complications.
**Discussion:** The role of vascular reconstruction of the IVC varies depending on the level and extent of the tumor, with options ranging from primary repair, ligation, or reconstruction dictated. Surgical resection with negative margins remains the treatment of choice due to the lack of efficacy of adjuvant therapies. Importantly, liver explantation offers a chance for complete surgical resection and reconstruction. Similarly, the complex nature of the tumor necessitated a pioneering approach involving direct hepato-atrial venous anastomosis.
**Conclusion:** To the best of our knowledge, this is the first reported case in which the hepatic veins were anastomosed directly to the right atrium while also replacing the native vena cava with a separate graft.

Abbreviations
IVC, inferior vena cava: the major and largest vein coming up from below the heart; LMS, leiomyosarcomas: an uncommon type of cancer originating from smooth muscle tissue.

KEYWORDS

*ex vivo* repair, en-bloc resection, inferior vena cava, leiomyosarcoma, retroperitoneum, right atrial anastomosis, hepatic vein anastomosis

# Introduction

Retro-hepatic inferior vena cava (IVC) leiomyosarcoma is a rare condition with special anatomic considerations that make resection and reconstruction difficult. Case reports detailing successful tumor removal are few (in the hundreds), speaking to the condition's rarity and the expertise required to perform a successful resection (1, 2). The techniques of resection described in the literature include:

- En-bloc liver and IVC resection.
- Resection of the retro-hepatic IVC with or without reconstruction.
- Chemoradiation therapy.

Of these, the most efficacious treatment is surgical resection, which confers a long-term survival benefit (3). We describe herein an *ex vivo*, retro-hepatic vena cava excision with liver re-implantation and reconstruction of the IVC, including a novel method of hepatic vein grafts to an atrial anastomosis.

# Case description

## Pre-operative patient evaluation

A 67-year-old male patient presented to his local emergency department for evaluation of lower abdominal pain. He was prescribed antibiotics with minimal relief. Upon return for re-evaluation, a CT scan found him to have a large retro-hepatic mass involving the IVC. An abdomen MRI then uncovered findings concerning sarcoma of the retro-hepatic IVC (**Figure 1**). A biopsy confirmed the diagnosis of leiomyosarcoma.

The patient was referred to our surgical oncology clinic, where he received a physical exam, which resulted in unremarkable showings; he denied any lower extremity swelling and was found without signs or symptoms of IVC compression. The consulted cardiac surgeons obtained a negative cardiac catheterization. A CT of the chest did not show metastatic disease. The clinic offered total liver explantation with back-table resection of the retro-hepatic IVC and tumor with a subsequent liver re-implantation on cardiopulmonary bypass.

## Intraoperative management

The surgeons performed a sternal incision, isolated the intrapericardial IVC, and then extended the incision to below the umbilicus. After liver mobilization and gallbladder removal, the common duct, cystic artery and duct were ligated and divided. Dissection of the hepatic artery followed in the operation and moved to ligation and division of the gastroduodenal artery. The portal vein was then dissected in preparation for veno-venous bypass. For explantation, the IVC was mobilized completely out of the retroperitoneum.

The patient was then placed on full cardiopulmonary bypass to excise the liver and vena cava. Each was excised from above the renal veins to below the atrium, before being taken to the back-table for tumor resection. At that point, the patient was placed on portal venous bypass, which was connected to the cardiopulmonary bypass circuit. The leiomyosarcoma was circumferentially dissected en-bloc with the IVC, leaving only the origins of the right hepatic vein and the confluence of the middle and left hepatic veins (**Figures 2A,B**). The cardiac surgeons anastomosed a 20 mm ringed Gore-Tex (GTX) interposition graft from above the renal veins to the IVC, below the diaphragm. They completed the *in situ* native vena reconstruction during back-table work.

After completing the IVC tumor resection, two separate, non-ringed 20 mm GTX grafts were utilized to reconstruct the hepatic veins before re-implantation. One graft was sewn to the origin of the right hepatic vein, and a separate graft was sewn to the confluence of the middle and left hepatic veins. These two grafts were then joined together to allow a single anastomosis directly to the right atrium anterior to the previously placed vena cava ringed GTX graft. Next, the surgeons removed the patient from the portal venous bypass. They re-anastomosed the portal vein end-to-end and perfused

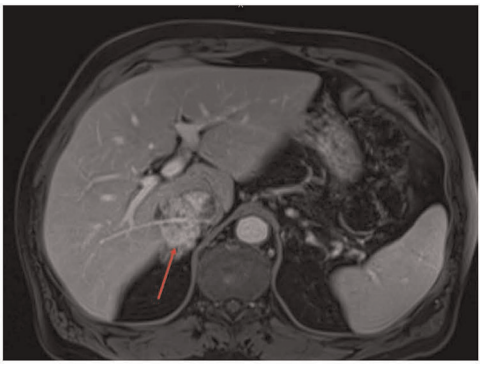

FIGURE 1
Pre-operative MRI showing involvement of the retro-hepatic IVC by leiomyosarcoma (red arrow). IVC, inferior vena cava.

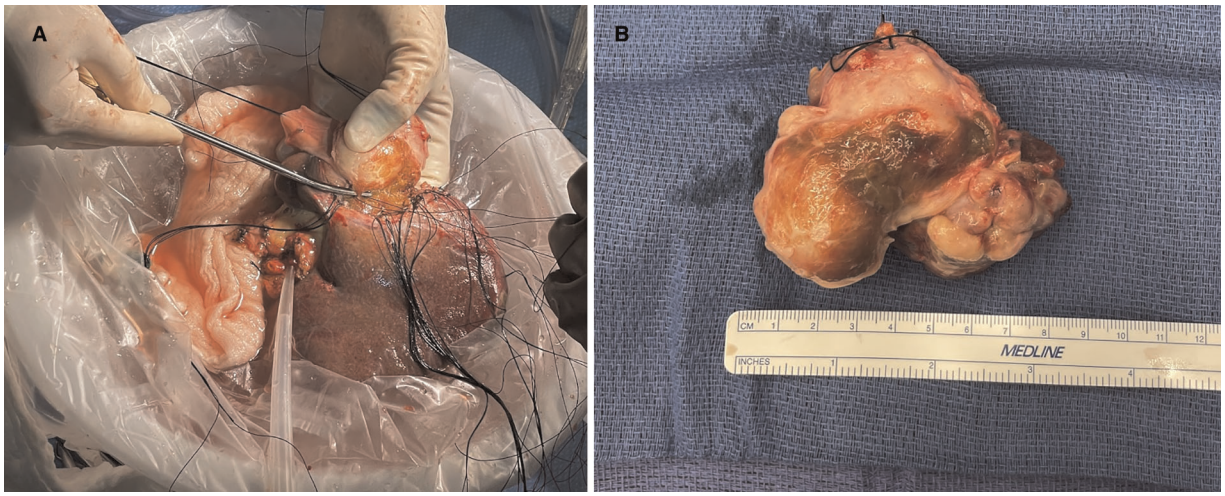


FIGURE 2
(A) Shows explanted liver on the back-table where the inferior IVC and leiomyosarcoma are being resected. (B) Shows the resected leiomyosarcoma and IVC. IVC, inferior vena cava.

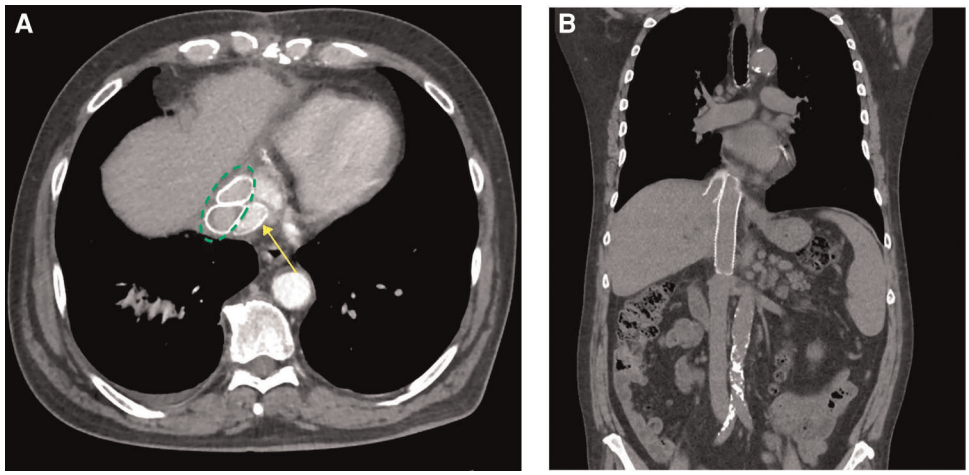


FIGURE 3
(A) Axial images showing the native vena cava GTX graft (posterior) (yellow arrow) and the two anterior hepatic vein GTX grafts (dotted green ellipse). (B) Coronal images showing the native vena cava graft (medial) and one of the hepatic vein GTX grafts (lateral). GTX, Gore-Tex.

the liver thereafter. The patient was able to be weaned from cardiopulmonary bypass at this time.

The procedure moved to hepatic artery anastomosis in another end-to-end fashion at the level of the gastroduodenal artery. Protamine was administered, and the patient was decannulated. After achieving meticulous hemostasis, the biliary anastomosis was performed end-to-end over a biliary stent. A segment of the patient's pericardium was harvested and utilized to patch the diaphragmatic opening triangularly, preventing compression of the GTX venous grafts. Last, the surgeons placed bilateral chest tubes along with an abdominal Blake drain in the patient prior to closing the pericardium, chest, and abdomen. The transesophageal echocardiogram revealed normal biventricular function. A total of one unit of packed red blood cells and one unit of cryoprecipitate were administered throughout the procedure.

## Post-operative care

The patient was extubated on the first post-operative day. His chest tubes were removed on the third post-operative day, and the intra-abdominal drain was removed on day 4. He was discharged home in stable condition on day 5. Other than

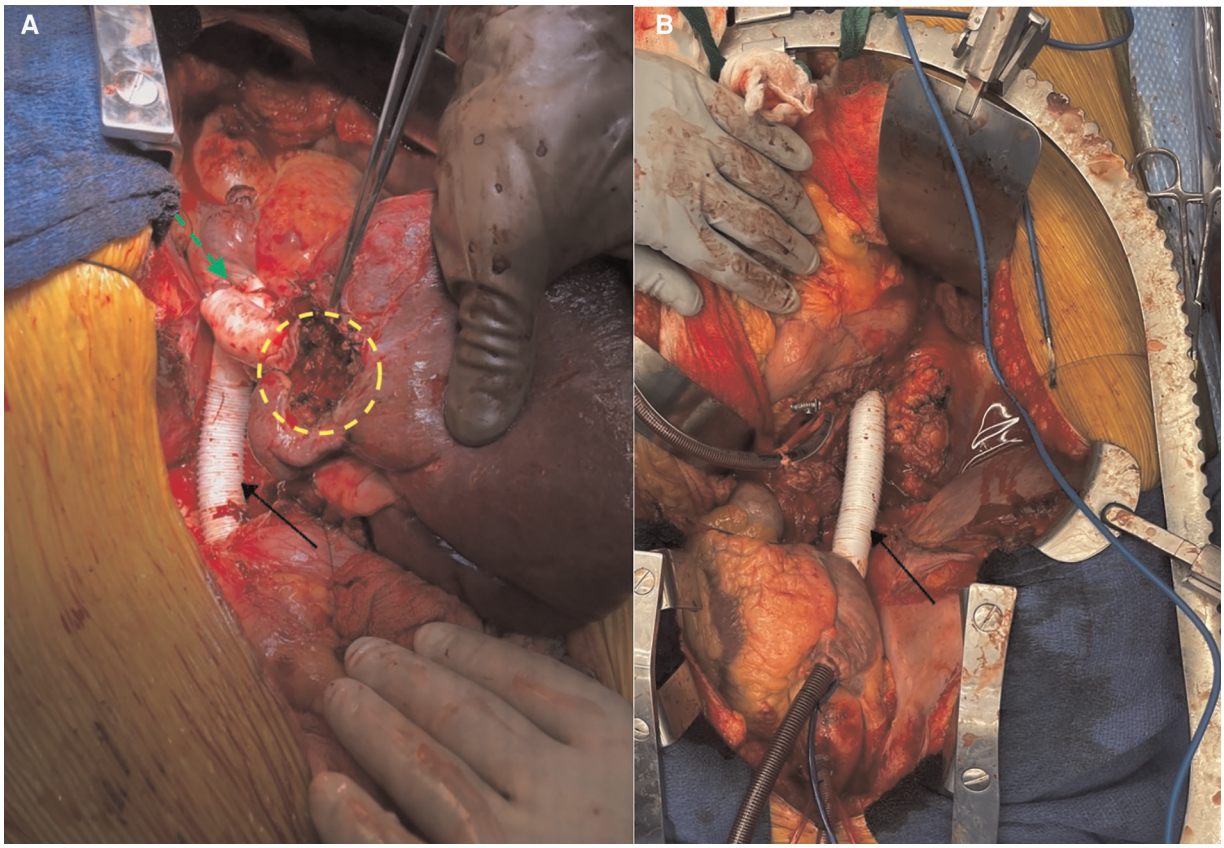


FIGURE 4
(A) Intraoperative view of the various graft reconstructions. Dotted green arrow = site of hepato-atrial anastomosis; dotted yellow circle = region of excised tumor; solid black arrow = vena caval GTX graft. (B) Vena caval graft (solid black arrow) before liver re-implantation. GTX, Gore-Tex.

intractable singultus, the hospital stay was usual. The patient's 3-month follow-up visit was unremarkable, as well as his 3-month post-operative abdominal and chest CT scans (**Figures 3A,B**).

## Discussion

Leiomyosarcomas (LMS) are classified as malignant neoplasms involving mesenchymal smooth muscle cells found within the vasculature, gastrointestinal tract, and portions of the genitourinary system. LMS originating from the IVC is extremely rare, representing 0.5% of all diagnosed sarcomas (estimated incidence of 1/100,000) (4). According to Roland et al., 5-year disease-specific survival rates after tumor resection were 65% (5). A retrospective chart review by Teixeira et al. compiled a range of 31%–66.7% for post-resection cava leiomyosarcoma patients (6).

The most common presentation of retro-hepatic cava leiomyosarcoma is abdominal pain; other regularly presenting symptoms are non-specific and include weight loss and fatigue. Site-specific presentation is typically due to venous outflow obstruction (7). Leiomyosarcoma of the IVC is stratified by location into segments I–III:

- Segment I involves the IVC inferior to the renal veins; lesions can cause nephrotic syndrome due to compression or occlusion of the renal vein(s).
- Segment II involves the IVC from the renal veins to the hepatic veins; lesions are typically asymptomatic and are the most common.
- Segment III involves the IVC superior to the hepatic veins. Segment III leiomyosarcoma can present with cardiac arrhythmia and Budd-Chiari syndrome (8, 9). (In all cases, there is an additional risk of lower extremity edema).

The main treatment of IVC leiomyosarcoma is surgical; however, resection and reconstruction techniques vary and are dependent on several factors (10). Surgical techniques include excision of the IVC, explantation of the liver with resection of the cava, resection of the cava utilizing total vascular exclusion with hypothermia, and liver transplantation with or without reconstruction of the IVC (2, 8, 11, 12). If resection

is performed, reconstruction of the IVC may or may not be necessary, depending on the degree and duration of obstruction and the presence of venous collaterals (2, 13).

In our case, the lack of radiographically significant local invasion of the patient's segment II tumor made the *ex vivo* approach to expose and resect the lesion a viable option. This option facilitated an end-to-end vena cava prosthetic graft anastomosis. Furthermore, the hepatic veins were amenable to anastomosis directly to the atrium. Through our literature review, this hepatic vein GTX conduit to atrium anastomosis appears to be a novel method of reconstruction not previously described. This pioneering approach to anastomosis was necessary for practical reasons. Because of the involvement of the hepatic veins by the leiomyosarcoma, the confluence of the hepatic veins had to be resected and reconstructed with two GTX grafts (one to the right and one to the confluence of the middle and left). The native vena cava between the renal veins and the atrium also required resection; this was subsequently reconstructed with a GTX graft in the heterotopic position. To reimplant the joined hepatic vein grafts into the vena, the caval graft would have required lengthy extensions to the hepatic vein grafts. To reach the vena caval grafts, the hepatic vein grafts would have to have been angled significantly posteriorly and would have been in danger of kinking with subsequent thrombosis. The atrial anastomosis was a straight shot for this anastomosis which allowed a much shorter length of hepatic vein GTX grafts and eliminated the risk of kinking/thrombosis. Intraoperative images shown in **Figure 4** highlight further details of the reconstruction.

Chemotherapy, which was previously thought to be of limited benefit in the treatment of cava leiomyosarcoma, has now been shown to have increased efficacy in the modern area of chemotherapeutics. Squires et al. performed a single-center experience evaluating neoadjuvant and adjuvant chemotherapy in patients diagnosed with cava leiomyosarcoma. They found that out of 11 patients evaluated, two were able to convert from an unresectable disease to an R1 resection with the addition of neoadjuvant tyrosine kinase inhibitor-based chemotherapy. Additionally, through proteomic analysis, *MYH11* also emerged as a potential diagnostic marker (14). Hines et al. noticed that in a single-center review when patients were treated with multimodality therapy (radical resection, radiation, or chemotherapy), the 10-year survival of IVC leiomyosarcoma was greater than leiomyosarcoma of the stomach, small intestine, retroperitoneum, or uterus (15). The role of radiation therapy and chemotherapy is difficult to fully characterize due to the rarity of the disease and the lack of ability to perform a randomized control trial.

The patient remains grateful for the procedure and continues to do well following surgery. Recently, he started showing radiological signs of metastatic disease following the discovery of a lung mass, but appreciates that the surgical resection and reconstruction have not only enhanced his quality of life, but have also potentially helped increase his overall survival. In his words, "The surgical team helped me enjoy a memorable Christmas with my family, that is what it's all about!"

## Conclusion

The challenging anatomic considerations involved in treating IVC LMS have led to numerous techniques for resection and reconstruction. However, no significant difference in disease-free survival has been noted based on excision or reconstruction techniques, allowing the surgeon to tailor the treatment with considerations for disease progression, local invasion, and surgeon expertise.

## Data availability statement

The original contributions presented in the study are included in the article/Supplementary Material, further inquiries can be directed to the corresponding author/s.

## Ethics statement

Ethical review and approval were not required for the study on human participants in accordance with the local legislation and institutional requirements. The patients/participants provided their written informed consent to participate in this study.

## Author contributions

JWM, CS, LMW, VB, and RL-S contributed to clinical management. NKS, JWM, JM, and UO contributed to writing the manuscript and making critical revisions. All authors contributed to the article and approved the submitted version.

## Acknowledgments

The authors would like to thank Bronson Herr from the department of surgery for his efforts in contributing to the editing of this work.

## Conflict of interest

The authors declare that the research was conducted in the absence of any commercial or financial relationships that could be construed as a potential conflict of interest.

## Publisher's note



## References

1. Bunting B, Marsh JW, Wei L, Hughes C, Gelzinis T. Surgical resection of a leiomyosarcoma involving atrial reconstruction, cardiopulmonary bypass, and ex-vivo liver resection and reimplantation. *J Cardiothorac Vasc Anesth*. (2017) 31(2):637–41. doi: 10.1053/j.jvca.2016.06.019

2. Das SAP, Paleela PS, Kuppuswamy MK, Venugopal B, Krishnan E. Retrohepatic caval leiomyosarcoma antesitum resection: a case report and a review of literature. *J Clin Exp Hepatol*. (2021) 11(6):742–6. doi: 10.1016/j.jceh.2021.01.002

3. Kato T, Hwang R, Liou P, Weiner J, Griesemer A, Samstein B, et al. Ex vivo resection and autotransplantation for conventionally unresectable tumors - an 11-year single center experience. *Ann Surg*. (2020) 272(5):766–72. doi: 10.1097/SLA.0000000000004270

4. Ducimetiere F, Lurkin A, Ranchere-Vince D, Decouvelaere AV, Peoc'h M, Istier L, et al. Incidence of sarcoma histotypes and molecular subtypes in a prospective epidemiological study with central pathology review and molecular testing. *PLoS One*. (2011) 6(8):e20294. doi: 10.1371/journal.pone.0020294

5. Roland CL, Boland GM, Demicco EG, Lusby K, Ingram D, May CD, et al. Clinical observations and molecular variables of primary vascular leiomyosarcoma. *JAMA Surg*. (2016) 151(4):347–54. doi: 10.1001/jamasurg.2015.4205

6. Teixeira Jr. FJR, Netto SDC, Perina ALF, Torricelli FCM, Teixeira LR, Zerati AE, et al. Leiomyosarcoma of the inferior vena cava: survival rate following radical resection. *Oncol Lett*. (2017) 14(4):3909–16. doi: 10.3892/ol.2017.6706

7. Mastoraki A, Leotsakos G, Mastoraki S, Papanikolaou I, Danias N, Smyrniotis V, et al. Challenging diagnostic and therapeutic modalities for leiomyosarcoma of inferior vena cava. *Int J Surg*. (2015) 13:92–5. doi: 10.1016/j.ijsu.2014.11.051

8. Kieffer E, Alaoui M, Piette JC, Cacoub P, Chiche L. Leiomyosarcoma of the inferior vena cava: experience in 22 cases. *Ann Surg*. (2006) 244(2):289–95. doi: 10.1097/01.sla.0000229964.71743.db

9. Penel N, Coindre JM, Giraud A, Terrier P, Ranchere-Vince D, Collin F, et al. Presentation and outcome of frequent and rare sarcoma histologic subtypes: a study of 10,262 patients with localized visceral/soft tissue sarcoma managed in reference centers. *Cancer*. (2018) 124(6):1179–87. doi: 10.1002/cncr.31176

10. Nooromid M, Martino RD, Squizzato F, Benedetto F, Caridi GD, Chou EL, et al. Surgical resection and graft replacement for primary inferior vena cava leiomyosarcoma: a multicenter experience. *J Vasc Surg Venous Lymphat Disord*. (2021) 10(3):617–25. doi: 10.1016/j.jvsv.2021.06.021

11. Buchholz BM, Boteon APC, Taniere P, Isaac JR, Gourevitch D, Muiesan P. Autotransplantation of the liver for ex vivo resection of intrahepatic caval leiomyosarcoma: a case report. *Exp Clin Transplant*. (2020) 18(3):396–401. doi: 10.6002/ect.2018.0183

12. Gaignard E, Bergeat D, Robin F, Corbiere L, Rayar M, Meunier B. Inferior vena cava leiomyosarcoma: what method of reconstruction for which type of resection? *World J Surg*. (2020) 44(10):3537–44. doi: 10.1007/s00268-020-05602-2

13. Daylami R, Amiri A, Goldsmith B, Troppmann C, Schneider PD, Khatri VP. Inferior vena cava leiomyosarcoma: is reconstruction necessary after resection? *J Am Coll Surg*. (2010) 210(2):185–90. doi: 10.1016/j.jamcollsurg.2009.10.010

14. Squires MH, Politano S, Pollock RE, Chen JL, Grignol V. Modern multimodality management of patients with caval leiomyosarcoma: new treatment paradigms and potential molecular insights. *J Surg Oncol*. (2021) 123(7):1618–23. doi: 10.1002/jso.26442

15. Hines OJ, Nelson S, Quinones-Baldrich WJ, Eilber FR. Leiomyosarcoma of the inferior vena cava: prognosis and comparison with leiomyosarcoma of other anatomic sites. *Cancer*. (1999) 85(5):1077–83. doi: 10.1002/(SICI)1097-0142(19990301)85:5<1077::AID-CNCR10>3.0.CO;2-0

frontiers | Frontiers in Oncology

TYPE Case Report
PUBLISHED 09 November 2022
DOI 10.3389/fonc.2022.1034563



OPEN ACCESS

EDITED BY
Jaques Waisberg,
Faculdade de Medicina do ABC, Brazil

REVIEWED BY
Sung Bin Park,
Chung-Ang University Hospital, South Korea
Shuhei Yoshida,
Hiroshima University, Japan
Paul Willemsen,
Hospital Network Antwerp (ZNA), Belgium

*CORRESPONDENCE
Jiaxin Li
407723080@qq.com

†These authors have contributed equally to this work

SPECIALTY SECTION
This article was submitted to Surgical Oncology, a section of the journal Frontiers in Oncology

RECEIVED 01 September 2022
ACCEPTED 19 October 2022
PUBLISHED 09 November 2022

CITATION
Feng X, Chen X, Feng Q, Liu X, Li H, Chen H, Cai Z and Li J (2022) Case report: A mesocolic lymphangioma in a 14-year-old child resected by laparoscopic surgery.
*Front. Oncol.* 12:1034563.
doi: 10.3389/fonc.2022.1034563



# Case report: A mesocolic lymphangioma in a 14-year-old child resected by laparoscopic surgery

Xuping Feng[1,2†], Xinyang Chen[3†], Qingbo Feng[1,2], Xiaoyin Liu[4], Hancong Li[3], Hao Chen[1,2], Zhaolun Cai[5] and Jiaxin Li[1,2,6*]

[1]Department of Liver Surgery & Liver Transplantation, State Key Laboratory of Biotherapy and Cancer Center, West China Hospital, Sichuan University and Collaborative Innovation Center of Biotherapy, Chengdu, Sichuan, China, [2]Laboratory of Liver Surgery, West China Hospital, Sichuan University, Chengdu, Sichuan, China, [3]West China School of Medicine, West China Hospital, Sichuan University, Chengdu, Sichuan, China, [4]Department of Neurosurgery, West China Hospital, Sichuan University, Chengdu, Sichuan, China, [5]Gastric Cancer Center, West China Hospital, Sichuan University, Chengdu, Sichuan, China, [6]DaFang County People's Hospital, Bijie, Guizhou, China

**Introduction:** Cystic lymphangioma is a benign malformation tumor of the lymphatic system. Its location is variable, and mesocolic localization remains extremely rare.

**Case presentation:** We report a case of right mesocolon giant cystic lymphangioma in a previously healthy 14-year-old boy who was successfully managed through a minimally invasive laparoscopic excision. The patient presented with 8 months of dull abdominal pain, sporadic, located on the peri-umbilicus, exacerbated for a month. An abdominal computed tomography (CT) revealed a large, multiseptated cystic mass on the right mesocolon. Right mesocolic excision using a laparoscope was performed on this patient. He was discharged on the fifth day without complications. Recurrence was not detected in three months of follow-up.

**Conclusion:** Cystic lymphangiomas in the mesocolon are rare benign neoplasms that pose diagnostic challenges. Complete resection is the optimal option for diagnostic confirmation and recurrence prevention. Laparoscopic surgery is feasible for children with mesocolic lymphangioma.

KEYWORDS

**mesocolon, cystic lymphangioma, case report, laparoscopic surgery, literature review**

## Introduction

Cystic lymphangiomas (CLs) are uncommon, benign malformations of the lymphatic system (1), which primarily occur during childhood, more than 80% of cases appear before the age of two (2). Most are located in the head-neck region (75%), and axilla(20%), while rarely arise in the abdomen (3). Abdominal cystic lymphangiomas (ACLs) constitute less than 5% of all cystic lymphangiomas (4), with the most common location in the mesentery and retroperitoneum and exceptionally rare in the mesocolon (5).

The clinical feature varies from incidental findings on imaging to acute abdomen mimicking a variety of pathologies including appendicitis, pancreatitis, and even malignancies (6). Due to their low frequency and acute abdominal condition, preoperative diagnosis remains challenging (7).

Herein, we describe a case of mesocolic cystic lymphangioma presenting with recurrent dull abdominal pain, in which laparoscopic surgery was performed successfully. Moreover, we updated the clinical features of this rare disease through a literature review. To our knowledge, our review contains the largest case series of mesocolic cystic lymphangioma to date.

## Case presentation

This study was reported under the principle of the CARE guideline (8). On April 18, 2022, a 14-year-old male was referred to West China Hospital for further investigations regarding the diagnosis of an intraabdominal mass. He had been experiencing recurrent dull abdominal pain for 8 months, which became aggravated one month ago. Persistent pain concentrated around the umbilicus for 1 to 2 hours, with gradual relief after resting. Any concomitant symptom, including fever, chill, vomiting, nausea, melena, and diarrhea, was denied. The patient reported unremarkable past medical history and family medical history. Physical examination revealed a palpable mass extending from the epigastric to the hypogastric region, particularly on the right side of the umbilicus. Neither routine laboratory investigations nor tumor marker testing revealed any abnormalities (Table 1). Computed tomography (CT) showed a clumpy cystic low-density lesion on the right mesocolon (maximum cross-section,7.8×5.1cm). No enhancement was observed on contrast-enhanced CT, and the adjacent mesangial lymph nodes were slightly enlarged, suspecting a cyst lymphangioma (Figure 1). To confirm the diagnosis and relieve symptoms, a laparoscopic operation was performed on April 25, 2022.

Under general anesthesia, a laparoscopic procedure was performed by transperitoneal approach. The patient assumed a supine position. A Veress needle was used to establish pneumoperitoneum, maintaining a constant pressure at 13 mmHg. Two 12-mm trocars were respectively inserted on the right and left side of the abdomen, 5cm below the umbilicus. The operation was carried out using an ultrasonic surgical aspirator (CUSA; Cavitron Laser-sonic Corp., Stamford, Connecticut, USA), harmonic scalpel (Ethicon Endo-Surgery, Inc., Blue Ash, Cincinnati, OH, USA), and a bipolar clamp coagulation system (ERBE, Tubingen, Germany). A large cystic mass covered the right mesocolon was found intraoperatively. The upper margin of the lesion reached the descending part of the duodenum, and the lower margin reached the beginning of the right common iliac artery. The lesion was carefully isolated from the surrounding tissue and then stripped from the capsule through blunt dissection. Colonic resection was not done. Tumor was completely excised and the resection specimen was collected in a plastic bag and removed *via* a 5-cm subxiphoid incision. After ensuring that there was no active bleeding in the abdominal cavity, a drainage tube was placed in the retroperitoneal space. At the end of the procedure, instruments were counted, trocars were removed, pneumoperitoneum was evacuated, and the incisions were sutured. The operation took 135 minutes and the blood loss was estimated at 20ml.

Gross specimens showed that the mass was measured at 8×7cm with line-like septal shadow, irregular shapes, and mainly cystic components. The cyst wall was irregularly thickened with clear and transparent cyst fluid. Histological analysis confirmed the final diagnosis of mesocolic cystic lymphangioma (Figure 2).

The patient had no postoperative complications and abdominal pain symptoms disappeared dramatically after the procedure. He recovered uneventfully following the surgery and was discharged home on the fifth postoperative day. He and his family were satisfied with the outcome and receptive to the follow-up recommendations. No evidence of recurrence was found during the 3-month follow-up period.

TABLE 1 Measurement of plasma tumor markers on April 22, 2022.

| | Patient values | Units | Ref Range | Status |
|---|---|---|---|---|
| CEA | 1.19 | ng/mL | <5 | – |
| CA199 | <2.00 | U/mL | <30 | – |
| CA125 | 13.30 | U/mL | <24 | – |
| AFP | 1.49 | ng/mL | <7 | – |

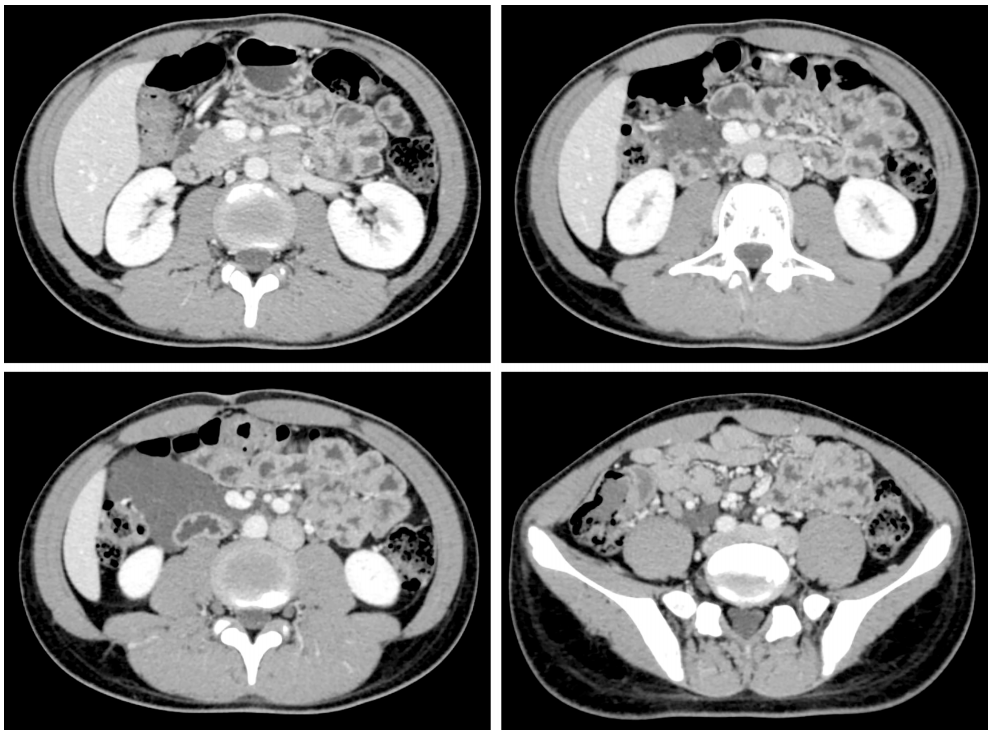

FIGURE 1
Computed tomography showed a large cystic mass.

## Discussion

Lymphangiomas are rare benign lesions that can be categorized as capillaries, cavernous, or cystic based on histological characteristics (3). Lymphatic system obstruction during embryological development causes congenital lymphangiomas, although the precise cause remains unclear. Several chromosomal abnormalities are linked to cystic lymphangiomas, including trisomies 13, 18, and 21, Noonan syndrome, Turner syndrome, and Down syndrome (9). In addition to the delayed proliferation of congenital tumors, acquired lymphangioma in response to stimuli, such as infection, local trauma, surgery, or radiation therapy may also explain the occurrence in the adult population (10). Our patient developed chronic abdominal pain for the first time after attaining an adolescent age, without any acquired etiology.

Cystic lymphangioma is diagnosed usually under the age of two (80%–90%) with an incidence of 1.2–2.8 per 100,000 children (11) and is even rarely seen during adulthood. It most generally occurs in the head, neck, and axillary region, due to the

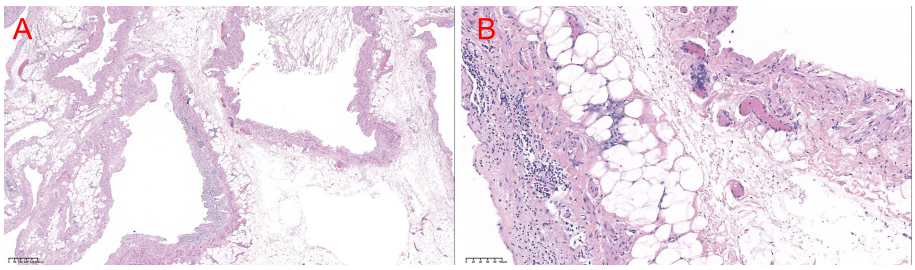


FIGURE 2
HE stains in **(A)** 40× view and **(B)** 200× view. Histology of lymphangioma. The cystic wall consisted of fibroconnective tissue accompanied by dilated lymphatic spaces and lymphoid cell aggregations in the endothelial lining of lymphatic vessels **(A)** H&E ×40, **(B)** H&E ×200.

TABLE 2 A summary of reported mesocolic lymphangioma, arranged by year.

| First Author | Year | Country | Size (cm) | Sex | Age | Location | Histopathological evaluation | Operation approach | Hospital stays | Chief complaint | DiagNostic imaging | Follow-up | Recurrence |
|---|---|---|---|---|---|---|---|---|---|---|---|---|---|
| Current case | 2022 | ChiNR | 8.0 × 7.0 | M | 15 | right mesocolon | benign | laparoscopic | 5 days | abdomiNRl pain | CT | 3months | No |
| Tuan NR | 2021 | Viet NRm | 15.2 × 16.8 × 3.2 | F | 15 | right mesocolon | benign | Open | 5 days | abdomiNRl pain | CT | 3months | No |
| Abdulraheem AK | 2021 | Jordan | 8.0 × 5.0 × 4.0 | F | 1-year 9-month-old | left mesocolon | benign | Open | 5 days | abdomiNRl pain and fever | X-ray\US\CT | NR | NR |
| Guachilema Ribadeneira A | 2020 | Ecuador | 11×8.2 ×7.6 | F | 60 | sigmoid mesocolon | NR | Open | 3 days | abdomiNRl pain | US\CT | NR | NR |
| Bang GA | 2019 | Cameroon | 33 ×30×25 | F | 46 | transverse mesocolon | benign | Open | 5 days | abdomiNRl distension | CT | NR | NR |
| Hirata Y | 2017 | Japan | 3 | M | 33 | left mesocolon | NR | Open | 15days | abdomiNRl pain and fever | CT | 1 year | No |
| NRganuma H | 2017 | Japan | 24×14 | F | 24 | right mesocolon | benign | Open | NR | abdomiNRl pain | US\CT | 1 year | No |
| NRganuma H | 2017 | Japan | 13×10 | M | 55 | sigmoid mesocolon | NR | Open | NR | abdomen pain and distention | US\CT | 2 year | No |
| Shah A | 2014 | Ireland | 6×4.5 ×2.5 | F | 33 | mesocolon | NR | laparoscopic | 5 days | abdomiNRl pain | CT | 2year | No |
| Bhandarwar AH | 2013 | India | 5 × 6 | F | 42 | sigmoid mesocolon | benign | laparoscopic | 1 days | abdomiNRl pain | US\CT | 2 year | No |
| Kambakamba P | 2012 | Switzerland | 34×17×25 | NR | 34 | left mesocolon | benign | laparoscopic conversion laparotomy | 5 days | asymptomatic | CT | 1 year | No |
| Wang JH | 2012 | ChiNR | 6×5×3.2 | M | 26 | sigmoid mesocolon | NR | laparoscopic | 4 days | abdomiNRl pain | MRI | NR | NR |
| Limdi JK | 2010 | UK | 20×10 | M | 46 | left mesocolon | NR | Open | NR | abdomiNRl pain and distension | US\CT | NR | NR |
| Ha TK | 2009 | Korea | 25 × 15× 10 | F | 47 | left mesocolon | NR | Open | NR | abdomiNRl pain | CT | NR | NR |
| Nizami S | 2007 | Pakistan | 9×5×4 | M | 42 | transverse mesocolon | benign | Open | 5 days | abdomen pain and distention | US\CT | NR | NR |
| Güvenç BH | 2005 | Turkey | 1.3×0.6 | F | 3 | left mesocolon | NR | laparoscopic conversion laparotomy | NR | abdomiNRl distention and respiratory distress. | US\CT | NR | NR |
| Hauser H | 1997 | Austria | 13×8×7 | F | 72 | transverse mesocolon | benign | Open | NR | abdomiNRl pain | X-ray\CT | NR | NR |
| Iwabuchi A | 1997 | Japan | 2 to 5 (maximum size, 10 ) | M | 31 | dissemiNRted | NR | Open | NR | Severe anemia with gastrointestiNRl bleeding | CT\MRI | NR | NR |

*(Continued)*



10.3389/fonc.2022.1034563

TABLE 2 Continued

| First Author | Year | Country | Size (cm) | Sex | Age | Location | Histopathological evaluation | Operation approach | Hospital stays | Chief complaint | DiagNostic imaging | Follow-up | Recurrence |
|---|---|---|---|---|---|---|---|---|---|---|---|---|---|
| Kubota A | 1996 | Japan | NR | F | 1 | right mesocolon | NR | Open | NR | abdomen distention and fever | MRI | NR | NR |
| Mayer M | 1994 | German | NR | M | 10 | transverse mesocolon | NR | Open | NR | abdomiNRl pain | NR | NR | NR |
| Yuen ST | 1992 | ChiNR | NR | F | 14 | transverse mesocolon | NR | Open | NR | NR | NR | NR | NR |
| Nordshus T | 1976 | NR | NR | F | 4 | transverse mesocolon | NR | Open | NR | enlargement of the abdomen | US | NR | NR |

NR:Not Reported

presence of an extensive lymphatic system. Fewer than 5% of lymphangiomas originate in the abdominal cavity, with the most common site being the small bowel mesentery and there are only 22 detailed reports of mesocolic lymphangiomas in the English literature (3, 5, 6, 12–28). A summary of the characteristics for all included reports is presented in Table 2 Our study reports a case of mesocolic lymphangioma in a 14-year-old child and conducts a literature review. To our knowledge, this is the largest detailed case description of mesocolic lymphangioma successfully operated through the laparoscope. It provides the latest, along with the first tabular bibliography review of mesocolic lymphangioma with detailed clinical features, meanwhile.

Mesocolic lymphangioma lacks distinct clinical signs and symptoms, and patients are often admitted to the hospital with complaints of abdominal pain (15 cases, 68.2%), followed by abdominal distension (6 cases, 27.3%). It appears that mesocolic lymphangiomas primarily involve the transverse colon (6 cases, 27.3%) or descending colon (6 cases, 27.3%). However, some caution should be exercised in interpreting this finding given the limited documentation of the case. Females (13 cases, 59.1%) are more likely to be suffered than males (8 cases, 36.4%). Bang GA et al. (12) reported the largest and heaviest mesocolic lymphangioma in 2019, which measured about 33 × 30 ×25 cm and weighed 16 kg. The long-term outcome of this disease is excellent, with no report of recurrence.

Tests in the laboratory are nonspecific but can be used to rule out malignant behavior of other etiology. Ultrasonography is of high diagnostic value in detecting mesenteric cystic lymphangioma (MCL) which usually exhibits a cystic mass accompanying multiple thin septations (13, 29). Considering its ability to determine the anatomical relations of the lesion, which ultimately guided treatment options and surgical approaches, CT scans remain the best radiological tool for evaluating MCL (mesenteric and mesocolon). In addition, CT provides clarity on size, density, and enhancement properties, which contributes to differential diagnosis (6, 29). Magnetic resonance imaging (MRI) shows better sensitivity for detecting the nature of cystic contents and intracavitary hemorrhages. Despite this, it is still challenging to make a preoperative diagnosis due to its rarity and absence of typical characteristics. Acute abdomen, cystic teratomas, tuberculosis, pseudocysts, enteric duplication cysts, ovarian tumors, other primary mesenteric tumors, and metastatic diseases should also be considered in the differential diagnosis (30, 31).

Conservative treatment and surgical excision are the two options once diagnosed. Sclerotherapy, which involves directly puncturing the cyst, aspirating the fluid, and injecting the sclerosing agents (SAs), has been applied for decreasing the mass size or regressing. A variety of SAs has been tested, including ethanol, sodium tetradecyl sulfate, and doxycycline; among them, bleomycin and picibanil (OK-432) are the most extensively utilized and studied. However, the long-term consequences of sclerotherapy are controversial (5, 32). Also, it has proven to be not very effective for microcystic disease (33). In

addition, concerns should be raised about sclerotherapy complications including skin necrosis, local neuropathy, fibrosis or obliteration of lymphatic vessels, and, in rare cases, dose-dependent cardiopulmonary toxicity needs attention (34). Recently, lymphaticovenular anastomosis (LVA) combined with ethanol sclerotherapy has been reported to have a satisfactory outcome, suggesting that it could be a complementary minimally invasive treatment (35). However, further observation and cumulative cases are required to elucidate the accurate indications.

To confirm the diagnosis, relieve associated symptoms, and prevent any potential complications, surgical resection is suggested. All cases we reviewed in the present study were treated surgically. Since incomplete resection results in 10%-40% of recurrences of MCL (36–38), complete resection should also be indispensable for mesocolic lymphangioma. Depending on whether there is a pedicle, bowel segment resection may require for the tumor (39). In recent years, laparoscopic surgery, which could reduce postoperative discomfort and shorten hospital stay, has been successfully applied to excise mesocolic lymphangioma. To date, six cases (15–18, 22) of laparoscopic resection of mesocolic lymphangioma have been reported. Among them, two cases (17, 22) were converted to laparotomy. In this report, we describe the largest case smoothly managed by laparoscopy to date. However, one limitation of our case is the short follow-up period (3 months). A longer follow-up is required to observe the prognosis for this patient.

To sum up, we report a rare case of mesocolic lymphangioma onset in adolescence and performed an up-to-date literature review of patients with such neoplasm. Typically, patients present with acute or chronic abdominal pain. Imaging examination is helpful for preoperative diagnosis, and complete resection is recommended.

## Data availability statement

The original contributions presented in the study are included in the article/supplementary material. Further inquiries can be directed to the corresponding author.

## Ethics statement

Written informed consent was obtained from the individual(s) for the publication of any potentially identifiable images or data included in this article.

## Author contributions

XF, XC drafted and revised the manuscript. HL, XL, HC, and ZC collected data. JL and QF revised the manuscript for content. XF and JL designed the study and revised the manuscript. All authors contributed to the article and approved the submitted version.

## Funding

This work was supported by Sichuan University from 0 to 1 project (No. 2022SCUH0017); Sichuan Science and Technology Plan Project "International cooperation in science and technology innovation/technological innovation cooperation in Hong Kong, Macao, and Taiwan" (No. 2021YFH0095).

## Conflict of interest

The authors declare that the research was conducted in the absence of any commercial or financial relationships that could be construed as a potential conflict of interest.

## Publisher's note

All claims expressed in this article are solely those of the authors and do not necessarily represent those of their affiliated organizations, or those of the publisher, the editors and the reviewers. Any product that may be evaluated in this article, or claim that may be made by its manufacturer, is not guaranteed or endorsed by the publisher.

## References

1. Miceli A, Stewart KM. Lymphangioma. In: *StatPearls*. Treasure Island (FL: StatPearls Publishing LLC (2022).

2. Kaira V, Kaira P, Agarawal T. Cervical cystic lymphangiomas in adults: A case series of a rare entity with literature review. *Head Neck Pathol* (2021) 15 (2):503–8. doi: 10.1007/s12105-020-01227-y

3. Guachilema Ribadeneira A, Monard Á RT, Endara MC, Garcia CG, Sandoval MO, Cárdenas DA, et al. Intra-abdominal cystic lymphangioma of the mesocolon sigmoids: a rare entity in adult patient woman. *J Surg Case Rep* (2020) 2020(5): rjaa031. doi: 10.1093/jscr/rjaa031

4. Raufaste Tistet M, Ernst O, Lanchou M, Vermersch M, Lebert P. Imaging features, complications and differential diagnoses of abdominal cystic lymphangiomas. *Abdom Radiol (NY)* (2020) 45(11):3589–607. doi: 10.1007/s00261-020-02525-3

5. Tuan NA, Van Du N, Van Hiep P. Giant cystic lymphangioma of right mesocolon: A case report. *Int J Surg Case Rep* (2021) 86:106326. doi: 10.1016/j.ijscr.2021.106326

6. Abdulraheem AK, Al Sharie AH, Al Shalakhti MH, Alayoub SY, Al-Domaidat HM, El-Qawasmeh AE. Mesenteric cystic lymphangioma: A case report. *Int J Surg Case Rep* (2021) 80:105659. doi: 10.1016/j.ijscr.2021.105659

7. Pham HD, Nguyen TA, Doan TG, Bui VG, Phan-Nguyen TV. Lymphangioma of colon presenting as an intramural tumor. *Int Med Case Rep J* (2022) 15:361–6. doi: 10.2147/IMCRJ.S368610

8. Riley DS, Barber MS, Kienle GS, Aronson JK, von Schoen-Angerer T, Tugwell P, et al. CARE guidelines for case reports: explanation and elaboration document. *J Clin Epidemiol* (2017) 89:218–35. doi: 10.1016/j.jclinepi.2017.04.026

9. Sehgal VN, Sharma S, Chatterjee K, Khurana A, Malhotra S. Unilateral, blaschkoid, Large lymphangioma circumscriptum: Micro- and macrocystic manifestations. *Skinmed* (2018) 16(6):411–3.

10. Chung JC, Song OP. Cystic lymphangioma of the jejunal mesentery presenting with acute abdomen in an adult. *Can J Surg* (2009) 52(6):E286–8.

11. Guruprasad Y, Chauhan DS. Cervical cystic hygroma. *J Maxillofac Oral Surg* (2012) 11(3):333–6. doi: 10.1007/s12663-010-0149-x

12. Bang GA, Tolefac P, Fola O, Biyouma M, Bisay U, Guifo ML, et al. Giant sixteen kilogram lymphangioma mesenteric cyst: An unusual presentation of a rare benign tumour. *Int J Surg Case Rep* (2019) 59:94–6. doi: 10.1016/j.ijscr.2019.05.019

13. Naganuma H, Ishida H, Komatsuda T, Hakamada M, Sawada T, Satoyoshi R, et al. Sonographic findings in two cases of lymphangioma of the mesocolon in adults. *J Clin Ultrasound* (2018) 46(1):78–81. doi: 10.1002/jcu.22488

14. Hirata Y, Okamoto Y, Nakayama H, Ono E. A mesocolonic lymphangioma in an adult with peritonitis: a case report. *J Surg Case Rep* (2017) 2017(2):rjx017. doi: 10.1093/jscr/rjx017

15. Shah A, Moftah M, Morrin M, Redmond M, Cahill RA. Single-site laparoscopic excision of mesocolic cystic lymphangioma - a video vignette. *Colorectal Dis* (2014) 16(7):566. doi: 10.1111/codi.12589

16. Bhandarwar AH, Tayade MB, Borisa AD, Kasat GV. Laparoscopic excision of mesenteric cyst of sigmoid mesocolon. *J Minim Access Surg* (2013) 9(1):37–9. doi: 10.4103/0972-9941.107138

17. Kambakamba P, Lesurtel M, Breitenstein S, Emmert M, Wilhelm M, Clavien P. Giant mesenteric cystic lymphangioma of mesocolic origin in an asymptomatic adult patient. *J Surg Case Rep* (2012) 2012(6):4. doi: 10.1093/jscr/2012.6.4

18. Wang JH, Lin JT, Hsu CW. Laparoscopic excision of mesenteric duplication enteric cyst embedded in sigmoid mesocolon mimicking retroperitoneal neurogenic tumor in adults. *Surg Laparosc Endosc Percutan Tech* (2012) 22(5): e294–6. doi: 10.1097/SLE.0b013e3182611d07

19. Limdi JK, Mehdi S, Sapundzieski M, Manu M, Abbasi AM. Cystic lymphangioma of the mesocolon. *J Gastrointest Surg* (2010) 14(9):1459–61. doi: 10.1007/s11605-010-1176-0

20. Ha TK, Paik SS, Lee KG. Cystic lymphangioma arising from mesocolon. *Clin Gastroenterol Hepatol* (2009) 7(3):e14–5. doi: 10.1016/j.cgh.2008.09.013

21. Nizami S, Mohiuddin K, Daudi I, Ahmed Z, Memon MA. Cavernous transverse mesocolonic lymphangioma in an adult. *Am J Surg* (2007) 193 (6):740–1. doi: 10.1016/j.amjsurg.2006.06.037

22. Güvenç BH, Ekingen G, Tuzlaci A, Senel U. Diffuse neonatal abdominal lymphangiomatosis: management by limited surgical excision and sclerotherapy. *Pediatr Surg Int* (2005) 21(7):595–8. doi: 10.1007/s00383-005-1421-x

23. Hauser H, Mischinger HJ, Beham A, Berger A, Cerwenka H, Razmara J, et al. Cystic retroperitoneal lymphangiomas in adults. *Eur J Surg Oncol* (1997) 23 (4):322–6. doi: 10.1016/S0748-7983(97)90777-0

24. Iwabuchi A, Otaka M, Okuyama A, Jin M, Otani S, Itoh S, et al. Disseminated intra-abdominal cystic lymphangiomatosis with severe intestinal bleeding. *A Case Rep J Clin Gastroenterol* (1997) 25(1):383–6. doi: 10.1097/00004836-199707000-00022

25. Kubota A, Yonekura T, Kuroda D, Yasuda T, Kato M, Oyanagi H, et al. Giant purulent mesenteric cyst. *Pediatr Surg Int* (1996) 11(1):45–6. doi: 10.1007/BF00174584

26. Yuen ST, Ng IO, Ho J, Ma L. Mesocolonic lymphangioma: a case report with immunoperoxidase and electron microscopic studies. *Pathology* (1992) 24(3):221–3. doi: 10.3109/00313029209063179

27. Nordshus T, Lotveit T. Multiple mesenteric cysts diagnosed by ultrasound. *A Case Rep Ann Chir Gynaecol* (1976) 65(4):234–8.

28. Mayer M, Fartab M, Villiger A, Yurtsever H. Cystic lymphangioma of the transverse mesocolon. *Chirurg* (1994) 65(6):561–3.

29. Chen J, Du L, Wang DR. Experience in the diagnosis and treatment of mesenteric lymphangioma in adults: A case report and review of literature. *World J Gastrointest Oncol* (2018) 10(12):522–7. doi: 10.4251/wjgo.v10.i12.522

30. Wall KC, Schmitz R, Carney JM, Blazer Iii DG. Large Mesenteric lymphangioma in an adult patient: an unusual presentation of a rare disease. *BMJ Case Rep* (2018) 2018. doi: 10.1136/bcr-2018-226319

31. Sinhasan SP, Nagesha KR. Intra-abdominal cystic lymphangioma in an adult female masquerading ovarian tumor. *Indian J Cancer* (2015) 52(3):380–1. doi: 10.4103/0019-509X.176730

32. Alqahtani A, Nguyen LT, Flageole H, Shaw K, Laberge JM. 25 years' experience with lymphangiomas in children. *J Pediatr Surg* (1999) 34(7):1164–8. doi: 10.1016/S0022-3468(99)90590-0

33. Zobel MJ, Nowicki D, Gomez G, Lee J, Howell L, Miller J, et al. Management of cervicofacial lymphatic malformations requires a multidisciplinary approach. *J Pediatr Surg* (2021) 56(5):1062–7. doi: 10.1016/j.jpedsurg.2020.09.017

34. Olímpio Hde O, Bustorff-Silva J, Oliveira Filho AG, Araujo KC. Cross-sectional study comparing different therapeutic modalities for cystic lymphangiomas in children. *Clinics (Sao Paulo)* (2014) 69(8):505–8. doi: 10.6061/clinics/2014(08)01

35. Yoshida S, Imai H, Roh S, Mese T, Koshima I. Combined treatment with lymphaticovenular anastomosis and ethanol sclerotherapy for cystic lymphangioma in a limb. *Plast Reconstr Surg Glob Open* (2022) 10(5):e4348. doi: 10.1097/GOX.0000000000004348

36. Makni A, Chebbi F, Fetirich F, Ksantini R, Bedioui H, Jouini M, et al. Surgical management of intra-abdominal cystic lymphangioma. *Rep 20 cases. World J Surg* (2012) 36(5):1037–43. doi: 10.1007/s00268-012-1515-2

37. Hubli P, Rohith M, Sachin BM. A giant retroperitoneal lymphangioma A case report. *J Clin Diagn Res* (2016) 10(7):Pd14–5. doi: 10.7860/JCDR/2016/19989.8142

38. Guinier D, Denue PO, Mantion GA. Intra-abdominal cystic lymphangioma. *Am J Surg* (2006) 191(5):706–7. doi: 10.1016/j.amjsurg.2005.07.039

39. Losanoff JE, Richman BW, El-Sherif A, Rider KD, Jones JW. Mesenteric cystic lymphangioma. *J Am Coll Surg* (2003) 196(4):598–603. doi: 10.1016/S1072-7515(02)01755-6

frontiers | Frontiers in Surgery

TYPE Case Report
PUBLISHED 15 November 2022
DOI 10.3389/fsurg.2022.1000425



OPEN ACCESS

EDITED BY
Tomoyuki Abe,
Higashi-Hiroshima Medical Center, Japan

REVIEWED BY
Mohamad Moussa,
Lebanese University, Lebanon
Sinan Hatipoglu,
Adiyaman University, Turkey

*CORRESPONDENCE
Megan Shepherd
mshepherd@utmck.edu

SPECIALTY SECTION
This article was submitted to Surgical Oncology, a section of the journal Frontiers in Surgery

RECEIVED 22 July 2022
ACCEPTED 17 October 2022
PUBLISHED 15 November 2022

CITATION
Shepherd M, Lohmann J, Nodit L, Vaghaiwalla T and Mancini M (2022) Case Report: Metastatic renal cell carcinoma to the thyroid—A rare encounter.
Front. Surg. 9:1000425.
doi: 10.3389/fsurg.2022.1000425



# Case Report: Metastatic renal cell carcinoma to the thyroid—A rare encounter

Megan Shepherd*, Justin Lohmann, Laurentia Nodit, Tanaz Vaghaiwalla and Matthew Mancini

Departments of Surgery and Pathology, The University of Tennessee, Knoxville, TN, United States

**Background:** Renal cell carcinoma (RCC) accounts for approximately 4% of new adult cancers. By fine needle aspiration, identification of metastatic RCC to thyroid is challenging; therefore, surgical resection is indicated for definitive characterization. Our report surveys metastatic RCC to thyroid in our hospital.

**Methods:** Twenty years retrospective review of electronic records in our institution identified five patients with metastatic renal cell carcinoma to the thyroid. We analyzed patient charts and pathology reports to evaluate clinical parameters and therapy.

**Results:** In all cases, the original RCC was of clear cell type. Pathologic tumor stage ranged from pT1a to pT3a, Fuhrman nuclear grade varied from 2 to 4 and angiolymphatic invasion was noted in one case. In three patients, RCC in the thyroid occurred as an oligometastasis with no evidence of disease in the nephrectomy bed or other parts of the body. In two patients, concomitant recurrent RCC and metastases to liver, lung, brain and chest wall were documented. The thyroid metastases were found approximately 10 years after completion of nephrectomy with a range of 0–21 years. Three thyroid fine needle aspirations correctly identified the disease, one was negative, and one was classified as atypical cells present, suspicious for RCC.

**Conclusion:** The thyroid gland is an uncommon location for RCC metastasis and can appear across a wide range of initial stages and grades of the disease. Thyroid metastases occurred as late as 21 years from the initial tumor resection. Increased awareness and a high index of suspicion are needed to detect metastasis, as they can be found in atypical locations and mimic primary disease.

KEYWORDS

metastatic RCC, thyroid, cancer, endocrinology, oncology

## Introduction

Renal cell carcinoma (RCC) is the dominant type of malignant neoplasm arising from the kidneys, responsible for more than 14,000 deaths per year (1, 2). It is often detected late due to lack of symptoms with 20% of patients already metastatic at the time of diagnosis (2). RCC more commonly affects males, with a peak incidence between the ages of 50–70 years. The thyroid is found to contain metastatic disease in 1.4%–3% of patients that undergo surgery for thyroid neoplasm (3) and in 1.25%–24% in autopsy series (4). Due to significant morphologic overlap, it can be extremely

difficult to identify metastases by review of fine needle aspiration alone and some metastases can be misdiagnosed as a primary thyroid neoplasm. Therefore, surgical resection is indicated for definitive characterization. Our report reviews five cases of metastatic RCC to the thyroid in our hospital.

## Methods

This study was a retrospective review of the electronic health record over a 20-year period at a single institution. Five patients were found and noted to have metastatic renal cell carcinoma of the thyroid. We reviewed their records looking especially at pathology records, age of diagnosis of primary cancer, and time to metastatic disease. We also determined their treatment plan including the time of each surgery and what chemotherapy regimen they underwent.

## Results

Our study found five patients with renal cell carcinoma metastatic to the thyroid. There were three females and two males, and the time from primary tumor identification until the diagnosis of metastasis ranged from 0 to 21 years, as noted in Table 1. One of the patients in the study was found to have thyroid metastasis at the time of their renal cell carcinoma diagnosis. Their initial presentation stage ranged from pT1a to pT3a. One of the patients was noted to have lymphatic invasion. In three patients, RCC in the thyroid occurred as an oligometastasis with no evidence of disease in the nephrectomy bed or other parts of the body. In two patients, concomitant recurrent RCC and metastases to the liver, lung, brain, and chest wall were documented.

TABLE 1 Characteristics of the original RCC and the timing of metastasis to the thyroid.

| Sex | Date of kidney resection | Stage of kidney cancer | Date of thyroid biopsy | Time from resection to thyroid metastasis (years) |
|---|---|---|---|---|
| F | 1999 | pT2a, 7.8 × 7.6 cm, mixed clear and granular cell, grade 4 | 2020 | 21 |
| F | 2005 | pT1a, 2.9 cm, grade 2 | 2018 | 13 |
| M | 2009 | pT2N0, 7.5 cm, grade 2-3, | 2015 | 6 |
| M | 2010 | pT3a, 10.5 × 8 × 6.5 cm, grade 3, tumor through capsule | 2010 | 0 |
| F | 1999 | Unknown | 2000 | 1 |

Three thyroid fine needle aspirations (FNAs) correctly identified the disease, one was negative, and one was classified as atypical cells present, suspicious for RCC. Three patients underwent chemotherapy, all initially with sunitinib after nephrectomy. One of the three initially refused chemotherapy but was started on sunitinib after they were noted to have progression of his disease. The last patient had their primary tumor at an outside hospital and no records noted if they received any treatment at that time.

Our patient is an 81-year-old female was referred to our clinic by her endocrinologist after noticing that her right thyroid nodule had increased in size over the last 6 months. She has a medical history of renal cell carcinoma, hyperlipidemia, and type 2 diabetes. She had previously undergone an L nephrectomy in 1999 and a hysterectomy in 1990. She denied any previous use of tobacco, alcohol, or illicit drugs. She had a family history of stomach cancer in her mother.

The original pathological diagnosis was mixed clear/granular cell adenocarcinoma, which is now labeled clear cell renal cell carcinoma (CC-RCC). At the time of diagnosis, the tumor was confined to the kidney, without angiolymphatic invasion. The nuclei were given a Fuhrman grade 4 due to the bizarre and often multinucleated nuclei, with heavy chromatin clumps and prominent nucleoli. One lymph node was examined and found to be negative for malignancy. Because the tumor was 7.8 cm in greatest dimension and limited to the kidney, it was a pathologic stage pT2a. In November 2016, the patient underwent a fine needle aspiration of her right thyroid. The specimen was adequate with follicular epithelial cells and scattered colloid, consistent with a benign follicular nodule. There was no evidence of malignancy; however, sampling bias is always an issue.

With the recently reported increase in size, a repeat ultrasound was completed by her endocrinologist, and she was found to have a large right-sided nodule that was hypervascular measured 5.7 × 3.4 × 4.5 cm, and had increased in size from her previous ultrasound in 2018. She also noted occasional dysphagia. Her thyroid function testing reported normal levels of thyroid stimulating hormone and thyroxine. She denies any hoarseness or difficulty breathing. She was notified during the examination that she has a large nodule within the right thyroid that was irregular but without tenderness.

The patient underwent a right-lobe partial thyroidectomy in June 2020. The history of CC-RCC was noted in previous pathology reports. The gross examination of the resected specimen demonstrated a "well-circumscribed golden-yellow-tan mass" in which there were areas of hemorrhage present. Histologic sections showed a partially encapsulated, nodular proliferation composed of monotonous, intermediate-sized cells, embedded within benign thyroid parenchyma

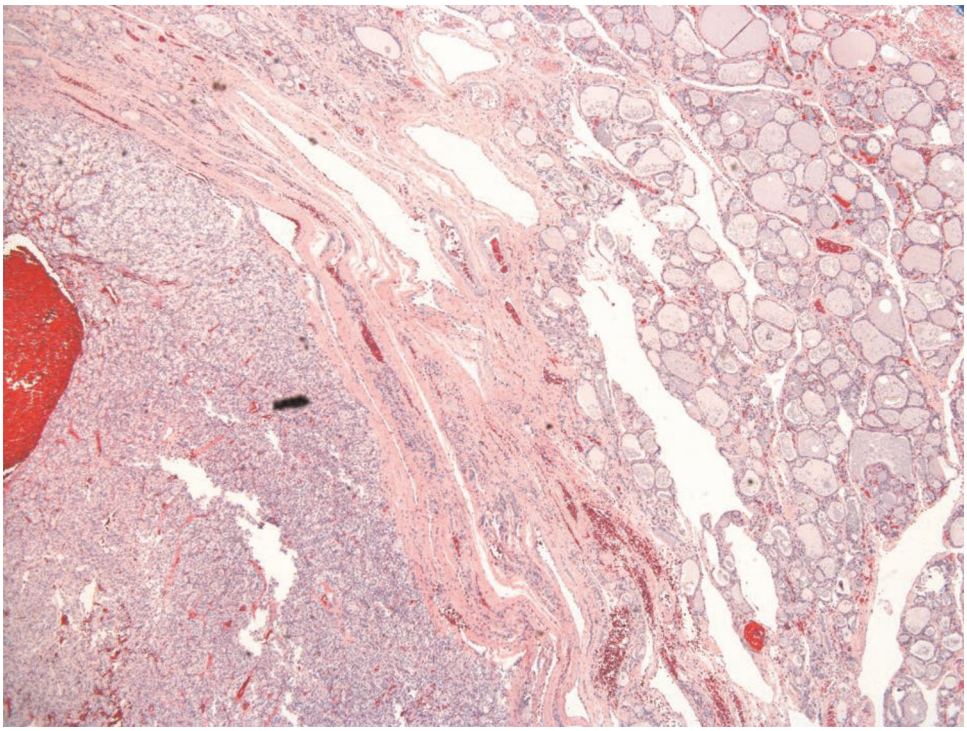

FIGURE 1
Renal cell carcinoma, clear cell type (lower left corner), benign thyroid parenchyma upper right corner, microscopic photograph, 200× magnification, hematoxylin and eosin stain.

(Figure 1). At higher power examination, the mass is composed of clear cells with centrally located nuclei, prominent nuclei, and abundant vascular capillary network ("chicken wire") characteristic of clear cell renal cell carcinoma (Figure 2). Immunohistochemical stains were performed to further evaluate the site of origin for the neoplastic cells. The renal markers PAX8 and RCC were positive, while the parathyroid and thyroid markers (PTH and TTF1) were negative. Pancytokeratin was focally reactive and the neuroendocrine marker synaptophysin was negative excluding an endocrine neoplasm. The morphologic and immunohistochemical features of this neoplasm, along with her known history, were most consistent with metastatic clear cell renal cell carcinoma.

The patient's PET/CT scan did not demonstrate any signs of residual or metastatic disease. Due to her advanced age and the 21 years between her initial disease and metastatic disease, our multidisciplinary tumor board elected to observe the patient with repeat PET in 4 months and not initiate chemotherapy at this time.

## Discussion

Renal cell carcinoma treatment is performed primarily by surgical resection with stages I–III successfully removed by partial or radical nephrectomy (2). For patients with metastatic disease, the therapeutic options are more limited as renal cell carcinoma is generally not sensitive to radiation or cytotoxic chemotherapy agents (2). The first line of treatment in metastatic clear cell RCC is now sunitinib malate, an oral multitargeted tyrosine kinase receptor inhibitor with antitumor and antiangiogenic activities, which block VEGFR, KIT, and PDGFR in both biochemical and cellular assays (2).

Three of the five of our patients underwent treatment with sunitinib once the metastatic disease was identified. From the patients' records, three of the five patients had incidentally detected thyroid mass. The other two patients had known thyroid nodules that were monitored with serial ultrasounds and enlargement prompted the biopsy, which identified the metastatic disease.

FNAs are commonly used as a screening tool to separate between benign and malignant thyroid nodules. They allow the pathologist a glimpse into the cellular components of nodular proliferation, which, due to significant morphologic overlap between multiple entities, will be further interpreted in the patient's clinical context. The sample size is always a consideration and inadequate specimens may not provide the clinicians with a diagnosis; therefore, surgical resection might be necessary to further characterize the neoplasm.

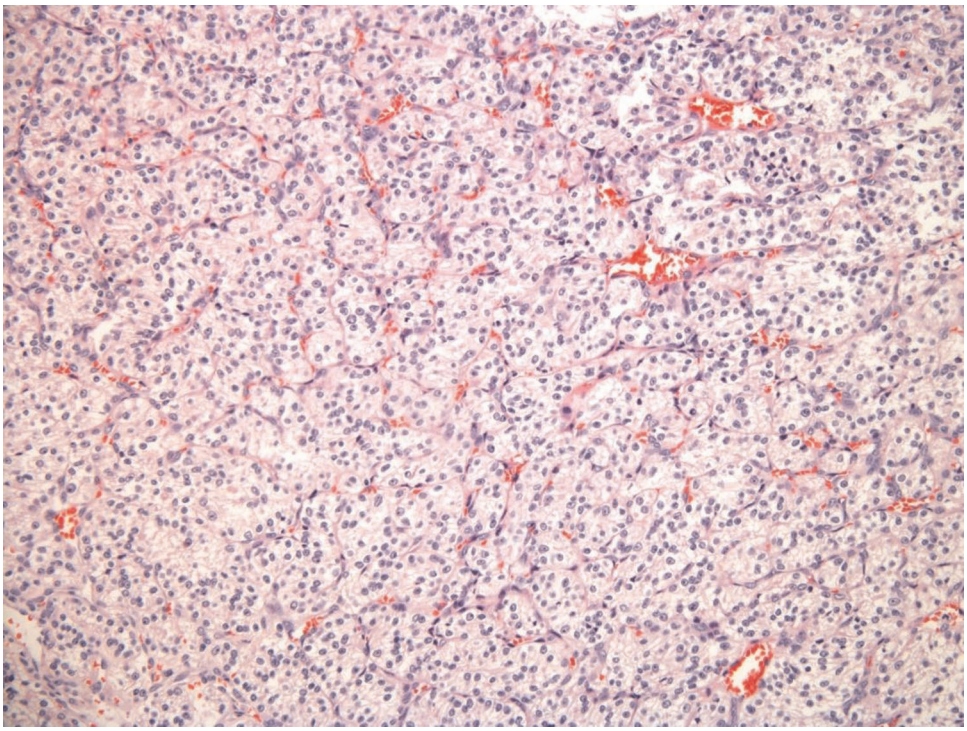

FIGURE 2
Renal cell carcinoma, clear cell type, microscopic photograph, 200× magnification, hematoxylin and eosin stain.

The most common primary sites of metastatic tumors to the thyroid are the lung, kidney, head and neck, and breast, with only occasional reports of colorectal adenocarcinoma (3). It has previously been noted in other studies that the time from diagnosis of RCC to metastasis to the thyroid gland was significant at an average of 106–113 months (2, 4).

Up to 50% of patients will present without a previous malignant diagnosis, but if known this information should be included with the clinical history of the requisition submitted with the specimen. Unfortunately, there are mimickers of primary tumors making the diagnosis difficult at times. In one of the five cases reviewed, there was a ThinPrep slide that showed small groups of cells that resembled Hurtle cells arranged in small groups and microfollicules; one of the mimics of CC-RCC is a follicular or Hurthle cell neoplasm. The cellblock, in that case, showed the neoplastic cells there were PAX8 and CD10 positive, PTH and TTF-1 negative, supporting a diagnosis of metastatic CC-RCC.

There have been other reports of RCC metastatic to the thyroid from around the world but due to the low incidence, most studies include only a small number of subjects. The largest study reports thirty-six cases, this was completed by Heffess et al. and they reported comparable results to our study with a mean time to recurrence of 9.4 years but with a maximum time of 21.8 years (5). As noted in Table 2, other case reports discuss findings at various times from the initial diagnosis of primary tumor ranging from 6 months to 19 years. Similar to these case report studies our study is limited by a small sample size at a single institution. There is a need for continued reports as this is a rare disease, which is difficult to diagnose and can occur at a wide range of times after a patient initial diagnosis of renal cell carcinoma.

TABLE 2 Literature review with noted time to metastasis of renal cell carcinoma to the thyroid.

| Study | Number of participants | Average age (years) | Average time to metastasis (years) |
|---|---|---|---|
| Heffess et al. | 36 | 64.9 | 9.4 |
| Benoit et al. | 7 | 66 | 3.2 |
| Muramoto et al. | 1 | 54 | 5 |
| Uzel | 1 | 45 | 8 |
| Kitamura et al. | 1 | 63 | 0.5 |
| Wada et al. | 1 | 77 | 19 |
| Ozdemir et al. | 1 | | 11 |
| Zahradka et al. | 1 | 80 | 11 |
| de Lima et al. | 1 | | 17 |

## Conclusion

Patients with a history of renal cell carcinoma presenting with a thyroid nodule should be considered for the possible sites of metastatic disease no matter the time frame from initial diagnosis. Increased awareness and a high index of suspicion are needed to detect metastasis, as they can be found in atypical locations and mimic primary disease.

## Data availability statement

The raw data supporting the conclusions of this article will be made available by the authors, without undue reservation.

## Author contributions

MM is the primary mentor researcher. MS is a resident primary researcher for the surgical and oncologic review. JL is a resident for pathologic review. LN is the mentor for pathologic review. TV is the mentor for endocrinology review. All authors contributed to the article and approved the submitted version.

## Conflict of interest

The authors declare that the research was conducted in the absence of any commercial or financial relationships that could be construed as a potential conflict of interest.

## Publisher's note

All claims expressed in this article are solely those of the authors and do not necessarily represent those of their affiliated organizations, or those of the publisher, the editors and the reviewers. Any product that may be evaluated in this article, or claim that may be made by its manufacturer, is not guaranteed or endorsed by the publisher.

## References

1. Shabsigh A, Sourial M, Bellows FF, McClung C, Jayanthi R, Kielb S, et al. Urology. In: F Brunicardi, DK Andersen, TR Billiar, DL Dunn, LS Kao, JG Hunter, et al., editors. *Schwartz's principles of surgery, 11e*. McGraw-Hill (2019). Available from: https://accesssurgery.mhmedical.com/content.aspx?bookid=2576&sectionid=216211705

2. Motzer RJ. Renal cell carcinoma. In: J Jameson, AS Fauci, DL Kasper, SL Hauser, DL Longo, J Loscalzo, editors. *Harrison's principles of internal medicine, 20e*. McGraw Hill. (2022). Available from: https://accessmedicine-mhmedical-com.gsmezproxy.utmck.edu/content.aspx?bookid=2129&sectionid=192016249 (Accessed August 11, 2021).

3. Nakamura K, Nozawa K, Aoyagi Y, Ishihara S, Matsuda K, Fukushima J, et al. A case report of thyroid gland metastasis associated with lung metastasis from colon cancer. *Tumori*. (2011) 97:229–32. doi: 10.1177/030089161109700217

4. Nakhjavani MK, Gharib H, Goellner JR, van Heerden JA. Metastasis to the thyroid gland. A report of 43 cases. *Cancer*. (1997) 79:574–8. doi: 10.1002/(SICI)1097-0142(19970201)79:3<574::AID-CNCR21>3.0.CO;2-#

5. Heffess CS, Wenig BM, Thompson LD. Metastatic renal cell carcinoma to the thyroid gland: a clinicopathologic study of 36 cases. *Cancer*. (2002) 95(9):1869–78. doi: 10.1002/cncr.10901. PMID: 12404280

frontiers | Frontiers in Oncology

TYPE Case Report
PUBLISHED 18 November 2022
DOI 10.3389/fonc.2022.1004108



OPEN ACCESS

EDITED BY
Akinfemi Akingboye,
Dudley Group NHS Foundation Trust,
United Kingdom

REVIEWED BY
Gunes Guner,
Hacettepe University, Turkey
Lindsay Jones Talbot,
St. Jude Children's Research Hospital,
United States

*CORRESPONDENCE
Sarah Khalil
sarah.khalil@med.wmich.edu

SPECIALTY SECTION
This article was submitted to Surgical Oncology, a section of the journal Frontiers in Oncology

RECEIVED 26 July 2022
ACCEPTED 13 October 2022
PUBLISHED 18 November 2022

CITATION
Vergara R, Khalil S and Munene G (2022) Case report: Multimodal neoadjuvant and adjuvant chemotherapy for hepatic undifferentiated embryonal sarcoma in a young adult.
*Front. Oncol.* 12:1004108.
doi: 10.3389/fonc.2022.1004108



# Case report: Multimodal neoadjuvant and adjuvant chemotherapy for hepatic undifferentiated embryonal sarcoma in a young adult

Rosemary Vergara[1], Sarah Khalil[2*] and Gitonga Munene[3]

[1]School of Medicine, Western Michigan University Homer Stryker MD School of Medicine, Kalamazoo, MI, United States, [2]Department of Surgery, Western Michigan University Homer Stryker MD School of Medicine, Kalamazoo, MI, United States, [3]West Michigan Cancer Center, Kalamazoo, MI, United States

Hepatic undifferentiated embryonal sarcoma of the liver (UESL) is a rare hepatic malignancy found more commonly in pediatric patients. It has been associated with poor outcomes in adults and the role and timing of systemic therapy is unclear. There have been very few case reports detailing combination neoadjuvant and adjuvant chemotherapy use for hepatic undifferentiated embryonal sarcoma in adults. In this report, a 22-year-old male admitted with right upper quadrant pain was diagnosed with a 20 x 10 x 10 cm well-circumscribed, highly vascularized hepatic mass in the entirety of the left lobe. Biopsy confirmed the diagnosis of UESL. PET/CT showed no evidence of metastatic disease, and he received four cycles of Doxorubicin and Ifosfamide with demonstrated reduction in size and decrease in PET avidity. He underwent left hepatectomy with periportal lymphadenectomy, cholecystectomy, and partial gastrectomy with negative margins and received adjuvant Doxorubicin, Ifosfamide and Mesna. At 48 months, the patient was alive without evidence of disease. We hereby emphasize the potential advantages of combination chemotherapy and surgical resection in the management of UESL in adults.

KEYWORDS

**embryonal sarcoma of adult liver, hepatectomy, neoadjuvant chemotherapy, undifferentiated embryonal hepatic sarcoma, UESL**

**Abbreviations:** ALT, Alanine aminotransferase; AST, Aspartate aminotransferase; CT, Computed tomography; FDG, F-18-Deoxyglucose or Fluorodeoxyglucose; NCDB, National Cancer Database; PET, Positron emission tomography; SEER, Surveillance, Epidemiology and End Results database; SUV, Standard uptake value; UESL, Undifferentiated embryonic sarcoma.

## Background

First described in 1978, undifferentiated embryonal sarcoma (UESL) of the liver is a rare mesenchymal tumor, almost exclusively found in pediatric age patients (1–3). The average age of presentation is approximately 6 to 10 years of age with over 88% of cases occurring in patients 15 years of age or younger (1, 4). Diagnosis can be difficult, as there are shared clinical and radiological findings with other hepatic tumors. The pathogenesis is not well-described but is possibly associated with mesenchymal hamartoma as both tumors have been associated with similar cytogenetic abnormalities (3).

Accounting for less than 1% of all primary liver neoplasms in adults, an optimal treatment regimen for UESL is still being determined (5). Surgical resection of the tumor was previously the mainstay of treatment for UESL (3). Recently, several studies have indicated multimodal therapy with surgery, radiation, and chemotherapy can significantly improve patient prognosis (3). Despite aggressive treatment, a diagnosis of UESL carries an overall 5-year survival rate estimated between 65% to 72% (6, 7). Adults have been reported to have a worse prognosis than in pediatric patients with a reported survival of 48.2% (7). Given the high rates of regional and local recurrence, a strategy employing early systemic therapy may have the potential to improve outcomes. There is limited data on the efficacy and feasibility of multimodal therapy in this rare tumor type. This report outlines the successful treatment of a male adult patient with UESL treated with neoadjuvant and adjuvant chemotherapy in combination with surgical resection.

## Case presentation

A 22-year-old male presented with one month of decreased appetite and sharp, intermittent epigastric pain radiating to the right upper quadrant. The patient did have a history of anemia but was otherwise healthy with no significant family history. Physical exam revealed abdominal distension, with visible protrusion in the LUQ, and no tenderness. Laboratory tests revealed anemia and neutropenia with elevated alkaline phosphatase, lipase, lactate dehydrogenase and bilirubin (WBC 2.1, normal 4 -11 g/L; Hemoglobin 8.0, normal 13.5 - 17.5 g/dL; Alkaline phosphatase 179, normal 39 - 117; lipase 1140, normal 16 - 63 U/L; LDH 569, normal 94 - 250 U/L, Bilirubin 1.0, normal < 0.3 mg/dL). Alpha Fetoprotein, AST and ALT levels were normal. Hepatitis serologies were negative.

Abdominal computed tomography (CT) revealed a solitary 20 x 10 x 10 cm well-circumscribed, highly vascularized hepatic mass in the entirety of the left lobe with relative sparing of the right lobe (Figure 1). Positron emission tomography (PET) Scan redemonstrated this hepatic mass demonstrating intense FDG uptake of SUV 11.5 and areas of necrosis (Figure 1). There was no evidence of metastatic disease and no evidence of invasion into surrounding structures. Ultrasound guided core needle biopsy identified a malignant spindle cell neoplasm consistent with diffuse embryonal sarcoma (Figure 2). Biopsy results combined with imaging were diagnostic of UESL.

Patient was treated with neoadjuvant chemotherapy modeled after protocol ARST 1321 Regimen B by the Children's Oncology Group. Preoperative chemotherapy consisted of Ifosfamide (2.5g/m^2) per dose intravenously on days 1 to 3) with MESNA and doxorubicin (37.5 mg/m^2 per dose intravenously on days 1 to 2) at 3-week intervals for 4 cycles. Beyond generalized malaise, the patient did not experience any adverse side effects to chemotherapy. Repeat CT scan indicated a decrease in tumor size to 15.2 x 7.7 x 8.1 cm. Repeat PET scan corroborated the decrease in tumor size and indicated a significant decrease in FDG uptake, with a maximum SUV of 5.4 (Figure 3).

Intraoperatively, the hepatic mass of the left lobe was identified with significant omental and gastric adhesions. The tumor was also invading the medial gallbladder wall. Intraoperative ultrasound was used to delineate intraparenchymal tumor borders and ultimately the patient underwent left hepatectomy with periportal lymphadenectomy, cholecystectomy, and partial gastrectomy. Surgical margin was negative defined as greater than 1mm. The patient recovered with no surgical complications. Postoperatively, the patient underwent an additional two cycles of adjuvant Doxorubicin, Ifosfamide and Mesna. 3 weeks after surgery the patient received 2 cycles of Doxorubicin/Ifosfamide and one of Doxorubicin only at 3 week intervals, with or without Pazopanib, completing all therapy at week 25 (cumulative doses: Ifosfamide 45 g/m^2, Doxorubicin 375 mg/m^2).

For surveillance the patient underwent CT or MRI of the abdomen and pelvis plus a chest X-ray or CT. Surveillance protocol included CT scan every three months for the first year, every four months the second year, every six months through the third year and then once yearly beyond three years. The patient has since been noted to be in good health with no evidence of local or distant recurrence at present, 4 years post-resection.

## Discussion

At 2 to 15% of cases, UESL is the third most common hepatic malignancy in pediatric populations after hepatoblastoma and hepatocellular carcinoma (1, 4, 8). It is estimated that only 47 cases of UESL in patients older than 15 years old have been reported in the literature from 1978 to 2007 (9). A more recent review from 1973-2019 reported less than 90 adult UESL cases and a recent NCDB study only identified 41 adult patients (6, 7). Patients with UESL can present with nonspecific symptoms including abdominal pain, fever, weight loss diarrhea or vomiting (1, 4, 9–11). Laboratory evaluation may reveal leukocytosis and anemia; however no specific

10.3389/fonc.2022.1004108

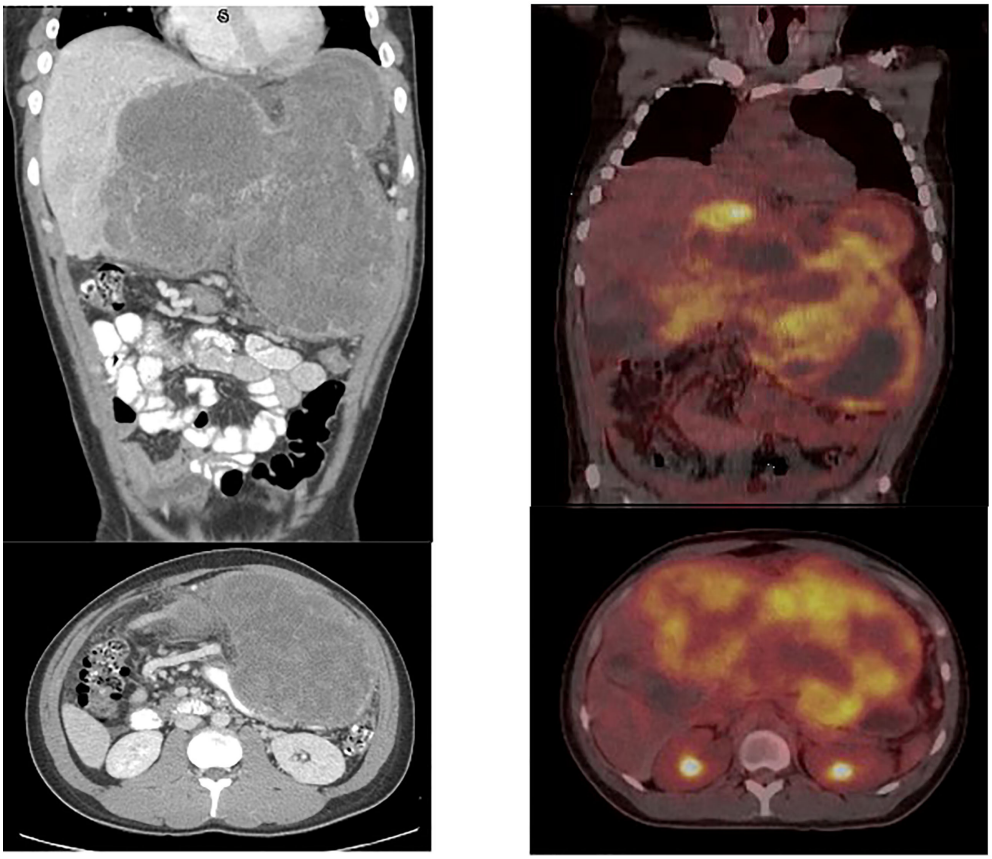

FIGURE 1
Initial CT scan demonstrating UESL. 20 x 10 x 10 cm well-circumscribed, solid mass of the entirety of the left lobe of the liver with relative sparing of the right lobe. Initial PET/CT demonstrating large hepatic mass measuring 25 x 13 cm with maximal SUV 11.5 as well as areas of necrosis, demonstrated by lack of FDG avidity.

serum markers identify UESL (1, 3). The differential diagnosis of UESL includes abscess, mesenchymal hamartoma, hydatid cyst, hepatocellular carcinoma, hepatoblastoma, biliary tract rhabdomyosarcoma, cystic metastasis, angiolipoma, leiomyosarcoma, liposarcoma, epithelioid hemangioendothelioma, and malignant melanoma (1, 3, 8). UESL does share chromosomal abnormalities seen with mesenchymal hamartoma, with some suggesting malignant transformation of mesenchymal hamartoma to develop UESL; abnormalities associated with 19q13.4 including balanced translocations t(11;19)(q13;q13.4) and t(15;19)(q15;q13.4) (1, 3, 12).

UESL can have a differential appearance on imaging. Ultrasound demonstrates a solid hepatic mass, generally isoechoic to normal liver, with anechoic areas corresponding to areas of tumor necrosis or degeneration (1, 13). CT demonstrates a well-defined hypodense mass with internal septations, almost cystic in appearance (1, 13). With contrast administration the tumor does progressively enhance (1, 13). MRI demonstrates low signal intensity on T1 weighted images and high signal intensity on T2 weighted images, again with enhancement on contrast administration (1, 13). Due to its differential appearance, image-guided biopsy is the mainstay of diagnosis, however cases have been reported of tumor rupture after biopsy (14). Rupture prior to complete surgical resection can be a consideration for treatment of residual disease and higher risk of recurrence (2, 4). The prognosis of UESL with rupture into the peritoneal cavity is less favorable in comparison to cancerous counterparts including hepatocellular carcinoma secondary to factors including increased risk of systemic metastases (15).

Histopathology demonstrates that UESL is composed of undifferentiated spindle cells with mitotic figures and myxoid stroma (9, 16). The high water content of the myxoid stroma is thought to be the reason for the differential appearance of UESL on imaging (1, 13). UESL tumors also show characteristic intracellular hyaline globules and anaplasia on a mesenchymal background (8, 17). These tumors tend to have a pseudocapsule made of compressed hepatic parenchyma, leading to a well circumscribed hepatic mass (9).

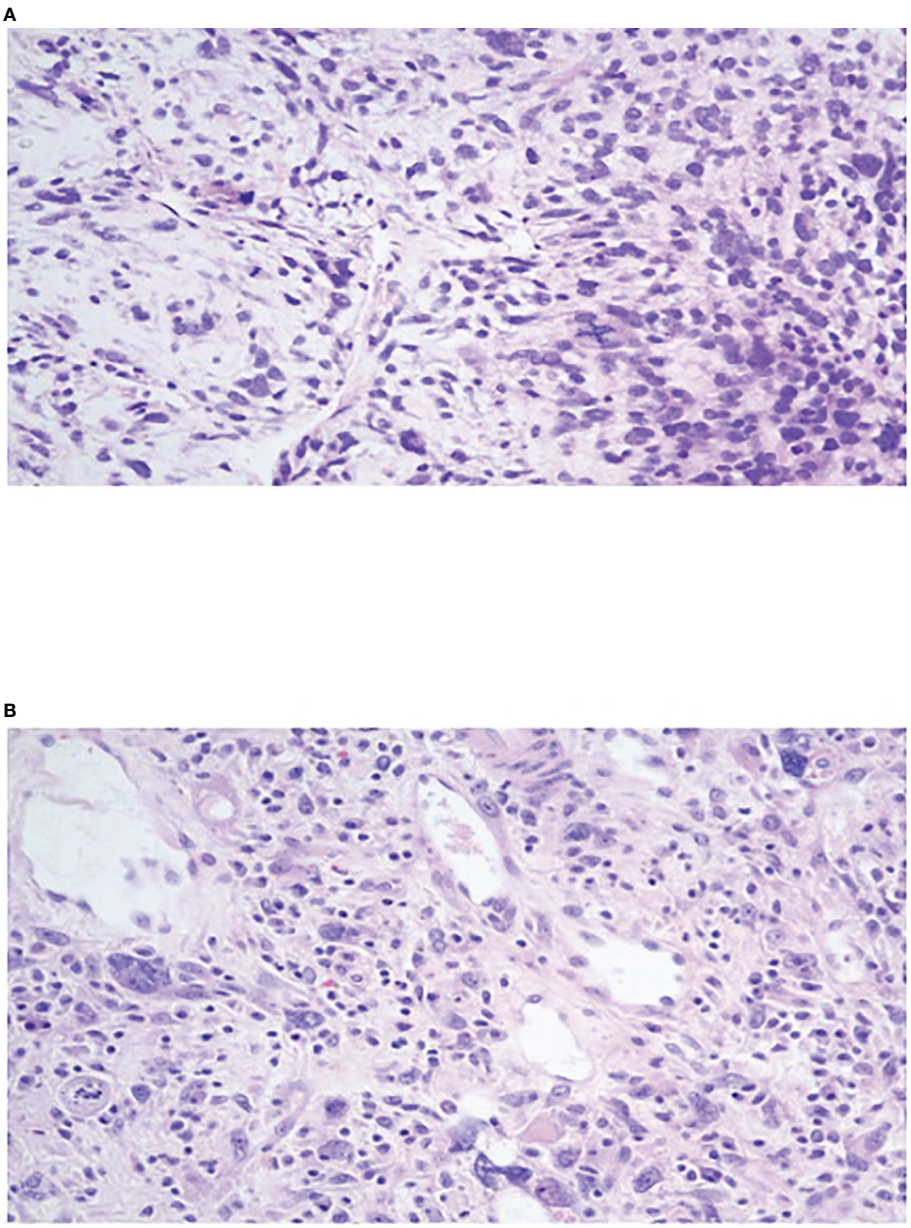


FIGURE 2
**(A)** Oval to stellate tumor cells with ill-defined cell borders loosely distributed in myxoid stroma with marked nuclear pleomorphism, hyperchromasia and brisk mitotic activity. **(B)** Tumor cells within a fibroinflammatory background showing marked nuclear pleomorphism, hyperchromasia, and frequent multinucleated and bizarre giant cells. Cytoplasmic and extracellular eosinophilic globules noted.

Prognosis for UESL has historically been considered dismal with reported 5-year overall survival rate of approximately 65% in all patients with worse outcomes reported in adults (6, 18). Factors that have been associated with improved survival are margin negative resection, receipt of chemotherapy and childhood. Treatment options for UESL include surgery, chemotherapy, and liver transplantation (1, 19–21). One retrospective study of UESL patients from 1975 to 2015 using the SEER database showed while 84% of patients underwent surgery, only 65% underwent chemotherapy and 9% underwent radiation therapy (18). While surgical resection of the primary tumor was previously the mainstay of treatment, recent studies have shown success with use of adjuvant chemotherapy and neoadjuvant chemotherapy, particularly in initially unresectable cases (3). Tumors are generally considered unresectable due to size, amount of liver involvement, and invasion into surrounding structures (14). Given the poorer outcome in

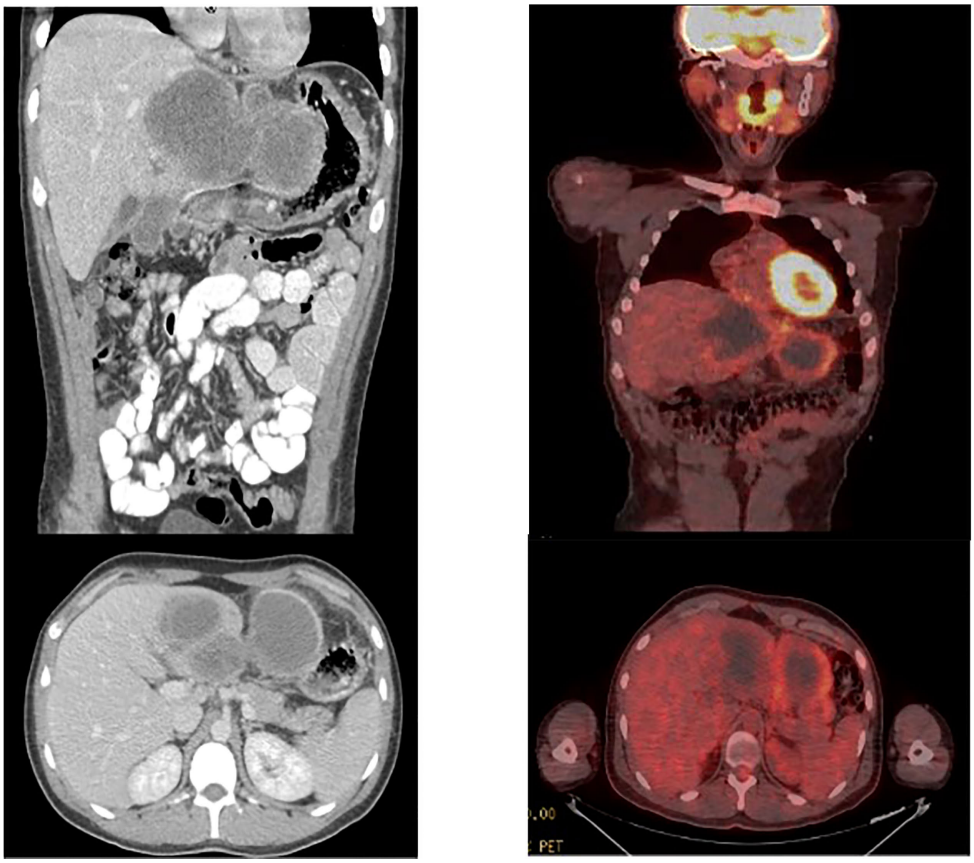


FIGURE 3
CT scan after completion of neodjuvant chemotherapy. Significant improvement was visualized with a decrease in lesion size to 15 x 7.7 x 8.1 cm. PET scan after completion of neodjuvant chemotherapy demonstrating reduction in size of mass to 14.5 x 6.8 x 8.9 cm as well as decreased FDG avidty of SUV 5.4.

adults and the propensity for early local and distant metastases a strategy employing combined neoadjuvant and adjuvant chemotherapy may result in improved outcomes. A recent review of NCDB patients with UESL from 2004 – 2015 showed that 92.7% of pediatric patients received chemotherapy as opposed to 65.9% of adults (7). Only 1 out of 41 adult patients receiving both surgery and chemotherapy also received neoadjuvant therapy as opposed to adjuvant therapy (7).

As shown in one study, 12 of 17 children with UESL treated with a multimodal approach between 1979 and 1995 were alive at 2.4 to 20 years follow-up (4). A separate study of five pediatric patients treated with resection followed by adjuvant chemotherapy demonstrated no disease recurrence at a median of 53 months post-treatment (22). A third study of five pediatric patients ages 10 to 19 were also treated with multimodal therapy, including orthotopic liver transplantation in unresectable cases, demonstrating 100% survival at 21 to 68 months of follow-up with instances of recurrence (23). Combinations of Vincristine, Cyclophosphamide, Dactinomycin, Doxorubicin, Etoposide and Ifosfamide are associated with longer survival and disease-free prognosis (4, 8, 10, 24). Chemotherapy for UESL is modeled after established regimens for pediatric rhabdomyosarcoma or Ewing sarcoma without cisplatin (8, 17, 25). UESL metastases have been reported in up to 15% of pediatric patients and are mainly seen during primary diagnosis in which sites most commonly include lungs, adrenal glands, peritoneum and extension into the heart (23, 26, 27). Available data regarding metastatic disease in UESL is limited but is a critical consideration for future optimization of multimodal treatment options.

A review of multimodal treatment regimens for UESL are outlined in Table 1. Also included are some cases of patients undergoing surgery alone with no chemotherapy, highlighting the improved success with neoadjuvant and adjuvant treatment strategies. Given the reported improvements associated with chemotherapy in pediatric patients, we elected to treat our patient with multimodal chemotherapy and surgical resection. The intended goal of this approach in our patient was decrease tumor size to enable resection, start early systemic therapy for a disease with a

10.3389/fonc.2022.1004108

TABLE 1 Cases of multimodal treatment of UES in adults.

| Reference | Year | Age/Sex | Tumor(s) | Treatment | Neoadjuvant Chemotherapy | Adjuvant Chemotherapy | Recurrence | Follow up (Months) |
|---|---|---|---|---|---|---|---|---|
| Present | 2021 | 22 M | 20 x 10 x 10 cm | Left hepatectomy. | DOX<br>IFO<br>MES | DOX<br>IFO<br>MES | None | 48 |
| Yu (19) | 2021 | 69 F | 16 cm | Surgical resection.<br>RFA | None | None | 6 months, | N/A |
| Pandit (20) | 2019 | 29 F | 15 x 12 cm | Surgical resection. | None | None | Yes at 4 months. | 8; deceased. |
| Pandit (15) | 2019 | 34 M | 16 x 14 cm | Laparotomy. | None | None | Tumor progression at 6 months. | 6 |
| Pinamonti (28) | 2018 | 60 F | 23 x 15 x 12 cm | hepatectomy | None | ACT<br>CYC<br>VIN | None | 30 |
| Sanchez-Morales (21) | 2018 | 53 F | Hypodense mass in the right lobe with satellite lesions. | Palliative radiotherapy and intravenous analgesia. | None | None | None | Deceased |
| Sanchez-Morales (21) | 2018 | 41 F | 20 x 16 cm mass in the right lobe. | Right hepatectomy. | None | Post-recurrence<br>DOX<br>ISO<br>Scheduled<br>DOCE<br>GEM | 24 months. | 60 |
| Khan (29) | 2017 | 21 M | 12.3 x 9.8 x 8.3 cm and 13.6 x 9.8 x 9.8 cm. | No tumor resection; unresectable. Orthotopic liver transplant. | DOX<br>IFO | N/A | None | 18 |
| Giakoustidis (30) | 2016 | 30 M | Voluminous mass in the right lobe. | Right portal vein embolization. Right trisegmentectomy. | None | CIS<br>CYC<br>DOX | Yes at 12 months. | 28; deceased. |
| Zanwar (31) | 2016 | 25 M | Hypodense mass in the right lobe. | Right hepatectomy. | ADRI<br>IFO<br>MES<br>VIN | ADRI<br>IFO<br>MES<br>VIN | None | 24 |
| Kim (32) | 2011 | 47 F | 12 x 10 cm well-demarcated mass in the left segment. | Left lateral sectionectomy. Radiotherapy. | DOX<br>DZN<br>IFO<br>MES | None | Yes at 24 months, metastatic lesion treated with radiotherapy. | 48 |
| Noguchi (5) | 2011 | 27 F | 21 x 19 x 14 cm mass in the right liver lobe. | Right trisegmentectomy. Radiation therapy. Peripheral blood stem cell transplantation. | None | First Course<br>ACT<br>ADRI<br>CIS<br>CYC<br>VIN<br>Second Course<br>CAB<br>CYC<br>ETP<br>RAN | None | 60 |
| Ma (33) | 2008 | 61 F | 12 x 9 x 8 cm mass to the right lobe. | Right hepatic lobectomy. Cholecystectomy. | None | None | None. | 8; deceased. |
| Pachera (9) | 2008 | 22 F | 19 x 14 x 11 cm mass. | Right portal vein embolization. Right trisectionectomy with extrahepatic bile duct resection. | None | ACT<br>CYC<br>VIN | None | 14 |
| Almogy (16) | 2005 | 21 F | 15 x 15 cm mass confined to the right lobe. Second smaller lesion in the left lateral segment. | Hepatic trisectionectomy | None prior to first resection<br>DOX<br>IFO | DOX<br>IFO<br>MES | None | 71 |

*(Continued)*

TABLE 1 Continued

| Reference | Year | Age/Sex | Tumor(s) | Treatment | Neoadjuvant Chemotherapy | Adjuvant Chemotherapy | Recurrence | Follow up (Months) |
|---|---|---|---|---|---|---|---|---|
| | | | | | MES<br>Prior to resection of secondary tumor | | | |

Adriamycin (Adri), Actinomycin D (Act), Carboplatin (Cab), Cisplatin (Cis), Cyclophosphamide (Cyc), Dacarbazine (Dzn), Docetaxel (Doce), Doxorubicin (Dox), Etoposide (Etp), Gemcitabine (GEM), Ifosfamide (Ifo), Isophosphamide (ISO), Mesna (Mes), Pembrolizumab (PMB), Ranimustine (Ran), Vincristine (Vin).

propensity for early metastases, and to assess tumor response *in vivo*. These advantages have been reported for other cancers such as gastric, gastroesophageal and pancreatic cancers (34, 35). Our patient thus far appears to have achieved some of the intended benefits of combination chemotherapy as well as disease free survival of 48 months. In conclusion, we believe this approach is well suited for this cancer given its underlying biology i.e. a propensity for early local and distant recurrence, and therefore warrants further study. This case study adds to the growing body of literature favoring combination of combined neoadjuvant and adjuvant chemotherapy with hepatic resection in treatment of UESL.

## Data availability statement

The raw data supporting the conclusions of this article will be made available by the authors, without undue reservation.

## Ethics statement

This case report is exempt from IRB approval. Patient did provide consent to publication of this manuscript.

## Authors contribution

RV and SK completed review of the literature, acquisition of data, drafting and completion of the manuscript. SK and GM participated in the critical review of the paper. All authors contributed to the article and approved the submitted version.

## Funding

Funding for publication was obtained from the Western Michigan University Homer Stryker MD School of Medicine Department of Surgery research fund.

## Acknowledgments

We would like to thank Bronson Methodist Hospital, West Michigan Cancer Center, and Western Michigan University for allowing us to conduct this project.

## Conflict of interest

The authors declare that the research was conducted in the absence of any commercial or financial relationships that could be construed as a potential conflict of interest.

## Publisher's note



## References

1. Gomes F, Melo D, Esteves C, Lima B, Carneiro F, Oliveira P. Undifferentiated embryonal sarcoma of the liver: A rare hepatic tumor and its related characteristic radiological features. *Radiol Case Rep* (2021) 16(3):646–50. doi: 10.1016/j.radcr.2020.12.017

2. Stocker JT. Hepatic tumors in children. *Clin Liver Dis* (2001) 5(1):259–ix. doi: 10.1016/s1089-3261(05)70163-x

3. Putra J, Ornvold K. Undifferentiated embryonal sarcoma of the liver: A concise review. *Arch Pathol Lab Med* (2015) 139(2):269–73. doi: 10.5858/arpa.2013-0463-RS

4. Bisogno G, Pilz T, Perilongo G, Ferrari A, Harms D, Ninfo V, et al. Undifferentiated sarcoma of the liver in childhood: A curable disease. *Cancer.* (2002) 94(1):252–7. doi: 10.1002/cncr.10191

5. Noguchi K, Yokoo H, Nakanishi K, Kakisaka T, Tsuruga Y, Kamachi H, et al. A long-term survival case of adult undifferentiated embryonal sarcoma of liver. *World J Surg Oncol* (2012) 10:65. doi: 10.1186/1477-7819-10-65

6. Wu Z, Wei Y, Cai Z, Zhou Y. Long-term survival outcomes of undifferentiated embryonal sarcoma of the liver: A pooled analysis of 308 patients. *ANZ J Surg* (2020) 90(9):1615–20. doi: 10.1111/ans.15684

7. Ziogas IA, Zamora IJ, Lovvorn Iii HN, Bailey CE, Alexopoulos SP. Undifferentiated embryonal sarcoma of the liver in children versus adults: A national cancer database analysis. *Cancers (Basel)* (2021) 13(12):2918. doi: 10.3390/cancers13122918

8. Childhood liver cancer treatment (PDQ)–health professional version *Targeted Therapy to Treat Cancer* (2022). (Bethesda, Maryland: National Cancer Institute). Available at: https://www.cancer.gov/types/liver/hp/child-liver-treatment-pdq.

9. Pachera S, Nishio H, Takahashi Y, Yokoyama Y, Oda K, Ebata T, et al. Undifferentiated embryonal sarcoma of the liver: Case report and literature survey. *J Hepatobiliary Pancreat Surg* (2008) 15(5):536–44. doi: 10.1007/s00534-007-1265-y

10. Walther A, Geller J, Coots A, Towbin A, Nathan J, Alonso M, et al. Multimodal therapy including liver transplantation for hepatic undifferentiated embryonal sarcoma. *Liver Transpl* (2014) 20(2):191–9. doi: 10.1002/lt.23773

11. Yu Y, Zhong Y, Wang J, Wu D. Sarcomatoid hepatocellular carcinoma (SHC): a case report. *World J Surg Oncol* (2017) 15(1):219. doi: 10.1186/s12957-017-1286-1

12. Stringer MD, Alizai NK. Mesenchymal hamartoma of the liver: a systematic review. *J Pediatr Surg* (2005) 40(11):1681–90. doi: 10.1016/j.jpedsurg.2005.07.052

13. Techavichit P, Masand PM, Himes RW, Abbas R, Goss JA, Vasudevan SA, et al. Undifferentiated embryonal sarcoma of the liver (UESL): A single-center experience and review of the literature. *J Pediatr Hematol/Oncol* (2016) 38(4):261–8. doi: 10.1097/MPH.0000000000000529

14. Babu BI, Bigam DL, Gilmour SM, Dajani KZ, Shapiro AMJ, Kneteman NM. Liver transplantation in locally unresectable, undifferentiated embryonal cell sarcoma. *Transplant Direct* (2021) 7(2):e654. doi: 10.1097/TXD.0000000000001106

15. Pandit N, Jaiswal LS, Shrestha V, Awale L, Adhikary S. Undifferentiated embryonal sarcoma of liver in an adult with spontaneous rupture and tumour thrombus in the right atrium. *ANZ J Surg* (2019) 89(9):E396–7. doi: 10.1111/ans.14670

16. Almogy G, Pappo O, Gips M, Lieberman S, Edden Y, Eid A. Improved survival with surgery and systemic chemotherapy for undifferentiated embryonal sarcoma of the liver. *Isr Med Assoc J* (2005) 7(10):672–3.

17. Stocker JT, Ishak KG. Undifferentiated (embryonal) sarcoma of the liver: report of 31 cases. *Cancer.* (1978) 42(1):336–48. doi: 10.1002/1097-0142(197807)42:1<336::aid-cncr2820420151>3.0.co;2-v

18. Pan L, Yin L, Liu XC, Ying RC, Kong WC. Adult versus paediatric undifferentiated embryonal sarcoma of the liver: a SEER database analysis. *ANZ J Surg* (2021) 91(12):2690–4. doi: 10.1111/ans.17290

19. Yu XH, Huang J, Ge NJ, Yang YF, Zhao JY. Recurrent undifferentiated embryonal sarcoma of the liver in adult patient treated by pembrolizumab: A case report. *World J Clin Cases* (2021) 9(10):2281–8. doi: 10.12998/wjcc.v9.i10.2281

20. Pandit N, Deo KB, Jaiswal LS, Pradhan A, Adhikary S. Hanging undifferentiated embryonal sarcoma of the liver in adult: an unusual presentation of an aggressive tumor. *J Gastrointest Canc* (2019) 50(3):689–92. doi: 10.1007/s12029-018-0119-y

21. Esteban SG, Emilio CU, Emmanuel AF, Oscar SJ, Paulina CE, Angel MM. Undifferentiated embryonal sarcoma of the liver in adult patient: A report of two cases. *Ann Hepatobiliary Pancreat Surg* (2018) 22(3):269–73. doi: 10.14701/ahbps.2018.22.3.269

22. May LT, Wang M, Albano E, Garrington T, Dishop M, Macy ME. Undifferentiated sarcoma of the liver: A single institution experience using a uniform treatment approach. *J Pediatr Hematol Oncol* (2012) 34(3):e114–6. doi: 10.1097/MPH.0b013e3182331fbe

23. Plant AS, Busuttil RW, Rana A, Nelson SD, Auerbach M, Federman NC. A single-institution retrospective cases series of childhood undifferentiated embryonal liver sarcoma (UELS): Success of combined therapy and the use of orthotopic liver transplant. *J Pediatr Hematol Oncol* (2013) 35(6):451–5. doi: 10.1097/MPH.0b013e318271c948

24. Mathias MD, Ambati SR, Chou AJ, Slotkin EK, Wexler LH, Meyers PA, et al. A single-center experience with undifferentiated embryonal sarcoma of the liver. *Pediatr Blood Canc* (2016) 63(12):2246–8. doi: 10.1002/pbc.26154

25. Ismail H, Dembowska-Bagińska B, Broniszczak D, Kaliciński P, Maruszewski P, Kluge P, et al. Treatment of undifferentiated embryonal sarcoma of the liver in children–single center experience. *J Pediatr Surg* (2013) 48(11):2202–6. doi: 10.1016/j.jpedsurg.2013.05.020

26. Shi M, Xu H, Sangster GP, Gu X. Pulmonary metastases from an undifferentiated embryonal sarcoma of the liver: A case report and review. *Case reports in oncological medicine. 2018* (2018) 7840865:1–6. doi: 10.1155/2018/7840865

27. Shi Y, Rojas Y, Zhang W, Beierle EA, Doski JJ, Goldfarb M, et al. Characteristics and outcomes in children with undifferentiated embryonal sarcoma of the liver: A report from the national cancer database. *Pediatr Blood Cancer* (2017) 64(4):e26272. doi: 10.1002/pbc.26272

28. Pinamonti M, Vittone F, Ghiglione F, Borasi A, Silvestri S, Coverlizza S. Unexpected liver embryonal sarcoma in the adult: Diagnosis and treatment. *Case Rep Surg* (2018) 2018:8362012. doi: 10.1155/2018/8362012

29. Khan ZH, Ilyas K, Khan HH, Ghazanfar H, Hussain Q, Inayat F, et al. Unresectable undifferentiated embryonal sarcoma of the liver in an adult Male treated with chemotherapy and orthotopic liver transplantation. *Cureus.* (2017) 9(10):e1759. doi: 10.7759/cureus.1759

30. Giakoustidis DE, Gargavanis AA, Katsiki ED, Salveridis NT, Antoniadis NA, Papanikolaou V. Undifferentiated embryonal sarcoma of the liver in a young female: treatment with portal vein embolization and liver trisectonectomy. *Korean J Hepatobiliary Pancreat Surg* (2016) 20(3):144–7. doi: 10.14701/kjhbps.2016.20.3.144

31. Zanwar S, Goel M, Patkar S, Ramaswamy A, Shetty N, Ramadwar M, et al. A case of ruptured adult embryonal sarcoma of the liver with excellent outcome after neoadjuvant chemotherapy. *J Gastrointest Canc* (2017) 48(1):100–2. doi: 10.1007/s12029-016-9877-6

32. Kim HH, Kim JC, Park EK, Hur YH, Koh YS, Cho CK, et al. Undifferentiated embryonal sarcoma of the liver presenting as a hemorrhagic cystic tumor in an adult. *Hepatobiliary Pancreat Dis Int* (2011) 10(6):657–60. doi: 10.1016/S1499-3872(11)60112-4

33. Ma L, Liu YP, Geng CZ, Tian ZH, Wu GX, Wang XL. Undifferentiated embryonal sarcoma of liver in an old female: case report and review of the literature. *World J Gastroenterol* (2008) 14(47):7267–70. doi: 10.3748/wjg.14.7267

34. Al-Batran SE, Homann N, Pauligk C, Goetze TO, Meiler J, Kasper S, et al. Perisoperative chemotherapy with fluorouracil plus leucovorin, oxaliplatin, and docetaxel versus fluorouracil or capecitabine plus cisplatin and epirubicin for locally advanced, resectable gastric or gastro-oesophageal junction adenocarcinoma (FLOT4): a randomised, phase 2/3 trial. *Lancet.* (2019) 393(10184):1948–57. doi: 10.1016/S0140-6736(18)32557-1

35. Oba A, Ho F, Bao QR, Al-Musawi MH, Schulick RD, Del Chiaro M. Neoadjuvant treatment in pancreatic cancer. *Front Oncol* (2020) 10:245. doi: 10.3389/fonc.2020.00245

frontiers | Frontiers in Oncology

TYPE Case Report
PUBLISHED 22 November 2022
DOI 10.3389/fonc.2022.992346



OPEN ACCESS

EDITED BY
Aali Jan Sheen,
Manchester Royal Infirmary,
United Kingdom

REVIEWED BY
Ayman Zaki Azzam,
Alexandria University, Egypt
Rahul Gupta,
Synergy Institute of Medical Sciences, India

*CORRESPONDENCE
Hui Su
suhuiningbo@163.com

SPECIALTY SECTION
This article was submitted to Surgical Oncology, a section of the journal Frontiers in Oncology

RECEIVED 12 July 2022
ACCEPTED 03 October 2022
PUBLISHED 22 November 2022

CITATION
Wang W, Chen Y, Wang C and Su H (2022) Giant desmoplastic small round cell tumor of the abdomen: A case report.
*Front. Oncol.* 12:992346.
doi: 10.3389/fonc.2022.992346



# Giant desmoplastic small round cell tumor of the abdomen: A case report

Wuke Wang [1], Yunjie Chen [1], Chunnian Wang [2] and Hui Su [1,3]*

[1]Department of General Surgery, Hwa Mei Hospital, University of Chinese Academy of Sciences, Ningbo No. 2 Hospital, Ningbo, China, [2]Department of Gastrointestinal Pathology, Ningbo Diagnostic Pathology Center, Ningbo, China, [3]Department of Gastrointestinal Surgery, First Affiliated Hospital of Jinan University, Guangzhou, China

**Background:** Desmoplastic small round cell tumor (DSRCT) is a rare, aggressive, mesenchymal malignancy of a separate clinicopathological entity. It has a predilection for young men, with no evidence of any ethnic predilection. The current diagnostic gold standard for DSRCT includes histopathologic, immunohistochemical, and cytogenetic studies in order to confirm the variable phenotypic expression and characteristic chromosomal translocation.

**Case summary:** A 65-year-old man presented with a sensation of an abdominal mass and a presentation of an incomplete bowel obstruction. Initial lab tests were in the normal range except for carbohydrate antigen. Contrast-enhanced CT showed that a large, mass-confounding density was occupied in the omentum majus area of the middle and lower abdominal wall. A 3D reconstruction of the images was performed to clarify the relationship between the tumor and the colon and was confirmed by a colonoscopy. After surgery, immunohistochemistry and fluorescence *in situ* hybridization (FISH) revealed EWSR1-WT1 gene rearrangement at 22q12, confirming the diagnosis of desmoplastic small round cell tumor.

**Conclusion:** Being different from the predilection of DSRCT for young men, the patient in our case is a 65-year-old man with a huge mass involving the transverse colon and the bladder.

KEYWORDS

**desmoplastic small round cell tumor, abdominopelvic tumor, medium-elderly male, DSRCT, case report**

## Introduction

The desmoplastic small round cell tumor (DSRCT) is a rare, aggressive, mesenchymal malignancy of uncertain differentiation with both a characteristic chromosomal translocation and immunohistochemical profile (1). Initially described in 1989 by Gerard and Rosai, DSRCT tumor cells were classified by express epithelial, neuronal, and skeletal

muscle and mesenchymal markers. However, by 1991, DSRCT was formally established as a separate clinicopathological entity (2). It has a predilection for young men, with ages ranging from 3 to 52 years, and with a peak incidence between the second and third decades of life. The mean age at diagnosis is 20.8 years, and it has a male-to-female ratio of 10:1, with no evidence of any ethnic predilection. The most common symptom of DSRCT is vague abdominal symptoms (3), and the more common is terminal disease on diagnosis with multiple intra-abdominal lesions (4). The current diagnostic gold standard for DSRCT includes histopathologic, immunohistochemical, and cytogenetic studies in order to confirm variable phenotypic expression and characteristic chromosomal translocation (5).

## Case presentation

A 65-year-old man presented with a sensation of an abdominal mass and a presentation of an incomplete bowel obstruction. He had a previous history of hypertension and hyperlipidemia; percutaneous internal coronary stenting was performed 9 years ago, and he is currently taking betaloc 47.5 mg, aspirin 100 mg, and rosuvastatin 10 mg, without a remarkable family history. Physical examination showed that his vital signs were within normal range. An abdominal examination could reach a massive mass extending from the middle abdomen to the pelvic cavity, which is about 16 cm in size, poor in mobility, and tough in texture; the rest abdomen was soft and non-tender, without signs of peritoneal irritation. Initial lab tests including complete blood count and tumor markers presented in the Table 1.

Contrast-enhanced CT of the abdomen showed that a large, mass-confounding density was occupied in the omentum majus area of the middle and lower abdominal wall (Figure 1A). A 3D reconstruction of the images was performed (Figure 1B). To clarify the relationship between tumor and colon, colonoscopy was performed (Figure 1C).

The preoperative diagnosis of the patient was intestinal obstruction and abdominal tumor, and he underwent surgery in May this year. During the operation, we observed that the tumor originated from the omentum majus and invaded the middle segment of the transverse colon, the anterior wall of bladder, and the abdominal wall. No other distant metastasis was found. The patient underwent surgical treatment that included a 5-cm transverse colon at each end with the mass involvement, the involved bladder tissue, and the lower umbilical range of about 10 * 10 cm of the adhesion peritoneum and rectus abdominal sheath. The complete tumor was removed and elevated colostomy was performed. (Figure 1D) The operation time of the patient was 282 minutes, the intraoperative bleeding was 100 ml, and there was no postoperative complication. Postoperatively, the patient was generally in a stable condition and discharged 9 days later.

The size of the tumor was 18 * 12 * 6 cm. The cut surface of the tumor was gray, with hemorrhage in the center. Histologically, the neoplasm was lobulated and consisted of small round cells with amphiphilic cytoplasm and round to ovoid mononuclear hyperchromatic nuclei. There was marked mitosis and necrosis. The neoplasm involved the surrounding adipose tissue and was infiltrated into the intestinal and bladder wall. (Figure 1E) Immunohistochemistry showed that the tumor cells differentiated into epithelium, muscle, and nerve. Tumor cells expressed an epithelial marker, such as CK(pan), CAM5.2, and EMA. Desmin, NSE, vimentin, and CD99 proteins were strongly expressed in the tumor cells. The positive rate of Ki-67 was about 60%. Some tumor cells expressed MC(HBME1). However, GATA-3, P63, CK5/6, Syn, CgA, CEA, Wilms tumor, MyoD1, myogenin, NKX2.2, calretinin, CD56, S-100, SOX-10, and PGP9.5 were negative. Fluorescence *in situ* hybridization (FISH) revealed EWSR1-WT1 gene rearrangement at 22q12, confirming the diagnosis of a desmoplastic small round cell tumor (Figure 1F). In August, the patient was reexamined with abdominal enhanced CT and chest CT, and was found with no tumor recurrence and metastasis. The patient has received chemotherapy four times since the operation. The chemotherapy regimen was oral dacarbazine 0.5 g d1–d4 and intravenous doxorubicin hydrochloride liposome 50 mg d1.

## Discussion

The desmoplastic small round cell tumor (DSRCT) is a soft tissue malignant neoplasm of the small round cell tumor family which occurs mainly in the abdominal and pelvic cavity of young patients (1). DSRCT has unique histology and immunohistochemical and molecular biology features, and is characterized by abdominopelvic sarcoma (6), including multi-lineage cellular nests of mesenchymal, epithelial, muscular, and neural differentiation admixed with desmoplastic stroma (7). In typical cases, the tumor is composed of oval cells with high nuclear to cytoplasmic ratio, which can also show striated features or clear cytoplasm, resulting in signet ring cells in a few cases. The exact incidence rate of DSRCT is unclear, although at least 1000 cases have been reported in the literature since its histopathological description. The 5-year overall survival rate in the retrospective study was approximately 10% (1, 8). Clinically, the signs and symptoms of DSRCT are no specific symptoms and most patients present with a single abdominal mass, as in our case. It is sometimes associated with pain, abdominal distention and/or ascites, constipation, weight loss, or other symptoms secondary to an extrinsic mass effect (bowel obstruction) or due to a compromise of abdominopelvic organs. This cancer is believed to originate from the surface of the peritoneum and to metastasize almost universally when it occurs. The common sites of metastasis include the liver, spleen, and lymph nodes above the diaphragm (9), although the

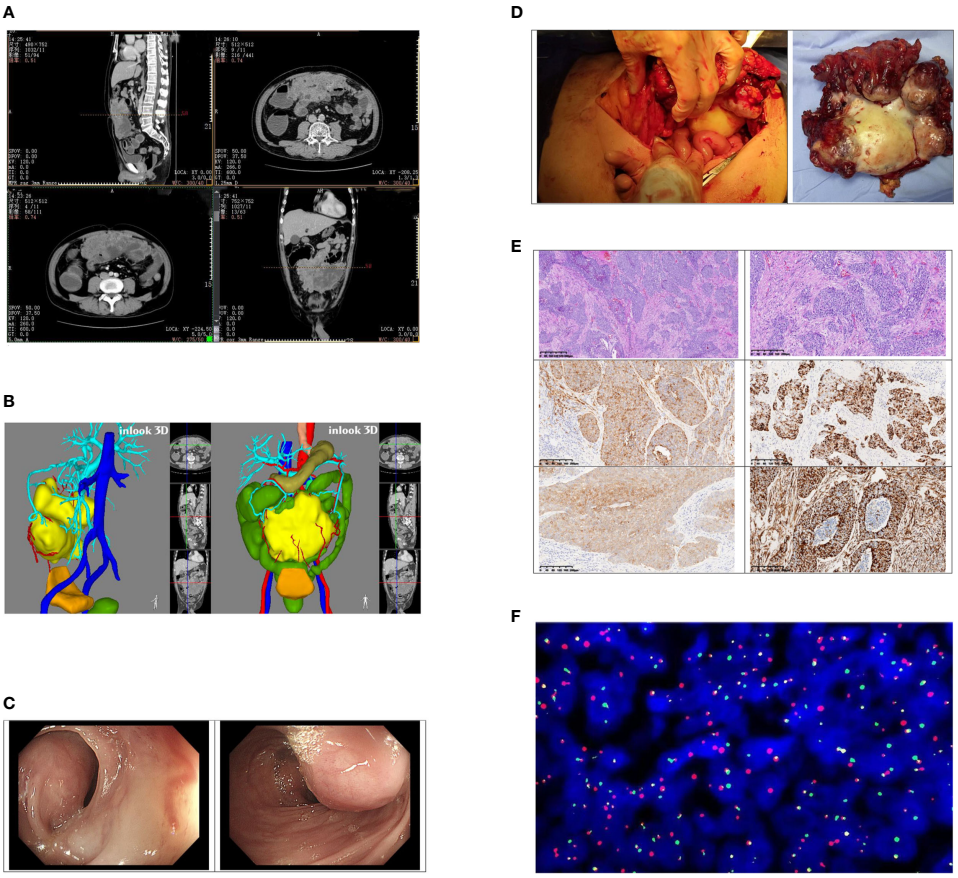


FIGURE 1
**(A)** Contrast-enhanced CT found that the larger cross-section range is about 167*149*65 mm; moderate uneven enhancement occurred after the enhancement; obscure boundary, unresolved from the adjacent transverse colon and part of the small intestine. Multiple effusion dilations were seen in the ascending colon and part of the small intestine. **(B)** The position of the tumor in the abdominal cavity and its relationship with various organs were displayed by 3D reconstruction imaging of CT. **(C)** A huge external pressure mass under the mucosa at the middle section of the transverse colon (approximately 65 cm away from the anus) made the intestinal lumen compressed, twisted, and narrow. **(D)** The tumor involved the middle part of the transverse colon and part of the bladder wall. The size was about 18 * 12 * 6 cm. **(E)** The pictures of tumor pathology sections; order is: ×40, ×100, CKpan (+), desmin (+), NSE (+), vim (+). **(F)** Project name: EWSR1/WT1 fusion gene test (FISH-tissue). Detection probe: LBPEWSR1/WT1 fusion gene probe. Chromosome loci: WTl (llpl3)/EWSRl (22ql2). Probe tag: green signal is GSPEWSR1, red signal (R) is the GSPWT1 detection result. Cell number analyzed: 200; Diagnostic opinion: The EWSR1/WT1 fusion gene was detected, 200 interval phase cells were analyzed, and each signal pattern was as follows: 1G1R1F39.0%, 1G1R2F20.0%, 1G1F4.0%, lG2F 5.0%, lRlF 5.0%, lR2F 4.0%, lGlR 9.0%, 2GlR 5.0%, lG2R 4.0%, 2G2R 5.0%.

disease may occur in different sites, including the testis and the central nervous system (10). DSRCT has many different staging methods, and the most recent uses imaging characteristics to define intermediate (no liver involvement or ascitic fluid), high-risk (either liver involvement or ascitic fluid), and very-high-risk disease (both liver involvement and ascitic fluid) (3).

Immunohistochemically, DSRCT had an immune spectrum of polyphenols with tumor cells expressing epithelium, mesenchymal, and neuroendocrine markers (11). Due to DSCRT and other tumor types, the final diagnosis depends on cytogenetics and molecular analysis of *in situ* hybridization or reverse transcription polymerase chain reaction. The specific molecular feature of DSRCT is the pathognomonic EWSR1-WT1 t(11;22) (p13:q12) translocation (12). In addition to the translocation defined by this disease, the understanding of recurrent carcinogenic changes or DSRCT subgroups defined by the genome is still limited (13). The genome-wide sequencing of DSRCT samples did not show any other information about secondary driving carcinogenic events other than the ewsr1–wt1 fusion. WT1 is considered as a useful antibody to diagnose DSRCT and distinguish it from other tumors with small blue cell morphology. Therefore, molecular detection is recommended to avoid diagnostic traps. We performed FISH analysis on this case to determine whether there was an ewsr1 gene break. Not surprisingly, the ewsr1 division signal was detected in tumor cells, which finally confirmed the diagnosis of DSRCT.

DSRCT is notorious for extensive metastasis. Patients usually have obvious tumor burden at the initial examination. The

TABLE 1 Leucocyte count was 12.9*10^9/L; neutrophil ratio was 86.9%, higher than the normal values; carbohydrate antigen was 125 216.30 U/ml, significantly higher than the normal values.

| Inspection item | Result | Reference ranges | Unit |
|---|---|---|---|
| Leucocyte count | 12.9 | 3.5–9.5 | *10^9/L |
| Classification of neutrophils | 86.9 | 40.0–75.0 | % |
| Absolute values of the monocytes | 0.62 | 0.1–0.6 | *10^9/L |
| Eosinophil count | 0.01 | 0.02–0.52 | *10^9/L |
| RBC | 4.55 | 4.30–5.80 | *10^12/L |
| Hemoglobin | 134 | 130–175 | g/L |
| Platelet count | 233 | 125–350 | *10^9/L |
| AFP | 3.5 | ≤7.00 | ng/ml |
| Carcinoembryonic antigen | 1.04 | ≤5.00 | ng/ml |
| Ferritin | 164.1 | 22.0–322.0 | ng/ml |
| Carbohydrate antigen 125 | 216.3 | ≤15.00 | U/ml |
| Carbohydrate antigen 19-9 | 12.55 | ≤34.00 | U/ml |
| Composite prostate antigen | 0.78 | <3.600 | ng/ml |
| Free prostate-specific antigen | 0.51 | <0.930 | ng/ml |
| Total prostate-specific antigen | 1.29 | <4.000 | ng/ml |
| Carbohydrate antigen 50 | 9.08 | <25.00 | U/ml |
| Carbohydrate antigen 242 | 13.27 | <25.00 | U/ml |
| Carbohydrate antigen 72-4 | 1.6 | <10.00 | U/ml |
| Neuron-specific enolase | 9.99 | <20.00 | ng/ml |
| Cytokeratin 19 fragment | 1.86 | <3.30 | ng/ml |
| Squamous cell carcinoma antigen | 0.26 | <1.50 | ng/ml |
| Acquisition time: | 2022/4/25 15:06 | Check time: | 2022/4/26 13:58 |

Other tumor indicators were in the normal range. Red color value means higher than normal value, and blue color value means lower than normal value.

symptoms are not obvious until the peritoneal surface is widely infiltrated by the tumor, and no definite operation can be performed (14). Given the rarity of this disease, no randomized trials addressing its treatment have been performed, and nearly all the available literature describes anecdotal or retrospective experiences. Therefore, there is no standard treatment at present. The treatment methods that have been used include high-dose alkylating agent chemotherapy and trial complete cytoreductive surgery. Other consolidation local control methods include the use of radiolabeled antibodies for research treatment and hyperthermic intraperitoneal chemotherapy (HIPEC). Despite intensive, multimodal treatment, recurrence is still common. Although, so far, the treatment methods for potential fusion oncogenes in DSRCT are not clear, drug development for this and other similar central drivers is still possible (15).

## Data availability statement

The original contributions presented in the study are included in the article/supplementary material. Further inquiries can be directed to the corresponding author.

## Author contributions

All persons who meet authorship criteria are listed as authors, and all authors certify that they have participated sufficiently in the work to take public responsibility for the content, including participation in the concept, design, analysis, writing, or revision of the manuscript.

## Funding

Funded by the Project of NINGBO Leading Medical & Health Discipline, Project Number: 2022-F19. Supported by Ningbo Natural Science Foundation, China (Grant No.2019A610215).

## Conflict of interest

The authors declare that the research was conducted in the absence of any commercial or financial relationships that could be construed as a potential conflict of interest.

## Publisher's note



## References

1. Sanguino A, Kaur G, Mao S. Desmoplastic small round-cell tumor: Retrospective review of institutional data and literature review. *Anticancer Res* (2021) 41(8):3859–66. doi: 10.21873/anticanres.15179

2. de Alava E, Marcilla D. Birth and evolution of the desmoplastic small round-cell tumor. *Semin Diagn Pathol* (2016) 33(5):254–61. doi: 10.1053/j.semdp.2016.05.003

3. Saltsman JA3rd, Price AP, Goldman DA, Hammond WJ, Danzer E, Magnan H, et al. A novel image-based system for risk stratification in patients with desmoplastic small round cell tumor. *J Pediatr Surg* (2020) 55(3):376–80. doi: 10.1016/j.jpedsurg.2018.02.068

4. Slim S, Zemni I, Bouida A, Bouhani M, Boujelbene N, Mrad K, et al. Intraabdominal and ganglionic desmoplastic small round cell tumor: A case series. *J Med Case Rep* (2021) 15(1):500. doi: 10.1186/s13256-021-03094-9

5. Wei G, Shu X, Zhou Y, Liu X, Chen X, Qiu M. Intra-abdominal desmoplastic small round cell tumor: Current treatment options and perspectives. *Front Oncol* (2021) 11::705760. doi: 10.3389/fonc.2021.705760

6. Ertoy Baydar D, Armutlu A, Aydin O, Dagdemir A, Yakupoglu YK. Desmoplastic small round cell tumor of the kidney: A case report. *Diagn Pathol* (2020) 15(1):95. doi: 10.1186/s13000-020-01015-w

7. Thway K, Noujaim J, Zaidi S, Miah AB, Benson C, Messiou C, et al. Desmoplastic small round cell tumor: Pathology, genetics, and potential therapeutic strategies. *Int J Surg Pathol* (2016) 24(8):672–84. doi: 10.1177/1066896916668637

8. Loktev A, Shipley JM. Desmoplastic Small round cell tumor (DSRCT): Emerging therapeutic targets and future directions for potential therapies. *Expert Opin Ther Targets* (2020) 24(4):281–5. doi: 10.1080/14728222.2020.1738392

9. Jin D, Chen M, Wang B, Gou Y. Mediastinal desmoplastic small round cell tumor. *Med (Baltimore)* (2020) 99(44):e22921. doi: 10.1097/MD.0000000000022921

10. Sedig L, Geiger J, Mody R, Jasty-Rao R. Paratesticular desmoplastic small round cell tumors: A case report and review of the literature. *Pediatr Blood Cancer* (2017) 64(12). doi: 10.1002/pbc.26631

11. Magro G, Broggi G, Zin A, Di Benedetto V, Meli M, Di Cataldo A, et al. Desmoplastic small round cell tumor with "Pure" spindle cell morphology and novel EWS-WT1 fusion transcript: Expanding the morphological and molecular spectrum of this rare entity. *Diagnostics (Basel)* (2021) 11(3):545. doi: 10.3390/diagnostics11030545

12. Gundem G, Gerstle JT, Heaton TE, LaQuaglia MP, Wexler LH, Meyers PA, et al. Comprehensive molecular profiling of desmoplastic small round cell tumor. *Mol Cancer Res* (2021) 19(7):1146–55. doi: 10.1158/1541-7786.MCR-20-0722

13. Dundr P, Drozenová J, Matěj R, Bártů M, Němejcová K, Robová H, et al. Desmoplastic small round cell tumor of the uterus: A report of molecularly confirmed case with EWSR1-WT1 fusion. *Diagnostics (Basel)* (2022) 12(5):1184. doi: 10.3390/diagnostics12051184

14. Hayes-Jordan A, LaQuaglia MP, Modak S. Management of desmoplastic small round cell tumor. *Semin Pediatr Surg* (2016) 25(5):299–304. doi: 10.1053/j.sempedsurg.2016.09.005

15. Silva MLG, Torrezan GT, Costa FD, Formiga MN, Nicolau U, Nascimento AG, et al. Desmoplastic small round cell tumor: A review of main molecular abnormalities and emerging therapy. *Cancers (Basel)* (2021) 13(3):498. doi: 10.3390/cancers13030498

frontiers | Frontiers in Oncology

TYPE Case Report
PUBLISHED 05 December 2022
DOI 10.3389/fonc.2022.1058211



OPEN ACCESS

EDITED BY
Riccardo Bertolo,
Hospital San Carlo di Nancy, Italy

REVIEWED BY
Giovanni Cochetti,
University of Perugia, Italy
Yoichiro Okubo,
Kanagawa Cancer Center, Japan

*CORRESPONDENCE
Jiaxin Li
407723080@qq.com

†These authors have contributed equally to this work

SPECIALTY SECTION
This article was submitted to Surgical Oncology, a section of the journal Frontiers in Oncology

RECEIVED 30 September 2022
ACCEPTED 16 November 2022
PUBLISHED 05 December 2022

CITATION
Feng Q, Li H, Chen X, Feng X and Li J (2022) Case report: Adrenal myelolipoma resected by laparoscopic surgery. *Front. Oncol.* 12:1058211. doi: 10.3389/fonc.2022.1058211



# Case report: Adrenal myelolipoma resected by laparoscopic surgery

Qingbo Feng[1†], Hancong Li[2†], Xinyang Chen[2†], Xuping Feng[1] and Jiaxin Li[1,3*]

[1]Department of Liver Surgery and Liver Transplantation Centre, West China Hospital, Sichuan University, Chengdu, Sichuan, China, [2]West China School of Medicine, West China Hospital, Sichuan University, Chengdu, Sichuan, China, [3]Department of General Surgery, Dafang County People's Hospital, Bijie, Guizhou, China

**Introduction:** Adrenal myelolipomas are benign tumors composed mainly of lipomatous elements with myeloid cells. With the development of medical imaging technology, the detection rate has gradually increased. We report a case of adrenal myelolipoma successfully excised through the laparoscope and reviewed existing literature in recent ten years to summarize the feasibility of the laparoscopic approach for this tumor.

**Case presentation:** Herein, we described a case of adrenal myelolipoma resected by laparoscope in a 63-year-old male patient. He did not have any other symptoms except the incidental finding of a left adrenal mass. An abdominal CT examination revealed a mixed-density lesion containing some amount of adipose tissue. In conjunction with the patient's willingness, we performed a laparoscopic operation to remove the lump. The definite diagnosis was confirmed as an adrenal myelolipoma according to the pathology. The patient recovered well postoperatively and without signs of recurrence at a 5-month follow-up.

**Conclusion:** Adrenal myelolipoma is commonly benign, asymptomatic, and hormonal inactivity. A surgical strategy is suggested for high-complication-risk patients. The laparoscopic approach is safe and effective with an obvious advantage over open procedures.

KEYWORDS

**adrenal myelolipoma, laparoscopic surgery, case report, literature review, adrenal incidentaloma**

## Introduction

Adrenal myelolipomas (AMLs) are rare, benign, mesenchymal neoplasms, consisting of mature adipose mixed with myeloid elements, which were initially described by Gierke in 1905 (1). The incidence of AML is 3.3% to 3.6% of all adrenal tumors in the general population, which has reached the second most common adrenal incidentalomas (1). Although prevailingly asymptomatic, enormous AML can present unregulated pain in the abdominal or flank due to compressing the surrounding tissue, further associated with hemorrhage or rupture (2). Imaging studies contribute to the diagnosis and detectable rate of AML; pathological examination reaches a definitive diagnosis (3). Generally, conservative treatment strategies are preferred. However, if symptoms develop, mass growth accelerates rapidly, or if it exceeds 6 cm, adrenalectomy will be the best option (4). While open surgical removal of giant AMLs is considered to be the treatment of choice, there have been increasing reports of giant AMLs successfully managed with minimally invasive techniques. Herein, we describe a case of AML and conduct a literature review on laparoscopic resection of AML in the last decade, emphasizing the feasibility of removing this kind of tumor by laparoscopic approaches.

## Case presentation

Our manuscript reporting adheres to CAse REport (CARE) guidelines (5).

We present a case of a 63-year-old male patient with no clinical symptoms but revealed a left adrenal mass in a CT scan for a regular physical checkup.

His past history included II diabetes mellitus treated with gliclazide, and he had been controlled with propranolol and amlodipine for hypertension. Upon admission, he had good general condition and stable vital signs, without palpable abdominal mass. Laboratory measurements demonstrated elevated blood Epinephrine (0.71 nmol/L, normal values <0.34 nmol/L). The serum levels of the tumor biomarker as well as thyroid hormones were normal. CT-scan showed a left adrenal mass of 5.1×5.1cm. The lesion manifested as a mixed-density shadow that contain certain amounts of adipose tissue (Figure 1). Based on imaging features, we highly suspected that was an adrenal myelolipoma. Even though the patient was asymptomatic and the tumor size was moderate, we planned to proceed with surgery combined with his wishes. On 29-04-2022, the patient underwent a left-sided laparoscopic procedure at our department.

During the operation, the patient was placed in the supine and parted-legs position. Using Veress needles, a 1-cm transverse incision near the right navel edge was made to establish pneumoperitoneum with a constant pressure of 13-14 mm Hg. Five trocars were used: a 5-mm trocar was inserted under the xiphoid process. A 12-mm trocar was placed below the left costal margin in the midclavicular line, and the other two 5-mm trocars were placed in the midaxillary and anterior axillary lines. The fifth trocar (12 mm) was installed a little to the left of the navel as a laparoscopic observation hole. The resection was carried out with an ultrasonic surgical aspirator (CUSA;

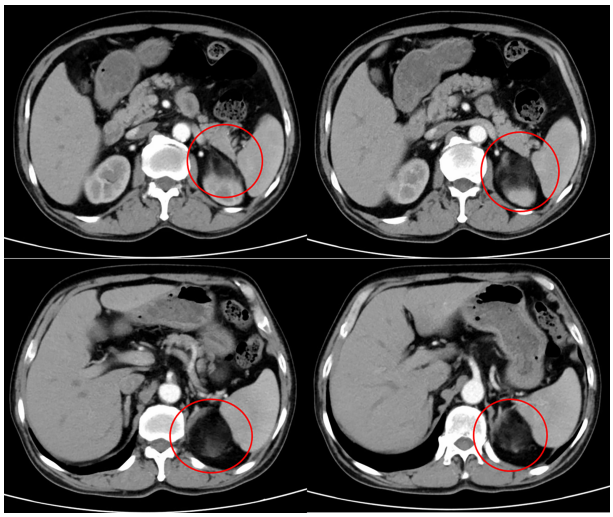

FIGURE 1
Abdominal computed tomography imaging, representing a left adrenal mass of 5.1×5.1cm.

Cavitron Laser-sonic Corp., Stamford, Connecticut, USA), harmonic scalpel (Ethicon Endo-Surgery, Inc., Blue Ash, Cincinnati, OH, USA), and a bipolar clamp coagulation system (ERBE, Tubingen, Germany). Intraoperative ultrasound sonography (IOUS) was performed for exploration and localization. The posterior peritoneum was gradually opened along the lower margin of the pancreatic body, and a 5×5cm neoplasm was observed behind the pancreatic body, demarcated clearly with the left kidney and spleen. The blood vessels around the left adrenal gland were separated and clipped, then severed with an ultrasound knife. The tumor was completely removed and the resection specimen was collected in a plastic bag and removed *via* a 6-cm incision on the low abdomen. A plasma drainage tube was placed to monitor the left retroperitoneal cavity drainage concerning volume, content, and color. Operating time was 270 min and blood loss was 50ml. However, free gas within the left pleural cavity was revealed in the immediate postoperative color-Doppler ultrasound examination. Pneumothorax was suspected after a CT scan of the left lung. Closed thoracic drainages were initiated following instant thoracic surgical consultation. Thoracentesis was smooth and the patient was transferred to the PACU (post-anesthesia care unit) for resuscitation. The postoperative course was uneventful and the patient was discharged after 4 days. He was satisfied with the operative outcome and complied with the follow-up recommendations. Neither dysfunction nor tumor recurrence was observed so far.

Grossly, a 5×5×4cm left adrenal tumor, in which, some necrosis and tumor-like changes were observed. Histopathology revealed a mixture of normal adrenal cells, adipose tissue, and three major hematopoietic components: myeloid, erythroid, and megakaryocytic lines (Figure 2). These findings confirmed the diagnosis of adrenal myelolipoma.

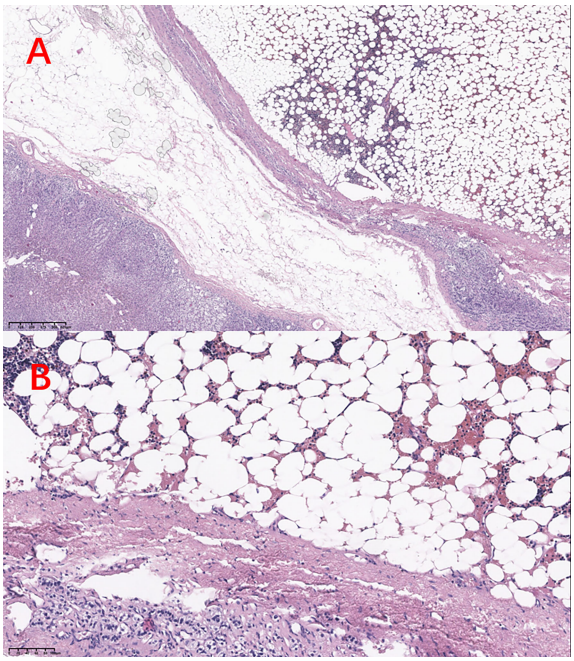


FIGURE 2
HE stains in **(A)** 10× view and **(B)** 40× view.

## Discussion

Adrenal lipomatous tumors are hormonally inactive and are often benign, myelolipoma is the most common type of them (6). Initially, it was mostly diagnosed as a postmortem finding. The prevalence at autopsy was estimated to be 0.08–0.4% in an autopsy series conducted in 1973 (7, 8). However, due to the widespread use of imaging techniques and especially high-resolution imaging procedures, incidental adrenal myelolipoma is increasingly reported. A clear explanation of adrenal myelolipoma etiology has not been determined. Several known risk factors contribute to its pathogenesis, including inflammation, degeneration, trauma, stress, obesity, hypertension, diabetes, and Cushing's syndrome (9, 10). Reticuloendothelial cell metaplasia of adrenal capillaries, emboli from bone marrow, and adrenal embryonic remnants of hematopoietic elements have been suggested as postulated mechanisms (3).

Most AMLs occur unilaterally (more frequent on the right adrenal), but the extra-adrenal localization, such as the presacral area, spleen, stomach, thoracic, retroperitoneal, pelvic, renal, hepatic, and osseous locations are also documented (11, 12). The sexes are affected equally, primarily during their 5th and 7th decades of life (13–15). The majority of AMLs are asymptomatic and hormonally inactive (10). Upon initial diagnosis, the myelolipoma typically with a median size of 2–2.5 cm (usually <4 cm), in diameter (1, 14, 16). Tumors of a larger size may be palpable or may cause symptoms as a result of mass effect, even complicated by spontaneous bleeding and pain, which ultimately lead to hemodynamic shock (17). While AMLs do not generally synthesize hormones, they might sometimes coexist with primary aldosteronism, congenital adrenal hyperplasia (CAH), phaeochromocytoma, adrenal adenoma, and Cushing's syndrome, creating excessive adrenal hormone levels (18).

The diagnosis of AMLs can be reliable by imaging techniques. A CT scan shows low-density fat (-10 to -30 Hounsfield units) mixed with higher-density marrow, which is a useful feature in identifying myelolipoma. In addition, areas of hemorrhage and calcification sometimes are found within the tumor (19). While MRI is more sensitive to detecting the macroscopic fatty tissue components, which usually hyperintense on the T1-weighted images and heterogeneously hyperintense on the T2-weighted images (20). On imaging, although infrequently, it needs to be differentiated from adrenocortical carcinomas with macroscopic fat,

retroperitoneal liposarcoma, adrenal lipomas, teratomas, and angiomyolipomas (2, 21–24).

Conservative management by surveillance with regular imaging follow-up is the therapy of choice for small, and asymptomatic lesions (4, 25). Adrenalectomy is indicated when symptomatology ensues, size greater than 4-7 cm, at a high risk of rupture and bleeding, and suspicion of malignancy in an imaging study (4, 9, 10). As for AMLs >10cm, open surgery is recommended, while just several reports of tumors being removed using minimally invasive strategies. The laparoscopic operation was once considered contraindicated for adrenal tumors exceeding 5-6 cm (26). However, the laparoscopic approach is being increasingly used and extended for larger-size adrenal tumors, and we found 18 articles published reported 23 cases in recent 10 years (3, 4, 17, 25, 27–40). Table 1 provides further details of these reports. Our literature review observes that AML with diameters up to 16 cm can be safely removed through transperitoneal laparoscopy (3, 4). Only one patient converted to open exploratory laparotomy due to multiple adhesions of the previous abdominal surgery which was conducted 6 years ago for a motor vehicle accident (27). Retroperitoneoscopic excision has also been reported as an option, though in limited case quantities (40, 41). Our literature review supports that laparoscopy is feasible and should be suggested as the procedure of choice concerning post-operative comfort, recovery time, scars, post-operative pain, and duration of hospitalization.

As a minimally invasive approach, laparoscopic surgery has well-known advantages over open procedures, including reduced postoperative complications, better cosmetic results, and shorter recovery time. Surgical site infection (SSI) is one of the common postoperative complications, constituting critical damage to surgery patients (42). While laparoscopic surgery shows better performance in decreasing the incidence of SSI due to the smaller incision, less blood loss, and fewer drainage times (43–45).

In addition, a small incision in the minimally invasive procedure can relieve postoperative pain and minimize scarring (46). Also, the time to first flatus, early oral diet restoration, mobilization, and length of hospital stay favor the minimally invasive operation (44). Therefore, more conducive to the rapid rehabilitation of patients after surgery compared with the open approach.

Although limited cases were reported, retroperitoneal routes could also be utilized by the surgeon. Retroperitoneal laparoscopic adrenalectomy, which provides more direct access to the adrenal gland, approaches the lesion from the back without cutting the peritoneum (47). The safety of retroperitoneal laparoscopy has been confirmed by several meta-analyses (47, 48). Despite the disadvantage of the limited operative space, the retroperitoneal approach is now widely accepted as a fast and safe operation, with the merit of shorter surgical time, less post-operative pain, reduced complication rate, and faster recovery (49, 50). Direct access to the adrenal gland, avoiding intraperitoneal organic injury, may probably be the reason for these advantages.

TABLE 1 A summary of reported adrenal myelolipoma resected by laparoscopic surgery in the last decade, arranged by published year.

| First Author | Year | Country | Size (cm) | Sex | Age | Location | Operation approach | Chief complaint | converted to open | Operative time | Blood loss volume | Hospital stays |
|---|---|---|---|---|---|---|---|---|---|---|---|---|
| *Current study* | 2022 | China | 5×5×4 | M | 63 | left adrenal | transperitoneal laparoscopic | asymptomatic | no | 270min | 50ml | 4 |
| Tinozzi FP | 2022 | Italy | 16 × 12 × 6 | M | 61 | right adrenal | transperitoneal laparoscopic | right hypochondrium pain | no | 160min | NR | 5 |
| Zulia YS | 2021 | USA | 15 | M | 50 | right adrenal | transperitoneal laparoscopic | right flank pain | no | NR | NR | NR |
| Kim DS | 2021 | Korea | 9 | M | 50 | right adrenal | transperitoneal laparoscopic | right flank pain | no | NR | NR | NR |
| Katsimantas A | 2020 | Greece | 16.5 × 15 × 6.5 | F | 66 | right adrenal | transperitoneal laparoscopic | asymptomatic | no | 146min | NR | 3 |
| Introini C | 2020 | Italy | 9×6 | M | 47 | right adrenal | transperitoneal laparoscopic | back pain | no | NR | NR | 5 |
| Alkhalifa AM | 2020 | Arabia | 6×4×6 | F | 46 | right adrenal | transperitoneal laparoscopic | abdominal pain | no | NR | NR | 2 |

(*Continued*)

TABLE 1 Continued

| First Author | Year | Country | Size (cm) | Sex | Age | Location | Operation approach | Chief complaint | converted to open | Operative time | Blood loss volume | Hospital stays |
|---|---|---|---|---|---|---|---|---|---|---|---|---|
| Alkhalifa AM | 2020 | Arabia | 6×5 | F | 35 | right adrenal | transperitoneal laparoscopic | asymptomatic | no | NR | NR | 3 |
| Alkhalifa AM | 2020 | Arabia | 9 × 7 × 6.6 | M | 45 | right adrenal | transperitoneal laparoscopic | right flank pain | yes | NR | NR | 2 |
| Alkhalifa AM | 2020 | Arabia | 6 × 5 × 4.5 | F | 47 | left adrenal | transperitoneal laparoscopic | left flank pain | no | NR | NR | 2 |
| Yamamoto T | 2019 | Japan | 14.3 | F | 69 | left adrenal | transperitoneal laparoscopic | asymptomatic | no | NR | NR | NR |
| Piskinpasa H | 2019 | Bangladesh | Right:8×7×5; Left:4.1×2.3 | M | 41 | bilateral adrenal | transperitoneal laparoscopic | asymptomatic | no | NR | NR | NR |
| Mhammedi WA | 2019 | Morocco | 8.5× 8.5× 4.5 | F | 20 | right adrenal | transperitoneal laparoscopic | abdominal pain | no | NR | NR | NR |
| Dotto RS | 2019 | Brazil | 7.0×6.0×8.4 | F | 28 | ectopic adrenal | transperitoneal laparoscopic | amenorrhea | no | 270min | 25ml | 2 |
| Liu N | 2018 | China | 13.5×10.5×6.5 | F | 26 | left adrenal | transperitoneal laparoscopic | secondary amenorrhea | no | NR | NR | NR |
| Molnar C | 2017 | Romania | 4×5 | F | 65 | right adrenal | transperitoneal laparoscopic | right flank pain | no | 120min | NR | 4 |
| Soveid M Md | 2016 | Iran | 6.5 | F | 26 | left adrenal | transperitoneal laparoscopic | left flank pain | no | NR | NR | NR |
| Chaudhary R | 2016 | India | 15×11 | M | 55 | left adrenal | transperitoneal laparoscopic | left upper abdomen pain | no | 210min | 50-60ml | 3 |
| Yang Y | 2015 | China | 4×4×3.3 | M | 40 | right adrenal | transperitoneal laparoscopic | asymptomatic | no | NR | NR | NR |
| Park BH | 2015 | Korea | 9.0×8.5 | F | 45 | right adrenal | transperitoneal laparoscopic | right flank pain | no | 110min | 50ml | NR |
| Yamashita S | 2014 | Japan | 4.5 | M | 49 | right adrenal | transperitoneal laparoscopic | asymptomatic | no | 117min | 20ml | 4 |
| Yamashita S | 2014 | Japan | 5 | F | 40 | right adrenal | transperitoneal laparoscopic | asymptomatic | no | 188min | 160ml | 4 |
| Yamashita S | 2014 | Japan | 3.5 | M | 45 | right adrenal | transperitoneal laparoscopic | asymptomatic | no | 152min | 50ml | 4 |
| Wu ZS | 2013 | Taiwan | 3.6 | M | 30 | right adrenal | posterior retroperitoneoscopic | asymptomatic | no | 160min | NR | 2 |

NR: Not Reported.



10.3389/fonc.2022.1058211

Notably, our patient suffered from pneumothorax immediately after the procedure. The injury to the diaphragm and pleura caused by electrocautery during the dissection of the left adrenal gland tumor was speculated to be the cause of the left-sided pneumothorax. A similar condition secondary to laparoscopic adrenalectomy has previously been observed and reported elsewhere (51–53). Even though the incidence was not high, this experience reminded us to pay close attention to the gentle operation and be vigilant of complications. Since the injury wound is typically small, the pneumothorax can be resolved by suturing the tear under laparoscopy (52). In the present study, we performed a thoracocentesis after the abdominal cavity was closed. The patient recovered well without chest pain or dyspnea.

In addition, histological grading has important prognostic implications. Therefore, exact histological grading is critical for guiding the following management (54). In future research, we will strengthen cooperation with the Pathology department, conducting a large pathological review of the adrenal myelolipoma and consequently better individual treatment and prognosis.

To sum up, the detection of adrenal myelolipoma increased with the development of imaging modalities. However, insufficient awareness of this adrenal incidentaloma exists among clinicians. Studies for establishing a common guideline on the management of adrenal myelolipoma are needed. We suggest laparoscopy could be a safe and effective surgical approach for the treatment strategy.

## Data availability statement

The original contributions presented in the study are included in the article/Supplementary Material. Further inquiries can be directed to the corresponding author.

## Ethics statement

Written informed consent was obtained from the individual(s) for the publication of any potentially identifiable images or data included in this article.

## Author contributions

QF and HL drafted and revised the manuscript. XC and XF collected data and revised the manuscript. QF revised the manuscript for content. JL designed the study and revised the manuscript. All authors contributed to the article and approved the submitted version.

## Funding

This work was supported by Sichuan University from 0 to 1 project (No. 2022SCUH0017); Sichuan Science and Technology Plan Project "International cooperation in science and technology innovation/technological innovation cooperation in Hong Kong, Macao and Taiwan" (No. 2021YFH0095).

## Conflict of interest

The authors declare that the research was conducted in the absence of any commercial or financial relationships that could be construed as a potential conflict of interest.

## Publisher's note

All claims expressed in this article are solely those of the authors and do not necessarily represent those of their affiliated organizations, or those of the publisher, the editors and the reviewers. Any product that may be evaluated in this article, or claim that may be made by its manufacturer, is not guaranteed or endorsed by the publisher.

## Supplementary material

The Supplementary Material for this article can be found online at: https://www.frontiersin.org/articles/10.3389/fonc.2022.1058211/full#supplementary-material

## References

1. Calissendorff J, Juhlin CC, Sundin A, Bancos I, Falhammar H. Adrenal myelolipomas. *Lancet Diabetes Endocrinol* (2021) 9(11):767–75. doi: 10.1016/S2213-8587(21)00178-9

2. Decmann Á, Perge P, Tóth M, Igaz P. Adrenal myelolipoma: a comprehensive review. *Endocrine* (2018) 59(1):7–15. doi: 10.1007/s12020-017-1473-4

3. Katsimantas A, Filippou D, Melloy A, Paparidis S, Ferakis N. Macroscopic appearance of giant adrenal myelolipoma during laparoscopy: An adjunct in differential diagnosis. *Cureus* (2020) 12(1):e6582. doi: 10.7759/cureus.6582

4. Tinozzi FP, Morone G, Calì B, Rebba A, Osman N, Albertario S, et al. Laparoscopic adrenalectomy for a giant adrenal myelolipoma: A case report. *Int J Surg Case Rep* (2022) 90:106678. doi: 10.1016/j.ijscr.2021.106678

5. Riley DS, Barber MS, Kienle GS, Aronson JK, von Schoen-Angerer T, Tugwell P, et al. CARE guidelines for case reports: explanation and elaboration document. *J Clin Epidemiol.* (2017) 89:218–35. doi: 10.1016/j.jclinepi.2017.04.026

6. Khater N, Khauli R. Myelolipomas and other fatty tumours of the adrenals. *Arab J Urol.* (2011) 9(4):259–65. doi: 10.1016/j.aju.2011.10.003

7. Olsson CA, Krane RJ, Klugo RC, Selikowitz SM. Adrenal myelolipoma. *Surgery* (1973) 73(5):665–70. doi: 10.5555/uri:pii:0039606073903279

8. Al Harthi B, Riaz MM, Al Khalaf AH, Al Zoum M, Al Shakweer W. Adrenal myelolipoma a rare benign tumour managed laparoscopically: Report of two cases. *J Minim Access Surg* (2009) 5(4):118–20. doi: 10.4103/0972-9941.59312

9. Shenoy VG, Thota A, Shankar R, Desai MG. Adrenal myelolipoma: Controversies in its management. *Indian J Urol.* (2015) 31(2):94–101. doi: 10.4103/0970-1591.152807

10. Cochetti G, Paladini A, Boni A, Silvi E, Tiezzi A, De Vermandois JAR, et al. Robotic treatment of giant adrenal myelolipoma: A case report and review of the literature. *Mol Clin Oncol* (2019) 10(5):492–6. doi: 10.3892/mco.2019.1823

11. Yamashita S, Ito K, Furushima K, Fukushima J, Kameyama S, Harihara Y. Laparoscopic versus open adrenalectomy for adrenal myelolipoma. *Ann Med Surg (Lond).* (2014) 3(2):34–8. doi: 10.1016/j.amsu.2014.04.001

12. Zattoni D, Balzarotti R, Rosso R. The management of bilateral myelolipoma: Case report and review of the literature. *Int J Surg Case Rep* (2015) 12:31–6. doi: 10.1016/j.ijscr.2015.04.021

13. Ebbehoj A, Li D, Kaur RJ, Zhang C, Singh S, Li T, et al. Epidemiology of adrenal tumours in Olmsted county, Minnesota, USA: a population-based cohort study. *Lancet Diabetes Endocrinol* (2020) 8(11):894–902. doi: 10.1016/S2213-8587(20)30314-4

14. Ichijo T, Ueshiba H, Nawata H, Yanase T. A nationwide survey of adrenal incidentalomas in Japan: the first report of clinical and epidemiological features. *Endocr J* (2020) 67(2):141–52. doi: 10.1507/endocrj.EJ18-0486

15. Al-Bahri S, Tariq A, Lowentritt B, Nasrallah DV. Giant bilateral adrenal myelolipoma with congenital adrenal hyperplasia. *Case Rep Surg* (2014) 2014:728198. doi: 10.1155/2014/728198

16. Ramirez M, Misra S. Adrenal myelolipoma: To operate or not? a case report and review of the literature. *Int J Surg Case Rep* (2014) 5(8):494–6. doi: 10.1016/j.ijscr.2014.04.001

17. Chaudhary R, Deshmukh A, Singh K, Biswas R. Is size really a contraindication for laparoscopic resection of giant adrenal myelolipomas? *BMJ Case Rep* (2016) 2016:1–4. doi: 10.1136/bcr-2016-215048

18. Hisamatsu H, Sakai H, Tsuda S, Shigematsu K, Kanetake H. Combined adrenal adenoma and myelolipoma in a patient with cushing's syndrome: case report and review of the literature. *Int J Urol.* (2004) 11(6):416–8. doi: 10.1111/j.1442-2042.2004.00815.x

19. Wale DJ, Wong KK, Viglianti BL, Rubello D, Gross MD. Contemporary imaging of incidentally discovered adrenal masses. *BioMed Pharmacother.* (2017) 87:256–62. doi: 10.1016/j.biopha.2016.12.090

20. Cyran KM, Kenney PJ, Memel DS, Yacoub I. Adrenal myelolipoma. *AJR Am J Roentgenol.* (1996) 166(2):395–400. doi: 10.2214/ajr.166.2.8553954

21. Craig WD, Fanburg-Smith JC, Henry LR, Guerrero R, Barton JH. Fat-containing lesions of the retroperitoneum: radiologic-pathologic correlation. *Radiographics* (2009) 29(1):261–90. doi: 10.1148/rg.291085203

22. Ferrozzi F, Bova D. CT and MR demonstration of fat within an adrenal cortical carcinoma. *Abdom Imaging.* (1995) 20(3):272–4. doi: 10.1007/BF00200415

23. Lam KY, Lo CY. Adrenal lipomatous tumours: a 30 year clinicopathological experience at a single institution. *J Clin Pathol* (2001) 54(9):707–12. doi: 10.1136/jcp.54.9.707

24. Lam AK. Lipomatous tumours in adrenal gland: WHO updates and clinical implications. *Endocr Relat Cancer* (2017) 24(3):R65–r79. doi: 10.1530/ERC-16-0564

25. Zulia YS, Gopireddy D, Kumar S, Singareddy A, Lall C. A rare case of hemorrhagic giant adrenal myelolipoma: Radiographic and pathologic correlation. *Cureus* (2021) 13(8):e17353. doi: 10.7759/cureus.17353

26. MacGillivray DC, Shichman SJ, Ferrer FA, Malchoff CD. A comparison of open vs laparoscopic adrenalectomy. *Surg Endosc.* (1996) 10(10):987–90. doi: 10.1007/s004649900220

27. Alkhalifa AM, Aldossary MY, Abusultan AJ, AlQattan AS, Alsomali M, Alquraish F, et al. Lipomatous tumors of adrenal gland: A case series of 5 patients and review of the literature. *Int J Surg Case Rep* (2020) 67:54–61. doi: 10.1016/j.ijscr.2020.01.027

28. Tang Q, Ji J, Zhou X, Tao R. Adrenal collision tumor: a case report of the coexistence of myelolipoma and ganglioneuroma. *Int J Clin Exp Pathol* (2019) 12(6):2302–4.

29. Piskinpasa H, Ciftci Dogansen S, Kusku Cabuk F, Guzey D, Sahbaz NA, Akdeniz YS, et al. BILATERAL ADRENAL AND TESTICULAR MASS IN a PATIENT WITH CONGENITAL ADRENAL HYPERPLASIA. *Acta Endocrinol (Buchar)* (2019) -5(1):113–7. doi: 10.4183/aeb.2019.113

30. Liu N, Zhang W, Tan J, Zhou J, Yu X, Ren N, et al. Adrenal myelolipoma with hyperandrogenemia and schizophrenia. *Cancer Manag Res* (2018) 10:177–80. doi: 10.2147/CMAR.S145332

31. Mhammedi WA, Ouslim H, Ouraghi A, Irzi M, Elhoumaidi A, Elhoumaidi A, et al. Adrenal myelolipoma: from tumorigenesis to management. *Pan Afr Med J* (2019) 34:180. doi: 10.11604/pamj.2019.34.180.20891

32. Kim DS, Lee JW, Lee SH. Spontaneous rupture of adrenal myelolipoma as a cause of acute flank pain: A case report. *World J Clin Cases.* (2021) 9(22):6552–6. doi: 10.12998/wjcc.v9.i22.6552

33. Dotto RS, Marx G, Bastos M, Machado JL, Glufke V, de Oliveira Freitas DM. A rare case of virilizing adult ectopic adrenal tumor. *Urol Case Rep* (2019) 27:100907. doi: 10.1016/j.eucr.2019.100907

34. Yamamoto T, Koizumi M, Kohno A, Numao N, Inamura K. A case report on 111In chloride bone marrow scintigraphy in management of adrenal myelolipoma. *Med (Baltimore).* (2019) 98(8):e14625. doi: 10.1097/MD.0000000000014625

35. Introini C, Campodonico F, Ennas M, Di Domenico A, Foppiani L. Non-secreting adrenal myelolipoma in a middle-aged male patient manifesting with sudden onset of severe lower back pain. *Arch Ital Urol Androl.* (2020) 92(3):205–6. doi: 10.4081/aiua.2020.3.205

36. Molnar C, Lata L, Pisica R, Russu C, Gherghinescu M, Molnar C, et al. Anterior transabdominal laparoscopic adrenalectomy, without ligatures, for a symptomatic right adrenal myelolipoma with intratumoral hemorrhage. *Chirurgia (Bucur).* (2017) 112(1):58–62. doi: 10.21614/chirurgia.112.1.58

37. Yang Y, Ye LY, Yu B, Guo JX, Liu Q, Chen Y. Two case reports of bilateral adrenal myelolipomas. *World J Clin Cases.* (2015) 3(9):853–60. doi: 10.12998/wjcc.v3.i9.853

38. Park BH, Lee SL, Seo KJ, Bae SR, Lee YS, Kang SH, et al. Laparoscopic hand-assisted adrenal sparing surgery for a giant adrenal myelolipoma: A case report. *Int Surg* (2015) 102(9–10):469–72. doi: 10.9738/INTSURG-D-14-00289.1

39. Soveid MM, Rais-Jalali GAM. Seventeen alpha-hydroxylase deficiency associated with absent gonads and myelolipoma: A case report and review of literature. *Iran J Med Sci* (2016) 41(6):543–7.

40. Wu ZS, Chiou SS, Lee JY, Chang YT. Intraperitoneal accessory spleen and adrenal myelolipoma: removal by simultaneous bilateral posterior retroperitoneoscopy. *Surg Laparosc Endosc Percutan Tech.* (2013) 23(1):e29–31. doi: 10.1097/SLE.0b013e3182680c13

41. Gong B, Ma M, Xie W, Yang X, Sun T. Retroperitoneal laparoscopic adrenalectomy with transient renal artery occlusion for large adrenal tumors (≥8 cm). *J Surg Oncol* (2018) 117(5):1066–72. doi: 10.1002/jso.25002

42. Shahane V, Bhawal S, Lele U. Surgical site infections: A one year prospective study in a tertiary care center. *Int J Health Sci (Qassim).* (2012) 6(1):79–84. doi: 10.12816/0005976

43. Li Z, Li H, Lv P, Peng X, Wu C, Ren J, et al. Prospective multicenter study on the incidence of surgical site infection after emergency abdominal surgery in China. *Sci Rep* (2021) 11(1):7794. doi: 10.1038/s41598-021-87392-8

44. de Vermandois JAR, Cochetti G, Zingaro MD, Santoro A, Panciarola M, Boni A, et al. Evaluation of surgical site infection in mini-invasive urological surgery. *Open Med (Wars).* (2019) 14:711–8. doi: 10.1515/med-2019-0081

45. Cochetti G, Boni A, Barillaro F, Pohja S, Cirocchi R, Mearini E. Full neurovascular sparing extraperitoneal robotic radical prostatectomy: Our experience with PERUSIA technique. *J Endourol.* (2017) 31(1):32–7. doi: 10.1089/end.2016.0477

46. Xiao H, Zhou H, Liu K, Liao X, Yan S, Yin B, et al. Development and validation of a prognostic nomogram for predicting post-operative pulmonary infection in gastric cancer patients following radical gastrectomy. *Sci Rep* (2019) 9(1):14587. doi: 10.1038/s41598-019-51227-4

47. Arezzo A, Bullano A, Cochetti G, Cirocchi R, Randolph J, Mearini E, et al. Transperitoneal versus retroperitoneal laparoscopic adrenalectomy for adrenal tumours in adults. *Cochrane Database Syst Rev* (2018) 12(12):Cd011668. doi: 10.1002/14651858.CD011668.pub2

48. Constantinides VA, Christakis I, Touska P, Palazzo FF. Systematic review and meta-analysis of retroperitoneoscopic versus laparoscopic adrenalectomy. *Br J Surg* (2012) 99(12):1639–48. doi: 10.1002/bjs.8921

49. Conzo G, Tartaglia E, Gambardella C, Esposito D, Sciascia V, Mauriello C, et al. Minimally invasive approach for adrenal lesions: Systematic review of laparoscopic versus retroperitoneoscopic adrenalectomy and assessment of risk factors for complications. *Int J Surg* (2016) 28 Suppl 1:S118–23. doi: 10.1016/j.ijsu.2015.12.042

50. Lee CR, Walz MK, Park S, Park JH, Jeong JS, Lee SH, et al. A comparative study of the transperitoneal and posterior retroperitoneal approaches for laparoscopic adrenalectomy for adrenal tumors. *Ann Surg Oncol* (2012) 19(8):2629–34. doi: 10.1245/s10434-012-2352-0

51. Naito S, Uozumi J, Shimura H, Ichimiya H, Tanaka M, Kumazawa J. Laparoscopic adrenalectomy: review of 14 cases and comparison with open adrenalectomy. *J Endourol.* (1995) 9(6):491–5. doi: 10.1089/end.1995.9.491

52. Aron M, Colombo JRJr., Turna B, Stein RJ, Haber GP, Gill IS. Diaphragmatic repair and/or reconstruction during upper abdominal urological laparoscopy. *J Urol.* (2007) 178(6):2444–50. doi: 10.1016/j.juro.2007.08.045

53. Maccora D, Walls GV, Sadler GP, Mihai R. Bilateral adrenalectomy: a review of 10 years' experience. *Ann R Coll Surg Engl* (2017) 99(2):119–22. doi: 10.1308/rcsann.2016.0266

54. Okubo Y, Yamamoto Y, Sato S, Yoshioka E, Suzuki M, Washimi K, et al. Diagnostic significance of reassessment of prostate biopsy specimens by experienced urological pathologists at a high-volume institution. *Virchows Arch* (2022) 480(5):979–87. doi: 10.1007/s00428-022-03272-0

frontiers | Frontiers in Oncology

TYPE Case Report
PUBLISHED 08 December 2022
DOI 10.3389/fonc.2022.1088803



OPEN ACCESS

EDITED BY
Zhaolun Cai,
Sichuan University, China

REVIEWED BY
Wanchun Zhu,
Shanghai Jiao Tong University, China
Maogui Li,
Qilu Hospital, Shandong University, China
Zhaohui Zhu,
Peking Union Medical College Hospital (CAMS), China

*CORRESPONDENCE
Dabiao Zhou
zhoudabiao@bjtth.org
Daqin Feng
13807713918@163.com

SPECIALTY SECTION
This article was submitted to Surgical Oncology, a section of the journal Frontiers in Oncology

RECEIVED 03 November 2022
ACCEPTED 23 November 2022
PUBLISHED 08 December 2022

CITATION
Li C, Feng D and Zhou D (2022) Case report: Clinical and single-cell transcriptome sequencing analysis of a mixed gangliocytoma-adenoma presenting as acromegaly. *Front. Oncol.* 12:1088803. doi: 10.3389/fonc.2022.1088803



# Case report: Clinical and single-cell transcriptome sequencing analysis of a mixed gangliocytoma-adenoma presenting as acromegaly

Chao Li[1], Daqin Feng[1]* and Dabiao Zhou[2]*

[1]Department of Neurosurgery, The First Affiliated Hospital, Guangxi Medical University, Nanning, China, [2]Department of Neurosurgery, Beijing Tiantan Hospital, Capital Medical University, Beijing, China

**Background:** Mixed gangliocytoma-adenoma (MGA) is a rare tumor of pituitary gland. It's difficult to distinguish it from pituitary adenoma by clinical manifestations, imaging features or serological testing. Thus, the histopathological examination is still the golden standard for diagnosis. Besides, studies on molecular level are still lacking.

**Case information:** In this case report, we described a 28-year-old male with MGA presenting as acromegaly, who suffered staging operation and post-operation gamma knife radiosurgery, but finally died of secondary hyperglycemic hyperosmolar collapse. A complete data including clinical, histopathological, ultrastructural and single-cell transcriptome level information were collected and analyzed.

**Conclusion:** This case report detailed the only clinical and molecular report of MGA following operation and radiotherapy. Complete clinical data enhanced the understanding of the diagnosis and treatment of this disease. Besides, the single-cell transcriptome sequencing analysis further disclosed the intra-tumoral heterogeneity and provided support for subsequent basic research.

KEYWORDS

**mixed gangliocytoma-adenoma, pituitary tumors, acromegaly, single-cell transcriptome sequencing, case report**

# Introduction

Mixed gangliocytoma-adenoma (MGA) is a kind of collision tumor of the pituitary gland, which was first written into World Health Organization (WHO) Classification of pituitary tumors in 2017 (1, 2). It is rarely seen among pituitary tumors, accounting for 0.29% approximately and often presenting the same kind of clinical symptoms as pituitary adenomas (3). Up to now, no more than 200 cases had been reported worldwide, and research on the diagnostic, therapeutic and molecular pathological aspects of the disease is still lacking (4). The aim of this study is to report a MGA, to be more precise, a growth hormone (GH) secreting type presenting as acromegaly. The clinical course, imaging features, blood hormone levels, histopathologic features, ultrastructural features and single-cell transcriptome characterization of the case were included in this study. This case report followed the CARE Guidelines (5).

# Case description

## Clinical course

The patient was a 20-year-old Chinese male who developed symptoms and signs of acromegaly within three years prior to hospitalization, including enlargement of the hands, feet, nose and jaw, thicker skin, deepening of the voice, and myocardial hypertrophy, etc. (Figure 1A). Over the one-month period before admition, he developed headache, hypertension, diabetes, reduced vision, visual field defects and polyuria. Blood hormone level screening showed the serum growth hormone level of him was over 40ng/mL (0.06-5.00ng/mL), and the Insulin-like growth factor-1(IGF-1) was 1567ng/mL (127~424ng/mL). The MRI revealed a solid-cystic lesion located in the enlarged and sunken sellar turcica, measuring about 44mm*27mm*37mm. The lesion presented with equal T1 and T2 signals, and showed significantly inhomogeneous enhancement. The MRI also showed an invasive behavior with mass effect on the optic chiasm, left cavernous sinus involvement, and internal carotid artery encased (Figure 1B).

Due to the relatively large size of the tumor and the location both within the sellar and supra-sellar, it was difficult to remove it at once. So, the doctor suggested a staged tumor resection plan. For the first time, the tumor was removed from the sellar using a transnasal-sphenoidal approach. Intraoperatively, the tumor was seen to be grayish-red in color, with a heterogeneous texture and a relatively rich blood supply. The operation was successful with no postoperative complications like cerebrospinal fluid leakage. After the first surgery, the serum GH level decreased to some extent but was not well controlled and remained at about 18ng/mL (0.06-5.00ng/mL). Eleven months later, the patient underwent a second surgery with the frontolateral approach to remove the suprasellar and parasellar part of the tumor. However, due to the hard texture of the tumor encircling the left internal carotid artery, some of the tumor body remained (Figure 1C), and the postoperative serum GH level still did not drop to normal level which was about 7ng/mL (0.06-5.00ng/mL). Three months after surgery, the patient further underwent gamma knife radiation therapy. Unluckily, it did not show significant efficacy after treatment. Then, the doctor suggested a growth inhibitor analog injection therapy, but the patients denied due to the weak economic condition. Four months later, the patient developed a severe hyperosmolar hyperglycemic syndrome with blood glucose exceeding 35 mmol/L, resulting in electrolyte disturbances and secondary coma. Finally, the patient died of

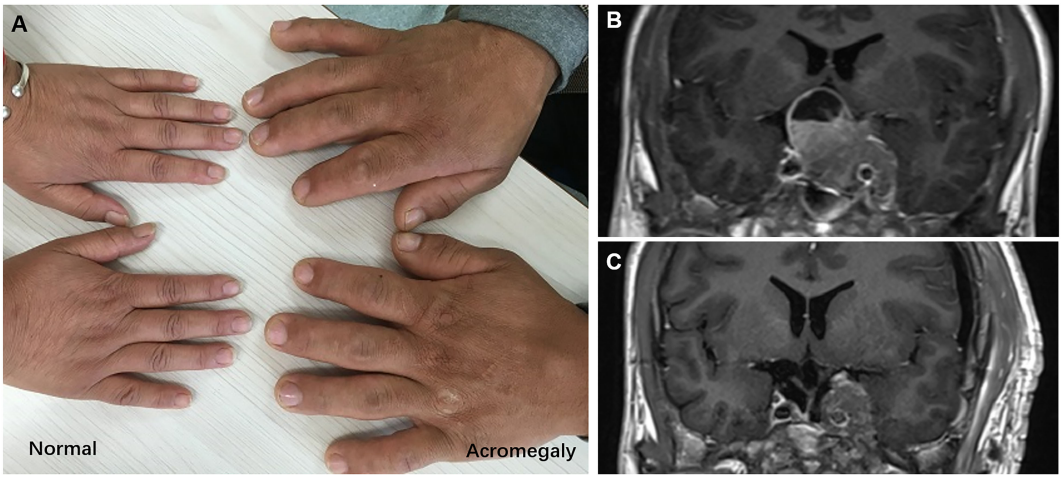


FIGURE 1
**(A)** The hands of normal and acromegaly people. **(B)** Preoperative MRI, 44mm× 27mm×37mm in size, with left cavernous sinus involvement, and internal carotid artery encased. **(C)** Postoperative MRI, show the residual tumor encircling the left internal carotid artery.

ineffective resuscitation in 33 months after the first surgery. Time line of the clinical course was shown in Figure S1.

## Histopathological examination

The hematoxylin-eosin (HE) staining revealed cap-like gangliocytoma cells surrounding the adenoma cells (Figure 2A). Further immunohistochemistry profile showed strongly positive for GH and Synapsin, scattered positive for Prolactin(PRL) and Ck8/18, and about 5% monoclonal antibody (MIB)-1 proliferative index positivity (Figures 2B–D). Immunofluorescent staining show strong positive for Pituitary transcript factor 1(Pit-1) (Figure 2E), which further proved its Pit-1 lineage origin. These findings are characteristic of the diagnosis of MGA. Further, the ultrastructure observed by electron microscope showed that tumor cells were densely distributed, with nuclei of different sizes, intracytoplasmic fibrous vesicles, round secretory granules within the fibrous vesicles, and scattered capillaries in the interstitium (Figure 2F). The suspicious gangliocytoma cells were large and contain abundant cytoplasm and Nissl granules.

## Single cell transcriptome sequencing analysis

Single-cell transcriptome sequencing analysis was performed on fresh tumor tissue obtained during two surgeries, 89 cells from the first surgery and 120 cells from the second surgery. First, a modified Single-cell Tagged Reverse Transcription sequencing (STRT-seq) technique (6) was applied and the single-cell RNA sequencing (scRNA-seq) data was obtained through Illumina sequencing. Then, information on chromosome copy number variation (CNV) was obtained by the InferCNV method based on scRNA-seq data, and a comparison of the CNV profiles of the two specimens revealed that two specimens had gain in chromosome 4, while chromosome 11 deletion was only detected in the specimen obtained from the first surgery, thus suggesting the possible existence of temporal and spatial heterogeneity within the tumor (Figure 3A). Then, all the 209 cells were analyzed by principal component analysis (PCA), and the results showed that the cells were almost clustered together, and only little part of cells (7/209) had cell cycle heterogeneity, which indicated that the heterogeneity within the tumor was small and about 3% of cells was in the process of mitosis (Figure 3B). At last, the differentially expressed genes of this case were analyzed and the biological processes (BP) corresponding to them were clarified by Gene Ontology (GO) enrichment analysis, in which the biological processes that were more involved were “Cytoskeleton Organization”, “anatomical structure development”, and “cellular component assembly involved in morphogenesis”(Figure 3C).

# Discussion

One category of tumors highlighted in 2017 WHO classification is neuronal and paraneuronal tumors, which

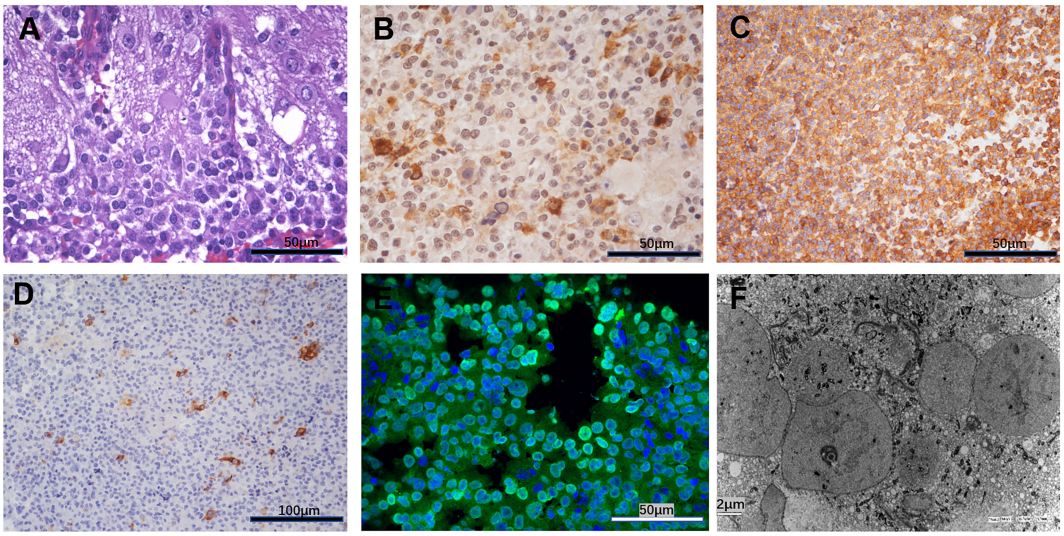


FIGURE 2
**(A)** Hematoxylin-eosin HE revealed cap-like gangliocytoma cells surrounding the adenoma cells. **(B)** Immunohistochemistry showed strongly positive for growth hormone. **(C)** Immunohistochemistry showed strongly positive for synapsin. **(D)** Immunohistochemistry showed scattered positive for Prolactin (PRL). **(E)** Immunofluorescent staining show strong positive for Pituitary Transcript Factor 1(Pit-1). **(F)** The ultrastructure observed by Electron microscope.

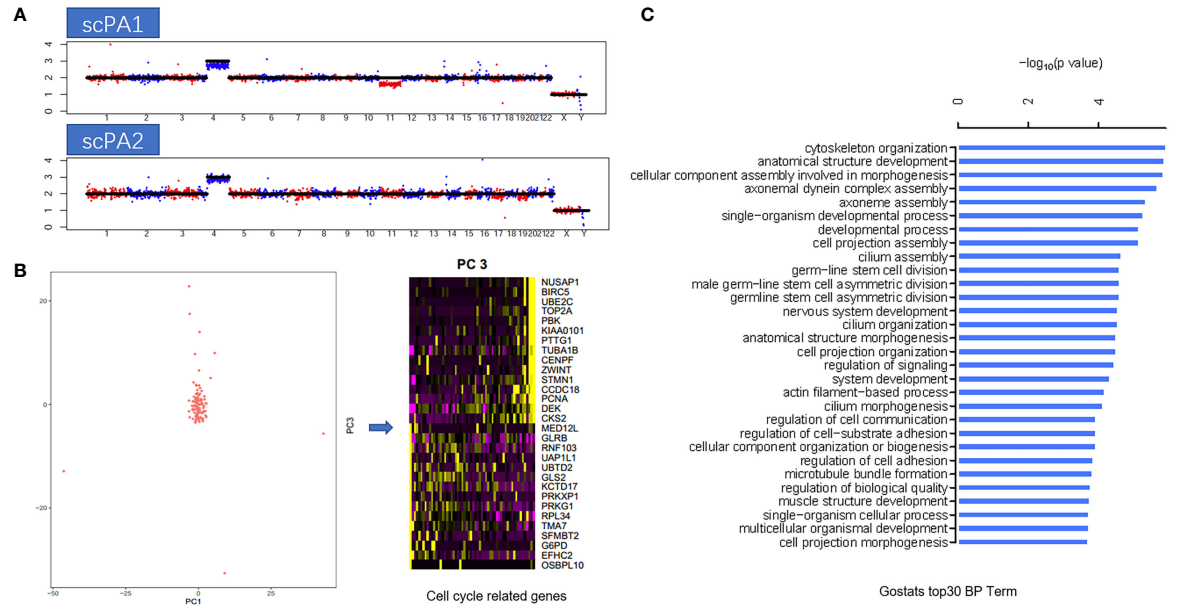


FIGURE 3
**(A)** Copy number variation (CNV) profiles of the two specimens: first surgery(scPA1) and second surgery(scPA2), show gain in chromosome 4 (both), and chromosome 11 deletion in scPA1 only, indicated the possible existence of temporal and spatial heterogeneity within the tumor. **(B)** Principal component analysis (PCA) showed that the cells were almost clustered together, and only little part of cells (7/209) had cell cycle heterogeneity (PC2 represented cell cycle related genes). **(C)** GO enrichment analysis of the differentially expressed genes of this case, the top 30 biological processes (BP) term were listed.

includes gangliocytoma and mixed gangliocytoma-adenoma, neurocytoma, paraganglioma and neuroblastoma, all of which are rare tumors, but they are of particular importance in the differential diagnosis of pituitary tumors (1, 2, 7, 8). This study highlights a case of mixed gangliocytoma-adenoma, which has a very low incidence, found to be only 0.29% (14/4891) in a retrospective German study that included 4891 pituitary lesions (3). Currently, there are three hypotheses regarding the pathogenesis of the disease: 1) Neuronal differentiation hypothesis. It is believed that most ganglion cell tumors in the sellar are the result of neuronal differentiation and chemosis in pituitary adenomas. Evidence supporting this hypothesis includes that both pituitary adenomas and ganglion cells can be observed microscopically (9). In a pathological study, Mikami et al. found that mixed gangliocytoma-adenoma is an intermediate morphological cell that lies between gangliocytoma and GH or PRL cell adenoma (10). It is generally believed that ganglion cells have no hormone-secreting capacity, but Li et al. found positive pituitary hormone expression in some tumor cells by performing neuron-related immunohistochemical staining of ganglion cell tumors in the sellar area (11). In addition, *in vitro* culture of anterior pituitary cells revealed that they can be converted into ganglion cells with different degrees of differentiation, providing a theoretical basis that pituitary adenomas can undergo neuronal transformation (12). 2) Residual ganglion cell hypothesis. It is believed that the ganglion cells that originally disappeared from the posterior pituitary gland due to excessive differentiation, like hypothalamic neurons, had the ability to release prohormone-releasing hormone, which can stimulate the occurrence of pituitary adenoma (13). At the same time, the ganglion cells are stimulated by the excessive secretion of prohormone-releasing hormone from the adenohypophysis and hypothalamic neurons, and eventually become tumorigenic (9). 3) Pituitary multipotent stem cell hypothesis (14). In 2006, Kontogeorgos et al. found that typical pituitary adenoma cells could express NFP, suggesting that pituitary adenomas have neuronal properties (15).

The clinical and imaging manifestations of mixed gangliocytoma-adenoma are essentially indistinguishable from pituitary adenoma, making preoperative diagnosis more difficult. This case presented clinically with acromegaly. On cranial MRI, the tumor was predominantly solid with occasional cystic changes. Also, it showed aggressive growth on imaging, invading the left cavernous sinus and encircling the internal carotid artery. So, a staged resection strategy was adopted. However, due to the tough texture of the cavernous sinus segment, a total dissection could not be achieved, and the

oculomotor nerve was disturbed during the operation which leaded to postoperative oculomotor nerve palsy. In recent years, with the development of endoscopic technique, some medical centers had attempted to resecting the intrasellar and parasellar lesions through a combined endoscopic transsphenoidal and craniotomy strategy (16, 17). Three months after the postoperative interval, the patient underwent Gamma Knife treatment, but the results were not satisfactory. Gamma knife radiosurgery has emerged as a relatively safe management option for patients (e.g., when cavernous sinus or dural invasion prevents total resection) with adjuvant treatment after sub-total resection of the lesion, or as primary treatment for selected patients when the risk of surgery is considered too high. The reported incidence of new endocrine disorders after radiosurgery was typically in the range of 25% to 40%, with a lower incidence of hypopituitarism approaching 20% (18). With recent multicenter study series showing that functional pituitary adenomas require higher therapeutic doses than nonfunctional pituitary adenomas and that patients with high doses of pituitary stalk irradiation in Gamma Knife treatment are at higher risk for post-Gamma Knife treatment endocrine disorders, the risk burden of achieving long-term endocrine remission remains a concern in current treatment approaches (18, 19). Eventually, the patient died of sudden syncope due to secondary hyperglycemic hyperosmolar syndrome. It has been reported that 15% to 38% of patients with acromegaly develop reduced glucose tolerance or diabetes, and high GH leads to abnormal glucose metabolism through several pathways, with insulin resistance being the predominant mechanism (20). High GH, advanced age, long duration of disease, family history of diabetes, and hypertension are risk factors for the development of abnormal glucose tolerance in patients with acromegaly (21). Through the diagnosis and treatment process of this case, we further understood the refractory nature of mixed gangliocytoma-adenoma, especially the growth hormone type, which is often accompanied by systemic damage, and can greatly affect the patient's quality and expectancy of life. The authors' opinion was: 1) Surgical resection remains the preferred first-line treatment; after all, surgery can immediately reduce GH and IGF-1 to lower levels as well as improve signs and symptoms and obtain a pathologic histologic confirmation. 2) In surgery, resection of pituitary adenomas extending into the cavernous sinus is aggressively pursued; however, residual tumor in the cavernous sinus is inevitable. 3) The efficacy of Gamma knife treatment of residual or recurrent MGA presenting as acromegaly still needs to be tested. 4) It has also been shown that appropriate use of growth-inhibiting drugs during Gamma Knife treatment, while waiting for IGF-1 normalization, may allow patients with acromegaly to achieve endocrine remission. However, the cost of treatment with growth inhibitors is very high and imposes a heavy financial burden on patients. Therefore, it is important to explore effective lifelong alternative treatment options for patients with persistent acromegaly after surgical resection.

Currently, the diagnosis of MGA relies on postoperative pathological examination, including histomorphological observation and immunohistochemical staining (4, 22). Ganglion cells are distributed in clusters or scattered in the rich nerve fiber network, with eosinophilic cytoplasm and binucleated or multinucleated; while pituitary adenoma cells are diffusely distributed, with round or ovoid nuclei, uniformly slender and loose chromatin, granular cytoplasm, partially vacuolated cytoplasm, and abundant interstitial blood sinuses. Often, these neuronal tumors are situated cap-like over the adenomas, with no obvious boundary between them. Immunohistochemical staining reveals positive expression of markers of ganglicytoma (e.g. SYN, Ck8/18, CgA, S-100, etc.) and positive expression of pituitary cell hormones (e.g. GH, PRL, TSH, ACTH, LH, FSH, etc.). It has also been reported that GHRH is expressed in ganglion cells in MGA with acromegaly (23), and CRH is expressed in ganglion cells in MGA with Cushing's syndrome (24). As for adenoma component in MGA, half is GH adenoma type as reported by Saeger in a Germany cohort with 14 cases included, but there are also reports related to prolactin adenoma, gonadotropin, and ACTH adenoma (3, 25, 26). In this case, tissue observation, immunohistochemistry, and electron microscopic ultrastructural observation were performed and were consistent with previous reports.

In addition, to explore the intratumoral heterogeneity of MGA, we also performed a pioneering single-cell transcriptome sequencing analysis of specimens from both surgeries to explore the tumor cell composition structure, intratumoral heterogeneity of the tumor, and functional types of cells at the single-cell level. Single-cell transcriptome sequencing is a relatively new technology for high-throughput transcriptome sequencing at the individual cell level, which can effectively address the challenges of cell heterogeneity and transcriptome heterogeneity within cell populations that are masked by bulk RNA-seq, and help discover new rare cell types and gain insight into the mechanisms of expression regulation during cell growth (27, 28). Through single-cell level studies, we found some temporal and spatial heterogeneity in the intratumoral cells of MGA, as evidenced by differences in the CNV profiles of the two specimens. However, at the transcriptomic level, the transcriptomic gene expression patterns of the cells obtained from the two specimens were extremely similar, with only a small fraction of cells in mitosis, which in turn suggested that MGA is a tumor with less intratumoral heterogeneity and inactive proliferation, which is consistent with previous studies of pituitary adenomas at the bulk level (29–31). We then focused on the functional properties of the

adenomatous component of growth hormone in MGA, and obtained the more active biological processes within the tumor by GO analysis. However, unfortunately, no ganglion cells were found in the 209 single cells we obtained by analyzing their gene signature. We speculated that this might be related to the insufficient number of cells taken, therefore, we also intended to further search for ganglicytoma cells by increasing the specimen volume in future studies.

## Conclusion

Mixed gangliocytoma-adenoma presenting as acromegaly is a rare CNS neoplasm which is not that benign, because it's growth hormone over-secretion behavior can cause severe damage to various systems of the body, and once it shows an invasive growth pattern, it is hard to achieve anatomic and functional resection, thus seriously affects the quality and span of patients' life. MRI findings are useful to make a surgery planning, but the histopathological examination, including a full immunohistochemistry panel, is essential to correctly diagnose MGA. With a high probability, single-cell molecular testing can help deeper understanding the pathogenesis of the disease, but more cases will be needed in the future.

## Data availability statement

The datasets presented in this study can be found in online repositories. The names of the repository/repositories and accession number(s) can be found in the article/Supplementary Material.

## Ethics statement

Written informed consent was obtained from the minor(s)' legal guardian/next of kin for the publication of any potentially identifiable images or data included in this article.

## Author contributions

CL wrote the manuscript. DZ and DF reviewed and edited the manuscript. All authors contributed to the article and approved the submitted version.

## Funding

This work was supported by the National Natural Science Foundation of China (Grant No. 31671109).

## Conflict of interest

The authors declare that the research was conducted in the absence of any commercial or financial relationships that could be construed as a potential conflict of interest.

## Publisher's note



## Supplementary material

The Supplementary Material for this article can be found online at: https://www.frontiersin.org/articles/10.3389/fonc.2022.1088803/full#supplementary-material

SUPPLEMENTARY FIGURE 1
The timeline of the clinical course of the case.

## References

1. Mete O, Lopes MB. Overview of the 2017 WHO classification of pituitary tumors. *Endocr Pathol* (2017) 28(3):228–43. doi: 10.1007/s12022-017-9498-z

2. Lopes MBS. The 2017 world health organization classification of tumors of the pituitary gland: A summary. *Acta Neuropathol* (2017) 134(4):521–35. doi: 10.1007/s00401-017-1769-8

3. Saeger W, Lüdecke DK, Buchfelder M, Fahlbusch R, Quabbe HJ, Petersenn S. Pathohistological classification of pituitary tumors: 10 years of experience with the German pituitary tumor registry. *Eur J endocrinol* (2007) 156(2):203–16. doi: 10.1530/eje.1.02326

4. Cossu G, Brouland JP, La Rosa S, Camponovo C, Viaroli E, Daniel RT, et al. Comprehensive evaluation of rare pituitary lesions: A single tertiary care pituitary center experience and review of the literature. *Endocr pathol* (2019) 30(3):219–36. doi: 10.1007/s12022-019-09581-6

5. Riley DS, Barber MS, Kienle GS, Aronson JK, von Schoen-Angerer T, Tugwell P, et al. CARE guidelines for case reports: Explanation and elaboration document. *J Clin Epidemiol* (2017) 89:218–35. doi: 10.1016/j.jclinepi.2017.04.026

6. Natarajan KN. Single-cell tagged reverse transcription (STRT-seq). *Methods Mol Biol (Clifton NJ)* (2019) 1979:133–53. doi: 10.1007/978-1-4939-9240-9_9

7. Castillo M, Mukherji SK. Intrasellar mixed gangliocytoma-adenoma. *AJR Am J roentgenol* (1997) 169(4):1199–200. doi: 10.2214/ajr.169.4.9308499

8. Kamel OW, Horoupian DS, Silverberg GD. Mixed gangliocytoma-adenoma: A distinct neuroendocrine tumor of the pituitary fossa. *Hum pathol* (1989) 20 (12):1198–203. doi: 10.1016/S0046-8177(89)80012-7

9. Geddes JF, Jansen GH, Robinson SF, Gmr E, Holton JL, Monson JP, et al. 'Gangliocytomas' of the pituitary: a heterogeneous group of lesions with differing

histogenesis. *Am J Surg pathol* (2000) 24(4):607–13. doi: 10.1097/00000478-200004000-00017

10. Mikami S, Kameyama K, Takahashi S, Yoshida K, Kawase T, Sano T, et al. Combined gangliocytoma and prolactinoma of the pituitary gland. *Endocr pathol* (2008) 19(2):117–21. doi: 10.1007/s12022-008-9027-1

11. Li JY, Racadot O, Kujas M, Kouadri M, Peillon F, Racadot J. Immunocytochemistry of four mixed pituitary adenomas and intrasellar gangliocytomas associated with different clinical syndromes: acromegaly, amenorrhea-galactorrhea, cushing's disease and isolated tumoral syndrome. *Acta neuropathologica* (1989) 77(3):320–8. doi: 10.1007/BF00687585

12. Vidal S, Horvath E, Bonert V, Shahinian K, Kovacs K. Neural transformation in a pituitary corticotroph adenoma. *Acta neuropathologica* (2002) 104(4):435–40. doi: 10.1007/s00401-002-0561-5

13. Koutourousiou M, Kontogeorgos G, Wesseling P, Grotenhuis AJ, Seretis A. Collision sellar lesions: Experience with eight cases and review of the literature. *Pituitary*. (2010) 13(1):8–17. doi: 10.1007/s11102-009-0190-2

14. Chen J, Hersmus N, Van Duppen V, Caesens P, Denef C, Vankelecom H. The adult pituitary contains a cell population displaying stem/progenitor cell and early embryonic characteristics. *Endocrinol* (2005) 146(9):3985–98. doi: 10.1210/en.2005-0185

15. Kontogeorgos G, Mourouti G, Kyrodimou E, Liapi-Avgeri G, Parasi E. Ganglion cell containing pituitary adenomas: Signs of neuronal differentiation in adenoma cells. *Acta neuropathologica* (2006) 112(1):21–8. doi: 10.1007/s00401-006-0055-y

16. Heng LJ, Jia D, Gong L, Zhang W, Ma J, Qu Y. Endoscopic endonasal resection of a mixed lesion of gangliocytoma and nonfunctioning pituitary adenoma. *World neurosurg* (2017) 106:1050.e1–.e6. doi: 10.1016/j.wneu.2017.05.064

17. Shepard MJ, Elzoghby MA, Ghanim D, Lopes MBS, Jane JAJr. Transsphenoidal surgery for mixed pituitary gangliocytoma-adenomas. *World neurosurg* (2017) 108:310–6. doi: 10.1016/j.wneu.2017.08.174

18. Pomeraniec IJ, Taylor DG, Cohen-Inbar O, Xu Z, Lee Vance M, Sheehan JP. Radiation dose to neuroanatomical structures of pituitary adenomas and the effect of gamma knife radiosurgery on pituitary function. *J neurosurg* (2019) 132 (5):1499–506. doi: 10.3171/2019.1.JNS182296

19. Gupta T, Chatterjee A. Modern radiation therapy for pituitary adenoma: Review of techniques and outcomes. *Neurol India* (2020) 68(Supplement):S113–S22. doi: 10.4103/0028-3886.287678

20. Vilar L, Vilar CF, Lyra R, Lyra R, Naves LA. Acromegaly: Clinical features at diagnosis. *Pituitary*. (2017) 20(1):22–32. doi: 10.1007/s11102-016-0772-8

21. Hannon AM, Thompson CJ, Sherlock M. Diabetes in patients with acromegaly. *Curr Diabetes Rep* (2017) 17(2):8. doi: 10.1007/s11892-017-0838-7

22. Xiao P, Xue L, Peng JJ, Feng ST, Liao B, Wen JM. An intrasellar mixed gangliocytoma-adenoma including ependymal component, and review of the literature. *BMJ Case Rep* (2009) 2009:733–745. doi: 10.1136/bcr.11.2008.1200

23. Kurosaki M, Saeger W, Lüdecke DK. Intrasellar gangliocytomas associated with acromegaly. *Brain tumor pathol* (2002) 19(2):63–7. doi: 10.1007/BF02478929

24. Saeger W, Puchner MJ, Lüdecke DK. Combined sellar gangliocytoma and pituitary adenoma in acromegaly or cushing's disease. a report of 3 cases. *Virchows Archiv: an Int J pathol* (1994) 425(1):93–9. doi: 10.1007/bf00193956

25. Sakata K, Fujimori K, Komaki S, Furuta T, Sugita Y, Ashida K, et al. Pituitary gangliocytoma producing TSH and TRH: A review of "Gangliocytomas of the sellar region". *J Clin Endocrinol Metab* (2020) 105(10):3109–21. doi: 10.1210/clinem/dgaa474

26. Bódi I, Martin AJ, Connor SE, Thomas NW, Lantos PL. Mixed pituitary gangliocytoma/adenoma (prolactinoma) with histogenetic implications. *Neuropathol Appl neurobiol* (2002) 28(3):252–5. doi: 10.1046/j.1365-2990.2002.00392.x

27. Tang F, Barbacioru C, Wang Y, Nordman E, Lee C, Xu N, et al. mRNA-seq whole-transcriptome analysis of a single cell. *Nat Methods* (2009) 6(5):377–82. doi: 10.1038/nmeth.1315

28. Jovic D, Liang X, Zeng H, Lin L, Xu F, Luo Y. Single-cell RNA sequencing technologies and applications: A brief overview. *Clin Trans Med* (2022) 12(3):e694. doi: 10.1002/ctm2.694

29. Melmed S. Pituitary-tumor endocrinopathies. *New Engl J Med* (2020) 382 (10):937–50. doi: 10.1056/NEJMra1810772

30. Barry S, Korbonits M. Update on the genetics of pituitary tumors. *Endocrinol Metab Clinics North America* (2020) 49(3):433–52. doi: 10.1016/j.ecl.2020.05.005

31. Ronchi CL, Peverelli E, Herterich S, Weigand I, Mantovani G, Schwarzmayr T, et al. Landscape of somatic mutations in sporadic GH-secreting pituitary adenomas. *Eur J Endocrinol* (2016) 174(3):363–72. doi: 10.1530/EJE-15-1064

frontiers | Frontiers in Oncology

TYPE Case Report
PUBLISHED 19 December 2022
DOI 10.3389/fonc.2022.1072485



OPEN ACCESS

EDITED BY
Ugo Grossi,
University of Padua, Italy

REVIEWED BY
Firdaus Hayati,
University of Malaysia Sabah, Malaysia
Faten Limaiem,
Hôpital Mongi Slim, Tunisia

*CORRESPONDENCE
Lie Yang
lie_222@163.com

SPECIALTY SECTION
This article was submitted to Surgical Oncology, a section of the journal Frontiers in Oncology

RECEIVED 17 October 2022
ACCEPTED 06 December 2022
PUBLISHED 19 December 2022

CITATION
Yang W, Cai Z, Nie P, Yuan T, Zhou H, Du Q, Qiu S, Zhang J and Yang L (2022) Case report and literature review: Small bowel intussusception due to solitary metachronous metastasis from renal cell carcinoma. *Front. Oncol.* 12:1072485. doi: 10.3389/fonc.2022.1072485



# Case report and literature review: Small bowel intussusception due to solitary metachronous metastasis from renal cell carcinoma

Wenming Yang[1], Zhaolun Cai[2], Pan Nie[3], Tao Yuan[4], Hang Zhou[1], Qiang Du[1], Siyuan Qiu[1], Jianhao Zhang[1] and Lie Yang[1]*

[1]Division of Gastrointestinal Surgery, Department of General Surgery, West China Hospital, Sichuan University, Chengdu, China, [2]Gastric Cancer Center, Department of General Surgery, West China Hospital, Sichuan University, Chengdu, China, [3]Department of Gastrointestinal Surgery, The Third People's Hospital of Chengdu, Chengdu, China, [4]Department of Anesthesiology, West China Hospital, Sichuan University, Chengdu, China

**Introduction:** Solitary metachronous small bowel metastasis from renal cell carcinoma (RCC) is rare. In contrast to idiopathic intussusception frequently occurring in children, adult intussusception is fairly uncommon and usually indicates a malignancy.

**Case presentation:** We presented an 84-year-old man with small bowel intussusception and obstruction due to a solitary metachronous metastasis from RCC. Computed tomography with intravenous contrast revealed small bowel obstruction and a 4 × 4 cm intraluminal soft-tissue mass with moderate enhancement. During urgent exploratory laparotomy, a pedunculated tumor of the distal ileum was found to be the lead point of intussusception. Hence, reduction of the intestinal invagination and segmental resection of the ileum with functional end-to-end anastomosis were performed. Histological examination finally confirmed the diagnosis. The postoperative recovery was uneventful. The patient was discharged without any complications on postoperative day 6.

**Conclusion:** The case report highlights the rarity of solitary metachronous small bowel metastases from RCC and suggests that life-long follow-up of RCC patients is critical due to its unpredictable behavior and the possibility of a long period of dormancy. Complete surgical resection remains the mainstay treatment for such patients.

KEYWORDS

**surgical oncology, case report, renal cell carcinoma, solitary metastasis, adult intussusception**

## Introduction

Renal cell carcinoma (RCC) is the third most frequently diagnosed cancer among urological tumors, with an estimated annual incidence of 0.4 million cases worldwide (1). RCC is a male-predominant (2:1 ratio) malignancy. It appears between 60 and 80 years old, with a median age of approximately 64 years and a near-normal distribution (2). Clear cell RCC (ccRCC) represents the most prevalent histological subtype of RCC (70-80%) and accounts for most RCC-related deaths (3). Partial or radical nephrectomy remains the gold standard in localized ccRCC therapy (4).

Nearly one-third of localized ccRCC patients will eventually develop metastases even after curative nephrectomy (5). Distant metastases in metastatic RCC (mRCC) patients are most frequently found in the lung (45.2%), followed by the bone (29.5%), lymph node (21.8%), liver (20.3%), and adrenal gland (8.9%), whereas the proportion of small bowel metastasis is extremely low (1.1%) (6). Portocaval venous shunts may facilitate small bowel involvement. Metachronous metastasis of RCC may occur more than a decade after the initial presentation and diagnosis. Despite significant progress in systemic treatment over the past two decades, *en bloc* resection of the oligometastatic disease is still a curative option for late RCC metastasis (≥ 2 years) (7).

Adults have intussusception less frequently than children, accounting for less than 5% of all intussusception and 1% of bowel obstruction cases (8). The most frequent pathologic condition that causes adult intussusception is malignancy, and the small bowel is the most affected site (9, 10). Nevertheless, gastrointestinal tract metastasis usually develops from breast cancer, melanoma, lung cancer, and esophageal squamous cell carcinoma, with the small bowel being the least involved site (2%) (11, 12). As a result, initial reduction combined with surgical resection remains the mainstay treatment in adult small bowel intussusception (13).

Following the principles of the CAse REport (CARE) guidelines (14), we reported a small bowel intussusception ascribed to an intramural cauliflower-like mass that proved to be a metastasis from a ccRCC 5 years after radical nephrectomy. In contrast to our case, most adult small bowel intussusceptions are benign illnesses, while large bowel involvement is likely to be malignant. The present case highlights the need for clinicians to maintain a high index of suspicion of metastasis when assessing the occurrence of new symptoms in these patients with a distant history of presumably curative cancer treatment.

## Case presentation

In September 2021, an 83-year-old male patient presented to the emergency department with intermittent abdominal pain and distention accompanied by cessation of passage of flatus and stool for 3 days. The concurrent medical problems included type 2 diabetes mellitus and pulmonary emphysema for more than 30 years. More significantly, he underwent left radical nephrectomy for ccRCC (pT3aN0M0, Fuhrman Grade 3) 5 years previously. The scheduled four cycles of adjuvant therapy with tyrosine kinase inhibitor sunitinib were discontinued because of patient intolerance. Computed tomography (CT) and serum tumor marker levels showed favorable local control and no signs of distant progression during intensive surveillance. The last follow-up visit was just 6 months before this admission.

On admission, he was afebrile with negative result of coronavirus disease 2019 testing. The blood pressure was 123/84 mmHg, and the heart rate was 105 beats per minute. Physical examination revealed pallor, mild dehydration, abdominal distention, and metallic bowel sounds, without rebound tenderness and palpable abdominal mass. Blood tests indicated iron deficiency anemia (hemoglobin, 9.8 g/dL; reference range, 13.0 – 17.5 g/dL) and an elevated percentage of neutrophils (87%; reference range, 40 – 75%). CT of the chest and abdomen with intravenous contrast demonstrated small bowel obstruction due to intussusception of the distal ileum containing an approximately 4 × 4 cm intraluminal soft-tissue mass with moderate enhancement (Figures 1A, B). No lung, bone, or liver metastasis or local relapse of RCC was visible on radiologic examination.

Complying with the multidisciplinary team's decision, the patient underwent an urgent exploratory laparotomy. After the reduction of intestinal invagination, a solitary ileal neoplasm was found to be the lead point of the intussusception (Figure 1C). Hence, segmental resection of the ileum was performed together with primary functional end-to-end anastomosis. Gross examination of the surgical specimen indicated a 4 × 3 × 3-cm taupe cauliflower-like, pedunculated tumor protruding into the ileum (Figure 1D).

Postoperatively, the patient was transferred back to the gastrointestinal surgical ward after spending 1 day in the surgical intensive care unit. Under the guidance of the enhanced recovery after surgery protocol, the patient's convalescence was unremarkable, with oral feeding beginning on postoperative day (POD) 3 and discharge on POD 6. The patient received no additional treatment due to his venerable age and underlying diseases. To date, the 1-year follow-up has been uneventful. The timeline with relevant data from the episode of care is shown in Figure 2.

Hematoxylin and eosin staining showed compact nests of tumor cells with clear cytoplasm separated by delicate vasculature (Figure 3A). The diagnosis of the ileal metastasis from ccRCC was established *via* the following immunohistochemical results: PAX-8 (+), CD10 (+), EMA (+), CK7 (-), CAIX (+), FH (+), SDHB (+), TFE3 (-), and Ki-67 (+, 30%) (Figures 3B-D). A total of 9 mesenteric lymph nodes were identified without tumor involvement. Additionally, genetic testing was declined by the patient's family members.

10.3389/fonc.2022.1072485

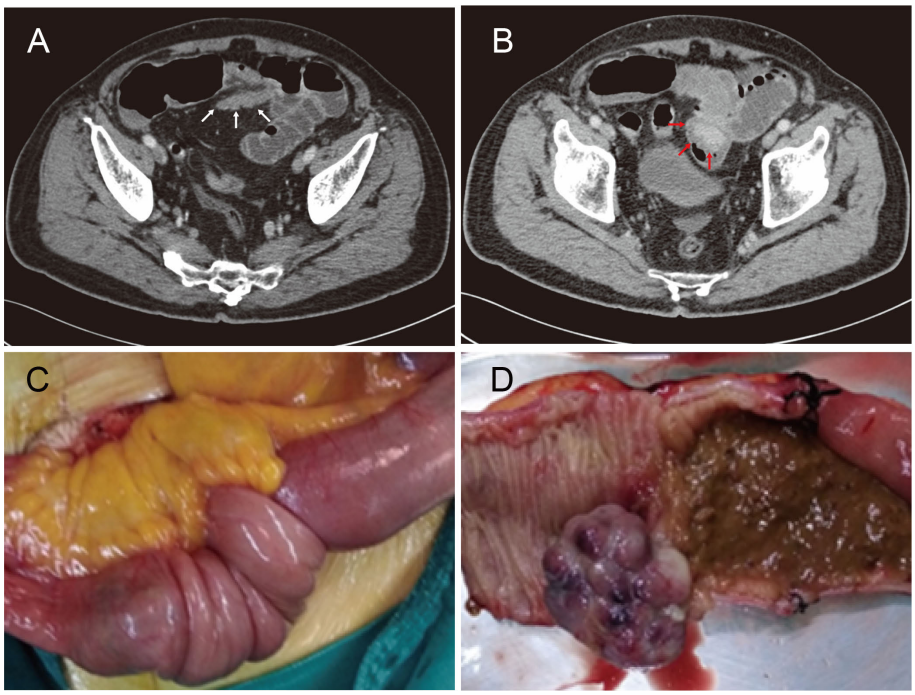


FIGURE 1
**(A, B)** Computed tomography images demonstrating small bowel obstruction due to intussusception of the distal ileum (*white arrows*) containing an approximately 4 × 4 cm intraluminal soft-tissue mass (*red arrows*). **(C)** An intraoperative photo confirming intussusception whose lead point was a solitary ileal neoplasm. **(D)** Gross image of the surgical specimen with a 4 × 3 × 3-cm taupe cauliflower-like, pedunculated tumor.

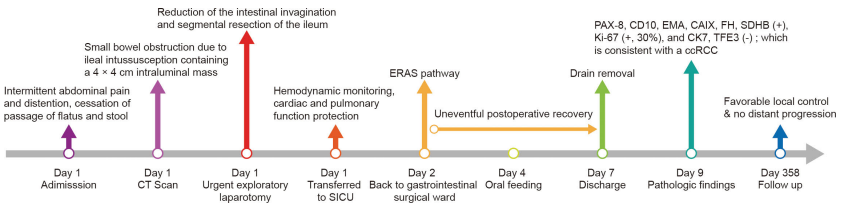


FIGURE 2
Timeline of the case presentation with relevant data. CT, computed tomography; SICU, surgical intensive care unit; ERAS, enhanced recovery after surgery; ccRCC, clear cell renal cell carcinoma.

## Discussion

A systematic electronic literature search was conducted in the PubMed, Embase (OVID interface), and Cochrane Central Register of Controlled Trials databases using medical subject headings and text words related to "solitary metachronous small bowel metastasis from RCC" to obtain relevant case reports published through 10 May 2022. The term "solitary metachronous small bowel metastasis from RCC" was defined as the small bowel metastasis diagnosed more than 6 months after partial or radical nephrectomy for localized RCC. The search strategy and syntax for the PubMed database are shown in the Supplementary material. Papers with non-English language, animal subjects, or unavailable full text were excluded. The general characteristics of the included studies were extracted and entered into a preplanned electronic form (Table 1). The pooled data were interpreted in a descriptive and narrative manner.

Finally, 48 potential studies were included for the evaluation, in which 21 cases with solitary metachronous small bowel

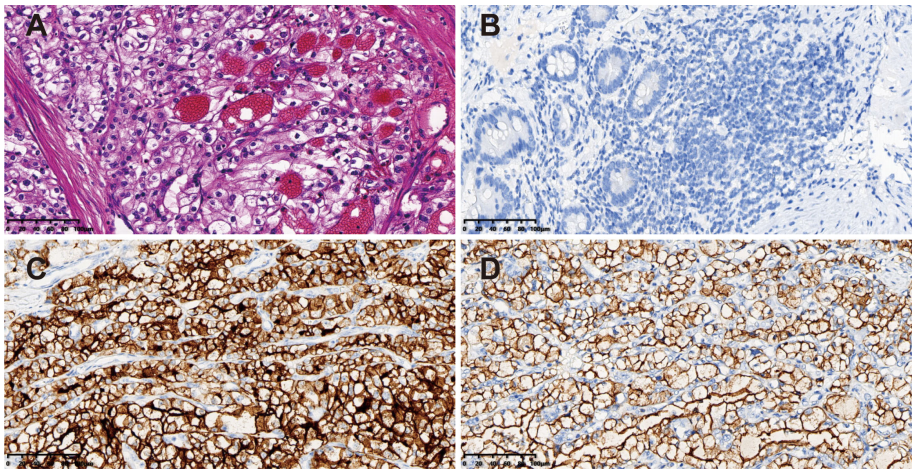


FIGURE 3
Pathological findings of the surgical specimen. **(A)** Hematoxylin & eosin staining showing compact nests of tumor cells with clear cytoplasm separated by delicate vasculature (magnification power: 20×). Immunohistochemical staining of the tumor revealing **(B)** PAX-8 (+), **(C)** CD10 (+), and **(D)** EMA (+) (magnification power: 20×).

metastases from RCC that had been reported between 1952 and 2020 met the inclusion criteria (15–34, 36, 37). The other cases in different publications were excluded due to synchronous, multiple metastases, or lack of additional radiological examination to check for metastases in other sites. The number of published case reports has increased in the last decade. Patients aged 60 years or older accounted for 81.8% of the enrolled instances (18/22). Like the primary RCCs, clear cell disease was the predominant histological subtype in these small bowel metastases (3). The disease course ranged from 8 months to 20 years post curative nephrectomy. Given the longer survival of RCC patients in the era of targeted therapy and immunotherapy, we are convinced that more late metastases will be identified (38, 39).

Ileal metastases from RCC were rather uncommon in our literature review when compared to duodenal and jejunal metastases. Although some subtypes might exhibit regional lymph node involvement, RCC is notable for hematogenous metastasis (40). Viadana et al. found that RCC first metastasizes to the lung *via* the renal vein and inferior vena cava before spreading systemically to multiple organs (41). However, our case revealed that small bowel metastasis may happen before lung metastasis. Furthermore, a clear cell sarcoma-like tumor of the gastrointestinal tract that primarily affects young-aged to middle-aged individuals is increasingly recognized as a primary neuroectodermal malignancy with clear cell morphology and a predilection for the small bowel (42). Besides, S-100 (+), SOX (+), and *EWSR1* gene fusions are essential to confirming the diagnosis (43).

Small bowel metastases from RCC exhibit various biological characteristics (44). We found that the most typical clinical presentations were gastrointestinal bleeding, melena, and secondary iron deficiency anemia. Willis et al. discovered that metastatic small bowel lesions typically form in the submucosa and cause mucosal rupture and ulceration (Borrmann classification type II or III) and bleeding (11, 45). Some individuals might experience non-specific symptoms, such as intermittent blunt abdominal pain, weakness, and weight loss. In addition, intussusception and perforation could occur in rare cases. Intestinal intussusception is primarily caused by the pedunculated small bowel tumor that originates from the submucosa and represents dimple formation on the serosa. Unlike idiopathic intussusception in children, intussusception in adults and the elderly is uncommon but typically associated with an underlying pathology (37).

The significance of radiological screening should be emphasized in patients with atypical symptoms and an RCC history. Small bowel series is inferior to CT as a practical and effective tool in assessing suspicious small bowel lesions, especially in the emergency setting (34). Capsule endoscopy can facilitate the localization of occult bleeding and intraluminal masses and shorten the diagnosis time (36). Besides, single- or double-balloon enteroscopy can assist in hemostasis and biopsy (26). The Tc-99m tagged red blood cell scan can be used for gastrointestinal hemorrhage to show the hypervascular characteristics of the intestinal lesion and guide additional angiography (21). Exploratory laparoscopy and laparotomy can be performed to help verify the diagnosis after getting informed consent.

Systemic treatment should be considered for individuals with medically inoperable RCC (3). Several immune checkpoint inhibitors were initially tested for RCC in the

TABLE 1 General characteristics of the reported cases of solitary metachronous small bowel metastasis from RCC.

| First author& Reference # | Year | Country | Age (years) & Gender | Years post-nephrectomy | Location of metastasis | Clinical presentation | Diagnostic tools | Type of RCC | Treatment Strategy | Follow-up period |
|---|---|---|---|---|---|---|---|---|---|---|
| Starr A (15) | 1952 | USA | 72 F | 20 | jejunum | anemia, occult bleeding in the stool | SBS & surgical exploration | clear cell | surgery | / |
| Nyhan AL (16) | 1987 | USA | 17 M | 1 | duodenum | massive upper gastrointestinal bleeding | arteriography & endoscopy | / | hemostasis | 6 months |
| Robertson GS (17) | 1990 | USA | 70 M | 12 | duodenum | weakness, melena | endoscopy & CT | / | surgery | / |
| Toh SK (18) | 1996 | UK | 69 F | 10 | duodenum | lethargy, colicky abdominal pain, indigestion, anorexia, weight loss, anemia | surgical exploration & pathologic examination | clear cell | surgery | 6 months |
| Leslie KA (19) | 1996 | USA | 78 F | 10 | duodenum | upper abdominal discomfort, pruritus | ERCP | clear cell | surgery | 2.5 years |
| Janzen RM (20) | 1998 | Canada | 75 M | 17.5 | duodenum | maroon-colored stools, anemia | ERCP with side-viewing endoscope | clear cell | surgery | / |
| Nguyen BD (21) | 1998 | USA | 67 M | 20 | ileum | intestinal bleeding | scintigraphy | / | surgery | / |
| Masselli G (22) | 2004 | Italy | 75 F | 4 | ileum | nausea, melena, loose stools | MRE | / | surgery | / |
| Chang WT (23) | 2004 | China | 63 F | 9 | duodenum | upper gastrointestinal bleeding | pathologic examination of frozen sections | clear cell | surgery | 10 moths |
| Bahli ZM (24) | 2007 | UK | 65 F | 1 | jejunum | tiredness, weight loss, intermittent abdominal pain | CE | / | surgery | / |
| Adamo R (25) | 2008 | USA | 86 F | 13 | duodenum | fatigue, anemia, anorexia, early satiety, weight loss | endoscopy & biopsy | clear cell | surgery | 7 moths |
| Takeda T (26) | 2011 | Japan | 75 M | 6 | jejunum | tarry stools | CE & DBE | clear cell | surgery | 6 months |
| Karahan N (27) | 2011 | Turkey | 69 M | 6 | jejunum | bloody vomiting | endoscopy & biopsy | / | surgery | / |
| Vazquez C (28) | 2011 | Uruguay | 68 M | 1 | jejunum | gastrointestinal bleeding | CE | clear cell | surgery | / |
| Cohen DL (29) | 2013 | USA | elderly M | 9 | jejunum | iron deficiency anemia, intermittent rectal bleeding | CE | clear cell | surgery | / |
| Chowdhury SD (30) | 2014 | India | middle-aged M | 6 | duodenum | cholestatic jaundice, recurrent cholangitis | endoscopy & biopsy | clear cell | PTBD | / |
| Ismail I (31) | 2015 | Australia | 66 M | 19 | jejunum | vomiting, abdominal pain | SBS & pathologic examination | clear cell | surgery | 18 months |
| Segura UV (32) | 2017 | Mexico | 48 F | 1 | duodenum | burning, sharp epigastric pain, hematemesis, melaena | endoscopy & biopsy | clear cell | discharge# | 1 week※ |
| Boullosa PE (33) | 2017 | Spain | 71 F | 6 | jejunum | melena, anemia | CE & CT | clear cell | surgery | 13 months |

*(Continued)*





10.3389/fonc.2022.1072485

TABLE 1 Continued

| First author& Reference # | Year | Country | Age (years) & Gender | Years post-nephrectomy | Location of metastasis | Clinical presentation | Diagnostic tools | Type of RCC | Treatment Strategy | Follow-up period |
|---|---|---|---|---|---|---|---|---|---|---|
| Mundath V (34) | 2017 | India | 68 F | 4 | jejunum | abdominal pain | CT & surgical exploration | clear cell | surgery | 6 months※ |
| Ignatavicius P (35) | 2018 | Lithuania | 62 M | 0.66 | duodenum | upper abdominal pain jaundice, general weakness, gastric outlet obstruction | duodenoscopy & biopsy | clear cell | surgery | 14 years |
| Lin KH (36) | 2020 | China | 59 M | 3 | jejunum | intermittent tarry stool | CE | clear cell | surgery | / |

#The patient requested voluntary discharge from the hospital. ※The patient died.
RCC, renal cell carcinoma; SBS, small bowel series; CT, computed tomography; ERCP, endoplasmic retrograde cholangiopancreatography; MRE, magnetic resonance enteroclysis; CE, capsule endoscopy; DBE, double-balloon enteroscopy; PTBD, percutaneous transhepatic biliary drainage.



10.3389/fonc.2022.1072485

adjuvant setting (46, 47). Nevertheless, more prospective phase III clinical trials are needed to provide high-quality evidence. It is necessary to conduct clinical and translational studies to determine the phenotypic predictors of response and resistance to each drug. Genetic testing can help select the optimal treatment regimen. Therefore, systemic and surgical treatments must be integrated to achieve a complete response and to obtain a thorough understanding of the biological features of RCC to explore new targets (48).

Meanwhile, complete metastasectomy of synchronous or metachronous solitary RCC metastasis could improve the patient survival (49). Thus, a conventional segmental resection of the ileum was performed with negative margins and lymph nodes in our case. Only one resected specimen reported by Mundath et al. in our literature review revealed the involvement of lymph nodes (34). Endoscopic hemostasis and transcatheter embolization can be utilized as a bridge to surgery in patients with massive gastrointestinal hemorrhage secondary to mRCC (16). Besides, diverting ostomy and gastrojejunostomy are recommended to ease obstruction-related symptoms in unresectable tumors. Definitive radiotherapy rather than no alternative treatment should be considered for RCC patients with medically inoperable duodenal metastases from RCC.

In conclusion, our case suggests that life-long follow-up of RCC patients is critical due to unpredictable tumor behavior and the possibility of a long period of dormancy. Complete resection of the solitary metachronous small bowel metastasis from RCC is indicated as a life-saving procedure and a curative treatment to cure metastasis-related complications. The present case report and review of the English-language literature emphasizes the rarity of this entity and recommends aggressive and tailored surgical treatment for these patients.

## Data availability statement

The original contributions presented in the study are included in the article/Supplementary Material. Further inquiries can be directed to the corresponding author.

## Ethics statement

The studies involving human participants were reviewed and approved by Ethical Committee on Biomedical Research, West China Hospital, Sichuan University. The patients/participants provided their written informed consent to participate in this study. Written informed consent was obtained from the individual for the publication of any potentially identifiable images or data included in this article.

## Author contributions

LY, WY, ZC, and PN conceptualized and designed the study. WY and ZC drafted the manuscript. TY and HZ were responsible for the literature search. QD, SQ, and JZ collected the clinical data. All authors contributed to the article and approved the submitted version.

## Funding

This study was supported by the 1·3·5 Project for Disciplines of Excellence–Clinical Research Incubation Project, West China Hospital, Sichuan University (Grant No. 2022HXFH028).

## Acknowledgments

We would like to thank Dr. Da-Gang Zhou (Department of Pathology, The Third Affiliated Hospital of Chengdu University of TCM/Chengdu Pidu District Hospital of Traditional Chinese Medicine) for the professional and valuable interpretation of the pathologic findings.

## Conflict of interest

The authors declare that the research was conducted in the absence of any commercial or financial relationships that could be construed as a potential conflict of interest.

## Publisher's note

# References

1. Sung H, Ferlay J, Siegel RL, Laversanne M, Soerjomataram I, Jemal A, et al. Global cancer statistics 2020: GLOBOCAN estimates of incidence and mortality worldwide for 36 cancers in 185 countries. *CA Cancer J Clin* (2021) 71(3):209–49. doi: 10.3322/caac.21660

2. Hsieh JJ, Purdue MP, Signoretti S, Swanton C, Albiges L, Schmidinger M, et al. Renal cell carcinoma. *Nat Rev Dis Primers* (2017) 3:17009. doi: 10.1038/nrdp.2017.9

3. Rini BI, Campbell SC, Escudier B. Renal cell carcinoma. *Lancet* (2009) 373 (9669):1119–32. doi: 10.1016/S0140-6736(09)60229-4

4. Ljungberg B, Bensalah K, Canfield S, Dabestani S, Hofmann F, Hora M, et al. EAU guidelines on renal cell carcinoma: 2014 update. *Eur Urol* (2015) 67(5):913–24. doi: 10.1016/j.eururo.2015.01.005

5. Frank I, Blute ML, Cheville JC, Lohse CM, Weaver AL, Zincke H. An outcome prediction model for patients with clear cell renal cell carcinoma treated with radical nephrectomy based on tumor stage, size, grade and necrosis: the SSIGN score. *J Urol* (2002) 168(6):2395–400. doi: 10.1097/01.ju.0000035885.91935.d5

6. Bianchi M, Sun M, Jeldres C, Shariat SF, Trinh QD, Briganti A, et al. Distribution of metastatic sites in renal cell carcinoma: a population-based analysis. *Ann Oncol* (2012) 23(4):973–80. doi: 10.1093/annonc/mdr362

7. Grüllich C, Vallet S, Hecht C, Duensing S, Hadaschik B, Jäger D, et al. Local salvage therapy for late (≥2 years) metastatic and local relapse of renal cell cancer is a potentially curative treatment irrespective of the site of recurrence. *Urol Oncol* (2016) 34(5):238.e9–17. doi: 10.1016/j.urolonc.2015.11.022

8. Azar T, Berger DL. Adult intussusception. *Ann Surg* (1997) 226(2):134–8. doi: 10.1097/00000658-199708000-00003

9. Cochran AA, Higgins GL3rd, Strout TD. Intussusception in traditional pediatric, nontraditional pediatric, and adult patients. *Am J Emerg Med* (2011) 29(5):523–7. doi: 10.1016/j.ajem.2009.11.023

10. Chiarelli M, Zago M, Tagliabue F, Burati M, Riva C, Vanzati A, et al. Small bowel intussusception due to rare cardiac intimal sarcoma metastasis: A case report. *Front Surg* (2021) 8:743858. doi: 10.3389/fsurg.2021.743858

11. Willis RA. Secondary tumors of the intestine. In: Willis RA, editor. *The spread of tumors in the human body, 3rd edition*. London: Butterworth & Co (1973). p. 209–13.

12. Hsu CC, Chen JJ, Changchien CS. Endoscopic features of metastatic tumors in the upper gastrointestinal tract. *Endoscopy* (1996) 28(2):249–53. doi: 10.1055/s-2007-1005437

13. Hong KD, Kim J, Ji W, Wexner SD. Adult intussusception: a systematic review and meta-analysis. *Tech Coloproctol* (2019) 23(4):315–24. doi: 10.1007/s10151-019-01980-5

14. Riley DS, Barber MS, Kienle GS, Aronson JK, von Schoen-Angerer T, Tugwell P, et al. CARE guidelines for case reports: explanation and elaboration document. *J Clin Epidemiol* (2017) 89:218–35. doi: 10.1016/j.jclinepi.2017.04.026

15. Starr A, Miller GM. Solitary jejunal metastasis twenty years after removal of a renal-cell carcinoma; report of a case. *N Engl J Med* (1952) 246(7):250–1. doi: 10.1056/NEJM195202142460703

16. Nyhan AL, Fishman EK, Kadir S. Diagnosis and management of massive gastrointestinal bleeding owing to duodenal metastasis from renal cell carcinoma. *J Urol* (1987) 138(3):611–3. doi: 10.1016/s0022-5347(17)43275-7

17. Robertson GS, Gertler SL. Late presentation of metastatic renal cell carcinoma as a bleeding ampullary mass. *Gastrointest Endosc* (1990) 36(3):304–6. doi: 10.1016/s0016-5107(90)71032-2

18. Toh SK, Hale JE. Late presentation of a solitary metastasis of renal cell carcinoma as an obstructive duodenal mass. *Postgrad Med J* (1996) 72(845):178–9. doi: 10.1136/pgmj.72.845.178

19. Leslie KA, Tsao JI, Rossi RL, Braasch JW. Metastatic renal cell carcinoma to ampulla of vater: an unusual lesion amenable to surgical resection. *Surgery* (1996) 119(3):349–51. doi: 10.1016/s0039-6060(96)80122-x

20. Janzen RM, Ramj AS, Flint JD, Scudamore CH, Yoshida EM. Obscure gastrointestinal bleeding from an ampullary tumor in a patient with a remote history of renal cell carcinoma: a diagnostic conundrum. *Can J Gastroenterol* (1998) 12(1):75–8. doi: 10.1155/1998/429832

21. Nguyen BD, Port JD, Petronis JD. Scintigraphy of ileal hemorrhage from metastasis of renal cell carcinoma. *Clin Nucl Med* (1998) 23(7):464–5. doi: 10.1097/00003072-199807000-00014

22. Masselli G, Brizi MG, Restaino G, Vecchioli A. MR enteroclysis in solitary ileal metastasis from renal cell carcinoma. *AJR Am J Roentgenol* (2004) 182(3):828–9. doi: 10.2214/ajr.182.3.1820828

23. Chang WT, Chai CY, Lee KT. Unusual upper gastrointestinal bleeding due to late metastasis from renal cell carcinoma: a case report. *Kaohsiung J Med Sci* (2004) 20(3):137–41. doi: 10.1016/S1607-551X(09)70098-1

24. Bahli ZM, Panesar KJ. Solitary jejunal metastasis from renal cell carcinoma. *J Ayub Med Coll Abbottabad* (2007) 19(2):62–3.

25. Adamo R, Greaney PJJr, Witkiewicz A, Kennedy EP, Yeo CJ. Renal cell carcinoma metastatic to the duodenum: treatment by classic pancreaticoduodenectomy and review of the literature. *J Gastrointest Surg* (2008) 12(8):1465–8. doi: 10.1007/s11605-007-0426-2

26. Takeda T, Shibuya T, Osada T, Izumi H, Mitomi H, Nomura O, et al. Metastatic renal cell carcinoma diagnosed by capsule endoscopy and double balloon endoscopy. *Med Sci Monit* (2011) 17(2):CS15–7. doi: 10.12659/msm.881380

27. Karahan N, Bozkurt KK, Cırış IM, Songür Y, Akin M, Cetın M, et al. Duodenojejunal invagination caused by small bowel metastasis of renal cell carcinoma. *Turk J Gastroenterol* (2011) 22(3):355–7. doi: 10.4318/tjg.2011.0231

28. Vazquez C, Berrueta J, De Simone F, Tcheckmedyian A, Gonzalez N, Bernachin J, et al. Small-intestinal bleeding due to metastatic renal cell cancer. *Endoscopy* (2011) 43(Suppl 2 UCTN):E13. doi: 10.1055/s-0030-1255821

29. Cohen DL. Small bowel metastasis from renal cell carcinoma identified on capsule endoscopy. *ACG Case Rep J* (2013) 1(1):3. doi: 10.14309/crj.2013.3

30. Chowdhury SD, Masih D, Chawla G, Pal S, Kurien RT, Augustine J. Metastasis of renal cell carcinoma to the duodenal papilla. *Indian J Gastroenterol* (2014) 33(5):493–4. doi: 10.1007/s12664-013-0398-y

31. Ismail I, Neuen BL, Mantha M. Solitary jejunal metastasis from renal cell carcinoma presenting as small bowel obstruction 19 years after nephrectomy. *BMJ Case Rep* (2015) 2015:bcr2015210857. doi: 10.1136/bcr-2015-210857

32. Segura UV, García-Leiva J, Nuñez BPJ. Duodenal metastases from sarcomatoid renal cell carcinoma: Case report. *Gastroenterol Hepatol* (2017) 40 (8):530–2. doi: 10.1016/j.gastrohep.2016.07.002

33. Boullosa PE, Turnes AM, Iglesias RC, Prada JIR. Jejunal metastasis of renal cell carcinoma. *Rev Esp Enferm Dig* (2017) 109(2):147–8.

34. Vani M, Nambiar A, Geetha K, Kundil B. Metastatic renal cell carcinoma causing small intestinal polyps with intussusception: A report of two cases. *J Clin Diagn Res* (2017) 11(4):ED13–5. doi: 10.7860/JCDR/2017/25513.9652

35. Ignatavicius P, Lizdenis P, Pranys D, Gulbinas A, Pundzius J, Barauskas G. Long-term survival of patient with ampulla of vater metastasis of renal cell carcinoma. *Prague Med Rep* (2018) 119(4):165–9. doi: 10.14712/23362936.2019.4

36. Lin KH, Hsu YC, Yen HH. Metastatic renal cell carcinoma of the jejunum: a rare cause of obscure gastrointestinal bleeding. *ANZ J Surg* (2020) 90(4):626–7. doi: 10.1111/ans.15270

37. Gayer G, Zissin R, Apter S, Papa M, Hertz M. Pictorial review: adult intussusception–a CT diagnosis. *Br J Radiol* (2002) 75(890):185–90. doi: 10.1259/bjr.75.890.750185

38. Albiges L, Tannir NM, Burotto M, McDermott D, Plimack ER, Barthélémy P, et al. Nivolumab plus ipilimumab versus sunitinib for first-line treatment of advanced renal cell carcinoma: extended 4-year follow-up of the phase III CheckMate 214 trial. *ESMO Open* (2020) 5(6):e001079. doi: 10.1136/esmoopen-2020-001079

39. Rini BI, Plimack ER, Stus V, Gafanov R, Hawkins R, Nosov D, et al. Pembrolizumab plus axitinib versus sunitinib for advanced renal-cell carcinoma. *N Engl J Med* (2019) 380(12):1116–27. doi: 10.1056/NEJMoa1816714

40. Dutcher JP. Update on the biology and management of renal cell carcinoma. *J Investig Med* (2019) 67(1):1–10. doi: 10.1136/jim-2018-000918

41. Viadana E, Bross ID, Pickren JW. The metastatic spread of kidney and prostate cancers in man. *Neoplasma* (1976) 23(3):323–32.

42. Wang J, Thway K. Clear cell sarcoma-like tumor of the gastrointestinal tract: an evolving entity. *Arch Pathol Lab Med* (2015) 139(3):407–12. doi: 10.5858/arpa.2013-0547-RS

43. Stockman DL, Miettinen M, Suster S, Spagnolo D, Dominguez-Malagon H, Hornick JL, et al. Malignant gastrointestinal neuroectodermal tumor: clinicopathologic, immunohistochemical, ultrastructural, and molecular analysis of 16 cases with a reappraisal of clear cell sarcoma-like tumors of the gastrointestinal tract. *Am J Surg Pathol* (2012) 36(6):857–68. doi: 10.1097/PAS.0b013e31824644ac

44. Farmer RG, Hawk WA. Metastatic tumors of the small bowel. *Gastroenterology* (1964) 47:496–504.

45. Borrmann R. Geschwulste des magens und des duodenums. In: Henke F, Lubarsch O, editors. *Handbuch der speziellen pathologischen anatomie und histology*, vol. Vol. IV/I . Berlin: Springer (1986). p. 812–1054.

46. Powles T, Tomczak P, Park SH, Venugopal B, Ferguson T, Symeonides SN, et al. Pembrolizumab versus placebo as post-nephrectomy adjuvant therapy for clear cell renal cell carcinoma (KEYNOTE-564): 30-month follow-up analysis of a multicentre, randomised, double-blind, placebo-controlled, phase 3 trial. *Lancet Oncol* (2022) 23(9):1133–44. doi: 10.1016/S1470-2045(22)00487-9

47. Pal SK, Uzzo R, Karam JA, Master VA, Donskov F, Suarez C, et al. Adjuvant atezolizumab versus placebo for patients with renal cell carcinoma at increased risk of recurrence following resection (IMmotion010): a multicentre, randomised, double-blind, phase 3 trial. *Lancet* (2022) 400(10358):1103–16. doi: 10.1016/S0140-6736(22)01658-0

48. Gao S, Yan L, Zhang H, Fan X, Jiao X, Shao F. Identification of a metastasis-associated gene signature of clear cell renal cell carcinoma. *Front Genet* (2021) 11:603455. doi: 10.3389/fgene.2020.603455

49. Thyavihally YB, Mahantshetty U, Chamarajanagar RS, Raibhattanavar SG, Tongaonkar HB. Management of renal cell carcinoma with solitary metastasis. *World J Surg Oncol* (2005) 3:48. doi: 10.1186/1477-7819-3-48

frontiers | Frontiers in Surgery

TYPE Case Report
PUBLISHED 29 December 2022
DOI 10.3389/fsurg.2022.985849



OPEN ACCESS

EDITED BY
Dimitrios Schizas,
National and Kapodistrian University of Athens, Greece

REVIEWED BY
Evangelos Chartampilas,
University General Hospital of Thessaloniki AHEPA, Greece
Stylianos Kykalos,
Laiko General Hospital, Greece

*CORRESPONDENCE
Mathilde Poras
✉ mathilde.poras@ulb.be

SPECIALTY SECTION
This article was submitted to Surgical Oncology, a section of the journal Frontiers in Surgery

RECEIVED 04 July 2022
ACCEPTED 05 December 2022
PUBLISHED 29 December 2022

CITATION
Poras M, Katsanos G, Agrafiotis AC, Demetter P, Pezzullo M and Lucidi V (2022) Case report: Sclerosed hemangioma of the liver: A diagnostic challenge.
Front. Surg. 9:985849.
doi: 10.3389/fsurg.2022.985849



# Case report: Sclerosed hemangioma of the liver: A diagnostic challenge

M. Poras[1,2]*, G. Katsanos[2], A. C. Agrafiotis[2], P. Demetter[3], M. Pezzullo[4] and V. Lucidi[2]

[1]Department of Abdominal Surgery, St Pierre University Hospital (Université Libre de Bruxelles), Brussels, Belgium, [2]Department of Abdominal Surgery, Erasme University Hospital (Université Libre de Bruxelles), Brussels, Belgium, [3]Department of Pathology, Erasme University Hospital (Université Libre de Bruxelles), Brussels, Belgium, [4]Department of Radiology, Erasme University Hospital (Université Libre de Bruxelles), Brussels, Belgium

Hemangiomas are the most common noncystic benign hepatic tumors and are usually incidentally discovered during routine radiological examinations. The diagnosis of hepatic hemangiomas with a typical presentation is generally easy with plain and cross-sectional imaging; however, it can be complicated when hemangiomas undergo histological changes such as fibrosis. Sclerosed hepatic hemangioma (SHH) is the extreme presentation of this fibrotic process. These atypical lesions can be misdiagnosed as primary hepatic malignancies or metastasis. Their diagnosis is established by histological examination. We report the case of a patient with an SHH, which was misdiagnosed as an intrahepatic cholangiocarcinoma. This article's aim is to draw attention to this infrequent pathology and underline the features of this benign tumor that could suggest its diagnosis prior to surgery to avoid unnecessary hepatic resections.

KEYWORDS
sclerosed, sclerosing, hemangioma, cholangiocarcinoma, liver

## Introduction

Hemangioma is the most common noncystic benign hepatic tumor with an incidence of 1%–20% in autopsy studies (1, 2). In a case series including 2008 patients who underwent hepatic resection, hemangiomas accounted for 41.7% of benign tumors (3). They present a female predilection around 30–50 years old (4, 5). In their vast majority, they are asymptomatic, and they are usually an incidental finding during routine radiological examinations or during laparotomy or laparoscopy for other abdominal pathologies (5, 6). When symptomatic, the main manifestation is abdominal pain or discomfort, and the prevalence of complications (pain, enlarging mass, rupture, Kasabach–Merritt syndrome) is extremely low (5, 7). Occasionally, tumor enlargement is possible during pregnancy or treatment with oral contraception (4). Spontaneous regression of hemangiomas occurs rarely (8).

Typical hemangiomas can be safely diagnosed during an ordinary radiological workup with ultrasonography (US), computed tomography (CT), and/or magnetic resonance imaging (MRI) (9). However, the diagnosis of hemangiomas can be challenging when the lesions are complicated with necrosis, fibrosis, or calcification

(10). Sclerosed hepatic hemangioma (SHH) is a rare entity, with only 78 cases described in the literature, including this report. Approximately 70% of SHH are diagnosed by surgical resection vs. 25% by biopsy or radiology (11).

In the case reported herein, an SHH was misdiagnosed as an intrahepatic cholangiocarcinoma, leading to surgical resection. The tumor presented atypical features on radiological examinations, and a definitive diagnosis was established on histological examination.

## Case report

We report the case of an 85-year-old Caucasian female patient who presented at the outpatient clinic of gastroenterology with the recent onset of vague abdominal pain localized in the epigastrium and the right subcostal area. There were no signs of jaundice. Clinical examination was normal.

Relevant clinical history included a right hemicolectomy and adjuvant chemotherapy for an adenocarcinoma of the colon, 16 years ago.

Laboratory tests were within normal limits.

Tumor markers such as carcinoembryonic antigen (CEA), alpha fetoprotein (a-fp), and CA 19-9 were within normal limits. Gastroscopy and colonoscopy did not detect any lesions. An abdominal US showed a hypoechogenic lesion at the level of the segment IV of the liver. On CT, the lesion showed no enhancement in the arterial phase and no dynamic changes between the portal venous phase and the delayed phase, showing weak and heterogeneous mainly peripheral enhancement. An abdominal MRI showed a mass (3 cm on its greatest diameter) with malignant features in segments III and IV. There was no intrahepatic biliary obstruction. A contrast-enhanced ultrasound (CEUS) was performed a few days after MRI confirmed the absence of any centripetal enhancement.

There were no previous examinations available for comparison in our archives.

The overall appearance was highly suggestive of an intrahepatic cholangiocarcinoma (**Figure 1**).

A fluorodeoxyglucose (FDG) positron emission tomography/CT (PET/CT) scan did not show any high FDG uptake in the liver or elsewhere. Despite a negative PET scan, with the rest of the imaging studies suggesting cholangiocarcinoma, the decision of a multidisciplinary reunion was in favor of a surgical resection.

During surgery, a white-colored, well-demarcated soft tumor was identified at the junction of segments III and IV. There were no enlarged lymph nodes in the hepatoduodenal ligament, and there were no signs of peritoneal carcinomatosis. Perioperative liver ultrasound did not detect other lesions.

During resection, the tumor was found to be in contact with the left hepatic duct, which was confirmed by a perioperative cholangiography and a left hepatectomy was performed (**Figure 2**). Intraoperative histological analysis was not performed.

The postoperative course was uneventful, and the patient was discharged on the seventh postoperative day.

Microscopic examination showed a fibrous stroma and the presence of vascular structures, with no malignant features (**Figures 3A,B**). The histological image was compatible with a sclerosed hemangioma.

## Discussion

SHH is an infrequent variant of hemangioma and is exceedingly difficult to differentiate from hepatic malignancies (11). There is an intense presence of fibrous tissue in which small vessels are occasionally detected (12).

Typical hemangiomas can be safely diagnosed during an ordinary radiological workup with US and CT/MRI (9). Hemangiomas present as hyperechoic, homogeneous lesions compared with normal parenchyma on US (4). Nevertheless, large or massive hemangiomas may also contain heterogeneous areas (7). On unenhanced CT scan, hemangiomas present as hypodense areas similar to liver vessels. After contrast injection, there is peripheral nodular enhancement and a fill-in of the lesion over time (5). Hemangiomas present with a hypointense signal on T1 IRM and a strongly hyperintense signal on T2-weighted images. The dynamic behavior with centripetal progressive enhancement is the same as described for CT (4, 5, 13, 14). MRI is the best performing imaging modality to diagnose liver hemangiomas with high specificity and sensitivity rates (4, 5, 14). Arteriography is rarely used prior to surgery (7). There is no uptake on PET scan (4). In a series of hepatic masses, including two typical hemangiomas, these lesions had no increased uptake on 18F-FDG PET, and on the other hand, they presented as hypometabolic regions on 11C-acetate PET imaging (15).

On the contrary, as stressed by Yamashita et al. in the case of SHH, the interpretation of radiological features alone can often lead to misdiagnosis, as they are similar to those of hepatic malignancies (2, 16, 17). In the radiological study by Jia et al. in 2021, 75% of SHH were misdiagnosed (18). With fewer than 80 cases of SHH found in the literature, it is a challenge to diagnose them preoperatively (11).

Doyle et al. in their retrospective study of 10 histologically proven SHH, found imaging features suggestive of the lesion, which, however, do not permit a definitive diagnosis. These features include a geographic pattern, capsular retraction, a decrease in size over time, and the loss of previously enhanced areas (1).

Mori et al. analyzed the imaging characteristics of 11 SHH, and when US was available, the lesions were hyperechoic (2).

On plain CT, SHH often presented a low density with irregular shape and heterogeneous density in the majority of

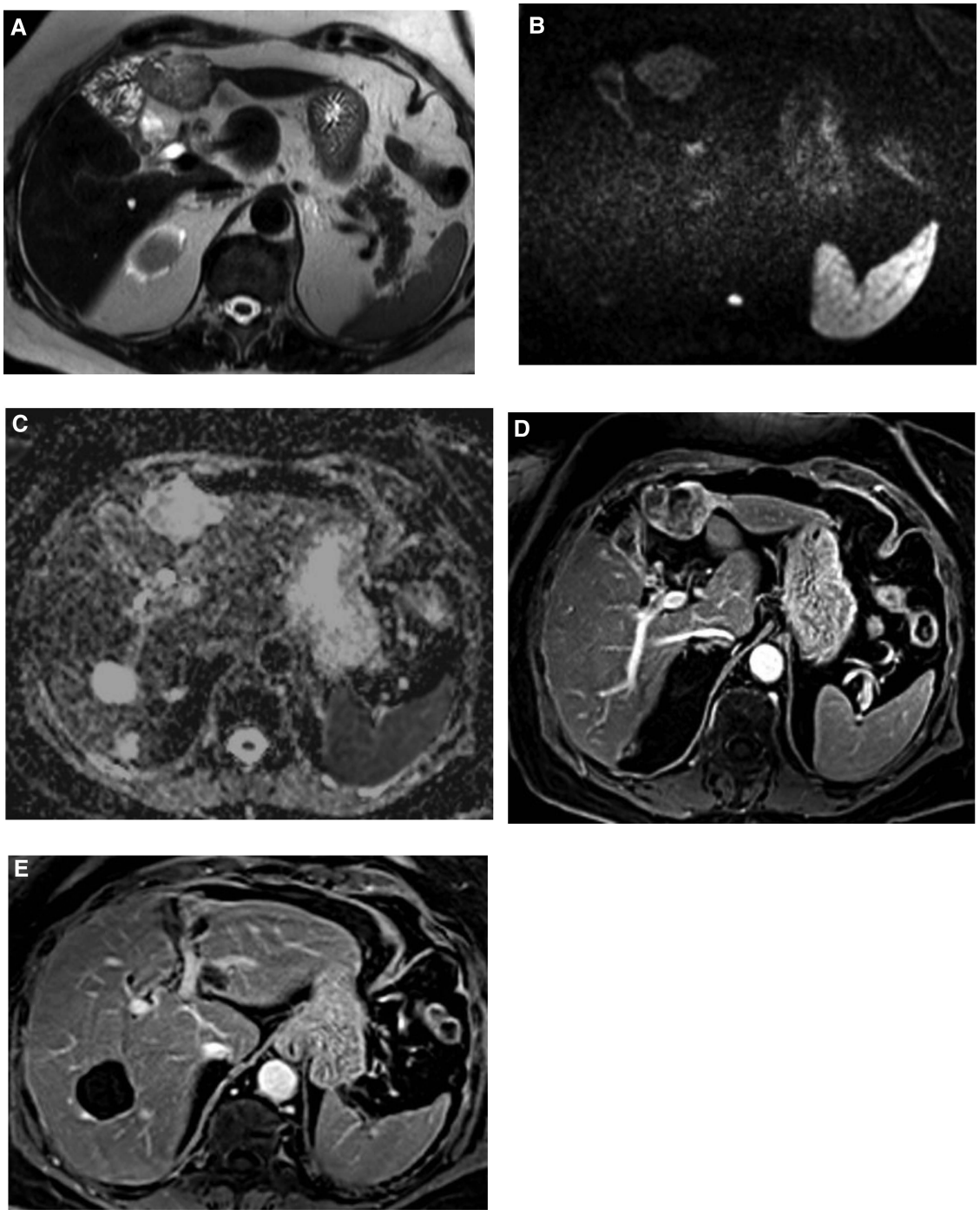


FIGURE 1
MRI images. Focal oval lesion straddling segments III and IVb showing sharp contours, heterogeneously high signal in T2 (A) and in diffusion-weighted imaging (B) corresponding to heterogeneous hypersignal on ADC map (C). Irregular and globally hypoenhancing behavior on T1 portal venous phase (D). (E) The lesion was located inferiorly to segmental left portal bifurcation, displaying a contact with the segmental branch for segment III without any major distortion or infiltration.

cases (18). After contrast injection, the majority of SHH had atypical enhancement characteristics, with little enhancement, or no enhancement during the arterial phase (2, 18). This atypical enhancement pattern could be related to the degree of degeneration with the obliteration of vascular channels and extensive tissue fibrosis (18).

The apparent diffusion coefficient (ADC) can be helpful in the differentiation between SHH and hepatic malignant tumors,

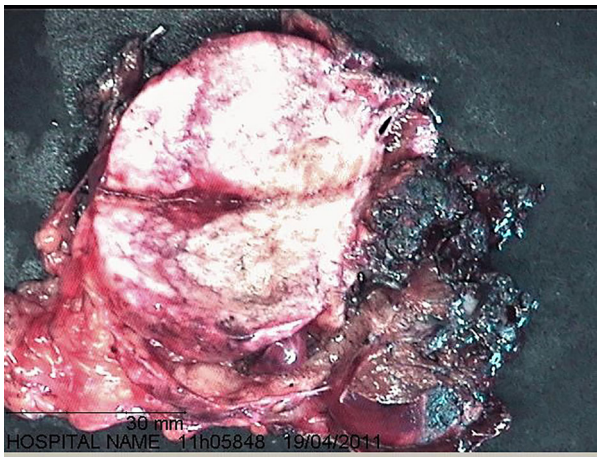


FIGURE 2
Predominantly extrahepatic indurated tumoral mass.

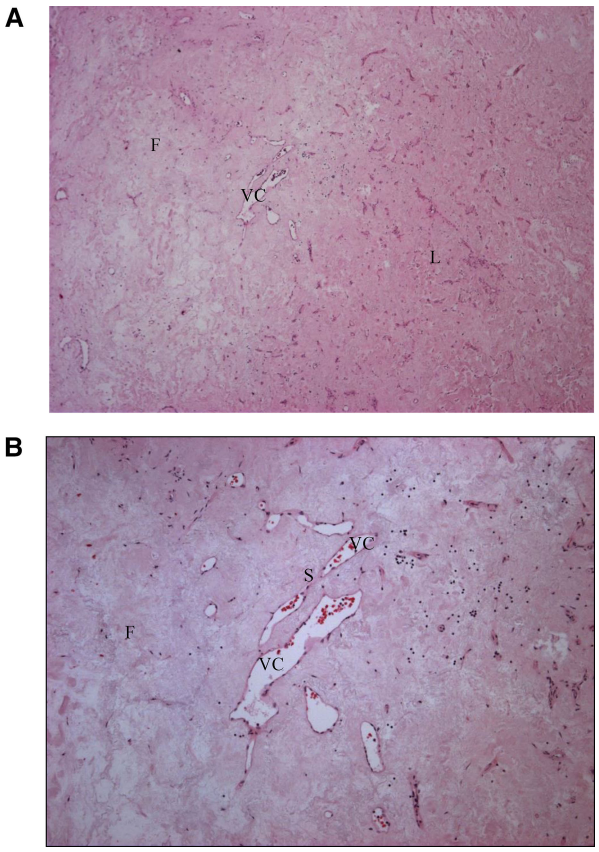


FIGURE 3
Sclerosed hemangioma, histological appearances. A rich paucicellular fibrous (F) stroma is distinguished from the Normal liver (L) tissue. Irregular vascular channels (VC) are separated by endothelial cells with thin fibrous septa (S). (**A**) Histology. Hematoxylin–eosin, magnification ×40. (**B**) Histology, Hematoxylin–eosin, magnification ×100.

as in SHH the ADC values are higher than the surrounding liver parenchyma, suggesting a benign lesion (18, 19). However, an ADC threshold value definition is not defined, because of the great individual variability (18). We do not receive help from this coefficient for the patient.

So, even with recent developments in radiological modalities, imaging alone cannot establish a definitive diagnosis. Small size or fibrosis can further accentuate the diagnostic challenge, as the amount of fibrosis in a sclerosing hemangioma figures out its morphological characteristics and the dynamic behavior that can shift progressively from the classical centripetal filling of typical hemangiomas to the weak and progressive enhancement of fibrotic tissue.

Fine needle aspiration or core biopsy procedures are generally safe with a low incidence of hemorrhagic complications especially in the case of SHH as it is less vascular than cavernous hemangioma (4, 12). Percutaneous fine needle biopsy should be the procedure of choice to distinguish degenerated hemangioma from hepatocellular carcinoma as advocated by Cheng et al. (20). CT-guided biopsy may be useful and can avoid major surgery (21). On the other hand, the risk of rupture or seeding in case of malignancy during biopsy should be taken into account in the decision-making process (2, 22). The above, along with the rarity of sclerosing hemangioma and the proposed diagnosis of cholangiocarcinoma, was the reason that we did not perform a preoperative biopsy in the present case.

At microscopic examination, cavernous hemangiomas present as vascular channels of different sizes with flattened endothelial cells separated by connective tissue septa (10). In fact, when partial fibrosis occurs, they are called sclerosing hemangiomas and when vascular spaces are extensively occupied by fibrous tissue, they are called sclerosed cavernous hemangiomas (2, 23). Makhlouf and Ishak describe the features of sclerosing and sclerosed hemangiomas and underline the role of mast cells in the pathogenesis of these variants of hepatic hemangiomas (23). The flattened cells show positivity for the endothelial marker, factor VIII-related antigen, marking the vascular origin of this tumor. This immunohistochemical staining is of paramount importance in differentiating SHH from malignant hepatic tumors, primary or metastatic (12).

Surgical resection is reserved for symptomatic patients, in cases where imaging techniques and histological examination after percutaneous biopsies are not helpful, and in cases with a high suspicion for malignancy due to medical history. In the other cases, a simple observation is sufficient.

## Conclusion

SHH is an extremely rare benign tumor, and it is a challenge to differentiate from hepatic malignant tumors. SHH has an

excellent prognosis and can be followed without surgery. Imaging interpretation alone can lead to a misdiagnosis; however, there are features that could raise the suspicion of an SHH. In that case, a preoperative biopsy or perioperative frozen section is important to avoid unnecessary hepatic resections. If neither imaging interpretation nor biopsy can establish a diagnosis, or if biopsy is contraindicated, the least invasive resection should be performed.

## Data availability statement

The original contributions presented in the study are included in the article/Supplementary Material, further inquiries can be directed to the corresponding author.

## Author contributions

MP is the first author, wrote the case report, and put together the different research. AA helped write the case report and participated in the surgery. PD participated in histology. MP participated in radiological analysis. GK coordinated the writing and scientific research. All authors contributed to the article and approved the submitted version.

## Conflict of interest

The authors declare that the research was conducted in the absence of any commercial or financial relationships that could be construed as a potential conflict of interest.

## Publisher's note

All claims expressed in this article are solely those of the authors and do not necessarily represent those of their affiliated organizations, or those of the publisher, the editors and the reviewers. Any product that may be evaluated in this article, or claim that may be made by its manufacturer, is not guaranteed or endorsed by the publisher.

## References


1. Doyle DJ, Khalili K, Guindi M, Atri M. Imaging features of sclerosed hemangioma. *Am J Roentgenol*. (2007) 189(1):67–72. doi: 10.2214/AJR.06.1076

2. Mori H, Ikegami T, Imura S, Shimada M, Morine Y, Kanemura H, et al. Sclerosed hemangioma of the liver: report of a case and review of the literature. *Hepatol Res*. (2008) 38(5):529–33. doi: 10.1111/j.1872-034X.2007.00306.x

3. Huang ZQ, Xu LN, Yang T, Zhang WZ, Huang XQ, Cai SW, et al. Hepatic resection: an analysis of the impact of operative and perioperative factors on morbidity and mortality rates in 2008 consecutive hepatectomy cases. *Chin Med J*. (2009) 122(19):2268–77. PMID: 20079125

4. Assy N, Nasser G, Djibre A, Beniashvili Z, Elias S, Zidan J. Characteristics of common solid liver lesions and recommendations for diagnostic workup. *World J Gastroenterol*. (2009) 15(26):3217–27. doi: 10.3748/wjg.15.3217

5. Terkivatan T, de Wilt JH, de Man RA, van Rijn RR, Zondervan PE, Tilanus HW, et al. Indications and long-term outcome of treatment for benign hepatic tumors: a critical appraisal. *Arch Surg*. (2001) 136(9):1033–8. doi: 10.1001/archsurg.136.9.1033

6. Vilgrain V, Boulos L, Vullierme MP, Denys A, Terris B, Menu Y. Imaging of atypical hemangiomas of the liver with pathologic correlation. *Radiographics*. (2000) 20(2):379–97. doi: 10.1148/radiographics.20.2.g00mc01379

7. Gedaly R, Pomposelli JJ, Pomfret EA, Lewis WD, Jenkins RL. Cavernous hemangioma of the liver: anatomic resection vs. enucleation. *Arch Surg*. (1999) 134(4):407–11. doi: 10.1001/archsurg.134.4.407

8. Okano H, Shiraki K, Inoue H, Ito T, Yamanaka T, Deguchi M, et al. Natural course of cavernous hepatic hemangioma. *Oncol Rep*. (2001) 8(2):411–4. doi: 10.3892/or.8.2.411

9. Choi YJ, Kim KW, Cha EY, Song JS, Yu E, Lee MG. Case report. Sclerosing liver haemangioma with pericapillary smooth muscle proliferation: atypical CT and MR findings with pathological correlation. *Br J Radiol*. (2008) 81(966):e162–5. doi: 10.1259/bjr/54210739

10. Jin SY. Sclerosed hemangioma of the liver. *Korean J Hepatol*. (2010) 16(4):410–3. doi: 10.3350/kjhep.2010.16.4.410

11. Sweed DM, Fayed ZA, Sweed EM, El-Sherif A, Mohamady M. Hepatic sclerosing hemangioma mimics hepatic malignancies: a case report and multidisciplinary approach. *Egypt Liver J*. (2019) 9:6. doi: 10.1186/s43066-019-0007-6

12. Aibe H, Hondo H, Kuroiwa T, Yoshimitsu K, Irie H, Tajima T, et al. Sclerosed hemangioma of the liver. *Abdom Imaging*. (2001) 26(5):496–9. doi: 10.1007/s002610000202

13. Tung GA, Vaccaro JP, Cronan JJ, Rogg JM. Cavernous hemangioma of the liver: pathologic correlation with high-field MR imaging. *Am J Roentgenol*. (1994) 162(5):1113–7. doi: 10.2214/ajr.162.5.8165993

14. Mathieu D, Rahmouni A, Vasile N, Jazaerli N, Duvoux C, Tran JV, et al. Sclerosed liver hemangioma mimicking malignant tumor at MR imaging: pathologic correlation. *J Magn Reson Imaging*. (1994) 4(3):506–8. doi: 10.1002/jmri.1880040344

15. Ho CL, Yu SC, Yeung DW. 11C-acetate PET imaging in hepatocellular carcinoma and other liver masses. *J Nucl Med*. (2003) 44(2):213–21. PMID: 12571212

16. Yamashita Y, Shimada M, Taguchi K, Gion T, Hasegawa H, Utsunomiya T, et al. Hepatic sclerosing hemangioma mimicking a metastatic liver tumor: report of a case. *Surg Today*. (2000) 30(9):849–52. doi: 10.1007/s005950070072

17. Yugawa K, Yoshizumi T, Harada N, Motomura T, Harimoto N, Itoh S, et al. Multiple hepatic sclerosing hemangiomas: a case report and review of the literature. *Surg Case Rep*. (2018) 4(1):60. doi: 10.1186/s40792-018-0468-6

18. Jia C, Liu G, Wang X, Zhao D, Li R, Li H. Hepatic sclerosed hemangioma and sclerosing cavernous hemangioma: a radiological study. *Jpn J Radiol*. (2021) 39(11):1059–68. doi: 10.1007/s11604-021-01139-z

19. Miyata T, Beppu T, Kuramoto K, Nakagawa S, Imai K, Hashimoto D, et al. Hepatic sclerosed hemangioma with special attention to diffusion-weighted magnetic resonance imaging. *Surg Case Rep*. (2018) 4(1):3. doi: 10.1186/s40792-017-0414-z

20. Cheng HC, Tsai SH, Chiang JH, Chang CY. Hyalinized liver hemangioma mimicking malignant tumor at MR imaging. *Am J Roentgenol*. (1995) 165(4):1016–7. doi: 10.2214/ajr.165.4.7676959

21. Li T, Klar MM, Alawad M, Abdul R, Zahiruddin A, Salifu MO, et al. Hepatic sclerosing hemangioma mimicking malignancy: a case and literature review. *Am J Med Case Rep*. (2021) 9(3):144–6. doi: 10.12691/ajmcr-9-3-2

22. Lee VT, Magnaye M, Tan HW, Thng CH, Ooi LL. Sclerosing haemangioma mimicking hepatocellular carcinoma. *Singapore Med J*. (2005) 46(3):140–3. PMID: 15735880

23. Makhlouf HR, Ishak KG. Sclerosed hemangioma and sclerosing cavernous hemangioma of the liver: a comparative clinicopathologic and immunohistochemical study with emphasis on the role of mast cells in their histogenesis. *Liver*. (2002) 22(1):70–8. doi: 10.1046/j.0106-9543.2001.01604.x

frontiers | Frontiers in Oncology

TYPE Case Report
PUBLISHED 05 January 2023
DOI 10.3389/fonc.2022.1099268



OPEN ACCESS

EDITED BY
Akinfemi Akingboye,
Dudley Group NHS Foundation Trust, United Kingdom

REVIEWED BY
Zeyu Wu,
Guangdong Provincial People's Hospital, China
Ankui Yang,
Sun Yat-sen University Cancer Center (SYSUCC), China
Xinying Li,
Xiangya Hospital, Central South University, China

*CORRESPONDENCE
Zhihui Li
rockoliver@vip.sina.com
Kun Zhang
zhangkun1989111@163.com

SPECIALTY SECTION
This article was submitted to Surgical Oncology, a section of the journal Frontiers in Oncology

RECEIVED 15 November 2022
ACCEPTED 13 December 2022
PUBLISHED 05 January 2023

CITATION
Peng X, Lei J, Li Z and Zhang K (2023) Case report: Visibly curative effect of dabrafenib and trametinib on advanced thyroid carcinoma in 2 patients.
*Front. Oncol.* 12:1099268.
doi: 10.3389/fonc.2022.1099268



# Case report: Visibly curative effect of dabrafenib and trametinib on advanced thyroid carcinoma in 2 patients

Xue Peng, Jianyong Lei, Zhihui Li* and Kun Zhang*

Thyroid and Parathyroid Surgery Center, West China Hospital of Sichuan University, Chengdu, China

**Background:** Differentiated thyroid cancer accounts for the majority of thyroid cancers and has a good prognosis after standard treatment. However, there are still some complex and refractory thyroid cancers, including locally advanced differentiated thyroid carcinoma and medullary carcinoma (MTC), poorly differentiated thyroid carcinoma (PDTC), and anaplastic thyroid carcinoma (ATC). Here, we report the therapeutic response of 2 advanced thyroid carcinoma patients treated with dabrafenib and trametinib.

**Case presentation:** Two elderly females presented to the clinic with neck masses, dyspnea, and dysphagia. Signs of the trachea and esophageal compression were markedly visible in computed tomography (CT) scan and ultrasonography. Pathologic diagnoses of PDTC were confirmed for both patients through ultrasound-guided fine-needle aspiration (US-FNA). Both patients were significantly relieved from dyspnea and dysphagia after a course of treatment with dabrafenib and trametinib, and their tumors gradually shrank during the follow-up period.

**Conclusion:** Overall, this treatment modality is rare, but effective. By sharing these 2 case reports, we hope to provide a reference for the treatment of clinically similar patients with advanced thyroid carcinoma.

KEYWORDS

**dabrafenib, trametinib, lymph node metastasis, thyroid carcinoma, targeted drug**

## Introduction

Locally advanced thyroid carcinoma is a type of thyroid cancer in which the tumor markedly invades surrounding organs and structures. Especially, poorly differentiated thyroid carcinoma is more aggressive and rapidly progresses to distant metastases. Poorly differentiated thyroid carcinoma is an aggressive form of follicular cell-derived thyroid

carcinoma with a behavior, morphology, and prognosis that is intermediate between indolent differentiated thyroid carcinoma (DTC) and rapidly growing and often fatal ATC (1). PDTC is a rare disease that was first described by Sakamoto in 1938 (2) and is reported to occur in 2% to 15% of all thyroid carcinomas (1, 3). Starting in 2004, the World Health Organization (WHO) classified PDTC as a non-follicular non-papillary, thyroglobulin-producing thyroid carcinoma with intermediate behavior between well-differentiated and anaplastic carcinoma (4–6). The 5-year disease-specific survival rate (DSS) for PDTC patients (51%) is also intermediate between DTC (91%) and ATC (0%) patients (7). PDTC patients usually miss the opportunity for surgery or have poor surgical outcomes due to the cancer's invasiveness and quick progression to distant metastasis. PDTC does not have a standard of treatment internationally (8). Surgery, chemotherapy, and radioiodine therapy (RAI) are commonly used treatment schemes, but the treatment options for PDTC patients with advanced, critical illness are very limited (9). In this case report, we describe 2 patients with advanced thyroid carcinoma who received dabrafenib and trametinib with good outcomes.

This study was reported in agreement with principles of the CARE guidelines (10).

## Case presentation

### Case 1

In December 2021, a 72-year-old woman with a neck mass, dysphagia with a cough and expectoration was referred to the Department of Thyroid Surgery & Western Medicine, West China Hospital, Sichuan University. Before visiting our hospital, the patient found a hard mass on the left side of her neck, along with tenderness and poor mobility. At that time, there was no dyspnea or dysphagia. The patient was treated at Sichuan Cancer Hospital, underwent ultrasound examination and received FNA. Ultrasound showed morphological abnormalities in the thyroid, abnormal lymph nodes were found on both sides of the neck, and FNA cytology revealed PTC (occupying the right lobe of the thyroid). The results of immunohistochemical analysis were as follows: positive TTF-1, G-3, CK19, MC (HBME-1), CD56, Ki67 (10%), negative (TG), PD-L1: 22c3, CPS: 65, negative control: negative, and positive control: positive. Gene testing revealed a *BRAF V600E* gene mutation (Ct value was 20.16). Because the patient's nutritional status was poor, and she could not afford immunotherapy, she was discharged from the hospital and took 3 cycles of anlotinib 12 mg qd (taking the medication for 2 weeks and stopping for 1 week). After completing the 3 cycles, the patient had dysphagia, increased coughing, and expectoration accompanied by blood in the sputum, so she was re-admitted to Sichuan Cancer Hospital. During hospitalization, the patient was unable to eat and was completely supported by parenteral nutrition.

Physical examination showed that she had a hoarse voice, clear consciousness and diffuse swelling of the neck, and was unable to touch her trachea because of the trachea was compressed by a huge mass. The thyroid mass was hard, and its size could not be measured. The laboratory examination revealed the following: FT3 1.64 pmol/L (reference range, 3.60–7.50 pmol/L), FT4 9.53 pmol/L (reference range, 12.0–22.0 pmol/L), TSH 7.34 mU/L (reference range, 0.27–4.20 mU/L), thyroglobulin (hTg) < 0.04 μg/l (reference range, 3.5–77 μg/l), anti-thyroglobulin antibodies (TGAb) > 4000 IU/ml (reference range, 0–115IU/ml), and tumor marker/carcinoembryonic antigen (CEA) 0.64 ng/ml (reference range, 0–5 ng/ml). Ultrasound re-examination revealed that the thyroid gland contained giant nodules encircling the bilateral common carotid arteries. In addition, bilateral neck areas I-IV had multiple lymph node fusions, the left neck was approximately 12×10×16 mm, the right side was approximately 20×19×14 mm, and the corticomedullary demarcation was unclear. We showed on computed tomography (CT) that the thyroid gland was unclear and there were lymph node metastases in the neck and upper mediastinum (Figure 1). The patient had a personal history of 20 years of hypothyroidism and had taken 50 μg levothyroxine (Euthyrox) for a long time. There was no history of neck surgery, neck radiotherapy, parathyroid disease, or hereditary disease.

To solve the patient's nutritional problems, the endoscopy center placed a jejunal nutrition tube. During this process, the patient had sudden dyspnea with a sharp drop in oxygen saturation and partial pressure of carbon dioxide of 164%, pH: 6.9. The anesthesiology department performed a successful emergency nasotracheal intubation, and the patient was transferred to the critical care medicine department. The multidisciplinary team (MDT) ruled out surgical treatment, because of the high risks involved, and because the tumor was poorly demarcated from surrounding tissues. dabrafenib and trametinib treatment was finally considered. dabrafenib and trametinib is approved by the FDA for the treatment of patients with ATC and *BRAF V600E* mutations. So, we obtained consent from the patient's family to tube feed the targeted agent dabrafenib mesylate (75 mg q12h) and trametinib (2 mg qd) on December 30, 2021. FDA recommends 150mg twice daily for the use of dabrafenib, but We had never used this scheme before in these two patients, so we could not evaluate the effectiveness and side effects. In addition, the patient's condition was bad and the basic condition was poor, so we tried to use half a dose to observe the efficacy, and subsequently adjusted the scheme according to the patient's condition. We sent the biopsy tissue for pathological re-examination, and the results of the cytology revealed malignant epithelial cells. Immunohistochemical staining of thyroid (Figure 2), which exhibited positive CK19, CD56 and G-3, and negative TTF-1, TG, HBME-1, CGA, SYN, p63, CD20. The Ki-67 positive rate was approximately 40%. Confirmed poorly differentiated thyroid

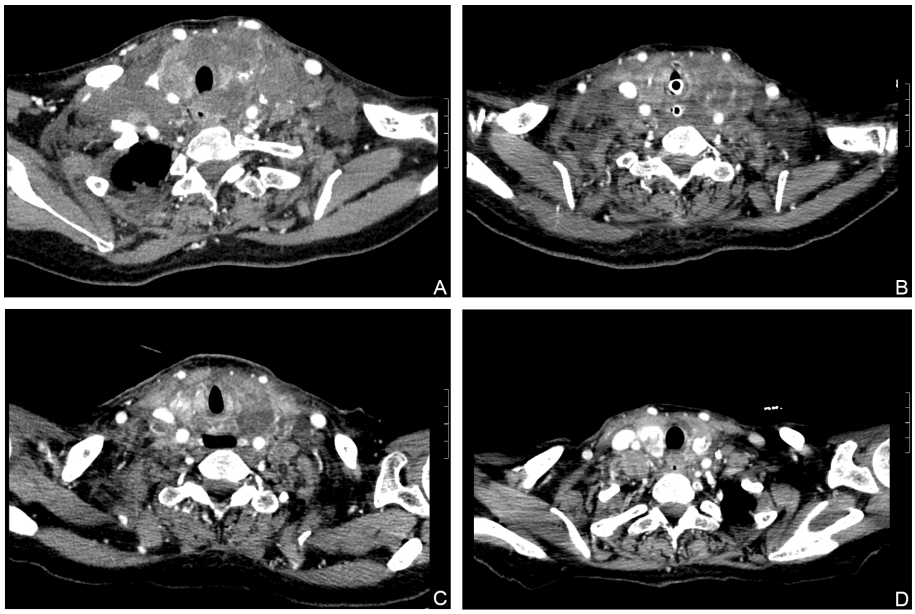


FIGURE 1
Hematoxylin and eosin (HE) stained FNAB of thyroid lobe **(A)**, 20× magnification) revealed malignant epithelial cells. IHC staining showed that malignant cells in thyroid were positive for G-3 **(B)**, 20× magnification), and negative for TTF1 **(C)**, 20× magnification), TG **(D)**, 20× magnification).

carcinoma. After 13 days of treatment, the patient's dyspnea and dysphagia symptoms had decreased, and she could sleep in a flat position and drink a small amount of liquid. Her neck circumference gradually decreased with daily measurements. However, she still had hoarseness and developed black stool (approximately 100-200 g/d) and hematuria on a daily basis. According to the patient's condition, the patient's above symptoms improved after treatment with proton pump inhibitor (PPI), somatostatin and oral Yunnan Baiyao. To clarify the cause of bleeding would require a gastroscope, after the patient's condition has improved. The patient continued oral dabrafenib 75 mg and trametinib 2 mg maintenance therapy and underwent thyroid stimulating hormone (TSH) repression therapy with levothyroxine 50μg after discharge. We compared the imaging reports at 3 days, 19days, 50days and found that the tumors significantly decreased in size. The author's department subsequently found that the tumor did not continue to grow or have any detectable distant metastasis through outpatient service and telephone. At the end of February 2022, the patient experienced fever and seizure. Moreover, a new mass was found in the right neck. After discontinuing dabrafenib and trametinib for 10 days, the mass grew rapidly, and blood culture suggested a serious infection. Therefore, after comprehensive consideration, we recommended that she continue to take dabrafenib and trametinib. The patient's condition progressed rapidly, and she died on March 10.

## Case 2

A 73-year-old woman presented to the emergency department of West China Hospital, Sichuan University, on January 31, 2022, because of a neck mass with chest and airway tightness. Previously, FNA was performed at her local hospital, and the results showed metastatic, poorly differentiated squamous cell carcinoma. Upon arrival in the emergency room, the patient suddenly lost consciousness. The emergency physicians immediately diagnosed respiratory failure and intubated the patient. To comprehensively evaluate the condition of patient, CT was performed and showed that there was a mass (6.3×5.6 cm) located in the left lobe region of the thyroid gland, which wrapped and invaded the trachea and esophagus, both of which were compressed to varying degrees, resulting in stenosis. Nodules of varying size were scattered throughout both lungs, with the largest nodule measuring 1.8 cm in diameter, which we suspect to be metastatic lesions (Figure 3). The laboratory examination upon admission revealed the following: FT3 2.08 pmol/L (reference range, 3.60–7.50 pmol/L), FT4 9.39 pmol/L (reference range, 12.0–22.0 pmol/L), TRAb 2.79 IU/l (reference range, <1.75 IU/l), WBC 12.99×10/L (reference range, 3.5–9.5 10^9/L), Hb 99 g/L (115–150 g/L), and PLT 259×10/L (100–300 10^9/L); TSH, hTg, TGAb, and CEA were unremarkable. She had a 13-year history of papillary thyroid cancer (PTC) and had previously undergone total

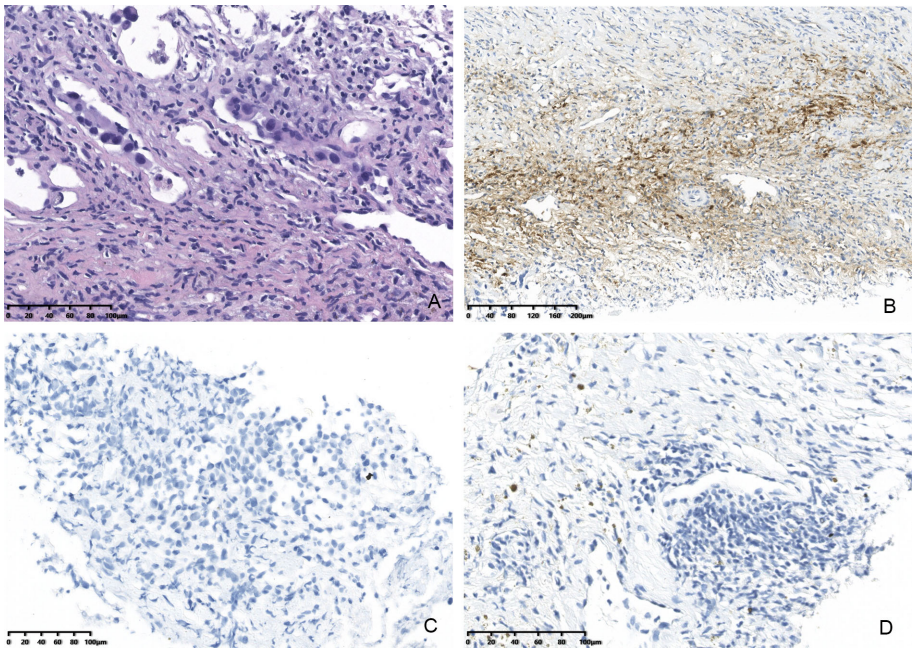


FIGURE 2
Computed tomography (CT) images showing that the size of the lesions had decreased. **(A)** Before treatment with dabrafenib and trametinib. **(B)** Dabrafenib and trametinib for 5 days. **(C)** Dabrafenib and trametinib for 19days. **(D)** Dabrafenib and trametinib for 50days.

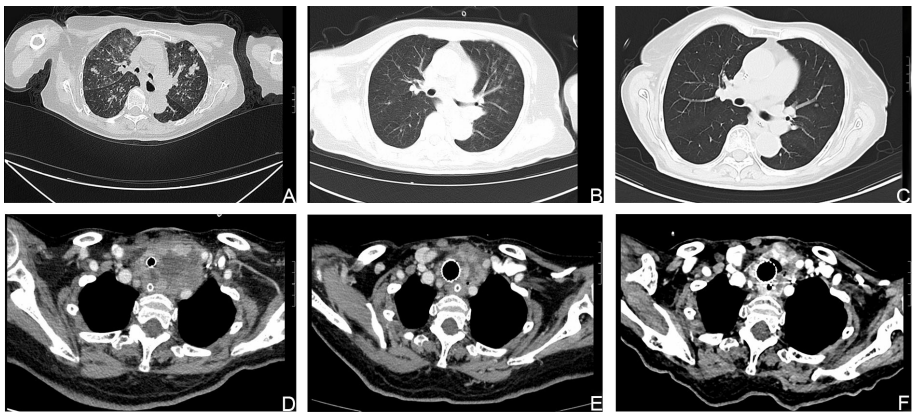


FIGURE 3
Computed tomography (CT) images showing that the size of the lesions had decreased. **(A, D)**. CT images of the metastatic lesions in the lung and neck respectively, before treatment with dabrafenib and trametinib. **(B, C, E, F)**. CT images of the metastatic lesions after treatment with dabrafenib and trametinib.

thyroidectomy, double central lymph node dissection, plus left cervical lymph node dissection in our hospital. Levothyroxine 75 μg in parallel with radioactive iodine [(131)I] therapy three times, were administered in after the operation. There was no personal or hereditary family history of cardiovascular or cerebrovascular disease. An appointment was set with a thyroid surgeon from our institution on the same day. After the completely treating the infection that emerged in the patient's lungs during the consultation on February 7, 2022, she was admitted to the Thyroid and Parathyroid Surgery Center. A covered stent was used instead of tracheal intubation with the assistance of the Department of Otorhinolaryngology. Due to the patient was critically ill after admission and had obvious symptoms of neck compression. In

an effort to strive for treatment time, while the patient underwent US-FNA, we communicated with the family and obtained the consent to empirically administer treatment with dabrafenib and trametinib (given the close similarity to that of case 1), and the final pathological results and genetic testing also confirmed the effectiveness of our medication. We selected a mass in the left lobe region of the thyroid gland by ultrasonographic localization, punctured the fine-needle into the interior of the nodule and multipoint aspiration was performed under the monitoring of ultrasound. Histological examination was performed postoperatively on fixed specimens with alcohol. Immunohistochemical analyses showed tissue positivity for the following markers: HBME-1, CK19, G-3, BRAF-VE, PCK, and PAX8. In addition, *TERT* promoter mutation (C288T) were identified by Molecular testing in the mass. Combined the morphology and all of the above findings led to a diagnosis of PTC with a mutation at position 228 of the *TERT* gene promoter (Figure 4). Under receiving comprehensive treatment from the nutrition, infection, and respiratory departments, the patient's condition improved after 5 days of dabrafenib and trametinib, and her symptoms of dyspnea, dysphagia, and hoarseness disappeared. Unexpectedly, she was required dose reductions of dabrafenib and adds radiotherapy because of edema of both lower extremities with petechiae. Three months later, the patient developed a tracheoesophageal fistula, which improved after conservative treatment. After ~8 months of treatment, numerous metastatic lesions had lessened on computed tomography. The survival time of the patient has reached 10 months since she diagnosis of PTC. At present, the patient is in a state of no recurrence and metastasis, and there is no obvious adverse reaction after taking dabrafenib and trametinib.

Both were approved by the ethics committee of the West China Hospital, Sichuan University, and written informed consent was provided by the patient for publication of this case publication.

## Discussion

These cases give us great confidence and a new strategy for the clinical treatment of a advanced thyroid carcinoma. Our discussion will focus on the effects of treatment.

Targeted drugs are emerging as a new option for the treatment of a variety of advanced tumors in the clinic, raising the hope of survival for many patients with refractory tumors. Thyroid cancer-targeted drugs have been gradually introduced to the clinic in recent years, and better efficacy is also seen in many reports for the treatment of advanced thyroid carcinoma. We report encouraging results in 2 consecutive patients with severe comorbidities who were admitted to the Thyroid and Parathyroid Surgery Center, West China Hospital of Sichuan University. Both patients presented with life-threatening metastatic thyroid cancer and were not eligible for surgery or radiotherapy. Dabrafenib, a

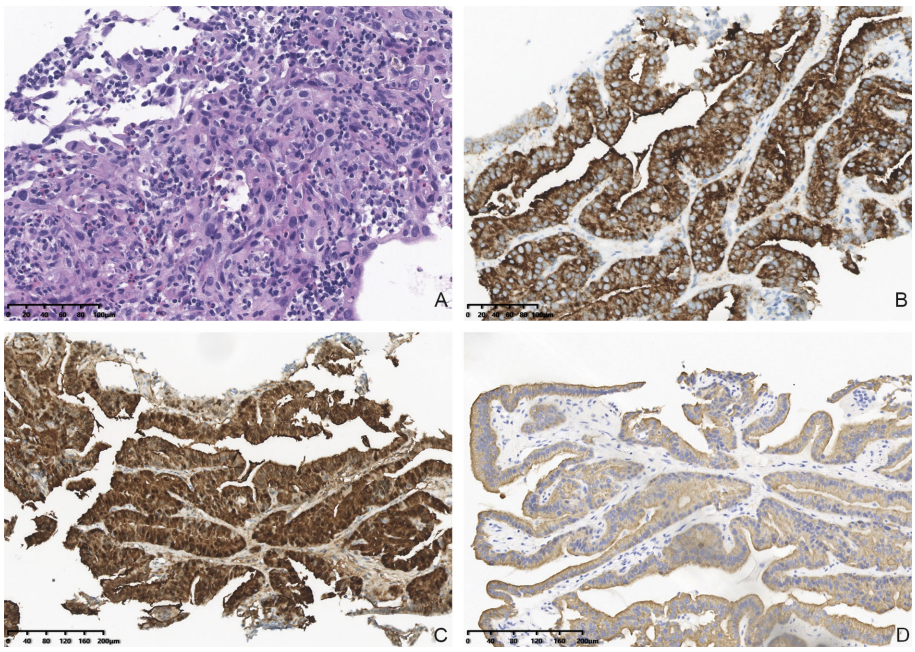


FIGURE 4
Hematoxylin and eosin (HE) stained FNAB of thyroid lobe **(A)**, 20× magnification) revealed malignant epithelial cells. IHC staining showed that malignant cells in thyroid were positive for BRAR-VE **(B)**, 20× magnification) and G-3 **(C)**, 20× magnification) and CK19 **(D)**, 20× magnification).

mutant BRAF kinase inhibitor, emerged from Glaxo Smith K's research program for the discovery of selective inhibitors of mutant *BRAF* kinase activity for the treatment of solid tumors (11). Trametinib is an orally administered, reversible selective allosteric inhibitor of MEK1 and MEK2, and is also approved as a single agent in the treatment of melanoma (12, 13). dabrafenib and trametinib was first approved by the FDA on May 29, 2013, for the treatment of unresectable or metastatic melanoma with *BRAF V600E* or *V600K* gene mutations. After confirmation by clinical studies (14), the FDA approved dabrafenib and trametinib for patients with ATC and *BRAF V600E* mutations on May 4, 2018 (14, 15). The effect of the combination of the 2 drugs had only been observed in the treatment of ATC, but we cannot estimate whether the application of these two drugs to other types of thyroid carcinoma will also achieve satisfactory results. We tried this approach to treat the 2 patients with advanced thyroid cancer and BRAF mutation, and the effect was better than expected. White PS (16) reported 2 cases of metastatic papillary thyroid carcinoma with major complications. Metastases decreased, and thyroglobulin antibodies consistently decreased after treatment with dabrafenib and trametinib. The protocol adopted by the authors was treated initially with dabrafenib 150 mg twice daily plus trametinib 2 mg once daily, first in continuous daily dosing, then in a five-week-on and three-week-off schedule. Whereas our regimen was continuous use of dabrafenib 150 mg and trametinib 2 mg once daily. As with White PS, both patients showed rapid clinical improvement upon starting the regimen. Since there is no consensus on the combination of these two drugs for the treatment of non-ATC advanced thyroid cancer, we speculate that it may also achieve good efficacy for advanced thyroid carcinoma without ATC or *BRAF V600E* mutation. Although we do not have enough evidence to support that this regimen is available, and see few relevant reports. The experiences in the 2 patients presented here illustrate that administering the 2 drugs are feasible, and suggest that this approach is efficacious, even in cases with serious comorbidities. However, few data are currently available on drug efficacy and/or response, and further preclinical and clinical studies are needed.

According to the relevant studies and the drug instructions of dabrafenib, dabrafenib and trametinib is known to cause the following adverse events: fever, chills, skin toxicity, arthralgia, myalgia, cough, hypophosphatemia, hyponatremia, hyperglycemia, increased alkaline phosphatase, bleeding (defined as bleeding from a critical site or organ), etc (17). In case 1, the patient had black stool and hematuria on a daily basis, denied any history of gastrointestinal and urinary diseases, and denied NSAID drug use. Case 2 patient developed edema of both lower extremities with petechiae. We consider these phenomena to be a side effect. Some studies also report retinopathy, renal failure, fatigue, and rhabdomyolysis (17). The symptoms may largely resolve upon discontinuation of the drugs, plus supportive therapy (18). Although the dabrafenib and trametinib achieved significant efficacy, the side effects that resulted were also obvious. Combined with the results of the study of 2 patients, we can conclude that dabrafenib and trametinib offers more advantages than disadvantages in the treatment of advanced thyroid carcinoma, and our treatment option is correct and certainly a new attempt for patients with advanced thyroid cancer. In the future, we may need to set up larger clinical trials to add evidence of the feasibility of this option.

## Conclusion

We report 2 rare cases of advanced thyroid carcinoma and point out the effectiveness of the combination of the 2 targeted drugs. The conclusion that dabrafenib and trametinib contributes to the management of advanced thyroid carcinoma remains to be further confirmed. We hope that our treatment procedures and initial outcomes can serve as a reference for the diagnosis and treatment of similar patients.

## Data availability statement

The original contributions presented in the study are included in the article/Supplementary material. Further inquiries can be directed to the corresponding authors.

## Ethics statement

The studies involving human participants were reviewed and approved by ethics committee of the West China Hospital, Sichuan University. The patients/participants provided their written informed consent to participate in this study. Written informed consent was obtained from the individual(s) for the publication of any potentially identifiable images or data included in this article.

## Author contributions

XP managed the cases, collected patient data and images, and wrote the manuscript. JL, ZL and KZ conducted the study and revised the manuscript. All authors contributed to the article and approved the submitted version.

## Acknowledgments

We thank the patients and their families for participating in this study.

## Conflict of interest

The authors declare that the research was conducted in the absence of any commercial or financial relationships that could be construed as a potential conflict of interest.

## Publisher's note

All claims expressed in this article are solely those of the authors and do not necessarily represent those of their affiliated organizations, or those of the publisher, the editors and the reviewers. Any product that may be evaluated in this article, or claim that may be made by its manufacturer, is not guaranteed or endorsed by the publisher.

## Supplementary material

The Supplementary Material for this article can be found online at: https://www.frontiersin.org/articles/10.3389/fonc.2022.1099268/full#supplementary-material

## References

1. Ibrahimpasic T, Ghossein R, Shah JP, Ganly I. Poorly differentiated carcinoma of the thyroid gland: Current status and future prospects. *Thyroid* (2019) 29(3):311–21. doi: 10.1089/thy.2018.0509

2. Sakamoto A, Kasai N, Sugano H. Poorly differentiated carcinoma of the thyroid. a clinicopathologic entity for a high-risk group of papillary and follicular carcinomas. *Cancer* (1983) 52(10):1849–55. doi: 10.1002/1097-0142(19831115)52:10<1849::aid-cncr2820521015>3.0.co;2-x

3. Sanders EMJr., LiVolsi VA, Brierley J, Shin J, Randolph GW. An evidence-based review of poorly differentiated thyroid cancer. *World J Surg* (2007) 31(5):934–45. doi: 10.1007/s00268-007-9033-3

4. Bellini MI, Biffoni M, Patrone R, Borcea MC, Costanzo ML, Garritano T, et al. Poorly differentiated thyroid carcinoma: Single centre experience and review of the literature. *J Clin Med* (2021) 10(22):5258. doi: 10.3390/jcm10225258

5. Nambiar A, Pv S, Susheelan V, Kuriakose MA. The concepts in poorly differentiated carcinoma of the thyroid: A review article. *J Surg Oncol* (2011) 103(8):818–21. doi: 10.1002/jso.21803

6. Xu B, Ghossein R. Poorly differentiated thyroid carcinoma. *Semin Diagn Pathol* (2020) 37(5):243–7. doi: 10.1053/j.semdp.2020.03.003

7. Patel KN, Shaha AR. Poorly differentiated and anaplastic thyroid cancer. *Cancer Control* (2006) 13(2):119–28. doi: 10.1177/107327480601300206

8. Huang J, Sun W, Zhang Q, Wang Z, Dong W, Zhang D, et al. Clinicopathological characteristics and prognosis of poorly differentiated thyroid carcinoma diagnosed according to the Turin criteria. *Endocr Pract* (2021) 27(5):401–7. doi: 10.1016/j.eprac.2020.11.008

9. Thiagarajan S, Yousuf A, Shetty R, Dhar H, Mathur Y, Nair D, et al. Poorly differentiated thyroid carcinoma (Pdtc) characteristics and the efficacy of radioactive iodine (Rai) therapy as an adjuvant treatment in a tertiary cancer care center. *Eur Arch Otorhinolaryngol* (2020) 277(6):1807–14. doi: 10.1007/s00405-020-05898-9

10. Riley DS, Barber MS, Kienle GS, Aronson JK, von Schoen-Angerer T, Tugwell P, et al. Care guidelines for case reports: Explanation and elaboration document. *J Clin Epidemiol* (2017) 89:218–35. doi: 10.1016/j.jclinepi.2017.04.026

11. Ballantyne AD, Garnock-Jones KP. Dabrafenib: First global approval. *Drugs* (2013) 73(12):1367–76. doi: 10.1007/s40265-013-0095-2

12. Flaherty KT, Robert C, Hersey P, Nathan P, Garbe C, Milhem M, et al. Improved survival with mek inhibition in braf-mutated melanoma. *N Engl J Med* (2012) 367(2):107–14. doi: 10.1056/NEJMoa1203421

13. Falchook GS, Lewis KD, Infante JR, Gordon MS, Vogelzang NJ, DeMarini DJ, et al. Activity of the oral mek inhibitor trametinib in patients with advanced melanoma: A phase 1 dose-escalation trial. *Lancet Oncol* (2012) 13(8):782–9. doi: 10.1016/S1470-2045(12)70269-3

14. Subbiah V, Kreitman RJ, Wainberg ZA, Cho JY, Schellens JHM, Soria JC, et al. Dabrafenib and trametinib treatment in patients with locally advanced or metastatic braf V600-mutant anaplastic thyroid cancer. *J Clin Oncol* (2018) 36(1):7–13. doi: 10.1200/JCO.2017.73.6785

15. Haddad RI, Nasr C, Bischoff L, Busaidy NL, Byrd D, Callender G, et al. Nccn guidelines insights: Thyroid carcinoma, version 2.2018. *J Natl Compr Canc Netw* (2018) 16(12):1429–40. doi: 10.6004/jnccn.2018.0089

16. White PS, Pudusseri A, Lee SL, Eton O. Intermittent dosing of dabrafenib and trametinib in metastatic Braf(V600e) mutated papillary thyroid cancer: Two case reports. *Thyroid* (2017) 27(9):1201–5. doi: 10.1089/thy.2017.0106

17. Odogwu L, Mathieu L, Blumenthal G, Larkins E, Goldberg KB, Griffin N, et al. Fda approval summary: Dabrafenib and trametinib for the treatment of metastatic non-small cell lung cancers harboring braf V600e mutations. *Oncologist* (2018) 23(6):740–5. doi: 10.1634/theoncologist.2017-0642

18. Finsterer J. Trametinib and dabrafenib induced rhabdomyolysis, renal failure, and visual loss. report of one case. *Rev Med Chil* (2020) 148(11):1684–9.

frontiers | Frontiers in Oncology

TYPE Case Report
PUBLISHED 06 January 2023
DOI 10.3389/fonc.2022.1096411



OPEN ACCESS

EDITED BY
Zhaolun Cai,
West China Hospital, Sichuan University, China

REVIEWED BY
Ugo Grossi,
University of Padua, Italy
Alessandro De Vita,
Scientific Institute of Romagna for the Study and Treatment of Tumors (IRCCS), Italy
Rahul Gupta,
Synergy Institute of Medical Sciences, India

*CORRESPONDENCE
Hsin-Hua Lee
dr.hh.lee@gmail.com

†These authors have contributed equally to this work and share first authorship

SPECIALTY SECTION
This article was submitted to Surgical Oncology, a section of the journal Frontiers in Oncology

RECEIVED 12 November 2022
ACCEPTED 05 December 2022
PUBLISHED 06 January 2023

CITATION
Cheng SH, Huang Y-S, Lee H-H, Yen H-H, Jhong Y-P and Chao T-Y (2023) Case report and literature review: Conversion surgery for initially unresectable huge retroperitoneal liposarcoma after preoperative radiotherapy.
*Front. Oncol.* 12:1096411.
doi: 10.3389/fonc.2022.1096411



# Case report and literature review: Conversion surgery for initially unresectable huge retroperitoneal liposarcoma after preoperative radiotherapy

Sarah Hsin Cheng[1†], Yen-Shuo Huang[2†], Hsin-Hua Lee[1,3,4,5,6*], Heng-Hsuan Yen[3], Ying-Pei Jhong[3] and Tzu-Yuan Chao[7]

[1]School of Medicine, College of Medicine, Kaohsiung Medical University, Kaohsiung, Taiwan, [2]Department of Pathology, Kaohsiung Medical University Hospital, Kaohsiung Medical University, Kaohsiung, Taiwan, [3]Department of Radiation Oncology, Kaohsiung Medical University Hospital, Kaohsiung Medical University, Kaohsiung, Taiwan, [4]Ph.D. Program in Environmental and Occupational Medicine, Kaohsiung Medical University and National Health Research Institutes, Kaohsiung, Taiwan, [5]Department of Radiation Oncology, Faculty of Medicine, College of Medicine, Kaohsiung Medical University, Kaohsiung, Taiwan, [6]Center for Cancer Research, Kaohsiung Medical University, Kaohsiung, Taiwan, [7]Department of Radiation Oncology, Kaohsiung Municipal Siaogang Hospital, Kaohsiung, Taiwan

**Background:** Retroperitoneal liposarcoma (RPLS) is a rare malignancy that is notorious for recurrence. Surgical resection with clean margin is the current treatment of choice. However, owing to the large retroperitoneal space, RPLSs often grow to significant sizes before being diagnosed. Neoadjuvant and adjuvant therapies have potentials to improve long term treatment outcome.

**Case presentation:** A 55-year-old Han Chinese male presented to the general surgery department with a one-year history of abdominal fullness and a one-week history of palpable right inguinal mass. At first, he was diagnosed with incarcerated inguinal hernia. However, abdominal computer tomography (CT) and biopsy confirmed his final diagnosis to be retroperitoneal well-differentiated liposarcoma, cT2bN0M0, stage IIb. The tumor, which measured 44.5cm in maximum diameter, was too large for primary surgical resection. Neoadjuvant radiotherapy with 70 Gy in 35 fractions was delivered to the tumor, which shrunk the target volume from 6300 cc to 4800 cc, as observed in the middle of the radiotherapy course. The right testicular mass also received 70Gy/35Fx. Conversion surgery was performed after radiotherapy. Unfortunately, due to residual tumor, adjuvant chemotherapy consisting of AIM (ifosfamide, Mesna, and doxorubicin) and MAID (Mesna, doxorubincin, ifosfamide, and dacarbazine) regimens were administered sequentially. Afterward, debulking surgery was conducted, plus another 18 cycles of ifosfamide monotherapy when residual tumor was still seen on CT. Since the completion of ifosfamide chemotherapy, the patient has been cancer free with no evidence of tumor recurrence for more than 26 months.

**Conclusion:** Despite conflicting evidence in the literature, our case supports the use of high dose neoadjuvant radiotherapy and adjuvant chemotherapy in treating large, unresectable RPLSs. It also highlights the importance of using individualized, multidisciplinary approach in achieving cure for large, unresectable rare tumors.

KEYWORDS

conversion surgery, retroperitoneal sarcoma, liposarcoma, inoperable, neoadjuvant radiotherapy, adjuvant chemotherapy, giant tumor

## 1 Introduction

Sarcomas develop from the connective tissues and the majority grows in the extremities (1). Only about 15% of sarcomas develop in the retroperitoneum (1). Out of all retroperitoneal sarcomas (RPSs), retroperitoneal liposarcomas (RPLSs) are the most common, accounting for 41% of RPSs (1, 2), while only accounting for 0.07% to 0.2% of all neoplasms (2). World Health Organization classification system subdivides liposarcomas into 5 distinct subgroups, each with its distinct clinical behavior and aggressive potential (3). The most commonly seen subgroup is the well-differentiated liposarcoma (WDLPS), which tends to be slow-growing and with less metastatic potential (2, 4). The 5-year survival rate of WDLPS is about 90% (2). However, it is known for recurrence. Even after complete surgical resection, the 5-year local recurrence rate is still 50% (1, 2). Most patients who succumb to RPLS die from the effect of local recurrence, not from distant metastases (1, 2).

Currently, the only definitive treatment for RPLSs is complete surgical resections with negative margins (1, 2, 5). However, owing to the large space in the retroperitoneum, RPLSs tend to be quite large before patients begin to show symptoms and seek medical help (2, 5). According to an analysis, approximately half of the RPLSs are greater than 20cm at diagnosis (2). Such size and proximity to vital retroperitoneal structures limit the surgeon's ability to achieve complete resection, a major predictor of survival and recurrence (1, 2, 5). Therefore, to improve complete resection rate, investigations into neoadjuvant and adjuvant therapies' efficacy were of great importance. Specifically, conversion surgery, defined as surgical treatment with curable intention after an initially unresectable tumor has responded to preoperative treatment, would be particularly beneficial. Unfortunately, the rare nature of RPSs and their heterogeneity make high level evidence difficult to come by (2, 5). To date, the roles of neoadjuvant and adjuvant therapies for RPLS have remained controversial (6). In this report, we present a case of huge RPLS, whose greatest diameter reached 44.5cm at presentation. The patient was initially deemed unsuitable for primary surgical resection. However, with the addition of high dose neoadjuvant radiotherapy (NART) and adjuvant chemotherapy (AC), he was cured and has remained cancer-free with minimal adverse effect for more than 26 months. To the best of our knowledge, no other published case reports have described the preoperative and postoperative therapies for a large RPLS in such details.

This study was reported in agreement with principles of the CARE guidelines (7).

## 2 Case description

A 55-year-old Han Chinese male presented to a local hospital with abdominal fullness and a palpable right inguinal mass. Both symptoms had been present for a year, but only worsened in the past few weeks, prompting the patient to seek medical attention. The patient had a history of intracerebral hemorrhage secondary to ruptured venous aneurysm 25 years ago. He recovered well and his activity of daily living was totally independent.

At first, the clinical impression following physical examination was incarcerated inguinal hernia. However, during the course of herniorrhaphy, bulging cord and scrotum were noted. Without prior computed tomography (CT) imaging studies, only the part of the tumor that was exposed during the surgery was excised. The excised specimen was sent for pathology studies. Subsequent abdominal and pelvic CT imaging revealed a right retroperitoneal mass with a maximum diameter of 44.5cm, protruding into the right inguinal space (Figures 1A, B). Histological examination of the surgical specimen showed the tumor to be composed of mature adipocytes with substantial size variation, which was appreciated alongside nuclear atypia in fat cells or stromal spindle cells. Scattered hyperchromatic and pleomorphic stromal spindle cells were easily identified within fibrous septa or blood vessel walls. Moreover, the neoplastic cells were immunoreactive for CDK4, p16 and MDM2 (Figures 2B–D). The final diagnosis was retroperitoneal WDLPS (FNCLCC, grade 1), cT2bN0M0, stage

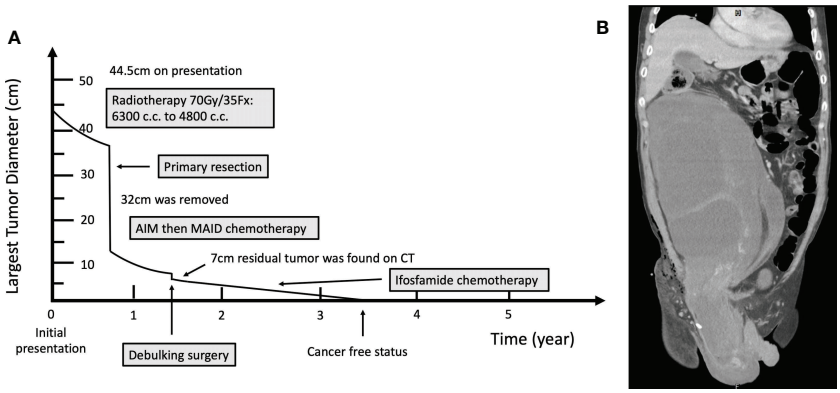


FIGURE 1
**(A)** Timeline of the occurrence of major clinical events. **(B)** Computed Tomography image before neoadjuvant radiotherapy.

IIb (Figure 2). Following the excision of the right scrotal tumor, the patient developed abdominal fullness with vomiting and fever up to 38.5 degree Celsius. Physical examination revealed abdominal distension with tenderness and redness surrounding an oozing surgical wound. Laboratory tests revealed marked elevation in CRP and leukocytosis. Abdominal wound infection with abscess was diagnosed. Fortunately, the infection resolved after proper wound care, drainage, and antibiotic treatment.

Due to the extensive nature of this tumor, complete surgical resection of this giant tumor was considered difficult, and primary chemotherapy was not recommended by medical oncologists. He was referred for radiotherapy at our cancer

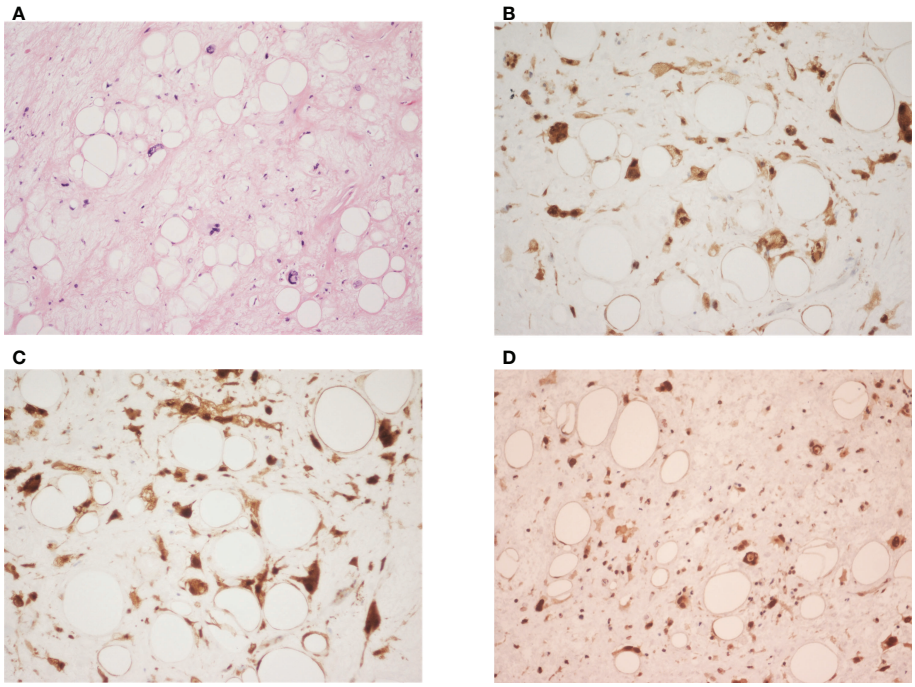


FIGURE 2
**(A)** It shows variably sized adipocytes with fibrous stroma, containing atypical cells with hyperchromatic nuclei and marked pleomorphism. (hematoxylin-eosin; original magnification ×200). **(B–D)** The neoplastic cells are immunoreactive for CDK4 (original magnification ×400), p16 (original magnification ×400), and MDM2 (original magnification ×200) respectively.

center. The organ at risk that needed to be considered first was the kidneys. Radiotherapy of 10MeV photon energy was delivered using manually chosen portals in order to maximally avoid the right kidney and completely avoid the left kidney. Thirty-five fractions of 2Gy were prescribed to the 95% isodose line. The radiation oncologist manually contoured on cross-sectional CT simulation images and measured target volume using segmentation tool programs, Eclipse and Pinnacle (Figure 3). The patient was monitored weekly. During the radiotherapy course, the patient reported less abdominal fullness and better digestion, which coincided with a reduction of the target volume from 6300cc to 4800cc, as noted in the adaptive treatment planning. Later on, the residual tumor mass in the right scrotum also received a total dose of 70Gy in 35 fractions (Figure 3). There was a grade 2 radiation-induced dermatitis in the scrotal area per the Common Terminology Criteria for Adverse Events (CTCAE) v4.0. Radiotherapy was well-tolerated without acute toxicities greater than 2. In addition, his kidney function, as measured by creatinine clearance, remained mostly the same throughout radiotherapy.

After significant volume reduction from the well-tolerated radiotherapy treatment, the patient became a candidate for surgery. He was referred to our surgical department where conversion surgery was carried out. A midline laparotomy incision was made to remove a yellowish soft, circumscribed retroperitoneal mass that measured 32cm in the greatest diameter and weighed 4.5kg. The surgery lasted around 3 hours and the blood loss was 200mL. The recovery process was smooth and no complication occurred after the surgery. However, microscopic examination revealed positive margin. Abdominal CT survey also suspected residual tumor (ycT2bN1M0, stage III) in the right inguinal area and the right pelvic wall (Figure 4A). Adjuvant chemotherapy was thus performed. At first, the patient received 4 cycles of AIM (ifosfamide, Mesna and doxorubicin) regimen. Then it was followed by 2 cycles of MAID regimen with Mesna, doxorubicin, ifosfamide and dacarbazine. During chemotherapy, the patient suffered from an episode of tumor site bacterial infection which was successfully treated with antibiotic and C-GSF injection. Otherwise, he mostly experienced grade 1 nausea/vomiting side effect per the CTCAE v4.0. At the completion of adjuvant chemotherapy (Figure 4B), the maximum tumor diameter decreased from approximately 11 cm to 8 cm. Debulking surgery for the remaining right inguinal tumor mass was thus performed. The resulting tissue fragments were 6.5cm in the greatest diameter without visible tumor cells in the section. Following the surgery, the patient developed poor wound healing, which resolved after proper wound care with Aquacel Tamponade and antibiotic use. Unfortunately, abdominal CT performed 20 days after the debulking surgery showed a 7-cm residual tumor mass in the right inguinal area and the pelvic peritoneum. This time, however, due to concern for doxorubicin's cumulative dose-dependent cardiotoxicity (8), the patient was started on ifosfamide monotherapy only. Fortunately, after 18 cycles of ifosfamide monotherapy, no evidence of recurrence was found on abdominal CT (Figure 4C). He experienced infection as a chemotherapy complication early on in the ifosfamide therapy. The infection was treated promptly without major sequala. At the time of the writing of the manuscript, the patient has remained cancer free for more than 26 months.

## 3 Discussion

The role of radiotherapy in treating RPLS has been controversial. Compared to adjuvant radiotherapy, NART offers several theoretical advantages. Firstly, the gross tumor volume could be clearly defined for precise treatment planning (9). Secondly, the tumor forms a natural tissue expander, displacing radiosensitive organs, such as the small bowel, from the radiation field (2, 5, 9). As a result, dose-limiting toxicity can be minimized. Moreover, traditional principle of sarcoma radiotherapy dictates that radiation be more biologically active

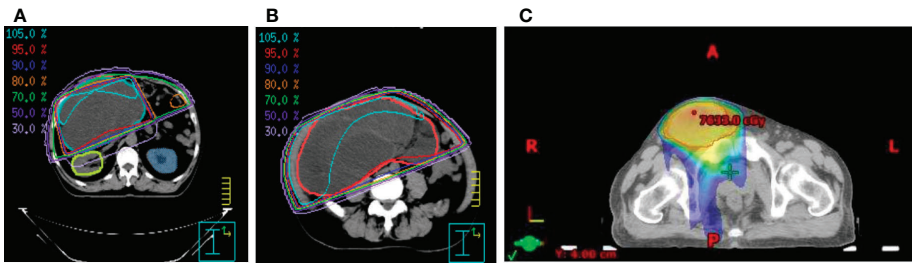


FIGURE 3
The isodose curves that show **(A)** renal parenchymal sparing and the coverage of the target tumor mass in **(B)** the peritoneal and **(C)** the inguinal area.

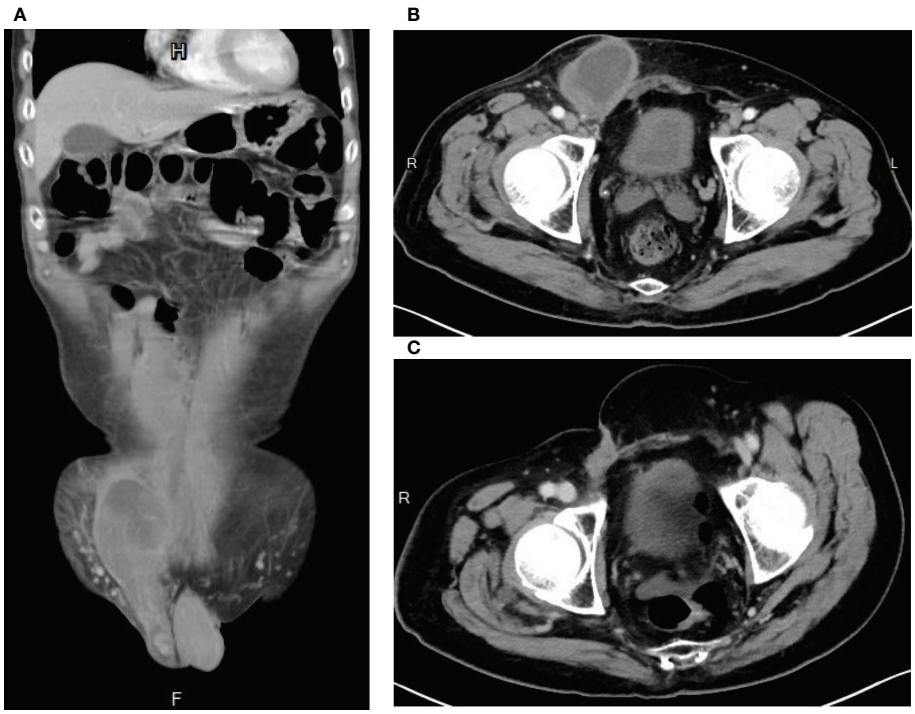


FIGURE 4
Computed Tomography images showing evidence of tumor shrinkage **(A)** after neoadjuvant radiotherapy plus conversion surgery, **(B)** after adjuvant chemotherapy AIM (ifosfamide, Mesna, and doxorubicin) and MAID (Mesna, doxorubincin, ifosfamide, and dacarbazine) regimens, and **(C)** after ifosfamide chemotherapy.

in the preoperative setting, allowing lower dosages to be prescribed (9). Finally, NART increases the possibility of achieving a complete resection, and thereby a cure, in tumors deemed unresectable (6). In the present case, the huge tumor was considered not suitable for either operation or chemotherapy at the discretion of surgeons and medical oncologists. Radiotherapy was his only option. It was not intended to be NART until the tumor drastically regressed and was later confirmed on adaptive treatment planning.

Indeed, these theoretical advantages seemed to have been proven in a number of small retrospective and prospective studies. NART plus curative resection were found to be better at achieving local control and prolonging survival than surgical resection only (5). Unfortunately, these studies were unable to assess the long-term benefit of NART (5, 10). To provide higher quality evidence, a randomized phase III multicenter clinical trial (STRASS) was published in 2020. Contrary to prior studies, STRASS found that NART cannot be considered a standard of care treatment for RPSs. According to the authors, abdominal recurrence-free survival (aRFS) and overall survival (OS) were similar between the NART plus surgery group and the surgery alone group at 3 years of follow-up (10). This result pointed to a lack of benefit with NART. Furthermore, STRASS also found a disproportionally high rate of adverse events among participants of the NART group, with 77% of participants experiencing grade 3-4 adverse effects (10). However, STRASS was not without criticism. Among the limitations of STRASS was defining aRFS as a composite endpoint (11). The author may have chosen such strategy so as to account for tumor progressing to unresectable during NART treatment (11). However, some critics worry that using composite endpoints would limit the ability of the study to truly capture local recurrence (11). Moreover, 3 years of follow-up was considered relatively short for a group of cancer whose 5-year local recurrence rate after complete gross resection could be as high as 80% in some histological subtypes (2). Furthermore, each histological subtype has its distinct clinical behavior. Yet, STRASS did not take such difference into account when designing the trial (11). It was not until the subgroup analysis did the authors perform a separate analysis of liposarcoma and found that in low grade sarcomas, such as WDLPS, radiotherapy seemed to have its values (10). Taken together, the benefit of NART in RPLS remains in question until higher quality evidence becomes available. However, individualized treatment incorporating NART in the present case was unexpectedly successful.

Like NART, adjuvant chemotherapy (AC) for RPLS is also poorly understood. Current evidence is contradictory with

different clinical trials showing contrasting results (12). Moreover, most of the studies were done on sarcomas of the extremities (6, 12). It is still unclear the extent to which we can extrapolate the data for use in primary RPS (6, 12). An updated meta-analysis of AC on soft tissue sarcomas (STS) of any sites demonstrated marginal benefit in local, distant, and overall recurrence, as well as OS (13). Doxorubicin plus ifosfamide appeared to offer greater benefit than doxorubicin alone (13). However, subsequent large, phase III randomised controlled trial published by the European Organization for Research and Treatment of Cancer (EORTC) found no OS or recurrence benefit with ifosfamide plus doxorubicin despite the regimen being well-tolerated (14). Recent long-term study by the Italian and Spanish Sarcoma Groups shows that three cycles of adjuvant epirubicin and ifosfamide is non-inferior to five cycles of the same regimen in STS of any sites (15). As is the case with NART, more higher-level evidence is needed to understand the role of AC in treating RPLS. Fortunately, besides NART and AC, there are now some promising new treatment options on the horizon. In systemic therapy, there are molecular therapies and new synthetic agents such as marine derived synthetics, Eribulin mesylate and trabectedin (3, 16). In the field of surgical oncology, compartmental surgery is also being explored (17). In radiation oncology, off-trial results regarding STS treatments are given more attention (18). Together, they offer hope for patients battling RPLSs and its other more aggressive variants.

To the best of our knowledge, this is the first case in the literature that describes in detail the use of both high dose NART and AC to treat large WDLPS (Table 1).

Due to the huge tumor size at presentation, the tumor was deemed unresectable. Without successful downstaging with a preoperative therapy, the patient had little chance of a cure. NART was thus administered, but with carefully chosen portals to prevent irradiation to critical organs. However, after surgical excision, remanent tumor mass was found on CT which could not be completed excised without causing significant morbidity to the patient. Likewise, radiotherapy would induce significant toxicity to adjacent retroperitoneal structures. Given the patient's relatively young age and fitness, chemotherapy was deemed an appropriate option. Therefore, AC regimen containing ifosfamide and doxorubicin was administered.

TABLE 1 Clinicopathological characteristics of reported case of large retroperitoneal liposarcoma treated with neoadjuvant and/or adjuvant therapy in the English literature.

| Authors | Publication Year | Patient Age (yr)/sex | Initial Tumor size | Tumor histology | Grade | Neoadjuvant treatment | Primary Treatment | Adjuvant Treatment | Outcome |
|---|---|---|---|---|---|---|---|---|---|
| Oh et al. (19) | 2014 | 39/F | 35 x 26 x 17cm | DDLPS | G2/3 | None | Surgical resection | RT with unknown dose, then doxorubicin +Ifosfamide | No recurrence during treatment |
| Choi et al. (20) | 2015 | 73/M | 23 x 15 x 7cm | Myxoid | G1 | None | Surgical resection | RT with 45Gy | No recurrence at 9 years |
| Khoury et al. (21) | 2015 | 72/F | 8.7cm | DDLPS | High grade | adriamycin/ dacarbazine + 50Gy RT | Surgical resection | none | Recurred in 1 year |
| Kus et al. (22) | 2015 | 40/F | 20 x 15 x 10cm | DDLPS | unknown | None | Surgical resection | AIM regimen | Bone metastasis after 3 months |
| Zheng et al. (23) | 2017 | 45/M | 65 x 45 x 30cm | WDLPS | G1 | None | Surgical resection | RT with unknown dose | No recurrence at 8 months |
| Da Silva et al. (24) | 2018 | 42/F | 8 x 16 x 7.7cm | WDLPS | High grade | None | Gemcitabine + docetaxel# | None | No recurrence at 8 months |
| Horowitz et al. (25) | 2020 | 73/M | 15 x 15 cm | DDLPS | high grade | None | Surgical resection | Doxorubicin then Palbociclib then Eribulin## | Cancer continues to progress, on palliative treatment now |
| Recinos et al. (26) | 2021 | 43/M | 17 cm | DDLPS | G3 | None | Surgical resection | Pazopanib monotherapy* | Cancer persists with |

*(Continued)*

TABLE 1 Continued

| Authors | Publication Year | Patient Age (yr)/sex | Initial Tumor size | Tumor histology | Grade | Neoadjuvant treatment | Primary Treatment | Adjuvant Treatment | Outcome |
|---|---|---|---|---|---|---|---|---|---|
| | | | | | | | | | evidence of radiographic and symptomatic improvement |
| Nakahashi et al. (27) | 2022 | 61/M | 11cm | DDLPS | G2 | None | Surgical resection | doxorubicin + ifosfamide | Recurred in 5 years |
| Suryabanshi et al. (28) | 2022 | 62/M | 30 x 28 x 21cm | WDLPS | Unknown | None | Surgical resection | AIM regimen | Local recurrence in 2 years** |
| Cheng et al., present case | 2022 | 55/M | 44.5cm | WDLPS | G1 | RT with 70Gy/ 35fr | Surgical resection | AIM followed by MAID; then ifsofamide monotherapy | Cancer free for 26 months |

#During the initial presentation, the cancer was surgically excised. However, on recurrence, chemotherapy alone was utilized to treat the recurrent tumor.
##Palbociclib then Eribulin are palliative for the patient with the goal of halting progression of the cancer.
*The patient did not tolerate postoperative radiotherapy of unknown dose and developed intolerable neurological side effect from doxorubicin and ifosfomide.
**The patient was inconsistent in follow up.
DDLPS, dedifferentiated liposarcoma; WDLPS, well-differentiated liposarcoma; RT, radiotherapy; AIM, Doxorubincin(Adriamycin), ifosfamide, and mesna; MAID, ifosfamide, doxorubicin, mesna, dacarbazine.

Another unique point about our case is the high radiation dosage (70Gy in 35 fractions) that was used. In our review of the literature, no other published studies have used such high dosage. For comparison, STRASS trial only used a radiation dosage of 50.4Gy in either 3D-Confromal RT or intensity modulated radiation therapy (10). The dosage we used correlates to a 2006 study that suggests a theoretical dose escalation of up to 80Gy could be considered in RPLS (29). Our patient responded well to 70Gy with good adherence. Grade 2 radiation-induced dermatitis was observed during radiotherapy, which subsided soon. To date, he has not developed any chronic radiotherapy-related adverse effect since completing the treatment more than 5 years ago. Furthermore, despite WDLPS' high recurrence rate, his cancer has not recurred for more than 2 years. The high NART dose may have contributed to his prolonged recurrence free survival since a number of studies have pointed to dose escalation as a possible solution to poor local control (29). However, the limitation of our present case report is the relatively short follow-up duration prior to its publication. As a malignancy known for recurrence, the patient has been cancer free for more than 2 years and will be followed up throughout his lifetime.

In conclusion, we present a case of RPLS who was cured by NART of 70Gy followed by surgical resection and AC. The case highlights the importance of individualized, multidisciplinary approach in treating large, rare malignancy. Although the role of NART and AC in RPLS treatment are still being debated, clinicians should not rule them out as viable options. For patients who are not candidates for standard therapies, these options, when carefully tailored, can be their only chance of a cure.

## 4 Patient perspective

I was shocked to see such a huge tumor residing inside my body on the CT scan. To put it simply, I had no debilitating symptoms, except some abdominal fullness and a visible inguinal mass. After the initial shock, the reality of treating the huge cancer sank in when surgeons and oncologists told me the tumor was too big for surgery or chemotherapy. My heart sank. By the time I had arrived at the Department of Radiation Oncology, I had lost most of my hope. However, during the course of the radiotherapy, when my bulging stomach began to flatten and I gradually regained my appetite, I began to feel hopeful again. After radiotherapy, I received an operation followed by chemotherapy. And then there was yet another surgery to the inguinal area followed by even more chemotherapy. The arduous journey took over 3 years. Along the way, there were multiple hospital visits for various treatments and checkups. Sometimes I had complications from these treatments, which further increase my hospital stays. Despite all these challenges, I survived the cancer and was declared cancer free. I am forever grateful to my family for their untiring support and to all the healthcare professionals for never giving up on me and whose expertise has allowed me a second chance at life. I feel more alive each day.

## Data availability statement

The original contributions presented in the study are included in the article/supplementary material. Further inquiries can be directed to the corresponding author.

## Ethics statement

Ethical review and approval was not required for the study on human participants in accordance with the local legislation and institutional requirements. The patients/participants provided their written informed consent to participate in this study.

## Author contributions

SC and Y-SH completed the first draft and generated graphs. H-HL designed the radiation field and critically revised the manuscript. H-HL, H-HY, Y-PJ and T-YC treated the patient and participated in treatment planning, dose calculation, and quality assurance. All authors contributed to the article and approved the submitted version.

## Acknowledgments

The authors would like to thank Dr. Yu-Ching Gao of Kaohsiung Medical University for her valuable comment and insight on RPLS chemotherapy treatment.

## Conflict of interest

The authors declare that the research was conducted in the absence of any commercial or financial relationships that could be construed as a potential conflict of interest.

## Publisher's note



## References

1. Park JO, Qin LX, Prete FP, Antonescu C, Brennan MF, Singer S. Predicting outcome by growth rate of locally recurrent retroperitoneal liposarcoma: The one centimeter per month rule. *Ann Surg* (2009) 250(6):977–82. doi: 10.1097/SLA.0b013e3181b2468b

2. Vijay A, Ram L. Retroperitoneal liposarcoma: A comprehensive review. *Am J Clin Oncol* (2015) 38(2):213–9. doi: 10.1097/COC.0b013e31829b5667

3. De Vita A, Mercatali L, Recine F, Pieri F, Riva N, Bongiovanni A, et al. Current classification, treatment options, and new perspectives in the management of adipocytic sarcomas. *Onco Targets Ther* (2016) 9:6233–46. doi: 10.2147/OTT.S112580

4. Choi JH, Ro JY. The 2020 WHO classification of tumors of soft tissue: Selected changes and new entities. *Adv Anat Pathol* (2021) 28(1):44–58. doi: 10.1097/PAP.0000000000000284

5. Cheng H, Miura JT, Lalehzari M, Rajeev R, Donahue AE, Bedi M, et al. Neoadjuvant radiotherapy for retroperitoneal sarcoma: A systematic review. *J Surg Oncol* (2016) 113(6):628–34. doi: 10.1002/jso.24221

6. Schmitz E, Nessim C. Retroperitoneal sarcoma care in 2021. *Cancers (Basel)* (2022) 14(5):1293. doi: 10.3390/cancers14051293

7. Riley DS, Barber MS, Kienle GS, Aronson JK, von Schoen-Angerer T, Tugwell P, et al. CARE guidelines for case reports: Explanation and elaboration document. *J Clin Epidemiol* (2017) 89:218–35. doi: 10.1016/j.jclinepi.2017.04.026

8. Von Hoff DD, Layard MW, Basa P, Davis HLJr., Von Hoff AL, Rozencweig M, et al. Risk factors for doxorubicin-induced congestive heart failure. *Ann Intern Med* (1979) 91(5):710–7. doi: 10.7326/0003-4819-91-5-710

9. Nielsen OS, O'Sullivan B. Retroperitoneal soft tissue sarcomas: A treatment challenge and a call for randomized trials. *Radiother Oncol* (2002) 65:133–6. doi: 10.1016/S0167-8140(02)00365-1

10. Bonvalot S, Gronchi A, Le Péchoux C, Swallow CJ, Strauss D, Meeus P, et al. Preoperative radiotherapy plus surgery versus surgery alone for patients with primary retroperitoneal sarcoma (EORTC-62092: STRASS): A multicentre, open-label, randomised, phase 3 trial. *Lancet Oncol* (2020) 21(10):1366–77. doi: 10.1016/S1470-2045(20)30446-0

11. Cardona K. The STRASS trial: An important step in the right direction. *Lancet Oncol* (2020) 21(10):1257–8. doi: 10.1016/S1470-2045(20)30429-0

12. Almond LM, Gronchi A, Strauss D, Jafri M, Ford S, Desai A. Neoadjuvant and adjuvant strategies in retroperitoneal sarcoma. *Eur J Surg Oncol* (2018) 44(5):571–9. doi: 10.1016/j.ejso.2018.02.001

13. Pervaiz N, Colterjohn N, Farrokhyar F, Tozer R, Figueredo A, Ghert M. A systematic meta-analysis of randomized controlled trials of adjuvant chemotherapy for localized resectable soft-tissue sarcoma. *Cancer* (2008) 113(3):573–81. doi: 10.1002/cncr.23592

14. Woll PJ, Reichardt P, Le Cesne A, Bonvalot S, Azzarelli A, Hoekstra HJ, et al. Adjuvant chemotherapy with doxorubicin, ifosfamide, and lenograstim for resected soft-tissue sarcoma (EORTC 62931): a multicentre randomised controlled trial. *Lancet Oncol* (2012) 13(10):1045–54. doi: 10.1016/S1470-2045(12)70346-7

15. Gronchi A, Stacchiotti S, Verderio P, Ferrari S, Martin Broto J, Lopez-Pousa A, et al. Short, full-dose adjuvant chemotherapy (CT) in high-risk adult soft tissue sarcomas (STS): Long-term follow-up of a randomized clinical trial from the Italian sarcoma group and the Spanish sarcoma group. *Ann Oncol* (2016) 27(12):2283–8. doi: 10.1093/annonc/mdw430

16. De Vita A, Recine F, Miserocchi G, Pieri F, Spadazzi C, Cocchi C, et al. The potential role of the extracellular matrix in the activity of trabectedin in UPS and l-sarcoma: Evidences from a patient-derived primary culture case series in tridimensional and zebrafish models. *J Exp Clin Cancer Res* (2021) 40(1):165. doi: 10.1186/s13046-021-01963-1

17. Munoz P, Bretcha-Boix P, Artigas V, Asencio JM. Surgical principles of primary retroperitoneal sarcoma in the era of personalized treatment: A review of the frontline extended surgery. *Cancers (Basel)* (2022) 14(17):4091. doi: 10.3390/cancers14174091

18. Dario C, Alessandro G. Radiotherapy in retroperitoneal liposarcoma: Are we looking for an answer in the wrong place? *Ann Surg Oncol* (2022). doi: 10.1245/s10434-022-12666-y

19. Oh SE, Kim HJ, Choi SJ, Oh SY, Roh CR, Kim JH. A case of huge retroperitoneal liposarcoma in pregnancy. *Obstet Gynecol Sci* (2014) 57(3):236–9. doi: 10.5468/ogs.2014.57.3.236

20. Choi JH, Hwang IG, Cha SJ, Lee TJ, Jang JS. Occurrence of colonic liposarcoma after retroperitoneal liposarcoma. *Korean J Intern Med* (2015) 30(1):125–8. doi: 10.3904/kjim.2015.30.1.125

21. Khoury M, Sim GC, Harao M, Radvanyi L, Amini B, Benjamin RS, et al. Multicystic dedifferentiated retroperitoneal liposarcoma: Tumour cyst fluid analysis and implications for management. *BMJ Case Rep* (2015) 2015. doi: 10.1136/bcr-2015-211218

22. Kus T, Aktas G, Kalender ME, Tutar E, Ulker E, Camci C. Complete response of a recurrent-metastatic liposarcoma with dedifferentiated histological features following the administration of trabectedin and review of literature. *J Cancer Res Ther* (2015) 11:974–6. doi: 10.4103/0973-1482.158032

23. Zeng X, Liu W, Wu X, Gao J, Zhang P, Shuai X, et al. Clinicopathological characteristics and experience in the treatment of giant retroperitoneal liposarcoma: A case report and review of the literature. *Cancer Biol Ther* (2017) 18(9):660–5. doi: 10.1080/15384047.2017.1345388

24. Da Silva FR, Lima AVJ, Albuquerque E, Moreira-Silva CA, De Oliveira NMF, Ohana JAL, et al. Complete remission of recurrent retroperitoneal liposarcoma after the administration of gemcitabine and docetaxel as first-line adjuvant chemotherapy: A case report. *Case Rep Oncol* (2018) 11:341–6. doi: 10.1159/000489393

25. Horowitz J, Singhal M, Marrero D, Bashjawish F, Leto D, Winters M, et al. A multi-modality treatment of retroperitoneal de-differentiated liposarcoma. *Am J Case Rep* (2020) 21:e919245. doi: 10.12659/AJCR.919245

26. Recinos LM, Mohapatra S, Santharaman A, Patel N, Broder A. Retroperitoneal liposarcoma presenting with malignant gastric outlet obstruction and acute pancreatitis: A case report. *Cureus* (2021) 13(1):e12775. doi: 10.7759/cureus.12775

27. Nakahashi K, Yokoyama Y, Fukaya M, Igami T, Mizuno T, Yamaguchi J, et al. A long-term survivor of advanced retroperitoneal dedifferentiated liposarcoma: A successful multimodal approach with extended resection and chemotherapy. *Nagoya J Med Sci* (2022) 84(1):200–7. doi: 10.18999/nagjms.84.1.200

28. Suryabanshi A, Timilsina B, Khadka N, Rijal A, Bhandari RS. Huge retroperitoneal liposarcoma encasing right kidney: A case report from Nepal. *Int J Surg Case Rep* (2022) 99:107647. doi: 10.1016/j.ijscr.2022.107647

29. Tzeng CW, Fiveash JB, Popple RA, Arnoletti JP, Russo SM, Urist MM, et al. Preoperative radiation therapy with selective dose escalation to the margin at risk for retroperitoneal sarcoma. *Cancer* (2006) 107(2):371–9. doi: 10.1002/cncr.22005

frontiers | Frontiers in Surgery

TYPE Case Report
PUBLISHED 06 January 2023
DOI 10.3389/fsurg.2022.1099416



OPEN ACCESS

EDITED BY
Zhaolun Cai,
Sichuan University, China

REVIEWED BY
Yonggang Ma,
Binzhou Medical University Hospital, China
Seiichi Yoshimoto,
National Cancer Center Hospital, Japan

*CORRESPONDENCE
Daqin Feng
✉ 13807713918@163.com;
Yu Luo
✉ 1048901826@qq.com

†These authors have contributed equally to this work and share first authorship

SPECIALTY SECTION
This article was submitted to Surgical Oncology, a section of the journal Frontiers in Surgery

RECEIVED 15 November 2022
ACCEPTED 05 December 2022
PUBLISHED 06 January 2023

CITATION
Li C, Lu J, Luo Y and Feng D (2023) Case report: Endovascular intervention of internal carotid artery pseudoaneurysm secondary to nasopharyngeal carcinoma radiotherapy. Front. Surg. 9:1099416. doi: 10.3389/fsurg.2022.1099416



# Case report: Endovascular intervention of internal carotid artery pseudoaneurysm secondary to nasopharyngeal carcinoma radiotherapy

Chao Li†, Jiachao Lu†, Yu Luo* and Daqin Feng*

Department of Neurosurgery, The First Affiliated Hospital, Guangxi Medical University, Nanning, China

**Background:** Internal carotid artery pseudoaneurysm (PSA) is a serious complication after radiotherapy for nasopharyngeal carcinoma, and once it ruptures and bleeds, it will seriously affect the patient's survival and prognosis. However, because of its relatively low incidence, many medical institutions lack experience in managing this type of emergency.

**Case information:** In this case report, we described two cases suffered ruptured internal carotid artery PSA after radiotherapy for nasopharyngeal carcinoma, including their history, diagnosis, and treatment. Both cases underwent emergency endovascular interventions, one of which with long-term healing after embolization of the PSA, and the other one with re-bleeding after embolization and was eventually stopped by embolization of the parent artery. Ultimately, both cases received timely and effective treatment.

**Conclusion:** This case report detailed the diagnosis and treatment course of internal carotid artery PSA after radiotherapy for nasopharyngeal carcinoma, which enhanced the understanding of this emergency, and provided valuable information and experience for the treatment strategy of similar PSA on the internal carotid artery.

KEYWORDS

internal carotid artery pseudoaneurysm, nasopharyngeal carcinoma, nasal bleeding, endovascular intervention, case report

## Introduction

Nasopharyngeal carcinoma is a common malignant tumor in southern China, because of its complex anatomy and high sensitivity to radiotherapy, the current clinical treatment adopts a comprehensive treatment based on radiotherapy, with a 5-year survival rate of 50% to 80% (1–3). With the prolongation of patient survival, nasopharyngeal haemorrhage caused after radiotherapy becomes a serious complication affecting the prognosis of patients. The incidence of nasopharyngeal hemorrhage after radiotherapy has been reported to be 2.7%, and ruptured internal carotid artery pseudoaneurysm bleeding accounts for approximately 1% of patients with hemorrhage (4, 5). The hemorrhage is characterized by rapid, recurrent, massive and not easily

controlled, and if resuscitation is not timely, the patient may die within a very short time due to asphyxia or circulatory collapse (6). However, for bleeding from pseudoaneurysms of the internal carotid artery, relying on simple nasal tamponade or surgical ligation often fails to solve the problem, and endovascular intervention is now a more effective treatment for this type of bleeding (7, 8). We will show two typical cases of endovascular intervention for bleeding from pseudoaneurysm secondary to nasopharyngeal carcinoma radiotherapy. This case report follows the CARE Guidelines (9).

# Case presentation

## Case one

A 40-year-old male was diagnosed with pathologically confirmed nasopharyngeal carcinoma (T4N2M0, undifferentiated non-keratinizing carcinoma) (**Figure 1**). One month later, he was treated with 3D conformal intensity-modulated radiotherapy (63 Gy to the lower neck and 73 Gy to the upper neck) and concurrent chemotherapy (cisplatin 40 mg + docetaxel 120 mg regimen). Three years later, MRI suggested tumor recurrence, and two cycles of GN (gemcitabine + nedaplatin) regimen chemotherapy was performed, after which further heavy proton radiation therapy was administered.Four years later, patient developed an intermittent nasal bleeding. Nine months later, he had a sudden nasal hemorrhage with a bleeding volume of 800 ml, and underwent emergency tracheotomy and bilateral external carotid artery embolization with spring coil. However, hemostasis was not effective. Another emergency DSA was applied, and finally found the real culprit- a pseudoaneurysm of the right internal carotid artery (rupture hole segment (C3)). Then, the operation named "internal carotid artery pseudoaneurysm embolization with stent-assisted spring coil and balloon-assisted onyx gel" was performed. The operation procedure details were shown in **Figure 2**. Intraoperative angiography showed that the pseudoaneurysm was completely embolized and the internal carotid artery was well reconstructed. The patient was successfully discharged three days after surgery without any neurological deficits. Up to now, the patient did not experience any further nasal bleeding. Time line of the clinical course was shown in **Supplementary Figure S1**.

## Case two

A 39-year-old male with pathologically confirmed nasopharyngeal carcinoma (T4N2M0, undifferentiated non-keratinizing carcinoma), and then underwent a combination of chemotherapy and radiotherapy (32 course). The CT examination suggested that the pterygoid body and occipital slope were invaded.One year later, the patient had a sudden onset of massive nasal bleeding with a volume of about 800 ml, and an emergency interventional operation named "internal carotid artery pseudoaneurysm embolization with stent-assisted spring coil and balloon-assisted onyx gel" was performed. The intraoperative angiography showed that the dissection aneurysm on right internal carotid artery C3 segment had been completely embolized, and the aneurysm-carrying artery was still patent.Three months later, however, the patient suffered another nasal hemorrhage with a volume of about 500 ml, and

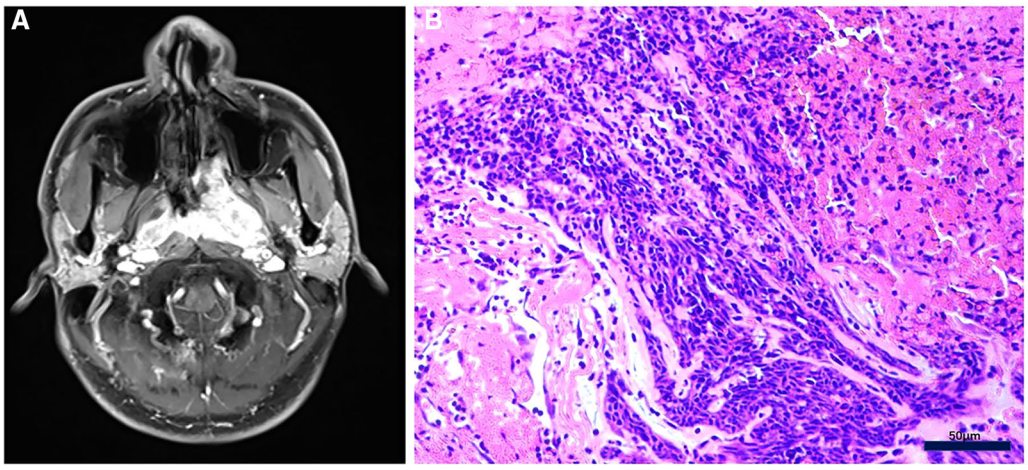


FIGURE 1
(**A**) MRI showed that nasopharyngeal carcinoma invaded the left postnaris, pterygopalatine fossa, cavernous sinus and skull base. (**B**) Morphological observation by HE staining was consistent with the diagnosis of undifferentiated non-keratinizing nasopharyngeal carcinoma, with no Keratinized beads of squamous cell carcinoma positive staining. Bar, 50 $\mu$m.

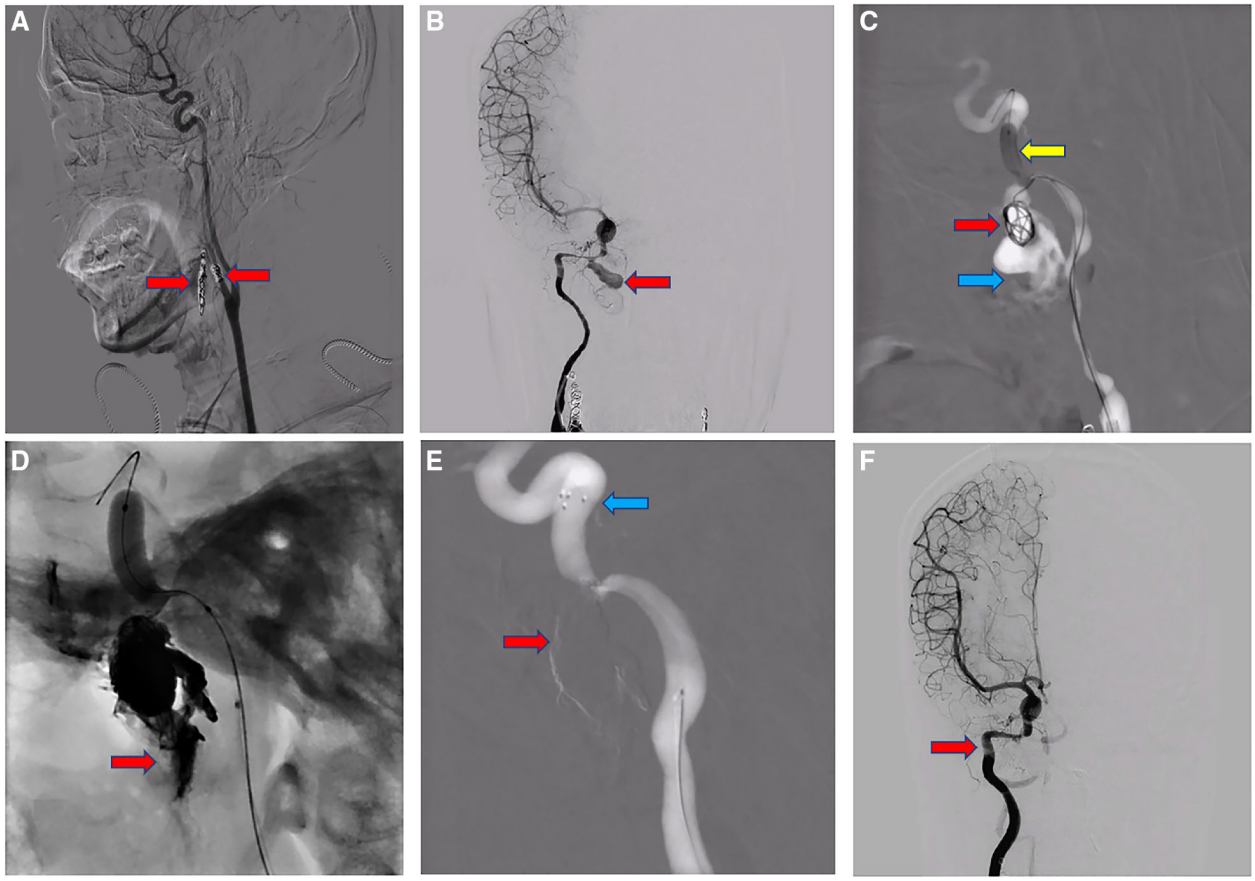


FIGURE 2
(**A**) bilateral external carotid arteries embolization with spring coil (red arrow). (**B**) Angiography suggests a narrow neck pseudoaneurysm in the right internal carotid artery rupture hole segment, diameter about 9.6 X 15.7 mm (red arrow). (**C**) Extravasation (blue arrow) of contrast medium into the nasal cavity was seen at the base, lateral and neck part of the aneurysm; The microcatheter was delivered into the aneurysm cavity, and the balloon (yellow arrow) was guided to the C4 segment and opened with a certain pressure to temporarily block the right internal carotid artery to prevent the thrombus from dislodging. Five spring coils (red arrow) were then sequentially placed and released in the aneurysm lumen *via* a microcatheter, and the imaging showed that the spring coils were well formed in the aneurysm lumen. (**D**) After imaging, we still saw extravasation (red arrow) of contrast into the sinus, and continued to use ONYX gel to fill and seal the fistula. (**E**) The imaging shows complete occlusion of the fistula (red arrow) and arterial stent (blue arrow) well released. (**F**) Well reconstruction of the internal carotid artery (red arrow) on imaging and the purpose of embolization is achieved.

an emergency DSA indicated that the clogged aneurysm was recurrent and larger than before, and located in C2 to C4 segment of the right internal carotid artery. After a hospital-wide multidisciplinary consultation (MDT) discussion, a treatment strategy of permanent occlusion of the aneurysm-carrying artery was decided to effectively prevent the recurrence of nasal hemorrhage. Cerebral angiography and balloon-assisted internal carotid artery occlusion with spring-ring and onyx gel were performed under general anesthesia. Intraoperative angiography showed complete occlusion of the right internal carotid artery, while the right cerebral hemisphere could receive adequate blood supply through the anterior communicating artery. The operation procedure details were shown in **Figure 3**. Up to now, the patient did not have any further nasal bleeding. Time line of the clinical course was shown in **Supplementary Figure S2**.

## Discussion

With the improvement of medical technology, the early diagnosis rate and 5-year survival rate of nasopharyngeal carcinoma have increased significantly (1, 10). Nasal hemorrhage caused by ruptured pseudoaneurysm of the internal carotid artery after radiotherapy for nasopharyngeal carcinoma has become one of the most common causes of death after surgery (1, 11). PSA rupture hemorrhage belongs to clinical intensive in otorhinolaryngology and neurosurgery, and related reports claimed that its mortality rate was high (1). The mechanism of its occurrence includes the following aspects: firstly, radiation causes damage to adjacent normal tissues, and the blood vessels invaded by tumor are exposed and become hardened and fibrotic (12); secondly, nasopharyngeal carcinoma can grow to the parapharynx and

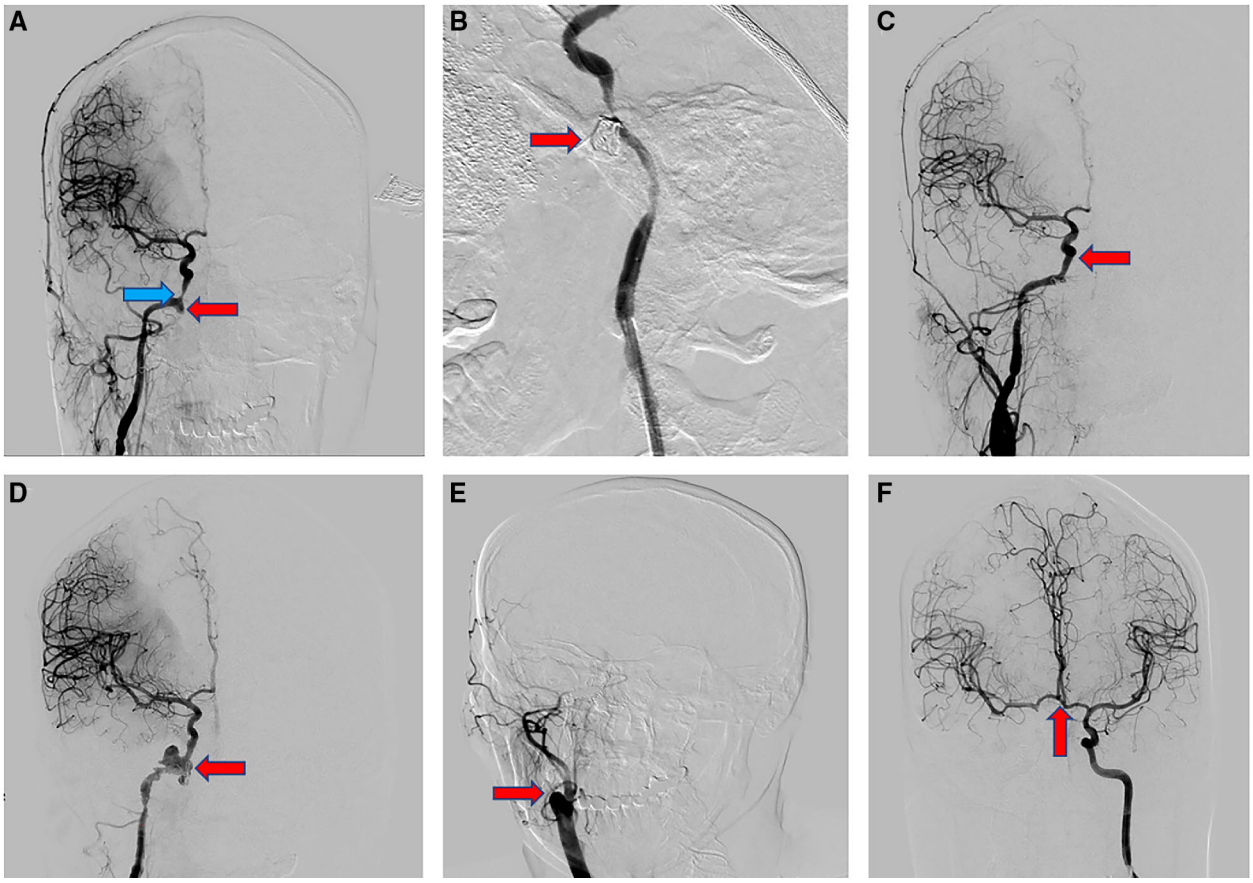


FIGURE 3
(**A**) the DSA examination showed that the pseudoaneurysm (red arrow) of the internal carotid artery located in the ruptured orifice segment of the right internal carotid artery, with a diameter of about 6*7 mm. The stenosis (blue arrow) of the cavernous sinus segment of the right internal carotid artery was about 50%. (**B**) With the assistance of stent and balloon, the pseudoaneurysm (red arrow) was successfully embolized with spring coils and ONXY gel. (**C**) Well reconstruction of the internal carotid artery (red arrow) on imaging. (**D**) The recurrent pseudoaneurysm (red arrow) located in the C2-4 segment of the right internal carotid artery, with a diameter of about 20*18.8 mm and a lobulated round shape. (**E**) After assessing the compensation of the internal carotid artery on the affected side by compression neck test, we completely and permanently occluded the right internal carotid artery (red arrow) with the aid of a balloon using spring coil and ONYX gel. (**F**) The anterior communicating artery (red arrow) was completely opened on the compression neck test.

directly invade the blood vessels in the neck, or indirectly erode the blood vessels by causing nasopharyngeal ulcer and infection, especially recurrent nasopharyngeal carcinoma is mostly located in the pharyngeal fossa, which easily invades the lateral internal carotid artery (11); finally, after the rupture and bleeding of the invaded artery, a hematoma is formed around the rupture of the vessel, which slowly liquefies over time, and the smooth muscle of the middle membrane of the vessel wall becomes thin or even absent, and connects to the aneurysm through the rupture, forming a pulsating pseudotumor (13, 14). Because of the thinness of the wall, it can rupture and bleed, and some patients can stop bleeding on their own when the blood pressure is lowered, thus showing the typical clinical symptoms of repeated bleeding (13).

Due to the concealment of nasopharyngeal bleeding and the special anatomical structure, nasopharyngeal hemorrhage is quite tricky to manage (15). The traditional methods are anterior and posterior nasal tamponade and nasal endoscopic radiofrequency cautery to stop bleeding (16, 17). The anterior and posterior nasal stuffing method is simple to operate and has good efficacy for small amount of nasopharyngeal bleeding, but most patients have limited mouth opening, nasal adhesions, and high risk of rebleeding when the stuffing is removed (17). Radiofrequency cautery under nasal endoscopy is accurate and reliable, but it is difficult to be effective when there is diffuse or rapid bleeding in the nasal cavity (12). In recent years, DSA has gained significant advantages in the treatment of nasopharyngeal carcinoma bleeding, which is the gold standard for identifying the site of vascular bleeding and the presence of vascular malformation (18, 19). Different treatment plans can be implemented according to the importance of the bleeding artery and the bleeding site. When

nasopharyngeal carcinoma bleeding is caused by the invasion of the external carotid artery alone, the bleeding artery can be embolized with gelatin sponge particles or spring ring (19); when the tumor invades the internal carotid artery and causes the formation of pseudoaneurysm of the internal carotid artery and rupture bleeding, the pseudoaneurysm can be embolized with stent/balloon assisted spring ring/ONXY glue, or isolation can be performed with overlapping stent; if the pseudoaneurysm is large in scope and difficult to embolize, then unilateral internal carotid artery occlusion is considered (12). But, intraoperative compression angiography of the affected internal carotid artery should be performed to fully assess the opening of the Willis ring, and postoperative attention should be paid to the serious complications (delayed cerebral infarction, etc.) of permanent embolization of the unilateral internal carotid artery (20).

Through the analysis of the cases, we have summarized some treatment experiences: 1) According to the relevant literature, for patients with nasopharyngeal carcinoma who underwent high-dose radiotherapy, multiple radiotherapy and recurrence after radiotherapy, it is especially important to perform regular color ultrasound examination of neck vessels, nasopharyngoscopy and CTA of head and neck for early detection of unruptured PSA (21). After detection, super-selective arterial embolization should be performed as much as possible to reduce embolization of non-diseased arteries. In order to avoid embolic particles from backflowing into the internal carotid artery by mistake and causing serious complications, injection of any kind of embolic material should be done in a low-pressure, slow and intermittent way under x-ray fluoroscopy, and assisted by applying stents or balloons. In the selection of embolic agent, the embolization of PSA in this group of cases is based on spring ring, supplemented by stent if necessary. For larger PSA, in order to achieve more complete embolization and reduce the cost, ONXY gel embolization with the assistance of balloon is applied in this group of cases, which is economical and has good hemostatic effect (22). 2) When patients with nasopharyngeal carcinoma repeatedly bleed heavily within a short period of time after posterior nasal cavity tamponade or interventional embolization of the external carotid artery, they should be alerted to the possibility of PSA rupture and bleeding. The authors suggest that DSA should be performed at an appropriate time to clarify the site of bleeding, and the scope of imaging should include the bilateral internal and external carotid arteries, and to assess the compensation of the Willis loop at the base of the brain (23). During the imaging process, attention should be paid to: whether there is extravasation of contrast agent, which can identify the site of hemorrhage once it appears; whether there is a pseudoaneurysm at the suspected site of hemorrhage; and whether there is vascular stenosis, distortion or disorder at the suspected site of hemorrhage, among which the internal carotid artery mainly shows severe lumen narrowing, suggesting tumor invasion, while the external carotid artery mainly shows vascular distortion and disorder. In addition, in patients with repeated hemorrhage after radiotherapy for nasopharyngeal carcinoma, the bleeding can be temporarily stopped because the blood pressure decreases, the bleeding rate slows down and blood clots are formed. When DSA imaging is performed, the pressure of contrast injection may cause re-bleeding or even violent and fatal hemorrhage, so we advocate to prepare for embolization before DSA, to buy time for resuscitation. 3) When the PSA is not suitable for isolation, it is still controversial whether to perform permanent embolization of unilateral internal carotid artery. Although this method is effective for hemostasis, it may affect the patient's expected survival, cause late cerebral infarction and other complications affecting the patient's quality of life after surgery (24, 25). In our case report, one of the patients accepted permanent unilateral internal carotid artery embolization, meanwhile, the internal carotid artery angiography on the healthy side immediately after embolization indicates that the healthy internal carotid artery has produced compensation, and the patient's quality of life after surgery is good and no large cerebral infarction occurred. However, preforming this method must be chosen carefully after full communication with the patient's family.

## Conclusion

Currently, endovascular intervention is the best option for managing hemorrhage secondary to postoperative internal carotid artery pseudoaneurysm in nasopharyngeal carcinoma patients. However, due to the rapid onset of the disease, emergency DSA is required for diagnosis, and a comprehensive assessment of the internal carotid artery, external carotid artery and intracerebral vascular substitution is also critical. In addition, in order to reduce surgical complications, it is important to detect the responsible vessel as accurately as possible and to select the appropriate embolization protocol and embolization material. Finally, the authors considered that early screening of patients at high risk for PSA and conversion of emergency surgery to elective surgery is the optimal treatment for this disease.

## Data availability statement

The original contributions presented in the study are included in the article/**Supplementary Material**, further inquiries can be directed to the corresponding author/s.

## Ethics statement

Written informed consent was obtained from the individual(s) for the publication of any potentially identifiable images or data included in this article.

## Author contributions

CL and JL wrote the manuscript. DF and YL reviewed and edited the manuscript. All authors contributed to the article and approved the submitted version.

## Acknowledgments

We thank the Information Department of First Affiliated Hospital, Guangxi Medical University for their comments and assistance with data collection.

## Conflict of interest

The authors declare that the research was conducted in the absence of any commercial or financial relationships that could be construed as a potential conflict of interest.

## Publisher's note



## Supplementary material

The Supplementary Material for this article can be found online at: https://www.frontiersin.org/articles/10.3389/fsurg.2022.1099416/full#supplementary-material.

## References

1. Chen YP, Chan ATC, Le QT, Blanchard P, Sun Y, Ma J. Nasopharyngeal carcinoma. *Lancet (London, England)*. (2019) 394(10192):64–80. doi: 10.1016/S0140-6736(19)30956-0

2. Tang LL, Chen YP, Chen CB, Chen MY, Chen NY, Chen XZ, et al. The Chinese society of clinical oncology (CSCO) clinical guidelines for the diagnosis and treatment of nasopharyngeal carcinoma. *Cancer Commun (London, England)*. (2021) 41(11):1195–227. doi: 10.1002/cac2.12218

3. Newton E, Valenzuela D, Foley J, Thamboo A, Prisman E. Outcomes for the treatment of locoregional recurrent nasopharyngeal cancer: systematic review and pooled analysis. *Head Neck*. (2021) 43(12):3979–95. doi: 10.1002/hed.26836

4. Alon EE, Lipschitz N, Bedrin L, Gluck I, Talmi Y, Wolf M, et al. Delayed sinonasal complications of radiotherapy for nasopharyngeal carcinoma. *Otolaryngol–Head and Neck Surg*. (2014) 151(2):354–8. doi: 10.1177/0194599814530858

5. Wong GK, Chan KK, Yu SC, Tsang RK, Poon WS. Treatment of profuse epistaxis in patients irradiated for nasopharyngeal carcinoma. *ANZ J Surg*. (2007) 77(4):270–4. doi: 10.1111/j.1445-2197.2007.04032.x

6. He CC, Si YF, Xie YA, Yu L. Management of intractable epistaxis in patients who received radiation therapy for nasopharyngeal carcinoma. *Eur Arch oto-Rhino-Laryngol*. (2013) 270(10):2763–7. doi: 10.1007/s00405-013-2598-6

7. Zeng L, Wan W, Luo Q, Jiang H, Ye J. Retrospective analysis of massive epistaxis and pseudoaneurysms in nasopharyngeal carcinoma after radiotherapy. *Eur Arch oto-Rhino-Laryngol*. (2022) 279(6):2973–80. doi: 10.1007/s00405-021-07111-x

8. Zhao Z, Huang L, Chen J, Huang W, Zhang X, Ma Y, et al. Comprehensive treatment strategy for internal carotid artery blowout syndrome caused by nasopharyngeal carcinoma. *Otolaryngol–Head and Neck Surg*. (2021) 164(5):1058–64. doi: 10.1177/0194599820963129

9. Riley DS, Barber MS, Kienle GS, Aronson JK, von Schoen-Angerer T, Tugwell P, et al. CARE Guidelines for case reports: explanation and elaboration document. *J Clin Epidemiol*. (2017) 89:218–35. doi: 10.1016/j.jclinepi.2017.04.026

10. Hua YJ, Han F, Lu LX, Mai HQ, Guo X, Hong MH, et al. Long-term treatment outcome of recurrent nasopharyngeal carcinoma treated with salvage intensity modulated radiotherapy. *Eur J Cancer*. (2012) 48(18):3422–8. doi: 10.1016/j.ejca.2012.06.016

11. Chen HC, Lin CJ, Jen YM, Juan CJ, Hsueh CJ, Lee JC, et al. Ruptured internal carotid pseudoaneurysm in a nasopharyngeal carcinoma patient with skull base osteoradionecrosis. *Otolaryngol–Head and Neck Surg*. (2004) 130(3):388–90. doi: 10.1016/j.otohns.2003.08.010

12. Lam JW, Chan JY, Lui WM, Ho WK, Lee R, Tsang RK. Management of pseudoaneurysms of the internal carotid artery in postirradiated nasopharyngeal carcinoma patients. *Laryngoscope*. (2014) 124(10):2292–6. doi: 10.1002/lary.24721

13. Nazari P, Tan LA, Wewel JT, Moftakhar R, Kasliwal MK. Massive epistaxis resulting from radiation-induced internal carotid artery pseudoaneurysm. *Neurol India*. (2017) 65(2):380–2. doi: 10.4103/neuroindia.NI_1259_15

14. Hua YJ, Chen MY, Qian CN, Hong MH, Zhao C, Guo L, et al. Postradiation nasopharyngeal necrosis in the patients with nasopharyngeal carcinoma. *Head Neck*. (2009) 31(6):807–12. doi: 10.1002/hed.21036

15. Sekhar LN, Schramm Jr. VL, Jones NF, Yonas H, Horton J, Latchaw RE, et al. Operative exposure and management of the petrous and upper cervical internal carotid artery. *Neurosurg*. (1986) 19(6):967–82. doi: 10.1227/00006123-198612000-00012

16. Shemesh R, Alon EE, Gluck I, Yakirevitch A. Endoscopic surgery for delayed sinonasal complications of radiation therapy for nasopharyngeal carcinoma: a subjective outcome. *Int J Radiat Oncol Biol Phys*. (2018) 100(5):1222–7. doi: 10.1016/j.ijrobp.2018.01.014

17. Zou L, Wu S, Liu Y, Wang S, Wen W, Liu H. Surgery option in the management of delayed diplopia after radiation therapy for nasopharyngeal carcinoma. *Eur J Ophthalmol*. (2018) 28(5):547–51. doi: 10.1177/1120672118757430

18. Low YM, Goh YH. Endovascular treatment of epistaxis in patients irradiated for nasopharyngeal carcinoma. *Clin Otolaryngol Allied Sci*. (2003) 28(3):244–7. doi: 10.1046/j.1365-2273.2003.00699.x

19. Xu X, Gopinathan A, Thong MKT, Loh KS, Ong YK. Endovascular embolisation of external carotid artery system haemorrhage in radiated nasopharyngeal carcinoma. *Eur Arch oto-Rhino-Laryngol*. (2022) 279(12):5851–8. doi: 10.1007/s00405-021-07111-x

20. Mok JS, Marshall JN, Chan M, van Hasselt CA. Percutaneous embolization to control intractable epistaxis in nasopharyngeal carcinoma. *Head Neck*. (1999) 21(3):211–6. doi: 10.1002/(SICI)1097-0347(199905)21:3<211::AID-HED5>3.0.CO;2-C

21. Xu X, Ong YK, Loh WS, Anil G, Yap QV, Loh KS. Clinical predictors of internal carotid artery blowout in patients with radiated nasopharyngeal carcinoma. *Head Neck*. (2021) 43(12):3757–63. doi: 10.1002/hed.26869

22. Li L, Cui JG, Liang ZH, Xu SB, Li J, Tian HQ, et al. Transvenous treatment of complex cavernous dural arteriovenous fistulae with onyx and coils. *Neurol India*. (2011) 59(1):92–6. doi: 10.4103/0028-3886.76877

23. Zhan J, Zhang S, Wei X, Fu Y, Zheng J. Etiology and management of nasopharyngeal hemorrhage after radiotherapy for nasopharyngeal carcinoma. *Cancer Manag Res*. (2019) 11:2171–8. doi: 10.2147/CMAR.S183537

24. Mak CH, Cheng KM, Cheung YL, Chan CM. Endovascular treatment of ruptured internal carotid artery pseudoaneurysms after irradiation for nasopharyngeal carcinoma patients. *Hong Kong Med J=Xianggang yi xue za zhi*. (2013) 19(3):229–36. doi: 10.12809/hkmj133833

25. Cheng KY, Lee KW, Chiang FY, Ho KY, Kuo WR. Rupture of radiation-induced internal carotid artery pseudoaneurysm in a patient with nasopharyngeal carcinoma–spontaneous occlusion of carotid artery due to long-term embolizing performance. *Head Neck*. (2008) 30(8):1132–5. doi: 10.1002/hed.20753

frontiers | Frontiers in Surgery

TYPE Case Report
PUBLISHED 06 January 2023
DOI 10.3389/fsurg.2022.1056831



OPEN ACCESS

EDITED BY
Zhaolun Cai,
Sichuan University, China

REVIEWED BY
Lin Xiaokun,
Wenzhou Medical University, China
Paul Willemsen,
Hospital Network Antwerp (ZNA), Belgium

*CORRESPONDENCE
Aijun Yu
ccw1979@126.com

SPECIALTY SECTION
This article was submitted to Surgical Oncology, a section of the journal Frontiers in Surgery

RECEIVED 14 October 2022
ACCEPTED 14 November 2022
PUBLISHED 06 January 2023

CITATION
Chen L, Gu J, Zhang X and Yu A (2023) Case report: Giant cystic ileal gastrointestinal stromal tumor with an atypical intratumoral abscess. Front. Surg. 9:1056831. doi: 10.3389/fsurg.2022.1056831



# Case report: Giant cystic ileal gastrointestinal stromal tumor with an atypical intratumoral abscess

Linguang Chen, Jiannan Gu, Xuejun Zhang and Aijun Yu*

Department of the First General Surgery, Affiliated Hospital of Chengde Medical University, Chengde, China

**Background:** Gastrointestinal stromal tumors (GISTs) are typically solid, sometimes with small cystic areas, but rarely manifest as predominantly cystic neoplasms. In addition, cystic intestinal GISTs with intratumoral abscess formation are rare.
**Case presentation:** We present the case of a 49-year-old male patient with a history of frequent and urgent urination for 2 weeks. Radiologic studies revealed a large cystic mass in the lower abdomen. The patient underwent abdominal laparotomy, which revealed a large cystic mass arising from the distal ileum invading the sigmoid mesocolon and apex vesicae. Partial resection of the ileum along with the tumor and the adjacent bladder was performed. Macroscopic examination revealed that the cystic mass contained a large amount of foul-smelling pus and a tumor-bowel fistula. The final pathology revealed an abdominal stromal tumor. Postoperative recovery was uneventful, and adjuvant imatinib mesylate 400 mg was administered daily. No tumor recurrence or metastasis was observed during the 9-month follow-up period.
**Conclusion:** Fingings of a cystic tumor in the abdomen should raise concern for cystic GISTs. This case report reviews a rare presentation of an ileal giant cystic GIST with atypical intratumoral abscess formation. Complete surgical resection and adjuvant imatinib is still the mainstay treatment for GISTs.

KEYWORDS

gastrointestinal stromal tumor, cystic neoplasm, intratumoral abscess, small intestine, case report

## Introduction

Gastrointestinal stromal tumors (GISTs) are the most common mesenchymal tumors of the gastrointestinal tract, accounting for 0.1%–3% of all gastrointestinal tumors (1), with an estimated annual incidence of 10–15 cases per million people (2). Most GISTs originate from the stomach (60%), with the small intestine being the second most common location. Small intestinal GISTs comprise approximately 30% of all GISTs (3), and most are located in the jejunum, followed by the duodenum and ileum (4). GISTs are typically solid tumors that rarely present with predominant cystic changes. Therefore, cystic intestinal GISTs with intratumoral abscess formation are rare. Herein, we report a case of cystic ileal GIST that presented as a large

abdominal cystic tumor preoperatively. In addition, a large amount of foul-smelling pus was observed within the tumor intraoperatively. A rapid frozen pathologic examination showed a mesenchymal tumor composed of spindle cells, and a postoperative pathological examination confirmed the diagnosis of GIST. Since a majority of previously reported cases of GISTs with an intratumoral abscess had findings of fever and significant abdominal pain, examination for an internal air-fluid level through imaging followed by emergency surgery should be performed (5–7). However, the present case had no such typical features; therefore, it was an "atypical abscess." To the best of our knowledge, this is the first report of an ileal giant cystic GIST (cGIST) with an atypical intratumoral abscess. This study was reported in agreement with principles of the CARE guidelines (8).

## Case report

A 49-year-old man was admitted to our hospital with a history of frequent and urgent urination for 45 the past 2 weeks. He did not have abdominal pain, fever, dysuria, or hematuria. His medical history was unremarkable except for hypertension. Physical examination revealed distention of the lower abdomen. A large, painless, immobile, and hard mass was palpable, having an estimated diameter of 17 cm. Laboratory testing revealed the following: C-reactive protein, 61.50 mg/L (normal range, 0–8 mg/L); white blood cell count, $14.94 \times 109$/L (normal range, $3.5–9.5 \times 109$/L); neutrophilic granulocytes, 80.8% (normal range, 40%–75%); hemoglobin, 101 g/L (normal range, 130–175 g/L); procalcitonin, 0.25 ng/ml (normal range, 0–0.05 ng/ml); interleukin-6, 43.49 pg/ml (normal range, 0–10 pg/ml); prothrombin time, 14.3 s (normal range, 9–13 s) and D-dimer, 1.60 ug/ml (normal range, 0–0.55 ug/ml). Routine urine tests, liver function tests, and tumor markers (AFP, CEA, CA 19-9) were all within the normal ranges. Ultrasonography revealed a large cystic mass, measuring approximately 17 cm in diameter, in the lower abdomen in front of the abdominal aorta and iliac vessels. Contrast-enhanced computed tomography (CT) revealed an abdominal cystic tumor with an unevenly thickened wall and mural nodules; air-fluid levels were not observed within the tumor. Enhancement was noted in the cyst wall and mural nodules during the arterial phase (**Figures 1A,B**). Magnetic resonance imaging (MRI) revealed a large cystic tumor with an internal fluid signal (**Figure 1C**). The nature and origin of the tumor could not be diagnosed preoperatively; therefore, a diagnostic laparotomy was performed through a midline abdominal incision. The procedure revealed a large cystic tumor arising from the distal ileum invading the sigmoid mesocolon and apex vesicae. Partial resection of the ileum along with the tumor and adjacent bladder was performed. The tumor was sent for frozen sectioning, revealing proliferated spindle-shaped tumor cells (**Figure 3A**). Anastomosis of the ileal was then performed using staples, side-to-side, without tumor rupture. Macroscopic examination revealed that the excised cystic mass measured 17 cm in the largest dimension and contained a large amount of foul-smelling pus.

Further examination revealed that the tumor communicated with the intestinal lumen *via* a mucosal fistula (**Figure 2**). The pus culture test result was positive for Salmonella enteritidis. Immunohistochemical staining showed that the tumor cells were positive for c-kit, DOG-1, CD34, and vimentin but negative for S-100 (**Figures 3B,C**). The Ki-67 index was approximately 6%. Mitotic count was less than 5/50 high-power fields. The resection margins were negative, and there was no lymph node metastasis. Gene analyses revealed the presence of a c-kit exon 11 mutations. The final diagnosis was high-risk GIST originating from the ileum. Postoperative recovery was uneventful, and there were no postoperative complications. The urine tube was removed 1 week after surgery, and the patient was discharged on the 13th postoperative day. Adjuvant imatinib mesylate (400 mg daily for 3 years) was administered. The patient did well during the 9-month follow-up visit without tumor recurrence or metastasis.

## Discussion

GISTs typically present as regular solid exoplastic masses, primarily found within the gastrointestinal tract and occasionally outside. GISTs rarely present as predominantly cystic tumors; in case of this rare occurrence, some researchers define them as cGISTs; if the proportion of cystic components is larger than 75% and the cyst wall is relatively regular according to the corresponding gross examination or preoperative radiological reports. The cGISTs should be considered a specific subtype of GISTs with relatively indolent behaviors and favorable prognoses, although similar to solid GISTs in terms of morphological and immunohistochemical features (9). The cause of cGISTs is related to degeneration, necrosis, and bleeding, although the exact mechanism remains unknown (9, 10). In addition, imatinib treatment can induce cystic changes (11).

Small bowel GISTs (SB GISTs) are the second most common type of GISTs in the digestive tract, with 5-, 10-, and 20-year disease-specific survival rates of 84.4, 71.2, and 54.2%, respectively (12). A retrospective study showed that patients with cGISTs had a 9:11 male-to-female ratio, with a mean age of 61 years (9). As SB GISTs often show an exophytic growth pattern and high activity, they tend to be asymptomatic in the early stages. Abdominal pain and gastrointestinal bleeding were the most common symptoms of cGISTs (9). Other rare presentations include obstruction, abdominal hemorrhage, tumor rupture, and peritonitis, which usually require emergency surgical intervention and are more common in the small

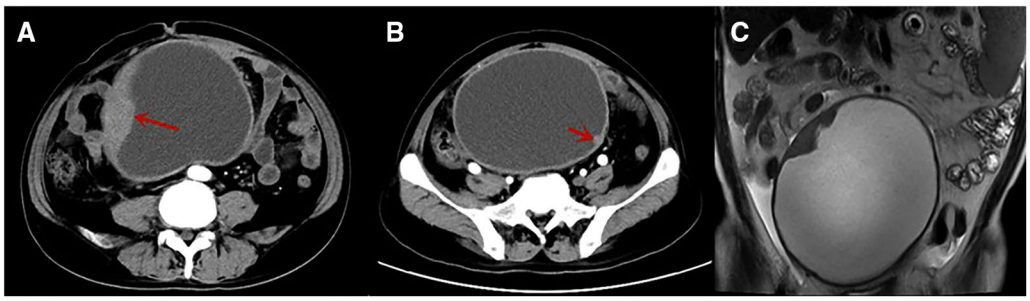


FIGURE 1
Ct scan showing a large cystic tumor in the lower abdomen with an unevenly thickened cystic wall, the solid component of the tumor (red arrow, A), and mural nodules (red arrow, B) with enhancement in the arterial phase. MRI revealed a large cystic tumor with an internal fluid signal (C). CT, computed tomography; MRI, magnetic resonance imaging.

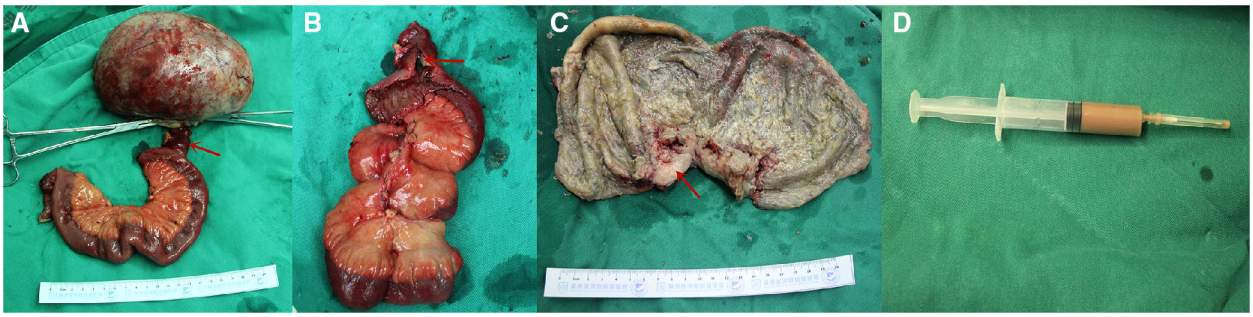


FIGURE 2
Intraoperative photograph showing a large cystic tumor arising from the ileum (A), communicating with the ileum *via* a small intestinal fistula (red arrow, A,B). The red arrow indicates the thickening of the cystic wall, which was the solid component of the tumor (red arrow, C). The last photo shows pus within the tumor (D).

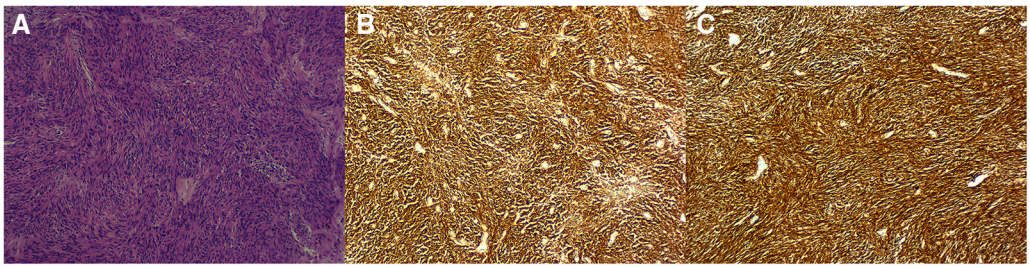


FIGURE 3
Hematoxylin and eosin staining showing a large number of spindle cells (10 × 10, A). Immunohistochemical staining showing tumor cells positive for c-kit (B) and DOG-1 (C).

intestine than in gastric GISTs (13). GIST-related fistulas and intratumoral abscesses are rare. Previous studies have suggested that the mechanism of intratumoral abscess formation comprises enteric bacteria entering the tumor cavity through the tumor-small intestinal fistula, which occurs due to GISTs' propensity to cause mucosal ulceration or defects, and eventually develops into an intratumoral abscess (5, 6, 14). There have been case reports of bacteremia and pyogenic liver abscesses resulting from enteric bacteria entering systemic circulation through the portal vein (14, 15). However, the present case had no typical features, such as a previously reported abdominal abscess or hyperpyrexia, severe abdominal pain, air-fluid level on imaging, and other indications for emergency surgery (5–7). He only had a mild elevation of inflammatory markers; therefore, it was referred to

as an "atypical abscess." We speculate that the patient was in the early stage of the disease without bacteremia or infection due to gas-producing bacteria.

CT or MRI is of great significance in diagnosing cGISTs. cGISTs usually demonstrated as an exophytic, well-defined, low-density mass with peripheral enhancement on contrast imaging (9).Tumor calcification was observed in 22% of patients, and tumor-related complications, such as tumor-bowel fistula, bowel obstruction, and intraperitoneal rupture, were observed in 32% of patients (16). However, CT or MRI is insufficient for preoperative diagnosis, especially for cGISTs. In addition, it is difficult to differentiate it from other cystic diseases such as duplication cysts, mucin-producing tumors, pancreatic pseudocysts, and cystic lymphangiomas. $^{18}$F-fluorodeoxyglucose positron emission tomography ($^{18}$FDG-PET) can be helpful in differentiating malignancy and ruling out metastatic disease as well as monitoring response to molecularly targeted therapy. Moreover, $^{18}$FDG-PET is more sensitive for the assessment of early therapy response than morphologic imaging modalities (17).

A recent systematic review and a retrospective cohort study showed diagnostic biopsies are safe procedures, with a very low risk of needle tract seeding and without an increase in local recurrence rates (18, 19). Endoscopic ultrasound-guided fine-needle aspiration (EUS-FNA) may provide an opportunity for preoperative pathological diagnosis of gastric cGISTs (20, 21). However, the safety for SB cGISTs needed to be further studied, especially for giant cystic lesions.

Histological examinations, immunohistochemical features and mutational analysis are useful for the final diagnosis of GISTs. Histologically, the most common cell morphology was the spindle cell type (86%), followed by the epithelial type (5%), and mixed type (9%). Immunohistochemical tests indicated that KIT, CD34, SMA, S-100, and desmin expression rates were 98%, 40%, 34%, 14%, and 0.2%, respectively (22). Mutational analysis showed that KIT mutations are present in 75% of GISTs, whereas 10% have platelet-derived growth factor receptor alpha mutations (23).

Surgical resection and imatinib are the most effective treatment for primary GISTs. For cGISTs, high attention should be paid intraoperatively to avoid abdominal dissemination due to tumor rupture. Partial resection of the ileum along with the tumor is the standard procedure for ileal cGISTs and lymphadenectomy should not be routinely performed if there is no evidence of lymph node metastasis. It is well accepted patients with high-risk features had prolonged overall survival (OS) with adjuvant imatinib (24). However, a previous study showed that oncologists tend to frequently underestimate the risk of GIST recurrence after initial tumor resection, especially in patients with intermediate tumor size (6–10 cm), intermediate-level mitotic count (6–10/50 HPF), and non-gastric origin, which affects the duration of postoperative adjuvant therapy and recurrence-free survival (25). In addition, preoperative imatinib therapy can effectively prevent tumor rupture and reduce post-surgical complication as well as improve prognosis for large GIST patients (26, 27). Therefore, for resectable cases of GISTs, accurate assessment of post-resection risk, standardized adjuvant/neoadjuvant therapy, and follow-up are crucial to improve prognosis and reduce postoperative recurrence.

## Conclusion

We present the case of a large cGIST located in the ileum with an intratumoral abscess diagnosed through histopathology after surgical excision. For intraperitoneal cystic lesions, especially those suspected to originate from the gut, the possibility of a GIST should be considered before surgery. We have shared our clinical experience to help guide the management of similar cases.

## Data availability statement

The original contributions presented in the study are included in the article/Supplementary Material, further inquiries can be directed to the corresponding author/s.

## Ethics statement

Written informed consent was obtained from the individual(s) for the publication of any potentially identifiable images or data included in this article.

## Author contributions

LC: collected the case data and wrote the manuscript. JG: prepared the photos. AY: guided article writing, and XZ and AY proofread the manuscript. All authors contributed to the article and approved the submitted version.

## Funding

This research was funded by the Natural Science Foundation of Hebei Province (grant no. H2021406047) and the Science and Technology Research and Development Program of Chengde City (grant no. 202006A087).

## Acknowledgments

We are thankful to Zhendong Cao of the Radiology Department for providing imaging data and Yang

Zhao of the Pathology Department for providing pathological images.

## Conflict of interest

The authors declare that the research was conducted in the absence of any commercial or financial relationships that could be construed as a potential conflict of interest.

## Publisher's note



## References

1. Miettinen M, Lasota J. Gastrointestinal stromal tumors: review on morphology, molecular pathology, prognosis, and differential diagnosis. *Arch Pathol Lab Med*. (2006) 130:1466–78. doi: 10.5858/2006-130-1466-GSTROM

2. Søreide K, Sandvik OM, Søreide JA, Giljaca V, Jureckova A, Bulusu VR. Global epidemiology of gastrointestinal stromal tumours (GIST): a systematic review of population-based cohort studies. *Cancer Epidemiol*. (2016) 40:39–46. doi: 10.1016/j.canep.2015.10.031

3. Nishida T, Goto O, Raut CP, Yahagi N. Diagnostic and treatment strategy for small gastrointestinal stromal tumors. *Cancer*. (2016) 122:3110–8. doi: 10.1002/cncr.30239

4. Qu H, Xu Z, Ren Y, Gong Z, Ju RH, Zhang F, et al. The analysis of prognostic factors of primary small intestinal gastrointestinal stromal tumors with R0 resection: a single-center retrospective study. *Med*. (2022) 101:e29487. doi: 10.1097/MD.0000000000029487

5. Rubini P, Tartamella F. Primary gastrointestinal stromal tumour of the ileum preoperatively diagnosed as an abdominal abscess. *Mol Clin Oncol*. (2016) 5:596–8. doi: 10.3892/mco.2016.1009

6. Ito S, Tsuchitani Y, Kim Y, Hashimoto S, Miura Y, Uemura T, et al. A gastrointestinal stromal tumor of the jejunum presenting with an intratumoral abscess: a case report and a literature review. *Int J Surg Case Rep*. (2018) 48:65–8. doi: 10.1016/j.ijscr.2018.05.012

7. Ballati A, Essaidi Z, El Attar L, Errguibi D, Hajri A, Boufettal R, et al. A gastrointestinal stromal tumor of stomach presenting with an intratumoral abscess: a case report. *Ann Med Surg*. (2021) 63:102143. doi: 10.1016/j.amsu.2021.01.091

8. Riley DS, Barber MS, Kienle GS, Aronson JK, von Schoen-Angerer T, Tugwell P, et al. CARE Guidelines for case reports: explanation and elaboration document. *J Clin Epi*. (2017) 89:218–35. doi: 10.1016/jclinepi.2017.04.026

9. Xue A, Yuan W, Gao X, Fang Y, Shu P, Xu C, et al. Gastrointestinal stromal tumors (GISTs) with remarkable cystic change: a specific subtype of GISTs with relatively indolent behaviors and favorable prognoses. *J Cancer Res Clin Oncol*. (2019) 145:1559–68. doi: 10.1007/s00432-019-02853-y

10. Miettinen M, Sobin LH, Lasota J. Gastrointestinal stromal tumors of the stomach: a clinicopathologic, immunohistochemical, and molecular genetic study of 1765 cases with long-term follow-up. *Am J Surg Pathol*. (2005) 29:52–68. doi: 10.1097/01.pas.0000146010.92933.de

11. Bechtold RE, Chen MY, Stanton CA, Savage PD, Levine EA. Cystic changes in hepatic and peritoneal metastases from gastrointestinal stromal tumors treated with Gleevec. *Abdom Imaging*. (2003) 28:808–14. doi: 10.1007/s00261-003-0021-2

12. Feng F, Wang F, Wang Q, Zheng G, Xu G, Liu S, et al. Clinicopathological features and prognosis of gastrointestinal stromal tumor located in the jejunum and ileum. *Dig Surg*. (2019) 36:153–7. doi: 10.1159/000487147

13. Sorour MA, Kassem MI, Ghazal A-H, El-Riwini MT, Abu Nasr A. Gastrointestinal stromal tumors (GIST) related emergencies. *Int J Surg*. (2014) 12:269–80. doi: 10.1016/j.ijsu.2014.02.004

14. Gorelik M, Sabates B, Elkbuli A, Dunne T. Ileal GIST presenting with bacteremia and liver abscess: a case report and review of literature. *Int J Surg Case Rep*. (2018) 42:261–5. doi: 10.1016/j.ijscr.2017.12.033

15. Kim BH, Lee JH, du Baik du S, Yun SW, Kim JH, Kong JH, et al. A case of malignant gastrointestinal stromal tumor of ileum with liver abscess. *Korean J Gastroenterol*. (2007) 50:393–7. PMID: 18159178

16. Baheti AD, Shinagare AB, O'Neill AC, Krajewski KM, Hornick JL, George S, et al. MDCT And clinicopathological features of small bowel gastrointestinal stromal tumours in 102 patients: a single institute experience. *Br J Radiol*. (2015) 88:20150085. doi: 10.1259/bjr.20150085

17. Dimitrakopoulou-Strauss A, Ronellenfitsch U, Cheng C, Pan L, Sachpekidis C, Hohenberger P, et al. Imaging therapy response of gastrointestinal stromal tumors (GIST) with FDG PET, CT and MRI: a systematic review. *Clin Transl Imaging*. (2017) 5(3):183–97. doi: 10.1007/s40336-017-0229-8

18. Jakob J, Salameh R, Wichmann D, Charalambous N, Zygmunt AC, Kreisel I, et al. Needle tract seeding and abdominal recurrence following pre-treatment biopsy of gastrointestinal stromal tumors (GIST): results of a systematic review. *BMC Surg*. (2022) 22:202. doi: 10.1186/s12893-022-01648-2

19. van Houdt WJ, IJzerman NS, Marjolein Schrijver A, Huis In 't Veld E, Thway K, Jones RL, et al. Oncological outcome after diagnostic biopsies in gastrointestinal stromal tumors: a retrospective cohort study. *Ann Surg*. (2021) 274(6):e1093–8. doi: 10.1097/SLA.0000000000003744

20. Takahashi K, Nihei T, Aoki Y, Konno N, Nakagawa M, Munakata A, et al. Gastric gastrointestinal stromal tumor with predominant cystic formation diagnosed by endoscopic ultrasound-fine needle aspiration. *Clin J Gastroenterol*. (2020) 13:359–64. doi: 10.1007/s12328-019-01058-7

21. Mangiavillano B, Chiari D, Auriemma F, Repici A. A rare case of cystic gastrointestinal stromal tumor and the crucial role of EUS-FNB (with video). *Dig Liver Dis*. (2021) 53(1):129–30. doi: 10.1016/j.dld.2020.05.028

22. Miettinen M, Makhlouf H, Sobin LH, Lasota J. Gastrointestinal stromal tumors of the jejunum and ileum: a clinicopathologic, immunohistochemical, and molecular genetic study of 906 cases before imatinib with long-term follow-up. *Am J Surg Pathol*. (2006) 30:477–89. doi: 10.1097/00000478-200604000-00008

23. Joensuu H, DeMatteo RP. The management of gastrointestinal stromal tumors: a model for targeted and multidisciplinary therapy of malignancy. *Annu Rev Med*. (2012) 63:247–58. doi: 10.1146/annurev-med-043010-091813

24. Cavnar MJ, Seier K, Curtin C, Balachandran VP, Coit DG, Yoon SS, et al. Outcome of 1000 patients with gastrointestinal stromal tumor (GIST) treated by surgery in the pre- and post- imatinib eras. *Ann Surg*. (2021) 273(1):128–38. doi: 10.1097/SLA.0000000000003277

25. Guérin A, Sasane M, Keir CH, Gauthier G, Macalalad AR, Wu EQ, et al. Physician underestimation of the risk of gastrointestinal stromal tumor recurrence after resection. *JAMA Oncol*. (2015) 1:797–805. doi: 10.1001/jamaoncol.2015.2407

26. Tang S, Yin Y, Shen C, Chen J, Yin X, Zhang B, et al. Preoperative imatinib mesylate (IM) for huge gastrointestinal stromal tumors (GIST). *World J Surg Oncol*. (2017) 15(1):79. doi: 10.1186/s12957-017-1143-2

27. Yang H, Shen C, Yin X, Cai Z, Wang Q, Zhang B. Clinicopathological features, clinical efficacy on 101 cases of rectal gastrointestinal stromal tumors, and the significance of neoadjuvant therapy. *BMC Surg*. (2021) 21(1):400. doi: 10.1186/s12893-021-01397-8

frontiers | Frontiers in Surgery

TYPE Case Report
PUBLISHED 06 January 2023
DOI 10.3389/fsurg.2022.1010050



OPEN ACCESS

EDITED BY
Riccardo Bertolo,
Hospital San Carlo di Nancy, Italy

REVIEWED BY
Nguyen Minh Duc,
Pham Ngoc Thach University of Medicine, Vietnam
Ilker Sengul,
Giresun University, Turkey

*CORRESPONDENCE
Junrong Zou
ydzjr@gmu.edu.cn
Quanliang Liu
liuquanliang2008@163.com

†These authors share first authorship

SPECIALTY SECTION
This article was submitted to Surgical Oncology, a section of the journal Frontiers in Surgery

RECEIVED 02 August 2022
ACCEPTED 07 November 2022
PUBLISHED 06 January 2023

CITATION
Yan S, Zou Y, Liao X, Zhong C, Liu S, Huang S, Zou J and Liu Q (2023) Giant superficial angiomyxoma of the male perineum: A case report.
Front. Surg. 9:1010050.
doi: 10.3389/fsurg.2022.1010050



# Giant superficial angiomyxoma of the male perineum: A case report

Sheng Yan[1†], Yuhua Zou[1†], Xinzhi Liao[1], Cunzhi Zhong[2], Shengyin Liu[1], Sigen Huang[1], Junrong Zou[3*] and Quanliang Liu[1*]

[1]Department of Urology, The First Affiliated Hospital of Gannan Medical University, Ganzhou, China, [2]Department of Anesthesiology, Operation Room, The First Affiliated Hospital of Gannan Medical University, Ganzhou, China, [3]Institute of Urology, Gannan Medical University, Ganzhou, China

Superficial angiomyxoma (SA) is a rare benign tumor that occurs either in the superficial dermis or subcutaneously. It often occurs in the trunk, neck, or limbs, and grows slowly. The diameter of the tumor is usually less than 5 cm. A giant SA of the perineum in men is very rare. We detailed the diagnosis and treatment of male patients with perineal SA and performed a literature review. We report a case of a 42-year-old male patient. He was admitted to hospital with a perineal mass found more than 1 year previously. A pelvic contrast-enhanced computed tomography scan in our hospital suggests that a round slightly hypointense foci of about 6.0 cm × 8.6 cm × 4.5 cm in size with still clear borders was seen below the penile corpus cavernosum in the perineum. We performed a perineal mass excision under continuous epidural anesthesia. A postoperative pathology report diagnosed perineal SA. There was no recurrence at follow-up for 27 months up to May 2022. Perineal SA is rare and should be combined with patient history and imaging to ensure complete excision of the mass margins. Adherence to long-term postoperative follow-up is the key to curing this case.

KEYWORDS
superficial angiomyxoma, perineal tumor, case report, surgical removal, clinical pathology

## Introduction

Superficial angiomyxoma (SA), also known as a cutaneous mucinous tumor, is a rare benign soft tissue tumor of the skin. SA was first reported by Carney et al. in 1985, with an incidence in the range of 0.008%–3% (1). Most SAs are isolated and can manifest themselves in association with Carney syndrome (2), which includes mucinous tumors, patchy skin pigmentation, and endocrine hyperfunctional disorders. Preoperative imaging examination has a certain significance for the estimation of tumor range and prognosis. However, imaging lacks typical features and a diagnosis is often made definitively by pathology. A giant SA in the perineum is extremely rare, and we report this case with the aim of providing a reference experience for clinical management.

## Case presentation

A male patient aged 42 years was admitted to the hospital after "finding a perineal mass for more than 1 year." The patient complained that he found a mass the size of peanut rice in the perineum 1 year previously, without tenderness and discomfort from ulceration. At that time, he did not pay attention to it, and the mass then gradually increased. A color Doppler ultrasound in the local hospital showed a slightly hypoechoic mass in the perineum, which was not treated at that time. During the physical examination, a hard and fixed mass of about 8.5 cm × 6 cm was palpable in the patient's perineum.

To understand the nature, blood supply, and anatomical location of the mass, a contrast-enhanced computed tomography (CE-CT) scan of the pelvis was performed. A round slightly hypointense foci of about 6.0 cm × 8.6 cm × 4.5 cm in size with still clear borders was seen below the penile corpus cavernosum in the perineum (Figure 1A), with a CT value of approximately 17 HU. During the arterial phase of enhanced scanning, an arterial vessel was seen (Figure 1B). The enhancement of the lesion was not obvious, and uneven enhancement was seen in the venous phase (Figure 1C), with a CT value of approximately 31 HU. The prostate was small, the edge was smooth, and the density in the parenchyma was uniform. The shape, size, and density of the seminal vesicle gland were normal. The bladder was well filled. The bladder wall was smooth, without thickening or nodule protrusion. The bladder seminal vesicle angle was normal. There was no effusion or enlarged lymph nodes in the pelvic cavity. Initially, a large benign tumor in the perineum was considered, but the type of tumor was not yet clear. In the past, the patient had been in good health. No abnormality was found in his chest x-ray, ECG, or routine biochemical examination after admission.

After communicating with the patient, he underwent a perineal mass resection under continuous epidural anesthesia. A lithotomy position and indwelling catheterization were used. A vertical incision was made in the middle of the lower

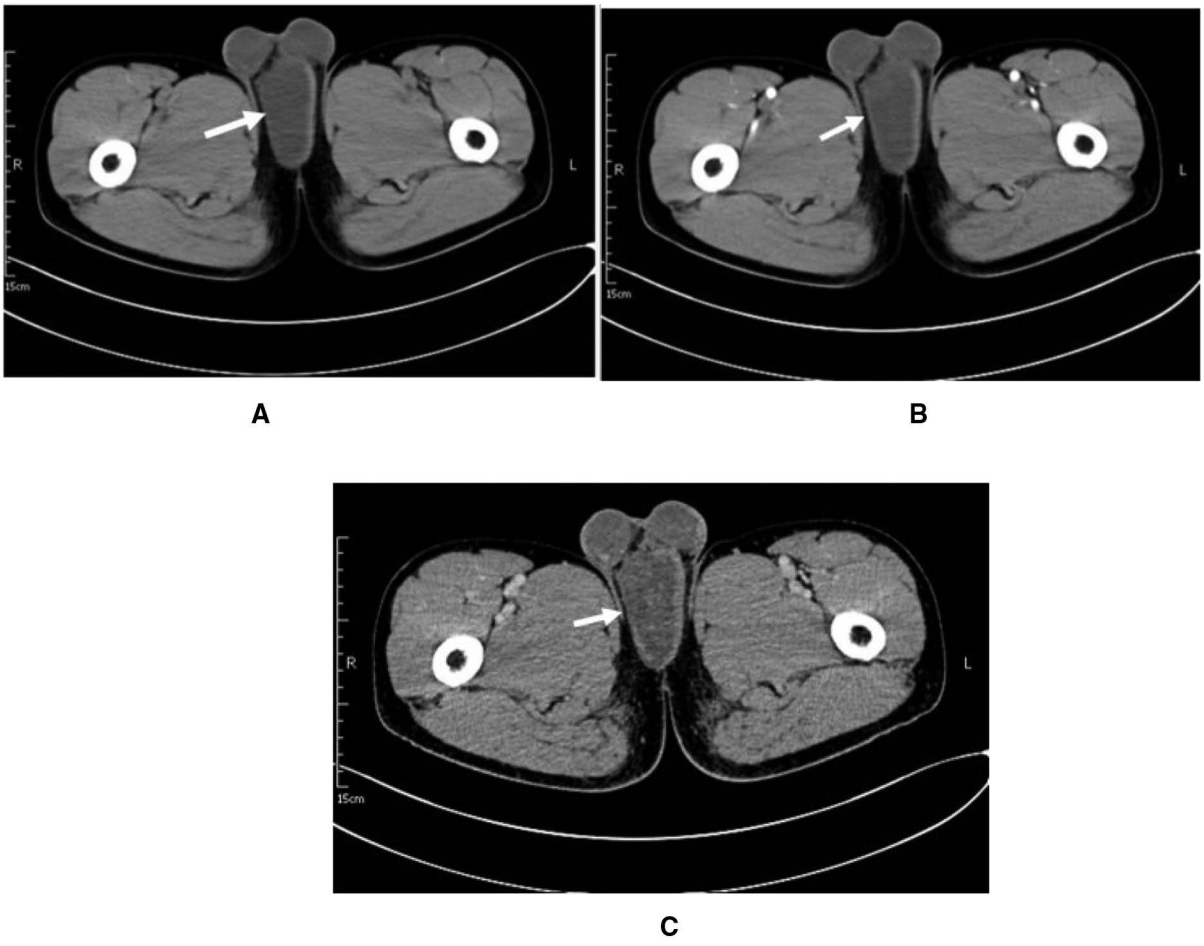


FIGURE 1
Patient imaging data. (A) CT plain axial image.(B) Arterial phase of the contrast. (C) Venous phase of the contrast.

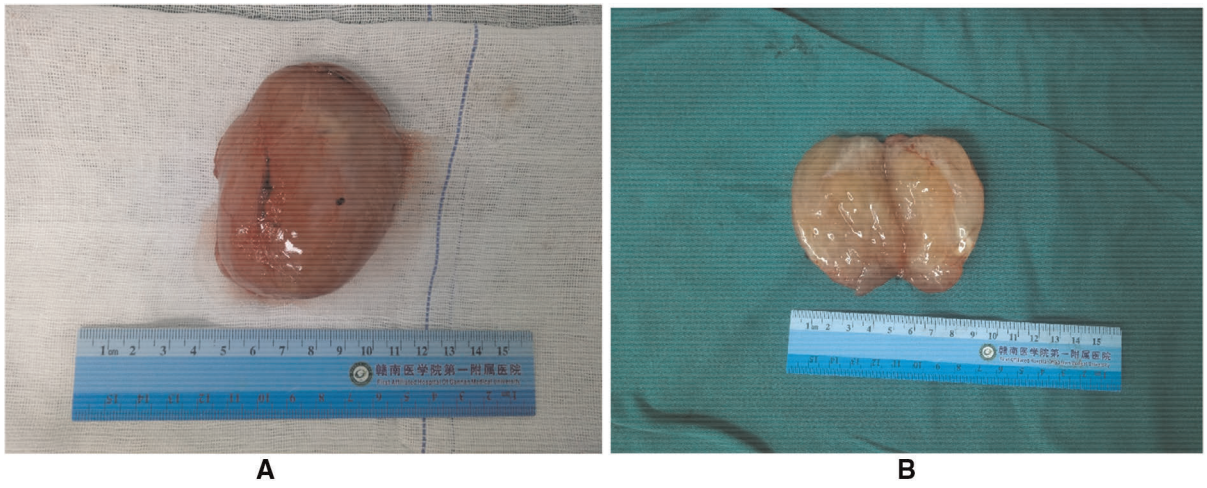


FIGURE 2
Patient tumor specimen. (A) The excised specimen was approximately 8.5 cm × 6 cm × 5 cm with clear margins. (B) The surface is grayish white, jelly-like, rubber-like.

part of the scrotum. After cutting into the superficial perineal muscle layer, the tumor capsule could be seen, which was free along the tumor capsule. The tumor was close to the urethral cavernous body above the tumor, and there were tumor nutrient vessels on the inner side. After carefully ligating the vessels, the tumor was completely removed and observed. The size of the tumor was approximately 8.5 cm × 6 cm × 5 cm in size (**Figure 2A**); the specimen was soft. The surface was off-white, jelly-like, and rubbery after cutting (**Figure 2B**). The pathological report from our hospital shows that under the microscope, there were abundant interstitial mucus, fibroblasts, more thin-walled vascular hyperplasia, and no epithelial cells (**Figure 3**). Based on these pathological findings, the diagnosis of perineal SA was confirmed. The patient recovered successfully and was discharged on the fourth postoperative day, and is still being followed up with no recurrence, and he expressed great satisfaction with the surgical treatment.

## Discussion

SA is a rare benign skin tumor, which is considered a special type of soft tissue tumor. They are difficult to diagnose because they lack unique features like fibroepithelial polyps (3). In recent years, SA has been clearly defined as an isolated soft tissue tumor entity. They can occur anywhere in superficial tissue and are painless (4), slow-growing masses. Allen et al. first reported 28 cases of SA in 1988 and named it superficial vascular mucinous adenoma (5). The clinical manifestations are mainly skin papules, nodular or polypoid masses, no pain, and a wave motion on palpation. The skin color on the surface is normal and mostly single lesion (6). In 2002, the World Health Organization classified SA as a benign tumor with undetermined differentiation (6). SA is rare in clinic and has not been reported in a large sample volume. At present, more than 30 cases have been reported in China. There is no significant gender difference in the incidence population, and the incidence is slightly higher in men than in women (4). The peak incidence is at the age of 40 years approximately (7). The disease can occur throughout the body (4, 8), mainly in the trunk, extremities, head and neck, and rarely in the perineum and vulva (3, 9). This case is a middle-aged man with a giant tumor in the perineum, which is rare.

Similar to other interstitial masses in the perineum, SAs are cystic in nature and are easily misdiagnosed as polyps or epidermoid cysts during physical examination (10). The surface of the SA is covered with epithelial tissue. It has a white, gray appearance, with occasional bleeding due to skin abrasion. It is an enveloped, soft, lobulated cystic tissue. The cut surface of the mass is shiny, colloid-like, translucent, gel-like tissue (2). The same is true for the surface of the mass incision in this case. Its pathogenesis is not yet clear. SAs may be sporadic or related to Carney syndrome, which is an autosomal dominant syndrome characterized by cardiac and mucosal skin myxoma, skin pigmentation, and a variety of endocrine gland hyperthyroidism (mainly endocrine adenoma) (11). This case is an isolated perineal SA in a man. No cardiac myxoma or other endocrine abnormalities were found during the preoperative examination.

The preoperative diagnosis of SA is difficult, and imaging helps to clarify the relationship between the SA and the surrounding tissues. On ultrasound, the SA appears as a confined round or oval mass with heterogeneous internal

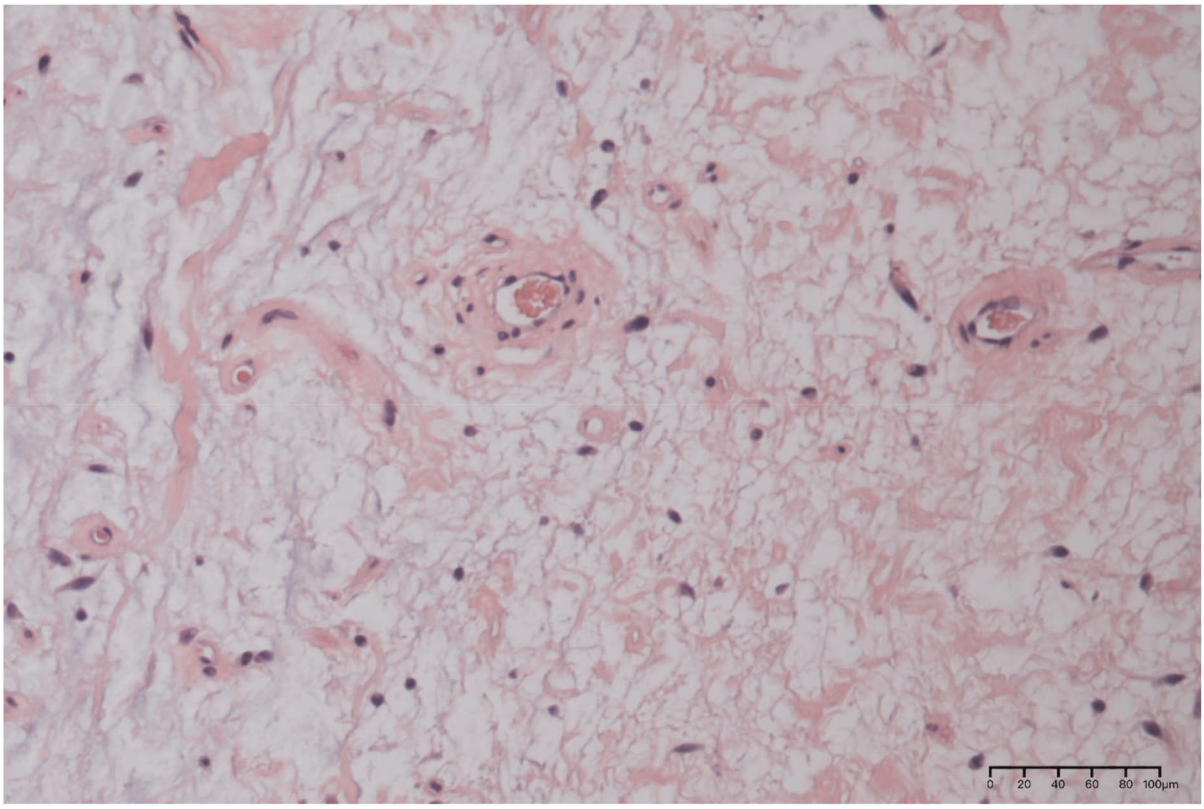


FIGURE 3
Pathological histological section of this case (HE × 200). Scattered spindle cells, stellate cells and perivascular inflammatory cells are visible against the background of a large amount of mucus stroma microscopically.

echogenicity. The CT/magnetic resonance imaging (MRI) scan of SA mostly shows a rounded/lobular soft tissue mass with well-defined borders and superficial lesions, with hypodense/low signal foci without significant enhancement. Its substance is the mucus-rich stromal component of the tumor. The separation of collagen bundles is also seen, showing isointensity (CT)/low signal (MRI). The literature reports a slightly dense or mixed signal with focal hemorrhage (12).

Clinically, SA usually has good boundaries and often extend to subcutaneous fat (12). Histologically, SA has an extensive mucus stroma consisting of loose spindle or stellate fibroblast-like lobular aggregates with an abundant mucus stroma containing thin-walled, medium-sized, hyaline vessels in a disorganized arrangement (13). The nuclei are ovoid, slightly darkly stained or vesicular, with inconspicuous nucleoli, no obvious heterogeneity, and rare nuclear division. In addition, a small number of inflammatory cells, mainly lymphocytes, neutrophils, and eosinophils, can be seen (14, 15). The presence of neutrophils can be a diagnostic clue, especially in the absence of skin ulceration or inflammation, as neutrophils are not present in other mucinous lesions of the skin. SA should be distinguished from all malignant and benign myxoid tumors on the surface, including aggressive angiomyxoma, myxoid neurofibroma, dermal nerve sheath myxoma, and low-grade fibromyxoid sarcoma.

Complete surgical excision is the best treatment for superficial hemangio mucinous tumors. Although SA is a benign tumor of the skin, there is a 30%–40% chance of local recurrence after surgery due to incomplete excision or blurred margins (16). A regular review and close follow-up should be done after surgery. No distant metastasis or malignancy has been reported so far (17).

## Conclusions

The incidence of SA is low and the clinical presentation lacks specificity, but SA should be considered when painless pelvic and perineal swellings without other features are found in young and middle-aged men. A pathological examination is the gold standard for diagnosing this disease. However, the relationship between the mass and the surrounding tissues and whether it invades deep tissues can be clarified by ultrasound, MRI, and CT auxiliary examination, which is a

reliable guide for judging the benignity and malignancy of the tumor and its prognosis. Extensive surgical excision is currently the main method of treatment, ensuring that the edges of the mass are removed intact to avoid postoperative recurrence. Although SA has a good prognosis, patients still need to be informed of regular follow-ups.

## Data availability statement

The raw data supporting the conclusions of this article will be made available by the authors, without undue reservation.

## Ethics statement

Written informed consent was obtained from the individual (s) for the publication of any potentially identifiable images or data included in this article.

## Author contributions

SY prepared and wrote the article. YZ was directly involved in the management of the patients. XL, SL, and SH were responsible for the collection and organization of the literature. CZZ prepared the intraoperative images. QL and JZ revised the manuscript and acted as corresponding authors. QL and YZ were the primary surgeons. All authors contributed to the article and approved the submitted version.

## Acknowledgments

We would like to thank QL for his guidance on this paper and for editing and proofreading this manuscript in English.

## Conflict of interest

The authors declare that the research was conducted in the absence of any commercial or financial relationships that could be construed as a potential conflict of interest.

## Publisher's note

All claims expressed in this article are solely those of the authors and do not necessarily represent those of their affiliated organizations, or those of the publisher, the editors and the reviewers. Any product that may be evaluated in this article, or claim that may be made by its manufacturer, is not guaranteed or endorsed by the publisher.

## References

1. Carney JA, Gordon H, Carpenter PC, Shenoy BV, Go VL. The complex of myxomas, spotty pigmentation, and endocrine overactivity. *Medicine (Baltimore)*. (1985) 64(4):270–83. doi: 10.1097/00005792-198507000-00007

2. Allen PW. Myxoma is not a single entity: a review of the concept of myxoma. *Ann Diagn Pathol*. (2000) 4(2):99–123. doi: 10.1016/s1092-9134(00)90019-4

3. Lee SH, Cho YJ, Han M, Bae JW, Park JW, Oh SR, et al. Superficial angiomyxoma of the vulva in a postmenopausal woman: a case report and review of literature. *J Menopausal Med*. (2016) 22(3):180–3. doi: 10.6118/jmm.2016.22.3.180

4. Calonje E, Guerin D, McCormick D, Fletcher CD. Superficial angiomyxoma: clinicopathologic analysis of a series of distinctive but poorly recognized cutaneous tumors with tendency for recurrence. *Am J Surg Pathol*. (1999) 23(8):910–7. doi: 10.1097/00000478-199908000-00008

5. Allen PW, Dymock RB, MacCormac LB. Superficial angiomyxomas with and without epithelial components. Report of 30 tumors in 28 patients. *Am J Surg Pathol*. (1988) 12(7):519–30. doi: 10.1097/00000478-198807000-00003

6. Murphey MD. World Health Organization classification of bone and soft tissue tumors: modifications and implications for radiologists. *Semin Musculoskelet Radiol*. (2007) 11(3):201–14. doi: 10.1055/s-2008-1038310

7. Kura MM, Jindal SR. Solitary superficial acral angiomyxoma: an infrequently reported soft tissue tumor. *Indian J Dermatol*. (2014) 59(5):529. doi: 10.4103/0019-5154.139893

8. Anehosur V, Adirajaiah S, Ghosh R. Intraoral superficial angiomyxoma: a case report. *J Maxillofac Oral Surg*. (2016) 15(Suppl 2):371–4. doi: 10.1007/s12663-016-0901-y

9. Wang YC, Li XM, Zhong GP, Xing Z, Wang ZP. Superficial angiomyxoma of penis: a case report of a 6-year follow-up. *Asian J Androl*. (2017) 19(2):262–3. doi: 10.4103/1008-682x.175784

10. Satter EK. Solitary superficial angiomyxoma: an infrequent but distinct soft tissue tumor. *J Cutan Pathol*. (2009) 36(Suppl 1):56–9. doi: 10.1111/j.1600-0560.2008.01216.x

11. Yun YI, Lee KS, Khwarg SI, Kim N. Rare case of isolated superficial angiomyxoma of the eyelid. *Korean J Ophthalmol*. (2020) 34(3):262–4. doi: 10.3341/kjo.2020.0010

12. Kim HS, Kim GY, Lim SJ, Ki KD, Kim HC. Giant superficial angiomyxoma of the vulva: a case report and review of the literature. *J Cutan Pathol*. (2010) 37(6):672–7. doi: 10.1111/j.1600-0560.2009.01333.x

13. Aberdein G, Veitch D, Perrett C. Mohs micrographic surgery for the treatment of superficial angiomyxoma. *Dermatol Surg*. (2016) 42(8):1014–6. doi: 10.1097/dss.0000000000000782

14. Hamzelou S, Ghanadan A, Daneshpazhooh M, Kiani A, Mahmoudi H. Superficial plantar angiomyxoma in a young man. *Australas J Dermatol*. (2017) 58(3):241–2. doi: 10.1111/ajd.12523

15. Zhu L, Zhao W, Shi Y, Lin B. Superficial angiomyxoma of the vulva complicated with condyloma acuminatum and Staphylococcus hominis infection. *Int J Dermatol*. (2014) 53(6):756–8. doi: 10.1111/j.1365-4632.2012.05572.x

16. Lee CU, Park SB, Lee JB, Park HJ, Kim MK, Chang IH. Sonographic findings of prescrotal superficial angiomyxoma. *Jpn J Radiol*. (2015) 33(4):216–9. doi: 10.1007/s11604-015-0395-4

17. Toth A, Nemeth T, Szucs A, Szollosi Z, Sziklai I. Retropharyngeal superficial angiomyxoma. *J Laryngol Otol*. (2010) 124(9):1017–20. doi: 10.1017/s002221510999274x

frontiers | Frontiers in Surgery

TYPE Case Report
PUBLISHED 06 January 2023
DOI 10.3389/fsurg.2022.1053852



OPEN ACCESS

EDITED BY
Zhaolun Cai,
Sichuan University, China

REVIEWED BY
Scott Leslie,
Royal Prince Alfred Hospital, Australia
Ioannis Sokolakis,
Martha-Maria Hospital Nuremberg, Germany

*CORRESPONDENCE
Chunyang Wang
wangchunyang001@hotmail.com

†These authors have contributed equally to this work and share first authorship

SPECIALTY SECTION
This article was submitted to Surgical Oncology, a section of the journal Frontiers in Surgery

RECEIVED 26 September 2022
ACCEPTED 07 November 2022
PUBLISHED 06 January 2023

CITATION
Ning Z, Zhang H, Wang B, Wang Y, Liu Y, Tao B, Zhang G, Liu H and Wang C (2023) Case report and literature review: Robot-assisted laparoscopic left renal mucinous cystadenocarcinoma radical nephrectomy. Front. Surg. 9:1053852. doi: 10.3389/fsurg.2022.1053852



# Case report and literature review: Robot-assisted laparoscopic left renal mucinous cystadenocarcinoma radical nephrectomy

Zikuan Ning[1†], Haoxun Zhang[1†], Bowen Wang[1], Yingwei Wang[2], Yiwen Liu[1], Boju Tao[1], Guoling Zhang[1], Hua Liu[1] and Chunyang Wang[1*]

[1]Department of Urology Surgery, The First Affiliated Hospital of Harbin Medical University, Harbin, China, [2]Department of Pathology, The First Affiliated Hospital of Harbin Medical University, Harbin, China

**Background:** Mucinous cystadenocarcinoma (MC) of the kidney is a rare renal epithelial tumor originating from the renal pelvic urothelium. There are only a few published reports on MC. Due to its rare and unknown tissue origin, its diagnosis is difficult which almost can be diagnosed through the pathological method.
**Case presentation:** In this case report, we report a female patient whose chief complaint was low back pain lasting for one month. The three-dimensional computed tomography scan of the urinary system detected approximately 7 cm of a left renal cystic mass. The renal cystic mass was diagnosed as MC after robot-assisted laparoscopic radical nephrectomy. The MC originated from the kidney after completing colorectal adenocarcinoma and ovarian adenocarcinoma.
**Conclusions:** We reported a case of MC of the kidney which was a rare renal tumor. We not only aimed to present an unusual case of MC and review the previous literature on its pathology and differential diagnosis, but also used new method to treat this type of tumor.

KEYWORDS
mucinous, cystadenocarcinoma, kidney, primary, robot-assisted surgery

## Introduction

The MC of the kidney is a rare tumor that accounts for less than 1% of malignant kidney tumors of the renal pelvis (1). However, its origin from the primary kidney is uncommon. Due to its rarity, it cannot be directly diagnosis in lieu of clinical and imaging features. It presents on computed tomography as a cystic renal mass, and a differential diagnosis mostly results in a misdiagnosis. Here, we reported a rare case of the MC of the primary kidney. This is the first case in which a Da Vinci robot was used to radically resect the left renal MC including the ports placement and operative details.

Abbreviations
MC, mucinous cystadenocarcinoma; CT, computed tomography; MRI, magnetic resonance imaging; IHC, immunohistochemistry.

We aimed to report this rare tumor and retrospectively review the pathology, radiology images, and surgery with challenges in cases of misdiagnosis of this type of neoplasm. This case report was reported in agreement with principles of the CARE guidelines (2) and its reporting checklist was as the **supplementary material**.

## Case report

A 46-year-old female patient presented with a complaint of left lower back pain for one month. One month prior, the patient had developed intermittent left lumbago without radiation pain. She had no urinary irritation, hematuria, fever, night sweats, or other uncomfortable feelings. She had a history of transvaginal myomectomy 7 years ago, left lumbar impact injury 9 years ago, and smoking for 10 years. She denied a history of hepatitis, tuberculosis, hypertension, diabetes, and coronary heart disease. There was no percussion pain in the double renal region, and a $6 \times 6$ cm mass in the left abdomen could be deeply palpated. In additional, there was no tenderness in the ureteral area or edema in either lower limb. An auxiliary examination revealed the following. Three-phase enhanced CT of the kidney showed decreased perfusion of the left kidney and a cystic low-density shadow in the left renal hilum, with a CT value of approximately $5 \pm 10$ HU and size of $7.4 \times 7.4$ cm. There were flocculent and high-density shadows in the cyst; however, there was no enhancement in the lesion and slight enhancement in the wall. In addition, the left renal pelvis was dilated, with no abnormal density shadow and a clear perirenal fat space. A small amount of fluid density under the left renal capsule were observed in the images. In general, no significant differences were found in the three-phase enhancement images. No abnormalities were observed in the right kidney. (**Figure 1**) Pulmonary CT findings were as follows. Nodules were observed under the pleura of the upper lobe of the right lung with a diameter of approximately 3 mm, and a punctate high-density shadow was observed in the upper lobe of the right lung. No abnormalities were found in the abdominal aorta, bilateral iliac artery, bilateral iliac vein, or inferior vena cava. On transvaginal three-dimensional ultrasound, cervical echo was found to be non-uniform. Routine blood examination showed no obvious abnormalities; blood, liver, kidney, and blood coagulation function were normal. The urine routine test results were abnormal: the erythrocyte count was 50.7/μl and leukocyte count was 171.8/μl. After comprehensive analysis, the admission diagnosis included a left renal tumor, left renal hydronephrosis, and left renal subcapsular effusion.

After admission to our hospital, perioperative preparation improved, and robot-assisted radical nephrectomy was performed under combined intravenous infusion and inhalation anesthesia. We used the da Vinci Xi surgical system of the fourth generation to perform the radical nephrectomy. The transperitoneal approach was adopted instead of the traditional retroperitoneal access approach to view the large tumor. The patient was placed in a lying position with the right oblique at 45°. The incision was at the lateral border of the left rectus abdominis under the 3 cm of the umbilical horizontal line. By cutting the subcutaneous tissue of the skin layer by layer, the sheath of the rectus abdominis, and the peritoneum, we put the first 8 mm trocar into the abdominal cavity, which connected to the robot's third arm, placing the monopolar curved scissors, with keeping the pneumoperitoneum pressure at the 14 mmHg level. Laparoscopy was inserted and the other trocars were established under direct vision. The second 8 mm trocar was established at the width of the two fingers under the xiphoid process, which connected to the robot's first arm, placing the maryland forceps bipolar. The third 8 mm trocar was established at the equidistant position between the above two trocars, which connected to the robot's second arm, placing

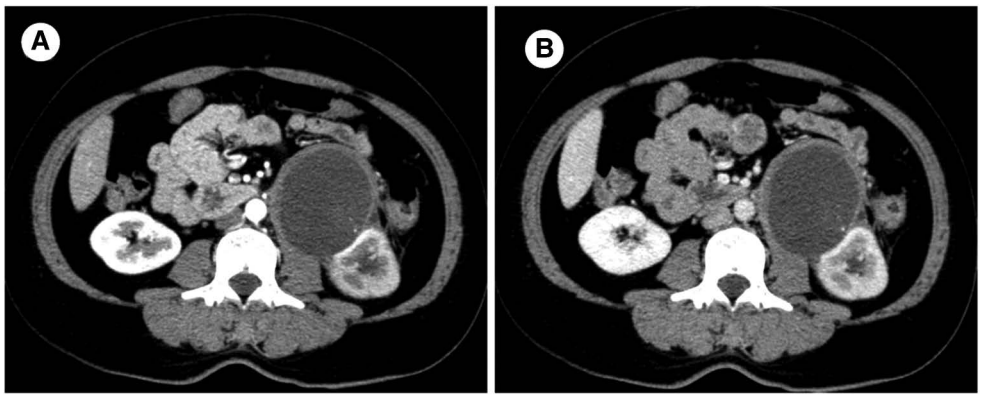


FIGURE 1
Enhanced computed tomography scan: A round low-denisty cystic mass located at the renal helium, measuring $7.4 \times 7.4$ cm in size with a width of 0.5 cm at the wall. (**A**) Arterial phase (**B**) Venous phase.

the laparoscopic lens. The area among the trocars and the operative region was kept as an isosceles triangle. Next, the fourth trocar was established at the position of the 2 cm medial to the iliac crest, which connected to the robot's fourth arm, placing a large needle driver. Finally, we established the fifth 10 mm trocar under the umbilicus as an auxiliary port. (Figure 2C) After examination, it was revealed that approximately 10 cm of the round eminence of the splenic curvature of the colon was protruding into the abdominal cavity. After releasing part of the adhesion, the descending colon adhered to the lateral abdomen, and the left peritoneum was cut along the para-colonic groove. The adhesion between kidney and surrounding tissue was severe, and the adhesion around the tumor was also serious, making it difficult to separate. The nature of the tumor was difficult to judge due to wound bleeding, the unclear relationship between between the tumor and kidney, and serious adhesion of the tumor with the psoas major muscle. Because the possibility of malignancy was high, we performed radical resection of the left kidney, including the tumor and part of the ureter. Dissociating the genital vein, and going upstream along it to the renal hilum, then we saw the renal vein. After using Hem-o-Lok clips to disconnect the genital vein, we then separated the renal vein and dissociated the renal artery in the rear. Next, clipping the renal artery and vein with Hem-o-Lok clips, we dissociated the inferior pole of the kidney to sever the ureter. Finally, with preserving the adrenal gland, the left kidney and tumor was removed completely. In the gross specimen, a mass measuring $7 \times 7$ cm was observed near the hilum of the left kidney and was associated with the ureter. (Figure 2A) After dissection along the vertical axis, there was an outflow of yellowish gelatinous material, and no neoplasm invasion was found in the renal pelvis or ureter. (Figure 2B) During surgery, approximately 800 ml blood was lost; therefore, 400 ml of plasma and 4 U of red blood cells were infused, and no transfusion reaction was observed. Pathology reports revealed that the volume of the left kidney was $11 \times 5 \times 7$ cm, and the volume of the gray-white cystic mass was $7 \times 6 \times 5$ cm at one pole. There was a large amount of mucus in the tumor, which was a focal grayish yellow color, similar to necrosis. There was a local grayish red color around the kidney, and part of the ureter was adherent. The ureter length was 5 cm, and the broken-end diameter was 0.6 cm. Microscopically, a wide range of mucus lakes was observed, in which floating and irregular glands showed large, deep staining of the tumor nucleus and obvious atypia. The image showed mucinous epithelium and a large amount of mucus. (Figure 3F) Immunohistochemical results were as follows: CDX-2(+), Villin(+), CK7(-), CK20(+), CEA(+), MUC2(+), MUC5AC(+), ER(-), PR(-), P16(-), and CA125(-). (Figures 3A–E) Low-grade mucinous adenocarcinoma of the left kidney was pathologically diagnosis; however metastasis

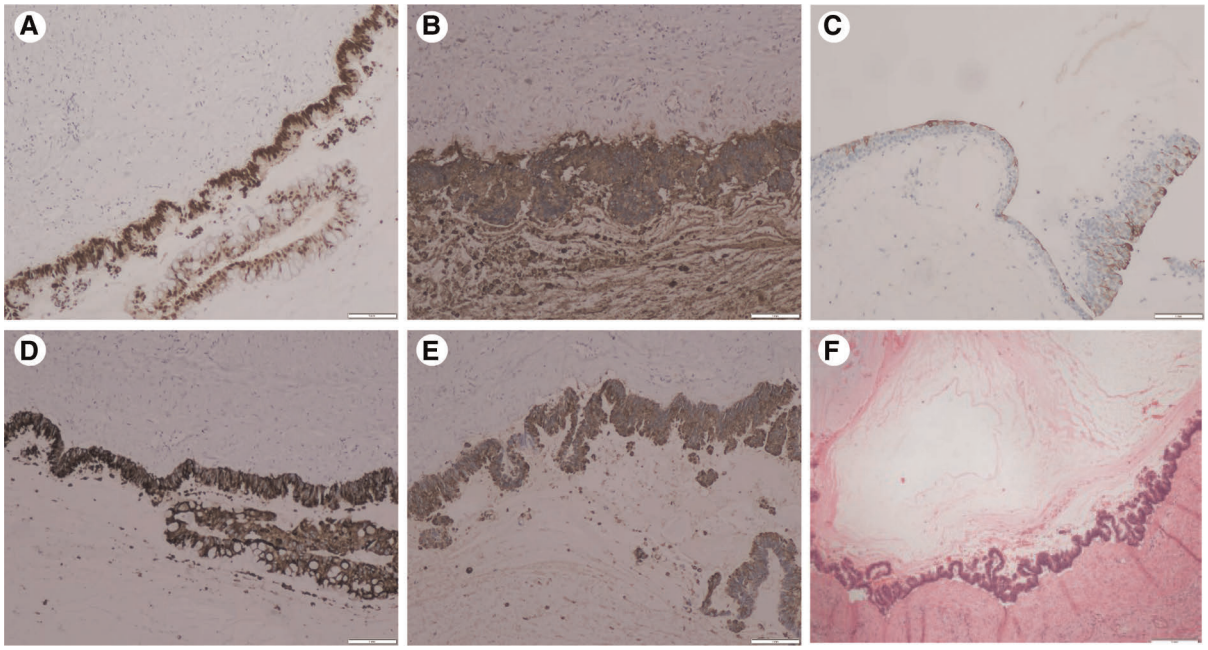


FIGURE 2
Immunohistochemistry results: (A) CDX2(+): diffuse and strong nuclear immunoreactivity for CDX2. (B) CEA(+): diffuse strong staining for the CEA. (C) CK20(+): atypical mucinous epithelium with patchy cytokeratin 20 staining. (D) MUC2(+) and (E) MUC5AC(+): atypical mucinous epithelium with diffuse strong staining for the MUC2 and MUC5AC gene products (×20) (F) pathology: a wide range of mucus lake was observed under the microscope, and the areas of the cyst wall are lined by atypical mucinous epithelium (H&E staining) (×20).

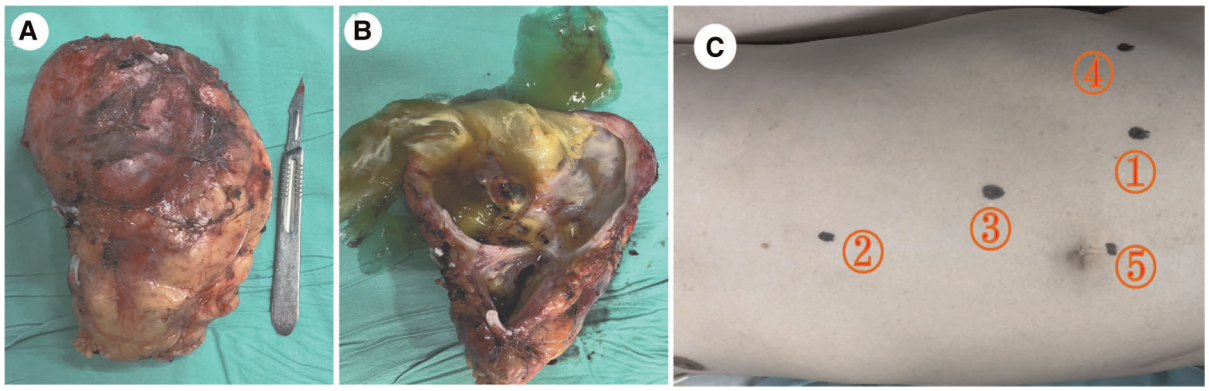


FIGURE 3
Fresh specimen of the left kidney with mass after radical resection. (A) Gross specimen: The tumor was associated with the kidney and located at the inferior pole. (B) Resection along the vertical axis: The tumor has a large amount of mucus with a focal grayish yellow appearance and thin wall. (C) The ports implacement.

was not diagnosed, suggesting the clinical examination of the appendix. No cancer was found at the end of the ureter or vascular end of the renal hilum.

Results of the routine blood examination on the first day after surgery were abnormal: the white blood cell count was $10.5 \times 10^9$/L and percentage of neutrophils was 85.9%. The catheter was removed on the second day after surgery. The CT of the upper, middle, lower abdomen was reexamined on the fourth day after surgery. A low-density shadow in the left accessory area, with a small amount of high-density shadow in the pelvic cavity, was observed; furthermore, no abnormalities were found in the other organs. The drainage tube was removed on the fifth day postoperatively, and the patient was discharged without any complaints of discomfort.

Our patient was very satisfied with our surgical method and therapeutic measures. There was no special discomfort after the operation, and she recovered quickly, feeling better than before. She suggested that we deal with her tumor properly and timely.

## Discussion

Primary mucinous adenocarcinoma of the kidney is rare, originating almost entirely from the epithelium of the renal pelvis. Although this type of tumor is located in the renal pelvis, it can also be located in the kidney, ureter, or bladder. To date, approximately 100 cases of mucinous adenocarcinomas of the renal pelvis have been reported. Van Langenhove et al. summarized eight cases of MC of the kidney in the last 10 years after searching the PubMed database (3). We found only one case of MC of the kidney originating from one pole of the kidney without invading the renal pelvis and ureter, which was resected through partial nephrectomy (4). In this paper, we report a case of the MC of the kidney that was located at the lower pole. The disease occurs frequently in men, and there are on specific symptoms, such as mucusuria, flank pain, hematuria, or symptoms that are generally caused by kidney stones and pyelonephritis. In addition, the tumor is generally large, and the abdominal mass is palpable (3, 5). The patient only presented symptoms of left lower back pain. Several theories about the histogenesis of MC in the kidney have been proposed to explain the metaplasia of glands in the pluripotent uroepithelium of the collecting system. The three histogenetic theories include chronic stimulation and differentiation of coelomic epithelial and renal dysplasia (6).

Radiological examinations included ultrasound, CT, or magnetic resonance imaging (MRI) to locate and evaluate the nature of the tumor. However, MC has no unique radiological characteristics. Therefore, distinguishing between benign or malignant tumors or determining the tumor origin are difficult using preoperative radiographic images. After summarizing 30 cases of mucinous adenocarcinomas of the renal pelvis, Li et al. found that mucinous adenocarcinomas presented as multiple renal pelvic calculi, severe hydronephrosis, calculous pyonephrosis, or ureteric junction obstruction, with few cases manifesting as a mass or tumor (5). Although, unique imaging features are lacking to differentiate mucinous adenocarcinomas from common renal tumors, there are also substantial proposals to involve urologists. Most papillary renal cell carcinomas are commonly associated with lymph node metastasis or renal vein infiltration (3). In our imaging findings, because the tumor secreted mucus, it turned into a low-density mass with a slightly thicker and smoother cyst wall on CT, with a CT value of $5 \pm 10$ HU and flocculent high-density shadow. Enhanced CT suggested no obvious enhancement in the content and slight enhancement in the cystic wall; the tumor

could be classified as a Bosniak III. After consulting with general orthopedic surgeons and performing an improved three-dimensional CT scan of the pancreas, an invasive relationship or serious adhesion between the tumor and surrounding tissues, including the psoas major and pancreas, was not found. Because the imaging findings were not specific, we considered the hematoma to be caused by a history of trauma or retroperitoneal tumor. Apart from imaging, special auxiliary examinations may also help in the diagnosis of mucinous adenocarcinomas of the kidney. Some cases have indicated that urine exfoliative cytology might serve as a useful tool when combined with clinical findings. In addition, several studies have also described the important role of CEA and CA199 plasma levels as useful markers before surgery to diagnose mucinous adenocarcinoma and as independent markers for prognosis and recurrence (7).

Renal MC generally have multiple cysts, and the tumor body is large and contains glue-like substances. Most of the cyst walls are smooth, white, or pink, and the local position may have nodular, granular, or micropapillary structures (8). According to the pathological examination results of this patient, a gray-white cystic mass measuring $7 \times 6 \times 5$ cm and a large amount of mucus in the tumor were observed in the lower pole of the kidney, which was closely related to the ureter. Many mucous lakes and mucoid columnar epithelium were observed under the microscope, which appeared highly similar to the cellular epithelium of colorectal adenocarcinomas. Unlike benign adenomas, we found that the tumor cells showed invasive growth microscopically. As stromal invasion is a definitive marker of malignancy, MC was diagnosed.

Considering that the pathological feature of the tumor is the secretion of a large amount of mucus, we analyzed the tumors from a neoteric perspective. The patient was thought to have either a mucinous tubular and spindle cell carcinoma (MTSCC), mixed epithelial and stomal tumor (MEST), or renal abscess. Particularly, MTSCC cells can secret mucus. Fine et al. categorized MTSCC into different subtypes according to the proportions of mucus, tubular, and fusiform components. One subtype is typical, which combines three components, and the other subtype is mucin-lacking, which has little mucus but is full of spindle cells or tubules (9). In addition, the tumor is located in the renal parenchyma with expansive growth and a cystic-solid tumor with a clear boundary as determined by imaging. Plain CT scans are generally isodense or have low density (10). Enhanced CT showed that the density of the tumor was significantly lower than that of the renal cortex and medulla (11). However, in this case, there were only mucous matrix and mucous epithelial cells, no tubular or spindle cells were found, and the imaging was not consistent; therefore, we ruled out the diagnosis.

Furthermore, MEST has a mucous matrix composition. It is a complex cystic and solid mass characterized by the presence of stromal components similar to the stroma of the ovary (composed of fusiform cells with full nuclei and rich cytoplasm) and epithelial component of cysts with an epithelial lining (12). MEST is a complex tumor composed of large cysts, microcapsules, and tubules. The largest cysts consist of columnar and cuboidal epithelia, which occasionally forms small papillary masses. The mucous stroma and fascicular area of the smooth muscle cells may protrude (13). Chu et al. reported a case of a borderline MEST-secreting myxoid matrix (14). The imaging manifestations are not specific. In a typical MEST, an expansive multilocular cystic mass may protrude into the renal pelvis with varying sizes and a thick cystic septum. The tumor does not have a thick fibrous wall, but the cystic septum is thicker than a typical cystic nephroma (13). In our case, there were no special structures observed under the microscope, except for the mucinous epithelium; therefore, MEST was excluded.

Lastly, renal abscesses had similar imaging findings. Renal abscesses are characterized by complex renal cysts with fluid density, uneven intensity, and thick and irregular walls. Owing to the presence of viscous pus, the liquid components show strong and uneven diffusion limitations on diffusion-weighted imaging. Contrast-enhanced CT showed well-defined, low-density round masses, often with thick edges or halos. The abscess had extended around the kidney. MRI showed inhomogeneous thick-edge lesions with low signal intensity on T1-weighted images and high signal intensity on T2-weighted images with limited diffusion (12, 15).

Renal MC can be primary or secondary. However, because primary mucinous adenocarcinoma of the kidney is relatively rare, metastasis from other primary origins, including the pancreas, ovary, colorectum, appendix, should first be excluded. The immunohistochemical results, CDX-2(+), CK20 (+), CEA(+), MUC2(+), MUC5AC(+), Villin(+), and CK7(-), were almost similar between the intestinal and ovarian phenotypes. However, combined with the imaging findings of the patient, the origin of the primary lesion could not be determined. Only one case of low-grade cystadenocarcinoma of the appendix presenting as a renal tumor was previously published by Gómez-Román et al. in 1995 (16). The three intestinal tumor markers, CDX2(+), CK20(+), and CK7(-), were similar to the immunophenotype of colorectal adenocarcinoma. Colorectal adenocarcinoma is characterized by CK7(-) and CK20(+) (17). Both the CK7-/CK20 + phenotype and CDX2 antibody expression are highly specific and sensitive markers of the origin of colorectal cancer, and the specificity of CK7-/CK20+ is 97.6% (18). Therefore, it is necessary to consider whether the tumor is of intestinal origin. CDX2 can also be expressed in ovarian mucinous adenocarcinoma, but most express CK7(+) and CK20(-). In addition, MUC2 and MUC5AC are secretory mucins, and the biological significance of their positive expression is mainly in the formation of high-viscosity gel-like mucus. These

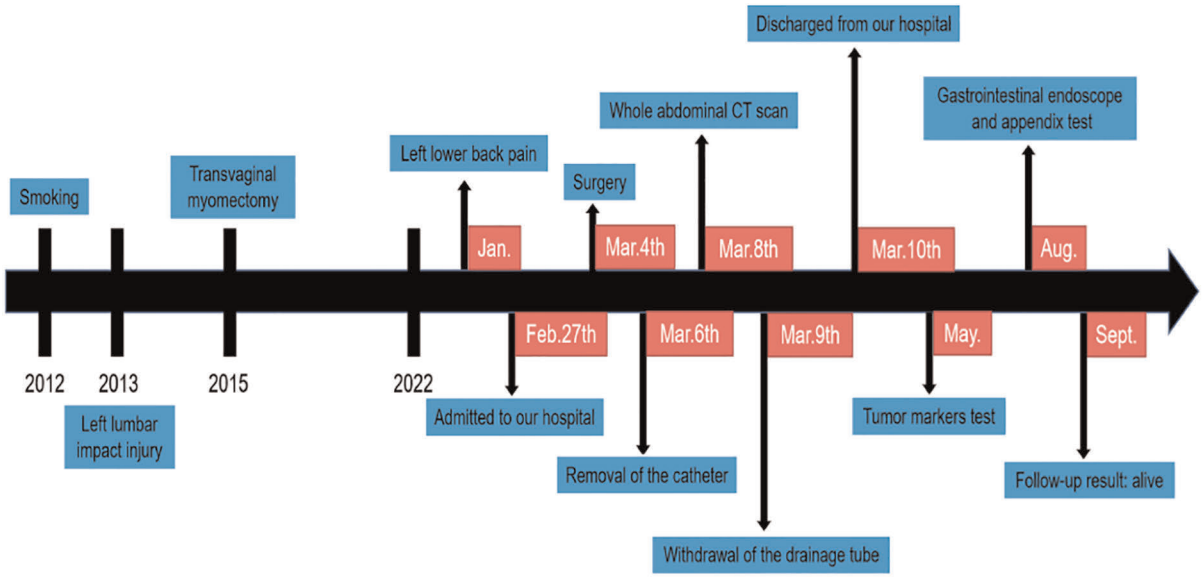


FIGURE 4
Timeline of the historical and current information from this episode of care.

immunostaining results support another differentiation theory of the histogenesis of the coelomic epithelium in MC in which the peritoneum (mesothelial) undergoes mucinous metaplasia and mucinous cystadenoma (4).

Radical nephrectomy is generally used in the surgical treatment of renal MC; however, Chung et al. reported the use of a partial nephrectomy (4). However, partial resection may be associated with the risk of recurrence and tumor rupture, leading to peritonitis. Some reports have also suggested an additional ureterectomy to improve prognosis, namely conventional nephroureterectomy with a bladder cuff, in case of mucusuria to prevent implantation of tumor cells, due to its development in areas such as the bladder and ureter where the urothelium was present (5). In this case, we performed robot-assisted laparoscopic radical resection of a left renal tumor, and the operation was completed using a transperitoneal approach because the relationship between the tumor and surrounding tissue was unclear and adherent. This was the first robot-assisted laparoscopic radical nephrectomy of MC of the kidney. We considered partial resection of the tumor; however, in view of the situation during the operation and after communicating with the family, we performed robot-assisted laparoscopic radical nephrectomy, and the tumor was completely removed. Compared with laparoscopic radical nephrectomy, robotic radical nephrectomy has obvious advantages, such as providing 3D visual effects with a wider and clearer range of observation and reducing the interference of the instrument, so that the operator can accurately view the anatomy for accurate suture and tremor of the surgeon's hand can be eliminated (19). Autorino et al. Concluded that patients who underwent robotic radical nephrectomy had a higher histological grade and pathological stage and shorter hospital stay, but no difference in operative complications were observed. These results suggest that robotic radical nephrectomy could treat patients with a more advanced and challenging MC (20). Similarly, this case adopted a transperitoneal approach, which is different from the traditional retroperitoneal access approach. The retroperitoneal approach is associated with an earlier recovery of intestinal function, shorter hospital stay, earlier recovery, shorter operation time, and shorter renal hilar vascular control time. However, the transperitoneal approach has a wider workspace and anatomical landmarks and locations can be identified easily (21). Considering the larger tumor size, risk of adhesion with other tissues, and practical needs, we chose transperitoneal access. In summary, we have provided a new method to treat renal MC. According to this case, the challenges of the robotic approach with a mucinous tumor included the fat saponification, severe adhesion with surrounding tissue, and difficult separation. Besides, the cystic renal occupied lesion was easy to be punctured, and leading to peritonitis if the tumor was ruptured. The patient recovered quickly postoperatively. The catheter was removed on the second postoperative day, and the drainage tube was removed on the fifth day after the operation.

The prognosis of primary adenocarcinoma of the renal pelvis is generally poor, with most patients dying during the 2–5 year follow-up period. The longest reported follow-up period with good prognosis was 79 months (22). Chemotherapy, radiotherapy, and chemoradiotherapy has

been recommended for the treatment of mucinous colorectal cancer and mucinous ovarian carcinoma (5). Therefore, we have adopted adjuvant therapy, such as chemotherapy after surgery, to prolong the survival time of patients. After following-up for half a year, the patient not only recovered well without any discomfort, but also the life and work of the patient were not affected with the weight increasing 10 kg. We did not give the patient adjuvant drug therapy, radiotherapy or chemotherapy. After discharging from our hospital, the patient improved gastrointestinal endoscope and appendix examination, the gastrointestinal tumor and appendix abnormality were not found, and no local recurrence and distant metastasis were found on the whole abdominal CT scan. (**Figure 4**) We will continue to follow up in future.

## Conclusion

We are the first to report a case of renal MC resected by robot-assisted laparoscopic radical nephrectomy. We have also reported another case in which the tumor was on the kidney without invading the renal pelvis and ureter. MC of the kidney is so rare that is cannot be diagnosed using radiological images; consequently, it can be misdiagnosed to a great extent. Although pathological diagnosis is the gold standard, we still considered the tumor as a local lesion or metastasis of intestinal or ovarian origin. In addition, preoperative examinations, including urine exfoliative cytology and serum levels of CEA and CA199, may improve the efficiency of diagnosis. In this study, we report a tumor that secreted mucus, the origin of the neoplasm, and the advantages of using robotic technology. When encountering a similar patient, we recommend following this situation.

## Data availability statement

The original contributions presented in the study are included in the article/**Supplementary Material**, further inquiries can be directed to the corresponding author/s.

## Ethics statement

The studies involving human participants were reviewed and approved by the ethics committee of The First Affiliated Hospital of Harbin Medical University. The patients/participants provided their written informed consent to participate in this study.

## Author contributions

NZK drafted the manuscript. ZHX treated the pictures. WYW collected the pathological pictures. NZK, WBW and LYW revised the manuscript. NZK, TPJ, ZGL and LH collected the clinical data. NZK and ZHX participated in the major revision of the manuscript. WCY reviewed the manuscript. All authors contributed to the article and approved the submitted version.

## Funding

This work was supported by the First Affiliated Hospital of Harbin Medical University Fund for Distinguished Young Medical Scholars (HYD2020JQ0020).

## Conflict of interest

The authors declare that the research was conducted in the absence of any commercial or financial relationships that could be construed as a potential conflict of interest.

## Publisher's note



## Supplementary material

The Supplementary Material for this article can be found online at: https://www.frontiersin.org/articles/10.3389/fsurg.2022.1053852/full#supplementary-material.

## References

1. Tepeler A, Erdem MR, Kurt O, Topaktas R, Kilicaslan I, Armağan A, et al. A rare renal epithelial tumor: mucinous cystadenocarcinoma case report and review of the literature. *Case Rep Med*. (2011) 2011:686283. doi: 10.1155/2011/686283

2. Riley DS, Barber MS, Kienle GS, Aronson JK, von Schoen-Angerer T, Tugwell P, et al. CARE Guidelines for case reports: explanation and elaboration document. *J Clin Epi*. (2017) 89:218–35. doi: 10.1016/jclinepi.2017.04.026

3. Tamsin A, Schillebeeckx C, Van Langenhove C, Vander Eeckt K, Ost D, Wetzels K. Mucinous cystadenocarcinoma in the renal pelvis: primary or secondary? Case report and literature review. *Acta Chir Belg*. (2020) 120 (6):417–24. doi: 10.1080/00015458.2019.1617515

4. Kim SH, Yuk HD, Park WS, Kim SH, Joung JY, Seo HK, et al. A case report of partial nephrectomy of mucinous cystadenocarcinoma in kidney and its literature review. *Cancer Res Treat*. (2016) 48(2):838–42. doi: 10.4143/crt.2014.219

5. Li H, Xie F, Zhao C, Yi Z, Chen J, Zu X. Primary mucinous adenocarcinoma of the renal pelvis misdiagnosed as calculous pyonephrosis: a case report and literature review. *Transl Androl Urol*. (2020) 9(2):781–8. doi: 10.21037/tau.2019.12.38

6. Ljungberg B, Bensalah K, Canfield S, Dabestani S, Hofmann F, Hora M, et al. EAU Guidelines on renal cell carcinoma: 2014 update. *Eur Urol*. (2015) 67 (5):913–24. doi: 10.1016/j.eururo.2015.01.005

7. Lai C, Teng XD. Primary enteric-type mucinous adenocarcinoma of the renal pelvis masquerading as cystic renal cell carcinoma: a case report and review of the literature. *Pathol Res Pract*. (2016) 212(9):842–8. doi: 10.1016/j.prp.2016.06.006

8. Gangane N A, Shende N, Sharma SM. Mucinous cystadenoma arising from renal pelvis: a report of 2 cases. *Urol J*. (2008) 5(3):197–9. doi: 10.22037/uj.v5i3.16

9. Fine SW, Argani P, DeMarzo AM, Delahunt B, Sebo TJ, Reuter VE, et al. Expanding the histologic spectrum of mucinous tubular and spindle cell carcinoma of the kidney. *Am J Surg Pathol*. (2006) 30(12):1554–60. doi: 10.1097/01.pas.0000213271.15221.e3

10. Alves AS, Gaivão AM, Marques RC, Matos C. Two rare entities in one patient: mucinous tubular and spindle cell carcinoma of the kidney and peritoneal adenomyomas. *Radiol Case Rep*. (2021) 16(8):1974–9. doi: 10.1016/j.radcr.2021.05.004

11. Young JR, Margolis D, Sauk S, Pantuck AJ, Sayre J, Raman SS. Clear cell renal cell carcinoma: discrimination from other renal cell carcinoma subtypes and oncocytoma at multiphasic multidetector CT. *Radiology*. (2013) 267 (2):444–53. doi: 10.1148/radiol.13112617

12. Wood 3rd CG, Stromberg 3rd LJ, Harmath CB, Horowitz JM, Feng C, Hammond NA, et al. CT And MR imaging for evaluation of cystic renal lesions and diseases. *Radiographics*. (2015) 35(1):125–41. doi: 10.1148/rg.351130016

13. Moch H. Cystic renal tumors: new entities and novel concepts. *Adv Anat Pathol*. (2010) 17(3):209–14. doi: 10.1097/PAP.0b013e3181d98c9d

14. Chu PG, Lau SK, Weiss LM, Jiang Z. Intestinal type of mucinous borderline tumor arising from mixed epithelial and stromal tumor of kidney. *Virchows Arch*. (2009) 455(4):389–94. doi: 10.1007/s00428-009-0831-x

15. Agnello F, Albano D, Micci G, Di Buono G, Agrusa A, Salvaggio G, et al. CT And MR imaging of cystic renal lesions. *Insights Imaging*. (2020) 11(1):5. doi: 10.1186/s13244-019-0826-3

16. Gómez-Román JJ, Val-Bernal JF, Fernández F. Mucinous cystadenocarcinoma of the vermiform appendix presenting as a renal tumor. *J Urol*. (1995) 154(3):1122–4. doi: 10.1016/S0022-5347(01)66994-5

17. Wong HH, Chu P. Immunohistochemical features of the gastrointestinal tract tumors. *J Gastrointest Oncol*. (2012) 3(3):262–84. doi: 10.3978/j.issn.2078-6891.2012.019

18. Bayrak R, Haltas H, Yenidunya S. The value of CDX2 and cytokeratins 7 and 20 expression in differentiating colorectal adenocarcinomas from extraintestinal gastrointestinal adenocarcinomas: cytokeratin 7-/20+phenotype is more specific than CDX2 antibody. *Diagn Pathol*. (2012) 7:9. doi: 10.1186/1746-1596-7-9

19. Singh I. Robotics in urological surgery: review of current status and maneuverability, and comparison of robot-assisted and traditional laparoscopy. *Comput Aided Surg*. (2011) 16(1):38–45. doi: 10.3109/10929088.2010.541620

20. Anele UA, Marchioni M, Yang B, Simone G, Uzzo RG, Lau C, et al. Robotic versus laparoscopic radical nephrectomy: a large multi-institutional analysis (ROSULA collaborative group). *World J Urol*. (2019) 37(11):2439–50. doi: 10.1007/s00345-019-02657-2

21. Desai MM, Strzempkowski B, Matin SF, Steinberg AP, Ng C, Meraney AM, et al. Prospective randomized comparison of transperitoneal versus retroperitoneal laparoscopic radical nephrectomy. *J Urol*. (2005) 173(1):38–41. doi: 10.1097/01.ju.0000145886.26719.73

22. Ye YL, Bian J, Huang YP, Guo Y, Li ZX, Deng CH, et al. Primary mucinous adenocarcinoma of the renal pelvis with elevated CEA and CA19-9. *Urol Int*. (2011) 87(4):484–8. doi: 10.1159/000329767

frontiers | Frontiers in Surgery

TYPE Case Report
PUBLISHED 06 January 2023
DOI 10.3389/fsurg.2022.1031284



OPEN ACCESS

EDITED BY
Riccardo Bertolo,
Hospital San Carlo di Nancy, Italy

REVIEWED BY
Gianni Lazzarin,
Abano Terme Hospital, Italy
Alessio Vagliasindi,
Santa Maria delle Croci Hospital, Italy

*CORRESPONDENCE
Zheng Lu
zdy527897470@126.com

SPECIALTY SECTION
This article was submitted to Surgical Oncology, a section of the journal Frontiers in Surgery

RECEIVED 29 August 2022
ACCEPTED 21 October 2022
PUBLISHED 06 January 2023

CITATION
Ma S, Zhang D, Zhao G, Ding S, Wu Q, Zhang X and Lu Z (2023) Gastric infiltration of hepatic sarcomatoid carcinoma: A case report and literature review.
Front. Surg. 9:1031284.
doi: 10.3389/fsurg.2022.1031284



# Gastric infiltration of hepatic sarcomatoid carcinoma: A case report and literature review

Shuoshuo Ma[1], Dengyong Zhang[1], Guanru Zhao[1], Sheng Ding[1], Qiong Wu[2], Xueli Zhang[3] and Zheng Lu[1]*

[1]Department of General Surgery, The First Affiliated Hospital of Bengbu Medical College, Bengbu, China, [2]Department of Pathology, Hospital of Bengbu Medical College, Bengbu, China, [3]Department of Radiology, Hospital of Bengbu Medical College, Bengbu, China

**Background:** Hepatic sarcomatoid carcinoma (HSC) is an extremely rare malignant tumor typically observed in clinical settings. HSC occurrence is predominantly noted in the right lobe and rarely in the left lobe of the liver. This report presents a case of sarcomatoid carcinoma that occurred in the left outer lobe of the liver, which was accompanied by gastrointestinal stromal tumors (GSTs) in the greater curvature of the stomach. In addition, the patient showed late-stage recurrence of HSC in gastric tissues.

**Case presentation:** A 63-year-old man was concomitantly diagnosed with HSC and GST. The main clinical manifestation was fever. Abdominal computer tomography (CT) and ultrasound-guided percutaneous liver biopsy at the local hospital revealed the presence of malignant hepatic tumors. The patient approached our hospital for further treatment. The subsequent electronic gastroscopy showed multiple submucosal tumors (SMT) in the stomach. Owing to the absence of multiple metastases in other regions of the body, we performed left hepatic lobe resection with gastric partial resection. The postoperative pathological analysis confirmed the presence of HSC and GST. The patient reported feeling well 1 month after the surgery, and no obvious space-occupying lesions in other areas were noted *via* imaging examinations. However, 3 months later, the patient presented with pain in the upper left abdomen, and examination revealed cancer recurrence in the stomach. The surgery was repeated, and the patient recovered favorably after the procedure. Unfortunately, the patient died owing to multiple metastatic diseases 4 months after the second surgical procedure.

**Conclusion:** HSC shows no characteristic clinical manifestations and is highly malignant. Surgical intervention is the first treatment of choice for patients with HSC. In cases of sarcomatoid cancer occurring in the left lobe of the liver, it is imperative to exercise strict vigilance against the tumor's invasion

Abbreviations
Hepatic sarcomatoid carcinoma, HSC; gastrointestinal stromal tumor, GST; computed tomography, CT; submucosal tumor, SMT; hepatocellular carcinoma, HCC; intrahepatic cholangiocarcinoma, ICC; hepatitis B virus, HBV; hepatitis C virus, HCV; carcinoembryonic antigen, CEA; alpha-fetoprotein, AFP; prostate-specific antigen, PSA; carbohydrate antigen 19-9, CA19-9; carbohydrate antigen 15-3, CA15-3; magnetic resonance imaging, MRI; diffusion-weighted imaging, DWI; immunohistochemistry, IHC; sarcomatoid carcinoma, SC; transcatheter hepatic artery chemoembolization, TACE; radiofrequency ablation, RFA; sarcomatoid hepatocellular carcinoma, SHC; intrahepatic sarcomatoid cholangiocarcinoma, ISCC; hepatitis B surface antigen, HBsAg; hepatitis C virus antibody, anti-HCV; Vimentin, Vim; epithelial membrane antigen, EMA; anion exchanger, AE; overall survival, OS; disease-free survival, DFS.

of the stomach tissue. This is particularly important when the tumor breaks through the capsule of the liver.

KEYWORDS

hepatic sarcomatoid carcinoma, gastric stromal tumor, case report, infiltration, review

# Introduction

Hepatic sarcomatoid carcinoma (HSC) is a particularly malignant tumor with unknown pathogenesis, and it accounts for 2% of surgically removed cases of hepatocellular carcinoma (HCC) and 3.9%–9.4% of autopsies (1, 2). HSC may be a tumor of monoclonal origin; however, its histological origin remains controversial (3). Compared with HCC and intrahepatic cholangiocarcinoma (ICC), HSC has a higher histological grade, recurrence rate, and metastasis rate; therefore, its prognosis is extremely poor. Currently, surgical treatment is the first choice of treatment, and adjuvant treatments include radiotherapy, chemotherapy, and interventional therapy among other comprehensive approaches.

In the current report, we present the case of a 63-year-old man who showed fever as the main clinical manifestation and had a postoperative pathological diagnosis of HSC and gastrointestinal stromal tumors (GST). We performed left hepatic lobectomy combined with partial gastrectomy on the patient, and the patient recovered favorably after the operation. However, 3 months later, the patient presented with gastric recurrence and received surgical intervention for the second time. In this paper, we share the clinical characteristics of and the diagnosis and treatment process for this patient with the aim to assist colleagues in their associated work.

# Case presentation

## Clinical history and laboratory findings

At the time of hospital admission, the patient was a 63-year-old male and showed fever as the main clinical manifestation. His body temperature fluctuated in the range of 37.5°C–38°C. The patient did not have jaundice, the abdomen was flat and soft, and showed no tenderness or rebound pain. The liver and spleen were not palpable under the ribs, and no mobile dullness was identified. The patient did not have a history of chronic diseases such as hypertension and diabetes, a history of infectious diseases including hepatitis B and tuberculosis, or a family history of tumors.

Blood routine tests showed increased levels of white blood cells ($11.14 \times 10^9$/L). The blood biochemical examination revealed that alanine aminotransferase (37 U/L) and aspartate transferase (18 U/L) were within the normal range. We noted a decrease in the total protein content (62.8 g/L) and the white ball ratio (1.0); however, the C-reactive protein (215.70 mg/L) levels had increased abnormally. Immune screening detected no hepatitis B virus (HBV) or hepatitis C virus (HCV) infection. Through the tumor marker screening, we determined that carcinoembryonic antigen (CEA) (1.24 ng/ml), alpha-fetoprotein (AFP) (4.47 ng/ml), prostate-specific antigen (2.98 ng/ml), carbohydrate antigen 19–9 (CA19–9) (6.32 IU/ml), and carbohydrate antigen 15–3 (CA15–3) (18.10 IU/ml) were within the normal range.

## Imaging examinations

The patient underwent a physical examination at the local hospital. Ultrasound examination of the liver, gallbladder, pancreas, and spleen showed the presence of space-occupying lesions in the left lobe of the liver. Computed tomography (CT) of the upper abdomen indicated a liver abscess and multiple lymphadenopathies in the abdominal cavity. However, a subsequent (1 week later) ultrasound-guided percutaneous liver biopsy revealed a malignant tumor in the left lobe of the liver.

To receive further treatment for liver tumors, the patient was admitted to the Department of Hepatobiliary Surgery at our hospital. The Color Doppler ultrasound (hepatobiliary, pancreatic, spleen, and portal vein) showed that the left outer lobe of the liver had a mixed echo of $103 \times 112 \times 110$ cm. The tumor was mainly hypoechoic with an irregular shape and clear boundaries. The internal echo was uneven, the color revealed the presence of dots of blood flow signals in and around the tumor, and no abnormality in the portal vein was noted. Irregular masses of long T1 (**Figure 1A**) and long T2 (**Figure 1B**) abnormal signals in the space between the liver and the stomach were detected through magnetic resonance imaging (MRI) of the tumor (plain scan + enhanced + functional imaging). In the images, the tumor size was approximately $9.5 \times 8.3$ cm, the circular short T1 and long T2 signals can be clearly visualized, and the tumor has a well-defined boundary. However, the lesion and the left lobe of the liver appear to be unclearly decomposed. Diffusion-weighted imaging (DWI) (**Figure 1C**) shows a strong signal, and the enhancement (**Figures 1D–F**) indicates progressive heterogeneous enhancement. Irregular thickening of the stomach wall was noted on the side of the corresponding lesser curvature of the fundus. The gallbladder was not enlarged, and its wall did not appear to be thickened. No dilation was

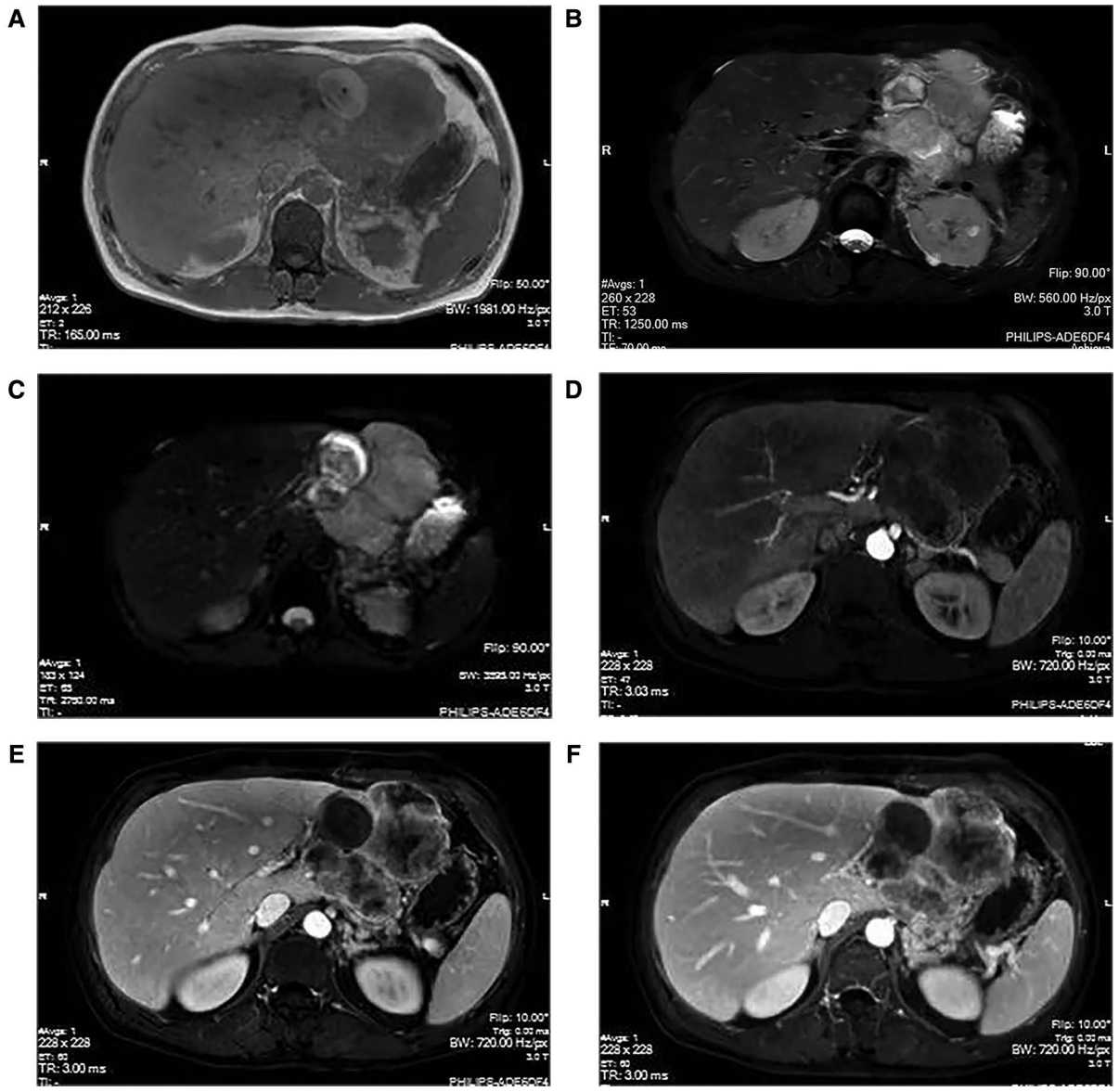


FIGURE 1
MRI manifestations of hepatic sarcomatoid carcinoma. The magnetic resonance imaging (plain scan + enhanced + functional imaging) shows abnormal signals of irregular mass in the liver, with a size of approximately 9.5 × 8.3 cm. The T1WI (**A**) shows a weak signal; however, the T2WI (**B**) and the DWI (**C**) show strong signals. The arterial phase (**D**) indicates slightly uneven enhancement at the edge of the lesion, with continuous uneven enhancement in the portal phase (**E**) and delayed phase (**F**).

observed in the intrahepatic and extrahepatic bile ducts and we noted no obvious filling defect in the main portal vein and its branches. We did not identify any abnormalities in the pancreas and spleen morphology or any obvious signal indicating irregularity. In the imaging range, multiple small lymph nodes could be identified in the retroperitoneum. Chest x-ray and CT images showed no abnormalities in the lungs, the heart, or the diaphragm. We used an electronic gastroscope and determined the presence of a submucosal bulge with a diameter of approximately 0.8 cm in the fornix and the greater curvature of the stomach. The surface of the protuberance was smooth, tough to touch with the biopsy forceps, and appeared to be inactive. This observation suggested that there were multiple SMTs within the protuberance. In the lesser curvature of the stomach near the corner, we noted that there was a sheet-like shallow erosion with smooth mucosa flushing in color; however, no ulcer or bleeding was observed. Pathologic examination of the biopsy revealed chronic superficial gastritis of the mucosa, which was severe, active, and locally accompanied by ulcers and *Helicobacter pylori* (HP) infection.

## Intraoperative situation

The patient was febrile and showed no characteristic clinical presentation. Results of laboratory tests, including tumor markers, were unremarkable. A combination of imaging findings and liver puncture results of the patient in the local hospital assisted us in determining that the patient had a malignant tumor in the left lobe of the liver, accompanied by greater curvature GST, without obvious metastatic lesions. Owing to the fact that only a small amount of pathological tissue was acquired through the liver puncture, the nature of the tumor required further elucidation *via* postoperative pathologic analysis. HCC, ICC, HSC, and other properties are not excluded. We performed left hepatic lobectomy combined with partial gastrectomy (wedge resection) with the patient's and his family's consent. We intraoperatively identified a mass of ∼10 cm in diameter in the left lobe of the liver, with off-white color and hard texture. The tumor had appeared to have broken through the liver capsule, the visceral surface densely adhered to the lesser curvature of the stomach, and enlarged lymph nodes were palpable in the suspensory ligament of the hepatoduodenum. Intraoperative biopsies were performed and all three enlarged lymph nodes tested negative upon pathologic examination. Two superficial tumors were observed on the greater curvature of the stomach wall. The right liver was normal in size and soft to the touch. The size of the gallbladder was approximately $7 \times 4 \times 3$ cm. No tumor metastatic nodules were detected in the omentum, diaphragm, jejunum, or pelvis. Intraoperative examination revealed that the liver tumor had invaded the left gastric artery, which was removed from the root. The operation was relatively successful, lasted for approximately 6 h, and the bleeding volume was approximately 200 ml.

## Pathology

The postoperative specimens were subjected to pathological examination and immunohistochemistry (IHC). The liver tumor tissue specimen was diagnosed as a high-grade pleomorphic malignant tumor of the left lateral lobe of the liver with necrosis. The immunological markers were as follows: CK (+) (**Figure 2B**), Vim (−), CD117 (−), Dog-1 (−), CD34 (−), SMA (−), Ki-67 (+, ∼60%), GPC-3 (−), and Hepar-1 (−). Additionally, the tissue specimen was sent to another hospital for consultation, and the IHC results showed AE1/AE3 (+) (**Figure 2C**), P16 (−), CDK4 (+), MDM2 (−), Desmin (−), Myogenin (−), and MyoD1 (−). Molecular detection: MDM2 gene status (−), no amplification. According to the outcomes of IHC analysis, a sarcomatoid carcinoma (SC) with a length of 10 cm, and a negative cut-off edge of the liver section was considered. The gastric tissue specimen was diagnosed as representing spindle cell proliferative disease, combined with immunological markers in line with low-risk GST, featuring 2 pieces with a length of 1.0–1.5 cm. The relevant immunohistochemical markers were as follows: Vim (+), CD117 (+) (**Figure 2E**), CD34 (+), Dog-1 (+) (**Figure 2F**), Ki-67 (+, ∼5%), SMA (−), S-100 (−).

## Outcome and follow-up

The patient recovered favorably and was discharged from our hospital on postoperative day 8. No adjuvant therapy was administered or prescribed. The patient was followed up in the outpatient clinic 1 month after discharge, and he presented no obvious symptoms or discomfort. The blood routine test and biochemical profile showed no abnormalities, and AFP (10.5 ng/ml) had no significant increase compared with the first measurement (4.47 ng/ml). The hepatobiliary, pancreatic and splenic ultrasound showed no obvious space-occupying lesions.

However, 3 months later, the patient presented with persistent pain in the upper left abdomen, which worsened paroxysmally. Imaging examinations revealed the presence of an irregular and substantial mass in the area between the greater curvature of the stomach and the omental sac (**Figure 3A**), and the enhanced CT scan showed uneven enhancement. The patient underwent gastric tumor resection with partial resection of the transverse colon. The tumor was $53 \times 78 \times 100$ mm in size, gray in color, and showed internal necrosis (**Figures 3B,C**). Results of postoperative pathology and IHC tests confirmed that the tumor in the stomach had metastasized from the HSC. The patient recovered well after the operation. Four months after the second operation, the patient died from multiple metastases to other sites.

# Discussion and conclusion

Cases of SC are extremely rare in clinical practice. SC may occur in multiple organs throughout the body and even occur concurrently. The lung and the bladder are the most common sites of occurrence (4, 5), whereas cases presenting with SCs in the liver are rare. HSC is a rare malignant tumor that typically occurs in the right lobe but rarely in the left lobe of the liver. HSC accounts for 1.8% of all surgically resected HCCs and 3.9%–9.4% of autopsy cases (1, 5). The age of onset of HSC patients is approximately 60 years, and the disease is more common in men, with its incidence 3–4 times that of women (6, 7). Herein, we have reported the case of a 63-year-old male patient, which is consistent with the characteristics of previous reports. HSC etiologies and pathogeneses require further elucidation; however, two main schools of thought exist in the medical field. One states that HSC is the sarcomatoid

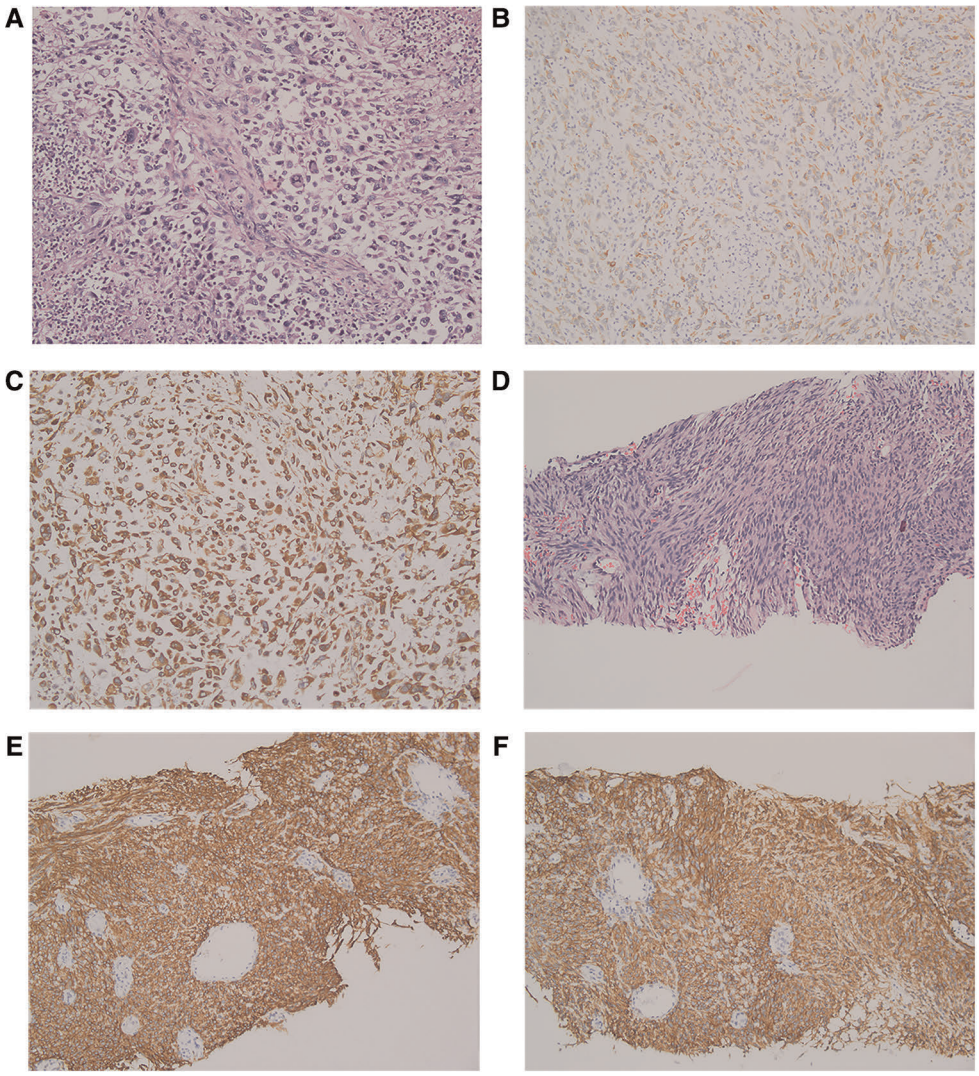


FIGURE 2
Pathology and immunohistochemistry of hepatic sarcomatoid carcinoma and gastrointestinal stromal tumors. Hematoxylin and eosin (H & E) staining of hepatic sarcomatoid carcinoma (**A**); the results of immunohistochemical staining of hepatic sarcomatoid carcinoma show CK positive ×200 (**B**) and AE1/AE3(+) positive ×200 (**C**); H&E staining of gastrointestinal stromal tumor (**D**); the results of immunohistochemical staining of the gastrointestinal stromal tumor shows CD117 positive ×200 (**E**) and DOG-1 positive ×200 (**F**).

transformation of HCC, whereas the other states that it is a combination of liver cancer and sarcoma. However, among the two, the former is more widely accepted by scholars (8). Previous studies have reported that sarcoma transformation may be related to certain preoperative anti-liver cancer treatments, including transcatheter hepatic artery chemoembolization (TACE), radiofrequency ablation (RFA), and percutaneous ethanol injection therapy (9–11). Conversely, in our case, the patient had no history of treatment. Under normal circumstances, the volume of HSC is larger than that of HCC, which helps to distinguish between the two. In a study of 28 HSCs, the average HSC size was 6.1 ± 2.8 cm, and 18 cases (64.3%) had tumors larger than 5 cm (12). Another study involving 17 cases of HSC pointed out that its long diameter was 6.12 ± 3.18 cm, whereas the HCC's long diameter was 4.21 ± 2.38 cm (13). In our case, the HSC had a long diameter of approximately 10 cm, which was consistent with the previous reports. For larger HSCs, the probability of false capsules and bleeding may increase. In the study including 28 patients, 9 (32.1%) had pseudocapsule formation, most of which were incomplete (12). HSC is highly aggressive and is associated with a particularly poor prognosis. In the abovementioned study, the researchers noted that up to 47.1% of HSC patients had intrahepatic metastasis, which was considerably greater than the 12% of HCC patients; however, this value was not significantly different from that of ICC (13). A total of 93% of HSC patients

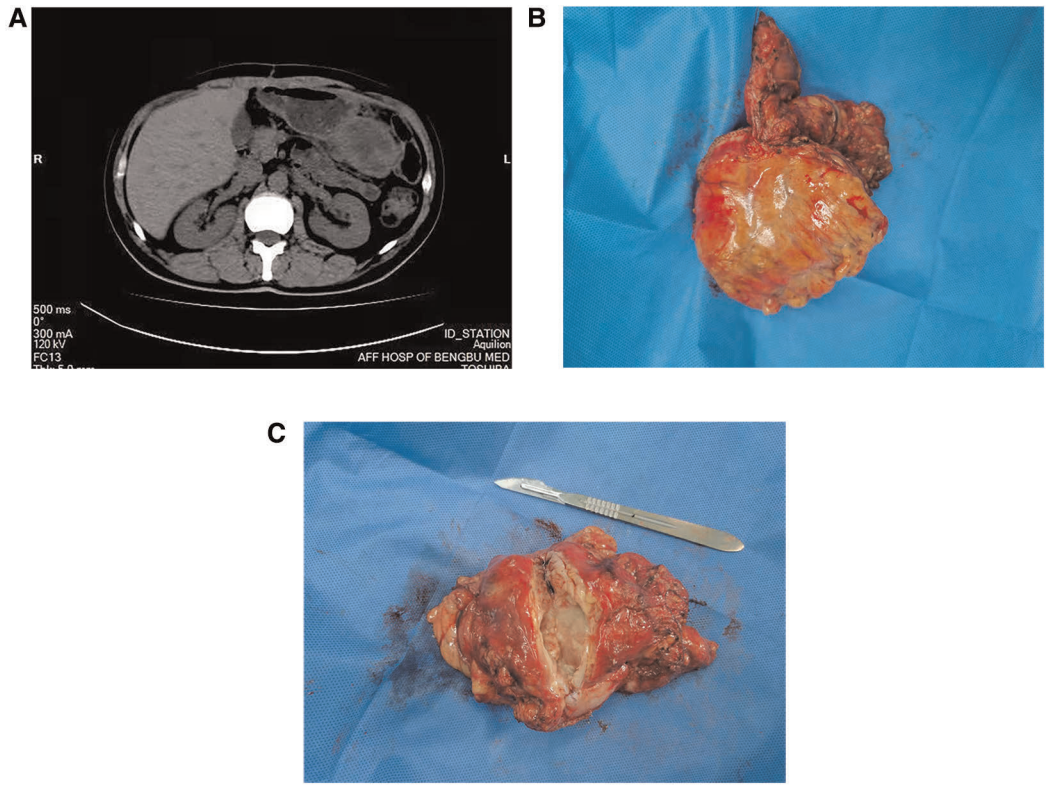


FIGURE 3
Related imaging data and clinical specimens of gastric recurrence of hepatic sarcomatoid carcinoma. A regular CT scan of the abdomen showed the presence of an irregularly shaped and uneven-density occupancy in the area between the greater curvature of the stomach and the omental sac (A), the size was approximately 53 × 78 × 100 mm; the specimen is off-white (B) and shows internal necrosis (C).

reportedly presented with extrahepatic metastases during treatment, with the most common metastatic organs being the lung, peritoneum, pleura, pancreas, adrenal gland, intestine, and spleen. A study with 28 patients reported that the number of patients with local invasion, vascular invasion, bile duct invasion, and lymph node metastasis was 6 (21.4%), 8 (28.6%), 3 (10.7%), and 7 (25%), respectively (12). Similar characteristics were observed in other study (14). In the present case, no other organ metastases were observed at the first visit; however, the tumor invaded the left gastric artery and gastric recurrence appeared 3 months after surgical intervention. A study involving univariate analysis (12) highlighted that the TNM stage, pseudocapsule formation, local invasion, vascular invasion, Child–Pugh classification, and radical resection are the prognostic factors of OS in HSC patients. A study involving 79 cases of HSC reported that the 1-year and 3-year overall survival rates were 63.3% and 35.4%, respectively (15). In addition to these poor survival rates, HSC is prone to recurrence. Notably, during the follow-up period, 25 of 28 (89.3%) patients who underwent radical surgical resection showed tumor recurrence, and the cumulative recurrence rate at 6, 12, and 24 months was 53.6%, 78.6%, and 85.7%, respectively (12).

Symptomatic HSC cases account for 68%–75% of cases. Abdominal pain is the most common symptom (7, 8, 12), followed by fatigue, fever, and jaundice. The typical systemic symptoms caused by liver decompensation are jaundice, fever, abdominal distension, and weight loss. In addition, patients with HSC may present with gastrointestinal symptoms, including persistent pain in the upper right quadrant, nausea, vomiting, weight loss, and palpable mass in the xiphoid (16). Our patient had fever as the main clinical presentation, which is common in other diseases. In addition, a small percentage of patients are asymptomatic (17.6%). To a certain degree, this observation is the opposite of liver cancer, which tends to exhibit no symptoms for most patients (70.0%) (13). Furthermore, 14 of 19 HSCs (73.7%) reportedly had a history of liver cirrhosis. A number of studies have also pointed out the potential relationship between chronic liver disease and HSC (17–19). However, in our case, liver function indicators (ALT and AST, among others) and tumor indicators (AFP and CEA, among others) were in the normal range. This is different from the features of liver cancer that we have observed previously, and it caught our attention.

On an enhanced MRI image, HSC is typically manifested as peripheral enhancement, central necrosis, and different

enhancements with and without a tumor envelope in the solid part (20). The varied tissue composition of HSC determines its mode of enhancement; therefore, this indicates that the imaging results of HSC are complex and diverse. In one example, more than half of HSC cases showed progressive enhancement in the Gd-DTPA-enhanced MRI scan, and approximately one-third of cases showed continuous high enhancement (20). Another study involving 10 cases of HSC reported that the enhancement mode of MRI was mainly "progressive" (21). The continuous enhancement mode of HSC is one of the crucial points to successfully identify the presence of HCC. This is attributable to the fact that the latter is primarily manifested as the "fast in and out" of the contrast agent. In our case, the T1WI showed a strong signal, the enhancement showed progressive unevenness and the lack of a "target sign." Although this is similar to previous reports, further differentiation from ICC should be noted. In addition, intrahepatic metastasis (17, 18), lymphadenopathy (13), and adjacent biliary tract dilation (19, 22) may assist in distinguishing between HSC from HCC as these characteristics are predominantly observed in HSC.

An accurate HSC diagnosis relies on a large number of pathological signs and IHC observations. HSC is composed of spindle cells and epithelial components that are identifiable in ultrastructure, IHC, and morphology (23). The IHC staining results of HSC were positive for the sarcoma-like component marker Vimentin (Vim), the epithelial component markers keratin (CK) and epithelial membrane antigen (EMA) (24, 25) as well as the anion exchanger (AE) 1/AE3, 34$\beta$E12, CAM 5.2, c-Kit, S-100 protein, HHF-35, kinesin-like protein-1, CD34, and HAM-56, which is helpful for the diagnosis of HSC (26). In the present case, the epithelial component markers keratin (CK) was negative; however, AE1/AE3 was positive. This is worth our attention. In cases when the microscopic features tend to indicate SC, but the IHC indicators appear to be inconsistent, adding other IHC indicators should be prioritized.

Reportedly, surgical resection has been an effective method for the treatment of HSC. Radical surgery can significantly prolong the overall survival of patients with HSC, and the associated survival period is significantly higher than that of palliative resection (12, 14). In the present case, we performed radical resection of the tumor. Unfortunately, the possibility of invasion of the gastric tissue by the tumor was overlooked, this was despite the fact that endoscopic biopsy suggested a negative result. This may have been the main etiology responsible for the subsequent gastric recurrence in the patient. For unresectable tumors, systemic chemotherapy and local radiotherapy can be selected (27). For multiple metastases, combined treatments, such as radiotherapy, chemotherapy, and hyperthermia, can alleviate symptoms, but they cannot change the overall survival (OS) (16). Owing to the poor differentiation of carcinogenesis and the aggressiveness of HSC, recurrence may be likely even in the early stages of the disease. Vascular invasion and local invasion are independent risk factors for short disease-free survival (DFS) (12). In this case, invasion of the left gastric artery and infiltration of the gastric wall may be important reasons for the recurrence and short survival period of our patient. Although previous studies found that HSC is mainly manifested as vascular clumps, adjuvant TACE is considered a risk factor related to poor prognosis (12). However, among patients with intrahepatic recurrence after hepatectomy, the median survival time of those who received TACE treatment was 14.6 months, which was significantly longer than the 8.1-month survival time of patients who received supportive treatment alone (12). These findings provide evidence that TACE may be beneficial for localized intrahepatic recurrence and may improve the survival rate of these patients.

HSC is highly malignant; thus, timely detection, accurate diagnosis, and personalized treatment are of paramount importance to positively impact disease prognosis. In cases presenting with SCs in the left lobe of the liver, clinicians should be vigilant regarding the possibility of gastric infiltration; this is a plausible outcome if the carcinoma breaks through the liver capsule. If available, gastric endoscopic ultrasonography should be used to evaluate the involvement of the gastric wall. In this report, we have shared our patient's clinical characteristics and the corresponding diagnosis and treatment process to provide a reliable reference for healthcare professionals in this field.

## Data availability statement

The original contributions presented in the study are included in the article/Supplementary Material, further inquiries can be directed to the corresponding author/s.

## Ethics statement

The studies involving human participants were reviewed and approved by the Ethics Committee of Bengbu Medical College. The patients/participants provided their written informed consent to participate in this study. Written informed consent was obtained from the individual(s) for the publication of any potentially identifiable images or data included in this article.

## Authors' contributions

MSS and ZDY were involved in collecting relevant medical history materials and writing drafts. ZGR and

DS were involved in gathering data and reviewing drafts. ZXL was involved in organizing and reviewing imaging materials. WQ helped by organizing and reviewing pathology materials. LZ conceptualized the study and performed the final revision. All authors contributed to the article and approved the submitted version.

## Funding

This work was supported by a grant from the Natural Science Foundation of Anhui Province (2008085MH256). The funding is used for page fees.

## Conflict of interest

The authors declare that the research was conducted in the absence of any commercial or financial relationships that could be construed as a potential conflict of interest.

## Publisher's note

All claims expressed in this article are solely those of the authors and do not necessarily represent those of their affiliated organizations, or those of the publisher, the editors and the reviewers. Any product that may be evaluated in this article, or claim that may be made by its manufacturer, is not guaranteed or endorsed by the publisher.

## References

1. Kakizoe S, Kojiro M, Nakashima T. Hepatocellular carcinoma with sarcomatous change. Clinicopathologic and immunohistochemical studies of 14 autopsy cases. *Cancer*. (1987) 59(2):310–6. doi: 10.1002/1097-0142 (19870115) 59:2<310::aid-cncr2820590224 > 3.0.co;2-s

2. Giunchi F, Vasuri F, Baldin P, Rosini F, Corti B, D'Errico-Grigioni A. Primary liver sarcomatous carcinoma: report of two cases and review of the literature. *Pathol Res Pract*. (2013) 209(4):249–54. doi: 10.1016/j.prp.2013.01.005

3. Thompson L, Chang B, Barsky SH. Monoclonal origins of malignant mixed tumors (carcinosarcomas): evidence for a divergent histogenesis. *Am J Surg Pathol*. (1996) 20(3):277–85. doi: 10.1097/00000478-199603000-00003

4. Kadouri Y, Ouskri S, Sayegh HE, Benslimane L, Nouini Y. Sarcomatoid carcinoma of the urinary bladder: analysis of five cases and literature review. *Pan Afr Med J*. (2020) 36:369. doi: 10.11604/pamj.2020.36.369.25036

5. Karmakar S, Ansari MHG, Thakur S, Rai DK. Sarcomatoid carcinoma of the lung. *Lung India*. (2021) 38(3):266–8. doi: 10.4103/lungindia.lungindia_67_20

6. Liao SH, Su TH, Jeng YM, Liang PC, Chen DS, Chen CH, et al. Clinical manifestations and outcomes of patients with sarcomatoid hepatocellular carcinoma. *Hepatol*. (2019) 69(1):209–21. doi: 10.1002/hep.30162

7. Okabayashi T, Shima Y, Iwata J, Iiyama T, Sumiyoshi T, Kozuki A, et al. Surgical outcomes for 131 cases of carcinosarcoma of the hepatobiliary tract. *J Gastroenterol*. (2014) 49(6):982–91. doi: 10.1007/s00535-013-0882-2

8. Kan A, Guo RP. The prognosis of subsequent surgical treatment in patients with sarcomatoid carcinoma in the liver: a retrospective study. *Int J Surg*. (2018) 55:145–51. doi: 10.1016/j.ijsu.2018.05.736

9. Koda M, Maeda Y, Matsunaga Y, Mimura K, Murawaki Y, Horie Y. Hepatocellular carcinoma with sarcomatous change arising after radiofrequency ablation for well-differentiated hepatocellular carcinoma. *Hepatol Res*. (2003) 27 (2):163–7. doi: 10.1016/s1386-6346 (03)00207-9

10. Komada N, Yamagata M, Komura K, Hayashi K, Maruyama T, Kataoka H, et al. Hepatocellular carcinoma with sarcomatous change arising in primary biliary cirrhosis. *J Gastroenterol*. (1997) 32(1):95–101. doi: 10.1007/bf01213303

11. Kojiro M, Sugihara S, Kakizoe S, Nakashima O, Kiyomatsu K. Hepatocellular carcinoma with sarcomatous change: a special reference to the relationship with anticancer therapy. *Cancer Chemother Pharmacol*. (1989) 23 (1):S4–8. doi: 10.1007/bf00647229

12. Lu J, Zhang J, Xiong XZ, Li FY, Ye H, Cheng Y, et al. Primary hepatic sarcomatoid carcinoma: clinical features and prognosis of 28 resected cases. *J Cancer Res Clin Oncol*. (2014) 140(6):1027–35. doi: 10.1007/s00432-014-1641-3

13. Zhang H, Chai S, Chen L, Wang Y, Cheng Y, Fang Q, et al. Mri features of hepatic sarcomatoid carcinoma different from hepatocellular carcinoma and intrahepatic cholangiocarcinoma. *Front Oncol*. (2021) 11:611738. doi: 10.3389/fonc.2021.611738

14. Wang QB, Cui BK, Weng JM, Wu QL, Qiu JL, Lin XJ. Clinicopathological characteristics and outcome of primary sarcomatoid carcinoma and carcinosarcoma of the liver. *J Gastrointest Surg*. (2012) 16(9):1715–26. doi: 10.1007/s11605-012-1946-y

15. Tang Y, Zhang T, Zhao Y, Chen Z, Ma X. Development and validation of a comprehensive radiomics nomogram for prognostic prediction of primary hepatic sarcomatoid carcinoma after surgical resection. *Int J Med Sci*. (2021) 18 (7):1711–20. doi: 10.7150/ijms.53602

16. Ma Q, Jiang L, Bonda S, Luo D, Zhang W. A rare case of hepatic sarcomatoid carcinoma: exceeding expectations in a stage iv primary hepatic sarcomatoid carcinoma patient. *Int J Clin Exp Pathol*. (2019) 12(1):378–83.

17. Gu KW, Kim YK, Min JH, Ha SY, Jeong WK. Imaging features of hepatic sarcomatous carcinoma on computed tomography and gadoxetic acid-enhanced magnetic resonance imaging. *Abdom Radiol (NY)*. (2017) 42(5):1424–33. doi: 10.1007/s00261-016-1038-7

18. Shi D, Ma L, Zhao D, Chang J, Shao C, Qi S, et al. Imaging and clinical features of primary hepatic sarcomatous carcinoma. *Cancer Imaging*. (2018) 18 (1):36. doi: 10.1186/s40644-018-0171-7

19. Seo N, Kim MJ, Rhee H. Hepatic sarcomatoid carcinoma: magnetic resonance imaging evaluation by using the liver imaging reporting and data system. *Eur Radiol*. (2019) 29(7):3761–71. doi: 10.1007/s00330-019-06052-8

20. Koo HR, Park MS, Kim MJ, Lim JS, Yu JS, Jin H, et al. Radiological and clinical features of sarcomatoid hepatocellular carcinoma in 11 cases. *J Comput Assist Tomogr*. (2008) 32(5):745–9. doi: 10.1097/RCT.0b013e3181591ccd

21. Honda H, Hayashi T, Yoshida K, Takenaka K, Kaneko K, Fukuya T, et al. Hepatocellular carcinoma with sarcomatous change: characteristic findings of two-phased incremental ct. *Abdom Imaging*. (1996) 21(1):37–40. doi: 10.1007/s002619900006

22. Kim SA, Lee JM, Lee KB, Kim SH, Yoon SH, Han JK, et al. Intrahepatic mass-forming cholangiocarcinomas: enhancement patterns at multiphasic ct, with special emphasis on arterial enhancement pattern–correlation with clinicopathologic findings. *Radiol*. (2011) 260(1):148–57. doi: 10.1148/radiol.11101777

23. Rossi G, Cavazza A, Sturm N, Migaldi M, Facciolongo N, Longo L, et al. Pulmonary carcinomas with pleomorphic, sarcomatoid, or sarcomatous elements: a clinicopathologic and immunohistochemical study of 75 cases. *Am J Surg Pathol*. (2003) 27(3):311–24. doi: 10.1097/00000478-200303000-00004

24. Shen XZ, Liu F. Primary sarcomatoid carcinoma of the mandibular gingiva: clinicopathological and radiological findings. *Singapore Med J*. (2014) 55(9): e152–5. doi: 10.11622/smedj.2014131

25. Giordano G, Berretta R, Silini E. Primary pure spindle cell carcinoma (sarcomatoid carcinoma) of the ovary: a case report with immunohistochemical study. *Diagn Pathol*. (2016) 11(1):70. doi: 10.1186/s13000-016-0521-3

26. Leng Q, Xiang XI, Tang Y, Yang Y, Qiu LI. Primary hepatic sarcomatoid carcinoma: a case report. *Exp Ther Med*. (2015) 10(3):1145–8. doi: 10.3892/etm.2015.2599

27. Shi Y, Rojas Y, Zhang W, Beierle EA, Doski JJ, Goldfarb M, et al. Characteristics and outcomes in children with undifferentiated embryonal sarcoma of the liver: a report from the national cancer database. *Pediatr Blood Cancer*. (2017) 64(4). doi: 10.1002/pbc.26272

frontiers | Frontiers in Surgery

TYPE Case Report
PUBLISHED 09 January 2023
DOI 10.3389/fsurg.2022.1068935



OPEN ACCESS

EDITED BY
Zhaolun Cai,
Sichuan University, China

REVIEWED BY
Lin Xiaokun,
Wenzhou Medical University, China
Agneta Nordenskjöld,
Karolinska University Hospital, Sweden

*CORRESPONDENCE
Yi Huang
✉ huangyi@medmail.com.cn
Shudong Zhang
✉ shootong@163.com

†These authors have contributed equally to this work

SPECIALTY SECTION
This article was submitted to Surgical Oncology, a section of the journal Frontiers in Surgery

RECEIVED 13 October 2022
ACCEPTED 05 December 2022
PUBLISHED 09 January 2023

CITATION
Hao Y, Xia L, Lu M, Liu C, Zhang F, Yan Y, Huang Y and Zhang S (2023) Case report and literature review: Primary leiomyosarcoma of the penis.
Front. Surg. 9:1068935.
doi: 10.3389/fsurg.2022.1068935



# Case report and literature review: Primary leiomyosarcoma of the penis

Yichang Hao[1†], Li Xia[1†], Min Lu[2], Chenhong Liu[1], Fan Zhang[1], Ye Yan[1], Yi Huang[1*] and Shudong Zhang[1*]

[1]Department of Urology, Peking University Third Hospital, Beijing, China, [2]Department of Pathology, Peking University Third Hospital, Beijing, China

**Background:** Leiomyosarcoma (LMS) is a malignant spindle-cell mesenchymal tumor originating from the smooth muscle cells, which mostly affects soft tissues and abdominopelvic organs over extremities. Primary LMS of the penis is a relatively uncommon mesenchymal tissue disease and a poorly understood condition.
**Case Report:** A 69-year-old man presented with a growing, painless mass protruding from the penis. The irregularly lobulated lump was roughly 3 cm × 2.5 cm, with a smooth surface, tough texture, distinct boundary, and no tenderness. It was determined to be a penile tumor during the preoperative radiological evaluation. The patient underwent resection of the penile mass, followed by extended resection in the second operation. The diagnosis of LMS was verified by pathological examination. During a 20-month follow-up, the patient made a smooth recovery and remained disease-free.
**Conclusion:** An immunohistochemical examination is essential for rendering this rare diagnosis. Radical excision of tumor lesions with negative cut margins is guaranteed to be the best treatment for primary penile LMS. Close follow-up should be provided due to the high rate of local recurrence.

KEYWORDS
penis, leiomyosarcoma (LMS), case report, malignant mesenchymal tumors, urogenital neoplasms

## Introduction

Malignant tumors of the penis are relatively rare, with an incidence of about 1 per 100,000 in developed countries such as North America and Europe; however, the incidence in less economically developed regions such as Asia, Africa, and South America is slightly higher than that in the aforementioned developed regions. The majority of penile malignant tumors (95%) are squamous cell carcinoma, while adenocarcinoma, malignant melanoma, and sarcoma are sporadic (1). Malignant mesenchymal tissue tumors (including Kaposi's sarcoma, smooth muscle sarcoma, rhabdomyosarcoma, and malignant fibrous histiocytoma) account for less than 5%, among which primary leiomyosarcoma (LMS) of the penis is incredibly uncommon, mostly affecting middle-aged and older males (2). In 1969, Pratt and Ross (3) first classified LMS of the penis into deep and superficial types according to the tumor

site. Since deep LMS has early metastasis and poor prognosis, early diagnosis and correct identification of the type are crucial.

A 69-year-old patient with primary penile LMS was admitted to our hospital in March 2021. This article, which is based on the CARE Guideline (4) and includes a reporting checklist in the **supplementary material**, analyzes the case data of this patient and reviews the pertinent literature to discuss the clinical manifestations, diagnosis, and treatment of primary penile LMS in order to better understand and diagnose it.

## Case presentation

A 69-year-old male patient was admitted to the hospital with a 3-year painless mass in the penis as his main complaint. Three years ago, the patient had a soy bean-sized, painless mass in the middle shaft of the penis with no obvious cause. No ulceration or effusion, urinary frequency, urgency, or urinary pain was present nor was there a fever or any other discomfort. The lump rapidly enlarged to a diameter of 3 cm 6 months ago, without any swelling, heat, pain, or any other discomfort. The patient had a history of hypertension and type 2 diabetes mellitus, both of which responded effectively to oral treatment.

Physical examination revealed an irregular lobulated mass measuring about 3 cm × 2.5 cm in the middle shaft part of the penis on the ventral side, with a smooth surface, tough texture, clear border, a moderate range of motion, and no tenderness. There was no visible skin ulceration on the surface, no redness or swelling of urethral orifice, and no aberrant secretion. The epididymis and bilateral testis were both normal, and there were no swollen lymph nodes in the inguinal region. The skin color of the scrotum was also normal.

Auxiliary examination revealed that the usual tests for blood, urine, stool, liver and kidney function, electrolytes, myocardial enzymes, coagulation function, and prostate-specific antigen were all normal. Preoperative pelvic magnetic resonance imaging (MRI) (male genital system) showed a nodular mixed signal shadow in the distal penis, with a size of about 31 mm × 27 mm × 22 mm, and a high signal on diffusion-weighted imaging (DWI). No noticeable large lymph nodes were seen in the pelvis (**Figure 1**). Preoperative ultrasonography showed that no enlarged lymph nodes were detected in the bilateral inguinal region.

Under intralesional anesthetic, the patient had the penile lump removed. The mass was in the lower fascia layer (Eberth fascia), totally excised, and there was no visible adhesion between it and the surrounding tissues.

Gross examination revealed a grey-yellow necrotic tumor, measuring 3 cm × 3 cm × 2.5 cm. Microscopic examination showed severe atypia and high mitoses. Immunohistochemical results showed that S-100 (−), CD34 (−), Ki-67 (about 70% +), P53 (consistent with wild type), smooth muscle actin (SMA) (+), Desmin (+), and Caldesmon (+). Results from immunohistochemistry and morphology were consistent with LMS (**Figure 2**).

Three weeks later, the patient was readmitted and an extended resection was performed under endotracheal anesthesia based on sufficient dialog with the patient and his families. The skin was excised from the surgical site within 3 cm, and subcutaneous tissue was dissected all the way to Buck's fascia. Postoperative pathology suggested no residual tumor cells.

There was no local discomfort after surgery and slight scarring at the wound; postoperative erectile function was basically the same as before. No local tumor recurrence, inguinal lymph node enlargement, and metastasis were noticed over the 20-month follow-up.

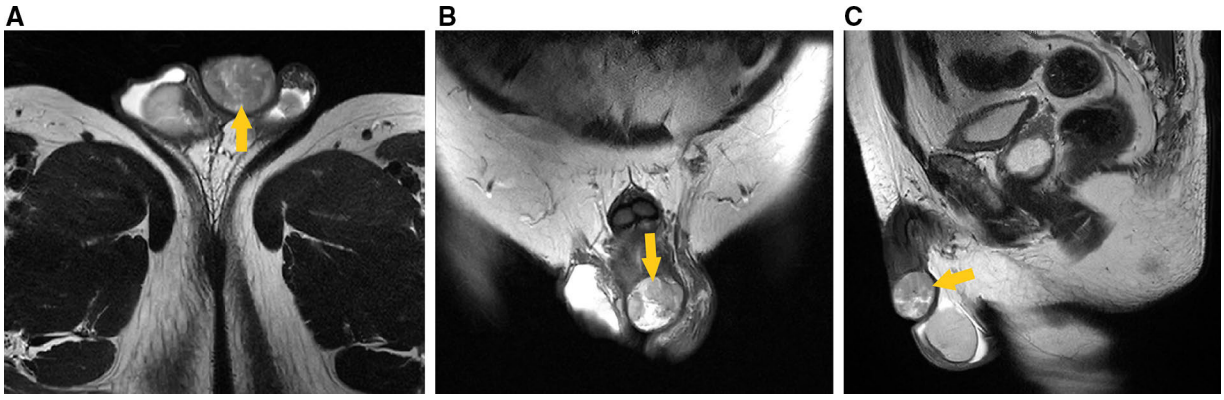


FIGURE 1
Preoperative pelvic MRI (male genital system) showed nodular mixed signal shadow in the distal penis (arrow head), with a size of about 31 mm × 27 mm × 22 mm, and a high signal on DWI. (A) Transverse section, T2-weighted imaging. (B) Coronal section, T2-weighted imaging. (C) Median sagittal section, T2-weighted imaging.

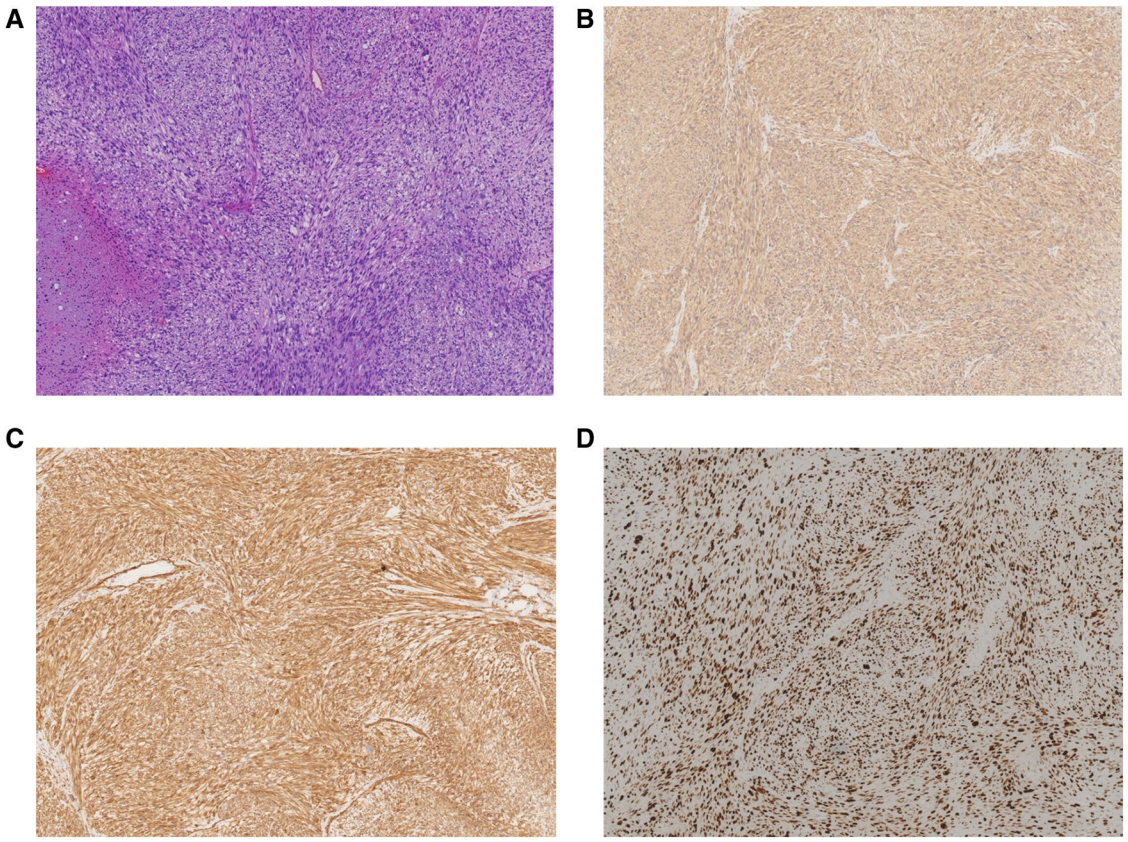


FIGURE 2
Pathological examination showing that the mass was composed of atypical spindle-shaped cells tumor with focal necrosis. (A) Hematoxylin and eosin (HE) staining with high mitoses and atypical mitoses (×40). (B) Immunohistochemistry staining of SMA (×40). (C) Immunohistochemistry staining of Caldesmon (×40). (D) Immunohistochemistry staining of Ki-67 (×40).

## Discussion

LMS is one of the most common subtypes of malignant mesenchymal tissue tumors, accounting for approximately 10%–20% of soft tissue sarcomas, which often affects the abdomen, retroperitoneum, large vessel wall, and uterus (5), and rarely involves the penis. Primary sarcomas of the penis also include Kaposi's sarcoma, epithelioid hemangioendothelioma, hemangiosarcoma, and rhabdomyosarcoma. Since Levi's initial report in 1930, 61 cases of primary LMS of the penis have been reported in English (**Table 1**), ranging in age from 6 to 84 years, with cases most frequently occurring in people in their forties and fifties (6–9). Penile LMS often originates from the following structures: (1) the dermal layer of the erector spinae; (2) the superficial fascial muscular layer of the penis; (3) the muscular layer of the superficial vessels outside the tunica albuginea; and (4) the muscular layer of the deep vascular complex that make up the corpus cavernosum and corpus spongiosum. With the tunica albuginea acting as the boundary, it can be divided into deep LMS and superficial LMS. Superficial LMS mostly appears on the surface of the distal penis or glans and is characterized by painless nodules, sluggish development, and a few deep infiltrations. Deep LMS, however, can involve the smooth muscle of the corpus cavernosum and invade the urethra and other surrounding structures (10).

LMS of the penis can present with a variety of clinical manifestations, such as painless nodules or masses, localized pain and swelling, superficial skin ulceration, hematuria, urethral obstruction, and enlargement of inguinal lymph node. In comparison to superficial LMS, deep LMS located below the deep fascia of the penis are more likely to manifest with hematuria and urethral obstruction (10). The most frequent location of tumor was the shaft, followed by the prepuce, whereas the coronal sulcus, the frenulum, and circumcision scars were additional uncommon locations (2).

Due to the rarity of penile LMS and the lack of distinct clinical symptoms, tumor excision and biopsy are typically required for diagnosis. A careful inspection of the lesion and palpation of the inguinal lymph nodes are required if a clinical suspicion of soft tissue sarcoma is strong. It is preferable to use MRI to demonstrate the depth of tumor invasion and evaluate

TABLE 1 Reported cases of leiomyosarcoma of the penis.

| Case | Author | Age (years) | Tumor size (cm) | Anatomic location | Treatment | Course and follow-up |
|---|---|---|---|---|---|---|
| 1 | Levi (1930) (11) | 38 | NA (small nodule) | Superficial on dorsum of distal shaft | Small nodule since childhood. Local excision at 36 | No follow-up |
| 2 | Kreibig (1931) (12) | 46 | NA (small nodule) | Superficial on dorsum of distal shaft | At ages 12 and 39, small nodule removed from prepuce; histology unknown. At 46, radical amputation after failed radiation | No follow-up |
| 3 | Meller (1932) (13) | 64 | NA | Superficial, proximal to coronal sulcus | Radiotherapy and eventual amputation | No follow-up |
| 4 | Ashley and Edwards (1957) (14) | 49 | NA (>2) | Superficial, proximal to coronal sulcus | Local excision followed by recurrence after 18 years | Well 18 months after second operation |
| 5 | Fagundes et al. (1962) (15) | 52 | NA | Deep, adherent to urethra at root of penis | Local excision with three recurrences over 5 years. Radiotherapy and eventual amputation | Well 10 months after amputation |
| 6 | Izdebski and Wiercinski (1962) (16) | 31 | NA | Deep, adherent to corpus cavernosum | Refused treatment | Dead 3 years later with widespread metastases |
| 7 | Pack et al. (1963) (17) | 83 | 4 | Deep, root of penis | Radiotherapy and eventual amputation | Dead 2 years later with lung metastases |
| 8 | Chaudhuri and Balasubrahmanyan (1966) (18) | 40 | 6 | Superficial on left side of prepuce | Radical amputation | Alive, well 3 years later |
| 9 | Bakken et al. (1968) (19) | 60 | 19 | Deep, bulbous portion of corpus spongiosum | Radical amputation | Dead 6 months later with widespread metastases |
| 10 | Hutcheson et al. (1969) (20) | 63 | NA (>4.5) | Superficial, dorsal aspect of midshaft of penis | Local excision with recurrences at 3 and 8 years. Radiotherapy and eventual amputation | No recurrence after radical excision |
| 11 | Pratt and Ross (1969) (3) | 38 | 3 | Deep, root of penis | Radical amputation | Alive, well 2 years after operation |
| 12 | Dehner and Smith (1970) (1) | 67 | NA | Superficial on dorsal shaft of distal penis | Local excision | No follow-up |
| 13 | Dehner and Smith (1970) (1) | 45 | 3 | Superficial on dorsum of shaft | Local excision | Well 1 year later |
| 14 | Greenwood et al. (1972) (21) | 64 | NA | Superficial near frenulum | Radiotherapy. Eventual partial amputation 2 years later | Alive, well 1 year after operation |
| 15 | Glucker et al. (1972) (22) | 6 | NA | Superficial, dorsum of glans | Local excision | Alive, free from recurrence at 1 year |
| 16 | Nkposong and Osunkoya (1972) (23) | 52 | NA | Deep in right corpus cavernosum | Local excision | Dead 3 months after operation |
| 17 | Gupta et al. (1973) (24) | 60 | 10.5 | Deep in distal part of shaft and glans | Radical amputation | Dead 5 months later with widespread metastases |
| 18 | Prabhakar et al. (1975) (25) | 54 | | | Penectomy | |

(*continued*)

TABLE 1 Continued

| Case | Author | Age (years) | Tumor size (cm) | Anatomic location | Treatment | Course and follow-up |
|---|---|---|---|---|---|---|
| | | | | Deep, anterior portion of shaft | | Dead 1 month after operation with lung metastases |
| 19 | Hamal (1975) (26) | 84 | NA | Glans penis at the coronal sulcus | Partial amputation | Alive, free from recurrence for 6 months |
| 20 | Blath and Manley (1975) (27) | 44 | 5 (multinodular) | Prepuce | Wide circumcision | Well 1 year later and free from recurrence |
| 21 | Armijo et al. (1978) (28) | 70 | NA | Glans and prepuce | Local excision, followed by another local excision | No recurrence after 8 months |
| 22 | Elem and Nieslanik (1979) (29) | 60 | NA | Deep, corpus spongiosum | Partial amputation | Dead 1 month after operation with lung metastases |
| 23 | Weinberger et al. (1982) (30) | 47 | 1 | Superficial, proximal to coronal sulcus | Local excision | Well 9 months after surgery |
| 24 | Jain et al. (1982) (31) | 55 | 5 | Superficial involving the glans of penis | Total amputation | Well 18 months after surgery |
| 25 | McDonald et al. (1983) (32) | 62 | 8 | Deep in right corpus cavernosum | Chemotherapy followed by emasculation and radiotherapy | Dead 7 months after initial diagnosis |
| 26 | Isa et al. (1984) (33) | 39 | NA (small nodule) | Superficial on dorsal shaft of penis | Local excision, then partial penectomy. Right groin dissection with radiotherapy 18 years later | Alive, well 1 year following groin dissection |
| 27 | Smart (1984) (34) | 61 | NA | Deep, root of penis | Radical penectomy and radiotherapy | Well at 6 months |
| 28 | Valadez and Waters (1986) (35)/Kathuria et al. (1986) (36)/Fetsch et al (2004) (37) | 45 | 2 | Superficial on prepuce | Circumcision | Well at 18 months |
| 29 | Koizumi, et al. (1987) (38) | 53 | NA | Glans | Partial penectomy | Well at 12 months |
| 30 | Pow-Sang and Orihuela (1994) (39) | 44 | NA | Superficial on prepuce | Wide circumcision | Well at 28 months |
| 31 | Dobos et al. (2001) (40) | 38 | 2.5, 0.4, and 0.3 | Glans and shaft | Radical amputation | Alive with widespread metastases, 6 months after surgery |
| 32 | Katsikas et al. (2002) (8) | 78 | 8, 8, and 14 | Penile root, midshaft | Radical penectomy | No recurrence after 2 years |
| 33 | Dominici et al. (2004) (10) | 53 | 2 × 1 | Superficial on prepuce | Circumcision. Partial penectomy at 4 year recurrence | Well 12 months after second operation |
| 34 | Fetsch et al. (2004) (37) | 43 | 2 | Circumcision scar | Local excision | NA |
| 35 | Fetsch et al. (2004) (37) | 45 | 2.4 | Dorsolateral midshaft | Local excision | NA |
| 36 | Fetsch et al. (2004) (37) | 49 | 1.5 | Circumcision scar and distal shaft | Local excision | Recurrence after 1 year → local excision → recurrence after 3 years → partial amputation → no recurrence after 5 years 8 months |
| 37 | Fetsch et al. (2004) (37) | 53 | 0.5 | Base of shaft at junction with abdominal wall | Local excision | No recurrence after 5 years 2 months |

(*continued*)

TABLE 1 Continued

| Case | Author | Age (years) | Tumor size (cm) | Anatomic location | Treatment | Course and follow-up |
|---|---|---|---|---|---|---|
| 38 | Fetsch et al. (2004) (37) | 53 | 0.9 | Lateral shaft, near base | Local excision | No recurrence after 11 years |
| 39 | Fetsch et al. (2004) (37) | 59 | 1.2 | Prepuce and distal shaft | Local excision | NA |
| 40 | Fetsch et al. (2004) (37) | 61 | 2 | Shaft | Local excision | No recurrence after 13 years 11 months |
| 41 | Fetsch et al. (2004) (37) | 62 | 0.7 | Circumcision scar | Local excision | No recurrence after 16 years 1 month |
| 42 | Fetsch et al. (2004) (37) | 43 | Multiple pieces to 2 | Periurethral (shaft) | Local excision | No recurrence after 18 years 7 months |
| 43 | Fetsch et al. (2004) (37) | 47 | 1.5 | Shaft | Local excision, local excision, wide local excision | Recurrence after 2 years 4 months → local excision → recurrence after 3 months → wide local excision → no recurrence after 10 years 4 months |
| 44 | Fetsch et al. (2004) (37) | 48 | 1.5 | Penis, NOS | Local excision | NA |
| 45 | Fetsch et al. (2004) (37) | 58 | 6 | Penile root | Local excision | NA |
| 46 | Fetsch et al. (2004) (37) | NA | NA | Shaft | Local excision 5 and lymph node dissection | Local recurrence 4, followed 10 months later by a metastasis to left arm, then lost to follow-up |
| 47 | Mendis et al. (2005) (41) | 51 | NA | Glans | Local excision | No recurrence after 5 months |
| 48 | Nanri et al. (2006) (42) | 27 | 10 × 7 | Deep in penile root | Total penectomy and chemotherapy | died from disseminated disease 14 months after surgery |
| 49 | Cibull et al. (2008) (6) | 68 | 1.5 | Glans | Partial penectomy | No recurrence after 13 months |
| 50 | Sundersingh et al. (2009) (43) | 56 | 3.5 × 3 × 3 | Deep, glans and distal shaft | Total penectomy | No recurrence after 6 months |
| 51 | Lacarrière et al. (2011) (44) | 64 | NA (bilateral masses) | Deep, penile root | Local excision, total penectomy, and chemotherapy | Lung metastases after 2 months operation |
| 52 | Brisciani et al. (2012) (45) | 63 | 1.3 nodule | Distal shaft | Local excision | No recurrence after 3 months |
| 53 | Cigna et al. (2013) (2) | 62 | 2.2 × 1.5 | Dorsum of glans | Local excision | No recurrence after 1 year |
| 54 | D'Cruze et al. (2014) (46) | 59 | 4 | Glans | Partial penectomy | No recurrence after 11 months |
| 55 | Romero Gonzalez et al. (2015) (47) | 39 | 1 | Distal shaft | Local excision | No recurrence after 3 years 6 months |
| 56 | Khobragade et al. (2015) (9) | 26 | 4.7 × 3.7 × 5.4 | Penile root | Local excision | No recurrence after 2 years |
| 57 | Khobragade et al. (2015) (9) | 38 | 3 × 4 (multinodular) | Glans, proximal shaft | Total penectomy | No recurrence after 9 months |
| 58 | Rabinovich (2018) (48) | 39 | 2 | Superficial, prepuce | Wide circumcision | No recurrence after 9 months |
| 59 | Ajmal et al. (2022) (49) | 70 | 3 × 2.2 × 1.5 | Prepuce | circumcision | NA |
| 60 | da Costa Junior et al. (2022) (50) | 54 | 2.0 × 1.0 | Glans | Local excision (the surgical margin had neoplasm) | No recurrence after 5 months |
| 61 | Goyal et al. (2022) (51) | 70 | 6.5 × 5.5 | Glans, distal shaft | Partial penectomy | NA |
| 62 | Current report (2022) | 69 | 3 × 2.5 | Superficial, shaft | Local excision | No recurrence after 17 months |

NA, not available; NOS, not otherwise specified.

both inguinal and pelvic lymph nodes. Deep LMS is prone to blood metastases, with the lung and liver being the most common sites of metastasis; therefore, a simultaneous CT scan of the chest and abdomen is recommended for high-risk tumors.

The pathologic diagnosis often includes a pretreatment biopsy and further pathologic evaluation after the tumor has been surgically removed to differentiate it from other sarcomas (52). It is important to note that fine needle aspiration frequently yields inadequate tissue to make a diagnosis. LMS consists of cells with a smooth muscle spectrum; both superficial and deep LMS have the same characteristic histologic features: spindle-shaped cells, with eosinophilic cytoplasm, long rod-shaped and darkly stained nuclei (53). The mitotic rate and other mitotic variables could predict the tendency of tumor invasion to adjacent structures or metastasis (8). In immunohistochemistry, SMA, Desmin, and Caldesmon are typically positive, but none of these markers are specific for smooth muscle differentiation (53). Cytokeratin and S100 were negative and could be differentiated from epithelial tissue (39). Negative CD34 could be identified from Kaposi's sarcoma (46). Immunopositive results for P16 and P53 with high Ki-67 proliferation index are highly sensitive and specific for the distinction of LMS and leiomyoma (52).

The principle of treatment for primary penile LMS is currently considered to be radical resection of the tumor lesion (R0 surgery) with maximum local organs preservation. Whether local lesion excision, partial penectomy, or total penectomy is performed depends on tumor type, size, and presence of metastasis. Tumor size is one of the best predictors of outcome for primary LMS of penis, when stratified as follows: $\leq$2 vs. >2 cm and $\leq$5 vs. >5 cm (37). First, local lesion and extensive resection is the best choice for superficial LMS and $\leq$2 cm in diameter, and the prognosis is better because distant metastasis of superficial LMS is rare. Due to the risk of recurrence, it is important to ensure a safe margin. The most critical factor for recurrence-free survival is the microscope-negative tumor margin. The majority of studies recommend a margin of at least 1 cm, while some have found that a margin of 2–5 cm is associated with a decreased rate of recurrence after resection (54). For subcutaneous LMS of the skin, it is recommended and desirable for complete excision of the subcutaneous tissue with at least 2–3 cm of the skin margin and subcutaneous tissue (55). A second surgery was performed in our patient that included a deep subcutaneous tissue excision that reached the penile fascia (Buck's fascia) and an expanded excision of the skin that was removed within 3 cm of the surgical site margin. However, partial penile resection or radical excision is typically the mainstay of treatment for profound LMS (9). When distant metastasis has occurred, the aim of treatment includes symptom relief, tumor volume reduction, and prolonging survival. Because of rare local lymph node metastasis in LMS and the distant metastasis is often present when the peripheral lymph nodes are involved, regional lymph node dissection is not advised in the absence of clearly clinical or imaging evidence of lymph node metastasis (52).

Adjuvant radiation treatment (RT) and chemotherapy may help in the treatment of LMS in order to preserve organ function and reduce local recurrence, although with a limited impact on survival rates (52). In a retrospective study of 14 patients with primary penile LMS in 1994 (39), local tumor recurrence was found in all patients treated with chemotherapy or radiotherapy only, and distant metastasis was found in 2 of them. Hensley et al. (56) reported that gemcitabine combined with docetaxel chemotherapy was significantly effective as first- and second-line treatment for primary penile LMS. The effectiveness of adjuvant radiation and chemotherapy in treating primary penile LMS has not been verified because of the small number of cases.

Tumor size, tumor depth, and histologic grade are the main factors affecting the risk and prognosis of primary penile LMS, as with other soft tissue sarcomas. The American Joint Committee on Cancer (AJCC) grading system has a grading system that takes into account characteristics such as tumor size, lymph node involvement, and distant metastasis; however, no research has determined if penile LMS falls within this system. In the TNM grading system, T stage is divided into T1 and T2 stages with the maximum diameter of 5 cm, but the majority of penile LMS is less than 5 cm. Thus, a lower cut-off value could be more applicable. In addition, for penile LMS, T stage should distinguish the superficial type from the deep type according to the depth of invasion, rather than just by the size of tumor. Moreover, poor differentiation (grade 3 or 4) results in upstaging to stages II or III irrespective of the tumor size (55). The Fédération Nationale des Centres de Lutte Contre Le Cancer (FNCLCC) grading system is the most widely used in the histological grading of soft tissue sarcomas. Based on the degree of differentiation, mitosis, and tumor necrosis, the FNCLCC grading can be divided into X, 1, 2, and 3 grades. The higher the grade is, the worse the prognosis will be (57). Eventually, superficial penile LMS has a better prognosis than deep LMS, especially for primary LMS with infiltration depth $\leq$2 cm and size $\leq$5 cm and being treated by extensive local excision with negative incisional margins. However, larger and deep LMS, especially located at the root of the penis, usually have a poor prognosis (33).

Local recurrence may occur after the surgery of primary penile LMS, and tumor cells often become poorly differentiated after recurrence. For superficial and deep lesions, the recurrence rates are 23% and 29%, respectively. However, the risk rate of distant metastasis was higher for deep-type LMS (50%) compared to 8% for superficial LMS. In addition, the risk of metastasis increased with tumor size, with a 29% and 50% chance of metastasis for tumors with a diameter of 5 cm and greater. Local lymph node metastasis is uncommon and occurs mostly

in the advanced stages of the disease, when distant metastases are often already present and the prognosis is poor (37).

Follow-up guideline for primary penile LMS are little standardized and adapted from the soft tissue sarcomas in general (55). A complete examination, especially the operation site and inguinal lymph nodes, should be carried out every 3 months for 3 years after resection, every 6 months for the following 2 years, and then annually for up to 10 years. In high-risk cases (>5 cm tumor size, deep LMS, local relapse, high-grade LMS), chest CT should be performed every 3–6 months together with MRI of the primary tumor site and sonography of regional lymph nodes and abdomen.

Additionally, the patient underwent surgery twice. As an improvement measure, it is recommended to be alert to the possibility of malignant mass, particularly given its rapid growth during the last period of the present case, and intraoperative frozen section analysis is necessary. In addition, after local excision, expanded resection of the margins and base of the lesion for biopsy is advised.

## Conclusion

In summary, though primary LMS of penis is very rare, it is not difficult to diagnose when pathology is included. Patients with deep lesions are likely to experience distant metastases at an early stage, which often has a bad prognosis. The best therapy for primary penile LMS to date is assured to be radical removal of malignant lesions with negative cut margins, and close monitoring should be administered.

## Data availability statement

The original contributions presented in the study are included in the article/**Supplementary Material**, further inquiries can be directed to the corresponding authors.

## Ethics statement

The studies involving human participants were reviewed and approved by Peking University Third Hospital Ethics Committee. The patients/participants provided their written informed consent to participate in this study.

## Author contributions

All authors listed have made a substantial, direct, and intellectual contribution to the work and approved it for publication.

## Conflict of interest

The authors declare that the research was conducted in the absence of any commercial or financial relationships that could be construed as a potential conflict of interest.

## Publisher's note



## Supplementary material

The Supplementary Material for this article can be found online at: https://www.frontiersin.org/articles/10.3389/fsurg.2022.1068935/full#supplementary-material.

## References

1. Dehner LP, Smith BH. Soft tissue tumors of the penis. A clinicopathologic study of 46 cases. *Cancer*. (1970) 25(6):1431–47. doi: 10.1002/1097-0142(197006)25:6<1431::AID-CNCR2820250624>3.0.CO;2-B

2. Cigna E, Maruccia M, Parisi P, Soda G, Nasca MR, Micali G, et al. Superficial leiomyosarcoma of the glans: report of a case and literature review. *Aesthetic Plast Surg*. (2013) 37(5):1052–8. doi: 10.1007/s00266-013-0199-9

3. Pratt RM, Ross RT. Leiomyosarcoma of the penis. A report of a case. *Br J Surg*. (1969) 56(11):870–2. doi: 10.1002/bjs.1800561122

4. Riley DS, Barber MS, Kienle GS, Aronson JK, von Schoen-Angerer T, Tugwell P, et al. CARE guidelines for case reports: explanation and elaboration document. *J Clin Epidemiol*. (2017) 89:218–35. doi: 10.1016/j.jclinepi.2017.04.026

5. George S, Serrano C, Hensley ML, Ray-Coquard I. Soft tissue and uterine leiomyosarcoma. *J Clin Oncol*. (2018) 36(2):144–50. doi: 10.1200/JCO.2017.75.9845

6. Cibull TL, Thomas AB, Badve S, Billings SD. Leiomyosarcoma of the penis presenting as a cutaneous lesion. *J Cutan Pathol*. (2008) 35(6):585–7. doi: 10.1111/j.1600-0560.2007.00846.x

7. Trivedi VAM, Rani R, Chauhan R, Singh U, Kuna N. Leiomyosarcoma of penis: an aggressive and exceptionally rare entity. *Gulf J Oncol*. (2017) 1(25):73–6. PMID: 29019335

8. Katsikas VS, Kalyvas KD, Ioannidis SS, Papathanasiou MV, Panagiotopoulou KP, Hitiroglou PM, et al. Leiomyosarcoma of the penis. *Sarcoma*. (2002) 6(2):75–7. doi: 10.1080/1357714021000022177

9. Khobragade KH, Tamhankar AS, Bakshi GK, Tongaonkar HB, Menon S. Leiomyosarcoma of penis. *Indian J Cancer*. (2015) 52(3):374–5. doi: 10.4103/0019-509X.176719

10. Dominici A, Delle Rose A, Stomaci N, Pugliese L, Posti A, Nesi G. A rare case of leiomyosarcoma of the penis with a reappraisal of the literature. *Int J Urol*. (2004) 11(6):440–4. doi: 10.1111/j.1442-2042.2004.00806.x

11. Levi I. On a case of primary fibrosarcoma of the skin of the penis: clinical and histological study. *G Ital Dermatol.* (1930) 71:1559–74.

12. Kreibig W. Beitrag zur Diagnostik der Penissarkome. *Deutsche Zeitschrift für Chirurgie*. (1931) 231(2):277–84. doi: 10.1007/BF02795646

13. Meller H. Beitrag zur Kenntnis der Penissarkome. *Wien Klin Wschr*. (1932) 45:49–50.

14. Ashley DJ, Edwards EC. Sarcoma of the penis; leiomyosarcoma of the penis: report of a case with a review of the literature on sarcoma of the penis. *Br J Surg*. (1957) 45(190):170–9. doi: 10.1002/bjs.18004519011

15. Fagundes LA, Hampe O, Brentano L, Johann D. Leiomyosarcoma of the penis: a case report. *J Urol*. (1962) 88:803–4. doi: 10.1016/S0022-5347(17)64885-7

16. Izdebski M, Wiercinski J. A case of leiomyoscarcoma of the caveronoous bodies of the penis. *Patol Pol*. (1962) 13:397–402. PMID: 13957147

17. Pack GT, Trinidad SS, Humphreys GA. Primary leiomyosarcoma of the penis: report of a case. *J Urol*. (1963) 89:839–40. doi: 10.1016/S0022-5347(17)64658-5

18. Chaudhuri S, Balasubrahmanyan M. Leiomyosarcoma of the penis. A case report. *Indian J Pathol Bacteriol*. (1966) 9(3):278–84. PMID: 5966972

19. Bakken CL, Hanna EA, Seybold HM. Leiomyosarcoma of the penis. *J Urol*. (1968) 99(6):769–71. doi: 10.1016/S0022-5347(17)62789-7

20. Hutcheson JB, Wittaker WW, Fronstin MH. Leiomyosarcoma of the penis: case report and review of literature. *J Urol*. (1969) 101(6):874–5. doi: 10.1016/S0022-5347(17)62446-7

21. Greenwood N, Fox H, Edwards EC. Leiomyosarcoma of the penis. *Cancer*. (1972) 29(2):481–3. doi: 10.1002/1097-0142(197202)29:2<481::AID-CNCR2820290237>3.0.CO;2-Q

22. Glucker E, Hirshowitz B, Gellei B. Leiomyosarcoma of the glans penis. Case report. *Plast Reconstr Surg*. (1972) 50(4):406–8. doi: 10.1097/00006534-197210000-00026

23. Nkposong EO, Osunkoya BO. Leiomyosarcoma of the penis. Report of a case. *West Afr Med J Niger Pract*. (1972) 21(2):34–6. PMID: 5064420

24. Gupta S, Gupta IM, Bhatnagar BN. A rapidly fatal leiomyosarcoma of the penis with widespread metastasis. *Indian J Pathol Bacteriol*. (1973) 16(4):71–3. PMID: 4791526

25. Prabhakar BR, Sethi RS, Singh H, Tung BS, Prabhakar H. Leiomyosarcoma of penis. *Indian J Cancer*. (1975) 12(1):103–6. PMID: 1184063

26. Hamal PB. Leiomyosarcoma of penis—case report and review of the literature. *Br J Urol*. (1975) 47(3):319–24. doi: 10.1111/j.1464-410X.1975.tb03974.x

27. Blath RA, Manley CB. Leiomyosarcoma of the prepuce. *J Urol*. (1976) 115(2):220–1. doi: 10.1016/S0022-5347(17)59141-7

28. Armijo M, Herrera E, de Dulanto F, Naranjo R, Camacho F. Penile leiomyosarcoma. Ultrastructural study (author's transl). *Ann Dermatol Venereol*. (1978) 105(3):267–74. PMID: 677694

29. Elem B, Nieslanik J. Leiomyosarcoma of the penis. *Br J Urol*. (1979) 51(1):46. doi: 10.1111/j.1464-410X.1979.tb04244.x

30. Weinberger GI, Wajsman Z, Beckley S, Simpson CL. Primary sarcoma of penis. *Urology*. (1982) 19(2):193–4. doi: 10.1016/0090-4295(82)90580-5

31. Jain SS, Vohra RR, Kohli PK, Bharti. Leiomyosarcoma of penis (a case report). *J Postgrad Med*. (1982) 28(2):120b–2. PMID: 7131344

32. McDonald MW, O'Connell JR, Manning JT, Benjamin RS. Leiomyosarcoma of the penis. *J Urol*. (1983) 130(4):788–9. doi: 10.1016/S0022-5347(17)51464-0

33. Isa SS, Almaraz R, Magovern J. Leiomyosarcoma of the penis. Case report and review of the literature. *Cancer*. (1984) 54(5):939–42. doi: 10.1002/1097-0142(19840901)54:5<939::AID-CNCR2820540533>3.0.CO;2-Y

34. Smart RH. Leiomyosarcoma of the penis. *J Urol*. (1984) 132(2):356–7. doi: 10.1016/S0022-5347(17)49624-8

35. Valadez RA, Waters WB. Leiomyosarcoma of penis. *Urology*. (1986) 27(3):265–7. doi: 10.1016/0090-4295(86)90287-6

36. Kathuria S, Jablokow VR, Molnar Z. Leiomyosarcoma of penile prepuce with ultrastructural study. *Urology*. (1986) 27(6):556–7. doi: 10.1016/0090-4295(86)90345-6

37. Fetsch JF, Davis Jr. CJ, Miettinen M, Sesterhenn IA. Leiomyosarcoma of the penis: a clinicopathologic study of 14 cases with review of the literature and discussion of the differential diagnosis. *Am J Surg Pathol*. (2004) 28(1):115–25. doi: 10.1097/00000478-200401000-00014

38. Koizumi H, Nagano K, Kosaka S. A case of penile tumor: combination of leiomyosarcoma and squamous cell carcinoma. *Hinyokika Kiyo*. (1987) 33(9):1489–91. PMID: 3324745

39. Pow-Sang MR, Orihuela E. Leiomyosarcoma of the penis. *J Urol*. (1994) 151(6):1643–5. doi: 10.1016/S0022-5347(17)35328-4

40. Dobos N, Nisenbaum HL, Axel L, Van Arsdalen K, Tomaszewski JE. Penile leiomyosarcoma: sonographic and magnetic resonance imaging findings. *J Ultrasound Med*. (2001) 20(5):553–7. doi: 10.7863/jum.2001.20.5.553

41. Mendis D, Bott SR, Davies JH. Subcutaneous leiomyosarcoma of the frenulum. *ScientificWorldJournal*. (2005) 5:571–5. doi: 10.1100/tsw.2005.76

42. Nanri M, Kondo T, Okuda H, Tanabe K, Toma H. A case of leiomyosarcoma of the penis. *Int J Urol*. (2006) 13(5):655–8. doi: 10.1111/j.1442-2042.2006.01376.x

43. Sundersingh S, Majhi U, Narayanaswamy K, Balasubramanian S. Primary leiomyosarcoma of the penis. *Indian J Pathol Microbiol*. (2009) 52(3):447–8. doi: 10.4103/0377-4929.55028

44. Lacarrière E, Galliot I, Gobet F, Sibert L. Leiomyosarcoma of the corpus cavernosum mimicking a Peyronie's plaque. *Urology*. (2012) 79(4):e53–4. doi: 10.1016/j.urology.2011.07.1410

45. Brisciani A, Brassetti A, Lauretti S, Mosca A, D'Alfonso V. Primary penile leiomyosarcoma: case report and review of the literature. *Urologia J*. (2012) 79(4):271–7. doi: 10.5301/RU.2012.9940

46. D'Cruze L, Boobala A, Balasubramanian S, Rajendiran S, Joseph LD. Primary leiomyosarcoma of the penis: a case report. *J Clin Diagn Res*. (2014) 8(1):162–3. doi: 10.7860/JCDR/2014/6723.3808

47. Romero Gonzalez EJ, Marenco Jiménez JL, Mayorga Pineda MP, Martínez Morán A, Castiñeiras Fernández J. Leiomyosarcoma of the penis, an exceptional entity. *Urol Case Rep*. (2015) 3(3):63–4. doi: 10.1016/j.eucr.2014.12.007

48. Rabinovich J. Leiomyosarcoma of the foreskin: a rare case of mesenchymal foreskin tumor. *Urol A*. (2018) 57(5):591–3. doi: 10.1007/s00120-018-0577-7

49. Ajmal Z, Khan AM, Zahra FT, McCarthy L, O'Malley R, Mehdi S. Leiomyosarcoma of the penis: a case report and re-appraisal. *Fed Pract*. (2022) 39(Suppl 2):S58–S61. doi: 10.12788/fp.0232

50. da Costa Junior RNG, Teixeira Júnior AAL, Rocha TMS, Sobrinho TBM, Barbosa LO, Silva RC, et al. Primary leiomyosarcoma of the glans. *Front Oncol*. (2022) 12:851003. doi: 10.3389/fonc.2022.851003

51. Goyal N, Menon S, Pal M. Primary leiomyosarcoma of the penis: a rare penile neoplasm. *Med J Armed Forces India*. (2022) 78(3):365–7. doi: 10.1016/j.mjafi.2022.02.004

52. Mangla A, Yadav U. *Leiomyosarcoma*. Treasure Island, FL: StatPearls (2021).

53. Serrano C, George S. Leiomyosarcoma. *Hematol Oncol Clin North Am*. (2013) 27(5):957–74. doi: 10.1016/j.hoc.2013.07.002

54. Tsutsumida A, Yoshida T, Yamamoto Y, Itoh T, Minakawa H, Sugihara T. Management of superficial leiomyosarcoma: a retrospective study of 10 cases. *Plast Reconstr Surg*. (2005) 116(1):8–12. doi: 10.1097/01.PRS.0000169711.70525.10

55. Zacher M, Heppt MV, Brinker TJ, Hayani KM, Flaig MJ, Berking C. Primary leiomyosarcoma of the skin: a comprehensive review on diagnosis and treatment. *Med Oncol*. (2018) 35(10):135. doi: 10.1007/s12032-018-1196-2

56. Hensley ML, Maki R, Venkatraman E, Geller G, Lovegren M, Aghajanian C, et al. Gemcitabine and docetaxel in patients with unresectable leiomyosarcoma: results of a phase II trial. *J Clin Oncol*. (2002) 20(12):2824–31. doi: 10.1200/JCO.2002.11.050

57. Kazlouskaya V, Lai YC, Khachemoune A. Leiomyosarcoma of the skin: review of the literature with an emphasis on prognosis and management. *Int J Dermatol*. (2020) 59(2):165–72. doi: 10.1111/ijd.14705

frontiers | Frontiers in Oncology

TYPE Case Report
PUBLISHED 10 January 2023
DOI 10.3389/fonc.2022.1062389



OPEN ACCESS

EDITED BY
Riccardo Bertolo,
Hospital San Carlo di Nancy, Italy

REVIEWED BY
Kirill Lyapichev,
University of Texas Medical Branch at Galveston, United States
Matteo Vittori,
Hospital San Carlo di Nancy, Italy

*CORRESPONDENCE
Marco Clementi
marco.clementi@univaq.it

SPECIALTY SECTION
This article was submitted to Surgical Oncology, a section of the journal Frontiers in Oncology

RECEIVED 05 October 2022
ACCEPTED 14 December 2022
PUBLISHED 10 January 2023

CITATION
Cappelli S, Marchesi F, Clementi M, Perracchio L, Palombi F, Pelle F, Botti C and Costantini M (2023) Reverse strategy to locally advanced breast implant-associated anaplastic large cell lymphoma: A case report. *Front. Oncol.* 12:1062389. doi: 10.3389/fonc.2022.1062389



# Reverse strategy to locally advanced breast implant-associated anaplastic large cell lymphoma: A case report

Sonia Cappelli[1], Francesco Marchesi[2], Marco Clementi[3*], Letizia Perracchio[4], Francesca Palombi[2], Fabio Pelle[1], Claudio Botti[1] and Maurizio Costantini[5]

[1]Department of Surgery, Division of Breast Surgery, Istituti di Ricovero e Cura a Carattere Scientifico (IRCCS) Regina Elena National Cancer Institute, Rome, Italy, [2]Hematology Unit, Department of Research and Clinical Oncology, Istituti di Ricovero e Cura a Carattere Scientifico (IRCCS) Regina Elena National Cancer Institute, Rome, Italy, [3]Department of Applied Clinical Sciences and Biotechnology, University of L'Aquila, L'Aquila, Italy, [4]Pathology Department, Istituti di Ricovero e Cura a Carattere Scientifico (IRCCS) Regina Elena National Cancer Institute, Rome, Italy, [5]Department of Surgery, Division of Plastic and Reconstructive Surgery, Istituti di Ricovero e Cura a Carattere Scientifico (IRCCS) Regina Elena National Cancer Institute, Rome, Italy

Breast implant-associated anaplastic large cell lymphoma (BIA-ALCL) is a rare T-cell lymphoma associated with textured breast implants. The most common presentation is a periprosthetic seroma that occurs at least 1 year after an aesthetic or reconstructive implantation, and in these cases, the surgical treatment seems to be successful. More rarely, BIA-ALCL presents with locally advanced mass-formed disease and a related regional lymph node involvement. In all these cases with worse prognosis, a multidisciplinary approach is required, including adjuvant chemotherapy, radiation therapy, and surgery. We present a clinical case of a 49-year-old woman who developed on the left side of the breast a mass-formed stage 3 BIA-ALCL 15 years after a bilateral breast augmentation with textured silicone implant. Our multidisciplinary team (MDT) scheduled the patient for a "reverse-strategy" sequential approach consisting of induction chemotherapy, hematopoietic stem cell mobilization, and harvest followed by autologous stem cell transplant (ASCT). After 100 days from the stem cell transplant, the patient showed a complete pathologic response and was a candidate for radical surgery. She underwent removal of both implants with total en bloc capsulectomy. On the left site, the periprosthetic mass was also en bloc removed. We did not perform any axillary dissection. Our surgical and hemato-oncological teams followed the patient every 3 months, and no local or systemic recurrences were observed 24 months after surgery. This case report has demonstrated the effectiveness of neoadjuvant chemotherapy

as part of a "reverse strategy" in selected cases of advanced-stage BIA-ALCL in which it was not possible to perform an immediate radical surgery. Furthermore, in our case, the de-escalation strategy adopted permitted a less demolitic surgery with good functional and aesthetic results.

KEYWORDS

**breast implant-associated anaplastic large cell lymphoma (BIA-ALCL), reverse-strategy, neoadjuvant chemotherapy, stem cell transplant, conservative surgery**

## Introduction

Breast implant-associated anaplastic large cell lymphoma (BIA-ALCL) is a recently recognized non-Hodgkin lymphoma of T-cell origin. Despite its low incidence, the increasing use of breast implants for aesthetic reconstruction or post-mastectomy purposes poses BIA-ALCL as an emerging medical challenge (1). All clinical case reports have demonstrated a strong relationship between BIA-ALCL and textured breast implants.

Although most patients with BI-ALCL have a relatively indolent clinical course presenting as a delayed effusion or persistent seroma around the implants, one-third of the cases develop a peri-capsular mass and a small number of lymph-node involvement or distant disease (2, 3).

The National Comprehensive Cancer Network (NCCN) guidelines and the UK guidelines on the Diagnosis and Treatment of BIA-ALCL suggest that during the early stage, surgical removal of the implant with the surrounding capsule intact usually has a curative effect. For mass-forming cases, surgery was also indicated with a total en bloc capsulectomy with removal of any associated mass and abnormal regional lymph nodes followed by adjuvant chemotherapy and/or radiotherapy (4, 5). In advanced-stage patients, the role of neoadjuvant therapy has not been investigated yet.

We report a case of a woman with locally advanced BIA-ALCL treated with an unconventional combined approach in which a sequential chemotherapeutic program was applied in a neoadjuvant setting (reverse strategy).

## Case report

A 49-year-old woman with a history of bilateral breast augmentation with silicone implant macro textured 15 years earlier presented with the appearance of a palpable large mass associated with a volumetric increase of the left breast. She had no postoperative complications or previous trauma to the breast, nor did she undergo any additional breast surgery before presentation to the clinic. The patient did not show any significant previous clinical history or relevant comorbidities. Clinical examination revealed swelling, erythema, palpable mass, and *peau d'orange* on the left breast (Figures 1A, B). The patient underwent breast ultrasound and magnetic resonance imaging. The latter showed signs of intracapsular ruptures.

On the same side, it had morbid tissue with a necrotic component localized in the external quadrant extending from the skin to the muscle layer (4 × 8 cm); the local swelling and the increase in skin thickness affect all the breast tissue. In addition, suspicious axillary lymph nodes have been reported in the same side. Given the complexity of the case, the patient was sent to our Breast Surgery Department of the "Regina Elena National Cancer Institute" in Rome, considered as a reference point in central-southern Italy for breast cancer (6, 7). We subjected the patient to 18-FDG positron emission tomography/computed tomography scan (PET/TC), which showed a focal increase of the left breast tissue intake (SUV max 39.4) going from the skin to the muscular layer of the outer quadrants and of the axillary and retro-pectoral lymph nodes (SUV max 7.8; dmt max 26 mm). Clinical and radiographic evaluations of the right breast did not show any abnormalities. The patient was subjected to fine needle aspiration of mass; cytology exam showed round, large cells with pleomorphic and cerebroid nuclei (CD45+++, Vimentin++, Keratin−). The following percutaneous biopsy of the mass demonstrated a proliferation of phenotypically aberrant population of large cells that expressed CD30 and CD45, negative for CD3, CD20, and ALK1, diagnostic for anaplastic large cell lymphoma, ALK-negative (ALK-ALCL) (Figures 2A, B) (8).

Following a multi-disciplinary tumor board discussion, involving hematologists, surgeons, pathologists, and radiotherapists, an immediate surgical treatment was considered not indicated, as a consequence of the extremely advanced disease stage not allowing a minimally invasive surgical intervention. After the administration of informed consent, we decided first to start a sequential chemotherapeutic approach consisting of induction chemotherapy, hematopoietic stem cell mobilization, and harvest followed by autologous stem cell transplant (ASCT), according to our institutional policy and international guidelines about treatment of advanced-stage ALK-negative peripheral T-

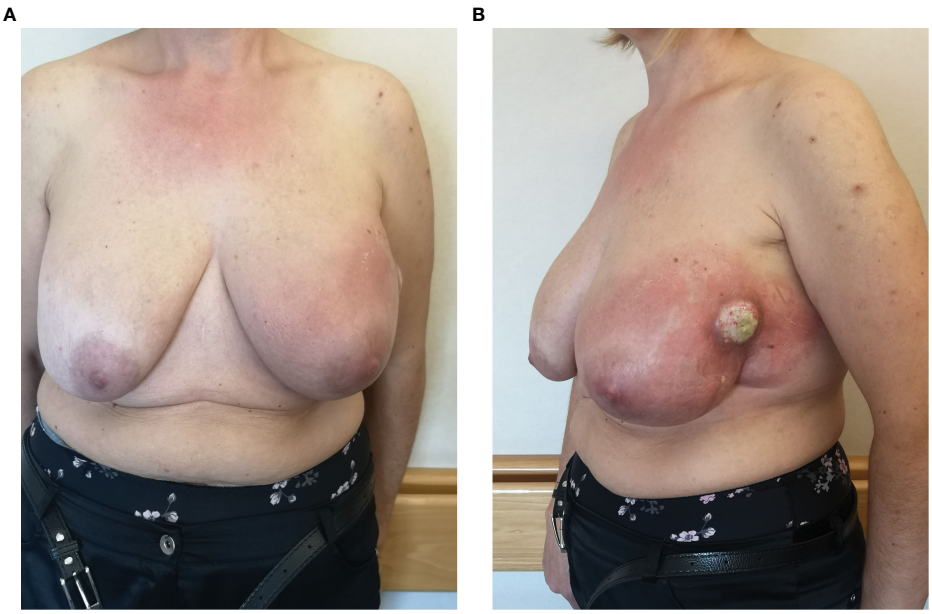

FIGURE 1
Clinical presentation at the recruitment: frontal view **(A)** and lateral view **(B)**.

cell lymphoid malignancies (9–12). In particular, induction chemotherapy consisted of six courses of alternating CHOEP (cyclophosphamide, vincristine, doxorubicin, etoposide, and prednisone; three cycles) and DHAP (cisplatin, cytarabin, and dexamethasone; three cycles). Hematopoietic stem cells were collected after the last DHAP cycle (CD34+ $\times$ $10^6$/kg collected: 7.024). At the end of the induction phase, a disease assessment performed by a CT/PET scan showed a complete remission. Afterwards, a consolidation treatment with ASCT after BEAM conditioning regimen (BCNU, etoposide, cytarabine, and melphalan) was finally performed (Figures 3A, B).

One hundred days after the stem cell transplant, she underwent removal of both implants with total en bloc capsulectomy. On the left, the site of the periprosthetic mass was also removed (Figures 4A, B).

We did not perform any axillary dissection. The histology, performed as reported by Lyapichev et al. (13), revealed a complete pathologic response with CD30 immunohistochemistry negative (Figures 5A, B).

Given his complete pathological response, multidisciplinary consensus did not consider adjuvant radiotherapy necessary. The patient was followed by our surgical and hemato-

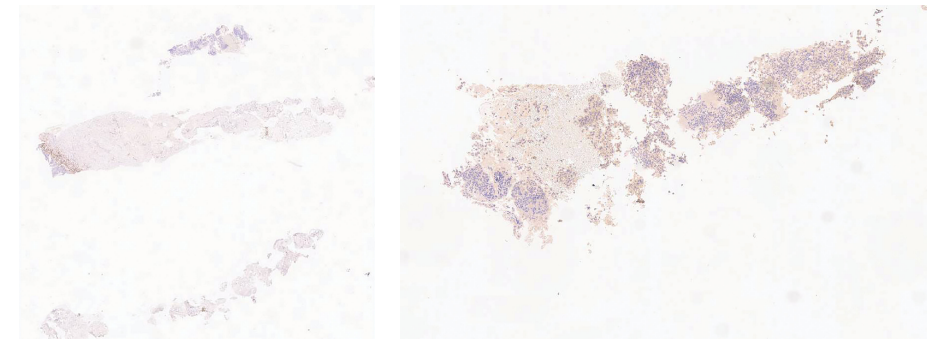

FIGURE 2
Fine needle cytology: neoplastic proliferation of large round cells with pleomorphic nuclei, negative for epithelial marker CK **(A)** and positive for linfoid marker and vimentin **(B)**.

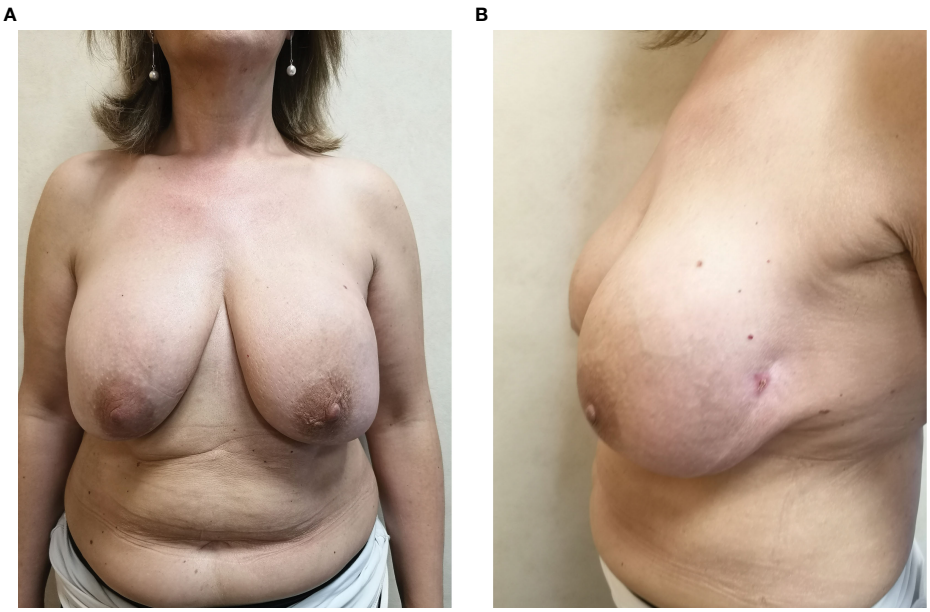

FIGURE 3
Clinical response after chemotherapy: frontal view **(A)** and lateral view **(B)**.

oncological teams every 3 months and no local or systemic recurrences were observed 24 months after surgery.

## Discussion

BIA-ALCL has been identified as an emerging disease entity and represents a novel variant of the clinic pathologic subtypes of anaplastic large cell lymphoma (ALCL) associated with breast implants with a textured outer. Since its first description in 1997 by Keech and Creech (1, 14), an increasing number of cases have been reported in literature (15), and recently, the World Health Organization has listed BIA-ALCL as a unique pathological entity (16).

The most common presentation of BIA-ALCL is a large spontaneous periprosthetic fluid collection occurring at least 1 year and on the average from 7 to 10 years following the implantation with a textured surface breast implant. In addition to large fluid collections and delayed seromas, 8% to 24% of patients present an associated palpable mass and 4% to 12% present with lymphadenopathy (4). Less than 5% of the cases are unfrequently described and manifest local and systemic signs, such as rash, fever, and capsular contracture (17).

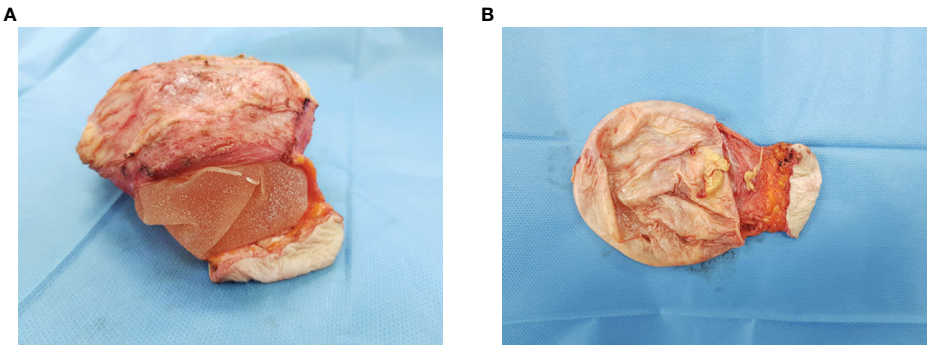

FIGURE 4
Surgical specimen: implants with total en bloc capsulectomy **(A)** and periprosthetic tissue previously involved by BIA-ALCL **(B)**.

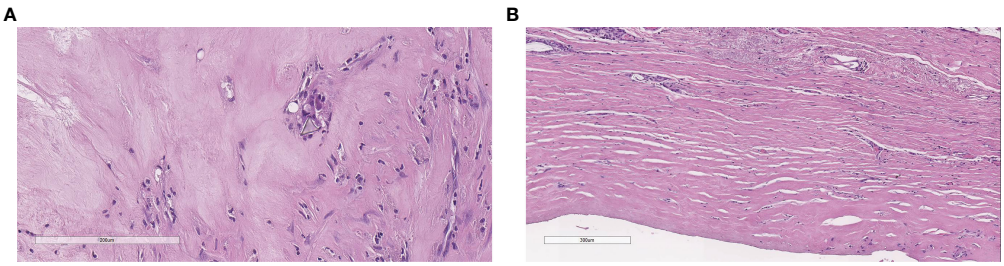


FIGURE 5
Complete pathological response: histology does not show neoplastic cells with a polyurethane crystal and rare inflammatory cells **(A)**, flat synovial metaplasia, and foreign body giant cell granulomas **(B)**.

Surgical excision is the established standard of care to treat the localized disease, but the BIA-ALCL treatment algorithm suggested by international guidelines is limited in case of unusual, progressive, or complex patient scenarios (18, 19). This smaller subset of patients that present with a tumor mass associated with the fibrous capsule or lymph node involvement are more likely to have worse prognosis. Miranda et al. found that only 72% of patients with tumor masses achieved remission, as opposed to 93% when disease was confined to the fibrous capsule (20). Ferrufino-Schmidt et al. found out a significant reduction in 5-year overall survival in patients with lymph node involvement compared to patients who are not clinically or radiologically suspected to have lymph node disease (75% vs. 97.8%) (21).

Our clinical case falls into one of those advanced BIA-ALCL stages (stage III) (13, 22) with worse prognosis. The patient had a large mass forming on the left side extending from the skin to the muscle layer and suspected ipsilateral axillary lymph nodes.

Our multidisciplinary oncology board, which involved hematologists, surgeons, pathologists, and radiotherapists, did not consider the patient as a candidate for immediate surgery due to the advanced stage of the disease. Such an intervention would have been extremely destructive and not safe. Keeping in mind the importance of obtaining safe negative surgical margins and conservative surgery with oncoplastic techniques, the patient was scheduled to administer chemotherapy and ASCT before surgery, reversing the commonly recommended strategy (reverse strategy).

In accordance with our institutional policy and international guidelines about treatment of advanced-stage ALK-negative peripheral T-cell lymphoid malignancies (9–12), patients were submitted to induction chemotherapy by six courses of alternating CHOEP and DHAP. Finally, a consolidation treatment with ASCT after BEAM conditioning regimen was performed. The chemotherapeutic regimen used in our patients is in line with the regimen proposed in literature to treat advanced BIA-ALCL in an adjuvant setting (4, 5). At the end of the induction phase, a clinical and radiological restaging manifested a complete remission of the disease.

Keeping in mind the pivotal role of "free" surgical margins to reduce local recurrences (22), the surgical procedure performed on treated tissue allows for a less destructive surgery without compromising its radical nature. In our case, a radiological complete remission was obtained, 100 days from the stem cell transplant; the patient underwent bilateral capsulectomy with, on the left side, a local excision of previous pericapsular mass to ensure that no tumor was present at the margins.

Contrary to guideline recommendations, we did not perform any axillary dissection, despite the initial suspicion of multi-lymphonodal involvement. A complete response was obtained for the concomitant axillary lymph node, as expected after the medical management of common ALCL so that we avoided needless axillary dissection. Our patient was not interested in maintaining an enlarged breast and asked to avoid an immediate reconstruction with smooth implants. At follow-up, a device-free reconstruction was planned, leaving the breast in a natural-looking shape. Two other cases, in which neoadjuvant therapy has been administered to treat advanced BIA-ALCL, have been reported in the literature (18, 19).

In both cases, a complete pathological response was achieved after neoadjuvant chemotherapy, and the adjuvant radiotherapy was deemed unnecessary, following a multidisciplinary consensus.

Our case has shown that the use of neoadjuvant chemotherapy is effective in cases of advanced BIA-ALCL, when immediate surgical treatment is not indicated for the extension of the disease. In these scenarios, the reverse strategy, which involves the use of neoadjuvant chemotherapy, may obtain near-clinical complete response allowing for conservative surgery.

The incidence of BIA-ALCL has continued to rise, but consistent data regarding recommendations for patients with a more aggressive presentation of BIA-ALCL are still lacking in the literature. In this optic, the role of unconventional therapeutic strategy should be investigated. Our report underlines the important role of neoadjuvant chemotherapy in BIA-ALCL to control disease burden before tumor resection in selected cases in which radical surgery is not possible or precluded due to the general condition of the patient.

## Consent to participate

Informed consent was obtained from the participant for the publication of this case report including all data and images.

## Data availability statement

The raw data supporting the conclusions of this article will be made available by the authors, without undue reservation.

## Ethics statement

The studies involving human participants were reviewed and approved by Central Ethics Committee IRCCS Lazio – IRCCS I.F.O. with number RS1719/22. The patients/participants provided their written informed consent to participate in this study. Written informed consent was obtained from the individual(s) for the publication of any potentially identifiable images or data included in this article.

## Author contributions

SC and FM wrote the main manuscript, its acquisition data, and the interpretation. LP, FPa, and FPe contributed to data acquisition. MCI made a critical review of the article. CB and MCo were in charge of the final approval of the version to be published. The final manuscript has been read and approved by all the authors.

## Funding

This work was financially supported through funding from the institutional "Ricerca Corrente" granted by the Italian Ministry of Health.

## Conflict of interest

The authors declare that the research was conducted in the absence of any commercial or financial relationships that could be construed as a potential conflict of interest.

## Publisher's note

All claims expressed in this article are solely those of the authors and do not necessarily represent those of their affiliated organizations, or those of the publisher, the editors and the reviewers. Any product that may be evaluated in this article, or claim that may be made by its manufacturer, is not guaranteed or endorsed by the publisher.

## References

1. Keech JA, Creech BJ. Anaplastic T-cell lymphoma in proximity to a saline-filled breast implant. *Plast Reconstr Surg* (1997) 100:554–5. doi: 10.1097/00006534-199708000-00065

2. Sheena Y, Smith S, Dua S, Morgan M, Ramakrishnan V. Current risk estimate of breast implant-associated anaplastic Large cell lymphoma in textured breast implants. *Plast Reconstr Surg* (2020) 145(2):446e. doi: 10.1097/PRS.0000000000006506

3. Marra A, Viale G, Pileri SA, Pravettoni G, Viale G, De Lorenzi F, et al. Breast implant-associated anaplastic large cell lymphoma: A comprehensive review. *Cancer Treat Rev* (2020) 84:101963. doi: 10.1016/j.ctrv.2020.101963

4. Clemens MW, Jacobsen ED, Horwitz SM. NCCN consensus guidelines on the diagnosis and treatment of breast implant-associated anaplastic Large cell lymphoma (BIA-ALCL). *Aesthet Surg J* (2019) 39(Suppl_1):S3–S13. doi: 10.1093/asj/sjy331

5. Turton P, El-Sharkawi D, Lyburn I, Sharma B, Mahalingam P, Turner SD, et al. UK Guidelines on the diagnosis and treatment of breast implant-associated anaplastic Large cell lymphoma on behalf of the medicines and healthcare products regulatory agency plastic, reconstructive and aesthetic surgery expert advisory group. *Br J Haematol* (2021) 192(3):444–58. doi: 10.1111/bjh.17194

6. Pelle F, Cappelli S, Graziano F, Piarulli L, Cavicchi F, Magagnano D, et al. Breast cancer surgery during the covid-19 pandemic: a monocentre experience from the Regina Elena national cancer institute of Rome. *J Exp Clin Cancer Res* (2020) 39(1):171. doi: 10.1186/s13046-020-01683-y

7. Cappelli S, Corallino D, Clementi M, Guadagni S, Pelle F, Puccica I, et al. Surgical site infections in patients undergoing breast oncological surgery during the lockdown: An unexpected lesson from the COVID-19 pandemic. *G Chir* (2022) 42 (2):e02. doi: 10.1097/IA9.0000000000000003

8. WHO Classification of Tumours Editorial Board. Haematolymphoid tumours. In: *Lyon (France): International agency for research on cancer; forthcoming, 5th ed* (2002) vol. 11 WHO Classificationof tumours series. Available at: https://publications.iarc.fr.

9. El-Asmar J, Reljic T, Ayala E, Hamadani M, Nishihori T, Kumar A, et al. Efficacy of high-dose therapy and autologous hematopoietic cell transplantation in peripheral T cell lymphomas as front-line consolidation or in the Relapsed/Refractory setting: A systematic Review/Meta-analysis. *Biol Blood Marrow Transplant* (2016) 22(5):802–14. doi: 10.1016/j.bbmt.2015.12.004

10. Fossard G, Broussais F, Coelho I, Bailly S, Nicolas-Virelizier E, Toussaint E, et al. Role of up-front autologous stem-cell transplantation in peripheral T-cell lymphoma for patients in response after induction: an analysis of patients from LYSA centers. *Ann Oncol* (2018) 29(3):715–23. doi: 10.1093/annonc/mdx787

11. Park SI, Horwitz SM, Foss FM, Pinter-Brown LC, Carson KR, Rosen ST, et al. The role of autologous stem cell transplantation in patients with nodal peripheral T-cell lymphomas in first complete remission: Report from COMPLETE, a prospective, multicenter cohort study. *Cancer* (2019) 125 (9):1507–17. doi: 10.1002/cncr.31861

12. D'Amore F, Gaulard P, Trümper L, Corradini P, Kim WS, Specht L, et al. Peripheral T-cell lymphomas: ESMO clinical practice guidelines for diagnosis, treatment and follow-up. *Ann Oncol* (2015) 26(Suppl 5):v108–15. doi: 10.1093/annonc/mdv201

13. Lyapichev KA, Piña-Oviedo S, Medeiros LJ, Evans MG, Liu H, Miranda AR, et al. A proposal for pathologic processing of breast implant capsules in patients with suspected breast implant anaplastic large cell lymphoma. *Modern Pathol* (2020) 33(3):367–79. doi: 10.1038/s41379-019-0337-2

14. Lyapichev KA, Medeiros LJ, Clemens MW, Ferrufino-Schmidt MC, Marques-Piubelli ML, Chai SM, et al. Reconsideration of the first recognition of breast implant-associated anaplastic large cell lymphoma: A critical review of the literature. *Ann Diagn Pathol* (2020) 45:151474. doi: 10.1016/j.anndiagpath.2020.151474

15. Wang Y, Zhang Q, Tan Y, Lv W, Zhao C, Xiong M, et al. Current progress in breast implant-associated anaplastic Large cell lymphoma. *Front Oncol* (2022) 11:785887. doi: 10.3389/fonc.2021.785887

16. WHO Classification of Tumours Editorial Board. Breast tumours. In: *Lyon (France): International agency for research on cancer, 5th ed*, vol. 2. (2019) WHO Classificationof tumours series. Available at: https://publications.iarc.fr.

17. Clemens MW, Brody GS, Mahabir RC, Miranda RN. How to diagnose and treat breast implant-associated anaplastic Large cell lymphoma. *Plast Reconstr Surg* (2018) 141(4):586e–99e. doi: 10.1097/PRS.0000000000004262

18. Caputo GG, Alban A, D'Alì L, Mariuzzi L, Galvano F, Parodi PC. Locally advanced breast implant-associated anaplastic large-cell lymphoma: a combined medical-surgical approach. *Eur Rev Med Pharmacol Sci* (2021) 25(9):3483–8. doi: 10.26355/eurrev_202105_25830

19. Thibodeau R, Fan KL, Wehner PB. Stage IV breast implant-associated anaplastic Large-cell lymphoma with complete pathologic response to neoadjuvant chemotherapy. *Plast Reconstr Surg Glob Open* (2019) 7(9):e2446. doi: 10.1097/GOX.0000000000002446

20. Miranda RN, Aladily TN, Prince HM, Kanagal-Shamanna R, De Jong D, Fayad LE, et al. Breast implant-associated anaplastic large-cell lymphoma: long-term follow-up of 60 patients. *J Clin Oncol* (2014) 32(2):114–20. doi: 10.1200/JCO.2013.52.7911

21. Ferrufino-Schmidt MC, Medeiros LJ, Liu H, Clemens MW, Hunt KK, Laurent C, et al. Clinicopathologic features and prognostic impact of lymph node involvement in patients with breast implant-associated anaplastic Large cell lymphoma. *Am J Surg Pathol* (2018) 42(3):293–305. doi: 10.1097/PAS.0000000000000985

22. Clemens MW, Medeiros LJ, Butler CE, Hunt KK, Fanale MA, Horwitz S, et al. Complete surgical excision is essential for the management of patients with breast implant-associated anaplastic Large-cell lymphoma. *J Clin Oncol* (2016) 34 (2):160–8. doi: 10.1200/JCO.2015.63.3412

frontiers | Frontiers in Oncology

TYPE Case Report
PUBLISHED 11 January 2023
DOI 10.3389/fonc.2022.1091877



OPEN ACCESS

EDITED BY
Zhaolun Cai,
Sichuan University, China

REVIEWED BY
Minggui Pan,
Kaiser Permanente, United States
Derek Allison,
University of Kentucky, United States
Jorge León,
University of São Paulo, Brazil

*CORRESPONDENCE
Huajun Li
chinalhj1967@126.com
Jie Qiao
jie.qiao@263.net

SPECIALTY SECTION
This article was submitted to Surgical Oncology, a section of the journal Frontiers in Oncology

RECEIVED 07 November 2022
ACCEPTED 08 December 2022
PUBLISHED 11 January 2023

CITATION
Jiang H, Wang C, Hou Z, Wang Y, Qiao J and Li H (2023) Case report: NUT carcinoma with MXI1::NUTM1 fusion characterized by abdominopelvic lesions and ovarian masses in a middle-aged female. *Front. Oncol.* 12:1091877. doi: 10.3389/fonc.2022.1091877



# Case report: NUT carcinoma with MXI1::NUTM1 fusion characterized by abdominopelvic lesions and ovarian masses in a middle-aged female

Huahua Jiang[1,2], Chao Wang[1,2], Zheng Hou[1,2], Yuxiang Wang[3], Jie Qiao[1,2,4,5]* and Huajun Li[1,2]*

[1]Department of Obstetrics and Gynecology, Peking University Third Hospital, Beijing, China, [2]National Clinical Research Center for Obstetrics and Gynecology, Peking University Third Hospital, Beijing, China, [3]Department of Pathology, School of Basic Medical Sciences, Third Hospital, Peking University Health Science Center, Beijing, China, [4]Beijing Advanced Innovation Center for Genomics, Peking University, Beijing, China, [5]Peking-Tsinghua Center for Life Sciences, Peking University, Beijing, China

**Background:** Nuclear protein of the testis (NUT) carcinoma is a rare subset of poorly differentiated, highly aggressive malignancy defined by NUTM1 gene rearrangements. Only three NUT cases of probable ovarian origin have been reported.

**Case presentation:** We report a case of NUT carcinoma in a 53-year-old female who presented with extensive abdominopelvic lesions and bilateral ovarian masses suggestive of advanced ovarian cancer. This patient was admitted to our hospital due to abdominal pain and distension for over two months. Imaging examinations suggested a possible malignancy of bilateral adnexal origin. This patient first underwent diagnostic laparoscopy. After receiving neoadjuvant chemotherapy, she underwent cytoreductive surgery. Surgical pathology showed infiltration of monotonous round tumor cells with no apparent differentiation characteristics. Immunohistochemistry (IHC) revealed nuclear expression of the NUT protein. And MXI1::NUTM1 fusion was identified by next-generation sequencing (NGS). Herein, we introduce an unusual NUT carcinoma and describe the clinical, imaging, and pathological features. In addition, we briefly reviewed the published literature and discussed the possibility of primary gynecological NUT carcinoma.

**Conclusions:** Identifying a NUT carcinoma arising from the abdominopelvic cavity is essential, and we underscore the need for NUT testing in undifferentiated malignant neoplasms that appear in this clinical setting. Although it is unclear from which origin this tumor arose, proper classification is essential for treatment planning.

KEYWORDS

**NUT carcinoma, ovarian neoplasms, undifferentiated pelvic neoplasms, case report, NUT rearrangement**

## Introduction

NUT carcinoma is a rare, aggressive, and relatively recently characterized subtype of poorly differentiated squamous cancer with remarkably unfavorable clinical outcomes (1). It was first described as thymic carcinoma in a young adult with the novel translocation t (15, 19) (q15; p13) in 1991 in Japan (2). NUT carcinoma most commonly harbors the BRD4-NUTM1 fusion oncoprotein. Other NUTM1-fusion partners include BRD3, NSD3, ZNF532, and ZNF592 (3). NUT carcinoma is an orphan disease with unknown origin. It can occur anywhere along the midline, with the typical sites being the upper aerodigestive tract (head, neck, thorax, and mediastinum), but also outside the midline (lung, salivary glands, pancreas, bladder, kidney, adrenal glands, ovary, and bone tissues.) (1, 4, 5). It most frequently occurs in adolescents and young adults but can occur at any age (0-81.7 years), with a median age varying from 16 to 24 years (6). The prognosis of NUT carcinoma is devastating; most patients progress rapidly and have hematologic or lymphatic metastases at diagnosis, with a median survival time of 6.7 months (7).

Although rare, the true incidence of NUT carcinoma is unknown because it is frequently misdiagnosed with other common malignancies, including poorly differentiated squamous cell carcinoma, sinonasal undifferentiated carcinoma, nasopharyngeal carcinoma, Ewing sarcoma, leukemia, thymic carcinoma, neuroblastoma and pancreatoblastoma, and even primary salivary gland carcinoma (1). It can be diagnosed with virtually 100% specificity and 87% sensitivity by positive (>50% of tumor nuclei) immunohistochemical (IHC) staining with the anti-NUT antibody, C52B1, which is normally restricted to expression in the testis (www.nmcregistry.org) (4, 6, 8). Characterization of the fusion gene by molecular analysis based on fluorescence *in situ* hybridization (FISH), reverse-transcriptase polymerase chain reaction (RT-PCR), cytogenetics, next-generation sequencing (NGS), or whole-exome sequencing (WES) can be an alternative to NUT IHC staining (6, 9).

In this study, we report a rare NUT carcinoma presenting with extensive abdominopelvic lesions and bilateral ovarian masses. This study was reported in agreement with the principles of the CARE guidelines (10).

## Case report

A 53-year-old Chinese female presented to the Emergency Department of our hospital for persistent abdominal pain and distension for over two months. Two months ago, the patient went to a local hospital and obtained a transvaginal ultrasound that revealed thickened bilateral fallopian, suggesting adnexitis. She was treated with antibiotics, but the pain persisted. The serum CA125 and CA724 levels were elevated (469U/ml and 33.4U/ml, respectively). Abdomen and pelvis computed tomography (CT) showed heterogeneous stomach and bilateral adnexal masses, suggesting adnexal lesions or the Krukenberg tumor. She was then referred to the emergency room of our hospital.

In our hospital, she received thorough examinations. A gynecological examination revealed an abdominopelvic mass with an unclear boundary. The transvaginal ultrasound showed a 3.9×2.3cm solid pelvic mass with ascites (Figure 1A; Supplemental Figures S1A, B). The abdominal and pelvic enhanced CT, the pelvic magnetic resonance imaging (MRI), and the positron emission computed tomography (PET-CT) all revealed irregular, heterogeneous, and plump bilateral adnexal masses with diffusely thickened peritoneum, omentum, and mesangium, multiple soft-tissue nodules, slightly thickened intestinal wall, abdominal and pelvic effusion, and multiple enlarged lymph nodes (Figures 1B–E; Supplemental Figures S1C–F). The serum CA125 level was 439U/mL. The chest X-ray showed no abnormality. The patient underwent bilateral tubal sterilization more than 20 years ago and was found with a Helicobacter pylori infection two months ago. She went into natural menopause for one year and gave birth to two children. Personal and family history were unremarkable.

## Treatment

Considering the possibility of ovarian or gastrointestinal malignancies, the patient was admitted to our hospital. After admission, the patient developed aggravated abdominal distension with an increase in body temperature to 39℃. After four days of intravenous anti-inflammatory, the patient underwent diagnostic laparoscopy with omentum and peritoneum biopsies in a stable condition, which suggested poorly differentiated carcinoma according to intraoperative consultation. About 2 liters of tawny ascites were drained for cytology confirmation during the operation, which revealed no tumor cells. The surgical findings showed multiple white granular tumor implants studding the omentum, peritoneum, and the surface of the diaphragm, liver, intestine, and uterus. A 9×9×3cm omental cake enclosed part of the intestine and was fixed. The omentum and intestine obscured bilateral ovaries and fallopian tubes. Combined with laboratory, imaging, and surgical findings, the possibility of advanced (stage IV) ovarian cancer was considered. Given the difficulty in performing satisfactory cytoreductive surgery, the patient was treated with three cycles of neoadjuvant chemotherapy with Paclitaxel-albumin, Carboplatin, and Bevacizumab.

After chemotherapy, the patient's serum CA125 level was reduced to 107 U/mL. Imaging examination showed reduced abdominal and pelvic effusion, while abdominopelvic lesions were roughly the same as before (Supplemental Figure S2). The

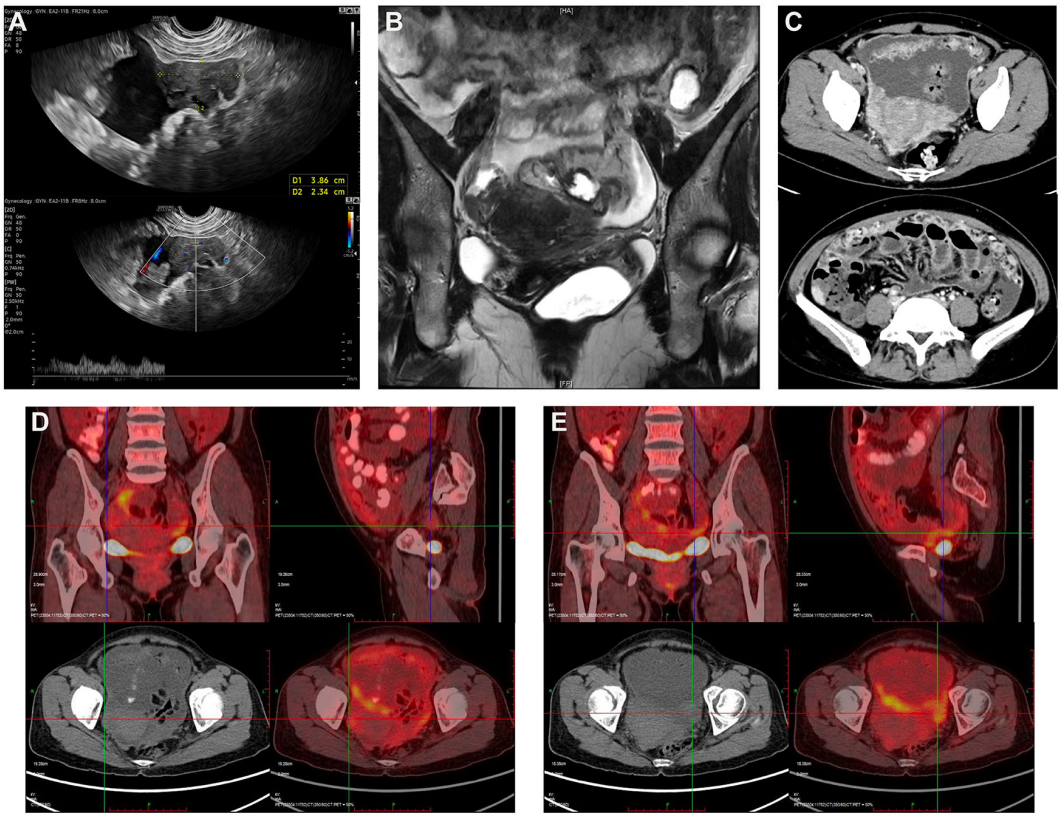


FIGURE 1
**(A)** Transvaginal ultrasound reveals a 3.9×2.3cm irregular hypoechoic mass in the right abdominal cavity with blood flow signals closely related to the peritoneum. **(B)** Pelvic MRI shows a suspicious mass in the right adnexal area and thickening of the omentum with pelvic effusion. **(C)** Abdominal and pelvic enhanced CT reveals plump bilateral adnexal masses, diffusely thickened peritoneum, omentum, and mesangium, slightly thickened intestinal wall, and abdominal and pelvic effusion. PET-CT displays plump bilateral adnexal areas, poorly demarcated from surrounding tissue, showing signs of hypermetabolism with **(D)** the SUVmax2.2 on the right and **(E)** the SUVmax3.1 on the left.

pathological findings of the previous operation excluded the common types of epithelial ovarian carcinoma, breast carcinoma, and neuroendocrine neoplasm. Still, the diagnosis could not be confirmed due to the poor differentiation characteristics of the tumor cells. Upper GI endoscopy and colonoscopy were performed to distinguish gastrointestinal tumors, but no mucosal lesions were identified (Supplemental Figure S3). The patient further underwent cytoreductive surgery, which showed a 20×10×4cm extensive gritty nodular omental cake densely adhered to the pelvic wall and part of the intestine and mesentery (Supplemental Figure S4A). The mesostenium and mesocolon were extensively thickened with contracture and stiff morphology. A heterogeneous mass about 2.5cm in diameter was found on the surface of the small intestine. The posterior wall of the uterus closely adhered to the rectum, and bilateral ovaries were enlarged with a solid nodular appearance (Supplemental Figure S4B). Total hysterectomy and bilateral salpingo-oophorectomy were performed. The omentum, small intestinal mass, and left pelvic lymph nodes were also removed. All specimen was submitted for pathological confirmation. It was an unsatisfactory cytoreductive surgery (R2), with the postoperative residuals being the diffuse thickened malignancy lesions in the mesentery. The patient recovered in a stable condition without any complications and was discharged home 13 days after surgery.

## Pathological findings

Microscopic examination showed malignancy infiltration in bilateral ovaries involving the omentum, peritoneum, mass on the small intestine surface, and the serosa of the uterus and bilateral fallopian tubes. The tumor cells were uniform monotonous medium-sized round and oval with small-to-moderate eosinophilic cytoplasm, enlarged nuclei, high nuclear/cytoplasmic ratio, and uneven chromatin (Figure 2A). Lymphatic vascular involvement and lymph node metastases were frequently observed (Figure 2B). Solid sheets and nests of typically undifferentiated cells infiltrating surrounding normal

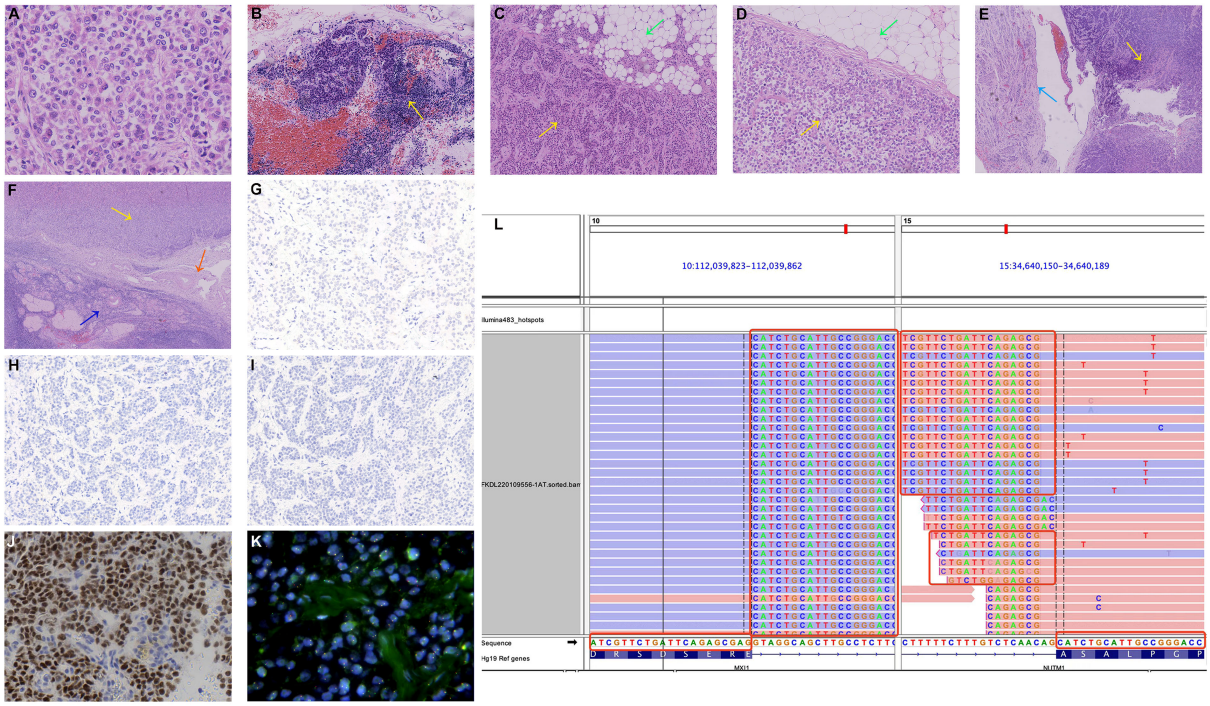


FIGURE 2
Microscopic findings. **(A)** Uniform monotonous medium-sized round and oval tumor cells with moderate eosinophilic cytoplasm, enlarged nuclei, high nuclear/cytoplasmic ratio, and uneven chromatin (hematoxylin and eosin (HE)). **(B)** Tumor cells infiltrate the pelvic lymph nodes (HE, yellow arrow). **(C)** A section of the omental biopsy specimen with the omental tissue at the upper right (HE, green arrow) and the tumor cells at the lower left (HE, yellow arrow). **(D)** A section of the omental specimen from cytoreductive surgery with no significant regression of tumor cells after chemotherapy (HE, omental tissue: green arrow, tumor cells: yellow arrow). **(E)** Tumor cells (HE, yellow arrow) infiltrate the serosa of the uterus (HE, azure arrow). **(F)** The tumor mass is close to the ovarian hilus (HE, yellow arrow), surrounded by large blood vessels (HE, orange arrow), with most of the typical stricture of ovarian cortical and corpus albicans preserved (HE, sapphire arrow). **(G)** Negative CK pan IHC staining. **(H)** Negative p40 IHC staining. **(I)** Negative p63 IHC staining. **(J)** Strong and diffuse nuclear reactivity for NUT in the tumor cells (NUT IHC staining). **(K)** Negative NUT FISH test. No significant red-green signal separation was observed. **(L)** NGS identified an MXI1::NUTM1 fusion consisting of MXI1 exon 5 and NUTM1 exon 3 obtained for the tumor specimens of the patient.

omental tissue were present, with no abrupt keratinization (Figure 2C). Comparing the two surgical specimens, there was no significant regression of tumor cells after neoadjuvant chemotherapy (Figures 2C, D). Malignancy infiltration was found on the serosa of the uterus, while typical structures of the endometrium and myometrium remained, suggesting that it was not a primary uterine neoplasm (Figure 2E). It is noteworthy that although the malignancies significantly infiltrated the ovary, most of the ovarian cortical and corpus albicans were intact. The lesions were mainly close to the ovarian hilus and surrounded by large blood vessels (Figure 2F), so the possibility of secondary ovarian malignancy cannot be excluded.

IHC was conducted to help confirm the diagnosis (Table 1). Tumor cells positively expressed monoclonal ER, INI1 (SMARCB1), BRG1(SMARCA4), and ARID1a, with patchy expressions of monoclonal PR, P16, Syn, SATB2, and CK8/18. The β-Catenin and P120 were positive in the cytoplasm. The Ki-67 labeling index was approximately 30%. There was no expression of CK pan (Figure 2G), p40 (Figure 2H), p63 (Figure 2I), and other IHC markers (i.e., CD56, CK7, WT-1, TTF-1, Desmin, C-myc, CgA, CDX2, INSM1, SSTR2, SSTR5). Details of all the IHC results were listed in Table 1. Based on the morphological and IHC features, 14 malignancies with similar morphology were compared, including ovarian serous carcinoma, ovarian clear cell carcinoma, ovarian germ cell neoplasms, ovarian sex cord-stromal neoplasms, neoplasms associated with the SWI/SNF complex, colorectal carcinoma, invasive lobular carcinoma of the breast, poorly differentiated hepatic cholangiocarcinoma, low grade endometrial stromal sarcoma, high grade endometrial stromal sarcoma, rhabdomyosarcoma, malignant peripheral nerve sheath tumors, histiocytic sarcoma, and plasmacytoma (Table 2). Additionally, to distinguish it from Ewing sarcoma, dual-color break-apart FISH was conducted to test for EWSR1 gene rearrangements, which revealed a negative result.

Finally, we conducted NUT immunostaining (clone C52B1) and revealed diffusely positive expression in the nucleus of tumor cells (Figure 2J). However, the FISH experiment found no disruption or translocation of the NUTM1 gene locus

TABLE 1 Immunohistochemical result[ab].

| Protein | Expression level | Clone | Manufacture |
|---|---|---|---|
| NUT | Nuclear positive | C52B1 | CST, Boston, USA |
| ER | Nuclear positive | SP1 | Genetech, Shanghai, China |
| PR | Few positive | 16 | Genetech, Shanghai, China |
| P16 | Faint positive | 1C1 | Zsbio, Beijing, China |
| PAX-8 | Negative | MRQ-50 | Zsbio, Beijing, China |
| P53 | Wtp53 positive | DO-7 | Zsbio, Beijing, China |
| WT-1 | Negative | 6F-H2 | Zsbio, Beijing, China |
| Ki-67 | Positive in 30% (hotspot) | MIB-1 | Genetech, Shanghai, China |
| CDX2 | Negative | EP25 | Genetech, Shanghai, China |
| CK7 | Negative | UMAB161 | Zsbio, Beijing, China |
| CK20 | Negative | EP23 | Zsbio, Beijing, China |
| Villin | Negative | UMAB230 | Zsbio, Beijing, China |
| NapsinA | Negative | IP64 | Zsbio, Beijing, China |
| TTF-1 | Negative | 8G7G3/1 | Zsbio, Beijing, China |
| HNF1β | Negative | EPR18644-13 | Biolynx, Hangzhou, China |
| β-Catenin | Cytoplasmic positive | UMAB15 | Zsbio, Beijing, China |
| E-Cadherin | Negative | UMAB184 | Zsbio, Beijing, China |
| P120 | Cytoplasmic positive | EP66 | Zsbio, Beijing, China |
| CK pan | Negative | AE1/AE3 | Zsbio, Beijing, China |
| GATA-3 | Negative | EP368 | Zsbio, Beijing, China |
| CgA | Negative | LK2H10 | Zsbio, Beijing, China |
| Syn | Few positive | SP11 | Genetech, Shanghai, China |
| CD56 | Negative | UMAB83 | Zsbio, Beijing, China |
| SATB2 | Faint positive | OTI5H7 | Zsbio, Beijing, China |
| Desmin | Negative | EP15 | Zsbio, Beijing, China |
| Hepatocyte | Negative | OCH1E5 | Zsbio, Beijing, China |
| HER2 | Negative | EP3 | Celnovte, Henan, China |
| S-100 | Negative | 15E2E2+4C4.9 | Zsbio, Beijing, China |
| AFP | Negative | OTI4D8 | Zsbio, Beijing, China |
| SF-1 | Negative | OTI1H2 | Zsbio, Beijing, China |
| CK8/18 | Dot-like positive | B22.1&B23.1 | Zsbio, Beijing, China |
| Glypican-3 | Negative | 1G12 | Zsbio, Beijing, China |
| CK19 | Negative | UMAB2 | Zsbio, Beijing, China |
| SALL4 | Negative | 6E3 | Zsbio, Beijing, China |
| CD68(KP1) | Negative | KP1 | Zsbio, Beijing, China |
| CD163 | Negative | 10D6 | Zsbio, Beijing, China |
| CD138 | Negative | EP201 | Zsbio, Beijing, China |

*(Continued)*

TABLE 1 Continued

| Protein | Expression level | Clone | Manufacture |
|---|---|---|---|
| CD38 | Negative | SPC32 | Zsbio, Beijing, China |
| CD10 | Negative | UMAB235 | Zsbio, Beijing, China |
| IFITM1 | Negative | Polyclonal | Sigma, Missouri, USA |
| INI1(SMARCB1) | Positive | 25 | Zsbio, Beijing, China |
| BRG1(SMARCA4) | Positive | E8V5B | Zsbio, Beijing, China |
| ARID1a | Positive | EP303 | Zsbio, Beijing, China |
| BCOR | Negative | C-10 | Zsbio, Beijing, China |
| CyclinD1 | Negative | SP4 | Genetech, Shanghai, China |
| SSTR2 | Negative | EP149 | Zsbio, Beijing, China |
| SSTR5 | Negative | Polyclonal | Novus, Colorado, USA |
| CD117 | Negative | YR145 | Genetech, Shanghai, China |
| Calretinin | Negative | SP13 | Maxim, Fujian, China |
| P40 | Negative | BC28 | Zsbio, Beijing, China |
| P63 | Negative | 4A4+UMAB4 | Zsbio, Beijing, China |
| C-MYC | Negative | EP121 | Zsbio, Beijing, China |

[a]All IHC staining except NUT antibody staining was performed on the Leica automated platform (Leica BOND-Max, Wetzlar, Germany) with validated commercial antibodies using appropriate positive and negative controls.
[b]NUT antibody staining was performed by the Pathology Laboratory of Peking University Third Hospital, with testicular tissue used for a positive control and phosphate-buffered saline used for a negative control.

TABLE 2 14 malignancies with similar morphology.

| Malignancies | Incongruent IHC indicators |
|---|---|
| Ovarian Serous Carcinoma | PAX-8 (-), WT-1 (-), P53 (Wtp53+), P16 (Faint+) |
| Ovarian Clear Cell Carcinoma | NapsinA (-), TTF1 (-) |
| Ovarian Germ Cell Neoplasms | SALL4 (-) |
| Ovarian Sex Cord-Stromal Neoplasms | SF-1 (-) |
| Neoplasms Associated with the SWI/SNF Complex | BRG1 (+), ARID1A (+), INI1 (+) |
| Colorectal Carcinoma | CK7 (-), CK20 (-), CDX2 (-), Villin (-), SATB2 (Faint+) |
| Invasive Lobular Carcinoma of the Breast | β-catenin (Cytoplasmic+), E-Cadherin (-), P120 (Cytoplasmic+), GATA-3 (-) |
| Poorly Differentiated Hepatic Cholangiocarcinoma | Hepatocyte (-), Glypican-3 (-), CK8/18 (Dot-like+), CK19 (-) |
| Low Grade Endometrial Stromal Sarcoma | CD10 (-), IFITM1 (-) |
| High Grade Endometrial Stromal Sarcoma | BCOR (-), CyclinD1 (-) |
| Rhabdomyosarcoma | Desmin (-) |
| Malignant Peripheral Nerve Sheath Tumors | S-100 (-) |
| Histiocytic sarcoma | CD68 (-), CD163 (-) |
| Plasmacytoma | CD38 (-), CD138 (-) |

(Figure 2K). We subsequently identified the gene fusion of MXI1 exon 5 (NM_130439.3) to NUTM1 exon 3 (NM_175741.3) *via* a targeted RNA-based NGS platform (DA8600, Daan Gene, Guangzhou, China) on tissue samples, which finally confirmed NUT carcinoma two months after cytoreductive surgery (Figure 2L). Besides, we also identified the gene fusion of MTMR3 exon 5 (NM_021090.4) to SFI1 exon 3 (NM_001007467.3).

## Follow-Up

One week after diagnosis, the patient developed fever and an increased burden of malignancy, with imaging of advanced diffusely thickened peritoneum, omentum, and mesangium, progressed multiple metastatic lymph nodes, and newly developed abdomino pelvic effusion. Unfortunately, although the patient was adequately informed and the potential feasibility of antitumor therapy was introduced, the patient refused further treatment due to financial difficulties and decided to be discharged to a local hospital for symptomatic relief and supportive treatment. She developed systemic symptoms and passed away four months and 18 days after cytoreductive surgery (Figure 3).

# Discussion

NUT, a protein product of the NUTM1 gene with highly specific physiologic expression in post-meiotic spermatids, is an emerging neoplastic driver when fused with genes related to transcription regulation (3). Although initially found to form fusion oncoproteins with bromodomain proteins in a series of fatal midline carcinomas, NUT has been identified with non-bromodomain partners in some non-midline neoplasms with varied histological morphology, including sarcoma, poroma, porocarcinoma, and acute lymphoblastic leukemias (11–14). Herein, we report a rare case of NUT carcinoma in a middle-aged woman presenting extensive abdominopelvic lesions and bilateral ovarian masses and initially considered advanced ovarian cancer.

Although increasingly reported outside midline sites, NUT carcinoma rarely presents ovarian lesions. As in our case, bilateral ovarian masses may raise concern for a gynecologic tract primary site of NUT carcinoma. Ovarian lesions are uncommon for NUT carcinoma, with only three case reports identified in the previous literature (5, 9, 11). The first patient was a 38-year-old white female presenting with mediastinal and bilateral ovarian masses; the possibility of primary ovarian lesions cannot be excluded (9). The second patient was a young female with ovarian and lung lesions, and the primary focus was uncertain (11). The third patient, similar to ours, was a middle-aged woman harboring a massive mass in the pelvic cavity with diffusely thickened peritoneum and multiple enlarged distant lymph nodes, indicating advanced ovarian cancer (5). In general, these patients and ours presented with extensive lesions involving the ovaries, so the possibility of the ovary origin should be considered. Of concern is that our patient's ovarian lesions were mainly distributed near the vessels of the ovarian hilus, with most of the typical structures

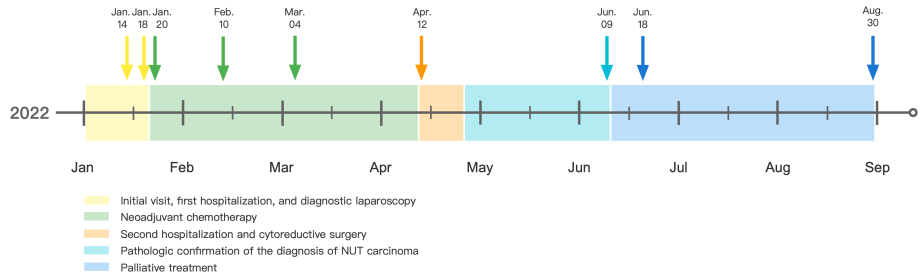


FIGURE 3
Time diagram from Jan 2022 to Sep 2022 of the patient: on Jan 14, 2022, abdominopelvic lesions and ovarian masses were identified by imaging examination; on Jan 18, 2022, diagnostic laparoscopy was performed. Pathological findings of the omentum and peritoneum biopsies suggested a poorly differentiated carcinoma. On Jan 20, 2022, the patient began the first course of neoadjuvant chemotherapy with Paclitaxel-albumin, Carboplatin, and Bevacizumab; on Feb 10, 2022, the patient received the second course of neoadjuvant chemotherapy; on Mar 4, 2022, the patient received the third course of neoadjuvant chemotherapy; on Apr 12, 2022, cytoreductive surgery was performed; on Jun 9, 2022, NUT carcinoma was confirmed by morphology, immunohistochemistry, and genetic alterations. On Jun 18, 2022, imaging examinations revealed a progressed malignancy burden. The patient refused antitumor therapy and passed away on Aug 30, 2022.

of the ovary intact. Therefore, the possibility of secondary ovarian malignancy cannot be ruled out. Given that this patient's lesions were predominantly in the abdominal and pelvic presenting with extensive thickened peritoneum, omentum, and mesangium, the possibility of primary NUT carcinoma in the peritoneum, omentum, or mesangium also cannot be ignored. These have not been previously reported or considered in the literature.

NUT carcinoma usually displays evidence of squamous differentiation either by histologic findings or immuno histochemically expression of p63, p40, CK-pan, and other markers associated with squamous differentiation (15). Similar to Jung et al., we observed strong ER expression, no expression of p63 or p40, and no abrupt squamous foci (5), and we also found weakly positive expression of PR and weak and dot-like CK8/18 expression, which is not common in classic NUT carcinoma (11). However, the IHC profiles of our study excluded 14 other morphologically similar malignancies and secured the diagnosis of a poorly differentiated NUT carcinoma. Recently, similar high ER reactivity was described in one report of the NUTM1-rearranged neoplasia with primary foot lesions, which was diagnosed as NUT sarcoma due to morphological consistency with extraskeletal myxoid chondrosarcoma (11). However, sarcomatoid differentiation is not remarkable in this case. The unique ER and PR expression may indicate that this tumor arose from a primary gynecologic site. Some reports of NUT carcinoma have shown some focal features of their possible origins. A recent rare report of an NSD3:NUTM1 fusion carcinoma arising in the thyroid showed retention of focal thyroglobulin production (16). In brief, the exact value of ER and PR expression in NUT carcinoma remains unclear, which may indicate a gynecologic origin and requires further investigation.

Myotubularin-related protein 3 (MTMR3) is an inositol lipid 3-phosphatase with extensive homology to myotubularin (17). It has been found to be related to inflammatory bowel disease (18), X-linked myotubular myopathy (17, 19), and type 4B Charcot-Marie-Tooth disease (20). SFI1 (SFI1 Centrin Binding Protein), essential for proper stability of centrioles and ciliogenesis regulation (21), is associated with diabetic nephropathy (22), neuroblastoma (23), and microcephaly (24). However, MTMR3::SFI1 fusion has not been previously reported. MAX interactor 1 (MXI1), the reported NUTM1 companion gene, belongs to the MAD family and encodes a transcription factor with a bHLH-Zip motif (25). MXI1 interacts specifically with transcription cofactor Max (25), regulates Myc activity *via* transcriptional inhibition, and plays a role in the regulation of cell proliferation (26, 27). So far, Three cases of MXI1::NUTM1 fusion neoplasm have been reported in published literature (28–30). Agreeing with previous cases, our case shows the appearance of a primitive small round cell morphology and is diagnosed based on the positive staining of the NUT protein. Although all four cases (including this case) generally show no expression of typical NUT carcinoma markers, the IHC profile of this case is slightly different with negative expression of Desmin and positive expressions of ER, PR, and CK8/18. Despite the negative expression of myc in MXI1::NUTM1 fusion neoplasm, evidence has shown that MXI1, which are normally repressors of MYC activity, can be converted into MYC-like mimics by fusion to NUTM1 (28). This may potentially be instructive in the therapeutic options.

NUT carcinoma was highly aggressive, remarkably refractory to chemotherapy and radiotherapy, and rapidly fatal. Most patients succumb to rapid disease progression with early locoregional invasion and distant metastases (7, 31). The prognosis is related to the fusion partners and malignancy sites. Analysis of 124 patients from the NUT Midline Carcinoma Registry (www.nmcregistry.org) found that the median overall survival (OS) of non-thoracic NUT carcinoma is longer than thoracic NUT carcinoma, so as non-BRD4-NUTM1 fusions compared with BRD4-NUTM1 fusion (32). In about 75% of cases, NUTM1 is fused with BRD4, a member of the dual bromodomain and extra terminal domain (BET) family proteins (15, 33). NUT-mediated genome-wide histone modification is vital in the pathogenesis of NUT carcinoma *via* activating the histone acetyltransferase (HAT) p300, a factor required for enhancer function achievement and the transcription of oncogenes or tumor suppressor genes like MYC and SOX2 (15).

Some cases have reported excellent tumor stabilization effects of Ewing sarcoma chemotherapy, concurrent Chemoradiotherapy (CCRT), and immunovirotherapy (34–37). Nasal NUT carcinoma has remarkably responded to Ewing sarcoma-based chemotherapy regimen and concurrent radiation in several cases (34, 35). And CCRT has been found helpful in achieving complete remission in several patients suffering from head, neck, and thoracic NUT carcinoma (36, 38). Recently, a case demonstrated the feasibility of an add-on immunovirotherapy regimen in a patent with thoracic NUT carcinoma, which includes an oncolytic virus (talimogene laherparepvec (T-VEC), IMLYGIC®) together with the immune checkpoint inhibitor pembrolizumab as an add-on to a basic therapy (cytostatic chemotherapy, radiation therapy, and epigenetic therapy) and shows a significant improvement of tumor stabilization and the patient's quality of life (37). And it has been reported that positive PD-L1 expression may be associated with better survival and may indicate the potential of immune checkpoint inhibitors in treating NUT carcinoma (15, 38).

Although the standard therapy for NUT carcinoma has not been well established, therapeutic epigenetic modifiers are emerging potential regimens for NUT carcinoma treatment. Promising epigenetic therapies include the inhibition of DNA binding by BET bromodomain inhibitors (BETis) and the modification of downstream histones by histone deacetylase

inhibitors (HDACis) (15, 39, 40). Several epigenetic therapies are under development and have shown some promising preclinical findings, including BETis (i.e., ABBV-075 (mivebresib), ABBV-744, and BI 894999), p300 BDi + BETi (i.e., GNE-781 + birabresib), CDK9 inhibition, CDK4/6i + BETi, DNA-damaging agents, and HDACis (15, 39–41). To date, several phase I/IIa clinical trials focused on BETi monotherapy have been completed and showed preliminary antitumor activity, including birabresib (aka MK-8628/OTX015, OncoEthix) (42), molibresib (aka iBET-762, GlaxoSmithKline) (43), ODM-207 (Orion Pharma) (44), RO6870810 (aka TEN-010, Roche) (45), and BMS-986158 (Bristol-Myers Squibb) (46). But more clinical trials are needed to confirm the safety and feasibility of these regimens for widespread use. Some ongoing phase I/II clinical trials include BETi combined with chemotherapy treatment (ZEN3694 + cisplatin/etoposide, CTEP 10507 and NCT05019716), dual BET and CBP/p300 inhibitor (EP31670, NCT05488548).

Of the three cases that reported NUT carcinoma with gynecological lesions, two described the treatment and prognosis. The first patient developed multiple diffuse progressive metastases throughout the body within three weeks of diagnosis, including liver, lung, brain, adrenal glands, pelvic cavity, bone, and lymph nodes. Although receiving chemoradiotherapy and targeted therapy, she died of a severe infection two months and 19 days after diagnosis (9). Another patient was a 54-year-old Korean woman who was treated with chemotherapy with bleomycin, etoposide, and cisplatin (BEP) but showed significant aggravated tumor burden with chest and lymph node metastases (5). Regardless of the therapies, conditions of NUT carcinoma patients with gynecologic tract lesions presented uncontrolled. Remarkably, the 38-year-old white female with mediastinal and ovarian masses received systemic chemotherapy with an HDACi (Romidepsin), but the tumor significantly progressed (9). Of the three cases that reported MXI1::NUTM1 fusion, two were not eligible for clinical trials and were too unwell to receive other basic therapies (28, 30), and one received an off-label use of Romidepsin but got progressively worse (29). Therefore, more experimental and clinical studies are required to characterize the drug resistance mechanisms and to screen the targeted therapies.

## Conclusion

We report the clinical and pathological findings of a rare NUT carcinoma with MXI1::NUTM1 fusion characterized by extensive abdominopelvic lesions and bilateral ovarian masses and share the difficulties and pitfalls of the diagnostic process. We emphasize the importance of NUT testing in undifferentiated malignant neoplasms with extensive abdominopelvic and ovarian involvement and put forward the possible gynecologic origin of NUT carcinoma, which is essential for proper classification and treatment planning.

## Data availability statement

The original contributions presented in the study are included in the article/Supplementary Material. Further inquiries can be directed to the corresponding authors.

## Ethics statement

Ethical review and approval was not required for the study on human participants in accordance with the local legislation and institutional requirements. The patients/participants provided their written informed consent to participate in this study. Written informed consent was obtained from the individual(s) for the publication of any potentially identifiable images or data included in this article.

## Author contributions

HL and JQ conceived, conducted, and participated in the whole process of this study. HJ carried out the entire procedure, including the medical records collection, manuscript drafting, and manuscript revision. CW and ZH revised the manuscript. YW provided figures and clinical pathological analysis. All authors contributed to the article and approved the submitted version.

## Funding

The study was supported by the National Natural Science Foundation of China (Grant No. 82201839).

## Acknowledgments

The authors sincerely thank all doctors and nurses in the Gynecology Ward One of Peking University Third Hospital. We gratefully acknowledge Dr. Bo Yu, Dr. Yingxi Wang, Dr. Jiaqi Huang, Dr. Shuxian Ren, Dr. Linlin Zhang, and Dr. Qizheng Wang for participating in the patient's clinical work. And we sincerely thank Prof. Bo Zhang and Dr. Zixiu Zhao of the Department of Pathology of Peking University Third Hospital for their advice on clinical pathological analysis.

## Conflict of interest

The authors declare that the research was conducted in the absence of any commercial or financial relationships that could be construed as a potential conflict of interest.

## Publisher's note

All claims expressed in this article are solely those of the authors and do not necessarily represent those of their affiliated organizations, or those of the publisher, the editors and the reviewers. Any product that may be evaluated in this article, or claim that may be made by its manufacturer, is not guaranteed or endorsed by the publisher.

## Supplementary material

The Supplementary Material for this article can be found online at: https://www.frontiersin.org/articles/10.3389/fonc.2022.1091877/full#supplementary-material

## References

1. French CA. Pathogenesis of NUT midline carcinoma. *Annu Rev Pathol* (2012) 7:247–65. doi: 10.1146/annurev-pathol-011811-132438

2. Kubonishi I, Takehara N, Iwata J, Sonobe H, Ohtsuki Y, Abe T, et al. Novel t (15;19)(q15;p13) chromosome abnormality in a thymic carcinoma. *Cancer Res* (1991) 51(12):3327–8.

3. Eagen KP, French CA. Supercharging BRD4 with NUT in carcinoma. *Oncogene.* (2021) 40(8):1396–408. doi: 10.1038/s41388-020-01625-0

4. French C. NUT midline carcinoma. *Nat Rev Cancer.* (2014) 14(3):149–50. doi: 10.1038/nrc3659

5. Jung M, Kim SI, Kim JW, Jeon YK, Lee C. NUT carcinoma in the pelvic cavity with unusual pathologic features. *Int J Gynecol Pathol* (2022) 41(3):292–7. doi: 10.1097/PGP.0000000000000801

6. Moreno V, Saluja K, Pina-Oviedo S. NUT carcinoma: Clinicopathologic features, molecular genetics and epigenetics. *Front Oncol* (2022) 12:860830. doi: 10.3389/fonc.2022.860830

7. Bauer DE, Mitchell CM, Strait KM, Lathan CS, Stelow EB, Lüer SC, et al. Clinicopathologic features and long-term outcomes of NUT midline carcinoma. *Clin Cancer Res* (2012) 18(20):5773–9. doi: 10.1158/1078-0432.CCR-12-1153

8. Haack H, Johnson LA, Fry CJ, Crosby K, Polakiewicz RD, Stelow EB, et al. Diagnosis of NUT midline carcinoma using a NUT-specific monoclonal antibody. *Am J Surg Pathol* (2009) 33(7):984–91. doi: 10.1097/PAS.0b013e318198d666

9. Dragoescu E, French C, Cassano A, Baker SJr., Chafe W. NUT midline carcinoma presenting with bilateral ovarian metastases: a case report. *Int J Gynecol Pathol* (2015) 34(2):136–42. doi: 10.1097/PGP.0000000000000129

10. Riley DS, Barber MS, Kienle GS, Aronson JK, von Schoen-Angerer T, Tugwell P, et al. CARE guidelines for case reports: explanation and elaboration document. *J Clin Epidemiol.* (2017) 89:218–35. doi: 10.1016/j.jclinepi.2017.04.026

11. Stevens TM, Morlote D, Xiu J, Swensen J, Brandwein-Weber M, Miettinen MM, et al. NUTM1-rearranged neoplasia: a multi-institution experience yields novel fusion partners and expands the histologic spectrum. *Mod Pathol* (2019) 32 (6):764–73. doi: 10.1038/s41379-019-0206-z

12. Khabirova E, Jardine L, Coorens THH, Webb S, Treger TD, Engelbert J, et al. Single-cell transcriptomics reveals a distinct developmental state of KMT2A-rearranged infant b-cell acute lymphoblastic leukemia. *Nat Med* (2022) 28(4):743–51. doi: 10.1038/s41591-022-01720-7

13. Tamura R, Nakaoka H, Yoshihara K, Mori Y, Yachida N, Nishikawa N, et al. Novel MXD4-NUTM1 fusion transcript identified in primary ovarian undifferentiated small round cell sarcoma. *Genes Chromosomes Cancer.* (2018) 57(11):557–63. doi: 10.1002/gcc.22668

14. McEvoy CR, Fox SB, Prall OWJ. Emerging entities in NUTM1-rearranged neoplasms. *Genes Chromosomes Cancer.* (2020) 59(6):375–85. doi: 10.1002/gcc.22838

15. French CA, Cheng ML, Hanna GJ, DuBois SG, Chau NG, Hann CL, et al. Report of the first international symposium on NUT carcinoma. *Clin Cancer Res* (2022) 28(12):2493–505. doi: 10.1158/1078-0432.CCR-22-0591

16. Allison DB, Rueckert J, Cornea V, Lee CY, Dueber J, Bocklage T. Thyroid carcinoma with NSD3::NUTM1 fusion: a case with thyrocyte differentiation and colloid production. *Endocr Pathol* (2022) 33(2):315–26. doi: 10.1007/s12022-021-09700-2

17. Walker DM, Urbé S, Dove SK, Tenza D, Raposo G, Clague MJ. Characterization of MTMR3. an inositol lipid 3-phosphatase with novel substrate specificity. *Curr Biol* (2001) 11(20):1600–5. doi: 10.1016/S0960-9822 (01)00501-2

18. Hoefkens E, Nys K, John JM, Van Steen K, Arijs I, van der Goten J, et al. Genetic association and functional role of crohn disease risk alleles involved in microbial sensing, autophagy, and endoplasmic reticulum (ER) stress. *Autophagy.* (2013) 9(12):2046–55. doi: 10.4161/auto.26337

19. Schaletzky J, Dove SK, Short B, Lorenzo O, Clague MJ, Barr FA. Phosphatidylinositol-5-phosphate activation and conserved substrate specificity of the myotubularin phosphatidylinositol 3-phosphatases. *Curr Biol* (2003) 13 (6):504–9. doi: 10.1016/S0960-9822(03)00132-5

20. Kim SA, Taylor GS, Torgersen KM, Dixon JE. Myotubularin and MTMR2, phosphatidylinositol 3-phosphatases mutated in myotubular myopathy and type 4B charcot-Marie-Tooth disease. *J Biol Chem* (2002) 277(6):4526–31. doi: 10.1074/jbc.M111087200

21. Laporte MH, Bouhlel IB, Bertiaux E, Morrison CG, Giroud A, Borgers S, et al. Human SFI1 and centrin form a complex critical for centriole architecture and ciliogenesis. *EMBO J* (2022) 41(21):e112107. doi: 10.15252/embj.2022112107

22. McDonough CW, Palmer ND, Hicks PJ, Roh BH, An SS, Cooke JN, et al. A genome-wide association study for diabetic nephropathy genes in African americans. *Kidney Int* (2011) 79(5):563–72. doi: 10.1038/ki.2010.467

23. Esposito MR, Binatti A, Pantile M, Coppe A, Mazzocco K, Longo L, et al. Somatic mutations in specific and connected subpathways are associated with short neuroblastoma patients' survival and indicate proteins targetable at onset of disease. *Int J Cancer.* (2018) 143(10):2525–36. doi: 10.1002/ijc.31748

24. Kodani A, Moyer T, Chen A, Holland A, Walsh CA, Reiter JF. SFI1 promotes centriole duplication by recruiting USP9X to stabilize the microcephaly protein STIL. *J Cell Biol* (2019) 218(7):2185–97. doi: 10.1083/jcb.201803041

25. Zervos AS, Gyuris J, Brent R. Mxi1, a protein that specifically interacts with max to bind myc-max recognition sites. *Cell.* (1993) 72(2):223–32. doi: 10.1016/0092-8674(93)90662-A

26. Dugast-Darzacq C, Grange T, Schreiber-Agus NB. Differential effects of Mxi1-SRalpha and Mxi1-SRbeta in myc antagonism. *FEBS J* (2007) 274(17):4643–53. doi: 10.1111/j.1742-4658.2007.05992.x

27. Wu W, Hu Z, Wang F, Gu H, Jiang X, Xu J, et al. Mxi1-0 regulates the growth of human umbilical vein endothelial cells through extracellular signal-regulated kinase 1/2 (ERK1/2) and interleukin-8 (IL-8)-dependent pathways. *PloS One* (2017) 12(6):e0178831. doi: 10.1371/journal.pone.0178831

28. McEvoy CR, Holliday H, Thio N, Mitchell C, Choong DY, Yellapu B, et al. A MXI1-NUTM1 fusion protein with MYC-like activity suggests a novel oncogenic mechanism in a subset of NUTM1-rearranged tumors. *Lab Invest.* (2021) 101 (1):26–37. doi: 10.1038/s41374-020-00484-3

29. Chen L, Larsen B, Dermawan JK, Zarka MA. Cytomorphology of NUTM1-rearranged sarcoma involving pleural fluid. *Diagn Cytopathol.* (2022) 50(9):E244–e7. doi: 10.1002/dc.24968

30. Duan FL, Hou J, Guo P, Tan H, Dai J, Tang Z, et al. Clinicopathologic features of an MXI1::NUTM1 fusion neoplasm; a new molecular variant of the

family of NUTM1-rearranged neoplasm. *Histopathology*. (2022) 81(4):536–9. doi: 10.1111/his.14720

31. Chau NG, Hurwitz S, Mitchell CM, Aserlind A, Grunfeld N, Kaplan L, et al. Intensive treatment and survival outcomes in NUT midline carcinoma of the head and neck. *Cancer*. (2016) 122(23):3632–40. doi: 10.1002/cncr.30242

32. Chau NG, Ma C, Danga K, Al-Sayegh H, Nardi V, Barrette R, et al. An anatomical site and genetic-based prognostic model for patients with nuclear protein in testis (NUT) midline carcinoma: Analysis of 124 patients. *JNCI Cancer Spectr* (2020) 4(2):pkz094. doi: 10.1093/jncics/pkz094

33. French CA, Miyoshi I, Kubonishi I, Grier HE, Perez-Atayde AR, Fletcher JA. BRD4-NUT fusion oncogene: a novel mechanism in aggressive carcinoma. *Cancer Res* (2003) 63(2):304–7.

34. Davis BN, Karabakhtsian RG, Pettigrew AL, Arnold SM, French CA, Brill YM. Nuclear protein in testis midline carcinomas: a lethal and underrecognized entity. *Arch Pathol Lab Med* (2011) 135(11):1494–8. doi: 10.5858/arpa.2010-0389-CR

35. Arimizu K, Hirano G, Makiyama C, Matsuo M, Sasaguri T, Makiyama A. NUT carcinoma of the nasal cavity that responded to a chemotherapy regimen for ewing's sarcoma family of tumors: a case report. *BMC Cancer* (2018) 18(1):1134. doi: 10.1186/s12885-018-5087-x

36. Muramatsu J, Takada K, Sugita S, Tsuchiya T, Yamamoto K, Takagi M, et al. Complete response induced by concurrent chemoradiotherapy in a patient with NUT carcinoma. *Intern Med* (2022) 61(8):1299–304. doi: 10.2169/internalmedicine.7741-21

37. Kloker LD, Calukovic B, Benzler K, Golf A, Böhm S, Günther S, et al. Case report: Immunovirotherapy as a novel add-on treatment in a patient with thoracic NUT carcinoma. *Front Oncol* (2022) 12:995744. doi: 10.3389/fonc.2022.995744

38. Pan M, Chang JS. Durable complete remission of PD-L1 positive NUT carcinoma treated with concurrent chemotherapy and radiation. *Perm J* (2020) 25:1–3. doi: 10.7812/TPP/20.251

39. Jung M, Kim S, Lee JK, Yoon SO, Park HS, Hong SW, et al. Clinicopathological and preclinical findings of NUT carcinoma: A multicenter study. *Oncologist*. (2019) 24(8):e740–e8. doi: 10.1634/theoncologist.2018-0477

40. Shiota H, Alekseyenko AA, Wang ZA, Filic I, Knox TM, Luong NM, et al. Chemical screen identifies diverse and novel histone deacetylase inhibitors as repressors of NUT function: Implications for NUT carcinoma pathogenesis and treatment. *Mol Cancer Res* (2021) 19(11):1818–30. doi: 10.1158/1541-7786.MCR-21-0259

41. Sun K, Atoyan R, Borek MA, Dellarocca S, Samson ME, Ma AW, et al. Dual HDAC and PI3K inhibitor CUDC-907 downregulates MYC and suppresses growth of MYC-dependent cancers. *Mol Cancer Ther* (2017) 16(2):285–99. doi: 10.1158/1535-7163.MCT-16-0390

42. Lewin J, Soria JC, Stathis A, Delord JP, Peters S, Awada A, et al. Phase ib trial with birabresib, a small-molecule inhibitor of bromodomain and extraterminal proteins, in patients with selected advanced solid tumors. *J Clin Oncol* (2018) 36 (30):3007–14. doi: 10.1200/JCO.2018.78.2292

43. Piha-Paul SA, Hann CL, French CA, Cousin S, Braña I, Cassier PA, et al. Phase 1 study of molibresib (GSK525762), a bromodomain and extra-terminal domain protein inhibitor, in NUT carcinoma and other solid tumors. *JNCI Cancer Spectr* (2020) 4(2):pkz093. doi: 10.1093/jncics/pkz093

44. Ameratunga M, Braña I, Bono P, Postel-Vinay S, Plummer R, Aspegren J, et al. First-in-human phase 1 open label study of the BET inhibitor ODM-207 in patients with selected solid tumours. *Br J Cancer*. (2020) 123(12):1730–6. doi: 10.1038/s41416-020-01077-z

45. Shapiro GI, LoRusso P, Dowlati A, TD K, CA J, Vaishampayan U, et al. A phase 1 study of RO6870810, a novel bromodomain and extra-terminal protein inhibitor, in patients with NUT carcinoma, other solid tumours, or diffuse large b-cell lymphoma. *Br J Cancer* (2021) 124(4):744–53. doi: 10.1038/s41416-020-01180-1

46. Hilton J, Cristea M, Postel-Vinay S, Baldini C, Voskoboynik M, Edenfield W, et al. BMS-986158, a small molecule inhibitor of the bromodomain and extraterminal domain proteins, in patients with selected advanced solid tumors: Results from a phase 1/2a trial. *Cancers (Basel)* (2022) 14(17). doi: 10.3390/cancers14174079

frontiers | Frontiers in Oncology

TYPE Case Report
PUBLISHED 12 January 2023
DOI 10.3389/fonc.2022.990600



OPEN ACCESS

EDITED BY
Zhaolun Cai,
Sichuan University, China

REVIEWED BY
Ziv Radisavljevic,
Harvard Medical School, United States
Yuichiro Ueda,
Fukuoka University Hospital, Japan

*CORRESPONDENCE
Meng Tang
1205469172@qq.com
Yang Qiu
qyangy@sina.com
Haidong Wang
xxwkwhd@sina.com

†These authors have contributed equally to this work

SPECIALTY SECTION
This article was submitted to Surgical Oncology, a section of the journal Frontiers in Oncology

RECEIVED 10 July 2022
ACCEPTED 19 December 2022
PUBLISHED 12 January 2023

CITATION
He B, Zhang S, Ren L, Zhou Y, Chen Q, Tang J, Zhang Y, Tang M, Qiu Y and Wang H (2023) Case report: Thyroid carcinoma invading trachea: Multidisciplinary resection and reconstruction assisted by extracorporeal membrane oxygenation. *Front. Oncol.* 12:990600. doi: 10.3389/fonc.2022.990600



# Case report: Thyroid carcinoma invading trachea: Multidisciplinary resection and reconstruction assisted by extracorporeal membrane oxygenation

Bo He[1†], Shixin Zhang[1†], Lin Ren[2†], Yi Zhou[1†], Qiao Chen[1], Jinghua Tang[1], Yi Zhang[2], Meng Tang[1*], Yang Qiu[1*] and Haidong Wang[1*]

[1]Department of Thoracic Surgery, Southwest Hospital, Army Medical University (Third Military Medical University), Chongqing, China, [2]Department of Breast and Thyroid Surgery, Southwest Hospital, Army Medical University (Third Military Medical University), Chongqing, China

**Background:** When thyroid cancer invades the trachea, tumor resection and trachea reconstruction are required. Although the traditional way of anesthesia and tracheal intubation can maintain the necessary ventilation function during the operation, tracheal intubation affects the surgical field of vision and is not conducive to the protection of the recurrent laryngeal nerve beside the trachea during the operation.

**Case presentation:** Extracorporeal membrane oxygenation (ECMO) is used to replace traditional tracheal intubation in the process of resection and end-to-end anastomosis of tracheal tumors, and complete tracheal tumor resection and trachea reconstruction are achieved.

**Conclusion:** Using ECMO for thyroid carcinoma resection, invaded trachea resection, and trachea reconstruction is safe and effective, which reduces the obstruction of endotracheal intubation on the operative field, guarantees the rapid and efficient end-to-end anastomosis in the upper trachea, and clearly avoids laryngeal recurrent nerve injury in the process of anastomosis.

KEYWORDS

**ECMO, thyroid tumor resection, trachea reconstruction, case report, safe and effective**

## Background

In 2020, the number of new cases of thyroid cancer in the world was about 580,000, and the incidence of thyroid cancer ranked 11th among all cancers (1). Thyroid tumors are the most common head and neck tumors involving the cervical trachea. For patients with a thyroid malignant tumor that has invaded the trachea, the operation requires that the thyroid and trachea invaded by the tumor are resected according to the scope of surgery, and tracheal respiration and neck dissection should be performed according to the situation (2, 3).

When thyroid cancer invades the trachea and recurrent laryngeal nerve, patients are at risk of respiratory distress, asphyxia, and even death. Sleeve resection of tracheal tumors and airway reconstruction are effective methods to treat tracheal tumors and save patients' lives. The simultaneous surgery of tracheal resection and tracheal reconstruction is also one of the most complicated and difficult operations, which is required a high level of surgical techniques and perioperative management. The difficulty of the operation is reflected in complete tumor resection, tracheal resection and reconstruction, and retention of functions of the recurrent laryngeal nerve and parathyroid gland at the same time. After multidisciplinary consultation, it was finally determined to complete the operation with extracorporeal membrane oxygenation (ECMO) assistance. This may be the first case of resection and reconstruction of the trachea invaded by thyroid cancer assisted by ECMO in China.

Although the traditional way of anesthesia and tracheal intubation can maintain the necessary ventilation function during the operation, tracheal intubation affects the surgical field of vision and is not conducive to the protection of the recurrent laryngeal nerve beside the trachea during the operation.

Therefore, in order to achieve the best surgical results and further expose the surgical field, we performed resection of thyroid cancer with invaded trachea and tracheal end-to-end anastomosis with the assistance of ECMO without mechanical ventilation and tracheal intubation in the surgical field.

Thyroid surgery was performed with radical thyroidectomy. During the operation, the recurrent laryngeal nerve monitoring technique was used to preserve the function of the invaded recurrent laryngeal nerve. The function of the parathyroid gland was preserved by using hyperfine dorsal membrane anatomy, negative imaging of the parathyroid gland, and parathyroid transplantation so as to ensure the postoperative quality of life.

This study was reported in agreement with the principles of the CARE guidelines (4).

## Case presentation

A 65-year-old woman was referred to our hospital after an examination revealed a right goiter due to an irritating dry cough. Computed tomography (CT) showed a mass in the right lobe and isthmus of the thyroid gland, and thyroid cancer was considered, which invaded the adjacent trachea and was accompanied by lymph node metastasis in cervical region 6 (Figure 1A). Fiberoptic bronchoscopy showed a protuberant tumor on the right anterior wall of the trachea, which was about 3 cm away from the glottis; the tracheal lumen was obviously narrow; no obvious abnormality was found in the remaining bilateral bronchus (Figure 1B). The cytological results of bronchial brushing showed abnormal cells of which the origin was not excluded from the thyroid.

Before the operation, the multidisciplinary consultation of thoracic surgery, thyroid and breast surgery, anesthesiology, cardiovascular medicine, and respiratory medicine was conducted, and relevant discussions and decisions were completed: 1) thyroid cancer invaded the trachea, and partial tracheal resection and tracheal reconstruction were required during the operation. 2) Preoperative assessment found the patient with mild chronic obstructive pulmonary disease, mild asthma, and airway resistance on the high side, which might lead to endotracheal mass dropping, bronchial foreign bodies blocked, and tumor cell implantation metastasis during induction of anesthesia. In order to ensure surgical safety, ECMO support was strongly recommended by respiratory and anesthesia specialists, which had indications. 3) The neck space was narrow, and the tracheal intubation seriously affected the operation field and hindered anastomosis. With the assistance of ECMO, tracheal intubation could be temporarily removed during intraoperative tracheal resection and reconstruction. 4) For neoplastic lesions with severe airway obstruction, prioritizing the establishment of ECMO during the induction of anesthesia is extremely important to ensure patient safety. In this case, preoperative CT showed that the diameter of the narrowest tracheal area was greater than 1 cm. After preoperative evaluation by the Department of Anesthesiology, it was considered safe and feasible to perform 8-mm outer diameter tracheal intubation. 5) After discussion with the Department of Thyroid and Breast Surgery, it was decided that the operation would be carried out in two stages: the first stage was carried out by the Department of Thyroid and Breast Surgery. After the resection of the thyroid tumor, the scope of tracheal invasion was further explored to accurately determine the way of tracheal anastomosis, minimize anastomotic tension, and also to ensure that the recurrent laryngeal nerve was not damaged during surgery. At this stage, ECMO was not required, and only conventional tracheal intubation was performed. The second stage was performed by the Thoracic Surgery Department. With the surgical field fully exposed under the assistance of ECMO, the Thoracic Surgery Department completed the tracheal tumor resection and end-to-end anastomosis as soon as possible.

After the patient's informed consent was obtained, the following was performed: total thyroidectomy + bilateral central

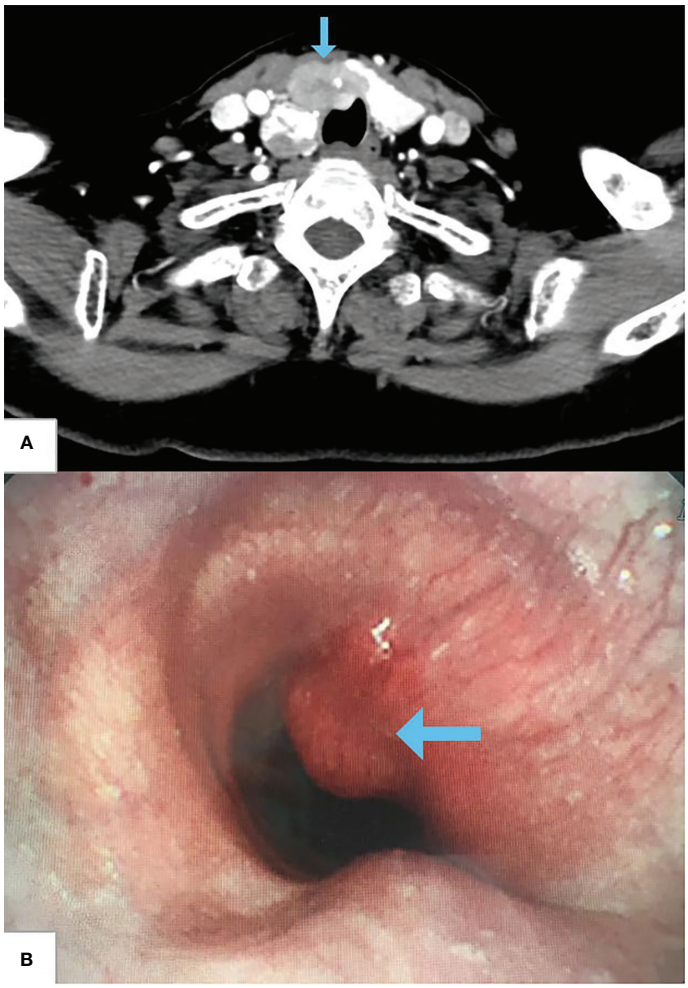


FIGURE 1
Preoperative cervical CT and fiberoptic bronchoscopy. **(A)** CT shows thyroid carcinoma invading trachea (arrow). **(B)** Fiberoptic bronchoscopy shows a protuberant tumor on the right anterior wall of the trachea, and the tracheal lumen is obviously narrow (arrow).

region lymph node dissection + bilateral recurrent laryngeal nerve exploration + right region 3 and 4 lymph node dissection + left upper parathyroid and left sternocleidomastoid muscle transplantation + ECMO-assisted tracheal tumor resection + tracheal end-to-end anastomosis. The patient was placed in a supine position for general anesthesia. The venous (V-V) ECMO cannulas of the left femoral vein to the right internal jugular vein were quickly established after heparinization.

The detailed operation process is as follows.

The patient was placed in a supine position, and after routine disinfection and towel spreading, 8-mm endotracheal intubation and ventilator ventilation were performed under the guidance of a fiberoptic bronchoscope, and the process was smooth. A 7-cm horizontal low collar incision on the neck was made along the dermatoglyph and 2 cm above the clavicle. Further separation and exploration revealed that the tumor was located in the right thyroid lobe, invading the anterior cervical muscle, the right recurrent laryngeal nerve, and the trachea. The length of the invaded trachea was about 2 cm, and the front wall and both side walls of the second and third cartilage rings were invaded occupying about 2/3 of the trachea, which made it difficult to peel off.

The Department of Thyroid and Breast Surgery operated at first. Nano-carbon suspension measuring 0.1 ml was injected into thyroid tissue for parathyroid negative development. The blood vessels of the superior pole of the thyroid were ligated. From top to bottom, the thyroid tissue was separated from the back of the thyroid gland to the surface of the trachea, and the blood vessels of the inferior pole of the thyroid were ligated. The right recurrent laryngeal nerve was seen surrounded by a tumor, and the recurrent laryngeal nerve was separated to be protected by blunt dissection. The upper and lower parathyroid glands were retained, the thyroid tissue was cut off at the isthmus of the thyroid, and the right and left thyroid glands were successfully removed, avoiding the invaded

trachea (Figure 2A). Then, bilateral central lymph node dissection was performed. During the operation, the monitoring instrument of the recurrent laryngeal nerve showed that the structure of the bilateral recurrent laryngeal nerve was intact, the electrophysiological activity of the left recurrent laryngeal nerve was intact, and that of the right recurrent laryngeal nerve was slightly weakened, which was considered to be caused by tumor invasion of nerve and edema after dissection.

The thoracic surgery team and the ECMO team performed partial tracheal resection and end-to-end sleeve anastomosis assisted by ECMO according to the plan discussed before surgery. Two thoracic surgeons subsequently performed intubation, and one extracorporeal perfusionist prefilled the ECMO tubes and heparinized the whole body. With the assistance of ultrasound, an intravenous cannula (CB96670-021, Medtronic, Shanghai, China) was placed at the opening between the inferior vena cava and the right atrium as an external drainage tube to draw venous blood out of the body, and an arterial cannula (CB96570-019, Medtronic) was placed at the opening between the right internal jugular vein and the right superior atrial vena cava as a return tube to bring external oxygenated blood into the body.

The MAQUET cardiopulmonary bypass package BE-PLS 2050 was used to prefill, exhaust, and connect ECMO tubes and cannulas. ECMO diversion was started, the endotracheal intubation retreated to the vicinity of the tracheal glottis, the ventilator was stopped, and oxygen was supplied by V-V ECMO diversion. Intraoperative ECMO parameters were as follows: centrifugal pump was maintained at 3,500 revolutions per minute, ECMO flow rate was maintained at 3.2 L/min, the fraction of inspiration $O_2$ was maintained at 45%, and airflow was maintained at 4.5 L/min. Oxygen saturation during the operation was between 98% and 100%.

The endotracheal tube was retracted near the trachea glottis, and the ventilator was stopped. The second and third tracheal rings and tumors were annularly resected 0.5 cm away from the

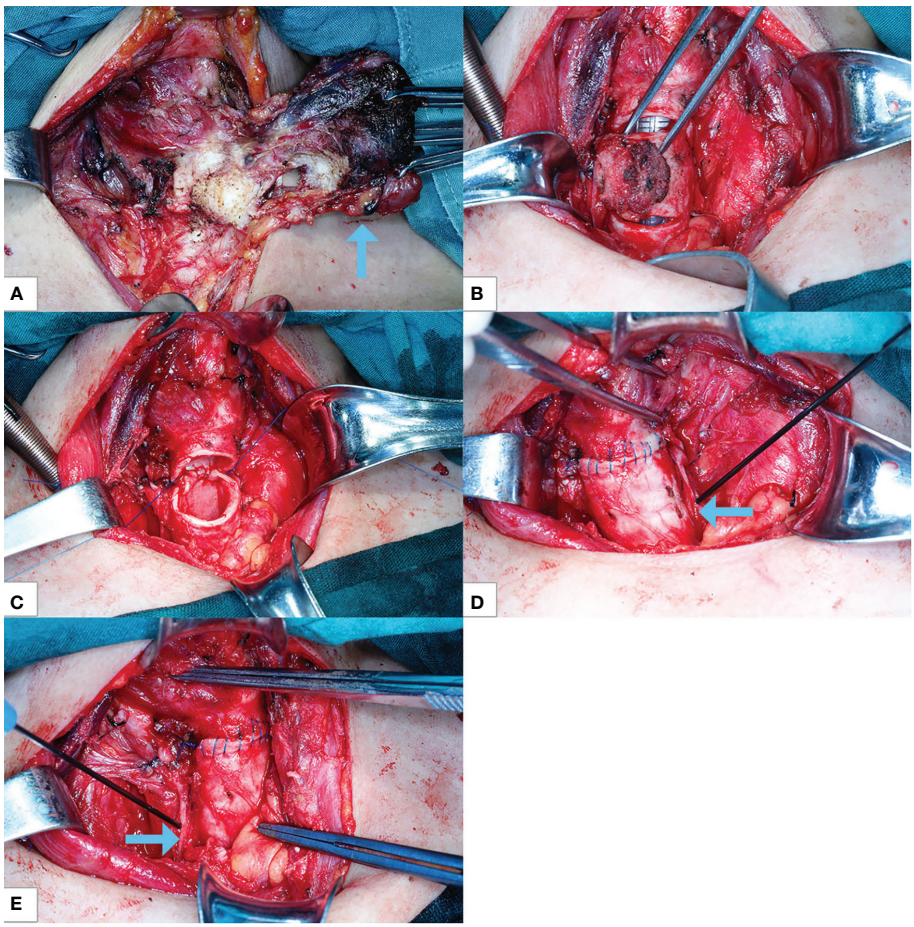


FIGURE 2
Intraoperative photographs. **(A)** Thyroid cancer invades the trachea (arrow). **(B)** The second and third tracheal rings and tumors are annularly resected with tracheal intubation ventilation condition. **(C)** The trachea end-to-end sleeve anastomosis is ongoing with ECMO ventilation. **(D)** The anastomosis is completed, with left recurrent laryngeal nerve with nerve detection and protection (arrow). **(E)** Right recurrent laryngeal nerve with nerve detection and protection (arrow). ECMO, extracorporeal membrane oxygenation.

upper and lower ends of the tracheal tumor (Figure 2B). The tracheal tumor specimens were taken out and sent for pathological examination, indicating chronic inflammation of the tracheal stump. The trachea end-to-end sleeve anastomosis of the trachea was completed without tension (Figures 2C–E). The monitoring technology of the recurrent laryngeal nerve was used to protect the recurrent laryngeal nerve in the whole process of tracheal resection and anastomosis. The endotracheal intubation was re-sent below the tracheal anastomosis, and the ventilator was resumed for assisted breathing. No air leakage was observed in the anastomosis. The morphology of tracheal end-to-end anastomosis was verified by fiberoptic bronchoscopy.

ECMO was discontinued, ECMO cannulas were removed, activated clotting time (ACT) was examined for 178 s, and 25 mg of protamine was used to neutralize heparin. The circulation time of ECMO was 50 min, during which the patient's blood pressure was stable and the oxygen saturation was 100%. The operation was smooth and successful, the intraoperative blood loss was about 400 ml, and no blood transfusion was given.

After the operation, the patient returned to the intensive care unit of thoracic surgery and recovered smoothly. She was discharged from the hospital after 11 days of operation and was required to wear a neck brace and maintain the head-down position for 2 weeks. The symptom of hoarseness was improved. Postoperative pathological results showed that there were three nodules in the right thyroid, two of which were papillary carcinoma involving striated muscle tissue and the whole trachea, and no cancer tissue was involved in the upper and lower stump of the trachea. Metastasis was observed in lymph nodes in the left central region, right central region, and right cervical lateral region. Postoperative neck–chest CT imaging of the respiratory tract showed that the right anterior wall of the cervical trachea returned to normal (Figures 3A, B).

## Discussion

Among thyroid cancer, 95% of thyroid cancers were differentiated thyroid cancer (DTC), mainly including papillary thyroid carcinoma (PTC), follicular thyroid carcinoma (FTC), and Hürthle cell carcinoma (HCC). Its clinical treatment involves ultrasound medicine, pathology, surgery, nuclear medicine, endocrinology, oncology, radiotherapy, interventional medicine and laboratory medicine, and many other disciplines. Surgery is the preferred treatment for most DTC patients, which plays a crucial role in the prognosis of the disease. Radical tumor resection is one of the

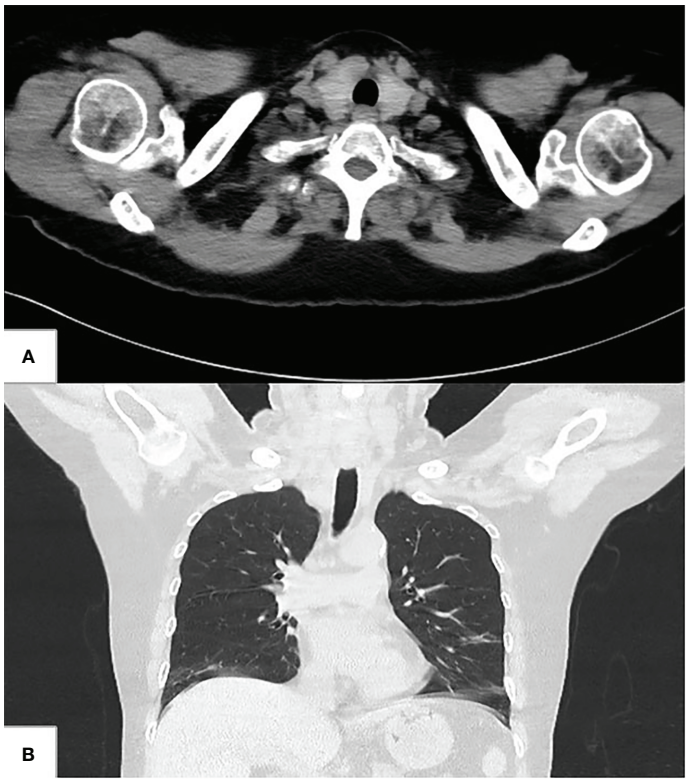


FIGURE 3
Postoperative neck–chest CT. **(A)** Transverse image shows the right anterior wall of the cervical trachea returned to normal. **(B)** coronal image shows the right anterior wall of the cervical trachea returned to normal.

important factors related to the prognosis of patients with DTC. T4 patients with a tumor that has invaded the surrounding structural organs generally are advised total thyroid gland resection; at the same time, the parts of the surrounding affected structures are needed to be removed, like the partial larynx and even the whole larynx, partial trachea, hypopharynx, partial esophagus, and so on. The treatment of DTC is mainly surgical treatment, supplemented by postoperative endocrine therapy, radionuclide therapy, radiotherapy, and targeted therapy in some cases (5).

Different types of thyroid tumors have different degrees and ways of tracheal involvement. The influence of thyroid benign tumors on the cervical trachea is mainly the compression of the trachea, and long compression time may lead to tracheomalacia. Thyroid malignant tumor not only directly compresses the trachea but also invades the trachea. McCaffrey et al. summarized the clinical data of 262 patients with papillary thyroid carcinoma invading the upper respiratory tract from 1940 to 1990 and found that upper respiratory tract involvement was an important factor affecting the survival rate of patients. At the same time, if the upper respiratory tract lumen was invaded, the mortality rate would be significantly increased (6).

Some foreign scholars believe that no matter how much scope of invasion, they are inclined to adopt tracheal circular resection and end-to-end anastomosis. Compared with window resection, this operation completely keeps the prototype of the airway, avoids the occurrence of airway stenosis, and maximizes the negative rate of incision margin. With the improvement of anastomosis technology, the risk of anastomotic leakage was not increased (21% *vs.* 25%), and patients could obtain a greater survival benefit (7).

During the operation, the diseased trachea was not only an important channel to ensure ventilation and maintain oxygenation during anesthesia operation but also the surgical site of surgeons, so the anesthesia management of partial tracheal resection and tracheal reconstruction was very complicated and tricky. There are no anesthetic guidelines and expert consensuses related to a tracheal tumor in China to determine airway opening strategies based on the size, location, characteristics, and degree of ventilation difficulty of tracheal masses (8, 9).

## Method 1

Patients with tumors located in the trachea are generally fit, have a satisfactory cardiopulmonary function, can lie down, have no dyspnea, and have mild tracheal stenosis. Their tumors have wide bases and non-annular growth and do not easily bleed when touched, in which situations rapid induction of endotracheal intubation is feasible. The tracheal tube with a smaller diameter than the narrowest place is selected, and the surface is fully lubricated. Guided by a fiberoptic bronchoscope, the tracheal intubation is completed through the tumor, and the tracheal balloon is placed below the tumor.

## Method 2

Patients have obvious dyspnea and severe tracheal stenosis, their lumen of the narrow section is irregular tubular, and the tumor surface easily bleeds when touched, which is a great risk. Such patients are advocated to keep spontaneous breathing, tracheotomy is conducted with local anesthesia below the tumor, and the endotracheal tube is inserted. Then, the tracheal tube is changed to be inserted through the mouth after resection of the tumor segment and end-to-end anastomosis, and the tracheal tube balloon passes over the anastomotic place.

## Method 3

If the inner diameter of the trachea is severely reduced, the trachea is distorted, or the tumor is free, and the forced insertion of the tracheal intubation will easily cause tumor shedding or bleeding and will cause ventilation dysfunction or suffocation. In this situation, right femoral arteriovenous intubation can be selected under local anesthesia to establish cardiopulmonary bypass and then induce anesthesia. The endotracheal tube is then placed at the proximal end of tracheal stenosis under the guidance of a fiberoptic bronchoscope. During the operation, the trachea is cut open in the lower segment of the stenosis, and tracheal intubation is performed to maintain ventilation. The cardiopulmonary bypass is removed early to reduce related complications such as coagulation dysfunction and intraoperative bleeding.

In 1965, Nevile et al. first reported the application of cardiopulmonary bypass in thoracic surgery (10). However, cardiopulmonary bypass may increase postoperative bleeding and potential complications such as liver and kidney function damage. Moreover, it is technically difficult and time-consuming to establish cardiopulmonary bypass, and at the same time, it can cause great trauma and late infection to patients, so it is not an ideal support method.

## Method 4

ECMO has been recently reported for carinal reconstruction surgery (11). In 2017, our team successfully completed ECMO-assisted tracheal tumor resection and carina reconstruction

(Thompson's operation). We used V-V ECMO to maintain a satisfactory oxygen supply without tracheal intubation, which proved that ECMO-assisted tracheal tumor resection and carina reconstruction is a safer and more effective technique as compared with traditional methods (12). ECMO support has also been used in neonatal trachea reconstruction with satisfactory results (13).

V-V ECMO can support partial or total lung function and can be used in patients with respiratory failure (14). ECMO can completely or partially replace cardiopulmonary function, and its auxiliary application provides the possibility and necessary guarantee for bronchoscopy and surgical treatment, which is a reasonable mode in airway reconstruction surgery.

The ECMO treatment used in this patient has the following advantages: 1) generally, systemic anticoagulation is required during ECMO diversion, which may increase the risk of bleeding during surgery. In this case, ECMO pipelines were established after thyroid tumor resection. The ECMO turnaround time was very short during tracheal resection and anastomosis. Protamine injection was used to neutralize heparin immediately after the removal of ECMO, so there would be no large blood loss during the operation. 2) There are many intubation modes that can be selected during ECMO operation, such as femoral arteriovenous intubation, internal jugular vein intubation, and common carotid artery intubation, which provide multiple anesthesia modes. 3) V-V ECMO is used to maintain a satisfactory oxygen supply without endotracheal intubation. 4) ECMO reduces the impact of tracheal intubation on the surgical field in a narrow space, improves the accuracy of anastomosis, and clearly avoids injury to the recurrent laryngeal nerve during anastomosis. There are also disadvantages in this case: ECMO does increase the cost of treatment, and the operation time will increase accordingly. However, we believe that under the condition of ECMO, the visual field of end-to-end tracheal anastomosis is more sufficient, and the anastomosis time can be greatly shortened, which actually shortens the operation time in another aspect.

In conclusion, this case proves that using ECMO for thyroid carcinoma resection, invaded trachea resection, and trachea reconstruction is safe and effective, which reduces the obstruction of endotracheal intubation on the operative field, guarantees the rapid and efficient end-to-end anastomosis in the upper trachea, and clearly avoids laryngeal recurrent nerve injury in the process of anastomosis, which provides another reference anesthesia and surgical method.

## Data availability statement

The raw data supporting the conclusions of this article will be made available by the authors, without undue reservation.

## Ethics statement

Written informed consent was obtained from the individual(s) for the publication of any potentially identifiable images or data included in this article.

## Author contributions

BH, SZ, LR, and YZho proceed the surgery. These authors contributed equally to this work and share first authorship. QC, JT, and YZha: assistant in nursing. MT and YQ prepared the first draft of the manuscript. HW finalized the manuscript and instructed the case. All authors contributed to the article and approved the submitted version.

## Funding

This work was supported by the fund from The Joint Medical Research Project of Chongqing Science and Technology Bureau & Chongqing Municipal Health Commission, No. 2019ZDXM003, to HW.

## Conflict of interest

The authors declare that the research was conducted in the absence of any commercial or financial relationships that could be construed as a potential conflict of interest.

## Publisher's note



## References

1. Sung H, Ferlay J, Siegel RL, Laversanne M, Soerjomataram I, Jemal A, et al. Global cancer statistics 2020: GLOBOCAN estimates of incidence and mortality worldwide for 36 cancers in 185 countries. *CA Cancer J Clin* (2021) 71(3):209–49. doi: 10.3322/caac.21660

2. Kim AW, Maxhimer JB, Quiros RM, Weber K, Prinz RA. Surgical management of well-differentiated thyroid cancer locally invasive to the respiratory tract. *J Am Coll Surg* (2005) 201(4):619–27. doi: 10.1016/j.jamcollsurg.2005.05.030

3. Suemitsu R, Takeo S, Hamatake M, Yamamoto T, Furuya K, Momosaki S. Thyroid cancer with a cystic mediastinal tumor invading the right main bronchus. *Ann Thorac Surg* (2010) 89(1):296–8. doi: 10.1016/j.athoracsur.2009.02.084

4. Riley DS, Barber MS, Kienle GS, Aronson JK, von Schoen-Angerer T, Tugwell P, et al. CARE guidelines for case reports: explanation and elaboration document. *J Clin Epidemiol.* (2017), 89:218–235. doi: 10.1016/j.jclinepi.2017.04.026

5. Haugen BR. American Thyroid association management guidelines for adult patients with thyroid nodules and differentiated thyroid cancer: What is new and what has changed? *Cancer* (2015) 123(3):372–81. doi: 10.1002/cncr.30360

6. McCaffrey TV, Bergstralh EJ, Hay ID. Locally invasive papillary thyroid carcinoma: 1940-1990. *Head Neck.* (1994) 16(2):165–72. doi: 10.1002/hed.2880160211

7. Brauckhoff M, Machens A, Thanh PN, Lorenz K, Schmeil A, Stratmann M, et al. Impact of extent of resection for thyroid cancer invading the aerodigestive tract on surgical morbidity, local recurrence, and cancer-specific survival. *Surgery.* (2010) 148(6):1257–66. doi: 10.1016/j.surg.2010.09.011

8. Schieren M, Böhmer A, Dusse F, Koryllos A, Wappler F, Defosse J. New approaches to airway management in tracheal resections-a systematic review and meta-analysis. *J Cardiothorac Vasc Anesth* (2017) 31(4):1351–8. doi: 10.1053/j.jvca.2017.03.020

9. Todd TRJ. Airway management following tracheal surgery. *Thorac Surg Clin* (2018) 28(2):219–26. doi: 10.1016/j.thorsurg.2018.01.007

10. Neville We, Langston Ht, Correll N, Maben H. Cardiopulmonary bypass during pulmonary surgery: preliminary report. *J Thorac Cardiovasc Surg* (1965) 50:265–76.

11. Lei J, Su K, Li XF, Zhou YA, Han Y, Huang LJ, et al. ECMO-assisted carinal resection and reconstruction after left pneumonectomy. *J Cardiothorac Surg* (2010) 5:89. doi: 10.1186/1749-8090-5-89

12. Qiu Y, Chen Q, Wu W, Zhang S, Tang M, Chen Y, et al. Extracorporeal membrane oxygenation (ECMO)-assisted intratracheal tumor resection and carina reconstruction: A safer and more effective technique for resection and reconstruction. *Thorac Cancer.* (2019) 10(5):1297–302. doi: 10.1111/1759-7714.13007

13. Kunisaki SM, Fauza DO, Craig N, Jennings RW. Extracorporeal membrane oxygenation as a bridge to definitive tracheal reconstruction in neonates. *J Pediatr Surg* (2008) 43(5):800–4. doi: 10.1016/j.jpedsurg.2007.12.014

14. Shekar K, Mullany DV, Thomson B, Ziegenfuss M, Platts DG, Fraser JF. Extracorporeal life support devices and strategies for management of acute cardiorespiratory failure in adult patients: a comprehensive review. *Crit Care* (2014) 18(3):219. doi: 10.1186/cc13865

frontiers | Frontiers in Oncology

TYPE Case Report
PUBLISHED 13 January 2023
DOI 10.3389/fonc.2022.1047738



OPEN ACCESS

EDITED BY
Zhaolun Cai,
Sichuan University, China

REVIEWED BY
Sachin Kolte,
Vardhman Mahavir Medical College and Safdarjung Hospital, India
Yongbin Chen,
Key Laboratory of Animal Models and Human Disease Mechanisms (CAS), China

*CORRESPONDENCE
Yan Chen
cheny658@mail.sysu.edu.cn
Ming Gao
gaoming2@mail.sysu.edu.cn

SPECIALTY SECTION
This article was submitted to Surgical Oncology, a section of the journal Frontiers in Oncology

RECEIVED 21 September 2022
ACCEPTED 28 December 2022
PUBLISHED 13 January 2023

CITATION
Chen Y, Qin T, Chen Y and Gao M (2023) Case report: Ewing sarcoma with EWSR–ERG fusion elevates procalcitonin extremely in the long term without infection.
*Front. Oncol.* 12:1047738.
doi: 10.3389/fonc.2022.1047738



# Case report: Ewing sarcoma with EWSR–ERG fusion elevates procalcitonin extremely in the long term without infection

Ying Chen[1], Tao Qin[2], Yan Chen[3]* and Ming Gao[4]*

[1]Sun Yat-sen Memorial Hospital, Sun Yat-sen University, Guangzhou, China, [2]Department of Medical Oncology, Sun Yat-sen Memorial Hospital, Sun Yat-sen University, Guangzhou, China, [3]Department of Hematology, The Eighth Affiliated Hospital of Sun Yat-sen University, Shenzhen, China, [4]Department of Radiology, Sun Yat-sen Memorial Hospital, Sun Yat-sen University, Guangzhou, China

**Background:** Ewing sarcoma (ES) represents a rare, aggressive bone and soft-tissue cancer. Unlike breast, liver, pancreatic, and prostate cancers, Ewing sarcoma has had no representative tumor marker until now. The use of procalcitonin (PCT) as a tumor marker is also rarely reported. PCT is a clinically recognized and widely used inflammatory marker in recent years. In rare cases, PCT may also be falsely positive due to non-infectious factors. In the few previously reported papers regarding the correlation between tumors and PCT, we learned that abnormalities of PCT level can also be impacted by individual cancers.

**Case presentation:** Here, we first reported a case of Ewing sarcoma with markedly elevated PCT without infection and carried out some literature review. The patient was a middle-aged man with extraskeletal Ewing sarcoma whose lesion was located in the distal abdominal ileum. He had a sudden and unprovoked onset of high fever during chemotherapy before surgery. After multiple examinations, the patient's blood routine, C-reactive protein, blood culture, and CT examination showed no signs of infection, and even the culture from the end of the central venous catheter showed no pathogen growth. Only PCT increased dramatically to more than 200 ng/ml. PCT remained at this level for several months until a single abdominal lumpectomy was performed before it dropped to near-normal levels.

**Conclusion:** In our report, PCT is significantly elevated in Ewing sarcoma in the absence of infection. Not only that, but we particularly highlighted the precipitous drop in PCT following tumor resection.

KEYWORDS

Ewing sarcoma, EWSR, procalcitonin, infection, case report, inflammatory marker

## 1 Introduction

Ewing sarcoma was first defined as an independent type of tumor in the early 20th century; it is also known as the Ewing sarcoma family of tumors (ESFT), which mainly includes classical Ewing sarcoma of the bone (ESB), extraskeletal Ewing sarcoma (EES), and primitive neuroectodermal tumor (PNET). It most often begins in the long bone

diaphysis, pelvis, and scapula, although it infrequently occurs in soft tissue. All of them share the common cellular histology and genetic mechanism characterized by small round cells expressing high levels of CD99 and Ewing sarcoma breakpoint region 1 protein (EWSR1) gene disruption. This provides a reliable basis for clinical diagnosis of Ewing sarcoma (1–3). Ewing sarcoma is a highly malignant tumor, most common in people aged 10 to 25 years, with a rare occurrence in older adults (4, 5). Patients with this cancer usually manifest pain, swelling, mass, unexpected tiredness, fever with no known cause, unintentional weight loss, or even anemia only (6). With the improvement of multimodality therapy, the overall survival (OS) has increased from approximately 70% a few years ago to approximately 80% in the past 2 years, although 5-year OS was 30% for patients with metastatic disease and less than 10% for patients who relapsed within 2 years of diagnosis (7–9).

Procalcitonin (PCT) is a prohormone consisting of 116 amino acids with a molecular weight of approximately 13 kDa. Under normal circumstances, PCT is secreted by thyroid C cells and then degraded by enzymes into calcitonin, with very little of it entering the peripheral blood (10, 11), while the PCT increases significantly after bacterial infection since multiple tissues can all express the PCT during sepsis (12). However, it is worth noting that elevated PCT levels can also be caused by non-infectious factors in the minority (13). There have been reports of it, and they include but are not limited to extensive surgery (14), pancreatitis (15, 16), end-stage renal disease (17), newborn (within 48 h of birth) (18), autoimmune diseases, and several neoplastic diseases (small-cell lung cancer, medullary thyroid C cell tumor, and cirrhosis combined with hepatic carcinoma) (19–22).

To the best of our knowledge, high serum levels of PCT have not been reported in Ewing sarcoma especially in the circumstances of no meaningful evidence of bacterial infection until now. Here, we present an adult male patient with extraskeletal Ewing sarcoma who had extremely high PCT levels (>200 ng/ml). Another mystery, in this case, is that the markedly elevated PCT value, which lasted for nearly 100 days, plunged precipitously after the resection of the lesion. This expands the clinical value of PCT in Ewing sarcoma. At the same time, in the absence of bacterial infection, Ewing sarcoma should be included in the differential diagnosis of elevated PCT. The patient has provided permission to publish information about his case, and the identity of the patient has been protected. This study was reported in agreement with the principles of the CAse REports (CARE) guidelines (23).

## 2 Case presentation

In November 2020, a 51-year-old man was examined at a local hospital for moderate anemia (hemoglobin level of 80 g/L) after a routine physical examination. Abdominal computed tomography (CT) findings showed uneven thickening of the terminal ileum (Figure 1). Positron emission tomography–computed tomography (PET/CT) showed a local soft tissue mass at the distal ileum with abnormally elevated glucose metabolism, which was considered a malignant lesion of the small intestine with multiple lymph node

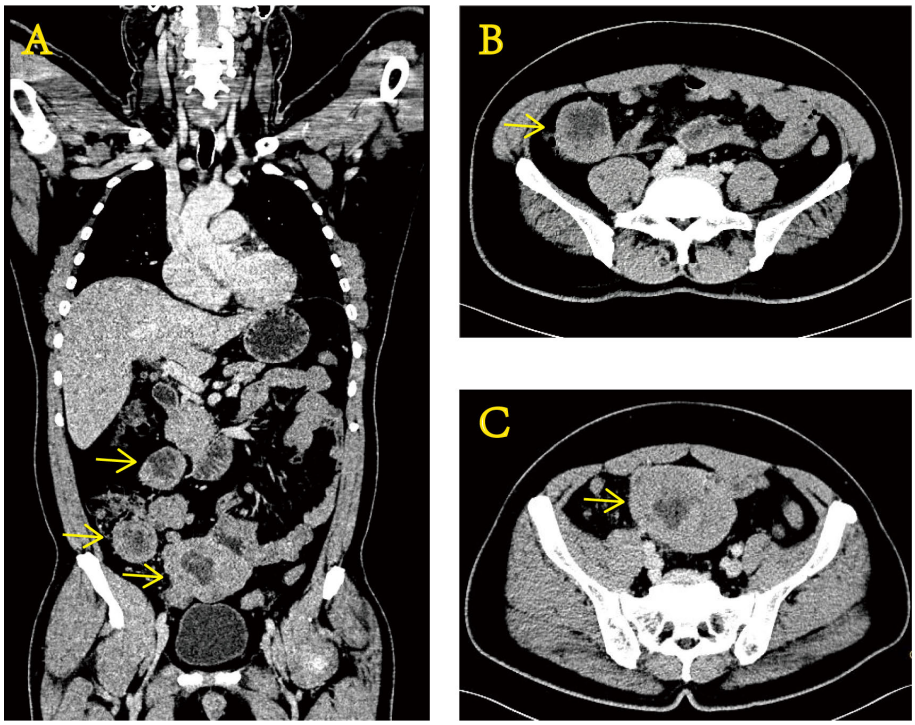


FIGURE 1
Enhanced CT images of the abdomen at the time of initial diagnosis show uneven thickening of the terminal ileum wall. Coronal section **(A)** and transverse section **(B, C)**.

metastases in the abdominal cavity. Then, a puncture aspiration biopsy of the abdominal neoplasm was performed on 3 December 2020. Immunohistochemistry (IHC) showed CD99 (+), vimentin (+), S-100 (+), CD117 (+), partial non-specific enolase (NSE) weakness (+), TdT (−), TTF-1 (−), CgA (−), and WT-1 (−). Fluorescence *in situ* hybridization (FISH) molecular assay revealed the presence of EWSR1 gene disruption. With immunohistochemical and molecular results combined, Ewing sarcoma was confirmed (4).

For further treatment, the patient presented to the oncology department of our hospital on 9 December 2020. We did a preliminary evaluation of the patient. On physical exam, he was lucid, generally in good condition, and without fever, and his vital signs were within the normal range. Cardiopulmonary and abdominal examination showed no obvious abnormalities. Laboratory results showed white blood cells 6.4 × $10^9$/L, red blood cells 4.73 × $10^{12}$/L, hemoglobin 93 g/L, and platelets 301 × $10^9$/L. Liver and kidney function was normal. Tumor markers were normal except for carbohydrate antigen 125 (45.1 U/ml), which was slightly elevated. Since PCT is not routinely required, we did not initially test for it. Based on the surgeon's consultation, we decided to administer chemotherapy first, closely review it during chemotherapy, and then change the treatment measures according to the evolution of the disease. According to the National Comprehensive Cancer Network (NCCN) guidelines, we selected the standard first-line treatment includes chemotherapy with a five-drug regimen of vincristine, Adriamycin, and cyclophosphamide, and alternating ifosfamide and etoposide (VAC/IE) for the patient with this tumor and began on the second day of hospitalization. On 9 February 2021, the patient had a sudden high fever without obvious causes outside the hospital. The auxiliary examination at the local hospital showed no abnormalities in blood routine, C-reactive protein (CRP), and blood culture. Also, the CT showed no signs of abscess or infection. Only PCT levels were shockingly over 200 ng/ml. To determine the cause of the fever, peripherally inserted central catheter (PICC) tubes were removed for culture. As in the blood culture, no pathogenic bacteria were found. After 8 days of treatment with ceftazidime and levofloxacin at the local hospital, the patient's temperature returned to normal and without any abnormal clinical symptoms or signs. However, the PCT levels were still over 200 ng/ml. Over the next 3 months or so, several imaging reviews were performed, and there was no finding of infection. Meanwhile, the efficacy assessment was stable disease (SD). During the same period, the PCT level was repeatedly reviewed also, with no exception, always over 200 ng/ml. In addition, other infection indicators were normal as usual, including CRP less than 5 mg/L each time, serum amyloid A (SAA) less than 4.8 mg/L each time, and white blood cells approximately 5 × $10^9$/L each time. The patient no longer had a fever or any discomfort.

On 6 May 2021, the patient returned to our hospital again for efficacy evaluation. Up to now, he has completed six cycles of chemotherapy of the five-drug regimen of VAC/IE. The enhanced magnetic resonance imaging (MRI) of his abdomen still indicates SD. Combined with the consultation opinions of gastrointestinal surgery and repeated film review, it was found that there is no engulfment of vessels of each lesion including lymph nodes, so it was considered that the abdominal mass could be removed. For the record, the PCT level at this time is still greater than 200 ng/ml. Other routine laboratory findings include white blood cells 5.29 × $10^9$/L, red blood cells 3.87 × $10^9$/L, hemoglobin 100 g/L, and platelets 243 × $10^9$/L. Serum creatinine and transaminase were normal, and serum albumin and serum calcium levels were normal. The patient had no fever or discomfort. After the exclusion of surgery-related contraindications, the patient underwent abdominal mass resection smoothly on 14 May 2021. Ewing sarcoma was diagnosed again by postoperative pathology. Immunohistochemistry showed CD99 (+), S-100 partial (+), CK minority (+), P53 partial weak (+), Syn minority (+), Ki67 approximately 60% (+), and CgA (−). Molecular assay (FISH) showed positive EWSR1 gene disruption (Figure 2). Unexpectedly, laboratory examination revealed 2.80 ng/mL of PCT on the first postoperative day, and there were no other special abnormalities except for a certain degree of increase in the white blood cells (17.35 × $10^9$/L), which was considered a normal postoperative change. Stunningly high levels of PCT, which lasted nearly 100 days in the absence of infection, dropped almost a hundredfold after one operation (Figure 3).

After approximately 0.5 months, we received the gene test report of the patient's tumor specimen and peripheral blood based on the detection method of 520-gene panel next-generation sequencing (NGS). The results showed EWSR–ERG gene rearrangement (fusion). After this operation (Figure 4), the patient regularly returned to the hospital for postoperative adjuvant chemotherapy


FIGURE 2
Pathological image of surgical specimens. **(A)** H&E. **(B)** CD99. **(C)** Detection of EWSR1 gene disruption by FISH. The probe type: Vysis LSI EWSR1 Probe (LOT 455960). Result of the patient's EWSR1 gene disruption test: positive (count 200 cells, approximately 90% show separation signal). FISH, fluorescence *in situ* hybridization.

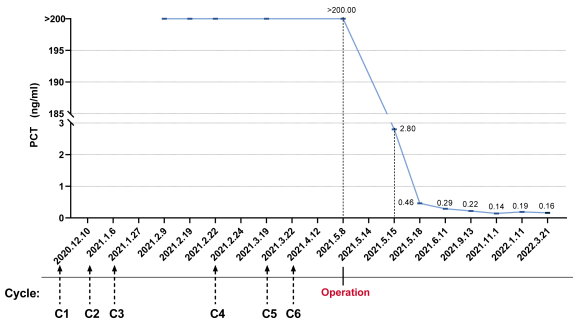


FIGURE 3
The trend of procalcitonin levels was from abnormally elevated initially to nearly normal after surgical resection.

with a two-drug regimen consisting of albumin-bound paclitaxel and gemcitabine. The efficacy assessment during each review was the status of no evidence of disease (NED). In addition, it cannot be ignored that the PCT level did not rise anymore. It never went above 0.5 ng/ml again. Until now, in March 2022, the patient still presents to our hospital for re-examination to monitor the change of the disease.

Finally, we reiterate that we have the patient's oral and written consent, which could confirm that the investigators obtained informed consent to publish information and images from the participant.

## 3 Discussion

At this point, we might marvel at the rarity of this case. Epidemiologically, the patient with Ewing sarcoma was a 51-year-old middle-aged Asian man, not a child or teenager of European descent (24–26). In terms of location, the tumor is of soft tissue origin rather than bone, not to mention trunk or long bone (1, 4). Based on cytogenetic and molecular genetic information, it is EWSR1–ERG that drives epigenetic reprogramming, rather than EWSR1–FLI1, the most common fusion protein, which accounts for 85% (4, 25).

The intimate connection between PCT and infection was first discovered by French oncologist Dr. Bohuon during the Gulf War in 1991. After more than 30 years of clinical verification, the diagnostic significance of PCT has been beyond doubt. Its serum level in healthy adults is usually no more than 0.05 ng/ml, while, when exposed to bacterial infection, PCT usually rises within 2–6 h, but there is little change when exposed to viral infection (27–29). Thus, it has long been reported that PCT exhibits advantages over conventional parameters in distinguishing between bacterial and viral infections (30).

PCT elevation was associated with malignant tumor progression, which was unknown. There has been no report of PCT's role in the prognosis of Ewing sarcoma. The previous study showed that the presence of a neuroendocrine component remained strongly associated with a positive PCT and unfavorable prognosis (31, 32). Here, we reported that the case might have a high tumor burden and poor prognosis with a high PCT level. After resection, the PCT level quickly decreased, meaning that sarcoma has a component of neuroendocrine, as Ewing sarcoma is derived from the neuroectoderm.

Moreover, we identified one and only one case of PCT high expression in another type of sarcoma, undifferentiated pleomorphic sarcoma (UPS), in the medical literature database (33). As in our case, after the exclusion of all potential sources of infection, it was speculated that the cause of the patient's elevated PCT was most likely secondary to malignancy. This somewhat extends the availability and traceability of our case report, although PCT levels were only mildly elevated in others' reports, and there was no decrease in PCT levels caused by surgical intervention. At present, there are few reports regarding Ewing sarcoma (or sarcoma) and PCT. More comparable cases should be collected and discussed in the future to bring new enlightenment and increase the application value of PCT.

In conclusion, the presentation of our case is intended to inspire future readers that, in addition to several tumor diseases that have been reported, in the absence of infection, high levels of PCT can be present persistently in Ewing sarcoma, although PCT has its

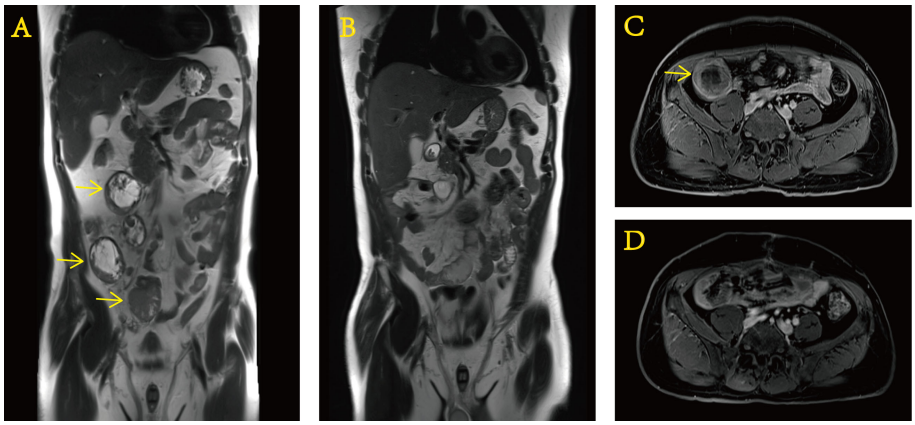


FIGURE 4
Preoperative and postoperative contrast-enhanced MRI of the abdomen. Preoperative **(A)** coronal and **(C)** transverse sections. Postoperative **(B)** coronal and **(D)** transverse sections.

specificity. At the same time, we highlighted the reduction of PCT due to tumor resection. This helps to broaden the significance of PCT in Ewing sarcoma. In contrast, in the absence of obvious bacterial infection, Ewing sarcoma should be included in the differential diagnosis of significantly elevated PCT, according to our experience.

## Data availability statement

The original contributions presented in the study are included in the article/supplementary materials. Further inquiries can be directed to the corresponding authors.

## Ethics statement

Written informed consent was obtained from the individual(s) for the publication of any potentially identifiable images or data included in this article.

## Author contributions

TQ guided disease treatment and contributed to the collection of original pathology and CT/MR images of the patient. YiC drafted the manuscript and contributed to the image presentation of clinical test data. MG contributed to disease surveillance and evaluation, particularly in imaging. YaC and TQ reviewed and modified the draft. All authors contributed to the article and approved the submitted version.

## Funding

This work was supported by a grant from the National Natural Science Foundation of China (82002819). The funding source had no role in the generating of ideas, data gathering, interpretation, writing of the manuscript, or the decision to submit the report for publication.

## Acknowledgments

The authors acknowledge the contributions of all the colleagues and institutions that aided their efforts.

## Conflict of interest

The authors declare that the research was conducted in the absence of any commercial or financial relationships that could be construed as a potential conflict of interest.

## Publisher's note



## References

1. Iwamoto Y. Diagnosis and treatment of ewing's sarcoma. *Jpn J Clin Oncol* (2007) 37 (2):79–89. doi: 10.1093/jjco/hyl142

2. Allegretti M, Casini B, Mandoj C, Benini S, Alberti L, Novello M, et al. Precision diagnostics of ewing's sarcoma by liquid biopsy: circulating EWS-FLI1 fusion transcripts. *Ther Adv Med Oncol* (2018) 10:1758835918774337. doi: 10.1177/1758835918774337

3. Hayashi M, Chu D, Meyer CF, Llosa NJ, McCarty G, Morris CD, et al. Highly personalized detection of minimal Ewing sarcoma disease burden from plasma tumor DNA. *Cancer* (2016) 122(19):3015–23. doi: 10.1002/cncr.30144

4. Balamuth NJ, Womer RB. Ewing's sarcoma. *Lancet Oncol* (2010) 11(2):184–92. doi: 10.1016/S1470-2045(09)70286-4

5. Antonescu C. Round cell sarcomas beyond Ewing: emerging entities. *Histopathology* (2014) 64(1):26–37. doi: 10.1111/his.12281

6. Horowitz ME, Tsokos MG, DeLaney TF. Ewing's sarcoma. *CA Cancer J Clin* (1992) 42(5):300–20. doi: 10.3322/canjclin.42.5.300

7. Gaspar N, Hawkins DS, Dirksen U, Lewis IJ, Ferrari S, Le Deley MC, et al. Ewing Sarcoma: Current management and future approaches through collaboration. *J Clin Oncol* (2015) 33(27):3036–46. doi: 10.1200/JCO.2014.59.5256

8. Grünewald TGP, Cidre-Aranaz F, Surdez D, Tomazou EM, de Álava E, Kovar H, et al. Ewing sarcoma. *Nat Rev Dis Primers* (2018) 4(1):5. doi: 10.1038/s41572-018-0003-x

9. Kallen ME, Hornick JL. The 2020 WHO classification: What's new in soft tissue tumor pathology? *Am J Surg Pathol* (2021) 45(1):e1–23. doi: 10.1097/PAS.0000000000001552

10. Gendrel D, Bohuon C. Procalcitonin as a marker of bacterial infection. *Pediatr Infect Dis J* (2000) 19(8):679–87. doi: 10.1097/00006454-200008000-00001

11. Becker KL, Nylén ES, White JC, Müller B, Snider RHJr. Clinical review 167: Procalcitonin and the calcitonin gene family of peptides in inflammation, infection, and sepsis: a journey from calcitonin back to its precursors. *J Clin Endocrinol Metab* (2004) 89 (4):1512–25. doi: 10.1210/jc.2002-021444

12. Müller B, White JC, Nylén ES, Snider RH, Becker KL, Habener JF. Ubiquitous expression of the calcitonin-i gene in multiple tissues in response to sepsis. *J Clin Endocrinol Metab* (2001) 86(1):396–404. doi: 10.1210/jcem.86.1.7089

13. Foushee JA, Hope NH, Grace EE. Applying biomarkers to clinical practice: a guide for utilizing procalcitonin assays. *J Antimicrob Chemother* (2012) 67(11):2560–9. doi: 10.1093/jac/dks265

14. Mokart D, Merlin M, Sannini A, Brun JP, Delpero JR, Houvenaeghel G, et al. Procalcitonin, interleukin 6 and systemic inflammatory response syndrome (SIRS): early markers of postoperative sepsis after major surgery. *Br J Anaesth* (2005) 94(6):767–73. doi: 10.1093/bja/aei143

15. Rau B, Steinbach G, Baumgart K, Gansauge F, Grünert A, Beger HG. The clinical value of procalcitonin in the prediction of infected necrosis in acute pancreatitis. *Intensive Care Med* (2000) 26 Suppl 2:S159–64. doi: 10.1007/BF02900730

16. Mofidi R, Suttie SA, Patil PV, Ogston S, Parks RW. The value of procalcitonin at predicting the severity of acute pancreatitis and development of infected pancreatic necrosis: systematic review. *Surgery* (2009) 146(1):72–81. doi: 10.1016/j.surg.2009.02.013

17. Meisner M, Lohs T, Huettemann E, Schmidt J, Hueller M, Reinhart K. The plasma elimination rate and urinary secretion of procalcitonin in patients with normal and impaired renal function. *Eur J Anaesthesiol* (2001) 18(2):79–87. doi: 10.1046/j.0265-0215.2000.00783.x

18. Chiesa C, Panero A, Rossi N, Stegagno M, De Giusti M, Osborn JF, et al. Reliability of procalcitonin concentrations for the diagnosis of sepsis in critically ill neonates. *Clin Infect Dis* (1998) 26(3):664–72. doi: 10.1086/514576

19. Scirè CA, Cavagna L, Perotti C, Bruschi E, Caporali R, Montecucco C. Diagnostic value of procalcitonin measurement in febrile patients with systemic autoimmune diseases. *Clin Exp Rheumatol* (2006) 24(2):123–8.

20. Algeciras-Schimnich A, Preissner CM, Theobald JP, Finseth MS, Grebe SK. Procalcitonin: a marker for the diagnosis and follow-up of patients with medullary thyroid carcinoma. *J Clin Endocrinol Metab* (2009) 94(3):861–8. doi: 10.1210/jc.2008-1862

21. Pardo-Cabello AJ, Manzano-Gamero V. Small cell lung cancer elevates procalcitonin levels in the absence of infection. *Lung Cancer* (2019) 134:272–3. doi: 10.1016/j.lungcan.2019.06.018

22. Lu J, Chen CL, Jin JD, Chen J, Yu CB. Continuous elevation of procalcitonin in cirrhosis combined with hepatic carcinoma: a case report. *BMC Infect Dis* (2021) 21(1):29. doi: 10.1186/s12879-020-05684-2

23. Riley DS, Barber MS, Kienle GS, Aronson JK, von Schoen-Angerer T, Tugwell P, et al. CARE guidelines for case reports: explanation and elaboration document. *J Clin Epidemiol* (2017), 89:218–235. doi: 10.1016/j.jclinepi.2017.04.026

24. Parkin DM, Stiller CA, Nectoux J. International variations in the incidence of childhood bone tumours. *Int J Cancer* (1993) 53(3):371–6. doi: 10.1002/ijc.2910530305

25. Dorfman HD, Czerniak B. Bone cancers. *Cancer* (1995) 75(1 Suppl):203–10. doi: 10.1002/1097-0142(19950101)75:1+<203::aid-cncr2820751308>3.0.co;2-v

26. Blay JY, De Pinieux G, Gouin F. Ewing's sarcoma. *N Engl J Med* (2021) 384 (15):1477. doi: 10.1056/NEJMc2102423

27. Assicot M, Gendrel D, Carsin H, Raymond J, Guilbaud J, Bohuon C. High serum procalcitonin concentrations in patients with sepsis and infection. *Lancet 1993 Feb* (8844) 27:341. doi: 10.1016/0140-6736(93)90277-n

28. Lippi G, Sanchis-Gomar F. Procalcitonin in inflammatory bowel disease: Drawbacks and opportunities. *World J Gastroenterol* (2017) 23(47):8283–90. doi: 10.3748/wjg.v23.i47.8283

29. Meisner M. Pathobiochemistry and clinical use of procalcitonin. *Clin Chim Acta* (2002) 323(1-2):17–29. doi: 10.1016/s0009-8981(02)00101-8

30. Chalupa P, Beran O, Herwald H, Kaspříková N, Holub M. Evaluation of potential biomarkers for the discrimination of bacterial and viral infections. *Infection* (2011) 39 (5):411–7. doi: 10.1007/s15010-011-0126-4

31. Avrillon V, Locatelli-Sanchez M, Folliet L, Carbonnaux M, Perino E, Fossard G, et al. Lung cancer may increase serum procalcitonin level. *Infect Disord Drug Targets* (2015) 15(1):57–63. doi: 10.2174/1871526515666150320162950

32. Patout M, Salaün M, Brunel V, Bota S, Cauliez B, Thiberville L. Diagnostic and prognostic value of serum procalcitonin concentrations in primary lung cancers. *Clin Biochem* (2014) 47(18):263–7. doi: 10.1016/j.clinbiochem.2014.09.002

33. Arce Gastelum A, Volberding T, Freeman SC, Dick M, Gbadamosi-Akindele M. Procalcitonin perplexity - prolonged idiopathic elevation in pleomorphic sarcoma: A case report and review of the literature. *Cureus* (2020) 12(5):e8215. doi: 10.7759/cureus.8215

frontiers | Frontiers in Surgery

TYPE Case Report
PUBLISHED 17 January 2023
DOI 10.3389/fsurg.2023.1074067



OPEN ACCESS

EDITED BY
Zhaolun Cai,
Sichuan University, China

REVIEWED BY
Miltiadis Lalountas,
General Hospital Polygyrou Chalkidiki, Greece
Francisco Sanchez Bueno,
Hospital Universitario Virgen de la Arrixaca, Spain

*CORRESPONDENCE
Defeng Song
✉ Sdf610613@jlu.edu.cn
Ye Feng
✉ fengye@jlu.edu.cn

SPECIALTY SECTION
This article was submitted to Surgical Oncology, a section of the journal Frontiers in Surgery

RECEIVED 19 October 2022
ACCEPTED 02 January 2023
PUBLISHED 17 January 2023

CITATION
Su T, Li C, Song B, Song D and Feng Y (2023) Case report and literature review: Giant retroperitoneal cystic lymphangioma. Front. Surg. 10:1074067. doi: 10.3389/fsurg.2023.1074067



# Case report and literature review: Giant retroperitoneal cystic lymphangioma

Tieshan Su[1], Chaoyuan Li[2], Bin Song[1], Defeng Song[1*] and Ye Feng[1*]

[1]Departments of Gastrointestinal Colorectal Anus Surgery, China-Japan Union Hospital, Jilin University, Changchun, China, [2]Departments of Orthopedics Surgery, China-Japan Union Hospital, Jilin University, Changchun, China

**Background:** Cystic lymphangioma is a rare benign tumor of the lymphatic system, which is most commonly observed in the neck, head and armpit.Less than 5% of lymphangiomas occur in the abdominal cavity and even less in the retroperitoneum.
**Case description:** A 65-year-old male patient was diagnosed with an "abdominal mass that had persisted for 1 year, accompanied by abdominal pain, abdominal distension and dyspnea for 7 days". After abdominal computerd tomography, a giant multilobed abdominal lymphangioma was suspected, which squeezed the intestinal canal and was closely related to the inferior vena cava. The patient underwent an exploratory laparotomy, during which, it was found that the tumor formed extensive adhesions to the transverse colon, small intestine and pelvic wall, and enveloped the abdominal aorta, superior mesenteric artery, inferior mesenteric artery and inferior vena cava to varying degrees. It was diffcult to remove the cyst completely. Postoperative pathology confirmed the diagnosis of retroperitoneal cystic lymphangioma. The patient recovered well after the operation, was eating normally by 5 days postoperatively,and was discharged 10 days postoperatively.The patient was followed up 1 month after postoperatively and no evidence of recurrence was observed.
**Conclusion:** In this case, we report a patient with giant retroperitoneal cystic lymphangioma who underwent exploratory laparotomy combined with preoperative abdominal computerd tomography and acute abdominal pain, abdominal distension and dyspnea. Because of the large volume of the tumor and its close relationship with the superior mesenteric artery and other blood vessels, the surgeon used scissors to separate the tumor sharply and removed the whole tumor completely.

KEYWORDS
cystic lymphangioma, retroperitoneal tumor, surgical resection, case report, literature review

## Introduction

Cystic lymphangioma is a non-cancerous vascular malformed conjunctival tumor consisting of thin-walled cysts. It is a rare benign tumor, which is most commonly observed in the neck, head,and armpit, while >5% of lymphangiomas occur in the abdominal cavity, including the mesentery and the greater omentum.The occurrence in the retroperitoneum is even rarer. Although cystic lymphangioma can occur at any age, it is mainly observed in children, in whom the prognosis is good (1, 2). In adults, cystic lymphangiomas account for approximately 7% of abdominal cysts (3). Retroperitoneal cystic lymphangioma is usually asymptomatic, but in some cases it is characterized by acute abdominal pain and distension caused by nausea, vomiting or intestinal obstruction. The tumor can be identified by imaging examinations such as ultrasound and computed tomography (CT), however histopathological examination remains the gold standard. Complete surgical resection of the tumor is the first choice for treatment (4–6). Here, we report the clinical features, diagnosis, treatment and

prognosis of a giant retroperitoneal cystic lymphangioma in a 63-year-old male patient. And this study is in accordance with the principles of CARE guidelines (7).

## Case description

The patient, a 65-year-old man, was diagnosed with abdominal swelling that had persisted for 1 year,and was accompanied by abdominal pain, abdominal distension and dyspnea for 7 days. A year prior, the patient found an"abdominal cystic mass (approximately 25 cm × 1.6 cm × 22 cm)" and attended an other hospital. He was admitted to the local hospital 7days prior due to sudden intermittent diffuse abdominal pain with abdominal distension, dyspnea, no fever, nausea, and vomiting. Abdominal CT suggested an "abdominal mass and intestinal obstruction", and the symptoms did not improve. The patient was admitted to the hospital for further diagnosis and treatment. The patient had had hypertension for 10 years and regularly took levamlodipine besylate tablets for 5 mg/days,which controlled his blood pressure within the normal range. A cardiac stent operation was performed 4 months prior because of myocardial infarction. Physical examination showed: no obvious heart abnormalities,although shortness of breath, obvious abdominal swelling, frog belly, no gastrointestinal type and peristaltic wave were noted,as well as a large mass that could be felt asoccupying most of the abdominal cavity. Regarding tumor markers: CA125:65.47 U/ml (reference value < 35 U/ml), other tumor markers were not abnormal. Abdominal enhanced CT: huge cystic space in the pelvis and abdominal cavity, with an irregular shape, linear septum, (approximately 24.2 cm × 16.7 cm × 27.8 cm), extending along the mesentery of the small intestine (**Figures 1A–D**). In contrast-enhanced scan, the cystic components were not enhanced, the septum was uniformly enhanced, the intestinal canal was displaced laterally under pressure (**Figures 1A,** Magi B), and the inferior vena cava was narrowed (**Figure 1C**). The preliminary diagnosis of the nature of abdominal mass pending diagnosis: cystic lymphangioma? An exploratory laparotomy was performed,during which a large cystic mass of approxmately 30 × 28 × 14 cm was observed retroperitoneally. The surface of the mass was smooth, white and red, with a light yellow exudate on the surface. The tumor formed extensive adhesion with the transverse colon, small intestine and pelvic wall, and enveloped the abdominal aorta, superior mesenteric artery, inferior mesenteric artery and inferior vena cava to varying degrees. We decided to surgically remove the cystic mass completely (**Figure 2**). Postoperative pathology: microscopically, necrosis and protein exudation in the cystic cavity, chronic inflammation with inflammatory granulation, obvious proliferation of interstitial vessels and fibrous tissue, scattered in clusters of smooth muscle bundles and more inflammatory cells, and occasional giant cells, as well as proliferation of small lymphatic vessels outside the cyst wall, consistent with cystic lymphangioma with chronic inflammation (**Figures 3A,B**).

The patient recovered well and could eat normally 5 days postoperatively. The patient was discharged 10 days after the surgery,at which point,he was in a good condition, with no pain or complications. In the initial recovery stage, he was advised to ingest high-quality protein that was easily absorbed and high in nutrition,and to avoid high-fat, high-fiber, indigestible and absorbed food, The patient was subjected to, regular re-examination and follow-up.

## Discussion

Cystic lymphangioma usually occurs in the head, neck and armpit, mostly in children, with no sex-related difference in incidence. Intraperitoneal lymphangioma is a rare intra-abdominal tumor. Less than 5% of lymphangiomas occur in the abdominal cavity, and the incidence of retroperitoneal tumors is even lower (1, 2). The etiology of cystic lymphangioma is unclear, and infection, lymphatic obstruction and surgery may be associated factors (8). According to the histological type, cystic lymphangioma can be divided into cystic, capillary and cavernous.Likewise, based on its clinical manifestations, it can be divided into macrocytic, microencapsulated, and mixed cysts. Microcapsules can be further subdivided into developing-cell microcapsules and closed-cell microcapsules based on whether the

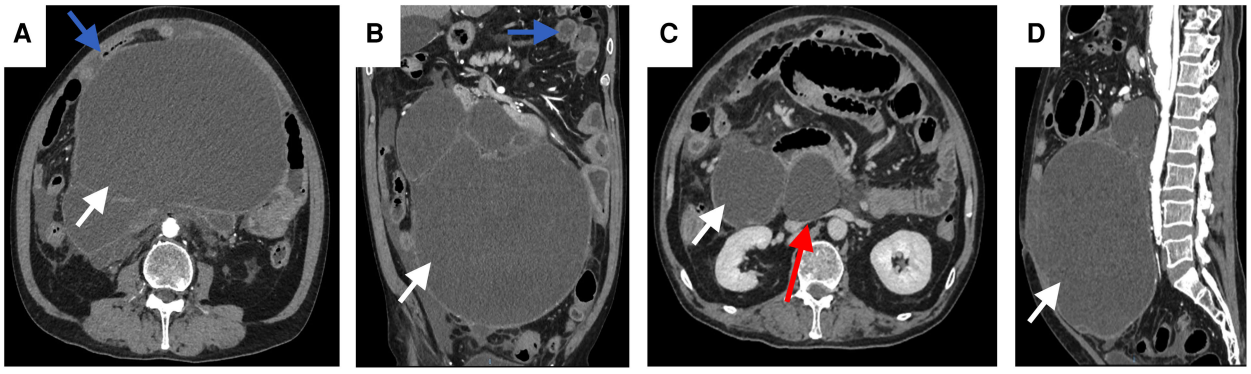


FIGURE 1
Abdominal enhanced CT axial arterial phase (A), coronary arterial phase (B), axial venous phase (C),and sagittal arterial phase (D) CT images show a retroperitoneal cystic mass (white solid arrow), extending along the mesentery to 24 cm. The tumor oppresses the surrounding intestine (blue solid arrow) and the inferior vena cava (B) (red solid arrow).

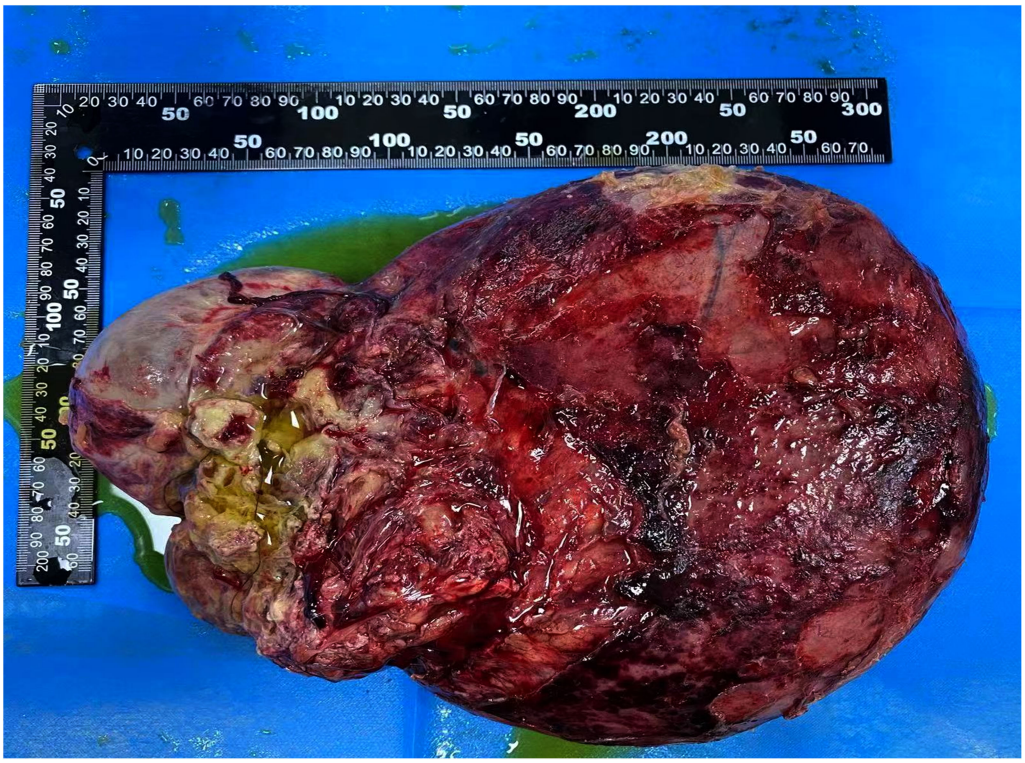

FIGURE 2
Image of the gross specimen.

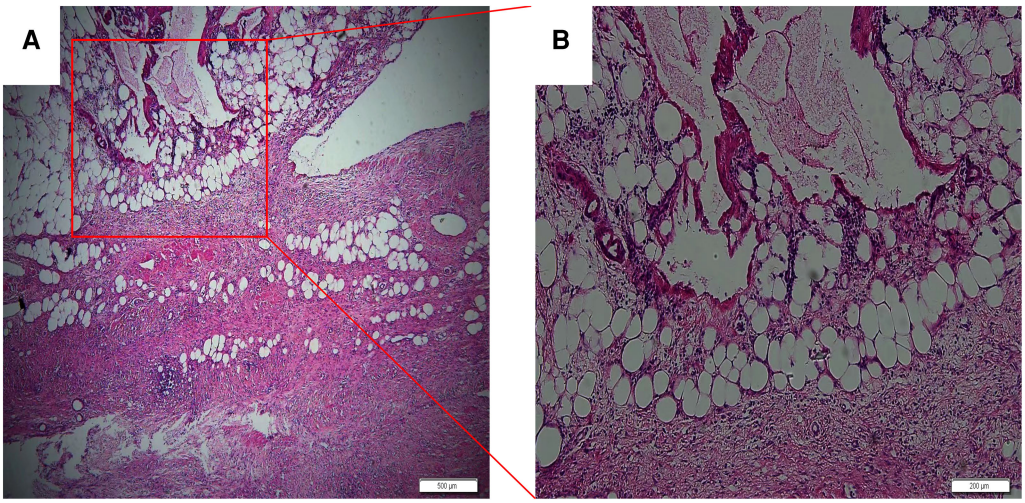


FIGURE 3
Necrosis and protein exudation in the cystic cavity, obvious proliferation of interstitial vessels and fibrous tissue, cystic lymphatic cavities of different sizes with inflammatory lymphocyte infiltration and lymphoid nodules; (**A**) hematoxylin and eosin (HE) × 40, scale 500 μm; (**B**) HE × 100, scale 200 μm.

cells are open or not (9).Here, we report a case of retroperitoneal giant cyst lymphangioma, which is consistent with other reports suggesting that the most common retroperitoneal lymphangioma is cystic type (10).

The clinical manifestations of retroperitoneal cystic lymphangioma are non specific and are related to the size and location of the tumor and the location of the surrounding tissues and organs, which makes diagnosis challenging. Initially, the tumor is small but asymptomatic; with the growth of the tumor, nausea, vomiting, abdominal pain and abdominal distension may occur due to compression of the abdominal organs, and in severe cases, acute abdominal pain and intestinal obstruction may even cause rupture, infection, bleeding and torsion of related organs and tissues (11–13). In the current case, abdominal contrast-enhanced

CT showed a huge retroperitoneal cystic mass, which occupied most of the abdominal cavity and pelvic cavity and squeezed the small intestine, resulting in abdominal pain, abdominal distension, dyspnea and other symptoms, and was admitted as "abdominal mass, intestinal obstruction". Cystic lymphangioma should be differentiated from abdominal lymphoma, mesenteric cyst, secondary metastasis of a malignant tumor, tuberculosis, echinococcosis, small intestinal adenocarcinoma and mesenteric related tumors (14). Imaging examination plays an important role in the diagnosis of retroperitoneal cystic lymphangioma. Ultrasound has a unique advantage in showing the size, location, content and boundary of the cyst. However, when there is hemorrhage and necrosis in the capsule, the echo of the contents will produce some changes, which will affect the judgment. Abdominal enhanced CT is the first choice.Abdominal enhanced CT can be used to observe the density of the tumor to determine the relationship with the surrounding tissue, blood vessels and organs, which can distinguish retroperitoneal lymphangioma from intraperitoneal lymphangioma. Magnetic resonance(MRI) is more sensitive in showing intra-cyst bleeding and content (15–17). However, a final diagnosis still requires pathological biopsy, which is characterized by abnormally dilated lymphatic vessels lined with flat endothelial cells with smooth muscle, blood vessels, fat and lymphatic matrix (18). CT was considered as cystic lymphangioma, and the final diagnosis was confirmed by postoperative pathology.

Without intervention, the volume of cystic lymphangioma will gradually increase, thus oppressing adjacent tissues, blood vessels, nerves, organs and so on, resulting in related complications (19). In our case, the volume increased by about 13 times over a year, leading to the occurrence of this symptom. Surgical resection of tumor is the first choice for the treatment of retroperitoneal lymphangioma. during the operation, attention should be paid to the relationship between tumor and surrounding tissue, blood vessels, nerves and organs, so as to remove the tumor completely and reduce the postoperative recurrence rate (20, 21). Recently some methods of nonsurgical treatment have emerged. Among them, sclerotherapy is the most commonly used alternative therapy for lymphangiomas that cannot be completely resected or diagnosed as difficult to operate. When compared with surgical resection, sclerotherapy has the advantages of being simple and causing less injury. Besides, several studies have reported that sclerosing agents can effectively treat large cystic lymphangioma, even though their curative effect on microcystic lymphangioma is much lower (22–24). Examples of such common hardeners include OK-432, doxycycline, bleomycin, and ethanol. Notably, OK-432 sclerotherapy can not only induce and activate leukocytes to produce cytokines, which in turn increase endothelial cell permeability, accelerate the speed and flow of lymphatic drainage, and facilitate lymphangioma cystic cavity shrinkage and lesion regression, but also reduce complications and focal fibrosis, making it a promising alternative to surgery, especially for patients with microcystic lymphangioma (25, 26). However, sclerotherapy has been reported to cause some adverse reactions, such as airway obstruction and skin necrosis. Therefore, the effectiveness of sclerotherapy needs to be further evaluated (27, 28). Another notable method is radiofrequency ablation, which destroys diseased tissues at low temperatures while causing less damage to the surrounding tissues. Presently, radiofrequency ablation is the first choice of treatment for treating oral and pharynx microcystic lymphangioma (29, 30). Some studies have also shown that radiofrequency ablation is an effective method for the treatment of superficial microcystic lymphangioma; however, further development and research are needed to better apply it for the treatment of microcystic lymphangioma found in other body parts.

Although the above-mentioned methods have greatly helped in the treatment of lymphangioma, clinicians still find it difficult to obtain optimal results for lymphangiomas with large lesion areas and invasive growth. Importantly, recent studies have shown the efficacy of several drugs in the treatment of lymphangioma, and some of these drugs have been used in treating patients with lymphangiomas, such as sildenafil, propranolol,sirolimus, and several inhibitors targeting the PI3K/AKT/mTOR signaling pathway (PI3K inhibitors, AKT inhibitors, MAPK inhibitors, sorafenib, etc.) (31, 32). However, some studies have demonstrated that sildenafil is not effective in the treatment of microcystic lymphangioma, whereas sirolimus has been demonstrated to have good efficacy in the treatment of microcystic lymphangioma and may become the focus of future research. In addition, studies have also shown that BMP and Wnt modulators, calcium channel blockers, and KATP activators (minoxidil) may also have some therapeutic potential (33).

Since a single treatment cannot achieve satisfactory results, clinicians are encouraged to use multiple methods of combined therapy. Consequently, surgical resection, as the main treatment, can be used to remove a significant volume of large cystic lesions, while the remaining diseased tissues can be treated with sclerotherapy. For instance, bleomycin is currently used in the treatment of residual small cystic diseases and has achieved some efficacy (34). However, sometimes lymphangiomas may require several rounds of sclerotherapy. For tumors that are large or widely enclosed and have invaded their surrounding tissues, blood vessels, and nerves, drugs or sclerotherapy can be taken first to reduce the size of the lesions before resecting them through surgery. Alternatively, postoperative sclerotherapy, drugs, radiofrequency ablation, and other combined therapy can be used. Unfortunately, there are currently no unified guidelines for the diagnosis and treatment of lymphangiomas, and further verification is still needed.

We provided a case report and on the basis of literature review, retroperitoneal cystic lymphangioma was investigated.PubMed was searched using these key words: ("Lymphangioma, Cystic" or "Cystic Lymphangioma" or "Cystic Lymphangiomas" or "Lymphangiomas, Cystic" or "Hygroma" or "Hygromas, Cystic" or "Cystic Hygroma Colli" or "Colli, Cystic Hygroma" or "Hygroma Colli, Cystic" or "Hygroma" or "Hygromas") and ("Retroperitoneal Space" or "Retroperitoneal Neoplasms" or "Retroperitoneal Fibrosis"). Key words referred to medical subject heading (MeSH). And the search terms used on PubMed were: ((["Lymphangioma, Cystic"(Mesh)] OR ((((((((((Cystic Lymphangioma(Title/Abstract)] OR [Cystic Lymphangiomas(Title/Abstract)]) OR [Lymphangiomas, Cystic(Title/Abstract)]) OR [Hygroma, Cystic(Title/Abstract)]) OR [Cystic Hygroma(Title/Abstract)]) OR [Cystic Hygromas(Title/Abstract)]) OR [Hygromas, Cystic(Title/Abstract)]) OR [Cystic Hygroma Colli(Title/Abstract)]) OR [Colli, Cystic Hygroma (Title/Abstract)]) OR [Hygroma Colli, Cystic(Title/Abstract)]) OR

[Hygroma(Title/Abstract)]) OR [Hygromas(Title/Abstract)]))) AND ([Retroperitoneal(Title/Abstract)] OR ((([" Retroperitoneal Space"(Mesh)] OR "Retroperitoneal Neoplasms"[Mesh]) OR "Retroperitoneal Fibrosis"[Mesh]))).

We systematically reviewed the studies returned from the literature searches.The inclusion criteria were as follows: (I) retroperitoneal cystic lymphangioma; (II) over 18 years old; (III) full text; (IV) manuscripts written in English. Studies were excluded for any of the following: (I) the study was a review, meeting abstract, non-clinical study, or *in vitro* study; (II) inferior quality literature or with insufficient outcome indicators; (III) The lesion is not retroperitoneal. Each abstract is carefully reviewed by two different authors (SS and DS). We conducted a systematic review of 240 records and finally included 29 articles involving 34 cases. Detailed characteristics of the reported cases are provided in supplemental (**Table 1**) (35–63). We made the statistics on the above date.There were 21 males and 13 females, aged from 25 to 76 years old, with an average age of 45.82 years old. 25 cases underwent laparotomy and 9 cases underwent laparoscopic surgery. The average diameter of tumor was 13.44 cm. Among the 34 patients, 1 case had postoperative complications, 20 cases had no postoperative complications, and the other 14 cases had no related data.

TABLE 1 Characteristics of the adult cases of retroperitoneal cystic lymphangioma reported in the literature.

| Auther | References No. | No. Patients | Open/Laparoscopy/ Conservative | Male/ Female | Age years (Means) | Tumer Size (cm) (Means) | Follow-up (mo) | Recurrence |
|---|---|---|---|---|---|---|---|---|
| Shayesteh et al. | (35) | 1 | 1/0/0 | 0/1 | 29 | 29 | NP | NP |
| Dunev et al. | (36) | 1 | 1/0/0 | 0/1 | 35 | 18.5 | NP | NP |
| Nuzzo et al. | (37) | 2 | 2/0/0 | 2/0 | 61.5 | 17.5 | 15 | 0 |
| Saadi et al. | (38) | 5 | 5/0/0 | 1/4 | 45 | 14 | 32.6 | 0 |
| Lim et al. | (39) | 1 | 1/0/0 | 1/0 | 74 | 9 | NP | NP |
| Kodera et al. | (40) | 1 | 1/0/0 | 0/1 | 39 | 5.5 | 24 | 0 |
| Cherk et al. | (41) | 1 | 1/0/0 | 0/1 | 41 | 9 | 30 | 0 |
| Bhavsar et al. | (42) | 1 | 1/0/0 | 1/0 | 54 | 12.2 | NP | NP |
| Aminian et al. | (43) | 1 | 1/0/0 | 1/0 | 50 | NP | NP | NP |
| Lai et al. | (44) | 1 | 0/1/0 | 1/0 | 47 | 5 | NP | 0 |
| Liedtke et al. | (45) | 1 | 1/0/0 | 1/0 | 61 | 19 | 3 | 0 |
| Kalish et al. | (46) | 1 | 1/0/0 | 1/0 | 22 | 14 | NP | NP |
| Suhani et al. | (47) | 1 | 1/0/0 | 0/1 | 22 | 22 | NP | NP |
| Tripathi et al. | (48) | 1 | 1/0/0 | 1/0 | 55 | 15 | 12 | 0 |
| Sato et al. | (49) | 1 | 0/1/0 | 0/1 | 30 | 5 | 24 | 0 |
| Chaker et al. | (50) | 1 | 1/0/0 | 1/0 | 68 | 4 | 50 | 0 |
| Olaoye et al. | (51) | 1 | 1/0/0 | 1/0 | 20 | NP | 36 | 0 |
| Rezaee et al. | (52) | 1 | 0/1/0 | 1/0 | 27 | 12.6 | 1 | 0 |
| Black et al. | (53) | 1 | 0/1/0 | 1/0 | 66 | 5 | 1 | 0 |
| Hubli et al. | (54) | 1 | 1/0/0 | 1/0 | 36 | 40 | 9 | 0 |
| Rajput et al. | (55) | 1 | 1/0/0 | 1/0 | 65 | 10 | 1 | 0 |
| Kasza et al. | (56) | 1 | 0/1/0 | 1/0 | 52 | 9.6 | 9 | 0 |
| Izumi et al. | (57) | 1 | 0/1/0 | 0/1 | 76 | 18 | NP | 1 |
| Ionescu et al. | (58) | 1 | 1/0/0 | 1/0 | 31 | 14.4 | NP | NP |
| Tsukamoto et al. | (59) | 1 | 0/1/0 | 0/1 | 36 | 10 | 12 | 0 |
| Mabrouk et al. | (60) | 1 | 1/0/0 | 1/0 | 70 | 19.5 | 6 | 0 |
| Suryawan et al. | (61) | 1 | 0/1/0 | 1/0 | 22 | 9.4 | 6 | 0 |
| Chung et al. | (62) | 1 | 1/0/0 | 1/0 | 56 | 4.5 | 0.3 | 0 |
| Colovic et al. | (63) | 1 | 0/1/0 | 0/1 | 26 | 5 | 6 | 0 |

Surgery (open, laparoscopy); No. patients, number of patients; NP, not precised.

Compared with the case reports in the existing literature, our case was first found during the physical examination a year ago, and the patient himself did not have obvious symptoms of discomfort, so there was no follow-up treatment. Preoperative abdominal contrast-enhanced CT showed that the case was a huge retroperitoneal cystic mass of approximately 24.2 cm × 16.7 cm × 27.8 cm. Up to the lower edge of the pancreas, down to the peritoneal reflex, left and right to the two abdominal walls, anterior to the anterior abdominal wall, and back to the front of the spinal lamina, occupying most of the abdominal cavity and pelvic cavity, squeezing the small intestine and oppressing the inferior vena cava. The nature can not be clear, consider the possibility of benign, but do not rule out the possibility of malignant. This time, due to the increase in the size of the cyst, it oppresses the surrounding intestines, causing the diaphragm to move upward, and some cysts rupture and bleeding, which irritates the intestinal tract, resulting in acute abdominal pain, abdominal distension, intestinal obstruction and dyspnea. Because of the critical condition, we decided to carry out exploratory laparotomy. During the operation, a huge retroperitoneal cystic mass was seen, which almost occupied the whole abdominal cavity and pelvic cavity. We found that the tumor was closely wrapped and adhered to the abdominal aorta, superior mesenteric artery, inferior mesenteric artery, inferior vena cava and other blood vessels, and pressed the surrounding intestinal lumen. Part of the tumor ruptured and bleeding could be seen on the surface. As the nature of the tumor was not clear, we decided to remove the tumor as completely as possible. The surgeon uses scissors to separate carefully and sharply to minimize the rupture and bleeding of the tumor and blood vessels. Accurate and meticulous operation during sharp separation of enclosing and adherent blood vessels to reduce the risk of hemorrhagic shock. When the tumor is completely removed, it is removed slowly to avoid sharp fluctuations in blood pressure. The patient recovered well after operation and was discharged smoothly 10 days later.

However, there are still some areas that need to be improved in our program. for example, in this operation, we can first extract the contents of the cyst to reduce the volume of the tumor, reduce the difficulty of the operation, and shorten the duration of the operation. it may make the patient recover faster and better. Secondly, we only use a single surgical resection, sometimes can not achieve satisfactory results, we should use a variety of methods combined treatment, surgical resection as the main treatment, and the remaining lesions can be treated with sclerotherapy. in addition, for invasive and recurrent people, targeted therapy is also essential.

The purpose of this case is to share our process of diagnosis and treatment of this rare abdominal cystic mass, and to provide some help for relevant people, institutions and fields, but the combined treatment of cystic lymphangioma is still lack of unified understanding. we still need to further explore.

## Conclusion

In this case, we report a patient with giant retroperitoneal cystic lymphangioma who underwent exploratory laparotomy combined with preoperative abdominal CT and acute abdominal pain, abdominal distension and dyspnea. Because of the large volume of the tumor and its close relationship with the superior mesenteric artery and other blood vessels, the surgeon used scissors to separate the tumor sharply and removed the whole tumor completely.

## Data availability statement

The original contributions presented in the study are included in the article/Supplementary Material, further inquiries can be directed to the corresponding author/s.

## Ethics statement

Written informed consent was obtained from the individual(s) for the publication of any potentially identifiable images or data included in this article.

## Author contributions

SS, BS and DS: contributed to the conception and design of the study. SS and CL: contributed to drafting the article. DS and YF: contributed to revising the article critically. All authors contributed to the article and approved the submitted version.

## Acknowledgments

We are grateful to the coauthors for the rereading of the article.

## Conflict of interest

The authors declare that the research was conducted in the absence of any commercial or financial relationships that could be construed as a potential conflict of interest.

## Publisher's note

All claims expressed in this article are solely those of the authors and do not necessarily represent those of their affiliated organizations, or those of the publisher, the editors and the reviewers. Any product that may be evaluated in this article, or claim that may be made by its manufacturer, is not guaranteed or endorsed by the publisher.

# References


1. de Perrot M, Rostan O, Morel P, Le Coultre C. Abdominal lymphangioma in adults and children. *Br J Surg*. (1998) 85:395–7. doi: 10.1046/j.1365-2168.1998.00628.x

2. Koenig TR, Loyer EM, Whitman GJ, Raymond AK, Charnsangavej C. Cystic lymphangioma of the pancreas. *AJR Am J Roentgenol*. (2001) 177:1090. doi: 10.2214/ajr.177.5.1771090

3. Hauser H, Mischinger HJ, Beham A, Berger A, Cerwenka H, Razmara J, et al. Cystic retroperitoneal lymphangiomas in adults. *Eur J Surg Oncol*. (1997) 23:322–6. doi: 10.1016/s0748-7983(97)90777-0

4. Thiam O, Faye PM, Niasse A, Seye Y, Gueye ML, Sarr IS, et al. Cystic mesenteric lymphangioma: a case report. *Int J Surg Case Rep*. (2019) 61:318–21. doi: 10.1016/j.ijscr.2019.07.051

5. Alfadhel SF, Alghamdi AA, Alzahrani SA. Ileal volvulus secondary to cystic lymphangioma: a rare case report with a literature review. *Avicenna J Med*. (2019) 9:82–5. doi: 10.4103/ajm.AJM_203_18

6. Cupido BD, Low G. Incidental cystic lymphangioma of the small bowel mesentery. *J Clin Imaging Sci*. (2015) 5:55. doi: 10.4103/2156-7514.166358

7. Riley DS, Barber MS, Kienle GS, Aronson JK, von Schoen-Angerer T, Tugwell P, et al. CARE Guidelines for case reports: explanation and elaboration document. *J Clin Epidemiol*. (2017) 89:218–35. doi: 10.1016/j.jclinepi.2017.04.026

8. Kogo H, Matsumoto S, Uchida E. Single-port laparoscopic-assisted resection for a large abdominal cystic lymphangioma: a case report. *Surg Case Rep*. (2018) 4:92. doi: 10.1186/s40792-018-0501-9

9. Dubois J, Thomas-Chaussé F, Soulez G. Common (cystic) lymphatic malformations: current knowledge and management. *Tech Vasc Interv Radiol*. (2019) 22:100631. doi: 10.1016/j.tvir.2019.100631

10. Gachabayov M, Kubachev K, Abdullaev E, Babyshin V, Neronov D, Abdullaev A. A huge cystic retroperitoneal lymphangioma presenting with back pain. *Case Rep Med*. (2016) 2016:1618393. doi: 10.1155/2016/1618393

11. Yagmur Y, Akbulut S, Gumus S, Babur M, Can MA. Case report of four different primary mesenteric neoplasms and review of literature. *Iran Red Crescent Med J*. (2016) 18:e28920. doi: 10.5812/ircmj.28920

12. Wei MY, Chua J, Cheng Y, Grossberg P. Small bowel volvulus in an adult with mesenteric lymphangioma and ascariasis. *ANZ J Surg*. (2018) 88:E859–60. doi: 10.1111/ans.13953

13. Tian C, Zheng Y, Ren X, Li B. A giant abdominal cystic tumour: mesentery cystic lymphangioma. *Dig Liver Dis*. (2015) 47:816–7. doi: 10.1016/j.dld.2015.05.008

14. Nagano H, Kimura T, Iida A, Togawa T, Goi T, Sato Y. Cystic lymphangioma in the peripheral jejunal mesentery in an adult and excision with laparoscopic-assisted surgery: a case report. *World J Surg Oncol*. (2019) 17:170. doi: 10.1186/s12957-019-1713-6

15. Hitzerd E, van Hamont D, Pijnenborg JM. Mesenteric lymphangioma mimicking a cystic ovarian mass on imaging. *BMJ Case Rep*. (2016) 2016:bcr2015213727. doi: 10.1136/bcr-2015-213727

16. Xu X, Zheng C, He X, Zhao Y, Hong T. Gastrointestinal: giant mesenteric cystic lymphangioma. *J Gastroenterol Hepatol*. (2017) 32:290. doi: 10.1111/jgh.13542

17. Lui SA, Nyo YL, Mali VP. Ileal cystic lymphangioma presenting with acute appendicitis. *J Indian Assoc Pediatr Surg*. (2018) 23:36–8. doi: 10.4103/jiaps.JIAPS_44_17

18. Okamoto D, Ishigami K, Yoshimitsu K, Irie H, Tajima T, Nishie A, et al. Hemorrhagic mesenteric cystic lymphangioma presenting with acute lower abdominal pain: the diagnostic clues on MR imaging. *Emerg Radiol*. (2009) 16:327–30. doi: 10.1007/s10140-008-0747-9

19. Zoguéreh DD, N'Tarundenga U, Provendier B, Gazaigne J. A giant retroperitoneal mass in adult. *Rev Med Interne*. (2003) 24:202–3. doi: 10.1016/s0248-8663(02)00810-x

20. Colbert SD, Seager L, Haider F, Evans BT, Anand R, Brennan PA. Lymphatic malformations of the head and neck-current concepts in management. *Br J Oral Maxillofac Surg*. (2013) 51:98–102. doi: 10.1016/j.bjoms.2011.12.016

21. Okazaki T, Iwatani S, Yanai T, Kobayashi H, Kato Y, Marusasa T, et al. Treatment of lymphangioma in children: our experience of 128 cases. *J Pediatr Surg*. (2007) 42:386–9. doi: 10.1016/j.jpedsurg.2006.10.012

22. Leung M, Leung L, Fung D, Poon WL, Liu C, Chung K, et al. Management of the low-flow head and neck vascular malformations in children: the sclerotherapy protocol. *Eur J Pediatr Surg*. (2014) 24:97–101. doi: 10.1055/s-0033-1354585

23. Farnoosh S, Don D, Koempel J, Panossian A, Anselmo D, Stanley P. Efficacy of doxycycline and sodium tetradecyl sulfate sclerotherapy in pediatric head and neck lymphatic malformations. *Int J Pediatr Otorhinolaryngol*. (2015) 79:883–7. doi: 10.1016/j.ijporl.2015.03.024

24. Acevedo JL, Shah RK, Brietzke SE. Nonsurgical therapies for lymphangiomas: a systematic review. *Otolaryngol Head Neck Surg*. (2008) 138:418–24. doi: 10.1016/j.otohns.2007.11.018

25. Jamal N, Ahmed S, Miller T, Bent J, Brook A, Parikh S, et al. Doxycycline sclerotherapy for pediatric head and neck macrocystic lymphatic malformations: a case series and review of the literature. *Int J Pediatr Otorhinolaryngol*. (2012) 76:1127–31. doi: 10.1016/j.ijporl.2012.04.015

26. Bagrodia N, Defnet AM, Kandel JJ. Management of lymphatic malformations in children. *Curr Opin Pediatr*. (2015) 27:356–63. doi: 10.1097/MOP.0000000000000209

27. Reismann M, Ghaffarpour N, Luvall E, Jirmo AC, Winqvist O, Radtke J, et al. Dynamic toll-like receptor expression predicts outcome of sclerotherapy for lymphatic malformations with OK-432 in children. *J Surg Res*. (2014) 187:197–201. doi: 10.1016/j.jss.2013.09.037

28. Ardıçlı B, Karnak İ, Çiftçi AÖ, Tanyel FC, Şenocak ME. Sclerotherapy with bleomycin versus surgical excision for extracervical cystic lymphatic malformations in children. *Surg Today*. (2016) 46:97–101. doi: 10.1007/s00595-015-1128-0

29. Thottam PJ, Al-Barazi R, Madgy DN, Rozzelle A. Submucosal resection of a microcystic oropharyngeal lymphatic malformation using radiofrequency ablation. *Int J Pediatr Otorhinolaryngol*. (2013) 77:1589–92. doi: 10.1016/j.ijporl.2013.05.037

30. Ryu NG, Park SK, Jeong HS. Low power radiofrequency ablation for symptomatic microcystic lymphatic malformation of the tongue. *Int J Pediatr Otorhinolaryngol*. (2008) 72:1731–4. doi: 10.1016/j.ijporl.2008.08.003

31. Blesinger H, Kaulfuß S, Aung T, Schwoch S, Prantl L, Rößler J, et al. PIK3CA Mutations are specifically localized to lymphatic endothelial cells of lymphatic malformations. *PLoS One*. (2018) 13:e0200343. doi: 10.1371/journal.pone.0200343

32. Boscolo E, Pastura P, Glaser K, Goines J, Hammill AM, Adams DM, et al. Signaling pathways and inhibitors of cells from patients with kaposiform lymphangiomatosis. *Pediatr Blood Cancer*. (2019) 66:e27790. doi: 10.1002/pbc.27790

33. Kim T, Tafoya E, Chelliah MP, Lekwuttikarn R, Li J, Sarin KY, et al. Alterations of the MEK/ERK, BMP, and Wnt/β-catenin pathways detected in the blood of individuals with lymphatic malformations. *PLoS One*. (2019) 14:e0213872. doi: 10.1371/journal.pone.0213872

34. Liu X, Cheng C, Chen K, Wu Y, Wu Z. Recent progress in lymphangioma. *Front Pediatr*. (2021) 9:735832. doi: 10.3389/fped.2021.735832

35. Shayesteh S, Salimian KJ, Fouladi DF, Blanco A, Fishman EK, Kawamoto S. Intra-abdominal lymphangioma: a case report. *Radiol Case Rep*. (2021) 16:123–7. doi: 10.1016/j.radcr.2020.10.052

36. Dunev VR, Genov PP, Kirilov IV, Mladenov VD. Retroperitoneal cystic lymphangioma-a case report. *Urol Case Rep*. (2021) 35:101555. doi: 10.1016/j.eucr.2020.101555

37. Nuzzo G, Lemmo G, Marrocco-Trischitta MM, Boldrini G, Giovannini I. Retroperitoneal cystic lymphangioma. *J Surg Oncol*. (1996) 61:234–7. doi: 10.1002/(SICI)1096-9098(199603)61:3<234::AID-JSO14>3.0.CO;2-7

38. Saadi A, Ayed H, Karray O, Kerkeni W, Bouzouita A, Cherif M, et al. Retroperitoneal cystic lymphangioma: about 5 cases and review of the literature. *Pan Afr Med J*. (2016) 25:73. doi: 10.11604/pamj.2016.25.73.10002

39. Lim HJ, Tan JW, Chia CS, Ong CJ. A rare case of retroperitoneal lymphangioma in a 74-year-old Chinese male. *J Surg Case Rep*. (2021) 2021:rjaa610. doi: 10.1093/jscr/rjaa610

40. Kodera K, Abe K, Kanehira M, Futagawa Y, Okamoto T, Ikegami T. Retroperitoneal lymphangioma mimicking malignant tumor treated by pancreaticoduodenectomy. *Clin J Gastroenterol*. (2021) 14:1791–7. doi: 10.1007/s12328-021-01492-6

41. Cherk M, Nikfarjam M, Christophi C. Retroperitoneal lymphangioma. *Asian J Surg*. (2006) 29:51–4. doi: 10.1016/S1015-9584(09)60297-9

42. Bhavsar T, Saeed-Vafa D, Harbison S, Inniss S. Retroperitoneal cystic lymphangioma in an adult: a case report and review of the literature. *World J Gastrointest Pathophysiol*. (2010) 1:171–6. doi: 10.4291/wjgp.v1.i5.171

43. Aminian A, Jafarian A, Mirsharifi R, Moulavi S, Dashti H, Ali FA. Retroperitoneal cystic lymphangioma. *Indian J Surg*. (2008) 70:150–1. doi: 10.1007/s12262-008-0043-7

44. Lai EC, Li AC, Leong HT, Lau WY. Retroperitoneal cystic lymphangioma. *ANZ J Surg*. (2005) 75:365–6. doi: 10.1111/j.1445-2197.2005.03359.x

45. Liedtke KR, Käding C, Döring P, Bekeschus S, Glitsch AS. A case of giant retroperitoneal lymphangioma and IgG4-positive fibrosis: causality or coincidence. *SAGE Open Med Case Rep*. (2021) 9:2050313X211016993. doi: 10.1177/2050313X211016993

46. Kalish M, Dorr R, Hoskins P. Retroperitoneal cystic lymphangioma. *Urology*. (1975) 6:503–6. doi: 10.1016/0090-4295(75)90641-x

47. Suhani S, Aggarwal L, Ali S, Thomas S. Giant retroperitoneal lymphangioma: a rare entity. *Indian J Surg*. (2014) 76:402–4. doi: 10.1007/s12262-013-0989-y

48. Tripathi M, Parshad S, Karwasra RK, Gupta A, Srivastva S, Sarwal A. Retroperitoneal lymphangioma in an adult: a case report of a rare clinical entity. *Case Rep Surg*. (2015) 2015:732531. doi: 10.1155/2015/732531

49. Sato T, Matsuo Y, Shiga K, Saito K, Morimoto M, Miyai H, et al. Laparoscopic resection of retroperitoneal lymphangioma around the pancreas: a case report and review of the literature. *J Med Case Rep*. (2015) 9:279. doi: 10.1186/s13256-015-0760-z

50. Chaker K, Sellami A, Ouanes Y, Zehani A, Jallouli W, Ben Chehida MA, et al. Retroperitoneal cystic lymphangioma in an adult: a case report. *Urol Case Rep*. (2018) 18:33–4. doi: 10.1016/j.eucr.2018.02.019

51. Olaoye IO, Adesina MD. Rare huge retroperitoneal cystic lymphangioma presenting as acute abdomen in an adult. *BJR Case Rep*. (2018) 4:20170120. doi: 10.1259/bjrcr.20170120

52. Rezaee ME, Alexakos SG, Taylor CE, Santis WF. A rare case of a retroperitoneal lymphangioma causing chronic flank pain in an adult. *Urol Case Rep*. (2020) 33:101408. doi: 10.1016/j.eucr.2020.101408

53. Black T, Guy CD, Burbridge RA. Retroperitoneal cystic lymphangioma diagnosed by endoscopic ultrasound-guided fine needle aspiration. *Clin Endosc*. (2013) 46:595–7. doi: 10.5946/ce.2013.46.5.595

54. Hubli P, Rohith M, Sachin BM. A giant retroperitoneal lymphangioma: a case report. *J Clin Diagn Res*. (2016) 10:PD14–5. doi: 10.7860/JCDR/2016/19989.8142

55. Rajput D, Srikanth K, Gupta A, Kumar A, Edem S, David LE, et al. Large retroperitoneal cystic lymphangioma mimicking mesenteric cyst: a case report. *Pan Afr Med J*. (2022) 42:115. doi: 10.11604/pamj.2022.42.115.30777

56. Kasza J, Brody FJ, Khambaty F, Vaziri K, Wallace B. Laparoscopic resection of a retroperitoneal cystic lymphangioma in an adult. *Surg Laparosc Endosc Percutan Tech*. (2010) 20:e114–6. doi: 10.1097/SLE.0b013e3181db79a7

57. Izumi D, Toyama E, Shigaki H, Iwagami S, Baba Y, Hayashi N, et al. Laparoscopic excision of an adult retroperitoneal cystic lymphangioma coexisting with an esophageal hiatus hernia. *Clin J Gastroenterol*. (2015) 8:130–3. doi: 10.1007/s12328-015-0571-1

58. Ionescu C, Ionescu M, Dumitrascu T. Retroperitoneal cystic lymphangioma in a patient with previous surgery for seminoma. A Case Report. *Maedica*. (2012) 7:180–2. PMID: 23399992

59. Tsukamoto T, Tanaka S, Yamamoto T, Kakinoki E, Uemichi A, Kubo S, et al. Laparoscopic excision of a retroperitoneal cystic lymphangioma: report of a case. *Surg Today*. (2003) 33:142–4. doi: 10.1007/s005950300032

60. Mabrouk A, Ennaceur F, Karoui Y, Nejma EB, Jedidi L, Moussa MB. Giant retroperitoneal lymphangioma in a 70-year-old male: a case report. *Pan Afr Med J*. (2022) 42:153. doi: 10.11604/pamj.2022.42.153.34175

61. Suryawanshi PR, Agrawal MM, Rathod MD, Mandhane AM. Laparoscopic excision of a large retroperitoneal lymphovascular malformation in an adult. *J Minim Access Surg*. (2017) 13:66–8. doi: 10.4103/0972-9941.181773

62. Chung SH, Park YS, Jo YJ, Kim SH, Jun DW, Son BK, et al. Asymptomatic lymphangioma involving the spleen and retroperitoneum in adults. *World J Gastroenterol*. (2009) 15:5620–3. doi: 10.3748/wjg.15.5620

63. Colovic RB, Grubor NM, Micev MT, Atkinson HD, Rankovic VI, Jagodic MM. Cystic lymphangioma of the pancreas. *World J Gastroenterol*. (2008) 14:6873–5. doi: 10.3748/wjg.14.6873

frontiers | Frontiers in Oncology

TYPE Case Report
PUBLISHED 26 January 2023
DOI 10.3389/fonc.2022.1031112



OPEN ACCESS

EDITED BY
Akinfemi Akingboye,
Dudley Group NHS Foundation Trust,
United Kingdom

REVIEWED BY
Valeria Maffeis,
Ospedale di Treviso, Italy
Sergei Tevosian,
University of Florida, United States

*CORRESPONDENCE
Lei Zhang
dw8316291@163.com
Long Xia
xialong@mail2.sysu.edu.cn

SPECIALTY SECTION
This article was submitted to Surgical Oncology, a section of the journal Frontiers in Oncology

RECEIVED 31 August 2022
ACCEPTED 05 December 2022
PUBLISHED 26 January 2023

CITATION
Xia Y, Wang S, Wang X, Du J, Zhang L and Xia L (2023) Case Report: A rare case of primary paraganglioma of the gallbladder with a literature review. *Front. Oncol.* 12:1031112. doi: 10.3389/fonc.2022.1031112



# Case Report: A rare case of primary paraganglioma of the gallbladder with a literature review

Yijun Xia[1], Shi Wang[1], Xidong Wang[1], Jiya Du[2], Lei Zhang[3]* and Long Xia[1]*

[1]Department of Hepatobiliary-Pancreatic-Splenic Surgery, Inner Mongolia Autonomous Region People's Hospital, Hohhot, China, [2]Department of Pathology, Inner Mongolia Autonomous Region People's Hospital, Hohhot, China, [3]Department of Pancreatic-Hepatobiliary Surgery, The Sixth Affiliated Hospital, Sun Yat-sen University, Guangzhou, China

**Introduction:** Paragangliomas of the gallbladder are exceptionally rare. To date, only a few cases of this disease have been reported globally, and the majority were found incidentally during surgery. Although complete resection can achieve a curative effect, specific targeted drugs may have survival benefits for patients with potential recurrence and metastasis risks.

**Case presentation:** A 48-year-old woman was scheduled for anatomical central hepatectomy due to the discovery of a liver mass. Surprisingly, a gallbladder tumor accompanied by intrahepatic invasion was found rather than primary liver lesions during the operation. Postoperatively, the lesion was confirmed to be a paraganglioma originating from the gallbladder with intrahepatic invasion detectable on histopathology. After surgery, the patient was treated with a new targeted drug, surufatinib {200 mg, q.d. [*quaque die* (every day)]}, and no recurrence was observed during the regular follow-up.

**Discussion:** Gallbladder paraganglioma is rare and occult, and surgeons do not know it well, so it is easily misdiagnosed before surgery. Postoperative pathological examination is the gold standard for diagnosis.

**Conclusion:** Given that the tumor contained abundant blood sinuses, the early and continuous enhancement of dynamic enhanced CT scanning was its characteristic manifestation. We presented a case in which a primary gallbladder paraganglioma was identified accidentally in a patient who was misdiagnosed with a liver lesion before surgery. Based on our experience in this work, the en bloc resection technique in combination with surufatinib might have a survival benefit to patients at risk of potential recurrence or metastasis; however, further follow-up observations are needed.

KEYWORDS

**gallbladder paraganglioma, neuroendocrine neoplasms (NENs), immunohistochemistry, differential diagnosis, surufatinib**

## Introduction

In recent years, compared with other solid tumors, the incidence rate of neuroendocrine neoplasms (NENs) has increased significantly. In general terms, NENs can be divided into the following classifications: well-differentiated neuroendocrine tumor (NET), poorly differentiated neuroendocrine carcinoma (NEC), pheochromocytoma (PHEO), and paraganglioma (PARA) (1). Paragangliomas are a special type of NENs called neurogenic NENs, which originate from the neural crest cells of the neuroectoderm. As a whole, they form the so-called paraganglion system, including the adrenal medulla and extra-adrenal neuroendocrine cell groups. Those located in the adrenal medulla are called pheochromocytoma and often produce a large amount of catecholamines (CA), causing a series of clinical symptoms, such as high blood pressure and metabolic alterations. Those located outside the adrenal gland are called paragangliomas, which can further be divided based on whether they arise from the sympathetic or parasympathetic ganglia (2). Paragangliomas originating from glossopharyngeal and vagal nerves distributed along the neck and skull base usually do not produce CAs because they come from the parasympathetic ganglia; instead, those from the sympathetic nervous system are widely distributed from the skull base to the pelvic floor, and have CA secretion functions, which are also called sympathetic paragangliomas (3).

In terms of the symptoms and histological features of "pheochromogenic reaction", sympathetic paraganglioma is closely related to pheochromocytoma. Given the similarities between sympathetic paraganglioma and pheochromocytoma, the treatment options are essentially the same (3). Paraganglioma can occur in multiple locations on the body, including multiple organs in the head and neck, and the retroperitoneal and urinary systems (4). However, it is worth noting that paraganglioma originating from the gallbladder is extremely rare and has only been reported in a few articles to date, most often after having been discovered incidentally during surgery (5, 6). In this study, we share the case of an interesting and complex patient with preoperatively diagnosed neoplasms in the middle lobe of the liver and an intraoperative finding of a gallbladder mass with a partial intrahepatic invasion rather than a liver tumor. Postoperative pathology confirmed that it was a rare paraganglioma of gallbladder origin. We hope that through a detailed and thorough description of this case, colleagues in hepatobiliary surgery can deepen their understanding of this rare disease.

## Case presentation

A 48-year-old woman was admitted with neoplasms in the middle lobe of the liver, which were diagnosed by abdominal ultrasonography. Abdominal enhanced computed tomography (CT) showed a poorly defined low-density lesion in the middle lobe of the liver (mainly located in the S4b and S5 segments), which was significantly enhanced, and was suspected to be an angiogenic liver tumor (Figure 1). Further examination revealed that the levels of neuron-specific enolase (NSE) of the patient were elevated (Figure 2B). Combined with her imaging characteristics and our previous clinical experience (7), it was determined that the lesion might be a liver neuroendocrine tumor. The rest of the patient's examination and laboratory indicators were all normal, and no obvious abnormality was found in the physical examination. Based on the above condition analysis, our preoperative diagnosis was a centrally located liver tumor and that a liver neuroendocrine neoplasm could not be excluded. We planned to perform anatomical central hepatectomy, namely a territory resection around the middle hepatic vein (Figure 2A). During the operation we were surprised by the discovery of a gallbladder tumor rather than the liver lesion suggested by CT imaging (Figure 2C). Therefore, we quickly adjusted the operative protocol and performed a cholecystectomy, hepatoduodenal ligament lymph node dissection, and partial hepatectomy (Figures 2E, F). Meanwhile, the rapid frozen pathological examination during the operation indicated that the margin of the cystic duct and liver was negative. This unexpected intraoperative situation triggered our profound reflection. After the operation, when we reviewed the CT images of the patients again and combined them with the intraoperative situation, we realized that this was an extremely complex gallbladder tumor. The bottom and body of the gallbladder had been filled with solid masses and enhanced significantly, whereas the density of the neck of the gallbladder was still normal (Figure 2D). As for the clear enhancement of the liver around the gallbladder (i.e., what we had mistaken for liver lesions before surgery), this was most likely related to abnormal perfusion or the existence of an arteriovenous fistula. Postoperative pathological analysis revealed that the size of gallbladder lesion was about 6.0 cm × 4.0 cm × 3.5 cm, which invaded the whole layer of gallbladder wall and partly involved the adjacent liver tissue. Combined with immunohistochemical staining, it was consistent with paraganglioma of gallbladder. Microscopically, the lesion was mainly located within the submucosa of the gallbladder. The tumor cells were diffusely distributed in clusters, mainly composed of principal cells and sustentacular cells. The chief cells were mostly arranged in nests, forming a characteristic "zellballen" architecture, and the cell clusters were filled with blood sinuses (Figure 3). Further detailed immunohistochemical analysis revealed that broad-spectrum pan-cytokeratin (CK-pan) antibody staining was negative, which means that the tumor originated from non-epithelial tissue. Chromogranin A (CgA), neuron-specific enolase (NSE), and synaptophysin (Syn), three important neuroendocrine markers, were all positive; S-100 highlighted surrounding sustentacular cells, and the Ki-67

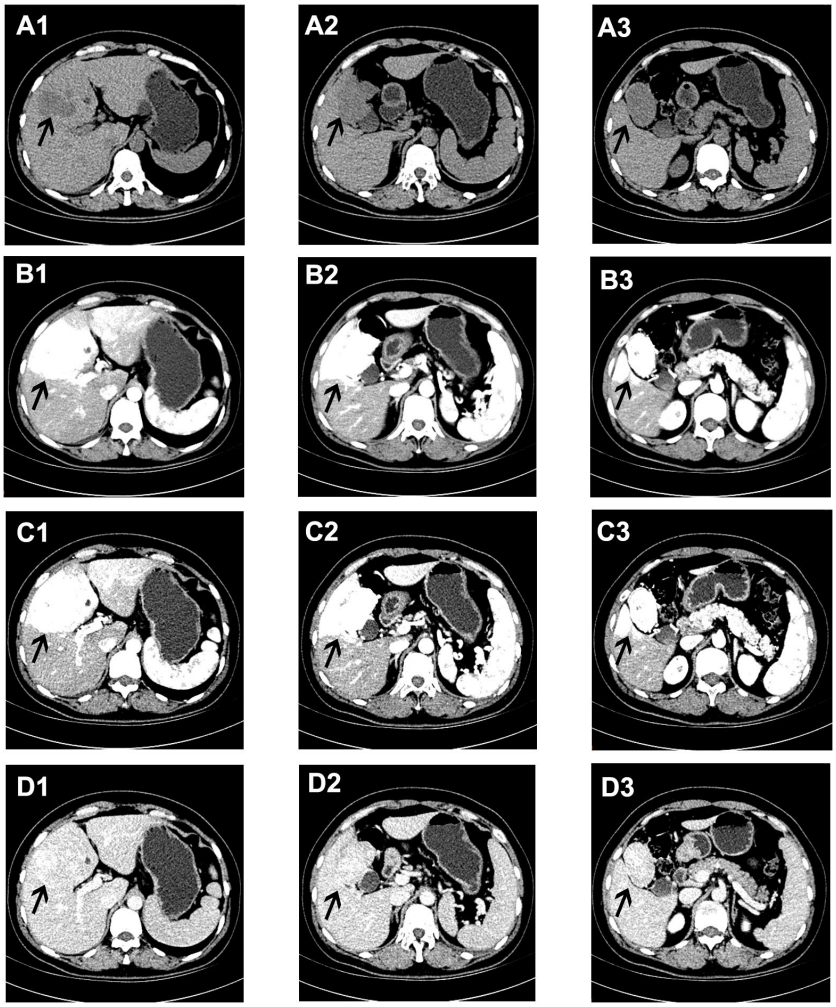


FIGURE 1
Abdominal enhanced CT manifestations of the lesions in the liver. **(A1–3)** On a plain CT scan, a poorly defined low-density lesion could be seen in the S4b and S5 segments of the liver. In the arterial phase **(B1–3)** and venous phase **(C1–3)** of a contrast-enhanced CT scan, the lesions showed continuous and obvious enhancement, while in the delayed phase **(D1–3)** the enhancement of the lesions decreased, and the density was similar to that of the normal liver, as shown by the black arrow.

proliferation index of tumor cells was 10% (Figure 4). To further exclude metastatic paraganglioma, the patient underwent a post-operative systemic positron emission tomography-computed tomography [specifically $^{18}$F-FDG (fluorodeoxyglucose F 18) PET-CT] scanning, which revealed no other hypermetabolic lesions. Collectively, the final diagnosis was primary gallbladder paraganglioma with partial liver invasion. In view of the abundant blood supply of the tumor and its potential for malignancy, we recommended that the patient take surufatinib, a new oral tyrosine kinase inhibitor developed completely independently in China at 1 month after surgery. Surufatinib has dual anti-angiogenic and immunomodulatory activity, and has been shown to be effective in clinical trials in non-pancreatic neuroendocrine tumor patients. We regularly followed up with the patient for half a year; her general condition was fine. Serum NSE levels showed a continuous downward trend (Figure 2B), and no obvious abnormality was found in biochemical tests and imaging examinations.

## Discussion

Paragangliomas are neoplasms originating from the paraganglia, which develop from neural crest cells and form the scattered nerve endocrine system around or within the autonomic nervous system, which extends from the skull base to the pelvic floor. In general, paragangliomas in the adrenal medulla are called pheochromocytoma, while those outside the

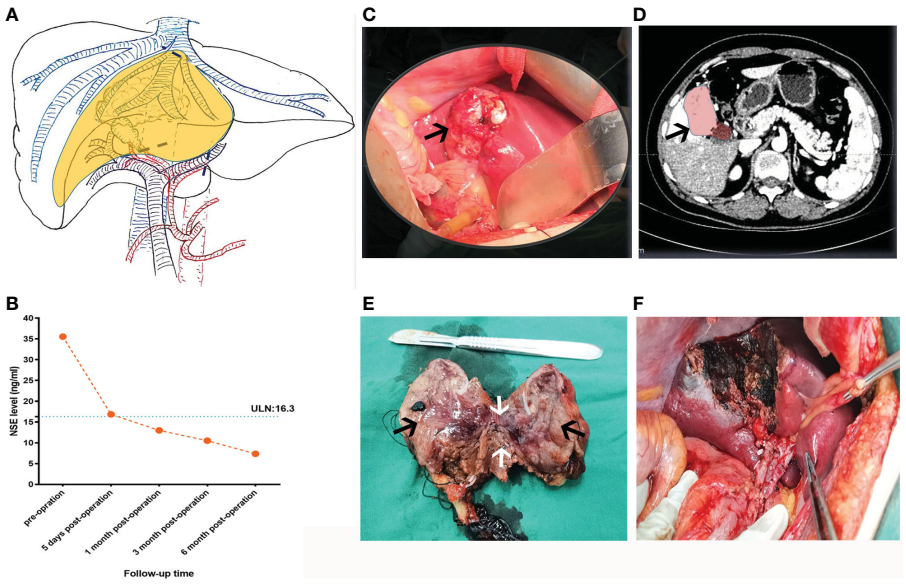


FIGURE 2
Preoperative planning and intraoperative status of patients. **(A)** According to the information from the two-dimensional enhanced CT image before operation, the hepatic lesion, the operative path **(the black dotted line),** and the resection area **(the yellow area)** were reconstructed by hand-drawing. **(B)** The tendency chart of NSE levels during patient follow-up. **(C)** Intraoperative gallbladder tumors (black arrow) and **(D)** corresponding CT images (black arrow). **(E)** Section of resected gallbladder tumor and part of the liver tissue, as shown, the black arrows indicate the gallbladder mass and the white arrow represents the liver tissue adjacent to the tumor **(F)** The wound condition after operation.

adrenal gland are designated extra-adrenal paragangliomas, also known as neurogenic NENs (2). Extra-adrenal paragangliomas are common in the body of the carotid artery or the bulb of the jugular vein, and, occasionally, occur in the bladder, prostate, and cauda equina; primary gallbladder paragangliomas are very rare in clinical practice (6). Theoretically, primary gallbladder paragangliomas arise from the migration of the hepatic plexus paraganglioma, which innervates the gallbladder, and is formed by sympathetic and parasympathetic fibers of the left vagus and celiac plexus (8).

At present, we still know very little about primary gallbladder paragangliomas. Since the first report of a gallbladder paraganglioma by Miller et al. in 1972 (9), the literature on gallbladder paraganglioma has been very limited, consisting entirely of case reports (Table 1) (5–7, 10–19). To our knowledge, our case is the largest tumor in all the current reports of the disease, and the pathology showed that it was accompanied by adjacent liver invasion, showing a certain degree of aggressiveness. Owing to the lack of typical clinical symptoms, some of these cases were found accidentally during cholecystectomy, and the others were due to the occurrence of accompanying symptoms or complications, such as right upper abdominal colic, obstructive jaundice, and bleeding. By reviewing these case reports, combined with our experience, we found that some of the clinical characteristics of primary gallbladder paraganglioma are as follows: (1) the patients were predominantly middle-aged women; (2) most patients lacked typical clinical symptoms and signs; (3) the CT scan of the lesion usually showed a soft tissue density mass with a clear boundary in the gallbladder, a small volume, and no obvious thickening and invasion of the surrounding gallbladder wall; (4) because the tumor contained abundant blood sinuses, most of them showed obvious enhancement in the early phase, the degree of enhancement could be close to the blood pool, the portal phase continued to enhance, and the delayed phase subsided; (5) the patients' serum NSE level may be elevated (at least in this case study); and (6) most of the tumors were located in the subserous layer of the gallbladder. It should be pointed out that these lesions still need to be differentiated from gallbladder polyps and mass-type gallbladder carcinoma. Gallbladder polyps are small and frequent, and the maximum diameter of the lesions is more than 1cm. Mass-type gallbladder carcinoma could also be manifested as a heterogeneous hyperenhancing soft-tissue mass, but often accompanied by necrosis, resulting in morphological changes of the gallbladder and the thickening or invasion of the gallbladder wall, but its degree of enhancement is significantly lower than that of paraganglioma. Although anatomical imaging for the precise localization of pheochromocytomas/paragangliomas (PGLs) is crucial, functional imaging is becoming an integral part of tumor imaging, especially for patients with multiple metastases. It was expected that patients with PHEO/PGL will benefit from

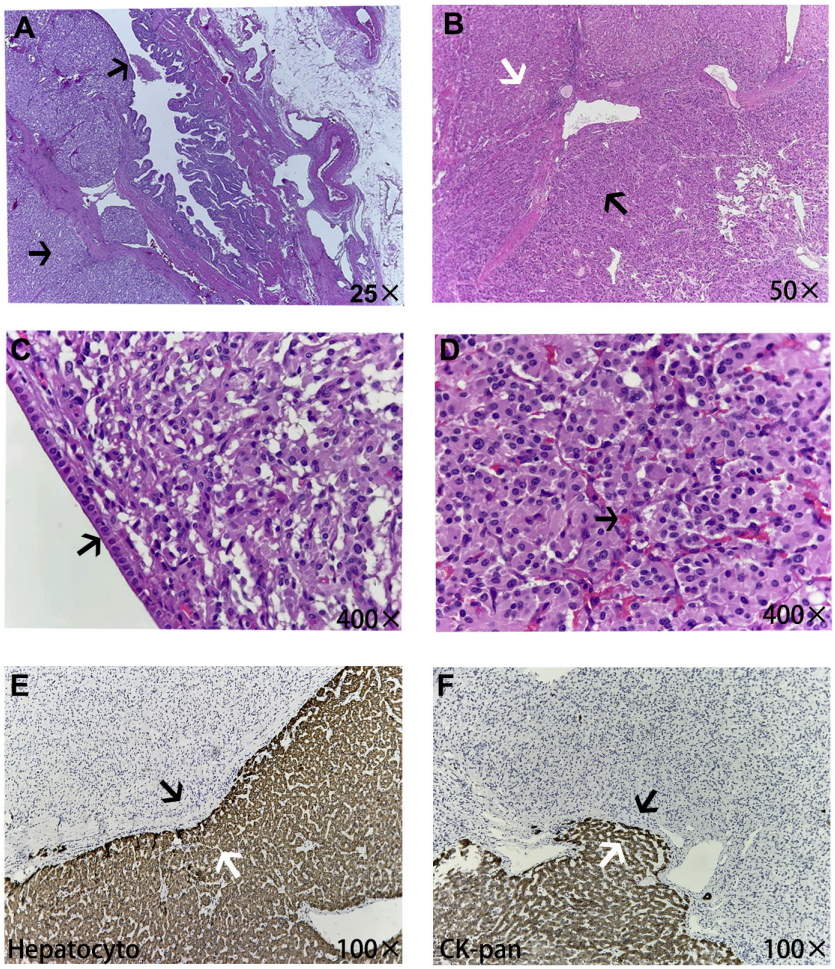


FIGURE 3
The microscopic pathological structure of tumor tissue. **(A)** The tumor was mainly located in the submucosa of the gallbladder (black arrow). **(B)** The white arrow shows normal liver tissue and the black arrow shows paragangliomas of the gallbladder tissue, in which tumor cells were diffusely distributed in clusters. **(C)** The gallbladder wall, which is surrounded by tumor cells, was covered with simple columnar epithelium structures (black arrow). **(D)** The paraganglioma demonstrated a characteristic zellballen architecture, rich in pink sinusoids inside (black arrow). Parts E and F show the junction structure of the tumor with adjacent liver tissues, and normal liver tissues all expressed the epithelial-derived markers Hepatocyto and CK-pan (white arrows), while non-epithelial paraganglioma tissue was negative (black arrows), which also indicated some degree of tumor invasion of the liver tissue.

the evaluation of functional characteristics of these tumors and new image-based treatment schemes (20, 21).

A thorough and detailed pathological examination after the operation was critically important for the diagnosis and differential diagnosis of NENs. The difference between NETs/NECs (neuroendocrine epithelial tumors) and PHEO/PARA (neuroendocrine non-epithelial tumors) is that the former has keratin expression, which was negative for spectral keratin in our patient (1). Microscopically, paraganglioma has its characteristic structure, which has the appearance of organoid "zellballen" architecture. The major and most common cell types are oval and granular chief cells, which are usually positive for CgA, NSE, and SYN, and negative for cytokeratin. Another cell-type component, which is usually less easily recognized in Hematoxylin eosin (HE), is a supportive sustentacular cell; usually presented as a fusiform hyperchromatic nucleus and an ambiguous vacuolar cytoplasm, it can be detected by positive immunostaining for S-100 (22). To sum up, pathological examination is the gold standard for the diagnosis of paraganglioma. Its characteristic immunohistochemical profile (i.e., positive for SYN, CgA, NSE, and S-100, and negative for cytokeratins) is helpful for the definite diagnosis and avoiding potential diagnostic pitfalls.

Currently, it is commonly believed that about 35%–40% of paragangliomas/pheochromocytomas (PPGLs) are genetically related (8). Therefore, patients with a definite diagnosis of

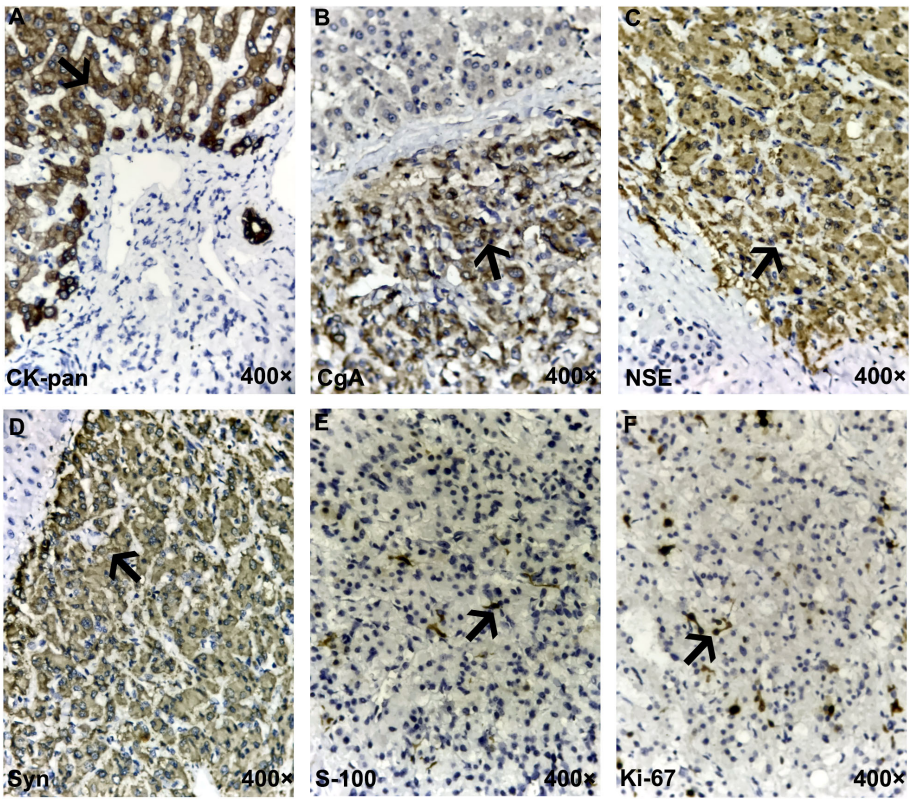


FIGURE 4
Immunohistochemistry for the gallbladder paraganglioma. **(A)** The difference between neuroendocrine epithelial tumor (NET/NEC) and neuroendocrine non-epithelial tumor (PHEO/PARA) is that the former expresses broad-spectrum pan-cytokeratin (CK-pan), which was negative here, meaning that the tumor was of non-epithelial origin. **(B–D)** Traditional general neuroendocrine markers, including chromogranin A (CgA), neuron-specific enolase (NSE), and synaptophysin (Syn), were all positive. **(E)** S-100 staining highlights surrounding sustentacular cells. **(F)** The Ki-67 proliferation index of tumor cells was 10%. The typical positive expression of each marker in the figures is indicated by black arrows.

PPGLs need to undergo pathogenic gene testing to determine whether or not their PPGLs are hereditary. In the case we reported, the patient did not have symptoms such as hypertension and palpitation. On detailed inquiry, there was no history of a similar condition in any family member. Because our hospital did not yet have the resources for genetic testing, and because of the high levels of COVID-19, the patient was unfortunately unable to undergo genetic testing. Since the fourth edition of the WHO classification, paragangliomas are no longer classified as benign and malignant because both may have metastatic potential and there are no well-defined features that can effectively predict metastatic behavior. This view was maintained in the fifth edition of the WHO bluebooks, which was published in 2022. Before recognizing that all PPGLs have variable metastatic potential, academics tried to develop multiple scoring or classification systems to predict metastatic risk. Although these assessment models have some predictive value, they lack universality and practicality. Therefore, the 2022 WHO bluebook did not highly recommend the metastatic risk assessment system of PPGLs (23).

In light of the fact that extra-adrenal tumors are more commonly clinically aggressive than adrenal tumors, and that in this case the tumor partially invaded the liver, although we had implemented a surgical scheme similar to the radical resection of a gallbladder carcinoma, postoperative recurrence problem is always a concern. As a new type of oral tyrosine kinase inhibitor, independently developed in China, surufatinib (24) has the dual activities of anti-angiogenesis and immune regulation. Encouragingly, it has shown good results in a Phase III clinical trial in China for patients with advanced non-pancreatic neuroendocrine tumors, solving the problem of patients with non-pancreatic neuroendocrine tumors lacking effective drug treatments (25, 26). Therefore, at 1 month after surgery, we recommend that the patient takes oral surufatinib to prevent the adverse consequences of recurrence and metastasis. So far, the patient from our case study has been followed up regularly for more than 6 months, and was in good condition at time of writing, with no signs of metastasis and recurrence.

TABLE 1 Summary of cases with paraganglioma of the gallbladder.

| Case no. | Source year | Age (years)/ sex | Clinical manifestation | Imaging characteristics | Size (cm) | Location | Associated findings | Hormone secretion |
|---|---|---|---|---|---|---|---|---|
| **1** | Miller (9), 1972 | 67/M | Recurrent hematemesis | Duodenal ulcer next to scarred duodenal bulb | 3.0 | NM | Tumor bleeding cholecystoduodenal fistula | NM |
| **2** | Wolff (10), 1973 | 32/F<br>52/F<br>59/F | Cholelithiasis<br>Cholelithiasis<br>Cholelithiasis | NM<br>NM<br>NM | NM<br>NM<br>NM | Subserosal<br>Subserosal<br>Subserosal | Chronic cholecystitis<br>Chronic cholecystitis<br>Chronic cholecystitis | NM<br>NM<br>NM |
| **3** | Kawabata (11), 1999 | 51/M<br>55/M | Hypochondralgia<br>Epigastralgia | Gallbladder stones<br>Hepatobiliary lithiasis | 0.5 × 0.3<br>0.3 × 0.2 | Subserosal<br>Subserosal | Liver dysfunction<br>Chronic cholecystitis | NM |
| **4** | Hirano (12), 2000 | 58/F | Right hypochondrial pain | Lesion in the neck of gallbladder | 1.3 × 0.9 | Submucosal | None | No |
| **5** | Cho et al. (13), 2001 | 45/F | Intermittent right upper quadrant pain | Fundal mass with diffusely thickened wall | 2.5 | NM | Tumor bleeding with chronic cholecystitis | No |
| **6** | Mehra (5), 2005 | 36/M | None | Normal | 1.5 | Subserosal | Chronic cholecystitis | NM |
| **7** | Sakuma (14), 2011 | 38/M | Hepatic hilus tumor | Heterogeneous mass and cholelithiasis | NM | Subserosal | Ectopic pheochromocytoma | NM |
| **8** | İlhan Ece (15), 2015 | 57/F | Intermittent right upper quadrant pain | Gallbladder stones and a mass within the triangle of Calot | 1.8 | Subserosal | Chronic cholecystitis | NM |
| **9** | Raha (16), 2018 | NM | Right upper quadrant pain | Gallbladder stones | NM | Subserosal | Paraganglioma of the cystic duct | No |
| **10** | Karel (17), 2019 | 36/M | Mild hypertension and tinnitus | A lesion with arterial enhancement adjacent to the gallbladder | 2.2 | NM | Elevated plasma dopamine level associated with SDHD mutation | Yes |
| **11** | Furrukh (6), 2020 | 63/F | Recurrent biliary colic | Mildly dilated gallbladder | NM | Submucosal | Chronic cholecystitis | No |
| **12** | Shukla (18), 2021 | 72/F | Discomfort in both ears accompanied by hearing loss | A lesion was seen in the neck of the gallbladder | 2.3 × 2.2 | NM | Familial paraganglioma syndromes | NM |
| **13** | Present case | 48/F | Physical examination revealed a liver mass | A tumor with a rich blood supply in the middle lobe of the liver | 6.0 × 4.0 | Submucosal | Paraganglioma of the gallbladder | No |

*NM indicates not mentioned.

## Conclusion

In conclusion, primary paragangliomas of the gallbladder are extremely rare in clinical settings and little is known about them. High levels of vigilance towards preoperative imaging is required for the detection of lesions that show significant and persistent enhancement early on the enhanced CT within the gallbladder. The characteristic immunohistochemical expression profile and the detection of pathogenic genes are critically important for diagnosis. In the era of targeted therapy, surufatinib might be a more effective treatment option for such tumors that have a risk of metastasis and recurrence, although more high-grade, high-quality clinical studies are needed to prove this in the future. We hope that through this case, more doctors can deepen their understanding of this rare disease and learn from our experiences and lessons.

## Data availability statement

The raw data supporting the conclusions of this article will be made available by the authors, without undue reservation.

## Ethics statement

The studies involving human participants were reviewed and approved by Ethics Review Board of the Inner Mongolia People's Hospital. The patients/participants provided their written informed consent to participate in this study. Written informed consent was obtained from the individual(s) for the publication of any potentially identifiable images or data included in this article.

## Author contributions

YX, SW, and LX collected imaging data and wrote the article, JD performed histopathological analysis of tissue sections, and LZ and LX reviewed and revised the manuscript. All authors contributed to the article and approved the submitted version.

## Conflict of interest

The authors declare that the research was conducted in the absence of any commercial or financial relationships that could be construed as a potential conflict of interest.

## Publisher's note

All claims expressed in this article are solely those of the authors and do not necessarily represent those of their affiliated organizations, or those of the publisher, the editors and the reviewers. Any product that may be evaluated in this article, or claim that may be made by its manufacturer, is not guaranteed or endorsed by the publisher.

## References

1. Bellizzi AM. Immunohistochemistry in the diagnosis and classification of neuroendocrine neoplasms: What can brown do for you? *Hum Pathol* (2020) 96:8–33. doi: 10.1016/j.humpath.2019.12.002

2. Corssmit EP, Romijn JA. Clinical management of paragangliomas. *Eur J Endocrinol* (2014) 171:R231–43. doi: 10.1530/EJE-14-0396

3. Jain A, Baracco R, Kapur G. Pheochromocytoma and paraganglioma-an update on diagnosis, evaluation, and management. *Pediatr Nephrol (Berlin Germany)* (2020) 35:581–94. doi: 10.1007/s00467-018-4181-2

4. Buffet A, Burnichon N, Favier J, Gimenez-Roqueplo AP. An overview of 20 years of genetic studies in pheochromocytoma and paraganglioma. *Best Pract Res Clin Endocrinol Metab* (2020) 34:101416. doi: 10.1016/j.beem.2020.101416

5. Mehra S, Chung-Park M. Gallbladder paraganglioma: A case report with review of the literature. *Arch Pathol Lab Med* (2005) 129:523–6. doi: 10.5858/2005-129-523-GPACRW

6. D'John M, Jabbar F. Primary gallbladder paraganglioma: A case report and review of literature. *Int J Surg Case Rep* (2020) 75:451–53. doi: 10.1016/j.ijscr.2020.09.095

7. Xia Y, Zhang L, Wu H, Qiao L, Xia L. Primary hepatic neuroendocrine tumor with multiple liver metastases: A case report with literature review. *J Int Med Res* (2020) 48:300060520932114. doi: 10.1177/0300060520932114

8. Fishbein L. Pheochromocytoma and paraganglioma: Genetics, diagnosis, and treatment. *Hematol/Oncol Clinics North A* (2016) 30:135–50. doi: 10.1016/j.hoc.2015.09.006

9. Miller TA, Weber TR, Appelman HD. Paraganglioma of the gallbladder. *Arch Surg (Chicago Ill 1960)* (1972) 105:637–9. doi: 10.1001/archsurg.1972.04180100080019

10. Wolff M. Paraganglioma of the gallbladder. *Arch Surg (Chicago Ill 1960)* (1973) 107:493. doi: 10.1001/archsurg.1973.01350210117035

11. Kawabata K. Paraganglia of the gallbladder: A report of two cases with an immunohistochemical study. *Pathol - Res Pract* (1999) 195:781–86. doi: 10.1016/S0344-0338(99)80121-6

12. Hirano T. Paraganglioma of the gallbladder: Report of a rare case. *Am J Gastroenterol* (2000) 95:1607–8. doi: 10.1111/j.1572-0241.2000.02120.x

13. Cho YU, Kim JY, Choi SK, Hur YS, Lee KY, Kim SJ, et al. A case of hemorrhagic gallbladder paraganglioma causing acute cholecystitis. *Yonsei Med J* (2001) 42:352–6. doi: 10.3349/ymj.2001.42.3.352

14. Sakuma T, Hirota M, Ohashi H, Kakudo K, Kawano K. Extensive ganglioneuromatosis of gallbladder. *Int J Surg Pathol* (2011) 19:524–6. doi: 10.1177/1066896908324129

15. Ece İ, Alptekin H, Çelik ZE, Şahin M. Gallbladder paraganglioma. *Ulusal cerrahi dergisi* (2015) 31:244–6. doi: 10.5152/UCD.2014.2691

16. AlMarzooqi R, AlJaberi L, Rosenblatt S, Plesec T, Berber E. A rare case of paraganglioma of the cystic duct. *Int J Surg Case Rep* (2018) 52:16–9. doi: 10.1016/j.ijscr.2018.09.041

17. Abdul Sater Z, Jha A, Mandl A, Mangelen SK, Carrasquillo JA, Ling A, et al. Gallbladder paraganglioma associated with SDHD mutation: A potential pitfall on (18)F-FDOPA PET imaging. *Nucl Med Mol Imaging* (2019) 53:144–47. doi: 10.1007/s13139-018-0558-1

18. Shreya S, Kashikar R, Shraddha SR, Shrinivas D. Case of the very rare gallbladder paraganglioma. *Indian J Radiol Imaging* (2021) 31:693–96. doi: 10.1055/s-0041-1736162

19. Rodríguez-Merchán B, Lozoya R, Allende E, Mesa J. [Paraganglioma of the gallbladder]. *Medicina Clin* (2006) 127:158. doi: 10.1157/13090388

20. Castinetti F, Kroiss A, Kumar R, Pacak K, Taieb D. 15 YEARS OF PARAGANGLIOMA: Imaging and imaging-based treatment of pheochromocytoma and paraganglioma. *Endocr Rel Cancer* (2015) 22:T135–45. doi: 10.1530/ERC-15-0175

21. Kroiss AS. Current status of functional imaging in neuroblastoma, pheochromocytoma, and paraganglioma disease. *Wiener Medizinische Wochenschrift (1946)* (2019) 169:25–32. doi: 10.1007/s10354-018-0658-7

22. Ramlal B, Voytek T, Ligato S. Paraganglia of the gallbladder: An underrecognized incidental finding and potential diagnostic pitfall. *Arch Pathol Lab Med* (2021) 145:437–40. doi: 10.5858/arpa.2020-0041-OA

23. Mete O, Asa SL, Gill AJ, Kimura N, de Krijger RR, Tischler A. Overview of the 2022 WHO classification of paragangliomas and pheochromocytomas. *Endocr Pathol* (2022) 33:90–114. doi: 10.1007/s12022-022-09704-6

24. Koumarianou A, Kaltsas G. Surufatinib - a novel oral agent for neuroendocrine tumours. *Nat Rev Endocrinol* (2021) 17:9–10. doi: 10.1038/s41574-020-00439-0

25. Xu J, Shen L, Zhou Z, Li J, Bai C, Chi Y, et al. Surufatinib in advanced extrapancreatic neuroendocrine tumours (SANET-ep): A randomised, double-blind, placebo-controlled, phase 3 study. *Lancet Oncol* (2020) 21:1500–12. doi: 10.1016/S1470-2045(20)30496-4

26. Lu X, Yan S, Koral KA, Chen Z. Surufatinib for the treatment of advanced extrapancreatic neuroendocrine tumors. *Expert Rev Anticancer Ther* (2021) 21:917–26. doi: 10.1080/14737140.2021.1944110

frontiers | Frontiers in Surgery

TYPE Case Report
PUBLISHED 30 January 2023
DOI 10.3389/fsurg.2023.1011152



OPEN ACCESS

EDITED BY
Riccardo Bertolo,
Hospital San Carlo di Nancy, Italy

REVIEWED BY
Lukas Rasulić,
University of Belgrade, Serbia
Rana Moshref,
King Faisal Specialist Hospital and Research Centre, Saudi Arabia

*CORRESPONDENCE
Dragan Jankovic
dragan.medicine@gmail.com

SPECIALTY SECTION
This article was submitted to Surgical Oncology, a section of the journal Frontiers in Surgery

RECEIVED 03 August 2022
ACCEPTED 02 January 2023
PUBLISHED 30 January 2023

CITATION
Jankovic D, Kalasauskas D, Keric N, Ottenhausen M and Ringel F (2023) Multiple myeloma presenting as a cervical intraforaminal tumor: A case report and review of literature. Front. Surg. 10:1011152. doi: 10.3389/fsurg.2023.1011152



# Multiple myeloma presenting as a cervical intraforaminal tumor: A case report and review of literature

Dragan Jankovic*, Darius Kalasauskas, Naureen Keric, Malte Ottenhausen and Florian Ringel

Department of Neurosurgery, University Medical Center, Johannes Gutenberg University Mainz, Mainz, Germany

Multiple myeloma (MM) is a hematological malignancy with characteristic clonal plasma cell proliferation and production of monoclonal immunoglobulins. Although it can often metastasize to the bony spine, completely extravertebral and extra-/intradural manifestations are exceedingly rare. In this case report, we describe a 51-year-old male patient with cervical extradural and intraforaminal MM who was surgically treated in our department. Clinical findings and radiological images were retrieved from medical records and an imaging system. This unusual localization of MM and similar cases in the literature are reviewed in detail. The patient underwent tumor resection via a ventral approach, and postoperative MRI demonstrated a sufficient decompression of neural structures. No new neurological deficits were observed at subsequent follow-ups. Although 7 cases of extramedullary extradural manifestations of multiple myeloma have been described in the literature so far, this is the first case of intraforaminal extramedullary multiple myeloma located in the cervical spine and treated by surgery.

KEYWORDS

case report, multiple myeloma, outcome, spine, surgery

## Introduction

Multiple myeloma (MM) represents 10% of all hematologic cancers with an annual incidence of 6.6 cases per 100,000 (1). It is characterized by the proliferation of neoplastic plasma cells, producing excessive monoclonal immunoglobulin (Ig) or free light chains (2). Multiple myeloma occurs as an extramedullary disease caused by hematogenous or continuous growth via the bone cortex. The most common site of manifestation of MM is the lower thoracic spine, followed by the lumbar spine. Vertebral destruction is primarily responsible for neurological symptoms, while the most frequent symptoms are pain and radiculopathy (3).

Here, we present a case of a patient with previously diagnosed and treated MM who was diagnosed with an intraspinal extradural tumor with an extension to the neuroforamen, resembling a spinal schwannoma, which finally turned out to be a manifestation of MM. We review the literature for the clinical course and management of this important differential diagnosis.

## Case description

A 51-year-old male patient presented to our department with pain in his left shoulder for approximately 9 months. The patient developed burning and piercing pain and dysesthesia in his left arm for 5 months, which corresponded to the C6 dermatome. His pain medication

consisted of hydromorphone and dexamethasone. On admission, the patient was awake and cooperative. Cranial nerve status was normal. Except for the tingling paraesthesia of Dig 1, there were no sensory or motor deficits in the extremities. There were no pathological findings in the standing and gait tests.

The patient was diagnosed with multiple myeloma 18 months ago, with manifestation in the 11th thoracic vertebral body, and treated with vertebral body replacement and dorsal spondylodesis T10–12. The surgery was followed by radiotherapy of the T10–12 up to a total dose of 46 Gy and two cycles of adjuvant chemotherapy (bortezomib–cyclophosphamide–dexamethasone). In the subsequent course, autologous stem cell transplantation was performed without complications.

Associated with his new radicular symptoms, an MRI of his cervical spine demonstrated an intraspinal, extradural, and intraforaminal contrast-enhancing lesion adjacent to the left-sided C6 root, without evidence of bone destruction. MRI features were suggestive of a C6 schwannoma (**Figure 1**).

A blood test showed normal values of hemoglobin (14.4 g/dl, reference range: 13.5–17.5 g/dl) and red cell count (4.72/pl; reference range: 4.2–5.6/pl). Serum LDH value was 275 U/I (reference range: <245 U/I). Tumor resection and decompression of the nerve root were scheduled via a ventral approach. A direct route to the lesion without retraction of the spinal cord was significantly more advantageous with a ventral approach.

As the intraoperative frozen section unexpectedly demonstrated a small blue cell tumor and the tumor diffusely infiltrated the nerve root, the decision was made to perform a partial resection and debulking of the tumor mass. A complete tumor resection could be taken into consideration after the completion of the histological analysis. The patient recovered well from the operation and reported significant pain relief. There were no new neurological deficits. Histologic analysis demonstrated cells with a narrow, poorly demarcated cytoplasm and relatively small, round, and hyperchromatic nuclei with numerous mitoses. The Ki67 proliferation index was >50%. Tumor cells were negative for CD45, CD3, CD20, CD138, synaptophysin, and S10. Positive immunoreactivity was observed only for vimentin antibodies. The final histological analysis revealed a manifestation of MM.

Postoperative MRI demonstrated a sufficient decompression of neural structures with a tumor remnant lateral to the nerve root (**Figure 2**). After an interdisciplinary case discussion, local ablative radiotherapy with a total dose of 45.0 Gy and adjuvant chemotherapy were performed. The patient has been followed for 9 months with no new neurological deficits and no tumor recurrence.

## Discussion

Although MM is the most common malignant tumor in the vertebrae, spinal cord compression occurs in only 5% of cases, usually due to extramedullary epidural tumor growth or a vertebral fracture (4) We searched the PubMed/MEDLINE databases using the following keywords: “multiple myeloma” AND extraosseous AND spinal cord compression. A literature search revealed only 7 cases of extradural manifestation of multiple myeloma (**Table 1**) (3, 5–10). To our knowledge, this is the first case of intraforaminal extramedullary multiple myeloma located in the cervical spine and

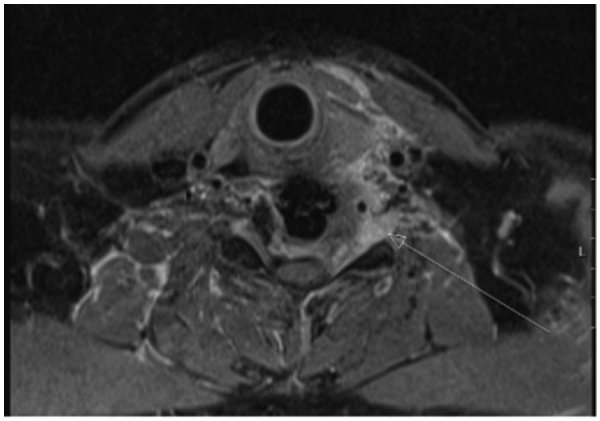

FIGURE 2
Postoperative axial T1-gadolinium MRI showing partial removal of tumor mass.

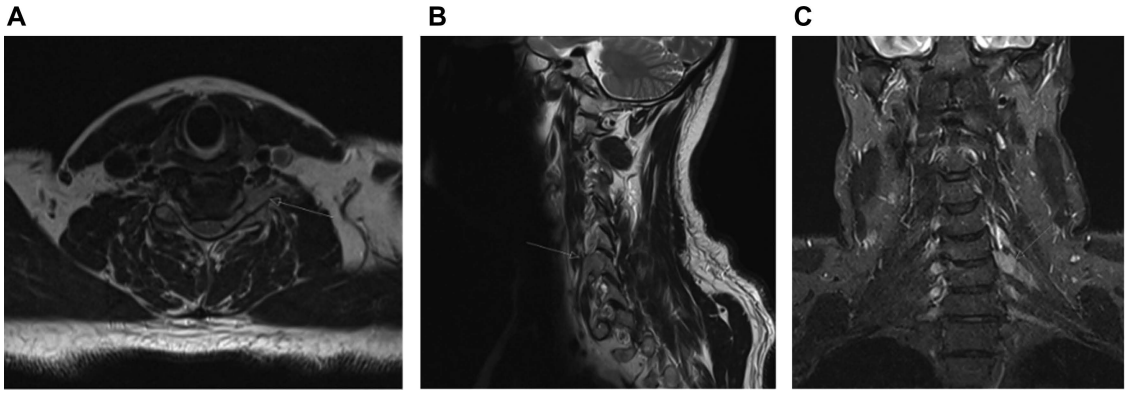


FIGURE 1
Axial (A), sagittal (B), and coronal (C) post-contrast T1 MRI showing extensive intraspinal, extradural tumor, including extension into the left C5/6 neural exit foramen.

treated by surgery. It is postulated that extramedullary hematopoietic (EMH) multiple myeloma arises from hematogenous spread or contiguous seeding from local lytic bone lesions (11). In this case, the manifestation of MM was localized extradural in the lateral spinal canal and neural foramen, without the affection of the adjacent vertebra. The tumor compressed the nerve root, which led to pain, motor, and sensory deficits.

It is known that multiple myeloma can be associated with chronic inflammatory demyelinating polyradiculoneuropathy (CIDP) (12). However, several studies have shown that idiopatic CIDP cannot be distinguished from CIDP related to monoclonal gammopathies (13, 14).

Given that pararoteinemia-neuropathy cannot be distinguished from CIDP, their work-up is still a debate. In addition to protein electrophoresis, some authors suggested that nerve biopsy could explain the etiology of neuropathy (15). Peripheral nerve ultrasound has been proposed to differentiate neuropathies associated with antimyelin, CIDP, and M-protein (16). However, due to variable neurotoxic patterns, ultrasound cannot provide relevant results in multiple myeloma.

The primary diagnostic tool for intraspinal tumors is MRI. MM manifests as a contrast-enhancing lesion. These lesions can be diffuse, spreading across multiple spinal levels (17).

The differential diagnoses for intraforaminal and spinal cord lesions usually include schwannoma, neurofibroma, hemangioblastoma, malignant peripheral nerve sheath tumor, spinal metastasis, solitary amyloidoma, and epidural abscess (5). However, the differentiation of intraforaminal lesions based on morphology and intensity may present a challenge for neuroradiologists. As a result, based on MRI features such as T1 iso- to hypointensity and T2 hyperintensity, as well as the configuration, a working diagnosis of schwannoma was made.

The median survival with MM is 2.5 years, while younger patients have a better prognosis. Some studies have reported that the median survival of a patient with EMH MM is 1–11 months (18–20) If the spine is affected, 75% of patients die within 1 year of diagnosis (21). Given the small number of papers published so far, MM's overall survival with extradural localization is unknown. In the cases of epidural extramedullary multiple myeloma reported so far, the cause of death was an infection or respiratory failure.

There are no guidelines for the management of treatment for intraspinal extradural multiple myeloma. In a longitudinal study of 1,003 patients by Varettoni et al., patients with an extramedullary manifestation of multiple myeloma had significantly lower hemoglobin and increased LDH levels (22). Similar findings were reported by studies of Barlogie et al. and Dimopoulus et al., confirming the association between LDH values and a more aggressive course and shorter survival of the patient with MM (23, 24). In our case, the serum LDH value on the day of admission was 275 U/I, which, with a Ki67 finding of >50%, confirms the aggressiveness of the tumor. Due to the extremely high proliferation activity, we hypothesized that MM has an aggressive phenotype, i.e., that there has been a plasmablastic transformation of MM.

An increased incidence of extramedullary relapse has been reported in patients undergoing allogeneic stem cell transplantation. In their retrospective study, Vincent et al. found that the number of previous therapies and age were associated with a higher risk of extramedullary relapse (25). Chemotherapy of extramedullary localizations of MM has so far not yielded satisfactory results (26).

Although extremely rare, a manifestation of multiple myeloma should be included in the differential diagnosis of extradural and

TABLE 1 Published cases of extradural multiple myeloma.

| Author | Age/ gender | Symptoms | Localization | MRI Signs of Myelopathy | Destruction of vertebral bodies | Intravertebral foramen involvement | Treatment | Follow-up |
|---|---|---|---|---|---|---|---|---|
| Avandhani et al. (5) | 60/female | Pain, spastic paraparesis | Posteriorly, T6-T7 | Yes | No | No | Total resection followed by local radiotherapy and chemotherapy | 6 months, improvement of motor power |
| Hu et al. (3) | 45/female | Pain, L5–S1 radiculopathy | L5–S1 | NS | No | NS | Surgical resection followed by chemotherapy | Died 5 months later due to pulmonary infection |
| Okacha et al. (6) | 47/male | Progressive paraplegia | Posteriorly, T4–T6 | Yes | No | Yes | Subtotal resection | Unchanged |
| Watanabe et al. (7) | 85/male | Paraplegie | C7–T2 | Yes | No | No | Chemotherapy | Unchanged |
| Matsui et al. (8) | 52/male | Pain with paresthesie | L3 | NS | Yes | Yes | Surgical resection, followed by chemotherapy | Died 5 months later due to respiratory dysfunctionmonths after the onset of symptoms |
| Lolin et al. (9) | 55/female | Pain | T4–5 | Yes | No | No | | Died 7 months later due to septicemic shock |
| Palmbach et al. (10) | 40/male | Paraplegia | C7–L2/L3 | NS | No | Yes | No | Died 3 months after admission due to respiratory insufficiency |

intraforaminal tumors in patients with a known MM. Early detection of the lesion is essential, especially if neurological symptoms appear. CSF cytology might be helpful in the diagnosis of intradural lesions, while tumor decompression can prevent neurological deterioration and improve the patient's quality of life. Given that it is difficult to distinguish multiple myeloma from other intraspinal pathology based on signal intensity and morphology on MRI scans, a rapid intraoperative tissue analysis should be considered to avoid unnecessary extensive tumor resections.

## Data availability statement

The original contributions presented in the study are included in the article/Supplementary Material, further inquiries can be directed to the corresponding author.

## Ethics statement

Written informed consent was obtained from the individual(s) for the publication of any potentially identifiable images or data included in this article.

## Author contributions

The authors that contributed to the conception and design of the study were DJ, DK, and NK. Data acquisition and interpretation were performed by DJ and DK. The first draft of the manuscript was written by DJ. DK, NK, and MO reviewed the manuscript. FR supervised and approved the final version of the report. All authors contributed to the article and approved the submitted version.

## Conflict of interest

The authors declare that the research was conducted in the absence of any commercial or financial relationships that could be construed as a potential conflict of interest.

## Publisher's note

All claims expressed in this article are solely those of the authors and do not necessarily represent those of their affiliated organizations, or those of the publisher, the editors and the reviewers. Any product that may be evaluated in this article, or claim that may be made by its manufacturer, is not guaranteed or endorsed by the publisher.

## References


1. Becker N. Epidemiology of multiple myeloma. *Recent Results Cancer Res.* (2011) 183:25–35. doi: 10.1007/978-3-540-85772-3_2

2. Rafae A, Malik MN, Abu Zar M, Durer S, Durer C. An overview of light chain multiple myeloma: clinical characteristics and rarities, management strategies, and disease monitoring. *Cureus*. (2018) 10(8):e3148, doi: 10.7759/cureus.3148

3. Hu KC, Lin J, Chuang YC, Cheng SJ, Chang KM. Multiple myeloma associated with extramedullary plasmacytoma causing nerve root compression: a case report. *J Formos Med Assoc.* (2001) 100(4):277–80.

4. Dispenzieri A, Kyle RA. Neurological aspects of multiple myeloma and related disorders. *Best Pract Res Clin Haematol.* (2005) 18(4):673–88. doi: 10.1016/j.beha.2005.01.024

5. Avadhani A, Shetty AP, Rajasekaran S. Isolated extraosseous epidural myeloma presenting with thoracic compressive myelopathy. *Spine J.* (2010) 10(4):e7–e10. doi: 10.1016/j.spinee.2010.01.007

6. Okacha N, Chrif E, Brahim E, Ali A, Abderrahman E, Gazzaz M, et al. Extraosseous epidural multiple myeloma presenting with thoracic spine compression. *Joint Bone Spine.* (2008) 75(1):70–2. doi: 10.1016/j.jbspin.2007.01.044

7. Watanabe Y, Endou A, Ooi S, Matsushima E, Shimisu Y, Nakashima K. Extraosseous epidural IgD myeloma presenting with compression myelopathy. *Psychiatry Clin Neurosci.* (2000) 54(6):665–7. doi: 10.1046/j.1440-1819.2000.00767.x

8. Matsui H, Fujie H, Tsuji H. Extraosseous epidural tumor of immunoglobulin D myeloma. *J Spinal Disord.* (1992) 5(3):366–9. doi: 10.1097/00002517-199209000-00017

9. Lolin YI, Lam CW, Lo WH, Au KL, Masarei JR. IgD multiple myeloma with thoracic spine compression due to epidural extra-osseous tumour spread. *J Clin Pathol.* (1994) 47(7):669–71. doi: 10.1136/jcp.47.7.669

10. Palmbach M, Hoffmann W, Grodd W, Postler E, Voigt K. Extraosseous, epidural tumour spread of multiple myeloma. *Eur J Radiol.* (1996) 22(2):146–8. doi: 10.1016/0720-048x(96)00754-1

11. Gozzetti A, Cerase A, Lotti F, Rossi D, Palumbo A, Petrucci MT, et al. Extramedullary intracranial localization of multiple myeloma and treatment with novel agents: a retrospective survey of 50 patients. *Cancer.* (2012) 118(6):1574–84. doi: 10.1002/cncr.26447

12. Fasanya AA, Loncharich MF, Gandhi V, Rana S, Balaan M. Multiple myeloma associated chronic inflammatory demyelinating polyradiculoneuropathy: the importance of continued surveillance. *Cureus.* (2016) 8(11):e899. doi: 10.7759/cureus.899

13. Rajabally YA. Neuropathy and paraproteins: review of a complex association. *Eur J Neurol.* (2011) 18(11):1291–8. doi: 10.1111/j.1468-1331.2011.03380.x

14. Simmons Z, Albers JW, Bromberg MB, Feldman EL. Long-term follow-up of patients with chronic inflammatory demyelinating polyradiculoneuropathy, without and with monoclonal gammopathy. *Brain.* (1995) 118(Pt 2):359–68. doi: 10.1093/brain/118.2.359

15. Van den Bergh PY, Rajabally YA. Chronic inflammatory demyelinating polyradiculoneuropathy. *Presse Med.* (2013) 42(6 Pt 2):e203–15. doi: 10.1016/j.lpm.2013.01.056

16. Athanasopoulou IM, Rasenack M, Grimm C, Axer H, Sinnreich M, Decard BF, et al. Ultrasound of the nerves—an appropriate addition to nerve conduction studies to differentiate paraproteinemic neuropathies. *J Neurol Sci.* (2016) 362:188–95. doi: 10.1016/j.jns.2016.01.055

17. Di L, Huang K, Kesayan T, Kroll D, Baz RC, Macaulay RJ, et al. Multiple myeloma presenting as an intramedullary spinal cord tumor: a case report and review of the literature. *J Med Case Rep.* (2020) 14(1):189. doi: 10.1186/s13256-020-02496-5

18. Dias A, Higashi F, Peres ALM, Cury P, Crusoe EQ, Hungria VTM. Multiple myeloma and central nervous system involvement: experience of a Brazilian center. *Rev Bras Hematol Hemoter.* (2018) 40(1):30–6. doi: 10.1016/j.bjhh.2017.09.004

19. Paludo J, Painuly U, Kumar S, Gonsalves WI, Rajkumar V, Buadi F, et al. Myelomatous involvement of the central nervous system. *Clin Lymphoma Myeloma Leuk.* (2016) 16(11):644–54. doi: 10.1016/j.clml.2016.08.010

20. Jurczyszyn A, Grzasko N, Gozzetti A, Czepiel J, Cerase A, Hungria V, et al. Central nervous system involvement by multiple myeloma: a multi-institutional retrospective study of 172 patients in daily clinical practice. *Am J Hematol.* (2016) 91(6):575–80. doi: 10.1002/ajh.24351

21. Bladé J, Kyle RA. Multiple myeloma in young patients: clinical presentation and treatment approach. *Leuk Lymphoma.* (1998) 30(5–6):493–501. doi: 10.3109/10428199809057562

22. Varettoni M, Corso A, Pica G, Mangiacavalli S, Pascutto C, Lazzarino M. Incidence, presenting features and outcome of extramedullary disease in multiple myeloma: a longitudinal study on 1003 consecutive patients. *Ann Oncol*. (2010) 21 (2):325–30. doi: 10.1093/annonc/mdp329

23. Barlogie B, Smallwood L, Smith T, Alexanian R. High serum levels of lactic dehydrogenase identify a high-grade lymphoma-like myeloma. *Ann Intern Med*. (1989) 110(7):521–5. doi: 10.7326/0003-4819-110-7-521

24. Dimopoulos MA, Barlogie B, Smith TL, Alexanian R. High serum lactate dehydrogenase level as a marker for drug resistance and short survival in multiple myeloma. *Ann Intern Med*. (1991) 115(12):931–5. doi: 10.7326/0003-4819-115-12-931

25. Vincent L, Ceballos P, Plassot C, Méniane JC, Quittet P, Navarro R, et al. Factors influencing extramedullary relapse after allogeneic transplantation for multiple myeloma. *Blood Cancer J*. (2015) 5(8):e341. doi: 10.1038/bcj.2015.48

26. Damaj G, Mohty M, Vey N, Dincan E, Bouabdallah R, Faucher C, et al. Features of extramedullary and extraosseous multiple myeloma: a report of 19 patients from a single center. *Eur J Haematol*. (2004) 73(6):402–6, tumour spread. J. Clin. Pathol. 1994; 47: 669–671. doi: 10.1111/j.1600-0609.2004.00331.x

frontiers | Frontiers in Oncology

TYPE Case Report
PUBLISHED 03 February 2023
DOI 10.3389/fonc.2023.1016232



OPEN ACCESS

EDITED BY
Riccardo Bertolo,
Hospital San Carlo di Nancy, Italy

REVIEWED BY
Fausto Fama',
University of Messina, Italy
Jiaxi He,
First Affiliated Hospital of Guangzhou Medical University, China

*CORRESPONDENCE
Zhendong Li
lz86153277@163.com

SPECIALTY SECTION
This article was submitted to Surgical Oncology, a section of the journal Frontiers in Oncology

RECEIVED 11 August 2022
ACCEPTED 13 January 2023
PUBLISHED 03 February 2023

CITATION
Liu Z and Li Z (2023) Case Report: Defect repair post-resection of cervical tracheal granular cell tumor by cervical anterior banded myofascial flap: A case study and literature review. *Front. Oncol.* 13:1016232. doi: 10.3389/fonc.2023.1016232



# Case Report: Defect repair post-resection of cervical tracheal granular cell tumor by cervical anterior banded myofascial flap: A case study and literature review

Zhu Liu and Zhendong Li*

Department of Head and Neck Tumor Surgery, Cancer Hospital of Dalian University of Technology, Cancer Hospital of China Medical University, Liaoning Cancer Hospital & Institute, Shenyang, Liaoning, China

**Objective:** A case of cervical tracheal granular cell tumor (CTGCT) is reported together with a discussion on the clinical manifestation, diagnosis, and treatment of CTGCT. Additional cases of tumors in the tracheal membrane are also discussed. A simple and viable tracheal reconstruction method was proposed. The research design involves a case report and literature review.

**Methods:** Twenty-four case reports on cervical GCT with complete clinical data were identified, with a specific focus on cases involving surgical treatment of tumors in the cervical tracheal membrane.

**Results:** Twenty-eight reports of GCT in the cervical trachea and six reports on cervical tracheal membrane tumors were identified. The clinical data of a middle-aged Asian woman with a cervical GCT was also discussed.

**Conclusion:** Cervical GCT is a rare disease, and tracheal resection is a reasonable treatment for cervical tracheal GCT. The proposed procedure is a simple and feasible method for reconstruction of the cervical tracheal membrane defect using a double-pedicled banded myofascial flap.

KEYWORDS

**granular cell tumor, tumor of the trachea, fascia tissue flap, tracheal membrane, tracheal reconstruction**

## Introduction

Granular cell tumors (GCTs) were first described by Abrikossoff in 1926 (1); the name derives from the presence of large numbers in eosinophilic granules in the tumor cell cytoplasm. GCT was initially considered a myogenic tumor and was described by Horn and Stout et al. (2) as a granular cell myoblastoma. Current pathological studies indicate that it is derived from neuronal tissue or Schwann cells (3, 4). It occurs most commonly in

patients between the ages of 30 and 50 years old with a higher incidence in females than in males (5). Most of the tumors are benign, and only 1–2% are malignant (6, 7). GCT in the respiratory system accounts for 2–6% of the overall cases; most respiratory-associated GCTs occur in the larynx and tracheal GCT is rare. The treatment of cervical tracheal GCT includes the use of simple endoscopic forceps combined with laser, electrosurgery, and argon ion-assisted resection, together with open surgery (8). Here, the case and treatment of a middle-aged Asian woman with a cervical GCT is presented, together with a summary of the clinical data of 26 cases of cervical tracheal GCT and an analysis of the clinical manifestations, diagnosis, and treatment of the disease. This study focuses on the surgical methods used for treating cervical tracheal membrane tumors, and introduces a simple and feasible method for tracheal membrane reconstruction.

## Case report

A 45-year-old Asian woman presented with a primary complaint of active dyspnea with irritant dry cough for two months. Bronchoscopy showed a bulging mass 2 cm below the voice box, which obstructed 80% of the lumen (Figure 1). The tumor was located in the submucosa, and biopsy specimens could not be obtained. There was no laryngeal vocalization, while the inspiratory and expiratory times were slightly prolonged, no swollen lymph nodes were found on the neck, and the breath sounds in both lungs were normal. No other abnormalities were observed. The patient was admitted to the hospital with clinical grade II dyspnea and moderate irritant airway spasm. The preoperative examination was completed within three days of admission. No biopsy was performed as the patient was unable to tolerate bronchoscopy. The assessment indicated no contraindications to surgery, and surgery was performed on the fourth day after admission. Prophylactic antibiotics were given half an hour before surgery, and the operation lasted for two hours. Postoperatively, the patient was admitted to the observation room in the ward. She had stable vital signs and did not experience respiratory distress, hoarseness, or hypocalcemia. Additionally, she was given continued cephalic antibiotics, phlegm, and intravenous nutrition treatment for a week. No local or intrapulmonary infection was observed. Hence, the patient was discharged after bronchoscopy on the ninth postoperative day.

Examinations showed that hematuria and stool routine were normal, coagulation routine was normal, and ECG was within the normal range. Enhanced computed tomography (CT) of the larynx and trachea revealed that the boundary between the tumor and the anterior wall of the esophagus was not clear, and the larger layer range was approximately 17 mm × 16 mm. This was apparent even after enhancement. The CT value of the plain scan was about 64 HU, and that of the enhanced scan was about 85 HU in the venous phase. Cervical posterior tracheal nodules were observed, and their nature was determined through microscopic examination (Figure 2). Enhanced MR in the neck revealed a nodular shadow in the cervical trachea of about 16 mm × 15 mm, and visible enhancement revealed long T1 and long T2 signals (Figure 3). Electronic duodenoscopy revealed no abnormality.

The tumor was exposed and removed after anesthesia induction, oral endotracheal intubation and mechanical ventilation, followed by the adjustment of the position of the endotracheal tube for tracheal defect repair. The tumor appeared as a smooth round-like shape in the tracheal cavity, located in the posterior membrane of the trachea. There was no stenosis in the trachea wall. The trachea cannula could pass through the tumor due to the elasticity of the posterior membrane. The patient was in the supine position. After intravenous anesthesia induction, a No. 6.5 reinforced endotracheal tube was used, and the cuff was 2 cm below the tumor, with cuff inflation. A low-collar incision in the neck was created. The left thyroid gland was exposed, and tissue separation was performed upward along the outer edge of the left thyroid gland. The middle thyroid vein and inferior thyroid artery were clamped and cut off under direct vision. The inferior thyroid pole was dissociated and exposed to protect the recurrent laryngeal nerve, and the lower parathyroid gland was retained *in situ*. The tissues along the surface of the recurrent laryngeal nerve were separated to the entrance point, with complete freeing of the lateral thyroid and retention of the upper parathyroid gland *in situ*, followed by the complete dissociation of the lower pole. The tissue block was then turned to the opposite side, and sharp dissection was performed on the surface of the trachea wall. The gland and isthmus were dissociated to the opposite lobe, and the recurrent laryngeal nerve was completely exposed and retained *in situ*. The tumor, with a length of approximately 2.0 cm, was located in the middle of the posterior of the second to fourth tracheal rings. The tumor was resected by an inter-tracheoesophageal approach, resulting in a tracheal membrane defect of approximately 3.0 cm × 2.0 cm after resection with a safe incision margin of 0.3 cm. Intraoperative

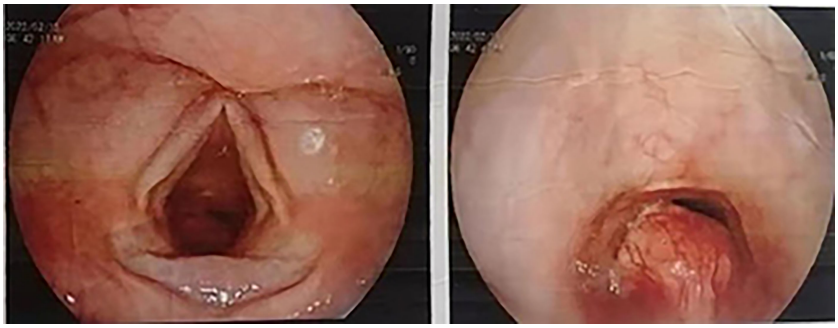

FIGURE 1
Bronchoscopic image; the scope positioned just cranial to the vocal cords shows the presence of a polypoid lesion within the infraglottic airway.

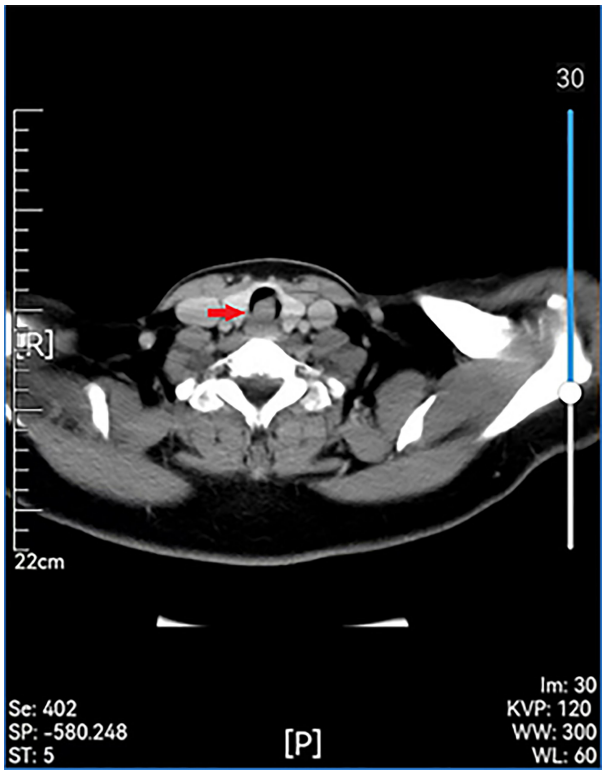


FIGURE 2
Preoperative enhanced CT scan showing a remodeled area of cervical with posterior wall erosion (red arrow).

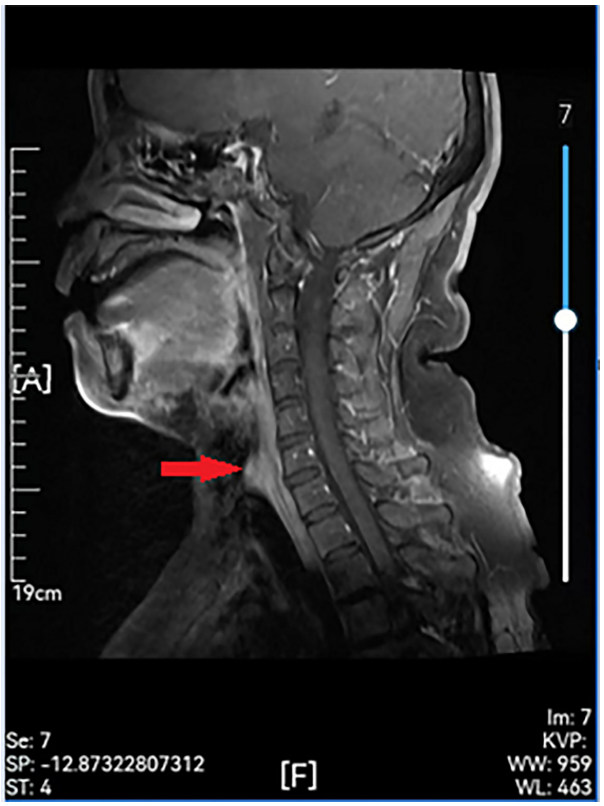


FIGURE 3
Preoperative enhanced MR showing a remodeled area of cervical with posterior wall erosion (red arrow).

pathological examination suggested the presence of a mesenchymal tumor. The fascia was cut on both sides of the left banded muscle to reach the muscle surface, and the full-thickness rectangular fascial flap of about 5×3×0.5 $cm^3$ on the muscle surface was lifted as a whole from top to bottom and from outside to inside to keep the upper and lower pedicle blood supplies. The double pedicle was moved to the defect site without torsion, and a 3-0 absorbable suture was used for suturing with a needle distance of about 0.5 cm. The defect was repaired by suturing the two lateral edges of the fascial tissue flap with the end of the second to fourth tracheal rings and soft tissue in opposite positions (Figure 4). The tissue was sutured from both ends to the center without knotting the retained suture. When sewing and knotting the middle part, the endotracheal tube was lifted intermittently with suspended ventilation. All stitches were knotted after the suture. A temporary tracheal cutaneous fistula was performed by transverse incision of 1 cm at the sixth to seventh tracheal rings without an endotracheal cannula. Postoperative nasal and oral respiration was smooth, antibiotics were given for one week, no postoperative complications were observed, and the tracheocutaneous fistula was closed. Bronchoscopy examination on the ninth day after surgery showed a slight bulge 2-6 cm below the glottis, behind the second to fourth tracheal rings, with white moss attached (Figure 5). No recurrence has been observed in postoperative follow-up examinations up to the present date.

Pathology: The gross specimen appeared as a white, smooth, shiny, nodular swelling of 2 cm × 1.5 cm, without an envelope, and was grayish-white on section with a medium texture and solid. Light microscopy revealed that the surface was covered with squamous epithelium and some areas of pseudostratified ciliated columnar epithelium, with a tightly packed mass in the submucosa. The tumor cells appeared spindle-shaped, round, polygonal, and irregularly arranged. The tumor cell cytoplasm appeared rich in eosinophilic red cytoplasm and filled with eosinophilic granules. The cell boundaries were indistinct. The nuclei were small, round, or oval, with no chromatin anisotropy, no nuclear fission phase, and obvious nucleoli. The pathological diagnosis indicated GCT. The immunohistochemical findings indicated S-100 (+), NSE (+), CD56 (+), and Ki67 3% (+). The microscopic findings are presented in Figure 6.

## Materials and method

The PubMed, EMBASE, and Google Scholar databases were searched with the following search terms: “tracheal granulosa cell tumor”, “granulosa cell tumor”, and “rare airway tumor”. The inclusion criteria were all articles published in PubMed and relevant only to humans. Articles without full texts were excluded. A total of 28 cases of cervical segmental tracheal GCT were identified in this search.

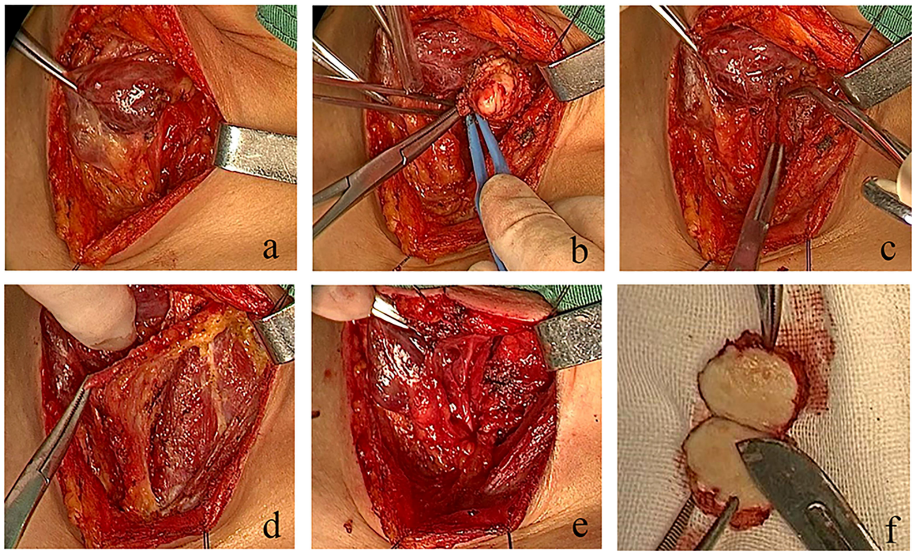


FIGURE 4
Real-time video of the operation process. In the case presented in this study, the defect was repaired by suturing the two lateral edges of the fascial tissue flap with the end of second to fourth tracheal rings and soft tissue in opposite positions. **(A)** Lateral freeing of the left thyroid gland, protection of the superior and inferior parathyroid glands, and the recurrent laryngeal nerve to expose the tumor. **(B)** Complete resection of the tracheal membrane tumor. **(C)** Tracheal membrane defect. **(D)** Preparation of a double-tipped banded myofascial flap. **(E)** No damage to the thyroid gland and recurrent laryngeal nerve after repair. **(F)** Specimen presentation.

## Results

Table 1 presents the clinical data of all 29 patients retrieved from the literature. Data were analyzed to elucidate the clinical features of cervical segmental tracheal GCT and assess the efficacy of different treatment modalities. The age range of the patients was 6-64 years, with a mean age of 31.4 years (n=29) and a median age of 31 years. Twenty-five of the 29 patients (86.2%) were female, and 22 had a clear ethnicity, of which 15 (51.7%) were black and three were Asian. Among the 25 patients, 21 (84%) presented with respiratory symptoms, mainly cough, shortness of breath, laryngeal tinnitus, and dyspnea. The mean tumor size at diagnosis was 2.67 cm (n=24), with a long axis range of 0.45-6 cm. Twenty-five cases (86.2%) had a single tumor. Most of the tumors (31) were intracavitary, eight were extracavitary, and five were both intra- and extracavitary. Seven tumors (35%), including the case presented in this study, were documented in the literature as occurring in the posterior tracheal wall. A review of the literature revealed a 62.5% incidence of recurrence or residual tumor in eight patients who underwent endoscopic resection; two of the recurrences were treated by trachelectomy, and two cases were supplemented with endoscopic laser-assisted resection. The incidence of recurrence or residual disease was 50% in the four patients who underwent shave resection and trachelectomy after recurrence in one case. No recurrence was reported in the 12 patients who underwent trachelectomy. One patient underwent electrosurgery and argon

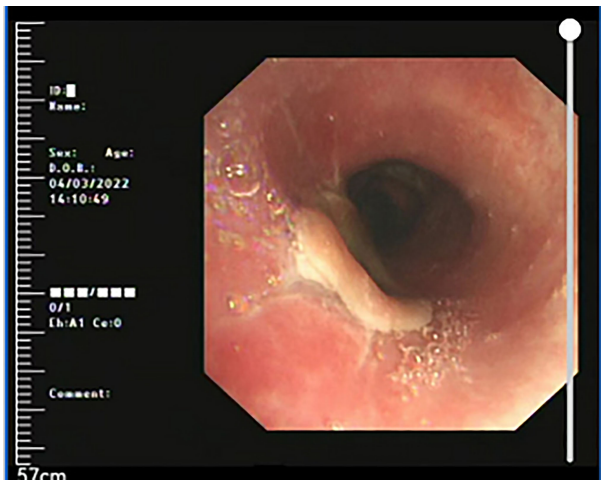


FIGURE 5
Three months after treatment, reexamination of bronchoscope showed a smooth surface of reconstruction site, with no tracheostenosis.

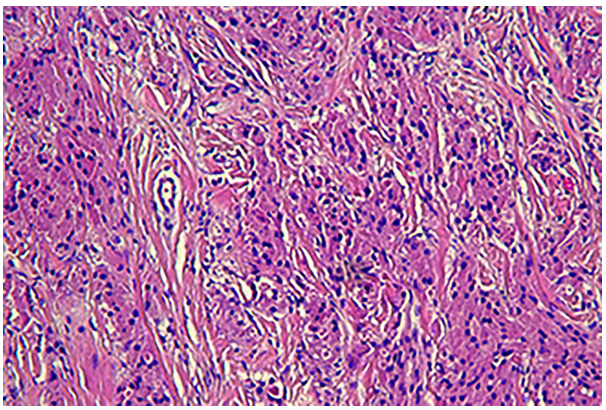

FIGURE 6
Hematoxylin and eosin staining revealed large cells with cytoplasmic granules.

TABLE 1 Published data on tracheal granular cell tumors.

| Source | Age/ Sex | Race | Complaint | Size (cm) | Solitary/ Multiple | Location | Intra/ Extraluminal | Results/ Follow-up | Surgical method/ Reconstruction method |
|---|---|---|---|---|---|---|---|---|---|
| Benisch (9) | 25/F | Black | Respiratory difficulty asthma | 1.5 | S | Posterior wall erosion | Intra | NED/15 mo | Tracheal resection and tracheotomy/end to end |
| Krouse (10) | 54/F | Black | NA | 2.5 | M | Cervical tracheal | Extra | Postmortem finding | None |
| Thawley (11) | 33/F | Black | Painless left neck mass | 3.0 | S | Left lateral tracheal wall, cricoid cartilage | Extra | Residual disease/8y | Tracheal wall shaving and Thyroid lobectomy/none |
| Carnalis (12) | 45/F | NA | Intermittent hemoptysis | 5.5 | S | Posterior wall erosion | Intra and extra | NED/3 y | Tracheal resection and tracheotomy/end to end |
| Polack (13) | 29/F | Black | Incidentally found | 2.0 | S | Anterior wall erosion | Extra | NED/4 wk | Tracheal wall shaving/none |
| Dunaway (14) | 6/F | Black | Intermittent wheezing | 2.0 | M | Left lateral tracheal wall | Intra | Residual disease/9y | Endoscopic excision |
| McLain (15) | 26/M | Black | Dyspnea | 2.0 | M | 8 cm below the vocal cords | Intra | NED/9 mo | Endoscopic laser excision Tracheal resection and tracheotomy/end to end |
| Mikaelian (16) | 20/F | Black | Cough associated with dyspnea | 2.0 | S | Posterior wall erosion | Intra | NED/2 y | Endoscopic laser excision Tracheal resection and tracheotomy/end to end |
| Thaller (17) | 31/F | Black | Increasing shortness of breath | 6.0 | S | Anterior wall erosion | Intra | NED/6 wk | Endoscopic laser excision and tracheotomy |
| Alessi (18) | 33/F | Black | Right upper extremity weakness and dygphngin | NA | S | Low in the neck | Extra | NED/7 y | Partial tracheal resection and thyroid lobectomy/none |
| Alessi (18) | 37/F | Black | Incidentally found | 3.0 | S | 6 cm above the carina, submucogal | Intra | NED/2y | Tracheal resection and tracheotomy/end to end |
| Solomons (19) | 10/M | NA | Acute respiratory distress | NA | S | Posterior tracheal wall and anterior oesophageal wall | Intra | Died postoperatively vocal cords in a paramedian position indicating bilateral recurrent nerve palsies | Partial tracheal resection and tracheotomy/Inferior turbinectomy and the turbinate mucosa sutured in to fill the defect |
| Oyama (20) | 30/F | Asian | Hemoptysis | 4.0 | S | Posterior tracheal wall | Intra | NED/1.5y | Tracheal resection and tracheotomy/end to end |
| Burton (21) | 14/F | Black | NA | NA | M | Cervical tracheal | Intra | NED/4 mo | Tracheal resection/end to end |
| Burton (21) | 37/F | Black | A chronic cough and upper respiratory infection | 4.0 | S | Right lateral tracheal wall erosion | Extra | NED/1 y | Tracheal shaving and partial tracheal resection Thyroid lobectomy |
| Burton (21) | 19/F | NA | Intractable asthma | 1.5 | S | Cervical tracheal | Intra | NED/8 y | Endoscopic excision, |
| Burton (21) | 43/F | Black | Severe asthma and new-onset dysphagia | 4.0 | S | Anterior wall erosion | Intra and extra | NED/6 mo | Tracheal resection and tracheotomy/end to end |
| Spandow (22) | 12/M | White | Increasing difficulty in breathing | 2.0 | S | Left lateral tracheal wall erosion | Intra and extra | NED/18 mo | Partial tracheal resection and thyroid lobectomy and tracheotomy/end to end |

*(Continued)*

TABLE 1 Continued

| Source | Age/ Sex | Race | Complaint | Size (cm) | Solitary/ Multiple | Location | Intra/ Extraluminal | Results/ Follow-up | Surgical method/ Reconstruction method |
|---|---|---|---|---|---|---|---|---|---|
| Thomas (23) | 46/F | NA | Dyspnea | 4.5 | S | Upper part of tracheal | Intra | Residual disease/9y | Successive endoscopic excision, laser |
| Frenckner (24) | 28/F | White | NA | NA | S | Cervical | Intra | NED/3 y | Transtracheal enucleation |
| Desai (25) | 10/F | NA | Obstructive sleep apnea and exercise-induced asthma | NA | S | Posterior tracheal wall | Intra | NED/10 y | Tracheal fissure and excision and tracheotomy/ |
| Kintanar (26) | 35/F | NA | Painless right neck mass | 2.2 | S | Right lateral tracheal wall | Extra | NA | Tracheal shaving/Thyroid lobectomy |
| Daniel M (27) | 29/F | Black | Dyspnea | 3.0 | S | Right lateral tracheal wall erosion | Intra and extra | NA | None |
| Ipakchi (8) | 22/F | Black | Shortness of breath, expiratory stridor | 3.0 | S | Right lateral tracheal wall | Intra | NED/18 mo | Endoscopic resection |
| Colella (28) | 58/M | White | trachyphonia and occasionally dysphonia Painless right neck mass | 1.1 | S | Right lateral tracheal wall erosion | Extra | NED/30 mo | Thyroidectomy, partial tracheal resection |
| Lee (29) | 45/F | Asian | Cough,shortness of breath | 3.0 | S | Anterior tracheal wall | Intra | NED/13 mo | Endoscopic resection, thyroid lobectomy |
| Guarnieri (6) | 64/F | White | Dyspnoea | 1.3 | S | Left lateral tracheal wall | Intra | NA | Electro surgery and argon plasma coagulation |
| Fama (30) | 26/F | NA | Painless right neck mass | 1.9 | S | Right lateral tracheal wall | Extra | NED/12 mo | Tracheal shaving/Thyroid lobectomy |
| Currentstudy | 45/F | Asian | Activities difficulty in breathing | 2.0 | S | Posterior wall erosion | Intra and extra | NED/3 mo | Partial posterior wall resection Reconstruction tracheal by two lateral edges of the fascia tissue flap |

NA, not available; F, female; M, male; S, solitary; M, multiple; Intra, intraluminal; Extra, extraluminal; NED, no evidence of disease; DWD, died with the disease.

plasma coagulation, and two patients underwent transtracheal resection of the mass. Seven of the 18 patients who underwent surgical treatment also underwent thyroidectomy; two cases were found to be cervical tracheal granulosa cell tumors with thyroid carcinoma. A total of 27 patients were treated, of whom one (3.7%) died of postoperative bilateral recurrent laryngeal nerve palsy. The follow-up period ranged from six weeks to nine years, except for two cases without intervention and one death.

## Discussion

GCT was discovered and first described in 1926 after a long case study. It is now known to originate from neuronal tissue, histiocytes, or Schwann cells. GCT can occur anywhere in the body, usually involving the skin, breast, and especially the gastrointestinal tract (e.g., mouth, tongue, and esophagus); however, GCT in the respiratory tract, especially in the trachea and bronchi, is rare (32). The majority of GCTs reported in the literature are benign, with only 1–2% being malignant, specifically in cervical tracheal GCTs.

The peak age of onset of GCT is between 30 and 50 years, with a higher prevalence in women and patients of black ethnicity. The observation that most GCT cases occur in females may support a correlation between hormones and disease (33), although there is a lack of data to establish a clear correlation. However, 86.2% of the patient data we retrieved were from females, and the cervical segment tracheal GCTs were consistent with this profile.

History and physical examination provide important clues to diagnosing GCT of the cervical trachea. A tumor located outside the cavity may appear as a painless mass in the neck. Therefore, GCT of the trachea is often misdiagnosed as bronchial asthma (34), chronic bronchitis, and tumors of thyroid origin. The differential diagnosis should include subsonic masses, benign and malignant tumors of the trachea, and esophageal and thyroid tumors. Specifically, two cases of thyroid carcinoma with cervical tracheal granulosa cell tumor (28, 30) were identified; these could easily lead to misdiagnosis and increase the likelihood of adverse events during the treatment course. Hence, examination methods and the capability to differentiate and diagnose diseases are particularly important. If a tumor arises intraluminally, endoscopy is the mode for visualization of tumor location, size, and

intraluminal status and can be used to define the pathology by tissue biopsy. Tomographic CT scans of the trachea and larynx, both of which are the primary methods of examining tracheal GCT, can determine the location and extent of tumor infiltration. If a tumor occurs adjacent to the thyroid gland outside the lumen, pathological examination and CT of ultrasonic guided neoplasm needle biopsy are key to the differential diagnosis.

Pathological examination is the gold standard for confirming the diagnosis of GCT, which typically shows loosely arranged polygonal cells of medium or large size. The cytoplasm is rich in eosinophilic granules, with rare nuclei and nucleoli. Immunohistochemistry provides an important diagnostic aid for pathological examination, and the expression of S-100 protein and neuron-specific enolase (NSE) can be important evidence for diagnosis (35).

The treatment modality for cervical segmental tracheal GCT should be selected according to the site of the tumor and the degree of infiltration. An analysis of the treatment outcomes of the retrieved cases showed a 62.5% incidence of recurrence or tumor residuals in endoscopic laser-assisted resection of intraluminal tumors, with no deaths, and a 50% incidence of recurrence or tumor residuals in shave resection of extraluminal tumors. Among the cases in which both procedures were used, three had tumor residuals, and although the progression-free survival period was between eight and nine years, there are currently insufficient data to suggest that this inert biological behavior of GCT is common. In intraluminal or extraluminal tumors without trachelectomy, enhanced management of the tumor base may be one way to reduce the recurrence rate, but again, data to support this are insufficient. Cervical trachelectomy has the highest cure rate with a mortality rate of 4%, while the cause of death in the case presented here was bilateral recurrent laryngeal nerve palsy due to intraoperative manipulation. The literature shows that trachelectomy has a high cure rate and a lower mortality rate than previously reported and is a reasonable approach for both radicality and safety; however, this procedure often requires tracheotomy, which is a factor affecting the patient's postoperative quality of life. Radical surgery usually needs to include thyroid lobectomy, depending on the extension and involvement of the tumor in the paratracheal region. To date, available data about laser resection are similarly sparse. Owing to limited data, a reasonable approach could be based on endoscopic therapy as the preferred treatment, and trachelectomy should be reserved for larger lesions that prevent disease recurrence or threaten airway patency (36). Because of the rarity of the disease, data on recurrence rates are lacking, and follow-up plans cannot be defined.

A literature survey yielded six cases with tumors in the cervical segment of the trachea. Four cases (66.6%) underwent tracheal sleeve resection with end-to-end anastomosis, and one underwent partial tracheal resection with the application of inferior turbinate mucosa to repair the tracheal membrane. Tracheotomy was performed in all six patients, and a tracheal tube was left in place. In the case presented in this study, we attempted to remove the membranous tumor while preserving the intact tracheal cartilage ring to avoid tracheotomy when it was clear that the mass did not invade the tracheal wall or the anterior esophageal wall. During the operation, we used the intertracheoesophageal approach to expose the tumor by freeing the lateral side of the thyroid gland; the procedure could retain the complete blood supply to the thyroid gland without affecting the function of the parathyroid gland and keep the recurrent laryngeal nerve above the tumor during the resection. Studies have shown that fascial tissues are hypometabolic, easily survivable, and resistant to saliva and infection, providing an excellent seal and structural stability for respiratory epithelialization (31). Furthermore, several reports on the successful repair of the residual larynx with banded myofascial flaps during laryngeal cancer surgery support the high survival rate of banded myofascial flaps (29). Therefore, we attempted to reconstruct the tracheal membrane after tumor resection by applying an adjacent double-tipped banded myofascial tissue flap. To prevent postoperative asphyxia, we created a 1-cm-long tracheal skin fistula without a tracheal tube, and the tracheal skin fistula of the patient was always sealed and facilitated oral and nasal breathing after surgery. We believe that the advantages of the banded myofascial flap for tracheal membrane repair include no additional incision, proximity to the recipient site, good blood supply in the form of an upper and lower double-tip, no twisting of the double-tip during suturing, moderate fascial tension, and avoidance of tracheotomy, making it an ideal graft for reconstruction of cervical tracheal membrane defects. However, the limitations of using banded myofascial flaps to repair tracheal defects, including the maximum distance between the double-tipped banded myofascial flap and the membranous defect, and the survival rate of single-tipped fascial flaps, remain unknown and need to be verified and promoted by more data in the future.

## Conclusions

GCT of the cervical segment trachea is a rare disease with a lack of specific information on its clinical presentation and imaging, and histopathological examination is the gold standard for diagnosis. Furthermore, while electronic bronchography is an important diagnostic method, it has limitations in terms of treatment. GCT trachelectomy is the best treatment for large infiltrating cervical tracheal tumors. Finally, in GCT of the cervical trachea, preservation of the tracheal cartilaginous ring and membrane reconstruction with a double-tipped banded myofascial flap is a feasible approach.

## Data availability statement

The original contributions presented in the study are included in the article/supplementary material. Further inquiries can be directed to the corresponding author.

## Ethics statement

Written informed consent was obtained from the individual(s) for the publication of any potentially identifiable images or data included in this article.

## Author contributions

All authors contributed to the drawing up and correction of the paper. All authors contributed to the article and approved the submitted version.

## Acknowledgments

The authors wish to thank Xinhui Li for her contributions to the project.

## Conflict of interest

The authors declare that the research was conducted in the absence of any commercial or financial relationships that could be construed as a potential conflict of interest.

## Publisher's note

All claims expressed in this article are solely those of the authors and do not necessarily represent those of their affiliated organizations, or those of the publisher, the editors and the reviewers. Any product that may be evaluated in this article, or claim that may be made by its manufacturer, is not guaranteed or endorsed by the publisher.

## References

1. Abrikossoff A. Uber myome, ausgehend von der quergestreiften willkürlichen muskulatur. *Virchows Arch Pathol Anat Physiol Klin Med* (1926) 260:215–33. doi: 10.1007/BF02078314

2. Hu F. *Clinical dermatology*. Demis DJ, McGuire J, editors. London: Harper and Row Publishers (1982) p. 1–5.

3. Frable MA, Fischer RA. Granular cell myoblastomas. *Laryngoscope* (1976) 86:36–42. doi: 10.1288/00005537-197601000-00007

4. Fliss DM, Puterman M, Zirkin H, Leiberman A. Granular cell lesions in head and neck: A clinicopathological study. *J Surg Oncol* (1989) 42:154–60. doi: 10.1002/jso.2930420305

5. Meyer MA, Becker JM, Quinones W. Endobronchial granular cell tumor: A case report. *J Radiol Case Rep* (2010) 4:29–35. doi: 10.3941/jrcr.v4i8.474

6. Guarnieri T, Cardinale L, Macchia G, Cortese G, Veltri A. Multiphasic multidetector computed tomography study of a rare tracheal 11 tumor: Granular cell tumor. *Case Rep Pulmonol* (2014) 2014:807430. doi: 10.1155/2014/807430

7. Fanburg-Smith JC, Meis-Kindblom JM, Fante R, Kindblom LG. Malignant granular cell tumor of soft tissue: Diagnostic criteria and clinicopathologic correlation. *Am J Surg Pathol* (1998) 22:779–94. doi: 10.1097/00000478-199807000-00001

8. Ipakchi R, Zager WH, de Baca ME, Bloedon E, McCue PA, Zwillenberg D. Granular cell tumor of the trachea in pregnancy: A case report and review of literature. *Laryngoscope* (2004) 114:143–7. doi: 10.1097/00005537-200401000-00026

9. Benisch BM, Abt AB, Abramson A. Granular cell myoblastoma of the trachea associated with pregnancy. *Chest* (1973) 63:832–3. doi: 10.1378/chest.63.5.832

10. Krouse TB, Mobini J. Multifocal granular cell myoblastoma. report of a case involving trachea, stomach, and anterior abdominal wall. *Arch Pathol* (1973) 96:95–9.

11. Thawley SE, Ogura JH. Granular cell myoblastoma of the head and neck. *South Med J* (1974) 67:1020–4. doi: 10.1097/00007611-197409000-00005

12. Carnalis RF, Dodson TA, Turkell SB, Maenza RM. Granular cell myoblastoma of the cervical trachea. *Arch Otolaryngol* (1976) 102:176–9. doi: 10.1001/archotol.1976.00780080098014

13. Polack EP. Pretracheal cervical granular cell myoblastoma. *Ann Plast Surg* (1979) 2:75–7. doi: 10.1097/00000637-197901000-00013

14. Dunaway CL, Brogdon BG, Robinson AE. Granular cell myoblastoma of the trachea. *Pediatr Radiol* (1981) 11:210–1. doi: 10.1007/BF00972053

15. McLain WC, Olsen GN, Wooldridge D, Almond CH, Boykin AB. Endotracheal granular cell myoblastoma: A failure of laser therapy. *Chest* (1984) 86:136–7. doi: 10.1378/chest.86.1.136

16. Mikaelian DO, Israel H, Cohn H, Jabourian Z. Granular cell tumor of the trachea. *Ann Otol Rhinol Laryngol* (1984) 93:457–9. doi: 10.1177/000348948409300507

17. Thaller S, Fried MP, Goodman ML. Symptomatic solitary granular cell tumor of the trachea. *Chest* (1985) 88:925–8. doi: 10.1378/chest.88.6.925

18. Alessi DM, Zimmerman MC. Granular cell tumors of the head and neck. *Laryngoscope* (1988) 98:810–4. doi: 10.1288/00005537-198808000-00003

19. Solomons NB. Extensive granular cell tumor of the larynx and trachea. *J Laryngol Otol* (1988) 102:658–60. doi: 10.1017/S0022215100106048

20. Oyama T, Nakanishi R, Yoshimatsu T, Osaki T, Yasumoto K. Granular cell tumors of the trachea: Case report and review of the literature. *J Bronchol Int Pulmonol* (1997) 4:145–7.

21. Burton DM, Heffner DK, Patow CA. Granular cell tumors of the trachea. *Laryngoscope* (1992) 102:807–13. doi: 10.1288/00005537-199207000-00010

22. Spandow O, Lindholm CE. Granular cell tumor in a child's trachea–a diagnostic and therapeutic challenge. *Int J Pediatr Otorhinolaryngol* (1994) 30:159–60. doi: 10.1016/0165-5876(94)90199-6

23. de Montpréville VT, Dulmet EM. Granular cell tumors of the lower respiratory tract. *Histopathology* (1995) 27:257–62. doi: 10.1111/j.1365-2559.1995.tb00218.x

24. Freckner P. The occurrence of so-called myoblastomas in the mouth and upper air passages: Report of five cases. *Acta Otolaryngol (Stockh)* (1938) 26:689–702. doi: 10.3109/00016483809118495

25. Desai DP, Maddalozzo J, Holinger LD. Granular cell tumor of the trachea. *Otolaryngol Head Neck Surg* (1999) 120:595–8. doi: 10.1053/hn.1999.v120.a84488

26. Kintanar EB, Giordano TJ, Thompson NW, Michael CW. Granular-cell tumor of trachea masquerading as hurtlecell neoplasm on fine needle aspirate: A case report. *Diagn Cytopathol* (1999) 22:379–82. doi: 10.1002/(SICI)1097-0339(200006)22:6<379::AID-DC10>3.0.CO;2-3

27. Suffin DM, Noori F, Kabak B, Ayoub RT, Pi J, Riar S, et al. Granular cell tumor of the trachea: A case report and review of the literature. *Clin Pulmonary Med* (2010) 17:53–5. doi: 10.1097/CPM.0b013e3181c794ba

28. Colella R, Sidoni A, Bellezza G, Cavaliere A. A unique simultaneous occurrence of paratracheal granular cell tumor and papillary thyroid carcinoma. *Int J Surg Pathol* (2007) 15:82–5. doi: 10.1177/1066896906295820

29. Lee DH, Yoon TM, Lee JK, Lim SC. Unusual granular cell tumor of the trachea coexisting with papillary thyroid carcinoma and masquerading as tracheal invasion of recurred thyroid carcinoma: A case report. *Med (Baltim)* (2016) 95:e3547. doi: 10.1097/MD.0000000000003547

30. Famà F, Pino A, Cavallari V, Fadda G, Ieni A, Dionigi G. Granular cell tumor of the trachea mimicking an infiltrating thyroid cancer. a case report. *Int J Surg Case Rep* (2022) 94:107031. doi: 10.1016/j.ijscr.2022.107031

31. Tunkeld DE, Bauerca CA, Sung GH, Rosenfeld RM, Chandrasekhar SS, Cunningham ER, et al. Clinical practice guideline: Tinnitus. *Otolaryngol Head Neck Surg* (2014) 151:S1–40. doi: 10.1177/0194599814545325

32. Lee SI, Park SW, Park JS, Lee WA. Jee KN. *A Case malignant granular Cell tumor Korean J Med* (2004) 67:S937–41.

33. Mahoney CP, Patterson SD, Ryan J. Granular cell tumor of the thyroid gland in a girl receiving high-dose estrogen therapy. *Pediatr Pathol Lab Med* (1995) 15:791–5. doi: 10.3109/15513819509027014

34. Muthuswamy PP, Alrenga DP, Marks P, Barker WL. Granular cell myoblastoma: Rare localization in the trachea. report of a case and review of the literature. *Am J Med* (1986) 80:714–8. doi: 10.1016/0002-9343(86)90831-4

35. Joung MK, Lee YJ, Chung CU, Lee JE, Jung SS, Kim SY, et al. A case of granular cell tumor of the trachea. *Korean J Int Med* (2007) 22:101–5. doi: 10.3904/kjim.2007.22.2.101

36. Rizzo A, Serban ED, Ricci AD, Nannini M, Saponara M, Cancellieri A, et al. Granular cell tumor of the trachea as a rare cause of dyspnea in a young woman. *Respir Med Case Rep* (2019) 28:100961. doi: 10.1016/j.rmcr.2019.100961

frontiers | Frontiers in Oncology

TYPE Case Report
PUBLISHED 16 February 2023
DOI 10.3389/fonc.2023.1101552



OPEN ACCESS

EDITED BY
Zhaolun Cai,
Sichuan University, China

REVIEWED BY
Hsin-Hua Lee,
Kaohsiung Medical University, Taiwan
Archya Dasgupta,
Tata Memorial Hospital, India
Chao Li,
Guangxi Medical University, China

*CORRESPONDENCE
Shota Tanaka
stanaka@m.u-tokyo.ac.jp

SPECIALTY SECTION
This article was submitted to Surgical Oncology, a section of the journal Frontiers in Oncology

RECEIVED 18 November 2022
ACCEPTED 31 January 2023
PUBLISHED 16 February 2023

CITATION
Matsuhashi A, Tanaka S, Takami H, Nomura M, Ikemura M, Matsubayashi Y, Shinoda Y, Yamada K, Sakai Y, Karasawa Y, Takayanagi S and Saito N (2023) Recurrent glioblastoma metastatic to the lumbar vertebra: A case report and literature review: Surgical oncology.
*Front. Oncol.* 13:1101552.
doi: 10.3389/fonc.2023.1101552



# Recurrent glioblastoma metastatic to the lumbar vertebra: A case report and literature review: Surgical oncology

Ako Matsuhashi[1], Shota Tanaka[1]*, Hirokazu Takami[1], Masashi Nomura[1], Masako Ikemura[2], Yoshitaka Matsubayashi[3], Yusuke Shinoda[4], Keisuke Yamada[1], Yu Sakai[1], Yasuaki Karasawa[1], Shunsaku Takayanagi[1] and Nobuhito Saito[1]

[1]Department of Neurosurgery, The University of Tokyo Hospital, Tokyo, Japan, [2]Department of Pathology, The University of Tokyo Hospital, Tokyo, Japan, [3]Department of Orthopedic Surgery, The University of Tokyo Hospital, Tokyo, Japan, [4]Department of Rehabilitation Medicine, Saitama Medical University Hospital, Saitama, Japan

**Background:** Glioblastoma is a malignant tumor, and its prognosis is as poor as 1.5 to 2 years. Most cases recur within one year even under the standard treatment. The majority of recurrences are local, and in rare cases, metastasize mostly within the centra nervous system. Extradural metastasis of glioma is exceedingly rare. Here, we present a case of vertebral metastasis of glioblastoma.

**Case presentation:** We present a 21-year-old man post total resection of the right parietal glioblastoma, diagnosed with lumbar metastasis. He originally presented with impaired consciousness and left hemiplegia and underwent gross total resection of the tumor. Given the diagnosis of glioblastoma, he was treated with radiotherapy combined with concurrent and adjuvant temozolomide. Six months after tumor resection, the patient presented with severe back pain, and was diagnosed as metastatic glioblastoma on the first lumbar vertebrae. Posterior decompression with fixation and postoperative radiotherapy were conducted. He went on to receive temozolomide and bevacizumab. However, at 3 months after the diagnosis of lumbar metastasis, further disease progression was noted, and his care was transitioned to best supportive care. Comparison on copy number status between primary and metastatic lesions on methylation array analysis revealed more enhanced chromosomal instability including 7p loss, 7q gain and 8 gain in the metastatic lesion.

10.3389/fonc.2023.1101552

**Conclusion:** Based upon the literature review and our case, younger age of initial presentation, multiple surgical interventions, and long overall survival seem to be the risk factors of vertebral metastasis. As the prognosis of glioblastoma improves over time, its vertebral metastasis is seemingly more common. Therefore, extradural metastasis should be kept in mind in the treatment of glioblastoma. Further, detailed genomic analysis on multiple paired specimens is mandated to elucidate the molecular mechanisms of vertebral metastasis.

KEYWORDS

**glioblastoma, vertebral metastasis, craniotomy, methylation array analysis, copy number alteration, chromosomal instability**

# 1 Introduction

Glioblastoma is a malignant tumor, classified as grade 4 in World Health Organization (WHO) classification of central nervous system (CNS) tumors 2021, and its prognosis is as poor as 1.5 to 2 years (1, 2). Most cases recur within one year even under the standard treatment of surgical resection, radiation therapy and chemotherapy. The vast majority of recurrences are local, and in rare cases, metastatic mostly within the CNS. Extradural metastasis is considered exceedingly rare due to the presence of blood brain barrier (3). Here, we report a case of vertebral metastasis of glioblastoma.

This study was reported in agreement with principles of the CARE guidelines (4). Written informed consent was obtained from the individual and the patient's legal guardian for the publication of any potentially identifiable images or data included in this article.

# 2 Case description

## 2.1 Clinical course

A 21-year-old man post total resection of the right parietal glioblastoma was diagnosed with lumber metastasis. At the age of 20, without any significant family history or past medical history, he presented to a local emergency department with impaired consciousness and left hemiplegia. Computed tomography (CT) showed intracranial hemorrhage in the right parietal lobe, and hematoma evacuation was conducted. Dilated veins were observed around the hematoma and the patient was diagnosed with intracranial hemorrhage from venous hemangioma. Five months after the operation, he began to complain of headache, and magnetic resonance imaging (MRI) showed an enhanced lesion in the right hemisphere which was rapidly increasing in size. Partial removal of the mass and external decompression was conducted. Then he was referred to our institute for resection of the remaining mass and adjuvant therapy. Gross total resection of the tumor, placement of carmustine wafer in the resection cavity and cranioplasty were conducted at our institute (Figure 1). Pathology was consistent with glioblastoma, isocitrate dehydrogenase (IDH)-wildtype. The patient was ambulatory post-operatively. Radiotherapy combined with concurrent and adjuvant temozolomide (75mg/m$^2$/day) per the Stupp regimen was conducted. Intensity Modulated Radiation Therapy (IMRT) of 60Gy was conducted at the edematous area surrounding the tumor, and IMRT of 50Gy at the tumor removal site. Four cycles of temozolomide (150mg/m$^2$/day) were administered during the maintenance phase. At the same time, bevacizumab (10mg/kg) was administered twice, two weeks apart.

At 6 months after the resection of tumor at our institute (14 months after the first operation), the patient presented with severe back pain. CT showed an osteolytic mass on the body of the first lumbar vertebrae and MRI showed an enhanced lesion constricting the spinal canal (Figure 2). There was no spinal metastasis. The patient did not present symptoms of spinal cord compression such as bladder and rectal disturbance or lower extremities paralysis. Brain MRI showed no intracranial recurrence, and whole spine MRI and whole-body CT showed no other lesions. Needle biopsy of the mass on the first lumbar vertebrae showed densely infiltrating spindle-

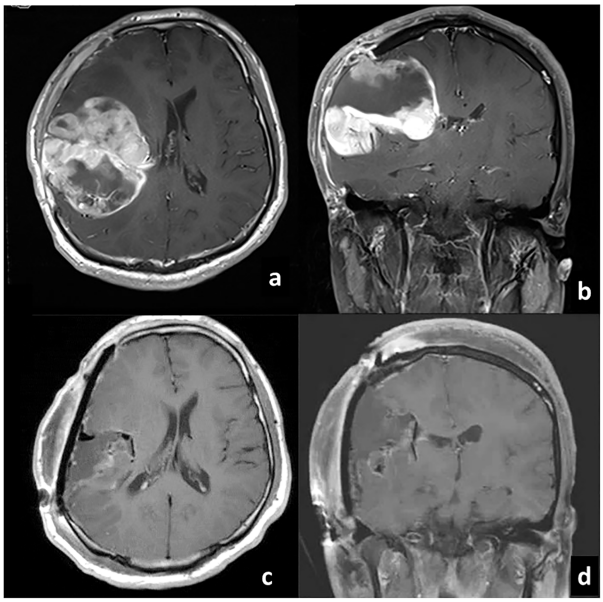


FIGURE 1
Gadolinium-enhanced T1-weighted MRI before **(A)** axial, **(B)** coronal and after **(C)** axial, **(D)** coronal) gross total resection of glioblastoma at our institute.

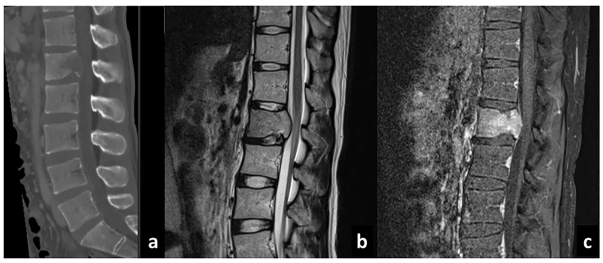


FIGURE 2
Sagittal CT **(A)**, T2-weighted **(B)**, and gadolinium-enhanced T1-weighted **(C)** MRI sequences of the spine showing development of metastatic lesion.

shaped cells with eosinophilic cytoplasm accompanied with regions of necrosis, which was consistent with glioblastoma (Figure 3). The cells were positive for glial fibrillary acidic protein (GFAP), and its MIB-1 index was 30%. Posterior decompression with fixation and postoperative radiotherapy of 30Gy were conducted to relieve the pain. He further received one more cycle of temozolomide (150mg/$m^2$/day) and two more administrations of bevacizumab (10mg/kg, two weeks apart). Three months after the diagnosis of lumbar metastasis, however, disease progression with multiple metastasis to the lymph nodes, the lungs, and the liver was found, prompting the transition to best supportive care.

## 2.2 Epigenetic analysis

This study was approved by the Ethics Committee of the University of Tokyo (#G10028). DNA was extracted from FFPE tissue samples and analyzed using the Illumina Infinium Human Methylation EPIC Bead Chip array according to the manufacturer's instructions. All DNA methylation analyses were performed using R version 4.1.0. Methylation values were calculated as β values. The following filtering criteria were applied: removal of probes overlapping with single-nucleotide polymorphisms, those mapped to chromosomes X and Y, or the Illumina control probes. Copy number alterations were calculated using signal data from the methylation array using the conumee Bioconductor package version 1.26.0.

Primary and metastatic samples had overall copy number status in common such as chromosome 1p loss, 16 loss and 22q loss; however, the metastatic sample had more prominent copy number alterations, including newly acquired 4 gain, 7p loss, 7q gain, 8 gain, 13q gain, 19q gain, and 20 loss (Figure 4).

# 3 Discussion

In this case illustration, we present an extremely rare case of glioblastoma which metastasized extracranially to the lumbar vertebra during the course of treatment. Glioblastoma was not believed to metastasize outside of the CNS until Davis first reported glioma meningeal metastasis in 1928 (5, 6). Extradural metastasis of glioblastoma is as rare as less than 2% (3). Dense dura around intracranial sinuses preventing tumor cell penetration and lack of a nurturing stroma in other organs to facilitate the survival of glioblastoma cells are some biological obstacles that prevent glioblastoma cells to infiltrate outside the CNS (7). Also, overall low median survival causes patients to die from intracranial hypertension or other complications before extracranial metastasis develop (6).

Vertebral metastasis is exceedingly rare; to the best of our knowledge, there has been 59 cases reported in the literature (Supplementary Tables 1, 2) (6, 8–58). Mean age of the 59 patients is 43.9 years (range, 11-70 years), which is much younger than the

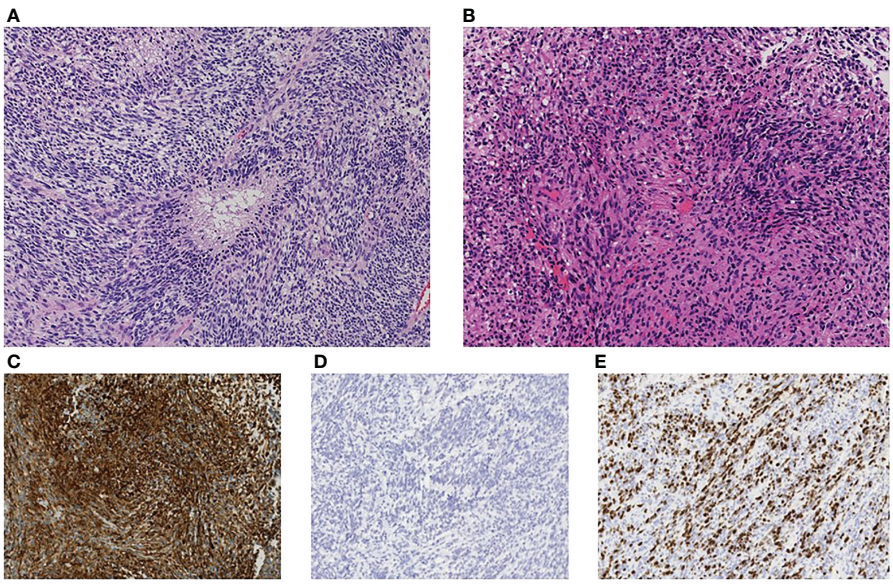


FIGURE 3
Immunohistopathological investigation showed densely infiltrating spindle-shaped cells with eosinophilic cytoplasm accompanied with regions of necrosis, consistent with glioblastoma **(A)** primary site, **(B)** lumbar metastasis). The cells were positive for glial fibrillary acidic protein (GFAP) **(C)** and negative for mutant isocitrate dehydrogenase 1 (IDH1-R132H) **(D)**. MIB-1 labeling index was 30% **(E)**. The original magnification was x200 **(A–E)**.

10.3389/fonc.2023.1101552

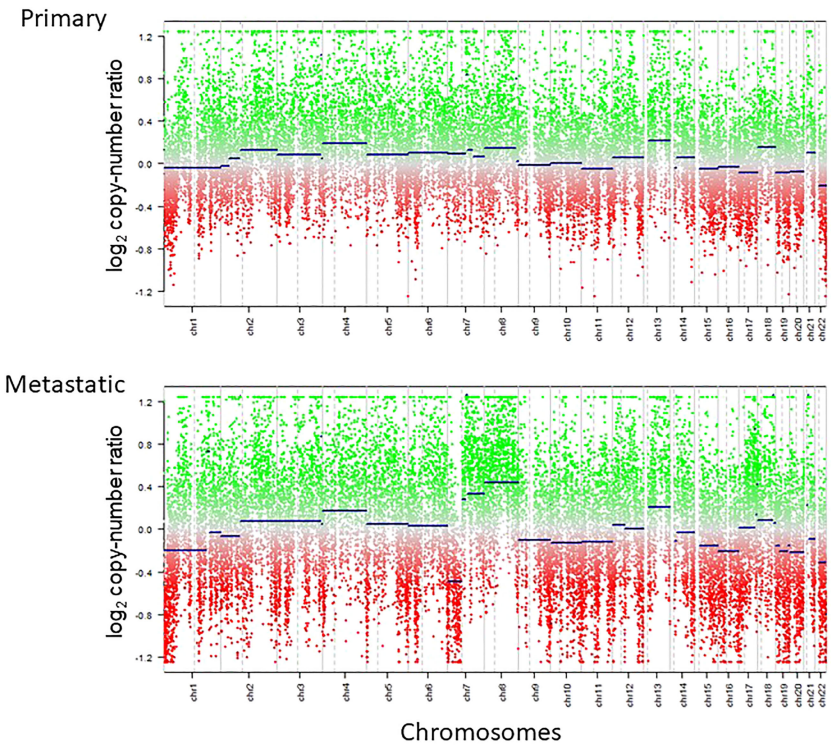


FIGURE 4
Copy number profiles of primary and metastatic lesions calculated by methylation array are shown. Copy number baseline imbalance was enhanced for the metastatic lesion compared with the primary lesion.

average age of patients diagnosed with glioblastoma. Moreover, in most cases, glioblastoma metastasis to the vertebral body is accompanied by metastasis to other locations such as the lung, lymph nodes, other bones and the liver. As for the cases with sufficient data, the mean overall survival of the cases is 28.0 months (range, 1-139 months) after the initial diagnosis of glioblastoma, and 8.5 months (range, 0-48 months) after the diagnosis of vertebral metastasis. Overall survival in these cases is longer than the average prognosis of glioblastoma. This suggests that long-surviving glioblastoma patients provide glioblastoma cells adequate time to cause extradural metastasis.

Considering the biological obstacles that prevent glioblastomas from infiltrating outside of the CNS, it can be speculated that deposition of tumor cells into the blood stream or excision of the dura due to surgical interventions may attribute to extracranial metastasis. As for the 59 reported cases, the mean number of surgeries conducted prior to vertebral metastasis was 1.5 (range, 0-5). In our case, the patient first presented with intracranial hemorrhage and the tumor was hypervascular enough to be misdiagnosed for venous hemangioma, allowing tumor cells to be feasibly deposited into the blood stream. Also, multiple surgeries including external decompression were conducted causing defects of the dura and the skull, which could have facilitated the extradural infiltration of glioblastoma cells. Based upon the literature and our case, younger age of initial presentation of glioblastoma and multiple surgical interventions seem to be the risk factors of vertebral metastasis of glioblastoma, though we still lack further statistical evaluation.

Little has been known about the genetic and epigenetic changes seen in the extracranial metastasis of glioblastoma. Copy number alterations have been known to be enhanced at the metastatic site compared with the primary site, in parallel with mutational burden, in systemic cancers such as lung, hepatocellular and urothelial malignancies among others (59–61). This is deemed to primarily reflect the clonal evolution and selection of the tumor cells at the primary site with the gain of metastatic potential (62, 63). Previously, a case of GBM with osseous metastasis was shown to harbor additional copy number alterations plus mutations compared with the intracranial tumor (64). In concordance, our case demonstrated the increased fluctuation of the copy number baseline (Figure 4), highly suggestive of the existence of tumor cells with the acquisition of metastatic capability. This is still an under-investigated finding in cases with metastatic glioblastoma and needs to be investigated in a larger cohort of samples.

Due to the improvement in the prognosis of the disease, vertebral metastasis is suspected to be encountered more commonly. Therefore, extradural metastasis of glioblastoma must be included in differential diagnoses in treating patients with glioblastoma. Further studies with detailed genomic analysis on multiple paired tumor specimens are warranted to unravel the molecular mechanisms of vertebral metastasis.

## Data availability statement

The data analyzed in this study is subject to the following licenses/restrictions: This is a case report. All the information is stored in the

medical chart. Requests to access these datasets should be directed to STan, stanaka@m.u-tokyo.ac.jp.

## Ethics statement

The studies involving human participants were reviewed and approved by The University of Tokyo. The patients/participants provided their written informed consent to participate in this study. Written informed consent was obtained from the individual and the patient's legal guardian for the publication of any potentially identifiable images or data included in this article.

## Author contributions

AM and STan contributed to conception and design of the study. AM organized the database. AM and HT performed the statistical analysis. AM and STan wrote the first draft of the manuscript. HT wrote sections of the manuscript. All authors contributed to manuscript revision, read, and approved the submitted version.

## Conflict of interest

The authors declare that the research was conducted in the absence of any commercial or financial relationships that could be construed as a potential conflict of interest.

## Publisher's note

All claims expressed in this article are solely those of the authors and do not necessarily represent those of their affiliated organizations, or those of the publisher, the editors and the reviewers. Any product that may be evaluated in this article, or claim that may be made by its manufacturer, is not guaranteed or endorsed by the publisher.

## Supplementary material

The Supplementary Material for this article can be found online at: https://www.frontiersin.org/articles/10.3389/fonc.2023.1101552/full#supplementary-material

## References


1. Stupp R, Hegi ME, Mason WP, van den Bent MJ, Taphoorn MJ, Janzer RC, et al. Effects of radiotherapy with concomitant and adjuvant temozolomide versus radiotherapy alone on survival in glioblastoma in a randomised phase III study: 5-year analysis of the EORTC-NCIC trial. *Lancet Oncol* (2009) 10:459–66. doi: 10.1016/S1470-2045(09)70025-7

2. Stupp R, Mason WP, van den Bent MJ, Weller M, Fisher B, Taphoorn MJ, et al. Radiotherapy plus concomitant and adjuvant temozolomide for glioblastoma. *N Engl J Med* (2005) 352:987–96. doi: 10.1056/NEJMoa043330

3. Ruff MW, Bhargav AG, Raghunathan A. A case of epidural glioblastoma metastasis presenting with a cervical myelopathy, torticollis, and l'hermitte's phenomenon. *Brain Tumor Pathol* (2018) 35:181–5. doi: 10.1007/s10014-018-0319-y

4. Riley DS, Barber MS, Kienle GS, Aronson JK, von Schoen-Angerer T, Tugwell P, et al. CARE guidelines for case reports: explanation and elaboration document. *J Clin Epidemiol* (2017) 89:218–35. doi: 10.1016/j.jclinepi.2017.04.026

5. Davis L. Spongioblastoma multiforme of the brain. *Ann Surg* (1928) 87:8–14.

6. Wu W, Zhong D, Zhao Z, Wang W, Li J, Zhang W. Postoperative extracranial metastasis from glioblastoma: a case report and review of the literature. *World J Surg Oncol* (2017) 15:231. doi: 10.1186/s12957-017-1300-7

7. Lun M, Lok E, Gautam S, Wu E, Wong ET. The natural history of extracranial metastasis from glioblastoma multiforme. *J Neurooncol* (2011) 105:261–73. doi: 10.1007/s11060-011-0575-8

8. Winkelman NWJr., Cassel C, Schlesinger B. Intracranial tumors with extracranial metastases. *J Neuropathol Exp Neurol* (1942) 11:149–68. doi: 10.1097/00005072-195204000-00004

9. Wisiol ES, Handler S, French LA. Extracranial metastases of a glioblastoma multiforme. *J Neurosurg* (1962) 19:186–94. doi: 10.3171/jns.1962.19.3.0186

10. Nigogosyan G, de la Pava S, Pickren JW. Brain tumor with extracranial metastases. report of two cases. *Arch Neurol* (1962) 6:300–6. doi: 10.1001/archneur.1962.00450220042007

11. Smith DR, Hardman JM, Earle KM. Contiguous glioblastoma multiforme and fibrosarcoma with extracranial metastasis. *Cancer* (1969) 24:270–6. doi: 10.1002/1097-0142(196908)24:2<270::AID-CNCR2820240210>3.0.CO;2-5

12. Smith DR, Hardman JM, Earle KM. Metastasizing neuroectodermal tumors of the central nervous system. *J Neurosurg* (1969) 31:50–8. doi: 10.3171/jns.1969.31.1.0050

13. Anzil AP. Glioblastoma multiforme with extracranial metastases in the absence of previous craniotomy. *Case Rep J Neurosurg* (1970) 33:88–94. doi: 10.3171/jns.1970.33.1.0088

14. Takeda F, Handa IK, Aiba T, Kawabuchi J, Fukai K. Autopsy case of malignant glioma with extreneural metastases. *Shinkei Kenkyu No Shimpo* (1971) 15:720–30.

15. Cooper PR, Budzilovich GN, Berczeller PH, Lieberman A, Battista A. Metastatic glioma associated with hypercalcemia. report of two cases. *J Neurosurg* (1974) 40:255–9. doi: 10.3171/jns.1974.40.2.0255

16. Hulbanni S, Goodman PA. Glioblastoma multiforme with extraneural metastases in the absence of previous surgery. *Cancer* (1976) 37:1577–83. doi: 10.1002/1097-0142(197603)37:3<1577::AID-CNCR2820370348>3.0.CO;2-0

17. Schatzki SC, McIlmoyle G, Lowis S. Diffuse osteoblastic metastases from an intracranial glioma. *AJR Am J Roentgenol* (1977) 128:321–3. doi: 10.2214/ajr.128.2.321

18. Slowik F, Balogh I. Extracranial spreading of glioblastoma multiforme. *Zentralblatt fur Neurochirurgie* (1980) 41:57–68.

19. Dietz R, Burger L, Merkel K, Schimrigk K. Malignant gliomas - glioblastoma multiforme and astrocytoma III-IV with extracranial metastases report of two cases. *Acta Neurochir* (1981) 57(1–2):99–105. doi: 10.1007/BF01665120

20. Sadik AR, Port R, Garfinkel B, Bravo J. Extracranial metastasis of cerebral glioblastoma multiforme: case report. *Neurosurgery* (1984) 15:549–51. doi: 10.1227/00006123-198410000-00014

21. Friedman JH, Liu HM, Spremulli E, Calabresi P. Distant metastases from a malignant glioma: unusual complications associated with treatment of a glioblastoma: distant metastases and focal white matter degeneration. *J Neurol Neurosurg Psychiatry* (1987) 50(2):237–8. doi: 10.1136/jnnp.50.2.237

22. Haddon M, Slavin JD, Spencer RP. Multiple bone metastases in a patient with glioblastoma multiforme. *Clin Nucl Med* (1989) 14(1):13–4. doi: 10.1097/00003072-198901000-00004

23. Lampl Y, Eshel Y, Gilad R, Sarova-Pinchas I. Glioblastoma multiforme with bone metastase and cauda equina syndrome. *J Neurooncol* (1990) 8(2):167–72. doi: 10.1007/BF00177841

24. Myers T, Egelhoff J, Myers M. Glioblastoma multiforme presenting as osteoblastic metastatic disease: case report and review of the literature. *AJNR Am J Neuroradiol* (1990) 11:802–3.

25. Chesnut RM, Abitbol JJ, Chamberlain M, Marshall LF. Vertebral collapse with quadraparesis due to metastatic gliobla multiforme: case report and review of the literature. *J Neurooncol* (1993) 16:135–40. doi: 10.1007/BF01324700

26. Mihara F, Ikeda M, Rothman MI, Numaguchi Y, Kristt D. Vertebral body metastasis of glioblastoma multiforme with epidural mass formation. contrast-enhanced MRI study. *Clin Imaging* (1994) 18:386–9. doi: 10.1016/0899-7071(94)90011-6

27. Kleinschmidt-Demasters BK. Diffuse bone marrow metastases from glioblastoma multiforme: the role of dural invasion. *Hum Pathol* (1996) 27(2):197–201. doi: 10.1016/S0046-8177(96)90376-7

28. Moriyama T, Kataoka H, Seguchi K, Nabeshima K, Kawano H, Goya T, et al. Establishment and characterization of a new human glioblastoma cell line (MGM-1) with highly motile phenotype. *Hum Cell* (1997) 10(1):105–10.

29. Solau-Gervais E, Flipo RM, Cotten A, Lecomte-Houcke M, Delcambre B. Metastasis from a glioblastoma and staphylococcus aureus spondylitis in the same vertebral body. *Rev Rhum Engl Ed* (1998) 65(1):75–6.

30. Frappaz D, Mornex F, Saint-Pierre G, Ranchere-Vince D, Jouvet A, Chassagne-Clement C, et al. Bone metastasis of glioblastoma multiforme confirmed by fine needle biopsy. *Acta Neurochir (Wien)* (1999) 141(5):551–2. doi: 10.1007/s007010050342

31. Beauchesne P, Soler C, Mosnier JF. Diffuse vertebral body metastasis from a glioblastoma multiforme: a technetium-99m sestamibi single-photon emission computerized tomography study. *J Neurosurg* (2000) 93:887–90. doi: 10.3171/jns.2000.93.5.0887

32. Park CC, Hartmann C, Folkerth R, Loeffler JS, Wen PY, Fine HA, et al. Systemic metastasis in glioblastoma may represent the emergence of neoplastic subclones. *J Neuropathol Exp Neurol* (2000) 59(12):1044–50. doi: 10.1093/jnen/59.12.1044

33. Cervio A, Piedimonte F, Salaberry J, Alcorta SC, Salvat J, Diez B, et al. Bone metastases from secondary glioblastoma multiforme: a case report. *J Neurooncol* (2001) 52 (2):141–8. doi: 10.1023/A:1010629618859

34. Fabi A, Vidiri A, Carapella C, Pace A, Occhipinti E, Caroli F, et al. Bone metastasis from glioblastoma multiforme without central nervous system relapse: a case report. *Anticancer Res* (2004) 24:2563–5.

35. Rajagopalan V, El Kamar FG, Thayaparan R, Grossbard ML. Bone marrow metastases from glioblastoma multiforme–a case report and review of the literature. *J Neurooncol* (2005) 72(2):157–61. doi: 10.1007/s11060-004-3346-y

36. Utsuki S, Tanaka S, Oka H, Iwamoto K, Sagiuchi T, Fujii K. Glioblastoma multiforme metastasis to the axis. *Case Rep J Neurosurg* (2005) 102:540–2. doi: 10.3171/jns.2005.102.3.0540

37. Astner ST, Pihusch R, Nieder C, Rachinger W, Lohner H, Tonn JC, et al. Extensive local and systemic therapy in extraneural metastasized glioblastoma multiforme. *Anticancer Res* (2006) 26(6c):4917–20.

38. Robert M, Wastie M. Glioblastoma multiforme: a rare manifestation of extensive liver and bone metastases. *BioMed Imaging Interv J* (2008) 4(1):e3–3. doi: 10.2349/biij.4.1.e3

39. Pham CT, Clarençon F, Ganem G, Cormier E, Guermazi Y, Rose M, et al. Spinal cervical metastasis from a glioblastoma multiform treated by percutaneous vertebroplasty: a case report. *J Neuroradiol* (2011) 38(5):323–5. doi: 10.1016/j.neurad.2010.08.006

40. Kalokhe G, Grimm SA, Chandler JP, Helenowski I, Rademaker A, Raizer JJ. Metastatic glioblastoma: case presentations and a review of the literature. *J Neurooncol* (2012) 107(1):21–7. doi: 10.1007/s11060-011-0731-1

41. Blume C, von Lehe M, van Landeghem F, Greschus S, Bostrom J. Extracranial glioblastoma with synchronous metastases in the lung, pulmonary lymph nodes, vertebrae, cervical muscles and epidural space in a young patient - case report and review of literature. *BMC Res Notes* (2013) 6:290. doi: 10.1186/1756-0500-6-290

42. Hamilton JD, Rapp M, Schneiderhan T, Sabel M, Hayman A, Scherer A, et al. Glioblastoma multiforme metastasis outside the CNS: three case reports and possible mechanisms of escape. *J Clin Oncol* (2014) 32(22):e80–84. doi: 10.1200/JCO.2013.48.7546

43. Kim W, Yoo H, Shin SH, Gwak HS, Lee SH. Extraneural metastases of glioblastoma without simultaneous central nervous system recurrence. *Brain Tumor Res Treat* (2014) 2(2):124–7. doi: 10.14791/btrt.2014.2.2.124

44. Khattab MH, Marciscano AE, Lo SS, Lim M, Laterra JJ, Kleinberg LR, et al. Antiangiogenic therapies and extracranial metastasis in glioblastoma: A case report and review of the literature. *Case Rep Oncol Med* (2015) 2015:431819. doi: 10.1155/2015/431819

45. Undabeitia J, Castle M, Arrazola M, Pendleton C, Ruiz I, Úrculo E. Multiple extraneural metastasis of glioblastoma multiforme. *Sist Sanit Navar* (2015) 38:157–61. doi: 10.4321/S1137-66272015000100022

46. Starnoni D, Yamgoue Y, Hottinger A, Bartanusz V. Multilevel severe radiculopathy from an extraneural glioblastoma cervical metastasis. *Surg Neurol Int* (2016) 7:S1028–9. doi: 10.4103/2152-7806.195588

47. Franceschi S, Lessi F, Aretini P, Mazzanti CM, Menicagli M, La Ferla M, et al. Molecular portrait of a rare case of metastatic glioblastoma: somatic and germline mutations using whole-exome sequencing. *Neuro Oncol* (2016) 18(2):298–300. doi: 10.1093/neuonc/nov314

48. Xu M, Wang Y, Xu J, Yao Y, Yu WX, Zhong P. Extensive therapies for extraneural metastases from glioblastoma, as confirmed with the OncoScan assay. *World Neurosurg* (2016) 90:698. e697–698.e611. doi: 10.1016/j.wneu.2016.01.074

49. Simonetti G, Silvani A, Fariselli L, Hottinger AF, Pesce GA, Prada F, et al. Extra central nervous system metastases from glioblastoma: a new possible trigger event? *Neurol Sci* (2017) 38(10):1873–5. doi: 10.1007/s10072-017-3036-0

50. Sun Q, Xu R, Xu H, Wang G, Shen X, Jiang H. Extracranial metastases of high-grade glioma: the clinical characteristics and mechanism. *World J Surg Oncol* (2017) 15 (1):181–1. doi: 10.1186/s12957-017-1249-6

51. Ricard JA, Cramer SW, Charles R, Gil Tommee C, Le A, Bell WR, et al. Infratentorial glioblastoma metastasis to bone. *World Neurosurg* (2019) 131:90–4. doi: 10.1016/j.wneu.2019.07.142

52. Li Z-G, Zheng M-Y, Zhao Q, Liu K, Du J-X, Zhang S-W. Solitary vertebral metastatic glioblastoma in the absence of primary brain tumor relapse: a case report and literature review. *BMC Med Imaging* (2020) 20(1):89. doi: 10.1186/s12880-020-00488-x

53. Colamaria A, Blagia M, Sacco M, Carbone F. Diffuse vertebral metastases from glioblastoma with vertebroepidural diffusion: a case report and review of the literature. *Surg Neurol Int* (2021) 12:437. doi: 10.25259/SNI_538_2021

54. den Hartog SJ, van der Kolk A, Bruggink A, Seute T, Wesseling P, Wilbers J. Pathology-proven extradural ("distant") metastases of gliomas in adults in the Netherlands between 1971 and 2018: a systematic case series. *Neurooncol Pract* (2021) 8(3):317–24.

55. Noch EK, Sait SF, Farooq S, Trippett TM, Miller AM. A case series of extraneural metastatic glioblastoma at memorial Sloan Kettering cancer center. *Neurooncol Pract* (2021) 8(3):325–36. doi: 10.1093/nop/npaa083

56. Zhang W, Cai Y, Wang X, Wang X, Li Y, Han G, et al. Bone metastases of glioblastoma: a case report and review of the literature. *Front Oncol* (2021) 11:705455. doi: 10.3389/fonc.2021.705455

57. Goodwin CR, Liang L, Abu-Bonsrah N, Hdeib A, Elder BD, Kosztowski T, et al. Extraneural glioblastoma multiforme vertebral metastasis. *World Neurosurg* (2016) 89:578–582 e573. doi: 10.1016/j.wneu.2015.11.061

58. Strong MJ, Koduri S, Allison JA, Pesavento CM, Ogunsola S, Ogunsola O, et al. Bone metastasis from glioblastoma: a systematic review. *J Neuro-Oncol* (2022) 158:379–92. doi: 10.1007/s11060-022-04025-4

59. Bambury RM, Bhatt AS, Riester M, Pedamallu CS, Duke F, Bellmunt J, et al. DNA Copy number analysis of metastatic urothelial carcinoma with comparison to primary tumors. *BMC Cancer* (2015) 15:242. doi: 10.1186/s12885-015-1192-2

60. Ouyang L, Lee J, Park CK, Mao M, Shi Y, Gong Z, et al. Whole-genome sequencing of matched primary and metastatic hepatocellular carcinomas. *BMC Med Genomics* (2014) 7:2. doi: 10.1186/1755-8794-7-2

61. Wang H, Ou Q, Li D, Qin T, Bao H, Hou X, et al. Genes associated with increased brain metastasis risk in non-small cell lung cancer: Comprehensive genomic profiling of 61 resected brain metastases versus primary non-small cell lung cancer (Guangdong association study of thoracic oncology 1036). *Cancer* (2019) 125:3535–44. doi: 10.1002/cncr.32372

62. Tew BY, Legendre C, Schroeder MA, Triche T, Gooden GC, Huang Y, et al. Patient-derived xenografts of central nervous system metastasis reveal expansion of aggressive minor clones. *Neuro Oncol* (2020) 22:70–83. doi: 10.1093/neuonc/noz137

63. Turajlic S, Xu H, Litchfield K, Rowan A, Horswell S, Chambers T, et al. Deterministic evolutionary trajectories influence primary tumor growth: TRACERx renal. *Cell* (2018) 173:595–610 e511. doi: 10.1016/j.cell.2018.03.043

64. Mohme M, Maire CL, Schliffke S, Joosse SA, Alawi M, Matschke J, et al. Molecular profiling of an osseous metastasis in glioblastoma during checkpoint inhibition: potential mechanisms of immune escape. *Acta Neuropathol Commun* (2020) 8:28. doi: 10.1186/s40478-020-00906-9

frontiers | Frontiers in Surgery

TYPE Case Report
PUBLISHED 17 February 2023
DOI 10.3389/fsurg.2023.1095591



OPEN ACCESS

EDITED BY
Zhaolun Cai,
Sichuan University, China

REVIEWED BY
Jad Ahmad Degheili,
Children's Hospital of Eastern Ontario (CHEO), Canada
Zhiping Xia,
Wuhan University, China

*CORRESPONDENCE
Xiaofeng Zou
gyfyzouxf@126.com
Quanliang Liu
liuquanliang2008@163.com

†These authors share first authorship

SPECIALTY SECTION
This article was submitted to Surgical Oncology, a section of the journal Frontiers in Surgery

RECEIVED 11 November 2022
ACCEPTED 24 January 2023
PUBLISHED 17 February 2023

CITATION
Zou Y, Xie X, Zhong C, Liu L, Wang Q, Yan S, Zou X and Liu Q (2023) Case report: Robot-assisted laparoscopic partial nephrectomy for renal cell carcinoma in a patient with situs inversus totalis and abdominal cocoon. Front. Surg. 10:1095591. doi: 10.3389/fsurg.2023.1095591



# Case report: Robot-assisted laparoscopic partial nephrectomy for renal cell carcinoma in a patient with situs inversus totalis and abdominal cocoon

Yuhua Zou[1†], Xiaojuan Xie[2†], Cunzhi Zhong[3], Li Liu[3], Qinlin Wang[3], Sheng Yan[1], Xiaofeng Zou[1*] and Quanliang Liu[1*]

[1]Department of Urology, The First Affiliated Hospital of Gannan Medical University, Ganzhou, China, [2]Department of Cardiology, The First Affiliated Hospital of Gannan Medical University, Ganzhou, China, [3]Department of Anesthesiology, Operation Rom, The First Affiliated Hospital of Gannan Medical University, Ganzhou, China

**Background:** Situs inversus totalis (SIT) is a congenital condition wherein organs in abdominal or thoracic cavity are mirrored from their normal positions. Abdominal cocoon, is a rare disease of unknown aetiology that is characterised by total or partial small intestine encapsulation by a compact fibrocollagenous membrane. Aside from having two extremely rare conditions (SIT and Abdominal cocoon), our patient developed renal cell carcinoma (RCC), which makes this case even more uncommon.

**Case Presentation:** We report the case of a 64-year-old man who was admitted to our hospital with an extremely rare case of localized RCC in the left kidney complicated with SIT and abdominal cocoon. Computer tomography urography (CTU) and angiography (CTA) showed that the patient was confirmed as having SIT, for the space-occupying lesion in the left kidney, clear cell RCC (ccRCC) was considered, the lesion in the right kidney was probably cystic. We diagnosed our patient as having a cT1aN0M0 left RCC, and the RENAL score was 7x. With partial nephrectomy (PN) being the preferred treatment approach, robot-assisted laparoscopic partial nephrectomy (RALPN) was performed after obtaining informed consent. After insertion of the laparoscope, adhesions were observed between the entire colon and the anterior abdominal wall. Then, abdominal cocoon was diagnosed. The surgery was uneventful, and the tumour was resected successfully while preserving the tumour capsule. No intestinal injury or any other complication occurred in the intraoperative or postoperative, and the patient recovered well after the operation.

**Conclusion:** PN is an extremely challenging procedure in patients with SIT and abdominal cocoon. The da Vinci Xi surgical system and thorough preoperative assessment allowed the surgeon to overcome stereotyping, visual inversion, and successfully perform PN in a patient with SIT and abdominal cocoon without increasing the risk of complications and preserving as much renal function as possible. Considering the satisfactory outcomes, this report may hopefully provide a practical reference for the treatment of RCC in patients with other special conditions.

KEYWORDS

situs inversus totalis, abdominal cocoon, renal cell carcinoma, robot-assisted laparoscopic, partial nephrectomy, case report

## Introduction

Situs inversus totalis (SIT) is a congenital condition wherein organs in the abdominal or thoracic cavity are mirrored from their normal positions. This rare anatomical anomaly has an incidence of approximately 0.005%–0.01% (1). Abdominal cocoon, which is also known as idiopathic sclerosing peritonitis, congenital small intestinal obstruction and fibromembranous encapsulation, is a rare disease of unknown aetiology that is characterised by total or partial small intestine encapsulation by a compact fibrocollagenous membrane (2).

Renal cell carcinoma (RCC) is a malignancy of the urinary system that accounts for 2%–3% of all adult malignancies (3). For patients with T1a RCC, partial nephrectomy(PN) is recommended (4). This report presents an extremely rare case of localized RCC in the left kidney in a patient with SIT and abdominal cocoon, and aims to address gaps in treating RCC with robot-assisted laparoscopic partial nephrectomy (RALPN) in these patients. In patients with SIT and abdominal cocoon, surgery may be extremely difficult as SIT is complicated by structural deformities, and lysis of extensive intestinal adhesions may cause secondary intestinal injury. In our case, the da Vinci Xi surgical system enabled successful RALPN of the left kidney, which not only avoids the unclear exposure of the mirror human anatomical structure under traditional laparoscopic surgery, but also solves the problem of the operator's right hand inversion during the operation.

## Case presentation

The reporting of this study conforms to CARE guidelines (5). In Dec. 3, 2021, a 64-year-old man with a solid space-occupying lesion that measured 25 × 36 mm in the inferior pole of the left kidney by Doppler ultrasound during physical examination one month prior. The body mass index (BMI) was 22.19 kg/m². Meanwhile, the patient was generally well, was afebrile, and did not experience low back pain or discomfort, frequent urination, urgency, painful urination and gross haematuria. Additionally, the patient denied gastrointestinal symptoms such as abdominal pain and distention, nausea and vomiting. The patient had a 6-year special history of hypertension, and his blood pressure was well controlled by regular oral antihypertensive drugs. During hospitalisation, his maximum monitored blood pressure (BP) was 135/97 mmHg, and his monitored heart rate ranged from 72 to 90 bpm. The patient denied any history of other medications, diabetes, abdominal surgery or trauma, abdominal tuberculosis, peritoneal dialysis, autoimmune disease, or chemotherapy. Preoperative blood tests and comprehensive metabolic panel suggested no abnormalities. Renal Doppler ultrasound showed a solid space-occupying lesion in the left kidney, which required further evaluation. Computer tomography urography (CTU) and angiography (CTA) showed that the stomach and spleen were located in the right abdominal cavity, while the right hepatic lobe, gallbladder and inferior vena cava were at the left side of his abdomen (Figures 1A–E), the bilateral kidneys were normal in size and shape, but a 24 × 35 mm isodense mass protruded from the outline of the left kidney (Figures 1B–E). On contrast-enhanced computed tomography (CT) scan, the mass was strongly enhanced in the arterial phase (Figure 1C), and the enhancement pattern was attenuated during the venous phase (Figure 1D). There was a 31 × 40 mm non-enhancing hypodense nodule and calcification of the wall in the right renal. Additionally, the left renal artery was supplied by one renal artery and one accessory renal artery (Figure 1E). Effusion or lymphadenopathy in the abdominopelvic cavity was not noted. Based on the above findings, the patient was confirmed as having SIT, for the space-occupying lesion in the left kidney, clear cell RCC (ccRCC) was considered, the lesion in the right kidney was probably cystic. Cardiac Doppler ultrasound demonstrated decreased diastolic function and normal systolic function of the left ventricle in the transposed heart. The estimated glomerular filtration rates (eGFR) were 29.76 and 28.8 ml/min for the left and right kidneys, respectively. Chest CT showed no space-occupying lesions or evident abnormalities. Before surgery, the patient was diagnosed with left RCC, SIT, right renal cyst and hypertension. We diagnosed our patient as having a cT1aN0M0 left RCC, and the RENAL score was 7x. With PN being the preferred treatment approach, left RALPN was performed after obtaining informed consent.

Surgery was performed under general anaesthesia with the patient being placed in a supine position and angled at 70° on the unaffected side. A 1.0 cm incision was created at the medial umbilical edge for insertion of a Veress needle and induction of $CO_2$ pneumoperitoneum that was maintained at 15 mmHg. A laparoscope was then inserted to observe the abdominal cavity, adhesions were observed between the entire colon and the anterior abdominal wall, particularly between the intestines (Figures 2A,B). Based on these findings, abdominal cocoon was diagnosed. Under direct laparoscopy, two 8-mm robotic ports were respectively placed in adhesion-free areas in the intestine 4 cm from the anterior superior iliac spine and under the costal margin (Figure 3A), while a 12-mm assistant port was inserted 5 cm under the umbilicus at the midline (Figure 3A). When the robotic laparoscopy system was ready, adhesions between the colon and the anterior abdominal wall were removed (Figure 2B–D). The transposed organs, including the liver, spleen, stomach and colon, were then noted (Figure 2C,D). The inferior vena cava was located on the left side (Figure 2E–H). A protruding tumour (Figure 2G) was found in the left kidney, three arterial branches were dissected (including one from the abdominal aorta to the lower pole of the kidney, and two from the main renal artery to the middle and lower poles of the kidney) (Figure 2F). The surgery was uneventful, and the tumour was resected successfully while preserving the tumour capsule (Figure 2I). The operation time was 180 min, which included 23 min of warm ischemia time. The intraoperative blood loss was 200 ml. A 23 × 36 mm specimen was removed from the left kidney and sectioned to confirm tumour capsule integrity (Figure 3B). Pathology revealed pT1aN0M0 Fuhrman Grade I ccRCC, which did not involve the surgical margins (Figure 4A,B). No intestinal injury or any other complication occurred in the intraoperative or postoperative. The patient was satisfied with the treatment. The patient was discharged at postoperative on day 7. Postoperatively, the patient was followed up for 10 months, and no recurrence, secondary infection, or intestinal obstruction was detected.

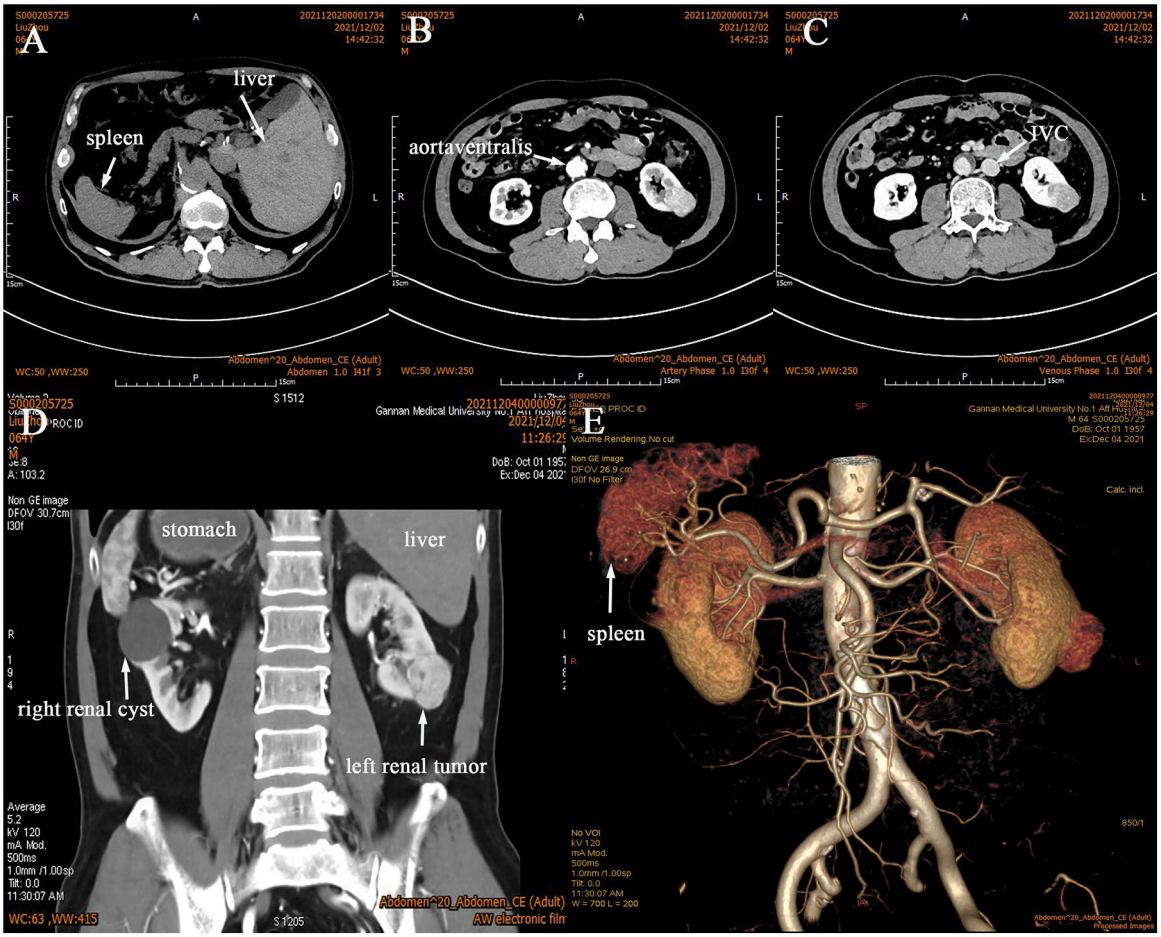


FIGURE 1
CTU and CTA was performed, and it confirmed SIT (A–E) with a tumor in the left kidney (B–E). It showed that the left renal artery had anatomical variation (E), the arterial phase (B), the venous phase (C), the coronal view (D).

## Discussion

SIT is the complete transposition of both the abdominal and thoracic organs that does not affect the anatomical relationships of the adjacent organs or their physiological functions, and anatomical variation of the great vessels, organ malformations and other congenital anomalies are common in patients with SIT (1). The mechanism responsible for such reversal is still unknown. Some believe that SIT involves autosomal recessive inheritance and genetic abnormalities, while others attribute SIT to malrotation during embryonic development (1). Recently, attention has focused on the association between SIT and cancer (6). Haruki et al. reported that KIF3 complex deficiency, a congenital characteristic in patients with SIT, appears to promote cancer development and progression (7).

Abdominal cocoon is a rare abdominal disorder first described by Foo et al. in 1978 (8). The syndrome lacks distinct clinical features and thus is difficult to diagnose before surgery. Although there is evidence of potential associations between abdominal cocoon and developmental abnormalities and medication, infection and surgery history, the underlying mechanism remains unknown (9). Abdominal cocoon can either be primary or secondary. Primary abdominal cocoon is idiopathic and commonly seen in patients without a history of abdominal surgery or trauma and may be linked to congenital dysplasia of the omentum majus and peritoneum (2). Secondary abdominal cocoon has a complex aetiology associated with previous surgery, peritoneal dialysis, tuberculous disease and gastrointestinal cancer (10, 11). Abdominal cocoon has nonspecific clinical manifestations, patients can be asymptomatic in mild cases. Common symptoms include an abdominal mass, persistent abdominal pain and incomplete bowel obstruction (12). Since preoperative diagnosis of abdominal cocoon is difficult, in most reported cases, the diagnosis is established based on intraoperative findings. In this report, the radiologist did not consider the possibility of abdominal cocoon. The patient was not diagnosed with abdominal cocoon until surgery, wherein bowel adhesions involving the descending colon, small intestine and peritoneum were observed.

Aside from having two extremely rare conditions (SIT and abdominal cocoon), our patient developed RCC, which makes this case even more uncommon. It is generally believed that laparoscopic surgery is safe and feasible even for patients with SIT. In fact, this approach has already been used in surgical conditions involving the gallbladder, bile duct, stomach, kidney and liver (1, 13). While several studies have reported open/laparoscopic radical nephrectomy (RN) (14, 15) or open PN (16) in patients with

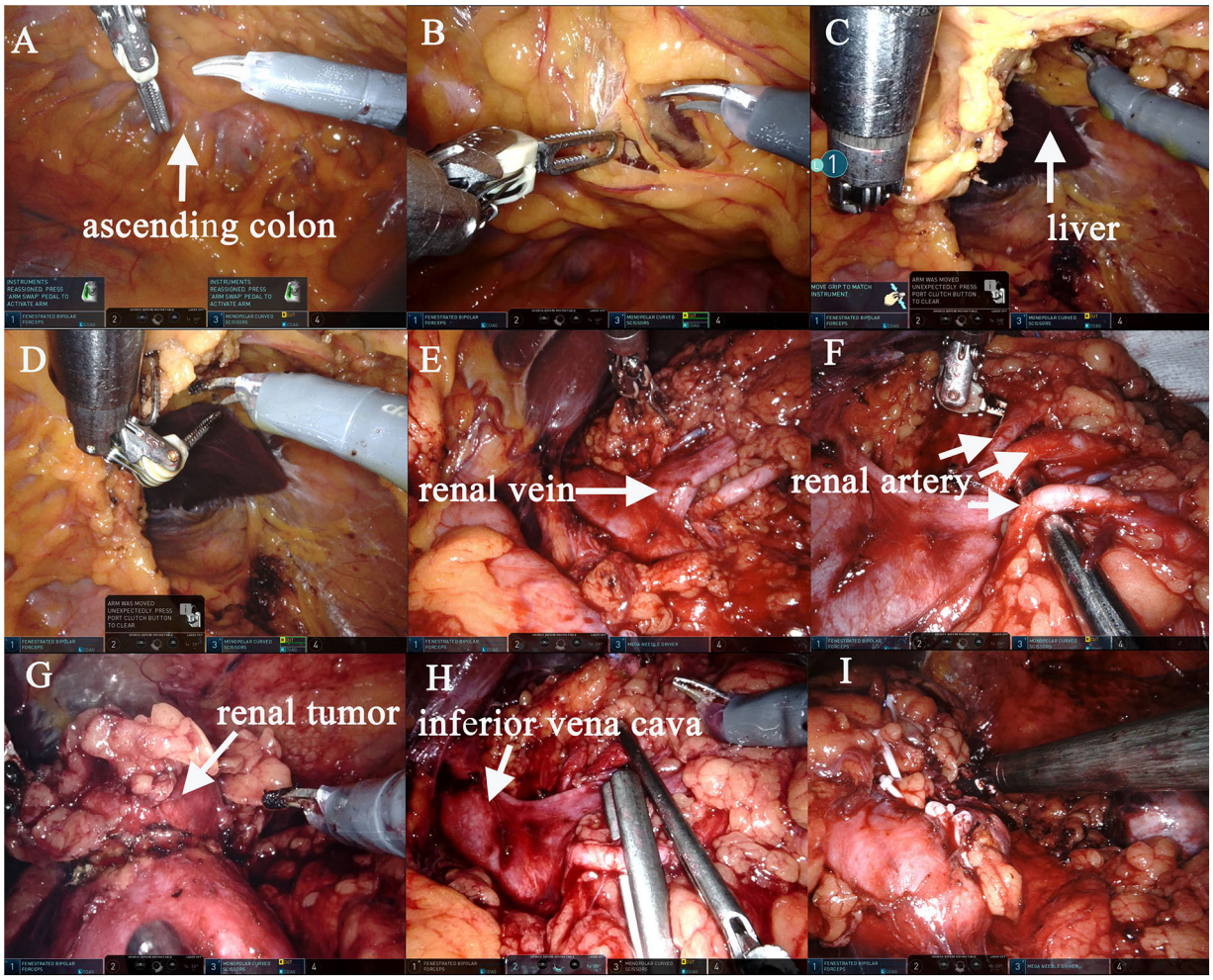


FIGURE 2
The left RALPN was performed. Adhesions were observed between the entire colon and the anterior abdominal wall, and the liver and the visual field of the surgical area could not be visualized (A,B). After adhesions between the colon and the anterior abdominal wall were removed, the liver and kidney areas on the left were exposed (B–D). The inferior vena cava was located on the left side (E,H), accurate dissection of the left renal hilar vessels (E), three arterial branches were dissected (including one from the abdominal aorta to the lower pole of the kidney, and two from the main renal artery to the middle and lower poles of the kidney) (F). The tumor was isolated and the margin was marked (G). Two branched renal arteries were blocked (H). The tumor was completely removed and the left renal margin was sutured accurately (I).

SIT and renal carcinoma, no case of simultaneous abdominal cocoon and RCC has been covered in these reports. Furthermore, there are no reports of RALPN in patients with SIT and abdominal cocoon.

In this case, given the transposition of internal organs and the goal of preserving as much renal parenchyma as possible, surgery was performed by an experienced surgeon who was thoroughly familiar with abdominal anatomy. Pneumoperitoneum was established to visualise the abdominal cavity, and abdominal cocoon was considered due to bowel encapsulation. Abdominal cocoon caused difficulties for the surgeon. Fortunately, we chose the medial side of the umbilical margin to insert the pneumoperitoneum needle and camera port first, which did not cause secondary intestinal injury. Additionally, other ports were inserted under direct laparoscopy and kept away from the bowel adhesions. So the port distribution was different from the conventional one. Despite the lack of international guidelines for abdominal cocoon management, the standard treatment for the disease includes removal of the sac and adhesiolysis (17). Because the patient was asymptomatic on weekdays, adhesiolysis was performed intraoperatively to separate the intestines and the peritoneum. However, adhesiolysis does not necessarily require complete removal of the sac or lysis of the bowel loops as long as the small intestines can be released and the intestines and mesentery can return to their normal positions without inflicting secondary injury.

The presence of vascular malformations, which often occur with SIT, should be considered when performing preoperative imaging tests. For patients with SIT and surgical disease, it is important to define the mirror-image characteristics to reduce the risk of vascular abnormalities before surgery (18). In our case, CTU and CTA were performed to visualise the tumour size and location as well as to determine the spatial relationship between the tumour and adjacent tissues. Additionally, the operation was performed based on a three-dimensional (3D) reconstruction of the renal vasculature that revealed the arterial orientation and variations of the affected kidney. Complete separation of the renal arterial divisions played a crucial role in reducing intraoperative bleeding

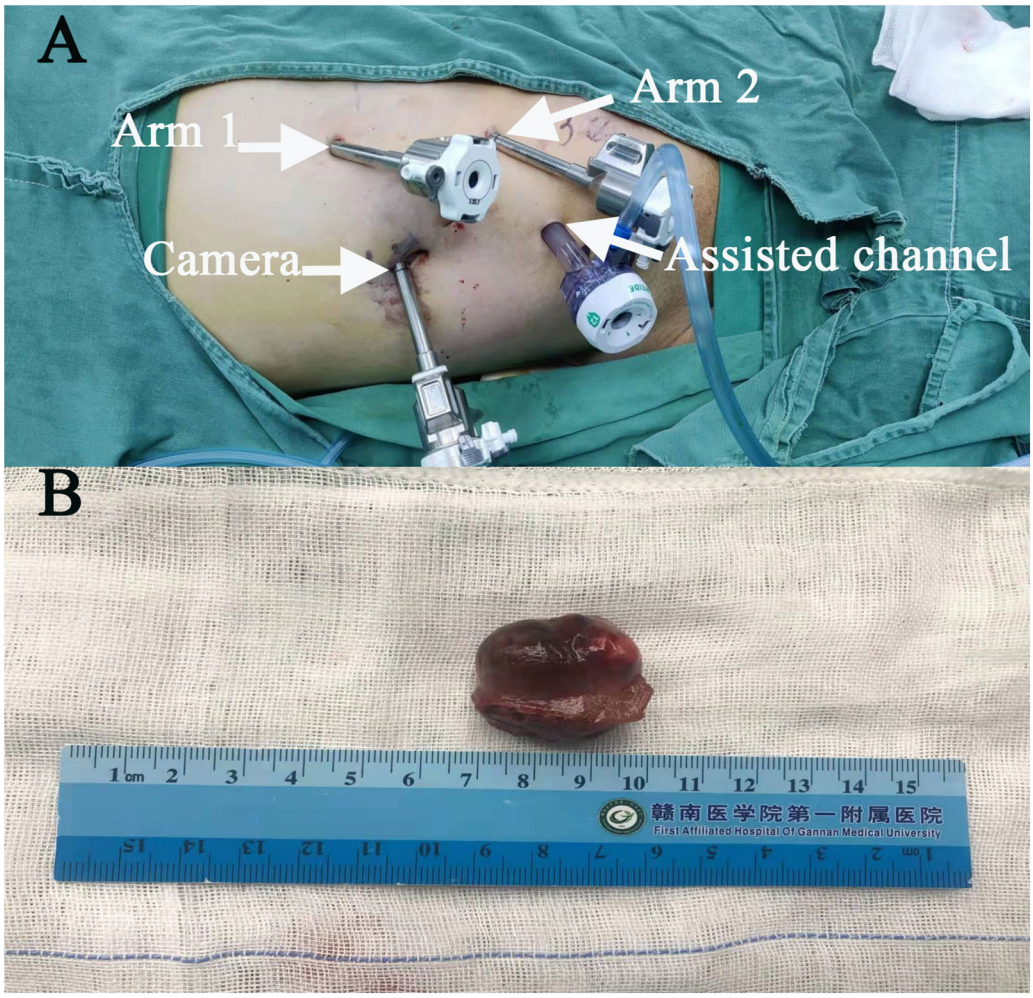


FIGURE 3
The distribution of ports in this case (A). Specimen: tumour capsule integrity (B).

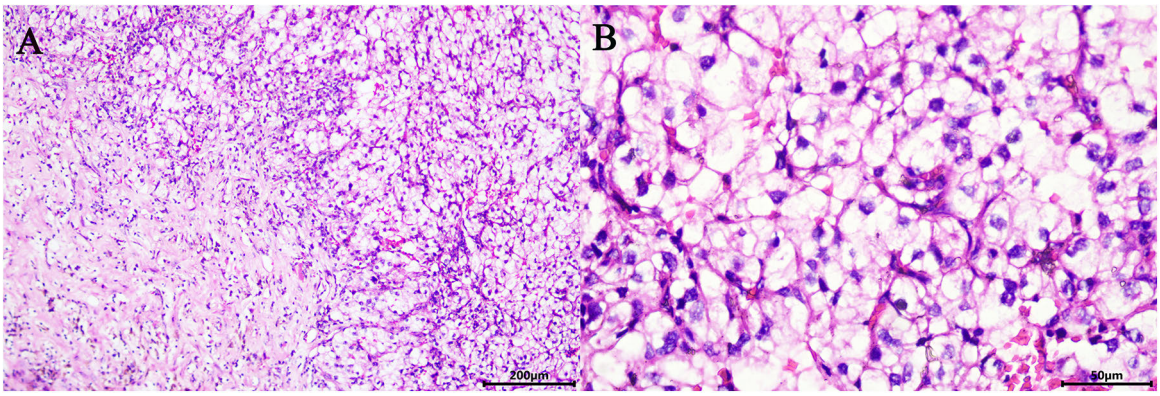


FIGURE 4
Microscopic appearance (A,B). Pathology revealed pT1aN0M0 Fuhrman Grade I ccRCC (hematoxilyn and eosin staining, ×200 (A), ×400 (B)).

and ensuring high visibility and effective tumour control. Intraoperative findings showed that the left renal artery had anatomical variation, which was consistent with the preoperative assessment, if this was incorrect, surgery may have damaged the renal artery and injured the kidney. In patients with SIT and abdominal cocoon, RALPN is technically demanding because it requires anti-conventional thinking and heightened awareness of the mirror-image reversal of internal organs. In this report, the da

Vinci Xi surgical system provided the operator with a surgical field magnified by >10-fold, high-definition 3D images, and robotic arms with seven planes of motion, and played an important role in all aspects (19), allowing for easier and safer separation of bowel adhesions, dissection of the renal hilum, separation of abnormal renal arteries, identification of surgical margins, tumour resection and wound closure with surgical precision.

## Conclusions

PN is an extremely challenging procedure in patients with SIT and abdominal cocoon. The da Vinci Xi surgical system and thorough preoperative assessment allowed the surgeon to overcome stereotyping, visual inversion, and successfully perform PN in a patient with SIT and abdominal cocoon without increasing the risk of complications and preserving as much renal function as possible. Considering the satisfactory outcomes, this report may hopefully provide a practical reference for the treatment of RCC in patients with other special conditions.

## Data availability statement

The original contributions presented in the study are included in the article/Supplementary Material, further inquiries can be directed to the corresponding author/s.

## Ethics statement

The studies involving human participants were reviewed and approved by The institutional research ethics committee of The First Affiliated Hospital of Gannan Medical University. The patients/participants provided their written informed consent to participate in this study. Written informed consent was obtained from the individual(s) for the publication of any potentially identifiable images or data included in this article.

## Author contributions

YHZ and XJX prepared and wrote the article. SY was directly involved in the management of the patients. CZZ, TP and QLW were responsible for the collection and organization of the literature. XFZ was the chief surgeon of the operation. QLL and XFZ revised the manuscript and acted as corresponding authors. All authors contributed to the article and approved the submitted version.

## Funding

This work was supported by the National Natural Science Foundation of China (No. 81860456), Key Project of Key Research and Development Plan of Jiangxi Province (No. 20212BBG71013).

## Acknowledgments

We would like to thank QLL for his guidance on this paper and for editing and proofreading this manuscript in English.

## Conflict of interest

The authors declare that the research was conducted in the absence of any commercial or financial relationships that could be construed as a potential conflict of interest.

## Publisher's note



## References

1. Eitler K, Bibok A, Telkes G. Situs Inversus totalis: a clinical review. *Int J Gen Med*. (2022) 15:2437–49. doi: 10.2147/IJGM.S295444

2. Tannoury JN, Abboud BN. Idiopathic sclerosing encapsulating peritonitis: abdominal cocoon. *World J Gastroenterol*. (2012) 18:1999–2004. doi: 10.3748/wjg.v18.i17.1999

3. Bahadoram S, Davoodi M, Hassanzadeh S, Bahadoram M, Barahman M, Mafakher L. Renal cell carcinoma: an overview of the epidemiology, diagnosis, and treatment. *G Ital Nefrol*. (2022) 39(3):2022–vol3. PMID: 35819037.

4. Campbell S, Uzzo RG, Allaf ME, Bass EB, Cadeddu JA, Chang A, et al. Renal mass and localized renal cancer: aUA guideline. *J Urol*. (2017) 198:520–9. doi: 10.1016/j.juro.2017.04.100

5. Agha RA, Franchi T, Sohrabi C, Mathew G, Kerwan A, SCARE Group. The SCARE 2020 guideline: updating consensus surgical CAse REport (SCARE) guidelines. *Int J Surg*. (2020) 84:226–30. doi: 10.1016/j.ijsu.2020.10.034

6. Hirokawa N, Tanaka Y, Okada Y, Takeda S. Nodal flow and the generation of left-right asymmetry. *Cell*. (2006) 125:33–45. doi: 10.1016/j.cell.2006.03.002

7. Haruki T, Maeta Y, Nakamura S, Sawata T, Shimizu T, Kishi K, et al. Advanced cancer with situs inversus totalis associated with KIF3 complex deficiency: report of two cases. *Surg Today*. (2010) 40:162–6. doi: 10.1007/s00595-009-4005-x

8. Foo KT, Ng KC, Rauff A, Foong WC, Sinniah R. Unusual small intestinal obstruction in adolescent girls: the abdominal cocoon. *Br J Surg*. (1978) 65:427–30. doi: 10.1002/bjs.1800650617

9. Sureka B, Mittal MK, Sinha M, Mittal A, Thukral BB. Abdominal cocoon. *Avicenna J Med*. (2013) 3:103–5. doi: 10.4103/2231-0770.120502

10. Mohamed FY, Alharbi YH, Almutairi MN, Azi NA, Aljreas AA, Alkhaldi EJ, et al. Abdominal cocoon: a rare complication of peritoneal dialysis in chronic kidney disease. *Cureus*. (2021) 13:e20341. doi: 10.7759/cureus.20341

11. Gadodia A, Sharma R, Jeyaseelan N. Tuberculous abdominal cocoon. *Am J Trop Med Hyg*. (2011) 84:1–2. doi: 10.4269/ajtmh.2011.10-0620

12. Hu Q, Shi JF, Sun YS. Abdominal cocoon with intestinal perforation: a case report. *Front Surg*. (2021) 8:747151. doi: 10.3389/fsurg.2021.747151

13. Abbey E, Yang F, Qi L, Wu JJ, Tong L, Zhen Z. Situs inversus totalis patients with gastric cancer: robotic surgery the standard of treatment?-A case report. *Int J Surg Case Rep*. (2021) 81:105818. doi: 10.1016/j.ijscr.2021.105818

14. Makiyama K, Sakata R, Yamanaka H, Tatenuma T, Sano F, Kubota Y. Laparoscopic nephroureterectomy in renal pelvic urothelial carcinoma with situs inversus totalis: preoperative training using a patient-specific simulator. *Urology*. (2012) 80:1375–8. doi: 10.1016/j.urology.2012.08.054

15. Ito J, Kaiho Y, Lwamura H, Anan G, Sato M. Laparoscopic radical nephrectomy for a right renal tumor with renal vein tumor thrombus in a patient with situs inversus totalis. *Asian J Endosc Surg*. (2019) 12:185–8. doi: 10.1111/ases.12608

16. Dergamoun H, Alaoui AE, Boualaou I, Sayegh H, Benslimane L, Nouini Y. Renal carcinoma and kartagener syndrome: an unusual association. *Case Rep Urol*. (2020) 2020:8260191. doi: 10.1155/2020/8260191 eCollection 2020.

17. Xu P, Chen LH, Li YM. Idiopathic sclerosing encapsulating peritonitis (or abdominal cocoon): a report of 5 cases. *World J Gastroenterol*. (2007) 13:3649–51. doi: 10.3748/wjg.v13.i26.3649

18. Chevli EM, Maiers TJ, Abramowitz DJ, Badkhshan S III, Bodkin JJ. Hand-assisted laparoscopic radical nephrectomy for renal cell carcinoma in a patient with situs inversus totalis. *Urol Case Rep*. (2019) 28:101076. doi: 10.1016/j.eucr.2019.101076

19. Raheem AA, Sheikh A, Kim DK, Alatawi A, Alabdulaali I, Han WK, et al. Da Vinci Xi and Si platforms have equivalent perioperative outcomes during robot-assisted partial nephrectomy: preliminary experience. *J Robot Surg*. (2017) 11:53–61. doi: 10.1007/s11701-016-0612-x

frontiers | Frontiers in Oncology

TYPE Case Report
PUBLISHED 09 March 2023
DOI 10.3389/fonc.2023.1078388



OPEN ACCESS

EDITED BY
Zhaolun Cai,
Sichuan University, China

REVIEWED BY
Yanfang Zheng,
Southern Medical University, China
Xing Niu,
China Medical University, China

*CORRESPONDENCE
Ying-Bin Liu
laoniulyb@shsmu.edu.cn
Mao-Lan Li
limaolan6@163.com
Yun Liu
liuyun05050650@renji.com

†These authors have contributed equally to this work

SPECIALTY SECTION
This article was submitted to Surgical Oncology, a section of the journal Frontiers in Oncology

RECEIVED 24 October 2022
ACCEPTED 20 February 2023
PUBLISHED 09 March 2023

CITATION
Yang J-X, Jia Z-Y, Liu F-T, Wu W-G, Li X-C, Zou L, Li H-F, Zhang F, Bao R-F, Peng S-Y, Lau WY, Liu Y, Li M-L and Liu Y-B (2023) Case report: A *de novo* ERBB3 mutation develops in a gallbladder cancer patient carrying BRCA1 mutation after effective treatment with olaparib.
*Front. Oncol.* 13:1078388.
doi: 10.3389/fonc.2023.1078388



# Case report: A *de novo* ERBB3 mutation develops in a gallbladder cancer patient carrying BRCA1 mutation after effective treatment with olaparib

Jing-Xiao Yang[1†], Zi-Yao Jia[1†], Fa-Tao Liu[2†], Wen-Guang Wu[1], Xue-Chuan Li[1,2,3], Lu Zou[1,2,3], Huai-Feng Li[4,5,6], Fei Zhang[4,5,6], Run-Fa Bao[4,5,6], Shu-You Peng[7], Wan Yee Lau[8], Yun Liu[2*], Mao-Lan Li[1*] and Ying-Bin Liu[1,2,3*]

[1]Department of Biliary-Pancreatic Surgery, Renji Hospital Affiliated to Shanghai Jiao Tong University School of Medicine, Shanghai, China, [2]Shanghai Cancer Institute, Shanghai, China, [3]State Key Laboratory of Oncogenes and Related Genes, Shanghai, China, [4]Shanghai Key Laboratory of Biliary Tract Disease Research, Shanghai, China, [5]Shanghai Research Center of Biliary Tract Disease, Shanghai, China, [6]Department of General Surgery, Xinhua Hospital Affiliated to Shanghai Jiao Tong University School of Medicine, Shanghai, China, [7]Department of General Surgery, The Second Affiliated Hospital of Zhejiang University School of Medicine, Hangzhou, Zhejiang, China, [8]Faculty of Medicine, The Chinese University of Hong Kong, Prince of Wales Hospital, Shatin, Hong Kong, Hong Kong SAR, China

**Background:** Gallbladder cancer (GBC) is highly lethal and resistant to most chemotherapeutic drugs. GBC was reported to carry multiple genetic mutations such as TP53, K-RAS, and ERBB2/3. Here, we unexpectedly identified a patient with GBC harboring germline BRCA1 p.Arg1325Lys heterozygous mutation. We sought to determine if olaparib, the poly ADP-ribose polymerase inhibitor (PARPi) commonly treated for BRCA mutation, can inhibit cancer development *via* a therapeutic trial on this patient.

**Case presentation:** The patient received GBC R0 resection after an 8-week olaparib treatment. After surgery and 6-month follow-up treatment with olaparib, the patient's blood carbohydrate antigen 19-9 (CA19-9) level declined from 328 to 23.6 U/ml. No recurrence in CT scanning was observed, indicating a disease-free survival of 6 months with conventional therapy. Two months later, CT examination and CA19-9 level showed cancer relapse. A blood biopsy revealed a new ERBB3 p.Gly337Arg mutation. GBC cell lines ectopically expressing BRCA1 p.Arg1325Lys together with ERBB3 p.Gly337Arg mutations were challenged with olaparib and/or afatinib, an ERBB2/3 inhibitor. The dual mutation cells were more responsive to the combined olaparib with afatinib than a single drug in the cell proliferation assay.

**Conclusion:** Olaparib is effective in a GBC patient with a BRAC1 mutation. The efficacy of olaparib and afatinib in both cultured BRAC1 and ERBB3 mutation cell lines suggests that a combined regimen targeting BRCA1/2 and ERBB2/3 mutations may be an optimal strategy to treat GBC patients who carry both gene mutations.

KEYWORDS

gallbladder cancer, dual targeted drugs therapy, olaparib, drug resistance, conversion therapy

# Introduction

Gallbladder cancer (GBC) is the most common type of biliary tract malignant tumor and resists most chemotherapeutic drugs (1). The incidence of gallbladder cancer in different regions varies, as it depends on multiple cancer risk factors, including geographical region, gender, age, and food intake (2). According to the database of the International Agency for Research on Cancer (IARC) Globocan in 2020, there were an estimated 115,949 new cases of GBC worldwide (contributing 0.6% of new cases, ranking 25th out of 36 cancers in 185 countries), and gallbladder cancer contributes to 0.9% of all cancer deaths annually.

Although divergent therapeutic approaches are currently available to treat GBC patients, surgery is still the most acceptable and effective means. However, a fairly large proportion of patients missed the opportunity of surgical resection due to the lack of early typical symptoms, thus accepting alternative non-surgical treatment including chemo- and/or radiotherapy. In order to improve early diagnosis, considerable efforts have been made to develop detecting technologies with minimally invasive approaches. For example, liquid biopsies containing circulating tumor cells (CTCs) and circulating tumor DNA (ctDNA) from the blood have received significant attention in the assistance of clinical diagnosis. The high sensitivity of these techniques allows us to reveal tumor genetic features with aberrant gene expressions and gene mutations, thus providing great value for early diagnosis and therapy.

A plethora of research evidence has established the paradigm that altered expressions of tumor oncogenes and/or suppressor genes drive tumor cell proliferation and transformation in tumor development. Elevated or mutated genes including ERBBs, TP53, EGF, CYP7A1, and CCR5 emerge to regulate a variety of human cancer development (1). For instance, mutation of BRCA1, a tumor suppressor gene, has been shown to be intimately associated with the formation of familial breast and ovarian cancer (3). Olaparib, a Food and Drug Administration (FDA)-approved drug targeting BRCA1 and BRCA2 (BRCA1/2) mutations, functions to inhibit poly ADP-ribose polymerase inhibitor (PARPi). In clinical trials, PARPi has improved outcomes of BRCA1/2 mutated cancer patients including breast, ovarian, pancreatic, and prostate cancers (4). While ERBB2/3 mutation was previously discovered to mediate the malignancy of GBC, we still lack sufficient knowledge on other gene mutations and the role of the co-existence of ERBB2/3 mutation with BRAC1/2 mutation in the malignant transformation of patients with GBC. Here, we reported that a gallbladder cancer patient with BRCA1 p.Arg1325Lys mutation responded well to olaparib, but 6 months later, the patient exhibited cancer relapse and developed ERBB3 mutation. Tumor cell lines carrying BRCA1 and ERRB3 mutations were responsive to olaparib and afatinib, suggesting that a combined regimen targeting BRCA1/2 and ERBB2/3 mutations may be an optimal strategy to treat GBC patients who carried both gene mutations.

This study is a case report and agreed with the principles of the CARE guidelines (5).

# Methods

## Clinical information

The patient provided informed consent before clinical examinations. A 52-year-old man diagnosed with gallbladder cancer was recruited who initially expressed right upper quadrant pain and obstructive jaundice. In the intravenous contrast-enhanced CT and positron emission tomography (PET)/CT, the images showed gallbladder cancer with liver invasion (Figure 1). In addition, the images contained enlarged retroperitoneal and left supraclavicular lymph nodes. Laboratory tests showed abnormal liver function, with an alanine transaminase level of 241 U/L and an aspartate aminotransferase level of 119 U/L. The levels of total bilirubin and direct bilirubin were elevated to 80.4 and 64.6 μmol/L, respectively. Serum tumor biomarkers revealed an elevated level of carbohydrate antigen 19-9 (CA19-9) to 328 U/ml (reference range, <39 U/ml). The patient was evaluated to have unresectable locally advanced gallbladder cancer finally.

## Treatment

An endoscopic metal biliary endoprosthesis (EMBE) was engaged first to release the biliary obstruction and the needle biopsy from the liver confirmed adenocarcinoma with gallbladder cancer origin (Figure 2A). After EMBE, liver function improved significantly, and alanine and oxalacetic transaminases decreased to 61 and 40, respectively. Total bilirubin and direct bilirubin decreased to 27.4 and 10.4, respectively. Jaundice basically subsided.

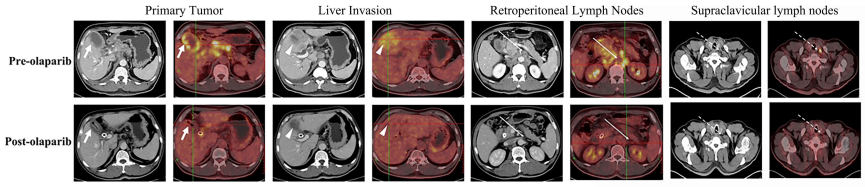


FIGURE 1
Representative pre- (upper row) and post-olaparib (lower row) treatment showing radiologic evidence in a 52-year-old man with gallbladder cancer harboring BRCA1 mutation. After 2 months of olaparib treatment, extensive metastatic lesions that involved the primary tumor (white arrow) and liver invasion (white arrowheads) became markedly reduced, while the retroperitoneal lymph nodes (long white arrows) and left supraclavicular lymph nodes (long white dotted arrows) disappeared when compared with those in the pre-olaparib treatment CT and PET/CT images.

The biopsy samples from liver metastasis were analyzed using the next-generation sequencing (NGS) method. A germline BRCA1 p.Arg1325Lys heterozygous mutation was detected and further confirmed by Sanger sequencing analysis. Subsequently, olaparib at 300 mg twice daily was given orally. The patient demonstrated remarkable clinical improvement with moderate adverse reactions such as nausea, diarrhea, or anemia in a course of 8-week treatment. CT and PET/CT exhibited favorable responses of the tumor to the treatment (Figure 1). The CA19-9 levels declined to 23.6 U/ml. His liver function levels, including alanine aminotransferase, aspartate aminotransferase, direct bilirubin, and indirect bilirubin, continued to improve. The tumor can be resected surgically after evaluation. As a result, the patient received radical surgery for the removal of the gallbladder, liver segments 4B and 5, common bile duct, and extended lymph node clearance. Histological examination of the resected surgical specimen showed cancer-free margins. All the resected lymph nodes were negative for metastasis. Thus, an R0 resection was achieved following olaparib treatment (Figure 2). Liquid biopsy with blood ctDNA after surgery showed the genetic signature of BRCA1 p.Arg1325Lys mutation. Following surgery, the patient kept receiving olaparib treatment at 300 mg twice daily for 6 months with mild adverse reactions similar to those described earlier at a local hospital. According to our follow-up, no tumor progression was found on the patient's examinations during the medication period.

## Genetic mutation studies

Two months later with no drug treatment, the patient visited our hospital again and displayed a poor quality of life. The CA19-9 levels of this patient showed an elevation to 38.4 from 26.3 U/ml, and tumor regrowth was detected by CT scan images (not shown) in a local hospital, indicating cancer relapse. According to ctDNA analysis from blood biopsy, a new ERBB3 p.Gly337Arg mutation was found. There was compelling evidence revealing the development of some gene mutations such as RAD51C (6) and Abcb1a after treatment with PARPi (7). In addition, our previous studies demonstrated that ERBB3 mutation mediates gallbladder cancer proliferation and progression (8, 9). Given this result, we evaluated the patient's general condition and devised the therapy strategy to add ERBB3 mutation inhibitors for combination treatment (olaparib plus afatinib). During the supportive treatment in order to attenuate intestinal obstruction, the patient exhibited cachexia and multiple organ functional failure with a performance status (PS) score of 4 out of 5. The patient and his family eventually chose to return to the local hospital for supportive treatment. According to our follow-up, the patient's general condition continued to deteriorate and never improved. The patient died in 43 days, missing the opportunity of the combined therapy.

## *In vitro* experiments

To examine if our early new therapeutic plan on the patient is reasonable and effective, we sought to use cultured cells exposed to olaparib and afatinib. Both wild-type and mutation constructs with single BRCA1 mutation and double BRCA1 and ERBB3 mutations were established in GBC cell lines GBC-SD and NOZ. After these cells stably expressed these genes, cell viability was analyzed in the presence of olaparib and/or afatinib. The results showed that GBC-SD cell lines with only BRCA1 p.Arg1325Lys mutation were more

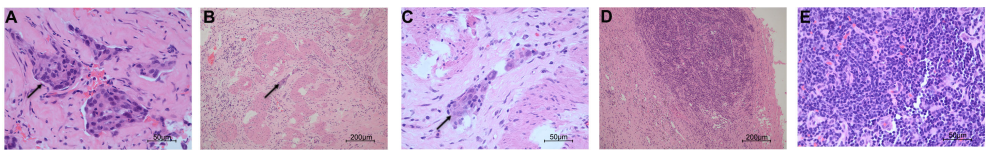


FIGURE 2
Histopathological examination of the specimens in pre- and post-olaparib treatment. **(A)** The cells (black arrow) from the infiltrating liver in pre-olaparib treatment are markedly pleomorphic with enlarged irregular nuclei (hematoxylin and eosin; magnification ×400). **(B, C)** After treatment with olaparib, only a very limited amount of cancer cells (black arrow) remained, and intense fibrosis developed (magnification ×100 in panel B and ×400 in panel **(C)**. **(D, E)** The resected lymph node was negative for malignancy (magnification ×100 in panel **D** and ×400 in panel **E**).

sensitive to olaparib when compared with the cells expressing the wild type (Figures 3A, B). However, cells with dual mutations of BRCA1 p.Arg1325Lys and ERBB3 p.Gly337Arg remarkably exhibited olaparib resistance (Figures 3A, B). Nevertheless, when afatinib was added, the sensitivity of these mutation cells to both these drugs resumed, and the effect of combined therapy was stronger than that of a single drug (Figures 3C, D). Similar results were obtained in colony formation and EdU assays of olaparib and/or afatinib on GBC cell lines ectopically expressing BRCA1 p.Arg1325Lys together with ERBB3 p.Gly337Arg mutations (Supplementary Material Figures 1, 2). The results suggest that the dual-targeted therapy may be more effective in gallbladder cancer patients with both BRCA1 and ERBB3 mutations than a single drug treatment.

## Statistical method

For comparisons of two groups, Student's t-test was applied if no significantly different variances were present; otherwise, the Mann–Whitney test was used $p < 0.05$ was considered statistically significant.

# Discussion

While BRCA1/2 mutation has frequently been identified in a wide spectrum of cancers, including breast (10), ovarian (11), pancreatic (12), and prostate (13) cancers, BRCA1 p.Arg1325Lys has not been reported in GBC. This is the first time to demonstrate that BRCA1 p.Arg1325Lys exists in GBC.

In concert with the sensitivities of mutated BRCA1/2 cancer cells to PARPi, the patient responded well to olaparib, the first line of targeted therapy approved by the FDA for BRCA1/2 mutated cancers (14). After treatment with olaparib, CT and PET/CT showed dramatic restriction of the tumor. Histopathological examination also showed only a few remaining tumor cells with no lymph node metastasis. The blood levels of CA19-9 declined from 328 U/ml to the normal range. All the results demonstrated favorable responses to BRCA1 mutation-targeted therapy. Although it is one case reported with BRCA1/2 mutation in GBC, the favorable clinical outcome has encouraged us to extend our research in clinical trials with GBCs expressing BRCA1/2 mutation in the near future.

Accumulating evidence indicated that cancer cells harboring BRCA1/2 mutation are defective in double-strand DNA break (DSB) repair, and these cells are sensitive to PARP inhibitors (15–18). However, prolonged treatment with PARPi can eventually lead to the occurrence of drug resistance. At present, at least four distinct molecular mechanisms have been documented to explain PARPi resistance (19): i) increased ability to export drugs, which could be caused by overexpression of drug-efflux transporter genes (Abcb1a and Abcb1b encoding for MDR1/P-gp and Abcg2) in cancer cells (7), ii) increased activity and level of PAR chains through loss of PARG (20) or PARP1 mutations that diminish trapping of protein on DNA (21), iii) increased homologous recombination (HR) (22), and iv) replication fork protection. For instance, there are defects of SMARCAL1, ZRANB3, and HLTF that mediate double DNA chain fork, MRE11-dependent degradation of nascent DNA in BRCA1/2-deficient human cell lines (23). In addition, other mechanisms that downregulate DNA repair pathways such as overexpression of histone methyltransferases EHMT1/2 have also been reported to mediate PARPi resistance (24, 25). It is worthwhile to further decipher the molecular mechanisms underpinning the acquired resistance to olaparib in our case.

The safety of PARPi has received significant attention, though no obvious adverse and unanticipated events were observed in this patient. Adverse events (AEs) may result in the termination of PARPi treatment when AE has threatened the patients' life. PARPi has a high risk of serious AE (SAE)- and AE-related discontinuation of treatment compared with placebo (26). This suggests that in the

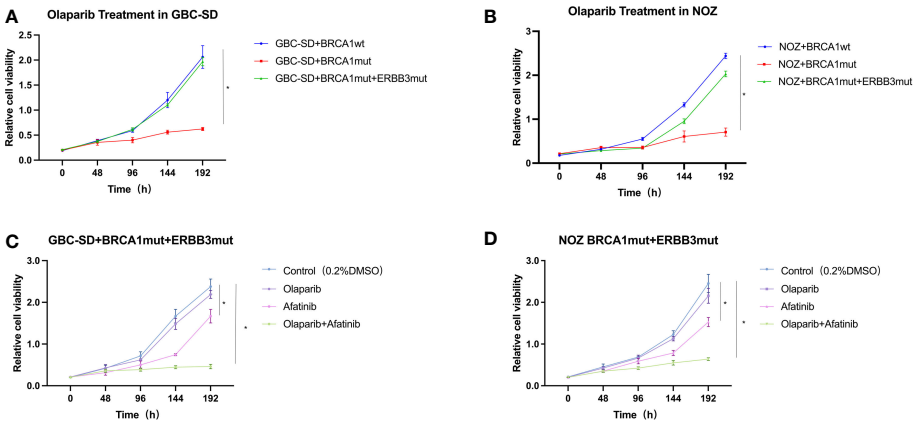


FIGURE 3
Cell viability of GBC-SD and NOZ cells expressing BRCA1 p.Arg1325Lys and ERBB3 p.Gly337Arg mutation. **(A)** GBC-SD cells expressing BRCA1 wild type (wt) or BRCA1 p.Arg1325Lys (mut) or both BRCA1 p.Arg1325Lys (mut) and ERBB3 p.Gly337Arg (mut) responded to olaparib (20 μM) over 192 h. **(B)** NOZ cells expressing both BRCA1 and ERBB3 wt or BRCA1 p.Arg1325Lys and ERBB3 p.Gly337Arg mutation responded to olaparib (20 μM) and afatinib (10 μM). **(C)** GBC-SD cells expressing both BRCA1 p.Arg1325Lys and ERBB3 p.Gly337Arg mutation responded to olaparib and afatinib. **(D)** NOZ cells expressing both BRCA1 p.Arg1325Lys and ERBB3 p.Gly337Arg mutation responded to olaparib and afatinib.

clinical application of PARPi, drug safety and AE should be particularly taken into account.

The combined therapy of PARPi with a DNA damage repair blocker such as topoisomerase I poison inhibitor was reported to sensitize tumor cell death and improve patient prognosis (27). In addition, a conjunction treatment of PARPi with anti-angiogenesis and anti-immune checkpoint drugs was also practiced in the clinical trials. However, the underlying mechanisms of these treatments remain to be clarified. Here, we found that the patient developed a new gene mutation with ERBB3 p.Gly337Arg when the disease did not respond to olaparib. It remains to be investigated if ERBB3 mutation is mechanistically associated with BRCA1 mutation. Nevertheless, our results with GBC cultured cell lines, which ectopically expressed both BRCA1 p.Arg1325Lys and ERBB3 p.Gly337Arg, developed resistance to olaparib. In contrast, single BRCA1 p.Arg1325Lys-mutated cells failed to grow in the presence of olaparib. Thus, dual inhibitors with olaparib and afatinib recapitulated the sensitivity of these cells to decreased cell growth, offering effective means to treat both mutations in GBC.

Compared with other previous cases of olaparib in the treatment of BRCA1 mutant gallbladder cancer (28, 29), the progression-free survival of the patient in our case was similar, but the mutation sites were different, which further demonstrated the feasibility of olaparib in the treatment of BRCA1 mutant gallbladder cancer. Different from other cases, the patient in this case was first treated with olaparib to shrink the tumor and successfully achieve R0 resection, thus achieving conversion therapy, which also provides a new idea for the surgical treatment of gallbladder cancer. In addition, this patient developed a new gene mutation with ERBB3 p.Gly337Arg, which was also one of the possible reasons for the progression of the disease. We also verified the effectiveness of dual-targeted drug therapy to a certain extent through an *in vitro* experiment, providing some ideas and references for similar situations that may occur in the future.

In summary, we reported that a patient with GBC harboring BRCA1 mutation initially responded well to olaparib. After a 6-month course of treatment, the patient developed an additional ERBB3 mutation, which led to the failure of the PARPi therapy. A dual BRCA1/2 and ERBB2/3 mutation-targeted therapy may suggest a benefit to GBC patients who carry both mutated genes.

## Data availability statement

The raw data supporting the conclusions of this article will be made available by the authors, without undue reservation.

## Ethics statement

Ethical review and approval was not required for the study on human participants in accordance with the local legislation and institutional requirements. The patients/participants provided their written informed consent to participate in this study. Written informed consent was obtained from the [individual(s) AND/OR minor(s)' legal guardian/next of kin] for the publication of any potentially identifiable images or data included in this article.

## Author contributions

(I) Conception and design: YL, M-LL and Y-BL. (II) Administrative support: M-LL, Y-BL, S-YP and WL. (III) Provision of study materials or patients: Y-DZ, W-GW, X-AW, H-FL, FZ and R-FB. (IV) Collection and assembly of data: Z-YJ, J-XY, X-CL and LZ. (V) Data analysis and interpretation: F-TL, Z-YJ, J-XY, X-CL and LZ. (VI) Manuscript writing: all authors. All authors contributed to the article and approved the submitted version.

## Funding

This study was supported by Shanghai Municipal Health Commission Health Industry Clinical Research Special Project (No. 20224Z0014), the National Key Research and Development Program of China (No. 2021YFE0203300), the National Natural Science Foundation of China (No. 82073206), the Shuguang Program of Shanghai Education Development Foundation and Shanghai Municipal Education Commission (No. 20SG14), the Basic Research Project of Science and Technology Commission of Shanghai Municipality (Nos. 20JC1419100, 20JC1419101, and 20JC1419102), the Clinical Science and Technology Innovation Project of Shanghai Shenkang Hospital Development Center (No. SHDC12019110), and Shanghai Clinical Medical Research Center for Digestive Diseases (No. 19MC1910200).

## Acknowledgments

We are very grateful to this patient and his family. We are very grateful to Professor Rong Shao of the Dept. of Pharmacology, Shanghai Jiao Tong University School of Medicine, for his editing and guidance.

## Conflict of interest

The authors declare that the research was conducted in the absence of any commercial or financial relationships that could be construed as a potential conflict of interest.

## Publisher's note



## Supplementary material

The Supplementary Material for this article can be found online at: https://www.frontiersin.org/articles/10.3389/fonc.2023.1078388/full#supplementary-material

# References

1. Schmidt MA, Marcano-Bonilla L, Roberts LR. Gallbladder cancer: epidemiology and genetic risk associations. *Chin Clin Oncol* (2019) 8:31. doi: 10.21037/cco.2019.08.13

2. Baiu I, Visser B. Gallbladder cancer. *JAMA* (2018) 320:1294. doi: 10.1001/jama.2018.11815

3. Wooster R, Weber BL. Breast and ovarian cancer. *N Engl J Med* (2003) 348:2339–47. doi: 10.1056/NEJMra012284

4. Kaufman B, Shapira-Frommer R, Schmutzler RK, Audeh MW, Friedlander M, Balmaña J, et al. Olaparib monotherapy in patients with advanced cancer and a germline BRCA1/2 mutation. *J Clin Oncol* (2015) 33:244–50. doi: 10.1200/JCO.2014.56.2728

5. Riley DS, Barber MS, Kienle GS, Aronson JK, von Schoen-Angerer T, Tugwell P, et al. CARE guidelines for case reports: explanation and elaboration document. *J Clin Epidemiol* (2017) 89:218–35. doi: 10.1016/j.jclinepi.2017.04.026

6. Kondrashova O, Nguyen M, Shield-Artin K, Tinker AV, Teng NNH, Harrell MI, et al. Secondary somatic mutations restoring and associated with acquired resistance to the PARP inhibitor rucaparib in high-grade ovarian carcinoma. *Cancer Discovery* (2017) 7:984–98. doi: 10.1158/2159-8290.CD-17-0419

7. Rottenberg S, Jaspers JE, Kersbergen A, van der Burg E, Nygren AOH, Zander SAL, et al. High sensitivity of BRCA1-deficient mammary tumors to the PARP inhibitor AZD2281 alone and in combination with platinum drugs. *Proc Natl Acad Sci U.S.A.* (2008) 105:17079–84. doi: 10.1073/pnas.0806092105

8. Li M, Zhang Z, Li X, Ye J, Wu X, Tan Z, et al. Whole-exome and targeted gene sequencing of gallbladder carcinoma identifies recurrent mutations in the ErbB pathway. *Nat Genet* (2014) 46:872–6. doi: 10.1038/ng.3030

9. Li M, Liu F, Zhang F, Zhou W, Jiang X, Yang Y, et al. Genomic / mutations promote PD-L1-mediated immune escape in gallbladder cancer: a whole-exome sequencing analysis. *Gut* (2019) 68:1024–33. doi: 10.1136/gutjnl-2018-316039

10. Tutt ANJ, Garber JE, Kaufman B, Viale G, Fumagalli D, Rastogi P, et al. Adjuvant olaparib for patients with - or -mutated breast cancer. *N Engl J Med* (2021) 384:2394–405. doi: 10.1056/NEJMoa2105215

11. Ray-Coquard I, Pautier P, Pignata S, Pérol D, González-Martín A, Berger R, et al. Olaparib plus bevacizumab as first-line maintenance in ovarian cancer. *N Engl J Med* (2019) 381:2416–28. doi: 10.1056/NEJMoa1911361

12. Golan T, Hammel P, Reni M, Van Cutsem E, Macarulla T, Hall MJ, et al. Maintenance olaparib for germline -mutated metastatic pancreatic cancer. *N Engl J Med* (2019) 381:317–27. doi: 10.1056/NEJMoa1903387

13. de Bono J, Mateo J, Fizazi K, Saad F, Shore N, Sandhu S, et al. Olaparib for metastatic castration-resistant prostate cancer. *N Engl J Med* (2020) 382:2091–102. doi: 10.1056/NEJMoa1911440

14. Helleday T. PARP inhibitor receives FDA breakthrough therapy designation in castration resistant prostate cancer: beyond germline BRCA mutations. *Ann Oncol* (2016) 27:755–7. doi: 10.1093/annonc/mdw048

15. Farmer H, McCabe N, Lord CJ, Tutt ANJ, Johnson DA, Richardson TB, et al. Targeting the DNA repair defect in BRCA mutant cells as a therapeutic strategy. *Nature* (2005) 434:917–21. doi: 10.1038/nature03445

16. Tutt A, Ashworth A. The relationship between the roles of BRCA genes in DNA repair and cancer predisposition. *Trends Mol Med* (2002) 8:571–6. doi: 10.1016/S1471-4914(02)02434-6

17. Moynahan ME, Chiu JW, Koller BH, Jasin M. Brca1 controls homology-directed DNA repair. *Mol Cell* (1999) 4:511–8. doi: 10.1016/S1097-2765(00)80202-6

18. Tutt A, Bertwistle D, Valentine J, Gabriel A, Swift S, Ross G, et al. Mutation in Brca2 stimulates error-prone homology-directed repair of DNA double-strand breaks occurring between repeated sequences. *EMBO J* (2001) 20:4704–16. doi: 10.1093/emboj/20.17.4704

19. Noordermeer SM, van Attikum H. PARP inhibitor resistance: A tug-of-War in BRCA-mutated cells. *Trends Cell Biol* (2019) 29:820–34. doi: 10.1016/j.tcb.2019.07.008

20. Gogola E, Duarte AA, de Ruiter JR, Wiegant WW, Schmid JA, de Bruijn R, et al. Selective loss of PARG restores PARylation and counteracts PARP inhibitor-mediated synthetic lethality. *Cancer Cell* (2018) 33(6):1078–93.e12. doi: 10.1016/j.ccell.2018.05.008

21. Pettitt SJ, Krastev DB, Brandsma I, Dréan A, Song F, Aleksandrov R, et al. Genome-wide and high-density CRISPR-Cas9 screens identify point mutations in PARP1 causing PARP inhibitor resistance. *Nat Commun* (2018) 9:1849. doi: 10.1038/s41467-018-03917-2

22. Bunting SF, Callén E, Wong N, Chen H-T, Polato F, Gunn A, et al. 53BP1 inhibits homologous recombination in Brca1-deficient cells by blocking resection of DNA breaks. *Cell* (2010) 141:243–54. doi: 10.1016/j.cell.2010.03.012

23. Maya-Mendoza A, Moudry P, Merchut-Maya JM, Lee M, Strauss R, Bartek J. High speed of fork progression induces DNA replication stress and genomic instability. *Nature* (2018) 559:279–84. doi: 10.1038/s41586-018-0261-5

24. Li H, Liu Z-Y, Wu N, Chen Y-C, Cheng Q, Wang J. PARP inhibitor resistance: the underlying mechanisms and clinical implications. *Mol Cancer* (2020) 19:107. doi: 10.1186/s12943-020-01227-0

25. Lee EK, Matulonis UA. PARP inhibitor resistance mechanisms and implications for post-progression combination therapies. *Cancers (Basel)* (2020) 12(8):2054. doi: 10.3390/cancers12082054

26. Cai Z, Liu C, Chang C, Shen C, Yin Y, Yin X, et al. Comparative safety and tolerability of approved PARP inhibitors in cancer: A systematic review and network meta-analysis. *Pharmacol Res* (2021) 172:105808. doi: 10.1016/j.phrs.2021.105808

27. Veneris JT, Matulonis UA, Liu JF, Konstantinopoulos PA. Choosing wisely: Selecting PARP inhibitor combinations to promote anti-tumor immune responses beyond BRCA mutations. *Gynecol Oncol* (2020) 156:488–97. doi: 10.1016/j.ygyno.2019.09.021

28. Li X, Gao L, Qiu M, Cao D. Olaparib treatment in a patient with advanced gallbladder cancer harboring BRCA1 mutation. *Onco Targets Ther* (2021) 14:2815–9. doi: 10.2147/OTT.S303594

29. Xie Y, Jiang Y, Yang X-B, Wang A-Q, Zheng Y-C, Wan X-S, et al. Response of BRCA1-mutated gallbladder cancer to olaparib: A case report. *World J Gastroenterol* (2016) 22:10254–9. doi: 10.3748/wjg.v22.i46.10254

frontiers | Frontiers in Surgery

TYPE Case Report
PUBLISHED 09 March 2023
DOI 10.3389/fsurg.2023.1110580



OPEN ACCESS

EDITED BY
Tomoyuki Abe,
Higashi-Hiroshima Medical Center, Japan

REVIEWED BY
Hsin-Hua Lee,
Kaohsiung Medical University, Taiwan
Giuseppe Emmanuele Umana,
Cannizzaro Hospital, Italy

*CORRESPONDENCE
Priyanshu Saha
✉ hellopriyanshu1@gmail.com

SPECIALTY SECTION
This article was submitted to Surgical Oncology, a section of the journal Frontiers in Surgery

RECEIVED 29 November 2022
ACCEPTED 19 January 2023
PUBLISHED 09 March 2023

CITATION
Saha P, Raza M, Fragkakis A, Ajayi B, Bishop T, Bernard J, Miah A, Zaidi SH, Abdelhamid M, Minhas P and Lui DF (2023) Case report: L5 tomita En bloc spondylectomy for oligometastatic liposarcoma with post adjuvant stereotactic ablative radiotherapy.
Front. Surg. 10:1110580.
doi: 10.3389/fsurg.2023.1110580



# Case report: L5 tomita En bloc spondylectomy for oligometastatic liposarcoma with post adjuvant stereotactic ablative radiotherapy

Priyanshu Saha[1,2]*, Mohsen Raza[2], Angelo Fragkakis[2], Bisola Ajayi[2], Timothy Bishop[2], Jason Bernard[2], Aisha Miah[3], Shane H. Zaidi[3], Mohamed Abdelhamid[4], Pawan Minhas[2] and Darren F. Lui[2]

[1]School of Medicine, St George's, University of London, United Kingdom, [2]Department of Complex Neurosurgery, St George's University Hospitals NHS Foundation Trust, United Kingdom, [3]Department of Sarcoma, Royal Marsden NHS Foundation Trust, United Kingdom, [4]Department of Vascular Surgery, St George's University Hospitals NHS Foundation Trust, United Kingdom

**Introduction:** Tomita En-bloc spondylectomy of L5 is one of the most challenging techniques in radical oncological spine surgery. A 42-year-old female was referred with lower back pain and L5 radiculopathy with a background of right shoulder liposarcoma excision. CT-PET confirmed a solitary L5 oligometastasis. MRI showed thecal sac indentation hence wasn't suitable for Stereotactic Ablative Radiotherapy (SABR) alone. The seeding nature of sarcoma prevents the indication of separation surgery hence excisional surgery is considered for radical curative treatment. This case report demonstrates dual-staged modified TES including the utilisation of novel techniques to allow for maximum radical oncological control in the era of SABR and lesser invasive surgery.

**Methods:** First-stage: Carbonfibre pedicle screws planned from L2 to S2AI-Pelvis, aligned, to her patient-specific rods. Radiofrequency ablation of L5 pedicles prior to osteotomy was performed to prevent sarcoma cell seeding. Microscope-assisted thecal sac tumour separation and L5 nerve root dissection was performed. Novel surgical navigation of the ultrasonic bone-cutter assisted inferior L4 and superior S1 endplate osteotomies. Second-stage: Vascular-assisted retroperitoneal approach at L4–S1 was undertaken protecting the great vessels. Completion of osteotomies at L4 and S1 to En-bloc L5: (L4 inferior endplate, L4/5 disc, L5 body, L5/S1 disc and S1 superior endplate). Anterior reconstruction used an expandable PEEK cage obviating the need for a third posterior stage. Reinforced with a patient-specific carbon plate L4–S1 promontory.

**Results:** Patient rehabilitated well and was discharged after 42 days. Cyberknife of 30Gy in 5 fractions was delivered two months post-op. Despite left foot drop, she's walking independently 9 months post-op.

**Conclusion:** These are challenging cases require a truly multi-disciplinary team approach. We share this technique for a dual stage TES and metal-free construct with post adjuvant SABR to achieve maximum local control in spinal oligometastatic disease. This case promotes our modified TES technique in the era of SABR and separation surgery in carefully selected cases.

KEYWORDS

spinal oligometastatic disease, sarcoma, case report, dual stage tomita *en bloc* spondylectomy, carbon fibre (CF), spine surgery, stereotactic ablative radiotherapy (SABR), oncological spine surgery

# Introduction

Total En Bloc Spondylectomy (TES) is a radical surgical technique first pioneered by Katsuro Tomita for solitary spinal metastases (1, 2). Its use in oligometastatic lesions of the spine aims to improve prognosis and oncological curability for patients *via* complete surgical resection rather than the piecemeal excision.

# Case presentation

A middle-aged African female underwent previous excision of lipoma of the right shoulder in 2018. She then had recurrence of the lump and was diagnosed with pleomorphic liposarcoma of the right shoulder. This was treated with pre-operative neo-adjuvant radiotherapy and *en bloc* resection in 2018. She was otherwise fit and well, working full time and regularly active and independent of all activities of daily living.

She reported low back pain with left leg radiculopathy radiating to the lateral foot in April 2020 with no bladder or bowel disturbance. Her oncology team organised a computed tomography scan which showed a solitary L5 lytic bone metastasis. After referral to our specialist unit, we obtained a single-photon emission computed tomography to confirm this was a solitary oligometastatic lesion. She was not eligible for SABR due to the fractured posterior wall and the lesion abutting the thecal sack. The lesion was already known to be radio insensitive. Piecemeal, palliative decompression is generally not advisable for sarcoma due to the risk of aggravation and further seeding.

She was referred to our complex Spine Multidisciplinary Team (MDT) meeting. The case was discussed between the oncologist, radio-oncologist and spinal team. The management plan was decided to be a L5 Tomita En bloc spondylectomy resection to provide maximal local control (**Figure 1**).

# Patient care timeline

## Pre-operative planning

The patient underwent Magnetic Resonance Imaging (MRI) whole spine, computerized tomography (CT) thorax, abdomen and pelvis, CT angiogram spine and whole-body Positron Emission Topography scan (PET). She underwent extensive pre-operative planning and was counselled on the risks of the surgery including high rate of morbidity and mortality. Consent for these procedures in view of Montgomery in the UK means that paternalistic medicine is not appropriate, and all options and risks must be advised to the patient. Particular note was given to permanent neurological deficit with L5 nerve root sacrifice but also injury to cauda equina. Vascular injury was of significant risk, and she was reviewed by the Vascular surgeon separately.

Carbon Fibre pedicle screws and rods were planned for this lady to ensure post-operative surveillance imaging could be optimal with no artefact. Furthermore, post adjuvant radiotherapy could be planned and delivered with more precision.

Carbon rods are rigid, and the pedicle screws have only 10 degrees of polyaxial movement making the insertion of this instrumentation technically challenging with little room for error. One method we employed to mitigate error was the use of 3-Dimensional printed model of the spine with bespoke jigs to allow pre-planned drilling of pedicles and insertion of carbon screws in a predetermined alignment.

En bloc resection of the posterior elements requires the pedicles to be osteotomised. Prior to this step, radiofrequency ablation of the pedicles was planned to help mitigate any living sarcoma tissue seeding.

A custom-built carbon spondylectomy cage was considered against an expandable poly-ether-ether-ketone (PEEK) cage. Fortuitously her pelvic incidence was 50 degrees and the L4–S1 lordosis of the PEEK Cage has an adaptable maximum lordosis of 25 degrees. A greater lordosis would have required a custom-made carbon cage.

Endoscopic equipment was prepared to help separate tumour from thecal sac as well as microscopic techniques to identify, isolate and preserve nerve roots but also to surgically sacrifice the right L5 nerve.

A multi-disciplinary team approach was required due to the complexity of the lesion and proximity to neurovascular structures. Teams involved included: Orthopaedic Complex Spine team, Neurosurgery, Vascular surgery, Anaesthetics, Radiologists, Intensive care, Physiotherapy and Occupational therapy.

## Surgical methods

The patient underwent a planned two-stage procedure with the primary aim being excision of L5 vertebra with stabilisation. She was categorised as an ASA 2 by the anaesthetic team. Spinal cord monitoring was undertaken for the duration of the operation.

First stage of the L5 Tomita en-bloc spondylectomy involved a posterior approach with dissection performed from L2 to pelvis. Skeletisation of the spine was performed, and the 3D printed navigation jigs were applied for segmental pedicle screw fixation with carbon fibre instrumentation. Carbon fibre pedicle screws were inserted from L2 to S2AI.

Intraoperative CT was performed to navigate the *en bloc* resection of the posterior elements of L5 requiring full removal of L4 and S1 posterior elements to fully visualise L5. Radiofrequency ablation was performed to the L5 pedicles with use of radiofrequency probes. The pedicles of L5 were cut with a navigated ultrasonic bone cutter allowing for precise cuts and protection of the nerve roots. Soft tissue dissection around the whole L5 posterior segment was performed.

Intraoperative microscope was utilised to perform careful separation of tumour from dura whilst preserving the tumour capsule and to safely mobilise nerve roots of L4–S1 and dissect surrounding soft tissue. An endoscopic set was at hand to assist in the separation of tumour from thecal sac. Epidural vessel bleeding was appropriately controlled.

A bovine dural patch was laid in front of the dura and anterior the thecal sac and to all nerve roots. Under navigation the ultrasonic bone cutter was then used to make posterior to anterior

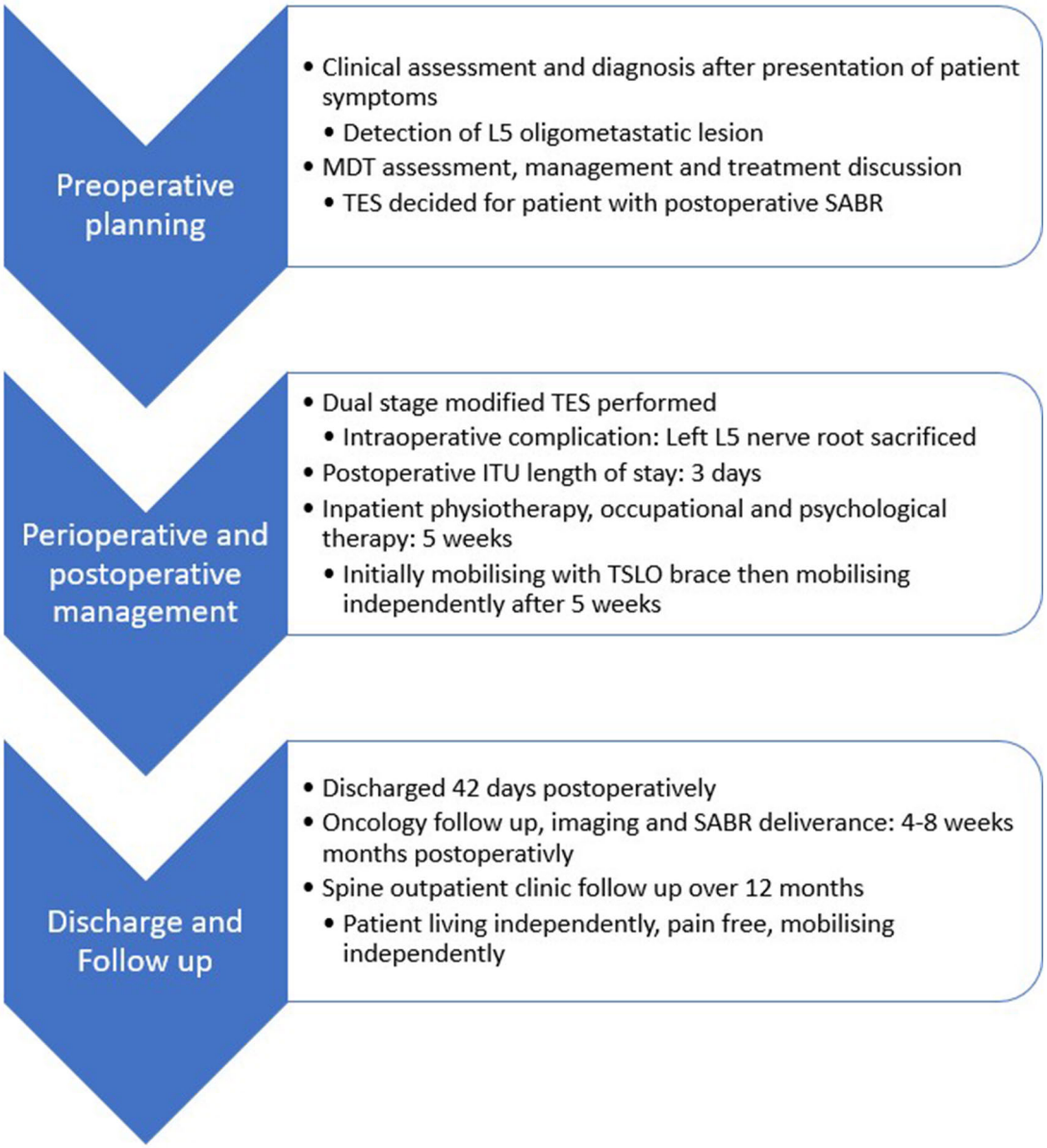


FIGURE 1
Patient Care Timeline.

cuts through the endplate of L4 and S1. The osteotomy gaps were filled with haemostat and sealed with bone wax. The posterior neural arch of L5 was removed *en bloc*.

Calibration of the ultrasonic bone cutter is possible with the 3D CT and spinal navigation set. After the soft tissue separation of tumour from thecal sac and the L5 nerve roots were freed, the Carbon Fibre Rods were inserted, and we used cross connectors for added stability. Even with the 3D printed navigation jigs inserting screws for pre-planned alignment for a rigid rod, there was still significant technical difficulties creating the posterior construct.

Antibiotic-impregnated beads were then laid into the wound. Closure was performed in layers with a drain inserted.

The first procedure was approximately 15 h and involved both Complex Spine and Neurosurgical teams operating. The operation was undertaken successfully, and the patient remained stable throughout. Spinal cord monitoring remained satisfactory throughout the operation. She was kept in ICU overnight in preparation for the second stage the next day.

The second stage commenced with an anterior approach (retroperitoneal) performed with the Vascular team. A long crescent shaped anterolateral oblique approach was chosen coming from the left side. The bowel and great vessels were mobilised, and careful dissection was performed to expose the anterior aspect of the lumbar spine from L3 to S1. The vasculature to L5 was identified and smaller contributing vessels such as the iliolumbar veins were ligated. Sympathetic chain was visualised and protected when possible.

The previous L4 and S1 osteotomy cuts were identified and completed with use of the ultrasonic bone cutter again by cutting from anterior to posterior to meet the former cuts under direct

vision and image intensifier. The L5 vertebra was removed and sent for histological analysis.

During the removal of L5 En bloc, a tear was caused to the left common iliac vein. This was repaired and the patient transfused intra-operatively. The removal of the L5 vertebrae also avulsed the left L5 nerve root taking the proximal root from within the thecal sac, a complication that was outlined as a strong possibility during the consenting process.

The expandable PEEK cage was assembled and filled with peptide enhanced bone graft. It was inserted under II guidance and expanded until press fit tightness and stability was achieved. The benefits of locking the posterior screws were expanding against a fixed point to deliver stability.

An overlying custom-made carbon plate and titanium screw construct was inserted covering L4 to S1. Cement augmentation was also applied for additional stability at two of the small screw sites holding the plate.

Closure was performed in layers and no further drains were inserted. Spinal cord monitoring showed some partial loss of left L5 nerve root, but activity was still noted due to cross over.

The second stage lasted approximately 9 h, with the total operating time over the two staged days equaling over 24 h. The patient was haemodynamically stable at the end of the surgery and was transferred directly to ICU.

## Post-operative management

The patient remained in Intensive Care Unit (ICU) and was transferred to the ward once stable a few days later. The patient made a steady recovery and had satisfactory post-operative check imaging (CT spine, MRI spine) with stable fixation noted.

She was reviewed daily by the Orthopaedic Complex Spine team with no major complications noted. Her left partial foot drop made small improvements during the time of her inpatient stay and she was fitted with an Ankle and Foot Orthosis splint for mobilising. She was able to mobilise as tolerated with the aid of a Thoracolumbar Sacral Orthosis brace. She received daily physiotherapy and occupational therapy and made good progress and was able to independently mobilise with the aid of a frame after 5 weeks.

She also received input from the pain team and cancer psychology support team during her admission. She developed no surgical site infections or post-operative complications such as chest infection, deep vein thromobis or pulmonary embolism.

A PET scan performed shortly prior to discharge revealed a right sided sacral fracture, although the patient was not symptomatic and did not affect her mobility. The scan also revealed the presence of possible metastases in the scapula and femur, and she was to be discussed at the Oncology MDT on discharge.

Patient was discharged after a total of 42 days. She continued her oncology follow-up which included Cyberknife deliverance of 30Gy in 5 fractions in accordance with UK consensus. The patient was well and mobilized independently pain-free 9 months postoperatively in spinal outpatient clinic with no local recurrence shown in PET scan.

# Discussion

The concept of "oligometastases" as an intermediate state between localised disease and widespread metastases was first proposed in 1995 by Hellman and Weichselbaum (3). The clinical implications of this are an opportunity to perform targeted local treatment of limited metastatic disease with the aim of potential curative treatment and progression-free survival. The spine is a common site of metastases and is a source of significant morbidity and mortality (4–6).

Tomita et al. developed the technique of Total En bloc spondylectomy (TES) *via* a two-step technique: an *en bloc* laminectomy *via* a posterior approach followed by *en bloc* resection of the anterior portion (vertebral body) with an oncological wide margin and subsequent insertion of vertebral prosthesis (1). Prior to this, conventional treatment involved piecemeal excision of malignant tissue which had a high possibility of tumour cell contamination of surrounding tissues, potentially contributing to incomplete tumour resection and recurrence of disease.

Previous reports of total corpectomy or spondylectomy for reducing local recurrence of a vertebral tumour showed positive clinical results (7–14). TES differs by involving En Bloc removal of the lesion *via* removal of the whole vertebra (both body and lamina) as one compartment (13).

Initial results for TES in thoracolumbar spinal metastases showed improved clinical outcomes such as pain relief, improved neurological deficit and prevention of impending paralysis (1). Longer-term follow up for patients undergoing TES showed mean length of survival was 38 months (rage 6–84 months) and 93% achieving local control and 32% still alive at last follow-up review (15). Similar encouraging prognostic outcomes have been shown with mortality rates less than 1%, morbidity less than 10% and median survival time longer than 3 years (16, 17).

## Stereotactic ablative radiotherapy

In relation to sarcoma, United Kingdom guidelines advise surgery as the gold standard for all adults with localised soft tissue sarcomas (18). The primary aim of surgery is to completely excise the tumour with a margin of normal tissue. Pre and/or post-operative radiotherapy is recommended along with surgical resection for majority of patients. Pre-operative treatment with chemotherapy and/or radiotherapy should also be considered depending on histology (18). Radiotherapy for intermediate and high grade sarcomas may be highly challenging, depending on the complexity of the affected body site, which could recommend the use of advanced stereotactic techniques (19).

Radiotherapy treatments for spinal oligometastatic disease include Stereotactic ablative radiotherapy (SABR). This method is beneficial as a precise high dose of radiation is targeted to the spinal lesions and causes tumour ablation whilst minimising damage to local healthy tissue (18). Several studies have shown the benefit of this treatment in oligometastatic spinal disease in outcomes such as tumour control, pain control, toxicity and morbidity (20–28).

CyberKnife is a non-surgical and non-invasive form of SABR that delivers effective tumour control (29, 30). In our patient, she was not eligible for this treatment due to the fractured posterior wall and the lesion abutting the thecal sack. In addition, the lesion was already known to be radio insensitive. Our MDT opted for surgical intervention in the form of L5 *en bloc* spondylectomy as piecemeal, palliative decompression is generally not advisable for sarcoma due to the risk of aggravation and further seeding. The patient underwent CyberKnife SABR post-operatively as part of her ongoing oncological management.

## Carbon fibre constructs

Carbon fibre implants have increasingly been used because metal hardware can limit post-operative radiotherapy due to its scattering effect of ionising radiation. Carbon fibre fixation systems (including rods and screws) can make post-operative radiotherapy easier and more effective due to its radiolucent nature and reduced interference with ionising radiation and accelerated particles (30). Studies have shown the benefit this intervention on improving radiotherapy treatment accuracy and its radiolucent benefit in the follow-up of patients to allow early detection of local recurrence (31–33). For these reasons, we decided to utilise carbon fibre pedicle screws and rods in combination with an expandable PEEK cage. To help protect the cage from migrating, we applied a custom carbon plate anteriorly.

Titanium within the target area introduces imaging artefact to the planning CT due to its very high electron density causing beam hardening, partial voluming and missing projection data, making it harder to visualize and accurately delineate the target for treatment. An MRI scan is used to help delineate the target and organs at risk, including the spinal cord / cauda equina; this scan is also affected by metal artefact which not only reduces its usefulness for delineation but also makes the task of registering the MRI to the planning CT much more difficult. Metal artefact on CT misrepresents the electron density in the area surrounding the metal, leading to inaccuracy in the calculation of dose in these regions. Furthermore, the dose calculation algorithms used by treatment planning systems are known to be less accurate at boundaries between tissues of different densities, under-estimating the dose at the interface between tissue and metal (caused by backscatter) and over-estimating the dose in the shadow of the metal (caused by increased attenuation) (34). When planning pelvic SABR treatment for patients with prosthetic hips, planning strategy would be to avoid allowing beams to enter through the prosthesis; however, this strategy is not practical for vertebral SABR, where the metalwork immediately surrounds the target area and may even pass through it.

For CyberKnife SABR treatments, the imaging artefact can also cause issues with the X-Sight Spine tracking method used to track the position of the target throughout treatment. (**Figure 2**) The tracking method uses a feature-based recognition algorithm to identify the patient position from kilovoltage images acquired every 45–90 s; this cannot be performed reliably if the images are compromised by metal artefact, so the tracking "mesh" has to be placed further away from the target.

Using carbon rather than titanium for the reconstruction resolves all these issues as the density of carbon (1.8 g/cm$^3$) is much lower than that of titanium (4.5 g/cm$^3$), so does not cause artefact in the planning image and can be modelled more accurately by the planning system.

## Cyberknife dosage fractionation

The Gross Tumour Volume and Clinical Target Volume were drawn following consensus guidelines (35) and expanded by 2 mm for PTV according to local protocol. Prescribed dose was 30Gy delivered in 5 fractions in order to meet the UK consensus dose constraint for bowel (36), with Planning Target Volume coverage compromised to meet the cauda equina (2 mm Planning Organ as Risk Volume) dose constraint. Treatment planning was performed using Accuray Precision version 2.0.1.1 and treatment was

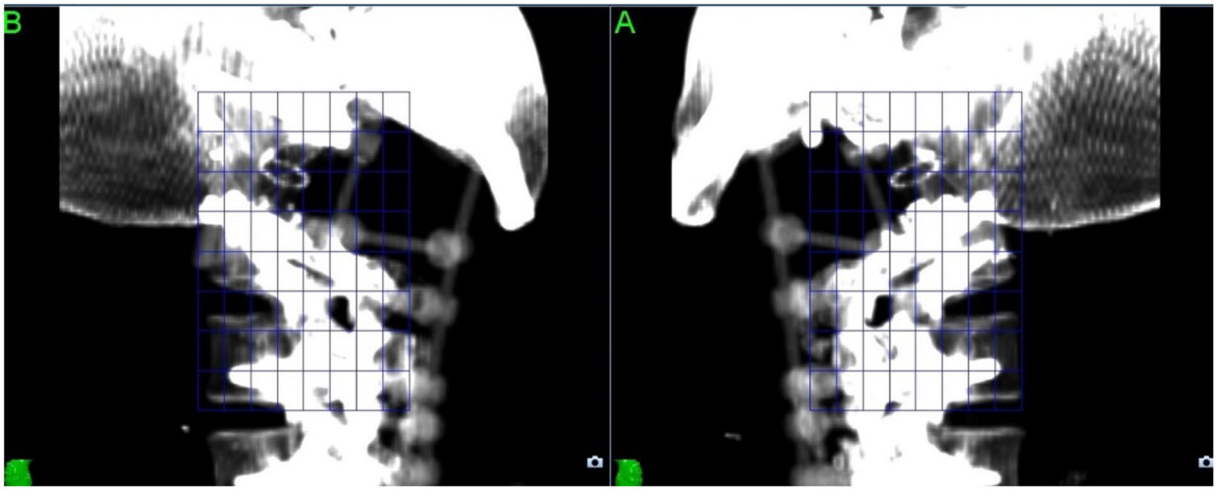


FIGURE 2
X-Sight Spine tracking DRRs from planning system.

delivered using a CyberKnife VSI with the Iris collimator. The treatment plan comprised 240 non-coplanar, non-isocentric beams with an estimated delivery time of 45 min per fraction. Because of the use of carbon fixtures for the reconstruction, we were able to track directly on the target area with no issues (**Figure 3**).

## Custom 3d printed surgical navigation guide

To aid with the carbon fibre pedicle screw placement, we used a custom 3D printed surgical navigation guide (37). Custom 3D printed guides have been shown in a recent systematic review and meta-analysis to reduce operative time, blood loss and achieve excellent screw placement compared with freehand techniques (38). We specifically required the guide to enable the S1 screws divergence to allow for the S1 cuts. The S2AI screw head alignment needed to be perfectly aligned with lumbar segment as there is no flexibility and is totally rigid with the construct. The low polyaxial nature of the screws makes them similar to monoblock screws which means cephalad caudal alignment is as important to medial lateral alignment so that the rod sits flush to the tulip at each level.

## Radiofrequency ablation

Prior to pedicle insertion, we used cool Radiofrequency Ablation System for theoretical destruction of sarcoma cells

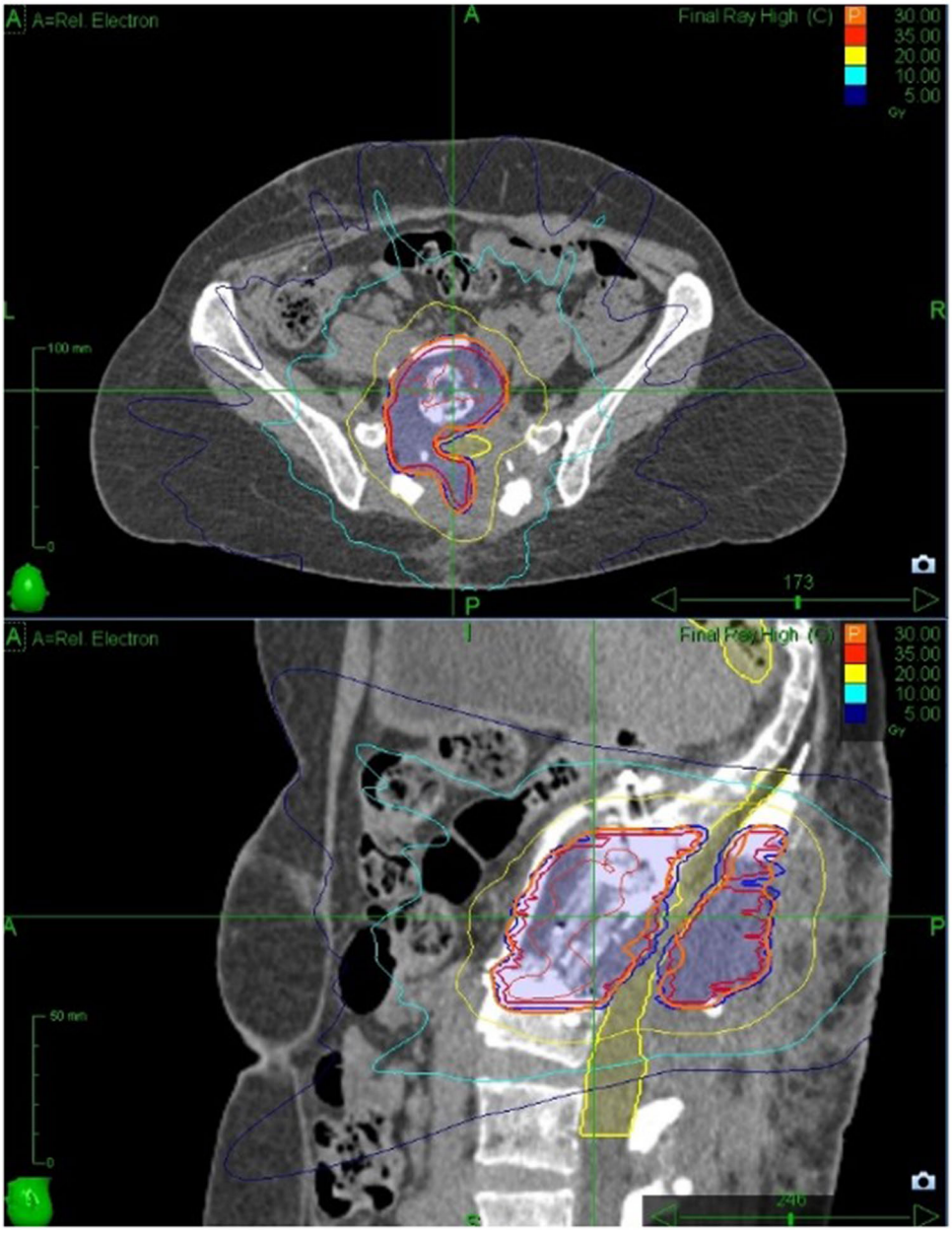


FIGURE 3
Dose distribution from planning system.

to prevent live tissue seeding. Studies have also shown its benefit in pain improvement in patients with metastatic bone disease (39).

### Spinal surgery infection prophylaxis

Following fixation of the cage construct, we applied antibiotic-impregnated calcium sulphate beads into the wound upon closure. These beads have been increasingly used in certain orthopaedic procedures as it has proven efficacy against biofilms and has predictable supra-therapeutic antibiotic elution profile over 40 days (40, 41). It has also been shown to be beneficial in several spinal implant fixation cases (42–44).

### Peptide enhanced bone graft

The expandable PEEK cage was filled a peptide enhanced bone graft which allows ectopic bone growth on the implant only. Studies have shown its high efficacy in spinal fusion rates with good post-surgical outcomes, including in patients with poor bone regenerative capacity quality (45, 46).

### Multidisciplinary approach

As this was a surgically complex case with high risk for morbidity and mortality, we adopted a multi-surgical specialty approach including the help of our hospital Vascular surgery team. The anterior approach to the lumbar spine is often not favoured by spinal surgeons or neurosurgeons due to the unfamiliarity and potential risk of serious vascular or visceral damage (47). Vascular complications are often related to the need to mobilise the great retroperitoneal vessels and other adjacent structures for exposure to the anterior lumbar spine. It is argued that the operating team should require vascular and general surgical skills in order to both perform the exposure and deal with any resulting complications (47). Although there has been debate about whether the presence of an "access surgeon" has a beneficial effect on complication rates for anterior lumbar spinal surgery, a recent systematic review and meta-analysis did report lower overall postoperative complication rates, lower reoperation rates and lower prosthesis complications and recommended availability of an access surgeon where exposure may be difficult (47–50). We greatly appreciated the expertise of our vascular surgeon and indeed required his specialist input intra-operatively when there was a tear to the left common iliac vein which was successfully repaired.

## Take-away lessons

We present a challenging case of an L5 *en bloc* spondylectomy for a case of oligometastatic liposarcoma performed at our specialist complex spinal unit. Our reported extensive pre-operative planning and specialist intra-operative techniques may be of assistance to others taking on these surgically challenging cases. We recommend a truly multi-disciplinary team approach for pre, intra and post-operative stages when managing such complex cases including Complex Spine team, Neurosurgery, Vascular surgery, Anaesthetics, Intensive care, Radiologists, Radiotherapy Physicists, Oncologists, Physiotherapy, Occupational therapists, Psychologists and specialist nursing staff.

## Patient perspective

Thank you very much to the spinal team and my doctors that performed this surgery and saving my life. I received excellent care before I got admitted, before my operation, during my hospital stay and was kindly looked followed up when I went home. The surgeons were very reassuring and provided me with good care. I also received lots of reassurance and support during my cancer hospital follow up when getting radiotherapy after my operation.

## Data availability statement

The raw data supporting the conclusions of this article will be made available by the authors, without undue reservation.

## Ethics statement

Ethical review and approval was not required for the study on human participants in accordance with the local legislation and institutional requirements. The patients/participants provided their written informed consent to participate in this study. Written informed consent was obtained from the individual(s) for the publication of any potentially identifiable images or data included in this article.

## Author contributions

PS—Writing—Original draft write up, Data curation, patient follow-up. MR—Writing –Original draft review & editing, Data curation, patient follow-up. AF—Writing—review & editing, patient Care—Orthopaedic Spine Surgeon. BA—Writing—review & editing, Patient Care—Physician Associate. TB—Writing—review & editing, Patient Care—Orthopaedic Spine Surgeon. JB—Writing—review & editing, Patient Care—Orthopaedic Spine Surgeon. SZ—Writing—review & editing, Patient Care—Sarcoma Specialist. AM—Writing—review & editing, Patient Care—Sarcoma Specialist. MA—Writing—review & editing, Patient Care—Vascular Surgeon. PM—Writing– review & editing, Patient Care -Neurological Surgeon. DL—Conceptualization, Data curation, Formal analysis, Investigation, Methodology, Project administration, Writing–review & editing, Patient Care—Orthopaedic Spine Surgeon. All authors contributed to the article and approved the submitted version.

## Conflict of interest

The authors declare that the research was conducted in the absence of any commercial or financial relationships that could be construed as a potential conflict of interest.

## Publisher's note

All claims expressed in this article are solely those of the authors and do not necessarily represent those of their affiliated organizations, or those of the publisher, the editors and the reviewers. Any product that may be evaluated in this article, or claim that may be made by its manufacturer, is not guaranteed or endorsed by the publisher.

## Supplementary material

The Supplementary Material for this article can be found online at: https://www.frontiersin.org/articles/10.3389/fsurg.2023.1110580/full#supplementary-material.

## References


1. Tomita K, Kawahara N, Baba H, Tsuchiya H, Nagata S, Toribatake Y. Total en bloc spondylectomy for solitary spinal metastases. *Int Orthop*. (1994) 18(5):291–8. doi: 10.1007/bf00180229

2. Tomita K, Kawahara N, Baba H, Tsuchiya H, Fujita T, Toribatake Y. Total en bloc spondylectomy. *Spine*. (1997) 22(3):324–33. doi: 10.1097/00007632-199702010-00018

3. Hellman S, Weichselbaum RR. Oligometastases. *J Clin Oncol*. (1995) 13(1):8–10. doi: 10.1200/jco.1995.13.1.8

4. Zeng KL, Tseng C-L, Soliman H, Weiss Y, Sahgal A, Myrehaug S. Stereotactic body radiotherapy (SBRT) for oligometastatic spine metastases: an overview. *Front Oncol*. (2019) 9:337. doi: 10.3389/fonc.2019.00337

5. Torregrossa F, Brunasso L, Musso S, Benigno UE, Gerardi RM, Bonosi L, et al. The palliative care in the metastatic spinal tumors. A systematic review on the radiotherapy and surgical perspective. *Life*. (2020) 12(4):571. doi: 10.3390/life12040571

6. Ferini G, Palmisciano P, Scalia G, Haider AS, Bin-Alamer O, Sagoo NS, et al. The role of radiation therapy in the treatment of spine metastases from hepatocellular carcinoma: a systematic review and meta-analysis. *Neurosurg Focus*. (2022) 53(5):E12. doi: 10.3171/2022.8.FOCUS2255

7. Roy-Camille R, Mazel CH, Saillant G, Lapresle PH. Treatment of malignant tumor of the spine with posterior instrumentation. In: N Sundaresan, HH Schmidek, AL Schiller, DI Rosenthal, editors. *Tumor of the spine*. Philadelphia: Saunders (1990). p. 473–87.

8. Abitbol J-J. Tumors of the spine: diagnosis and clinical management, by N. Sundaresan, HH schmidek, Al Schiller, Di Rosenthal, editors. W.B. Saunders, Philadelphia, 1990 574 pp., 512 illus. *J Orthop Res*. (1991) 9(2):306–306. doi: 10.1002/jor.1100090220

9. Roy-Camille R, Saillant G, Bisserié M, Judet T, Hautefort E, Mamoudy P. Résection vertébrale totale dans la chirurgie tumorale au niveau du rachis dorsal par voie postérieure pure. Technique—indications [total excision of thoracic vertebrae (author's Transl)]. *Rev Chir Orthop Reparatrice Appar Mot*. (1981) 67(3):421–30. Roy-Camille R. Nouvelles perspectives en chirurgie du rachis. *Int Orthop*. (1989) 13(2). doi: 10.1007/bf00266367

10. Stener B. Total spondylectomy in chondrosarcoma arising from the seventh thoracic vertebra. *J Bone Joint Surg Br*. (1971) 53-B(2):288–95. doi: 10.1302/0301-620x.53b2.288

11. Stener B. Complete removal of vertebrae for extirpation of tumors. *Clin Orthop Relat Res*. (1989) 245:72–82. doi: 10.1097/00003086-198908000-00013

12. Stener B. Technique of complete spondylectomy in the thoracic and lumbar spine. In: N Sundaresan, HH Schmidek, AL Schiller, DI Rosenthal, editors. *Tumor of the spine*. Philadelphia: Saunders (1990). p. 432–7.

13. Sundaresan N, Rosen G, Huvos AG, Krol G. Combined treatment of osteosarcoma of the spine. *Neurosurgery*. (1988) 23(6):714–9. doi: 10.1097/00006123-198812000-00005

14. Boriani S, Biagini R, De Iure F, Di Fiore M, Gamberini G, Zanoni A. Lumbar vertebrectomy for the treatment of bone tumors: surgical technique. *Chir Organi Mov*. (1994) 79(2):163–73.

15. Tomita K, Kawahara N, Murakami H, Demura S. Total en bloc spondylectomy for spinal tumors: improvement of the technique and its associated basic background. *J Orthop Sci*. (2006) 11(1):3–12. doi: 10.1007/s00776-005-0964-y

16. Tomita K, Kawahara N, Kobayashi T, Yoshida A, Murakami H, Akamaru T. Surgical strategy for spinal metastases. *Spine*. (2001) 26(3):298–306. doi: 10.1097/00007632-200102010-00016

17. Yao KC, Boriani S, Gokaslan ZL, Sundaresan N. En bloc spondylectomy for spinal metastases: a review of techniques. *Neurosurg Focus*. (2003) 15(5):E6. Published 2003 Nov 15. doi: 10.3171/foc.2003.15.5.6.

18. Dangoor A, Seddon B, Gerrand C, Grimer R, Whelan J, Judson I. UK Guidelines for the management of soft tissue sarcomas. *Clin Sarcoma Res*. (2016) 6:20. Published 2016 Nov 15. doi: 10.1186/s13569-016-0060-4

19. Ferini G, Palmisciano P, Zagardo V, Viola A, Illari SI, Marchese V, et al. Combining a customized immobilization system with an innovative use of the ExacTrac system for precise volumetric modulated arc therapy of challenging forearm sarcomas. *Pract Radiat Oncol*. (2022) 12(6):S1879-8500(22)00328-9. doi: 10.1016/j.prro.2022.10.005

20. Clinic M. Stereotactic Radiosurgery. Mayo Clinic. https://www.mayoclinic.org/tests-procedures/stereotactic-radiosurgery/about/pac-20384526 Published April 27, 2019. Accessed October 24, 2022.

21. Ho JC, Tang C, Deegan BJ, Allen PK, Jonasch E, Amini B, et al. The use of spine stereotactic radiosurgery for oligometastatic disease. *J Neurosurg Spine*. (2016) 25(2):239–47. doi: 10.3171/2016.1.SPINE151166

22. Chang JH, Gandhidasan S, Finnigan R, Whalley D, Nair R, Herschtal A, et al. Stereotactic ablative body radiotherapy for the treatment of spinal oligometastases. *Clin Oncol (R Coll Radiol)*. (2017) 29(7):e119–25. doi: 10.1016/j.clon.2017.02.004

23. Koontz BF. Stereotactic body radiation therapy for oligometastatic prostate cancer: the hunt for the silver bullet. *Int J Radiat Oncol Biol Phys*. (2017) 99(4):761–3. doi: 10.1016/j.ijrobp.2017.05.020

24. Barzilai O, Versteeg AL, Sahgal A, Rhines LD, Bilsky MH, Sciubba DM, et al. Survival, local control, and health-related quality of life in patients with oligometastatic and polymetastatic spinal tumors: a multicenter, international study. *Cancer*. (2019) 125(5):770–8. doi: 10.1002/cncr.31870

25. Ahmed KA, Stauder MC, Miller RC, Bauer HJ, Rose PS, Olivier KR, et al. Stereotactic body radiation therapy in spinal metastases. *Int J Radiat Oncol Biol Phys*. (2012) 82(5):e803–9. doi: 10.1016/j.ijrobp.2011.11.036

26. Silva SR, Gliniewicz A, Martin B, Prabhu VC, Germanwala AV, Melian E, et al. Oligometastatic disease state is associated with improved local control in patients undergoing three or five fraction spine stereotactic body radiotherapy. *World Neurosurg*. (2019) 122:e342–8. doi: 10.1016/j.wneu.2018.10.044

27. Thibault I, Al-Omair A, Masucci GL, Masson-Côté L, Lochray F, Korol R, et al. Spine stereotactic body radiotherapy for renal cell cancer spinal metastases: analysis of outcomes and risk of vertebral compression fracture. *J Neurosurg Spine*. (2014) 21(5):711–8. doi: 10.3171/2014.7.SPINE13895

28. Yamada Y, Bilsky MH, Lovelock DM, Venkatraman ES, Toner S, Johnson J, et al. High-dose, single-fraction image-guided intensity-modulated radiotherapy for metastatic spinal lesions. *Int J Radiat Oncol Biol Phys*. (2008) 71(2):484–90. doi: 10.1016/j.ijrobp.2007.11.046

29. Kam TY, Chan OSH, Hung AWM, Yeung RMW. Utilization of stereotactic ablative radiotherapy in oligometastatic & oligoprogressive skeletal metastases: results and pattern of failure. *Asia Pac J Clin Oncol*. (2019) 15(Suppl 2):14–9. doi: 10.1111/ajco.13115

30. Pontoriero A, Iatì G, Cacciola A, Conti A, Brogna A, Siragusa C, et al. Stereotactic body radiation therapy with simultaneous integrated boost in patients with spinal metastases. *Technol Cancer Res Treat*. (2020) 19:19. doi: 10.1177/1533033820904447

31. Tedesco G, Gasbarrini A, Bandiera S, Ghermandi R, Boriani S. Composite PEEK/carbon fiber implants can increase the effectiveness of radiotherapy in the management of spine tumors [published correction appears in J spine surg. 2018 mar;4(1):167]. *J Spine Surg*. (2017) 3(3):323–9. doi: 10.21037/jss.2017.06.20

32. Boriani S, Tedesco G, Ming L, Ghermandi R, Amichetti M, Fossati P, et al. Carbon-fiber-reinforced PEEK fixation system in the treatment of spine tumors: a preliminary report. *Eur Spine J*. (2018) 27(4):874–81. doi: 10.1007/s00586-017-5258-5

33. Laux CJ, Hodel SM, Farshad M, Müller DA. Carbon fibre/polyether ether ketone (CF/PEEK) implants in orthopaedic oncology. *World J Surg Oncol*. (2018) 16(1):241. Published 2018 Dec 28. doi: 10.1186/s12957-018-1545-9

34. Wang X, Yang JN, Li X, Tailor R, Vassilliev O, Brown P, et al. Effect of spine hardware on small spinal stereotactic radiosurgery dosimetry. *Phys Med Biol*. (2013) 58(19):6733–47. doi: 10.1088/0031-9155/58/19/6733

35. Redmond KJ, Lo SS, Soltys SG, Yamada Y, Barani IJ, Brown PD, et al. Consensus guidelines for postoperative stereotactic body radiation therapy for spinal metastases: results of an international survey. *J Neurosurg Spine*. (2017) 26(3):299–306. doi: 10.3171/2016.8.SPINE16121

36. Hanna GG, Murray L, Patel R, Jain S, Aitken KL, Franks KN, et al. UK Consensus on normal tissue dose constraints for stereotactic radiotherapy. *Clin Oncol (R Coll Radiol)*. (2018) 30(1):5–14. doi: 10.1016/j.clon.2017.09.007

37. Costanzo R, Ferini G, Brunasso L, Bonosi L, Porzio M, Benigno UE, et al. The role of 3D-printed custom-made vertebral body implants in the treatment of spinal tumors: a systematic review. *Life*. (2022) 12(4):489. doi: 10.3390/life12040489

38. Wallace N, Butt BB, Aleem I, Patel R. Three-dimensional printed drill guides versus fluoroscopic-guided freehand technique for pedicle screw placement: a systematic review and meta-analysis of radiographic, operative, and clinical outcomes. *Clin Spine Surg*. (2020) 33(8):314–22. doi: 10.1097/BSD.0000000000001023

39. Levy J, Hopkins T, Morris J, Tran ND, David E, Massari F, et al. Radiofrequency ablation for the palliative treatment of bone metastases: outcomes from the multicenter OsteoCool tumor ablation post-market study (OPuS one study) in 100 patients. *J Vasc Interv Radiol*. (2020) 31(11):1745–52. doi: 10.1016/j.jvir.2020.07.014

40. Delury C, Aiken S, Thomas H. *Determining the efficacy of antibiotic-loaded calcium sulfate beads against Pre-formed biofilms: An in vitro study, in ASM microbe*. San Francisco, USA: Biocomposites, STIMULAN (2019).

41. Cooper JJ, Aiken SS, Laycock PA. *Antibiotic stability in a synthetic calcium sulphate carrier for local delivery, in 32nd annual meeting of the European bone and joint infection society*. Prague: Czech Republic (2013).

42. Upendra B, Kanna R, Khurjekar K, Mahesh B, Badve S. The spine clinics – postoperative spinal infections—clinical scenarios. *Indian Spine J*. (2018) 1(1):32–45. doi: 10.4103/isj.isj_38_17

43. Chang MY, Chen MH, Chang CJ, Huang JS. Preliminary clinical experience with polyetheretherketone cages filled with synthetic crystallic semihydrate form of calcium sulfate for anterior cervical discectomy and fusion. *Formos J Surg [Internet]*. (2013) 46 (4):109–15. doi: 10.1016/j.fjs.2013.04.005

44. Stathakpoulos DP, Kyratzoulis IM. Percutaneous Injectable Synthetic Calcium Sulfate for the Enhancement of Percutaneous Spinal Fusion (Poster presentation) Injectable and Implantable Biomaterials and Biologics for Tissue Regeneration 17th Interdisciplinary Research Conference on Biomaterials. St. Catherine's College, Oxford, UK., Tissue Engineering. (2007) 13:1367–92.

45. Arnold PM, Sasso RC, Janssen ME, Fehlings MG, Smucker JD, Vaccaro AR, et al. Efficacy of i-factor bone graft versus autograft in anterior cervical discectomy and fusion: results of the prospective, randomized, single-blinded food and drug administration investigational device exemption study. *Spine*. (2016) 41(13):1075–83. doi: 10.1097/BRS.0000000000001466

46. Jacobsen MK, Andresen AK, Jespersen AB, Støttrup C, Carreon LY, Overgaard S, et al. Randomized double blind clinical trial of ABM/P-15 versus allograft in noninstrumented lumbar fusion surgery. *Spine J*. (2020) 20(5):677–84. doi: 10.1016/j.spinee.2020.01.009

47. Asha MJ, Choksey MS, Shad A, Roberts P, Imray C. The role of the vascular surgeon in anterior lumbar spine surgery. *Br J Neurosurg*. (2012) 26(4):499–503. doi: 10.3109/02688697.2012.680629

48. Jarrett CD, Heller JG, Tsai L. Anterior exposure of the lumbar spine with and without an "access surgeon": morbidity analysis of 265 consecutive cases. *J Spinal Disord Tech*. (2009) 22(8):559–64. doi: 10.1097/BSD.0b013e318192e326

49. Quraishi NA, Konig M, Booker SJ, Shafafy M, Boszczyk BM, Grevitt MP, et al. Access related complications in anterior lumbar surgery performed by spinal surgeons. *Eur Spine J*. (2013) 22 Suppl 1(Suppl 1):S16–20. doi: 10.1007/s00586-012-2616-1

50. Phan K, Xu J, Scherman DB, Rao PJ, Mobbs RJ. Anterior lumbar interbody fusion with and without an "access surgeon": a systematic review and meta-analysis. *Spine*. (2017) 42(10):E592–601. doi: 10.1097/BRS.0000000000001905

frontiers | Frontiers in Surgery

TYPE Case Report
PUBLISHED 17 March 2023
DOI 10.3389/fsurg.2023.1094472



OPEN ACCESS

EDITED BY
Zhaolun Cai,
Sichuan University, China

REVIEWED BY
Yi Lu,
Peking Union Medical College Hospital (CAMS), China
Nikolaos Zavras,
University General Hospital Attikon, Greece

*CORRESPONDENCE
Jun Qi
qijun@xinhuamed.com.cn

SPECIALTY SECTION
This article was submitted to Surgical Oncology, a section of the journal Frontiers in Surgery

RECEIVED 10 November 2022
ACCEPTED 20 February 2023
PUBLISHED 17 March 2023

CITATION
Yu M, Zhou J, Shangguan X, Qian S, Ding J and Qi J (2023) Nephron sparing surgery for a patient with a complicated solitary functioning kidney and a giant pT3 renal cell carcinoma: A case report.
Front. Surg. 10:1094472.
doi: 10.3389/fsurg.2023.1094472



# Nephron sparing surgery for a patient with a complicated solitary functioning kidney and a giant pT3 renal cell carcinoma: A case report

Minghao Yu, Jiatong Zhou, Xun Shangguan, Subo Qian, Jie Ding and Jun Qi*

Department of Urology, Xinhua Hospital Affiliated to Shanghai Jiaotong University School of Medicine, Shanghai, China

A solitary functioning kidney (SFK) with renal cell carcinoma (RCC) is an imperative indication for nephron-sparing surgery (NSS). Nevertheless, a giant pT3 RCC mass (maximum diameter >20 cm) on the functioning side of a patient with SFK is extremely rare. However, whether NSS is more beneficial than radical nephrectomy (RN) in such patients is controversial. Here, we present the case of a 71-year-old female patient with a 20 cm*16 cm RCC mass in the SFK, who initially presented with hematuria and acute urinary tract obstructive anuria caused by renal calculi. The patient underwent NSS treatment after our evaluation, and the 26-month follow-up revealed that her renal function recovered to the state before the tumor formation. In addition, no relapse or metastasis was detected.

KEYWORDS

solitary functioning kidney, nephron-sparing surgery, renal cell carcinoma, acute upper ureteral obstruction, case report, open nephrectomy

## Introduction

Solitary functioning kidneys (SFK), whether congenital or acquired, are very common in the clinic. However, when malignant tumors occur in the unilaterally functioning kidney, the condition of patients with SFK becomes much more complicated. Providing proper management for these patients and improving the prognosis remains a knotty problem for urologists.

Nephron-sparing surgery (NSS) is the standard treatment for patients with tumors in the SFK. Although partial renal parenchyma has been reserved after NSS, the question of whether patients could achieve oncological control and renal function preservation depends on the tumor size, together with the presence of serosal infiltration, lymph node involvement, and distant metastasis. In addition, the surgical scheme, the skills of surgeons, and rational adjuvant therapy are also closely related to good long-term prospects. Owing to the difficulty of achieving total excision during the operation, tumors with a locally extensive size have a higher relapse or metastasis rate than small ones after NSS (1). Therefore, the National Comprehensive Cancer Network Clinical Practice Guidelines in Oncology (NCCN Guidelines, V1.2021) recommend only NSS for patients with stage pT3 when it is clinically indicated (2). However, both the American Urological Association Guidelines (AUA Guidelines, 2021) and the European Association of Urology Guidelines (EUA Guidelines, 2022) do not recommend NSS for patients with pT3 RCC (3). Selecting NSS or radical nephrectomy (RN) for patients with RCC in the SFK remains a matter of controversy.

Herein, we report the case of a patient with pT3aN0M0 renal cell carcinoma (RCC) in the SFK. The patient displayed symptoms of acute upper ureteral obstruction and was

diagnosed with a 20 cm*16 cm malignant tumor mass in the right kidney by positron emission tomography-computed tomography (PET-CT) imaging, in addition to a pathological examination in Shanghai, China. After a multidisciplinary discussion, our surgery team implemented an NSS scheme on the patient that included open right partial nephrectomy, together with the removal of calculi, pyeloureteroplasty, and nephrostomy. The most recent renal function examination showed that the serum creatine (SCr) level, the blood urea nitrogen (BUN) level and the estimated glomerular filtration rate (eGFR) were close to those before RCC formation. So far, no serious surgical complications or acute renal injury (AKI) have occurred, and a postoperative follow-up revealed no metastasis. We present the following article under the CARE reporting checklist.

## Case presentation

A 71-year-old female was referred to the outpatient clinic of our hospital because of non-induced hematuria for 1 week and anuria for 1 day, accompanied by a fever (38.7°C) (4 July 2020). The patient was in poor health since she had suffered from hypertension and diabetes for many years. Her left kidney failed to function because of atrophy caused by unilateral renal calculi 20 years ago (eGFR of the left kidney: 2.64 ml/min/1.73 $m^2$). Bilateral multiple renal calculi were found under a B-ultrasound. In addition, CT imaging of the abdomen showed a right renal mass (211 mm × 159 mm) but revealed no hemorrhagic foci around the mass or thrombi in the renal vein (Figure 1A). The SCr level indicated serious renal decompensation (456.7 umol/L). Since the right renal mass showed no signs of rupture, we initially attributed the hematuria and fever symptoms to the acute upper ureteral obstruction caused by renal calculi. In order to alleviate the symptoms of urinary tract obstruction and infection, we performed ureteroscopic lithotripsy and double-J stent placement in the right ureter along with anti-infection treatment (5 July 2020). However, the patient presented with gross hematuria, dysuria, and fever again only a few days after the double-J stent was removed (30 July 2020). A PET/CT scan revealed a space-occupying lesion with increased metabolism at the lower pole of the right kidney but no obvious metastasis in the whole body. Several enhancement patterns around the mass were also presented by the scan, and we considered them to be signs of hemorrhage (30 July 2020). The laboratory examination revealed that the SCr level was 187.6 μmol/L, and the BUN level was 19 mmol/L, which indicated that renal decompensation still existed. The renal function test showed that the eGFR of the right kidney was 23.9 ml/min/1.73 $m^2$ (31 July 2020). To study the characteristics of the giant mass, an ultrasound-guided renal biopsy was performed, and pathology reported RCC [renal adenocarcinoma, grade IV according to the International Society of Urological Pathology (ISUP) grading system, with transcription factor EB (TFEB) amplification] (31 July 2020) (Figure 2A). As the patient and her family requested to preserve renal function, our surgical team decided to perform NSS on the patient after a discussion, using RN and emergency hemodialysis as alternate schemes.

Considering the large size of the renal mass, our surgical team settled on an open partial nephrectomy (OPN) to remove it. The operation was scheduled 18 days after the biopsy (18 August 2020). We prescribed Amlodipine Besylate and Novolin to control blood pressure and blood glucose, in addition to Aztreonam for anti-infection before the operation. The CT angiography (CTA) presented the origin of the extrarenal arterial blood supply of the tumor mass but revealed no vascular abnormalities in the functioning kidney (5 August 2020). The preoperative dialysis was performed to depress the SCr level, and the SCr level was 234.6 umol/L before the operation (17 August 2020). In addition, steps were taken to ensure that the liver and kidney functioned normally so that the patient could tolerate the surgery. During the operation, an L-shaped incision was made by the surgeon in the right upper abdomen, finding the giant RCC mass on the ventral side of the lower right kidney with ureteral dilatation. The surgeon completed the dissection of the perirenal adipose tissue in order to expose the tumor mass and shifted a considerable part of the mass out of the body for the convenience of surgical operations. In addition to the tumor resection, the surgeon removed the calculi in the upper segment of the renal pelvis and ureter and a part of the renal calyces and then performed the right pyeloureteroplasty procedure to help maintain renal function and a nephrostomy to facilitate postoperative drainage. The renal artery was clamped during the mass resection, and the total ischemia time was 110 min. Thus, our surgical team placed ice crumbles around the surgical field to reduce the renal surface temperature and preserve renal function. The total bleeding volume was 800 mL, and the transfused red blood cells (RBCs) and plasma levels were 4U and 400 mL, respectively. The resected mass weighed 5.8 kg (Figures 2B–D). A postoperative abdominal CT scan (August 25, 2020) indicated the total resection of the RCC mass (Figure 1B), and a pathological examination of the RCC mass showed that the renal sinus adipose tissue was involved locally, with no obvious breakthrough of fibrous capsule and no tumor involvement in the renal cutting edge or perirenal adipose tissue (pT3aM0N0, UISS III). After nearly 2 weeks of the surgery, the result of a renal function examination revealed that the SCr level was 240.8 μmol/L and the BUN level was 10 mmol/L (30 August 2020). The patient did not take any medicine after NSS and was followed up every 3 months. Now, 26 months have passed since the operation, and the latest chest and abdominal CT scanning showed no sign of relapse or metastasis (June 3, 2022) (Figure 1C). In addition, the most recent follow-up revealed that the SCr level was 189.5 umol/L (Figure 1D), the BUN was 17.74 mmol/L, and the eGFR of the right kidney was 30.3 ml/min/1.73 $m^2$ (22 August 2022). The complete timeline is shown in Figure 3.

## Discussion

SFK refers to a condition in which patients have two kidneys anatomically but have to rely on one to support normal physiological activity since the other one has failed to function.

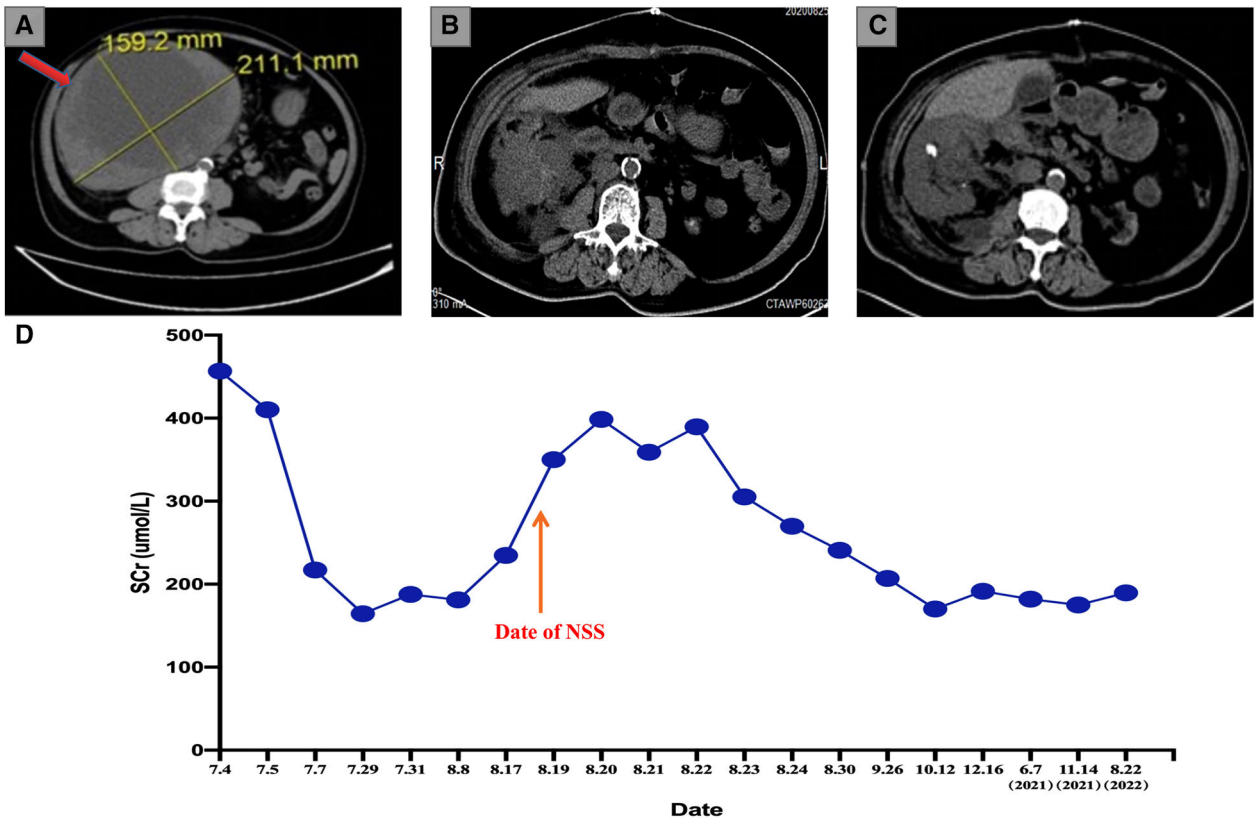


FIGURE 1
(A) Preoperative abdominal CT examination showing a 20 cm*16 cm RCC mass (the red arrow). (B) Abdominal CT scan after 1 week of the operation indicates a complete resection of the giant RCC mass. (C) The most recent abdominal CT scan indicates no sign of relapse. (D) The tendency chart presents the changes in the SCr level along with the progression of disease and treatment. CT, computed tomography; RCC, renal cell carcinoma; SCr, serum creatine.

Acquired SFK usually results from unilateral renal trauma or severe calculus obstruction. When the acquired SFK is complicated with RCC, the tumor mass on the functioning side always leads to renal failure. Thus, for those patients with acquired SFK and RCC in whom surgery is indicated, a timely resection of the tumor mass is vital for saving their lives. Choosing the appropriate type of operation is the key to reliable oncological control and decreasing the probability of postoperative complications for these patients.

SFK is considered the imperative indication for NSS, while NSS is not recommended for pT3/pT4 RCC patients (2, 3). For patients with pT3 RCC, most guidelines recommend RN for tumor resection. When surgeons deal with pT3 RCC in patients with SFK, the question of which type of treatment, NSS or RN, could benefit patients more begs an answer. The major advantage of NSS for patients with SFK is to preserve a partially functioning kidney and prevent them from submitting to renal replacement therapy or renal transplantation. In addition, accumulating evidence supports that NSS could achieve similar overall survival (OS) and cancer-specific survival (CSS) rates with RN, and the preservation of renal function helps patients improve their quality of life after the operation. Moreover, NSS significantly reduces the incidence of long-term cardiovascular accidents and chronic kidney disease (CKD). However, performing NSS on patients with pT3 RCC is a great challenge for surgeons, as the radical resection of RCC masses is difficult to perform during NSS. Studies have shown that for patients with pT2-pT4 RCC, margin positive rates are higher in those who receive NSS than in those who receive RN. Due to the relatively long operation and ischemia time, patients with a large-volume RCC who undergo NSS are prone to having short-term complications (4–6). In summary, we can conclude from the above comparison that NSS and RN have their own advantages and disadvantages in dealing with patients with pT3 RCC. In terms of the surgical approach, laparoscopic nephrectomy has been proven to have many advantages, while we chose OPN for our patient because of its ease of operation and to avoid tumor rupture during resection. No serious complication occurred after the OPN procedure, which proves that OPN is still a good choice when handling locally complicated and large RCCs.

Preoperative examination and treatment are indispensable steps in the process of resection. A general examination should be carried out to check whether general health conditions such as blood pressure, cardiac function, pulmonary function, and so on enable patients to withstand surgery. Adjustments for comorbidities in addition to abnormal bleeding and coagulation

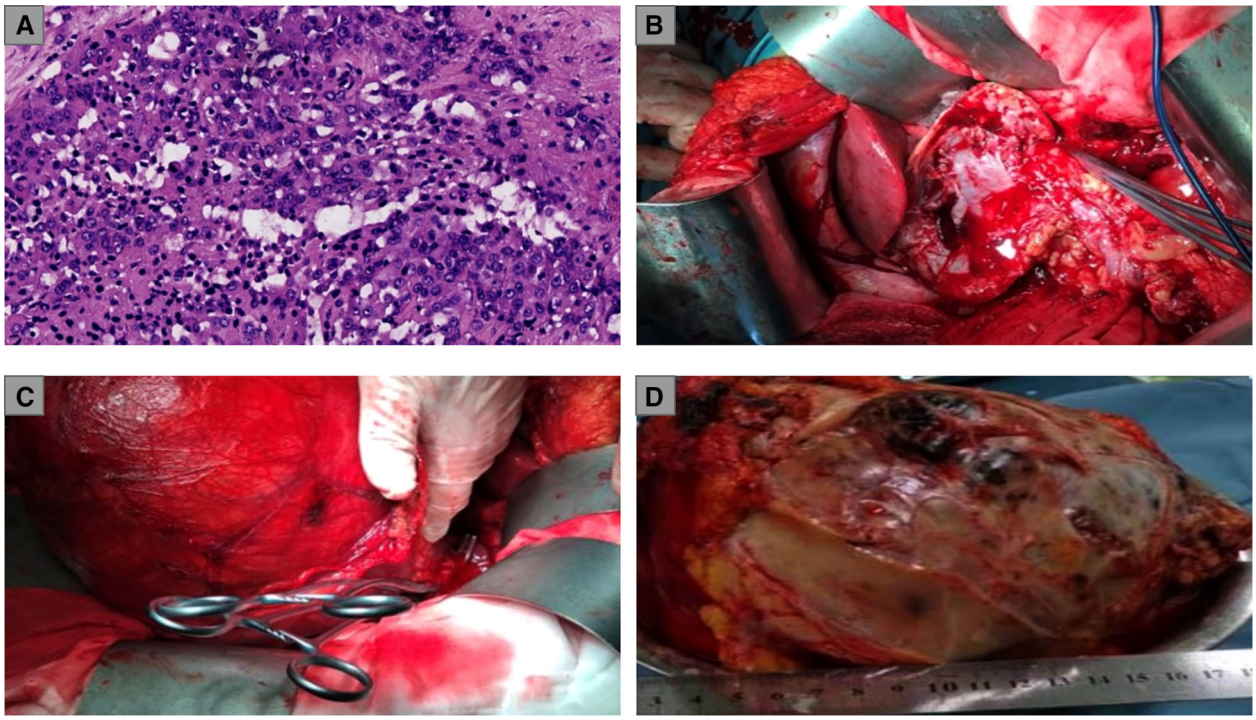


FIGURE 2
(A) Pathological examination of renal biopsies: renal adenocarcinoma, ISUP grade IV; (B) Exposure of the surgical field and the clamping of the renal artery; (C) A considerable part of the RCC mass was shifted out of the body for the convenience of surgical operations; (D) weighing and measurement of the RCC mass. ISUP, International Society of Urological Pathology; RCC, renal cell carcinoma.

function are necessary. For patients with poor general conditions, NSS is not recommended (7). The preoperative eGFR and Scr levels need to be evaluated to check renal function before surgery. The abdominal CT scan and CTA assist surgeons to assess the tumor complexity and uncover aberrant vessels, which are crucial for the evaluation of surgical complexity and outcomes. Clinical trials of neoadjuvant TKI-drug therapy found that high-risk RCC patients (pT3, pT4, and N+) enjoyed disease-free survival (DFS) benefits and a reduction in tumor volume (8). The results indicated that preoperative neoadjuvant therapy with targeted drugs could help some patients switch from RN to NSS. The patient in our case did not receive neoadjuvant therapy before the operation. Owing to the symptoms of acute ureteral obstruction and the huge volume of RCC mass, urgent surgery was required, and hence, we dealt with only her basic disease condition and decreased the SCr level.

Surgeons might choose RN to ensure the total resection of RCC masses from patients with pT3 RCC in an SFK, which will reduce the risk of tumor relapse. However, the most prominent disadvantage of this surgical choice is that patients need to receive renal transplantation or long-term hemodialysis after RN. This will severely affect their daily lives and place a huge economic burden on their families. Therefore, in addition to a comprehensive evaluation of the patient and tumor, the opinions of the patient and their family are also very important when choosing the type of surgery. Before a decision is made on the surgical scheme, surgeons should fully communicate with patients and their families and honor the wishes of patients. Our patient and her family strongly requested that we preserve the functioning kidney, and in response, we carefully considered the opinions of the patient and her family before making the decision.

We have summarized some key points that were worth noting during NSS. Before blocking the renal artery, the size and firmness of the artery clamp should be checked in order to avoid incomplete blocking of vessels, which might cause intraoperative bleeding. The surgeon has to mark the resection range of the tumor mass along

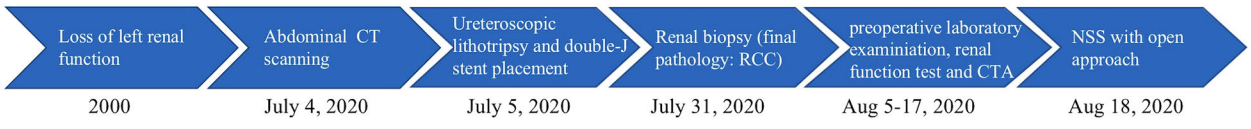


FIGURE 3
Timeline of the medical history, examination, and treatment.

the edge of the normal renal tissue to make sure that the mass or the pseudocapsule is not ruptured, and then, carefully cut approximately 0.5 cm–1 cm away from the edge of the mass to maintain the integrity of the tumor capsule, which is significant for complete excision and preventing tumor rupture during NSS. It is widely recognized that a short ischemia time is crucial for preserving renal function after the operation. Previous research suggested that human kidneys could tolerate 30–60 min of controlled clamp ischemia with minor damage renal parenchyma and no acute renal function loss. However, Bravi et al. reported that a distinct difference existed in the risk of AKI between patients who had an ischemia time <10 min vs. >20 min (9). In our patient, the ischemia time was much longer than 60 min. Nevertheless, the patient still successfully preserved her renal function, and AKI did not occur after the operation. We believe that the ice in the surgical field greatly helped in preserving the renal parenchyma to the maximum extent. Along with the experience from other NSS cases, we suggest that surgeons lower the temperature of the surgical field to approximately 15–0°C, which could preserve the renal function from being damaged within 2 h. Postoperatively, the exact suture of the wound is critical for preventing bleeding. As OPN always results in deep wounds, a multilayer suture is recommended. We hope our tips could provide some reference for peers who handle similar cases.

Regular postoperative follow-up could help surgeons detect tumor recurrence, metastasis, renal insufficiency, and other problems on time and deal with them immediately. The follow-up should include renal function tests, a chest and abdominal CT examination, and laboratory examinations that measure the serum parameter of renal function. The patient reported in our case was followed up every 3 months, and the chest and abdominal CT examination revealed no signs of relapse or metastasis to date.

## Conclusions

Our case provides evidence that NSS is a reasonable option for SFK patients with a local pT3 RCC. We believe that a comprehensive evaluation of the patient's general condition, renal function, and tumor complexity is crucial for the formulation of the surgical plan. In addition, there are many important points to consider during NSS for the preservation of postoperative renal function and the prevention of perioperative complications. We hope to share our experience with our peers who handle similar cases.

## Data availability statement

The original contributions presented in the study are included in the article/Supplementary Material; further inquiries can be directed to the corresponding author.

## Ethics statement

Written informed consent was obtained from the individual(s) for the publication of any potentially identifiable images or data included in this article.

## Author contributions

MY initiated the study. JQ and SQ performed the surgery. JZ, XS, and JD collected details of the medical history and follow-up information of patients. All authors contributed to the article and approved the submitted version.

## Funding

The National Natural Science Foundation of China (81970657).

## Conflict of interest

The authors declare that the research was conducted in the absence of any commercial or financial relationships that could be construed as a potential conflict of interest.

## Publisher's note



## References

1. Berdjis N, Hakenberg OW, Novotny V, Manseck A, Oehlschlager S, Wirth MP. Nephron-sparing surgery for renal cell carcinoma in the solitary kidney. *Scand J Urol Nephrol.* (2007) 41(1):10–3. doi: 10.1080/00365590600911225

2. Motzer RJ, Jonasch E, Boyle S, Carlo MI, Manley B, Agarwal N, et al. NCCN guidelines insights: kidney cancer, version 1.2021. *J Natl Compr Canc Netw.* (2020) 18(9):1160–70. doi: 10.6004/jnccn.2020.0043

3. Ljungberg B, Albiges L, Abu-Ghanem Y, Bedke J, Capitanio U, Dabestani S, et al. European association of urology guidelines on renal cell carcinoma: the 2022 update. *Eur Urol.* (2022) 82(4):399–410. doi: 10.1016/j.eururo.2022.03.006

4. Becker F, Roos FC, Janssen M, Brenner W, Hampel C, Siemer S, et al. Short-term functional and oncologic outcomes of nephron-sparing surgery for renal tumours ≥7 cm. *Eur Urol.* (2011) 59(6):931–7. doi: 10.1016/j.eururo.2011.02.017

5. Karellas ME, O'Brien MF, Jang TL, Bernstein M, Russo P. Partial nephrectomy for selected renal cortical tumours of ≥7 cm. *BJU Int*. (2010) 106(10):1484–7. doi: 10.1111/j.1464-410X.2010.09405.x

6. Breau RH, Crispen PL, Jimenez RE, Lohse CM, Blute ML, Leibovich BC. Outcome of stage T2 or greater renal cell cancer treated with partial nephrectomy. *J Urol*. (2010) 183(3):903–8. doi: 10.1016/j.juro.2009.11.037

7. Rintoul-Hoad S, Fernando A, Nair R, Challacombe B, O'Brien T. Open nephron-sparing surgery in patients with a complex tumour in a solitary kidney: technical, oncological and functional outcomes. *BJU Int*. (2021) 128(4):431–4. doi: 10.1111/bju.15400

8. Bindayi A, Hamilton ZA, McDonald ML, Yim K, Millard F, McKay RR, et al. Neoadjuvant therapy for localized and locally advanced renal cell carcinoma. *Urol Oncol*. (2018) 36(1):31–7. doi: 10.1016/j.urolonc.2017.07.015

9. Bravi CA, Mari A, Larcher A, Amparore D, Antonelli A, Artibani W, et al. Toward individualized approaches to partial nephrectomy: assessing the correlation between ischemia time and patient health Status (RECORD2 project). *Eur Urol Oncol*. (2021) 4(4):645–50. doi: 10.1016/j.euo.2020.05.009

frontiers | Frontiers in Oncology

TYPE Case Report
PUBLISHED 28 March 2023
DOI 10.3389/fonc.2023.1109643



OPEN ACCESS

EDITED BY
Zhaolun Cai,
Sichuan University, China

REVIEWED BY
Yang Yang,
First Affiliated Hospital of Sun Yat-sen University, China
Rafael De La Garza Ramos,
Montefiore Medical Center, United States

*CORRESPONDENCE
Shanyong Zhang
jzhangshanyong@yeah.net

SPECIALTY SECTION
This article was submitted to Surgical Oncology, a section of the journal Frontiers in Oncology

RECEIVED 01 December 2022
ACCEPTED 08 March 2023
PUBLISHED 28 March 2023

CITATION
Ge W, Qu Y, Hou T, Zhang J, Li Q, Yang L, Cao L, Li J and Zhang S (2023) Case report: Surgical treatment of a primary giant epithelioid hemangioendothelioma of the spine with total en-bloc spondylectomy. *Front. Oncol.* 13:1109643. doi: 10.3389/fonc.2023.1109643



# Case report: Surgical treatment of a primary giant epithelioid hemangioendothelioma of the spine with total en-bloc spondylectomy

Wanbao Ge[1], Yuan Qu[1], Tingting Hou[1], Jiayin Zhang[1], Qiuju Li[1], Lili Yang[1], Lanqing Cao[2], Jindong Li[3] and Shanyong Zhang[1]*

[1]Department of Spine Surgery, Second Affiliated Hospital of Jilin University, Changchun, Jilin, China, [2]Department of Pathology, Second Affiliated Hospital of Jilin University, Changchun, Jilin, China, [3]Department of Thoracic Surgery, Second Affiliated Hospital of Jilin University, Changchun, Jilin, China

**Background:** Epithelioid hemangioendothelioma (EHE) is an extremely uncommon malignant neoplasm that originates from vascular endothelial or pre-endothelial cells. In this report, we present the case of patient who was diagnosed with a primary giant EHE of the spine and underwent treatment with total en-bloc spondylectomy (TES).

**Case presentation:** A 43-year-old male patient with a history of he presented to our hospital with chronic and progressive back pain. Physical examination revealed weakened sensation of acupuncture and touch on the left costal arch, while relatively normal neurological functions were preserved. Radiological examinations identified a giant destructive soft tissue lesion occupying the T8 vertebral region, with moderate destruction of the pedicle and lamina, as well as the 7$^{th}$ left rib. A preoperative biopsy of the 8th vertebra resulted in a diagnosis of epithelioid hemangioendothelioma(EHE). Postoperative immunohistochemical and pathological reports confirmed the presence of EHE in the left ribs and T8 ribs. The patient underwent resection of the 7th left rib and posterior pedicle screw fixation with 8 pairs of screws and a titanium mesh cage. Subsequently, thoracic en bloc spondylectomy was performed on the T8 vertebra. The patient did not receive radiation or chemotherapy following surgery. Over a period of 3 years, the patient remained free of disease and relapse.

**Conclusion:** The use of transarterial embolization with spherical embolic agents (TES) has been demonstrated to be a safe, effective, and reliable treatment option for hepatic epithelioid hemangioendothelioma (EHE). Nevertheless, it is crucial to conduct long-term follow-up of this patient in order to assess their clinical outcome.

KEYWORDS

**epithelioid hemangioendothelioma, total en-bloc spondylectomy, vertebral lesion, vascular neoplasm, giant**

## Introduction

Epithelioid hemangioendothelioma (EHE) is an exceedingly uncommon tumor that originates from vascular endothelial or pre-endothelial cells. This neoplasm exhibits histological properties that fall in between those of hemangiomas and high-grade angiosarcomas. Although EHE can manifest in any organ of the body, it is most frequently observed in the liver, lung, and skin, but rarely affects the spine (1, 2). Epithelioid hemangioendothelioma (EHE) has a prevalence of one in a million (3). Although mortality is generally low, some cases can lead to death due tometastases (4). Atypical localized pain is the most frequent early symptom of EHE, which serve as an indication of the disease that can later progress into a chronic illness (5). Consequently, the exclusion of other diseases in patients with primary spinal tumors can occasionally lead to an accidental diagnosis of EHE.

Despite its relatively low mortality, delayed diagnosis and treatment of EHE can result in a protracted and potentially fatal illness. Nonetheless, we report a case of primary giant EHE of the spine in which the patient underwent early wide-margin resection without postoperative adjuvant therapy. As a result, the patient achieved long-term survival free from disease and without any instrument-related complications.

## Case report

A 43-year-old man presented to our hospital on foot with chronic and progressive back pain. He had been experiencing paroxysmal back pain for approximately 1 year., which was more pronounced at night and not relieved by rest. In the 15 days leading up to his admission, the back pain had intensified, accompanied by mild radiating pain and numbness in his lower limbs. The patient did not report any other physical discomfort, except for the pain, and denied any disease-related complaints. Upon further inquiry, he reported a slight weight over the past month. The patient had no significant strong family medical history of cancer or congenital diseases.

Upon physical examination, the patient exhibited weakened sensation to fine-touch and pinprick along his left costal arch, as well as grade 4 strength in his lower extremities. Pressure and percussion pain were observed over the T8 vertebra. However, the straight-leg raising test and the Babinski sign were bilaterally negative. The patient's bilateral deep tendon reflexes for the Achilles tendon and knee jerk reflexes were normal. And no anomalies in the spinal cord or neurological conditions in the upper extremity were noted. Nonetheless, the patient exhibited evident anxiety and a strong desire for surgery.

Diagnostic tests were conducted to identify cancer cell markers, and routine laboratory tests were performed to determine the patient's condition. The laboratory results were almost within the normal range, which increased uncertainty regarding the diagnosis of EHE, except for the elevated levels of carcinoembryonic antigen alpha-fetoprotein was elevated (16.81 ng/ml, normal: <8.78 ng/ml) and cytokeratin 19 fragment Cyra21-1 (2.74 ng/ml,normal: <2.08 ng/ml). A thoracic magnetic resonance imaging (MRI) revealed a vertebral lesion, which was assessed to determine the degree of flexibility of the vertebral spine, and a surgical intervention approach was finalized as the treatment course.

The MRI showed a giant destructive soft tissue lesion occupying the T8 vertebral region with moderate destruction of the pedicle and lamina (Figures 1A, B). Another lesion was found on the seventh left rib (Figure 1C). The preoperative medical tests, including an electrocardiogram and chest CT scan (Figure 2).

Previous studies have recommended preoperative embolization to generally "shrink" the tumor (5). Therefore, vascular embolization was planned and performed. Preoperative angiography showed abundant blood supply in the tumor (Figure 3). To decrease intraoperative blood flow volume and maintain vital signs, four segmental arteries were embolized 12 hours preoperatively. EHE was ultimately diagnosed by a standard biopsy to determine the therapy course. Neuroelectromyography testing was not performed and an IV infusion of cephalosporin was administered 30 minutes before surgery to prevent infection. Tranexamic acid was not administered for prophylactic hemostasis. In consultation with a thoracic surgeon and an anesthesiologist, resection of the 7th rib and total en-bloc spondylectomy (TES) were performed sequentially. The patient was positioned right lateral decubitus and the rib was resected. During costectomy, a mass measuring 4.5 × 11 cm could be recognized, and no implant nodules, hydrothorax, or visible abnormality in the lungs were found around the 7th rib (Figure 4A). The patient was then transferred to prone location of TES. During TES, the pedicles of T6, T7, T9, and T10 were fixed with routine screws first (Screws are made of titanium alloy. Lengths are T6:35mm, T7:35mm, T9:35mm, T10:40mm, respectively. Diameters are T6:40mm, T7:40mm, T9:40mm, T10:45mm, respectively). C-arm fluoroscopy showed satisfactory positioning of the pedicle screws bilaterally. The left 8th vertebral body was exposed, and a giant tumor invading the vertebral body and the costovertebral joint was resected (Figure 4B). An appropriate titanium mesh cage was implanted and the incision was closed with drains. The whole surgical procedure was successful, and the intraoperative blood loss was only about 1000 ml. The proper placement of the surgical implants was immediately checked by X-ray.

Postoperative pathology reports confirmed the diagnosis of EHE. Microscopic examination revealed that mostly eosinophilic endothelial cells constituted the tumor, without any well-formed vessels (Figure 5). Immunohistochemical staining was performed for friend leukemia integration 1 (FLI-1), CD31, and CD34 expression. Combined CD31 and FLI-1 staining suggested the diagnosis of EHE (Figure 6). In this case, the tumor sample was also positive for endothelial markers such as smooth muscle alpha-actin. Moreover, cytokeratin (AE1/AE3), indicating epithelial origin, was positive, with 8% of the cells being Ki-67-positive.

**Abbreviations:** EHE, epithelioid hemangioendothelioma; TES, total en-bloc spondylectomy; MRI, magnetic resonance imaging; CT, computed tomography; FLI-1, friend leukemia integration 1 transcription factor; WWTR1, WW domain-containing transcription regulator 1; CAMTA1, calmodulin-binding transcription activator 1.

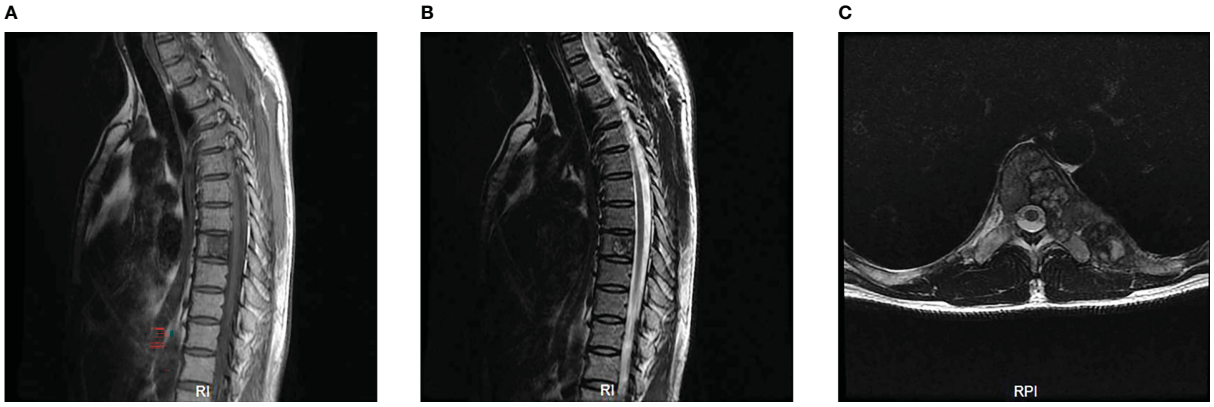


FIGURE 1
Preoperative MRI scan of the patient's thoracic spine **(A–C)**. Sagittal scan revealed the density of obvious bone destruction in the T8 on T1 and T2-weighted images **(A, B)**. Transverse MRI scan showed a 6.5cm x 2.0cm sized and well-defined lesion occupying the T8 vertebral body, pedicle and lamina **(C)**.

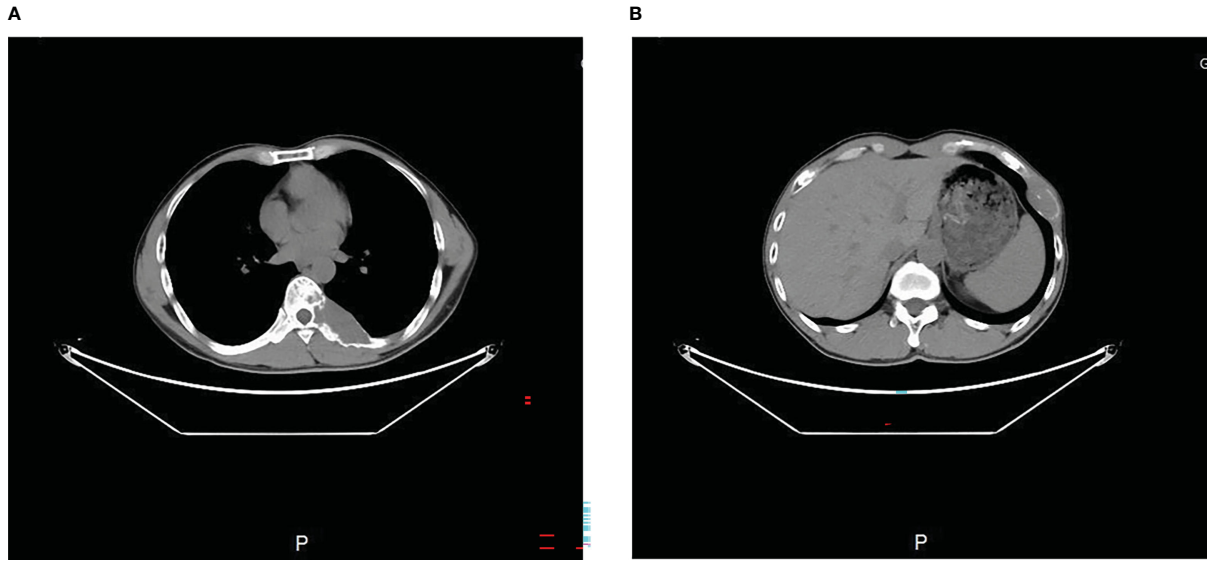


FIGURE 2
Preoperative transverse CT scan **(A, B)** showed the tumor occupied the 8th thoracic vertebral body and 7th rib.

During a recent postoperative follow-up after the surgery, there was no indication of any tumor progression or the emergence of any new symptoms (Figure 7). However, the patient and their family have politely declined radiation treatment. Currently, the patient's back pain has been relieved, and the sensory function, including fine-touch and pinprick sensation, of the left costal arch has returned to normal.

## Discussion

Primary spinal EHE is a rare type of malignancy, accounting for only 1% of all malignant bone tumors (6). EHE is characterized by polygonal or round epithelioid endothelial cells with abundant eosinophilic hyaline cytoplasm and vesicular nuclei. Due to its local aggressiveness and metastatic potential, EHE is considered to have histological features that fall between those of hemangioma and high-grade angiosarcoma. Typically, most patients in the early stages of EHE development are asymptomatic, and the accidental discovery of the tumor during routine physical examinations is a common way to achieve early diagnosis. Although patients may not place importance on the most common symptom of atypical local pain, EHE can still lead to complications and mortality (Table 1). However, our study demonstrated significant therapeutic effects during the follow-up period.

Pathological examination is considered the gold standard for EHE diagnosis. In this case, we performed immunohistochemistry, and the examination results were consistent with diagnosis of EHE.

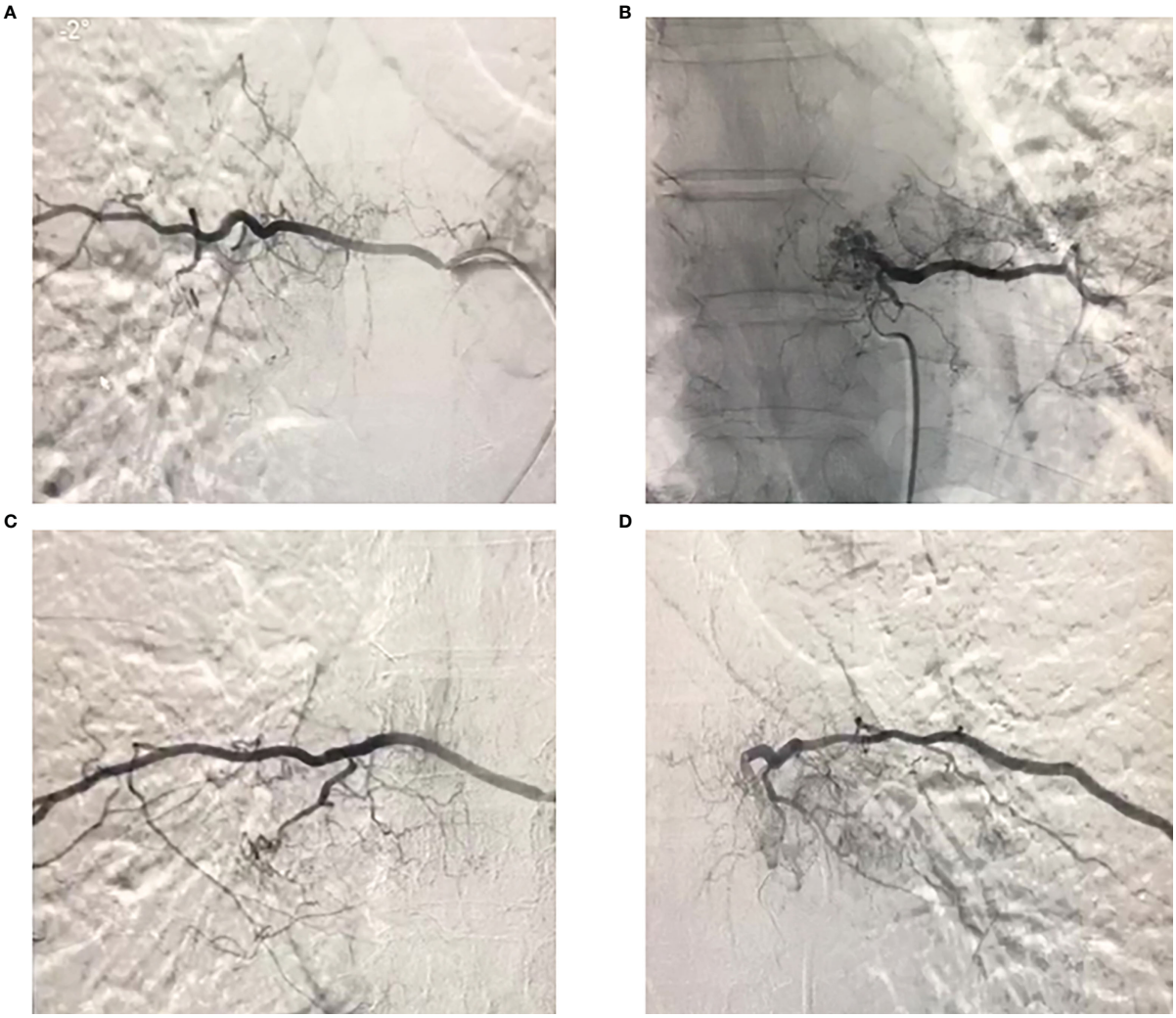


FIGURE 3
Preoperative angiography of the 7th and 8th thoracic vertebral segment arteries showed that the tumor had a rich blood supply, and embolization was performed.

However, with advancements in medical technology, new approaches such as molecular genetic testing can be applied to further clarify the diagnosis of EHE. A specific recurrent WWTR1-CAMTA1 gene fusion has been detected in the majority of EHE patients, and this genetic hallmark can be used as a new diagnostic indicator of EHE (11). Additionally, the detection of the WWTR1-CAMTA1 gene fusion can distinguish EHE from other benign or malignant vascular tumors (11, 12). Some recent studies have suggested that an alternate YAP1-TFE3 fusion, found in a subset of cases, may also be meaningful in EHE diagnosis. However, it remains unclear whether the YAP1-TFE3 gene fusion should be used to identify EHE (12). In the present case, preoperative puncture biopsy, clinical symptoms, and imaging features suggested that the patient required surgical intervention. Therefore, we performed TES, which resulted in satisfactory clinical results. We also recommended that the patient and his family undergo genetic testing. However, although we suggested genetic testing, the family members refused, and we believe that this did not affect the patient's treatment and prognosis.

There are no standard treatment courses available for the management of spinal EHE. Preoperative embolization and surgical resection, followed by postoperative radiotherapy and/or chemotherapy, are the alternative options. Surgical resection is generally considered the optimal treatment approach (13). However, en-bloc resection of spinal EHE can be challenging due to the highly vascular nature of the tumor and the risk of intraoperative bleeding. The extent of surgical can range from wide margin to marginal or intralesional resection. Several clinical studies suggest that wide resection (i.e., TES), should be performed to achieve favorable outcomes (14). Luzzati et al. reported the largest case series of ten spinal EHE patients and found that patients who received relatively broad or marginal resection had better prognoses (15). While TES is currently considered the preferred choice to control spinal EHE progression, further

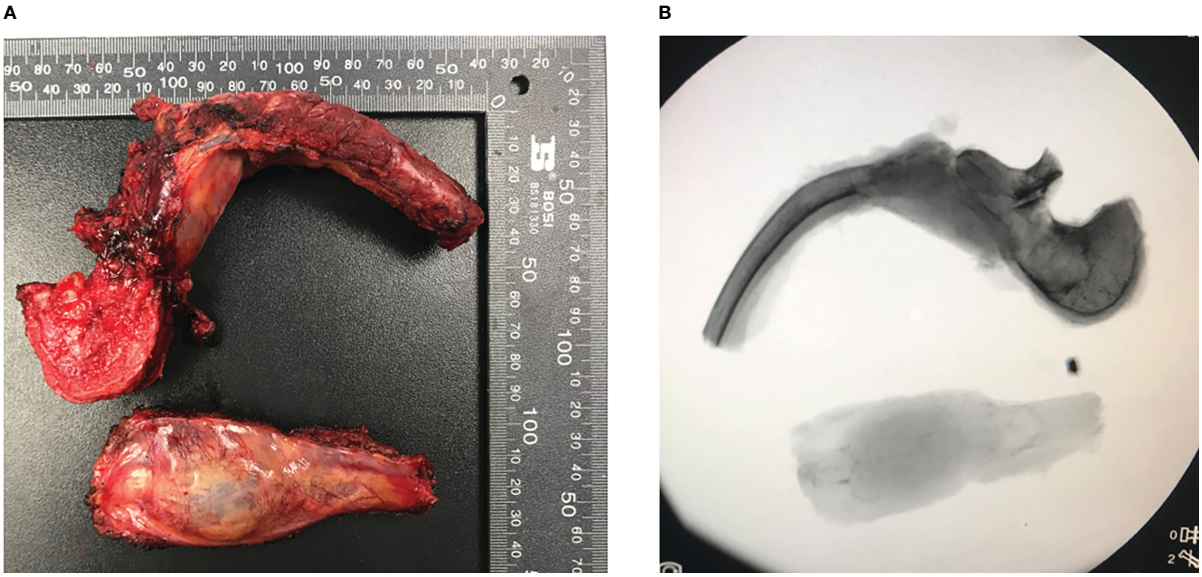


FIGURE 4
En-bloc excision tumor specimen in T8 and part of 7th rib of the patient and corresponding perspective image **(A, B)**. Both images showed the integrity of tumor and the lesion was completely removed.

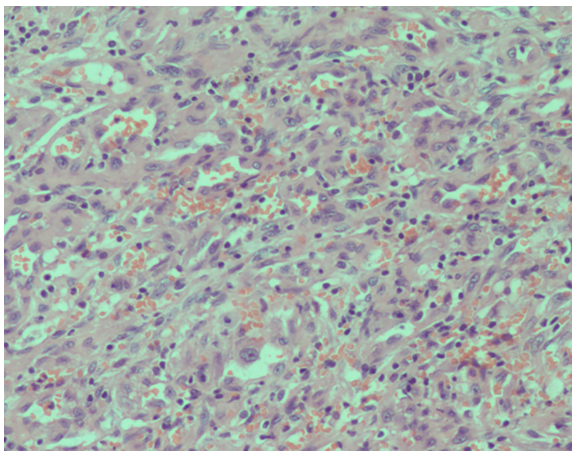

FIGURE 5
Histopathology of the resected mass. High-power magnification (200×) shows cords and groups of epithelioid cells in a dense without well-formed vascular structures.

analysis of large volumes of clinical outcomes and substantial experimental data is needed to establish the ultimate conclusion. In our case, we successfully performed a wide resection and achieved a clear resection margin.

In addition to surgery, systemic therapy, including chemotherapy and radiotherapy, may also benefit patients with spinal epithelioid hemangioendothelioma (EHE) According to a few reports, radiotherapy for partially excised spinal EHE lesions can be effective (8). Moreover, some clinical centers use radiation (45–50 Gy) as a postoperative systemic treatment to achieve long-term local control and pain relief (16). While systemic therapy can provide physiological support for patients who refuse other treatments (17, 18), surgery remains the optimal treatment choice. However, there is currently no evidence to support a strong correlation between chemotherapy or radiotherapy and good prognosis in patients with spinal EHE. In our case, the patient declined radiation or chemotherapy treatment, and we followed the patient for 3 years without observing tumor recurrence. We plan to extend the follow-up period if necessary. Our patient, who received only extensive resection surgery with favorable outcomes, may provide insight for developing a standardized treatment plan for EHE in the future. In contrast, expectant observation may be an alternative approach for unresectable tumors or those that may lead to severe complications if resected.

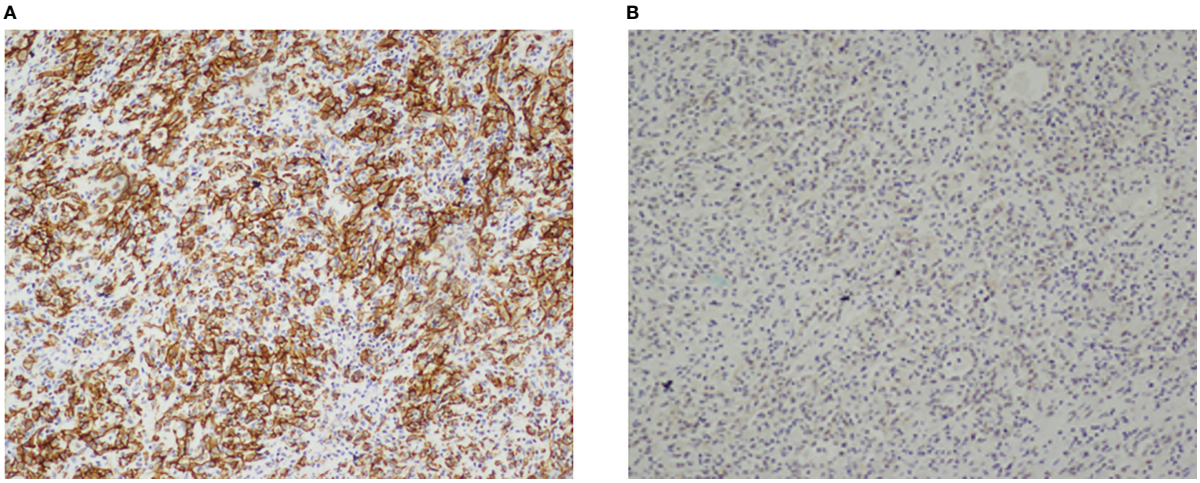


FIGURE 6
Immunohistochemical stain of the resected mass. **(A, B)** Tumor cells expressed CD31 **(A)** and FIL-1 **(B)**. Both immunohistochemical stain were in 100×magnification.

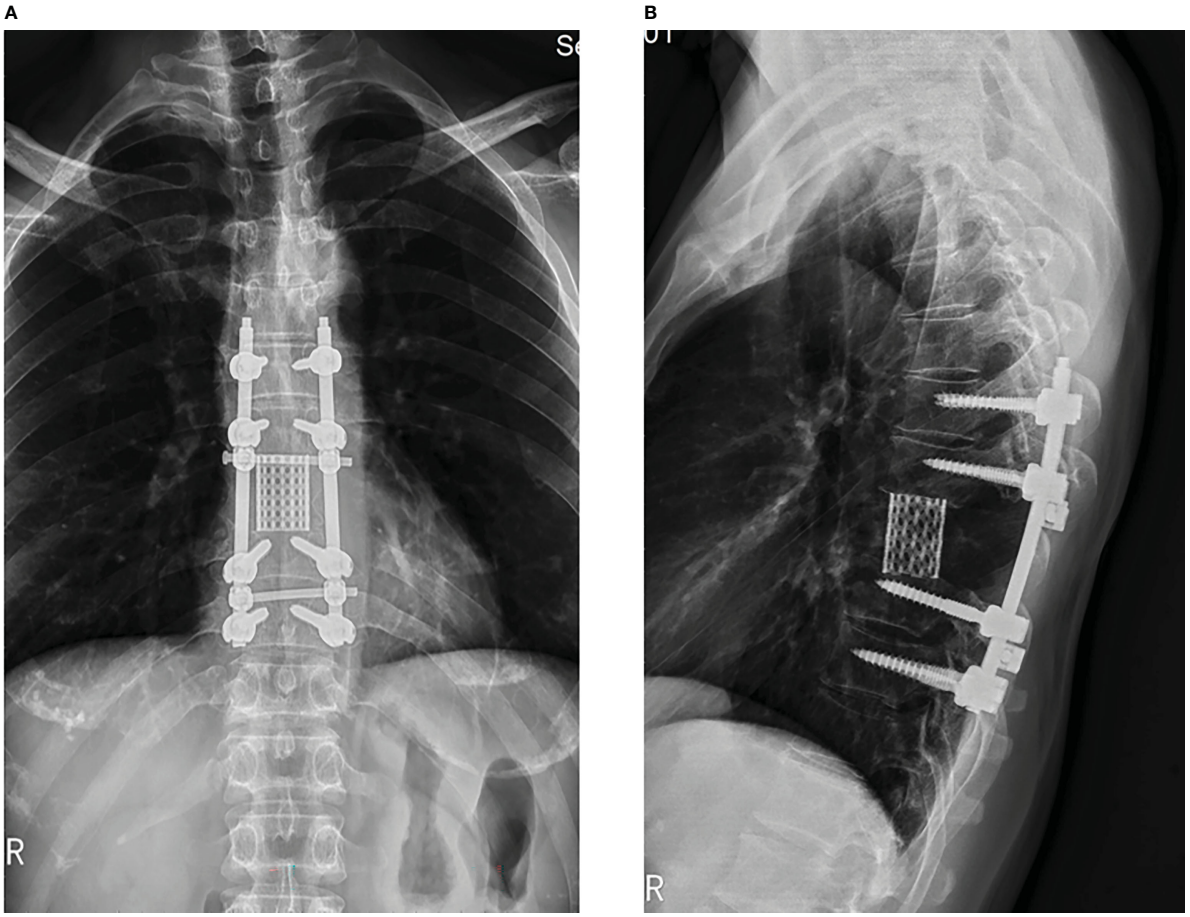


FIGURE 7
3 months follow-up after the surgery, x-ray display of thoracic spine showing transpedicular screw and a titanium mesh were used in the reconstruction of the stability of the spine in patient. (**A**: orthotopic position, **B**: side position).

TABLE 1 Complications and mortality of EHE in the references of other authors.

| Author | Case number | Patient age [&] | Segment | Therapeutic regimen | Follow-up time [#] | Complication | Mortality |
|---|---|---|---|---|---|---|---|
| Kitaichi, Nagai (7) | Male [8] | 14–69 | Lung | Surgical resection;Chemotherapy. | 320 | Pleural effusion; Ascites; | 23.8% |
| | Female [13] | 15–62 | | | | | |
| Aflatoon, Staals (8) | Male [3] | 21–31 | Spine | Surgical resection;Radiation therapy. | 120 | Postirradiation sarcoma; Back pain; Lung Metastatic disease. | 12.5% |
| | Female [5] | 25–74 | | | | | |
| Rosenbaum (9) | Male [4] | 28–62 | Lung; Liver; Bone; Soft tissue. | Surgical resection; Systemic treatment. | 300 | Acute myeloid leukemia; Disease. | 25% |
| | Female [6] | | | | | | |
| Shiba, Imaoka (10) | Male [22] | 18–78 | Lung; Liver; Bone; | Surgical resection;Chemotherapy | 120 | Metastatic disease. | 28% |
| | Female [20] | | | | | | |
| Deyrup, Tighiouart (4) | Male [28] | 9–93 | Head and neck; Extremities; Mediastinum; Trunk; Genitals and retroperitoneum. | Surgical resection;Chemotherapy; Radiation therapy. | 60 | Metastatic disease. | 19% |
| | Female [21] | | | | | | |

[&] represents years; [#] indicates months.

Regarding prognosis, patients with multifocality, pleural involvement, lymph node invasion, or remote metastases generally have considerably poor outcomes. Conversely, patients without these adverse factors have an average 5-year survival rate of >70% (9). In this case, only one lesion was presented, and there was no evidence of multifocality, pleural involvement, lymph node involvement, or metastasis. According to Rosenbaum et al. (9), satisfactory clinical outcomes can be achieved after standard surgical treatment and 3 years of tumor-free survival. However, according to recent research, the WWTR1-CAMTA1 gene fusion may indicate that other genetic anomalies can lead to more aggressive biological behavior (9). Simultaneously, the 5-year survival for WWTR1-CAMTA1 fusion is 59%, compared to 86% for YAP1-TFE3 fusion (9). Some asymptomatic patients may also have a good prognosis through careful monitoring, as spontaneous regressions have been reported (7). Unfortunately, our patient declined the proposal for genetic testing. We believe that genetic detection is significant for the prognosis of EHE patients and for EHE prevention in their families. Screening for the gene mutation causing EHE in other family members can enable early diagnosis and prompt treatment, particularly for asymptomatic family members, to prevent distant metastases and poor prognosis. The prognosis of EHE varies depending on anatomical site. EHE of soft tissues can be indolent. However, EHE arising in the lung or bone have a worse prognosis than soft tissue tumors, and patients often present with metastatic disease. Additionally, in the recently identified YAP1-TFE3 subset of cases, the metastatic rate may be higher. A traditional risk stratification is based on mitotic activity and tumor size. During the one-year follow-up, the patient reported remission of back pain and no recurrence of pain.

This case report has several limitations that should be acknowledged. The follow-up period is less than 5 years, and the study involves only one patient. Therefore, to accurately evaluate the therapeutic effect of TES, multicenter, large-sample, long-follow-up randomized controlled trials are necessary. Additionally, the patient did not undergo genetic testing, which limits the ability to make definitive conclusions regarding the impact of genetic anomalies on the clinical outcomes of EHE. As such, genetic counseling and education should be offered to patients and their family members for prevention, early diagnosis, and treatment.

## Conclusion

TES has been demonstrated to be safe, effective, and reliable for the treatment of EHE, and in this case, we were able to successfully diagnose and treat the patient. Nonetheless, the patient requires long-term follow-up to assess the clinical outcome and to determine if any recurrence or metastasis occurs. This is especially important given that EHE is known to have a variable clinical course and prognosis, which can be influenced by a range of factors such as genetic anomalies, tumor location, and disease stage. Long-term follow-up will also provide additional insight into the efficacy and safety of TES as a treatment modality for EHE. This study was reported in agreement with principles of the CARE guidelines (19).

## Data availability statement

The datasets used and/or analyzed during the current study are available from the corresponding author on reasonable request.

## Ethics statement

Ethical review and approval was not required for the study on human participants in accordance with the local legislation and institutional requirements. The patients/participants provided their written informed consent to participate in this study. Written

informed consent was obtained from the participant/patient(s) for the publication of this case report.

## Author contributions

Data Curation: Writing - Original Draft: WG, YQ. Writing - Review and Editing: SZ. Visualization: TH, JZ, LY. Supervision: LC. Project administration: QL, JL. All authors contributed to the article and approved the submitted version.

## Acknowledgments

The authors would like to acknowledge the financial support from the Natural Science Foundation of Science and Technology Department of Jilin Province (20200201551JC).

## Conflict of interest

The authors declare that the research was conducted in the absence of any commercial or financial relationships that could be construed as a potential conflict of interest.

## Publisher's note

All claims expressed in this article are solely those of the authors and do not necessarily represent those of their affiliated organizations, or those of the publisher, the editors and the reviewers. Any product that may be evaluated in this article, or claim that may be made by its manufacturer, is not guaranteed or endorsed by the publisher.

## References

1. Mentzel T, Beham A, Calonje E, Katenkamp D, Fletcher C. Epithelioid hemangioendothelioma of skin and soft tissues: Clinicopathologic and immunohistochemical study of 30 cases. *Am J Surg Pathol* (1997) 21:363–74. doi: 10.1097/00000478-199704000-00001

2. Mendlick MR, Nelson M, Pickering D, Johansson SL, Seemayer TA, Neff JR, et al. Translocation t(1;3)(p36.3;q25) is a nonrandom aberration in epithelioid hemangioendothelioma. *Am J Surg Pathol* (2001) 25:684–7. doi: 10.1097/00000478-200105000-00019

3. Sardaro A, Bardoscia L, Petruzzelli M, Portaluri M. Epithelioid hemangioendothelioma: An overview and update on a rare vascular tumor. *Oncol Rev* (2014) 8:259. doi: 10.4081/oncol.2014.259

4. Deyrup A, Tighiouart M, Montag A, Weiss S. Epithelioid hemangioendothelioma of soft tissue: A proposal for risk stratification based on 49 cases. *Am J Surg Pathol* (2008) 32:924–7. doi: 10.1097/PAS.0b013e31815bf8e6

5. Munier O, Muckensturm B, Fesneau M, Wachter T. Epithelioid hemangioendothelioma of the spine: A case report. *Cancer Radiother* (2017) 21:222–5. doi: 10.1016/j.canrad.2016.11.006

6. Kerry G, Marx O, Kraus D, Vogel M, Kaiser A, Ruedinger C, et al. Multifocal epithelioid hemangioendothelioma derived from the spine region: Case report and literature review. *Case Rep Oncol* (2012) 5:91–8. doi: 10.1159/000336947

7. Kitaichi M, Nagai S, Nishimura K, Itoh H, Asamoto H, Izumi T, et al. Pulmonary epithelioid haemangioendothelioma in 21 patients, including three with partial spontaneous regression. *Eur Respir J* (1998) 12:89–96. doi: 10.1183/09031936.98.12010089

8. Aflatoon K, Staals E, Bertoni F, Bacchini P, Donati D, Fabbri N, et al. Hemangioendothelioma of the spine. *Clin Orthop Relat Res* (2004) 418:191–7. doi: 10.1097/00003086-200401000-00031

9. Rosenbaum E, Jadeja B, Xu B, Zhang L, Agaram NP, Travis W, et al. Prognostic stratification of clinical and molecular epithelioid hemangioendothelioma subsets. *Modern Pathol* (2020) 33:591–602. doi: 10.1038/s41379-019-0368-8

10. Shiba S, Imaoka H, Shioji K, et al. Clinical characteristics of Japanese patients with epithelioid hemangioendothelioma: A multicenter retrospective study. *BMC Cancer* (2018) 18:993. doi: 10.1186/s12885-018-4934-0

11. Flucke U, Vogels R, de Saint Aubain Somerhausen N, et al. Epithelioid hemangioendothelioma: Clinicopathologic, immunhistochemical, and molecular genetic analysis of 39 cases. *Diagn Pathol* (2014) 9:131. doi: 10.1186/1746-1596-9-131

12. Doyle L, Fletcher C, Hornick J. Nuclear expression of CAMTA1 distinguishes epithelioid hemangioendothelioma from histologic mimics. *Am J Surg Pathol* (2016) 40:94–102. doi: 10.1007/s00586-011-1798-2

13. Ma J, Wang L, Mo W, Yang X, Xiao J. Epithelioid hemangioendotheliomas of the spine: Clinical characters with middle and long-term follow-up under surgical treatments. *Eur Spine J* (2011) 20:1371–6. doi: 10.1007/s00586-011-1798-2

14. Lee S, Lee J. Surgical treatment of asymptomatic epithelioid hemangioendothelioma originating from the superior vena cava: A case report. *Medicine* (2020) 99:e19859. doi: 10.1097/MD.0000000000019859

15. Luzzati A, Gagliano F, Perrucchini G, Scotto G, Zoccali C. Epithelioid hemangioendothelioma of the spine: Results at seven years of average follow-up in a series of 10 cases surgically treated and a review of literature. *Eur Spine J* (2015) 24:2156–64. doi: 10.1007/s00586-014-3510-9

16. O'Shea B, Kim J. Epithelioid hemangioma of the spine: Two cases. *Radiol Case Rep* (2014) 9:984. doi: 10.2484/rcr.v9i4.984

17. Agulnik M, Yarber JL, Okuno SH, von Mehren M, Jovanovic BD, Brockstein BE, et al. An open-label, multicenter, phase II study of bevacizumab for the treatment of angiosarcoma and epithelioid hemangioendotheliomas. *Ann Oncol* (2013) 24:257–63. doi: 10.1093/annonc/mds237

18. Chevreau C, Le Cesne A, Ray-Coquard I, Italiano A, Cioffi A, Isambert N, et al. Sorafenib in patients with progressive epithelioid hemangioendothelioma: A phase 2 study by the French sarcoma group (GSF/GETO). *Cancer* (2013) 119:2639–44. doi: 10.1002/cncr.28109

19. Riley DS, Barber MS, Kienle GS, Aronson JK, von Schoen-Angerer T, Tugwell P, et al. CARE guidelines for case reports: Explanation and elaboration document. *J Clin Epidemiol* (2017) 89:218–35. doi: 10.1016/j.jclinepi.2017.04.026

frontiers | Frontiers in Surgery

TYPE Case Report
PUBLISHED 30 March 2023
DOI 10.3389/fsurg.2023.1081326



OPEN ACCESS

EDITED BY
Zhaolun Cai,
Sichuan University, China

REVIEWED BY
Antonio Giovanni Solimando,
University of Bari Aldo Moro, Italy
Vagan Bokhian,
Russian Cancer Research Center NN Blokhin, Russia

*CORRESPONDENCE
Bi-Xiang Zhang
✉ bixiangzhang@163.com

SPECIALTY SECTION
This article was submitted to Surgical Oncology, a section of the journal Frontiers in Surgery

RECEIVED 27 October 2022
ACCEPTED 07 March 2023
PUBLISHED 30 March 2023

CITATION
Zhang Z-Y, Wang Y-W, Zhang W and Zhang B-X (2023) Case Report: Solitary metastasis to the appendix after curative treatment of HCC. Front. Surg. 10:1081326. doi: 10.3389/fsurg.2023.1081326



# Case Report: Solitary metastasis to the appendix after curative treatment of HCC

Zun-Yi Zhang, Yu-Wei Wang, Wei Zhang and Bi-Xiang Zhang*

Research Laboratory and Hepatic Surgery Center, Department of Hepatic Surgery, Tongji Hospital, Tongji Medical College, Huazhong University of Science and Technology, Wuhan, China

**Background:** Liver cancer is now the fourth most common cancer in China. The most important factor in decreasing the overall survival is recurrence. Nearly 40%–70% of patients would be detected with intrahepatic or extrahepatic recurrence in 5 years after R0 resection. The intestine is not a usual site for extrahepatic metastasis. Only one case of hepatocellular carcinoma (HCC) metastasis to the appendix has been reported so far. So, it poses a difficulty for us to develop treatment plan.
**Case presentation:** Here, we report a very rare case of a recurrent HCC patient. R0 resection was first performed on this 52-year-old men who was diagnosed with Barcelona Clinic Liver Cancer stage A HCC. Different from other cases, a solitary metastasis to the appendix was detected 5 years after the R0 resection. After discussing with the multidisciplinary team, we decided to perform surgical resection again. The final postoperative pathology confirmed HCC. Complete responses were detected in this patient after the combined treatment of transarterial chemoembolization, angiogenesis inhibitors, and immune checkpoint inhibitors.
**Conclusion:** Because solitary metastasis to the appendix in HCC is very rare, this case might be the first reported in HCC patients after R0 resection. This case report highlights the efficacy of the combination of surgery, local regional therapy, angiogenesis inhibitors, and immune treatment in HCC patients with solitary metastasis to the appendix.

KEYWORDS
HCC, metastasis, appendix, resection, systemic treatment

## Introduction

Liver cancer is now the fourth most common cancer in China (1, 2). Hepatocellular carcinoma (HCC) represents the majority of primary liver cancer. Nearly 40%–70% of patients would be detected with intrahepatic or extrahepatic recurrence in 5 years after R0 resection (3). The most common recurrence pattern is intrahepatic recurrence. Extrahepatic metastasis is relatively low in incidence. The most common sites of extrahepatic metastasis are the lungs, bones, lymph nodes, and adrenal glands (4). The intestine is not a usual site for extrahepatic metastasis. So far, only one case of HCC metastasis to the appendix has been reported (5). Also, the appendix was found with metastasis because the tumor lesion in the liver ruptured. Solitary metastasis after R0 resection of HCC might be the first reported after we reviewed the domestic and international literature.

Because this kind of metastasis is rare and lacks imaging features, it is easily misdiagnosed as appendicitis. We need to solve the problem of improving the accuracy of the diagnosis and prolonging the patient's survival time. According to the conventional

view, extrahepatic metastasis of HCC usually means a worse prognosis (6). Most advanced-stage HCC patients would die of liver failure because of the progression of intrahepatic lesions rather than extrahepatic metastasis (7). Although with a high risk of recurrence, the selected patients with resectable extrahepatic metastasis could achieve an acceptable prognosis after R0 resection. With the improvement of medicine in liver cancer, the evolving role of immune checkpoint inhibitors (ICIs), angiogenesis inhibitors, and local regional treatment offers great promise in treating HCC patients with a high risk of recurrence (7). Nonetheless, no well-designed large samples of clinical control study have been reported. Thus, this poses a difficult problem for clinicians.

Herein, we report one case of an HCC patient with solitary metastasis to the appendix 5 years after R0 resection of the intrahepatic lesion. In this case report, we have two objectives. The first is to highlight that the appendix might be a site of tumor recurrence after R0 resection of the primary site of the liver. The second is to highlight that resection of the solitary metastasis to the appendix combined with local regional treatment, immune checkpoint inhibitors, and angiogenesis inhibitors could prolong the survival time of such patients. This study was reported in agreement with the principles of the CARE guidelines (8).

## Case presentation

A 52-year-old men with hepatitis B virus-associated chronic hepatitis was diagnosed with HCC at the clinic in 2016. No other specific family and psychosocial history including relevant genetic information should be reported. Physical examination showed no positive results. The patient's alpha-fetoprotein (AFP) was 49.36 ng/mL. A computed tomography (CT) scan showed that liver tumors were located in segments 5 and 6 (**Figures 1A,B**). The Child–Pugh Score was A with five points. The BCLC stage for this patient was A. After confirmation of no surgical contraindications, robotic-assisted laparoscopic segmentectomy 5–6 was performed on this patient. The surgery went without a hitch. The resected specimen was extracted from the lower abdomen with a specimen bag. The pathologic result confirmed the hepatic lesion was primary middle differentiated HCC (**Figures 1C,D**). After the resection, this patient accepted the antiviral treatment. Every 3 months, this patient came back to our department to recheck his tumor biomarkers (AFP, abnormal prothrombin DCP) and to undergo radiology tomography (ultrasonography, MRI, or CT). There was no sign of recurrence until 3 years after the surgery. On 29 December 2019, this patient returned to our department because of the elevated level of AFP. After an MRI scan, a new tumor lesion with a diameter of 2 cm was detected in

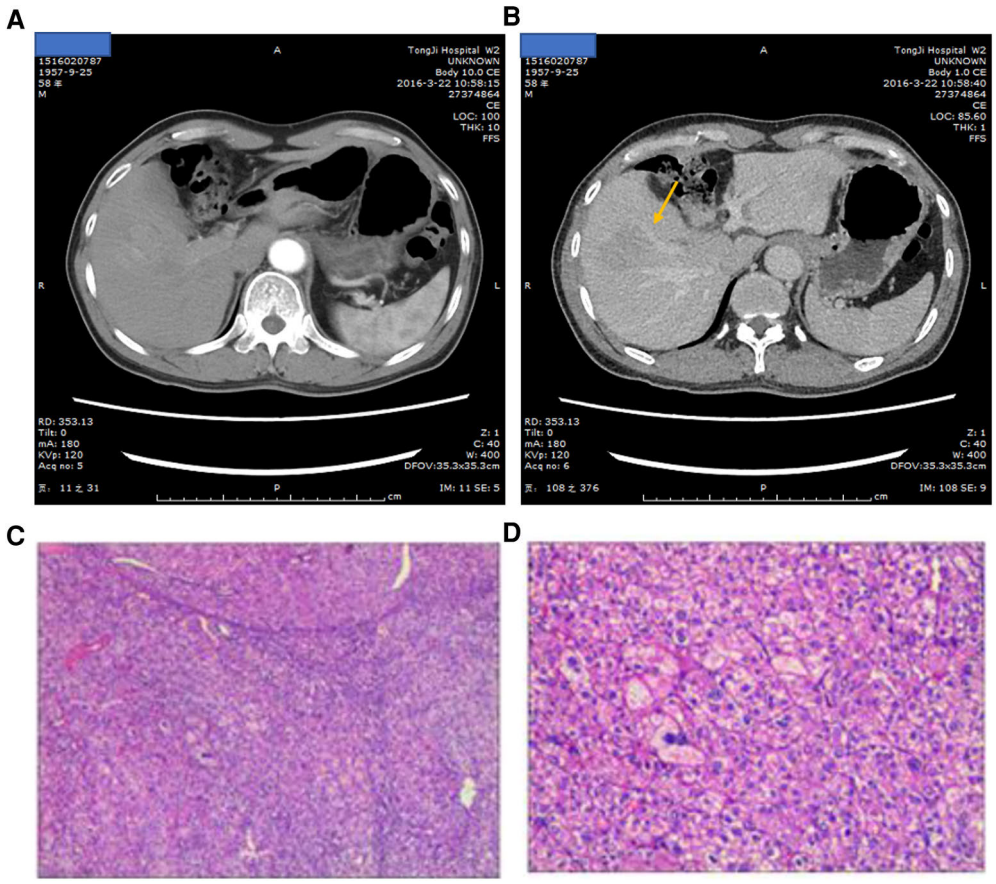


FIGURE 1
(A) Arterial phase of the liver-enhanced CT scan showing the tumor lesion in segments 5 and 6. (B) Portal venous phase of the liver-enhanced CT scan showing the tumor lesion in segments 5 and 6; the arrow points at the liver lesion. (C,D) HE staining of pathological diagnosis.

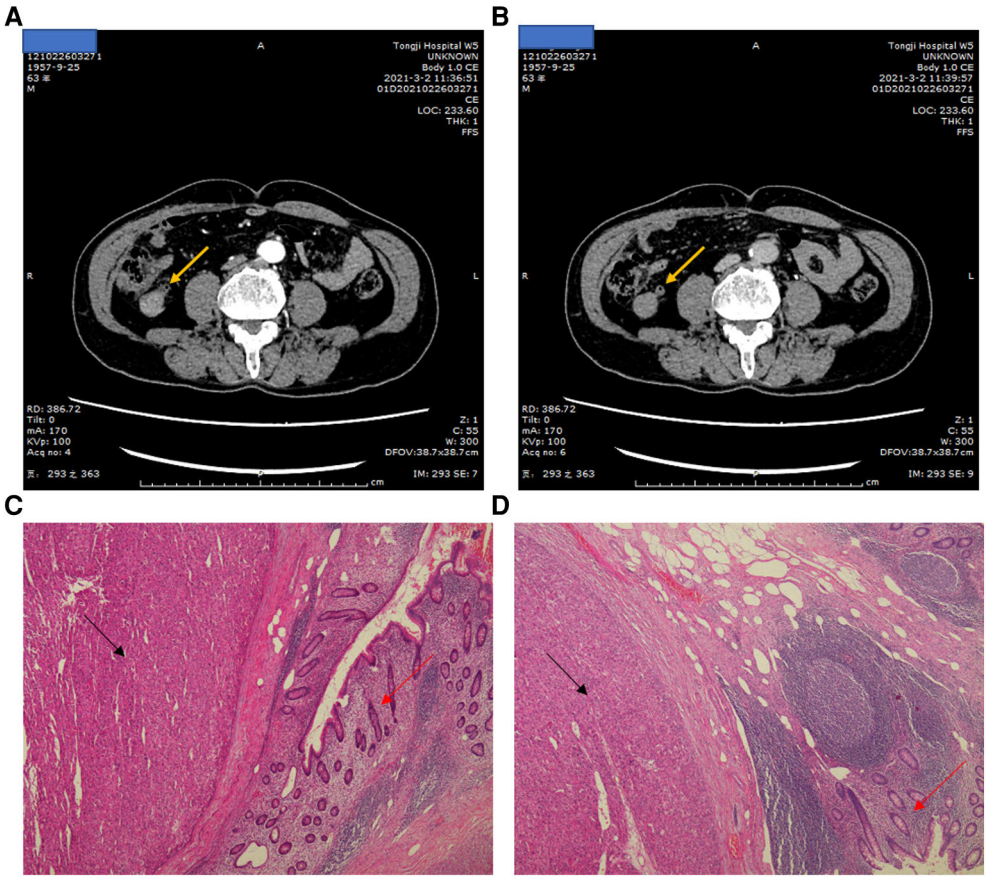


FIGURE 2
(A) Arterial phase of the Liver-enhanced computed tomography (CT) showing the tumor lesion in the appendix, the arrow point at the appendix. (B) portal venous phase of the the Liver-enhanced computed tomography (CT) showing the tumor lesion in the appendix, the arrow point at the appendix. (C, D) The HE stain of pathological diagnosis. The black arrow point at tumor lesion. The red arrow point at the appendix.

segment 7. Then, microwave ablation was performed on this hepatic lesion. The AFP level soon came back to the normal range after the surgery. On 6 March 2021, this patient returned to our department for the symptoms of acute appendicitis. The AFP and DCP levels were found to be elevated slightly. After the enhanced CT scan, a tumor with a diameter of 2 cm was found to adhere to the tip of the appendix (**Figures 2A,B**). No sign of recurrence was detected in the remnant liver at the same time. Although it is very rare, this patient was diagnosed with solitary metastasis of HCC to the appendix. After discussing with the multidisciplinary team, laparoscopic appendectomy was performed on this patient on 12 March 2021. The pathologic diagnosis confirmed that the lesion adhered to the appendix was a metastatic HCC (**Figures 2C,D**). The metastatic lesion had invaded all the layers from the serous membrane submucosa. After appendectomy, this patient followed the routine follow-up every 3 months in our clinic. On 15 January 2022, this patient was found to have elevated AFP and DCP levels. After the MRI scan, we found multiple recurrent intrahepatic lesions in the right half of the liver. The maximum diameter of the recurrent intrahepatic lesion was 2 cm (**Figures 3A,B**). After multidisciplinary team discussion, transarterial chemoembolization (TACE) combined with angiogenesis inhibitors (lenvatinib) and ICIs (PD-1 antibodies) was administrated to this patient. After 4 months, the CT scan showed that the typical site of liver metastasis had been covered by iodized oil (**Figures 3C,D**). The AFP level was found to decrease to the normal range (**Figure 4A**). So far, this patient has survived for 7 years, and the disease was found to be in a stable state. The timeline for this patient's treatment is summarized in **Figure 4B**.

## Discussion

Based on the latest report from China (9), HCC is now the fourth-most malignancy and the third leading cause of mortality. Surgical treatment including hepatectomy and liver transplantation as the only way to cure the disease is the most commonly used treatment to improve the survival of patients. However, postoperative recurrence within 5 years still could be observed in 40%–70% of patients (7). The most common sites of extrahepatic recurrence are the lungs, bone, lymph nodes, adrenal glands, and brain, in that order (4). Intestinal metastasis is not a common site of metastasis, which was reported in 0.5%–4% of HCC patients (10, 11). So far, there is only one case that has reported a patient with tumor lesions in the liver and appendix concurrently (5). The cause of metastasis to the appendix was thought to be the rupture

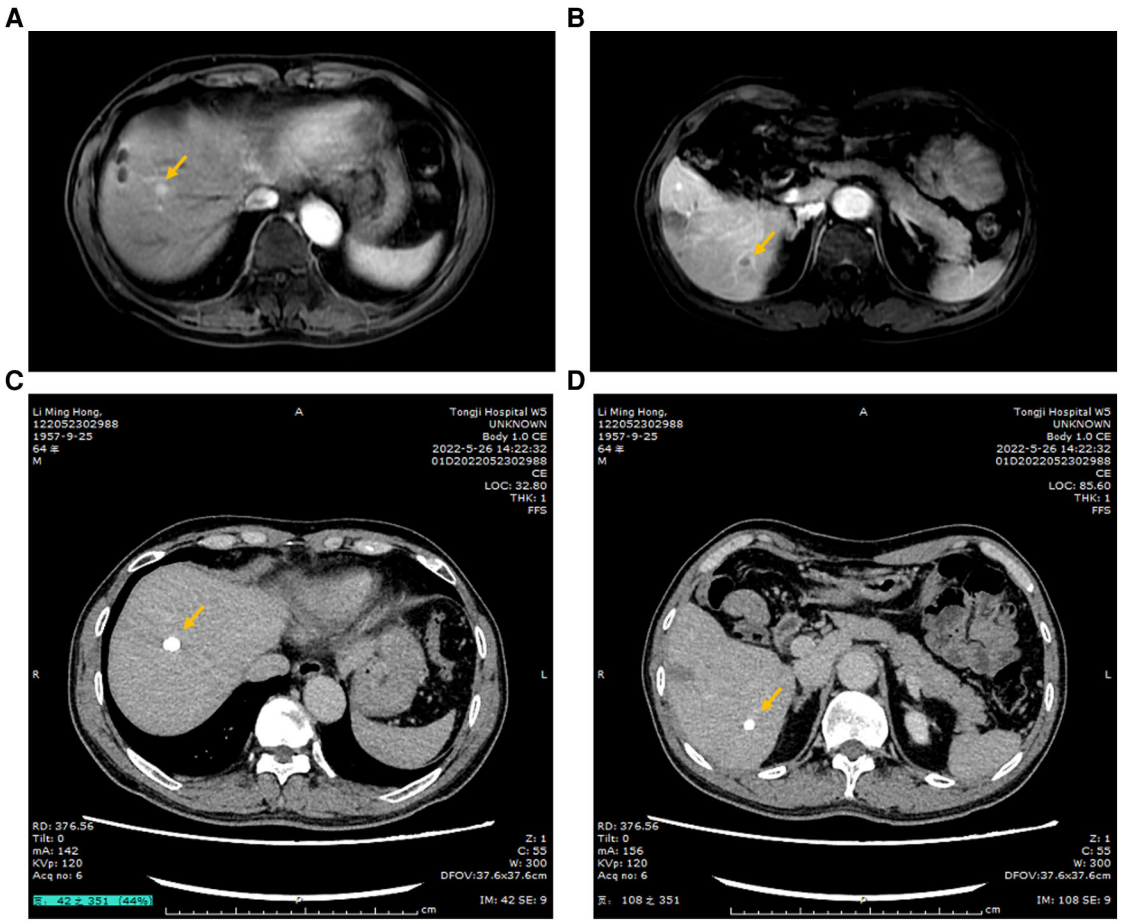


FIGURE 3
(A,B) PWI of the MRI scan showing the typical metastatic tumor in the liver; the arrow points at the lesion. (C,D) After TACE combined with angiogenesis inhibitors and ICIs, the typical lesions of the liver were covered by iodized oil, which were shown in the CT scan.

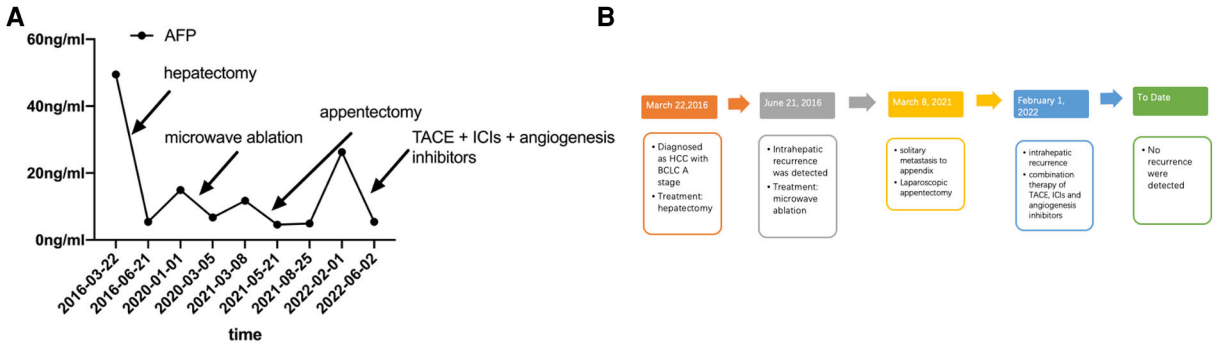


FIGURE 4
(A) AFP level of this patient from the first detection of HCC to the last treatment. (B) Timeline of the treatment for this patient.

of an exophytic HCC into the peritoneal cavity and subsequent implantation of the tumor nodule onto the serosal surface of the bowel (5). Compared with metastatis to the appendix, metastatis to the colon was relatively common. The cause of metastasis to the colon could be stratified into two major reasons. One is the implantation of tumor cells. The other one is hematogenous metastasis (5, 12). Table 1 shows a summary of patients with colon/appendix metastasis from HCC obtained after research in the domestic and international literature. The median time from initial HCC to colon/appendix metastasis is 7 years (Table 1). Among the reported cases, only two cases had a history of tumor rupture (5, 13). Three patients had metastasis to the colon/

TABLE 1 Summary of cases reported in HCC patients with colon/appendix metastasis.

| Case | Year | Author | Age | Sex | Previous treatment | Time from initial HCC to colorectal/appendix metastasis (years) | History of tumor rupture | Site of metastasis | Treatment after finding of metastasis | Survival after the treatment |
|---|---|---|---|---|---|---|---|---|---|---|
| 1 | 2021 | Miyauchi et al. (20) | 80 | Male | Segment hepatectomy and radio-frequency ablation (RFA) | 5.3 | No | Ascending colon | Resection and lenvatinib | 30 months |
| 2 | 2021 | Mu et al. (15) | 86 | Male | TACE and microwave ablation | 10 | No | Hepatic flexure | Colostomy | 10 months |
| 3 | 2020 | Yu et al. (13) | 60 | Male | Hemihepatectomy and TACE | 10 | Yes | Descending colon | Hartmann Procedure | Over 3 months |
| 4 | 2020 | Kim et al. (18) | 72 | Male | Hemihepatectomy | 3 | No | Ascending colon | Resection | 6 weeks |
| 5 | 2019 | Pham et al. (19) | 60 | Male | TACE | 1 | No | Sigmoid colon | Resection | Not mentioned |
| 6 | 2019 | Tagliabue et al. (14) | 70 | Male | TACE | No mentioned | No | Sigmoid colon | Resection | Not mentioned |
| 7 | 2016 | Wu et al. (21) | 54 | Male | Segment-hepatectomy | 5 | No | Ileocecal junction | Right-half colon resection | 4 years |
| 8 | 2010 | Yoo et al. (16) | 47 | Male | TACE | 1.5 | No | Sigmoid colon | Anterior resection | Over 4 months |
| 9 | 2008 | Kim et al. (5) | 50 | Male | None | At the same time | Yes | Appendix | Appendectomy | Not mentioned |

appendix without a history of tumor rupture or hepatectomy (14–16). So, the cause of the metastasis to the colon or appendix may be complex. Implantation or hematogenous metastasis could both be a major cause. Our patient reported here was found to have appendix metastatis 5 years after when the tumor was R0-resected. We thought that the reason for metastasis for this patient was implantation. During the first surgery, the HCC specimen was taken out of the patient by a specimen bag from the lower abdomen. Although we were careful during the process, cell exfoliation still could happen. After we rechecked the pathological figure, we finally confirmed that tumor tissues had invaded all the layers from the serous membrane to the submucosa.

According to the Barcelona Clinic Liver Cancer (BCLC) staging system (17), the detection of extrahepatic metastasis indicates an advanced stage. Rather than resection, systemic treatment or conservative treatment would be recommended for such patients based on the BCLC staging system. The prognosis of such patients would be extremely poor, and the median survival time is expected to be nearly 1 year. However, according to the Chinese National Liver cancer stage system and the consensus on multidisciplinary management of recurrent and metastatic HCC after resection, resection could be recommended for patients with solitary metastasis (1, 7). The prognosis of recurrent HCC patients after repeat resection was found to be associated with the clinicopathologic characteristics of primary HCC and recurrence interval (7). In most reported cases mentioned in **Table 1**, surgery was performed to cure abdominal pain or intestinal obstruction rather than to cure HCC (13, 18–21). The overall survival since the detection of colon/appendix metastasis of the reported cases varied from 6 weeks to 5 years. The overall survival depends mainly on the liver function, tumor burden, and performance status of the patient. If the performance status is acceptable and complete resection is possible, aggressive resection might lead to a prolonged prognosis. For this patient, we found only recurrence in the tip of the appendix, which could be R0-resected at the first time, which means resection might be an acceptable choice.

Although R0 resection could be performed on HCC patients with solitary extrahepatic metastasis, a high risk of recurrence still existed (22). Because extrahepatic metastasis usually means that the tumor cell has penetrated into the blood vessel. Therapy used in patients with a high risk of recurrence was still under exploration. For now, only TACE has been confirmed with the effect of reducing the recurrent rate in random clinical trials (23). In this clinical trial, patients who received adjuvant TACE had a significantly longer 3-year recurrence free survival (RFS) than those who received conservative treatment (56% versus 42.1%). After 3 months, this patient returned to the department for adjuvant TACE. However, we found multiple intrahepatic recurrence in the routine examination. Recent advancements in tumor biology are currently attracting great interest in new antitumor drugs including ICIs and angiogenesis inhibitors (24). Given that the conventional locoregional therapies and angiogenesis inhibitors could induce the release of local inflammatory factors and neoantigens (25), several trials are assessing combination therapy for HCC patients without decompensation of liver function and surgical opportunity (26, 27). After combination therapy of conventional locoregional therapies, angiogenesis inhibitors, and ICIs, 33.3%–52.3% of unresectable patients could regain the opportunity of R0 resection. Among the reported cases, observative response rates are between 41.7% and 77.4%. With the inspiring results from recent clinical trials of TACE, immunotherapy, and target therapy (28), a combination of such treatment was suggested to this patient, and we received outstanding outcomes. After combining angiogenesis inhibitors, ICIs, and TACE, tumor markers came down to the normal range. In the routine examination, no sign of recurrence was detected.

For this patient, we did not perform a genetic test after we found tumor recurrence in the appendix or liver. Unlike other tumors, the genomic test is not necessary to treat advanced HCC. According to one investigation of phase III clinical trials (SHARP), angiogenesis markers [angiopoietin 2 (Ang2) and vascular endothelial growth factor (VEGF)] are predictors of overall survival in patients with HCC. However, neither Ang2 nor VEGF could predict a response to sorafenib (29). Lenvatinib, an oral inhibitor of vascular endothelial growth factor receptors (VEGFRs), fibroblast growth factor receptor 1-4 (FGFR1-4), ret proto-oncogene (RET), KIT proto-oncogene receptor tyrosine

kinase, and Platelet-derived growth factor receptor α (PDGFRa), has been tested in phase III trials in advanced HCC (30). In this clinical trial, lenvatinib has been proven to be noninferior to sorafenib in terms of overall survival. Similarly, no biomarker-predicting responses to lenvatinib have been reported (31). ICIs, including agents targeting cytotoxic T lymphocyte protein 4, PD-1, or its ligand PD-L1, have been proven effective in many clinical trials (32, 33). Different from other tumors, data presented on nivolumab and pembrolizumab (PD-1 inhibitors) have not shown any correlation between PDL-1 expression or other biomarkers and treatment efficacy (31, 34). To date, in the angiogenesis inhibitors or ICIs used in HCC, no specific gene mutation has been confirmed that could stratify patients, and this may be the reason why no clinical guidelines for HCC highly recommended genetic test.

Overall, solitary metastasis to the appendix 5 years after R0 resection of the intrahepatic lesion is a really rare phenomenon in HCC. This case might be the only one reported so far. Because of its scarcity, no well-designed clinical trials could provide treatment suggestions for this situation. Appendectomy might be an acceptable choice for patients with solitary metastasis to the appendix. Metastasis of extrahepatic lesions usually means dissemination of tumor cells into the body and a high risk of recurrence. Combined therapy of local regional treatment, angiogenesis inhibitors, and ICIs might be used to deal with this situation even after R0 resection of metastatic lesions.

## Patient perspective

We contacted this patient in October 2022 and asked him for his views on our therapy. No complaints or questions were proposed. Before the surgery, this patient suffered from lower abdominal pain. After the surgery, no pain was found. With the following medical treatment, the tumor was controlled with complete response. He thought the treatment therapy was successful.

## Data availability statement

The original contributions presented in the study are included in the article/Supplementary Material; further inquiries can be directed to the corresponding author.

## Ethics statement

Written informed consent was obtained from the individual(s) for the publication of any potentially identifiable images or data included in this article.

## Author contributions

Z-YZ performed most of the writing and prepared the figures and tables. Y-WW and B-XZ performed data and writing accusation. WZ designed the outline of this paper. All authors contributed to the article and approved the submitted version.

## Funding

This work is supported by the National Natural Science Foundation of China (grant no. 81802767 and 81860117).

## Conflict of interest

The authors declare that the research was conducted in the absence of any commercial or financial relationships that could be construed as a potential conflict of interest.

## Publisher's note

All claims expressed in this article are solely those of the authors and do not necessarily represent those of their affiliated organizations, or those of the publisher, the editors and the reviewers. Any product that may be evaluated in this article, or claim that may be made by its manufacturer, is not guaranteed or endorsed by the publisher.

## References

1. Xie D-Y, Ren Z-G, Zhou J, Fan J, Gao Q. 2019 Chinese clinical guidelines for the management of hepatocellular carcinoma: updates and insights. *Hepatobiliary Surg Nutr*. (2020) 9:452–63. doi: 10.21037/hbsn-20-480

2. Zhou M, Wang H, Zeng X, Yin P, Zhu J, Chen W, et al. Mortality, morbidity, and risk factors in China and its provinces, 1990–2017: a systematic analysis for the Global Burden of Disease Study 2017. *Lancet Lond Engl*. (2019) 394:1145–58. doi: 10.1016/S0140-6736(19)30427-1

3. Tabrizian P, Jibara G, Shrager B, Schwartz M, Roayaie S. Recurrence of hepatocellular cancer after resection: patterns, treatments, and prognosis. *Ann Surg*. (2015) 261:947–55. doi: 10.1097/SLA.0000000000000710

4. Kudo M, Izumi N, Kokudo N, Sakamoto M, Shiina S, Takayama T, et al. Report of the 21st nationwide follow-up survey of primary liver cancer in Japan (2010–2011). *Hepatol Res*. (2021) 51:355–405. doi: 10.1111/hepr.13612

5. Kim HC, Yang DM, Jin W, Kim GY, Choi SI. Metastasis to the appendix from a hepatocellular carcinoma manifesting as acute appendicitis: CT findings. *Br J Radiol*. (2008) 81:e194–6. doi: 10.1259/bjr/79390979

6. Farges O, Dokmak S. Malignant transformation of liver adenoma: an analysis of the literature. *Dig Surg*. (2010) 27:32–8. doi: 10.1159/000268405

7. Wen T, Jin C, Facciorusso A, Donadon M, Han H-S, Mao Y, et al. Multidisciplinary management of recurrent and metastatic hepatocellular carcinoma

after resection: an international expert consensus. *Hepatobiliary Surg Nutr*. (2018) 7:353–71. doi: 10.21037/hbsn.2018.08.01

8. Riley DS, Barber MS, Kienle GS, Aronson JK, von Schoen-Angerer T, Tugwell P, et al. CARE guidelines for case reports: explanation and elaboration document. *J Clin Epidemiol*. (2017) 89:218–35. doi: 10.1016/j.jclinepi.2017.04.026

9. Chen W, Zheng R, Baade PD, Zhang S, Zeng H, Bray F, et al. Cancer statistics in China, 2015. *CA Cancer J Clin*. (2016) 66:115–32. doi: 10.3322/caac.21338

10. Ou TM, Tsai WC, Hsieh TY, Shih YL. Hepatocellular carcinoma with colonic metastasis. *Singapore Med J*. (2014) 55:e93–5. doi: 10.11622/smedj.2013262

11. Katyal S, Oliver JH, Peterson MS, Ferris JV, Carr BS, Baron RL. Extrahepatic metastases of hepatocellular carcinoma. *Radiology*. (2000) 216:698–703. doi: 10.1148/radiology.216.3.r00se24698

12. Park M-S, Kim KW, Yu J-S, Kim M-J, Yoon S-W, Chung K-W, et al. Radiologic findings of gastrointestinal tract involvement in hepatocellular carcinoma. *J Comput Assist Tomogr*. (2002) 26:95–101. doi: 10.1097/00004728-200201000-00014

13. Yu Y-M, Cao Y-S, Wu Z, Huang R, Shen Z-L. Colon metastasis from hepatocellular carcinoma: a case report and literature review. *World J Surg Oncol*. (2020) 18:189. doi: 10.1186/s12957-020-01960-2

14. Tagliabue F, Burati M, Chiarelli M, Marando A, Simone MD, Cioffi U. Left colonic metastasis from primary hepatocellular carcinoma: a case report. *World J Clin Cases*. (2019) 7:2044–8. doi: 10.12998/wjcc.v7.i15.2044

15. Mu M, Yu J, Liang P, Yu X, Cheng Z. Colonic metastasis from hepatocellular carcinoma after treated by ablation and transarterial chemoembolization manifested by intestinal obstruction: a case report and review of the literature. *J Cancer Res Ther*. (2021) 17:814–7. doi: 10.4103/jcrt.JCRT_217_20

16. Yoo DJ, Chung YH, Lee YS, Kim SE, Jin YJ, Lee YM, et al. Sigmoid colon metastasis from hepatocellular carcinoma. *Korean J Hepatol*. (2010) 16:397–400. doi: 10.3350/kjhep.2010.16.4.397

17. Llovet JM, Brú C, Bruix J. Prognosis of hepatocellular carcinoma: the BCLC staging classification. *Semin Liver Dis*. (1999) 19:329–38. doi: 10.1055/s-2007-1007122

18. Kim R, Song J, Kim SB. Concurrent hepatocellular carcinoma metastasis to stomach, colon, and brain: a case report. *World J Clin Cases*. (2020) 8:3534–41. doi: 10.12998/wjcc.v8.i16.3534

19. Pham BV, Phan HH, Ngo LL, Nguyen HTT, Le KV, Dinh TC, et al. A rare colonic metastasis case from hepatocellular carcinoma. *Open Access Maced J Med Sci*. (2019) 7:4368–71. doi: 10.3889/oamjms.2019.837

20. Miyauchi W, Yamamoto M, Masahiro M, Shishido Y, Miyatani K, Matsunaga T, et al. Colonic metastasis of hepatocellular carcinoma with repeated retroperitoneal bleeding: a case report. *Surg Case Rep*. (2021) 7:261. doi: 10.1186/s40792-021-01349-7

21. Wu D, Wei S, Liu B, Wu X, Feng Y, Luo C, et al. Effect of immune suppression on metastasis in a patient with hepatocellular carcinoma metastasized to the colon and stomach: a case report. *Exp Ther Med*. (2016) 11:1741–7. doi: 10.3892/etm.2016.3108

22. Ohta M, Nakanishi C, Kawagishi N, Hara Y, Maida K, Kashiwadate T, et al. Surgical resection of recurrent extrahepatic hepatocellular carcinoma with tumor thrombus extending into the right atrium under cardiopulmonary bypass: a case report and review of the literature. *Surg Case Rep*. (2016) 2:110. doi: 10.1186/s40792-016-0241-7

23. Wang Z, Ren Z, Chen Y, Hu J, Yang G, Yu L, et al. Adjuvant transarterial chemoembolization for HBV-related hepatocellular carcinoma after resection: a randomized controlled study. *Clin Cancer Res*. (2018) 24:2074–81. doi: 10.1158/1078-0432.CCR-17-2899

24. Leone P, Solimando AG, Fasano R, Argentiero A, Malerba E, Buonavoglia A, et al. The evolving role of immune checkpoint inhibitors in hepatocellular carcinoma treatment. *Vaccines*. (2021) 9:532. doi: 10.3390/vaccines9050532

25. Yi C, Chen L, Lin Z, Liu L, Shao W, Zhang R, et al. Lenvatinib targets FGF receptor 4 to enhance antitumor immune response of anti-programmed cell death-1 in HCC. *Hepatol Baltim Md*. (2021) 74:2544–60. doi: 10.1002/hep.31921

26. Wu J-Y, Yin Z-Y, Bai Y-N, Chen Y-F, Zhou S-Q, Wang S-J, et al. Lenvatinib combined with anti-PD-1 antibodies plus transcatheter arterial chemoembolization for unresectable hepatocellular carcinoma: a multicenter retrospective study. *J Hepatocell Carcinoma*. (2021) 8:1233–40. doi: 10.2147/JHC.S332420

27. Huang Y, Zhang Z, Liao W, Hu K, Wang Z. Combination of sorafenib, camrelizumab, transcatheter arterial chemoembolization, and stereotactic body radiation therapy as a novel downstaging strategy in advanced hepatocellular carcinoma with portal vein tumor thrombus: a case series study. *Front Oncol*. (2021) 11:650394. doi: 10.3389/fonc.2021.650394

28. Li Z, Han N, Ren X, Zhang Y, Chu X. Effectiveness of TKI inhibitors combined with PD-1 in patients with postoperative early recurrence of HCC: a real-world study. *Front Oncol*. (2022) 12:833884. doi: 10.3389/fonc.2022.833884

29. Llovet JM, Peña CEA, Lathia CD, Shan M, Meinhardt G, Bruix J, SHARP Investigators Study Group. Plasma biomarkers as predictors of outcome in patients with advanced hepatocellular carcinoma. *Clin Cancer Res*. (2012) 18:2290–300. doi: 10.1158/1078-0432.CCR-11-2175

30. Kudo M, Finn RS, Qin S, Han K-H, Ikeda K, Piscaglia F, et al. Lenvatinib versus sorafenib in first-line treatment of patients with unresectable hepatocellular carcinoma: a randomised phase 3 non-inferiority trial. *Lancet Lond Engl*. (2018) 391:1163–73. doi: 10.1016/S0140-6736(18)30207-1

31. Llovet JM, Montal R, Sia D, Finn RS. Molecular therapies and precision medicine for hepatocellular carcinoma. *Nat Rev Clin Oncol*. (2018) 15:599–616. doi: 10.1038/s41571-018-0073-4

32. Sové RJ, Verma BK, Wang H, Ho WJ, Yarchoan M, Popel AS. Virtual clinical trials of anti-PD-1 and anti-CTLA-4 immunotherapy in advanced hepatocellular carcinoma using a quantitative systems pharmacology model. *J Immunother Cancer*. (2022) 10:e005414. doi: 10.1136/jitc-2022-005414

33. Qin S, Finn RS, Kudo M, Meyer T, Vogel A, Ducreux M, et al. RATIONALE 301 study: tislelizumab versus sorafenib as first-line treatment for unresectable hepatocellular carcinoma. *Future Oncol Lond Engl*. (2019) 15:1811–22. doi: 10.2217/fon-2019-0097

34. El-Khoueiry AB, Sangro B, Yau T, Crocenzi TS, Kudo M, Hsu C, et al. Nivolumab in patients with advanced hepatocellular carcinoma (CheckMate 040): an open-label, non-comparative, phase 1/2 dose escalation and expansion trial. *Lancet Lond Engl*. (2017) 389:2492–502. doi: 10.1016/S0140-6736(17)31046-2

frontiers | Frontiers in Oncology

TYPE Case Report
PUBLISHED 02 May 2023
DOI 10.3389/fonc.2023.1073728



OPEN ACCESS

EDITED BY
Raffaele Ratta,
Hôpital Foch, France

REVIEWED BY
Takeshi Yuasa,
Japanese Foundation For Cancer Research, Japan
Lori Wood,
Queen Elizabeth II Hospital, Canada

*CORRESPONDENCE
Jean Courcier
jean.courcier@aphp.fr

RECEIVED 18 October 2022
ACCEPTED 31 March 2023
PUBLISHED 02 May 2023

CITATION
Courcier J, De La Taille A, Bertolo R, Amparore D, Erdem S, Kara O, Marchioni M, Pavan N, Roussel E, Mamodaly M, Campi R and Ingels A (2023) Surgical and oncological management of renal medullary carcinoma in a young patient: a case report.
*Front. Oncol.* 13:1073728.
doi: 10.3389/fonc.2023.1073728



# Surgical and oncological management of renal medullary carcinoma in a young patient: a case report

Jean Courcier[1,2]*, Alexandre De La Taille[1], Riccardo Bertolo[3], Daniele Amparore[4], Selcuk Erdem[5], Onder Kara[6], Michele Marchioni[7], Nicola Pavan[8], Eduard Roussel[9,10], Maria Mamodaly[11], Riccardo Campi[12,13] and Alexandre Ingels[1]

[1]Department of Urology, Henri Mondor Hospital, University of Paris Est Créteil (UPEC), Créteil, France, [2]Université Paris-Saclay, CEA, CNRS, Inserm, BioMaps, Villejuif, France, [3]Department of Urology, San Carlo Di Nancy Hospital, Rome, Italy, [4]Division of Urology, Department of Oncology, School of Medicine, San Luigi Hospital, University of Turin, Orbassano, Italy, [5]Division of Urologic Oncology, Department of Urology, Istanbul University Istanbul Faculty of Medicine, Istanbul, Türkiye, [6]Department of Urology, Kocaeli University School of Medicine, Kocaeli, Türkiye, [7]Urology Unit, Department of Medical, Oral and Biotechnological Sciences, "G. d'Annunzio" University of Chieti, Chieti, Italy, [8]Urology Clinic, Department of Medical Surgical and Health Science, University of Trieste, Trieste, Italy, [9]Department of Urology, Onze-Lieve-Vrouwziekenhuis (OLV) Hospital, Aalst, Belgium, [10]Department of Urology, University Hospitals Leuven, Leuven, Belgium, [11]Pathology Department, University of Paris Est Créteil (UPEC), Henri Mondor Hospital, Créteil, France, [12]Unit of Urological Robotic Surgery and Renal Transplantation, Careggi Hospital, University of Florence, Florence, Italy, [13]Department of Experimental and Clinical Medicine, University of Florence, Florence, Italy

Renal medullary carcinoma (RMC) is a rare form of renal cell carcinoma that has a poor prognosis. It is known to be associated with sickle cell trait or disease, although the exact underlying mechanisms are still unclear. The diagnosis is made through immunochemical staining for SMARCB1 (INI1). In this report, we present a case of a 31-year-old male patient with sickle cell trait who was diagnosed with stage III right RMC. Despite the poor prognosis, the patient survived for a remarkable duration of 37 months. Radiological assessment and follow-up were primarily performed using 18F-FDG PET/MRI. The patient underwent upfront cisplatin-based cytotoxic chemotherapy before surgical removal of the right kidney and retroperitoneal lymph node dissection. Identical adjuvant chemotherapy was administered post-surgery. Disease relapses were detected in the retroperitoneal lymph nodes; these were managed with chemotherapy and surgical rechallenges. We also discuss the oncological and surgical management of RMC, which currently relies on perioperative cytotoxic chemotherapy strategies, as there are no known alternative therapies that have been shown to be superior to date.

KEYWORDS

**non-clear cell RCC, renal medullary carcinoma, SMARCB1, chemotherapy, onco-urological management**

## 1 Introduction

Renal carcinoma represents approximatively 2%–3% of solid cancers. Clear cell renal cell carcinoma is the most common type, accounting for 75% of cases, followed by papillary renal cell carcinoma (10%) and chromophobe renal cell carcinoma (<5%) (1). There are other rare pathological entities that present with a wide diversity of histological types. Among these rare entities is renal medullary carcinoma (RMC), which accounts for approximatively 0.5% of renal carcinoma (2). RMC mostly affects men (gender ratio: 2:1), and most commonly affects adolescents and young adults (median age at diagnosis: 28 years), with the right kidney being preferentially involved (3). This pathology is almost exclusively associated with heterozygous sickle cell trait or disease and other hemoglobinopathies (4). Thus, the practice of high-intensity exercise in such patients could hypothetically be a risk factor (5). The diagnosis is commonly made by investigating general symptoms such as abdominal pain, fatigue, weight loss, and, more specifically, by gross hematuria or clinical palpation of a flank or abdominal mass (6). The disease is more likely to be diagnosed at an advanced or metastatic stage (7). In addition, several reports have described rapid metastatic dissemination even in patients who were treated early for localized RMC (4, 6, 8). Radiological evaluation of the disease relies on enhanced computed tomography (CT), which typically shows a weakly and heterogeneously enhanced tumor, a central localization in the kidney with respect of the kidney's outline. (9, 10). The radiological aspect on CT scan can mimic a urothelial upper tract tumor invading the renal parenchyma. This medical condition has a poor prognosis, with a reported median overall survival (OS) of 13 months (95% CI: 9.0–17.9 months) (6). The physiopathology of RMC is still hypothetical, but chronic stress hypoxia associated with sickle cell disease is suspected to play a role (11). The first histological characterization of this cancer dates back to 1995 (12). On histopathological examination, an infiltrative tumor is readily visible, originating from the medullary boundary with the kidney's excretory tract. The tumor is composed of poorly differentiated cells and shows neutrophil infiltration. Cystic components may also be present. Finally, the loss of expression of SMARCB1 (INI1) is suspected to play a central role in the pathogenesis of RMC, and confirmation of this loss of expression through immunohistochemistry confirms the diagnosis (13–16). In this report, we present a case of the management of RMC.

**Abbreviations:** RMC, renal medullary carcinoma; SMARCB1, SWI/SNF-related, matrix-associated, actin-dependent regulator of chromatin, subfamily B, member 1; INI1, integrase interactor 1; 18F-FDG PET/MRI, 2-deoxy-2-[18F] fluoroglucose positron emission tomography coupled with magnetic resonance imaging; CT, computed tomography; OS, overall survival; 95% CI, 95% confidence interval; EMA, epithelial membrane antigen; CK, cytokeratin; CD, cluster of differentiation; PAX8, paired-box gene 8; GATA 3, G-A-T-A nucleotide sequence binding protein 3; PD-L1, programmed death ligand 1; PD-1, programmed death 1; TNM, tumor node metastasis classification; AJCC/UICC, American Joint Committee on Cancer and International Union Against Cancer; TP53, tumor protein 53; TMB, tumor mutational burden; MSS, microsatellite stability; MSI, microsatellite instability; MVAC, Methotrexate, Vinblastine, Adriamycin, Cisplatin; ORR, overall response rate; HR, hazard ratio; ccRCC, clear cell renal cell carcinoma; EZH2, enhancer of zeste homologue 2; IO, immuno-oncology; CTLA4, cytotoxic T-lymphocyte-associated protein 4.

## 2 Case presentation

In April 2019, a 31-year-old male patient was referred by a practitioner for evaluation of right lower back pain that had been ongoing for 3 months, along with weight loss of 6 kg over a 6-month period. The patient reported experiencing a sense of heaviness in the right hypochondrium towards the end of 2018, accompanied by colicky abdominal pain that increased in intensity over the following months. However, no symptoms of altered bowel movements or hematuria were reported. The patient had a history of heterozygous sickle cell trait and had suffered from malaria infection at the age of 12. He had no other significant medical history and reported no family history of neoplasia. Abdominal ultrasound imaging revealed a 50-mm mass in the patient's right kidney. Subsequent CT scans showed a heterogeneous 50 × 47 × 45 mm parenchymal renal mass involving the renal sinus (Figure 1), along with lymph node involvement in para-aortic and inter-aortocaval locations. There was no extension to the renal vein, and no abnormalities were found in the liver or at the thoracic or skeletal levels.

Whole-body 18F-FDG PET/MRI revealed a 43-mm hypermetabolic lesion in the right kidney, which was accompanied by hypermetabolic retroperitoneal lymph node invasion and a single hypermetabolic lymph node above the diaphragm in the left sub-clavicular position. There was no evidence of invasion in the viscera or bones.

The diagnosis of RMC was established based on a biopsy of the renal mass: analysis of eight biopsy samples revealed proliferation of a poorly differentiated carcinoma tumor consisting of basophilic cellular elements with increased nuclear–cytoplasmic ratio, irregular hyperchromatic nuclei, and frequent mitotic figures. The proliferation exhibited a trabecular-cord architecture, and there was

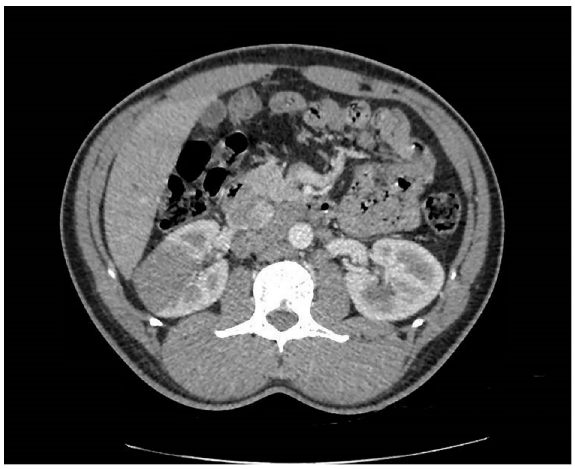

FIGURE 1
Axial enhanced CT scan showing the poorly delimited right renal mass at diagnosis.

no evidence of glandular inflection. It was located within a highly inflammatory stroma, and the entire tumor was separated by sclerohyaline areas in which residual renal tubules and numerous congestive vessels without embolism were observed. There was no evidence of a lymphomatous process. Immunohistochemical analysis revealed positive staining of the tumor cells for Vimentin, EMA, CK7, PAX8, and E-Cadherin, and negative staining for CD117, CD10, CK20, CK5-6, P40, and GATA 3. These immunohistochemical findings excluded the possibility of urothelial carcinoma. The histological appearance was consistent with an epithelial tumor of renal origin. The pathological report further indicated tumor proliferation, with an immunohistochemical profile (SMARCB1/INI1 negative) consistent with the proposed diagnosis of RMC. Notwithstanding, 20% of tumoral cell membranes were positive for PD-L1 staining in immunohistochemistry.

At the time of diagnosis, the patient's general condition was good, with a body mass index of 25.6 kg/$m^2$ and a performance status of 0. The case was discussed in a multidisciplinary meeting, and systemic therapy was recommended. The initial treatment plan included three cycles of paclitaxel (80 mg/$m^2$ on days 1 and 8), gemcitabine (1,000 mg/$m^2$ on days 1 and 8), and cisplatin (70 mg/$m^2$ on day 1), given in 21-day cycles. The patient commenced chemotherapy in June 2019.

After completion of three cycles of chemotherapy, 18F-FDG PET/MRI showed a partial response, with reduction in the size of the primary tumor from 43 mm to 26 mm, and no uptake observed in the supra-diaphragmatic lymph node. However, a hypermetabolic 23-mm inter-aortocaval lymph node and multiple weakly metabolic retroperitoneal nodes smaller than 1 cm were still present.

In September 2019, the patient underwent an open right nephrectomy with retroperitoneal lymph node dissection, which took 180 min and resulted in an estimated blood loss of 700 ml. No post-operative complications of grade higher than CLAVIEN-DINDO level 1 were reported.

Histological examination revealed a remnant of RMC with evidence of a therapeutic response, as indicated by 60% fibrotic involution of the renal tumor. The pathologist described in his report a specimen of total right nephrectomy, which contained residual tumor of medullary carcinoma with extensive fibrous and inflammatory changes related to adjuvant chemotherapy. The therapeutic response was estimated to be 60% (60% fibrosis and 40% viable tumor) of the overall surface area of the macroscopically observed scarred zone, measuring 2.5 cm in its largest dimension. The residual tumor was composed of more-or-less cohesive masses of cells, with abundant eosinophilic cytoplasm that was clarified in places with an irregular nucleus, strongly nucleolated within a myxoid stroma. No sarcomatoid or rhabdoid features were observed. On immunohistochemical examination, these tumor cells expressed cytokeratins 7 and 903, vimentin, and PAX8, but not INI1. PD-L1 was expressed in 5% of tumor cells. The tumor was strictly intrarenal and did not invade the renal vein or small vessels. The collecting system and adrenal gland were not involved. The inter-aortocaval lymph node dissection revealed a metastatic lymph node measuring 4 cm in its largest dimension, without capsular rupture, with fibrous changes, one node measuring 0.3 cm with complete fibrous remodeling in favor of a tumor response, and four negative nodes (one positive out of six nodes). There were microfoci of tumor cells in the periganglionic connective tissue. The surgical margins were clear. Overall, the tumor was classified as ypT1aN1R0 according to the TNM 2018 classification, AJCC/UICC 8th edition. Histologic features are shown in Figure 2.

Subsequently, adjuvant therapy under the same cytotoxic chemotherapy protocol was administered for three cycles, and surveillance was conducted until a relapse was detected in October 2020, through 18F-FDG PET/MRI, which revealed progression of the retroperitoneal lymph nodes, with two hypermetabolic lymph nodes (14-mm inter-aortocaval and 10-mm latero-aortic). The case was reviewed at a multidisciplinary meeting, and it was decided that a rechallenge of chemotherapy should be pursued before the possibility of surgical reintervention was contemplated. In the absence of validated therapeutic alternatives, it was decided to administer gemcitabine at 1,250 mg/$m^2$ (on days 1 and 8) in association with cisplatin at 70 mg/$m^2$ (on day 1), which was reduced to 65 mg/$m^2$ after the third cycle due to grade 3 neutropenia. Following three cycles of treatment, a partial response was observed, as evidenced by a reduction in the size of the inter-aortocaval lymph node from 14 mm to 7 mm and the latero-aortic lymph node from 10 mm to 5 mm. Following six cycles, the patient was proposed for surgical management of the remaining retroperitoneal disease, and underwent extensive retroperitoneal lumbo-aortic and aorto-cava lymph node dissection in April 2021. The operative time was 195 min, with an estimated blood loss of 1,300 ml. The histology report indicated malignancy in 11 out of 16 lumbo-aortic nodes (11N+/16), and in 2 out of 10 inter-aorto-cava nodes (2N+/10).

Progression of the disease was diagnosed 10 months after the last surgery: the patient described intense right flank pain that had been present for several weeks, requiring a significant increase in oral morphine doses. The CT scan that was then performed to explore these symptoms showed a reappearance of retroperitoneal lymph nodes without any other identifiable lesions, suggestive of disease progression. The patient's case was presented at a specialized multidisciplinary consultation meeting to search for molecular anomalies. A liquid biopsy "Foundation One Liquid CDx" was performed but did not allow for inclusion in a therapeutic trial or specific therapeutic orientation [TP53 mutation negative, low tumor mutational burden (TMB at 4 MBs), no loss of heterozygosity, microsatellite stable (MSS)]. The patient was therefore proposed for systemic treatment with carboplatin, doxorubicin, and bortezomib, but he did not wish to resume chemotherapy and requested some time to reflect. Inclusion in the phase I therapeutic trial PEMBIB (17) was proposed, but unfortunately, the patient's general condition no longer allowed for inclusion in the protocol, with the appearance of symptomatic ascites effusion requiring evacuative punctures.

The patient presented to the emergency department 4 months after being diagnosed with recurrent disease. He reported persistent asthenia for several weeks without significant worsening, but with the gradual appearance of edema in the lower limbs and tense ascites requiring two trans-abdominal punctures for evacuation. A deterioration of the general condition was noted from the end of May 2022, with an inability to eat and the onset of anuria 24 h prior to presentation to the emergency department. He was subsequently

10.3389/fonc.2023.1073728

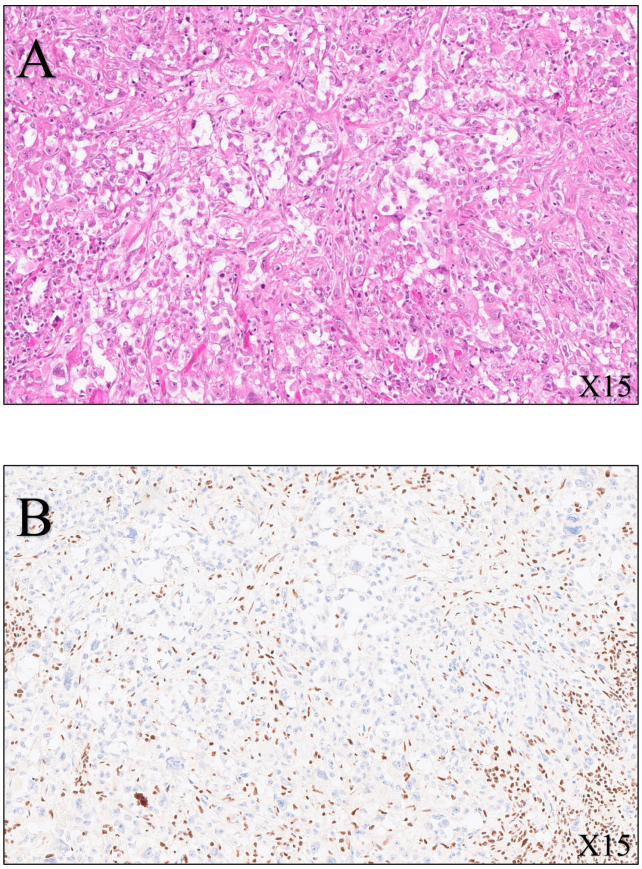


FIGURE 2
Histological features of the radical nephrectomy of the right kidney. **(A)** SMARCB1-deficient renal medullary carcinoma (hematoxylin–eosin–saffron, ×15 magnification): tumor cells are pleomorphic with enlarged nuclei, vesicular chromatin, proeminent nucleoli, and eosinophilic cytoplasm. **(B)** Immunohistochemistry (SMARCB1, ×15 magnification) shows loss of expression of SMARB1 (also known as INI1, SNF5, or BAF47) within the tumor cells, whereas intratumoral lymphocytes are strongly positive (nuclear stain).

admitted to the intensive care unit due to multiorgan failure. A non-enhanced thoracoabdominal-pelvic CT scan was performed due to renal insufficiency: this showed the appearance of multiple hypodense nodular lesions in the liver suggestive of secondary lesions; large retroperitoneal nodules in the right nephrectomy bed; an increase in the number and size of aortocaval, iliac, and inguinal lymph nodes; the appearance of bilateral pleural effusion; and a large amount of intra-abdominal fluid accumulation. The appearance of a lytic lesion of the L2 vertebral body, suggestive of a secondary lesion, was also indicated. Given the severity of the clinical picture and the absence of therapeutic resources, a collective decision (involving oncologists and intensivists) not to perform invasive resuscitation procedures was taken.

This patient unfortunately passed away in June 2022, 37 months after initial diagnosis. A timeline depicting patient care is shown in Figure 3.

## 3 Discussion

Despite advancements in the understanding of this disease, no significant improvement in disease-specific survival has been observed over the past decade, and treatment is currently based on chemotherapy and nephrectomy, despite a lack of solid scientific evidence (18–20). In 2016, Beckermann et al. proposed clinical guidelines, developed in collaboration with a panel of experts, to aid in the clinical management of these patients (8). These guidelines were subsequently updated in 2019 by Msaouel et al., with a major change in the form of the proposal that nephrectomy should only be

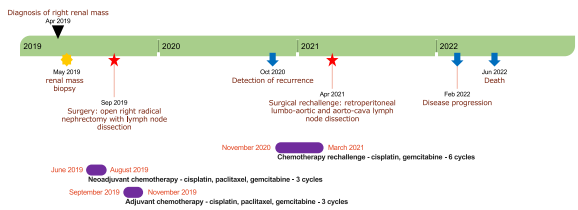


FIGURE 3
A timeline depicting patient care with the main notable events during follow-up. The timeline is represented by a green stripe divided into years. The black triangle indicates the date of diagnosis; the yellow star denotes the timing of renal mass biopsy; the red stars indicate the timing of surgeries; the blue arrows denote the timing of recurrence and death; and the violet stripes represent periods of chemotherapy.

performed in the event of a response to chemotherapy in a perioperative scheme (21).

We report a single patient with a prolonged OS of 37 months, in contrast to the data reported by Shah et al., who found a median OS of 16.4 months in 38 patients treated with nephrectomy before or during cytotoxic chemotherapy (6). This highlights the exceptional nature of this patient's response. The current expert consensus, as reported by Msaouel et al., supports the use of platinum-based cytotoxic chemotherapy as prior systemic therapy for RMC treatment (21). Cisplatin-based chemotherapy (specifically, cisplatin plus gemcitabine in combination with doxorubicin or high-dose MVAC) is the best-described and most effective known treatment for RMC, with an overall response rate (ORR) of 29% according to literature sources (6, 8, 18, 19, 22–24). However, this treatment strategy appears to be based on weak scientific foundations, approaching historical treatments of metastatic upper tract urothelial cancer or collecting duct carcinoma, in the absence of alternative therapies. Patients who demonstrate a radiological response to the disease should be considered for nephrectomy in conjunction with retroperitoneal lymphadenectomy. Systemic therapy should then be continued, with close clinical and radiological follow-up every 6 to 12 weeks.

The supposed benefit of cytoreductive nephrectomy in RMC patients is based on a retrospective study of 52 patients (6). The comparison between patients who underwent nephrectomy and those who received only systemic therapy suggested a benefit in favor of the nephrectomy group, with a median OS of 16.4 months compared to 7.0 months, respectively ($p < 0.001$, HR = 0.22, 95% CI: 0.09–0.51).

With significant advancements in the diagnosis and understanding of this disease having occurred over the past two decades, it is noteworthy that the rarity of RMC may contribute to the lack of scientific evidence regarding its management. Nonetheless, ongoing phase II clinical trials are exploring alternative treatment options based on identified molecular pathways and plausible physiopathological hypotheses. Among these research axes are therapeutics targeting the proteasome, such as bortezomib, which promotes cell death in SMARCB1-deficient tumors (25). Studies evaluating proteasome inhibitors as systemic treatments for RMC have been conducted. For instance, a phase II study published in 2004 assessed bortezomib for patients with advanced RCC and reported clinical activity, with 4 out of 37 evaluable patients showing partial response (11% ORR). Interestingly, only one of the four responders had RMC, despite being the only one with this histology, while the other three had ccRCC (26, 27). In addition, there have been reports of prolonged responses in children with metastatic RMC who were treated with a combination of bortezomib and platinum-based chemotherapy. Two cases of exceptional complete responses with no evidence of disease at 23 months and 7 years from diagnosis were reported by Carden et al. (28). A phase II trial (NCT03587662) is currently recruiting patients to evaluate the safety and efficacy of ixazomib, a second-generation proteasome inhibitor, in combination with gemcitabine and doxorubicin in patients with SMARCB1-negative renal tumors (29).

EZH2 (enhancer of zeste homologue 2) inhibitors are a type of anticancer drug that regulate DNA transcription by inhibiting histone methylation. In mice with SMARCB1-deleted tumors, these inhibitors have been found to be effective in halting histone methylation (30, 31). EZH2 inhibitors work by demethylating lysine 27 of histone H3, which can enhance the effectiveness of other drugs like doxorubicin (32). Through demethylation of histone H3, EZH2 inhibitors can also restore the expression of proapoptotic genes in cancerous cells, promoting programmed death. One particular EZH2 inhibitor, known as tazemetostat, is currently undergoing evaluation in a phase II basket study. The study is recruiting patients with SMARCB1-negative tumors, including refractory synovial sarcoma and RMC patients. Recruitment was active at the time of writing, with an estimated primary completion date of December 2022 (NCT02601950). The authors of the study reported clinical activity in a subset of a cohort of 62 patients treated for epithelioid sarcoma with tazemetostat (800 mg, oral drug, twice daily), with a 15% ORR (95% CI: 7%–26%) (33). Unfortunately, no results on RMC patients treated with tazemetostat in this study have yet been reported.

Lastly, immune-oncology (IO) using anti-PD-1 and anti-CTLA4 antibodies has demonstrated clinical activity in RMC. In one study, Sodji et al. reported clinical activity in a single patient with metastatic RMC who was treated with nivolumab (anti-PD-1 antibody) for 15 months after recurrence following initial nephrectomy and six adjuvant cycles of cisplatin-based chemotherapy (34). The patient experienced stability of retroperitoneal lesions and regression of pulmonary secondary lesions while on nivolumab. The authors did not suggest any predictive role of PD-L1 tumoral expression in response to nivolumab. Three RMC patients were included in a phase I study that evaluated the safety of nivolumab plus cabozantinib (a tyrosine kinase inhibitor) ± ipilimumab (anti-CTLA4 antibody) for patients with metastatic urothelial carcinoma and other genitourinary tumors (35). Two of these patients were evaluated for treatment response, with one achieving a partial response and the other showing progressive disease during treatment. The use of ipilimumab in these patients was not mentioned. Furthermore, another study reported the use of pembrolizumab (an anti-PD-1 antibody) in four RMC patients (36).

Regrettably, it appears evident that the scarcity of RMC patients (who are rare and medically complex) constrains the enrollment of participants in clinical trials and obstructs the successful completion of phase III research. Consequently, it is of paramount importance to incorporate RMC patients in phase II studies, as indicated in the accompanying table (Table 1).

## 4 Conclusion

We report here the case of a 31-year-old patient with RMC who received appropriate treatment consisting of initial cisplatin-

TABLE 1 Ongoing phase II trials for RMC.

| Trial | Phase | Drugs | Recruitment status | Related publications |
|---|---|---|---|---|
| Ixazomib, Gemcitabine, and Doxorubicin in Treating Patients With Locally Advanced or Metastatic Kidney Cancer—NCT03587662 | II | Ixazomib + doxorubicin + gemcitabine | Recruiting | Msaouel et al. (29) |
| A Phase II, Multicenter Study of the EZH2 Inhibitor Tazemetostat in Adult Subjects with INI1-Negative Tumors—NCT02601950 | II | Tazemetostat | Active, not recruiting | Gounder et al. (33) |
| Phase II Trial of Nivolumab Plus Ipilimumab in Patients with Renal Medullary Carcinoma—NCT03274258 | II | Nivolumab + ipilimumab | Active, not recruiting | Msaouel et al. (37) |
| Secured Access to Nivolumab for Adult Patients with Selected Rare Cancer Types (AcSe)—NCT03012581 | II | Nivolumab | Active, not recruiting | Albiges et al. (38) |

based chemotherapy, followed by nephrectomy with retroperitoneal lymphadenectomy and continued adjuvant chemotherapy. He survived for 37 months after the initial diagnosis, supporting the therapeutic strategy employed here based on expert consensus. However, novel therapies are urgently needed to improve outcomes for patients with this rare and life-threatening disease. Ongoing phase II clinical trials are currently recruiting RMC patients.

## Data availability statement

The original contributions presented in the study are included in the article/supplementary material. Further inquiries can be directed to the corresponding author.

## Ethics statement

Written informed consent was obtained from the individual(s) for the publication of any potentially identifiable images or data included in this article.

## Author contributions

Study concept and design: JC, AT, AI. Drafting of the manuscript: JC, AI, RC, MMam, RB, DA, SE, OK, MMar, NP, and ER. Critical revision of the manuscript: AT, AI, and MMam. All authors contributed to the article and approved the submitted version.

## Conflict of interest

The authors declare that the research was conducted in the absence of any commercial or financial relationships that could be construed as a potential conflict of interest.

## Publisher's note

All claims expressed in this article are solely those of the authors and do not necessarily represent those of their affiliated organizations, or those of the publisher, the editors and the reviewers. Any product that may be evaluated in this article, or claim that may be made by its manufacturer, is not guaranteed or endorsed by the publisher.

## References

1. Moch H, Cubilla AL, Humphrey PA, Reuter VE, Ulbright TM. The 2016 WHO classification of tumours of the urinary system and Male genital organs–part a: Renal, penile, and testicular tumours. *Eur Urol* (2016) 70:93–105. doi: 10.1016/j.eururo.2016.02.029

2. Amin MB, Smith SC, Agaimy A, Argani P, Compérat EM, Delahunt B, et al. Collecting duct carcinoma versus renal medullary carcinoma: an appeal for nosologic and biological clarity. *Am J Surg Pathol* (2014) 38:871–4. doi: 10.1097/PAS.0000000000000222

3. Gupta R, Billis A, Shah RB, Moch H, Osunkoya AO, Jochum W, et al. Carcinoma of the collecting ducts of Bellini and renal medullary carcinoma: clinicopathologic analysis of 52 cases of rare aggressive subtypes of renal cell carcinoma with a focus on their interrelationship. *Am J Surg Pathol* (2012) 36:1265–78. doi: 10.1097/PAS.0b013e3182635954

4. Blas L, Roberti J, Petroni J, Reniero L, Cicora F. Renal medullary carcinoma: A report of the current literature. *Curr Urol Rep* (2019) 20:4. doi: 10.1007/s11934-019-0865-9

5. Shapiro DD, Soeung M, Perelli L, Dondossola E, Surasi DS, Tripathi DN, et al. Association of high-intensity exercise with renal medullary carcinoma in individuals with sickle cell trait: Clinical observations and experimental animal studies. *Cancers* (2021) 13:6022. doi: 10.3390/cancers13236022

6. Shah AY, Karam JA, Malouf GG, Rao P, Lim ZD, Jonasch E, et al. Management and outcomes of patients with renal medullary carcinoma: a multicentre collaborative study. *BJU Int* (2017) 120:782–92. doi: 10.1111/bju.13705

7. Iacovelli R, Modica D, Palazzo A, Trenta P, Piesco G, Cortesi E. Clinical outcome and prognostic factors in renal medullary carcinoma: A pooled analysis from 18 years of medical literature. *Can Urol Assoc J* (2015) 9:E172–177. doi: 10.5489/cuaj.2373

8. Beckermann KE, Sharma D, Chaturvedi S, Msaouel P, Abboud MR, Allory Y, et al. Renal medullary carcinoma: Establishing standards in practice. *J Oncol Pract* (2017) 13:414–21. doi: 10.1200/JOP.2017.020909

9. Blitman NM, Berkenblit RG, Rozenblit AM, Levin TL. Renal medullary carcinoma: CT and MRI features. *AJR Am J Roentgenol* (2005) 185:268–72. doi: 10.2214/ajr.185.1.01850268

10. Sandberg JK, Mullen EA, Cajaiba MM, Smith EA, Servaes S, Perlman EJ, et al. Imaging of renal medullary carcinoma in children and young adults: A report from the children's oncology group. *Pediatr Radiol* (2017) 47:1615–21. doi: 10.1007/s00247-017-3926-6

11. Msaouel P, Tannir NM, Walker CL. A model linking sickle cell hemoglobinopathies and SMARCB1 loss in renal medullary carcinoma. *Clin Cancer Res* (2018) 24:2044–9. doi: 10.1158/1078-0432.CCR-17-3296

12. Davis CJ, Mostofi FK, Sesterhenn IA. Renal medullary carcinoma the seventh sickle cell nephropathy. *Am J Surg Pathol* (1995) 19:1–11. doi: 10.1097/00000478-199501000-00001

13. Carvalho JC, Thomas DG, McHugh JB, Shah RB, Kunju LP. p63, CK7, PAX8 and INI-1: An optimal immunohistochemical panel to distinguish poorly differentiated urothelial cell carcinoma from high-grade tumours of the renal collecting system. *Histopathology* (2012) 60:597–608. doi: 10.1111/j.1365-2559.2011.04093.x

14. Lopez-Beltran A, Cheng L, Raspollini MR, Montironi R. SMARCB1/INI1 genetic alterations in renal medullary carcinomas. *Eur Urol* (2016) 69:1062–4. doi: 10.1016/j.eururo.2016.01.002

15. Calderaro J, Masliah-Planchon J, Richer W, Maillot L, Maille P, Mansuy L, et al. Balanced translocations disrupting SMARCB1 are hallmark recurrent genetic alterations in renal medullary carcinomas. *Eur Urol* (2016) 69:1055–61. doi: 10.1016/j.eururo.2015.09.027

16. Cheng JX, Tretiakova M, Gong C, Mandal S, Krausz T, Taxy JB. Renal medullary carcinoma: Rhabdoid features and the absence of INI1 expression as markers of aggressive behavior. *Mod Pathol* (2008) 21:647–52. doi: 10.1038/modpathol.2008.44

17. Baldini C, Danlos F-X, Varga A, Texier M, Halse H, Mouraud S, et al. Safety, recommended dose, efficacy and immune correlates for nintedanib in combination with pembrolizumab in patients with advanced cancers. *J Exp Clin Cancer Res* (2022) 41:217. doi: 10.1186/s13046-022-02423-0

18. Amato RJ. Chemotherapy for renal cell carcinoma. *Semin Oncol* (2000) 27:177–86.

19. Strouse JJ, Spevak M, Mack AK, Arceci RJ, Small D, Loeb DM. Significant responses to platinum-based chemotherapy in renal medullary carcinoma. *Pediatr Blood Cancer* (2005) 44:407–11. doi: 10.1002/pbc.20292

20. Su Y, Hong AL. Recent advances in renal medullary carcinoma. *IJMS* (2022) 23:7097. doi: 10.3390/ijms23137097

21. Msaouel P, Hong AL, Mullen EA, Atkins MB, Walker CL, Lee C-H, et al. Updated recommendations on the diagnosis, management, and clinical trial eligibility criteria for patients with renal medullary carcinoma. *Clin Genitourinary Cancer* (2019) 17:1–6. doi: 10.1016/j.clgc.2018.09.005

22. Swartz MA, Karth J, Schneider DT, Rodriguez R, Beckwith JB, Perlman EJ. Renal medullary carcinoma: Clinical, pathologic, immunohistochemical, and genetic analysis with pathogenetic implications. *Urology* (2002) 60:1083–9. doi: 10.1016/s0090-4295(02)02154-4

23. Wilson NR, Wiele AJ, Surasi DS, Rao P, Sircar K, Tamboli P, et al. Efficacy and safety of gemcitabine plus doxorubicin in patients with renal medullary carcinoma. *Clin Genitourin Cancer* (2021) 19:e401–8. doi: 10.1016/j.clgc.2021.08.007

24. Rathmell WK, Monk JP. High-Dose-Intensity MVAC for advanced renal medullary carcinoma: Report of three cases and literature review. *Urology* (2008) 72:659–63. doi: 10.1016/j.urology.2008.05.009

25. Genovese G, Carugo A, Tepper J, Robinson FS, Li L, Svelto M, et al. Synthetic vulnerabilities of mesenchymal subpopulations in pancreatic cancer. *Nature* (2017) 542:362–6. doi: 10.1038/nature21064

26. Kondagunta GV, Drucker B, Schwartz L, Bacik J, Marion S, Russo P, et al. Phase II trial of bortezomib for patients with advanced renal cell carcinoma. *J Clin Oncol* (2004) 22:3720–5. doi: 10.1200/JCO.2004.10.155

27. Ronnen EA, Kondagunta GV, Motzer RJ. Medullary renal cell carcinoma and response to therapy with bortezomib. *J Clin Oncol* (2006) 24:e14. doi: 10.1200/JCO.2005.05.0344

28. Carden MA, Smith S, Meany H, Yin H, Alazraki A, Rapkin LB. Platinum plus bortezomib for the treatment of pediatric renal medullary carcinoma: Two cases. *Pediatr Blood Cancer* (2017) 64:e26402. doi: 10.1002/pbc.26402

29. Msaouel P, Slack-Tidwell R, Genovese G, Daw NC, Siefker-Radtke AO, Tannir NM. Phase II trial of ixazomib combined with gemcitabine and doxorubicin in patients with SMARCB1-deficient kidney malignancies. *JCO* (2019) 37:TPS678–8. doi: 10.1200/JCO.2019.37.7_suppl.TPS678

30. Kim KH, Roberts CWM. Targeting EZH2 in cancer. *Nat Med* (2016) 22:128–34. doi: 10.1038/nm.4036

31. Knutson SK, Warholic NM, Wigle TJ, Klaus CR, Allain CJ, Raimondi A, et al. Durable tumor regression in genetically altered malignant rhabdoid tumors by inhibition of methyltransferase EZH2. *Proc Natl Acad Sci U.S.A.* (2013) 110:7922–7. doi: 10.1073/pnas.1303800110

32. Porazzi P, Petruk S, Pagliaroli L, De Dominici M, Deming D, Puccetti MV, et al. Targeting chemotherapy to decondensed H3K27me3-marked chromatin of AML cells enhances leukemia suppression. *Cancer Res* (2022) 82:458–71. doi: 10.1158/0008-5472.CAN-21-1297

33. Gounder M, Schöffski P, Jones RL, Agulnik M, Cote GM, Villalobos VM, et al. Tazemetostat in advanced epithelioid sarcoma with loss of INI1/SMARCB1: an international, open-label, phase 2 basket study. *Lancet Oncol* (2020) 21:1423–32. doi: 10.1016/S1470-2045(20)30451-4

34. Sodji Q, Klein K, Sravan K, Parikh J. Predictive role of PD-L1 expression in the response of renal medullary carcinoma to PD-1 inhibition. *J Immunother Cancer* (2017) 5:62. doi: 10.1186/s40425-017-0267-9

35. Apolo AB, Nadal R, Girardi DM, Niglio SA, Ley L, Cordes LM, et al. Phase I study of cabozantinib and nivolumab alone or with ipilimumab for advanced or metastatic urothelial carcinoma and other genitourinary tumors. *JCO* (2020) 38:3672–84. doi: 10.1200/JCO.20.01652

36. Naing A, Meric-Bernstam F, Stephen B, Karp DD, Hajjar J, Rodon Ahnert J, et al. Phase 2 study of pembrolizumab in patients with advanced rare cancers. *J Immunother Cancer* (2020) 8:e000347. doi: 10.1136/jitc-2019-000347

37. Msaouel P, Slack-Tidwell R, Tannir NM. Phase II trial of nivolumab (nivo) plus ipilimumab (ipi) in patients with SMARCB1-deficient kidney malignancies. *JCO* (2019) 37:TPS677–7. doi: 10.1200/JCO.2019.37.7_suppl.TPS677

38. Albiges L, Pouessel D, Beylot-Barry M, Bens G, Pannier D, Gavoille C, et al. Nivolumab in metastatic nonclear cell renal cell carcinoma: First results of the AcSe prospective study. *JCO* (2020) 38:699–9. doi: 10.1200/JCO.2020.38.6_suppl.699

# Frontiers in Surgery

**Explores and improves surgical practice and clinical patient management**

A multidisciplinary journal which explores surgical practices - from fundamental principles to advances in microsurgery and minimally invasive techniques. It fosters innovation and improves the clinical management of patients.

---

## Discover the latest Research Topics

See more →


**Frontiers**

Avenue du Tribunal-Fédéral 34
1005 Lausanne, Switzerland
frontiersin.org

**Contact us**

+41 (0)21 510 17 00
frontiersin.org/about/contact